COMPREHENSIVE COORDINATION CHEMISTRY

The Synthesis, Reactions, Properties & Applications of Coordination Compounds

Editor-in-Chief
SIR GEOFFREY WILKINSON, FRS

Executive Editors
ROBERT D GILLARD
JON A McCLEVERTY

Volume 1
Theory
&
Background

COMPREHENSIVE COORDINATION CHEMISTRY

IN 7 VOLUMES

PERGAMON MAJOR REFERENCE WORKS

Comprehensive Inorganic Chemistry (1973)

Comprehensive Organic Chemistry (1979)

Comprehensive Organometallic Chemistry (1982)

Comprehensive Heterocyclic Chemistry (1984)

International Encyclopedia of Education (1985)

Comprehensive Insect Physiology, Biochemistry & Pharmacology (1985)

Comprehensive Biotechnology (1985)

Physics in Medicine & Biology Encyclopedia (1986)

Encyclopedia of Materials Science & Engineering (1986)

World Encyclopedia of Peace (1986)

Systems & Control Encyclopedia (1987)

Comprehensive Coordination Chemistry (1987)

Comprehensive Polymer Science (1988)

Comprehensive Medicinal Chemistry (1989)

COMPREHENSIVE COORDINATION CHEMISTRY

The Synthesis, Reactions, Properties & Applications of Coordination Compounds

Volume 1

Theory & Background

EDITOR-IN-CHIEF

SIR GEOFFREY WILKINSON, FRS

Imperial College of Science & Technology, University of London, UK

EXECUTIVE EDITORS

ROBERT D. GILLARD

University College, Cardiff, UK

JON A. McCLEVERTY

University of Birmingham, UK

PERGAMON PRESS

OXFORD · NEW YORK · BEIJING · FRANKFURT
SÃO PAULO · SYDNEY · TOKYO · TORONTO

U.K. Pergamon Press, Headington Hill Hall, Oxford OX3 0BW, England

U.S.A. Pergamon Press, Maxwell House, Fairview Park, Elmsford, New York 10523, U.S.A.

PEOPLE'S REPUBLIC OF CHINA Pergamon Press, Room 4037, Qianmen Hotel, Beijing, People's Republic of China

FEDERAL REPUBLIC OF GERMANY Pergamon Press, Hammerweg 6, D-6242 Kronberg, Federal Republic of Germany

BRAZIL Pergamon Editora, Rue Eça de Queiros, 346, CEP 04011, São Paulo, Brazil

AUSTRALIA Pergamon Press Australia, P.O. Box 544, Potts Point, NSW 2011, Australia

JAPAN Pergamon Press, 8th Floor, Matsuoka Central Building, 1-7-1 Nishishinjuku, Shinjuku-ku, Tokyo 160, Japan

CANADA Pergamon Press Canada, Suite No. 271, 253 College Street, Toronto, Ontario M5T 1R5, Canada

---

First edition 1987

Library of Congress Cataloging-in-Publication Data

Comprehensive coordination chemistry.
Includes bibliographies.
Contents: v. 1. Theory and background - v. 2. Ligands - v. 3. Main group and early transition elements - [etc.]
1. Coordination compounds.
I. Wilkinson, Geoffrey, Sir, 1921-
II. Gillard, Robert D.
III. McCleverty, Jon A.
QD474.C65 1987 541.2'242 86-12319

British Library Cataloguing in Publication Data

Comprehensive coordination chemistry: the synthesis, reactions, properties and applications of coordination compounds.
1. Coordination compounds.
I. Wilkinson, Geoffrey, 1921-
II. Gillard, Robert D.
III. McCleverty, Jon A.
541.2'242 QD474

ISBN 0-08-035944-2 (vol. 1)
ISBN 0-08-026232-5 (set)

Printed in Great Britain by A. Wheaton & Co. Ltd., Exeter

Contents

Reaction Mechanisms

Complexes in Aqueous and Non-aqueous Media

Preface

Since the appearance of water on the Earth, aqua complex ions of metals must have existed. The subsequent appearance of life depended on, and may even have resulted from, interaction of metal ions with organic molecules. Attempts to use consciously and to understand the metal-binding properties of what are now recognized as electron-donating molecules or anions (ligands) date from the development of analytical procedures for metals by Berzelius and his contemporaries. Typically, by 1897, Ostwald could point out, in his 'Scientific Foundations of Analytical Chemistry', the high stability of cyanomercurate(II) species and that 'notwithstanding the extremely poisonous character of its constituents, it exerts no appreciable poison effect'. By the late 19th century there were numerous examples of the complexing of metal ions, and the synthesis of the great variety of metal complexes that could be isolated and crystallized was being rapidly developed by chemists such as S. M. Jørgensen in Copenhagen. Attempts to understand the 'residual affinity' of metal ions for other molecules and anions culminated in the theories of Alfred Werner, although it is salutary to remember that his views were by no means universally accepted until the mid-1920s. The progress in studies of metal complex chemistry was rapid, perhaps partly because of the utility and economic importance of metal chemistry, but also because of the intrinsic interest of many of the compounds and the intellectual challenge of the structural problems to be solved.

If we define a coordination compound as the product of association of a Brönsted base with a Lewis acid, then there is an infinite variety of complexing systems. In this treatise we have made an arbitrary distinction between coordination compounds and organometallic compounds that have metal–carbon bonds. This division roughly corresponds to the distinction — which most but not all chemists would acknowledge as a real one — between the cobalt(III) ions $[Co(NH_3)_6]^{3+}$ and $[Co(\eta^5\text{-}C_5H_5)_2]^+$. Any species where the number of metal–carbon bonds is at least half the coordination number of the metal is deemed to be 'organometallic' and is outside the scope of our coverage; such compounds have been treated in detail in the companion work, 'Comprehensive Organometallic Chemistry'. It is a measure of the arbitrariness and overlap between the two areas that several chapters in the present work are by authors who also contributed to the organometallic volumes.

We have attempted to give a contemporary overview of the whole field which we hope will provide not only a convenient source of information but also ideas for further advances on the solid research base that has come from so much dedicated effort in laboratories all over the world.

The first volume describes general aspects of the field from history, through nomenclature, to a discussion of the current position of mechanistic and related studies. The binding of ligands according to donor atoms is then considered (Volume 2) and the coordination chemistry of the elements is treated (Volumes 3, 4 and 5) in the common order based on the Periodic Table. The sequence of treatment of complexes of particular ligands for each metal follows the order given in the discussion of parent ligands. Volume 6 considers the applications and importance of coordination chemistry in several areas (from industrial catalysis to photography, from geochemistry to medicine). Volume 7 contains cumulative indexes which will render the mass of information in these volumes even more accessible to users.

The chapters have been written by industrial and academic research workers from many countries, all actively engaged in the relevant areas, and we are exceedingly grateful for the arduous efforts that have made this treatise possible. They have our most sincere thanks and appreciation.

We wish to pay tribute to the memories of Professor Martin Nelson and Dr Tony Stephenson who died after completion of their manuscripts, and we wish to convey our deepest sympathies to their families. We are grateful to their collaborators for finalizing their contributions for publication.

Because of ill health and other factors beyond the editors' control, the manuscripts for the chapters on Phosphorus Ligands and Technetium were not available in time for publication. However, it is anticipated that the material for these chapters will appear in the journal *Polyhedron* in due course as Polyhedron Reports.

We should like to acknowledge the way in which the staff at the publisher, particularly Dr Colin Drayton and his dedicated editorial team, have supported the editors and authors in our

However, it is anticipated that the material for these chapters will appear in the journal *Polyhedron* in due course as Polyhedron Reports.

We should also like to acknowledge the way in which the staff at the publisher, particularly Dr Colin Drayton and his dedicated editorial team, have supported the editors and authors in our endeavour to produce a work which correctly portrays the relevance and achievements of modern coordination chemistry.

We hope that users of these volumes will find them as full of novel information and as great a stimulus to new work as we believe them to be.

ROBERT D. GILLARD
Cardiff

JON A. McCLEVERTY
Birmingham

GEOFFREY WILKINSON
London

Contributors to Volume 1

Professor A. W. Adamson
Chemistry Department, University of Southern California, Los Angeles, CA 90089, USA

Professor J. C. Bailar, Jr.
School of Chemical Sciences, University of Illinois, Urbana, IL 61801, USA

Professor D. St. C. Black
School of Chemistry, University of New South Wales, PO Box 1, Kensington, NSW 2033, Australia

Professor I. G. Dance
School of Chemistry, University of New South Wales, PO Box 1, Kensington, NSW 2033, Australia

Professor B. N. Figgis
Department of Physical and Inorganic Chemistry, University of Western Australia, Nedlands, WA 6009, Australia

Dr J. MacB. Harrowfield
Department of Physical and Inorganic Chemistry, University of Western Australia, Nedlands, WA 6009, Australia

Professor H. M. N. H. Irving
Department of Analytical Science, University of Cape Town, Rondebosch, 7700 Cape Town, South Africa

Professor G. B. Kauffman
Department of Chemistry, California State University, Fresno, CA 93740, USA

Dr D. L. Kepert
Department of Physical and Inorganic Chemistry, University of Western Australia, Nedlands, WA 6009, Australia

Dr C. Kutal
Chemistry Department, University of Georgia, Athens, GA 30601, USA

Professor H. E. LeMay, Jr.
Department of Chemistry, College of Arts and Science, Chemistry Building, University of Nevada, Reno, NV 89557, USA

Professor T. J. Meyer
Kenan Laboratories, Department of Chemistry, University of North Carolina, Chapel Hill, NC 27514, USA

Dr C. J. Pickett
AFRC Unit of Nitrogen Fixation, University of Sussex, Falmer, Brighton BN1 9RQ, UK

Dr T. E. Sloan
Chemical Abstracts Service, 2540 Olentangy River Road, PO Box 3012, Columbus, OH 43210, USA

Professor H. Taube
Chemistry Department, Stanford University, Stanford, CA 94305, USA

Professor M. L. Tobe
Chemistry Department, University College London, 20 Gordon Street, London WC1H 0AJ, UK

Dr. D. H. Vaughan
Department of Chemistry, Paisley College of Technology, High Street, Paisley, Renfrewshire, PA1 2BE, UK

Dr S. B. Wild
Research School of Chemistry, Australian National University, Canberra, ACT 2600, Australia

Contents of All Volumes

Volume 1 Theory & Background

Volume 2 Ligands

Volume 3 Main Group & Early Transition Elements

Volume 4 Middle Transition Elements

Volume 5 Late Transition Elements

Volume 6 Applications

Volume 7 Indexes

1.1

General Historical Survey to 1930

GEORGE B. KAUFFMAN
California State University, Fresno, CA, USA

1.1.1 INTRODUCTION

Coordination chemistry encompasses a great diversity of substances and phenomena. In order to survey its history within a single chapter, the author has had to limit his discussion to what he considers the major discoveries, both experimental and theoretical, in the development of the field and to forgo many of the interesting but minor events. We shall first consider, in approximately chronological order, some historically significant coordination compounds, followed by several pre-Werner theories of their formation and constitution. Werner's theory and his most important discoveries will then be dealt with, followed by post-Werner developments through the third decade of the twentieth century. For more detailed treatment of the various topics dealt with here, the reader is referred to the author's previously published articles and books[1–5] on Werner and coordination chemistry, which he has drawn upon in preparing this chapter.

1.1.2 SOME HISTORICALLY SIGNIFICANT COORDINATION COMPOUNDS

Coordination chemistry is, quite simply, the chemistry of coordination compounds. The coordinated groups, called ligands,[6] may be neutral molecules or ions. Historically, the accumulation of information and experimental data about these compounds has been a very slow and gradual process.

1.1.2.1 Alizarin

Different historians ascribe different dates to the discovery of the first coordination compound. Perhaps the earliest known of all coordination compounds is the bright-red alizarin dye, a calcium aluminum chelate compound of hydroxyanthraquinone. It was first used in India and known to the ancient Persians and Egyptians long before it was used by the Greeks and Romans. Joseph's 'coat of many colors' may possibly have been treated with it.

Alizarin was mentioned by Herodotus (*ca.* 450 B.C.). It was probably the red dye used by Alexander the Great to win a battle against a much larger Persian army 120 years later. In possibly the first recorded example of chemical warfare or camouflage, Alexander dyed his soldiers' clothing with blood-like splotches and enticed the Persians into heedlessly attacking what they thought was a demoralized force of badly wounded men. In more recent times, madder dyes were an integral part of American Revolutionary history, being the dye used in the British 'redcoats'.[7]

1.1.2.2 Tetraamminecopper(II) Ion

Probably the first scientifically recorded observation of a completely inorganic coordination compound is the formation of the familiar tetraamminecopper(II) ion, $[Cu(NH_3)_4]^{2+}$. The 16th century German physician and alchemist Andreas Libavius (1540?–1616) noticed that *aqua calcis* (limewater or saturated calcium hydroxide solution) containing *sal ammoniac* (ammonium chloride) became blue in contact with brass (an alloy of copper and zinc).[8]

1.1.2.3 Prussian Blue

Another candidate for the first coordination compound is Prussian Blue, potassium iron(III) hexacyanoferrate(II), a complex of empirical formula $KCN{\cdot}Fe(CN)_2{\cdot}Fe(CN)_3$. It was first obtained accidentally in 1704 by Diesbach, a manufacturer of artist's colors from Berlin. Initially it was described[9] as a nontoxic pigment suitable for oil colors, but its method of preparation was kept secret, probably because Diesbach wished to benefit monetarily from his discovery.

A recipe for the preparation of Prussian Blue was published 20 years after its discovery.[10,11] Since materials containing iron, potash and nitrogenous matter such as blood or animal hooves may have been heated together in more remote times, ferrocyanides [hexacyanoferrates(II)] probably antedate Diesbach's discovery. They contain Fe—CN bonds and may thus possibly be considered as the first known examples of coordination compounds containing transition metal–carbon bonds (organometallic compounds).

1.1.2.4 Hexaamminecobalt(III) Ion

Most authorities attribute the discovery of the first metal ammine to Tassaert, a Parisian chemist about whom virtually nothing is known — not even his first name. In his short article[12] he is identified only as Citoyen Tassaert — Citizen Tassaert. Some chemists imply or even openly state that Tassaert was the first to prepare hexaamminecobalt(III) chloride, $[Co(NH_3)_6]Cl_3$, the parent compound from which all cobalt ammines may be considered to be derived. Yet he merely observed the brownish mahogany color of the solution formed when excess aqueous ammonia is added to a solution of cobalt chloride or cobalt nitrate, and he failed to follow up his accidental discovery.

1.1.2.5 Vauquelin's Salt and Magnus' Green Salt[13]

Louis-Nicolas Vauquelin (1763–1829) discovered the pink compound tetraamminepalladium(II) tetrachloropalladate(II), $[Pd(NH_3)_4][PdCl_4]$.[14] This compound, which contains coordinated palladium in both the cation and the anion, is still known as Vauquelin's Salt after its discoverer. The corresponding platinum compound, $[Pt(NH_3)_4][PtCl_4]$, was discovered by Heinrich Gustav Magnus (1802–1870).[15] It constitutes the first discovered platinum ammine and is known as Magnus'

Green Salt. The two salts are also so-called 'polymerization isomers' of the *cis* and *trans* isomers of the dichlorodiammine complexes of the corresponding metals, which for platinum are *cis*- and *trans*-$[PtCl_2(NH_3)_2]$ (see Section 1.1.2.8).

1.1.2.6 Gmelin's Compounds

According to some authorities, the first metal ammine to be isolated in the solid state was the reddish yellow hexaamminecobalt(III) oxalate $[Co(NH_3)_6]_2(C_2O_4)_3$, described in 1822 by Leopold Gmelin (1788–1853).[16] Gmelin also discovered several new double salts: potassium ferricyanide, or potassium hexacyanoferrate(III), $K_3[Fe(CN)_6]$,[17] the cobalticyanides or hexacyanocobaltates(III), $M_3[Co(CN)_6]$,[18] and the platinocyanides or tetracyanoplatinates(II), $M_2[Pt(CN)_4]$.[19]All these substances certainly deserve to rank among the earliest known coordination compounds.

1.1.2.7 Zeise's Salt

An extremely interesting compound which played an important role in the development of bonding theory in both inorganic and organic chemistry is potassium trichloro(ethylene)platinate(II) monohydrate, which was discovered by William Christoffer Zeise (1789–1847).[20] It was the first discovered organometallic compound to contain an unsaturated organic ligand and is known as Zeise's Salt. Its discovery led to the preparation and characterization of many other platinum–alkene compounds. Its structure and bonding were not understood until the preparation and characterization of the first 'sandwich' compound, ferrocene [bis(cyclopentadienyl)iron(II)], by Kealy and Pauson[21] (1951) in the United States and by Miller *et al.*[22] (1952) in England.

1.1.2.8 Peyrone's Salt and Reiset's Second Chloride

Two other extremely important platinum(II) compounds were discovered during the first half of the 19th century. Both possess the same formula, $PtCl_2(NH_3)_2$, and were discovered in the same year (1844). They differ in physical and chemical properties and constitute the simplest, best known, and longest known case of stereoisomerism among platinum compounds. One isomer, called platosemidiammine chloride or Peyrone's Salt, was first prepared by the action of aqueous ammonia on potassium tetrachloroplatinate(II),[23] while the other isomer, called platosammine chloride or Reiset's Second Chloride, was first prepared by Jules Reiset (1818–1896) by the action of heat or concentrated hydrochloric acid on tetraammineplatinum(II) chloride.[24] Werner, in his first paper on the coordination theory,[25] discussed these compounds at length and considered them to be geometric isomers with a square-planar configuration. The explanation of the course of the reactions involved in the preparation of these isomers was finally given in generalized form by Il'ya Il'ich Chernyaev in his famous *trans* effect[26] (see Section 1.1.5.7).

1.1.2.9 Gibbs' and Genth's Researches[27]

Except for Gmelin's work, there were few other investigations of cobalt–ammonia compounds during the first half of the 19th century. Credit for the first distinct recognition of the existence of perfectly well-defined and crystallized solid salts of cobalt ammines belongs to Frederick Augustus Genth (1820–1893).[28] It was in 1847 at the University of Marburg that Genth made his accidental discovery. Before he was able to complete his research on and analysis of these new compounds, he emigrated to the United States. In 1851 he published his results in an obscure Philadelphia journal for German physicians.[29] He described salts of two cations, roseocobalt [modern, aquapentaamminecobalt(III)] and luteocobalt [modern, hexaamminecobalt(III)]. As we have seen, a few similar compounds of platinum had been prepared in Europe before Genth, but his work drew attention to the neglected field of coordination compounds.

In 1852, Oliver Wolcott Gibbs (1822–1908)[30] began to collaborate with Genth on an investigation which has since become famous in the annals of coordination chemistry. In 1856 Gibbs' and Genth's joint results appeared in a 67-page monograph.[31] They described the preparation, properties, analytical data and reactions of 35 salts of four cobalt–ammine cations: (1) Genth's roseocobalt or aquapentaamminecobalt(III), $[Co(NH_3)_5H_2O]X_3$; (2) purpureocobalt or chloropentaamminecobalt(III), $[CoCl(NH_3)_5]X_2$, described by Claudet;[32] (3) Genth's luteocobalt or hexaamminecobalt(III), $[Co(NH_3)_6]X_3$; and (4) Gibbs' xanthocobalt or nitropentaamminecobalt(III), $[CoNO_2(NH_3)_5]X_2$. For the first time, roseo and purpureo compounds were clearly differentiated although Gibbs and Genth erred in supposing them to be isomeric. They correctly predicted coordination compounds in which one or more equivalents of ammonia are replaced by an equal number of equivalents of an organic amine as well as compounds in which cobalt could be replaced by other metals. Gibbs and Genth deserve credit for attracting chemists to a field which today is experiencing a renaissance of activity. Their experimental results form a direct transitional link from the primitive, qualitative observations of Libavius, Diesbach and Tassaert to the most recent of sophisticated, quantitative, contemporary investigations.

1.1.3 EARLY THEORIES OF COORDINATION COMPOUNDS

In most fields of science, theory generally lags behind practice; sufficient experimental data must be accumulated before attempts are made to explain these experimental facts and to predict new phenomena. During the first half of the 19th century, discoveries of coordination compounds were few, sporadic and often accidental, and it was not until after Gibbs' and Genth's classic memoir that chemists devoted themselves to a systematic study of this field. We thus might think that few theories of coordination compounds were advanced until late in the second half of the 19th century, but this was not the case. In coordination chemistry, the lag of theory behind practice was not great because of the tremendous importance of coordination compounds to the general question of chemical bonding.

1.1.3.1 Graham's Ammonium Theory[33,34]

As the number of known coordination compounds increased, theories to explain their constitution were devised.[35] Thomas Graham (1805–1869) is credited with originating the first theory of metal ammines, the so-called ammonium theory, in which metal ammines are considered as substituted ammonium compounds. Graham attempted to explain the constitution of compounds such as diamminecopper(II) chloride by the formula (**1**).

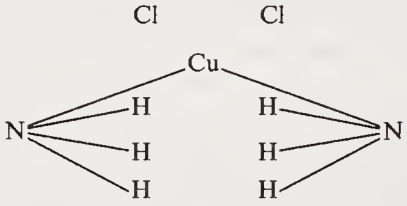

(1)

Because of the close analogy between copper and hydrogen, he suggested that two hydrogen atoms, one from each ammonia molecule, had been displaced by the copper atom. He viewed the salt as a 'chloride of cuprammonium' similar to the 'chloride of ammonium'[36] and thus accounted for the strong retention of the ammonia in the complex. The theory shows a remarkably close similarity to the modern Lewis acid–base approach to the formation of coordinate covalent bonds. Despite the fact that Graham's ammonium theory could be applied only when the number of ammonia molecules in the coordination compound equaled the electrovalence of the metal, it met with a fair degree of success, largely because of the modifications of it that were proposed by other chemists such as Gerhardt,[37] Wurtz,[38] Reiset,[24] von Hofmann[39] and Weltzien.[40]

1.1.3.2 Berzelius' Conjugate Theory[34]

In 1841, Jöns Jacob Berzelius (1779–1848)[41] proposed his conjugate theory, using terms and ideas (*corps copulés*) that he borrowed from Gerhardt. Berzelius viewed metal ammines as conjugated or copulated compounds consisting of ammonia and a conjugate or copula. The conjugate cannot be removed by reaction with an acid and neither increases nor decreases the saturation capacity of a base. In other words, a metal in conjugation with ammonia is still capable of combining with other substances.

Berzelius had introduced his theory of copulae in order to reconcile his electrochemical theory of 1811 with the new phenomena obtained in the organic field which seemed incompatible with it. As time passed, the number of supporters of his theory diminished, and the number of its opponents increased. More and more complicated and improbable formulas became necessary to make the theory agree with experimental facts. Berzelius' stratagem of regarding some compounds as conjugated compounds bore little resemblance to reality in many cases, and although Claus in

1854 and Blomstrand in 1869 in his chain formulas attempted to revive and modify Berzelius' ideas, Berzelius' theory otherwise was of little value.

1.1.3.3 Claus' Ammonia Theory

The next major theory of metal ammines was proposed by Carl Ernst Claus (1796–1864). In 1854, Claus rejected the ammonium theory and suggested a return to Berzelius' view of complexes as conjugated compounds. He compared the platinum ammines not with ammonium salts nor with ammonium hydroxide but with metal oxides. He designated the coordinated ammonia molecule as 'passive, in contrast to the active, alkaline state in the ammonium salts, where it can easily be detected and replaced by other bases'.

Claus' propositions were summarized as three statements in his more widely read paper of 1856.[42] (1) 'If several equivalents of ammonia (from two to six) combine with an equivalent of certain metal chlorides, neutral substances are formed, in which the basic property of ammonia has been destroyed and simultaneously the ammonia can be neither detected by the usual methods nor eliminated by double decomposition'. (2) 'If the chlorine in these compounds is replaced by oxygen, strong bases are obtained, whose saturation capacity is always determined by the oxygen equivalents contained in them but not by the number of equivalents of ammonia present in them'. (3) 'The number of equivalents of ammonia entering into these substances is not a random one; as is evident from a number of facts, it is determined by the number of equivalents of water contained in the hydrates of the metal oxides which can enter into such compounds along with the ammonia'.

Claus' first postulate was vigorously attacked by Karl Weltzien (1813–1870),[40] while Hugo Schiff (1834–1915)[43] attacked not only Claus' first postulate but also his second. All of Claus' three postulates reappeared modified almost four decades later in Werner's coordination theory. Claus' third postulate closely adumbrates Werner's concepts of the coordination number and of the transition series between metal ammines and metal salt hydrates.

1.1.3.4 Constant Valence and Kekulé's 'Molecular Compounds'[44]

At about the time that Claus proposed his ammonia theory, the concept of valence was being formulated and developed by a number of chemists — in particular, Kekulé, Frankland, Williamson, Odling, Kolbe and Couper. During the late 19th and early 20th centuries the principal difficulty in the field of valence was its application to *all* types of chemical compound, and one of the main controversies involved whether or not a given element could possess more than one valence. Since coordination compounds pose a number of basic constitutional problems, it is not surprising that they became involved in the question of variable *vs.* constant valence.

Most of the pioneers in the theory of valence readily admitted the possibility of variable valence. On the other hand, August Kekulé (1829–1896)[45] adopted and rigidly adhered to the principle of constant valence. In spite of the mass of data that soon accumulated to contradict this, he insisted that atomicity (his term for valence) was 'a fundamental property of the atom which is just as constant and unchangeable as the atomic weight itself'. The simplicity of this principle, however, was more than outweighed by the complicated and unrealistic formulas required to maintain it, and eventually Kekulé stood virtually alone in its defense.

Kekulé's dichotomy of compounds into 'atomic compounds' and 'molecular compounds' was an attempt to buttress his theory of constant valence. Since he regarded the valences of nitrogen, phosphorus and cobalt as invariably three, and of copper as invariably two, he was forced to consider phosphorus(V) chloride, ammonium chloride, copper(II) sulfate pentahydrate and hexaamminecobalt(III) chloride as 'molecular compounds' with the formulas $PCl_3{\cdot}Cl_2$, $NH_3{\cdot}HCl$, $CuSO_4{\cdot}5H_2O$ and $CoCl_3{\cdot}6NH_3$, respectively. At most, Kekulé's artificial division of compounds into 'atomic compounds', which obeyed the rules of classical valence theory, and into 'molecular compounds', which did not obey these rules, had some limited value as a formal classification. It did not explain the nature or operation of the forces involved in the formation of 'molecular compounds' except to assume that the forces were acting between molecules rather than between atoms. Since the forces acting between molecules were supposedly weaker than the forces acting between atoms, the resulting 'molecular compounds' should be less stable than 'atomic compounds'. Indeed, some of the substances of limited thermal stability cited by Kekulé as prototypes of 'molecular compounds', such as phosphorus(V) chloride, ammonium chloride and copper(II) sulfate pentahydrate, did decompose in the vapor state. However, this was a relative rather than an absolute phenomenon. Therefore many chemists began to regard Kekulé's classification as meaningless.

Kekulé's instability criterion failed completely in the case of many coordination compounds, which were classified as 'molecular compounds' by sheer dint of necessity although they were extremely resistant to heat and chemical reagents. For example, although hexaamminecobalt(III) chloride contains ammonia, it neither evolves this ammonia on mild heating nor does it react with acids to form ammonium salts. Also, addition of a base to its aqueous solution fails to precipitate hydrated cobalt(III) hydroxide.

1.1.3.5 The Blomstrand–Jørgensen Chain Theory[46]

Whereas Kekulé disposed of complex compounds by banishing them to the limbo of 'molecular compounds', other chemists developed highly elaborate theories to explain their constitution and properties. The most successful and widely accepted of such pre-Werner theories was the chain theory,[47] advanced by Christian Wilhelm Blomstrand (1826–1897)[48] and developed by Sophus Mads Jørgensen (1837–1914).[46,49,50] Although Werner's ideas eventually triumphed, this did not invalidate Jørgensen's observations. On the contrary, his experiments have proven completely reliable and provided the experimental foundation not only for the Blomstrand–Jørgensen chain theory but also for Werner's coordination theory.

The latter half of the 19th century was a period of tremendous progress in organic chemistry, which exerted a predominant influence on other branches of chemistry. Blomstrand suggested that ammonia molecules could link together as $-NH_3-$ chains, analogous to $-CH_2-$ chains in hydrocarbons. These chains involved 'quinquevalent' nitrogen. Today we know that nitrogen can form at most four bonds, but in Blomstrand's time formulas depicting nitrogen atoms with five bonds were quite common.

The number of ammonia molecules associated with the metal (the length of the chain) depended on the metal and its valence, a point later accounted for more adequately by Werner's concept of the coordination number. Jørgensen made provision for different reactivities of various atoms and groups. Halogen atoms that could not be precipitated immediately by silver nitrate were called 'nearer' and were considered to be bonded directly to the metal atom. Halogen atoms that could be precipitated immediately by silver nitrate were called 'farther' and were considered to be bonded through ammonia chains. These two different kinds of bonding were later explained more satisfactorily by Werner's terms 'non-ionogenic' and 'ionogenic', respectively, and by his concepts of inner and outer spheres of coordination. Despite the chain theory's admitted limitations, it permitted the correlation of a considerable amount of empirical data.

In 1883, Jørgensen demonstrated that tertiary amines, which contain no replaceable hydrogen, can form compounds completely analogous to the metal ammines. Graham's ammonium theory (Section 1.1.3.1) conceived of metal ammines as salts in which some of the hydrogen atoms of the ammonium group were replaced by metal atoms. Since tertiary amines contain no replaceable hydrogen, Jørgensen's discovery effectively eliminated the ammonium theory from serious consideration. Therefore chemists had to assume the existence of ammonia chains copied from hydrocarbons or to conceive of metal ammines as 'molecular compounds'. Since Kekulé's theory really explained nothing and only 'substituted a beautiful word for a confused concept', to quote Werner, the Blomstrand–Jørgensen chain theory became the most popular and satisfactory way of accounting for metal ammines and held sway for almost a quarter of a century until displaced by Werner's coordination theory.

Although Jørgensen created no new structural theory of his own, he logically and consistently extended and modified Blomstrand's chain theory to interpret the many new series of complexes that he, Jørgensen, had prepared for the first time. In 1893, Alfred Werner (1866–1919)[51] challenged this theory with a revolutionary new theory based, according to Werner's own admission, on the sturdy foundation of Jørgensen's painstaking experimental investigations. Jørgensen's work bore the seeds of the Blomstrand–Jørgensen theory's destruction, for some of the compounds first prepared by Jørgensen later proved instrumental in demonstrating the validity of Werner's views.

1.1.4 THE COORDINATION THEORY AND THE WERNER–JØRGENSEN CONTROVERSY

1.1.4.1 Werner's Coordination Theory

The circumstances surrounding the creation of Werner's coordination theory provide us with a classic example of the 'flash of genius'. One night in late 1892, Werner awoke at 2 a.m. with the solution to the problem of the constitution of 'molecular compounds', which had come to him like a flash of lightning. He arose from his bed and wrote furiously and without interruption. By 5 p.m. of the following day he had finished his most famous paper, 'Beitrag zur Konstitution anorganischer Verbindungen' (Contribution to the Constitution of Inorganic Compounds).[1,25,50,52,53]

In his revolutionary theory, which marked an abrupt break with the classical theories of valence and structure, Werner postulated two types of valence: *Hauptvalenz* (primary or ionizable valence) and *Nebenvalenz* (secondary or non-ionizable valence). Every metal in a particular oxidation state (with a particular primary valence) also has a definite *coordination number* (a fixed number of secondary valences that must be satisfied). Whereas primary valences can be satisfied only by anions, secondary valences can be satisfied not only by anions but also by neutral molecules. The secondary valences are directed in space around the central metal atom, and the combined aggregate forms a 'complex', which usually exists as a discrete unit in solution. Typical configurations are octahedral for coordination number six and square planar or tetrahedral for coordination number four. Werner's view of the two types of linkage, ionizable ('ionogenic') and non-ionizable ('non-ionogenic'), did much to clarify ideas of chemical bonding a generation before the views of Kossel and Lewis in 1916 led to our present concepts of ionic and covalent bonding.

In our comparison between the chain theory and the coordination theory, we shall confine ourselves to the most common type of complexes, namely, the octahedral hexacovalent ammines of cobalt(III). Although we are concentrating on coordination number six, Werner used similar arguments to prove the constitution and configuration for compounds of coordination number four. Our survey here, which includes only the most important aspects of the controversy, will be organized on the basis of compound type, *i.e.* in a logical rather than strictly chronological sequence. We will consider type MA_6 in which the coordination number of the central metal atom is satisfied by six ammonia molecules. We shall then proceed to replace these ammonia molecules one at a time with other groups.[46,52–54]

The acknowledged test of a scientific theory is its ability to explain known facts and to predict new ones. In examining the comparative successes of the chain theory and the coordination theory in meeting these criteria, we shall examine the metal ammines under two aspects: (1) *constitution* (the manner of bonding of the constituent atoms and groups) and (2) *configuration* (the spatial arrangement of these atoms and groups).

1.1.4.2 Constitution of Cobalt Ammines

1.1.4.2.1 Hexaammines (type MA_6)

Luteocobaltic chloride (modern, $[Co(NH_3)_6]Cl_3$, hexaamminecobalt(III) chloride) is a stable yellow-orange compound.[55] In solution, all the chlorine is immediately precipitated by silver nitrate. Treatment with hydrochloric acid at 100 °C does not remove any ammonia. Treatment with sulfuric acid does not remove any ammonia, but yields the compound $Co_2(SO_4)_3{\cdot}12NH_3$, *i.e.* the chlorine atoms are replaced by sulfate groups. Clearly, some sort of very stable metal–ammonia bonding but much less stable metal–chlorine bonding is indicated.

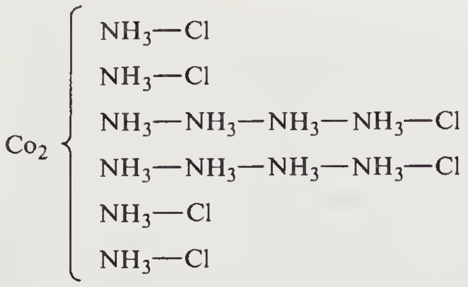

$$Co_2\left\{\begin{array}{l} NH_3{-}Cl \\ NH_3{-}Cl \\ NH_3{-}NH_3{-}NH_3{-}NH_3{-}Cl \\ NH_3{-}NH_3{-}NH_3{-}NH_3{-}Cl \\ NH_3{-}Cl \\ NH_3{-}Cl \end{array}\right.$$

(2)

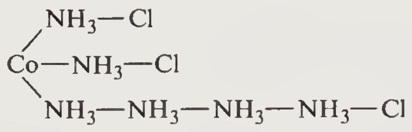

(3) Jørgensen

$[Co(NH_3)_6]Cl_3$

(4) Werner

On heating, one-sixth of the ammonia is lost, and only two-thirds of the chlorine in the resulting purpureocobaltic chloride ($[CoCl(NH_3)_5]Cl_2$) can now be precipitated by silver nitrate. Jørgensen postulated that halogen atoms bonded to the metal atom through other groups such as ammonia can be precipitated by silver nitrate, while those bonded directly to the metal atom cannot.[56] Jørgensen[57] proposed the formula (**2**) for the luteo salt. Both Jørgensen's (**3**) and Werner's (**4**) structures are compatible with the experimental observations. (For simplicity, monomeric formulas will be used for this discussion although they were not used by Jørgensen until 1890.)[58] Their formulas, however, differ in that Jørgensen regarded the chlorine atoms as attached to the metal atom through ammonia molecules, while Werner regarded them as ionogenic and outside the coordination sphere. Werner regarded the central metal atom and the ammonia molecules as comprising a discrete unit, a complex cation. Such a structure should yield four ions in solution, and this was later confirmed by conductance studies.[59,60]

1.1.4.2.2 Pentaammines (type MA_5B)

These compounds may be regarded as luteo salts in which one-sixth of the ammonia has been replaced by another group. Depending on the replacing group, this type can be subdivided into several series. Purpureo salts are pentaammines in which the replacing group is sulfate, nitrate, oxalate or a halogen. Purpureocobaltic chloride, $[CoCl(NH_3)_5]Cl_2$, is formed by heating luteocobaltic chloride.[55] The ammonia molecules are strongly bonded to the cobalt atom, as shown by the fact that ammonia is not evolved even on heating to 100 °C. Jørgensen showed that cold concentrated sulfuric acid does not react with the ammonia in the salt but yields the compound $[CoCl(NH_3)_5]SO_4$, which, although it contains chlorine, gives no immediate precipitate with silver nitrate. He also found that only two-thirds of the chlorine in the original salt can be immediately precipitated by silver nitrate, while the remaining third is precipitated only on long boiling.[55,61]

To account for this difference in reactivity, Jørgensen suggested, as did Werner after him, that the 'unreactive' or 'masked' chlorine was bonded directly to the metal atom. The structures proposed by these two investigators, (**5**) and (**6**) respectively, are both compatible with the experimental facts but differ again in the mode of attachment of the 'reactive' chlorine atoms. Jørgensen regarded these atoms as linked to the metal atom through ammonia molecules, while Werner considered them as not linked to any particular atom, but attracted to the complex cation as a whole by electrostatic forces. Werner's structure requires that a solution of purpureocobaltic chloride furnish three ions, a fact confirmed by conductance studies.[59,60] Other pentaammine series over which Jørgensen and Werner clashed included roseopentammines (aquapentaammines, $[M(NH_3)_5H_2O]X_3$) and xantho and isoxantho salts (nitropentaammines and nitritopentaammines, $[MNO_2(NH_3)_5]X_2$ and $[MONO(NH_3)_5]X_2$).[31,57,60,62]

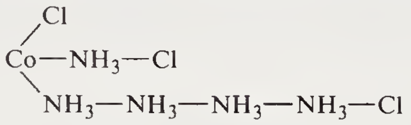

(**5**) Jørgensen

$[CoCl(NH_3)_5]Cl_2$

(**6**) Werner

1.1.4.2.3 Tetraammines (type MA_4B_2)

These compounds may be regarded as luteo salts in which one-third of the ammonia has been replaced by other groups. It is among such compounds that the possibility of stereoisomerism is first encountered, and our consideration of these compounds will be postponed until the section on configuration. As far as constitution is concerned, both the Blomstrand–Jørgensen (**7**) and Werner (**8**) formulas for this type of compound agreed in the number of ions predicted, *viz.* two ions, and this fact was confirmed by conductance studies.[59,60]

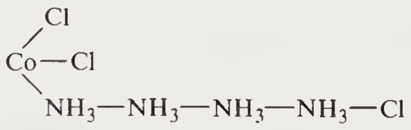

(**7**) Jørgensen

$[CoCl_2(NH_3)_4]Cl$

(**8**) Werner

1.1.4.2.4 Triammines (type MA_3B_3)

These compounds may be regarded as luteo salts in which one-half of the ammonia has been replaced by other groups. We have seen how Jørgensen's and Werner's formulations for hexaammines, pentaammines and tetraammines, both systems reasonably compatible with experimental facts, permitted two rival hypotheses to exist side by side for a limited time. However, as more experimental evidence accumulated, the scales began to tip in favor of Werner's theory.

When successive ammonia molecules in a hexaammine are replaced by negative groups such as chlorine atoms, these enter the coordination sphere and thus become non-ionic or 'masked'. With the replacement of the first two ammonia molecules, the ionic character of the compounds as predicted by the two theories is in complete agreement, but with that of the third ammonia molecule, the ionic character of the resulting compounds (**9**) and (**10**) differs radically according to the two theories.

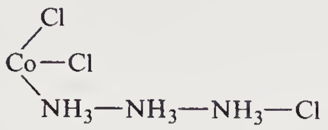

(**9**) Jørgensen: two ions

$[CoCl_3(NH_3)_3]^0$

(**10**) Werner: non-electrolyte

Table 1 shows a comparison of the formulas and predicted numbers of ions for the transition series $[Co(NH_3)_6](NO_2)_3$ ... $K_3[Co(NO_2)_6]$ according to the two theories, and Figure 1 shows the results of Werner's first published experimental work in support of his coordination theory, a study of conductances carried out in collaboration with his friend and former fellow student Arturo Miolati (1869–1956).[63]

Table 1 A Comparison of Blomstrand–Jørgensen's Chain Theory with Werner's Coordination Theory[a]

	BLOMSTRAND–JØRGENSEN		*WERNER*	
Class of compound	*Formula*	*No. of ions*	*Formula*	*No. of ions*
Hexaammines MA_6	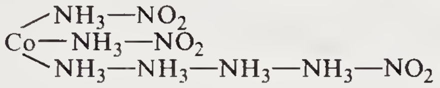	4	$[Co(NH_3)_6](NO_2)_3$	4
	$\downarrow$ −NH_3		$\downarrow$ −NH_3	
Pentaammines MA_5B	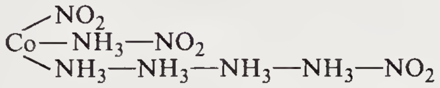	3	$[CoNO_2(NH_3)_5](NO_2)_2$	3
	$\downarrow$ −NH_3		$\downarrow$ −NH_3	
Tetraammines MA_4B_2	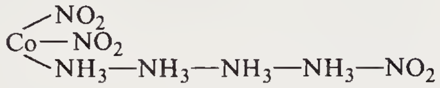	2	$[Co(NO_2)_2(NH_3)_4]NO_2$	2
	$\downarrow$ −NH_3		$\downarrow$ −NH_3	
Triammines MA_3B_3	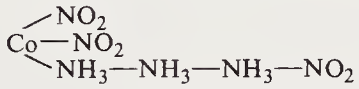	2	$[Co(NO_2)_3(NH_3)_3]$	0
			$\downarrow$ −NH_3	
Diammines MA_2B_4	Unaccountable	—	$K[Co(NO_2)_4(NH_3)_2]$	2
			$\downarrow$ −NH_3	
Monoammines MAB_5	Unaccountable	—	Unknown for cobalt	(3)
			$\downarrow$ −NH_3	
Double salts, MB_6	Unaccountable	—	$K_3[Co(NO_2)_6]$	4

[a] Ref. 3, p. 96.

In their first publication on this subject,[59] Werner and Miolati showed that the molecular conductances (μ) of coordination compounds decreased as successive molecules of ammonia were replaced by acid residues (negative groups or anions). For cobalt(III) salts, they found that μ for luteo salts (hexaammines) > μ for purpureo salts (acidopentaammines) > μ for praseo salts (diacidotetraammines). The conductance fell almost to zero for the triacidotriammine $Co(NO_2)_3(NH_3)_3$ and then rose again for tetracidodiammines, in which the complex behaved as an anion. By such measurements, Werner and Miolati determined the number of ions in complexes of cobalt(III), platinum(II) and platinum(IV). They not only found support for the coordination theory, but they also elucidated the process of dissociation of salts in aqueous solution and followed the progress of aquations.

In their second article on the conductances of complexes, Werner and Miolati[60] showed the complete agreement in magnitude, variation and pattern between their experimentally measured conductances and those predicted according to the coordination theory. The graph of experimentally measured conductances for the $[Co(NH_3)_6]Cl_3$ ... $K_3[Co(NO_2)_6]$ transition series (Figure 1) agreed completely with the numbers of ions predicted according to the coordination theory (Table 1). The conductance results were also concordant with the number of 'masked' and 'unmasked' acid radicals. Furthermore, in its explanation of anionic complexes and its demonstration of the existence of a continuous transition series (*Übergangsreihe*) between metal ammines (MA_6) and double salts (MB_6), the Werner theory succeeded in an area in which the Blomstrand–Jørgensen theory could not compete.

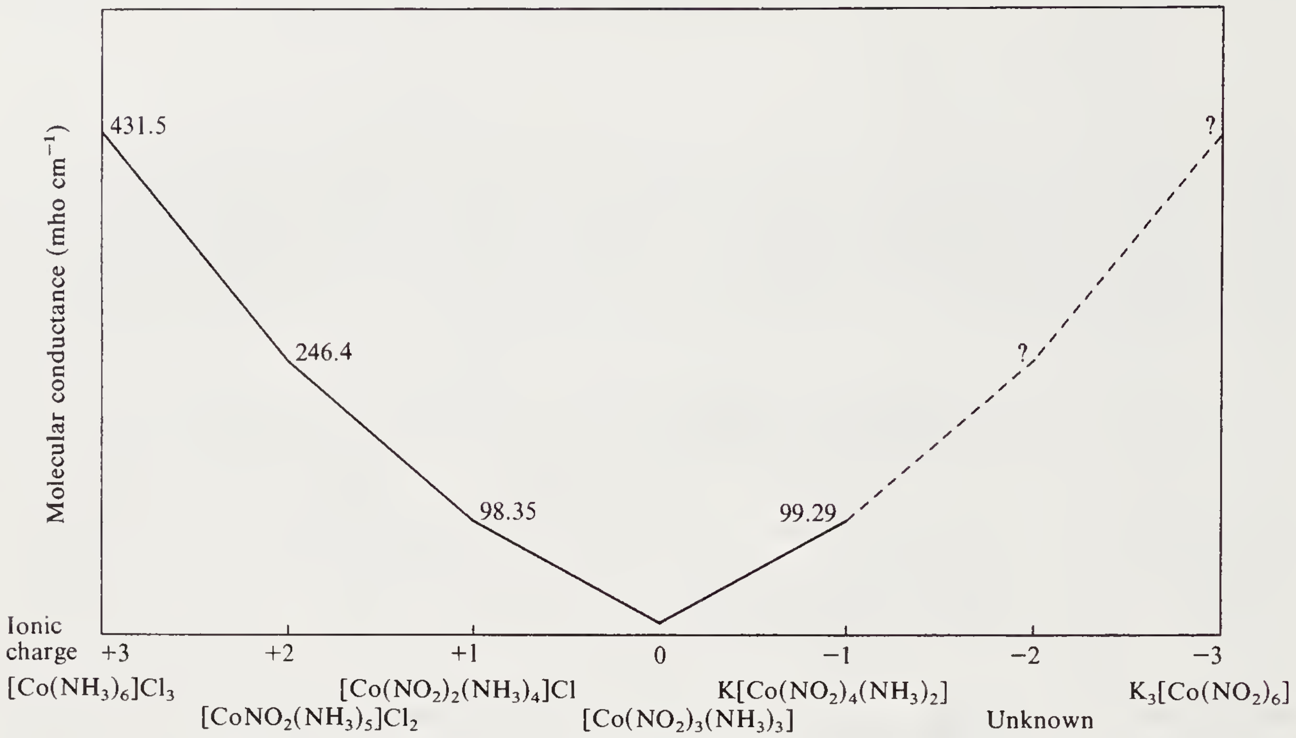

Figure 1 Conductances of cobalt(III) coordination compounds[60] (ref. 3, p. 94)

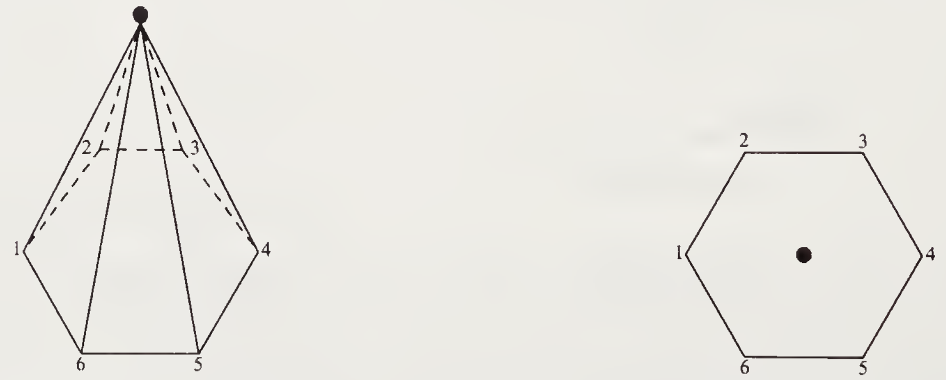

(I) Hexagonal pyramidal

(II) Hexagonal planar

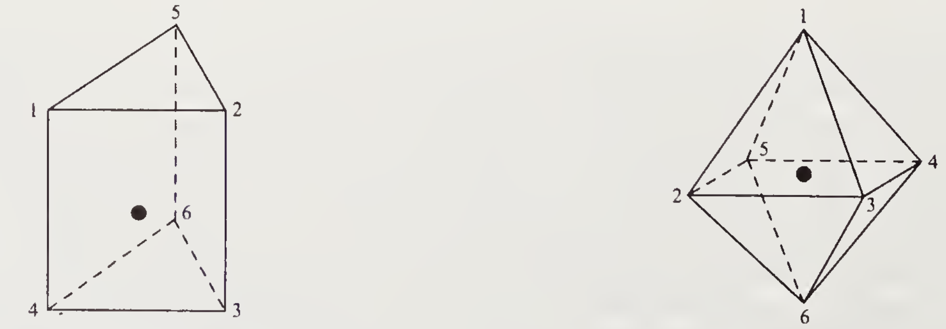

(III) Trigonal prismatic

(IV) Octahedral

Figure 2 Configurational possibilities for coordination number six (ref. 3, p. 97)

1.1.4.3 Configuration of Cobalt Ammines

Let us now examine the means used by Werner to establish the configuration of cobalt ammines.[53] The technique of 'isomer counting' that Werner used as a means of proving configuration admittedly did not originate with him.[64] Yet the technique of comparing the number and type of isomers actually prepared with the number and type theoretically predicted for various configurations probably reached the height of its development with Werner's work. By this method he was able not only to discredit completely the rival Blomstrand–Jørgensen chain theory but also to demonstrate unequivocally that trivalent cobalt possesses an octahedral configuration rather than another possible symmetrical arrangement such as hexagonal planar or trigonal prismatic. The method is summarized in Figure 2 and Table 2. In considering Werner's proof of the configuration of the cobalt ammines, we shall examine two types of stereoisomerism, *viz.* geometric isomerism and optical isomerism.

Table 2 Proof of Configuration for Coordination Number Six by 'Isomer Counting'[a]

	Theoretically predicted isomers				*Experimentally found isomers*	
Compound type	*I Hexagonal pyramidal*	*II Hexagonal planar (a special case of I)*	*III Trigonal prismatic*[c]	*IV Octahedral*	*V*	*Result VI*
MA_6	One form only	One form only	One form only	One form only	One form only	None
MA_5B	One form only	One form only	One form only	One form only	One form only	None
$M(\overline{AA})B_4$[b]	One form only	One form only	Two geometric	One form only	One form only	Provisionally eliminates trigonal prismatic (III)
MA_4B_2	Three geometric (1,2; 1,3; 1,4)	Three geometric (1,2; 1,3; 1,4)	Three geometric (1,2; 1,3; 1,4)	Two geometric (1,2 *cis*; 1,6 *trans*)	Two or less geometric	Provisionally proves octahedral (IV); discovered 1907
MA_3B_3	Three geometric (1,2,3; 1,2,4; 1,3,5)	Three geometric (1,2,3; 1,2,4; 1,3,5)	Three geometric (1,2,3; 1,2,5; 1,2,6)	Two geometric (1,2,3 *facial*; 1,2,6 *peripheral*)	Two or less geometric	Provisionally proves octahedral (IV)
$M(\overline{AA})_2B_2$[b] or $M(\overline{AA})_2BC$[b]	Two geometric	Two geometric	Four geometric, one of which is asymmetric	Two geometric (1,2 *cis*; 1,6 *trans*), the first of which is asymmetric	Two geometric (1,2 *cis*; 1,6 *trans*), the first of which was resolved	Unequivocally proves octahedral (IV); discovered 1911
$M(\overline{AA})_3$[b]	One form only	One form only	Two geometric	One asymmetric pair	One pair optical resolved	Unequivocally proves octahedral (IV); discovered 1912

[a] Ref. 3, p. 98.

[b] $\overline{AA}$ represents a symmetrical bidentate (chelate) ligand. Such ligands coordinate at two adjacent positions. They can span *cis* positions but not *trans* positions.

[c] Coordination compounds with this configuration have been synthesized (R. Eisenberg and J. A. Ibers, *J. Am. Chem. Soc.*, 1965, **87**, 3776–3778; *Inorg. Chem.*, 1966, **5**, 411–416; E. I. Stiefel and H. B. Gray, *J. Am. Chem. Soc.*, 1965, **87**, 4012–4013; H. B. Gray, R. Eisenberg and E. I. Stiefel, in 'Werner Centennial', G. B. Kauffman, Symposium Chairman, American Chemical Society, Washington, DC, 1967, pp. 641–650).

1.1.4.3.1 Geometric isomerism[27,46,53,66]

Through the years, Werner and his students prepared and characterized, in most cases for the first time, geometric isomers of no less than 53 series of cobalt and chromium complexes.[64,65] In most cases, as a comparison of columns IV and V of Table 2 shows, the number and type of isomers prepared corresponded to the expectations for the octahedral arrangement, but there were a few exceptions, and Werner required more than 20 years to accumulate a definitive proof for his structural ideas. For example, the best known case of geometric (*cis–trans*) isomerism was observed by Jørgensen[67] not among simple tetraammines MA_4B_2 but among salts $M(\overline{AA})_2B_2$, in which the four ammonia molecules had been replaced by two molecules of the bidentate (chelate) organic base ethylenediamine (en), *i.e.* among the so-called praseo (green) and violeo (violet) series of formula $CoCl_3{\cdot}2en$. Jørgensen regarded the difference in color as due to *structural* isomerism connected with the linking of the two ethylenediamine molecules, whereas Werner regarded the compounds as *stereoisomers, i.e.* compounds composed of the same atoms and bonds but differing only in the orientation of these atoms and bonds in space (Figure 3).

If this type of isomerism was merely a geometric consequence of the octahedral structure as Werner maintained, it should also be observed among simple tetraammines MA_4B_2 which do not contain ethylenediamine. Yet for compounds $[CoCl_2(NH_3)_4]X$, only one series (praseo, green) was

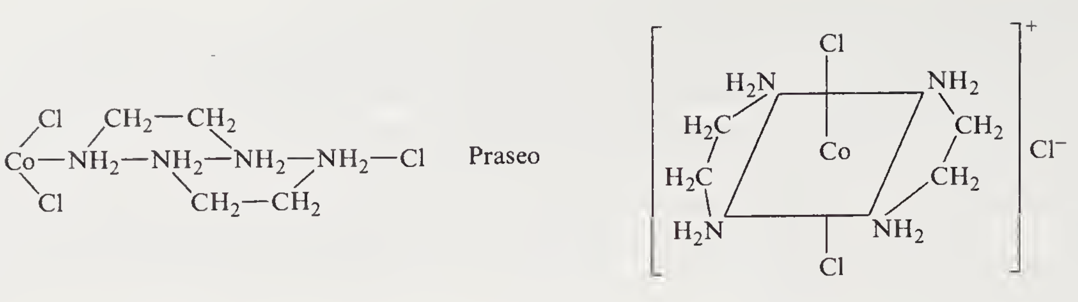

Jørgensen Werner

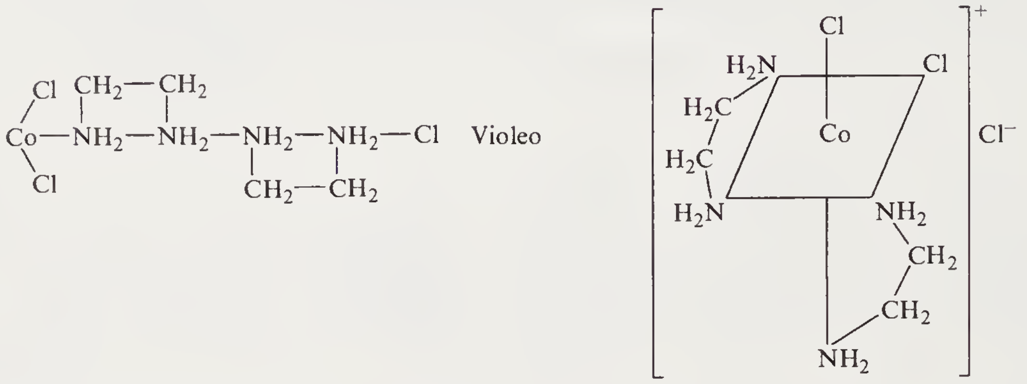

Figure 3 Jørgensen's and Werner's formulae for praseo and violeo ethylenediamine isomers (ref. 3, p. 99)

known.[31] Jørgensen, a confirmed empiricist, quite correctly criticized Werner's theory on the ground that it implied the existence of unknown compounds. It was not until 1907 that Werner finally succeeded in synthesizing the unstable, highly crucial violeo tetraammines, *cis*-$[CoCl_2(NH_3)_4]X$,[68] which were a necessary consequence of his theory but not of Jørgensen's (Figure 4). His Danish opponent immediately conceded defeat.

Praseo (*trans:* 1,6)
Gibbs and Genth (1857)

Violeo (*cis:* 1,2)
Werner (1907)

Figure 4 Ammonia praseo and violeo isomers (ref. 3, p. 100)

1.1.4.3.2 Optical isomerism

Even though the discovery of the long-sought violeo salts in 1907 convinced Jørgensen that his own views could not be correct, Werner's success in preparing two, and only two, isomers of the $[CoCl_2(NH_3)_4]X$ salts as well as numerous compounds of the MA_4B_2 type was not sufficient to prove conclusively his proposed octahedral configuration. Despite such 'negative' evidence, it could still be argued logically that failure to isolate a third isomer of these compounds did not necessarily prove their nonexistence. A more 'positive' proof was necessary. This proof involved the resolution into optical isomers of certain types of asymmetric coordination compounds containing chelate groups.[69] The agreement of Werner's empirical results with the predictions of his octahedral hypothesis can clearly be seen by comparing Column V with Columns I–IV in Table 2.

As early as 1899,[70] Werner recognized that the resolution into optical isomers of certain types of coordination compounds, containing chelate groups which can span *cis* positions only, could provide the 'positive' proof that he needed. After many unsuccessful attempts, in 1911 he succeeded. His resolution, with his American student Victor King (1886–1958), of *cis*-chloroamminebis(ethylenediamine)cobalt(III) salts by means of the resolving agent silver *d*-α-bromocamphor-π-sulfonate was sufficient to prove conclusively the octahedral configuration for cobalt(III) (Figure 5).[71]

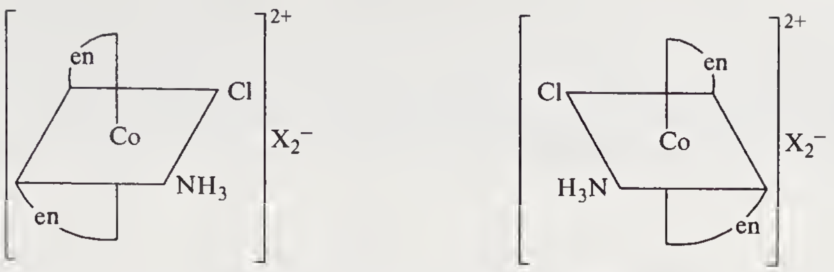

Figure 5 Optical antipodes of *cis*-$[Co(Cl)(NH_3)(en)_2]X_2$ (ref. 3, p. 100)

The resolution of optically active coordination compounds, a feat which 'shook chemistry to its innermost foundations',[72] gained for the coordination theory the widespread recognition for which Werner had been striving for so long. Nor was the theory's founder neglected, for two years later, largely in recognition of 'the most brilliant confirmation of [his] stereochemical views',[73] Werner was awarded the Nobel Prize in chemistry for 1913.[74]

Yet because of the prevalent view that optical activity was almost always connected with carbon atoms, a number of Werner's contemporaries argued that the optical activity of these, and the many other mononuclear and polynuclear coordination compounds subsequently resolved by him,[75] was somehow due to the organic chelate groups present, even though these symmetrical ligands were all optically inactive. Any vestige of doubt was finally dispelled by Werner's resolution in 1914[76] of completely carbon-free coordination compounds — the tris[tetraammine-μ-dihydroxo-cobalt(III)]cobalt(III) salts (**11**), first prepared by Jørgensen.[77] These salts are compounds of the $M(\overline{AA})_3$ type, in which $\overline{AA}$ is the inorganic bidentate ligand (**12**).

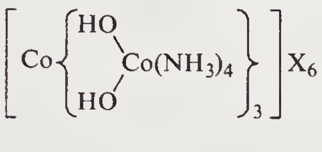

$\left[Co\left\{(HO)_2Co(NH_3)_4\right\}_3\right]X_6$

(**11**)

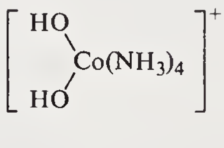

$\left[(HO)_2Co(NH_3)_4\right]^+$

(**12**)

At the beginning of his career, Werner had destroyed the carbon atom's monopoly on geometric isomerism. In his doctoral dissertation,[78] he had explained the isomerism of oximes as due to the tetrahedral configuration of the nitrogen atom. Now, at the peak of his career, he had likewise forced the tetrahedron to relinquish its claim to a virtual monopoly on optical isomerism. One of the major goals of his life's work, the demonstration that stereochemistry is a general phenomenon not limited to carbon compounds and that no fundamental difference exists between organic and inorganic compounds, had been attained.

The validity of Werner's structural views was later amply confirmed by X-ray diffraction studies (see Section 1.1.5.5). Yet, despite the advent of more *direct* modern techniques, Werner's classical configurational determinations by simple *indirect* methods still remain today a monument to his intuitive vision, experimental skill and inflexible tenacity. In the words of Henry Eyring, 'The ingenuity and effective logic that enabled chemists to determine complex molecular structures from the number of isomers, the reactivity of the molecule and of its fragments, the freezing point, the empirical formula, the molecular weight, *etc.*, is one of the outstanding triumphs of the human mind'.[79]

1.1.5 TWENTIETH-CENTURY DEVELOPMENTS

1.1.5.1 Inner Complexes: Ley and Bruni (1904)

Werner's coordination theory[25] was a watershed in the history of coordination chemistry and gave the field its name. With a few exceptions, the majority of chemists accepted Werner's views, and most 20th century contributions have been developments, extensions or confirmations of Werner's theory rather than ideas incompatible with or opposed to it. Ley's concept of inner complex salts is one of the earliest of such post-Werner developments.[80]

Although metal chelates were known in the late 19th century, the first person to recognize clearly the special significance and consequences of the cyclic structure in coordination compounds was the German chemist Heinrich Ley (1872–1938). In 1904, by observations of color, transference and distribution experiments, and determinations of molecular weight and electrical conductance, he explained the constitution of copper glycinate and related compounds by applying Werner's concepts of *Hauptvalenzen* (primary valencies) and *Nebenvalenzen* (secondary valencies).[80,81] He showed that the compound was not an ordinary simple salt or even an ordinary complex salt but rather a special type of metal chelate that he called an inner metal complex salt (*inneres Metallkomplexsalz*) (**13**), in which each bidentate ligand is bonded to the central metal ion by both a primary valency and a secondary valency, forming a cyclic structure. The concept of inner complexes is also sometimes associated with the name of Giuseppe Bruni (1873–1946), who, with C. Fornara, proposed a constitutional formula for copper glycinate analogous to Ley's formula.[82]

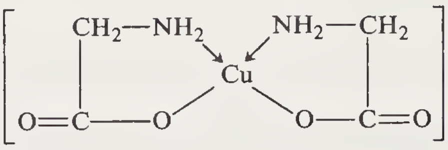

(**13**) Bis(glycinato)copper(II)

1.1.5.2 Cyclic Bonding and Stability: Chugaev's Rule of Rings (1906)

Closely related to Ley's concept of inner complexes is Chugaev's so-called rule of rings. In order for a molecule with two potentially coordinating groups, such as a diamine, $NH_2(CH_2)_nNH_2$, or an amino acid, $NH_2(CH_2)_nCOOH$, to function as a chelate group, it must be geometrically possible to form a ring of low strain. From organic chemistry it is known that five- and six-membered rings are the most stable, whereas four-membered rings are less stable and three-membered rings are quite unstable (Baeyer's strain theory).[83] That these relationships were completely applicable to complex compounds was shown by Lev Aleksandrovich Chugaev, Professor of Chemistry at St. Petersburg University (1873–1922), as early as 1906 (Chugaev's rule of rings). This rule served as a point of departure for stereochemical research not only by Chugaev but also by many other workers.[84] The method for determining the configuration of coordination compounds of Pt^{II} by reaction with oxalic acid, subsequently developed by Grinberg, provides an excellent example of the stability of a five-membered ring.[85] Chugaev also clearly showed the stability of pentatomic and hexatomic ring systems by comparing the ease of formation of complexes of Co^{III}, Ni^{II} and Pt^{II} with various diamines.[86]

1.1.5.3 Alternative Theories of Coordination Compounds

1.1.5.3.1 Friend (1908)

In 1908, John Albert Newton Friend (1881–1966) criticized Werner's theory and offered an alternative explanation of complex compounds.[87] Friend noted that the classical theory of valency could not explain why the valency of most elements apparently varies, why electropositive elements readily combine with electronegative ones to form the most stable compounds, why electropositive and electronegative elements combine both with themselves and with other elements of the same sign to form fairly stable molecules, and why molecules can combine with other molecules to form highly stable complexes. To resolve these difficulties, Friend distinguished three kinds of valency: (1) free positive, (2) free negative and (3) residual or latent valency. His third type referred to positive and negative valencies, which differ from the free valencies in that they can only be called out in pairs of equal and opposite sign. Friend's free valencies correspond to Werner's *Hauptvalenzen* and his latent valencies to Werner's *Nebenvalenzen*, with certain differences in the latter case.

Friend[88] specifically criticized Werner's theory and emphasized the differences between his own latent valencies and Werner's *Nebenvalenzen*. He applied his new theory of valency to ammonium salts, metal ammines and halide 'double salts', and he proposed that for hexacoordinate central atoms a 'hexatomic shell' forms around the metal but that all the elements or groups are joined *together* by latent valencies and not necessarily to the metal itself. In 1916, Friend applied his cyclic theory of complexes in detail to the structures of the chlorides of hexaamminecobalt(III), chloropentaamminecobalt(III) and dichlorotetraamminecobalt(III) and emphasized four basic differences between his theory and Werner's.[89]

1.1.5.3.2 Briggs (1908)

Samuel Henry Clifford Briggs (1880–1935) devised formulas for coordination compounds that he claimed fulfilled the conditions required by experimental data and that indicated the manner in which the affinities of the atoms are disposed in the molecule.[90] He did not claim to be proposing a new theory of valency; like Werner, he believed that 'a totally comprehensive and satisfactory theory of valency will not be possible until we have a much more complete knowledge of the constitution of molecular compounds, and also of the nature of chemical affinity, than we possess today'. Briggs later reinterpreted his formulas in terms of the electronic theory of valency, distinguished between what he called primary and secondary affinity, concepts similar to Werner's *Hauptvalenz* and *Nebenvalenz*, and characterized three different types of chemical combination.[91]

1.1.5.3.3 Povarnin (1915)

In 1915, in a series of four papers, Georgii Georgievich Povarnin (1880–1946) criticized Werner's theory on the grounds that: (1) it necessitates the assumption of two kinds of valencies, with a further differentiation of groups into 'ionogens' and 'non-ionogens', thus making three varieties of affinity bonds; (2) it makes a distinction between atomic and molecular compounds; (3) it assumes that while the number of principal valences of an element depends on its position in the periodic table, the number of its auxiliary valences is not related to the table; (4) in many cases it makes it difficult to predict the number of possible isomers; and (5) it explains the structure of the inner sphere where atoms or groups are linked directly to the central atom but fails to show how this sphere is united with the outer sphere where union with the central atom is through the intermediacy of other atoms.[92]

To overcome these difficulties, Povarnin proposed his theory of polar affinities, in which he assumed that atoms themselves are complex systems of positive and negative affinities in unequal amounts so that an element is positive when the positive charge exceeds the negative, and negative when the situation is *vice versa.* He therefore regarded the classical unit of valency as composed of two polar charges not identical in absolute magnitude. He postulated that bonds between atoms have the power to oscillate and that atoms tend to form four- or six-membered cyclic molecules.

1.1.5.3.4 Pfeiffer (1920)

Even so great an admirer of Werner as Paul Pfeiffer (1875–1951),[93] Werner's former student and one-time 'chief of staff' at the University of Zürich and the man who first applied Werner's theory to crystal structures (see Section 1.1.5.4), proposed modifications of the coordination theory. He applied what he called the principle of 'affinity adjustment of the valencies' to overcome certain shortcomings of Werner's theory.[94] He considered the ionizable radicals or atoms in the outer sphere to be combined with the complex radical as a whole and not attached definitely to the central atom or to any of its associated molecules. He also applied this idea to complex organic molecular compounds. However, Pfeiffer's modifications should not be interpreted as attacks on Werner's ideas.

1.1.5.4 'Crystals as Molecular Compounds': Pfeiffer (1915)

Werner apparently did not realize that the polynuclear complexes which he investigated so extensively[95] constituted a transition between the usual mononuclear coordination compounds and the infinite structure of the crystal lattice. It remained for Paul Pfeiffer, Paul Niggli (1888–1953) and others to point out that crystal structures were in beautiful agreement with his coordination theory, as revealed by the then new experimental technique of X-ray diffraction.[96]

Pfeiffer suggested that crystals be regarded as extremely high-molecular-weight coordination compounds, in which atoms act as coordination centers, about which further atoms group themselves in definite symmetrical relationships.[97] According to him, crystals are constructed according to the same structural chemical and steric laws as coordination compounds. He regarded the forces holding together the atoms or groups of atoms in crystals as identical with the chemical forces operative in coordination compounds. He thus extended the coordination theory into areas in which it had previously been inapplicable.

Pfeiffer dealt with sodium chloride, which he regarded as a high-molecular-weight coordination compound $(NaCl)_n$ made up of equal amounts of $[NaCl_6]$ and $[ClNa_6]$ units. He showed that in crystals of symmetrical compounds, the difference between primary valencies *(Hauptvalenzen)* and secondary valencies *(Nebenvalenzen)* disappears. He extended his treatment to other crystals, and he showed that coordination centers could be groups of atoms as well as single atoms.[98] He also pointed out that coordination numbers as high as 12 must sometimes be considered,[99] and he suggested that in crystals of simple organic molecular compounds of type AB each constituent acts as a coordination center so that AB_6 and BA_6 units interpenetrate just as they do in the rock salt crystal.[94]

1.1.5.5 Determination of Configuration by X-Ray Diffraction

1.1.5.5.1 Wyckoff and Posnjak (1921)

As a result of Pfeiffer's suggestion of applying Werner's coordination theory to crystals and the advent of new experimental techniques, a number of scientists in various countries simultaneously began to investigate the crystal structures of coordination compounds by means of X-rays. Ralph W. G. Wyckoff (b. 1897) 'chose ammonium hexachloroplatinate(IV) as a crystal that should provide a clear-cut test of Werner coordination'.[100] The results of his investigation, published together with Eugen Posnjak (1888–1949), constitute the first published experimental crystallographic study of a coordination compound.[101] In Wyckoff's words, 'All six chlorine atoms in $(NH_4)_2PtCl_6$ ... were crystallographically identical. They were equally distant from the metal atom, and hence there was no difference in the bonds they formed with it. Furthermore, chlorines were found to be at the corners of a regular octahedron having the platinum atom at its center. A more complete agreement with the predictions of the Werner theory could scarcely have been imagined'.[100] Others quickly applied the X-ray diffraction technique and confirmed the octahedral configuration of the six halogen atoms in similar hexacoordinate complexes.

1.1.5.5.2 Dickinson (1922)

Within a year of Wyckoff and Posnjak's confirmation of the octahedral configuration for platinum(IV) (coordination number six), Roscoe Gilkey Dickinson (1894–1945) used the X-ray diffraction method to confirm Werner's prediction of a planar configuration for platinum(II) (coordination number four).[102] Dickinson followed up his determination of the crystal structure of ammonium hexachlorostannate(IV) ($(NH_4)_2[SnCl_6]$), isomorphous with Wyckoff and Posnjak's $(NH_4)_2[PtCl_6]$, with determinations of the crystal structures of potassium tetrachloroplatinate(II) ($K_2[PtCl_4]$) and potassium and ammonium tetrachloropalladates(II) ($K_2[PdCl_4]$ and $(NH_4)_2[PdCl_4]$). In the three cases each platinum or palladium atom was found to be surrounded by four equidistant and equivalent chlorine atoms situated in a plane. A similar arrangement has been found for the ammonia molecules in $[Pt(NH_3)_4]Cl_2$.

Since Dickinson's first determinations, crystal structures of many other complexes of various coordination numbers have been determined. All these investigations and others have provided a complete and *direct* confirmation of Werner's views to support his *indirect* configurational proofs obtained during the previous decades by preparation of isomers and resolution of optically active compounds (see Section 1.1.4), and today the terminology and concepts of coordination theory are routinely used in crystallography.

1.1.5.6 The Effective Atomic Number Concept: Sidgwick (1923)

The first attempts to interpret Werner's views on an electronic basis were made in 1923 by Nevil Vincent Sidgwick (1873–1952) and Thomas Martin Lowry (1874–1936).[103] Sidgwick's initial concern was to explain Werner's coordination number in terms of the sizes of the sub-groups of electrons in the Bohr atom.[104] He soon developed the attempt to systematize coordination numbers into his concept of the 'effective atomic number' (EAN).[105] He considered ligands to be Lewis bases which donated electrons (usually one pair per ligand) to the metal ion, which thus behaves as a Lewis acid. Ions tend to add electrons by this process until the EAN (the sum of the electrons on the metal ion plus the electrons donated by the ligand) of the next noble gas is achieved. Today the EAN rule is of little theoretical importance. Although a number of elements obey it, there are many important stable exceptions. Nevertheless, it is extremely useful as a predictive rule in one area of coordination chemistry, that of metal carbonyls and nitrosyls.

1.1.5.7 The *Trans* Effect: Chernyaev (1926)

Almost every beginning student of organic chemistry knows that substitutions do not occur in a random manner. For example, according to the Crum Brown–Gibson Rule governing the path of substitution in aromatic compounds, certain groups on the benzene nucleus are *ortho-* or *para*-orienting, while others are *meta*-orienting. In a similar manner, substitutions among coordination compounds are not random. However, the general principle underlying the directive influences of coordinated ligands was not enunciated until well into the third decade of the present century. Such influences are most pronounced and well investigated among square planar complexes, especially those of platinum(II).[106]

The chemical behavior of dipositive platinum complexes was studied by many of the early investigators in coordination chemistry, and the well-known regularities observed in substitutions were cited by Werner in his assignment of *cis* and *trans* configurations for platinum(II) complexes, to which he ascribed a square-planar arrangement.[25] The compounds chosen by Werner were among the simplest and longest known platinum isomers, *viz.* platosemidiammine chloride or Peyrone's Salt and platosammine chloride or Reiset's Second Chloride, both with the formula $PtCl_2(NH_3)_2$ (see Section 1.1.2.8). Werner, on the basis of transformation reactions, assigned them the configurations (**14**).

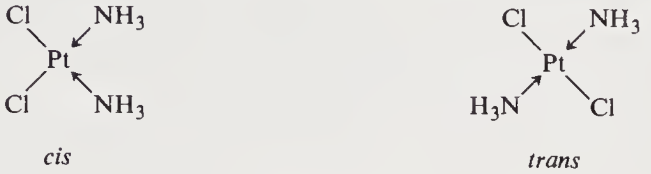

(**14**)

The synthesis of each of these compounds involved directive influences, and the preparative reactions were known as Peyrone's reaction and Jørgensen's reaction, respectively, and were said to exemplify Peyrone's rule (*cis* orientation) and Jørgensen's rule (*trans* orientation) (Scheme 1).

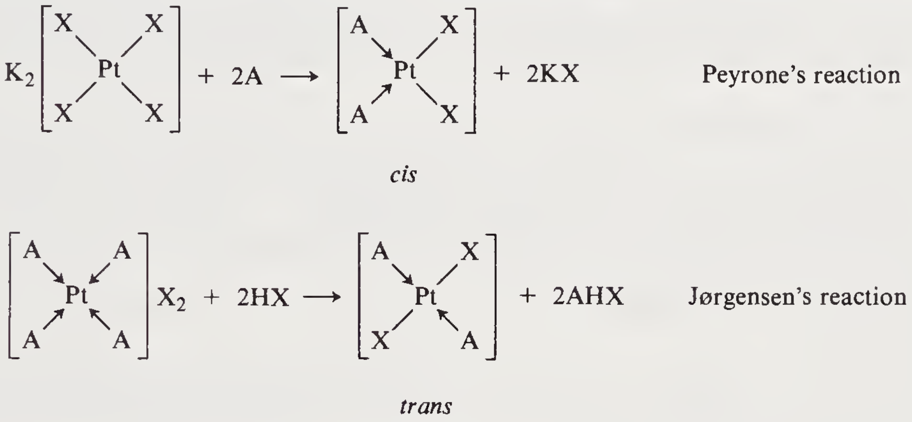

(A = NH_3 or an amine, X = halogen)

Scheme 1

In 1893 a third important regularity was observed by Nikolaĭ Semenovich Kurnakov (1860–1941).[107] While investigating the substitution of ligands by thiourea and thioacetamide, Kurnakov found that replacement occurs with all the ligands of the *cis* compound but only with the acid radicals of the *trans* compound (Scheme 2). Since the two isomers yield different products, this reaction, known as Kurnakov's reaction or Kurnakov's test, may be used to differentiate *cis* from *trans* isomers of dipositive platinum or palladium. Kurnakov's classic reaction played a crucial role in Werner's proof of the square planar configuration of Pt^{II} and in Chernyaev's formulation of the *trans* effect.

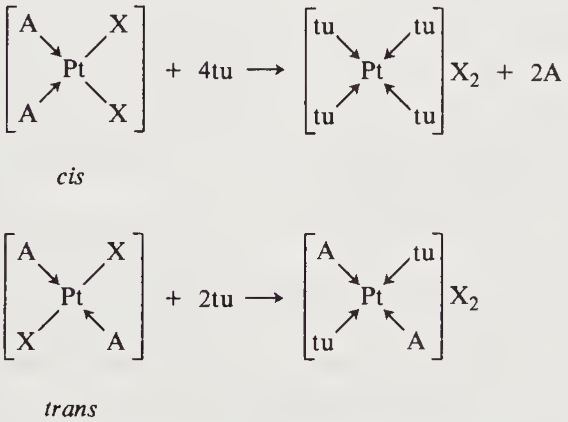

(A = NH_3 or an amine, X = halogen or acid radical, tu = thiourea)

Scheme 2

Peyrone's, Jørgensen's and Kurnakov's reactions are all specialized cases of a more general directive influence and hence are explainable by and derivable from it. Although Werner recognized the principle of '*trans* elimination' as early as 1893, it was not until 1926 that Il'ya Il'ich Chernyaev (1893–1966) pointed out the general regularity of what he called the *trans* effect in order to describe the influence of a coordinated ligand on the practical ease of preparing compounds in which the group *trans* to it had been replaced.[26]

Chernyaev generalized that a negative group coordinated to a metal atom loosens the bond of any group *trans* to it and thus explained not only Peyrone's, Jørgensen's and Kurnakov's reactions but also many other features of the reactions of divalent and tetravalent platinum.[108] He also investigated substitutions of complexes of chromium, cobalt, tellurium and osmium. He postulated that the *trans* effects of atoms are inversely proportional to their metallic character, *i.e.* directly proportional to their electronegativities. Electronegative ligands such as NO_2^-, NCS^-, F^-, Cl^-, Br^- and I^- have a greater '*trans* influence' than neutral ligands such as NH_3, amines or H_2O. Chernyaev's original *trans*-directing series has been extended to include a variety of ligands: $CN^- \approx CO \approx C_2H_4 \approx NO^- > CH_3^- \approx SC(NH_2)_2 \approx SR_2 \approx PR_3 > SO_3H^- > NO_2^- \approx I^- \approx SCN^- > Br^- > Cl^- > C_5H_5N > RNH_2 \approx NH_3 > OH^- > H_2O$.

Acknowledgement. The author wishes to thank Sharon Turner for technical assistance.

1.1.6 REFERENCES

1. G. B. Kauffman, 'Alfred Werner: Founder of Coordination Chemistry', Springer-Verlag, Berlin, 1966.
2. G. B. Kauffman, 'Classics in Coordination Chemistry, Part I: The Selected Papers of Alfred Werner', Dover, New York, 1968.
3. G. B. Kauffman, 'Classics in Coordination Chemistry, Part II: Selected Papers (1798-1899)', Dover, New York, 1976.
4. G. B. Kauffman, 'Classics in Coordination Chemistry, Part III: Twentieth-Century Papers (1904-1935)', Dover, New York, 1978.
5. G. B. Kauffman, 'Inorganic Coordination Compounds', Heyden, London, 1981.
6. For the origin and dissemination of the term 'ligand' in coordination chemistry see W. H. Brock, K. A. Jensen, C. K. Jørgensen and G. B. Kauffman, *Ambix*, 1981, **28**, 171; *J. Coord. Chem.*, 1982, **11**, 261; *J. Chem. Inf. Comput. Sci.*, 1982, **22**, 125; *Polyhedron*, 1983, **2**, 1; *J. Chem. Educ.*, 1983, **60**, 402.
7. D. F. Martin and B. B. Martin, 'Coordination Compounds', McGraw-Hill, New York, 1964, pp. 25–26.
8. A. Libavius, 'Commentationum Metallicarum Libri Quatuor de Natura Metallorum ...', Frankfurt, vi p. II, c. 19.
9. Anonymous, *Miscellanea Berolinensia*, 1710, **I**, 377.
10. J. Woodward, *Philos. Trans. R. Soc. London*, 1724, **33**, 15 (in Latin). For an English translation see H. M. Powell, *Proc. Chem. Soc.*, 1959, 73.
11. J. Browne, *Philos. Trans. R. Soc. London*, 1724, **33**, 17.
12. Tassaert, *Ann. Chim. (Paris)*, 1798, **28**, 92. For a discussion and partial English translation see ref. 3, pp. 2–3.
13. G. B. Kauffman, in 'Dictionary of Scientific Biography', ed. C. C. Gillispie, Charles Scribner's Sons, New York, 1974, vol. 9, pp. 18–19; *Platinum Met. Rev.*, 1975, **20**, 21.
14. L.-N. Vauquelin, *Ann. Chim. (Paris)*, 1813, **88**, 188.
15. G. Magnus, *Pogg. Ann. Phys. Chem.*, 1828, **14**, 239. For a discussion and annotated English translation see ref. 3, pp. 7–16.
16. L. Gmelin, 'Handbuch der theoretischen Chemie', 2nd edn., Varrentrapp, Frankfurt, 1822, p. 928.
17. L. Gmelin, *Schweigger's J. Chem. Phys.*, 1822, **34**, 325.
18. L. Gmelin, *Schweigger's J. Chem. Phys.*, 1822, **36**, 230.
19. L. Gmelin, ref. 16, vol. II, p. 1692.
20. W. C. Zeise, *Pogg. Ann. Phys. Chem.*, 1827, **9**, 632; 1831, **21**, 497. For a discussion and annotated English translation of the second article see ref. 3, pp. 17–37.
21. T. J. Kealy and P. L. Pauson, *Nature (London)*, 1951, **168**, 1039. For a brief discussion of the discovery of ferrocene see G. B. Kauffman, *J. Chem. Educ.*, 1983, **60**, 185 and *Revista Chilena Educación Química*, 1979, **4**, 107.
22. S. A. Miller, J. A. Tebboth and J. F. Tremaine, *J. Chem. Soc.*, 1952, 632.
23. M. Peyrone, *Ann. Chim. (Paris)*, 1844, **51**, 1.
24. J. Reiset, *Compt. Rend.*, 1844, **18**, 1100; *Ann. Chim. (Paris)*, 1844, [3] **11**, 417.
25. A. Werner, *Z. Anorg. Chem.*, 1893, **3**, 267. For a discussion and annotated English translation see ref. 2, pp. 5-88.
26. I. I. Chernyaev, *Izvestiya Instituta po Izucheniyu Platiny i Drugikh Blagorodnykh Metallov*, 1926, **4**, 243. For a discussion and annotated English translation see ref. 4, pp. 143–195. See also ref. 5, pp. 158–162.
27. G. B. Kauffman, *Isis*, 1977, **68**, 392; ref. 5, pp. 64–68.
28. G. B. Kauffman, in 'Dictionary of Scientific Biography', ed. C. C. Gillispie, Charles Scribner's Sons, New York, 1972, vol. 5, pp. 349–350; *J. Chem. Educ.*, 1975, **52**, 155.
29. F. A. Genth, *Keller–Tiedemann's Nordamerikanischer Monatsbericht für Natur- und Heilkunde*, 1851, **2**, 8.
30. G. B. Kauffman, *Platinum Met. Rev.*, 1972, **16**, 101.
31. W. Gibbs and F. A. Genth, 'Researches on the Ammonia-Cobalt Bases', Smithsonian Institution, Washington, 1856; reprinted in *Am. J. Sci.*, 1856, [2] **23**, 235, 248, 319; 1857, [2] **24**, 86.
32. F. Claudet, *Philos. Mag.*, 1851, **2**, 253.
33. G. B. Kauffman, in 'Dictionary of Scientific Biography', ed. C. C. Gillispie, Charles Scribner's Sons, New York, 1972, vol. 5, pp. 492–495.
34. G. B. Kauffman, *J. Chem. Educ.*, 1974, **51**, 522; ref. 5, pp. 69–70.
35. For discussions of some of these theories see F. Reitzenstein, *Z. Anorg. Chem.*, 1898, **18**, 152; and J. C. Bailar, Jr., in 'The Chemistry of the Coordination Compounds', ed. J. C. Bailar, Jr., Reinhold, New York, 1956, chap. 2.
36. T. Graham, 'Elements of Chemistry', Baillière, London, 1837. This book is rare and is better known through its German translation, 'Lehrbuch der Chemie', transl. F. J. Otto, Vieweg und Sohn, Braunschweig, 1840, vol. 2, p. 741. For an annotated excerpt of Graham's theory from T. Graham, 'Elements of Chemistry', Lea and Blanchard, Philadelphia, 1843, pp. 296–297 see ref. 3, pp. 43–45.

37. C. Gerhardt, *Jahresbericht*, 1850, **3**, 335.
38. C.-A. Wurtz, *Ann. Chim. Phys.*, 1850, [3] **30**, 488.
39. A. W. von Hofmann, *Ann. Chem.*, 1851, **78**, 253.
40. K. Weltzien, *Ann. Chem.*, 1856, **97**, 19.
41. J. J. Berzelius, *Jahresbericht*, 1841, **21**, 108; ref. 3, pp. 47–48; ref. 5, pp. 72–74.
42. C. Claus, *Ann. Chem.*, 1856, **98**, 317. For an annotated English translation see ref. 3, pp. 52–67. See also G. B. Kauffman, in 'Dictionary of Scientific Biography', ed. C. C. Gillispie, Charles Scribner's Sons, New York, 1971, vol. 3, pp. 301–302; ref. 5, pp. 74–76.
43. H. Schiff, *Ann. Chem.*, 1862, **123**, 1.
44. G. B. Kauffman, *J. Chem. Educ.*, 1972, **49**, 813; ref. 3, pp. 69–71; ref. 5, pp. 76–81.
45. A. Kekulé, *Compt. Rend.*, 1864, **58**, 510.
46. G. B. Kauffman, *J. Chem. Educ.*, 1959, **36**, 521; reprinted in 'Selected Readings in the History of Chemistry', ed. A. J. Ihde and W. F. Kieffer, Journal of Chemical Education, Easton, PA, 1965, pp. 185-191; *Chymia*, 1960, **6**, 180; ref. 3, pp. 92-102; ref. 5, pp. 81-85.
47. C. W. Blomstrand, 'Die Chemie der Jetztzeit vom Standpunkt der electrochemischen Auffassung aus Berzelius Lehre entwickelt', Carl Winter's Universitätsbuchhandlung, Heidelberg, 1869. See also C. W. Blomstrand, *Ber.*, 1871, **4**, 40 and a discussion and annotated English translation in ref. 3, pp. 71–92; ref. 5, pp. 81–82.
48. G. B. Kauffman, in 'Dictionary of Scientific Biography', ed. C. C. Gillispie, Charles Scribner's Sons, New York, 1970, vol. 2, pp. 199–200; *Annals of Science*, 1975, **32**, 12; *Centaurus*, 1977, **21**, 44.
49. G. B. Kauffman, in 'Dictionary of Scientific Biography', ed. C. C. Gillispie, Charles Scribner's Sons, New York, 1973, vol. 7, pp. 179–180.
50. G. B. Kauffman, *J. Chem. Educ.*, 1976, **53**, 445.
51. G. B. Kauffman, in 'Dictionary of Scientific Biography', ed. C. C. Gillispie, Charles Scribner's Sons, New York, 1976, vol. 14, pp. 264–272.
52. G. B. Kauffman, *Chemistry*, 1966, **39** (12), 14.
53. G. B. Kauffman, *Educ. Chem.*, 1967, **4** (1), 11; ref. 3, pp. 93–102; ref. 5, chap. 6.
54. G. B. Kauffman, 'Coordination Chemistry: Its History through the Time of Werner' (audiotape and book), American Chemical Society, Washington, 1977.
55. S. M. Jørgensen, *Z. Anorg. Chem.*, 1899, **19**, 78, 109. For a discussion and annotated English translation of the second article see ref. 3, pp. 92–164.
56. S. M. Jørgensen, *J. Prakt. Chem.*, 1887, [2] **35**, 417.
57. S. M. Jørgensen, *Z. Anorg. Chem.*, 1894, **5**, 147; 1894, **7**, 289.
58. S. M. Jørgensen, *J. Prakt. Chem.*, 1890, [2] **41**, 429; J. Petersen, *Z. Phys. Chem.*, 1892, **10**, 580.
59. A. Werner and A. Miolati, *Z. Phys. Chem.*, 1893, **12**, 35. For a discussion and annotated English translation see ref. 2, pp. 89–115.
60. A. Werner and A. Miolati, *Z. Phys. Chem.*, 1894, **14**, 506. For a discussion and annotated English translation see ref. 2, pp. 117–139.
61. S. M. Jørgensen, *J. Prakt. Chem.*, 1878, [2] **18**, 209.
62. G. B. Kauffman, *Coord. Chem. Rev.*, 1973, **11**, 161.
63. G. B. Kauffman, *Isis*, 1970, **61**, 241.
64. See, *e.g.*, J. H. van't Hoff, *Maandblad voor Natuurwetenschappen*, 1875, **6**, 37; W. Körner, *Gazz. Chim. Ital.*, 1874, **4**, 305.
65. A. Werner, *Ann. Chem.*, 1912, **386**, 1.
66. G. B. Kauffman, *Coord. Chem. Rev.*, 1975, **15**, 1.
67. S. M. Jørgensen, *J. Prakt. Chem.*, 1889, [2] **39**, 1.
68. A. Werner, *Ber.*, 1907, **40**, 4817. For a discussion and annotated English translation see ref. 2, pp. 141–154.
69. G. B. Kauffman, in 'Van't Hoff–Le Bel Centennial', ed. O. B. Ramsay, American Chemical Society, Washington, 1975, pp. 126–142; *Isis*, 1975, **65**, 38.
70. A. Werner and A. Vilmos, *Z. Anorg. Chem.*, 1899, **21**, 145.
71. A. Werner and V. L. King, *Ber.*, 1911, **44**, 1887. For a discussion and annotated English translation see ref. 2, pp. 155–173. See also V. L. King, *J. Chem. Educ.*, 1942, **19**, 345 and G. B. Kauffman and E. V. Lindley, Jr., *J. Chem. Educ.*, 1974, **51**, 424; *Inorg. Synth.*, 1976, **16**, 93; G. B. Kauffman, *J. Prakt. Chem.*, 1966, [4] **33**, 295.
72. P. Karrer, *Helv. Chim. Acta*, 1920, **3**, 196.
73. I. Lifschitz, *Z. Elektrochem.*, 1920, **26**, 514.
74. A. Werner, in 'Les Prix Nobel en 1913', Norstedt & Fils, Stockholm, 1914; *Naturwissenschaften*, 1914, **2**, 1; *J. Chim. Phys.*, 1914, **12**, 133; 'Nobel Lectures in Chemistry, 1901-1921', ed. Nobel Foundation, Elsevier, Amsterdam, 1966, pp. 253-269.
75. G. B. Kauffman, *Coord. Chem. Rev.*, 1974, **12**, 105.
76. A. Werner, *Ber.*, 1914, **47**, 3087. For a discussion and annotated English translation see ref. 2, pp. 175–184.
77. S. M. Jørgensen, *Z. Anorg. Chem.*, 1898, **16**, 184.
78. A. Hantzsch and A. Werner, *Ber.*, 1890, **23**, 11. For a discussion and annotated English translation see G. B. Kauffman, *J. Chem. Educ.*, 1966, **43**, 155.
79. H. Eyring, *Chem. Eng. News*, Jan. 7, 1963, **41** (1), 5.
80. G. B. Kauffman, *J. Chem. Educ.*, 1973, **50**, 693.
81. H. Ley, *Z. Elektrochem.*, 1904, **10**, 954. For an annotated English translation see G. B. Kauffman, *J. Chem. Educ.*, 1973, **50**, 698; ref. 4, pp. 5–19; ref. 5, pp. 137–140.
82. G. Bruni and C. Fornara, *Atti Accad. Naz. Lincei, Cl. Sci. Fis., Mat., Nat., Rend.*, 1904, [5] **13**, 11, 26.
83. A. Baeyer, *Ber.*, 1885, **18**, 2269.
84. G. B. Kauffman, *J. Chem. Educ.*, 1963, **40**, 656; *Platinum Met. Rev.*, 1973, **17**, 144; ref. 4, pp. 20–25; ref. 5, pp. 141–144.
85. A. A. Grinberg, *Helv. Chim. Acta*, 1931, **14**, 445.
86. L. A. Chugaev, *Ber.*, 1906, **39**, 3190; *J. Prakt. Chem.*, 1907, [2] **75**, 153. For an annotated English translation of the second article see ref. 4, pp. 26–44.
87. G. B. Kauffman, in 'Dictionary of Scientific Biography', ed. C. C. Gillispie, Charles Scribner's Sons, New York, 1972, vol. 5, pp. 189–190; ref. 4, pp. 49–51; ref. 5, pp. 146–147.
88. J. A. N. Friend, *J. Chem. Soc.*, 1908, **93**, 1006; reprinted with annotations in ref. 4, pp. 52–59.

89. J. A. N. Friend, *J. Chem. Soc.*, 1916, **109**, 715; reprinted with annotations in ref. 4, pp. 60-73.
90. S. H. C. Briggs, *J. Chem. Soc.*, 1908, **93**, 1564; ref. 4, pp. 46-48; ref. 5, pp. 147-148.
91. S. H. C. Briggs, *J. Chem. Soc.*, 1917, **111**, 253.
92. G. Povarnin, *J. Russ. Phys. Chem. Soc.*, 1915, **47**, 217, 501, 989, 1787, 2073; ref. 4, p. 48; ref. 5, pp. 148-149.
93. G. B. Kauffman, in 'Dictionary of Scientific Biography', ed. C. C. Gillispie, Charles Scribner's Sons, New York, 1974, vol. 10, p. 578.
94. P. Pfeiffer, *Z. Anorg. Allg. Chem.*, 1920, **112**, 81; *Z. Angew. Chem.*, 1920, **33**, 37.
95. G. B. Kauffman, *Coord. Chem. Rev.*, 1973, **9**, 339.
96. G. B. Kauffman, *J. Chem. Educ.*, 1973, **50**, 277.
97. P. Pfeiffer, *Z. Anorg. Chem.*, 1915, **92**, 376. For a discussion and annotated English translation see ref. 4, pp. 74-84. See also ref. 5, pp. 150-151.
98. P. Pfeiffer, *Z. Anorg. Chem.*, 1916, **97**, 161.
99. P. Pfeiffer, *Z. Anorg. Chem.*, 1918, **105**, 26.
100. R. W. G. Wyckoff, in 'Werner Centennial', ed. G. B. Kauffman, American Chemical Society, Washington, 1967, pp. 114–119.
101. R. W. G. Wyckoff and E. Posnjak, *J. Am. Chem. Soc.*, 1921, **43**, 2292; reprinted with annotations and discussion in ref. 4, pp. 85–111. See also ref. 5, pp. 151–153.
102. R. G. Dickinson, *J. Am. Chem. Soc.*, 1922, **44**, 2404; reprinted with annotations and discussion in ref. 4, pp. 112–126. See also ref. 5, pp. 153–155.
103. T. M. Lowry, *Chem. Ind. (London)*, 1923, **43**, 316, 412, 711, 1004.
104. N. V. Sidgwick, *J. Chem. Soc.*, 1923, **123**, 725; reprinted with annotations and discussion in ref. 4, pp. 127–143. See also ref. 5, pp. 155–157.
105. N. V. Sidgwick, *Nature (London)*, 1923, **111**, 808; *Trans. Faraday Soc.*, 1923, **19**, 469; *Chem. Ind. (London)*, 1923, **42**, 1203; 'The Electronic Theory of Valency', Oxford University Press, London, 1927, chap. 10.
106. G. B. Kauffman, *Platinum Met. Rev.*, 1976, **20**, 126; *J. Chem. Educ.*, 1977, **54**, 86; V. A. Golovnya, T. N. Leonova, W. Craig and G. B. Kauffman, *Ambix*, 1976, **23**, 187.
107. G. B. Kauffman and A. Beck, *J. Chem. Educ.*, 1962, **39**, 44; reprinted in 'Selected Readings in the History of Chemistry', ed A. J. Ihde and W. F. Kieffer, Journal of Chemical Education, Easton, PA, 1965, pp. 191-196; G. B. Kauffman, *Polyhedron*, 1983, **2**, 855.
108. I. I. Chernyaev, *Izvestiya Instituta po Izucheniyu Platiny i Drugikh Blagorodnykh Metallov*, 1927, **5**, 118.

1.2

Development of Coordination Chemistry since 1930

JOHN C. BAILAR, JR.
University of Illinois, Urbana, IL, USA

1.2.1 INTRODUCTION

The long awaited renaissance in inorganic chemistry finally arrived during the 1940s and since that time there has been great activity in all branches of the science, particularly in the chemistry of coordination compounds. The tenets of Werner's theory have not been discarded, but they have been refined and greatly extended. For example, early workers considered coordination compounds of only a few metals (*e.g.* Pt, Co, Cr) and coordination numbers of four and six. More recent research on coordination compounds has been concerned with nearly all the metals in the periodic table, with all coordination numbers from two to twelve and in many (even fractional) oxidation states. For example, compounds of palladium(I), palladium(V) and platinum(V) are well established. In the metal carbonyls and related substances, the metal is assigned a zero oxidation state, *viz.* $Ni(CO)_4$, $Ni(PF_3)_4$ and $Ni(PhNC)_4$. Herzog has reported a variety of oxidation states — even negative states — in compounds containing bipyridyl or 1,10-phenanthroline.[1] It is possible, however, that in these compounds the ligand is showing a reduced state rather than the metal. Klemm and his coworkers have shown the importance of the coordination number in the preparation of such compounds as K_3VF_6, K_2VF_6, KVF_6, K_3CuF_6 and $KAgF_4$. In each case the heavy metal fills its coordination sphere and assumes whatever oxidation state is dictated by the number of potassium ions present.[2] New synthetic methods and physical methods of studying structure have been essential to these developments. The growth of interest in coordination chemistry has been greatly stimulated by developments in catalysis and in the role of metals in biochemistry.

Among the metals which have achieved prominence only recently, molybdenum must certainly occupy first place. It has attracted interest chiefly because of its role in biological processes and also because it shows a great variety of oxidation states and coordination numbers. Steifel's extensive review of molybdenum complexes covers their chemistry up to 1977.[3] Because of their use in nuclear medicine, the complexes of technetium have received recent interest.[4]

Among the newer types of compound which have received wide study are Vaska's compound (with its ease of oxidative addition and reductive elimination), the phthalocyanines, macrocycles, crown ethers, metal–metal bonded compounds, and complexes in which hydrogen, ethylenes, organic phosphines and carbon monoxide behave as ligands. The importance of the catalytic hydrogenation of carbon–carbon double bonds gives the hydrido and ethylenic coordination compounds special importance. Alkene coordination was not accounted for by the early theories of coordination, although the compound $K[PtCl_3(C_2H_4)]$ had been known since 1829. This compound has now been studied extensively. The complex is planar, with the ethylene molecule perpendicular to this plane, and attached to the metal through the π-electrons of the carbon atoms. Many other ethylenic compounds of the platinum metals have been prepared, and their structures are well known. Alkenes containing two suitably placed double bonds can attach themselves through both double bonds, forming a pseudo chelate ring, or can bind themselves to two metal atoms.[5]

Hydrido complexes can be prepared by the oxidative addition of hydrogen to coordinatively unsaturated metals (*e.g.* Vaska's compound) or by reduction of higher valent compounds with borohydride or similar reagents.

1.2.2 SYNTHESIS

New procedures for the synthesis of inorganic complexes have made it possible to prepare several new types of compound. Particularly noteworthy is the discovery by Shibata and his coworkers that the carbonato groups of $[Co(CO_3)_3]^{3-}$ can be displaced stepwise, so that ligands of three different kinds can be introduced readily; and compounds such as $[Co(en)(pn)(NO_2)_2]^+$ and $[Co(NH_3)_2(H_2O)_2(CN)_2]^+$ can be prepared.[6] The tris-carbonato complex can be obtained in optically active form.

Ogino and his students have observed that the use of dimethyl sulfoxide as a solvent allows the formation of very large chelate rings on cobalt(III) complexes. Rings of intermediate size do not form.[7] The conformations of these large rings, and application of the method to the synthesis of complexes of other metals, await investigation.

The template method of forming multidentate, cyclic complexes, as developed by Curtis and by Busch, has made it possible to synthesize complexes which were previously unknown and unavailable. Most of these macrocycles are planar, but some are known to be folded or crumpled, either because the metal atom in the center of the ring is too large to fit between the four nitrogen atoms, or because of substituents on the carbon atoms of the ring.[8] In those cases in which the ring is large enough, two metal ions can be attached. This is particularly true of complexes of the alkali metals with phthalocyanines[9] and crown ethers.[10]

Reactions of coordinated ligands have been used to prepare new types of complexes. A striking example is shown in Sargeson's synthesis of the 'sepulchrate' cobalt(III) ion from $[Co(en)_3]^{3+}$ by treatment with formaldehyde and ammonia, in which the open faces of the octahedron are bridged by —$N(CH_2)_3$— groups. The metal ion, thus completely enclosed, shows quite remarkable properties.[11] Sargeson and his group have also done interesting work on the use of the triflate ion ($CF_3SO_3^-$) as a good 'leaving group'; this greatly simplifies the preparation of many types of complexes.[12]

Another advance was made by Collman,[13] who observed that the acetylacetonate chelate ring has semi-aromatic character and can be nitrated and brominated much as benzene can. Reactions of these derivatives can lead to new types of complexes. Insertions can also lead to new types of complex, as shown by reaction (1).

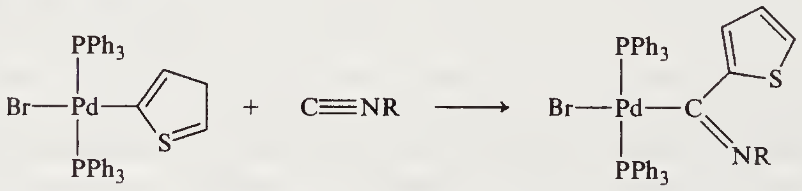

(1)

Werner and the other early coordination chemists produced a good many di- and poly-nuclear compounds in which the metal atoms were bound together through ^-OH, $^-NH_2$ or halo bridges. In many of those compounds there were double or triple bridges. It was shown later that the heavy metal cyanides such as Prussian blue and the insoluble metal hydroxides are high polymers containing cyano, oxo or hydroxo bridges. Thomas based a theory of colloidal oxides on this observation.[14] In more recent years the number of bridge groups has been greatly increased to include O_2, O_2^-, O_2^{2-}, O_2H^-, S^{2-}, SO_4^{2-}, N_2, NO_2^-, $N_2O_2^{2-}$, HPO_4^{2-}, $C_2O_4^{2-}$ and $MeCO_2^-$. The compounds (1) containing carboxylate ions as bridges are of particular interest, as some of them also contain metal–metal bonds.[16]

Polymeric chromium(III) compounds containing carboxylate and hydroxo bridges have found practical application as water and grease repellents. These are shown conventionally as (**2**). In Quilon (trade name), the R groups are long hydrocarbon chains; in Volan, they are allyl groups to which other groups can be attached after the chromium complex has been applied to the surface which is being treated; in Scotch Guard, they are perfluorocarbon chains which are both water and oil repellent, and this is used in treating fabrics to be used in upholstery and clothing. Most bridge ligands are quite simple in structure, but there are some which are much more complex. An interesting example is shown in the recent work of Reedijk, who used 3,5-bis(2-pyridyl)-1,2,4-1*H*-triazole to form the planar dinuclear complex (**3**).

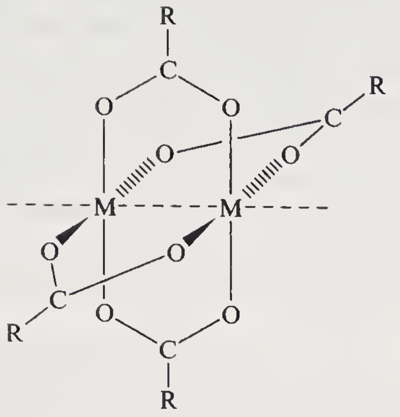

(1)

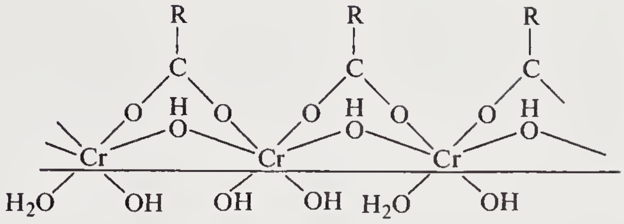

(2)

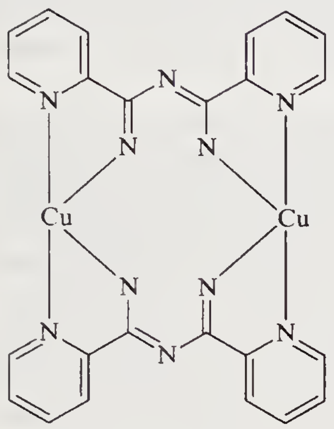

(3)

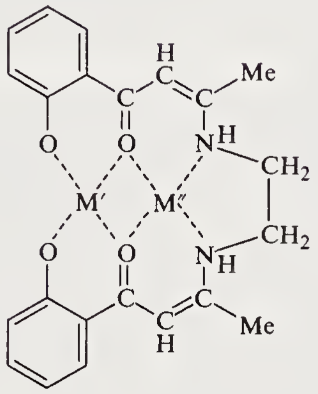

(4)

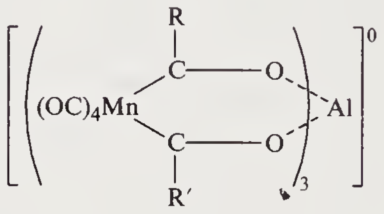

(5)

The development of 'compartmental' ligands has given us a new type of dinuclear complex.[14a] In recent years a good many have been prepared, but a single example (**4**) must suffice to illustrate them. M′ and M″ may be the same metal or different. The first metal ion to be introduced goes into the N_2O_2 ring, and the second one into the O_4 ring.

Another type of polynuclear complex has been developed by Lukehart and his students.[15] Starting with manganese pentacarbonyl, for example, they have prepared complexes of the type (**5**). Formally, these resemble the complexes of 1,2-diketones and, indeed, they have some of the properties of those substances.

1.2.3 STRUCTURE

Many advances have been made in the synthesis of compounds of unusual structure, and in the determination of structures by spectral, X-ray and magnetic methods. The development of the crystal field and molecular orbital theories has aided greatly in the understanding of structure.[16] Werner's hypothesis that all six-coordinate complexes are octahedral has been found to be too simplistic: most of them are octahedral, but there are some that are triangular prismatic and a few that are pentagonal pyramidal. Many of those that are octahedral are highly distorted,[17] the distortions being brought about by steric factors and charges on the ligands. Rings which Werner assumed to be flat are in fact twisted, especially if they carry bulky substituents. The discovery of coordination numbers which Werner did not suspect has also introduced new structural factors.

A new group of compounds, those containing metal–metal bonds, has been an exciting development and has opened new avenues of investigation. In many of these there are non-metallic atoms or groups also — hence their classification as coordination compounds. In many cases the non-metallic groups serve as bridges between metal atoms, but not always. The case of the octachlorodirhenium ion is a striking example of a dinuclear compound without bridges: not only are the rhenium atoms joined by a quadruple bond, but the square groups of four chloro groups on each rhenium atom are eclipsed. This is explained by the presence of a quadruple bond between the two metal atoms, which consists of one σ, two π, and one δ bond.[16] The chlorides Mo_6Cl_{12} and Ta_6Cl_{14} are interesting examples of bridged complexes: in each case the six metal atoms are at the centers of the faces of a cube (thus describing a regular octahedron). In the molybdenum compound, only eight of the chloro groups are covalently bound. They occupy the corners of the cube, each of them being bound to three metal atoms; in the tantalum compound, 12 chloro groups occupy the centers of the cube edges, each being bound to two metal atoms.

The discovery in 1965 that tris(*cis*-1,2-diphenylethylene-1,2-dithiolato)rhenium, $Re(S_2C_2Ph_2)_3$, is trigonal prismatic rather than octahedral came as a surprise to many. Since that time, however, a number of other structures of that shape have been discovered, as well as some that are intermediate between the prismatic and octahedral forms. Still another, and rather surprising, six-coordinate structure has been determined for $CrO(O_2)_2(NC_5H_5)$, which is a distorted pentagonal pyramid with the non-peroxo oxygen at the apex. The peroxo oxygen atoms in each pair are too far apart to be considered to be occupying a single position.

In recent years, X-ray methods have also shown a variety of configurations for complexes of coordination number eight. It was long thought that all were either antiprismatic or dodecahedral, but some are cubic (*e.g.* the $[U(NCS)_8]^{4-}$, $[U(bipy)_4]^{4+}$ and $[PaF_8]^{3-}$ ions) and some are hexagonal pyramidal (*e.g.* the $[UO_2(MeCO_2)_3]^-$ ion).

The lanthanide ions are so large that they show coordination numbers of 10, 11 and even 12. Hoard and his students have shown that when ethylenediaminetetraacetate (edta) combines with the larger lanthanide ions, the sexidentate edta covers only a portion of the metal ion, the remainder being coordinated with water molecules.[18]

Many unusual ligands have been devised and synthesized, in most cases to test some point of stereochemistry, stability or other property. Long chain amines, cyclic polyamines, cyclic polyethers (crown ethers) and combinations of these have become popular as ligands. The use of organic phosphines and arsines has also become common. Complexes of the phosphines are particularly useful in many types of catalyst, especially those used in stereoselective reactions. In recent years, ambidentate ligands have received a good deal of attention, among them the thiocyanato and selenocyanato ions. With many ambidentate ligands, one linkage isomer converts spontaneously into the other, but little attention has been paid to the mechanism of such isomerizations. The nitrito–nitro isomerism of cobalt(III) complexes is an exception. Taube and his students, Sargeson and coworkers, and others have studied it in detail.

1.2.4 MECHANISMS OF REACTIONS

Most reactions of coordination compounds can be classified as either substitutions or oxidation–reductions. The classic book by Basolo and Pearson[19] discusses both types in detail. The oxidation–reductions can occur either by simple electron transfer or by atom transfer. Taube's work on the reduction of cobalt(III) complexes by Cr^{II} is especially important in this regard. Among the many reactions which he has studied, the best known, perhaps, is[20]

$$Co(NH_3)_5Cl^{2+} + Cr^{II} \rightarrow CrCl^{2+} + Co^{2+} + 5NH_3 \qquad (2)$$

The crux of Taube's method is that Co^{III} and Cr^{III} complexes are inert, whereas those of Co^{II} and Cr^{II} are labile.

Reactions other than oxidations and reductions can take place by a momentary dissociation of a donor molecule (decrease in coordination number), by a momentary increase or by a twist mechanism. Basolo, Pearson and their students have studied the rates, enthalpies and entropies of a great many substitutions and have used them for a variety of purposes. For example, they have demonstrated that solutions of $[Ni(bipy)_3]^{2+}$ and $[Ni(phen)_3]^{2+}$ racemize only by dissociation, but in the case of the Fe^{II} analogues, dissociation can account only in part for the racemization. The other mechanism is thought to involve a twist of the complex about the metal ion. In the solid state, racemizations and other rearrangements do not, in most cases, involve dissociation, so must take place by a twist mechanism. Several twist mechanisms have been suggested, the best known being the Bailar (or trigonal) twist and the Rây–Dutt (or tetragonal) twist.[21] The latter is applicable to mono- and bi-dentate ligands; the former also to most polydentate ligands.

1.2.5 ISOMERISM

The concept of isomerism and isomer counts were used extensively in the development of Werner's theory. They are still important, but on a much more sophisticated level than Werner could have imagined; some of the structures which he used are now known to be greatly distorted[22] and others are not as simple as he believed. Geometric isomers may exist in one form or another, depending upon the solvent, temperature and other conditions, or they may change their coordination numbers. For example, it has been found that $[Co(PEt_3)_2(NCS)_2]$ is planar in the solid state, but tetrahedral when in solution in a non-polar solvent. Similarly, optical isomers may change their configurations during substitutions.

A minor change in the nature of the ligands sometimes produces a great change in the nature of a complex. Thus, if R″ is —$(CH_2)_2$— in the branched quadridentate ligand (**6**), the nickel complex is a dimer in which each half is planar and diamagnetic, but if R″ is —$(CH_2)_3$— the complex is polymeric and paramagnetic; each nickel atom is at the center of a tetrahedron.[23]

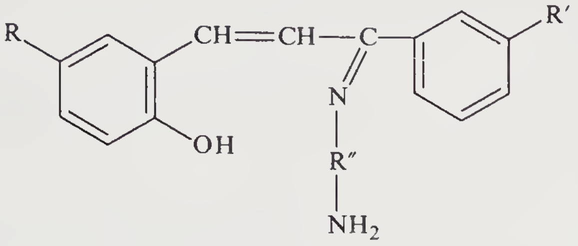

(**6**)

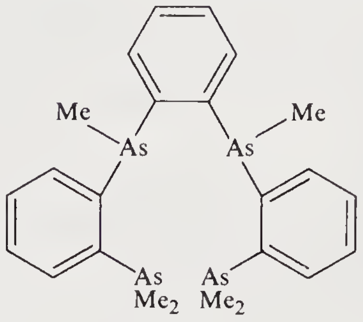

(**9**)

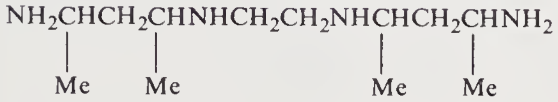

$$NH_2\underset{\underset{Me}{|}}{C}HCH_2\underset{\underset{Me}{|}}{C}HNHCH_2CH_2NH\underset{\underset{Me}{|}}{C}HCH_2\underset{\underset{Me}{|}}{C}HNH_2$$

(**7**)

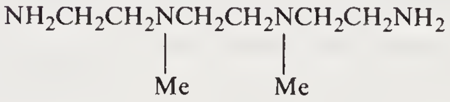

$$NH_2CH_2CH_2\underset{\underset{Me}{|}}{N}CH_2CH_2\underset{\underset{Me}{|}}{N}CH_2CH_2NH_2$$

(**8**)

It was the optical resolution of $[Co(en)_2(NH_3)Cl]^{2+}$ that firmly established Werner's theory and which initiated the study of the optical activity of complex ions. The realization that some octahedral complexes are chiral evidently did not occur to Werner until several years after he published his theory of coordination. He then realized that the demonstration of this property would furnish an almost irrefutable argument in favor of his theory, and he and his students devoted several years to attempts to effect such resolution. Had he but known it, the problem could have been easily solved, for *cis*-$[Co(en)_2(NO_2)_2]X$ ($X = Cl, Br$) crystallizes in hemihedral crystals which can be separated mechanically, just as Pasteur separated the optical isomers of sodium ammonium tartrate.

Optical activity may be achieved in at least three ways: (a) by the asymmetric arrangement of ligands about the central metal ion; (b) by the use of a ligand which is itself optically active; and (c) by the use of a ligand in which an atom (or atoms) becomes chiral upon attachment to the metal. The second of these is illustrated by propylenediamine and the tetradentate (**7**) and the last by (**8**)[24] and by (**9**). Neither the nitrogen atoms nor the arsenic atoms[25] in these last two ligand molecules are chiral, but the ones near the centers of their respective molecules become so when they are coordinated to a metal ion. In each case, they can be of the same or of opposite chirality. Thus complexes with a six-coordinate metal can theoretically exist in a large number of isomeric forms; these differ in stability and not all of them have been isolated.

The presence of a chiral ligand not only introduces its own optical activity, but it may also exert a stereoselective effect on the complex as a whole. Early attempts to explain this relied upon molecular symmetry, but were not very successful. The observation that even simple chelate rings are puckered, and that the introduction of a substituent would favor one conformation over another, has now been generally accepted.[26] Both $[Co(en)_3]^{3+}$ and $[Co(pn)_3]^{3+}$ can exist in different conformations which are in rapid equilibrium. The carbon–carbon bond in each ring may be approximately parallel to the trigonal axis of the octahedron (*'lel'* form) or it may be quite oblique to it (*'ob'* form). The *lel,lel,lel* form of the compound is more stable than the *ob,ob,ob* form, the hydrogen atoms on the organic part of the ring being almost completely staggered. In the tris(propylenediamine)cobalt(III) complex, the presence of the added methyl group enhances this effect markedly: the methyl group tends to be equatorial. Similar effects can be calculated for other chelate rings, such as those containing *cis*-1,2-cyclohexanediamine and stilbenediamine. The latter contains two asymmetric carbon atoms, and because of the effects just cited, *d,l*-stilbenediamine gives more stable complexes than does the *meso* isomer. It should be noted in passing that because of the dis-symmetry of the propylenediamine molecule end for end, another type of isomerism is possible. This type has received little attention.

Several other types of isomerism have been studied in recent years. For example, a bis-tridentate complex containing an unsymmetrical ligand can exist, theoretically, in three geometric forms: meridional, symmetrical-facial and chiral unsymmetrical-facial. With ligands which are rigid (*e.g.* phen) and with those of small normalized bite, the meridional form is favored. With flexible ligands (*e.g.* dien), all the forms of the cobalt(III) complex have been isolated.[22] Another type of ligand, exemplified by tris[1,1,1-(trisaminomethyl)]ethane, can coordinate only facially. When the opposite face of the octahedron is filled with a monodentate group and an unsymmetrical bidentate group or with three different monodentate groups, a chiral complex is formed.[27]

Werner's final triumph in support of his theory came in the optical resolution of a purely inorganic synthetic complex. Such compounds are still rare, but a few have been prepared in optically active form: *cis*-$[Rh(NHSO_2NH)_2(H_2O)_2]^-$, $[Pt(S_5)_3]^{2-}$ and *cis,cis,cis*-$[Co(NH_3)_2(H_2O)_2X_2]^+$ (X = CN or NO_2),[28] though the cyano group does contain carbon.

Methods of optical resolution have been greatly improved by the use of adsorption and column chromatography. Many adsorbents have been used, *e.g.* quartz powder, lactose and, by far the best of all, SP-Sephadex. An improvement in the classical method of forming diastereoisomers has been effected by the use of optically active inorganic complexes as resolving agents. This has not yet become popular among organic chemists, but is increasingly used by coordination chemists. Bacterial attack to destroy one isomer of a racemic pair has also been shown to be possible.[29]

Werner based some of his conclusions on the supposition that a chelate ring could span only the *cis* positions in a complex. While this is valid for the small rings with which he was familiar, it does not necessarily hold for larger rings. Several investigators have prepared compounds in which a single bidentate ligand occupies *trans* positions in a planar complex.

Paul Pfeiffer discovered a very interesting stereochemical phenomenon, which now bears his name — the Pfeiffer effect; this has received a good deal of attention.[30] When an optically active substance which is stable in solution is added to a solution of a labile chiral substance, the optical rotation of the solution changes, reaching a new level in some hours. Several theories have been advanced to explain the phenomenon, the most satisfactory based on the supposition that the optically active ion or molecule forms an association with one isomer of the racemic pair of the labile substance and thus shifts the *dextro–levo* equilibrium. In general it is not possible to use this as a means of resolution, for when the added optically active substance is removed from the labile material, the latter immediately racemizes.

1.2.6 *TRANS* EFFECT

The *trans* effect, which is defined as the labilization of a ligand *trans* to some other, *trans*-directing ligand, was observed by Werner who referred to it as a '*trans* elimination effect'; he used it in determining the configurations of *cis* and *trans* isomers of planar platinum(II) complexes. It is a very significant effect in these substances, and much less important in the chemistry of palladium(II) compounds. There is also a *trans* effect in octahedral complexes, but it is minor. It is a kinetic effect; the related thermodynamic effect is referred to as the '*trans* influence'. Several theories have been advanced to explain the *trans* effect, the most popular of which was first stated by Grinberg, and which has been restated in terms of molecular orbital theory by later investigators. Essentially, it assumes that an easily polarized donor group will induce a polarization of the metal to which it is attached; this, in turn, weakens the bond *trans* to it. The Russians have utilized the *trans* effect in the synthesis of platinum(IV) compounds containing a large number of different groups. They first prepare planar platinum(II) compounds of known configuration by using the *trans* effect, then oxidize these to the octahedral platinum(IV) compounds. By this means they have made such compounds as $[Pt(en)(py)(NH_3)Cl_2]Cl_2$, $[Pt(en)(py)(NH_3)ClBr]Cl_2$ and even five of the possible 15 geometric isomers of $[Pt(NH_3)(py)ClBrI(NO_2)]$.[31]

1.2.7 NON-AQUEOUS SOLVENTS

As in other fields of inorganic chemistry, some research on coordination compounds has been carried out in non-aqueous media. There are several reasons for this: first, some compounds are not soluble in water, but will dissolve in other solvents (of course, solubilities can often be modified by judicious selection of the counter ion). In those cases in which the coordination compound reacts with water, the use of a non-aqueous solvent may be advantageous. A familiar example is the determination of the number of ions in a compound by measuring the conductivity in nitromethane or other highly polar solvent. In studying the self-exchange rate of the $[Co(NH_3)_6]^{2+/3+}$system, Geselowitz and Taube used liquid ammonia as the solvent to avoid the danger that the labile cobalt(II) compound might be $[Co(NH_3)_5H_2O]^{2+}$ rather than $[Co(NH_3)_6]^{2+}$.[32]

The oxidation–reduction potentials of metal ions differ in different solvents due chiefly to differences in the strength of coordination of the solvents to the metal ions. Thus, Schaap and coworkers,[33] who measured reduction potentials polarographically in anhydrous ethylenediamine, found the order of half-wave potentials to be $Cd^{2+} > Pb^{2+} > Cu^{2+} \rightarrow Cu^{+} > Ti^{+}$, whereas, in aqueous solution, the order is $Cd^{2+} > Ti^{+} > Pb^{2+} > Cu^{2+} \rightarrow Cu^{+}$. Oxidation–reduction potentials have been measured in a great variety of non-aqueous solvents, both protonic and non-protonic. Among the former are liquid ammonia and concentrated sulfuric acid.[34] Among the latter are acetonitrile, cyanopropane, cyanobenzene, dimethyl sulfoxide, methylene chloride, acetone, tetrahydrofuran, dimethylformamide and pyridine.[34]

The compounds which exist in molten salt baths may not be typical Werner type complexes, but many of them are, indeed, coordination compounds. The most interesting of these (at least to this reviewer) are the halide complexes. Many of these contain metal–metal bonds in addition to metal–halide bonds and some of them are large clusters. As examples one might consider Sc_5Cl_8, Sc_7Cl_{10} and Sc_7Cl_{12} (all made by melting $ScCl_3$ and metallic scandium together at different temperatures). Other examples are Ta_6Cl_{15}, Zr_6Cl_{12}, Zr_6I_{12} and the laminar $(ZrCl)_n$.[35]

Reactions of coordination compounds in the solid state have been studied extensively for many years. There are very few cases of two complexes reacting with each other; the important examples are those in which a complex loses one or more volatile ligand molecules upon heating, or which undergoes rearrangement or racemization without loss of a volatile component. If a volatile ligand is lost, several different results may ensue:

An anion may enter the coordination sphere, as in the reaction:

$$Cr(en)_3Cl_3 \rightarrow \textit{cis}\text{-}Cr(en)_2Cl_2Cl \tag{3}$$

A coordinated group may change its mode of coordination to maintain the coordination number:

$$Co(en)_2(H_2O)SO_4NO_3 \ \ (\text{unidentate } SO_4) \rightarrow Co(en)_2SO_4NO_3 \ \ (\text{bidentate } SO_4)$$

Dimerization may take place with the formation of a bridge, or bridges:

$$2Co(NH_3)_4(OH)(H_2O)X_2 \rightarrow (NH_3)_4Co(OH)_2Co(NH_3)_4X_4 \tag{4}$$

$$Cr(NH_3)_6Al(C_2O_4)_3 \rightarrow Cr(C_2O_4)_3Al_x + 6NH_3 \tag{5}$$

An uncoordinated group which is part of a potentially multidentate ligand such as edta may coordinate:

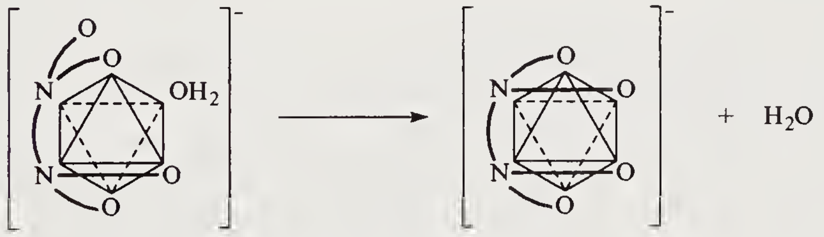

(6)

The coordination number of the metal may change:

$$Ni(NH_3)_6Cl_2 \rightarrow Ni(NH_3)_4Cl_2 + 2NH_3 \tag{7}$$

Many studies of reactions of this sort have been made by Tsuchiya and his coworkers.[36]

If no volatile ligand is lost, again several different types of reactions have been found to take place:

Cis–trans rearrangement:

$$\textit{trans,cis}\text{-}Co(en)(NH_3)_2Cl_2Br \rightarrow \textit{cis,trans}\text{-}Co(en)(NH_3)_2Cl_2Br$$

$$\textit{trans}\text{-}Cr(NH_3)_4(H_2O)BrBr_2 \rightarrow \textit{cis}\text{-}Cr(NH_3)_4(H_2O)BrBr_2$$

Racemization of an optically active complex:

$$\textit{d}\text{-}Co(en)_3I_3 \rightarrow \text{racemic-}Co(en)_3I_3$$

Exchange of a ligand with a counter anion:

$$\textit{trans,cis}\text{-}Co(en)(NH_3)_2Cl_2SCN \rightarrow \textit{cis,cis}\text{-}Co(en)(NH_3)_2(NCS)ClCl$$

A remarkable reaction in which a monomer reacts to form a polymer has been observed by Foxman and his students.[37] They prepared $[Ni\{P(CH_2CH_2CH_2NH_2)_3\}_2Br_2]$, in which the bromine and phosphorus atoms are coordinated to the tetracovalent nickel. Upon heating, the nickel becomes hexacovalent, combining with nitrogen atoms from two other molecules of the complex, and thus forming a polymer.

There has been little study of coordination compounds in the vapor state because most complexes are not volatile. Some of those that can be obtained in the gaseous state have been studied by electron diffraction and microwave spectroscopy, and a good deal has been learned about their structures. There is an advantage to studying them in the gaseous state, for in that condition the molecules are almost independent of each other and there are no packing or solvent effects.[38] Many metallic chlorides are volatile and have been shown to be dimeric in the vapor state, though they tend to dissociate at higher temperatures. Some are trimeric (*e.g.* Cu_3Cl_3 and Re_3Br_9) and some are tetramers (*e.g.* Nb_4F_{20} and Ta_4Cl_{20}). In all of these the molecules have been found to be cyclic with halo bridges between the metal atoms. Volatile derivatives are known and are often monomeric; thus $[AlCl_3{\cdot}NMe_3]$ and $[AlBr_3{\cdot}SbBr_3]$ contain tetrahedral aluminum, and nitrogen or antimony respectively, with the other non-metallic atoms occupying staggered positions.

A somewhat surprising group of coordination compounds consists of the volatile heavy metal nitrates, such as those of copper, zinc, mercury, titanium, zirconium and hafnium. The structures of some of these, in the gaseous state, have been determined; thus $Cu(NO_3)_2$ contains two bidentate, almost planar, staggered nitrato groups. Some derivatives of metal nitrates have also been found to be volatile; for example, $Fe(NO_3)_3{\cdot}N_2O_4$ and $Al(NO_3)_3{\cdot}2MeCN$.[39]

Sievers and his coworkers have used the volatility of the metal diketonates in the separation and analysis of heavy metals and have done interesting stereochemical work on a few of them. They have achieved at least partial resolution of the optical isomers of tris(hexafluoroacetylacetonato)chromium(III) by passing the vapor through a column of quartz powder at 55 °C, and have separated the facial and meridional isomers of tris(trifluoroacetylacetonato)chromium(III) by gas chromatography at 115 °C.[40]

Matrix isolation methods of synthesis have also been used to prepare and study coordination compounds. These involve the vaporization of a metal and a potential ligand, which are then rapidly carried in a stream of inert gas to a very cold surface, where the compound which has been formed is quickly trapped in the solid matrix. It is possible to determine the type of bonding, the structure and the thermodynamic properties of the compounds formed. Only small ligand molecules have been used thus far: carbon monoxide, nitric oxide, nitrogen and oxygen, for example, but molecules of great interest have been formed. Some such are $[Pd(C_2H_4)]$, $[Pd(N_2)_3]$, $[Ni(N_2)_2O_2]$, $[Ni(N_2)_4]$ and $[Ni(CO)(N_2)_3]$.[41]

1.2.8 APPLICATIONS

The early workers in coordination chemistry were more interested in the theory of bonding and structure than in any practical usefulness which the compounds might have. In more recent times, however, applications have developed. Perhaps the most important of these is in catalysis, especially for hydrogenation and the activation of carbon–hydrogen bonds. Metal carbonyls and their derivatives have played a large part in this application, as well as in carbonylation reactions such as the recently developed process for converting methanol to acetic acid:[42]

$$MeOH + CO \xrightarrow{Rh_2(CO)_8} MeCOOH \tag{8}$$

Platinum complexes containing diphosphines and other chelating ligands containing asymmetric carbon atoms have found a place in the chemical industry as stereospecific catalysts. Some of them give products with a high degree (85–90%) of specificity. This is important in the manufacture of some drugs (*e.g.* *levo*-dihydroxyphenylalanine, used in the treatment of Parkinson's disease).

The great growth of interest in the role of metal ions in biological processes has stimulated work in bioinorganic chemistry to the extent that several large books have been written on the subject (*e.g.* ref. 43) and there is a journal devoted entirely to it.[44] Coordination compounds of many of the metals are involved in life processes. One thinks first, of course, of iron and magnesium, but there are many others (*e.g.* copper, zinc, cobalt, molybdenum and manganese). It is known that all of the metals in the periodic table from vanadium to zinc are essential to human life. Complexes of even the alkali and alkaline earth metals with crown ethers and other cyclic ligands play important biological roles. Other coordinated metals have found use in the treatment of disease, *e.g.* gold compounds for arthritis and platinum compounds for some cancers. Still others are ingested inadvertently and cause disease, *e.g.* cadmium.

Attempts to develop synthetic oxygen carriers during the 1940s did not produce commercially useful materials[45] because, in their use, there was always some irreversible oxidation which soon destroyed the inorganic complex. More recent work has been concerned chiefly with the mechanism of oxygen bonding and the structure of the oxygen-containing compounds. However, there is current interest in dioxygen carriers as oxygen activators.[46] There has been interest, too, in nitrogen-carrying compounds, particularly those that might be used in nitrogen fixation.[47]

Attempts in the late 1950s and early 1960s to form high-temperature plastic polymers by coordination of organic materials to metal ions were not successful. The presence of the metal ion does, in many cases, give the ligand increased thermal stability, but this extends only to atoms adjacent to the metal. The presence of only a small amount of organic matter does not give a plastic material.

Some coordination compounds have been used as dyes and pigments, but it must be admitted that these applications developed without reference to the fact that the compounds are complexes. Examples of paint pigments are Prussian blue and the phthalocyanines; metallized azo dyes are common in the textile industry.

1.2.9 REFERENCES

1. S. Herzog, *J. Inorg. Nucl. Chem.*, 1958, **8**, 557.
2. W. Liebe, E. Weise and W. Klemm, *Z. Anorg. Allg. Chem.*, 1961, **311**, 281.
3. E. I. Stiefel, *Prog. Inorg. Chem.*, 1977, **22**, 1.
4. S. C. Srivastava and P. Richards, *J. Indian Chem. Soc.*, 1982, **59**, 1209.
5. J. K. Nicholson and B. L. Shaw, *J. Chem. Soc. (A)*, 1966, 807; L. Guggenberger, *Chem. Commun.*, 1968, 512.
6. M. Shibata, 'Topics in Current Chemistry', Springer Verlag, Berlin, 1983.
7. H. Ogino, *Bull. Chem. Soc. Jpn.*, 1977, **50**, 2459.
8. D. K. Cabbiness and D. W. Margerum, *J. Am. Chem. Soc.*, 1969, **91**, 6540.
9. R. F. Ziola and M. Extine, *Inorg. Chem.*, 1981, **20**, 2709; R. F. Ziola, W. W. H. Gunther and J. M. Troup, *J. Am. Chem. Soc.*, 1981, **103**, 4629.
10. C. J. Pederson, *J. Am. Chem. Soc.*, 1970, **92**, 386. For a fuller account on crown ethers see C. J. Pederson and H. K. Frensdorff, *Angew. Chem., Int. Ed. Engl.*, 1972, **11**, 16.
11. A. M. Sargeson, *Chem. Br.*, 1979, **15**, 23.
12. N. E. Dixon, W. G. Jackson, G. A. Lawrance and A. M. Sargeson, *Inorg. Synth.*, 1983, **22**, 103.
13. J. P. Collman, *Angew Chem., Int. Ed. Engl.*, 1965, **4**, 132.
14. (a) D. Fenton, U. Casellato, P. A. Vigato and M. Vidali, *Inorg. Chim. Acta*, 1982, **62**, 57; (b) T. H. Whitehead, *Chem. Rev.*, 1937, **21**, 113.
15. C. M. Lukehart, G. P. Torrence and J. V. Zerle, *Inorg. Chem.*, 1976, **15**, 2393; *Inorg. Synth.*, 1978, **18**, 56.
16. F. A. Cotton and M. H. Chisholm, *Chem. Eng. News*, 1982, June 8, 40; E. L. Muetterties, *Chem. Eng. News*, 1982, August 30, 28.
17. D. L. Kepert, 'Inorganic Stereochemistry', Springer Verlag, Berlin, 1982.
18. J. L. Hoard, M. D. Lind and B. K. Lee, *Proc. Conf. Rare Earth Res., 4th, Phoenix, AZ*, Gordon and Breach, New York, 1964, p. 403.
19. F. Basolo and R. G. Pearson, 'Mechanisms of Inorganic Reactions', Wiley, New York, 1967.
20. H. Taube, *Rec. Chem. Prog.*, 1956, **17**, 25.
21. J. C. Bailar, Jr., *J. Inorg. Nucl. Chem.*, 1958, **8**, 165; R. Priyadaranjan and N. K. Dutt, *J. Indian Chem. Soc.*, 1943, **20**, 81.
22. D. L. Kepert, *Prog. Inorg. Chem.*, 1972, **22**, 1; 'Inorganic Stereochemistry', Springer Verlag, Berlin, 1982.
23. (a) S. D. Patil and V. H. Kulkarni, *Inorg. Chim. Acta*, 1983, **73**, 125; (b) I. Bernal and G. B. Kauffman, *J. Chem. Educ.*, 1985, in press.
24. G. H. Searle, M. Petkovic and F. R. Keene, *Inorg. Chem.*, 1974, **13**, 399.
25. B. Bosnick, S. T. D. Lo and E. A. Sullivan, *Inorg. Chem.*, 1975, **14**, 2305.
26. E. J. Corey and J. C. Bailar, Jr., *J. Am. Chem. Soc.*, 1959, **81**, 2620.
27. K. Yamanari, J. Hidoka and Y. Shimurai, *Bull. Chem. Soc. Jpn.*, 1975, **48**, 1653; S. Shimba, S. Fujinami and M. Shibata, *Chem. Lett.*, 1979, 783.
28. F. G. Mann, *J. Chem. Soc.*, 1933, 412; R. D. Gillard and F. L. Wimmer, *J. Chem. Soc., Chem. Commun.*, 1978, 936; also ref. 6.
29. J. C. Bailar, Jr., H. Itatani, M. J. S. Crespi and J. Geldard, *Adv. Chem. Ser.*, 1967, No. 62, 103; R. D. Gillard and C. Thorpe, *Chem. Commun.*, 1970, 997.
30. P. E. Schipper, *Inorg. Chim. Acta*, 1975, **12**, 199.
31. I. I. Chernyaev, T. N. Fedatova and O. N. Adrianova, *Zh. Neorg. Khim.*, 1966, **11**, 1349; I. I. Chernyaev and T. D. Fedotova, *ibid.*, 1729; L. N. Essen, F. A. Zakharova and A. D. Gel'man, *Zh. Neorg. Khim.*, 1958, **3**, 2654.
32. D. Geselowitz and H. Taube, in 'Advances in Inorganic and Bioinorganic Mechanisms', ed. A. G. Sykes, Academic, London, 1982, p. 391.
33. W. B. Schaap, A. E. Messner and F. C. Schmidt, *J. Am. Chem. Soc.*, 1955, **77**, 2683.
34. G. F. Reynolds, 'Progress in Polarography', Wiley, New York, 1962, p. 243.
35. J. D. Corbett, *Acc. Chem. Res.*, 1981, **14**, 239 and related papers.
36. R. Tsuchiya, A. Uehara and E. Kyuno, *Bull. Chem. Soc. Jpn.*, 1973, **46**, 3737 and related papers.
37. K. Cheng and B. M. Foxman, *J. Am. Chem. Soc.*, 1977, **99**, 8102; K. Cheng, B. M. Foxman and S. W. Gersten, *Mol. Cryst. Liq. Cryst.*, 1979, **52**, 77.
38. M. Hargittai and I. Hargittai, 'Molecular Geometries of Coordination Compounds in the Vapor Phase', Elsevier, Amsterdam, 1977.
39. C. C. Addison, *Adv. Chem. Ser.*, 1962, **36**, 131; C. C. Addison and N. Logan, *Adv. Inorg. Chem. Radiochem.*, 1964, **6**, 71.
40. R. E. Sievers, R. W. Moshier and M. L. Morris, *Inorg. Chem.*, 1962, **1**, 966; R. E. Sievers, B. W. Ponder, M. L. Morris and R. W. Moshier, *Inorg. Chem.*, 1963, **2**, 693; R. W. Moshier and R. E. Sievers, 'Gas Chromatography of Metal Chelates', Pergamon, Oxford, 1965.

41. 'Cryochemistry', ed. M. Maskovits and G. Ozm, Wiley, New York, 1976.
42. Anon., *Chem. Eng. News*, 1984, February 27, p. 21.
43. 'Metal Binding in Medicine', ed. M. J. Seven, Lippincott, Philadelphia, 1960; 'Inorganic Biochemistry', ed. G. Eichhorn, Elsevier, Amsterdam, 1973 (two volumes); 'Bioinorganic Chemistry', ed. R. Dessy, J. Dillard and L. Taylor, American Chemical Society, Washington, DC, 1971.
44. *Journal of Inorganic Biochemistry* (formerly called *Bioinorganic Chemistry*), Elsevier, Amsterdam.
45. H. Diehl and coworkers, many papers in the *Iowa State College Journal of Science* in 1947 and 1949; M. Calvin and coworkers, many papers in *J. Am. Chem. Soc.*, 1946.
46. B. R. James, *Adv. Chem. Ser.*, 1980, **191**, 253.
47. 'Current Perspectives in Nitrogen Fixation', Proc. 4th Int. Symp., ed. A. H. Gibson and W. E. Newton, 1980, Elsevier, Amsterdam, especially the papers by J. Chatt (p. 15), T. A. George (p. 22) and M. Hidai (p. 26); G. E. Bossard and T. A. George, *Inorg. Chim. Acta*, 1981, **54**, L239 and references therein.

2

Coordination Numbers and Geometries

DAVID L. KEPERT
University of Western Australia, Nedlands, Australia

2.1 VALENCE SHELL ELECTRON PAIR REPULSION THEORY

2.1.1 Introduction

The most useful approach in predicting the stereochemistry of coordination compounds is the Valence Shell Electron Pair Repulsion theory (VSEPR theory), which is based on the idea that the electron pairs around an atom will be arranged so as to minimize the repulsion between them. The qualitative foundations of this field were laid by Sidgwick and Powell[1] in 1940 and by Gillespie and Nyholm[2] in 1957.

In 1963, Hoard and Silverton used a more quantitative approach when they considered that the arrangement of the eight cyanide groups about the metal atom in $K_4[Mo(CN)_8]\cdot 2H_2O$ was determined by the repulsion between all carbon atoms.[3] They also calculated the stereochemical constraints arising from the introduction of chelate rings, as in the eight-coordinate acetylacetonate complex [Zr(acac)$_4$]. This quantitative approach has been developed into a more comprehensive scheme in a monograph by Kepert[4] and this chapter consists of a shortened description of that work.

The quantitative use of VSEPR theory involves three distinct parts. In each, the details of the calculation method are obtained empirically using the very large amount of accurate structural data that is now available. The first part concerns the nature of the repulsion law, which allows the calculation of the stereochemistries of complexes containing any number of identical unidentate ligands. The second part deals with the steric constraints brought about when the ligands are connected to form bidentates or multidentates, such ring systems being extremely important throughout chemistry. The third part makes use of effective bond length ratios, which allows the calculation of the distortions that occur when the ligands are not all identical. An important feature of this third part is the treatment of molecules in which one of the electron pairs around the atom is non-bonding.

2.1.2 The Repulsion Law

The basis of the VSEPR theory is the assumption that the stereochemical arrangement of ligands about a central atom (for convenience, referred to as the metal atom) is determined by the mutual repulsion between all metal–ligand bonds. The repulsion due to any ligand will, of course, be made up of contributions from the metal–ligand bond, from the donor atoms, and from the remainder of the ligand molecule. The relative importance of these terms will not be the same for all compounds, but a large contribution will be from those parts close to the metal atom simply because these are the closest to the adjacent metal–ligand system.

It is assumed that this very complicated repulsion can be simply represented by a model in which each metal–ligand bond is considered to act as a point, the 'effective centre' of the bond. The repulsion u_{ij} between two effective centres of repulsion, i and j, is taken to be inversely proportional to some power n of the distance d_{ij} between them:

$$u_{ij} = \frac{a}{d_{ij}^{\,n}}$$

where a is the proportionality constant. The total repulsion energy, U, is obtained by summing the repulsion over every pair of metal–ligand bonds:

$$\begin{aligned} U &= \sum_{ij} u_{ij} \\ &= \sum_{ij} a d_{ij}^{\,-n} \end{aligned}$$

If all bonds are equal, that is, if the effective centres of all bonds lie on the surface of a sphere of radius r, then the total repulsion energy can be expressed as:

$$U = aXr^{-n}$$

where X is the numerical repulsion energy coefficient, which is a function of n and the geometry of the coordination polyhedron. The most stable stereochemistry is simply calculated by the minimization of X as a function of geometry.

The most appropriate value of n to use in the repulsion law cannot be known exactly. The lower limit is $n = 1$, which unrealistically assumes coulombic repulsion among bonds considered as points. The geometry obtained as n approaches infinity is the same as that obtained for the hard sphere model, where incompressible spheres are at each vertex of the coordination polyhedron, the spheres touching each other at the midpoint of the short edges. Comparison between calculated and experimental structures shows that the best agreement is obtained for $n \approx 6$, this value being reasonable for repulsion between electron clouds. All results quoted in this chapter were obtained using $n = 6$. It is fortunate that the calculated stereochemistry is usually fairly independent of the exact value chosen for n, at least within the approximate range $n \approx 3-10$.

For molecules containing only one type of metal–ligand bond, the above energy relation is sufficient to enable very accurate stereochemical predictions to be made.

The repulsion energy coefficient X can be separated into the individual ligand repulsion energy coefficients Y_i for each ligand:

$$X = \sum_i Y_i$$

It is predicted that those atoms with the largest individual ligand repulsion energy coefficients, that is those which are the most sterically crowded, will have the longest bond lengths. Differences in repulsion energy can lead to differences in bond length of about 5%.

2.1.3 The Basic Stereochemistries

The minimum value for the repulsion energy coefficient X obtained for the most stable stereochemistry for each coordination number is shown in Table 1. A plot of X against coordination number shows that the regular tetrahedron, octahedron and icosahedron are approximately 20% more stable than would be predicted from the smooth curve passing through the remaining points that correspond to the less regular structures. Precise energy units cannot be associated with these repulsion energy coefficients, but it is generally found that distortions corresponding to an increase in X by 0.01–0.05 units are of chemical significance.

Table 1 Repulsion Energy Coefficients, X, for the Most Stable Stereochemistry for Each Coordination Number

Coordination number	*Stereochemistry*	X
2	Linear	0.016
3	Equilateral triangle	0.111
4	Tetrahedron	0.316
5	Trigonal bipyramid	0.877
6	Octahedron	1.547
7	Capped octahedron	3.230
8	Square antiprism	5.185
9	Tricapped trigonal prism	8.105
10	Bicapped square antiprism	12.337
11	Edge-coalesced icosahedron	18.562
12	Icosahedron	23.531

Table 2 shows the difference in repulsion energy between the most stable stereochemistry and the next most stable stereochemistry for each coordination number. There are clearly two classes of behaviour:

(a) For each of the coordination numbers five, seven, eight, nine, ten and eleven, there are two or three stereochemistries of almost equal stability. Moreover, the repulsion energy calculations show that there are no energy barriers between any pair of these structures allowing facile interconversions between them. Repetition of any of these interconversions about different axes leads to a scrambling of all ligand sites, as is observed in solution. In the solid state, structures are commonly observed that are intermediate between the pairs of structures listed in Table 2.

(b) In contrast, the tetrahedron, octahedron and icosahedron are substantially more stable than any other four-, six- or twelve-coordinate structure. Thus not only are tetrahedral and octahedral molecules rigid, but complexes containing a mixture of ligands may have them arranged in different ways. The separation and independent examination of optical and geometrical isomers is a very important part of the chemistry of tetrahedral and octahedral molecules.

Table 2 Repulsion Energy Coefficients X' for Various Stereochemistries Compared with the Repulsion Energy Coefficient X for the Most Stable Stereochemistry of the Same Coordination Number

Coordination number	*Stereochemistry*	X'	$X'-X$
4	Tetrahedron	0.316	
	Square	0.531	0.215
5	Trigonal bipyramid	0.877	
	Square pyramid	0.890	0.013
6	Octahedron	1.547	
	Trigonal prism	1.935	0.388
7	Capped octahedron	3.230	
	Capped trigonal prism	3.231	0.001
	Pentagonal bipyramid	3.266	0.036
8	Square antiprism	5.185	
	Triangular dodecahedron	5.245	0.060
9	Tricapped trigonal prism	8.105	
	Capped square antiprism	8.117	0.012
10	Bicapped square antiprism	12.337	
	Sphenocorona	12.362	0.025
	Trirhombohedron	12.363	0.026
11	Edge-coalesced icosahedron	18.562	
	Capped pentagonal antiprism	18.571	0.009
12	Icosahedron	23.531	
	Bicapped pentagonal prism	25.928	2.397

2.1.4 Multidentate Ligands

To calculate the stereochemistries of molecules containing chelate groups, it is assumed that each bonded bidentate ligand is sufficiently rigid that interaction between its metal—ligand bonds can be considered constant, and is therefore omitted when summing the electron-pair repulsions. The chelate geometry is given by the 'normalized bite', *b*, defined as the distance between the effective bond centres divided by *r*.

The distance between the donor atoms of any chelate group is relatively constant, depending to only a small extent upon the coordination number and the size of the metal atom. For example:

β-diketonates $(RCOCHCOR)^-$:	O···O ~2.8 ± 0.1 Å
dithiocarbamates, xanthates, *etc.* $(S_2CX)^-$:	S···S ~2.8 ± 0.1 Å
nitrate $(NO_3)^-$:	O···O ~2.1 ± 0.05 Å

Any particular ligand will tend to form higher coordination numbers with larger metal atoms, although there may be some overlap between different groups. For example:

$(RCOCHCOR)^-$:	$[M(bidentate)_3]^{x\pm}$ for M—O	< ~2.1 Å
	$[M(bidentate)_4]^{x\pm}$ for M—O	> ~2.1 Å
$(S_2CX)^-$:	$[M(bidentate)_3]^{x\pm}$ for M—S	< ~2.5 Å
	$[M(bidentate)_4]^{x\pm}$ for M—S	> ~2.5 Å
$(NO_3)^-$:	$[M(bidentate)_3]^{x\pm}$ for M—O	< ~2.0 Å
	$[M(bidentate)_4]^{x\pm}$ for M—O	~2.0 to ~2.4 Å
	$[M(bidentate)_4]^{x\pm}$ for M—O	~2.4 to 2.6 Å
	$[M(bidentate)_6]^{x\pm}$ for M—O	> ~2.6 Å

It is shown in more detail in Section 2.3.3.5 that the normalized bite decreases as the number of atoms in the chelate ring decreases, and as the size of those atoms decreases. Typical values for six-coordinate metal atoms and the larger eight-coordinate metal atoms are shown in Table 3.

The extension from bidentate ligands to multidentate ligands is outside the scope of this chapter, but has been dealt with elsewhere.[4]

2.1.5 Effective Bond Length Ratios

For complexes containing different donor atoms it is necessary to introduce another empirical parameter to account for the small distortions observed compared with compounds containing only one type of metal—ligand bond. The parameter chosen is the distance between the central atom and the effective centre of the bond. That is, the relative repulsion of the metal—ligand bond

Table 3 Normalized Bites for Typical Bidentate Ligands Attached to Six-coordinate and Eight-coordinate Metal Atoms

Chelate ring	*Normalized bite, b* *[M(bidentate)$_3$]*	 *[M(bidentate)$_4$]*
Six-membered (*e.g.* acetylacetonate)	~1.4	~1.2
Five-membered (*e.g.* tropolonate)	~1.3	~1.1
Four-membered: 3 large atoms (*e.g.* dithiophosphate)	~1.3	~1.1
2 large atoms (*e.g.* dithiocarbamate)	~1.2	~1.1
0 large atoms (*e.g.* nitrate)	~1.1	~1.0
Three-membered (*e.g.* peroxide)	—	~0.8

M—*i* and the metal–ligand bond M—*j* is determined by the 'effective bond length ratio', $R(i/j)$. These empirical parameters can be successfully transferred from one stereochemistry to another, and even between different coordination numbers.

These effective bond length ratios are obtained by fitting experimental structures against structures calculated as a function of $R(i/j)$. A simple example is a tetrahedral molecule containing one ligand different to the other three, [M(unidentate A)(unidentate B)$_3$]. The effective bond length ratio between the unique metal–ligand A bond lying on the threefold axis and the other three metal-ligand B bonds is defined as R(A/B).

For $R(\mathrm{A/B}) = 1$, the tetrahedron is regular, with AMB = BMB = 109.5°. The repulsion energy calculations show that AMB increases, and BMB decreases, as R(A/B) is decreased. For example, for trifluoromethyl groups bonded to carbon atoms, the experimental FCC and FCF bond angles are 112.4° and 106.4° respectively, which correspond to $R(\mathrm{C/F}) = 0.86$, or $R(\mathrm{F/C}) = 1.16$. Note that the carbon–carbon effective bond length is approximately 14% *shorter* than the carbon–fluorine effective bond length, although the real carbon–carbon bond length is 15% *longer* than the real carbon-fluorine bond length. The same R(F/C) values are obtained for trifluoromethyl groups attached to phosphorus atoms where the real carbon–phosphorus bond length is 42% longer than the real carbon–fluorine bond length. The large effective bond length of a carbon–fluorine bond is readily attributed to the high electronegativity of the fluorine atom, which attracts the bonding electron pair towards itself. Examination of a large number of tetrahedral molecules in this way indicates that a self-consistent set of effective bond length ratios can be obtained for various groups attached to the light elements, for example, $R(\mathrm{Cl/R}) = 1.05$, $R(\mathrm{H/R}) = 1.09$ and $R(\mathrm{F/R}) = 1.16$ (where R = alkyl).[4] Much greater distortions from regular tetrahedral bond angles are observed for alkyl groups attached to the metallic elements of the *p*-block, as in $[\mathrm{AlCl_3R}]^-$, $[\mathrm{GaCl_3R}]^-$, $[\mathrm{InCl_3R}]^-$ and $[\mathrm{SnCl_3R}]$, implying that these metal–alkyl effective bond lengths are unusually short.[4]

Any physical meaning attached to these $R(i/j)$ values is more uncertain for groups which can be considered as potentially bonding through multiple bonds; for example, oxygen can be considered to be bonded as X=O, X→O or $\mathrm{X^{2+}{\leftarrow}O^{2-}}$. It is most convenient to treat these bonds in the same way as before. For example, triphenylphosphine oxide is significantly distorted from regular tetrahedral geometry, Ph—P—O = 112.0°, Ph—P—Ph = 106.8°, corresponding to an effective bond length ratio for the phosphorus–oxygen bond of $R(\mathrm{O^{2-}/Ph}) = 0.87$.[4] The analogous phosphine sulfides, phosphine selenides and phosphine carbenes are very similar [$R(\mathrm{O^{2-}/Ph}) \approx R(\mathrm{S^{2-}/Ph}) \approx R(\mathrm{Se^{2-}/Ph}) \approx R(\mathrm{{=}CR/Ph})$],[4] again showing that the distance between the effective centre of repulsion and the central atom is not a simple function of bond length. As expected, the most distorted tetrahedron is the trifluorosulfonium oxide ion:[5]

$(\mathrm{F_3SO})^+$: FSO = 116.0°, FSF = 102.2°, $R(\mathrm{O^{2-}/F}) = 0.68$

The effective bond length of a singly bonded group relative to that of a double bonded group can also be obtained for compounds of the type $(\mathrm{X{=}})_3\mathrm{M}$(unidentate). Thus in the alkyl perchlorate $\mathrm{O_3ClOR}$,[6] O—Cl—OR = 103.8°, O—Cl—O = 114.5° and $R(\mathrm{OR/O^{2-}}) = 1.29$, the reciprocal of which is $R(\mathrm{O^{2-}/OR}) = 0.78$ and is in reasonable agreement with the value obtained for compounds containing a single M=O group. The decrease in R(OX/O) values from $\mathrm{O_3Cl{-}OX}$ (1.29) to $^{-}\mathrm{O_3S{-}OX}$ (1.20) to $^{2-}\mathrm{O_3P{-}OX}$ (1.16) reflects the decrease in formal bond order to the non-bridging oxygen atoms from 2.00 to 1.67 and 1.33, respectively.[7] The greatest departure from regular tetrahedral geometry is again observed for the oxofluoro complexes $(\mathrm{O_3F})^{x-}$:

$\mathrm{O_3ClF}$:[8] OClF = 100.8°, OClO = 116.6°, $R(\mathrm{F/O^{2-}}) = 1.46$, bond order = 2.00
$\mathrm{O_3SF^{-}}$:[9] OSF = 103.4°, OSO = 114.8°, $R(\mathrm{F/O^{2-}}) = 1.31$, bond order = 1.67
$\mathrm{O_3PF^{2-}}$:[4] OPF = 104.3°, OPO = 114.1°, $R(\mathrm{F/O^{2-}}) = 1.26$, bond order = 1.33

Structural parameters of compounds containing two double bonds and two single bonds are very similar, as shown, for example, by:

$[SO_2Me_2]$:[10] OSO = 117.9°, MeSMe = 103.0°, $R(O^{2-}/Me) = 0.83$
$[PO_2R_2]$:[7] OPO = 117.7°, RPR = 103.0°, $R(O^{2-}/R) = 0.83$

Tetrahedral complexes of a first-row transition metal ion $[M^{II}X_3L]^-$, where X = Cl, Br or I, and L is an uncharged unidentate ligand, generally have LMX and XMX angles of about 105° and 114° respectively,[4] showing that the effective bond lengths of the charged ligands are about 20% shorter than the uncharged ligands: $R(\text{ligand}/X^-) \approx 1.2$ or $R(X^-/\text{ligand}) \approx 0.8$. Complexes between the first-row transition metal dichlorides and two uncharged ligands, $[MCl_2L_2]$, have bond angles ClMCl ≈ 115° and LML ≈ 102°,[4] again corresponding to $R(Cl^-/\text{ligand}) = 0.85$.

The same values for $R(X^-/L)$ are obtained for higher coordination numbers as in, for example, $[MX_5L]^{x-}$, $[MX_4L_2]^{x-}$ and $[MX_3L_4]^{x-}$ provided the transition metal is in a relatively high oxidation state.[4] (More complex stereochemical behaviour is found for organometallic complexes with the metal atom in a lower oxidation state.) The same fitting procedure has been carried out for complexes of higher coordination numbers containing bidentate ligands, for example $[M(\text{bidentate})_3L]^{x-}$, $[M(\text{bidentate})_3X]^{x-}$ and $[M(\text{bidentate})_2X_4]^{x-}$ to yield $R(L/\text{bidentate}) \approx 1.0$ and $R(X^-/\text{bidentate}) \approx 0.8$. The charge on the chelate group does not appear to greatly affect these effective bond length ratios. Similarly, polyatomic unidentate ligands such as thiocyanate behave more like uncharged ligands than like chloride, bromide or iodide.

The ligands oxide and nitride, O^{2-} and N^{3-}, occupy even more space than do halide ions and have correspondingly lower effective bond length ratios: $R(O^{2-}/L) \approx 0.6$; $R(O^{2-}/X^-) \approx 0.8$.

2.1.6 Elements Containing a Non-bonding Pair of Electrons

For the particularly interesting compounds where there is a non-bonding pair of electrons attached to the central atom the $R(\text{lone pair}/j)$ values found are not constant, the lone pair of electrons being constricted closer to the central atom for atoms further down the Periodic Table.

The stereochemical parameters for the Group V halides, $[MX_3(\text{lone pair})]$, are summarized in Table 4, the X-ray data being augmented by recent electron diffraction and microwave data on the gaseous molecules, agreement between the two sets of results being very good for the smaller Group V atoms. However, the interpretation of the X-ray results for the larger atoms becomes increasingly complicated by the presence of short intermolecular contacts. For example, in SbF_3 the three Sb—F bonds are 1.92 Å long, but distorted octahedral coordination about the antimony atom is completed by three Sb···F contacts of 2.61 Å. Similarly, in $SbCl_3$ there are three Sb—Cl bonds of 2.75 Å, with an additional five Sb···Cl contacts at about 3.6 Å. Antimony trichloride forms weak adducts with a large number of molecules, in which low ClSbCl angles, 90–94°, are observed, and in addition to the three Sb—Cl bonds of ~2.35 Å, further contacts to the antimony atom occur at ~3.0–3.5 Å.

Table 4 Stereochemical Parameters[4] for Group V Halides, $[MX_3(\text{lone pair})]$

Compound	*Crystal*		*Vapour*	
	XMX (°)	*R(lone pair/X)*	*XMX (°)*	*R(lone pair/X)*
NF_3	—	—	102.4	0.68
NCl_3	106.8	0.88	107.4	0.91
NBr_3	—	—	—	—
NI_3	—	—	—	—
PF_3	—	—	97.4	0.47
PCl_3	100.1	0.58	100.1	0.58
PBr_3	100.5	0.60	101.0	0.62
PI_3	102.0	0.67	—	—
AsF_3	—	—	96.0	0.41
$AsCl_3$	98.2	0.51	98.6	0.53
$AsBr_3$	97.7	0.50	99.7	0.58
AsI_3	102.0	0.67	100.2	0.60
SbF_3	87.3	—	95.0	0.36
$SbCl_3$	94.1	0.30	97.2	0.47
$SbBr_3$	—	—	98.2	0.52
$SbI_3 \cdot 3S_8$	96.6	0.44	—	—

For these Group V halides (Table 4), it is observed that $R(\text{lone pair}/X)$ decreases on descending the periodic table and also decreases along the series I > Br > Cl > F, as the bonding pairs of electrons are drawn out closer to the halogen atoms. The X-ray structural parameters for the Group VI cations $[MX_3(\text{lone pair})]^+$ (Table 5) agree with those for the uncharged Group V molecules.

Table 5 Stereochemical Parameters[4] for Group VI Compounds, $[MX_3(\text{lone pair})]^+$

Compound	*XMX (°)*	*R(lone pair/X)*
$(SF_3)(BF_4)$	97.5	0.48
$(SCl_3)(ICl_4)$	101.3	0.64
$(SeF_3)A$ (A = NbF_6, Nb_2F_{11})	94.7	0.34

The same type of fitting procedure for $[MX_4(\text{lone pair})]^{x\pm}$ and $[MX_5(\text{lone pair})]^{x\pm}$ yields similar R(lone pair/X) values for five- and six-coordinate complexes (Table 6). However, complexes of the type $[MX_6(\text{lone pair})]^{x-}$ may show steric activity of the lone pair, as in $[XeF_6(\text{lone pair})]$, R(lone pair/F) $\approx$ 0.2, or no steric activity, R(lone pair/X) ≈ 0, and is discussed in more detail in Section 2.4.1.4. The lone pair of electrons shows less steric activity as the steric crowding in the molecule increases, although the R(lone pair/j) value may increase if the steric crowding is reduced by replacing the unidentate ligands with bidentate ligands which hold the donor atoms closer together. For example:

	R(lone pair/j)
$[Sb^{III}Cl_6]^{3-}$	0.0
$[Sb^{III}(S_2COEt)_3]$	0.15

Table 6 Effective Bond Length Ratios[4] for a Non-bonding Pair of Electrons, R(lone pair/X)

Coordination no. 4		*Coordination no. 5*		*Coordination no. 6*	
N^{III}	0.8	—	—	—	—
P^{III}	0.5	S^{IV}	0.5	—	—
As^{III}	0.5	Se^{IV}	0.4	—	—
Sb^{III}	0.4	Sb^{III}, Te^{IV}	0.3	Sb^{III}, Te^{IV}, Xe^{VI}	0.3

There are no known eight-coordinate complexes in which the lone pair occupies a coordination site, even in compounds containing bidentate ligands.

The structures of the oxoanions $[XO_3(\text{lone pair})]^{2-}$ (X = S, Se, Te) and $[XO_3(\text{lone pair})]^-$ (X = Cl, Br) (Table 7) are again consistent with the general picture. In addition to the three short X—O bonds, the larger elements again have additional longer interactions, but there is again a clear contraction of the non-bonding electron pair down the series sulfite, selenite, tellurite, or chlorate, bromate. The larger OXO angles for chlorate and bromate compared with the Group VI anions are clearly due to the increase in bond order from 1.33 to 1.67.

Table 7 Effective Bond Length Ratios[4,11] for a Non-bonding Pair of Electrons in $[MO_3(\text{lone pair})]^{x-}$

	Compound		*OMO (°)*	*R(lone pair/O)*
12078	*Bond order* $= 1\frac{1}{3}$			
	$A_2(SO_3)\cdot xH_2O$	(A = Li, Na, Cs, NH_4)	105.3	0.81
	$NaH_3(SeO_3)_2$		101.0	0.62
	$A_2(TeO_3)\cdot xH_2O$	(A = K, ½Ba)	99.9	0.58
12079	*Bond order* $= 1\frac{2}{3}$			
	$A(ClO_3)$	(A = Na, K)	106.6	0.87
	$Na(BrO_3)$		104.1	0.76

The existence of sterically active lone pairs of electrons is thus well established in elements of the p-block, although it is generally considered that electrons in d-orbitals do not show stereochemical activity. However, their presence can be invoked to explain the structure of square planar complexes. In the absence of the other effects, the repulsion between four metal–ligand bonds leads to a tetrahedral structure rather than a square planar structure (Table 2). Merely as a means of illustrating the effect on four metal–ligand bonds of a relatively small amount of electron density along the z-axis, imagine one electron pair in an orbital, half above and half below the metal atom (Figure 1). Each half is considered to act at a point, distance R_e from the metal atom (defining the distance between the metal atom and each bonding pair of electrons as unity). The dependence of AMC (or BMD) on R_e is shown in Figure 2. As the electron pair spreads out along the z-axis, the tetrahedron becomes progressively squashed into a square, this being achieved at $R_e \geqslant 0.13$. This spread of electron density is more likely to occur for the d^8 electron configuration in which a non-bonding electron pair is located in the d_{z^2} orbital, particularly for second- and third-row transition metal ions in which the d orbitals are generally expanded, and for π-bonding ligands which can further interact with this orbital. Square-planar complexes are also favoured by reducing the steric crowding in the molecule as occurs for the larger second- and third-row transition metal ions and for complexes containing chelate rings of small normalized bite.

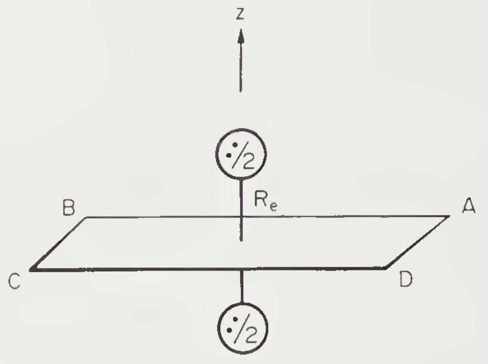

Figure 1 General stereochemistry for square-planar complexes containing one non-bonding pair of electrons

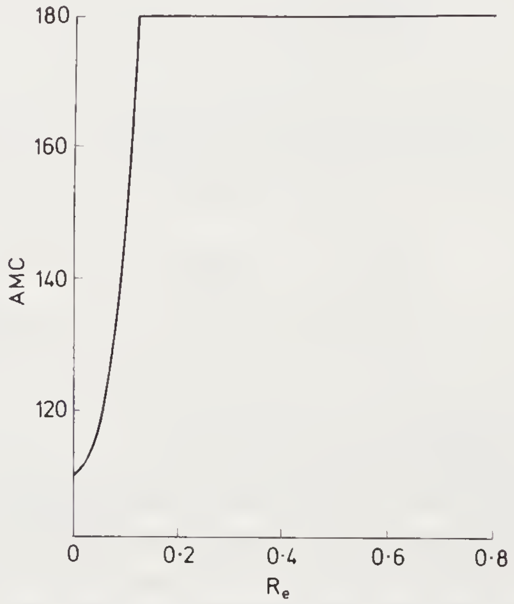

Figure 2 Dependence of bond angle AMC (degrees) upon distance R_e for four-coordinate complexes containing one non-bonding pair of electrons

The existence of some electron density on each side of the square plane can also be used to explain the *trans* influence in square complexes, in which the bond *trans* to a strong metal–ligand bond is weakened.[12] For the case where the non-bonding electron density along the z-axis is relatively expanded, $R_e \geqslant 0.3$, a decrease in the effective bond length R(A) to ligand A shifts this region of non-bonding electron density towards atom C. Atom C therefore experiences a greater repulsion than do atoms B and D, and the M—C bond is weaker than the M—B and M—D bonds. The calculated *trans* influence, Y_C/Y_B, is shown as a function of R_e in Figure 3.

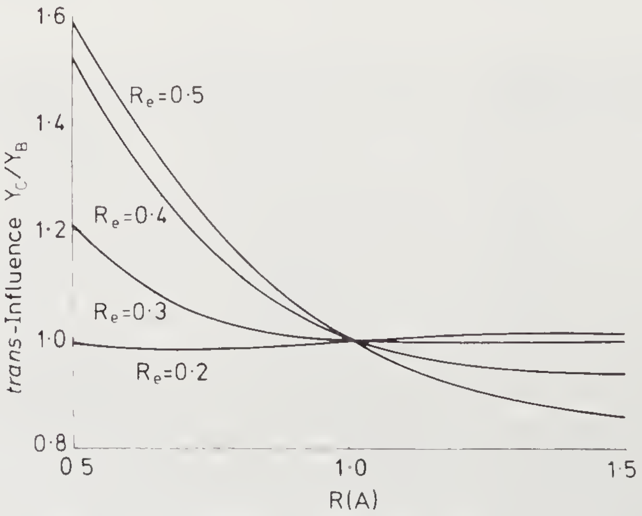

Figure 3 The *trans* influence, Y_C/Y_B, as a function of R(A) and R_e for square-planar [M(unidentate A)(unidentate B)$_3$] containing one non-bonding pair of electrons

This picture of the *trans* influence differs from the conventional π-bonding picture, where the metal π-electrons are displaced *toward* the more strongly bonding ligand A and cannot effectively π-bond the *trans*-ligand C.

2.2 FIVE-COORDINATE COMPOUNDS

2.2.1 [M(Unidentate)$_5$]

The starting point for five-coordination is to consider the trigonal bipyramid and the square pyramid, and the relation between them. Both are examples of the more general stereochemistry shown in Figure 4. A twofold axis passes through the metal atom M and the donor atom E, the other four atoms lying on a pair of vertical mirror planes. Descriptions of the stereochemical changes without enforcing this full C_{2v} symmetry are considered later in this section. The angles between this axis and the bonds to each of the pairs of donor atoms A,C and B,D are denoted by ϕ_A and ϕ_B, respectively. The trigonal bipyramid is defined by $\phi_A = 90.0°$ and $\phi_B = 120.0°$ (or $\phi_A = 120.0°$ and $\phi_B = 90.0°$), and the square pyramid is defined by $\phi_A = \phi_B$.

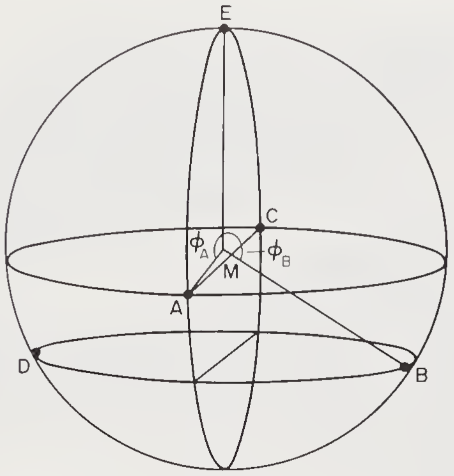

Figure 4 General stereochemistry for [M(unidentate)$_5$] with C_{2v} symmetry

The potential energy surface displayed in Figures 5a and 5b shows that there is no potential energy barrier between the square pyramid at $\phi_A = \phi_B = 101.3°$ and the two trigonal bipyramids situated at the two minima. Movement along the 'reaction coordinate' connecting the two trigonal bipyramids is usually described as the Berry pseudo-rotation.[13]

An important feature of five-coordination is the large differences among the different ligand sites. For example, the apical site of a trigonal bipyramid has three nearest neighbours at $2^{1/2}r$, whereas the equatorial sites have only two such close neighbours. Thus the apical sites experience greater repulsion than the equatorial sites, leading to the expectation of a longer metal–ligand bond: $Y(\text{apical})/Y(\text{equatorial}) = 1.21$. Similarly, each ligand at a square basal site of a square pyramid experiences more repulsion than does the single atom at the apical site: $Y(\text{basal})/Y(\text{apical}) = 1.27$.

Structurally characterized molecules of the type [M(unidentate)$_5$]$^{x\pm}$ cover the complete range from the trigonal bipyramid ($\phi_A = 90.0°$, $\phi_B = 120.0°$) to the square pyramid ($\phi_A = \phi_B \approx 100°$), some simple examples being shown in Table 8. Whether a compound is near the trigonal bipyramid end of the potential energy surface, or near the square pyramid, must be attributed to crystal-packing forces. For example, the structure of $SbPh_5$ is nearer the square-pyramidal end of the range, whereas the solvate $SbPh_5 \cdot \frac{1}{2}C_6H_{12}$ is trigonal bipyramidal. In molecules towards the trigonal bipyramidal end of the range, the axial bonds are about 5% longer than the equatorial bonds, whereas for molecules towards the square pyramidal end of the range, the axial bond is about 4% shorter than the four basal bonds. These observations are in agreement with the predictions made above.

However, a much more complicated pattern of bond lengths is observed for many transition metal complexes, particularly those with the d^8, d^9 or d^{10} electron configuration.[4] These have a much wider range of metal–ligand bond lengths and can be considered as having two, three or four 'normal' metal–ligand bonds, with the remaining ligands being more weakly bonded. For example, the anion in *cubic*-[Cr(NH$_3$)$_6$][HgCl$_5$] has a linear Cl—Hg—Cl group with Hg—Cl = 2.52 Å, with three weaker interactions completing a trigonal bipyramid, Hg—Cl = 2.64 Å.[27] However in the *rhombohedral* modification of [Cr(NH$_3$)$_6$][HgCl$_5$] there are three chlorine atoms coplanar with the mercury atom at Hg—Cl = 2.43 Å, with the two *trans*-ligands further away

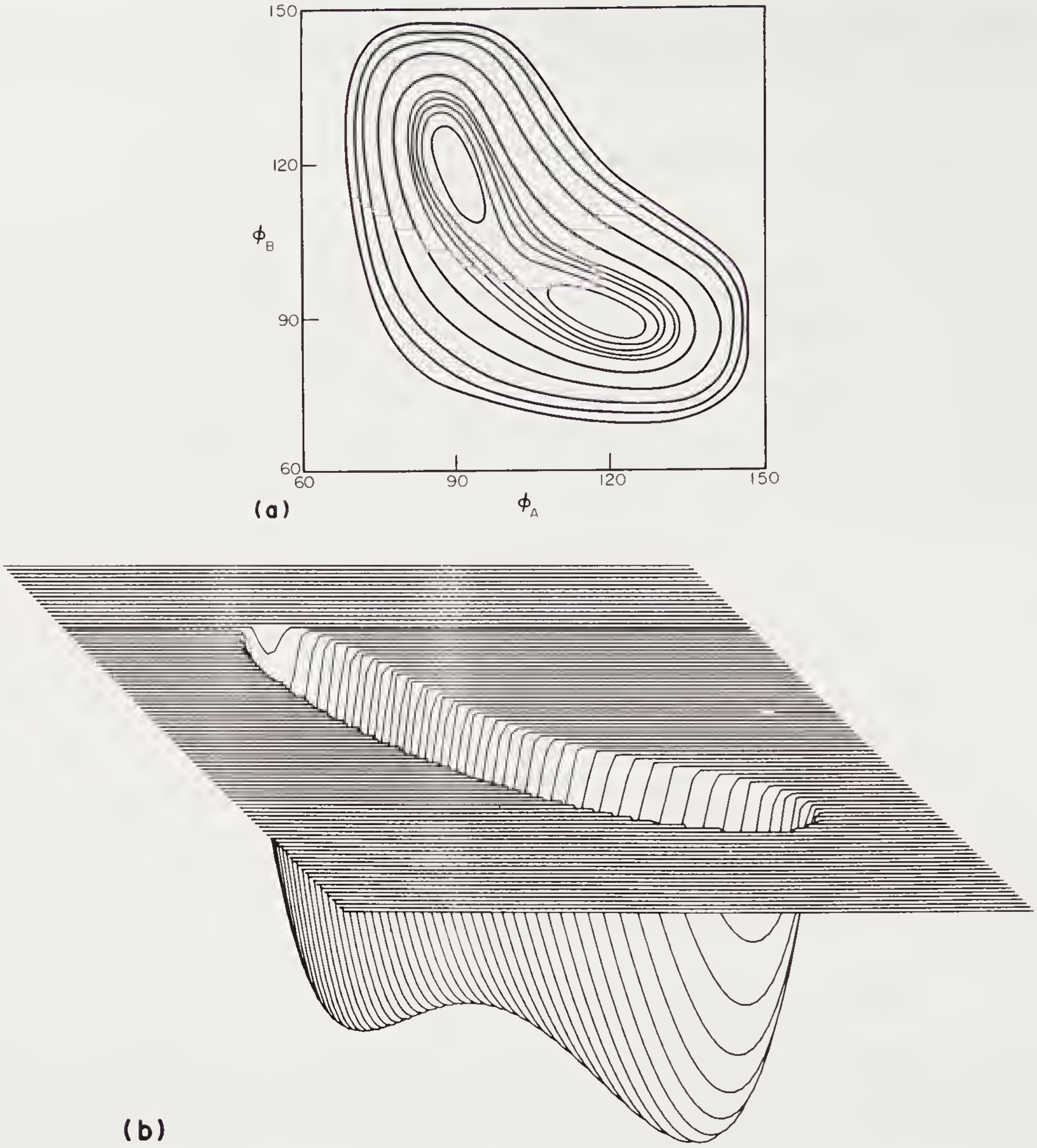

Figure 5 (a) Projection of the potential energy surface for [M(unidentate)$_5$] on to the $\phi_A - \phi_B$ plane (in degrees). The five faint contour lines are for successive 0.01 increments in X above the minima, and the five heavy contour lines are for successive 0.1 increments above the minima. (b) As in (a), but with truncation at $X = 0.05$

Table 8 Stereochemical Parameters for Some [M(unidentate)$_5$] Complexes

Complex	ϕ_A	ϕ_B	*Ref.*
[$SbPh_5$]·½C_6H_{12}	90.3	119.2	14
[$AsPh_5$]·½C_6H_{12}	90	120	15
[PPh_5]	91.5	118.7	16
(PCl_4)[VCl_5]	89.1	116.3	17
[$P(OPh)_5$]	91.6	116.9	18
$(Ph_4As)_2[Fe(N_3)_5]$	93.1	118.3	19
[$Sb(C_6H_4Me)_5$]	91.1	114.9	20
$[Co(MeC_5H_4NO)_5](ClO_4)_2$	93.0	114.0	21
[$Nb(NMe_2)_5$]	101.5	109.1	22
[$SbPh_5$]	98.3	105.4	23
$[Mg(Me_3AsO)_5](ClO_4)_2$	99.8	107.6	24
$[Mg(Me_3PO)_5](ClO_4)_2$	99.9	106.4	25
[$Nb(NC_5H_{10})_5$]	98.4	110.5	22
	100.4	108.4	22
$(Et_4N)_2[InCl_5]$	103.0	104.7	26

at 2.95 Å.[28] For the d^8, d^9 and d^{10} complexes nearer the square pyramid end of the range, the axial metal–ligand bond is *longer* than the four basal bonds and the stereochemistry can be considered to be approaching square planar with one additional weakly bonded ligand. A typical example is $[Cr(NH_3)_6][Ni(CN)_5]\cdot 2H_2O$, where $Cr—CN_{basal} = 1.88$ Å and $Cr—CN_{axial} = 2.10$ Å.[29]

Many five-coordinate molecules exhibit very rapid intramolecular rearrangements, leading to all five ligands being equivalent over the NMR timescale, with the energy barriers to interconversion being less than approximately 20 kJ mol^{-1}. For example, the ^{19}F NMR spectrum of PF_5 shows all fluorine atoms equivalent, over the temperature range 60 to −197 °C.[30] Proton NMR studies on $SbMe_5$ in carbon disulfide down to about −100 °C also show the presence of only one type of methyl group.[31] The ^{13}C NMR spectra of $[Fe(CO)_5]$ and $[Fe(CNBu)_5]$ show only a single resonance at temperatures as low as −170 °C and −80 °C respectively.[32,33] Both ^{19}F NMR and ^{31}P NMR studies on $[Fe(PF_3)_5]$, $[Ru(PF_3)_5]$ and $[Os(PF_3)_5]$ down to −160 °C in $CHClF_2$ show all ligands are equivalent.[33,34] In contrast, metal ions with the d^8 electron configuration bonded to five phosphite ligands are rigid trigonal bipyramids at low temperature, but show simultaneous exchange between two axial ligands and two equatorial ligands at higher temperatures, corresponding to rapid movement along the trough in the potential energy surface shown in Figure 5.[33,35,36]

Finally, for purposes of comparison with results described later, a potential energy surface is required in which the high C_{2v} symmetry enforced when calculating Figure 5 is absent. The general stereochemistry is now shown in Figure 6, and contains a mirror plane through MBDE as the only symmetry element. The axes are defined so that $\phi_A = \phi_B = \phi_C$, the structure being completely defined by ϕ_A, θ_A, ϕ_D and ϕ_E.

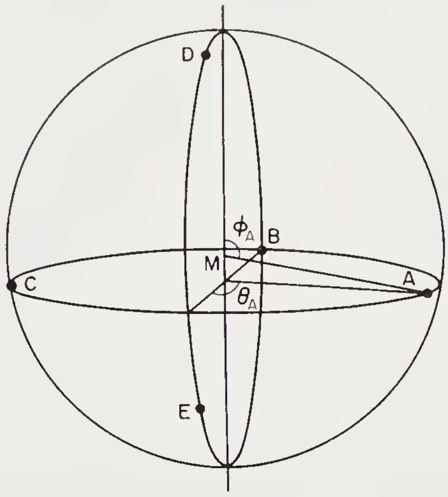

Figure 6 General stereochemistry for [M(unidentate)$_5$] complexes containing one mirror plane, through BDE

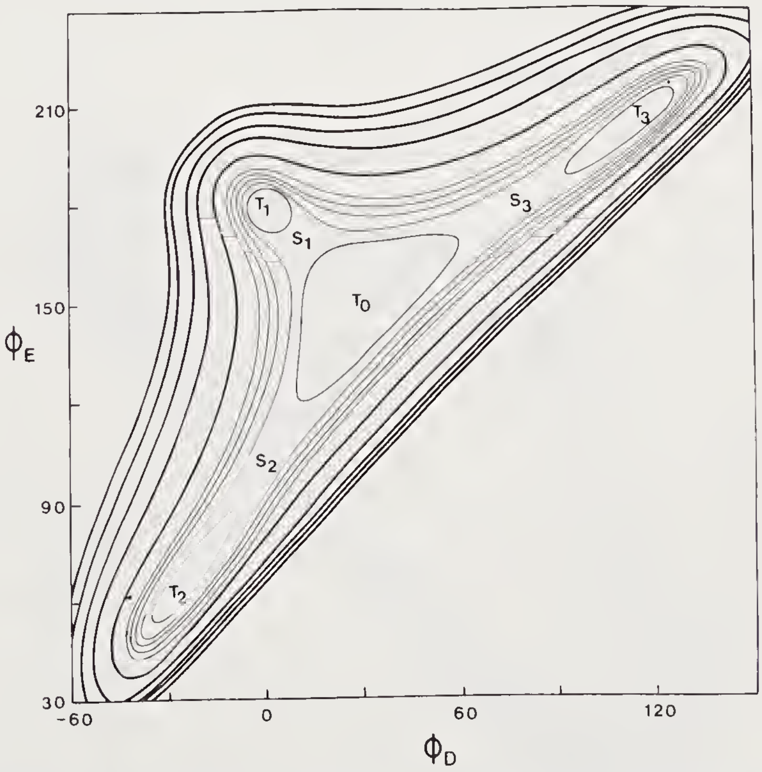

Figure 7 Projection of the potential energy surface for [M(unidentate)$_5$] on to the ϕ_D–ϕ_E plane (in degrees). The five faint contour lines are for successive 0.01 increments in X above the minima, and the five heavy contour lines are for successive 0.1 increments above the minima, at T_0, T_1, T_2 and T_3. The locations of the stereochemistries are shown by T (trigonal bipyramid) and S (square pyramid)

The potential energy surface projected on to the ϕ_D–ϕ_E plane is shown in Figure 7. There are now three identical transformations starting from the central trigonal bipyramid T_0 at $\phi_D = 30.0°$, $\phi_E = 150.0°$, depending on which of the three equivalent atoms forming the trigonal plane, B, D and E, becomes the apical atom of the square pyramid, S_1, S_2 and S_3 respectively. Each of these square pyramids exists on a saddle between the trigonal bipyramid T_0 and the trigonal bipyramids T_1,T_2 and T_3, respectively. These stereochemical changes are shown in Figure 8.

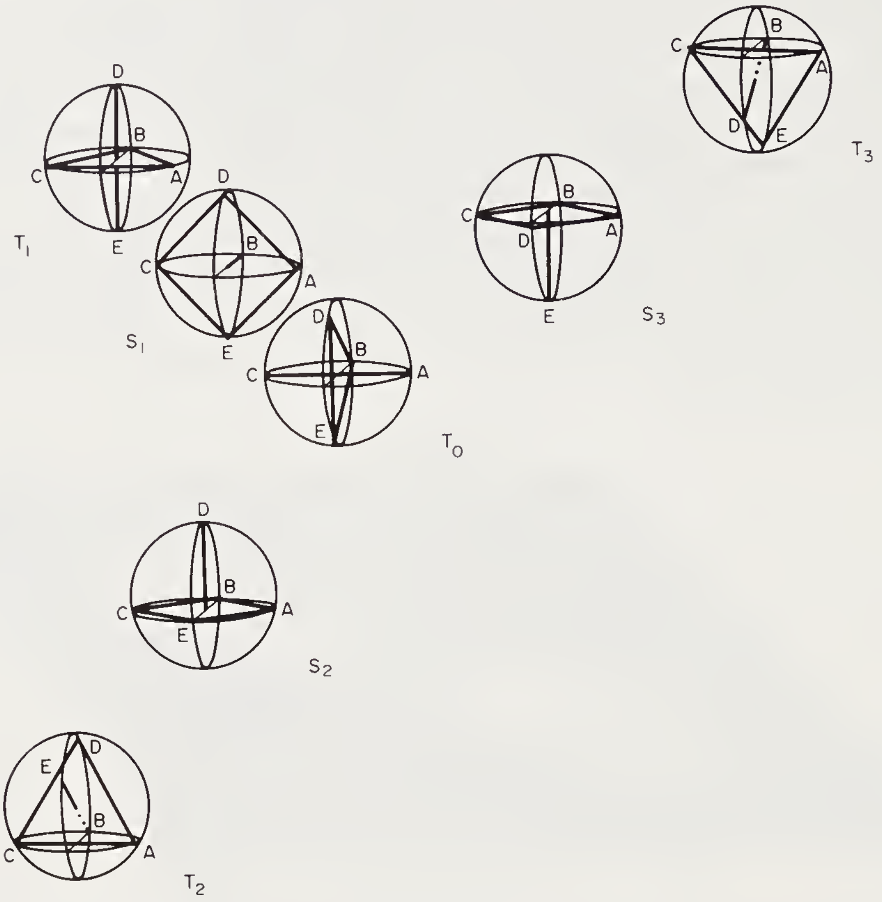

Figure 8 The relation among the stereochemistries corresponding to Figure 7

2.2.1.1 *[M(unidentate A)(unidentate B)$_4$]*

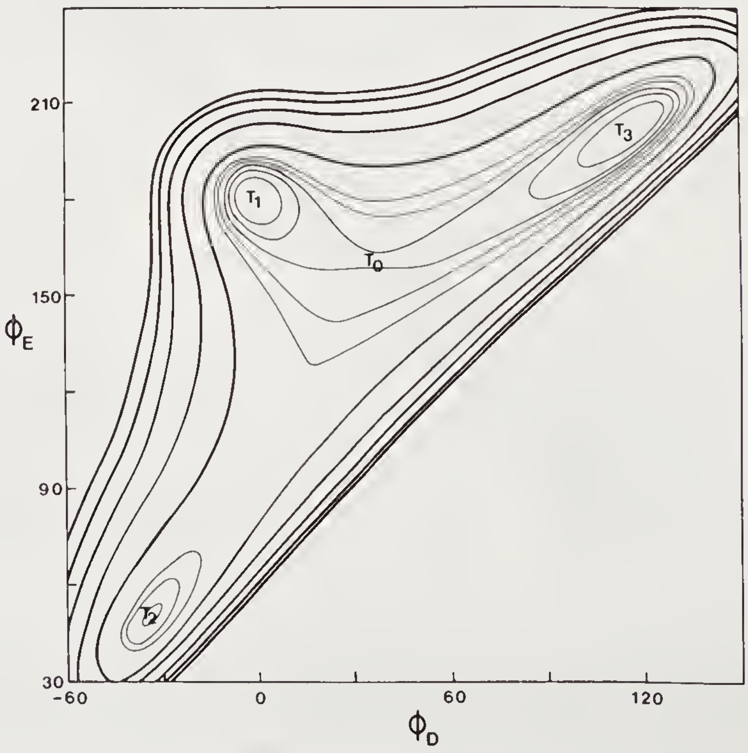

Figure 9 Projection of the potential energy surface for [M(unidentate A)(unidentate B)$_4$] on to the ϕ_D–ϕ_E plane (in degrees). The five faint contour lines are for successive 0.01 increments in X above the minima and the five heavy contour lines are for successive 0.1 increments above the minima, at T_1 and T_3. $R = 1.2$. The positions of the trigonal bipyramids (T) are shown

The general stereochemistry for complexes with one ligand different from the other four is the same as that shown in Figure 6, but now the effective bond length of the M—D bond is defined as R, with the other four remaining at unity.

Typical potential energy surfaces for $R = 1.2, 0.8$ and 0.2 are shown in Figures 9–11 respectively, and should be compared with Figure 7 calculated for $R = 1.0$.

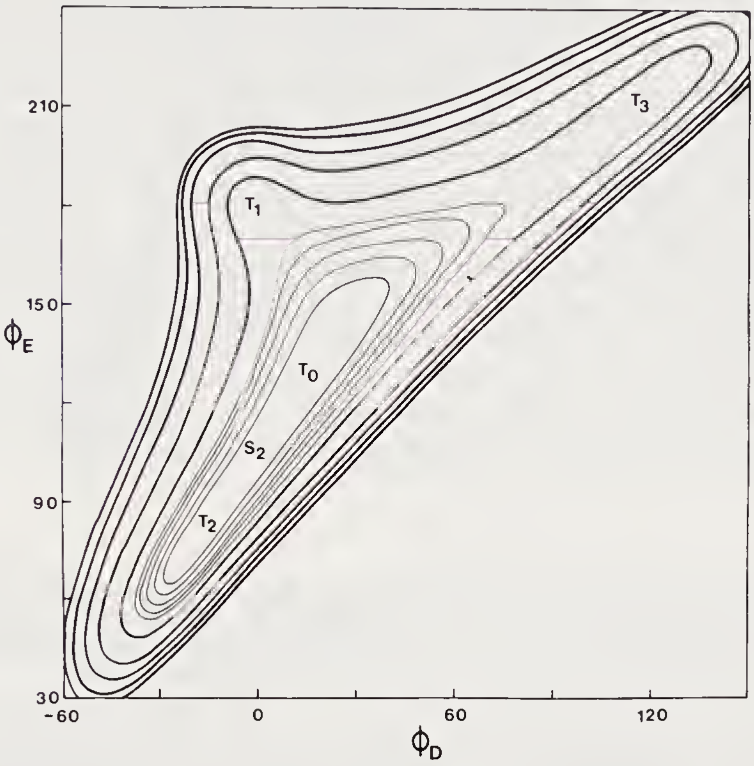

Figure 10 Projection of the potential energy surface for [M(unidentate A)(unidentate B)$_4$] on to the ϕ_D–ϕ_E plane (in degrees). The five faint contour lines are for successive 0.01 increments in X above the minima, and the five heavy contour lines are for successive 0.1 increments above the minima, at T_0 and T_2. $R = 0.8$. The positions of the trigonal bipyramids (T) and square pyramid (S) are shown

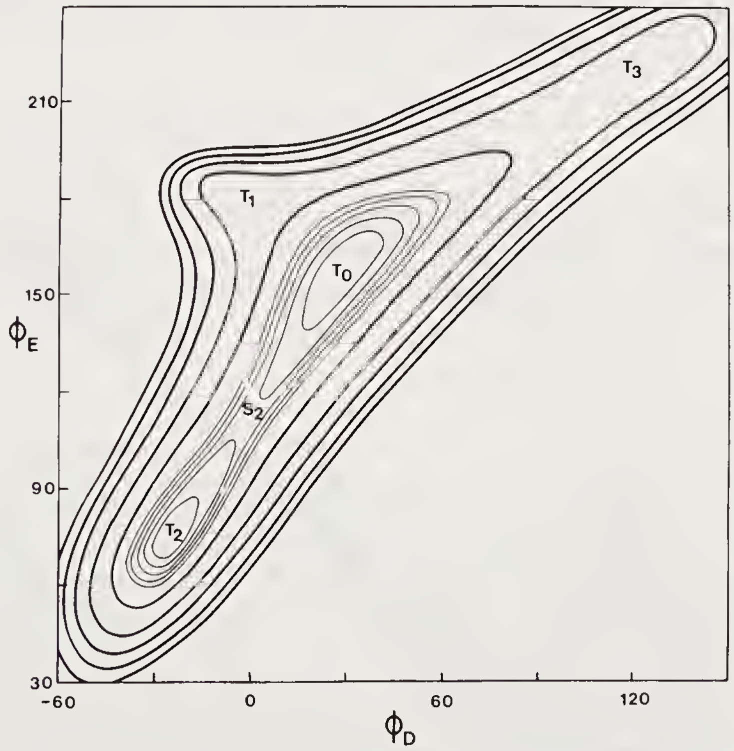

Figure 11 Projection of the potential energy surface for [M(unidentate A)(unidentate B)$_4$] on to the ϕ_D–ϕ_E plane (in degrees). The five faint contour lines are for successive 0.01 increments in X above the minima, and the five heavy contour lines are for successive 0.1 increments above the minima, at T_0 and T_2. $R = 0.2$. The positions of the trigonal bipyramids (T) and square pyramid (S) are shown

As one centre of repulsion is withdrawn from the central atom (Figure 9), the trigonal bipyramids T_1 and T_3 are stabilized, and the unique ligand occupies one of the axial sites of a trigonal bipyramid. Examples of this stereochemistry include complexes containing one uncharged ligand

and four charged ligands, as in the (1-adamantoxo)molybdenum(IV) complex $[Mo(OC_{10}H_{15})_4(Me_2NH)]$[37] and the osmium tetroxide–quinuclidine complex $[Os\{N(CH_2CH_2)_3CH\}O_4]$.[38]

For one effective bond length shorter than the other four, $R = 0.8$ (Figure 10), it is the trigonal bipyramids T_0 and T_2 that are stabilized, with the unique ligand in the equatorial plane. These trigonal bipyramids are connected by the square pyramid S_2, in which the unique ligand occupies the apical site. As R is further decreased, the minima corresponding to T_0 and T_2 move closer together until at $R = 0.7$ they coalesce to form the square pyramid S_2 as the sole minimum on the potential energy surface. The equatorially substituted trigonal bipyramid is found in transition metal complexes containing one charged ligand and four uncharged ligands, as in $[NiBr(PMe_3)_4](BF_4)$[39] and $[Ni(CH_3)(PMe_3)_4](BPh_4)$.[40] This is also found for $[MoO(OC_4F_9)_4]$,[41] although the dominant stereochemistry for monooxo complexes is the axially substituted square pyramid, examples including $[ReOCl_4]$ and $(Ph_4As)[MOCl_4]$ (M = Cr, Mo, Re), as well as the nitrido complexes $(Ph_4As)[MNCl_4]$ (M = Mo, Re, Ru, Os) and the thiohalide $[WSCl_4]$.[4] On reduction to $R = 0.4$, the minimum due to the S_2 square pyramid again divides into two minima corresponding to a return to T_0 and T_2, which move further apart as R is decreased. The structures of Rb[Bi(lone pair)$(SCN)_4$][42] and [Te(lone pair)$(Ph)_4$]$\cdot \frac{1}{8}C_6H_6$[43] can be considered to have this trigonal bipyramidal structure if it is assumed that the lone pair of electrons occupies an equatorial site. The detailed bond angles imply R(lone pair/ligand) ≈ 0.2. The lone pair of electrons has been experimentally observed in the closely related [Te(lone pair)Cl_2Me_2].[44]

2.2.1.2 [M(unidentate A)$_2$(unidentate B)$_3$]

The description of the general stereochemistry is the same as that used for [M(unidentate)$_5$] and [M(unidentate A)(unidentate B)$_4$] (Figure 6). Two ligands lie on the mirror plane with M—D = M—E = R, the remaining effective bond lengths being defined as unity.

The potential energy surface calculated for $R = 1.2$ is shown in Figure 12 and should be compared with Figure 7 calculated for $R = 1.0$, and Figure 8. It can be seen that stereochemically T_1 is stabilized, with the two extended bonds at the apices of a trigonal bipyramid. Conversely, as R is decreased to 0.8 (Figure 13), it is the trigonal bipyramid T_0 that is stabilized, with the two shorter effective bond lengths in equatorial sites. As R is decreased even further, the repulsion between these two contracted bonds becomes the dominant term, and the minimum deepens and shifts so that there is a continuous change in stereochemistry from T_0, through the square pyramid S_1 with the pair of substituents in basal sites, to T_1 in which the pair of ligands again occupy the two axial sites of a trigonal bipyramid.

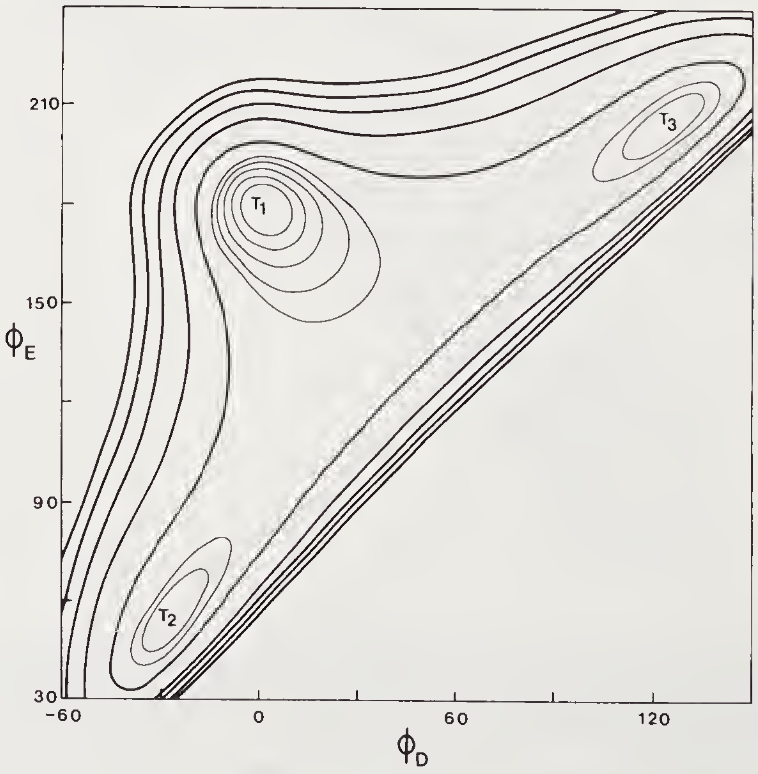

Figure 12 Projection of the potential energy surface for [M(unidentate A)$_2$(unidentate B)$_3$] on to the ϕ_D–ϕ_E plane (in degrees). The five faint contour lines are for successive 0.01 increments in X above the minimum, and the five heavy contour lines are for successive 0.1 increments above the minimum, at T_1. $R = 1.2$. The positions of the trigonal bipyramids (T) are shown

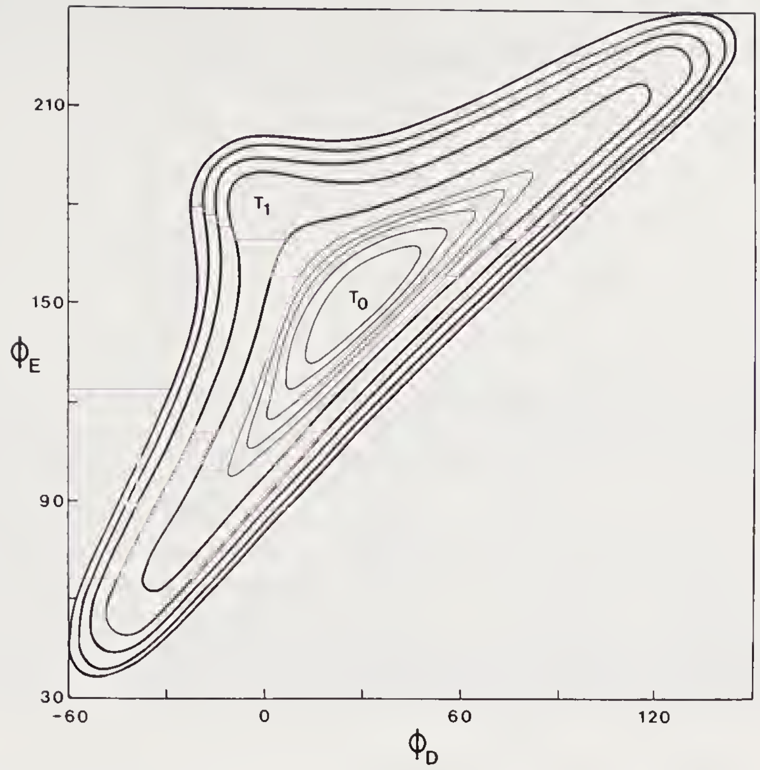

Figure 13 Projection of the potential energy surface for [M(unidentate A)$_2$(unidentate B)$_3$] on to the ϕ_D–ϕ_E plane (in degrees). The five faint contour lines are for successive 0.01 increments in X above the minimum, and the five heavy contour lines are for successive 0.1 increments above the minimum, at T_0. $R = 0.8$. The positions of the trigonal bipyramids (T) are shown

These structural predictions are followed in real molecules. For transition metal complexes containing two uncharged and three charged ligands, [M^{III}(ligand)$_2Cl_3$] and [M^{II}(ligand)$_2Cl_3$]$^-$ with R(ligand/Cl$^-$) $\approx$ 1.2, isomer T_1 is observed with the uncharged ligands axial and the chlorine atoms in the equatorial sites of a trigonal bipyramid. Examples include [Al(OC$_4$H$_8$)$_2$Cl$_3$],[45] [V(NMe$_3$)$_2$Cl$_3$],[46] [Fe(NC$_5$H$_4$CN)$_2$Cl$_3$],[47] [Co(PEt$_3$)$_2$Cl$_3$][48] and [Ni{N(CH$_2$CH$_2$)$_3$NMe}$_2$Cl$_3$]-(ClO$_4$).[49] The same factors also lead to this structure for (Ph$_4$P)[Mo(CO)$_2$(SC$_6$H$_2$Pr$_3$)$_3$].[50]

Atoms with two bonds of shorter effective bond length than the other three adopt the trigonal bipyramidal T_0 structure. Transition metal complexes [$M^{II}X_2$(ligand)$_3$] (X = Cl, Br, I) are of this type, with the two halogen atoms equatorial, typical examples being [CoBr$_2$(PF$_2$Ph)$_3$],[51] [CoBr$_2$(Ph$_2$PH)$_3$],[52] [NiBr$_2$(PMe$_3$)$_3$][53] and [NiI$_2${P(OMe)$_3$}$_3$].[54] The related bi(basal substituted) square pyramidal S_1 structure is observed for [RuCl$_2$(PPh$_3$)$_3$].[55]

The trifluoro complexes ClF$_3$[56] and XeF$_3^+$[57–59] are T-shaped, but can be considered to be of stereochemistry T_0 if lone pairs of electrons occupy two of the equatorial sites, completing a five-coordinate trigonal bipyramidal arrangement of electron pairs. The linear trihalide ions such as (I—I—I)$^-$ can likewise be regarded as being of stereochemistry T_1 with three non-bonding pairs of electrons in the three equatorial sites.[60–62]

2.2.2 [M(Bidentate)(Unidentate)$_3$]

The interconversions between the trigonal bipyramid and square pyramid described above for [M(unidentate)$_5$] involve relatively large changes in the length of the polyhedral edges, the limits being $3^{1/2}r = 1.73r$ for the edges linking the equatorial sites of a trigonal bipyramid, and $1.39r$ for the edges linking the basal sites of a square pyramid. The introduction of a chelating ligand of fixed normalized bite must substantially alter the form of the potential energy surface, and a more rigid and well-defined structure might be expected. The results of the calculations outlined below show that this expectation is not realized for bidentate ligands of low normalized bite where the potential energy surfaces are even flatter than those calculated for [M(unidentate)$_5$], and is only partially realized for those of high normalized bite.

The axes for the general stereochemistry are defined by placing the bidentate ligand symmetrically across the 'North Pole' at $\phi = 0$, with $\theta_A = 0$ and $\theta_B = 180°$ (Figure 14). The angles ϕ_i and θ_i are defined by Figure 14. The potential energy surfaces are shown projected on to the θ_C–θ_D plane (Figure 15), which most clearly separates the different stereochemistries. To prevent the overlap of several minima on these projections, due merely to an interchange of labels on the donor atoms, it is also convenient to impose the conditions $\phi_E \geqslant \phi_C$, $\phi_E \geqslant \phi_D$ and $\theta_D \leqslant \theta_E \leqslant (360°$

+ θ_C). For values of the normalized bite b less than 1.3, the single minimum consists of an extraordinarily long and level valley encompassing stereochemistries I and II (Figure 15).

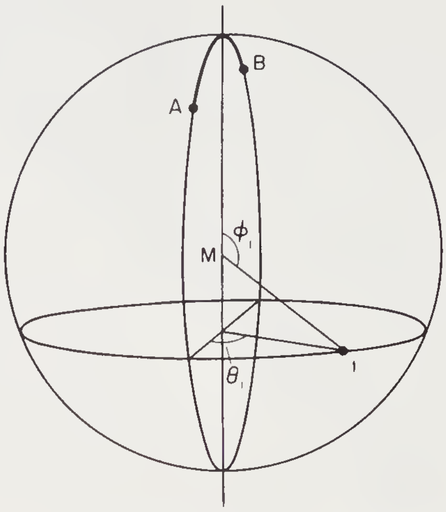

Figure 14 General stereochemistry of [M(bidentate)(unidentate)$_3$]. The coordinate system used to define the positions of the unidentate ligands C, D and E is indicated for the generalized unidentate ligand i

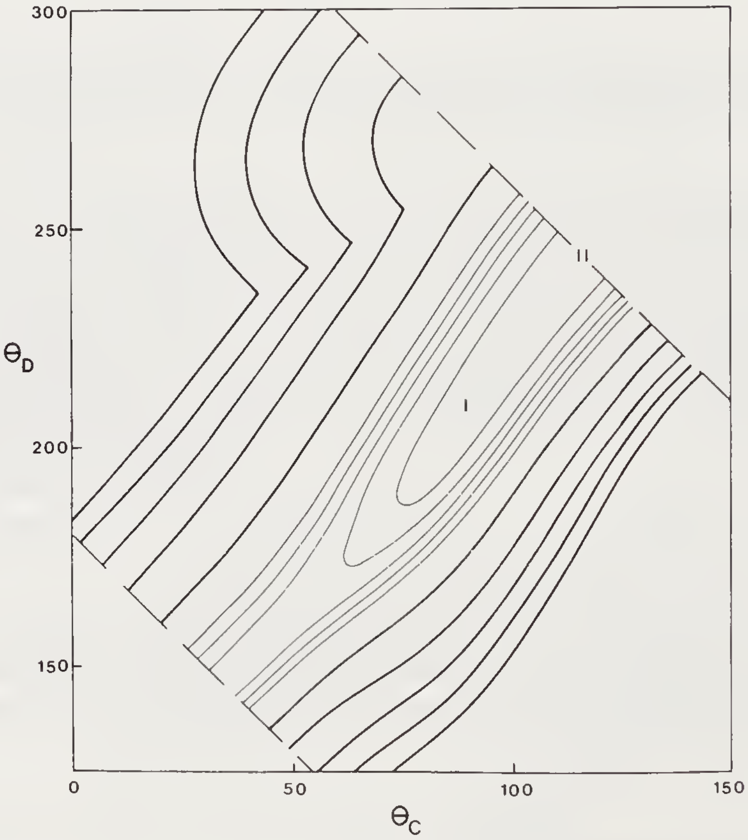

Figure 15 Projection of the potential energy surface of [M(bidentate)(unidentate)$_3$] on to the $\theta_C-\theta_D$ plane (in degrees). The five faint contour lines are for successive 0.01 increments in X above the minimum, and the five heavy contour lines are for successive 0.1 increments above the minimum, at II. b = 1.2. The positions of stereochemistries I and II are shown

In both stereochemistries I and II, $\phi_C \approx \phi_D \approx \phi_E \approx 120°$, and $|\theta_C-\theta_D| \approx |\theta_D-\theta_E| \approx |\theta_E-\theta_C| \approx 120°$, and the structures may be considered to consist of the bidentate ligand lying above and parallel to an approximately equilateral triangular arrangement of the three unidentate ligands (Figure 16). The interconversion between I and II can be readily envisaged as free spinning of the bidentate ligand above the triangular array of unidentate ligands.

In stereochemistry I, the bidentate ligand AB is parallel to the edge DE, and this stereochemistry may alternatively be pictured as a distorted square pyramid with the bidentate ligand spanning one of the basal edges. In stereochemistry II, the projection of the bidentate ligand AB is normal to the edge CD and this stereochemistry may be pictured as an irregular trigonal bipyramid.

The difference in energies between stereochemistries I and II is small and, for small or medium normalized bites, it can only be predicted that the observed stereochemistry will lie somewhere in the valley between these extremes. This is in agreement with the known structures. For example, $[Sb(O_2C_6H_4)Ph_3][Sb(O_2C_6H_4)Ph_3[H_2O)]$[63] has stereochemistry I, $[Sb(C_6H_4C_6H_4)Ph_3]$[64] and [Fe-

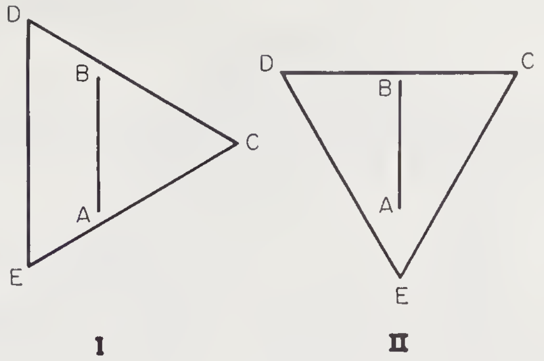

Figure 16 Stereochemistries I and II for [M(bidentate)(unidentate)$_3$] at low *b*

{$C_6H_4(AsMe_2)_2$}$(CO)_3$][65] have stereochemistry II, whereas [$Fe(Ph_2PCH_2PPh_2)(CO)_3$][66] and [$Sn(NO_3)(SnPh_3)_3$][67] have intermediate structures.

The very flat floor in the potential energy surface connecting stereochemistries I and II agrees with the observed non-rigid behaviour of a number of substituted iron carbonyls, [Fe(bidentate)$(CO)_3$].[66,68,69] However, more rigid behaviour is expected at higher normalized bites,[4] and it is therefore relevant that the ^{19}F NMR spectrum of $(CH_2)_4PF_3$ is temperature dependent, the molecule becoming rigid below −70 °C. On the other hand, $(CH_2)_5PF_3$, in which the normalized bite will be larger, shows no evidence of an intramolecular exchange process up to ~ 100 °C.[70]

2.2.3 [M(Bidentate)$_2$(Unidentate)]

Figure 17 defines the general stereochemistry, the bidentate ligands spanning the AB and CD edges. Two representative potential energy surfaces are shown in Figures 18 and 19, and should be compared with Figure 5, calculated for five unidentate ligands.

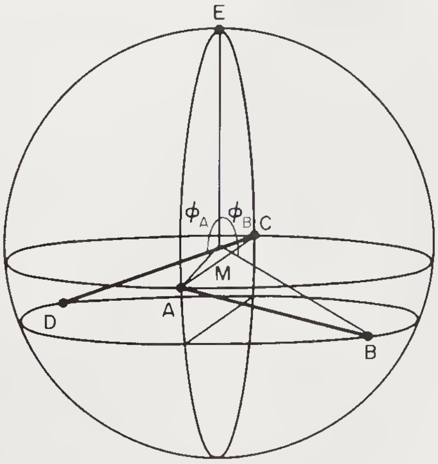

Figure 17 General stereochemistry for [M(bidentate)$_2$(unidentate)] with C_2 symmetry

For small values of the normalized bite (Figure 18), a single minimum on the potential energy surface occurs at $\phi_A = \phi_B$, corresponding to the square pyramid (or more correctly, a rectangular pyramid). As the normalized bite is progressively increased to $b = 1.28$, the minimum symmetrically splits into two minima corresponding to two equivalent irregular bipyramids. These minima progressively deepen and move further apart as the normalized bite is further increased (Figure 19).

Common examples of compounds of the type [M(bidentate)$_2$(unidentate)] range from [$P(O_2C_6H_4)_2X$], where X = halide, alkyl, etc.[4] with normalized bites of ~1.42 and stereochemistries intermediate between a square pyramid and a trigonal bipyramid, to [$Fe(S_2CNR_2)_2X$],[4] $b \approx 1.23$, that are close to square pyramidal.

Superimposed on this effect of normalized bite upon stereochemistry is the effect due to the unidentate ligand having a different effective bond length to those of the bidentate ligands.[4] Thus compounds containing O^{2-} as the unidentate ligand are expected to have a structure close to a square pyramid even for large chelate rings, as is observed, for example, for [$V(MeCOCHCOMe)_2O$] ($b = 1.38$),[71,72] as well as for [$V(S_2CNEt_2)_2O$] ($b = 1.21$).[73]

The repulsion energy calculations also show that significant distortion with loss of the twofold axis is possible, particularly in the direction toward a square pyramid in which the unidentate ligand now occupies a basal site.[4] Such distortions are frequently observed, particularly for ions such as copper(II) and iridium(I).[4]

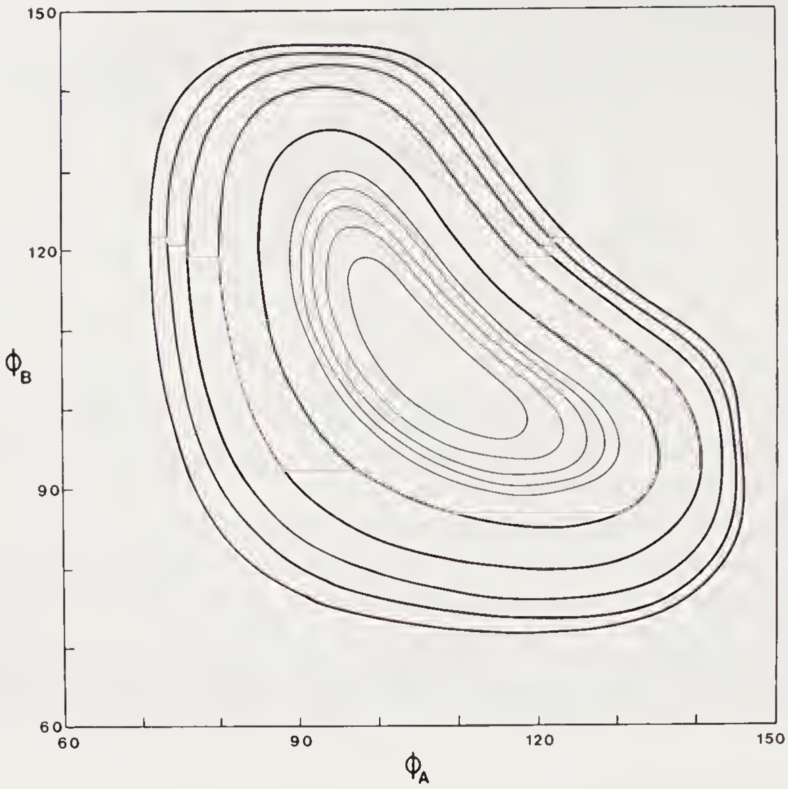

Figure 18 Projection of the potential energy surface for [M(bidentate)$_2$(unidentate)] on to the ϕ_A–ϕ_B plane (in degrees). The five faint contour lines are for successive 0.01 increments in X above the minimum, and the five heavy contour lines are for successive 0.1 increments above the minimum. b = 1.2

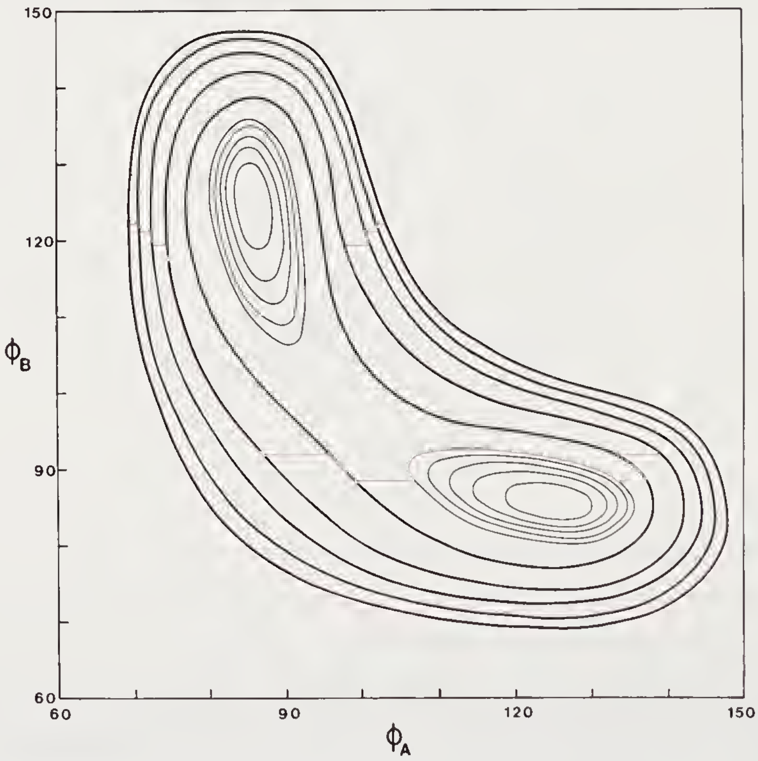

Figure 19 Projection of the potential energy surface for [M(bidentate)$_2$(unidentate)] on to the ϕ_A–ϕ_B plane (in degrees). The five faint contour lines are for successive 0.01 increments in X above the minima, and the five heavy contour lines are for successive 0.1 increments above the minima. b = 1.5

A number of compounds of the *p*-block elements containing two bidentate ligands can be considered to be five-coordinate and trigonal bipyramidal if a non-bonding pair of electrons occupies one of the equatorial sites, for example [Sn(S$_2$CNR$_2$)$_2$(lone pair)] and [Pb(RCOCHCOR)$_2$(lone pair)].[4] The greater repulsion observed from this line pair implies *R*(lone pair/bidentate) values of 0.6 for sulfur(IV) compounds, decreasing to ~0.4 for selenium(IV) and ~0.2 for tellurium(IV), antimony(III), tin(II) and lead(II).[4]

As expected from the calculated potential energy surfaces, the barriers to intramolecular rearrangement are generally higher for [M(bidentate)$_2$(unidentate)] complexes than for [M(unidentate)$_5$] complexes.[74–77]

2.3 SIX-COORDINATE COMPOUNDS

2.3.1 [M(Unidentate)$_6$]

The octahedron is the dominant stereochemistry for complexes containing six unidentate ligands. Nevertheless, significant distortions are observed when there are different types of ligand.

2.3.1.1 [M(unidentate A)(unidentate B)$_5$]

The general stereochemistry for octahedral molecules containing one ligand different to the other five is shown in Figure 20. The effective bond length to the unique ligand A lying on the fourfold axis is R, the other five metal–ligand bond lengths being defined as unity. As R is decreased from 1.0, the increase in AMB and decrease in BMF (Figure 21) increases the repulsion experienced by atom F relative to atom B (Figure 22). It is therefore expected that the bond *trans* to the unique ligand will be longer than the four *cis* bonds. However, it is important to note that at much lower values, $R < 0.4$, the opposite *trans* influence is expected, $Y_F/Y_B < 1.0$.

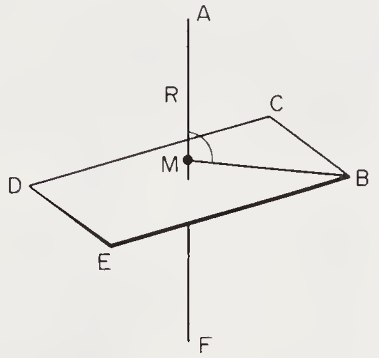

Figure 20 General stereochemistry for [M(unidentate A)(unidentate B)$_5$]

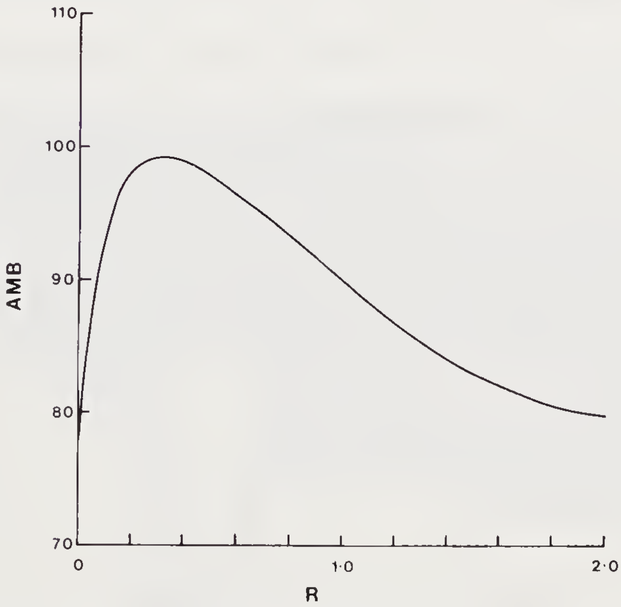

Figure 21 Bond angles (degrees) for [M(unidentate A)(unidentate B)$_5$], as a function of effective bond length ratio R

Experimental bond angles AMB, the corresponding R(A/B) values and the length of the *trans* metal–ligand bond relative to the length of the *cis* metal–ligand bonds, (M—F)/(M—B), for a selection of compounds, are collected in Table 9.

For nitrido, oxo and thiohalide complexes $[MNX_5]^{x-}$, $[MOX_5]^{x-}$ and $[MSX_5]^{x-}$, the NMX, OMX and SMX bond angles of about 95° correspond to $R(N^{3-}/X^-)$, $R(O^{2-}/X^-)$ and $R(S^{2-}/X^-)$ values of about 0.7. In these nitrido, oxo and thio complexes the predicted large weakening of the bond *trans* to the N^{3-} or O^{2-} group is observed, this bond being about 10% longer than the four *cis* metal–ligand bonds. Electron diffraction and microwave studies[89] on [IOF$_5$] yield structural parameters similar to those obtained for the above transition metal complexes:

$$OIF = 98.0°, (I—F)_{trans}/(I—F)_{cis} = 1.03, R(O/F) = 0.50$$

As expected, AMB angles of less than 90° are observed for [M(uncharged ligand)X$_5$]. For example, the $[M(H_2O)Cl_5]^{x-}$ complexes have OMCl angles of 88° corresponding to $R(\text{ligand}/X^-)$

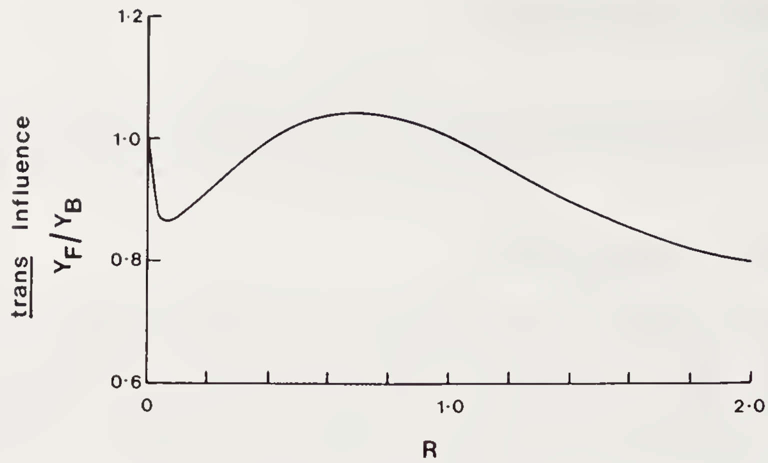

Figure 22 The *trans* influence, Y_F/Y_B, as a function of R for [M(unidentate A)(unidentate B)$_5$]

Table 9 Stereochemical Parameters for Some Octahedral Transition Metal Complexes, [M(unidentate A)(unidentate B)$_5$]

Complex	*AMB (°)*	*(M—F)/(M—B)*	*R(A/B)*	*Ref.*
$K_2[OsNCl_5]$	96.2	1.10	0.63	78
$(C_2H_{10}N_2)[VOF_5]$	98.2	1.17	0.48	79
$(N_2H_6)[NbOF_5]H_2O$	98.0	1.14	0.50	80
$K_2[NbOF_5]$	94.5	1.12	0.74	81
$K_2[MoOCl_5]$	95.6	1.08	0.67	82
$(Ph_3BzP)[WSCl_5]$	95.1	1.07	0.70	83
$[Cr(NH_3)_6][Mn(H_2O)Cl_5]$	87.6	0.98	1.15	84
$(NH_4)_2[Fe(H_2O)Cl_5]$	87.6	0.98	1.15	85
$(H_3O)_2[Fe(H_2O)Cl_5]$	88.3	0.98	1.10	86
$(NH_4)_2[Mo(H_2O)Cl_5]$	89.1	0.99	1.06	87
$(NH_4)_2[Rh(H_2O)Cl_5]$	89.6	0.98	1.03	88

= 1.1. As predicted, the *trans* M—X bond is now shorter than the four *cis* M—X bonds, $(M-X)_{trans}/(M-X)_{cis} = 0.98$.

A particularly important type of complex is $[M(\text{lone pair})(\text{unidentate})_5]^{x\pm}$. The series $[SbF_5(\text{lone pair})]^{2-}$,[90] $[TeF_5(\text{lone pair})]^{-}$,[91,92] $[IF_5(\text{lone pair})]$[93,94] and $[XeF_5(\text{lone pair})]^{+}$[95–98] have the expected square pyramidal structure, with a non-bonding pair of electrons presumed to occupy the sixth octahedral site. The structures are grossly distorted, the (lone pair)—M—F angles of ~ 100° corresponding to R(lone pair/F) ≈ 0.3. In contrast to the nitrido, oxo and thio complexes above, the *trans* M—F bond is now *shorter* than the *cis* M—F bond, (M—F)/(M—B) = 0.96, this behaviour being in complete agreement with the predictions made above.

2.3.1.2 [M(unidentate A)$_2$(unidentate B)$_4$]

(i) The theoretical stereochemistries

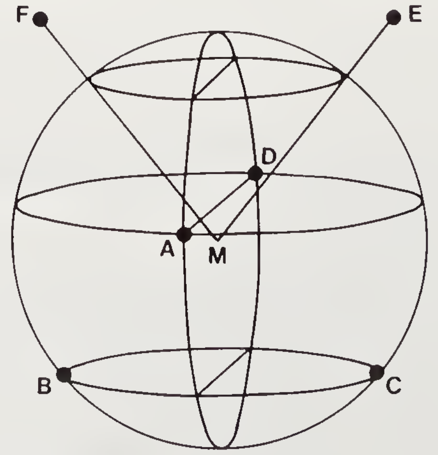

Figure 23 General stereochemistry for [M(unidentate A)$_2$(unidentate B)$_4$]. The ϕ angular coordinates are defined as the angles between the metal–ligand bonds and the twofold axis passing through the metal atom M and the midpoint of EF. The θ angular coordinates are defined relative to $\theta_E = 90°$ and $\theta_F = -90°$

The general stereochemistry for complexes of the type [M(unidentate A)$_2$(unidentate B)$_4$] is shown in Figure 23. The M—A, M—B, M—C and M—D effective bond lengths are defined as unity, and the M—E and M—F effective bond lengths are defined as R, the axes being defined so that $\phi_E = \phi_F$, $\theta_E = 90°$, and $\theta_F = -90°$.

The potential energy surface is shown projected on to the $\theta_A-\theta_B$ plane in Figures 24a and 24b, calculated for six equal metal–ligand bonds, $R = 1.0$. The deep minima at $\theta_A = 0$, $\theta_B = -90°$, and at $\theta_A = 90°$, $\theta_B = 0$, correspond to the *cis* octahedron, whereas the equally deep minimum at $\theta_A = 0$, $\theta_B = 0$ corresponds to the *trans* octahedron. These three minima are connected *via* high saddles corresponding to two of the three possible disubstituted trigonal prisms.

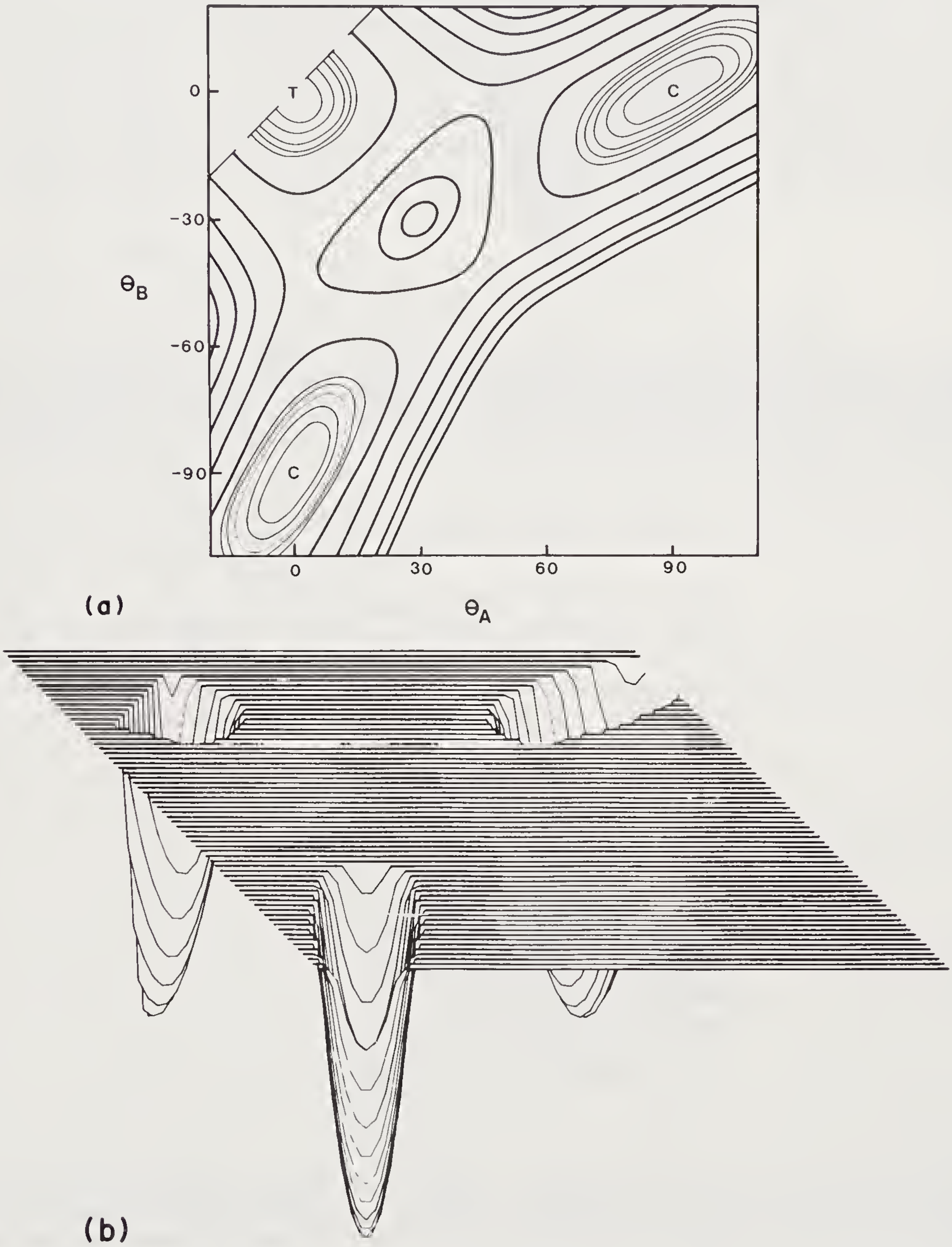

Figure 24 (a) Projection of the potential energy surface for [M(unidentate A)$_2$(unidentate B)$_4$] on to the $\theta_A-\theta_B$ plane (in degrees). The five faint contour lines are for successive 0.02 increments in X above the minima, and the five heavy contour lines are for successive 0.2 increments above the minima, at C and T. $R = 1.0$. The positions of the *cis* (C) and *trans* isomers (T) are shown. (b) As in (a), but with truncation at $X = 0.1$

Reducing R to 0.7 results in the *trans* octahedral structure existing as an even deeper minimum (Figure 25). Conversely, increasing R to 1.5 stabilizes the *cis* structure and, in addition, results in a much flatter potential energy surface (Figure 26). It should be noted that a *cis* to *trans* interconversion, or a *cis* to *trans* to *cis* interconversion, is possible, but not a direct *cis* to *cis* interconversion.

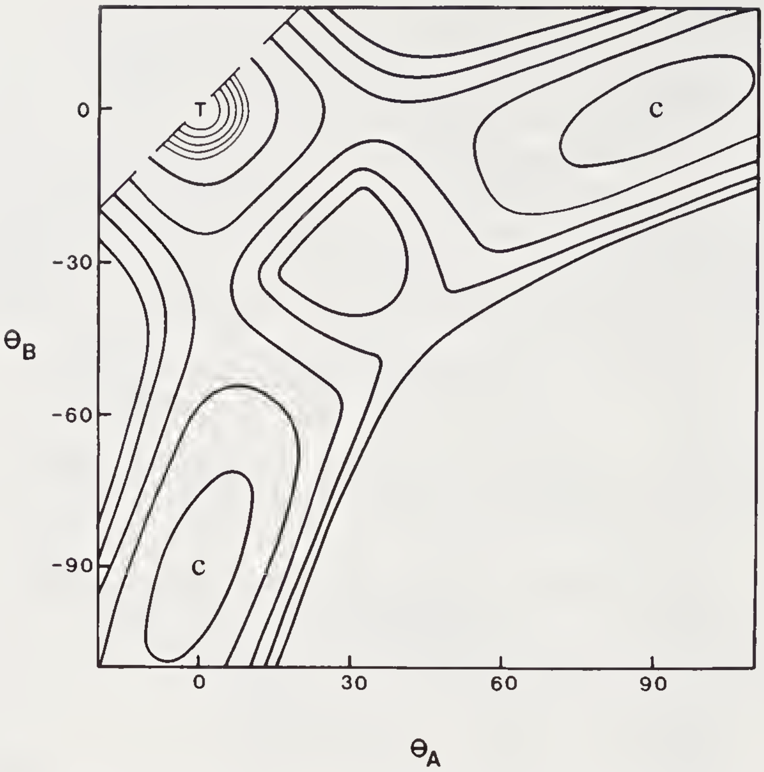

Figure 25 Projection of the potential energy surface for [M(unidentate A)$_2$(unidentate B)$_4$] on to the θ_A-θ_B plane (in degrees). The five faint contour lines are for successive 0.02 increments in X above the minimum, and the five heavy contour lines are for successive 0.2 increments above the minimum, at T. R = 0.7. The positions of the *cis* (C) and *trans* isomers (T) are shown

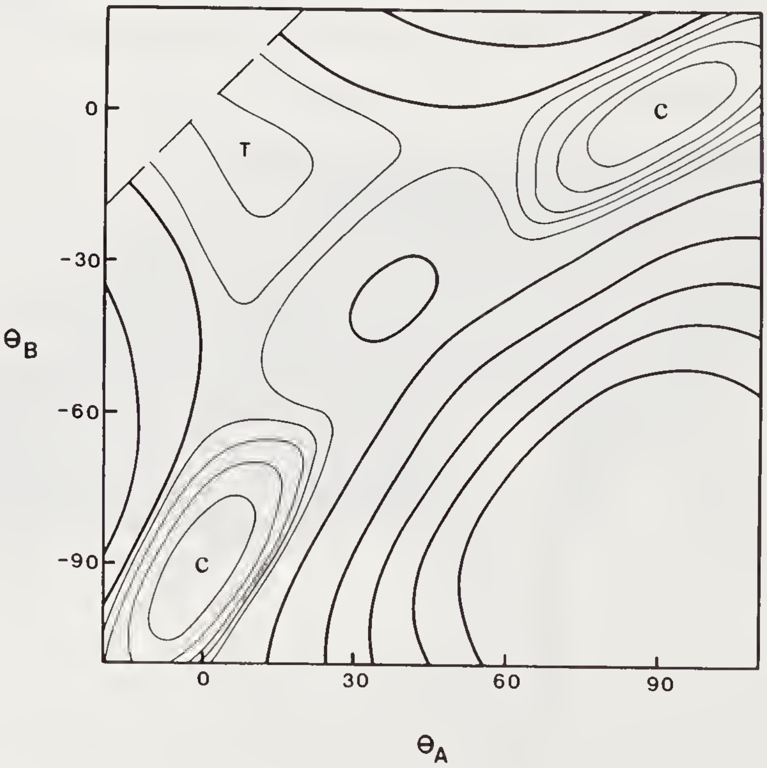

Figure 26 Projection of the potential energy surface for [M(unidentate A)$_2$(unidentate B)$_4$] on to the θ_A–θ_B plane (in degrees). The five faint contour lines are for successive 0.02 increments in X above the minima, and the five heavy contour lines are for successive 0.2 increments above the minima, at C. R = 1.5. The positions of the *cis* (C) and *trans* isomers (T) are shown

(ii) Comparison with experiment

For $R \approx 0.8-1.4$, the *cis* and *trans* structures are of comparable stability, and both structures would be expected. Indeed, the ability to form both these octahedral isomers has been recognized since the beginning of coordination chemistry.[99]

The *trans* structure is expected for $R < \sim 0.7$ (Figure 25), the two important experimental cases being [M(lone pair)$_2$(unidentate)$_4$] and [MO$_2$(unidentate)$_4$]. Compounds containing two non-bonding pairs of electrons and four unidentate ligands are invariably observed to be square planar, with a presumed *trans* arrangement of the non-bonding electron pairs completing the octahedron. Examples include $[\mathrm{Te^{II}(ligand)_4(lone\ pair)_2}]^{2+}$,[100–103] $[\mathrm{I^{III}Cl_4(lone\ pair)_2}]^{-}$[104,105] and $[\mathrm{Xe^{IV}F_4(lone\ pair)_2}]$.[106–109] Uranyl complexes $[\mathrm{UO_2X_4}]^{2-}$ have only been observed as the *trans* isomer,[110–112] other examples of *trans* dioxo complexes being $[\mathrm{ReO_2(C_5H_5N)_4}]\mathrm{Cl{\cdot}2H_2O}$,[113] $\mathrm{K_3[ReO_2(CN)_4]}$[114,115] and $\mathrm{NaK_3[MoO_2(CN)_4]{\cdot}6H_2O}$.[116] However, complexes with more complex stoichiometry, that is containing two different unidentate ligands in addition to $\mathrm{O^{2-}}$, are known as both *cis* and *trans* isomers.

In agreement with predictions made from the potential energy surfaces, intramolecular rearrangements are restricted to compounds which have two long effective bond lengths, and four short effective bond lengths. The rearrangement of *cis*-$[\mathrm{M(ER_3)_2(CO)_4}]$ (where M = Fe, Ru, Os; E = Si, Ge, Sn, Pb; R = alkyl, Ph, Cl) has been studied in some detail.[117–120] Detailed ^{13}C NMR lineshape analysis shows that the CO scrambling proceeds by a *cis* to *trans* to *cis* isomerization process, the results not being consistent with a *cis* to *cis* process, in agreement with the potential energy surface shown in Figure 26. The intramolecular isomerization of *cis*-$[\mathrm{Mo(PBu_3)_2(CO)_4}]$ in tetrachloroethylene at 65–80 °C has been examined by studying the C—O stretching vibration in the infrared.[121] It was noted that there was no exchange between the two pairs of carbonyl groups prior to formation of the *trans* isomer, again showing the absence of the direct *cis* to *cis* process.

(iii) Copper(II) complexes

Octahedral compounds with an odd number of electrons in the e_g orbitals, for example manganese(III) ($t^3_{2g}e^1_g$) and copper(II) ($t^6_{2g}e^3_g$), are often observed to be distorted.

Complexes of the type $[\mathrm{Cu(ligand)_6}]^{x\pm}$ are relatively rare, being restricted to those where the ligand is $\mathrm{H_2O}$, $\mathrm{OH^-}$, $\mathrm{NH_3}$, $\mathrm{NO_2^-}$ and a few organic molecules. The imidazole complex $[\mathrm{Cu(C_3H_4N_2)_6}](\mathrm{NO_3})_2$[122] is tetragonally elongated, two *trans* copper–nitrogen bonds being 28% longer than the other four. This is in contrast to the cobalt,[123] nickel,[124] and cadmium[125] analogues which have regular octahedral structures. The 2-pyridone complex $[\mathrm{Cu(C_5H_5NO)_6}](\mathrm{ClO_4})_2$ similarly has two *trans* copper–oxygen bonds 31% longer than the other four.[126] In these cases the two *trans* ligands have clearly been 'pushed back' by some non-bonding electron density each side of the plane, that is, in the copper d_{z^2} orbital.

In contrast, the pyridine 1-oxide complexes $[\mathrm{Cu(C_5H_5NO)_6}](\mathrm{ClO_4})_2$[127,128] and $[\mathrm{Cu(C_5H_5NO)_6}](\mathrm{BF_4})_2$[127] have regular octahedral structures, with six equal copper–oxygen bond lengths. However, these X-ray results are still consistent with the idea that each static $[\mathrm{Cu(C_5H_5NO)_6}]^{2+}$ ion is tetragonally distorted if it is assumed that there is either a rapid oscillation between the three mutually perpendicular tetragonal distortions at each cation site, or a random orientation of the distorted cations over all sites in the crystal.

The stereochemistry of $[\mathrm{Cu(NO_2)_6}]^{4-}$ has been extensively studied, and may be tetragonally compressed, tetragonally elongated or regular octahedral, depending upon the choice of cations and the temperature.[129–133] For example, $\mathrm{K_2Pb[Cu(NO_2)_6]}$ has a small tetragonal compression at 3 °C (two *trans* Cu—N bonds 5% shorter than the other four), but is regular octahedral above 7 °C. On the other hand, the cobalt[134] and nickel[132] analogues are regular octahedral.

Associated with these distortions is the tendency of copper(II) to form complexes of stoichiometry $[\mathrm{Cu(unidentate\ A)_2(unidentate\ B)_4}]^{x\pm}$. These complexes typically have a large tetragonal elongation, and there is a continuous series from *trans* octahedral complexes to square planar $[\mathrm{Cu(unidentate\ B)_4}]$ complexes. It must be remembered that in any square planar molecule in the solid state, or in solution, the very open spaces outside the square faces inevitably allow the approach of other atoms, for example anions, other square planar molecules, or solvent molecules, which can sometimes be regarded as forming one (as in five-coordinate copper(II) complexes) or two additional weak bonds. It may be noted that repulsion energy calculations show that the two unidentate A ligands need only approach to $R(\mathrm{A/B}) \leqslant 1.4$ to enforce a square planar structure. However, even genuine four-coordinate copper(II) complexes are not necessarily tetrahedral. For example, $[\mathrm{CuCl_4}]^{2-}$ is most commonly a squashed tetrahedron, although it has also been observed as a regular tetrahedron and as a square plane. In Section 2.1.6 it was noted that the squashing of a tetrahedron into a square requires only a small amount of electron density on each side of the metal atom, for example from an electron pair in the d_{z^2} orbital.

2.3.2 [M(Bidentate)$_2$(Unidentate)$_2$]

2.3.2.1 *Relative stability of* cis *and* trans *octahedral complexes*

The two stereochemistries usually envisaged for complexes of the type $[\mathrm{M(bidentate)_2(unidentate)_2}]$ are the *cis* and *trans* octahedral structures (Figures 27a and 27b). It will be shown in more detail below that both these structures become significantly distorted for bidentate ligands of small normalized bite. It is sufficient to note at this stage that the *trans* octahedral structure distorts to form the skew-trapezoidal bipyramidal structure (Figures 27c and 27d).

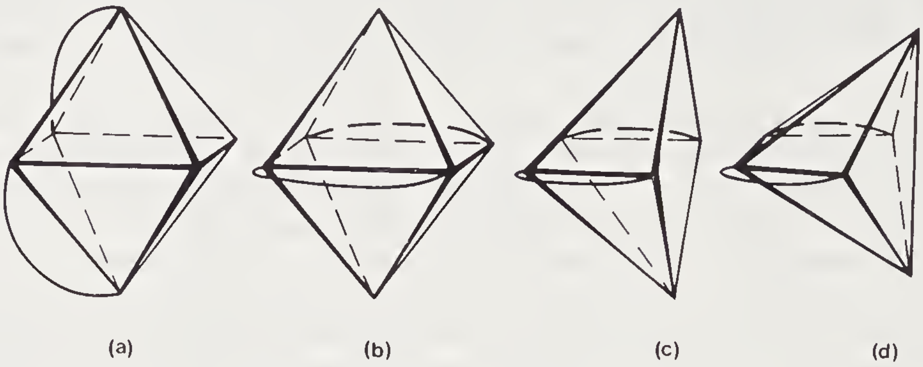

Figure 27 Stereochemistries of [M(bidentate)$_2$(unidentate)$_2$]: (a) *cis* octahedral; (b) *trans* octahedral; (c,d) skew-trapezoidal bipyramidal

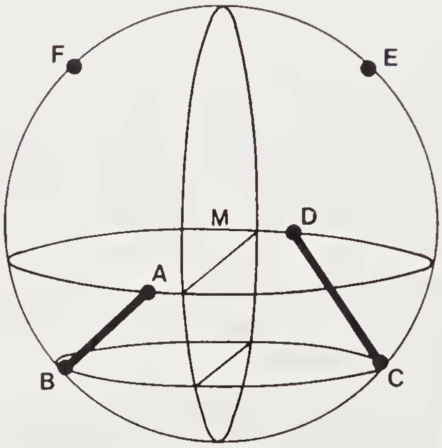

Figure 28 General stereochemistry for *cis*-[M(bidentate)$_2$(unidentate)$_2$]. The ϕ angular coordinates are defined as the angles between the metal–ligand bonds and the twofold axis passing through the metal atom M and the midpoint of EF. The θ angular coordinates are defined relative to $\theta_E = 90°$ and $\theta_F = -90°$

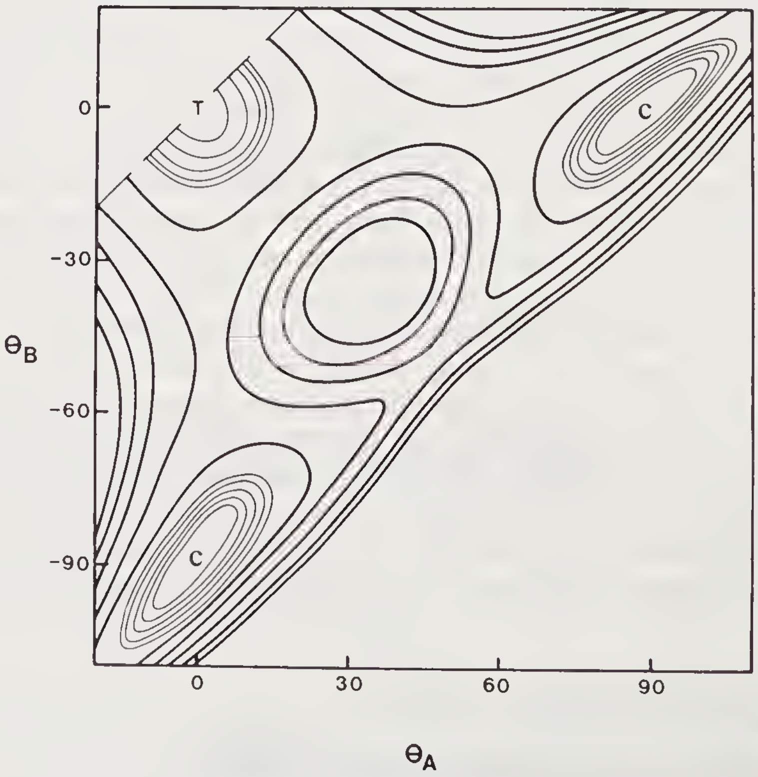

Figure 29 Projection of the potential energy surface for [M(bidentate)$_2$(unidentate)$_2$] on to the θ_A–θ_B plane (in degrees). The five faint contour lines are for successive 0.02 increments in X above the minima, and the five heavy contour lines are for successive 0.2 increments above the minima, at C. b = 1.4. The positions of the *cis* (C) and *trans* isomers (T) are shown

The general stereochemistry is shown in Figure 28, where AB and CD are the two bidentate ligands, and E and F the two unidentate ligands. A twofold axis passes through $\phi = 0$ and $\phi = 180°$, the θ coordinates being defined relative to $\theta_E = 90°$ and $\theta_F = -90°$.

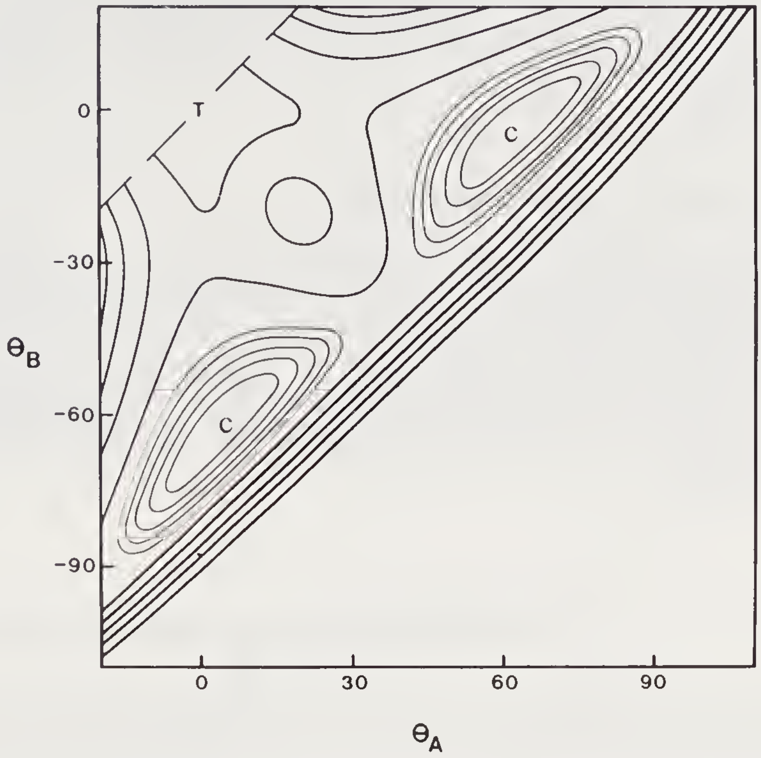

Figure 30 Projection of the potential energy surface for [M(bidentate)$_2$(unidentate)$_2$] on to the θ_A–θ_B plane (in degrees). The five faint contour lines are for successive 0.02 increments in X above the minima, and the five heavy contour lines are for successive 0.2 increments above the minima, at C. $b = 1.1$. The positions of the *cis* (C) and *trans* isomers (T) are shown

Typical potential energy surfaces projected on to the θ_A–θ_B plane are shown in Figures 29–31 and should be compared with the similar surface calculated for [M(unidentate A)$_2$(unidentate B)$_4$] (Figure 24). The angular distortion of the *cis* isomer as the normalized bite is reduced is evident in these Figures, and is discussed in more detail in the next section. At $b = 2^{1/2}$, both the *cis* and the *trans* structures have the same energy, but as the normalized bite is reduced the *cis* structure becomes significantly more stable than the *trans* structure (Figure 30), and below $b = 0.90$ the *trans* structure ceases to remain as a discrete minimum (Figure 31). However, the *trans* structure remains possible at low b when the effective bond length ratio, R(unidentate/bidentate) > 1.0.[135]

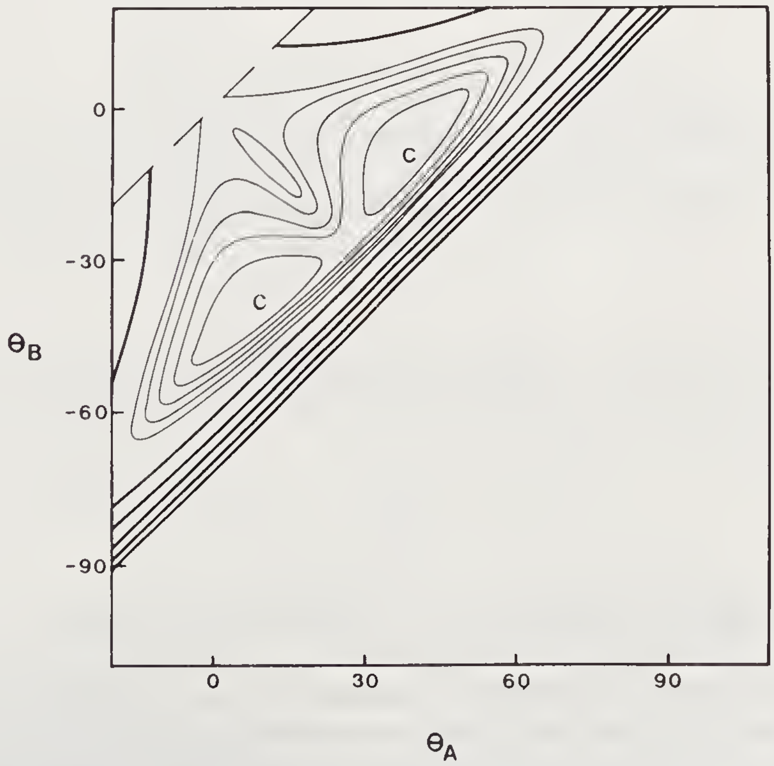

Figure 31 Projection of the potential energy surface for [M(bidentate)$_2$(unidentate)$_2$] on to the θ_A–θ_B plane (in degrees). The five faint contour lines are for successive 0.02 increments in X above the minima, and the five heavy contour lines are for successive 0.2 increments above the minima, corresponding to the *cis* isomer (C). $b = 0.8$

A survey[4] of all compounds having two identical and symmetrical bidentate ligands and two identical unidentate ligands, with known crystal structures, shows that for compounds with bidentate ligands having $b < \sim 1.3$, there are approximately an equal number of *cis* and *trans* structures. However, compounds with four-membered chelate rings and $b < \sim 1.2$ show a strong preference for the *cis* structure (Sections 2.3.2.2 and 2.3.2.3) with a small number of skew-trapezoidal bipyramidal structures (Section 2.3.2.4), in agreement with the results from the repulsion energy calculations.

2.3.2.2 Angular distortions in cis *octahedral complexes*

The angular coordinates of the *cis* isomer are shown in Figure 32, axes being defined by Figure 28. The variation with normalized bite is not as may have been intuitively expected. If decreasing b from the regular octahedral value of 1.414 merely resulted in atoms A and B moving uniformly toward one another, then θ_A would move to negative values, and θ_B would increase above −90 °C. However, Figure 32 shows that θ_A is predicted to *increase*, with a corresponding very large increase in θ_B. This distortion corresponds to a rotation of both bidentate ligands about the twofold axis to higher values of θ (Figure 33).

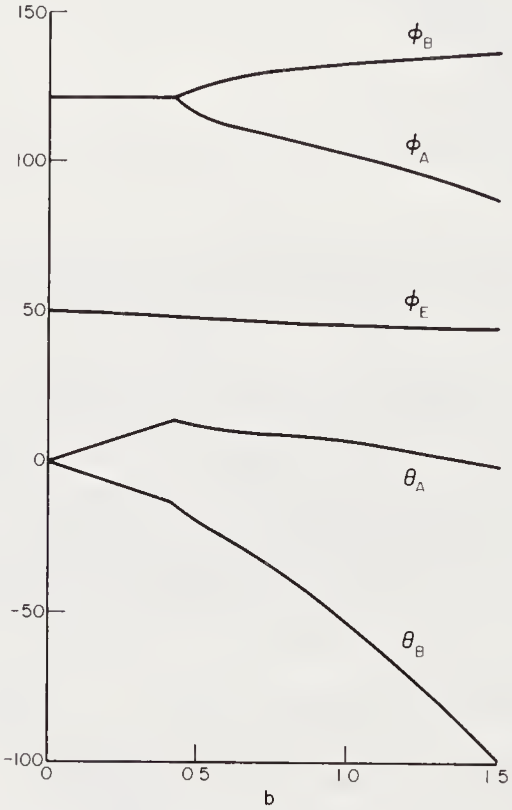

Figure 32 Angular coordinates (degrees) for *cis*-[M(bidentate)$_2$(unidentate)$_2$] as a function of normalized bite b

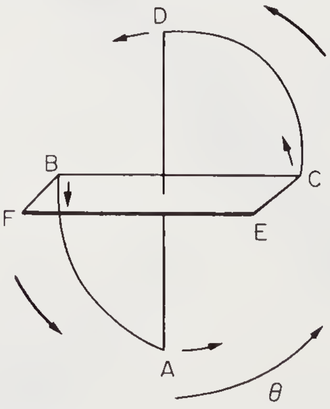

Figure 33 Angular distortions in *cis*-[M(bidentate)$_2$(unidentate)$_2$]

This increase in θ_A and θ_B is experimentally observed and is shown in Table 10, which is restricted to molecules with bidentate ligands that form four-membered chelate rings with small normalized bites. Exact agreement is not expected with Figure 32, which was calculated for R(unidentate/bidentate) = 1.0. Nevertheless, in all cases the largest distortion from the parameters of the regular octahedron is the increase in θ_B, whereas θ_A slightly *increases*.

Table 10 Angular Parameters (°) of Octahedral *cis*-[M(bidentate)$_2$(unidentate)$_2$] Containing Four-membered Chelate Rings

Complex	*b*	ϕ_A	ϕ_B	ϕ_E	θ_A	θ_B	*Ref.*
Regular octahedron	1.41	90	135	45	0	−90	
$[Co(NO_3)_2(Me_3PO)_2]$	0.96	101	138	53	−1	−53	136
$[Co(NO_3)_2\{(Me_2N)_3PO\}_2]$	0.96	100	139	54	1	−50	137
$[Co(O_2CMe)_2(N_2C_3H_3Me)_2]$	0.99	111	136	49	2	−65	138
$[Sn(S_2CNEt_2)_2Ph_2]$	1.11	103	140	51	5	−65	139
$[Mo(S_2CNMe_2)_2(N_2MePh)_2]$	1.12	99	141	54	6	−60	140
$[Mo(S_2CNMe_2)_3(N_2Ph_2)_2]\cdot Me_2CO$	1.12	99	141	54	7	−59	140
$[Mo(S_2CNPr_2)_2O_2]$	1.12	104	139	53	14	−59	141
$[Mo(S_2CNEt_2)_2O_2]$	1.13	106	140	57	15	−60	142
$[Mo(S_2CNEt_2)_2(NPh)_2]$	1.13	104	140	52	6	−64	143
$[Sn(S_2COEt)_2(SCSOEt)_2]$	1.14	103	136	46	0	−78	144
$[Sn(S_2COEt)_2I_2]$	1.14	102	139	49	5	−68	145
$[Sn(S_2COEt)_2Br_2]$	1.16	99	136	48	2	−69	145
$[Sn(S_2COEt)_2Cl_2]$	1.16	100	136	47	4	−68	146
$[Sn(S_2CNEt_2)_2(SCSNEt_2)_2]$	1.16	102	131	41	1	−73	147
$[Fe\{S_2CN(CH_2)_5\}_2(CO)_2]$	1.21	99	135	46	1	−77	148
$[Sn(S_2PEt_2)_2I_2]$	1.27	97	136	46	5	−75	149

2.3.2.3 *Bond-length distortions in* cis *octahedral complexes*

As the normalized bite of the bidentate ligand is reduced from 1.414, the A end of each ligand is associated with less repulsion than is the B end (Figure 34). It is therefore predicted that the bidentate ligand will be unsymmetrically coordinated, with the M—A bond being shorter than the M—B bond, the latter being *trans* to a unidentate ligand. This effect increases as *R*(unidentate/bidentate) decreases (Figure 34).

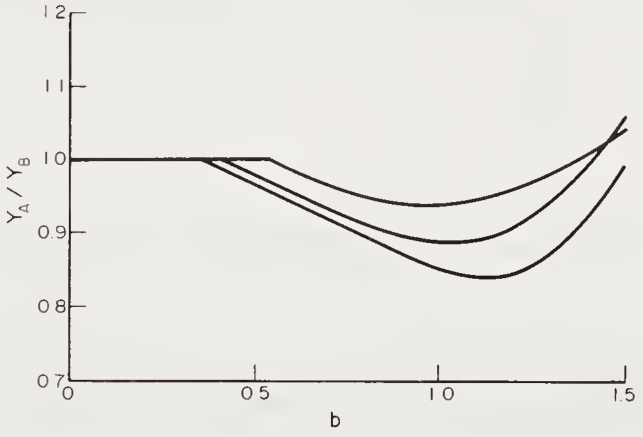

Figure 34 Ratio of individual atom-repulsion coefficients for the two ends of each bidentate ligand in *cis*-[M(bidentate)$_2$(unidentate)$_2$] as a function of normalized bite *b*. Upper curve, *R*(unidentate/bidentate) = 1.5; middle curve, *R*(unidentate/bidentate) = 1.0; lower curve, *R*(unidentate/bidentate) = 0.75

This predicted behaviour is experimentally observed, and is shown most clearly in compounds in which the unidentate ligand is O^{2-} (Table 11). The M—A bond, which is *cis* to both unidentate ligands, is about 9% shorter than the M—B bond. As expected, the effect is much smaller for unidentate ligands of lower charge,[135] a typical example being the unsymmetrical bonding of the nitrate group in $[Co(NO_3)_2(Me_3PO)_2]$, (M—A)/(M—B) = 0.98.

Table 11 Bond-length Ratios for *cis*-[M(bidentate)$_2$O$_2$]

Complex	*b*	*(M—A)/(M—B)*	*Ref.*
$[Mo(S_2CNPr_2)_2O_2]$	1.12	0.92	141
$[Mo(S_2CNEt_2)_2O_2]$	1.13	0.93	142
$(NH_4)_3[V(C_2O_4)_2O_2]\cdot 2H_2O$	1.23	0.90	150
$K_3[V(C_2O_4)_2O_2]\cdot 3H_2O$	1.23	0.91	151
$[Mo(MeCOCHCOMe)_2O_2]$	1.29	0.90	152
$[Mo(PhCOCHCOPh)_2O_2]$	1.29	0.92	153

2.3.2.4 *Distortion of the* trans *octahedral structure to the skew-trapezoidal bipyramidal structure*

Bidentate ligands that form five- or six-membered chelate rings and have relatively large normalized bites ($b \approx 1.2-1.5$) normally form undistorted *trans* structures. As the normalized bite is further decreased, however, repulsion energy calculations show that the rectangle formed by the two coplanar bidentate ligands becomes distorted and forms a planar trapezoid. The unidentate ligands are simultaneously skewed toward (Figure 27c), or even past (Figure 27d), the long edge of the trapezoid. Two mirror planes are retained throughout this distortion, and the stereochemistry is completely described by three angular parameters, the angles the metal–ligand bonds make with the twofold axis (Figure 35). The dependence of these parameters, ϕ_A, ϕ_B and ϕ_E, on the normalized bite is shown in Figure 36. This structure does not remain as a discrete minimum on the potential energy surface at very low values of the normalized bite, as indicated by the extent of the lines in Figure 36. The repulsion energy calculations also show that the distortion to the skew-trapezoidal bipyramidal structure commences at larger values of the normalized bite as R(unidentate/bidentate) decreases.

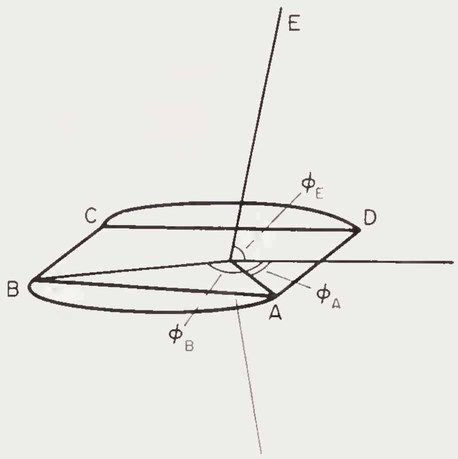

Figure 35 General stereochemistry for *trans* octahedral and skew-trapezoidal bipyramidal [M(bidentate)$_2$(unidentate)$_2$]

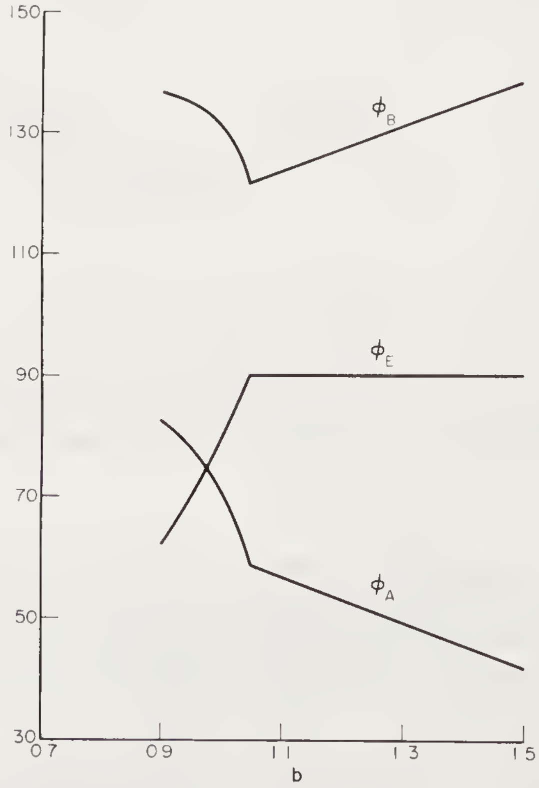

Figure 36 Angular coordinates (degrees) for *trans* octahedral and skew-trapezoidal bipyramidal [M(bidentate)$_2$(unidentate)$_2$] as a function of normalized bite *b*

The only examples of skew-trapezoidal bipyramidal structures found with two equivalent unidentate ligands and two symmetrical bidentate ligands are four tin complexes containing four-membered chelate rings. The detailed structural parameters are given in Table 12, and the trapezoids illustrated in Figure 37, together with [Sn(MeCOCHCOMe)$_2$Me$_2$] which has a larger normalized bite and an undistorted *trans* structure.[157]

Table 12 Stereochemical Parameters of Skew-trapezoidal Bipyramidal [$Sn(bidentate)_2R_2$] Complexes ($R = Me, Ph$)

Complex	*b*	ϕ_A	ϕ_B	ϕ_E	*(M—A)/(M—B)*	*Ref.*
[$Sn(NO_3)_2Me_2$]	0.92	88.1	142.6	71.8	1.19	154
[$Sn(S_2CNMe_2)_2Me_2$]	1.06	74.5	138.6	68	1.20	155
[$Sn(S_2PMe_2)_2Me_2$]	1.13	71.2	140.1	61.3	1.34	149
[$Sn\{S_2P(OEt_2)_2\}_2Ph_2$]	1.14	68.4	137.8	67.5	1.29	156

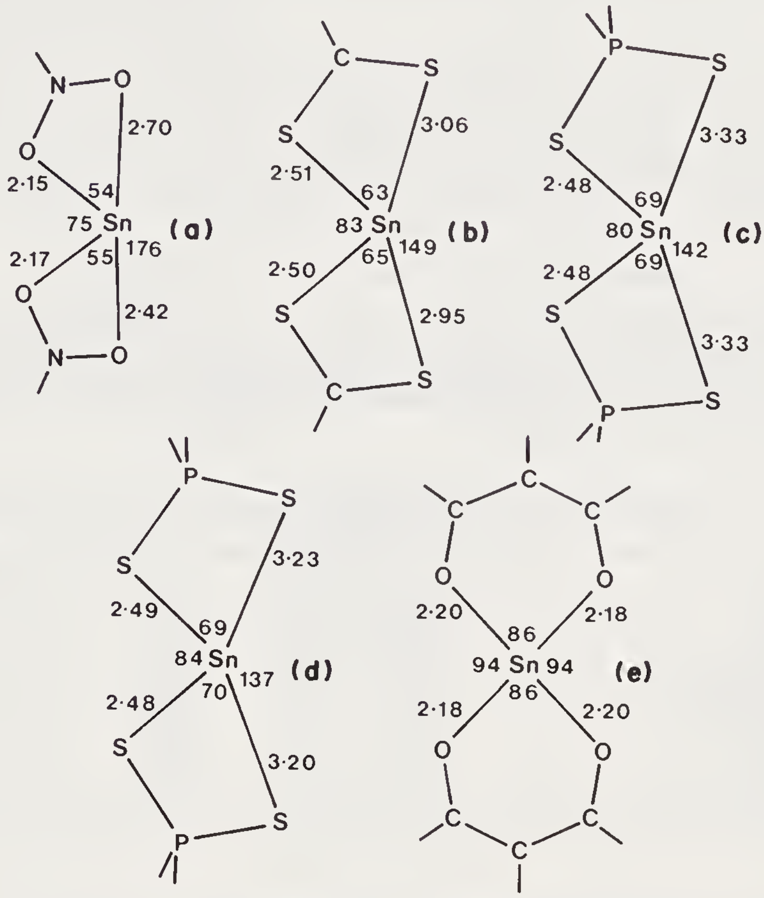

Figure 37 Geometries, degrees and Å, of the $Sn(bidentate)_2$ planes in: (a) [$Sn(NO_3)_2Me_2$]; (b) [$Sn(S_2CNMe_2)_2Me_2$]; (c) [$Sn(S_2PMe_2)_2Me_2$]; (d) [$Sn\{S_2P(OEt)_2\}_2Ph_2$]; (e) [$Sn(MeCOCHCOMe)_2Me_2$]

A notable feature of these complexes is the very unsymmetrical bonding of the bidentate ligands, the tin–ligand(A) bonds being 20–35% longer than the tin–ligand(B) bonds (Table 12 and Figure 37). This arises from the considerably greater repulsion energy associated with the A end of the bidentate ligand than with the B end (Figure 38).

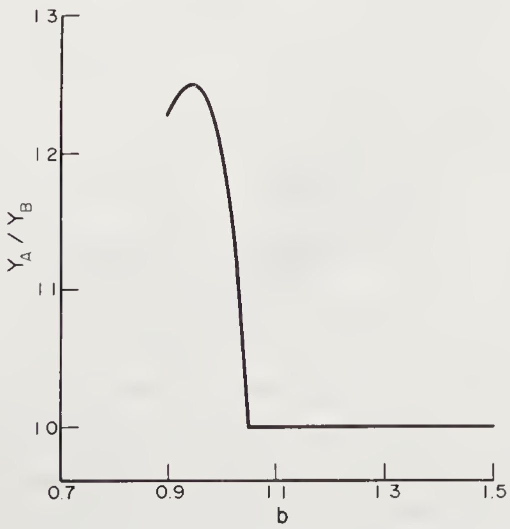

Figure 38 Ratio of individual atom-repulsion coefficients for the two ends of each bidentate ligand in *trans* octahedral and skew-trapezoidal bipyramidal [$M(bidentate)_2(unidentate)_2$] as a function of normalized bite *b*

2.3.2.5 *Bis(dithiochelate) complexes of selenium(II) and tellurium(II)*

The thiourea complexes $[Te^{II}\{SC(NH_2)_2\}_4]Cl_2$ and $[Te^{II}\{SC(NH_2)_2\}_4]Cl_2{\cdot}2H_2O$ have a square-planar arrangement of sulfur atoms about the tellurium atom (Section 2.3.1.2(ii)). Selenium(II) and tellurium(II) xanthates, dithiocarbamates and diselenocarbamates, on the other hand, have a planar trapezoid structure (see Figure 39 for typical dimensions). These compounds have bidentate ligands with normalized bites of $b = 1.0{-}1.2$ and can clearly be regarded as having skew-trapezoidal bipyramidal stereochemistry, with the *trans* apical sites being occupied by the two non-bonding pairs of electrons. It is important to note that one central atom–donor atom bond to each chelate is 10–20% longer than the other, as predicted in the previous section.

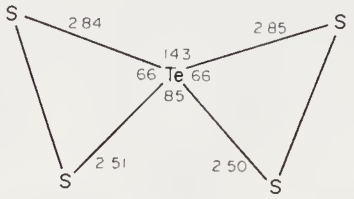

Figure 39 Geometries, degrees and Å, of $[Te(S_2COMe)_2]$

Detailed structural parameters are given in Table 13. On the other hand, the bidentate sulfur donor ligands in $[Te\{(SPPh_2)_2N\}_2]$ form six-membered chelate rings with large normalized bites, $b = 1.37$, and the complex has an undistorted planar rectangular structure, $\phi_A = 47.0°$, $\phi_B = 133.0°$, $(M{-}A)/(M{-}B) = 1.01$.[164]

Table 13 Stereochemical Parameters of Bis(dithiochelate) Complexes of Selenium(II) and Tellurium(II)

Complex	*b*	ϕ_A	ϕ_B	*(M—A)/(M—B)*	*Ref.*
$[Te(S_2COMe)_2]$	1.09	71.1	137.4	1.14	158
$[Te(S_2COEt)_2]$	1.09	72.2	138.2	1.16	159
$[Te\{S_2CN(C_4H_8O)\}_2]$	1.10	72.8	139.5	1.13	160
$[Se\{S_2CN(C_4H_8O)\}_2]$	1.15	67.5	137.7	1.21	161
$[Se(S_2CNEt_2)_2]$	1.15	65.7	136.2	1.18	162
$[Se(Se_2CNEt_2)_2]$	1.20	61.6	135.5	1.14	163

2.3.2.6 *Pentagonal pyramidal [M(bidentate)$_2$(unidentate A)(unidentate B)] complexes*

Compounds containing two bidentate ligands and two chemically similar unidentate ligands can exist as the usual *cis* and *trans* octahedral isomers, or as the skew-trapezoidal bipyramidal structure observed for bidentate ligands of small normalized bite. However, a different stereochemistry, which can be represented as a pentagonal pyramid, is found under the combined conditions of small normalized bite and a large difference between the natures of the two unidentate ligands.

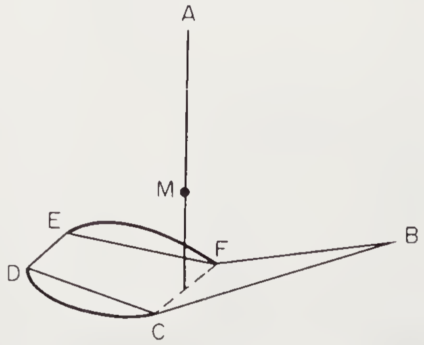

Figure 40 Pentagonal pyramidal [M(bidentate)$_2$(unidentate A)(unidentate B)]

The stereochemistry is shown in Figure 40. The two unidentate ligands lie on a mirror plane, the effective bond lengths being given by R_A and R_B respectively, the other four effective bond lengths being defined as unity. Repulsion energy calculations show that this structure is expected provided the normalized bite is less than about 0.9, and provided the difference $(R_B{-}R_A) > {\sim}0.4$. Both unidentate ligands lie on the same side of the CDEF plane, which distinguishes this stereochemistry from the skew-trapezoidal bipyramid where the two unidentate ligands lie on opposite sides of the trapezoid formed by the two chelate rings.

The known pentagonal pyramidal molecules are $[Cr(O_2)_2O(C_5H_5N)]$,[165] $(NH_4)[V(O_2)_2O(NH_3)]$[166] and $(NH_4)_4[\{V(O_2)_2O\}_2O]$,[167] where two peroxide groups behave as bidentate ligands with $b = 0.77$, and the unidentate A ligand is O^{2-}. These structures are in contrast to those of related complexes containing bidentate ligands of larger normalized bite such as $(NH_4)_2[V(C_2O_4)_2O(H_2O)]$[168] and $[V(oxine)_2O(OPr)]$[169] ($b = 1.24$), which have conventional *cis* octahedral structures.

2.3.3 [M(Bidentate)$_3$]

2.3.3.1 The theoretical stereochemistry

Repulsion energy calculations show that the stereochemistry corresponding to the single minimum on any potential energy surface always contains a threefold axis. The stereochemistry is, therefore, completely defined by the normalized bite of the bidentate ligand b and the angle of twist θ between the upper and lower triangular faces (Figure 41). The regular octahedron corresponds to $\theta = 30°$ and $b = 2^{1/2}$. The trigonal prism is the eclipsed arrangement with $\theta = 0°$.

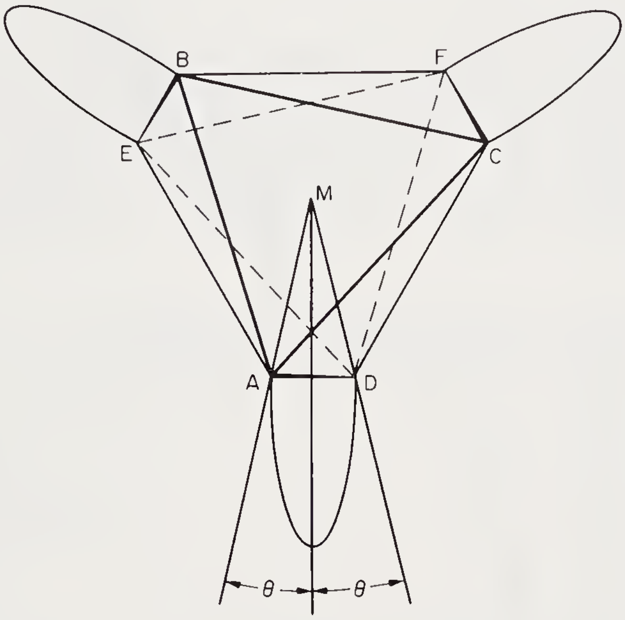

Figure 41 General stereochemistry for [M(bidentate)$_3$]

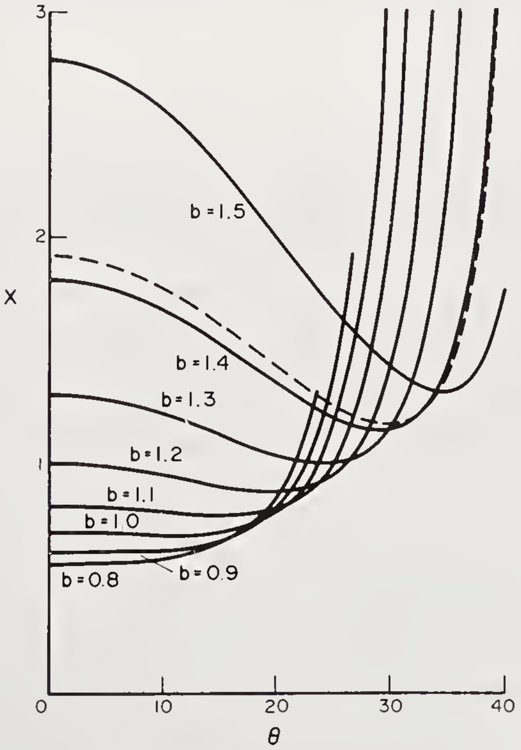

Figure 42 Repulsion-energy coefficient X for [M(bidentate)$_3$] as a function of angle of twist θ (degrees) and normalized bite b. Broken line corresponds to $b = 2^{1/2}$

The repulsion energy coefficient X is shown as a function of the angle of twist θ and the normalized bite b in Figure 42. For normalized bites of $b = 2^{1/2} = 1.414$, the regular octahedron at $\theta = 30°$ exists as a deep minimum. The energy difference between this minimum and the maximum at $\theta = 0°$ is the activation energy for racemization of these optically active compounds by this simple twist mechanism. As the normalized bite of the bidentate ligands is progressively decreased, two important effects are observed. Firstly, the upper triangular face ABC of the octahedron is brought into a more eclipsed configuration relative to the lower triangular face DEF, and the energy minimum moves to lower values of θ. The location of this minimum, θ_{min}, is plotted as a function of b in Figure 43. Secondly, the decrease in b causes the potential energy surface to become much shallower, resulting in structures which are easier to distort and which have lower activation energies for racemization.

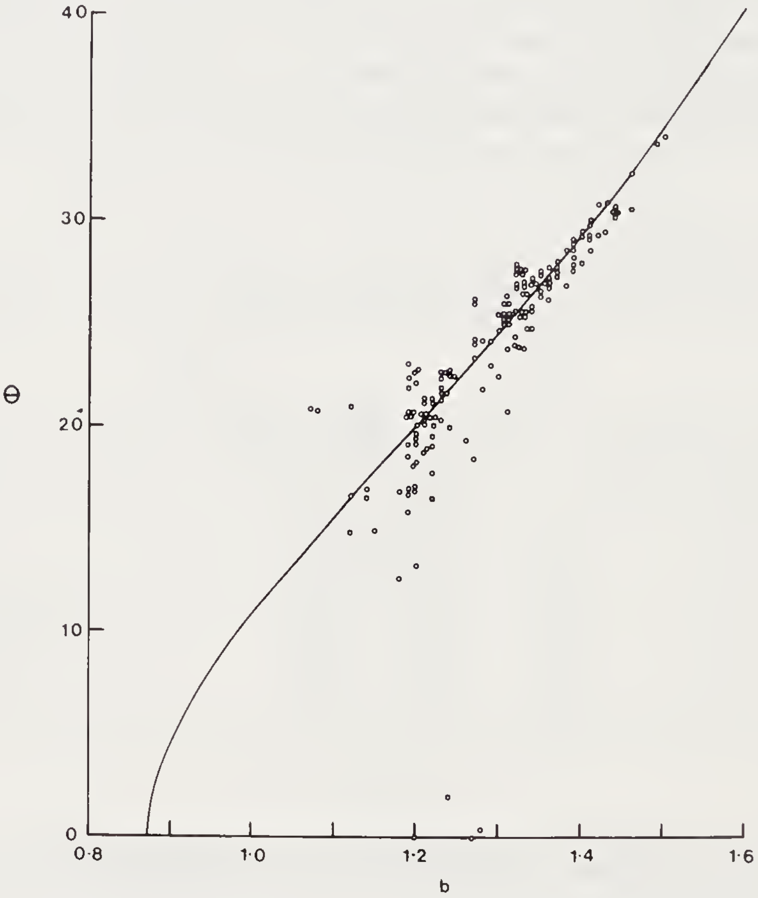

Figure 43 Angle of twist θ (degrees) and normalized bite b for complexes of the type $[M(\mathrm{bidentate})_3]$. Theoretical curve for most stable stereochemistry also shown

2.3.3.2 Comparison with experiment

The overwhelming majority of tris(bidentate ligand) complexes have structures close to D_3 symmetry, intermediate between the octahedron and trigonal prism. The structural parameters of those molecules that contain three identical symmetrical bidentate ligands are shown in Figure 43 (results from a 1980 literature search[4]). The structures of the majority conform reasonably well with the above predictions. The structures range from distorted octahedral structures that are twisted *away* from the trigonal prism for normalized bites $b > 2^{1/2}$, for example $[\mathrm{Co(MeCOCHCOMe)_3}]$, $b = 1.50$, $\theta = 34.0°$,[170] to $(\mathrm{Bu_4N})[\mathrm{Cd(S_2CNEt_2)_3}]$ which is approaching a trigonal prismatic structure, $b = 1.08$, $\theta = 8.5°$.[171] The scatter about the theoretical line is less than $\theta \approx \pm 1°$ for large normalized bites ($b \approx 1.4-1.5$) but increases to $\theta \approx \pm 5°$ for small normalized bites ($b \approx 1.1-1.3$), corresponding to about 0.05 units in the repulsion energy coefficient X. Distortions from D_3 symmetry are also more frequently observed as the normalized bite is decreased, which is also in accord with the repulsion energy calculations.[4]

The very large amount of data available for these compounds allows the recognition of three general types of molecule that do not exactly agree with either the theoretical prediction or with the great majority of experimentally known structures. These are discussed separately in the next section, and that type with the most marked discrepancy, the tris(dithiolate) molecules, have been deleted from Figure 43. Complexes of manganese(III) and copper(II) have also been deleted from Figure 43 and are discussed separately in Section 2.3.3.4.

2.3.3.3 Some 'anomalous' complexes

(i) Dithiolate complexes

Tris(bidentate) complexes $[M(S_2C_2R_2)_3]^{x-}$ (R = H, CN, Ph, CF_3, CO_2Me) form complexes that are much further distorted away from the octahedron toward the trigonal prism than would be expected from simple repulsion energy calculations. There is also considerable difficulty in formulating these complexes, which may be described as either dithiolate (**1**) or dithiolene (**2**). The latter is obviously unrealistic for complexes such as $[V(S_2C_2Ph_2)_3]$, which would require the formation of vanadium(VI). Evidence from C—C and C—S bond lengths shows that the bonding is intermediate between these extremes, with extensive electron delocalization between the metal and ligands. Similar complexes are formed with benzenedithiolate, $o\text{-}C_6H_4S_2{}^{x-}$, and aminobenzene thiolate, $o\text{-}NHC_6H_4S^{x-}$.

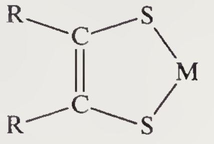

(**1**) Dithiolate

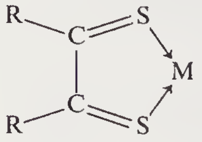

(**2**) Dithiolene

Values of the normalized bite b and the twist angle θ for these complexes are given in Table 14. In sharp contrast to other tris(chelate) complexes, it is very clear that θ is not a simple function of b. In all cases θ is lower than predicted, and in many cases the trigonal prism with $\theta = 0°$ is observed. These dithiolate ligands are clearly different from other bidentate ligands, even other sulfur donors such as $MeSCH{=}CHS^-$, dithioacetylacetonate, dithiooxalate, dithiophosphates, dithiocarbamates and xanthates.

Table 14 Structural Parameters for Tris(dithiolate) and Related Complexes

Complex	*b*	*θ*	*Ref.*
$(Ph_4As)_2[Fe\{S_2C_2(CN)_2\}_3]$	1.39	~24.5	172
$(Me_4N)_2[V\{S_2C_2(CN)_2\}_3]$	1.33	17.0	173
$[Mo(S_2C_2H_2)_3]$	1.33	0	174
$[Mo\{S_2C_2(CF_3)_2\}_3]$	1.33	0	175
$(Ph_4As)_2[Mo\{S_2C_2(CN)_2\}_3]$	1.32	14.0	176
$(Ph_4As)_2[W\{S_2C_2(CN)_2\}_3]$	1.32	14.0	176
$[Mo(S_2C_6H_4)_3]$	1.31	0	177
$[V(S_2C_2Ph_2)_3]$	1.31	0	178
$[Re(S_2C_2Ph_2)_3]$	1.30	0	179
$(Ph_4As)[Ta(S_2C_6H_4)_3]$	1.30	~16	180
$(Ph_4As)[Nb(S_2C_6H_4)_3]$	1.29	0.6	181
$(Ph_4P)_2[Mo\{S_2C_2(CO_2Me)_2\}_3]HCONMe_2\cdot C_6H_6$	1.29	~4	182
$(Me_4N)_2[Zr(S_2C_6H_4)_3]$	1.28	19.4	183
$[Tc(NHC_6H_4S)_3]$	1.27	4.6	184
$[Mo(NHC_6H_4S)_3]$	1.26	6.2	185

It is not clear why dithiolate ligands stabilize the trigonal prism. As the octahedron is twisted toward the trigonal prism the S—S distance between the three ligands necessarily decreases. Bonding within these S_3 triangles, together with the utilization of metal *d*-orbitals, may well be important.

(ii) Tris(bipyridyl) and tris(1,10-phenanthroline) complexes

Sufficient structural data on tris(bipyridyl) and tris(1,10-phenanthroline) complexes have accumulated to suggest that these complexes may be closer to the octahedral limit than predicted theoretically. The structural data are collected in Table 15 and compared with the theoretical curve derived from repulsion theory in Figure 44. Also shown in Figure 44 is the result from a linear regression of the 141 points in Figure 43, that gave:

$$\theta = -36.4 + 46.6b$$

The only compounds deleted from this treatment are the tris(bipyridyl) and tris(phenanthroline) complexes, and the three exceptional β-diketonates discussed in the next section.

The complexes contributing to the least squares line in Figure 44 contain either two-coordinate donor atoms with very little steric hindrance (for example, acetylacetonate, oxalate, dithiocarbamates or xanthates), or tetrahedrally coordinated donor atoms (for example, 1,2-diaminoethane or 1,3-diaminopropane). The agreement between the theoretical curve and the experimental line is very good. The observation that the line of best fit lies 0.5° below the calculated line may be

Table 15 Structural Parameters for Tris(bipyridyl) and Tris(1,10-phenanthroline) Complexes

Complex	*b*	*θ*	*Ref.*
$[Co(phen)_3](ClO_4)_3 \cdot 2H_2O$	1.34	28.3	186
$[Co(bipy)_3][Fe(CN)_6] \cdot 8H_2O$	1.33	28.3	187
$[Fe(phen)_3]I_2 \cdot 2H_2O$	1.33	26.5	188
$[Fe(phen)_3][S_2MoS_2FeCl_2]$	1.32	27.0	189
$[Fe(phen)_3](ClO_4)_3 \cdot H_2O$	1.32	27.8	190
$[Fe(phen)_3](SbC_4O_6H_2)_2 \cdot 8H_2O$	1.32	27.6	191
$(bipy\ H)[Fe(bipy)_3](ClO_4)_4$	1.32	27.6	192
$[Fe(bipy)_3][Fe_2OCl_6]$	1.31	27.3	193
$K[Ni(phen)_3][Co(C_2O_4)_3] \cdot 2H_2O$	1.29	22.9	194
$[Ni(phen)_3][Mn(CO)_5]_2$	1.28	24.1	195
$[Os(phen)_3](ClO_4)_2 \cdot H_2O$	1.27	26.1	196
$[Ru(bipy)_3](PF_6)_2$	1.27	25.9	197
$[Ni(bipy)_3]_2Cl_2(C_4H_4O_6) \cdot nH_2O$	1.27	24.1	198
$[Ni(bipy)_3](SO_4) \cdot 7.5H_2O$	1.27	24.0	199
$[Co(bipy)_3]Cl \cdot H_2O$	1.24	22.6	200
$[Co(bipy)_3]Cl_2 \cdot 2H_2O \cdot EtOH$	1.24	22.4	200
$[Hg(phen)_3](CF_3SO_3)_2$	1.15	14.9	201

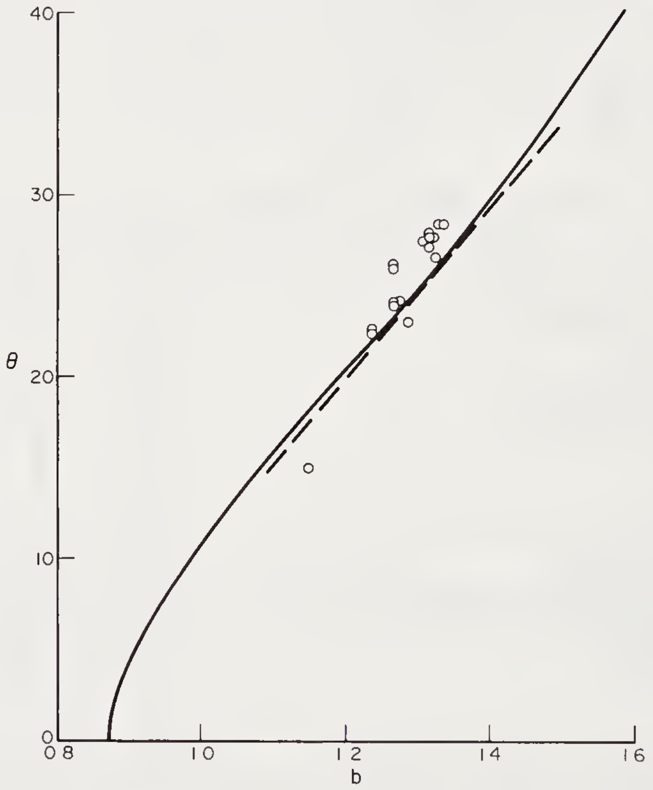

Figure 44 Angle of twist θ (degrees) and normalized bite b for tris(bipyridyl) and tris(phenanthroline) complexes. Full line, theoretical curve for most stable stereochemistry. Broken line, line of best fit through 141 structurally characterized complexes

attributed to the asymmetric nature of the potential energy well (Figure 42), so that experimental deviations will be larger on the low-θ side of the minimum than on the high-θ side.

Figure 44 shows that the bipyridyl and 1,10-phenanthroline complexes have angles of twist approximately 1° *higher* than predicted by theory, or approximately 1.5° higher than all other complexes. If this effect is real, it may be attributed to the clash between the *ortho*-hydrogen atoms of one ligand and the adjacent ligands hindering the twist towards the trigonal prism. An alternative explanation may be that the lone pairs of electrons in the bipyridyl and 1,10-phenanthroline ligands are unusually rigidly directed, resulting in slightly bent metal–ligand bonds. If the effective bond angle at the metal atom is approximately 2° larger than the angle between the metal–nitrogen vectors, there would be an increase in the effective normalized bite of approximately 0.02, bringing the bipyridyl and phenanthroline complexes into coincidence with all other complexes. Similar distortions appear to be found in tris(2-methyl-1, 10-phenanthroline)iron(II) ($b = 1.23$, $\theta = 24.9°$),[202] tris(diphenylazenato)cobalt(III) ($b = 1.08$, $\theta = 20.7°$),[203,204] and a tris(diimine)ruthenium complex ($b = 1.25$, $\theta = 24.7°$).[205]

(iii) Some tris(β-diketonate) complexes

Of the 158 compounds in Figure 43, three tris(β-diketonate) complexes have angles of twist grossly at variance with predictions and it is necessary to seek other explanations for their structures. The structural parameters of all tris(β-diketonate) complexes are listed in Table 16 and also shown in Figure 45. It is clear that the four molecules for which $b < 1.3$ are much closer to the trigonal prism than predicted. These have metal–oxygen bond lengths > 2.2 Å and are sterically very uncrowded molecules that are relatively easy to distort. The small steric interactions are shown, for example, by the formation of eight-coordinate tetrakis(β-diketonate) complexes between these ligands and transition metals of this size.

Table 16 Structural Parameters for Tris(β-diketonate) Complexes

Complex	*b*	*θ*	*Ref.*
$[Co(MeCOCHCOMe)_3]$	1.50	34.0	170
$[Co(MeCOCHCOMe)_3]\cdot 2(NH_2)_2CSe$	1.49	33.0	206
$[Ru(MeCOCHCOMe)_3]$	1.46	32.2	207
$[Ge(MeCOCHCOMe)_3](ClO_4)$	1.46	30.7	208
$[Ga(MeCOCHCOMe)_3]$	1.44	30.6	209
$[Al(MeCOCHCOMe)_3]$	1.44	30.4	170
$[Cr(MeCOCHCOMe)_3]$	1.43	30.8	210
$[Cr(MeCOCHCOMe)_3]\cdot 2(NH_2)_2CS$	1.43	30.1	211
$[Cr(MeCOCHCOMe)_3]$	1.42	30.7	212
$[Mo(MeCOCHCOMe)_3]$	1.39	28.9	213
$[Co(CNC_6H_4Me)_5][Co(HCOC(NO_2)COH)_3]$	1.39	28.9	214
$[Fe(MeCOCHCOMe)_3]\cdot AgClO_4\cdot H_2O$	1.39	28.2	215
$[Fe(MeCOCHCOMe)_3]$	1.38	26.8	216
$[Fe(CF_3COCHCOCF_3)_3]$	1.38	28.5	217
$[Fe(PhCOCHCOPh)_3]$	1.37	26.8	218
$[Ir(MeCOCHCOMe)_3]$	1.36	26.1	219
$(C_{14}H_{19}N_2)[Mg(CF_3COCHCOCF_3)_3]$	1.35	26.5	220
$[Ti(MeCOCHCOMe)_3](ClO_4)$	1.34	24.7	221
$[Sc(MeCOCHCOMe)_3]$	1.31	23.7	222
$(NH_4)[Cd(CF_3COCHCOC_4H_3O)_3]$	1.30	17.5	223
$K[Cd(MeCOCHCOMe)_3]\cdot H_2O$	1.28	0.4	224
$Rb_2[Na(CF_3COCHCOCF_3)_3]$	1.24	2	225
$[Er(Bu^tCOCHCOBu^t)_3]$	1.20	0.0	226

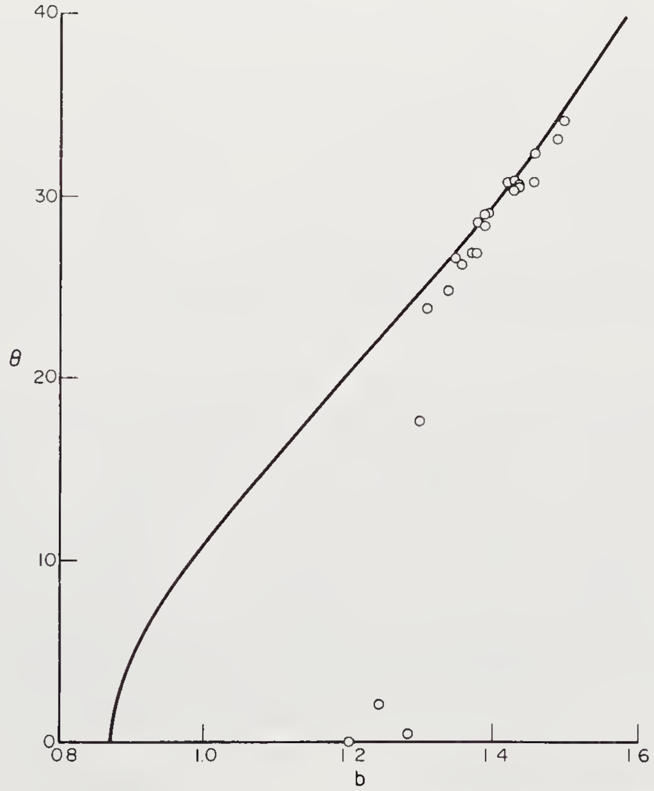

Figure 45 Angle of twist θ (degrees) and normalized bite b for tris(β-diketonate) complexes. Theoretical curve for most stable stereochemistry also shown

The distortion towards the trigonal prism of $(NH_4)[Cd(CF_3COCHCOC_4H_3O)_3]$, $K[Cd(MeCOCHCOMe)_3]\cdot H_2O$ and $Rb_2[Na(CF_3COCHCOCF_3)_3]$ appears to be due to extraordinary crystal packing energies. In these three compounds the small cation sits on, or close to, the threefold axis of the anion and the close contacts between the cation and triangular faces of the anion result in the formation of infinite linear polymers. Any twist towards octahedral geometry must enlarge these triangular faces with a weakening of the cation–anion bonding. On the other hand, salts formed between *large* cations and tris(β-diketonate) anions, namely $(C_{14}H_{19}N_2)[Mg(CF_3COCHCOCF_3)_3]$ and $[Co(CNC_6H_4Me)_5][Co\{OCHC(NO_2)CCHO\}_3]$ have normal structures.

In the erbium complex, $[Er(Bu^tCOCHCOBu^t)_3]$, it may be that the large bulk of the tertiary butyl groups result in considerable intramolecular steric hindrance and prevent the complex twisting towards the octahedron.

2.3.3.4 Manganese(III) and copper(II) complexes

Manganese(III) and copper(II) complexes have been excluded from Figure 44, since experience with complexes containing unidentate ligands leads to the expectation that the octahedral stereochemistry will be tetragonally distorted (Section 2.3.1.2.iii). If, as a rough approximation, the bond angles are averaged assuming D_3 symmetry, then the values of b and θ are again in reasonable accord with the repulsion energy calculations (Figure 46).[4]

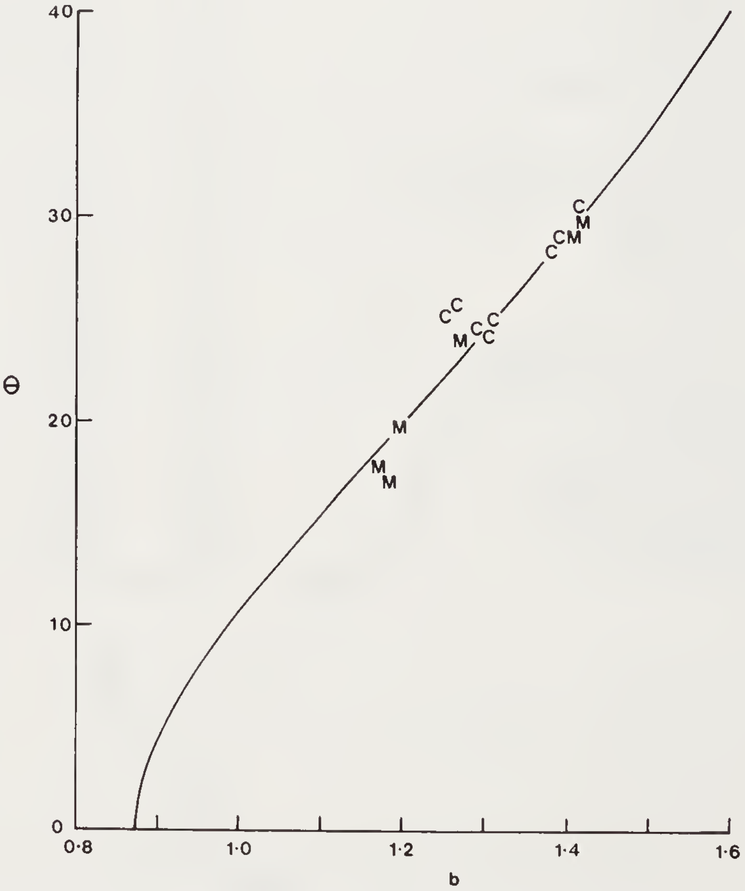

Figure 46 Angle of twist θ (degrees) and normalized bite b for complexes of the type $[Mn^{III}(bidentate)_3]^{x\pm}$ (M) and $[Cu^{II}(bidentate)_3]^{x\pm}$ (C). Theoretical curve for most stable stereochemistry also shown

The difference between the shortest and longest bond length is much less than that observed in complexes containing unidentate ligands, but the type of distortion is very variable. In $(C_{14}H_{19}N_2)[Cu(CF_3COCHCOCF_3)_3]$,[220] $[Cu(HOCH_2CH_2OH)_3](SO_4)$,[227] $[Cu(NH_2CH_2CH_2NH_2)_3]Cl_2\cdot\frac{3}{4}C_2H_8N_2$[228] and $[Cu(phen)_3](ClO_4)_2$[229] there is a fairly obvious tetragonal elongation of the octahedron, two *trans* bonds being 8–16% longer than the other four. On the other hand, $[Cu\{OP(NMe_2)_2OP(NMe_2)_2O\}_3](ClO_4)]_2$[230] and $[Cu(NH_2CH_2CH_2NH_2)_3](SO_4)$[231] (at room temperature) have six equal copper–ligand bond lengths, and it is again necessary to propose rapid oscillation between the three mutually perpendicular tetragonal distortions at each lattice site (see Section 2.3.1.2.iii). More complex distortions are found for many of the complexes in Figure 46.[4]

2.3.3.5 Some comments on ligand design

If the only way of obtaining the normalized bite of a bidentate ligand was from the crystal structure, the repulsion energy approach to stereochemistry would be limited. No matter how useful the theory may be in rationalizing the relation between different stereochemical parameters, it would have little predictive use since these other parameters are precisely determined at the same time as the normalized bite. Therefore, to utilize fully this repulsion approach to stereochemistry, it is essential to be able to make some estimate of the expected normalized bite of any coordinated ligand.

Figure 47 again displays some of the data in Figures 43 and 46. The data are now restricted to complexes of the first-row transition metals from chromium to copper to avoid large variations in central atom size, the 12-coordinate metallic radii being in the range 1.2–1.3 Å.

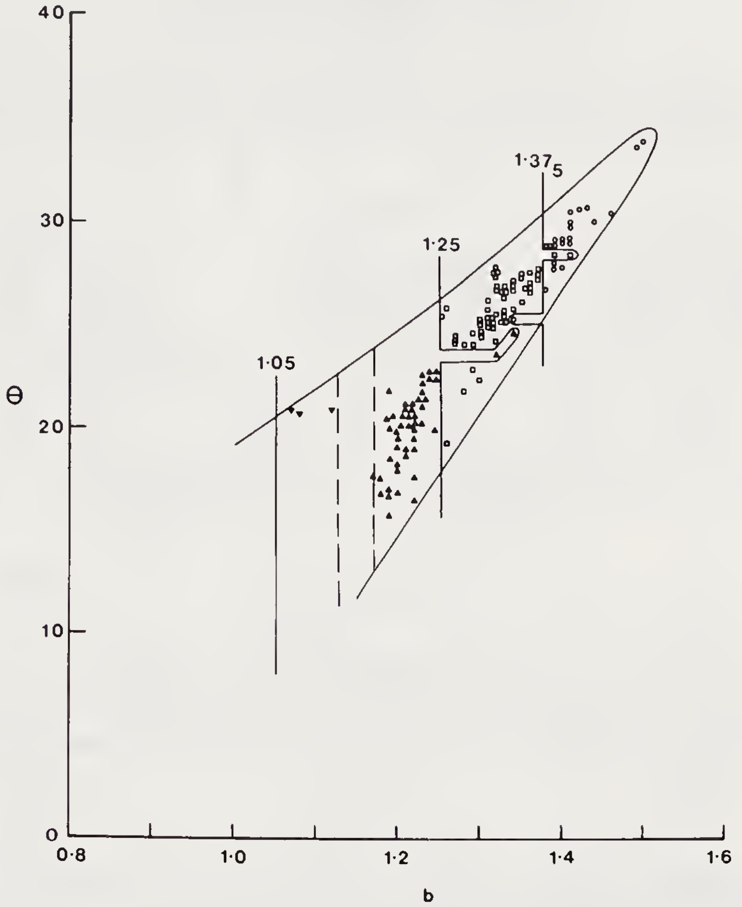

Figure 47 Angle of twist θ (degrees) and normalized bite b for complexes of the type $[M(\text{bidentate})_3]^{x\pm}$ (M = Cr, Mn, Fe, Co, Ni, Cu)

To a first approximation the ligands divide into three groups. The first group is contained within the limits $b = 1.37_5$ to $b = 1.50$ and consists of those ligands that form six-membered chelate rings, such as acetylacetonate and trimethylenediamine. The second group is contained within the limits $b = 1.25$ to $b = 1.37_5$ and contains the complexes with five-membered chelate rings, such as *o*-phenanthroline and ethylenediamine. The third group is contained within $b = 1.05$ to $b = 1.25$ and contains the complexes with four-membered rings, such as nitrate and dithiocarbamates. This strikingly simple and important correlation is further illustrated in Figure 48 with three representative examples: $[Co(MeCOCHCOMe)_3]$,[232] $[Co(NH_2CH_2CH_2NH_2)_3]^{3+}$,[4] and $[Co(NO_3)_3]$.[233]

Extension to flexible seven-membered rings does not necessarily increase the normalized bite, as indicated by $[Co(NH_2CH_2CH_2CH_2CH_2NH_2)_3]Br_3$, for which the parameters are $b = 1.40$ and $\theta = 27.9°$.[234] This is achieved by substantial buckling of the seven-membered ring.

Further subdivisions can be made according to the size of the non-metal atoms in the chelate ring. For example, the four-membered chelate ring group may be divided into four subgroups. The subgroup containing ligands of lowest normalized bite ($b = 1.05$–1.12_5) consists of $(PhN_3Ph)^-$ and NO_3^-, where three small second-row elements complete the chelate ring. There are no known examples of the second subgroup. The third subgroup of normalized bite 1.17–1.25 contains ligands with one second-row element and two larger elements in the chelate ring, such as the dithiocarbamates and xanthates. The fourth subgroup contains the dithiophosphates with three large ring atoms, and this subgroup intrudes into the group containing the five-membered chelate rings. A comparison of the ring geometries of $[Co(NO_3)_3]$,[233] $[Co(S_2COEt)_3]$[235] and $[Co\{S_2P(OMe)_2\}_3]$[236] is shown in Figure 49.

Unusually large normalized bites may be achieved with five-membered chelate rings by again incorporating large atoms into the ring. The intrusion of the five-membered ring region into the six-membered ring region in Figure 47 is due to a dithiooxalate complex containing two sulfur atoms in the chelate ring, all other five-membered rings in Figure 47 containing only carbon,

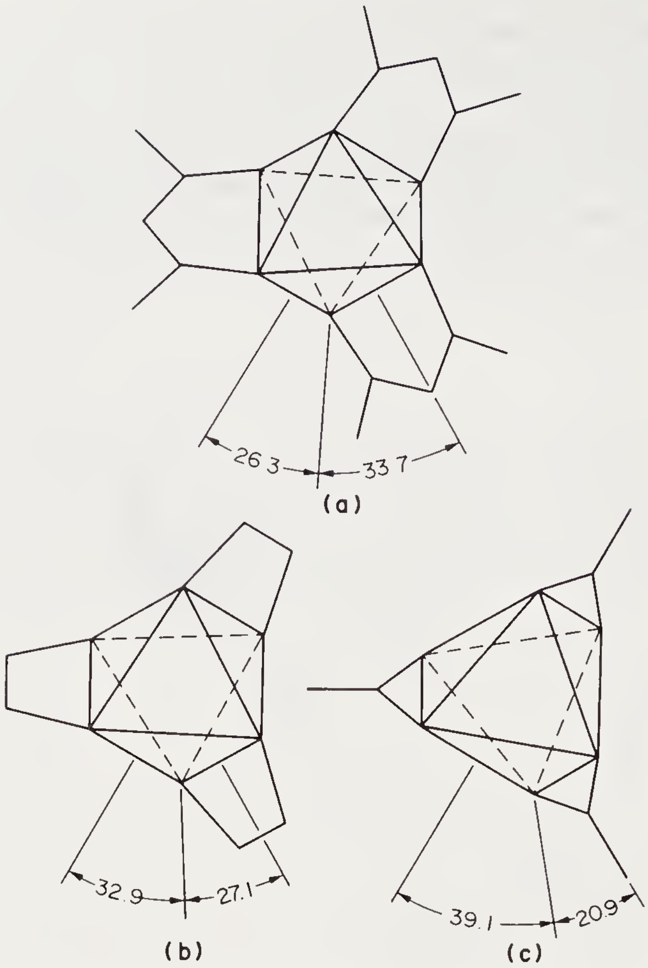

Figure 48 (a) $[Co(acac)_3]$, (b) $[Co(en)_3]^{3+}$ and (c) $[Co(NO_3)_3]$; angles in degrees

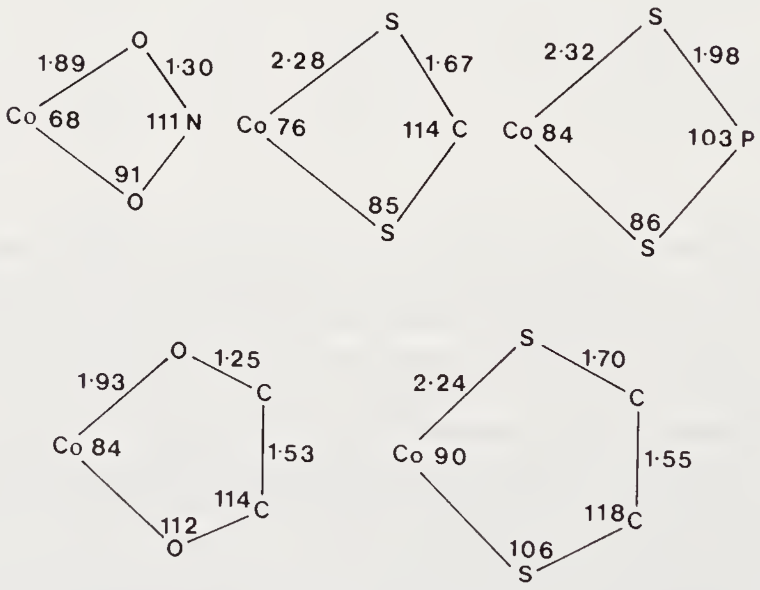

Figure 49 Ring geometries, degrees and Å, in $[Co(NO_3)_3]$, $[Co(S_2COEt)_3]$, $[Co\{S_2P(OMe)_2\}_3]$, $[Co(C_2O_4)_3]^{3-}$ and $[Co(S_2C_2O_2)_3]^{3-}$

nitrogen and oxygen atoms. Comparative ring geometries in $[Co(C_2O_4)_3]^{3-}$[237] and $[Co(S_2C_2O_2)_3]^{3-}$[238] are also shown in Figure 49.

The size of the metal atom is also important in determining the normalized bite, the smaller normalized bites being obtained with the larger metal atoms. Thus the lowest normalized bite for a six-membered ring containing a transition metal ion is that observed for $[Sc(MeCOCHCOMe)_3]$[222] in which the normalized bite of 1.31 is similar to complexes of the other transition metals containing five-membered chelate rings. Similarly, the lowest normalized bite for a transition metal complex containing a five-membered ring is $b = 1.20$, observed for the tropolonate complex $[Sc(O_2C_7H_5)_3]$.[239] The metal–oxygen distance and the O···O intraligand distance are not completely independent of each other. For example, in β-diketonate complexes, an increase in the metal ion radius of about 10% causes a general loosening of the coordination sphere, with a small increase of about 2–5% in the O···O distance.

2.4 SEVEN-COORDINATE COMPOUNDS

2.4.1 [M(Unidentate)$_7$]

The starting point for the consideration of seven coordination is the consideration of three structures with very similar values for the repulsion energy coefficient X:

capped octahedron: $X = 3.230$
capped trigonal prism: $X = 3.231$
pentagonal bipyramid: $X = 3.266$

It is important to note that these structures, shown in Figure 50, contain two or three different types of ligand site, and different sized faces and edge lengths. Detailed structural parameters have been given elsewhere.[4]

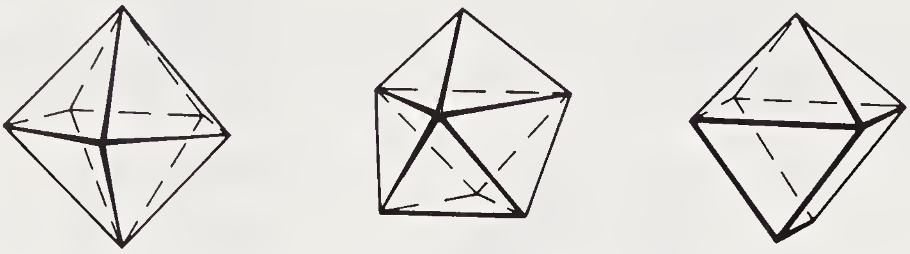

Figure 50 The pentagonal bipyramid, capped octahedron and capped trigonal prism

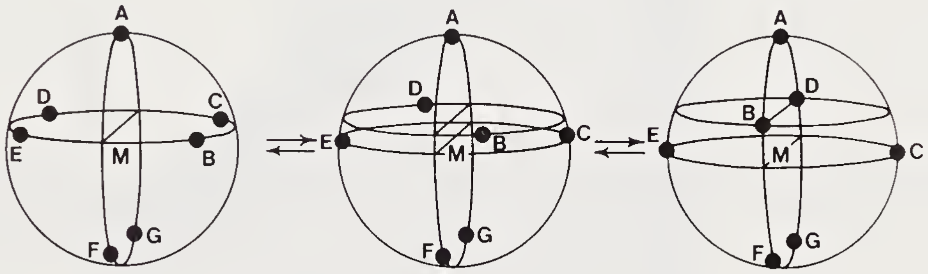

Figure 51 Transformation of the capped trigonal prism (left) to the pentagonal bipyramid (right) with retention of a twofold axis. The ϕ angular coordinates are defined as the angles between the metal—ligand bonds and the twofold axis along the M—A bond. The θ angular coordinates are defined relative to $\theta_F = 0$ and $\theta_G = 180°$

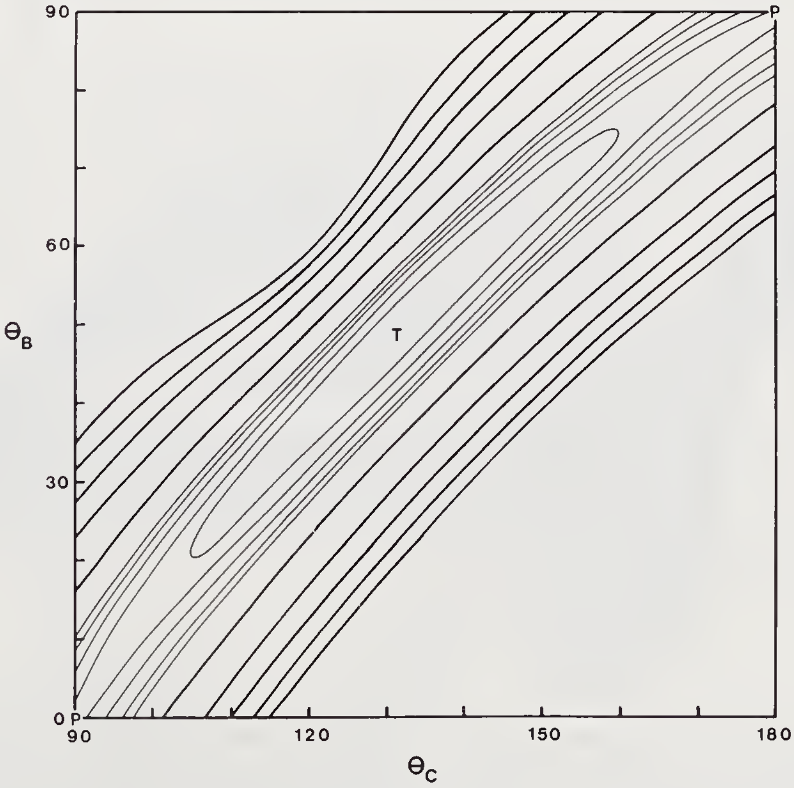

Figure 52 Projection of the potential energy surface for [M(unidentate)$_7$] on to the θ_B–θ_C plane (in degrees), with retention of a twofold axis. The five faint contour lines are for successive 0.02 increments in X above the minimum, and the five heavy contour lines are for successive 0.2 increments above the minimum, at T. The locations of the pentagonal bipyramid (P) and capped trigonal prism (T) are indicated

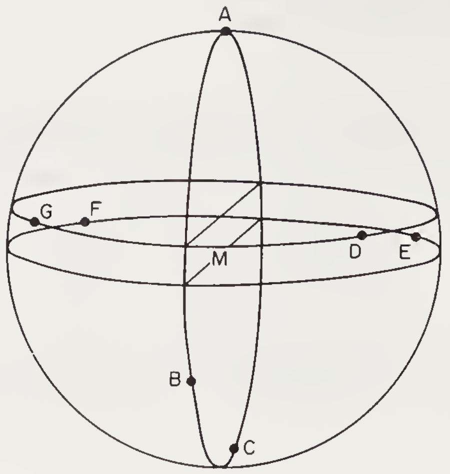

Figure 53 General stereochemistry for [M(unidentate)$_7$] with retention of a mirror plane. The ϕ angular coordinates are defined as the angles between the metal–ligand bonds and the M–A bond. The θ angular coordinates are defined relative to the mirror plane through MABC

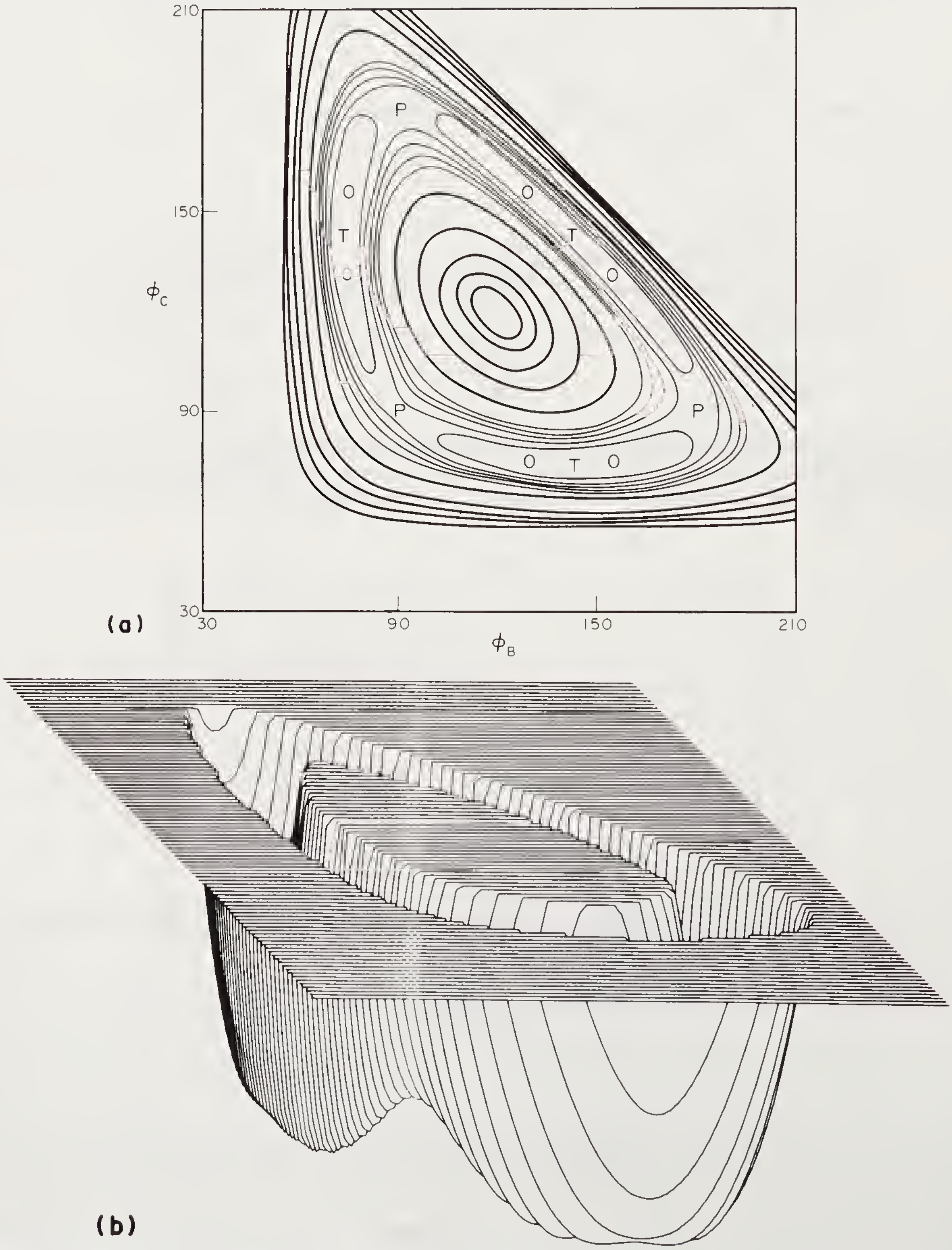

Figure 54 (a) Projection of the potential energy surface for [M(unidentate)$_7$] on to the ϕ_B–ϕ_C plane (in degrees), with retention of a mirror plane. The five faint contour lines are for successive 0.02 increments in X above the minima, and the five heavy contour lines are for successive 0.2 increments above the minima, at T. The locations of the pentagonal bipyramids (P), capped octahedra (O), and capped trigonal prisms (T) are indicated. (b) As in (a), but with truncation at X = 0.1

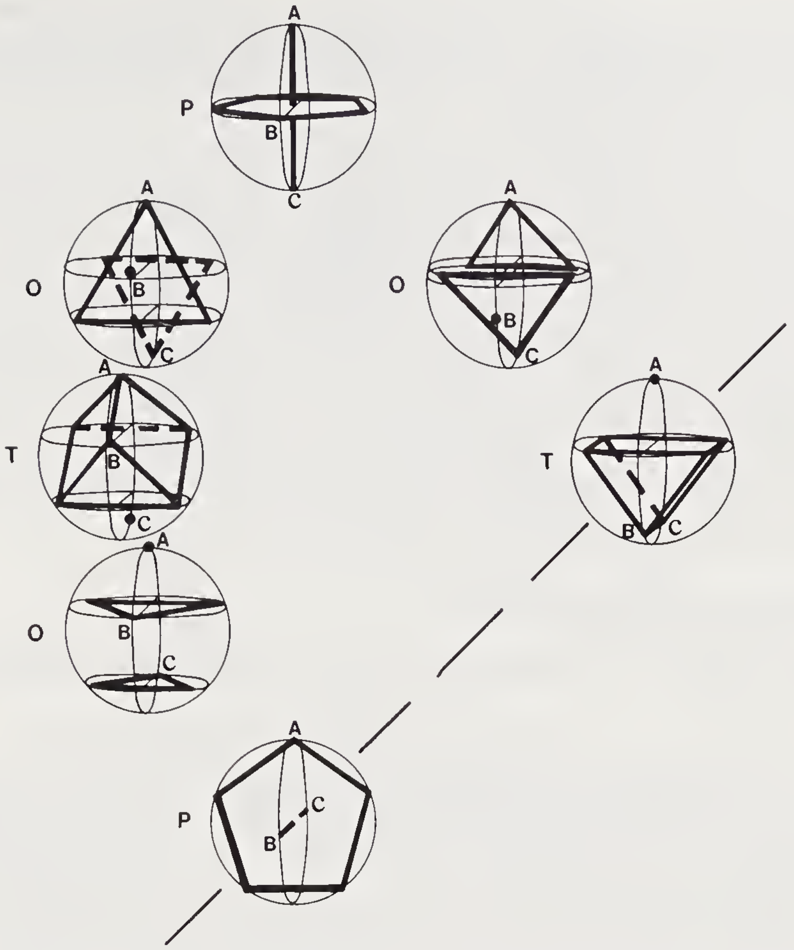

Figure 55 Stereochemistries corresponding to the locations marked on the upper left-hand side of Figure 54. (P) Pentagonal bipyramids; (O) capped octahedra; (T) capped trigonal prisms

2.4.1.1 Relations between the pentagonal bipyramid, capped octahedron and capped trigonal prism

The three polyhedra in Figure 50 are of comparable stability, and it is shown in this section that there are no potential energy barriers between them.Two types of interconversion are illustrated, the first in which a twofold axis is maintained, and the second in which a mirror plane is maintained throughout the transformations.

The transformation of a pentagonal bipyramid to a capped trigonal prism with retention of a twofold axis is shown in Figure 51. The twofold axis passes through atom A, while the θ_B and θ_C coordinates are defined relative to $\theta_F = 0$ and $\theta_G = 180°$. The potential energy surface for this transformation is shown projected on to the $\theta_B - \theta_C$ plane in Figure 52. Movement along the flat valley corresponds to free rotation of the four BCDE atoms relative to the two FG atoms.

The general stereochemistry containing a mirror plane is shown in Figure 53. Atoms A, B and C lie on the mirror plane, and the axes are defined by $\phi_A = 0$, $\theta_B = 0$, $\theta_C = 180°$. The potential energy surface projected on to the $\phi_B - \phi_C$ plane is shown in Figures 54a and 54b. The locations of the pentagonal bipyramid (P), capped octahedron (O) and capped trigonal prism (T) are marked and lie along the bottom of a 'moat'. Each stereochemistry occurs more than once on the potential energy surface, but this apparent redundancy is useful when comparison is made with related surfaces (see later).

The stereochemistry at each of these locations is shown in Figure 55. It can be seen that the capped octahedron can be considered as an intermediate between the pentagonal bipyramid and the capped trigonal prism, but it is much closer in energy and stereochemistry to the latter.

2.4.1.2 Comparison with experiment

Structurally characterised molecules with seven identical ligands are restricted mainly to some fluoro complexes $[MF_7]^{x-}$, aquo complexes $[M(H_2O)_7]^{2+}$, isonitrile complexes $[M(CNR)_7]^{2+}$ and cyanide complexes $[M(CN)_7]^{x-}$. The stereochemistries are distributed along the long valley connecting the capped trigonal prism and the pentagonal bipyramid.

The X-ray data on IF_7 are not sufficient to obtain the precise stereochemistry.[240,241] The ^{19}F NMR spectrum shows equivalence of all seven fluorine atoms, consistent with rapid intramolecular rearrangement.[242-244] The anion in $K_2[NbF_7]$ has approximately capped trigonal prismatic stereochemistry.[245] The small distortion corresponds to the molecule moving along the potential energy surface (Figures 54a and 54b) about 20% of the way to the capped octahedron, or about 5% of the way to the pentagonal bipyramid.

In the calcium polyiodide compound $[Ca(H_2O)_7](I_{10})$ the stereochemistry appears to be intermediate between a capped octahedron and a pentagonal bipyramid, whereas $[Sr(H_2O)_7](I_{12})$ and $[Ca(H_2O)_7]_2[Cd_6Cl_{16}(H_2O)_2]\cdot H_2O$ contain capped trigonal prismatic cations.[246,247]

A close approximation to a capped trigonal prism is also observed for $[Mo(CNBu)_7](PF_6)_2$.[248] However, the closely related compounds $[Cr(CNBu)_7](PF_6)_2$,[249] $[Mo(CNPh)_7](PF_6)_2$,[250] $[Mo(CNMe)_7](BF_4)_2$[251] and $[W(CNBu)_7](W_6O_{19})$[252] lie considerably further along the potential energy valley and are closer to capped octahedra than to capped trigonal prisms. Solutions of $[Mo(CNBu)_7]^{2+}$ yield only a single ^{13}C NMR signal even down to −135 °C, showing the expected stereochemical non-rigidity.[253]

The structures of $K_4[V(CN)_7]\cdot 2H_2O$,[254] $K_5[Mo(CN)_7]\cdot H_2O$, $Na_5[Mo(CN)_7]\cdot 10H_2O$[255] and $K_4[Re(CN)_7]\cdot 2H_2O$[256] are close to pentagonal bipyramids.

2.4.1.3 *[M(unidentate A)$_6$(unidentate B)]*

Figure 56 shows a typical potential energy surface calculated for one effective bond length shorter than the other six:

$$MA = R = 0.8, \quad MB = MC = MD = ME = MF = MG = 1.0$$

A mirror plane has been assumed, and Figure 56 should be compared with Figure 54, which was calculated for seven equal bond lengths. It can be seen that the continuous 'moat' in Figure 54 contracts to two 'ponds' at $\phi_B \approx 93°$ and $\phi_C = 180°$ (and *vice versa*), corresponding to a pentagonal bipyramid with the short bond in one of the axial sites. Also shown in Figure 56 are the locations of the capped octahedron with the short bond in the capping site at $\phi_B \approx 79°$, $\phi_C \approx 131°$ (O), the capped trigonal prism with the short bond in the capping site at $\phi_B = \phi_C \approx 144°$ (T), and the pentagonal bipyramid with the short bond occupying one of the equatorial sites at $\phi_B = \phi_C \approx 91°$ (P′).

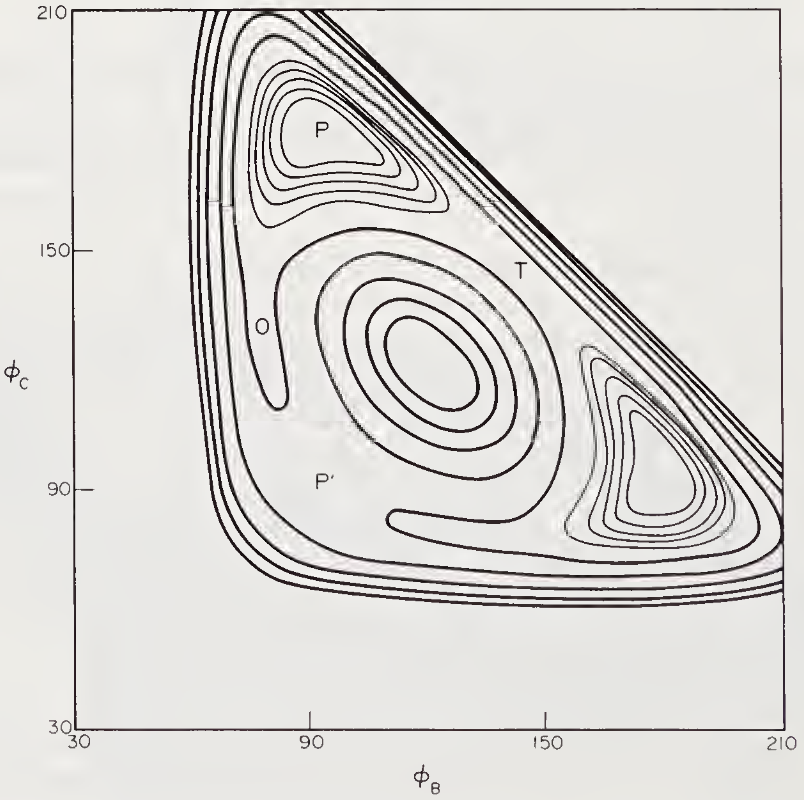

Figure 56 Projection of the potential energy surface for [M(unidentate A)$_6$(unidentate B)] on to the ϕ_B–ϕ_C plane (in degrees) with retention of a mirror plane. The five faint contour lines are for successive 0.02 increments in X above the minima, and the five heavy contour lines are for successive 0.2 increments above the minima, at P. R = 0.8. The locations of the pentagonal bipyramids (P and P′), capped octahedron (O) and capped trigonal prism (T) are indicated

A typical potential energy surface calculated for a single long bond, MA = R = 1.2, is shown in Figure 57. Destabilization of the pentagonal bipyramid with the single long bond in an axial site (at $\phi_B \approx 88°$, $\phi_C = 180°$ and *vice versa*) results in a bridging of the 'moat' at this stereochemistry with the creation of two 'lagoons', one deeper than the other. The deepest minimum at $\phi_B \approx 70°$, $\phi_C \approx 129°$ corresponds to the capped octahedron with the long bond occupying the capping site.

This minimum is fairly flat, and the capped trigonal prism with the long bond occupying one of the sites *trans* to the capping atom is of comparable energy. The saddle at $\phi_B = \phi_C \approx 88°$ shows that the pentagonal bipyramid with the long bond in an equatorial site is also readily accessible. The second, less deep minimum at $\phi_B = \phi_C \approx 142°$ is the capped trigonal prism with the long bond in the capping site.

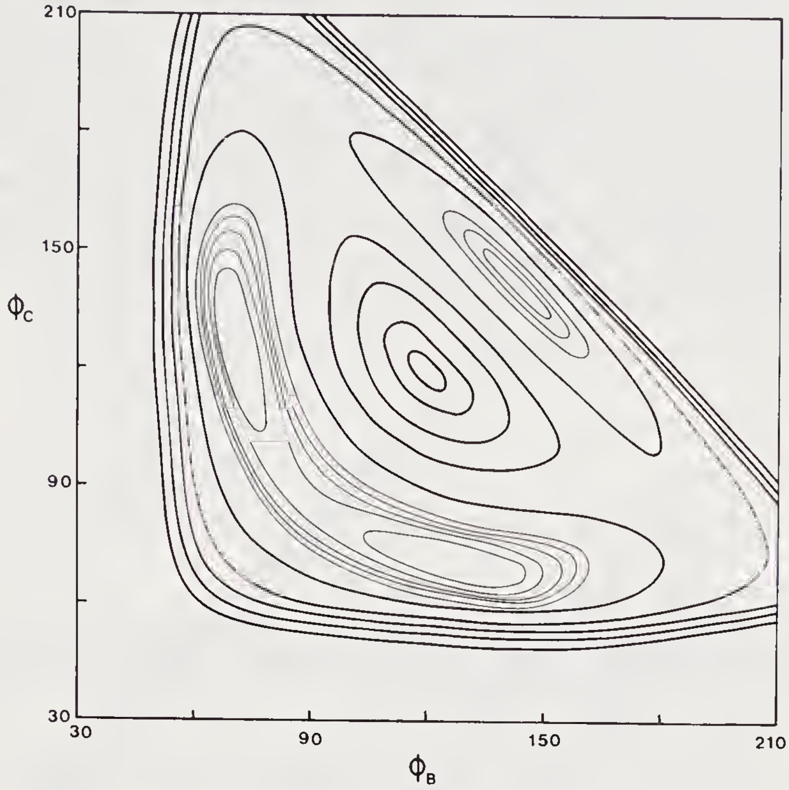

Figure 57 Projection of the potential energy surface for [M(unidentate A)$_6$(unidentate B)] on to the ϕ_B–ϕ_C plane (in degrees) with retention of a mirror plane. The five faint contour lines are for successive 0.02 increments in X above the minima, and the five heavy contour lines are for successive 0.2 increments about the minima. $R = 1.2$

Although little structural information concerning compounds of the type [M(unidentate A)$_6$(unidentate B)] is available, there are known examples of all the predicted structures. The anion in $Na_3[NbOF_6]$ is pentagonal bipyramidal with the oxygen atom in an axial site, as clearly predicted in Figure 56.[257] The molybdenum isonitrile complexes $[Mo(CNBu)_6I]I$[258] and $[Mo(CNBu)_6Br]Br$[259] have capped trigonal prismatic stereochemistries, with the halogen atoms in the unique capping sites, $\phi_B \approx \phi_C \approx 145°$. On the other hand, $[Mo(CNBu)_6(SnCl_3)][(Ph_3B)_2CN]$ lies in the alternative potential energy hollow in Figure 57 at $\phi_B = 72°$, $\phi_C = 112°$, with a stereochemistry intermediate between a pentagonal bipyramid with the tin atom in an equatorial site, and a capped octahedron with the tin atom in the axial site.[260] Capped octahedral stereochemistry, with crystallographic threefold symmetry, is observed for $[U(Me_3PO)_6Cl]Cl_3$[261] and $[V(CO)_6(AuPPh_3)]$.[262] The structure of $[Er\{OC(NHMe)_2\}_6(H_2O)](ClO_4)_3$ has been described as a pentagonal bipyramid with the water molecule in one of the equatorial sites.[263]

2.4.1.4 *[M(unidentate)$_6$(lone pair)]*

The following compounds of the *p*-block elements contain seven electron pairs in the valence shell, but the six unidentate ligands are octahedrally arranged, with only small distortions:[264]

Group IV	*Group V*	*Group VI*
	$Sb^{III}Cl_6^{3-}$	$Te^{IV}Cl_6^{2-}$
	$Sb^{III}Br_6^{3-}$	$Te^{IV}Br_6^{2-}$
	$Bi^{III}Cl_6^{3-}$	
	$Bi^{III}Br_6^{3-}$	
	$Bi^{III}I_6^{3-}$	
$[Pb^{II}(ligand)_6]^{2+}$	$[Bi^{III}(ligand)_6]^{3+}$	

The non-bonding pair of electrons has no marked influence on the stereochemistry, in sharp contrast to the complexes of the *p*-block elements with lower coordination numbers, $[MX_3(lone\ pair)]^{x\pm}$ (Section 2.1.6), $[MX_4(lone\ pair)]^{x\pm}$ (Section 2.2.1.1) and $[MX_5(lone\ pair)]^{x\pm}$ (Section 2.3.1.1). At first sight, it might be expected from these repulsion energy calculations, and from Figure 56 in particular, that there would be a pentagonal bipyramidal arrangement of electron pairs with the lone pair occupying one of the axial sites. It is clear that in these sterically crowded molecules the non-bonding pair of electrons plays no significant stereochemical role.

Xenon hexafluoride, on the other hand, is less sterically crowded than the above $MX_6^{x\pm}$ compounds and has a non-octahedral structure in the vapour phase in which the lone pair of electrons exhibits some stereochemical influence.[265,266] The model proposed for the vapour state, however, is not the pentagonal bipyramid with the electron pair in an axial site, but a fluxional structure in which an octahedron is distorted by the lone pair projecting towards one face (that is, a capped octahedron with the lone pair in a capping site) and/or by the lone pair projecting towards one edge (that is, a pentagonal bipyramidal structure with the lone pair in an equatorial site). This behaviour is reproduced from the repulsion energy calculations if a small effective bond length ratio R(lone pair/F^-) is used. For example, at R(lone pair/F^-) = 0.1 (Figure 58), the potential energy surface shows stabilization of the capped octahedron (O). Two such capped octahedra are connected by a low saddle (P′), and the movement across this saddle corresponds to the stereochemical change deduced for the gas-phase structure of XeF_6.

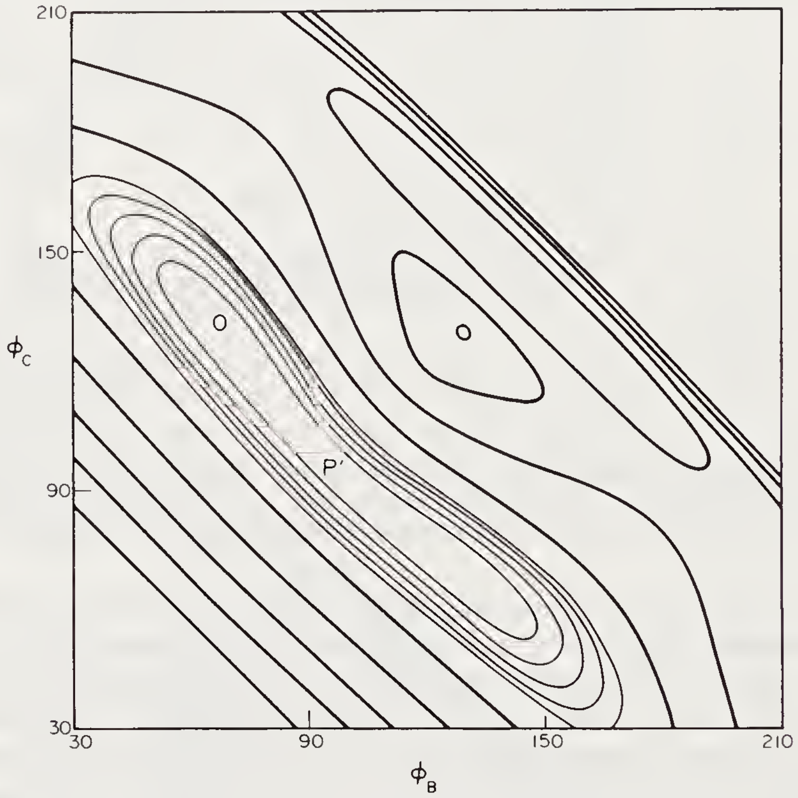

Figure 58 Projection of the potential energy surface for [M(unidentate A)$_6$(unidentate B)] on to the ϕ_B–ϕ_C plane (in degrees) with retention of a mirror plane. The five faint contour lines are for successive 0.02 increments in X above the minima, and the five heavy contour lines are for successive 0.2 increments above the minima, at O. $R = 0.1$. The locations of the pentagonal bipyramid (P′), and capped octahedra (O) are indicated

2.4.1.5 [M(unidentate A)$_5$(unidentate B)$_2$]

Potential energy surfaces in which the effective bond lengths to two ligands is 0.8, the other five being defined as unity, are shown in Figure 59 where a twofold axis is retained (compare with Figure 52 calculated for [M(unidentate)$_7$]), and in Figure 60 in which a mirror plane is retained (compare with Figure 54). In both surfaces the single deep minimum corresponds to a pentagonal bipyramid with the two short effective bond lengths in the two axial sites.

This predicted structure has been observed in $K_3[UO_2F_5]$,[267] $[UO_2(H_2O)_5](ClO_4)_2\cdot 2H_2O$,[268] $[UO_2(OSMe_2)_5](ClO_4)_2$,[269] $[UO_2\{OC(NH_2)_2\}_5](NO_3)_2$[270] and $Cs_3[UO_2(NCS)_5]$.[271]

2.4.2 [M(Bidentate)(Unidentate)$_5$]

2.4.2.1 The theoretical stereochemistries

The potential energy surfaces for [M(bidentate)(unidentate)$_5$] are complex, and contain a number of minima.[4] A summary of the more important stereochemistries, corresponding to calculated potential energy minima, is given in Figure 61.

Below a normalized bite of 1.1 there is a shallow potential energy trough that incorporates the capped trigonal prism with the bidentate ligand spanning the prism edge *trans* to the capping atom

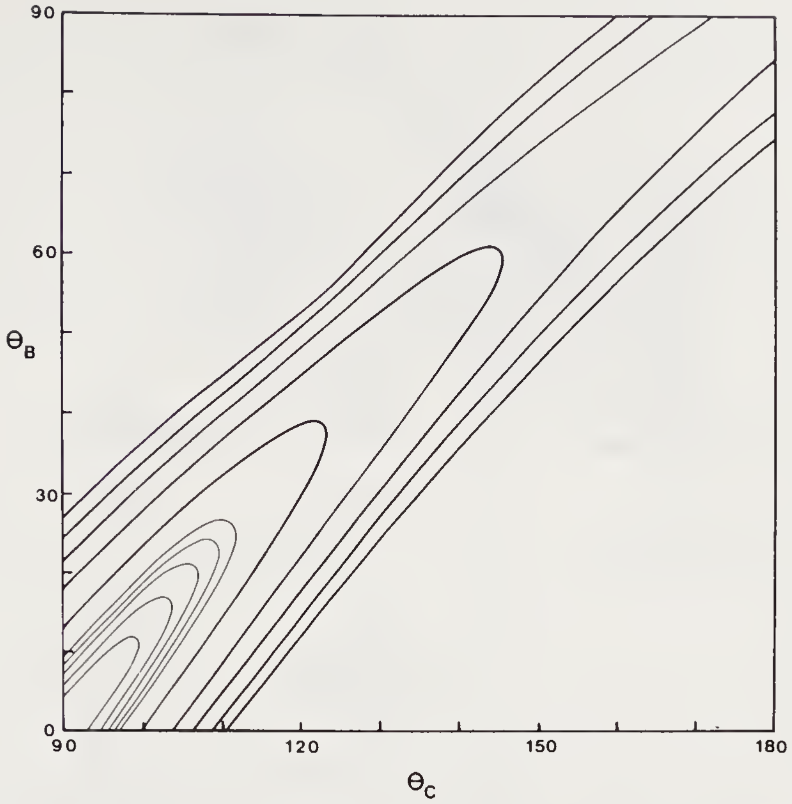

Figure 59 Projection of the potential energy surface for [M(unidentate A)$_5$(unidentate B)$_2$] on to the θ_B–θ_C plane (in degrees) with retention of a twofold axis. The five faint contour lines are for successive 0.02 increments in X above the minimum, and the five heavy contour lines are for successive 0.2 increments above the minimum. R = 0.8

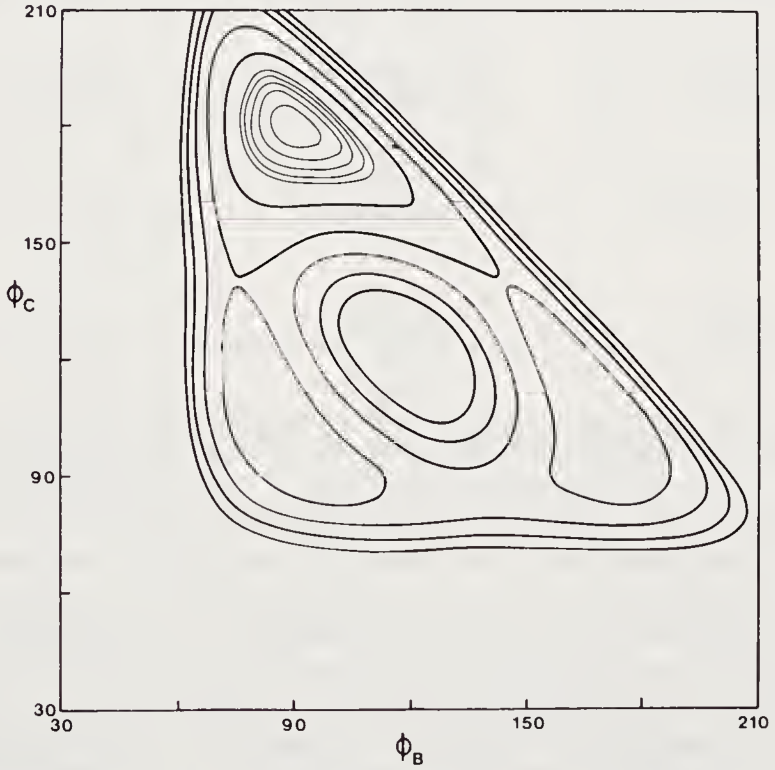

Figure 60 Projection of the potential energy surface for [M(unidentate A)$_5$(unidentate B)$_2$] on to the ϕ_B–ϕ_C plane (in degrees) with retention of a mirror plane. The five faint contour lines are for successive 0.02 increments in X above the minimum, and the five heavy contour lines are for successive 0.2 increments above the minimum. R = 0.8

(stereochemistry A) and the pentagonal bipyramid with the bidentate ligand spanning one of the pentagonal edges (stereochemistry B) (Figure 61). The potential energy surface is similar to that shown in Figure 52, which was calculated for [M(unidentate)$_7$]. The transformation is similar to that shown in Figure 51, but with the bidentate ligand spanning the F and G sites, and can be envisaged as free rotation of the bidentate ligand about the twofold axis.

As the value of the normalized bite increases, both these stereochemistries progressively distort. The distortion of stereochemistry A corresponds to the bidentate ligand on the mirror plane moving towards the unidentate ligand on the mirror plane, towards the formation of a pentagonal bipyramid with the bidentate ligand spanning an axial and equatorial site (Figure 62). The capped

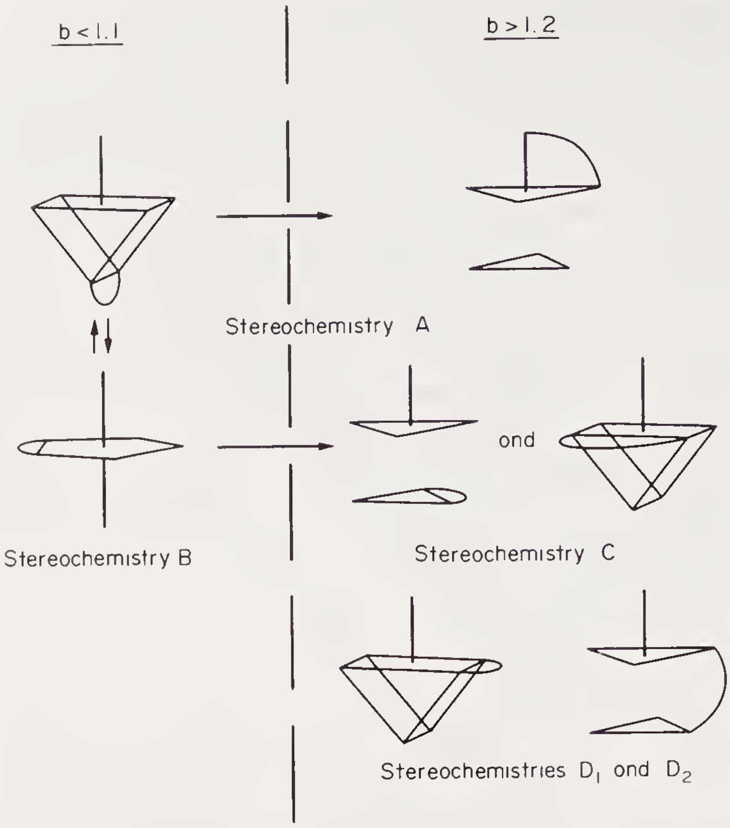

Figure 61 Stereochemistries for [M(bidentate)(unidentate)$_5$]

trigonal prism–pentagonal bipyramid interconversion also traverses the capped octahedron at $b = 1.21$. Atom B is the capping atom, and CDG and AEF are the two triangular planes normal to the threefold axis.

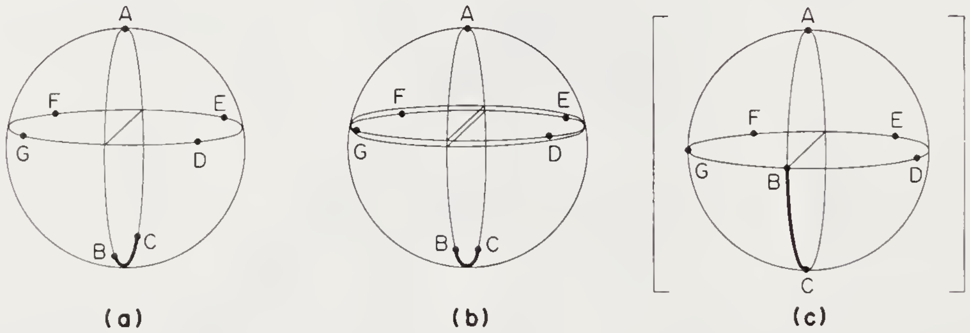

Figure 62 Stereochemistry A for [M(bidentate)(unidentate)$_5$]: (a) $b = 1.1$; (b) $b = 1.2$; (c) $b = 2^{1/2}$ (not a discrete minimum)

At small normalized bites, stereochemistry B is a pentagonal bipyramid with the bidentate ligand spanning one of the pentagonal edges, and exists as a minimum on the potential energy surface at $\phi_B \approx 90°$, $\phi_C \approx 180°$. Above $b = 1.2$ this minimum divides into two minima (Figure 63) corresponding to two different orientations of stereochemistry C. These minima move further apart on further increasing b. A mirror plane is retained and the surface shown in Figure 63 is directly comparable with the much flatter surface calculated for [M(unidentate)$_7$], shown in Figure 54. As before, this continuous change in stereochemistry from the pentagonal bipyramid traverses the capped octahedron and capped trigonal prism (Figure 64). The capped octahedron is formed at $b = 1.32$, where B is the capping atom, and the capped trigonal prism occurs at $b = 1.48$.

Stereochemistry D exists as a potential energy minimum only above $b = 1.16$, and is reasonably well represented as a capped trigonal prism (Figure 61). There is negligible difference in energy between this capped trigonal prism (stereochemistry D$_1$) and the capped octahedron shown in Figure 61 (stereochemistry D$_2$). The difference in stereochemistry is also small.[264] The capped octahedral description rather than the more symmetrical capped trigonal prismatic description is expected to be favoured for complexes with a greater diversity of ligands.

2.4.2.2 *Comparison with experiment*

The peroxide ion behaves as a bidentate ligand in the complexes $[Nb(O_2)F_5]^{2-}$ and $[Ta(O_2)F_5]^{2-}$ and has a normalized bite $b \approx 0.74$. The structures of a number of salts have been determined and

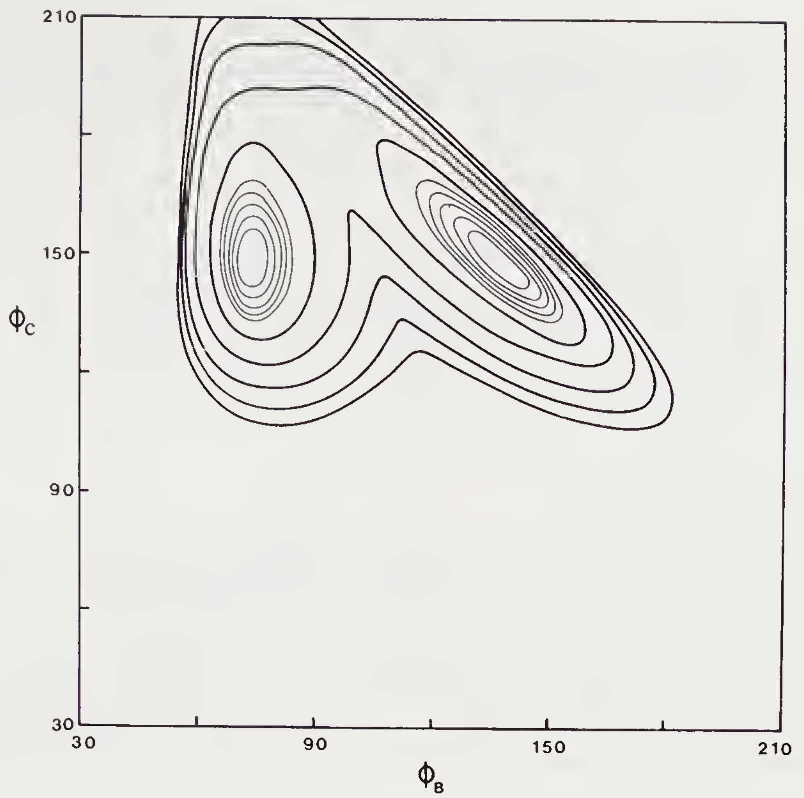

Figure 63 Projection of the potential energy surface for [M(bidentate)(unidentate)$_5$] on to the ϕ_B–ϕ_C plane (in degrees) with retention of a mirror plane. The five faint contour lines are for successive 0.02 increments in X above the minima, and the five heavy contour lines are for successive 0.2 increments above the minima. b = 1.4

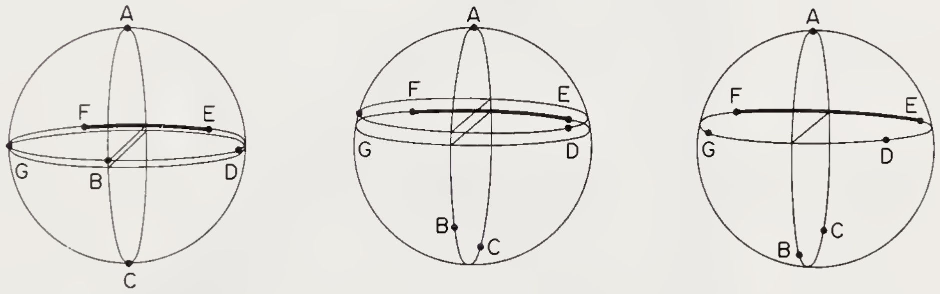

(a) (b) (c)

Figure 64 Stereochemistries B and C of [M(bidentate)(unidentate)$_5$]: (a) b = 1.0; (b) b = 1.3; (c) b = 1.5

they all contain pentagonal bipyramidal anions with the peroxide ligand spanning adjacent equatorial sites, that is stereochemistry B, which is in agreement with predictions.[272–274] The same structure is found for [Sn(NO$_3$)Ph$_2$(Me$_2$SO)$_3$](NO$_3$) containing the chelated nitrate group, b = 0.87.[275]

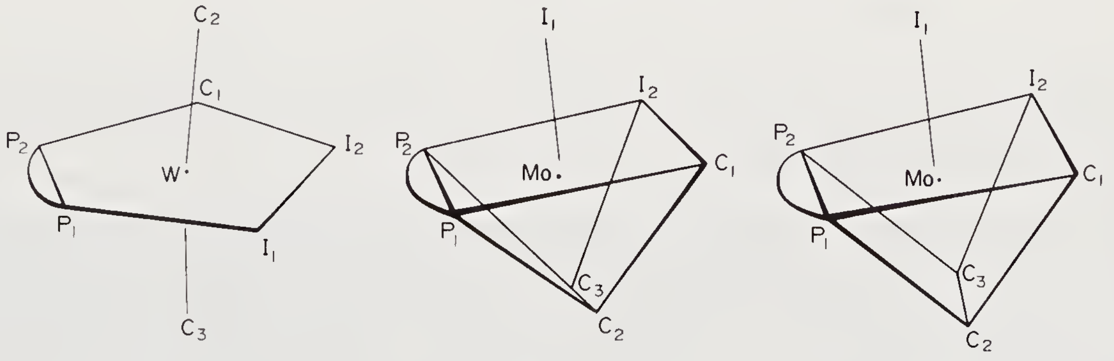

(a) (b) (c)

Figure 65 The stereochemistries of (a) [W(Ph$_2$PCH$_2$PPh$_2$)I$_2$(CO)$_3$]; (b) [Mo(Ph$_2$PCH$_2$CH$_2$PPh$_2$)I$_2$(CO)$_3$]·CH$_2$Cl$_2$; (c) [Mo(Ph$_2$PCH$_2$CH$_2$CH$_2$PPh$_2$)I$_2$(CO)$_3$]

At larger normalized bites, $b \approx 1.1-1.3$, that is, for ligands forming five- or six-membered chelate rings and/or having large atoms in the chelate rings, stereochemistries B, C and D are all observed. Stereochemistry B is found for a number of molybdenum isocyanide complexes, [Mo(Ph$_2$PCH$_2$PPh$_2$)(CNC$_6$H$_{11}$)$_5$](PF$_6$)$_2$,[276] [Mo(Ph$_2$PCH$_2$PPh$_2$)(CNMe)$_5$](PF$_6$)$_2$[277] and [Mo(Ph$_2$PCH$_2$CH$_2$PPh$_2$)(CNMe)$_5$](PF$_6$)$_2$.[277] Stereochemistry C is observed for [Ta(bipy)Cl$_2$Me$_3$].[278] The most common type of structurally characterized complex is the diphosphine or diarsine complex of molybdenum or tungsten, $[M(bidentate)X_2(CO)_3]$, where X is Cl, Br or I. The majority contain five- or six-membered chelate rings and can be adequately represented by stereochemistry D_1, with distortions depending on the particular mix of ligands present.[4] However, it does not follow that all such substituted carbonyl halides must be of stereochemistry D, as this potential energy minimum disappears at low *b*. It is therefore important to note that $[W(Ph_2PCH_2PPh_2)I_2(CO)_3]$, which has the lowest value of *b* for these compounds, has the pentagonal bipyramidal stereochemistry B. This point is further emphasized by Figure 65, which compares the stereochemistries of $[W(Ph_2PCH_2PPh_2)I_2(CO)_3]$, $[Mo(Ph_2PCH_2CH_2PPh_2)I_2(CO)_3]\cdot CH_2Cl_2$ and $[Mo(Ph_2PCH_2CH_2CH_2PPh_2)I_2(CO)_3]$; in all cases the metal–ligand bonds have been made equal, and the view is such that the chelate ring is on the same projection to the page.[279]

2.4.3 [M(Bidentate)$_2$(Unidentate)$_3$]

At large normalized bites, $b > \sim 1.2$, the repulsion energy calculations indicate that several structures are possible, which have been described in detail elsewhere.[4] However, at lower normalized bites one stereochemistry is significantly more stable than any other. For example, at $b = 1.1$, the three deep minima on the potential energy surface (Figure 66) correspond to the three possible orientations of the pentagonal bipyramid with both bidentate ligands spanning edges of the pentagon, with the three unidentate ligands in both of the axial sites and one of the equatorial sites. This surface should be compared with Figure 55 calculated for $[M(unidentate)_7]$.

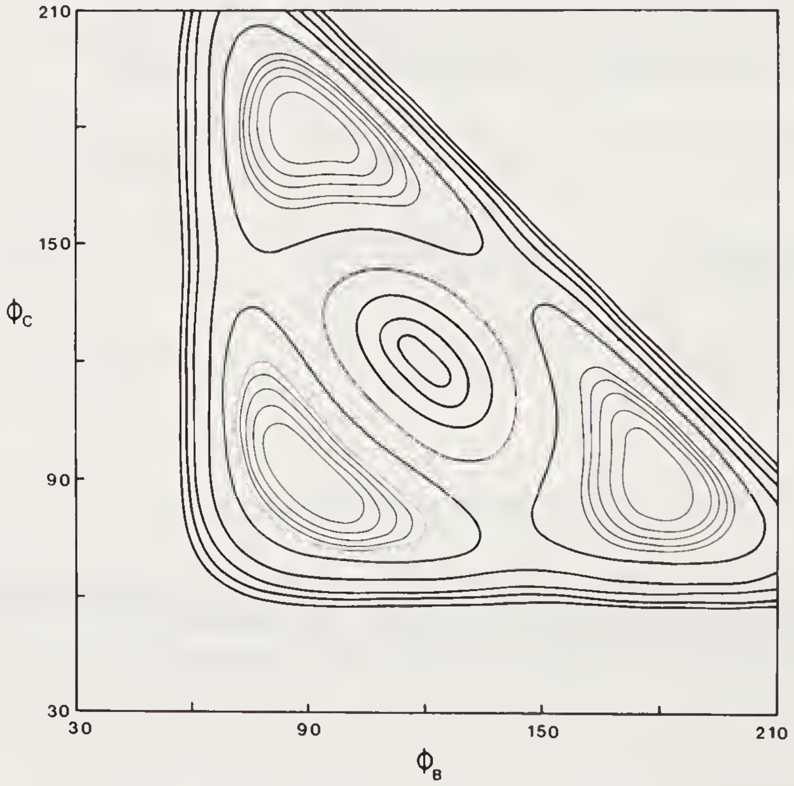

Figure 66 Projection of the potential energy surface for $[M(bidentate)_2(unidentate)_3]$ on to the ϕ_B–ϕ_C plane (in degrees) with retention of a mirror plane. The five faint contour lines are for successive 0.02 increments in *X* above the minima, and the five heavy contour lines for successive 0.2 increments above the minima. $b = 1.1$

There are a large number of molecules with this pentagonal bipyramidal structure. These include compounds with the peroxo three-membered chelate ring, $[Cr(O_2)_2(NH_3)_3]$[280] and $K_3[Cr(O_2)_2(CN)_3]$,[281] compounds with four-membered chelate rings such as $[Cd(NO_3)_2(C_5H_5N)_3]$,[282] $[Hg(O_2CCF_3)_2(C_5H_5N)_3]$,[283] $[Cd(O_2CC_6H_4OH)_2(C_5H_5N)_3]$[284] and $[Sm\{S_2P(OEt)_2\}_2(OPPh_3)_3][S_2P(OEt)_2]$,[285] and five-membered chelate rings as in $Cs[Ti(C_2O_4)_2(H_2O)_3]\cdot 2H_2O$.[286] This stereochemistry is also observed for a large number of dioxouranium complexes, $[U(bidentate)_2O_2(unidentate)]$.[4]

2.4.4 [M(Bidentate)$_3$(Unidentate)]

2.4.4.1 The theoretical stereochemistries

The repulsion energy calculations show the existence of three major stereochemistries. If the unidentate ligand A is placed at $\phi = 0$ and the bidentate ligands are labelled BC (with $\theta_B = 0$), DE and FG, the relation among the three stereochemistries is most readily depicted by projecting the potential energy surface on to the $\phi_D - \theta_D$ plane (Figure 67). The stereochemistries associated with the points indicated in Figure 67 are shown in Figure 68, and as polyhedra in Figure 69.

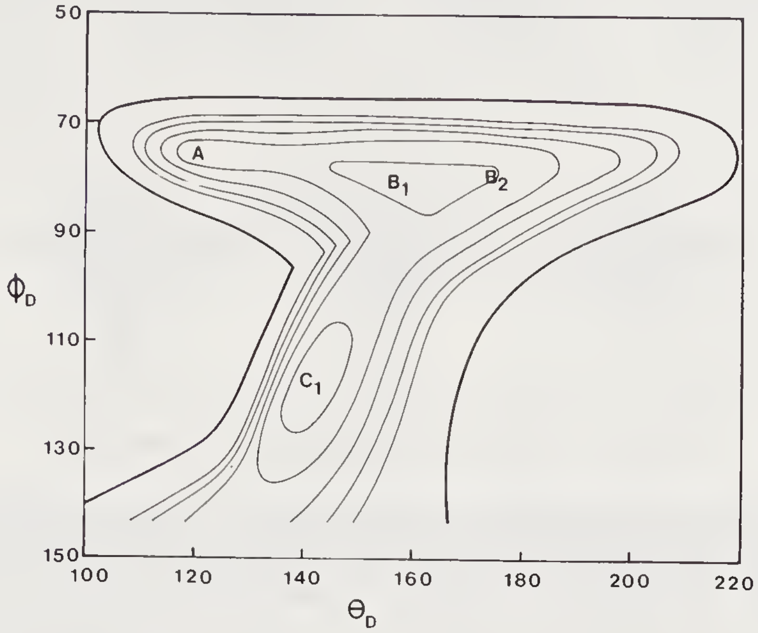

Figure 67 Projection of the potential energy surface for [M(bidentate)$_3$(unidentate)] on to the $\phi_D-\theta_D$ plane (in degrees). The five faint contour lines are for successive 0.02 increments in X above the minimum, and the heavy contour line is 0.2 above the minimum, at C_1. $b = 1.2$. The locations of stereochemistries A, B_1, B_2 and C_1 are indicated

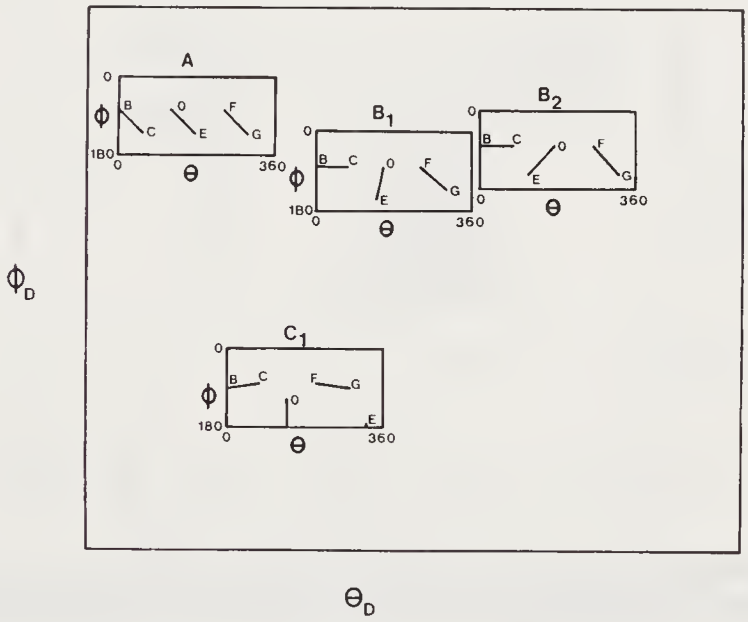

Figure 68 Projections of the four stereochemistries for [M(bidentate)$_3$(unidentate)] that were located in Figure 67. In all cases the unidentate ligand at $\phi = 0°$ is not shown

Stereochemistry A contains a threefold axis and is a capped octahedron with the unidentate ligand in the unique capping site. Stereochemistry B_1 contains no elements of symmetry and the polyhedron chosen to best describe the stereochemistry is somewhat arbitrary, two common examples being shown in Figure 69. However, the closely related stereochemistry B_2 contains a mirror plane which contains only the unidentate ligand (Figure 69). Stereochemistry C contains a mirror plane through ADE, and is intermediate between a pentagonal bipyramid (BCDFG as the pentagonal plane) and a capped trigonal prism (A the capping atom, BCFG as the capped face). As mentioned several times, this stereochemistry is also related to the capped octahedron, with D as the capping atom and CEF and ABG as the two triangular planes normal to the threefold axis. It is clear from the potential energy surface (Figure 67) that structures between these ideal limits are also expected.

The form of this potential energy surface is critically dependent on the effective bond length ratio *R*(unidentate/bidentate). As *R*(unidentate/bidentate) becomes less than unity, stereochemistry C becomes very stable, a typical potential energy surface being shown in Figure 70. Conversely, as *R*(unidentate/bidentate) increases, it is the other end of the potential energy trough that deepens,

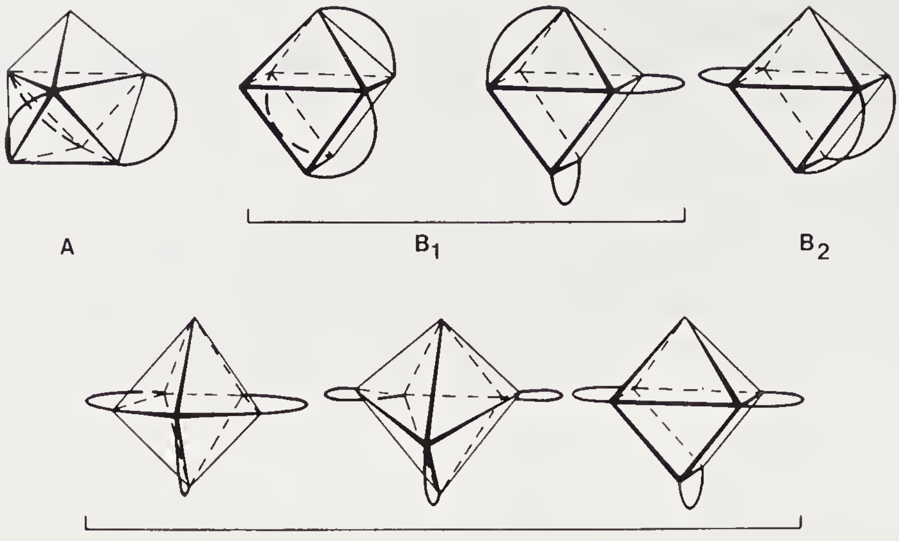

Figure 69 Stereochemistries for [M(bidentate)$_3$(unidentate)]

corresponding to the capped octahedron (Figure 71). The relative energies of these two limits, stereochemistry A and stereochemistry C, are shown in Figure 72. It can be seen that they are of comparable stabilities at very low values of R(unidentate/bidentate) (as well as at R(unidentate/bidentate) $\approx$ 1.0), which is of particular relevance when discussing [M(bidentate)$_3$(lone pair)].

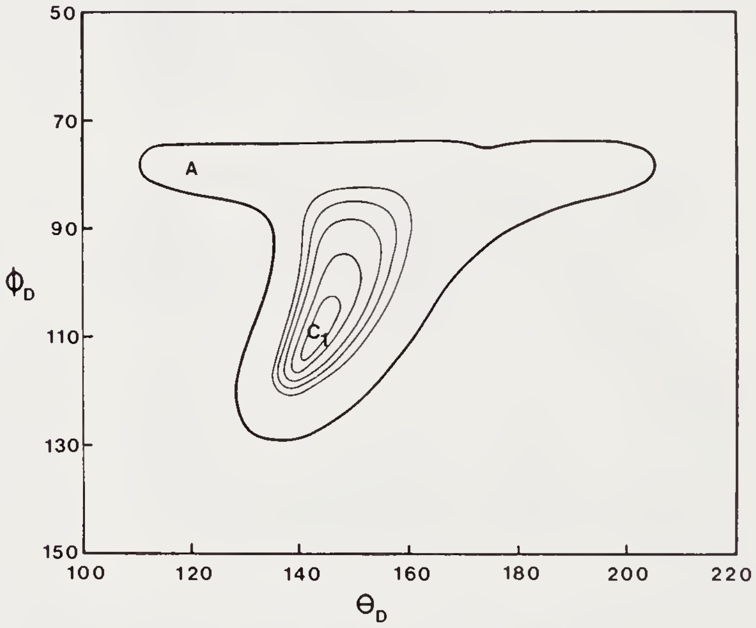

Figure 70 Projection of the potential energy surface for [M(bidentate)$_3$(unidentate)] on to the ϕ_D–θ_D plane (in degrees). The five faint contour lines are for successive 0.02 increments in X above the minimum, and the heavy contour line is 0.2 above the minimum, at C_1. b = 1.2, R(unidentate/bidentate) = 0.8. The locations of stereochemistries A and C_1 are indicated

2.4.4.2 Comparison with experiment

There are many known examples of all three of the stereochemistries predicted for [M(bidentate)$_3$(unidentate)], some typical examples being shown in Table 17. It is apparent that uncharged ligands such as H_2O, R_2CO and R_3N with R(unidentate/bidentate) < 1.0 favour stereochemistries A and B in agreement with Figure 71, whereas charged unidentate ligands such as Cl^-, Me^-, and O^{2-} with R(unidentate/bidentate) > 1.0 favour stereochemistry C in agreement with Figure 70.

The experimental bond angles for any compound can be fitted against those calculated as a function of b and R(unidentate/bidentate), and hence a value for the effective bond length ratio obtained.[264] For example, for the complexes [M(bidentate)$_3$(uncharged ligand)] in Table 17, the value of R(unidentate/bidentate) is close to unity, indicating no gross differences in bond type. However much lower values are obtained for charged ligands, as expected:

$R(X^-/\text{bidentate}) \sim 0.7$
$R(O^{2-}/\text{bidentate}) \approx 0.4$
$R(\text{lone pair/bidentate}) \approx 0.1$

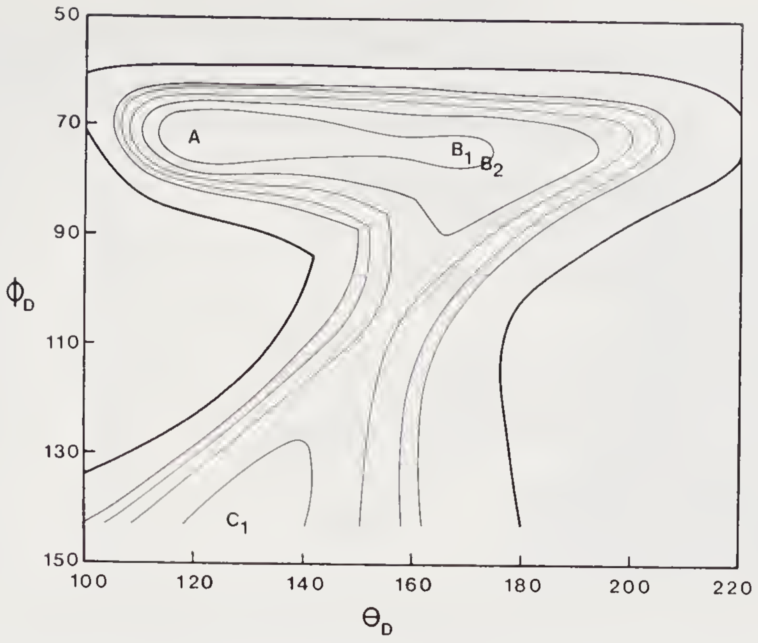

Figure 71 Projection of the potential energy surface for [M(bidentate)$_3$(unidentate)] on to the ϕ_D–θ_D plane (in degrees). The five faint contour lines are for successive 0.02 increments in X above the minimum, and the heavy contour line is 0.2 above the minimum, b = 1.2, R(unidentate/bidentate) = 1.2. The locations of stereochemistries A, B_1, B_2 and C_1 are indicated

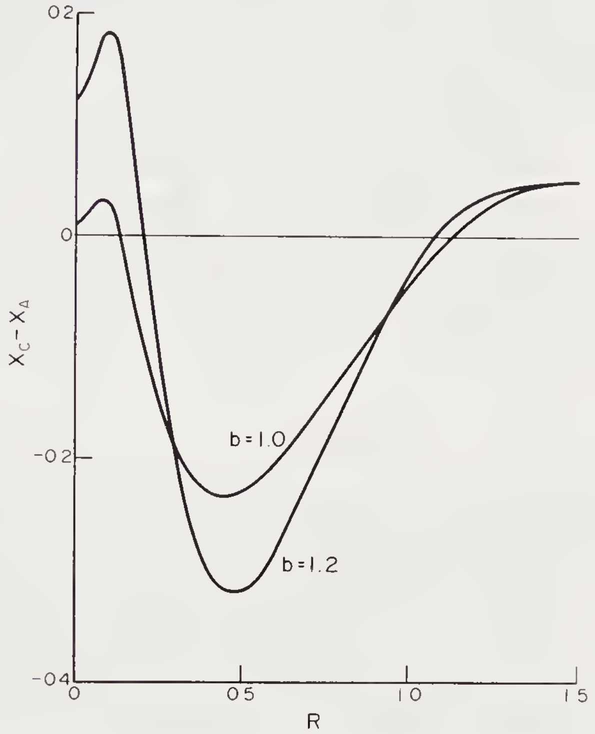

Figure 72 Repulsion energy coefficient of stereochemistry C relative to stereochemistry A of [M(bidentate)$_3$(unidentate)] as a function of R(unidentate/bidentate)

Table 17 Stereochemistries of Some [M(bidentate)$_3$(unidentate)] Complexes

Complex	*b*	*Ref.*
Stereochemistry A		
[P(S$_2$CNMe$_2$)$_3$(lone pair)]	1.13	287
[As(S$_2$CNEt$_2$)$_3$(lone pair)]	1.13	288
[Sb{S$_2$P(OPr)$_2$}$_3$(lone pair)]	1.18	289
[Bi{S$_2$P(OPr)$_2$}$_3$(lone pair)]	1.18	290
[Eu(Bu^{t}COCHCOBu^t)$_3$(NC$_7$H$_{13}$)]	1.18	291
[Ho(PhCOCHCOPh)$_3$(H$_2$O)]	1.21	292
[Y(PhCOCHCOMe)$_3$(H$_2$O)]	1.21	293
Stereochemistry B		
[Dy(Bu^{t}COCHCOBu^t)$_3$(H$_2$O)]	1.20	294
[Yb(MeCOCHCOMe)$_3$(H$_2$O)]·$\frac{1}{2}$C$_6$H$_6$	1.22	295
[Lu(Bu^{t}COCHCOBu^t)$_3$(NC$_5$H$_4$Me)]	1.22	296
[Yb(MeCOCHCOMe)$_3${MeCOCH=C(NH$_2$)Me}]	1.23	297
[Lu(C$_3$F$_7$COCHCOBu^t)$_3$(H$_2$O)]	1.23	298
[Yb(MeCOCHCOMe)$_3$(H$_2$O)]	1.24	299

Table 17 *continued*

Complex	*b*	*Ref.*
Stereochemistry C		
$[Sn(NO_3)_3Me]$		300
$[Co\{P(OCH_2)_3CMe\}_5][Co(NO_3)_3(NCMe)]$	0.98	301
$(Et_4N)[Pb(S_2COEt)_3(\text{lone pair})]$	1.00	302
$[Te(S_2CNEt_2)_3Ph]$	1.05	303
$[Sb(S_2COEt)_3(\text{lone pair})]\cdot \frac{1}{2}C_{10}H_8N_2$	1.07	304
$[Ta(S_2CNEt_2)_3S]$	1.11	305
$[Nb(S_2CNEt_2)_3O]$	1.11	306
$[Mo(S_2CNEt_2)_3N]$	1.11	307
$[Mo(S_2CNMe_2)_3(N_2Ph)]\cdot CH_2Cl_2$	1.12	308
$[V(S_2CNEt_2)_3O]$	1.13	306
$A_3[Sb(C_2O_4)_3(\text{lone pair})]\cdot 4H_2O$ $(A = NH_4, K)$	1.14	309
$[Ru(S_2CNMe_2)_3I](I_2)$	1.15	310
$[Sb(S_2PPh_2)_3(\text{lone pair})]$	1.18	311
$(NH_4)_3[Nb(C_2O_4)_3O]\cdot H_2O$	1.19	312
$[Sn(O_2C_7H_5)_3Cl]CHCl_3$	1.20	313
$[Zr(MeCOCHCOMe)_3Cl]$	1.25	314

The expected asymmetries of the bidentate ligands in compounds of stereochemistries A and C are fairly independent of *b*, but increase as *R*(unidentate/bidentate) decreases (Figure 73). The predicted behaviour is experimentally observed. For compounds containing uncharged unidentate ligands the bonding of the bidentate ligands is fairly symmetric, but markedly unsymmetric in compounds containing a lone pair of electrons, with low *R*(lone pair/bidentate) values. For example, in compounds with stereochemistry A, the interaction with the lone pair lengthens the three bonds *cis* to it, as expected from $Y_B/Y_C > 1.0$:

$[P(S_2CNMe_2)_3(\text{lone pair})]$	MB/MC = 1.36
$[As(S_2CNEt_2)_3(\text{lone pair})]$	MB/MC = 1.21
$[Sb\{S_2P(OPr)_2\}_3(\text{lone pair})]$	MB/MC = 1.19
$[Bi\{S_2P(OPr)_2\}_3(\text{lone pair})]$	MB/MC = 1.06

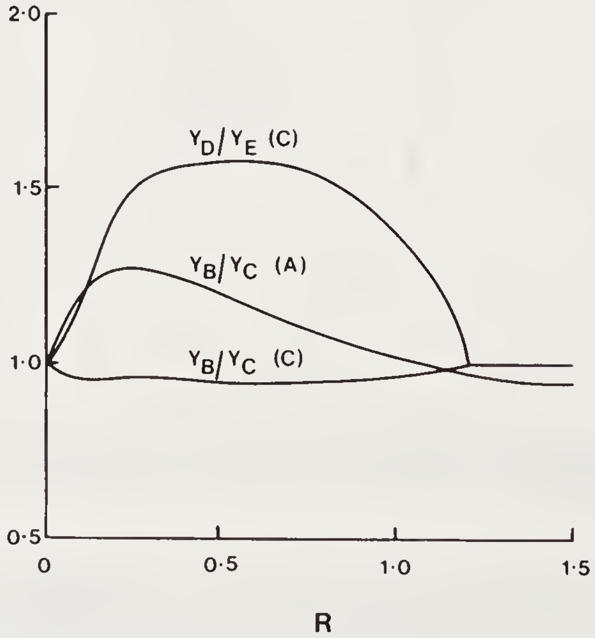

Figure 73 Ratio of the individual atom repulsion coefficients for the two ends of each bidentate ligand in stereochemistries A and C of [M(bidentate)$_3$(unidentate)] as a function of *R*(unidentate/bidentate). $b = 1.2$

Figure 73 shows that for compounds with stereochemistry C, the BC (and FG) bidentate ligand will be more symmetrically bonded than the DE bidentate ligand, $Y_B/Y_C < 1.0$ and $Y_D/Y_E \gg 1.0$. These predicted distortions are again observed, for example:

$(Et_4N)[Pb(S_2COEt)_3(\text{lone pair})]$	MB/MC = 0.96	MD/ME = 1.12
$[Sb(S_2COEt)_3(\text{lone pair})]\cdot \frac{1}{2}C_{10}H_8N_2$	MB/MC = 0.91	MD/ME = 1.25
$A_3[Sb(C_2O_4)_3(\text{lone pair})]\cdot 4H_2O$ $(A = NH_4, K)$	MB/MC = 0.97	MD/ME = 1.11
$[Sb(S_2PPh_2)_3(\text{lone pair})]$	MB/MC = 0.88	MD/ME = 1.30

Stereochemistry C is intermediate between a pentagonal bipyramid and a capped trigonal prism, and the repulsion energy calculations show that as the normalized bite increases, the bidentate ligand DE progressively swings further away from the pentagonal bipyramid position towards the capped trigonal prism position. This rotation as a function of normalized bite is shown in the isomorphous pair [Nb(S_2CNEt_2)$_3$O] and [V(S_2CNEt_2)$_3$O],[306] where the decrease in metal–sulfur distance from 2.60 to 2.50 Å results in an increase in normalized bite from 1.11 to 1.13. The decrease in ϕ_D and ϕ_E, as measured by the O═M—S angles, is from 95° to 98° and from 161° to 166°, respectively (Figure 74).

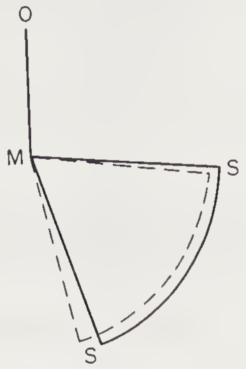

Figure 74 MADE geometry in [Nb(S_2($CNEt_2$)$_3$O] (——) and [V(S_2CNEt_2)$_3$O] (- - -)

2.5 EIGHT-COORDINATE COMPOUNDS

2.5.1 [M(Unidentate)$_8$]

The starting point for the consideration of eight coordination is the following three structures:

square antiprism: $X = 5.185$
triangular dodecahedron: $X = 5.245$
cube: $X = 5.758$

The two most stable structures, the square antiprism and the dodecahedron, are considered in more detail below. The square antiprism is observed to be much more common than the dodecahedron, in agreement with the above repulsion energy coefficients.

2.5.1.1 *The square antiprism*

The square antiprism is shown in Figure 75. All ligand sites are identical, and the stereochemistry is completely defined by α, the angle the eight metal–ligand bonds make with the fourfold axis. It should be noted that there is also a twofold axis passing through the midpoint of every edge connecting triangular faces, the symmetry being D_{4d}.

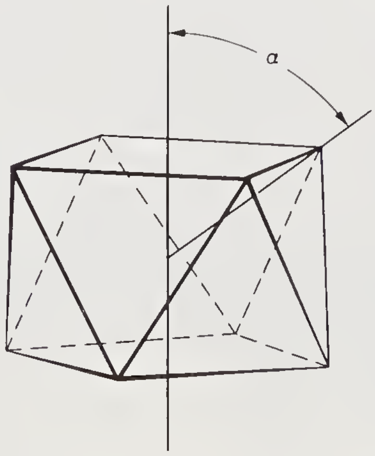

Figure 75 The square antiprism

For a square antiprism based on equal edge lengths (the hard sphere model) and all metal–ligand bond lengths equal to r, $\alpha = 59.26°$ and the edge length is $1.2156r$. However, the stereochemistry of the polyhedron calculated by minimization of the repulsion energy is elongated along the major axis, $\alpha = 57.1°$, with a contraction of the larger square faces. This predicted small decrease in α from 59.3° to about 57° is observed in those square antiprismatic molecules whose structure has been precisely determined (Table 18).

Table 18 Square Antiprismatic [M(unidentate)$_8$]

Complex	*α (°)*	*Ref.*
$H_4[W(CN)_8]\cdot 6H_2O$	57.6	315
$Na_3[W(CN)_8]\cdot 4H_2O$	59.1	316
$H_4[W(CN)_8]\cdot 4HCl\cdot 12H_2O$	56.1	317
$[Nd(ONC_5H_5)_8](ClO_4)_3$	56.1	318
$[Sr(H_2O)_8](AgI_2)_2$	58.2	319
$[Cu(H_2O)_6]_2[ZrF_8]$	57.1	320
$Cs_4[U(NCS)_8]$	56.7	321
$Na_3[TaF_8]$	—	322
$Cd_2[Mo(CN)_8]\cdot 2N_2H_4\cdot 4H_2O$	—	323
$[La\{OC(CHCMe)_2O\}_8](ClO_4)_3$	—	324
$[Sr(H_2O)_8]_2(Bi_2Br_{10})$	—	325
$[Y(H_2O)_8](Tc_2Cl_8)\cdot H_2O$	—	326

2.5.1.2 *The dodecahedron*

The dodecahedron is shown in Figure 76. One set of four donor atoms is necessarily different from the other set of four donor atoms. The four A atoms constitute a tetrahedron that has been elongated along the fourfold inversion axis. The set of B atoms form a tetrahedron that has been squashed along the same axis, creating a puckered square interposed between the two pairs of A atoms. A twofold axis passes through the midpoint of each B—B edge, the symmetry being D_{2d}. An alternative useful way of viewing the dodecahedron is to consider it as two interpenetrating planar trapezoids, $B_1A_1A_2B_2$ and $B_3A_3A_4B_4$, which are at right angles to each other (Figure 76).

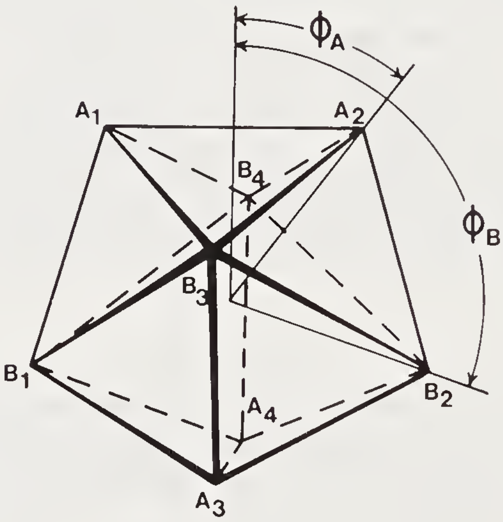

Figure 76 The dodecahedron

The detailed geometry of the dodecahedron is described by two angular variables, ϕ_A and ϕ_B, the angles the M—A and M—B bonds make with the fourfold inversion axis, and the bond length ratio MA/MB (Figure 76).

For a 'hard sphere model', and all metal–ligand distances equal to r, A—A = A—B = $1.1993r$, but $B{-}B = 1.4986r = 1.2496A{-}A$, so that there are significant holes in the structure along the B—B edges. For this hard sphere model, $\phi_A = 36.85°$ and $\phi_B = 110.54°$. However, the repulsion energy calculations predict a further flattening of the B_4 tetrahedron, the minimum occurring at $\phi_A = 37.3°$, $\phi_B = 108.6°$ with a shortening of the long B—B edges. This distortion is observed for $K_4[Mo(CN)_8]\cdot 2H_2O$ ($\phi_A = 36.0°$, $\phi_B = 107.1°$)[327] and $(Bu_4N)_3[Mo(CN)_8]$ ($\phi_A = 37.2°$, $\phi_B = 107.5°$),[328] but the larger distortion observed for $[Gd(H_2(O)_8]Cl_3\cdot 2C_{10}H_8N_2$[329] and $[Y(H_2O)_8]Cl_3\cdot 2C_{10}H_8N_2$[330] is at least partly attributable to the strong hydrogen-bonding network.

2.5.1.3 *Relations between the square antiprism, dodecahedron and cube*

The general stereochemistry is shown in Figure 77. The points are arranged in two sets of four, with a D_2 axis passing through the metal atom.

The potential energy surface projected onto the θ_A–θ_B plane is shown in Figures 78a and 78b. The centre of the surface, at $\theta_A = \theta_B = 45°$, corresponds to the dodecahedron, labelled D_1. Distortion of this dodecahedron by decreasing θ_A to 30.9° and increasing θ_B to 55.3° produces a square antiprism (A_1) with $A_1B_1A_4B_4$ and $A_2B_2A_3B_3$ comprising the two square faces. The potential

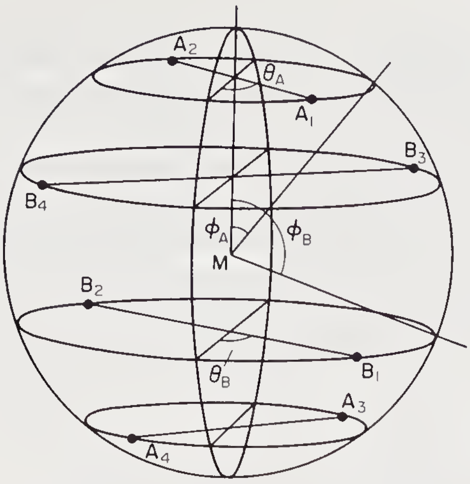

Figure 77 General stereochemistry for [M(unidentate)$_8$]

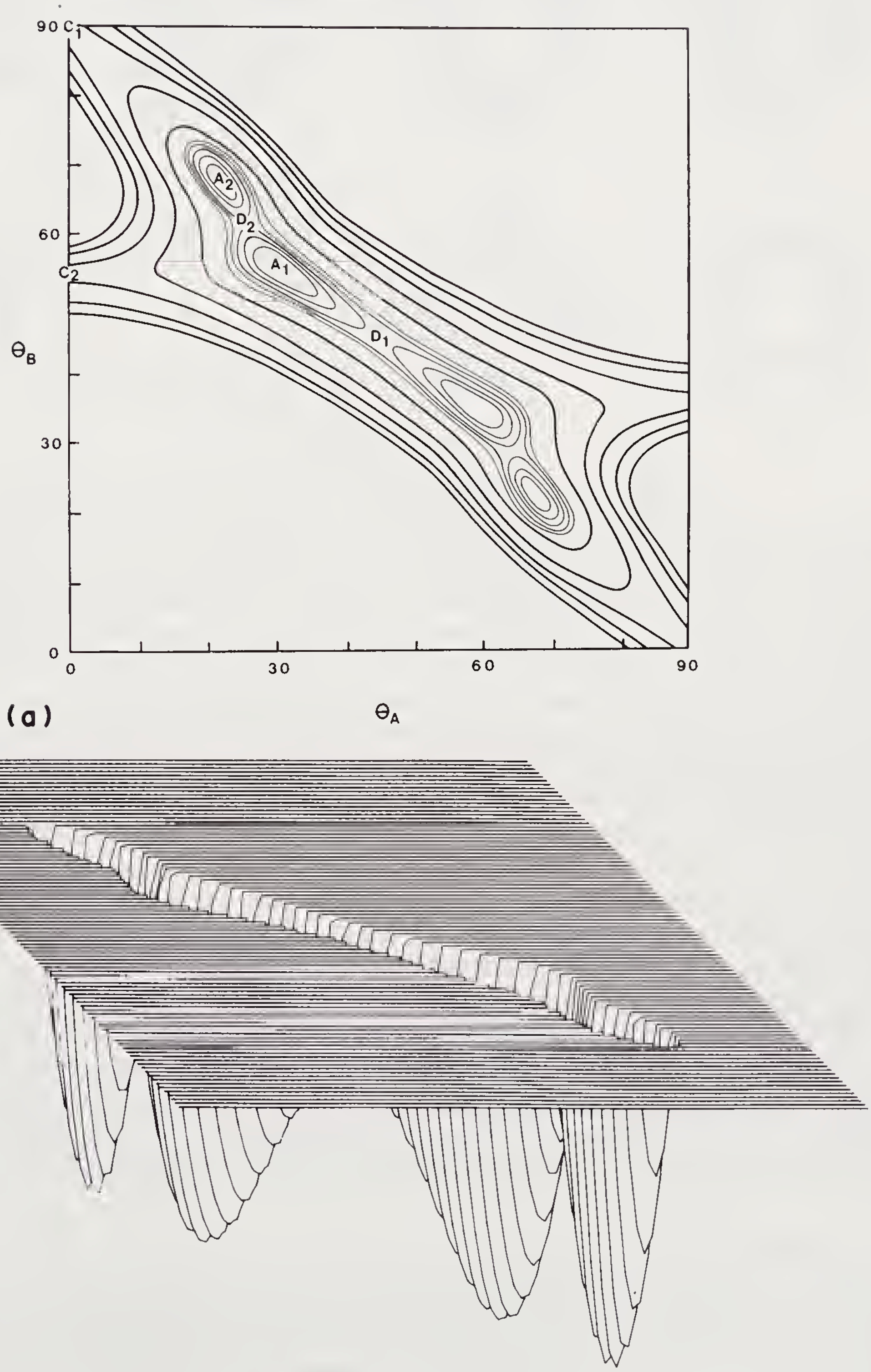

Figure 78 (a) Projection of the potential energy surface for [M(unidentate)$_8$] on to the θ_A–θ_B plane (in degrees). The five faint contour lines are for successive 0.02 increments in X above the minima, and the five heavy contour lines are for successive 0.2 increments above the minima. The locations of the dodecahedra (D), square antiprisms (A) and cubes (C) are shown. (b) As in (a), but with truncation at X = 0.1

energy surface is symmetrical about D_1, since the A_1A_2 atoms can be twisted away from 90° relative to the A_3A_4 atoms in either a clockwise or anticlockwise direction. Further continuation along the reaction coordinate in Figure 78a generates an alternative dodecahedron D_2 at $\theta_A = 25.5°$ and $\theta_B = 61.7°$, which is identical to the original dodecahedron D_1 but with the A and B labels interchanged. This dodecahedron is then converted into a square antiprism A_2, at $\theta_A = 22.5°$ and $\theta_B = 67.5°$, the square faces being $A_1B_3A_2B_4$ and $A_3B_2A_4B_1$. Continuation up this potential energy valley in the same direction to $\theta_A = 0$ and $\theta_B = 90°$ leads to the cube, labelled C_1. Moving up a different potential energy valley from the first square antiprism leads to the cube C_2 and $\theta_A = 0$ and $\theta_B = 54.7°$. Direct distortion from the dodecahedron D_1 to a third cube, C_3, also situated at $\theta_A = \theta_B = 45°$, can also occur. Views of the polyhedra corresponding to D_1, A_1, D_2, A_2, C_1, C_2, and C_3 are shown in Figure 79.

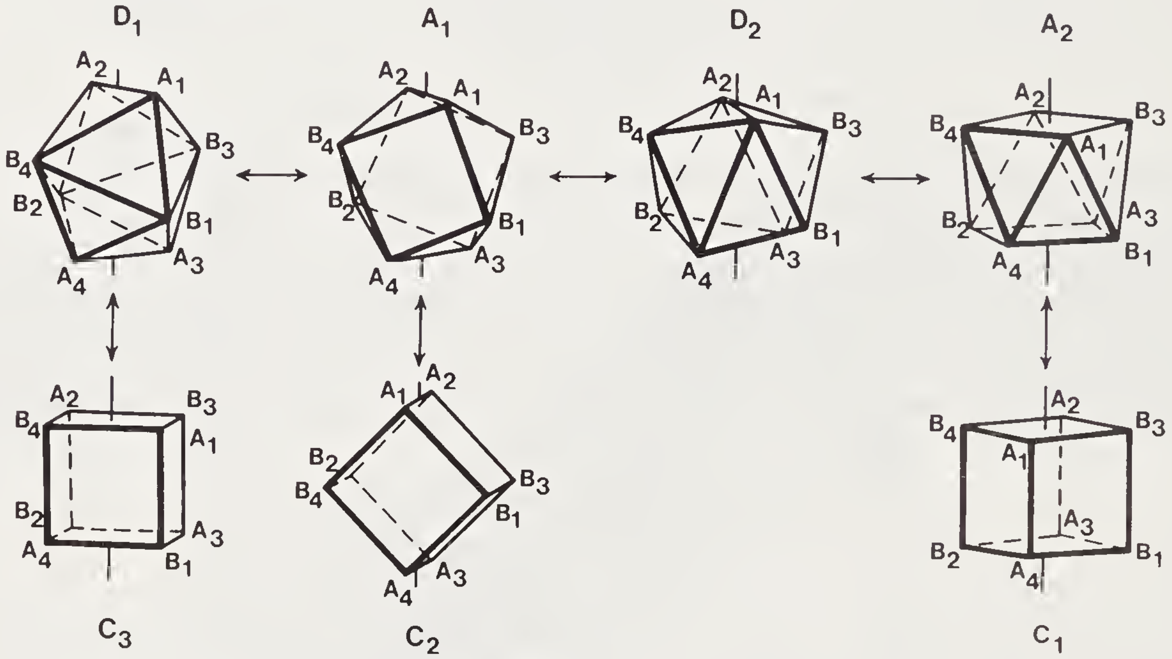

Figure 79 The relation between the polyhedra corresponding to Figure 78

Potential energy surfaces of the type shown in Figures 78a and 78b indicate that structures intermediate between a square antiprism and a dodecahedron might be expected, with smaller distortions in the direction of a cube also permitted. The octacyanomolybdate anion has been observed as both a square antiprism and a dodecahedron (see above), but in $(Et_3NH)_2(H_3O)_2[Mo(CN)_8]$ appears to be approximately midway between these structures.[331] In $Li_6(BeF_4)[ZrF_8]$,[332] the dodecahedral structure is distorted towards the C_3 cube, the most obvious reason for the distortion being interaction with the lithium ions which lie outside all the A—B edges, but not outside the A—A or B—B edges. In contrast to $Cs_4[U(NCS)_8]$, which is close to the ideal square antiprism (Table 18), the structure of the tetraethylammonium salt, $(Et_4N)_4[U(NCS)_8]$,[333] is cubic. This cubic structure is not retained in solution. The structure must be attributed to the tetraethylammonium groups, which are disordered and sit outside each face of the cube so that half-ethyl groups are projected between every pair of thiocyanate groups. Cubic stereochemistry is also found in Na_3PaF_8.[334] The structure is closely related to the fluorite structure, with both sodium and protactinium occupying the cubic sites.

The potential energy surface in Figures 78a and 78b shows that there is no potential barrier between the square antiprism and dodecahedron, and very rapid rearrangements may be expected. As shown above, the structures of $[M(CN)_8]^{4-}$ and $[M(CN)_8]^{3-}$ where M is Mo or W, in the solid state may be square antiprismatic, dodecahedral or an intermediate stereochemistry. In solution, only a single ^{13}C NMR signal is observed for $[Mo(CN)_8]^{4-}$ in $CH_2Cl_2{-}CHClF_2$ mixtures at temperatures as low as −165 °C, consistent with very rapid intramolecular rearrangements.[335]

2.5.1.4 *[M(unidentate A)$_x$(unidentate B)$_{8-x}$]*

It has been shown above that for eight equivalent unidentate ligands, the square antiprism is slightly more stable than the dodecahedron. However, the energy difference is not large, leading to the occurrence of both structures in the solid state. A major difference between the square antiprism and the dodecahedron is that the former has eight identical ligand sites, whereas the dodecahedron has four A sites associated with higher repulsion energy than the four B sites. It follows that for compounds of the type [M(unidentate A)$_x$(unidentate B)$_{8-x}$], in which there are significant differences between the two types of ligand, the sorting into the appropriate A and B sites may stabilize the dodecahedron relative to the square antiprism.

Charged monoatomic ligands such as halide, with short effective bond lengths, are expected to occupy preferentially the B sites of a dodecahedron, as observed for $[UCl(OCHNMe_2)_7]_2[UO_2Cl_4]_3$[336] and $[ThCl_4(OSPh_2)_4]$.[337] On the other hand, $[EuCl_2(OH_2)_6]Cl$[338] retains the square antiprismatic structure. The thiocyanate ion has an effective bond length similar to that of uncharged ligands, and complexes such as $[U(NCS)_4\{OP(NMe_2)_3\}_4]$ also have the square antiprismatic structure.[339]

The stabilization of the dodecahedron for complexes of the type [M(unidentate A)$_4$(unidentate B)$_4$] is shown by the potential energy surface in Figure 80, calculated for the effective bond length ratio $R(A/B) = 1.20$. Figure 80 is directly comparable to Figure 78a, in which all metal–ligand bonds were equal. Figure 80 clearly shows that the dodecahedron at $\theta_A = \theta_B = 45°$ has been stabilized relative to all other stereochemistries, and corresponds to the long bonds occupying the A sites of the dodecahedron. Conversely, the dodecahedron at $\theta_A \approx 29°$ and $\theta_B \approx 58°$, corresponding to the long bonds occupying the B sites, has been significantly destabilized. There is a smooth change in stereochemistry from the square antiprism to the dodecahedron as $R(A/B)$ is increased from 1.0 to 1.2.

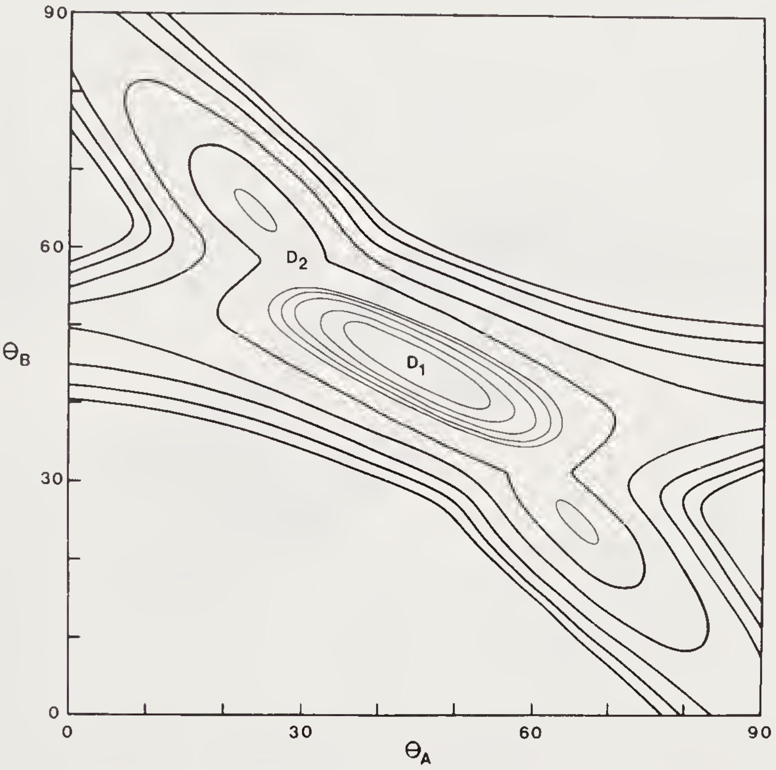

Figure 80 Projection of the potential energy surface for [M(unidentate A)$_4$(unidentate B)$_4$] on to the θ_A–θ_B plane (in degrees). The five faint contour lines are for successive 0.02 increments in X above the minimum, and the five heavy contour lines are for successive 0.2 increments above the minimum, at D_1. $R(A/B) = 1.2$. The positions of the dodecahedra D_1 and D_2 are shown

2.5.2 [M(Bidentate)$_2$(Unidentate)$_4$]

With values of the normalized bite from 1.20 to 1.25, which are appropriate for the bidentate ligands fitting along various edges of polyhedra calculated for [M(unidentate)$_8$], seven separate isomers have been located as potential energy minima. These are most readily envisaged as various ways of arranging ligands along the edges of distorted square antiprisms (isomers A–F), or a distorted dodecahedron (isomer G) (Figure 81). These seven isomers all contain some elements of symmetry, namely three twofold axes in isomer A, one twofold axis in isomers B, E and F, a twofold axis and two mirror planes in isomer D, and one mirror plane in isomers C and G. Both bidentate ligands are symmetrical and equivalent and all four unidentate ligands are equivalent only in isomers A and D.

Potential energy surfaces analogous to that shown in Figure 78a for [M(unidentate)$_8$] may be calculated for isomer A if the chelate rings span the A_1A_2 and A_3A_4 edges shown in Figure 77. At large normalized bites (Figure 82), the minima correspond to the above square antiprism, but these minima progressively move closer together as b is reduced, until a single minimum is obtained at $\theta_A = \theta_B = 45°$ (Figure 83), corresponding to a dodecahedron with the bidentate ligands spanning the two A—A edges, and the four unidentate ligands occupying the B sites. The dodecahedron is additionally stabilized by the effect examined in Section 2.5.1.4, decreasing the effective bond length to the unidentate ligands, R(unidentate/bidentate).

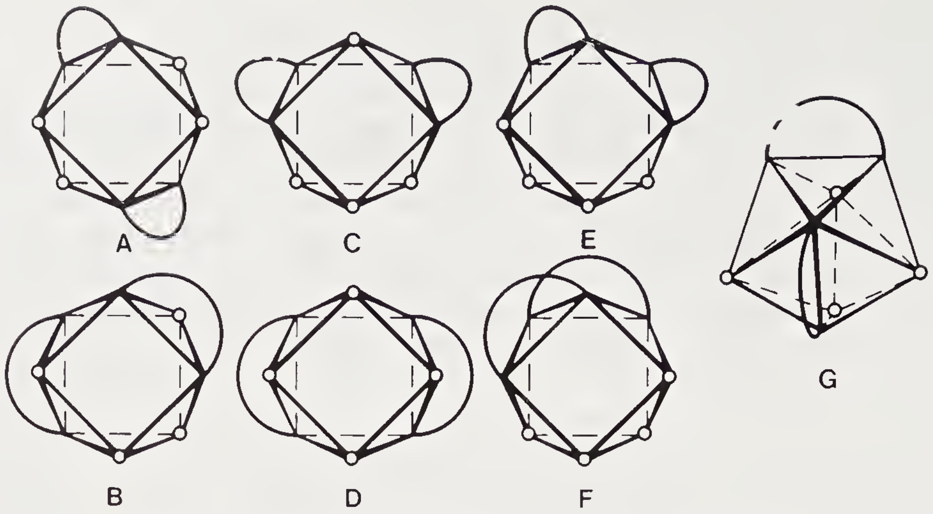

Figure 81 Stereochemistries for [M(bidentate)$_2$(unidentate)$_4$]

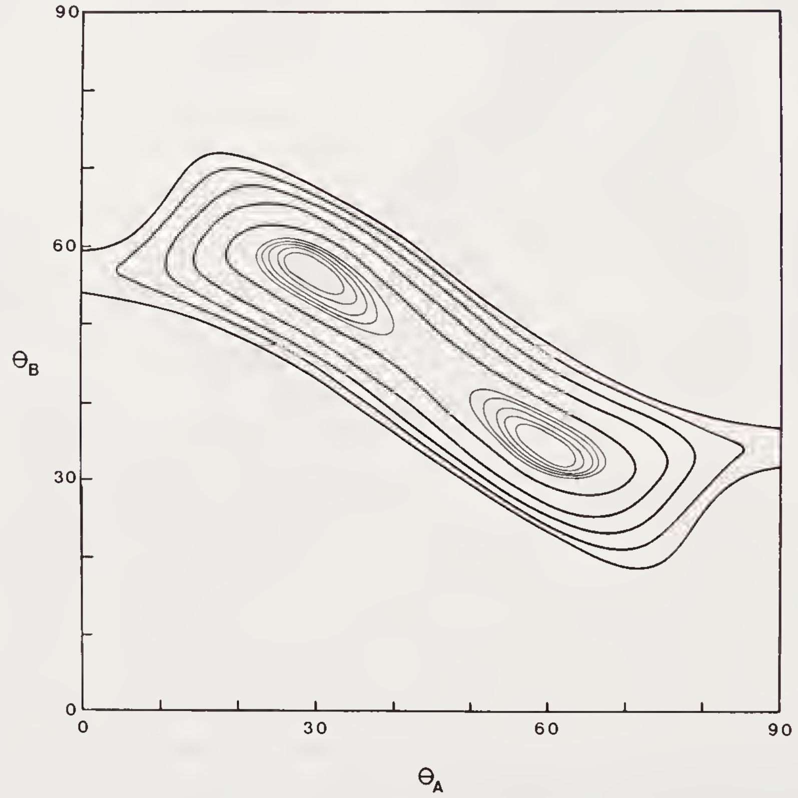

Figure 82 Projection of the potential energy surface for isomer A of [M(bidentate)$_2$(unidentate)$_4$] on to the θ_A–θ_B plane (in degrees). The five faint contour lines are for successive 0.02 increments in X above the minima, and the five heavy contour lines are for successive 0.2 increments above the minima. b = 1.3

Similar changes occur in the stereochemistries of the other isomers as b is reduced. Isomer B distorts towards a dodecahedron where one trapezoid is formed from the bidentate ligands, and one from the four unidentate ligands. At low b, isomer C approximates to a bicapped trigonal prism, with the bidentate ligands spanning edges linking capping sites and prism sites. Isomer D also forms a bicapped trigonal prism, but with the two bidentate ligands forming the uncapped rectangular face of the prism. Isomers E and F are converted into isomer D below $b = 1.0$. The stereochemistry of isomer G is relatively insensitive to the value of b.

The relative energies of each of these isomers, and also its range of existence as a discrete potential energy minimum, are shown in Figure 84. Isomers A, C and E are of equal stability at $b = 1.26$, which is the value appropriate for bidentate ligands spanning the non-square edges of a square antiprism, and isomers B, D and F are of equal stability at $b = 1.19$, corresponding to the square edges of a square antiprism.

This order of stability changes dramatically at R(unidentate/bidentate) < 1.0, where isomer A is greatly stabilized with respect to all other isomers (Figure 85). This stereochemistry will therefore be strongly stabilized for charged unidentate ligands.

All tetrahalo complexes [M(bidentate)$_2$X$_4$]$^{x\pm}$ are observed to have stereochemistry A as predicted. The diarsine ligands in [M{C$_6$H$_4$(AsMe$_2$)$_2$}$_2$X$_4$]$^{x+}$, where M is Ti^{IV}, Nb^{IV}, Nb^{V}, Ta^{V}, Mo^{V}

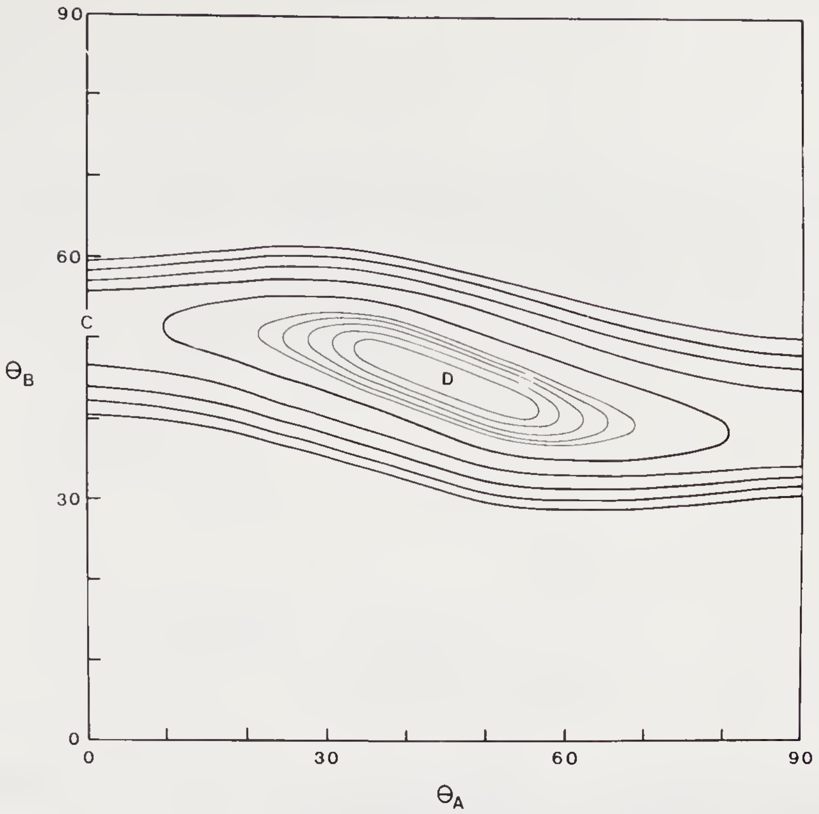

Figure 83 Projection of the potential energy surface for isomer A of [M(bidentate)$_2$ (unidentate)$_4$] on to the $\theta_A-\theta_B$ plane (in degrees). The five faint contour lines are for successive 0.02 increments in X above the minimum, and the five heavy contour lines are for successive 0.2 increments above the minimum, at D. b = 0.9. The locations of the dodecahedron (D) and 'cube' (C) are indicated

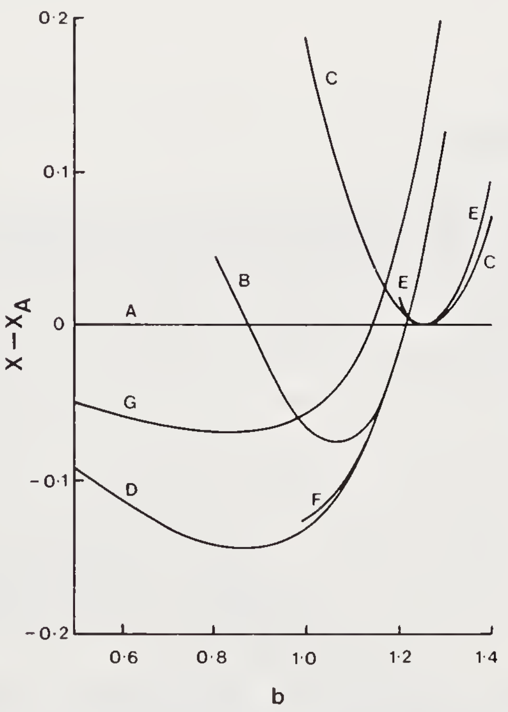

Figure 84 Repulsion energy coefficients for [M(bidentate)$_2$(unidentate)$_4$] stereochemistries relative to those for stereochemistry A, as a function of normalized bite, b. R(unidentate/bidentate) = 1.0

or Tc^V and X is Cl or Br,[340–345] span the two A—A edges of a dodecahedron and range in normalized bite from 1.18 to 1.23, depending on the metal atom and its oxidation state. The complexes $(Me_4P)[Ta(Me_2PCH_2CH_2PMe_2)_2Cl_4]_3Cl_4{\cdot}4Me_2S$ and $[Ta(Me_2PCH_2CH_2PMe_2)_2Cl_4]$, b = 1.18 and 1.20 respectively, are likewise stereochemistry A, but now the tantalum(V) complex is dodecahedral whereas the tantalum(IV) complex is closer to square antiprismatic.[346] Isomer A is also observed, for example, in $[Th\{OP(NMe_2)_2OP(NMe_2)_2O\}_2Cl_4]$,[347] $[Zr(bipy)_2(NCS)_4]$ [348] and $[U(Me_2PCH_2CH_2PMe_2)_2(OPh)_4]$.[349] Examples of other isomers are listed below:

isomer B:	$[U\{OP(NMe_2)_2OP(NMe_2)_2O\}_2(NCS)_4]$[347]	b = 1.16
isomer C:	$[Ca(picrate)_2(H_2O)_4]{\cdot}H_2O$[350]	b = 1.06
isomer D:	$[W\{ONN(Me)O\}_2Me_4]$[351]	b = 1.14
isomer G:	$[Ca(NO_3)_2(MeOH)_4]$[352]	b = 0.85

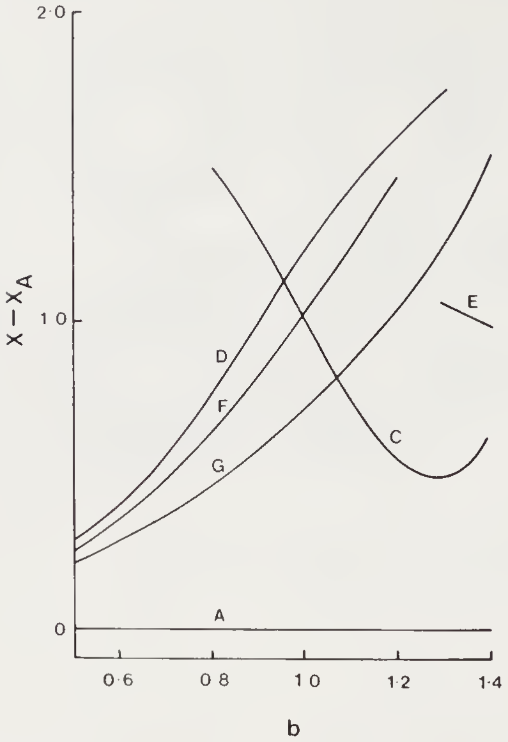

Figure 85 Repulsion energy coefficients for [M(bidentate)$_2$(unidentate)$_4$] stereochemistries relative to those for stereochemistry A, as a function of normalized bite, *b*. *R*(unidentate/bidentate) = 0.75

2.5.3 [M(Bidentate)$_3$(Unidentate)$_2$]

Eight-coordinate compounds containing three bidentate ligands can be classified into the following three types, depending on the normalized bite of the bidentate ligands:

1. $b < \sim 0.9$. These compounds are all of hexagonal bipyramidal stereochemistry, with a linear unidentate–metal–unidentate group. The hexagonal plane formed by the three bidentate ligands may be slightly puckered. This structure is observed for $(Me_4N)[Pb(O_2CMe)_3Ph_2]$[353] and a number of dioxouranium complexes with bidentate ligands that form four-membered chelate rings, such as acetate, nitrate, carbonate and dithiocarbamate.[4]
2. $b \approx 1.1-1.2$. These compounds are adequately described as distorted square antiprisms or distorted dodecahedra. There are 17 different ways (not counting optical isomers) three bidentate ligands can be arranged around the edges of a square antiprism or a dodecahedron (excluding the longer B—B edges). These structures are common for a number of lanthanoid β-diketonate complexes that form six-membered chelate rings, [Ln(RCOCHCOR)$_3$(unidentate)$_2$].[4]
3. $b \approx 1.0$. The only example of intermediate normalized bite is found in $[Nb(O_2CNMe_2)_5]$, in which two of the carbamate ligands act only as unidentate ligands.[354] This structure is very unusual and can be described as two interpenetrating pentagons (Figure 86). However, the repulsion energy calculations show that it is predicted to form from one of the square antiprismatic isomers of [M(bidentate)$_3$(unidentate)$_2$] as the normalized bite is reduced from ~1.2 to ~1.0.[4]

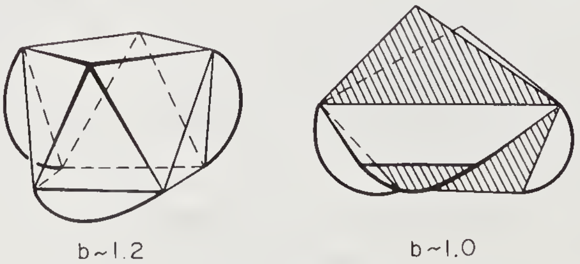

Figure 86 The change in stereochemistry from a square antiprism to two interpenetrating pentagons as *b* is reduced for one of the possible isomers of [M(bidentate)$_3$(unidentate)$_2$]

2.5.4 [M(Bidentate)$_4$]

2.5.4.1 *The theoretical stereochemistries*

The general stereochemistry is the same as that shown (Figure 77), with the added condition that bidentate ligands span the A_1B_1, A_2B_2, A_3B_3 and A_4B_4 edges. Representative potential energy surfaces are shown in Figures 87–90, and are directly comparable with those calculated above (Figures 78a and 80). The minima on the potential energy surfaces correspond to three different stereochemistries, the relative stabilities of which depend on the choice of normalized bite *b*.

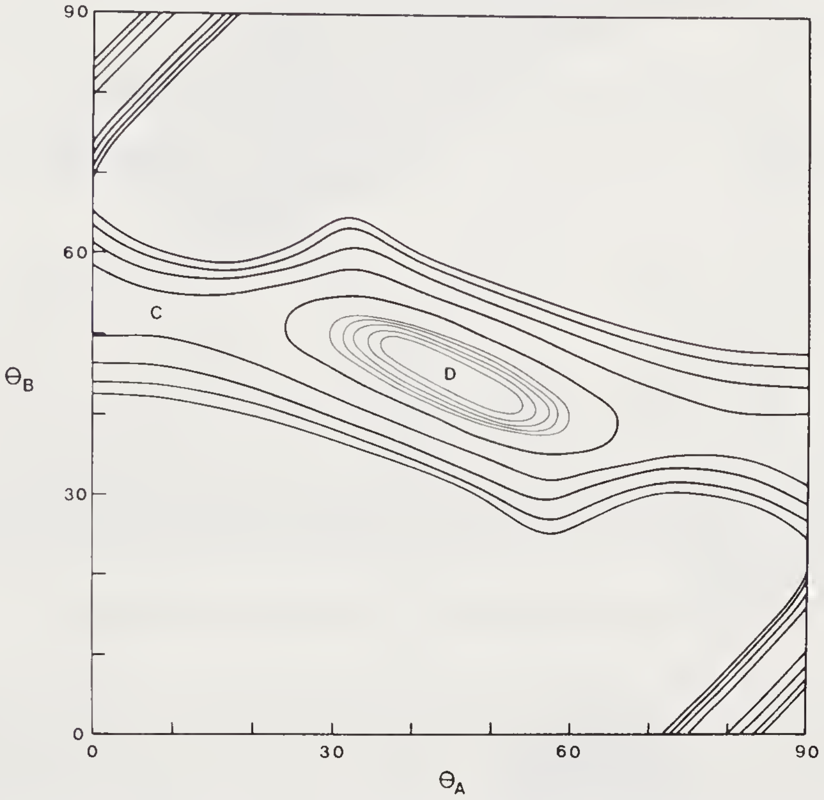

Figure 87 Projection of the potential energy surface for [M(bidentate)$_4$] on to the θ_A–θ_B plane (in degrees). The five faint contour lines are for successive 0.02 increments in *X* above the minimum, and the five heavy contour lines are for successive 0.2 increments above the minimum, at D. b = 1.0. The locations of the dodecahedron (D) and 'cube' (C) are indicated

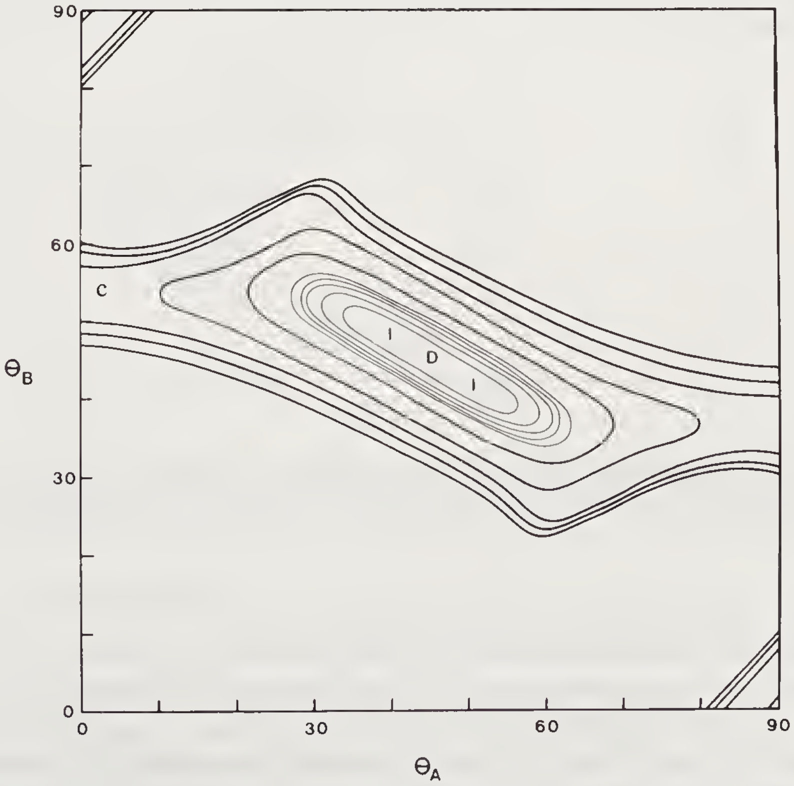

Figure 88 Projection of the potential energy surface for [M(bidentate)$_4$] on to the θ_A–θ_B plane (in degrees). The five faint contour lines are for successive 0.02 increments in *X* above the minima, and the five heavy contour lines are for successive 0.2 increments above the minima, at I. b = 1.1. The locations of the dodecahedron (D), intermediate stereochemistries (I) and 'cube' (C) are indicated

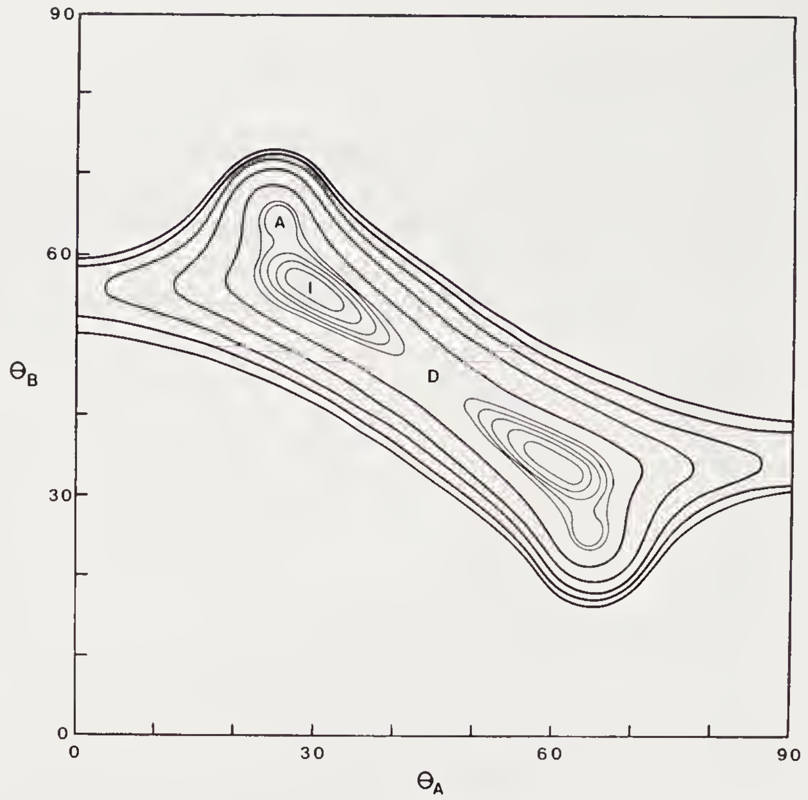

Figure 89 Projection of the potential energy surface for [M(bidentate)$_4$] on to the θ_A-θ_B plane (in degrees). The five faint contour lines are for successive 0.02 increments in X above the minima, and the five heavy contour lines are for successive 0.2 increments above the minima, at I. b = 1.2. The locations of the dodecahedron (D), intermediate stereochemistries (I) and square antiprism (A) are indicated

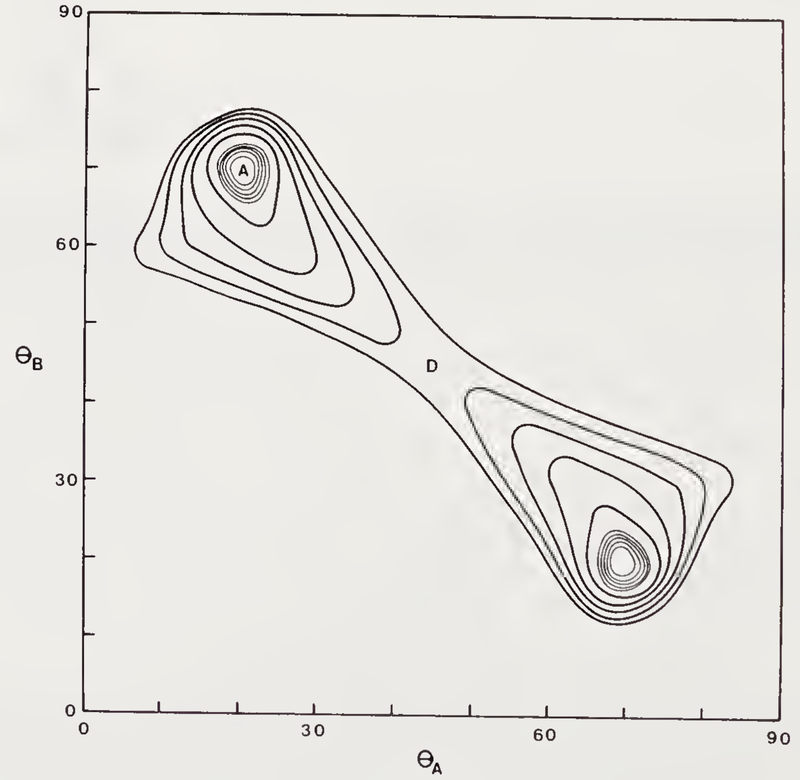

Figure 90 Projection of the potential energy surface for [M(bidentate)$_4$] on to the θ_A–θ_B plane (in degrees). The five faint contour lines are for successive 0.02 increments in X above the minima, and the five heavy contour lines are for successive 0.2 increments above the minima, at A. b = 1.3. The locations of the dodecahedron (D) and square antiprism (A) are indicated

At low normalized bites (Figure 87) the minimum at $\theta_A = \theta_B = 45°$ corresponds to the dodecahedron of overall molecular symmetry D_{2d} (Figure 91).

As the normalized bite is progressively increased (Figure 88), this central minimum becomes increasingly shallow and then divides into two identical minima. These minima then move further apart as b is increased further (Figure 89). These minima correspond to the intermediate stereochemistry, and the polyhedron chosen to best describe the structure depends upon the value of b. At the low end of the range, $b \approx 1.1$, the stereochemistry is adequately represented as a distorted D_{2d} dodecahedron. At $b = 1.19$, the structure is a square antiprism with the bidentate ligands along the square edges (Figure 92a). At other values of the normalized bite these square faces are creased,

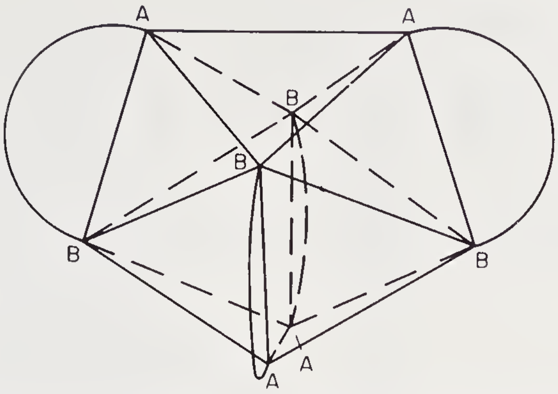

Figure 91 The D_{2d} dodecahedral isomer of [M(bidentate)$_4$]

and one of the dodecahedral isomers shown in Figures 92b and 92c may be the preferred description.

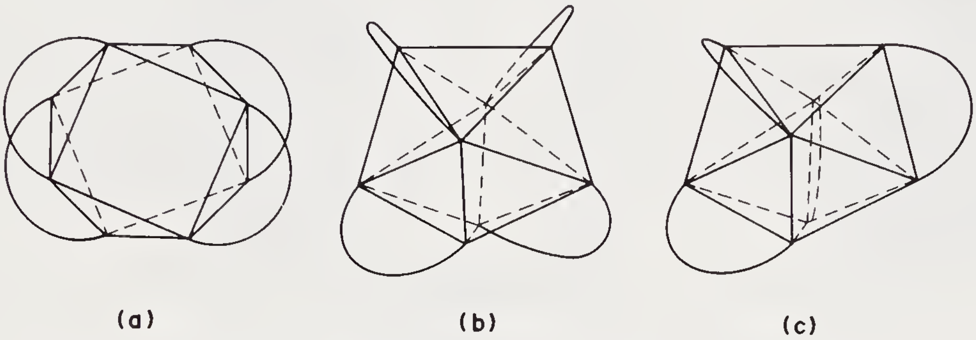

Figure 92 The intermediate stereochemistry of [M(bidentate)$_4$] represented as a square antiprism (a) and as dodecahedra (b and c)

Figure 89 shows that at b = 1.2 an additional feature has appeared on the potential energy surface, which at b = 1.3 has formed a deep minimum (Figure 90). The two minima correspond to the two optical isomers of the D_4 square antiprism (Figure 93). It may be noted that in contrast to the 'three-bladed propeller', which is the dominant stereochemistry for tris(bidentate) complexes (Section 2.3.3), this 'four-bladed propeller' is only expected in tetrakis(bidentate) complexes where the bidentate ligands have exceptionally large normalized bites. At b = 1.26, the angle of twist θ = 22.5° and the two square faces are staggered with respect to each other (Figure 93). In an analogous way to the behaviour of tris(bidentate) complexes, a decrease in b leads to a decrease in θ.

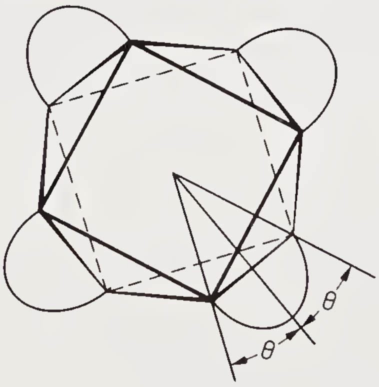

Figure 93 The D_4 square antiprismatic isomer of [M(bidentate)$_4$]

2.5.4.2 *Comparison with experiment*

The above predictions, that the stereochemistry is largely controlled by the normalized bite of the bidentate ligands, is in general agreement with the known structures, a representative selection being given in Table 19.

Compounds with normalized bites less than ~1.1 generally have the D_{2d} dodecahedral structure, with some distorted structures occurring at the higher end of the range. As b is increased from ~1.1 to ~1.2, the D_{2d} dodecahedral structures are progressively replaced by the intermediate stereochemistries (Table 19). The only compound with the bidentate ligand having a large normalized bite, [Nb(Bu^{t}COCHCOBu^t)$_4$] with b = 1.28, has the D_4 square antiprismatic structure

Table 19 Stereochemistries of $[M(bidentate)_4]$

Complex	*b*	*Stereochemistry*	*Ref.*
$K_3[Cr(O_2)_4]$	0.78	D_{2d} dodecahedron	355
$[Zn(NH_3)_4][Mo(O_2)_4]$	0.79	D_{2d} dodecahedron	356
$[Sn(NO_3)_4]$	0.99	D_{2d} dodecahedron	357
$[Sn(O_2CMe)_4]$	1.00	D_{2d} dodecahedron	358
$(Et_4N)[Bi(S_2COEt)_4]$	1.02	D_{2d} dodecahedron	359
$[Ti(NO_3)_4]$	1.03	D_{2d} dodecahedron	360
$[Te(S_2CNEt_2)_4]$	1.07	D_{2d} dodecahedron	361
$[Mo(S_2CPh)_4]$	1.10	D_{2d} dodecahedron	362
$[W(S_2CSEt)_4]$	1.10	D_{2d} dodecahedron	363
$(Ph_4As)[Ce\{S_2P(OMe)_2\}_4]$	1.10	D_{2d} dodecahedron	364
$[V(S_2CPh)_4]$	1.11	D_{2d} dodecahedron	365
$[Ti(S_2CNEt_2)_4]$	1.11	D_{2d} dodecahedron	366
$[Ta(S_2CNMe_2)_4]Cl{\cdot}CH_2Cl_2$	1.11	D_{2d} dodecahedron	367
$[Mo(S_2CNEt_2)_4]Cl$	1.11	D_{2d} dodecahedron	368
$[W(S_2CNEt_2)_4]Br$	1.12	D_{2d} dodecahedron	369
$Na_4[Ce(O_2C_6H_4)_4]{\cdot}21H_2O$	1.12	D_{2d} dodecahedron	370
$(Ph_4P)[Pr(S_2PMe_2)_4]$	1.12	Intermediate	371
$[Th(S_2PMe_2)_4]$	1.13	D_{2d} dodecahedron	372
$H[Sc(O_2C_7H_5)_4]$	1.13	Distorted D_{2d} dodecahedron	373,374
$[Hf(O_2C_7H_5)_4]HCONMe_2$	1.14	D_{2d} dodecahedron	375
$[Th(MeCOCHCOMe)_4]{\cdot}\frac{1}{2}C_6H_6$	1.14	Intermediate	376
$[U(PhCOCHCOPh)_4]$	1.16	Intermediate	377
$Na_4[Zr(C_2O_4)_4]{\cdot}3H_2O$	1.17	Distorted D_{2d} dodecahedron	378
$[Ce(MeCOCHCOMe)_4]$	1.17	Intermediate	379,380
$Cs[Eu(CF_3COCHCOCF_3)_4]$	1.18	Intermediate	381
$[Zr(MeCOCHCOMe)_4]$	1.22	Intermediate	382
$[Nb(Bu^tCOCHCOBu^t)_4]$	1.28	*D* square antiprism	383

as predicted. The angle of twist θ for this structure (Figure 93) is 24°, in excellent agreement with that calculated for this normalized bite.

One unusual feature of the D_{2d} dodecahedral molecules is that the asymmetry predicted for the bidentate ligands changes sign as the normalized bite is increased. Below a normalized bite of approximately 1.0, it is predicted that the ligand atoms at the A sites of the dodecahedron are associated with a smaller repulsion energy than are those at the B sites (Figure 94). However, for larger chelate rings the atoms at the A site are predicted to be more hindered than those at the B sites, $Y_A/Y_B > 1.0$ (Figure 94). This prediction is experimentally confirmed, for example, by the two molybdenum complexes shown in Figure 95. In the peroxo complex the Mo—A bond is 3% shorter than the Mo—B bond, whereas in the dithiobenzoate complex the Mo—A bond is 3% longer than the Mo—B bond.

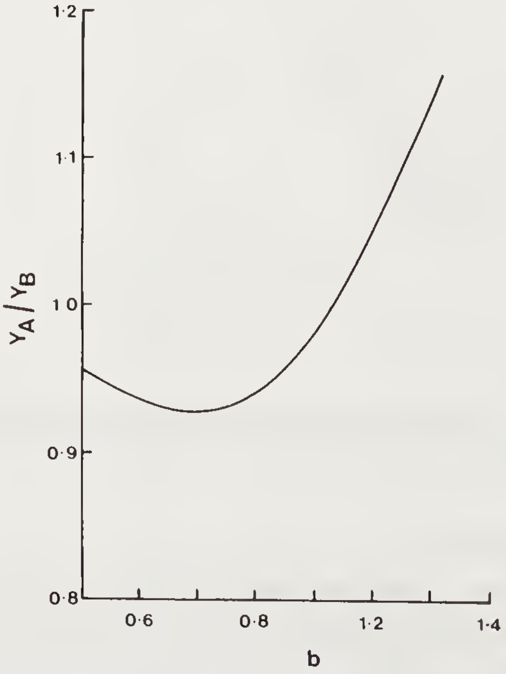

Figure 94 Ratio of the individual atom repulsion coefficients for the two ends of each bidentate ligand in the D_{2d} dodecahedral $[M(bidentate)_4]$ as a function of normalized bite *b*

There are a small number of anomalous structures that are not included in Table 19.[4] For example, cubic stereochemistry is observed for $[U(bipy)_4]$[384] but, as is common with this ligand, the unusual structure can be attributed to the peculiar steric requirements of bipyridyl.[4]

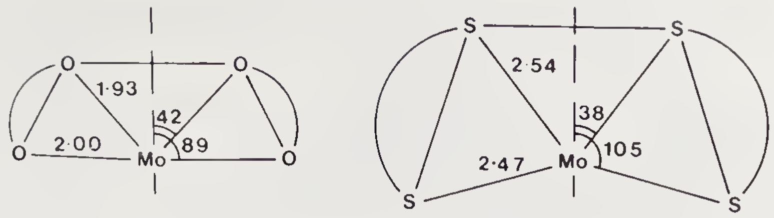

Figure 95 Trapezoid geometries, degrees and Å, in $[Zn(NH_3)_4][Mo(O_2)_4]$ and $[Mo(S_2CPh)_4]$

2.6 NINE-COORDINATE COMPOUNDS

2.6.1 [M(Unidentate)$_9$]

Only two stereochemistries need be considered for nine-coordinate compounds:

tricapped trigonal prism: $X = 8.105$
capped square antiprism: $X = 8.117$

The tricapped trigonal prism is shown in Figure 96, where atoms ABCGHI form the trigonal prism, capped by atoms DEF. If all ligands lie on the surface of a sphere of radius r, the stereochemistry is defined by ϕ_A, the angle the six 'prismatic' metal–ligand bonds make with the threefold axis. For a 'hard sphere model' each unidentate ligand is in contact with four neighbouring unidentate ligands, that is, $\phi_A = \arcsin(2/3) = 41.81°$, the polyhedral edge lengths being AB = AD = $2/3^{1/2}r = 1.1547r$ and AG = $(2/3)5^{1/2}r = 1.4907r$.

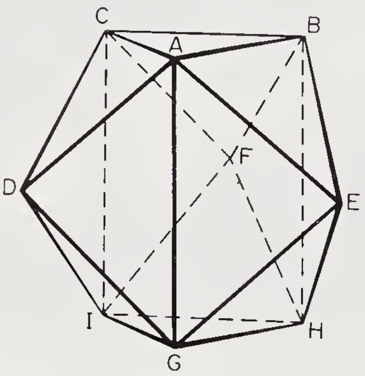

Figure 96 The tricapped trigonal prism

The most favourable polyhedron formed by minimization of the total repulsion energy is squashed along the threefold axis, ϕ_A being increased to 44.7°. This results in a decrease in all four ligand–ligand distances to each capping atom, increasing the repulsion experienced by these atoms, $Y_D/Y_A = 1.138$. The resultant increase in metal–capping atom bond length will lead to a further increase in ϕ_A, e.g. for $R(D/A) = 1.0$ and 1.1, $\phi_A = 44.7°$ and 45.6° respectively.[385]

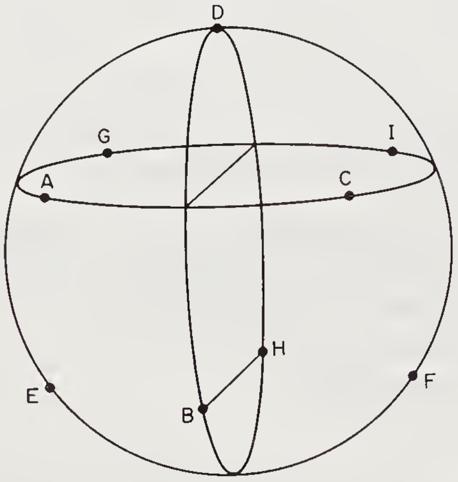

Figure 97 General stereochemistry for [M(unidentate)$_9$]

The capped square antiprism is closely related to the tricapped trigonal prism. The general structure, with C_{2v} symmetry, is shown in Figure 97, the symmetry axis being coincident with the M—D bond. The capped square antiprism is defined by $\phi_B = \phi_F$, creating a square BFHE face, and $\theta_C = 45°$. The potential energy surface for [M(unidentate)$_9$] is shown in Figures 98a and 98b projected on to the $\phi_B - \phi_F$ plane. There is no potential energy barrier between the two tricapped

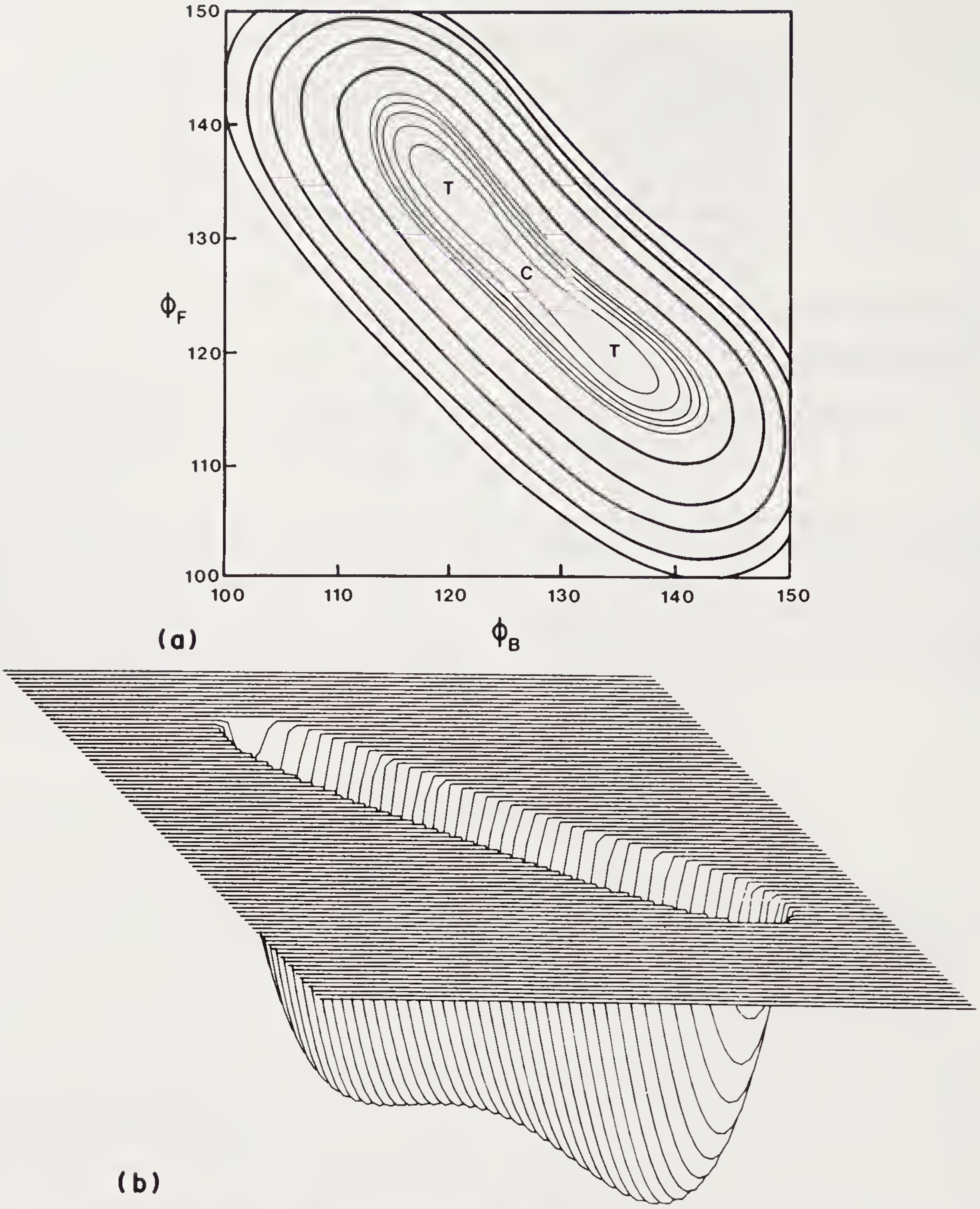

Figure 98 (a) Projection of the potential energy surface for [M(unidentate)$_9$] on to the ϕ_B–ϕ_F plane (in degrees). The five faint contour lines are for successive 0.02 increments in X above the minima, and the five heavy contour lines are for 0.2 increments above the minima, at T. The location of the tricapped trigonal prisms (T) and the capped square antiprism (C) are indicated. (b) As in (a), but with truncation at $X = 0.1$

trigonal prisms and the capped square antiprism. Movement along the valley between the two stereochemistries necessarily scrambles all nine atoms, as any one of the three capping atoms of the tricapped trigonal prism can be selected to become the unique capping atom of the capped square antiprism.

Structurally characterized compounds containing nine equivalent unidentate ligands are restricted to the lanthanoid nonahydrates $[Ln(H_2O)_9](BrO_3)_3$,[386,387] $[Ln(H_2O)_9](EtSO_4)_3$[387–389] and $[Ln(H_2O)_9](CF_3SO_3)_3$[390] and the hydride complex $K_2[ReH_9]$.[391,392] All have the tricapped trigonal prismatic structure and the stereochemical parameters of $\phi_A \approx 46°$ and (M—D)/(M—A) $\approx$ 1.06 are in reasonable agreement with predictions.

2.6.2 [M(Bidentate)$_3$(Unidentate)$_3$]

A number of stereochemistries may be envisaged for complexes of the type [M(bidentate)$_3$(unidentate)$_3$], which are based on the tricapped trigonal prism and the capped square antiprism. The most important of these is the tricapped trigonal prism with the bidentate ligands spanning the DG, EH and FI edges (Figure 96). The main effect of reducing the normalized bite is to twist the lower GHI triangular face relative to the ABC and DEF triangles. For example, the angle of twist between the DEF and GHI triangles decreases from 60° at $b = 1.1387$ to 44° at $b = 0.87$ (as in the complexes below).

This tricapped trigonal prismatic structure is observed in a number of trinitrato complexes, including $[Tl(NO_3)_3(H_2O)_3]$,[393] $[Y(NO_3)_3(H_2O)_3]2C_{10}H_8N_2$,[394] $[Yb(NO_3)_3(OSMe_2)_3]$[395] and $[Nd(NO_3)_3(OC_3HN_2Me_2Ph)_3]$.[396] The observed normalized bites of ~0.87 and the angles of twist between the DEF and GHI triangles of ~46° are in good agreement with theory.

A notable feature of this stereochemistry is that the dihedral angle between any two bidentate ligands is close to 90°.[397] For example, in the above trinitrato complexes it is ~88°. The three bidentate ligands can therefore be considered to form half an icosahedral $[M(bidentate)_6]$ unit (Section 2.9.2), whereas the three unidentate ligands form half an octahedral $[M(unidentate)_6]$ unit.

The repulsion energy calculations also predict that each bidentate ligand will be unsymmetrically bonded, the capping atom experiencing more repulsion than the prismatic atom. This is experimentally observed: $(M—D)/(M—G) \approx 1.05$ for the above trinitrato complexes.

Different structural isomers of $[M(bidentate)_3(unidentate)_3]$ are found for $(Eu(NO_3)_3\{OC(NMe_2)_2\}_3]$,[398] $[Sm\{NH_2NHC(C_5H_4N)O\}_3(H_2O)_3](NO_3)_3$,[399] $[C(NH_2)_3]_5[Th(CO_3)_3F_3]$[400] and $[Ho(NO_3)_3(H_2O)_3]\cdot2C_{10}H_8N_2$.[394]

2.6.3 [M(Bidentate)$_4$(Unidentate)]

Four equivalent bidentate ligands can be wrapped around a nine-coordinate metal atom by forming a capped square antiprism, with the bidentate ligands spanning edges linking the two square faces of the antiprism (Figure 99). This structure is observed for $[Th(CF_3COCHCOCH_3)_4(H_2O)]$.[401] A distorted form is found for $[Pb(phen)_4(ClO_4)](ClO_4)$.[402]

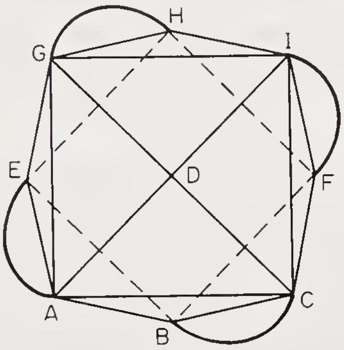

Figure 99 One of the capped square antiprismatic isomers of $[M(bidentate)_4(unidentate)]$

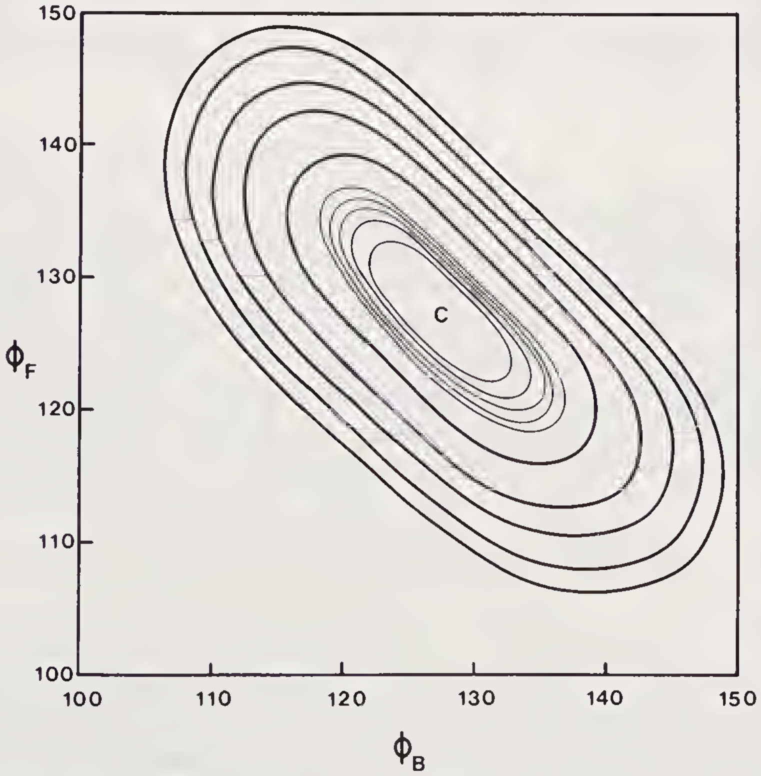

Figure 100 Projection of the potential energy surface for $[M(bidentate)_4(unidentate)]$ on to the ϕ_B-ϕ_F plane (in degrees). The five faint contour lines are for successive 0.02 increments in X above the minimum, and the five heavy contour lines are for 0.2 increments above the minimum, at C. The location of the capped square antiprism (C) is indicated

Repulsion energy calculations carried out over the range $b = 0.5-1.4$ confirm that this isomer exists as a discrete potential energy minimum. The stabilization of the capped square antiprism compared with the tricapped trigonal prism is shown by the typical potential energy surface in Figure 100, and should be contrasted with that calculated for [M(unidentate)$_9$] (Figure 98a) which shows the stabilization of the tricapped trigonal prism.

The ACIG and BFHE square faces of the antiprism are staggered at $b = 1.1746$, and the angle of twist between these faces decreases from 45° at $b = 1.1746$ to 0° at $b = 0.75$. The angle of twist of 42° at $b = 1.15$ observed for [Th(CF$_3$COCHCOCH$_3$)$_4$(H$_2$O)] is in excellent agreement with the calculated value of 43°.

The repulsion energy calculations predict that the bidentate ligands in capped square antiprismatic molecules will be unsymmetrically bonded, the atoms forming the capped face experiencing considerably less repulsion than the atoms forming the uncapped face, $Y_C/Y_B \approx 0.88$ for $b \approx 0.8-1.4$. This agrees with the observed Th—O bond lengths of 2.39 and 2.46 Å respectively in [Th(CF$_3$COCHCOCH$_3$)$_4$(H$_2$O)].

Other, less symmetrical, isomers are observed for other complexes of the type [M(bidentate)$_4$(unidentate)], including [Sr(MeCONHCOMe)$_4$(H$_2$O)](ClO$_4$),[403] [Th(O$_2$C$_7$H$_5$)$_4$(Me$_2$NCHO)],[404] [Th(C$_4$H$_3$SCOCHCOCF$_3$)$_4${(C$_8$H$_{17}$)$_3$PO}],[405] [Th(O$_2$C$_7$H$_4$Pr)$_4$(H$_2$O)]·H$_2$O,[406] [Th(O$_2$C$_7$H$_5$)$_4$(H$_2$O)][407] and (NO)$_2$[Sc(NO$_3$)$_4$(ONO$_2$)].[408]

2.7 TEN-COORDINATE COMPOUNDS

2.7.1 [M(Unidentate)$_{10}$]

There is as yet no structurally characterized compound containing ten unidentate ligands. Nevertheless the geometry of these hypothetical compounds is a useful introduction to the stereochemistry of known ten-coordinate complexes containing chelate groups such as [M(NO$_3$)$_3$(H$_2$O)$_4$][409,410] and [M(bidentate ligand)$_5$] (see below).

The repulsion energy calculations show that the following three structures are possible for ten-coordination:

bicapped square antiprism:	$X = 12.337$
sphenocorona:	$X = 12.362$
trirhombohedron:	$X = 12.363$

These structures are shown in Figure 101. The sphenocorona can be considered as a distorted bicapped square antiprism if atoms C and E are the capping atoms, and AGID and BFJH the two square faces of the antiprism. Similarly the trirhombohedron can be considered as a distorted bicapped square antiprism if atoms B and F are taken as the two capping atoms, the two square faces being AGHE and CDJI. The differences in energy between these three polyhedra are small and all three stereochemistries, or intermediates lying along various reaction coordinates connecting them, would be possible.

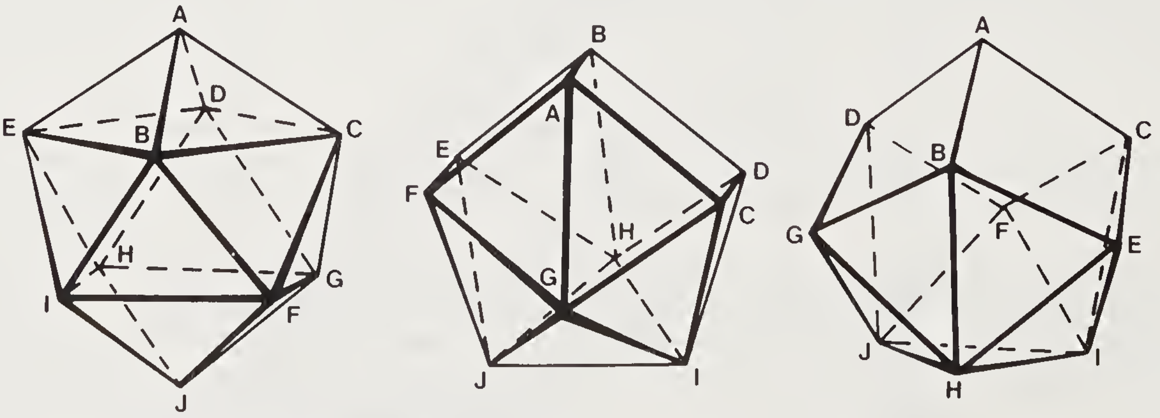

Figure 101 The bicapped square antiprism, sphenocorona and trirhombohedron

2.7.2 [M(Bidentate)$_5$]

There are three important minima on the potential energy surfaces calculated for [M(bidentate)$_5$]. At $b \approx 1.1$, isomers I and II correspond to two of the possible ways of arranging bidentate ligands around a bicapped square antiprism, whereas isomer III is a sphenocorona (Figure 102).

The differences between the repulsion energy coefficients for these stereochemistries are shown in Figure 103. Compounds of stereochemistries II and III are expected only above $b \approx 0.95$,

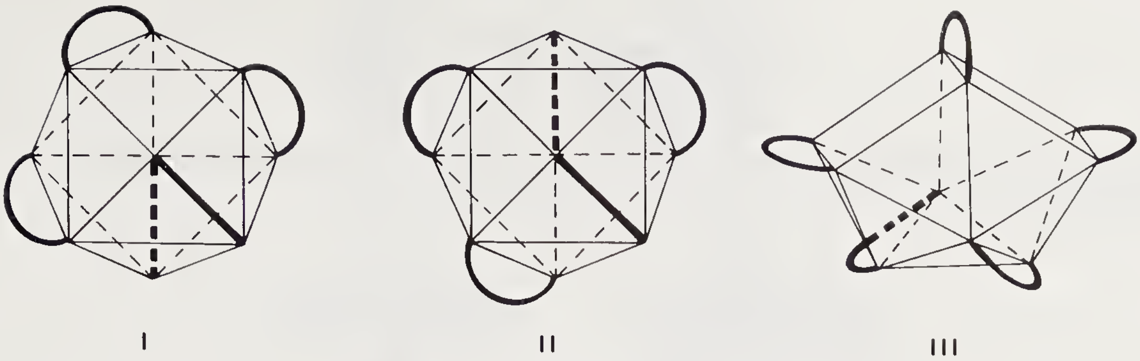

Figure 102 Isomers of [M(bidentate)$_5$]

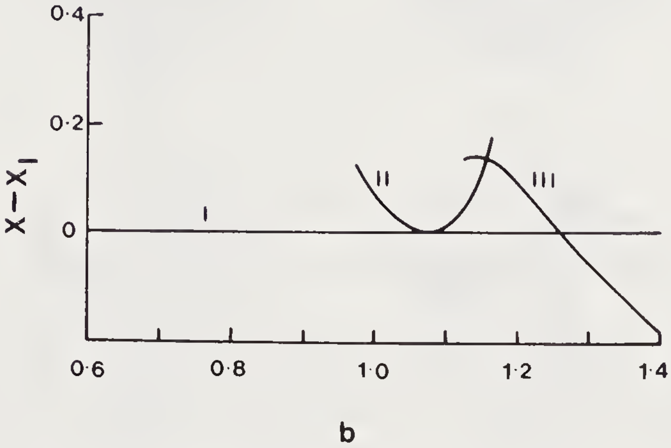

Figure 103 Repulsion energy coefficients, relative to those for isomer I, for the various isomers of [M(bidentate)$_5$], as a function of *b*

whereas stereochemistry I is stable at all values of the normalized bite. There are a number of lanthanoid and actinoid complexes with four-membered nitrate or carbonate rings and normalized bites in the range 0.8−0.9. As predicted from the calculations, they are all of stereochemistry I. Examples include $(Ph_4As)_2[Eu(NO_3)_5]$,[411] $(NO)_2[Ho(NO_3)_5]$,[412] $Na_6[Ce(CO_3)_5]\cdot 12H_2O$[413] and $[Co(NH_2)_3]_6[Th(CO_3)_5]\cdot 4H_2O$.[414] The only monomeric molecule in which the isomer II structure is observed is the barium diacetamide complex $[Ba(MeCONHCOMe)_5](ClO_4)_2$.[415] The normalized bite of 0.98 is within the range where this stereochemistry is expected. This stereochemistry is also observed in the triclinic modification of $K_4[U(C_2O_4)_4]\cdot 4H_2O$ (b = 1.07) in which the anion is a linear polymer with bridging oxalate groups. The orthorhombic modification of $K_4[U(C_2O_4)_4]\cdot 4H_2O$ (b = 1.07) is the only example of stereochemistry III.[416]

2.8 ELEVEN-COORDINATE COMPOUNDS

There are no known compounds [M(unidentate)$_{11}$] and it does not appear likely that any could be prepared. However, the geometry of these hypothetical compounds is a useful starting point to the stereochemistries of eleven-coordinate complexes containing chelate groups, such as $[Th(NO_3)_4(H_2O)_3]\cdot 2H_2O$[417,418] and $[La(NO_3)_3(H_2O)_5]\cdot H_2O$.[419]

The repulsion energy calculations show that the most stable structure is formed by replacing two adjacent atoms at the vertices of an icosahedron by a single atom at the midpoint of that edge. This 'edge coalesced icosahedron' is slightly more stable than the closely related capped pentagonal antiprism formed by removal of one of the vertices formed by an icosahedron:

edge coalesced icosahedron:	X = 18.562
capped pentagonal antiprism:	X = 18.571.

2.9 TWELVE-COORDINATE COMPOUNDS

2.9.1 [M(Unidentate)$_{12}$]

As for ten- and eleven-coordination, there are no twelve-coordinate complexes containing only unidentate ligands. The most common twelve-coordinate molecules are those of the type [M(bidentate)$_6$]. The relevant stereochemistries are shown in Figure 104, and the repulsion energy coefficients listed below:

icosahedron: $X = 23.531$
bicapped pentagonal prism: $X = 25.928$
anticuboctahedron: $X = 26.280$
cuboctahedron: $X = 26.483$

The icosahedron is clearly the most stable structure and is expected to be by far the most chemically important.

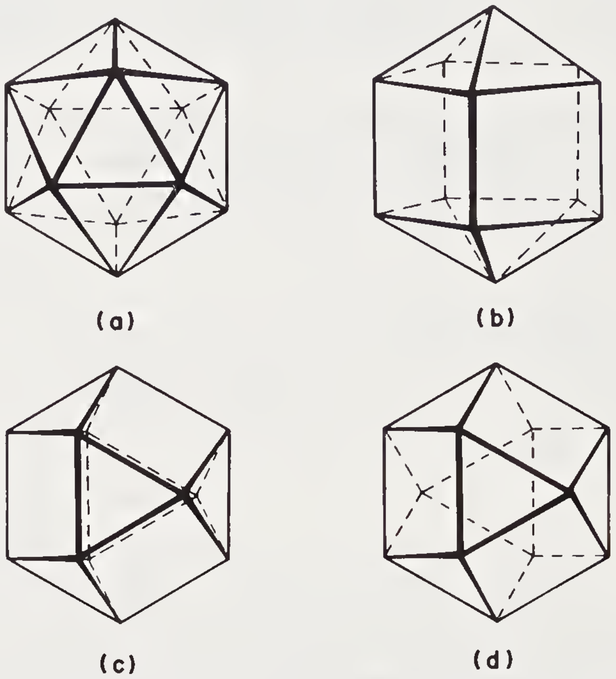
(a) (b) (c) (d)

Figure 104 (a) The icosahedron; (b) the bicapped pentagonal prism; (c) the anticuboctahedron; (d) the cuboctahedron

2.9.2 [M(Bidentate)$_6$]

Three structural isomers may be formed by wrapping six bidentate ligands with $b = 1.0515$ along the edges of a regular icosahedron (Figure 105). Stereochemistry I is highly symmetrical, with the very rare point group symmetry T_h. On reducing the normalized bite the symmetry remains unaltered and all vertices remain identical. All polyhedral edge lengths not spanned by a bidentate ligand are equal, and of length a:

$$a = \left[2 - \left(b^2 - \frac{b^4}{4}\right)^{1/2}\right]^{1/2}$$


I II III

Figure 105 Regular icosahedral isomers of [M(bidentate)$_6$]

A clear distinction between isomers I and II is shown by the angles between vectors joining the central metal atom and the midpoint of each bidentate ligand. For isomer I there are twelve angles of 90.0° and three of 180.0° at all values of the normalized bite, with the midpoint of each bidentate ligand situated at the apex of a regular octahedron about the metal atom. For isomer II of the regular icosahedron, $b = 1.0515$, there are three angles of 72.0°, six of 90.0°, three of 120.0° and three of 144.0°. The first twelve angles approach 90°, and the last three approach 180°, as b is progressively decreased to zero.

The relative energies of these three isomers are shown in Figure 106. Isomer III is unstable for $b < 1.0$, and the existence of compounds with this structure is not expected. Isomers I and II are both expected, the latter being more stable.

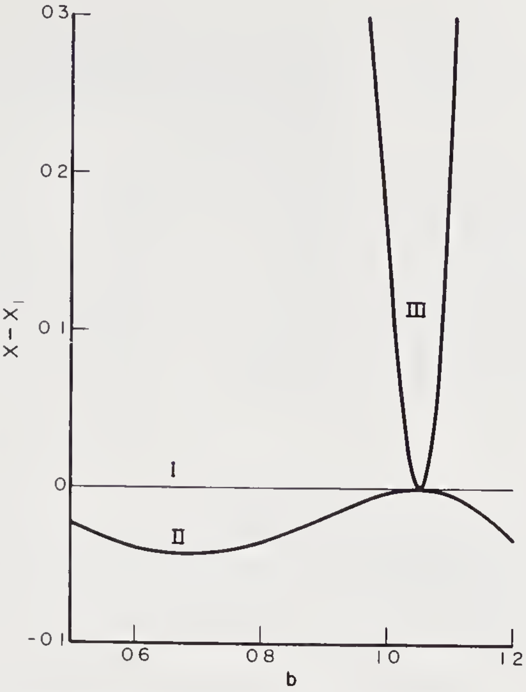

Figure 106 Repulsion energy coefficients, relative to those for isomer I, for the various isomers of [M(bidentate)$_6$] as a function of *b*

Structure I is observed for a number[4] of hexanitrato complexes, $b = 0.80-0.82$, for example $[Mg(H_2O)_6]_3[La(NO_3)_6]_2 \cdot 6H_2O$[420] and $[Mg(H_2O)_6][Th(NO_3)_6] \cdot 2H_2O$.[421] Structure II has been observed only for the praseodymium(III) naphthyridine complex, $[Pr(napy)_6](ClO_4)_3$.[422]

2.10 REFERENCES

1. N. V. Sidgwick and H. M. Powell, *Proc. R. Soc. London, Ser. A*, 1940, **176**, 153.
2. R. J. Gillespie and R. S. Nyholm, *Q. Rev., Chem. Soc.*, 1957, **11**, 339.
3. J. L. Hoard and J. V. Silverton, *Inorg. Chem.*, 1963, **2**, 235.
4. D. L. Kepert, 'Inorganic Stereochemistry', Springer-Verlag, Berlin, 1982.
5. C. Lau, H. Lynton, J. Passmore and P. Y. Siew, *J. Chem. Soc., Dalton Trans.*, 1973, 2535.
6. J. B. F. N. Engberts, H. Morssink and A. Vos, *J. Am. Chem. Soc.*, 1978, **100**, 799.
7. M. C. Favas and D. L. Kepert, *Prog. Inorg. Chem.*, 1980, **27**, 325.
8. A. H. Clark, B. Beagley, D. W. J. Cruickshank and T. G. Hewitt, *J. Chem. Soc. (A)*, 1970, 872.
9. Z. Zak and M. Kosicka, *Acta Crystallogr.*, 1978, **B34**, 38.
10. D. E. Sands, *Z. Kristallogr.*, 1963, **119**, 245.
11. F. Daniel, J. Moret, M. Maurin and B. Philippot, *Acta Crystallogr.*, 1982, **B38**, 703.
12. Yu. N. Kukushkin, *Russ. J. Inorg. Chem.*, 1976, **21**, 481.
13. R. S. Berry, *J. Chem. Phys.*, 1960, **32**, 933.
14. C. Brabant, B. Blanck and A. L. Beauchamp, *J. Organomet. Chem.*, 1974, **82**, 231.
15. C. P. Brock and D. F. Webster, *Acta Crystallogr.*, 1976, **B32**, 2089.
16. P. J. Wheatley, *J. Chem. Soc.*, 1964, 2206.
17. M. L. Ziegler, B. Nuber, K. Wiedenhammer and G. Hoch, *Z. Naturforsch., Teil B*, 1977, **32**, 18.
18. R. Sarma, F. Ramirez, B. McKeever, J. F. Maracek and S. Lee, *J. Am. Chem. Soc.*, 1976, **98**, 581, 4691.
19. J. Drummond and J. S. Wood, *Chem. Commun.*, 1969, 1373.
20. C. Brabant, J. Hubert and A. L. Beauchamp, *Can. J. Chem.*, 1973, **51**, 2952.
21. I. Bertini, P. Dapporto, D. Gatteschi and A. Scozzafava, *Inorg. Chem.*, 1975, **14**, 1639.
22. C. Heath and M. B. Hursthouse, *Chem. Commun.*, 1971, 143.
23. A. L. Beauchamp, M. J. Bennett and F. A. Cotton, *J. Am. Chem. Soc.*, 1968, **90**, 6675.
24. Y. S. Ng, G. A. Rodley and W. T. Robinson, *Inorg. Chem.*, 1976, **15**, 303.
25. Y. S. Ng, G. A. Rodley and W. T. Robinson, *Acta Crystallogr.*, 1978, **B34**, 2837.
26. G. Joy, A. P. Gaughan, I. Wharf, D. F. Shriver and J. P. Dougherty, *Inorg. Chem.*, 1975, **14**, 1795.
27. W. Clegg, D. A. Greenhalg and B. P. Straughan, *J. Chem. Soc., Dalton Trans.*, 1975, 2591.
28. W. Clegg, *J. Chem. Soc., Dalton Trans.*, 1982, 593.
29. F. A. Jurnak and K. N. Raymond, *Inorg. Chem.*, 1974, **13**, 2387.
30. E. L. Muetterties, *Acc. Chem. Res.*, 1970, **3**, 266.
31. E. L. Muetterties, W. Mahler, K. J. Packer and R. Schmutzler, *Inorg. Chem.*, 1964, **3**, 1298.
32. J. M. Bassett, M. Green, J. A. K. Howard and F. G. A. Stone, *J. Chem. Soc., Chem. Commun.*, 1977, 853.
33. P. Meakin and J. P. Jesson, *J. Am. Chem. Soc.*, 1973, **95**, 7272.
34. P. Meakin, E. L. Muetterties and J. P. Jesson, *J. Am. Chem. Soc.*, 1972, **94**, 5271.
35. A. D. English, S. D. Ittel, C. A. Tolman, P. Meakin and J. P. Jesson, *J. Am. Chem. Soc.*, 1977, **99**, 117.
36. J. P. Jesson and P. Meakin, *J. Am. Chem. Soc.*, 1974, **96**, 5760.
37. M. Bochmann, G. Wilkinson, G. B. Young, M. B. Hursthouse and K. M. A. Malik, *J. Chem. Soc., Dalton Trans.*, 1980, 901.
38. W. P. Griffith, A. C. Skapski, K. A. Woode and M. J. Wright, *Inorg. Chim. Acta*, 1978, **31**, L413.
39. M. Dartiguenave, Y. Dartiguenave, A. Gleizes, C. Saint-Joly, J. Galy, P. Meier and A. E. Merbach, *Inorg. Chem.*, 1978, **17**, 3503.

40. A. Gleizes, A. Kerkeni, M. Dartiguenave, Y. Dartiguenave and H. F. Klein, *Inorg. Chem.*, 1981, **20**, 2372.
41. D. A. Johnson, J. C. Taylor and A. B. Waugh, *J. Inorg. Nucl. Chem.*, 1980, **42**, 1271.
42. Z. Galdecki, M. L. Glowka and B. Goliński, *Acta Crystallogr.*, 1976, **B32**, 2319.
43. C. S. Smith, J.-S. Lee, D. D. Titus and R. F. Ziolo, *Organometallics*, 1982, **1**, 350.
44. R. F. Ziolo and J. M. Troup, *J. Am. Chem. Soc.*, 1983, **105**, 229.
45. A. H. Cowley, M. C. Cushner, R. E. Davis and P. E. Riley, *Inorg. Chem.*, 1981, **20**, 1179.
46. P. T. Greene and P. L. Orioli, *J. Chem. Soc. (A)*, 1969, 1621.
47. J.-C. Daran, Y. Jeannin and L. M. Martin, *Inorg. Chem.*, 1980, **19**, 2935.
48. W. J. P. van Enckevort, H. M. Hendriks and P. T. Beurskens, *Cryst. Struct. Commun.*, 1977, **6**, 531.
49. W. J. Rozell and J. S. Wood, *Inorg. Chem.*, 1977, **16**, 1827.
50. J. R. Dilworth, J. Hutchinson and J. A. Zubieta, *J. Chem. Soc., Chem. Commun.*, 1983, 1034.
51. O. Stelzer, W. S. Sheldrick and J. Subramanian, *J. Chem. Soc., Dalton Trans.*, 1977, 966.
52. J. A. Bertrand and D. L. Plymale, *Inorg. Chem.*, 1966, **5**, 879.
53. J. W. Dawson, T. J. McLennan, W. Robinson, A. Merle, M. Dartiguenave, Y. Dartiguenave and H. B. Gray, *J. Am. Chem. Soc.*, 1974, **96**, 4428.
54. L. J. Vande Griend, J. C. Clardy and J. G. Verkade, *Inorg. Chem.*, 1975, **14**, 710.
55. S. J. La Placa and J. A. Ibers, *Inorg. Chem.*, 1965, **4**, 778.
56. R. D. Burbank and F. N. Bensey, *J. Chem. Phys.*, 1953, **21**, 602.
57. P. Boldrini, R. J. Gillespie, P. R. Ireland and G. J. Schrobilgen, *Inorg. Chem.*, 1974, **13**, 1690.
58. R. J. Gillespie, D. Martin, G. J. Schrobilgen and D. R. Slim, *J. Chem. Soc., Dalton Trans.*, 1977, 2234.
59. D. E. McKee, A. Zalkin and N. Bartlett, *Inorg. Chem.*, 1973, **12**, 1713.
60. M. J. Nolte, E. Singleton and E. van der Stok, *Acta Crystallogr.*, 1978, **B34**, 1684.
61. H. Pritzkow, *Acta Crystallogr.*, 1975, **B31**, 1505.
62. J. Runsink, S. Swen-Walstra and T. Migchelsen, *Acta Crystallogr.*, 1972, **B28**, 1331.
63. M. Hall and D. B. Sowerby, *J. Am. Chem. Soc.*, 1980, **102**, 628.
64. P. L. Millington and D. B. Sowerby, *J. Chem. Soc., Dalton Trans.*, 1981, 2011.
65. D. S. Brown and G. W. Bushnell, *Acta Crystallogr.*, 1967, **22**, 296.
66. F. A. Cotton, K. I. Hardcastle and G. A. Rusholme, *J. Coord. Chem.*, 1973, **2**, 217.
67. M. Nardelli, C. Pelizzi, G. Pelizzi and P. Tarasconi, *Z. Anorg. Allg. Chem.*, 1977, **431**, 250.
68. M. Akhtar, P. D. Ellis, A. G. MacDiarmid and J. D. Odom, *Inorg. Chem.*, 1972, **11**, 2917.
69. G. R. Langford, M. Akhtar, P. D. Ellis, A. G. MacDiarmid and J. D. Odom, *Inorg. Chem.*, 1975, **14**, 2937.
70. E. L. Muetterties, W. Mahler and R. Schmutzler, *Inorg. Chem.*, 1963, **2**, 613.
71. R.P. Dodge, D. H. Templeton and A. Zalkin, *J. Chem. Phys.*, 1961, **35**, 55.
72. P. K. Hon, R. L. Belford and C. E. Pfluger, *J. Chem. Phys.*, 1965, **43**, 3111.
73. K. Henrick, C. L. Raston and A. H. White, *J. Chem. Soc., Dalton Trans.*, 1976, 26.
74. H. Goldwhite, J. Grey and R. Teller, *J. Organomet. Chem.*, 1976, **113**, C1.
75. R. R. Holmes, *J. Am. Chem. Soc.*, 1974, **96**, 4143.
76. J. S. Miller and K. G. Caulton, *J. Am. Chem. Soc.*, 1975, **97**, 1067.
77. E. F. Perozzi, J. C. Martin and I. C. Paul, *J. Am. Chem. Soc.*, 1974, **96**, 6735.
78. D. Bright and J. A. Ibers, *Inorg. Chem.*, 1969, **8**, 709.
79. H. Rieskamp and R. Mattes, *Z. Naturforsch., Teil B*, 1976, **31**, 1453.
80. V. A. Sarin, V. Ya. Dudarev, L. E. Fykin, Yu. E. Gorbunova, E. G. Il'yin and Yu. A. Buslaev, *Dokl. Akad. Nauk SSSR*, 1977, **236**, 393.
81. G. Z. Pinsker, *Sov. Phys.-Crystallogr.*, 1967, **11**, 634.
82. V. V. Tkachev, O. N. Krasoschka and L. O. Atovmyan, *J. Struct. Chem.*, 1976, **17**, 807.
83. M. G. B. Drew, G. W. A. Fowles, E. M. Page and D. A. Rice, *J. Chem. Soc., Dalton Trans.*, 1981, 2409.
84. W. Clegg, *Acta Crystallogr.*, 1978, **B34**, 3328.
85. B. N. Figgis, C. L. Raston, R. P. Sharma and A. H. White, *Aust. J. Chem.*, 1978, **31**, 2717.
86. I. Sotofte and K. Nielsen, *Acta Chem. Scand., Ser. A*, 1981, **35**, 821.
87. R. G. Cavell and J. W. Quail, *Inorg. Chem.*, 1983, **22**, 2597.
88. G. Bugli and C. Potvin, *Acta Crystallogr.*, 1981, **B37**, 1394.
89. L. S. Bartell, F. B. Clippard and E. J. Jacob, *Inorg. Chem.*, 1976, **15**, 3009.
90. R. R. Ryan and D. T. Cromer, *Inorg. Chem.*, 1972, **11**, 2322.
91. J. C. Jumas, M. Maurin and E. Philippot, *J. Fluorine Chem.*, 1977, **10**, 219.
92. S. H. Mastin, R. R. Ryan and L. B. Asprey, *Inorg. Chem.*, 1970, **9**, 2100.
93. R. D. Burbank and G. R. Jones, *Inorg. Chem.*, 1974, **13**, 1071.
94. G. R. Jones, R. D. Burbank and N. Bartlett, *Inorg. Chem.*, 1970, **9**, 2264.
95. N. Bartlett, B. G. DeBoer, F. J. Hollander, F. O. Sladky, D. H. Templeton and A. Zalkin, *Inorg. Chem.*, 1974, **13**, 780.
96. N. Bartlett, F. Einstein, D. F. Stewart and J. Trotter, *J. Chem. Soc. (A)*, 1967, 1190.
97. N. Bartlett, M. Gennis, D. D. Gibler, B. K. Morrell and A. Zalkin, *Inorg. Chem.*, 1973, **12**, 1717.
98. K. Leary, D. H. Templeton, A. Zalkin and N. Bartlett, *Inorg. Chem.*, 1973, **12**, 1726.
99. A. Werner, *Z. Anorg. Allg. Chem.*, 1893, **3**, 267.
100. H. K. Ault and S. Husebye, *Acta Chem. Scand., Ser. A*, 1978, **32**, 157.
101. R. C. Elder, T. Marcuso and P. Boolchand, *Inorg. Chem.*, 1977, **16**, 2700.
102. S. Hauge and M. Tysseland, *Acta Chem. Scand.*, 1971, **25**, 3072.
103. K. Fosheim, O. Foss, A. Scheie and S. Solheimsnes, *Acta Chem. Scand.*, 1965, **19**, 2336.
104. A. J. Edwards, *J. Chem. Soc., Dalton Trans.*, 1978, 1723.
105. R. J. Elema, J. L. de Boer and A. Vos, *Acta Crystallogr.*, 1963, **16**, 243.
106. J. H. Burns, P. A. Agron and H. A. Levy, *Science*, 1963, **139**, 1208.
107. J. H. Burns, R. D. Ellison and H. A. Levy, *Acta Crystallogr.*, 1965, **18**, 11.
108. J. A. Ibers and W. C. Hamilton, *Science*, 1963, **139**, 106.
109. D. H. Templeton, A. Zalkin, J. D. Forrester and S. M. Williamson, *J. Am. Chem. Soc.*, 1963, **85**, 242.
110. C.Bois, Nguyen Quy Dao and N. Rodier, *Acta Crystallogr.*, 1976, **B32**, 1541.
111. L. Di Sipio, E. Tondello, G. Pelizzi, G. Ingletto and A. Montenero, *Cryst. Struct. Commun.*, 1974, **3**, 297, 301, 527, 731; 1977, **6**, 723.
112. R. Graziani, G. Bombieri, E. Forsellini and G. Paolucci, *J. Cryst. Mol. Struct.*, 1975, **5**, 1.

113. C. J. L. Lock and G. Turner, *Acta Crystallogr.*, 1978, **B34**, 923.
114. R. H. Fenn, A. J. Graham and N. P. Johnson, *J. Chem. Soc. (A)*, 1971, 2880.
115. R. K. Murmann and E. O. Schlemper, *Inorg. Chem.*, 1971, **10**, 2352.
116. V. W. Day and J. L. Hoard, *J. Am. Chem. Soc.*, 1968, **90**, 3374.
117. R. K. Pomeroy and W. A. G. Graham, *J. Am. Chem. Soc.*, 1972, **94**, 274.
118. R. K. Pomeroy, L. Vancea, H. P. Calhoun and W. A. G. Graham, *Inorg. Chem.*, 1977, **16**, 1508.
119. L. Vancea, M. J. Bennett, C. E. Jones, R. A. Smith and W. A. G. Graham, *Inorg. Chem.*, 1977, **16**, 897.
120. L. Vancea, R. K. Pomeroy and W. A. G. Graham, *J. Am. Chem. Soc.*, 1976, **98**, 1407.
121. D. J. Darensbourg, *Inorg. Chem*, 1979, **18**, 14.
122. D. L. McFadden, A. T. McPhail, C. D. Garner and F. E. Mabbs, *J. Chem. Soc., Dalton Trans.*, 1975, 263.
123. E. Prince, A. D. Mighell, C. W. Reimann and A. Santoro, *Cryst. Struct. Commun.*, 1972, **1**, 247.
124. A. Santoro, A. D. Mighell, M. Zocchi and C. W. Reimann, *Acta Crystallogr.*, 1969, **B25**, 842.
125. A. D. Mighell and A. Santoro, *Acta Crystallogr.*, 1971, **B27**, 2089.
126. D. Taylor, *Aust. J. Chem.*, 1975, **28**, 2615.
127. C. J. O'Connor, E. Sinn and R. L. Carlin, *Inorg. Chem.*, 1977, **16**, 3314.
128. D. Taylor, *Aust. J. Chem.*, 1978, **31**, 713.
129. D. L. Cullen and E. C. Lingafelter, *Inorg. Chem.*, 1971, **10**, 1264.
130. M. D. Joesten, S. Takagi and P. G. Lenhert, *Inorg. Chem.*, 1977, **16**, 2680.
131. D. Mullen, G. Heger and D. Reinen, *Solid State Chem.*, 1975, **17**, 1249.
132. S. Takagi, M. D. Joesten and P. G. Lenhert, *Acta Crystallogr.*, 1975, **B31**, 596; 1976, **B32**, 326, 1278, 2524.
133. S. Takagi, P. G. Lenhert and M. D. Joesten, *J. Am. Chem. Soc.*, 1974, **96**, 6606.
134. J. A. Bertrand and D. A. Carpenter, *Inorg. Chem.*, 1966, **5**, 514.
135. D. L. Kepert, *Prog. Inorg. Chem.*, 1977, **23**, 1.
136. F. A. Cotton and R. H. Soderberg, *J. Am. Chem. Soc.*, 1963, **85**, 2402.
137. A. Michelet, B. Viossat, P. Khodadad and N. Rodier, *Acta Crystallogr.*, 1981, **B37**, 678.
138. W. D. Horrocks, J. N. Ishley and R. R. Whittle, *Inorg. Chem.*, 1982, **21**, 3270.
139. P. F. Lindley and P. Carr, *J. Cryst. Mol. Struct.*, 1974, **4**, 173.
140. J. Chatt, B. A. L. Crichton, J. R. Dilworth, P. Dahlstrom, R. Gutkoska and J. Zubieta, *Inorg. Chem.*, 1982, **21**, 2383.
141. L. Ricard, J. Estienne, P. Karagiannidis, P. Toledano, J. Fischer, A. Mitschler and R. Weiss, *J. Coord. Chem.*, 1974, **3**, 277.
142. A. Kopwillem, *Acta Chem. Scand.*, 1972, **26**, 2941.
143. B. L. Haymore, E. A. Maatta and R. A. D. Wentworth, *J. Am. Chem. Soc.*, 1979, **101**, 2063.
144. C. L. Raston, P. R. Tennant, A. H. White and G. Winter, *Aust. J. Chem.*, 1978, **31**, 1493.
145. R. W. Gable, C. L. Raston, G. L. Rowbottom, A. H. White and G. Winter, *J. Chem. Soc., Dalton Trans.*, 1981, 1392.
146. S. W. Cowan, R. W. Gable, B. F. Hoskins and G. Winter, *Inorg. Chim. Acta*, 1983, **77**, L225.
147. C. S. Harreld and E. O. Schlemper, *Acta Crystallogr.*, 1971, **B27**, 1964.
148. J. S. Ricci, C. A. Eggers and I. Bernal, *Inorg. Chim. Acta*, 1972, **6**, 97.
149. K. C. Molloy, M. B. Hossain, D. van der Helm, J. J. Zuckerman and F. P. Mullins, *Inorg. Chem.*, 1981, **20**, 2172.
150. W. R. Scheidt, C. Tsai and J. L. Hoard, *J. Am. Chem. Soc.*, 1971, **93**, 3867.
151. R. E. Drew, F. W. B. Einstein and S. E. Gransden, *Can. J. Chem.*, 1974, **52**, 2184.
152. B. Kamenar, M. Penavic and C. K. Prout, *Cryst. Struct. Commun.*, 1973, **2**, 41.
153. B. Kojic-Prodic, Z. Ruzic-Toros, D. Grdenic and L. Golic, *Acta Crystallogr.*, 1974, **B30**, 300.
154. J. Hilton, E. K. Nunn and S. C. Wallwork, *J. Chem. Soc., Dalton Trans.*, 1973, 173.
155. T. Kimura, N. Yasuoka, N. Kasai and M. Kukuda, *Bull. Chem. Soc. Jpn.*, 1972, **45**, 1649.
156. B. W. Liebich and M. Tomassini, *Acta Crystallogr.*, 1978, **B34**, 944.
157. G. A. Miller and E. O. Schlemper, *Inorg. Chem.*, 1973, **12**, 677.
158. H. Graver and S. Husebye, *Acta Chem. Scand., Ser. A*, 1975, **29**, 14.
159. S. Husebye, *Acta Chem. Scand.*, 1967, **21**, 42.
160. S. Husebye, *Acta Chem. Scand.*, 1970, **24**, 2198.
161. O. P. Anderson and S. Husebye, *Acta Chem. Scand.*, 1970, **24**, 3141.
162. S. Husebye and G. Helland-Madsen, *Acta Chem. Scand.*, 1970, **24**, 2273.
163. R. O. Gould, C. L. Jones, W. J. Savage and T. A. Stephenson, *J. Chem. Soc., Dalton Trans.*, 1976, 908.
164. S. Bjornevag, S. Husebye and K. Maartmann-Moe, *Acta Chem. Scand.*, 1982, **36**, 195.
165. R. Stomberg, *Arkiv Kemi*, 1964, **22**, 29.
166. R. E. Drew and F. W. B. Einstein, *Inorg. Chem.*, 1972, **11**, 1079.
167. I. B. Svensson and R. Stomberg, *Acta Chem. Scand.*, 1971, **25**, 898.
168. G. E. Form, E. S. Raper, R. E. Oughtred and H. M. M. Shearer, *J. Chem. Soc., Chem. Commun.*, 1972, 945.
169. W. R. Scheidt, *Inorg. Chem.*, 1973, **12**, 1758.
170. P. K. Hon and C. E. Pfluger, *J. Coord. Chem.*, 1973, **3**, 67.
171. J. A. McCleverty, S. Gill, R. S. Z. Kowalski, N. A. Bailey, H. Adams, K. W. Lumbard and M. A. Murphy, *J. Chem. Soc., Dalton Trans.*, 1982, 493.
172. A. Sequeira and I. Bernal, *J. Cryst. Mol. Struct.*, 1973, **3**, 157.
173. E. I. Stiefel, Z. Dori and H. B. Gray, *J. Am. Chem. Soc.*, 1967, **89**, 3353.
174. A. E. Smith, G. N. Schrauzer, V. P. Mayweg and W. Heinrich, *J. Am. Chem. Soc.*, 1965, **87**, 5798.
175. C. G. Pierpont and R. Eisenberg, *J. Chem. Soc. (A)*, 1971, 2285.
176. G. F. Brown and E. I. Stiefel, *Inorg. Chem.*, 1973, **12**, 2140.
177. M. Cowie and M. J. Bennett, *Inorg. Chem.*, 1976, **15**, 1584.
178. R. Eisenberg and H. B. Gray, *Inorg. Chem.*, 1967, **6**, 1844.
179. R. Eisenberg and J. A. Ibers, *Inorg. Chem.*, 1966, **5**, 411.
180. J. L. Martin and J. Takats, *Inorg. Chem.*, 1975, **14**, 1358.
181. M. Cowie and M. J. Bennett, *Inorg. Chem.*, 1976, **15**, 1589.
182. M. Draganjac and D. Coucouvanis, *J. Am. Chem. Soc.*, 1983, **105**, 139.
183. M. Cowie and M. J. Bennett, *Inorg. Chem.*, 1976, **15**, 1595.
184. J. Baldas, J. Boas, J. Bonnyman, M. F. Mackay and G. A. Williams, *Aust. J. Chem.*, 1982, **35**, 2413.
185. K. Yamanouchi and J. H. Enemark, *Inorg. Chem.*, 1978, **17**, 2911.
186. E. C. Niederhoffer, A. E. Martell, P. Rudolph and A. Clearfield, *Cryst. Struct. Commun.*, 1982, **11**, 1951.

187. K. Yanagi, Y. Ohashi, Y. Sasada, Y. Kaizu and H. Kobayashi, *Bull. Chem. Soc. Jpn.*, 1981, **54**, 118.
188. L. Johansson, M. Molund and A. Oskarsson, *Inorg. Chim. Acta*, 1978, **31**, 117.
189. J. A. Broomhead, J. R. Dilworth, J. Hutchinson and J. Zubieta, *Cryst. Struct. Commun.*, 1982, **11**, 1701.
190. J. Baker, L. M. Engelhardt, B. N. Figgis and A. H. White, *J. Chem. Soc., Dalton Trans.*, 1975, 530.
191. A. Zalkin, D. H. Templeton and T. Ueki, *Inorg. Chem.*, 1973, **12**, 1641.
192. B. N. Figgis, B. W. Skelton and A. H. White, *Aust. J. Chem.*, 1978, **31**, 57.
193. P. C. Healy, B. W. Skelton and A. H. White, *Aust. J. Chem.*, 1983, **36**, 2057.
194. K. R. Butler and M. R. Snow, *J. Chem. Soc. (A)*, 1971, 565.
195. B. A. Frenz and J. A. Ibers, *Inorg. Chem.*, 1972, **11**, 1109.
196. H. A. Goodwin, D. L. Kepert, J. M. Patrick, B. W. Skelton and A. H. White, *Aust. J. Chem.*, 1984, **37**, 1817.
197. D. P. Rillema, D. S. Jones and H. A. Levy, *J. Chem. Soc., Chem. Commun.*, 1979, 849.
198. A. Wada, C. Katayama and J. Tanaka, *Acta Crystallogr.*, 1976, **B32**, 3194.
199. A. Wada, N. Sakabe and J. Tanaka, *Acta Crystallogr.*, 1976, **B32**, 1121.
200. D. J. Szalda, C. Creutz, D. Mahajan, and N. Sutin, *Inorg. Chem.*, 1983, **22**, 2372.
201. G. B. Deacon, C. L. Raston, D. Tunaley and A. H. White, *Aust. J. Chem.*, 1979, **32**, 2195.
202. H. A. Goodwin, E. S. Kucharski and A. H. White, *Aust. J. Chem.*, 1983, **36**, 1115.
203. M. Corbett and B. F. Hoskins, *Aust. J. Chem.*, 1974, **27**, 665.
204. W. R. Krigbaum and B. Rubin, *Acta Crystallogr.*, 1973, **B29**, 749.
205. B. Chaudret, C. Cayret, H. Koster and R. Poilblanc, *J. Chem. Soc., Dalton Trans.*, 1983, 941.
206. W. B. Wright and E. A. Meyers, *Cryst. Struct. Commun.*, 1980, **9**, 1173.
207. G. K.-J. Chao, R. L. Sime and R. J. Sime, *Acta Crystallogr.*, 1973, **B29**, 2845.
208. T. Ito, K. Toriumi, F. B. Ueno and K. Saito, *Acta Crystallogr.*, 1980, **B36**, 2998.
209. K. Dymock and G. J. Palenik, *Acta Crystallogr.*, 1974, **B30**, 1364.
210. B. Morosin, *Acta Crystallogr.*, 1965, **19**, 131.
211. W. B. Wright and E. A. Meyers, *Cryst. Struct. Commun.*, 1973, **2**, 477.
212. R. Kuroda and S. F. Mason, *J. Chem. Soc., Dalton Trans.*, 1979, 273.
213. C. L. Raston and A. H. White, *Aust. J. Chem.*, 1979, **32**, 507.
214. G. Albertin, E. Bordignon, A. Orio, G. Pelizzi and P. Tarasconi, *Inorg. Chem.*, 1981, **20**, 2862.
215. L. R. Nassimbeni and M. M. Thackeray, *Acta Crystallogr.*, 1974, **B30**, 1072.
216. J. Iball and C. H. Morgan, *Acta Crystallogr.*, 1967, **23**, 239.
217. C. E. Pfluger and P. S. Haradem, *Inorg. Chim. Acta*, 1983, **69**. 141.
218. B. Kaitner and B. Kamenar, *Cryst. Struct. Commun.*, 1980, **9**, 487.
219. J. G. Rodriguez, F. H. Cano and S. Garcia-Blanco, *Cryst. Struct. Commun.*, 1979, **8**, 53.
220. M. R. Truter and B. L. Vickery, *J. Chem. Soc., Dalton Trans.*, 1972, 395.
221. U. Thewalt and T. Adam, *Z. Naturforsch., Teil B*, 1978, **33**, 142.
222. T. J. Anderson, M. A. Neuman and G. A. Melson, *Inorg. Chem.*, 1973, **12**, 927.
223. W. O. McSharry, M. Cefola and J. G. White, *Inorg. Chim. Acta.*, 1980, **38**, 161.
224. T. M. Greaney, C. L. Raston, A. H. White and E. N. Maslen, *J. Chem. Soc., Dalton Trans.*, 1975, 876.
225. D. E. Fenton, C. Nave and M. R. Truter, *J. Chem. Soc., Dalton Trans.*, 1973, 2188.
226. J. P. R. de Villiers and J. C. A. Boeyens, *Acta Crystallogr.*, 1971, **B27**, 2335.
227. B.-M. Antti, B. K. S. Lundberg and N. Ingri, *Acta Chem. Scand.*, 1972, **26**, 3984.
228. I. Bertini, P. Dapporto, D. Gatteschi and A. Scozzafava, *J. Chem. Soc., Dalton Trans.*, 1979, 1409.
229. O. P. Anderson, *J. Chem. Soc., Dalton Trans.*, 1973, 1237.
230. M. D. Joesten, M. S. Hussain and P. G. Lenhert, *Inorg. Chem.*, 1970, **9**, 151.
231. D. L. Cullen and E. C. Lingafelter, *Inorg. Chem.*, 1970, **9**, 1858.
232. G. J. Kruger and E. C. Reynhardt, *Acta Crystallogr.*, 1974, **B30**, 822.
233. J. Hilton and S. C. Wallwork, *Chem. Commun.*, 1968, 871.
234. S. Sato and Y. Saito, *Acta Crystallogr.*, 1975, **B31**, 1378.
235. S. Merlino, *Acta Crystallogr.*, 1969, **B25**, 2270.
236. J. F. McConnell and A. Schwartz, *Acta Crystallogr.*, 1972, **B28**, 1546.
237. K. R. Butler and M. R. Snow, *J. Chem. Soc. (A)*, 1971. 565.
238. K. R. Butler and M. R. Snow, *Acta Crystallogr.*, 1975, **B31**, 354.
239. T. J. Anderson, M. A. Neuman and G. A. Melson, *Inorg. Chem.*, 1974, **13**, 158.
240. R. D. Burbank, *Acta Crystallogr.*, 1962, **15**, 1207.
241. J. Donohue, *Acta Crystallogr.*, 1965, **18**, 1018.
242. N. Bartlett, S. Beaton, L. W. Reeves and E. J. Wells, *Can. J. Chem.*, 1964, **42**, 2531.
243. R. J. Gillespie and J. W. Quail, *Can. J. Chem.*, 1964, **42**, 2671.
244. E. L. Muetterties and K. J. Packer, *J. Am. Chem. Soc.*, 1964, **86**, 293.
245. G. M. Brown and L. A. Walker, *Acta Crystallogr.*, 1966, **20**, 220.
246. R. Thomas, 1980, personal communication.
247. H. Leligny and J. C. Monier, *Acta Crystallogr.*, 1983, **C39**, 947.
248. D. L. Lewis and S. J. Lippard, *J. Am. Chem. Soc.*, 1975, **97**, 2697.
249. J. C. Dewan, W. S. Mialki, R. A. Walton and S. J. Lippard, *J. Am. Chem. Soc.*, 1982, **104**, 133.
250. J. C. Dewan and S. J. Lippard, *Inorg. Chem.*, 1982, **21**, 1682.
251. P. Brant, F. A. Cotton, J. C. Sekutowski, T. E. Wood and R. A. Walton, *J. Am. Chem. Soc.*, 1979, **101**, 6588.
252. W. A. LaRue, A. T. Liu and J. S. Filippo, *Inorg. Chem.*, 1980, **19**, 315.
253. S. J. Lippard, *Prog. Inorg. Chem.*, 1976, **21**, 91.
254. R. A. Levenson and R. L. R. Towns, *Inorg. Chem.*, 1974, **13**, 105.
255. M. G. B. Drew, P. C. H. Mitchell and C. F. Pygall, *J. Chem. Soc., Dalton Trans.*, 1977, 1071.
256. J-M. Manoli, C. Potvin, J-M. Bregeault and W. P. Griffith, *J. Chem. Soc., Dalton Trans.*, 1980, 192.
257. R. Stomberg, *Acta Chem. Scand., Ser. A*, 1983, **37**, 453.
258. D. F. Lewis and S. J. Lippard, *Inorg. Chem.*, 1972, **11**, 621.
259. C. T. Lam, M. Novotny, D. L. Lewis and S. J. Lippard, *Inorg. Chem.*, 1978, **17**, 2127.
260. C. M. Giandomenico, J. C. Dewan and S. J. Lippard, *J. Am. Chem. Soc.*, 1981, **103**, 1407.
261. G. Bombieri, E. Forsellini, D. Brown and B. Whittaker, *J. Chem. Soc., Dalton Trans.*, 1976, 735.
262. M. G. B. Drew, *Acta Crystallogr.*, 1982, **B38**, 254.

263. M. C. Mattos, E. Surcouf and J.-P. Mornon, *Acta Crystallogr.*, 1977, **B33**, 1855.
264. D. L. Kepert, *Prog. Inorg. Chem.*, 1979, **25**, 41.
265. L. S. Bartell and R. M. Gavin, *J. Chem. Phys.*, 1968, **48**, 2466.
266. R. D. Burbank and N. Bartlett, *Chem. Commun.*, 1968, 645.
267. W. H. Zachariasen, *Acta Crystallogr.*, 1954, **7**, 783.
268. N. W. Alcock and S. Esperas, *J. Chem. Soc., Dalton Trans.*, 1977, 893.
269. J. MacB. Harrowfield, D. L. Kepert, J. M. Patrick, A. H. White and S. F. Lincoln, *J. Chem. Soc., Dalton Trans.*, 1983, 393.
270. A. Zalkin, H. Ruben and D. H. Templeton, *Inorg. Chem.*, 1979, **18**, 519.
271. N. W. Alcock, M. M. Roberts and D. Brown, *Acta Crystallogr.*, 1982, **B38**, 2870.
272. Z. Ruzic-Toros, B. Kojic-Prodic, F. Gabela and M. Sljukic, *Acta Crystallogr.*, 1972, **B33**, 692.
273. W. Massa and G. Pausewang, *Z. Anorg. Allg. Chem.*, 1979, **456**, 169.
274. R. Stomberg, *Acta Chem. Scand., Ser. A*, 1981, **35**, 389, 489; 1982, **A36**, 101, 423.
275. L. Coghi, C. Pelizzi and G. Pelizzi, *J. Organomet. Chem.*, 1976, **114**, 53.
276. P. W. R. Corfield, J. C. Dewan and S. J. Lippard, *Inorg. Chem.*, 1983, **22**, 3424.
277. J. C. Dewan, T. E. Wood, R. A. Walton and S. J. Lippard, *Inorg. Chem.*, 1982, **21**, 1854.
278. M. G. B. Drew and J. D. Wilkins, *J. Chem. Soc., Dalton Trans.*, 1973, 1830.
279. R. M. Foy, D. L. Kepert, C. L. Raston and A. H. White, *J. Chem. Soc., Dalton Trans.*, 1980, 440.
280. R. Stomberg, *Arkiv Kemi*, 1964, **22**, 49.
281. R. Stomberg, *Arkiv Kemi*, 1965, **23**, 401.
282. A. F. Cameron, D. W. Taylor and R. H. Nuttall, *J. Chem. Soc., Dalton Trans.*, 1972, 1608.
283. J. Halfpenny and R. W. H. Small, *Acta Crystallogr.*, 1978, **B34**, 3758.
284. N. G. Charles, E. A. H. Griffith, P. F. Rodesiler and E. L. Amma, *Inorg. Chem.*, 1983, **22**, 2717.
285. A. A. Pinkerton and D. Schwarzenbach, *J. Chem. Soc., Dalton Trans.*, 1976, 2466.
286. M. G. B. Drew and D. J. Eve, *Acta Crystallogr.*, 1977, **B33**, 2919.
287. R. W. Light, L. D. Hutchins, R. T. Paine and C. F. Campana, *Inorg. Chem.*, 1980, **19**, 3597.
288. C. L. Raston and A. H. White, *J. Chem. Soc., Dalton Trans.*, 1975, 2425.
289. D. B. Sowerby, I. Haiduc, A. Barbul-Rusu and M. Salajan, *Inorg. Chim. Acta*, 1983, **68**, 87.
290. S. L. Lawton, C. J. Fuhrmeister, R. G. Haas, C. S. Jarman and F. G. Lohmeyer, *Inorg. Chem.*, 1974, **13**, 135.
291. E. Bye, *Acta Chem. Scand., Ser. A*, 1974, **28**, 731.
292. A. Zalkin, D. H. Templeton and D. G. Karraker, *Inorg. Chem.*, 1969, **8**, 2680.
293. F. A. Cotton and P. Legzdins, *Inorg. Chem.*, 1968, **7**, 1777.
294. C. S. Erasmus and J. C. A. Boeyens, *J. Cryst. Mol. Struct.*, 1971, **1**, 83.
295. E. D. Watkins, J. A. Cunningham, T. Phillips, D. E. Sands and W. F. Wagner, *Inorg. Chem.*, 1969, **8**, 29.
296. S. J. S. Wasson, D. E. Sands and W. F. Wagner, *Inorg. Chem.*, 1973, **12**, 187.
297. M. F. Richardson, P. W. R. Corfield, D. E. Sands and R. E. Sievers, *Inorg. Chem.*, 1970, **9**, 1632.
298. J. C. A. Boeyens and J. P. R. de Villiers, *J. Cryst. Mol. Struct.*, 1971, **1**, 297.
299. J. A. Cunningham, D. E. Sands, W. F. Wagner and M. F. Richardson, *Inorg Chem.*, 1969, **8**, 22.
300. G. S. Brownlee, A. Walker, S. C. Nyburg and J. T. Szymanski, *Chem. Commun.*, 1971, 1073.
301. J. O. Albright, J. C. Clardy and J. G. Verkade, *Inorg. Chem.*, 1977, **16**, 1575.
302. S. G. Hardin, P. C. Healy, W. G. Mumme, A. H. White and G. Winter, *Aust. J. Chem.*, 1982, **35**, 2423.
303. S. Esperas and S. Husebye, *Acta Chem. Scand.*, 1972, **26**, 3293.
304. D. L. Kepert, C. L. Raston, A. H. White and G. Winter, *Aust. J. Chem.*, 1978, **31**, 757.
305. E. J. Peterson, R. B. Von Dreele and T. M. Brown, *Inorg. Chem.*, 1978, **17**, 1410.
306. J. C. Dewan, D. L. Kepert, E. N. Maslen, C. L. Ralston, D. Taylor and A. H. White, *J. Chem. Soc., Dalton Trans.*, 1973, 2082.
307. M. B. Hursthouse and M. Motevalli, *J. Chem. Soc., Dalton Trans.*, 1979, 1362.
308. G. A. Williams and A. R. P. Smith, *Aust. J. Chem.*, 1980, **33**, 717.
309. M. C. Poore and D. R. Russell, *Chem. Commun.*, 1971, 18.
310. B. M. Mattson and L. H. Pignolet, *Inorg. Chem.*, 1977, **16**, 488.
311. M. J. Begley, D. B. Sowerby and I. Haiduc, *J. Chem. Soc., Chem. Commun.*, 1980, 64.
312. G. Mathern and R. Weiss, *Acta Crystallogr.*, 1971, **B27**, 1610.
313. J. J. Park, D. M. Collins and J. L. Hoard, *J. Am. Chem. Soc.*, 1970, **92**, 3636.
314. R. B. VonDreele, J. J. Stezowski and R. C. Fay, *J. Am. Chem. Soc.*, 1971, **93**, 2887.
315. S. S. Basson, L. D. C. Bok and J. G. Leipoldt, *Acta Crystallogr.*, 1970, **B26**, 1209.
316. L. D. C. Bok, J. G. Leipoldt and S. S. Basson, *Acta Crystallogr.*, 1970, **B26**, 684.
317. L. D. C. Bok, J. G. Leipoldt and S. S. Basson, *Z. Anorg. Allg. Chem.*, 1972, **392**, 303.
318. A. R. Al-Karaghouli and J. S. Wood, *Inorg. Chem.*, 1979, **18**, 1177.
319. S. Geller and T. O. Dudley, *J. Solid State Chem.*, 1978, **26**, 321.
320. J. Fischer, R. Elchinger and R. Weiss, *Acta Crystallogr.*, 1973, **B29**, 1967.
321. G. Bombieri, P. T. Moseley and D. Brown, *J. Chem. Soc., Dalton Trans.*, 1975, 1520.
322. J. L. Hoard, W. J. Martin, M. E. Smith and J. F. Whitney, *J. Am. Chem. Soc.*, 1954, **76**, 3820.
323. J. Chojnacki, J. Grochowski, L. Lebioda, B. Oleksyn and K. Stadnicka, *Rocz. Chem.*, 1969, **43**, 273.
324. C. Castellani Bisi, A. Della Giusta, A. Coda and V. Tazzoli, *Cryst. Struct. Commun.*, 1974, **3**, 381.
325. F. Lazarini and I. Leban, *Acta Crystallogr.*, 1980, **B36**, 2745.
326. F. A. Cotton, A. Davison, V. W. Day, M. F. Fredrich, C. Orvig and R. Swanson, *Inorg. Chem.*, 1982, **21**, 1211.
327. J. L. Hoard, T. A. Hamor and M. D. Glick, *J. Am. Chem. Soc.*, 1968, **90**, 3177.
328. B. J. Corden, J. A. Cunningham and R. Eisenberg, *Inorg. Chem.*, 1970, **9**, 356.
329. M. Bukowska-Strzyzewska and A. Tosic, *Acta Crystallogr.*, 1982, **B38**, 265.
330. M. Bukowska-Strzyzewska and A. Tosic, *Acta Crystallogr.*, 1982, **B38**, 950.
331. J. G. Leipoldt, S. S. Basson and L. D. C. Bok, *Inorg. Chim. Acta*, 1980, **44**, L99.
332. D. R. Sears and J. H. Burns, *J. Chem. Phys.*, 1964, **41**, 3478.
333. R. Countryman and W. S. McDonald, *J. Inorg. Nucl. Chem.*, 1971, **33**, 2213.
334. D. Brown, J. F. Easey and C. E. F. Rickard, *J. Chem. Soc. (A)*, 1969, 1161.
335. E. L. Muetterties, *Inorg. Chem.*, 1973, **12**, 1963.
336. D. L. Kepert, J. M. Patrick and A. H. White, *J. Chem. Soc., Dalton Trans.*, 1983, 381.
337. C. E. F. Rickard and D. C. Woollard, *Acta Crystallogr.*, 1980, **B36**, 292.

338. D. L. Kepert, J. M. Patrick and A. H. White, *Aust. J. Chem.*, 1983, **36**, 477.
339. D. L. Kepert, J. M. Patrick and A. H. White, *J. Chem. Soc., Dalton Trans.*, 1983, 385.
340. J. C. Dewan, D. L. Kepert, C. L. Raston and A. H. White, *J. Chem. Soc., Dalton Trans.*, 1975, 2031.
341. D. L. Kepert, B. W. Skelton and A. H. White, *J. Chem. Soc., Dalton Trans.*, 1981, 652.
342. R. J. H. Clark, J. Lewis, R. S. Nyholm, P. Pauling and G. B. Robertson, *Nature (London)*, 1961, **192**, 222.
343. K. A. Glavan, R. Whittle, J. F. Johnson, R. C. Elder and E. Deutsch, *J. Am. Chem. Soc.*, 1980, **102**, 2103.
344. M. G. B. Drew, A. P. Wolters and J. D. Wilkins, *Acta Crystallogr.*, 1975, **B31**, 324.
345. M. G. B. Drew, G. M. Egginton and J. D. Wilkins, *Acta Crystallogr.*, 1974, **B30**, 1895.
346. F. A. Cotton, L. R. Falvello and R. C. Najjar, *Inorg. Chem.*, 1983, **22**, 770.
347. D. L. Kepert, J. M. Patrick and A. H. White, *J. Chem. Soc., Dalton Trans.*, 1983, 559.
348. E. J. Peterson, R. B. Von Dreele and T. M. Brown, *Inorg. Chem.*, 1976, **15**, 309.
349. P. G. Edwards, R. A. Andersen and A. Zalkin, *J. Am. Chem. Soc.*, 1981, **103**, 7792.
350. V. Diakiw, T. W. Hambley, D. L. Kepert, C. L. Raston and A. H. White, *Aust. J. Chem.*, 1979, **32**, 301.
351. S. R. Fletcher and A. C. Skapski, *J. Organomet. Chem.*, 1973, **59**, 299.
352. A. Leclaire, *Acta Crystallogr.*, 1974, **B30**, 2259.
353. N. W. Alcock, *J. Chem. Soc., Dalton Trans.*, 1972, 1189.
354. M. H. Chisholm and M. Extine, *J. Am. Chem. Soc.*, 1975, **97**, 1623.
355. R. Stomberg, *Acta Chem. Scand.*, 1963. **17**, 1563.
356. R. Stomberg, *Acta Chem. Scand.*, 1969, **23**, 2755.
357. C. D. Garner, D. Sutton and S. C. Wallwork, *J. Chem. Soc. (A)*, 1967, 1949.
358. N. W. Alcock and V. L. Tracy, *Acta Crystallogr.*, 1979, **B35**, 80.
359. C. L. Raston, A. H. White and G. Winter, *Aust. J. Chem.*,1978, **31**, 2207.
360. C. D. Garner and S. C. Wallwork, *J. Chem. Soc. (A)*, 1966, 1496.
361. S. Husebye and S. E. Svaeren, *Acta Chem. Scand.*, 1973, **27**, 763.
362. M. Bonamico, G. Dessy, V. Fares and L. Scaramuzza, *J. Chem. Soc., Dalton Trans.*, 1975, 2079.
363. K. Hanewald, G. Kiel and G. Gattow, *Z. Anorg. Allg. Chem.*, 1981, **476**, 89.
364. S. Spiliadis, A. A. Pinkerton and D. Schwarzenbach, *Inorg. Chim. Acta*, 1983, **75**, 115.
365. M. Bonamico, G. Dessy, V. Fares and L. Scaramuzza, *J. Chem. Soc., Dalton Trans.*, 1974. 1258.
366. M. Colapietro, A. Vaciago, D. C. Bradley, M. B. Hursthouse and I. F. Rendall, *J. Chem. Soc., Dalton Trans.*, 1972, 1052.
367. D. F. Lewis and R. C. Fay, *Inorg. Chem.*, 1976, **15**, 2219.
368. C. D. Garner, N. C. Howlader, F. E. Mabbs, A. T. McPhail, R. W. Miller and K. D. Onan, *J. Chem. Soc., Dalton Trans.*, 1978, 1582.
369. J. G. Wijnhoven, *Cryst. Struct. Commun.*, 1973, **2**, 637.
370. S. R. Sofen, S. R. Cooper and K. N. Raymond, *Inorg. Chem.*, 1979, **18**, 1611.
371. A. A. Pinkerton and D. Schwarzenbach, *J. Chem. Soc., Dalton Trans.*, 1976, 2464.
372. A. A. Pinkerton, A. E. Storey and J.-M. Zellweger, *J. Chem. Soc., Dalton Trans.*, 1981, 1475.
373. T. J. Anderson, M. A. Neuman and G. A. Melson, *Inorg. Chem.*, 1974, **13**, 1884.
374. A. R. Davis and F. W. B. Einstein, *Inorg. Chem.*, 1974, **13**, 1880.
375. D. Tranqui, A. Tissier, J. Laugier and P. Boyer, *Acta Crystallogr.*, 1977, **B33**, 392.
376. M. Lenner, *Acta Crystallogr.*, 1978, **B34**, 3770.
377. D. L. Kepert, J. M. Patrick and A. H. White, *J. Chem. Soc., Dalton Trans.*, 1983, 567.
378. G. L. Glen, J. V. Silverton and J. L. Hoard, *Inorg. Chem.*, 1963, **2**, 250.
379. B. Matkovic and D. Grdenic, *Acta Crystallogr.*, 1963, **16**, 456.
380. H. Titze, *Acta Chem. Scand.*, 1969, **23**, 399.
381. J. H. Burns and M. D. Danford; *Inorg. Chem.*, 1969, **8**, 1780.
382. J. V. Silverton and J. L. Hoard, *Inorg. Chem.*, 1963, **2**, 243.
383. T. J. Pinnavaia, B. L. Barnett, G. Podolsky and A. Tulinsky, *J. Am. Chem. Soc.*, 1975, **97**, 2712.
384. G. Del Piero, G. Perego, A. Zazzetta and G. Brandi, *Cryst. Struct. Commun.*, 1975, **4**, 521.
385. D. L. Kepert, *J. Chem. Soc.*, 1965, 4736.
386. S. K. Sikka, *Acta Crystallogr.*, 1969, **A25**, 621.
387. J. Albertsson and I. Elding, *Acta Crystallogr.*, 1977, **B33**, 1460.
388. R. W. Broach, J. M. Williams, G. P. Felcher and D. G. Hinks, *Acta Crystallogr.*, 1979, **B35**, 2317.
389. C. R. Hubbard, C. O. Quicksall and R. A. Jacobson, *Acta Crystallogr.*, 1974, **B30**, 2613.
390. J. MacB. Harrowfield, D. L. Kepert, J. M. Patrick and A. H. White, *Aust. J. Chem.*, 1983, **36**, 483.
391. S. C. Abrahams, A. P. Ginsberg and K. Knox, *Inorg. Chem.*, 1964, **3**, 558.
392. K. Knox and A. P. Ginsberg, *Inorg. Chem.*, 1964, **3**, 555.
393. R. Faggiani and I. D. Brown, *Acta Crystallogr.*, 1978, **B34**, 1675.
394. T. J. R. Weakley, *Inorg. Chim. Acta*, 1982, **63**, 161.
395. K. K. Bhandary, H. Manohar and K. Vankatesan, *J. Chem. Soc., Dalton Trans.*,1975, 288.
396. K. K. Bhandary, H. Manohar and K. Vankatesan, *Acta Crystallogr.*, 1976, **B32**, 861.
397. M. C. Favas and D. L. Kepert, *Prog. Inorg. Chem.*, 1981, **28**, 309.
398. C. Chieh, G. E. Toogood, T. D. Boyle and C. M. Burgess, *Acta Crystallogr.*, 1976, **B32**, 1008.
399. L. B. Zinner, D. E. Crotty, T. J. Anderson and M. D. Glick, *Inorg. Chem.*, 1979, **18**, 2045.
400. S. Voliotis, *Acta Crystallogr.*, 1979, **B35**, 2899.
401. T. W. Hambley, D. L. Kepert, C. L. Raston and A. H. White, *Aust. J. Chem.*, 1978, **31**, 2635.
402. A. V. Ablov, A. Yu. Kon, I. F. Burshtein, T. I. Malinovskii and Z. G. Levitskaya, *Dokl. Akad. Nauk SSSR*, 1974, **217**, 1317.
403. P. S. Gentile, M. P. Dinstein and J. G. White, *Inorg. Chim. Acta*, 1976, **19**, 67.
404. V. W. Day and J. L. Hoard, *J. Am. Chem. Soc.*, 1970, **92**, 3626.
405. J. G. Leipoldt, G. F. S. Wessels and L. D. C. Bok, *J. Inorg. Nucl. Chem.*, 1975, **37**, 2487.
406. E. Huber-Buser, *Cryst. Struct. Commun.*, 1975, **4**, 731.
407. R. J. Hill and C. E. F. Rickard, *J. Inorg. Nucl. Chem.*, 1975, **37**, 2481.
408. C. C. Addison, A. J. Greenwood, M. J. Haley and N. Logan, *J. Chem. Soc., Chem. Commun.*, 1978, 580.
409. D. J. Rogers, N. J. Taylor and G. E. Toogood, *Acta Crystallogr.*, 1983, **C39**, 939.
410. K. Al-Rasoul and T. J. R. Weakley, *Inorg. Chim. Acta*, 1982, **60**, 191.

411. J.-C. G. Bunzli, B. Klein, G. Chapuis and K. J. Schenk, *J. Inorg. Nucl. Chem.*, 1980, **42**, 1307.
412. G. E. Toogood and C. Chieh, *Can. J. Chem.*, 1975, **53**, 831.
413. S. Voliotis and A. Rimsky, *Acta Crystallogr.*, 1975, **B31**, 2620.
414. S. Voliotis and A. Rimsky, *Acta Crystallogr.*, 1975, **B31**, 2612.
415. P. S. Gentile, J. White and S. Haddad, *Inorg. Chim. Acta*, 1975, **13**, 149.
416. M. C. Favas, D. L. Kepert, J. M. Patrick and A. H. White, *J. Chem. Soc., Dalton Trans.*, 1983, 571.
417. T. Ueki, A. Zalkin and D. H. Templeton, *Acta Crystallogr.*, 1966, **20**, 836.
418. J. C. Taylor, M. H. Mueller and R. L. Hitterman, *Acta Crystallogr.*, 1966, **20**, 842.
419. B. Eriksson, L. O. L. Larsson and L. Niinisto, *J. Chem. Soc., Chem. Commun.*, 1978, 616.
420. M. R. Anderson, G. T. Jenkin and J. W. White, *Acta Crystallogr.*, 1977, **B33**, 3933.
421. S. Scavnicar and B. Prodic, *Acta Crystallogr.*, 1965, **18**, 698.
422. A. Clearfield, R. Gopal and R. W. Olsen, *Inorg. Chem.*, 1977, **16**, 911.

3

Nomenclature of Coordination Compounds

THOMAS E. SLOAN
Chemical Abstracts Service, Columbus, OH, USA

3.1 INTRODUCTION

This chapter presents a concise overview of the present conventions in coordination nomenclature. Generally, the IUPAC rules and recommendations have been followed. For the cases where the IUPAC practices seemed to be out of date or incomplete, the author has drawn upon the vast expertise in nomenclature available at Chemical Abstracts Service. Sections 3.2.3 and 3.4 deal with ligand locant notation and the numbering of polynuclear complexes may be considered provisional. These concepts are still under active consideration in the various national and international nomenclature commissions and committees. The presentation is relatively brief, but it is hoped that the nomenclature principles are evident, especially when examples presented are closely examined.

3.1.1 History

Chemical nomenclature has evolved from the mystical terminology of alchemy into the two general patterns of present day terminology, the ‘additive’ nomenclature of inorganic chemistry and the 'substitutive' nomenclature prevalent in organic chemistry. Inorganic additive nomenclature developed along with the science of chemistry as it evolved from alchemy in the 17th and 18th centuries, and it still contains practices directly traceable to the last quarter of the 18th century. Acid nomenclature and binary nomenclature for salts were the first attempts to classify and name chemical substances based on their compositions and chemical generic relationships.

3.1.2 Parent–Substitutive Nomenclature

Organic chemistry developed as a separate branch of chemistry in the 19th century. Plant and animal origins of compounds provided the largest source of names for these substances, *e.g.* citric acid, malic acid and urea. Source names still provide important root word resources in organic nomenclature, *e.g.* prostane and strychnine. As organic chemistry developed, name endings came to denote classes of similar compounds as 'ol' for alcohols, 'one' for ketones and 'ine' for alkaloids. With the advent of the radical theory in organic chemistry, it became apparent that various parts of a compound could react and maintain their separate identities, and that radicals and atoms of one type substitute for other radicals or atoms in reactions of carbon skeleton compounds. Parent and substituent nomenclature developed as a natural consequence along with these discoveries. The *parent* part of an organic name denotes a large structural portion of the compound, usually with an ending indicating a primary reactive feature of the molecule, and the *substituent* expresses groups substituted on to the parent compound, *e.g.* parent 'benzoic acid' and substituent 'ethyl'. Since organic chemistry deals mainly with the study of large assemblies of a relatively small number of elements, this pattern of nomenclature has great practical and economic advantages over nomenclature designating atomic composition by *addition* of the element names, *e.g.* benzene *vs.* hexahydrogen cyclohexacarbon.

3.1.3 Additive Nomenclature

Inorganic additive nomenclature, however, names both simple and complex entities of more than 100 elements. Inorganic nomenclature also provides several degrees of complexity in order to enable a name for a compound to indicate empirical composition, molecular composition, composition and connectivity, and complete qualitative three-dimensional compound structure.

With the discoveries that led to the founding of coordination chemistry by Alfred Werner and others at the start of the 20th century, and the concomitant demise of constant valency theories, the utility of additive nomenclature once again became evident and was the nomenclature pattern used by Werner and his contemporaries in their publications.

Additive nomenclature[1] is based on the combination of element names or roots of element names and/or ligand names. The simplest and oldest additive nomenclature is binary nomenclature that expresses two components, *e.g.* sodium chloride. The cationic or electropositive portion of the compound expressed in a binary name is the element name unchanged or a group name ending in '-ium', and the anionic or electronegative portion of a compound expressed in the name ends in -ide, -ite or -ate. The proportions of cations and anions in neutral compounds are indicated by Stock numbers or simple or multiplicative prefixes (see Section 3.3.2). Additive nomenclature denotes composition. For examples see Table 1.

Table 1 Binary Nomenclature

1. RbBr	Rubidium bromide Rubidium(I) bromide	8. $AlCl_3$	Aluminum trichloride[c] Aluminum(III) chloride[c]
2. $CaCl_2$	Calcium dichloride Calcium(II) chloride	9. $La(I_3)_3$	Lanthanum tris(triiodide) Lanthanum(III) (triiodide)
3. $(NH_4)(NO_3)$	Ammonium nitrate	10. $(SO_2)Cl_2$	Sulfuryl chloride[d]
4. SCl_4	Sulfur tetrachloride[a] Sulfur(IV) chloride[a]	11. $CH_3{-}C({=}O)Cl$	Acetyl chloride[d]
5. $Al_2(SO_4)_3$	Dialuminum tris(sulfate)[b] Aluminum(III) sulfate(VI)[b]	12. CH_2Cl_2	Methylene chloride[d]
6. $Na(ClO_2)$	Sodium chlorite Sodium(I) chlorite(III)	13. $Mg(OH)_2$	Magnesium dihydroxide Magnesium(II) hydroxide
7. K_3N	Potassium nitride	14. $Na(ClO_4)$	Sodium perchlorate Sodium(I) perchlorate(VII)

[a] The substitutive name is tetrachloro-λ^4-sulfane.

[b] Trisulfate is the $(S_3O_{10})^{2-}$ ion. Sulfate(VI) may be considered a contracted form of the tetraoxosulfate(VI). This contraction is only acceptable for common oxo anions.

[c] The structural connectivity name for Al_2Cl_6 is di-μ-chloro-tetrachlorodialuminum.

[d] Occasionally radical names are used for cations in trivial usage.

The nomenclature pattern established in binary nomenclature is also used to indicate the composition of more complex entities, including ionic coordination compounds. Electropositive constituents are cited in alphabetical order before the electronegative constituents, which are also cited in alphabetical order. For examples see Table 2.

Table 2 Compositional Nomenclature of More Complex Compounds

Ag_2ScZnF_7	Scandium disilver zinc heptafluoride Scandium(III) disilver(I) zinc(II) fluoride
Co_2CuO_4	Dicobalt copper tetraoxide Dicobalt(III) copper(II) oxide
$Cu_2(OH)_3(NO_3)$	Dicopper trihydroxide nitrate Dicopper(II) trihydroxide nitrate
$CuIn_2BrSe_3$	Copper diindium bromide tris(selenide)
$Cr(OH)(SO_4)$	Chromium hydroxide sulfate Chromium(III) hydroxide sulfate
$FePb_2ReO_6$	Iron dilead ruthenium hexaoxide
$[Cr(NH_3)_6][FeCl_6]$	Hexaamminechromium(III) hexachloroferrate(III)

3.1.4 Coordination Nomenclature

The name for a coordination compound is derived by selecting a central atom and naming surrounding bonded species as ligands. Ligands may be monatomic or polyatomic and may be formally derived from anions (chloro, trifluoromethanesulfonato), neutral molecules (ammine, ethylene), and cations [(2-aminoethyl)triethylammonium, cycloheptatrienylium]. Polyatomic ligands may bond through a single atom and are termed monodentate. Ligands that form rings by bonding to the central atom through two or more separate atoms are said to be chelated. Chelating ligands are termed bidentate, tridentate, tetradentate, pentadentate, hexadentate, heptadentate, *etc.* Ligands may also bridge two or more central atoms.

The geometric shape of the fixed positions occupied by ligating atoms is the coordination polyhedron. The common coordination polyhedra are the tetrahedron, square plane, trigonal bipyramid, square pyramid, octahedron and trigonal prism, for coordination numbers four, five and six. Distortions from the idealized coordination polyhedra occur due to size requirements of ligands and electronic .effects such as the Jahn–Teller effect. Nevertheless, it is common practice to describe the overall geometry of the ligand environment as an idealized coordination polyhedron.

3.2 LIGANDS

3.2.1 Neutral Ligands

Neutral ligand names, with the exception of NH_3 (ammine), H_2O (aqua), CO (carbonyl) and NO (nitrosyl), are expressed in coordination nomenclature by their unmodified names. The ligand names for all neutral ligands except for the four listed above are enclosed in punctuation (parentheses – ( ), square brackets – [ ], and braces – { }). For examples see Table 3.

Table 3 Neutral Ligand Names

Formula	*Systematic name*	*Common name*
Br_2	(dibromine)	
O_2	(dioxygen)	
S_8	(octasulfur)	
N_2	(dinitrogen)	
(CS)		(thiocarbonyl), (carbonothioyl)
(NS)		(thionitrosyl)
(H_2S)	(sulfane)	(hydrogen sulfide)
(PH_3)	(phosphane)	(phosphine)
$(CH_2{=}CH_2)$	(ethene)	(ethylene)
(PH_2PH_2)	(diphosphane)	(diphosphine)
$[P(C_6H_5)_3]$	(triphenylphosphane)	(triphenylphosphine)
$[NH_2(CH_3)]$	(methanamine)	(methylamine)
$[N(CH_3)_3]$	(*N*,*N*-dimethylmethanamine)	(trimethylamine)
(NC_5H_5)		(pyridine)
$(H_2NC_6H_5)$	(benzenamine)	(aniline)
$(OCHC_6H_5)$		(benzaldehyde)

3.2.2 Anionic and Cationic Ligands

Anionic ligand names generally end in ‘o’. When the anion name of a species ends in -ide, -ite or -ate, the ligand name is formed by replacing the final -e with -o to give -ido, -ito or -ato. Punctuation is used to set off inorganic anionic ligand names containing numerical prefixes, as in (disulfato), and for thio, seleno and telluro analogs of oxo anions, as in (thiophosphato) for example. The formal anionic charge of anionic ligands derived from polybasic acids, and most multiple charges on other ligands, are indicated by the Ewens–Bassett number, *e.g.* [phosphato(1−)], [phosphato(2−)], [phosphato(3−)] and [diazanido(3−)], for $(H_2PO_4)^-$, $(HPO_4)^{2-}$, $(PO_4)^{3-}$ and $(NH{-}N)^{3-}$, respectively. Ligand names with formal charges indicated by the Ewens–Bassett number are always enclosed in punctuation. Common practice has allowed that the -ato suffix on anionic ligands derived from polybasic acids may indicate the loss of all commonly acknowledged acid protons to form the ligand of highest possible negative charge. In this context the Ewens–Bassett number is not used to indicate formal charge and all non-ionized protons are named in the ligand, *e.g.* phosphato, (hydrogen phosphato) and (dihydrogen phosphato) for $(PO_4)^{3-}$, $(HPO_4)^{2-}$ and $(H_2PO_4)^-$, respectively. For examples see Table 4.

Table 4 Anionic Inorganic Ligand Names

Formula	*Systematic name*	*Common name*
H^-	hydrido	hydro
F^-	fluoro	
Cl^-	chloro	
$(I_3)^-$	[triiodo(1−)]	
$[ClF_2]^-$	[difluorochlorato(1−)]	
$[IF_4]^-$	[tetrafluoroiodato(1−)]	
$(ClO)^-$	[oxochlorato(1−)]	hypochlorito
$(ClO_2)^-$	[dioxochlorato(1−)]	chlorito
$(ClO_3)^-$	[trioxochlorato(1−)]	chlorato
$(ClO_4)^-$	[tetraoxochlorato(1−)]	perchlorato
$(IO_5)^{3-}$	[pentaoxoiodato(3−)]	mesoperiodato
$(IO_6)^{5-}$	[hexaoxoiodato(5−)]	orthoperiodato
$(I_2O_9)^{4-}$	[μ-oxo-octaoxodiiodato(4−)]	(dimesoperiodato)
$(ClS)^-$	[sulfidochlorato(1−)]	(thiohypochlorito)
O^{2-}	oxido	oxo
S^{2-}	sulfido	thio, thioxo
Se^{2-}	selenido	seleno, selenoxo
Te^{2-}	tellurido	telluro, telluroxo
$(O_2)^{2-}$	(dioxido)	peroxo
$(S_2)^{2-}$	(disulfido)	(dithio)
$(S_3)^{2-}$	(trisulfido)	(trithio)
$(O_3)^{2-}$	(trioxido)	ozonido
$(O_2)^{1-}$	[dioxido(1−)]	hyperoxido, superoxido
$(OH)^-$		hydroxo
$(HS)^-$	(sulfanido)	mercapto, (hydrosulfido)
$(O_2H)^-$		(hydrogenperoxo), (hydroperoxo)
$(HS_2)^-$	(disulfanido)	(hydrogendisulfido)
$(SO_2)^-$	[dioxosulfato(2−)]	sulfoxylato
$(SO_3)^{2-}$	[trioxosulfato(2−)]	sulfito
$(SO_3H)^-$	[hydridotrioxosulfato(1−)]	(hydrogensulfito)
$(S_2O_3)^{2-}$		(thiosulfato)
$(SO_4)^{2-}$	[tetraoxosulfato(2−)]	sulfato
$(S_2O_7)^{2-}$	[μ-oxo-hexaoxodisulfato(2−)]	(disulfato)
N^{3-}	nitrido	
P^{3-}	phosphido	
$(N_2)^{2-}$	[dinitrido(2−)]	
$(N_2)^{4-}$	[dinitrido(4−)]	
$(N_3)^-$	(trinitrido)	azido
$(P_2)^{2-}$	[diphosphido(2−)]	
$(NH)^{2-}$	[azanido(2−)]	imido
$(NH_2)^-$	(azanido)	amido
$(PH)^{2-}$	[phosphanido(2−)]	phosphinidene
$(PH_2)^-$	(phosphanido)	phosphino
$(FN)^{2-}$	[fluoroazanido(2−)]	(fluorimido)
$(ClHN)^-$	(chloroazanido)	(chloramido)
$(Br_2N)^-$	(dibromoazanido)	(dibromamido)
$(FP)^{2-}$	[fluorophosphanido(2−)]	(fluorophosphinidene)
$(F_2P)^-$	(difluorophosphanido)	(difluorophosphino)
$(HN{=}N)^-$	(diazenido)[a]	(diiminido)
$(NNH)^{3-}$	[diazanido(3−)]	[hydrazinido(3−)]

Table 4 *(continued)*

Formula	*Systematic name*	*Common name*
$(H_2NN)^{2-}$	[diazanido(2−)]	[hydrazinido(2−)]
$(H_2NNH)^-$	(diazanido)	(hydrazinido)
$(NHOH)^-$	(hydroxylaminato)	(hydroxyamido)
$(NOH)^{2-}$	[hydroxylaminato(2−)]	(hydroxyimido)
$(PO_3)^{3-}$	[trioxophosphato(3−)]	phosphito
$(HPO_2)^{2-}$	[hydridodioxophosphato(2−)]	phosphinito
$(H_2PO)^-$	(dihydridooxophosphato)	phosphenito
$(PO_4)^{3-}$	[tetraoxophosphato(3−)]	phosphato
$(HPO_3)^{2-}$	[hydridotrioxophosphato(2−)]	phosphonato
$(H_2PO_2)^-$	(dihydridodioxophosphato)	phosphinato
$(NO_2)^-$	(dioxonitrato)	nitrito-*N* or -*O*
$(NO_3)^-$	(trioxonitrato)	nitrato

[a] IUPAC 'The Nomenclature of Hydrides of Nitrogen and Derived Cations, Anions, and Ligands', *Pure Appl. Chem.*, 1982, **54**, 2545.

Anionic ligands derived from organic compounds by formal loss of a proton are named by appending the -ato suffix to the compound name, *e.g.* (benzenethiolato). Punctuation is used to set off all organic ligand names ending in -ato. Common practice allows for some exceptions. Anionic ligands derived from common alcohols may end in -oxo as in ethoxo. Alkyl (R—), alkylidene (R═), alkylidyne (R≡), aryl (Ar—), *etc.* ligands are considered to be formally anionic in organometallic compounds and are given organic radical names without alteration in coordination and organometallic compound nomenclature. For examples see Table 5.

The name of a cationic ligand is used without change, *e.g.* cycloheptatrienylium and (1-amino-*N*,*N*,*N*-trimethylmethanaminium).

Table 5 Organic Ligand Names

Formula	*Systematic name*	*Common name*
$(CH_3O)^-$	(methanolato)	methoxo
$(C_2H_5O)^-$	(ethanolato)	ethoxo
$(CH_3S)^-$	(methanethiolato)	
$(C_6H_5O)^-$	(phenolato)	phenoxo
$(C_2O_4)^{2-}$		(oxalato)
$(HCO_2)^-$	(methanoato)	(formato)
$(CH_3N)^{2-}$	[methanaminato(2−)]	(methylimino)
$(CH_3NH)^-$	(methanaminato)	(methylamido)
$[(CH_3)_2N]^-$	(*N*-methylmethanaminato)	(dimethylamido)
$(CH_3P)^{2-}$	[methylphosphanato(2−)]	(methylphosphinidene)
$(CH_3PH)^-$	(methylphosphanato)	(methylphosphino)
CH_3— (Me—)	methyl	
CH_3CH_2— (Et—)	ethyl	
$CH_3CH_2CH_2$— (Pr—)	propyl	
$(CH_3)_2CH$—	(1-methylethyl)	isopropyl
$CH_2{=}CH{-}CH_2$—	(2-propenyl)	allyl
$CH_3CH_2CH_2CH_2$— (Bu—)	butyl	
$(CH_3)_2CHCH_2$—	(2-methylpropyl)	isobutyl
$CH_3CH_2CH(CH_3)$—	(1-methylpropyl)	*sec*-butyl
$(CH_3)_3C$—	(1,1-dimethylethyl)	*tert*-butyl
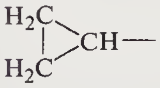	cyclopropyl	
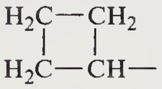	cyclobutyl	
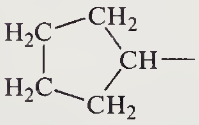	cyclopentyl	
C_5H_5—	cyclopentadienyl	
C_6H_5— (Ph—)	phenyl	
$C_6H_5CH_2$—	(phenylmethyl)	benzyl
$C_{10}H_7$—	1- or (2-naphthalenyl)	1- or 2-naphthyl
C_9H_7—	(1*H*-indenyl)	indenyl

Table 5 *(continued)*

Formula	*Systematic name*	*Common name*
$C_{10}H_{17}-$	(1,7,7-trimethylbicyclo[2.2.1]hept-2-yl)	2-bornyl
$CH_3-C(=O)-$	(1-oxoethyl)	acetyl
$CH_3CH_2C(=O)-$	(1-oxopropyl)	propionyl
$CH_3CH_2CH_2C(=O)-$	(1-oxobutyl)	butyryl
$CH_2=$	methylene	
$CH_3CH=$	ethylidene	
$CH_3CH_2CH=$	propylidene	
$CH_2=CH-CH=$	(2-propen-1-ylidene)	allylidene
$(CH_3)_2C=$	(1-methylethylidene)	isopropylidene
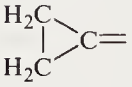	cyclopropylidene	
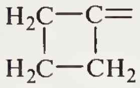	cyclobutylidene	
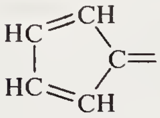	(2,4-cyclopentadien-1-ylidene)	
$C_6H_5CH=$	(phenylmethylene)	benzylidene
$CH\equiv$	methylidyne	
$CH_3C\equiv$	ethylidyne	
$CH_3CH_2-C\equiv$	propylidyne	
$C_6H_5C\equiv$	(phenylmethylidyne)	benzylidyne

3.2.3 Polydentate Ligands

3.2.3.1 Ligating atom symbol locants

Polydentate ligands may bond to central atoms through one of several ligating atoms or through two or more ligating atoms to form chelate rings. Because of these added considerations it is sometimes necessary to distinguish between, or indicate, specific donor atoms within a ligand. For small or uncomplicated ligands this is simply accomplished by appending the italicized atomic symbol and, where necessary, a superscript locant for the donor atom at the end of the ligand name. The symbols are listed in alphabetical order. For examples see Table 6.

Table 6 Atomic Symbol Locants

1.	M—NCS	(thiocyanato-*N*)
2.	M—SCN	(thiocyanato-*S*)
3.	M—ONO	(nitrito-*O*)
4.	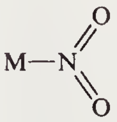	(nitrito-*N*)
5.	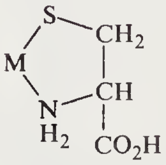	(cysteinato-*N*,*S*)
6.	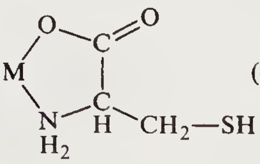	(cysteinato-*N*,*O*)
7.	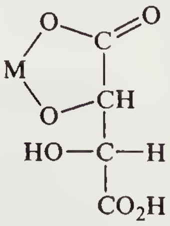	[tartrato(2−)-O^1,O^2]
8.	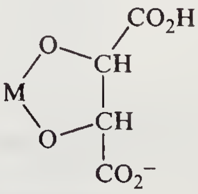	[tartrato(3−)-O^2,O^3]

3.2.3.2 Kappa notation

As more complex ligand structures are derived the usefulness of this simple notation diminishes, due particularly to the complicated nature of organic systematic substitutive nomenclature for the complex ligand structures, and because italic atomic symbols are used as locants in organic nomenclature. The italic atomic symbol set off by the Greek letter 'κ' is used within the name of a complicated polydentate ligand to indicate clearly the bonding atom.^{2} The ligand donor atom locant prefixed by 'κ ', *e.g.* -κ*N*, is placed after that portion of the ligand name which denotes the particular function, ring, chain or radical prefix in which the ligating atom is named. Ligating atoms occurring in functional suffixes, chains, rings and radical prefixes which contain other potential donor atoms, are uniquely indicated by a superscript numeral, letter or prime on the italic element symbol. These indexes denote the position of the ligating atom within the indicated portion of the ligand name. For examples see Table 7.

Table 7 Coordinating Atom Locants

1.	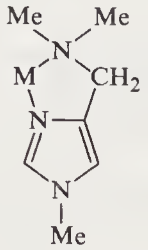	(*N*,*N*,1-Trimethyl-1*H*-imidazole-κN^3-4-methanamine-κ*N*)
2.	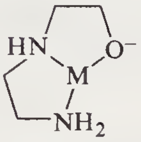	[2-[(2-Amino-κ*N*-ethyl)amino-κ*N*]ethanolato-κ*O*]
3.	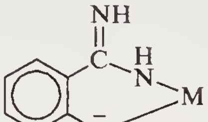	(2-Mercapto-κ*S*-benzenecarboximidamidato-κ*N*)
4.	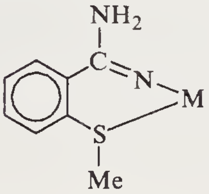	[2-(Methylthio-κ*S*)benzenecarboximidamidato-κ*N*′]

For identically bonded ligating atoms a right superscript numeral is given on the κ symbol to indicate the number of identical ligating atoms, *e.g.* (diethylenetriamine-$\kappa^3 N$). Multiplicative prefixes such as 'bis', 'tris', 'tetrakis', *etc.* operate on the locant. Thus the substituent is written '...bis(2-amino-κ*N*-ethyl)... ' not '...bis(2-amino-$\kappa^2 N$-ethyl...)', as shown by the two isomers of the tetraamine ligand *N*,*N*′-bis(2-aminoethyl)-1,2-ethanediamine (examples 2 and 3 in Table 8). Also, the monodentate bonding of the ...-1,2-ethanediamine (example 2 in Table 8) is indicated by '...1,2-ethanediamine-κ*N*)' compared with the bidentate chelation indicated by '...1,2-ethanediamine-$\kappa^2 N,N'$)' (example 3 in Table 8). The designation of bonding for 1,2-ethanediamine is shown in two ways in example 1 of Table 8. When the κ*N* notation is placed within the punctuation, the multiplicative prefix operates to multiply the notation. In the second name the κ*N* notation is placed outside the parentheses with the superscript six ('$\kappa^6 N$') to indicate six metal–nitrogen bonds. This second practice is useful in polynuclear complexes. For examples see Table 8.

Table 8 Multiplication of κ Locants

1.	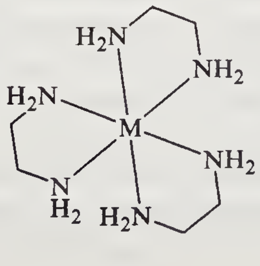	a) Tris(1,2-ethanediamine-$\kappa^2 N,N'$) or b) Tris(1,2-ethanediamine)-$\kappa^6 N$

Table 8 *(continued)*

2.	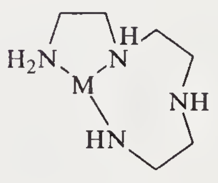	[*N*-(2-Amino-κ*N*-ethyl)-*N*′-(2-aminoethyl)-1,2-ethanediamine-κ^2*N*,*N*′]
3.	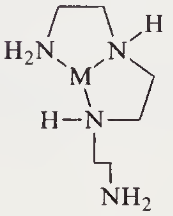	[*N*-(2-Amino-κ*N*-ethyl)-*N*′-(2-aminoethyl)-1,2-ethanediamine-κ^2*N*′]
4.	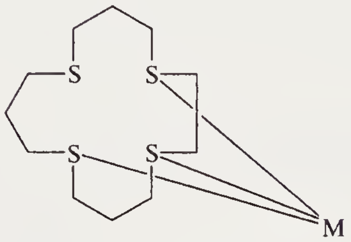	(1,4,8,12-Tetrathiacyclopentadecane-κ^3*S*^{1},*S*^{4},*S*^{8}) or (1,4,8,12-Tetrathiacyclopentadecane-κ^3*S*^{1,4,8})
5.	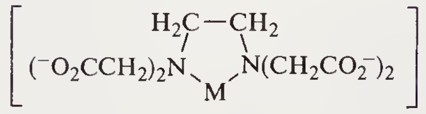	[[(1,2-Ethanediyldinitrilo-κ^2*N*,*N*′)tetraacetato](4−)]
6.	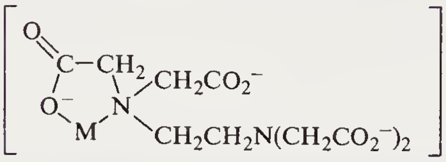	[[(1,2-Ethanediyldinitrilo-κ*N*)tetraacetato-κ*O*](4−)]
7.	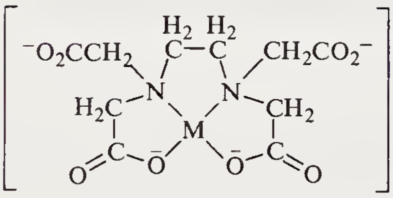	[[(1,2-Ethanediyldinitrilo-κ^2*N*,*N*′)tetraacetato-κ^2*O*,*O*′](4−)]
8.	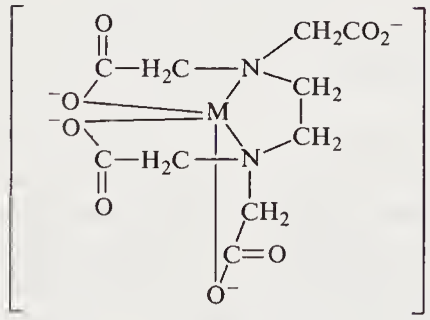	[[(1,2-Ethanediyldinitrilo-κ^2*N*,*N*′)tetraacetato-κ^3*O*,*O*′](4−)]

3.2.3.3 Hapto notation

The unique nature of the bonding of hydrocarbon π-electronic systems to metals in organometallic compounds, and the complex structures of these compounds, has rendered conventional nomenclature impotent. To overcome the difficulties due to the unique bonding and structure of these compounds the hapto nomenclature symbol, 'η', was devised.[3] The hapto symbol, 'η', with numerical right superscript, is prefixed to the ligand name or that portion of the ligand name most appropriate to indicate the connectivity, *e.g.* (η^2-ethenylcyclopentadiene) or (ethenyl-η^5-cyclopentadiene). The right superscript numerical index indicates the number of connected ligating atoms in the ligand. In the compounds in which the superscript index is not sufficient to specify a unique structure, locants of the ligating atoms are given before the hapto symbol 'η'. When ligating atom numerical locants are used, the locants and hapto symbol 'η' are enclosed in parentheses, *e.g.* (1,2,3-η)-. When locants are used the hapto superscript index is omitted. In polynuclear compounds the numerical locant of the central atom (see Section 3.4.4) is given before the hapto symbol and the hapto symbol is always enclosed in parentheses, *e.g.* [3(η^5)-... and [2(1,2,3,4-η)-.... For examples see Table 9.

Table 9 Hapto Notation

1.	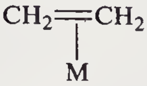	(η^2-ethene)
2.	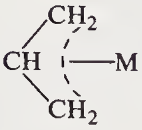	(η^3-allyl)
3.	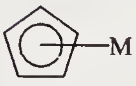	(η^5-cyclopentadienyl)
4.	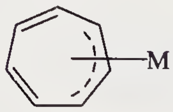	[(1,2,3-η)-2,4,6-cycloheptatrien-1-yl]
5.	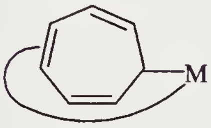	[(1,4,5-η)-2,4,6-cycloheptatrien-1-yl]
6.	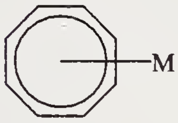	(η^8-1,3,5,7-cyclooctatetraene)
7.	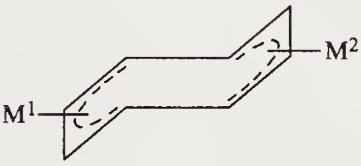	μ-[1(1,2,3,4-η):2(5,6,7,8-η)-1,3,5,7-cyclooctatetraene]
8.	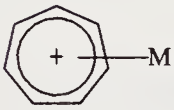	(η^7-cycloheptatrienylium)

3.2.3.4 *Bridging ligand notation*

Bridging ligands are indicated in a coordination name by the Greek letter prefix 'μ'. The bridging index, the number (greater than two) of coordination centers connected by a bridging ligand, is indicated by a right subscript on μ, *e.g.* 'μ_3', and the bridging ligand name is separated from the rest of the complex name by punctuation. Bridging ligands are cited in alphabetical order with the other ligands, but with a bridging ligand given before a corresponding nonbridging ligand, *e.g.* di-μ-bromo-tetrabromo..., μ-(diphenylphosphino)-bis(diphenylphosphino).... Multiple bridging is cited in descending order of complexity, *e.g.* di-μ_3-thio-μ-thio-tetrathio....

3.2.4 Ligand Abbreviations

A list of commonly encountered ligand abbreviations is given in Table 10. While it is generally accepted to use abbreviations for ligands in a pseudo formula ($[Co(edta)(H_2O)]^-$) within textual material to stand for a cumbersome name, it should be recognized that ambiguities in interpretation can always occur with this type of notation. Thus, all abbreviations should be defined within a suitable span of text. Scientific publications should certainly contain at least one formula per compound which is composed only of the internationally accepted atomic symbols, and which accurately defines the composition of the compound or compounds of primary interest reported in the publication.

Table 10 Ligand Abbreviations

Systematic name	*Abbreviation*	*Common name*
	Diketones	
1,3-Butanedione, 1-phenyl-	Hba	benzoylacetone
3,5-Heptanedione, 2,2,6,6-tetramethyl-	Hdpm	dipivaloylmethane
3,5-Octanedione, 6,6,7,7,8,8,8-heptafluoro-2,2-dimethyl-	Hfod	4,6-octanedione, 1,1,1,2,2,3,3-heptafluoro-7,7-dimethyl-
2,4-Pentanedione	Hacac	acetylacetone
2,4-Pentanedione, 1,1,1,5,5,5-hexafluoro-	Hhfa	hexafluoroacetylacetone
2,4-Pentanedione, 1,1,1-trifluoro-	Hfta	trifluoroacetylacetone
1,3-Propanedione, 1,3-diphenyl-	Hdbm	dibenzoylmethane
	Amino alcohols	
Ethanol, 2-amino-	Hea	ethanolamine
Ethanol, 2,2′-iminobis-	H_2dea	diethanolamine
Ethanol, 2,2′,2″-nitrilotris-	H_3tea	triethanolamine
	Amino acids and related compounds	
Adenosine	Ado	adenosine
Adenosine 5′-(tetrahydrogen triphosphate)	ATP	adenosine triphosphate
Adenosine 5′-(trihydrogen diphosphate)	ADP	adenosine diphosphate
Alanine	Ala	alanine
Arginine	Arg	arginine
Aspartic acid	Asp	aspartic acid
Cysteine	Cys	cysteine
Glutamic acid	Glu	glutamic acid
Glycine	Gly	glycine
Guanosine	Guo	guanosine
Histidine	His	histidine
Inosine	Ino	inosine
Isoleucine	Ile	isoleucine
Leucine	Leu	leucine
Lysine	Lys	lysine
Lysine, 5-hydroxy-	Hyl	hydroxylysine
Methionine	Met	methionine
Norleucine	Nle	norleucine
Norvaline	Nva	norvaline
Ornithine	Orn	ornithine
Phenylalanine	Phe	phenylalanine
Proline	Pro	proline
Proline, 4-hydroxy-	Hyp	hydroxyproline
1*H*-Purin-6-amine	Ade	adenine
1*H*-Purine	Pur	purine
Serine	Ser	serine
Threonine	Thr	threonine
Tryptophan	Trp	tryptophan
Tyrosine	Tyr	tyrosine
Valine	Val	valine
	Organics	
Acetyl	Ac	acetyl
Benzyl	Bz	benzyl
Bicyclo[2.2.1]hepta-2,5-diene	nbd	norbornadiene
Butyl	Bu	butyl
Cyclohexyl	Cy	cyclohexyl
1,5-Cyclooctadiene	Cod	cycloocta-1,5-diene
1,3,5,7-Cyclooctatetraene	Cot	cyclooctatetraene
Cyclopentadienyl	Cp	cyclopentadienyl
Ethyl	Et	ethyl
Methyl	Me	methyl
Phenyl	Ph	phenyl
Propyl	Pr	propyl
	Heterocyclic	
1*H*-Benzimidazole	bim	benzimidazole
2,2′-Bipyridine	bpy	2,2′-bipyridine
Borate(1−), tetrakis(1*H*-pyrazolato-*N*)-, hydrogen	Hbpz	hydrogen tetra(1-pyrazolyl)borate(1−)
1,4-Diazabicyclo[2.2.2]octane	dabco	1,4-diazabicyclo[2.2.2]octane
Furan, tetrahydro-	thf	tetrahydrofuran
1*H*-Imidazole	im	imidazole
1,10-Phenanthroline	phen	1,10-phenanthroline
Piperidine	pip	piperidine
3-Pyridinecarboxamide	nia	nicotinamide

Table 10 *(continued)*

Systematic name	*Abbreviation*	*Common name*
4-Pyridinecarboxamide	isn	isonicotinamide
1*H*-Pyrazole	pz	pyrazole
Pyridine	py	pyridine
Pyridine, 2,6-dimethyl-	lut	2,6-lutidine
Pyridine, methyl-	pic	picoline
2,2′:6′,2″-Terpyridine	terpy	2,2′,2″-terpyridine
	Common	
Acetic acid, (1,2-ethanediyldinitrilo)tetra-	H_4edta	ethylenediaminetetraacetic acid
Arsine, 1,2-phenylenebis(dimethyl-	diars	*o*-phenylenebis(dimethylarsine)
2,3-Butanedione dioxime	H_2dmg	dimethylglyoxime
2-Butenedinitrile, 2,3-dimercapto-	H_2mnt	maleonitriledithiol
Carbamodithioic acid, diethyl-	HEt_2dtc	diethyldithiocarbamic acid
1,2-Cyclohexanediamine	chxn	*trans*-1,2-diaminocyclohexane
1,2-Ethanediamine	en	ethylenediamine
1,2-Ethanediamine, *N*-(2-aminoethyl)-	dien	diethylenetriamine
1,2-Ethanediamine, *N*,*N*-bis(2-aminoethyl)-	tren	tris(2-aminoethyl)amine
1,2-Ethanediamine, *N*,*N*′-bis(2-aminoethyl)-	trien	triethylenetetramine
1,2-Ethanediamine, *N*,*N*,*N*′,*N*′-tetramethyl-	tmen	*N*,*N*,*N*′,*N*′-tetramethylethylenediamine
Ethenetetracarbonitrile	tcne	tetracyanoethylene
Formamide, *N*,*N*-dimethyl-	dmf	dimethylformamide
Glycine, *N*,*N*-bis(carboxymethyl)-	H_3nta	nitrilotriacetic acid
Glycine, *N*,*N*-bis[2-[bis(carboxymethyl)amino]-ethyl]-	H_5dtpa	*N*,*N*,*N*′,*N*″,*N*″-diethylenetriaminepentaacetic acid
Glycine, *N*-(carboxymethyl)-	H_2ida	iminodiacetic acid
Glycine, *N*,*N*′-1,2-cyclohexanediylbis[*N*-(carboxy-methyl)-	H_4cdta	*trans*-cyclohexanediaminetetraacetic acid
Hydrazinecarbothioamide	Hthsc	thiosemicarbazide
Imidodicarbonimidic diamide	Hbig	biguanide
Methane, sulfinylbis-	dmso	dimethyl sulfoxide
Phosphine, [2-[(diphenylphosphino)methyl-2-methyl-1,3-propanediyl]bis(diphenyl-	triphos	1,1,1-tris(diphenylphosphinomethyl)ethane
Phosphine, 1,2-ethanediylbis(diethyl-	depe	1,2-bis(diethylphosphino)ethane
Phosphine, 1,2-ethanediylbis(diphenyl-	dppe	1,2-bis(diphenylphosphino)ethane
Phosphoric triamide, hexamethyl-	hmpa	hexamethylphosphoric triamide
1,2-Propanediamine	pn	propylenediamine
1,3-Propanediamine	tn	trimethylenediamine
1,3-Propanediamine, *N*,*N*′-bis(2-aminoethyl)-	2,3,2-tet	1,4,8,11-tetraazaundecane
1,3-Propanediamine, *N*,*N*′-bis(3-aminopropyl)-	3,3,3-tet	1,5,9,13-tetraazatridecane
Propanedinitrile, 2,2′-(2,5-cyclohexadiene-1,4-diylidene)bis-	tcnq	tetracyanoquinodimethane
1,3,5,7-Tetraazatricyclo[3.3.1.1^{3,7}]decane	hmta	hexamethylenetetramine
Thiourea	tu	thiourea
Urea	ur	urea
	Schiff base	
Benzenethiol, 2,2′-[1,2-ethanediylbis(nitrilo-methylidyne)]bis-	H_2tsalen	bis(2-mercaptobenzylidene)ethylenediamine
Glycine, *N*-[2-hydroxyphenyl]methylene-	H_2salgly	salicylideneglycine
2-Pentanone, 4,4′-(1,2-ethanediyldinitrilo)bis-	H_2acacen	bis(acetylacetone)ethylenediamine
Phenol, 2,2′-[1,2-ethanediylbis(nitrilo-methylidyne)]bis-	H_2salen	bis(salicylidene)ethylenediamine
Phenol, 2,2′-iminobis(1,2-ethanediylnitrilo-methylidyne)]bis-	H_2saldien	bis(salicylidene)diethylenetriamine
Phenol, 2,2′-[1,3-propanediylbis(nitrilo-methylidyne)]bis-	H_2saltn	bis(salicylidene)-1,3-diaminopropane
	Macrocycles	
1,4,7,10,13-Benzopentaoxacyclopentadecin, 2,3,5,6,8,9,11,12-octahydro-	benzo-15-crown-5	2,3-benzo-1,4,7,10,13-pentaoxacyclopentadec-2-ene, 6,7,9,10,18-hexahydro-
1,10-Dioxa-4,7,13,16-tetraphosphacyclooctadecane	[18]aneP_4O_2	1,10-dioxa-4,7,13,16-tetraphosphacyclooctadecane
1,4,7,10,13,16-Hexaoxacyclooctadecane	18-crown-6	1,4,7,10,13,16-hexaoxacyclooctadecane
4,7,13,16,21,24-Hexaoxa-1,10-diazabicyclo-[8.8.8]hexacosane	cryptand 222	4,7,13,16,21,24-hexaoxa-1,10-diazabicyclo[8.8.8]-hexacosane
29*H*,31*H*-Phthalocyanine	H_2pc	phthalocyanine
21*H*,23*H*-Porphine-2,18-dipropanoic acid, 7,12-diethenyl-3,8,13,17-tetramethyl-	PPIX	protoporphyrin IX
21*H*,23*H*-Porphine, 2,3,7,8,12,13,17,18-octaethyl-	H_2oep	octaethylporphyrin
21*H*,23*H*-Porphine, 5,10,15,20-tetraphenyl-	H_2tpp	tetraphenylporphyrin
1,4,8,11-Tetraazacyclotetradecane, 2,3,9,10-tetra-methyl-	Me_4[14]aneN_4	2,3,9,10-tetramethyl-1,4,8,11-tetraazacyclotetra-decane
1,4,8,11-Tetraazacyclotetradeca-1,3-diene	[14]1,3-dieneN_4	1,4,8,11-tetraazacyclotetradeca-1,3-diene

Table 10 *(continued)*

Systematic name	*Abbreviation*	*Common name*
1,4,8,11-Tetraazacyclotetradecane	$[14]aneN_4$	1,4,8,11-tetraazacyclotetradecane
Tetrabenzo[*b*,*f*,*j*,*n*][1,5,9,13]tetraazacyclohexadecine	$Bz_4[16]$-tetraeneN_4	3,4:7,8:11,12:15,16-tetrabenzo-1,5,9,13-tetraazacyclohexadeca-1,5,9,13-tetraene
4,7,13,18-Tetraoxa-1,10-diazabicyclo[8.5.5]eicosane	cryptand 211	4,7,13,18-tetraoxa-1,10-diazabicyclo[8.5.5]eicosane
1,4,7,10-Tetrathiacyclododecane	[12]aneS	1,4,7,10-tetrathiacyclododecane

3.3 MONONUCLEAR COMPLEXES

3.3.1 Order of Citation of Ligands

The ligands in coordination names are listed in alphabetical order before the central atom name. Numerical prefixes that indicate the number of ligands are not considered in determining the ligand alphabetical order, *e.g.* tri*c*arbonyl*h*ydrido(*t*ributylphosphine)cobalt.

3.3.2 Numerical Prefixes

Numerical prefixes used to indicate the number of ligands are of two types. The simple numerical prefixes: di, tri, tetra, penta, hexa, hepta, octa, nona, deca, undeca, dodeca, trideca... are used before simple ligands. Simple ligands are those ligand names that do not start with numerical prefixes and that are not enclosed in punctuation. There is no elision of vowels or hyphenation in the use of numerical prefixes, *e.g.* hexaammine and dioxo. The multiplicative prefixes: bis, tris, tetrakis, pentakis, hexakis, heptakis, octakis, nonakis, decakis, undecakis, dodecakis, tridecakis... are used before ligands whose names are enclosed in punctuation, *e.g.* tris(ethene), bis(diphosphato), tetrakis(1,2-dimethylbenzoato) (for enclosing punctuation of ligands see Sections 3.2.1 and 3.2.2). The nesting order of punctuation in coordination nomenclature is [{[( )]}].

3.3.3 Indication of Oxidation State and Ionic Charge

The element names for central atoms in neutral and cationic complexes are used unchanged. The element names for central atoms in anionic complexes take the -ate ending. The six elements silver, gold, copper, iron, lead and tin form the anion names from the Latin, *e.g.* argentate, aurate, cuprate, ferrate, plumbate and stannate, respectively. The oxidation number of a central atom is indicated by the Stock number, a Roman numeral in parentheses given after the central atom name. The oxidation number may be positive, zero or negative and by convention is indicated as (III), (0) and (−II), respectively. The ionic charge on a complex ion is indicated by the Ewens−Bassett number, which is the Arabic number followed by the sign of the charge all enclosed in parentheses and cited after the ion name, *e.g.* (2+) and (4−). A zero charge is not indicated for neutral compounds.

The simplest names for mononuclear compounds list the ligands followed by the name of the central atom and indicate only composition. The bonding of the ligand to the central atom can be indicated by the notations given in Section 3.2.3. The stereochemistry of mononuclear compounds can be given by the notation developed in Section 3.8. For examples see Tables 11, 12 and 13.

Table 11 Mononuclear Neutral Compounds

1.	$[Li(CH_3)]$	Methyllithium
2.	$[PtCl_2(NH_3)_2]$	Diamminedichloroplatinum(II)
3.	$[Cu(C_5H_7O_2)_2]$	Bis(2,4-pentanedionato)copper(II)
4.	$[CoH(N_2)\{P(C_6H_5)_3\}_3]$	(Dinitrogen)hydridotris(triphenylphosphine)-cobalt
5.	$[Fe(CH_3CO)(CO)_2I\{P(CH_3)_3\}_2]$	Acetyldicarbonyliodobis(trimethylphosphine)-iron(II)
6.	$[W\{CH(C_6H_5)\}(CO)_4(C_2H_3N)]$	(Acetonitrile)tetracarbonylbenzylidenetungsten
7.	$[W\{S(C_6H_5)\}(CO)_4[C\{N(CH_3)_2\}]]$	(Benzenethiolato)tetracarbonyl[(dimethylamino)-methylidyne]tungsten
8.	$[\overline{Pt\{CH(C_6H_5)CH(C_6H_5)C}H(C_6H_5)\}\{P(C_6H_5)_3\}_2]$	(1,2,3-Triphenyl-1,3-propanediyl)bis(triphenyl-phosphine)platinum
9.	$[V(C_2H_5NO)O(SO_4)]$	Bis(acetamide-*O*)oxo(sulfato-*O*,*O*′)vanadium(IV)
10.	$[Ni(C_4H_7N_2O_2)_2]$	Bis(2,3-butanedione dioximato-$\kappa^2 N,N'$)nickel(II)

Table 11 *(continued)*

11.	$[\overline{Mn\{(C_6H_4)N}N(C_6H_5)\}(CO)_4]$	Tetracarbonyl[2-(phenyldiazo-κN^2)phenyl-κC^1]manganese
12.	$[\overline{Ni(COCH_2CH_2N}CH_3)\{P(C_6H_5)_2CH_2CH_2P(C_6H_5)_2\}]$	[1,2-Ethanediylbis(diphenylphosphine-κP)][3-(methylamino-κN)propanalato(2−)-κC^1]nickel
13.	$[Pt(NH_3)Cl_2(\eta^2\text{-}C_2H_4)]$	Amminedichloro(η^2-ethene)platinum(II)
14.	$[Fe(CO)_3(C_4H_4SO)]$	Tricarbonyl(2,5-dihydro-η^2-thiophene-1-oxide-κO)iron
15.	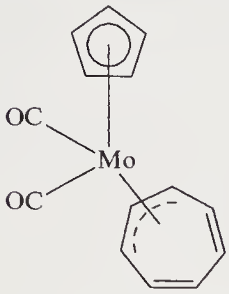	Dicarbonyl[(1,2,3-η)-2,4,6-cycloheptatrien-1-yl](η^5-cyclopentadienyl)molybdenum
16.	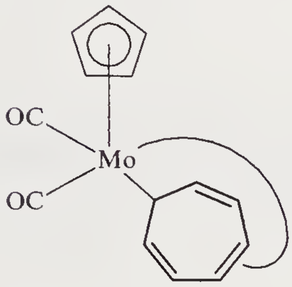	Dicarbonyl[(1,4,5-η)-2,4,6-cycloheptatrien-1-yl](η^5-cyclopentadienyl)molybdenum

Table 12 Compounds Containing Complex Cations

1.	$[Co(NH_3)_6]Cl(SO_4)$	Hexaamminecobalt(III) chloride sulfate
2.	$[Al(OH)(H_2O)_5]^{2+}$	Pentaaquahydroxoaluminum(III) ion
3.	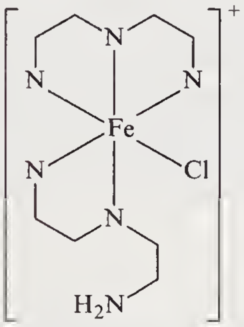	[N-(2-Aminoethyl)-1,2-ethanediamine-κ^2N,N'][N-(2-amino-κN-ethyl)-1,2-ethanediamine-κ^2N,N']chloroiron(2+) ion
4.	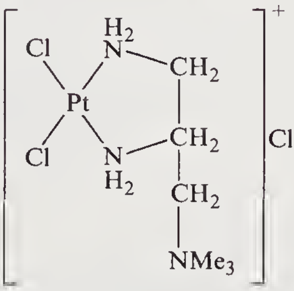	Dichloro(2,3-diamino-κ^2N^2,N^3-N,N,N-trimethyl-1-propanaminium)platinum(II) chloride
5.	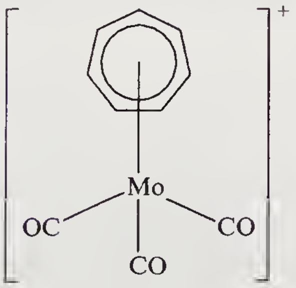	Tricarbonyl(η^7-cycloheptatrienylium)molybdenum(1+) ion

Table 13 Compounds Containing Complex Anions

1.	$Na_2[WBr_6]$	Disodium hexabromotungstate(IV)
2.	$K_2[Fe(CN)_5(NO)]$	Dipotassium pentacyanonitrosylferrate(2−)
3.	$[SeCl_3][FeCl_4]$	Trichloroselenium(II) tetrachloroferrate(III)
4.	$[BrF_4]^-$	Tetrafluorobromate(III) ion
5.	$K[B(C_6H_5)_4]$	Potassium tetraphenylborate(1−)
6.	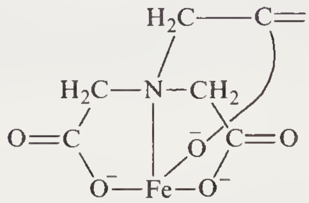	[*N*,*N*-Bis(carboxy-κ*O*-methyl)glycinato(3−)-κ*N*,κ*O*]-ferrate(II) ion
7.	$[Co(CO)_4]^-$	Tetracarbonylcobaltate(1−) ion
8.	$[Cr\{COCH{=}P(CH_3)_3\}\text{-}(\eta^5\text{-}C_5H_5)(CO)(NO)]^-$	Carbonyl (η^5-cyclopentadienyl)nitrosyl-[(trimethylphosphoranylidene)acetyl-κC^1]chromate(1−) ion
9.	$[\overline{Co(NH_2{-}CH_2CH_2{-}N}H_2)_3]_2\text{-}[W(C_2O_4)O_2F_2]_3$	Bis[tris(1,2-ethanediamine-κ^2*N*,*N*′)cobalt(III)] tris[difluoro(oxalato)dioxotungstate(VI)]

3.4 POLYNUCLEAR COORDINATION COMPOUNDS

Polynuclear compounds may be either of such large extended structures as to make rational structure-based nomenclature impractical, or the structures may be undefined or partially elucidated. In these instances compositional nomenclature is most suited.

3.4.1 Compositional Nomenclature

In compositional nomenclature, ligands are given in alphabetical order before central atoms. Central atoms are listed in alphabetical order as well. Bridging ligands to the extent known are indicated by the 'μ' notation (see Section 3.2.3.4). The numbers of ligands and central atoms are indicated by the appropriate numerical prefixes (see Section 3.3.2). Anions, cations, oxidation states and ionic charges are indicated in the same manner as in mononuclear compounds (see Section 3.3.3). For examples see Table 14.

Table 14 Compositional Nomenclature for Polynuclear Compounds

1.	$Ca_{14}[Al_{14}F_2O_{33}]$	Tetradecacalcium difluorotritriacontaoxotetradecaaluminate(III)
2.	$[CoCu_2Sn\{\mu\text{-}(C_2H_3O_2)\}_2(C_5H_5)(CH_3)]$	Bis(μ-acetato)-cyclopentadienylmethylcobaltdicoppertin
3.	$[Os_8(\mu\text{-}CO)_2(CO)_{20}]^{2+}$	Di-μ-carbonyl-icosacarbonyloctaosmium(2+) ion
4.	$[Fe_6Mo_2(C_6H_5S)_9S_8]^{3-}$	Nonakis(benzenethiolato)octathiohexairondimolybdate(3−) ion

3.4.2 Dinuclear Coordination Compounds

Bridging ligands in dinuclear complexes are indicated by the 'μ' prefix and are listed as noted in Section 3.2.3.4. Bridging accomplished by multiatom bridges is indicated by the 'κ' ligating notation with the symbols separated by a colon, *e.g.* μ-(nitrito-κ*N*:κ*O*). If the molecular symmetry permits, the bridging ligand may be stated before other alphabetically preferred ligands and simpler names formed by multiplying symmetrical portions of the name. For examples see Table 15.

Table 15 Symmetrical Dinuclear Compounds

1.	$[Fe_2(\mu\text{-}CO)_3(CO)_6]$	Tri-μ-carbonyl-bis(tricarbonyliron)
2.	$[Pt_2Br_4\{\mu\text{-}S(CH_3)_2\}]$	Bis[μ-thiobis(methane)]-bis[dibromoplatinum(II)]
3.	$[Ru_2(NH_3)_{10}(\mu\text{-}N{\equiv}CCH{=}CH{-}C{\equiv}N)]^{6+}$	[μ-(2-Butenedinitrile)-κN^1:κN^4]-bis[pentaammineruthenium(III)] ion

3.4.3 Metal–Metal Bonding

Metal to metal bonding is indicated by the italicized atomic symbols separated by a long dash and enclosed in parentheses. Bond order may be indicated by an Arabic number above the long dash, *e.g.* $(\mathrm{Mo}\overset{3}{\text{—}}\mathrm{Mo})$. The bond order notation is listed after the central atom names and before the charge or Stock number. For examples see Table 16.

Table 16 Compounds Containing Metal–Metal Bonds

1.	$[Mn_2(CO)_{10}]$	Bis(pentacarbonylmanganese)(*Mn*—*Mn*)
2.	$[Re_2Br_8]^{2-}$	Bis(tetrabromorhenate)($Re\overset{4}{—}Re$)(2–)

3.4.4 Central Atom Numbering

Unsymmetrical homo-dinuclear compounds are numbered based first on the number of ligands and second on the alphabetical order of the ligand names. The central atom with the greatest number of ligands is numbered 1 or, if no choice can be made based on the number of ligands, the central atom with the greatest number of alphabetically preferred ligands is numbered 1. Unsymmetrical hetero-dinuclear compounds are numbered based on the priorities of the central atoms listed in Table 17, the higher priority (more metallic) central atom being numbered 1.

Table 17 Element Sequence

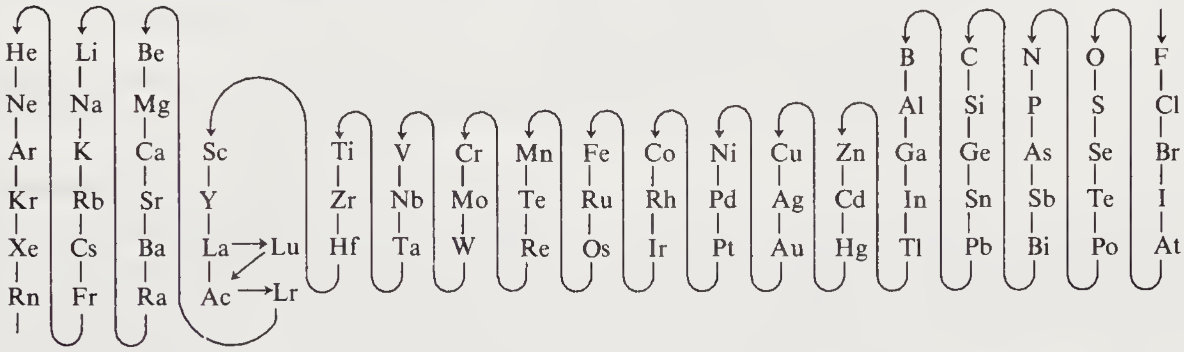

The ligating atom 'κ' italic atomic symbol notation is used to indicate ligand bonding. Bridging and unsymmetrical ligand distribution is shown by the numerical locant of the central atom to which the ligand is bonded. The locant of the central atom is cited on the line before the 'κ', *e.g.* (4-nitrobenzimidato-2κ*O*), indicating that the 4-nitrobenzimidate is bonded to the number 2 central atom. The right superscript numeral is again employed to indicate the number of identically bonded ligating atoms, *e.g.* $[\overset{(1)}{Re}(CO)_5\overset{(2)}{Ni}(CO)_3]$ is octacarbonyl-1κ^5*C*,2κ^3*C*-nickelrhenium(*Ni*—*Re*).

Bridging is indicated by the 'μ' prefix before the bridging ligand name, and unsymmetrical bridging by multiatom bridges is denoted by the ligating atom notation and central atom locant number separated by a colon: μ-(hydroxyamido)-2κ*N*:1κ*O*-. For examples see Table 18.

Table 18 Unsymmetrical Dinuclear Compounds

1.	$[Cr(NH_3)_5(\mu\text{-}OH)Cr(NH_3)_4\{NH_2(CH_3)\}]Cl_5$	Nonaammine-μ-hydroxo-(methanamine)dichromium(III) pentachloride
2.	$Br_2\overset{(1)}{Al}\,(\mu\text{-}Cl)_2\overset{(2)}{Al}\,Cl_2$	Dibromo-1κ^2*Br*-di-μ-chloro-dichloro-2κ^2*Cl*-dialuminum
3.	$[[\overset{(1)}{Ir}(CO)Br_2\{P(CH_3)_3\}_2](\overset{(2)}{Hg}Br)]$	Tribromo-1κ^2*Br*,2κ*Br*-carbonyl-1κ*C*-bis(triphenylphosphine-1κ^2*P*)mercuryiridium(*Hg*—*Ir*)
4.	$[\{Co(NH_3)_3\}_3(\mu\text{-}O)_2(\mu\text{-}NO_2)]Cl$	(μ-Nitrito-κ*N*:κ*O*)di-μ-oxo-bis(triamminecobalt)(1+) chloride
5.	$[\{\overset{(1)}{Co}(NH_3)_3\}(\mu\text{-}O)_2(\mu\text{-}NO_2)\{\overset{(2)}{Co}(NH_3)_2\}(C_5H_5N)]Cl$	Pentaammine-1κ^3*N*,2κ^2*N*1-(μ)nitrito-1κ*N*,2κ*O*)di-μ-oxo-(pyridine-2κ*N*)dicobalt(1+) chloride
6.	$[\overset{(1)}{Cu}(en)(H_2O)(\mu\text{-}OH)_2\overset{(2)}{Cu}(en)(SO_4)]$	Aqua-1κ*O*-bis(1,2-ethanediamine)-1κ^2*N*,*N*′,2κ^2*N*,*N*′-di-μ-hydroxo-sulfato-2κ*O*-dicopper(II)
7.	$[\overset{(1)}{Ni}(NH_3)_4Br\{\mu\text{-}(C_2H_3OS)\}\overset{(2)}{Ni}(NH_3)_3Br_2]$	Heptaammine-1κ^4*N*,2κ^3*N*-tribromo-1κ*Br*,2κ^2*Br*-[μ-(thioacetato)-2κ*O*:1κ*S*]-dinickel
	and the isomer:	Heptaammine-1κ^4*N*,2κ^3*N*-tribromo-1κ*Br*,2κ^2*Br*-[μ-(thioacetato)-1κ*O*:2κ*S*]-dinickel

3.4.5 Trinuclear and More Complex Structures

Structural nomenclature for more complex polynuclear compounds is based on the description of the fundamental structural unit, and a logical procedure for numbering the atoms of the fundamental or central structural unit. For nonlinear clusters, descriptors such as *tetrahedro*, *dodecahedro*, *etc.* have traditionally been used to describe a central structural unit (CSU). However, synthetic chemistry has now advanced far beyond the utility of the limited CSU set associated with these descriptors (see below). A more comprehensive CSU descriptor and a numbering system have been developed specifically for fully triangulated polyboron polyhedra (deltahedra).[4] The Casey, Evans, Powell descriptors (CEP) that may be employed as systematic alternatives to the traditional descriptors for metal deltahedral frameworks are listed in Table 19.

Table 19 Structural Descriptors

Central atoms	*Descriptor*	*Point group*	*CEP descriptor*
3	*triangulo*	D_{3h}	
4	*quadro*	D_{4h}	
4	*tetrahedro*	T_d	$[T_d$-(13)-Δ^4-*closo*]
5		D_{3h}	$[D_{3h}$-(131)-Δ^6-*closo*]
6	*octahedro*	O_h	$[O_h$-(141)-Δ^8-*closo*]
6	*triprismo*	D_{3h}	
8	*antiprismo*	S_6	
8	*dodecahedro*	D_{2d}	$[D_{2d}$-(2222)-Δ^6-*closo*]
8	*hexahedro* (cube)	O_h	
12	*icosahedro*	I_h	$[I_h$-(1551)-Δ^{20}-*closo*]

Metal–metal bonding need not be indicated in names for clusters in which the cluster descriptors are given, *e.g.* -*triangulo*-triosmium not *triangulo*-triosmium(3*Os*—*Os*) nor *cyclo*-triosmium-(3*Os*—*Os*).

Numbering of the CSU is based on locating a reference axis and planes of atoms perpendicular to the reference axis. The reference axis is the axis of highest rotational symmetry. The end of the reference axis with a single atom (or smallest number of atoms) is the first plane to be numbered. The CSU is oriented so that the first position to receive a locant, in the first plane with more than one atom, is in the 12 o'clock position. Locant numbers are assigned to the axial position or to each position in the first plane, beginning at the 12 o'clock position and moving in either the clockwise or anticlockwise direction. From the first plane move to the next position and continue numbering in the same direction (clockwise or anticlockwise), always returning to the 12 o'clock position or the position nearest to it in the forward direction before assigning locants in that plane. Numbering in this manner is continued until all positions are numbered. A complete discussion of numbering deltahedra is given in reference 4.

Central structural units may thus be specifically identified and numbered for nomenclature practices. However, many symmetrical CSUs may not require a full set of locants in the name because these compounds may exhibit only one possible isomer.

Locants for bridging ligands are cited in the same manner as in dinuclear compounds. Central atom locants will at times be necessary for monoatomic bridges in more complicated polynuclear compounds. For these compounds the locants are cited on the line before the ligand indicator 'κ' and are separated by a colon, *e.g.* tri-μ-chloro-1:2κ*Cl*,1:3κ*Cl*,2:3κ*Cl*-. For examples see Table 20.

Table 20 Cluster Compounds

1. $[\{Co(CO)_3\}_3(\mu_3\text{-}CI)]$	Nonacarbonyl-μ_3-(iodomethylidyne)-*triangulo*-tricobalt
2. $Cs_3[Re_3Cl_{12}]$	Cesium dodecachloro-*triangulo*-trirhenate(3−)
3. $[Cu_4I_4\{P(C_2H_5)_3\}_4]$	Tetra-μ_3-iodo-tetrakis(triethylphosphine)-*tetrahedro*-tetracopper
	Tetra-μ_3-iodo-tetrakis(triethylphosphine)$[T_d$-(13)-Δ^4-*closo*]tetracopper
4. $[Co_4(\mu\text{-}CO)_3(CO)_9]$	Tri-μ-carbonyl-1:2κ*C*,1:3κ*C*,2:3κ*C*-nonacarbonyl-$1\kappa^2C,2\kappa^2C,3\kappa^2C,4\kappa^3C$-*tetrahedro*-tetracobalt
	Tri-μ-carbonyl-1:2κ*C*,1:3κ*C*,2:3κ*C*-nonacarbonyl-$1\kappa^2C,2\kappa^2C,3\kappa^2C,4\kappa^3C$-$[T_d$-(13)-$\Delta^4$-*closo*]tetracobalt
5. $[Mo_6S_8]^{2-}$	Octa-μ_3-thio-*octahedro*-hexamolybdate(2−) ion
	Octa-μ_3-thio-$[O_h$-(141)-Δ^8-*closo*]hexamolybdate(2−) ion
6. $[Pt(\mu_3\text{-}1)(CH_3)_3]_4$	Tetra-μ_3-iodo-tetrakis(trimethylplatinum)(II)
	Tetra-μ_3-iodo-dodecamethyl-$1\kappa^3C,2\kappa^3C,3\kappa^3C,4\kappa^3C$-*tetrahedro*-tetraplatinum
	Tetra-μ_3-iodo-dodecamethyl-$1\kappa^3C,2\kappa^3C,3\kappa^3C,4\kappa^3C$-$[T_d$-(13)-$\Delta^4$-*closo*]tetraplatinum(II)
7. $[Be_4(\mu_4\text{-}O)(\mu\text{-}C_2H_3O_2)_6]$	Hexakis(μ-acetato-κ*O*:κ*O′*)μ_4-oxo-*tetrahedro*-tetraberyllium
	Hexakis(μ-acetato-κ*O*:κ*O′*)μ_4-oxo-$[T_d$-(13)-Δ^4-*closo*]tetraberyllium
8. $[\{Hg(CH_3)\}_4(\mu_4\text{-}S)]^{2+}$	μ_4-Thio-tetrakis(methylmercury)(2+) ion
	Tetramethyl-1κ*C*,2κ*C*,3κ*C*,4κ*C*-μ_4-thio-*tetrahedro*-tetramercury(2+) ion
	Tetramethyl-1κ*C*,2κ*C*.3κ*C*,4κ*C*-μ_4-thio-$[T_d$-(13)-Δ^4*closo*]tetramercury(2+) ion
9. $[Fe_2Pt(CO)_8\{P(C_6H_5)_3\}_2]$	Octacarbonyl-$1\kappa^4C,2\kappa^4C$-bis(triphenylphosphine-3κ*P*)-*triangulo*-diironplatinum

Central atoms in noncaged polynuclear structures are numbered from one end along the path containing the greatest number of central atoms to the remote end. The number *one* terminal central atom is chosen: first, by the priorities of the central atoms listed in Table 17, the highest priority (more metallic) central atom being given last in that sequence; second, by deciding which central atom gives the lowest locant set for ligands at the first point of difference; and lastly, by the alphabetical order of ligands. The terminal central atom or the terminal central atom adjacent, as one proceeds along the path of central atoms to the central atom with the greatest number of alphabetically preferred ligands, is numbered 1. The ligand indicator kappa 'κ' with central atom locant and italicized donor atom symbol is used as necessary to indicate positioning of the ligands. For examples see Table 21.

Table 21 Complex Polynuclear Compounds

1.	$[Os_3(SiCl_3)_2(CO)_{12}]$	Dodecacarbonyl-1κ^4C,2κ^4C,3κ^4C-bis(trichlorosilyl)-1κSi,3κSi-triosmium(2*Os*—*Os*)
2.	$[Rh_3(CO)_3(\mu\text{-}Cl)Cl\text{-}[\mu_3\text{-}\{(C_6H_5)_2P(CH_2)(C_6H_5)P(CH_2)P(C_6H_5)_2\}]_2]Cl$	Tricarbonyl-1κC,2κC,3κC-μ-chloro-1:2κCl-chloro-3κCl-bis-μ_3-[bis[(diphenylphosphino)-1$\kappa P'$:3$\kappa P''$-methyl]phenylphosphine-2κP]-trirhodium(1+) chloride
3.	$[CrCo_2(\mu_3\text{-edta})(\mu\text{-}OH)_2(NH_3)_6(H_2O)]^{3+}(ClO_4)_3$	Hexaammine-2κ^3N,3κ^3N-aqua-1κO-μ_3-[(1,2-ethanediyldinitrilo-1κ^2N,N')tetraacetato-1κ^3O^1,O^2,O^3:2κO^4:3κO^4]-di-μ-hydroxo-2:3κ^4O-chromiumdicobalt(3+) triperchlorate
4.	$[Ni_3(C_5H_7O_2)_6]$	Bis-μ_3-(2,4-pentanedionato)-1:2κ^4O^2:2:3κ^4O^4-bis-μ-(2,4-pentanedionato)-1κ^2O^2,O^4,1:2κ^2O^2,3κ^2O^2,O^4,2:3κ^2O^2-bis(2,4-pentanedionato)-1κ^2O^2,O^4,3κ^2O^2,O^4-trinickel

3.4.6 Cyclic Coordination Compounds

Central atoms in bridged cyclic compounds are numbered: first, by the priorities of the central atoms listed in Table 17, the highest priority (more metallic) central atom being given last in that sequence; second, by deciding which central atom gives the lowest locant set for ligands at the first point of difference; and lastly, by the alphabetical order of ligands. The central atom with the greatest number of alphabetically preferred ligands is numbered 1. The prefix '*cyclo*' is used for noncluster monocyclic compounds and the prefix is italicized and cited before all ligands. Central atom locants and ligand locant notations are employed according to the same principles as in linear structures above. For examples see Table 22.

Table 22 Cyclic Polynuclear Compounds

1.	$[Pt_3(\mu\text{-}OH)_3(NH_3)_6]^{3+}$	*cyclo*-Tri-μ-hydroxo-tris(diammineplatinum)(3+) (not Hexaamminetri-μ-hydroxo-*triangulo*-triplatinum(3+))
2.	$[Pt_2\{Pd(NH_3)(NH_2Me)\}(\mu\text{-}OH)_3(NH_3)_4]^{3+}$	*cyclo*-Pentaammine-1κ^2N,2κ^2N,3κN-tri-μ-hydroxo-1:2κO,1:3κO,2:3κO-(methanamine-3κN)palladiumdiplatinum(3+)
3.	$[Rh_4\{\mu\text{-}C_3N_2H_2(CH_3)\}_4(CO)_8]$	*cyclo*-Tetrakis-μ-(2-methyl-1*H*-imidazolato)-κ^4N^1:κ^4N^3-tetrakis(dicarbonylrhodium)
4.	$[Rh_4\{\mu\text{-}(C_3N_2H_2(CH_3)\}_4(CO)_6(PMe_3)_2]$	*cyclo*-Hexacarbonyl-1κ^2C,2κC,3κ^2C,4κC-tetrakis-μ-(2-methyl-1*H*-imidazolato)-1:2κ^2N^1:N^3,1:4κ^2N:N^3,2:3κ^2N^1:N^3,3:4κ^2N^1:N^3-bis(trimethylphosphine)-2κP,4κP-tetrarhodium

3.5 COORDINATION POLYMERS

Compounds of known composition but uncertain polymeric structure can be conveniently named by selecting a suitable subunit and prefixing 'poly' to the compositional coordination name of the subunit. Bridging and other bonding notations are not generally employed, unless limited bonding and specific structural detail is known about the internal structure of the polymer subunit. The 'poly' prefix is not italicized and the name of the subunit given after 'poly' is enclosed in square brackets. For examples see Table 23.

Table 23 Compositional Polymer Nomenclature

1.	$[\,\overline{Gd\{OC(O)CH_2O}H\}_3]_n$	Poly[tris(hydroxyacetato)gadolinium(III)]
2.	$[K[CdCl_3]]_n$	Poly[potassium [trichlorocadmate(II)]]
3.	$[Fe\{As(CH_3)_2\}(CO)_2(NO)]_n$	Poly[dicarbonyl(dimethylarsino)nitrosyliron]

Single-strand and quasi-single-strand coordination polymers are named based on the IUPAC provisional recommendations.[5] These nomenclature recommendations are designed to provide unique and unambiguous nomenclature for regular linear coordination polymers. In order to assign unique nomenclature, lengthy and necessarily complex directions are included to select and orient the unique constitutional repeating unit (CRU). This is necessary for many nomenclature applications and the complete recommendations in reference 5 should be consulted whenever a unique and unambiguous name is desirable.

An unambiguous name[6] may be sufficient for many applications and is simply derived by selecting a rational, convenient constitutional repeating unit (CRU) and naming the arbitrarily selected CRU by the recommended principles.

The name of the linear CRU starts with the italic prefix '*catena*' and the non-italic prefix 'poly' and is based on a backbone consisting of central atoms and bridging ligands where present. All coordination polymers have one or more central atoms and may, or may not, contain bridging ligands. Coordination polymers, mononuclear or polynuclear and their associated ligands (except for ligands between central atoms in the backbone, if present), are named by the usual principles of coordination nomenclature. Bridging ligands as noted in Section 3.2.3.4 are named by prefixing with 'μ' and ligating atom locants where necessary. The bridging ligand that continues the chain of CRU is given last in the polymer name. This is an obvious departure from common coordination practice. Thus, the essential elements for deriving a name for a linear polymeric coordination compound are: selecting the CRU; naming the part of the CRU that does not include terminal bridging ligands; and following this by the names of the bridging ligands separated by the bridging notation 'μ'. For examples see Table 24.

Table 24 Linear Polymers

1.	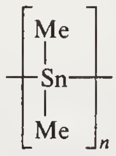 $[\mathrm{-Sn(Me)_2-}]_n$	*catena*-Poly[dimethyltin]
2.	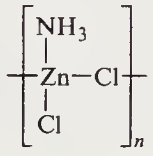 $[\mathrm{-Zn(NH_3)(Cl)-Cl-}]_n$	*catena*-Poly[(amminechlorozinc)-μ-chloro]
3.	$[\mathrm{Ag{-}CN}]_n$	*catena*-Poly[silver(μ-cyano-*C*: *N*)] (unique name *catena*-poly[silver(μ-cyano-*N*: *C*)]) (see ref. 5)
4.	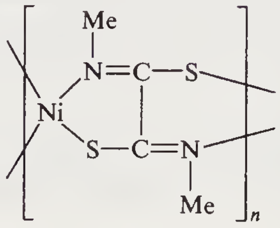	*catena*-Poly[nickel[μ-*N*,*N*′-dimethyldithiooxalimidato(2−)-κ*N*,κ*S*′:κ*N*′, κ*S*]]
5.	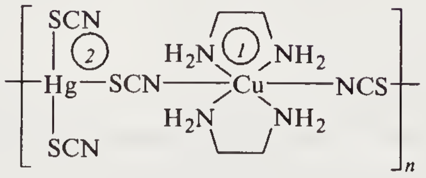	*catena*-Poly[[bis(thiocyanato-2κ*S*)mercury]-(μ-thiocyanato-1κ*N*:2κ*S*)-[*bis*(1,2-ethanediamine-1κ^2*N*,*N*′)-copper]-(μ-thiocyanato-1κ*N*:κ*S*)]
6.	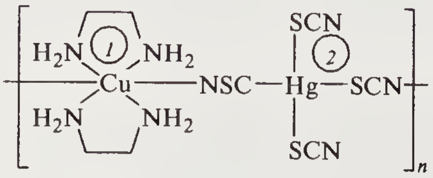	(unique name) *catena*-Poly[[bis(1,2-ethanediamine-1κ^2*N*,*N*′)copper]-(μ-thiocyanato-1κ*N*:2κ*S*)-[bis(thiocyanato-2κ*S*)mercury]-(μ-thiocyanato-2κ*S*:κ*N*)]

3.6 METALLOCENES (BIS(η^5-CYCLOPENTADIENYL) COMPOUNDS)

The traditional names ferrocene, manganocene, ruthenocene, nickelocene, *etc.* are given to the respective bis(η^5-cyclopentadienyl)metal complexes. 'Ocene' names should not be coined for isoelectronic species such as chromocene for bis(η^6-benzene)chromium, for structurally analogous species such as uranocene for bis(η^8-1,3,5,7-cyclooctatetraene)uranium, or for other condensed rings such as benzo- or dibenzo-ferrocene for bis[(1,2,3,3a,7a-η)-indenyl]iron.

Metallocene derivatives may be named by either standard organic suffix (functional)[7] or prefix nomenclature. Substituents are given the lowest numerical locants in the usual manner on the equivalent cyclopentadienyl rings of the ocene entity. The first ring is numbered 1 to 5 and the second ring is numbered 1′ to 5′. In metallocenes composed of multiple ocene groupings the cyclopentadienyl rings are further numbered 1″ to 5″, 1‴ to 5‴, *etc.* The radical names -ocenyl, -ocenediyl, -ocenetriyl, *etc.* are used. For examples see Table 25.

Table 25 Metallocene Nomenclature

1.	$[Fe(\eta^5\text{-}C_5H_5)_2]$	Ferrocene
2.	$[Os(\eta^5\text{-}C_5H_5)_2]$	Osmocene
3.	$[Ni(CH_3\text{-}\eta^5\text{-}C_5H_4)_2]$	1,1′-Dimethylnickelocene
4.	$[Os(\eta^5\text{-}C_5H_5)(HOCH_2CH_2\text{-}\eta^5\text{-}C_5H_4)]$	2-Osmocenylethanol (1-Hydroxyethyl)osmocene
5.	$[Os(\eta^5\text{-}C_5H_5)(CH_3CO\text{-}\eta^5\text{-}C_5H_4)]$	Methyl osmocenyl ketone Acetylosmocene
6.	$[Fe(\eta^5\text{-}C_5H_4\text{-}CH_2CH_2CH_2\text{-}\eta^5\text{-}C_5H_4)]$	1,3-(1,1″-Ferrocenediyl)propane 1,1′-Trimethyleneferrocene
7.	$[Fe_2(\mu\text{-}\eta^5\text{-}C_5H_4\text{-}CH_2CH_2\text{-}\eta^5\text{-}C_5H_4)(\eta^5\text{-}C_5H_5)_2]$	1,1″-Ethylenediferrocene
8.	$[Fe(\eta^5\text{-}C_5H_5)\{\eta^5\text{-}C_5H_4As(C_6H_5)_2\}]$	Ferrocenyldiphenylarsine (Diphenylarsino)ferrocene
9.	$[Fe(\eta^5\text{-}C_5H_5)_2][BF_4]$	Ferrocenium(1+) tetrafluoroborate(1−)
10.	$[Fe\{(CH_3)_5\text{-}\eta^5\text{-}C_5\}_2]Cl_2$	Decamethylferrocenium(2+) dichloride
11.	$[Fe_2(\mu\text{-}\eta^5\text{-}C_5H_4\text{-}CH_2\text{-}\eta^5\text{-}C_5H_4)_2]$	[1.1]Ferrocenophane
12.	$[Fe_3(\mu\text{-}\eta^5\text{-}C_5H_4\text{-}CH_2CH_2\text{-}\eta^5\text{-}C_5H_4)_3]$	[2.2.2]Ferrocenophane

3.7 FORMULAS

The formulas for coordination compounds identify the coordination entity. This is done by listing first the central atom or atoms in alphabetical order of the element symbols, followed by the ligands and enclosing the complete coordination entity in square brackets, *e.g.* $K_3[CrCl_6]$. Ligands presumed to be ionic are listed next and are given in alphabetical order according to the symbol of the ligating atoms. Neutral ligands follow also in alphabetical order according to the symbols of the ligating atoms. Polydentate organic ligands are listed at CH, which precedes other atomic symbols of the ligand which then follow in alphabetical order. A ligand with fewer C atoms precedes one with more. Ligands may be indicated by abbreviations (bpy, dppe, *etc.*). Polyatomic ligand formulas are enclosed in parentheses. The nesting order of punctuation in coordination formulas is: [( )], [{( )}], [[{( )}]], *etc.*

Differing contexts require considerable flexibility in writing formulas. Thus, the goal of any context should be to give the formula as clearly and definitively as possible regardless of these guidelines noted above. For examples see Table 26.

Table 26 Formulas

1.	$[PtCl(NH_3)_2\{NH_2(CH_3)\}][BF_4]$
2.	$Na[OsBrCl(NO_2)(NH_3)]$
3.	$[CoCl_2(en)_2]$
4.	$[Rh(CO)(PPh_3)(\mu\text{-}CO)_2Rh(PPh_3)_2]$

3.8 STEREOCHEMISTRY

The terms *cis*, *trans*, *fac*, *mer*, *sym*, *asym*, *endo*, *exo*, *syn*, *anti*, *dextro*, *levo* and others have been coined to describe various diastereomers. The terms most commonly used in inorganic chemistry are *cis* and *trans* to describe the square planar $[MX_2Y_2]$ system, *fac* and *mer* to describe the octahedral $[MX_3Y_3]$, $[MX_3Y_2Z]$ and $[MX_3UYZ]$ systems, *sym* and *asym* to generally distinguish symmetrical from asymmetrical systems in any coordination polyhedron, and *dextro* and *levo*, usually written *d* and *l*, to indicate the right- or left-handed rotation of a plane polarized beam of light. As coordination systems become more complicated, as with the tetradentate ABBA chelate shown in Figure 1, these binary terms are rendered useless.

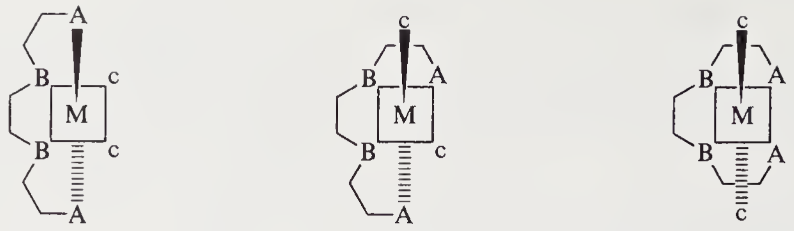

α-cis
I

β-cis
II

trans
III

Figure 1 Geometric isomers of octahedral complexes with linear tetradentate ligands

A general method of stereochemical notation based on the ligand priority sequence rule of Cahn, Ingold, and Prelog (CIP),[8,9] developed at Chemical Abstracts Service,[10,11] has been in use in Chemical Abstracts Chemical Substance Indexes for mononuclear coordination compounds since 1972.

3.8.1 Stereochemical Notation

Stereochemical notation is based on the awareness that to describe fully the configuration of a coordination compound, the coordination polyhedron, the relative arrangement of the ligands in space, the chirality of the central atom and the ligand stereochemistry must be in some way noted. This is done with a notation descriptor composed of four parts:[12] (a) the site symmetry symbol to describe the coordination polyhedron around the central atom; (b) the configuration index to indicate the geometrical arrangement of the ligating atoms on the coordination polyhedron; (c) the central atom chirality to indicate the spatial relationship of the ligating atoms; and (d) the ligand stereochemical notation that indicates the various stereochemical features of the ligand. This latter set of symbols are generally the notations used in organic chemistry.

The site symmetry symbols for the most common coordination polyhedra of coordination numbers 2–9 are shown in Table 27. The configuration index is a one- to nine-digit number that identifies ligand atoms on symmetry elements of a structure. The configuration index numbers are composed of the CIP priority numbers of the donor ligating atoms. Three different sets of chirality symbols are employed to designate the chirality at a coordination center (*R*, *C* and Δ indicate right-handed or clockwise, and *S*, *A* and Λ indicate left-handed or anti-clockwise), the principles defining right- and left-handed are different for each set of symbols. Because of the differing assignment principles, there is no exact translation of *R* to *C* or *C* to Δ. For this reason the different sets of chirality symbols are retained.

Table 27 Site Symmetry Symbol

	Coord. no.	*Site symmetry symbol*
Linear	2	*L*-2
Angular	2	*A*-2
Trigonal plane	3	*TP*-3
Trigonal pyramid	3	*TPY*-3
Tetrahedron	4	*T*-4
Square plane	4	*SP*-4
Square pyramid	4	*SPY*-4
Trigonal bipyramid	5	*TB*-5
Square pyramid	5	*SPY*-5
Octahedron	6	*OC*-6
Trigonal prism	6	*TPR*-6
Pentagonal bipyramid	7	*PB*-7
Octahedron, face monocapped	7	*OCF*-7
Trigonal prism, square face monocapped	7	*TPRS*-7
Cube	8	*CU*-8
Square antiprism	8	*SA*-8
Dodecahedron	8	*DD*-8
Hexagonal bipyramid	8	*HB*-8
Octahedron, *trans*-bicapped	8	*OCT*-8
Trigonal prism, triangular face bicapped	8	*TPRT*-8
Trigonal prism, square face bicappped	8	*TPRS*-8
Trigonal prism, square face tricapped	9	*TPRS*-9
Heptagonal bipyramid	9	*HB*-9

Stereochemical symbols and terms associated with ligand atoms may be given in the ligand portion of the name, for example tris[L-aspartato(2−)]cobaltate(3−), or more preferably after the central atom chirality label, for example the [*OC*-6-21-Δ-(*R*),(*R*),(*R*)]-tris(1,2-propanediamine)-cobalt(III) ion. In the latter cases the CIP priority number of the ligating atom may be used as a locant for defining the position of the closest ligand stereocenter in an ambiguous context. The lowest CIP priority number should be used for multidentate ligands.

The structures in Figures 2–6 illustrate the utility of a ligand index-based stereochemical notation for coordination compounds.

The tris(1,2-propanediamine-*N*,*N*′)cobalt(3+) structure of Figure 2 has two geometric configurations each for the *R*,*R*,*R* and *S*,*S*,*S* ligand configurations, both of which have Δ and Λ forms to give eight isomers. The *R*,*R*,*S* and *R*,*S*,*S* ligand configurations have two facial and six meridional configurations, each in a Δ and a Λ form, to give 16 isomers. This results in a total of 24 possible isomers. In the structure shown, the asymmetric carbon atoms are in a meridional configuration. The principal axis is determined by the maximum difference in the *trans* CIP priority numbers, the 1−2 axis. The configuration number is determined by noting the priority numbers of the atoms *trans* to the highest CIP priority atoms on the principal axis and in the plane, *e.g.* 21. The helical configuration of the chelate rings is right-handed and is symbolized by Δ. The complete stereodescriptor is [*OC*-6-21-Δ-(*R*),(*R*),(*R*)]. The stereodescriptors for all 24 isomers are tabulated in Table 28.

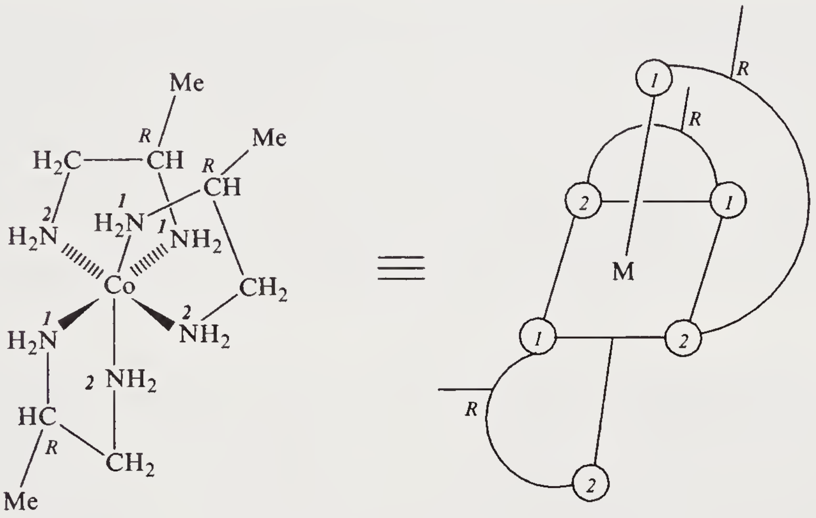

Configuration number = 21
Chirality symbol = Δ

Figure 2 $[Co(1,2\text{-}pn)_3]^{3+}$, [*OC*-6-21-Δ-(*R*),(*R*),(*R*)]-tris(1,2-propanediamine-*N*,*N*′)cobalt(3+)

Table 28 Stereonotation for 24 Isomers of $[Co(1,2\text{-}pn)_3]^{3+}$

[*OC*-6-21-Δ-(*R*),(*R*),(*R*)]	[*OC*-6-21-Λ-(*S*),(*S*),(*S*)]
[*OC*-6-22-Δ-(*R*),(*R*),(*R*)]	[*OC*-6-22-Λ-(*S*),(*S*),(*S*)]
[*OC*-6-21-Δ-(*S*),(*S*),(*S*)]	[*OC*-6-21-Λ-(*R*),(*R*),(*R*)]
[*OC*-6-22-Δ-(*S*),(*S*),(*S*)]	[*OC*-6-22-Λ-(*R*),(*R*),(*R*)]
[*OC*-6-43-Δ-(*R*),(*R*),(*S*)]	[*OC*-6-44-Λ-(*R*),(*S*),(*S*)]
[*OC*-6-44-Δ-(*R*),(*S*),(*S*)]	[*OC*-6-43-Λ-(*R*),(*R*),(*S*)]
[*OC*-6-32-Δ-(*R*),(*R*),(*S*)]	[*OC*-6-24-Λ-(*R*),(*S*),(*S*)]
[*OC*-6-13-Δ-(*R*),(*R*),(*S*)]	[*OC*-6-42-Λ-(*R*),(*S*),(*S*)]
[*OC*-6-42-Δ-(*R*),(*R*),(*S*)]	[*OC*-6-23-Λ-(*R*),(*S*),(*S*)]
[*OC*-6-24-Δ-(*R*),(*S*),(*S*)]	[*OC*-6-32-Λ-(*R*),(*R*),(*S*)]
[*OC*-6-42-Δ-(*R*),(*S*),(*S*)]	[*OC*-6-13-Λ-(*R*),(*R*),(*S*)]
[*OC*-6-23-Δ-(*R*),(*S*),(*S*)]	[*OC*-6-42-Λ-(*R*),(*R*),(*S*)]

[[*N*,*N*′-1,2-Ethanediylbis(glycinato)](2−)][oxalato(2−)]cobaltate(1−), an octahedral structure with a tetradentate ligand, is shown in Figure 3. The oxalate oxygen atoms are CIP priority number 1, the glycine oxygen atoms are priority number 2, and the nitrogen atoms are priority number 3. The tetradentate ligand is primed to give the maximum difference on the principal axis, 1−3′. The configuration number is 33, with the glycine nitrogens *trans* to the oxalate oxygens. Primes are not generally necessary in the configuration numbers for octahedral complexes, but they are used to determine the chirality descriptor. The chirality is determined by the increasing sequence 1232′ or clockwise, *C*. The complete descriptor is (*OC*-6-33-*C*) for the α-*cis* isomer and (*OC*-6-3-*C*) for the β-*cis* isomer.

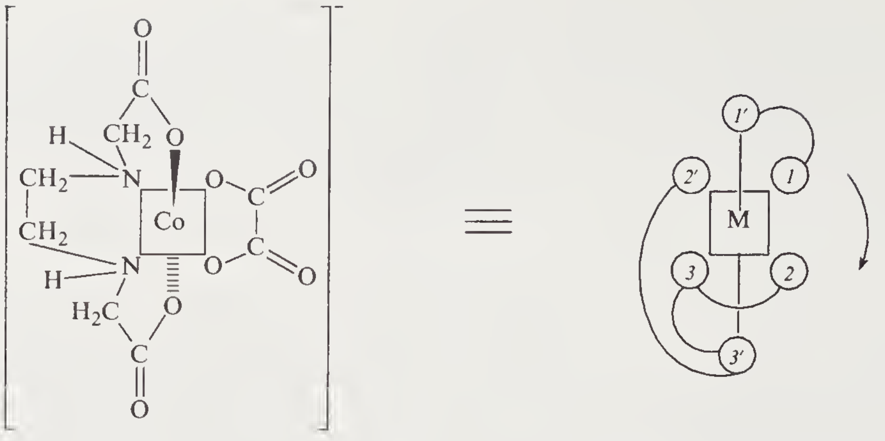

α-*cis*

Configuration number = 33
Chirality symbol = *C*

Figure 3 $[Co\{(CH_2)_2[NH(C_2H_2O_2)]_2\}(C_2O_4)]$, [*OC*-6-33-*C*]-[(*N*,*N*′-1,2-ethanediylbis(glycinato))(2−)]-[oxalato(2−)]cobaltate(1−)

Bromochloro(2-ethyl-13-methyl-3,6,9,12,18-pentaazabicyclo[12.3.1]octadeca-1(18),2,12,14,16-pentaene-$\kappa^5N^{3,6,9,12,18}$)iron(1+), a seven-coordinate pentagonal bipyramidal structure with a planar macrocyclic ligand, is shown in Figure 4. The bromine atom is priority number 1, the chlorine is 2, the imine nitrogens are 3 and 4, the pyridine nitrogen is 5, and the amine nitrogens have priority numbers of 6 and 7 as shown. The configuration number starts with the priority numbers of the atoms on the C_5 axis, 12, and continues with the priority numbers for the atoms in the pentagonal plane in the increasing sequential order 35476. When viewed from atom priority number 1 on the C_5 axis, this sequence is clockwise of *C*. The complete descriptor is (*PB*-7-12-35476-*C*).

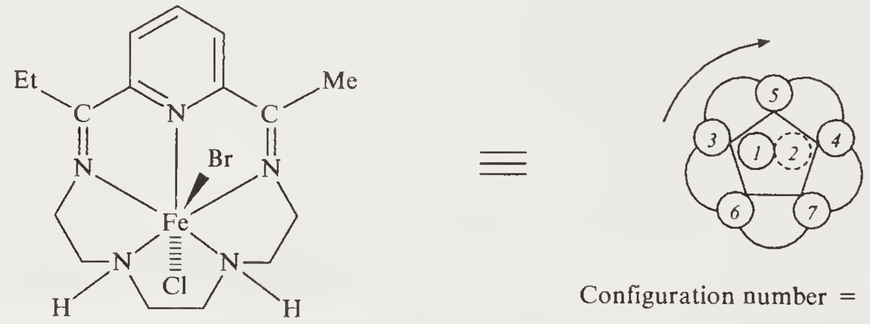

Configuration number = 12-35476
Chirality symbol = *C*

Figure 4 $[FeBrCl(C_{16}H_{25}N_5)]$, (*PB*-7-12-35476-*C*)-bromochloro(2-ethyl-13-methyl-3,6,9,12,18-pentaazabicyclo[12.3.1]-octadeca-1(18),2,12,14,16-pentaene-$\kappa^5N^{3,6,9,12,18}$)iron(1+)

Bis[*N*-(2-amino-κ*N*-ethyl)-1,2-ethanediamine-κ^2N]bromochloropraseodymium(1+), an eight-coordinate, triangular face, bicapped trigonal prismatic structure, is shown in Figure 5. The structure is viewed from the atom of highest priority on the C_3 axis, priority number 4. The configuration number begins with the priority numbers for the donor atoms on the C_3 axis given in lowest sequential order, 4,4′, and continues with the priority number of the highest priority atom in the adjacent plane, 1, along with the priority number for the atom it eclipses, 3′. The configuration number sequence continues either right or left to the donor atom of next highest priority in the first plane. This is the atom of priority number 3. This and the atom it eclipses, 2, are cited next. The sequence continues in a like manner to give 44′-13′324′4. The sequence increases in clockwise direction when viewed from atom priority number 4 on the C_3 axis. The complete descriptor is (*TRPT*-8-44′-13′324′4-*C*).

Tetraaqua(2,4,5,6(1*H*,3*H*)-pyrimidinetetrone-κO^4-5-oximato-κN^5)(2,4,5,6(1*H*,3*H*)-pyrimidinetetrone-κO^4-5-oximato-κO^5)strontium, the structure in Figure 6, is an eight-coordinate, square face, bicapped trigonal prism. The structure is viewed from a point on the C_3 axis above the uncapped square or rectangular face. The first digit of the configuration number is the priority number of the most-preferred atom in the square face, 1. The second number is that of the atom encountered next on the structure projection as one proceeds either right or left to the atom in the plane adjacent to the square face, priority number 3. The priority numbers for the remaining atoms are given as they are encountered, continuing in the same direction on the projection of the structure

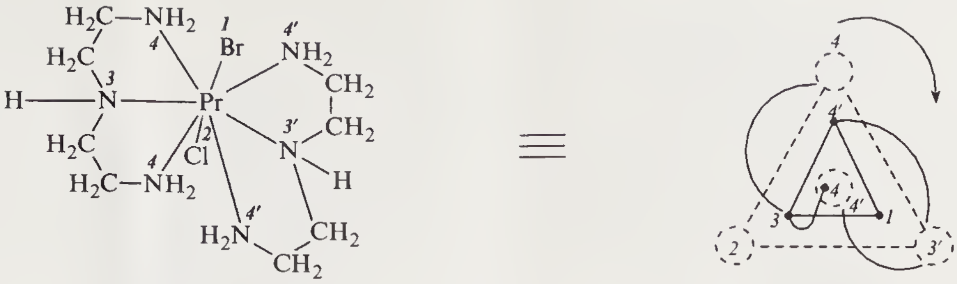

Configuration number = 44'-13'324'4

Chirality symbol = *C*

Figure 5 $[\mathrm{Pr(C_4H_{13}N_3)_2BrCl}]^+$, (*TRPT*-8-44'-13'324'4-*C*)-bis[*N*-(2-amino-κ*N*-ethyl)-1,2-ethanediamine-κN^2]-bromochloropraseodymium(1+)

to give 13445244. As viewed from above the square face, the sequential order increases in the anticlockwise direction, symbolized *A*. The complete descriptor is (*TPRS*-8-13445244-*A*).

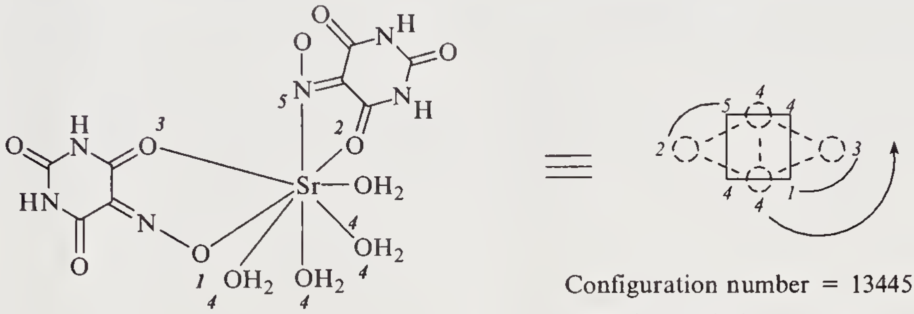

Configuration number = 13445244

Chirality symbol = *A*

Figure 6 $[\mathrm{Sr(H_2O)_4(C_4H_2N_3O_4)_2}]$, (*TPRS*-8-13445244-*A*)-tetraaqua(2,4,5,6(1*H*,3*H*)-pyrimidinetetrone-κO^4-5-oximato-κN^5)(2,4,5,6(1*H*,3*H*)-pyrimidinetetrone-κO^4-5-oximato-κO^5)strontium

This stereochemical notation provides a vehicle for inorganic and coordination chemists to describe the gross symmetry of the central atom, the geometric distribution of ligands on the coordination polyhedron, and the stereochemical configurations at the central atom and at chiral centers in the ligands. This notation is especially useful for describing the more complicated types of stereochemical configurations (Table 28), for the compounds of higher coordination numbers, and for compounds with lower symmetry coordination polyhedra that have potentially thousands of possible isomers.

3.8.2 Hapto Compounds

The stereochemistry of bis(η^5-cyclopentadienyl)iron (ferrocene), tricarbonyl(η^5-cyclopentadienyl)-manganese, and (η^6-benzene)tricarbonylchromium has been extensively reviewed by Schlögl.[13] His review is primarily concerned with ring substitution, and his stereonotation is the extension of the CIP sequence rule, *R*,*S*, to the cyclopentadiene ring. This is achieved by considering the hapto attachment to the metal atom equivalent to a single bond. This device results in a four-coordinate center (not tetrahedral), which can be ranked by the normal CIP procedures. The ranking and notation for 1-acetyl-2-methylferrocene is shown in Figure 7. Iron, atomic number 26, is the highest ranking atom, priority number 1. The methyl-substituted ring atom has a priority number of 2; the α-unsubstituted ring atom has a priority number of 3; and the carbonyl atom has a priority number of 4. The chirality symbol is given to the highest CIP priority cyclopentadienyl ring atom. When this atom is viewed from opposite the lowest priority ligand, number 4, the sequence 1,2,3 is right-handed and is given the chirality symbol *R*. This application of the CIP sequence rule has been generally accepted and is used in Chemical Abstracts indexes to assign chirality symbols to polysubstituted bis(η^5-cyclopentadienyl)metal complexes. Before the concept of centrochirality was adopted in 1967,[13] cyclopentadienyl metal compounds were assigned *R* and *S* descriptors according to the concept of planar chirality.

Following the planar chirality procedure, the molecule is viewed from a point above the substituted ring on the C_5 axis. The ring substituents are ranked by CIP procedures and the *R* or *S* chirality symbol is assigned, based on the clockwise or anticlockwise sense of the resulting sequence. According to the rules of planar chirality, the ferrocene complex in Figure 7 would be assigned the symbol *S*. However, this approach has been abandoned.

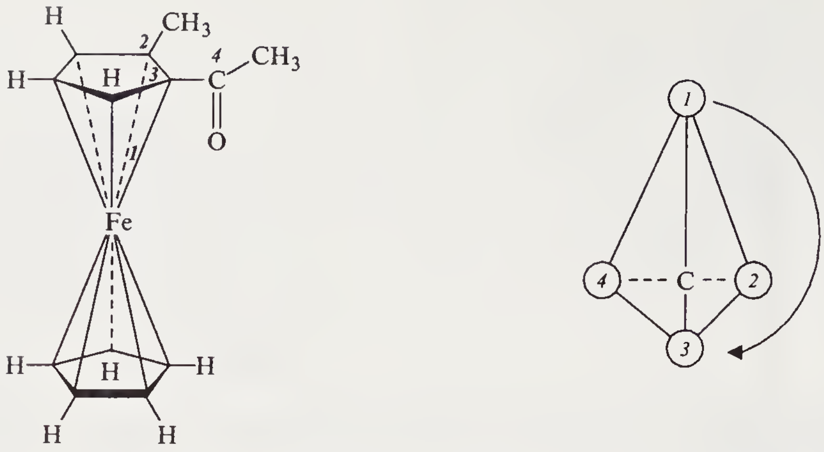

Figure 7 $[Fe(\eta^5\text{-}C_5H_5)[\eta^5\text{-}(CH_3CO)(CH_3)C_5H_3]]$, (*R*)-1-acetyl-2-methylferrocene

Optically active η^5-cyclopentadienyl metal complexes, in which the metal is a chiral center, are becoming increasingly available. Stanley and Baird have suggested an extension of the CIP sequence rule to be applied to the metal center.[14] This proposal states that polyhapto ligands 'be considered pseudo-atoms of atomic weight equal to the sum of the atomic weight of all the atoms bonded to the metal atom'. This proposal has been accepted and employed by several researchers in this field. It should be noted that to keep within the generally accepted priorities of the CIP sequence rule, the first priority is 'higher atomic number precedes lower'. Thus the pseudo-atom proposal might be altered such that polyhapto ligands would be considered pseudo-atoms of atomic number equal to the sum of the atomic numbers of all atoms bonded to the metal atom, to be consistent with the CIP sequence rule. Thus, $\eta^8\text{-}C_8H_8$, $\eta^7\text{-}C_7H_7$, $\eta^6\text{-}C_6H_6$, $\eta^5\text{-}C_5H_5$, $\eta^4\text{-}C_4H_6$ and $\eta^3\text{-}C_3H_5$ would be treated as pseudo-atoms of atomic number $48 > 42 > 36 > 30 > 24 > 15$. This places η^5-cyclopentadienyl, the most common polyhapto ligand, between the second and third periods of the periodic table (*e.g.* between Cl, atomic number 17, and As, atomic number 33) when considering only common donor atoms. This is approximately the same relative priority obtained by comparison of atomic weights (*e.g.* $\eta^5\text{-}C_5H_5$, 60; Cl, 35.5; and As, 75) for the same donor atoms.

Applying the pseudo-atom convention to the iron complex in Figure 8, the iodine atom is priority 1, the $\eta^5\text{-}C_5H_3R_2$ ligand is priority number 2, the phosphorus atom is priority number 3, and carbon is priority number 4.[15] When the iron is viewed from the side opposite the priority number 4, the sequence is 1,2,3 in the anticlockwise or *S* direction. The highest priority carbon in the cyclopentadienyl ligand, indicated by an asterisk, is designated with the *R* chirality symbol by application of the extended CIP sequence rule.

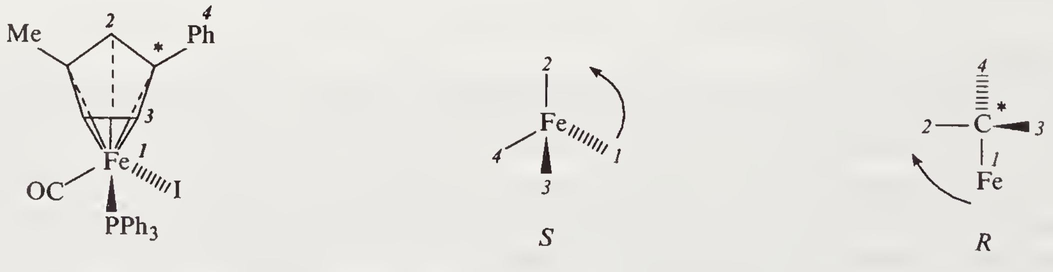

Figure 8 $[Fe[3\text{-}(CH_3)\text{-}1\text{-}(C_6H_5)\text{-}\eta^5\text{-}C_5H_3][P(C_6H_5)_3](CO)]I$

Bernal *et al.* have further extended the pseudo-atom priorities to a series of five-coordinate molybdenum complexes, one of which is shown in Figure 9.[16] They assign the chirality symbol according to the octahedral sequence rule, by treating the square pyramid as an octahedron with a vacant sixth position. Accordingly, the ligand positions on the octahedron are numbered 1 to 6 such that 1 and 6 are always *trans*, and 2 to 5 will advance either right or left around the belt of the octahedron according to the priorities of the belt donor atoms. The structure is then viewed from opposite the triangular face 4,5,6. The sequence 1,2,3 is clockwise, and the chirality symbol *R* is assigned.

The assignment of descriptors and configuration is sometimes arbitrary, at best, when based on model structures and pseudo-atom coordination numbers. A more explicit stereochemical notation is achieved by using this notation, which states within the stereodescriptor the model structure on which the notation is based. In this notation the pseudo-square pyramidal structure is [*SPY*-5-14-*C*(*R*)]. This structure can be expected to result in geometric isomers when one of the

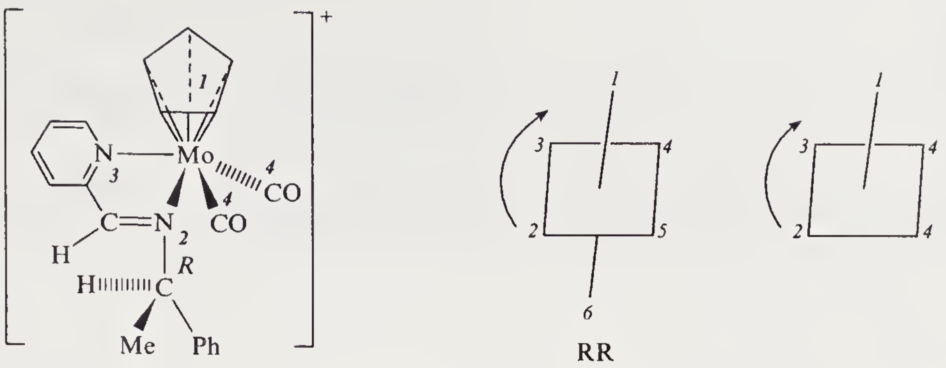

Figure 9 $[[Mo(\eta^5\text{-}C_5H_5)(CO)_2]^{2-}([\{[1\text{-}(C_6H_5)C_2H_5]N\}CH]C_5H_4N)]$, [*SPY*-5-14-*C*-(*R*)]

carbonyls is substituted by a ligand such as a phosphine. This is easily noted in the configuration number.

The definition of a pseudo-atom coordination number for polyhapto ligands will be a difficult one on which to achieve a consensus. For example, η^5-cyclopentadienyl can be thought to be either five-coordinate (having five nearest neighbor carbon atoms to the coordination center), three-coordinate (due to the donation of six valence electrons and the usual replacement of three monohapto ligands) or monocoordinate (in the pseudo-atom concept above). Whatever coordination number or coordination geometry is chosen, this systematic notation is unambiguous because the necessary information is stated exactly as an integral part of the stereodescriptor.

3.8.3 Polynuclear and Cluster Compounds

Bridged binuclear, trinuclear and tetranuclear chelated octahedral structures were examined by Schäffer,[17] who used the skew line helical definition for the chirality symbols Δ and Λ. The configurational isomers for a tetrakisbidentate, edge-fused-bis-octahedral structure are ΔΔ, ΔΛ, ΛΔ, and ΛΛ.

Many polynuclear and cluster compounds with challenging stereochemical properties are now frequently being prepared. For example, asymmetric metallocarboranes have been prepared by Miller *et al.*,[18] and an asymmetric tetrahedral cluster with four different atoms at the tetrahedral apexes was recently reported by Richter and Vahrenkamp.[19] Casey *et al.* have recently considered stereochemical notation for large clusters.[20] Polynuclear and cluster compounds, especially those with polyhapto ligands and ligands that contain involved stereochemistry in themselves, have potentially tens of thousands, if not hundreds of thousands, of isomeric configurations. Intermediate size chemical systems with relatively simple and straightforward stereochemical relationships can be described by the various notations already outlined. These notations will require some extensions and further elaboration, such as an appropriate set of locants to place a stereodescriptor at an exact position in an extended structure. Undoubtedly, further refinements will be needed that cannot be foreseen until a particular configuration is demonstrated. However, larger compounds with very complicated stereochemical relationships, in all probability, will require the more powerful and rapid analysis available only through the application of computer systems.

3.9 REFERENCES

1. IUPAC, 'Nomenclature of Inorganic Chemistry: Definitive Rules 1970', 2nd edn., Butterworths, London, 1971; *Pure Appl. Chem.*, 1971, **28**, 1.
2. T. E. Sloan and D. H. Busch, *Inorg. Chem.*, 1978, **17**, 2043.
3. F. A. Cotton, *J. Am. Chem. Soc.*, 1968, **90**, 6230.
4. J. B. Casey, W. J. Evans and W. H. Powell, *Inorg. Chem.*, 1981, **20**, 1333.
5. IUPAC, 'Nomenclature for Regular Single-Strand and Quasi-Single-Strand Inorganic and Coordination Polymers', *Pure Appl. Chem.*, 1981, **53**, 2283.
6. Unambiguous systematic names may be generally considered to be those names derived by applying systematic principles without regard to the various hierarchical principles necessary to choose one unique variation, *e.g.* for $[NiBr(NH_3)(\mu\text{-}Cl)_2CuCl(NH_3)]$, diammine-1,2$\kappa^2$*N*-bromo-2$\kappa$*Br*-di-μ-chloro-chloro-1κ*Cl*-copper(II)nickel(II) and di-μ-chloro-chloroamminebromoamminecopper(II)nickel(II) are two unambiguous systematic names derived from different principles.
7. IUPAC, 'Nomenclature of Organic Chemistry', 1979 edn., Rule C-22, Pergamon Press, Oxford, 1979, p. 112.
8. R. S. Cahn, C. Ingold and V. Prelog, *Angew. Chem., Int. Ed. Engl.*, 1966, **5**, 385.
9. V. Prelog and G. Helmchen, *Angew. Chem., Int. Ed. Engl.*, 1982, **21**, 567.
10. M. F. Brown, B. R. Cook and T. E. Sloan, *Inorg. Chem.*, 1975, **14**, 1273.
11. M. F. Brown, B. R. Cook and T. E. Sloan, *Inorg. Chem.*, 1978, **17**, 1563.

12. T. E. Sloan, in 'Topics In Stereochemistry', vol. 12, ed. G. Geoffroy, N. L. Allinger and E. L. Eliel, Wiley, New York, 1981, p. 1.
13. K. Schlögl, in 'Topics In Stereochemistry', vol. 1, ed. N. L. Allinger and E. L. Eliel, Wiley, New York, 1967, p. 39.
14. K. Stanley and M. C. Baird, *J. Am. Chem. Soc.*, 1975, **97**, 6598.
15. T. G. Attig, R. G. Teller, S. M. Wu, R. Bau and A. Wojcicki, *J. Am. Chem. Soc.*, 1979, **101**, 619.
16. T. Bernal, S. J. LaPlaca, J. Korp, H. Brunner and W. Herrmann, *Inorg. Chem.*, 1978, **17**, 382.
17. U. Thewalt, K. A. Jensen and C. E. Schäffer, *Inorg. Chem.*, 1972, **11**, 2129.
18. V. R. Miller, L. G. Sneddon, D. C. Beer and R. N. Grimes, *J. Am. Chem. Soc.*, 1974, **96**, 3090.
19. F. Richter and H. Vahrenkamp, *Angew. Chem., Int. Ed. Engl.*, 1978, **17**, 864.
20. J. B. Casey, W. J. Evans and W. H. Powell, *Inorg. Chem.*, 1981, **20**, 3556.

4

Clusters and Cages

IAN G. DANCE
University of New South Wales, Sydney, Australia

4.1 INTRODUCTION

4.1.1 Overview

A new field of coordination chemistry is that of polymetallic cage and cluster complexes $[\mathrm{M}_m(\mu\text{-X})_x\mathrm{L}_l]^z$ with molecular (*i.e.* discrete) structure. They contain at least three metal atoms, frequently with bridging ligands X and terminal ligands L. These compounds link the classical complexes ($m = 1$) and the non-molecular ($m \rightarrow \infty$) binary and ternary compounds of the metals.[1] Molecular polymetallic clusters (with finite radius) also provide a link with the surfaces (infinite radius) of metals and their binary compounds.[2–5] Polymetallic complexes are known for almost all metals except the actinides.

A key property of these polymetallic complexes is geometrical structure, more variable and diverse than the coordination stereochemistries of monometallic complexes or the symmetrical lattices of non-molecular compounds. The following well-defined aggregation modes illustrate the geometrical scope of the field.

(1) Staphylometallic aggregates such as $[\mathrm{Cu_5Cl_{16}}]^{11-}$ have no cyclic connections.
(2) At the other extreme, aggregates containing the maximum number of cyclic connections occur as molecular fragments of non-molecular structures. For instance, polycyclic $[\mathrm{S_4Zn_{10}(SPh)_{16}}]^{4-}$, structure (**10a**), is a fragment of the cubic ZnS lattice.[6]
(3) The metals, bridging ligands and terminal ligands are frequently arrayed as concentric regular polyhedra, which may be empty or contain a central ligand or metal atom. Thus, in onion-shell polyhedral description, the filled cage $[\mathrm{ClZn_8(SPh)_{16}}]^-$ (**8f**) is *centro*-(μ_4-Cl)-*tetrahedro*-$\mathrm{Zn_4}$-*icosahedro*-(μ-SPh)$_{12}$-*tetrahedro*-$\mathrm{Zn_4}$-*tetrahedro*-$(\mathrm{SPh})_4$.[7]
(4) One extreme type is held together only by metal–metal bonds, with no bridging ligands. Most gold clusters (Section 4.12.1) are in this category; an even more exotic class devoid of ligands contains the 'naked' polymetal anions, such as $\mathrm{Pb_9}^{4-}$(Section 4.9.3).

These illustrative aggregation modes draw attention to the two cohesive forces: ligand bridges and direct metal–metal bonds. The dual terms 'cluster' and 'cage' have been suggested[8] to distinguish species with and without metal–metal bonds, respectively. This differentiation can be useful but there are now many known polymetallic complexes where the presence of M—M bonding is partial, or uncertain and debatable. In this chapter description of M—M bonding in specific complexes will be explicit when significantly present or absent, and the words 'cage' and 'cluster' have no special implications.

Metal clusters occur in metal storage proteins and redox metalloenzymes. The record for cluster size is held by the iron-storage protein ferritin,[9] where an ordered aggregate $\{(\mathrm{FeOOH})_8\text{-}(\mathrm{FeO{\cdot}H_2PO_4})\}_n$ containing up to 4500 $\mathrm{Fe^{III}}$ atoms occurs within a protein cavity of 80 Å diameter, and the growth and dispersal processes occur with iron in the reduced $\mathrm{Fe^{II}}$ state.

In many instances the syntheses of polymetallic clusters have been serendipitous, and recognized only after the determination of the crystal structure of the product. The rational synthesis of a predicted polymetallic complex is rare. Nonetheless, some patterns and principles of cluster synthesis are recognized, the main factor being modification of the ligand-to-metal ratio. With a mono- or oligo-metallic precursor the preparative reaction involves reduction of the ligand/metal ratio, while a non-molecular precursor can be fragmented into clusters by reaction with a limited proportion of terminal ligand.

The question of M—M bonding is part of the general question of electronic structure and bonding. The concepts applicable to monometallic complexes, namely of the metal *s*, *p* and *d* orbitals forming molecular orbitals which are (a) M—L bonding, (b) non-bonding, (c) weakly M—L antibonding and (d) strongly M—L antibonding, are now supplemented by cluster MOs which are (e) M—M bonding, (f) M—M non-bonding and (g) M—M antibonding. In general the M—M MOs of type (e), (f) and (g) (which in a cluster often replace the type (b) mono-metal orbitals) are frontier orbitals not distant in energy from the metal *d* AOs. Therefore these M—M MOs may be empty (pre- or early-transition metals), partially filled (transition metals) or fully filled (late- and post-transition metals), corresponding to zero, variable and zero M—M bond order, respectively. The variable electron population of these orbitals correlates with the variable oxidation states often obtainable for a cluster. Relationships between observed M—M distance, cluster electron population and MO descriptions are well advanced (see Section 4.4.4). Magnetic exchange, ferro- and/or antiferro-magnetic, is often observed for polymetallic complexes. The measurable interaction energies (<5 kJ $\mathrm{mol^{-1}}$) are, however, at least an order of magnitude less than the bond energies of interest.

The development of the relatively youthful class of polymetallic complexes has depended on the advent of routine X-ray structure determination, and consequently the bulk of the information and understanding at present involves geometrical structure. This metrical bias, reinforced by the intriguing unpredictability of many aggregate structures, determines the content and organization of this chapter. The primary classification of compounds is structural, according to increasing numbers of metal atoms.

Lack of space has forced exclusion of some clusters, and topics described in reviews elsewhere are afforded reduced coverage. Literature citation for established classes of aggregates such as the polyoxometallates is limited to contemporary leading references. Dimetallic and linear polymetallic complexes are excluded.

4.1.2 Reviews

Recent accounts of clusters and cages are contained in the book ‘Transition Metal Clusters’ (1980),[10] and in reviews emphasizing trimetallic clusters (1980),[11] biological clusters and synthetic analogs (1977,[12,13] 1981,[14] 1982,[15] 1983[16]), gold clusters (1982),[17] polyoxometallates (1974,[18] 1976[19]), thio- and seleno-bridged cages (1983)[20] and polymetallic carboxylates (1977).[21] Contemporary reviews of related fields emphasize clusters and surfaces (1979),[2] catalysis by clusters (1983),[5] coordinatively unsaturated clusters (1980),[3] organometallic and carbonyl clusters (1980,[22] 1981[23]), condensed metal clusters (1981)[1] and ligand-free metal clusters (1983).[24]

4.1.3 Terminology and Notation*

The terms ‘molecular’ and ‘non-molecular’ describe *geometrical* structure, namely the presence or absence of discrete polyatomic units separated by non-bonding boundaries. The infinite linkages characteristic of structural non-molecularity can be classified as one-, two- or three-dimensional: the first two types correspond to chain and layer structures, respectively. Structurally molecular complexes may have any charge or size.

General symbols are: X, bridging anionic ligand; Y, anionic terminal ligand; Z, anionic central ligand; and L, uncharged terminal ligand. In some diagrams smaller open circles represent metal atoms and larger dotted circles denote ligand donor atoms. Where necessary the superscripts ^{i} and ^{o} are used to differentiate inner and outer ligands or metal atoms. ‘Centrifugal’ ligands radiate from the cluster centre.

4.2 POLYHEDRA, PATTERNS AND PROGRESSIONS

4.2.1 Cluster Symmetry

The salient characteristic of most clusters is the occurrence of high symmetry, exact or virtual, manifest in the polyhedra constituted by the cluster atoms. In evaluating the cluster polyhedra it is frequently appropriate to consider three subsets of cluster atoms, namely metals M, bridging ligands X and terminal ligands L, and to describe the polyhedra formed by the subsets separately or combined. This global analysis of polyhedra and symmetry is usually the primary stage, followed by the traditional consideration of individual metal coordination stereochemistry. An alternative approach to aggregate structure focuses on the local environment, describing first the metal coordination polyhedra around individual metal atoms, and then describing the modes of polyhedra

---

* In this chapter, structure designations in bold figures indicate the number of metal atoms in the cluster, *e.g.* **(3a)**, **(5b)** and **(9c)** are structures with three-, five- and nine-atom clusters respectively.

linkage. A tertiary stage of cluster topological analysis concentrates on the array of ligand substituents, and their possible influence on cluster geometry.

4.2.2 Cluster Polyhedra

There are five regular (Platonic) polyhedra with equivalent faces and equivalent vertices. Of these, the tetrahedron, octahedron, cube (hexahedron) and icosahedron are *widely* represented in cluster polyhedra. The structure descriptions in Table 1 illustrate the occurrence of regular polyhedra in cages $X_xM_mL_l$, and demonstrate the descriptive notation based on expanding concentric polyhedra of metals and ligands. A fascinating approach to a large Platonic cage molecule occurs in $[M_6S_{17}]^{4-}$ (**6h**; M = Nb, Ta),[25] which is one half of *centro*-S-*icosahedro*-M_{12}-*pentagonal dodecahedro*-$(\mu_3\text{-S})_{20}$-*icosahedro*-S_{12} (Section 4.6.5).

Table 1 Concentric Regular Polyhedra

Cluster structure	*Diagram*	*Example*
Tetrahedro-$(\mu_3\text{-X})_4$-*tetrahedro*-M_4		$(TlOMe)_4$
Tetrahedro-$(\mu_3\text{-X})_4$-*tetrahedro*-M_4-*tetrahedro*-L_4	(**4w**)	$S_4Fe_4(NO)_4$
Octahedro-$(\mu\text{-X})_6$-*tetrahedro*-M_4	(**4s**)	$[Cu_4I_6]^{2-}$
Octahedro-$(\mu\text{-X})_6$-*tetrahedro*-M_4-*tetrahedro*-L_4	(**4t**)	$[Co_4(SPh)_{10}]^{2-}$
Tetrahedro-$(\mu_3\text{-X})_4$-*tetrahedro*-$(\mu_3\text{-X}')_4$-*octahedro*-M_6	(**6m**)	$O_4Sn_6(OMe)_4$
Hexahedro-$(\mu_3\text{-X})_8$-*octahedro*-M_6-*octahedro*-L_6	(**6m**)	$[S_8Fe_6(PEt_3)_6]^{2+}$
Octahedro-$(\mu_4\text{-X})_6$-*hexahedro*-M_8-*hexahedro*-L_8	(**8b**)	$[S_6Co_8(SPh)_8]^{4-}$
Centro-$(\mu_8\text{-Z})$-*icosahedro*-$(\mu\text{-X})_{12}$-*hexahedro*-M_8	(**8d**)	$[ICd_8(SCH_2CH_2OH)_{12}]^{3+}$
Centro-$(\mu_4\text{-Z})$-*tetrahedro*-M_4-*icosahedro*-$(\mu\text{-X})_{12}$-*tetrahedro*-M_4-*tetrahedro*-L_4	(**8f**)	$[ClZn_8(SPh)_{16}]^-$

Semi-regular polyhedra (all vertices identical, all edges same length, all faces regular polygons, but not all faces identical) prevalent in cages and clusters include prisms (particularly trigonal and hexagonal prisms), the cuboctahedron and the (tetra)truncated tetrahedron. Very large face-centred cuboctahedra are postulated for the metal cores of $Au_{55}(PPh_3)_{12}Cl_6$ and $Rh_{55}(PBu^t_3)_{12}Cl_{20}$ (Section 4.12.3), while an instance of the truncated tetrahedron is found in *octahedro*-M_6-*tetrahedro*-$(\mu_3\text{-E})_4$-*truncated tetrahedro*-$(\mu\text{-SPh})_{12}$-*tetrahedro*-M_4-*tetrahedro*-$(SPh)_4$ (Section 4.10.1.2).

Sometimes the metal and ligand sets combined comprise a higher symmetry polyhedron than the sets separated: an example is *hexagonal prismo*-$(RMXR')_6$ (Section 4.6.6). Coplanar metal atoms occur in regular triangular, square, pentagonal, hexagonal or octagonal molecules.

4.2.3 Structural Patterns and Progressions

The body of the description of clusters and cages in Sections 4.3–4.12 is organized primarily by the number of metal atoms, and consequently topological relationships between aggregates with different metal counts may be obscured. Attention to these relationships is drawn here.

4.2.3.1 Ligand connectivities

There are four modes of connection of non-chelating ligands to the metal polyhedron: terminal, edge-bridging, face-bridging and central. Table 2 lists and indexes most of the major structure types according to the metal polyhedron and the ligand connectivity modes. Inspection of the columns permits recognition of sequences of structure types with similar connectivity but different size or symmetry. Where the metal polyhedron is semi-regular and not all faces or edges are equivalent, different ligand connection arrangements can occur within the same mode column.

4.2.3.2 Uncharged cages

The metal/ligand ratios in the complexes listed in Table 2 are obviously related to the proportions of vertices, edges and faces of the various metal polyhedra. The charges of the metals and ligands need not balance in these compounds. There is, however, another set of complexes $(MX)_p$ or $(RMXR')_p$ with no net charge, where the thermodynamics of solvation rather than symmetry might appear to be the primary determinant of composition and structure. In these cages the structure must adapt to the fixed M/X ratio.

Trends in cage size according to bulk of ligand substituents are apparent: (i) $(HAlNBu^t)_4$ $(HAlNPr^i)_6$ and $(HAlNEt)_8$, with structures (**4w**), (**6j**) and (**8h**); and (ii) $(MeZnSBu^t)_5$ and $(MeZnSPr^i)_8$, with structures (**5g**) and (**8h**). A subset of the $(MX)_p$ or $(LMX)_p$ group involves

Table 2 Major Structure Types, Classified by Metal Polyhedron and Ligand Connectivity

General formula	*Ligand positions*				*Structure/ section number*
		bridging			
	central	*face*	*edge*	*terminal*	
M_3 Triangle					
$(\mu\text{-X})_3\mathrm{M_3L_3}$	0	0	3	3	4.3.1.1
$(\mu\text{-X})_3\mathrm{M_3L_6}$	0	0	3	6	4.3.1.2
$(\mu\text{-X})_3\mathrm{M_3Y_6L_3}$	0	0	3	9	**(3a)**
$(\mu\text{-X})_6\mathrm{M_3L_3}$	0	0	6	3	**(3b)**
$(\mu\text{-XRX})_6\mathrm{M_3}$	0	0	6	0	**(3c)**
$(\mu_3\text{-X})_2\mathrm{M_3L_6}$	0	2	0	6	**(3d)**
$(\mu_3\text{-X})(\mu\text{-X})_3\mathrm{M_3Y_3}$	0	1	3	3	**(3e)**,**(3f)**
$(\mu_3\text{-X})(\mu\text{-X})_3\mathrm{M_3L_9}$	0	1	3	9	**(3g)**
$(\mu_3\text{-X})_2(\mu\text{-X})_3\mathrm{M_3}$	0	2	3	6	**(3h)**
$(\mu_3\text{-X})(\mu\text{-XRX})_6\mathrm{M_3L_3}$	0	1	6	3	**(3i)**
$(\mu_3\text{-X})_2(\mu\text{-XRX})_3\mathrm{M_3}$	0	2	3	0,9	**(3j)**
$(\mu_3\text{-X})_2(\mu\text{-XRX})_6\mathrm{M_3}$	0	2	6	3	**(3k)**
M_4 Square					
$\mathrm{M_4Y_4L_4}$	0	0	0	8	**(4a)**
$(\mu\text{-X})_4\mathrm{M_4}$	0	0	4	0,2,12	**(4b)**,**(4c)**
$(\mu\text{-XRX})_4\mathrm{M_4}$	0	0	4	0	**(4d)**
$(\mu\text{-XRX})_8\mathrm{M_4}$	0	0	8	0	**(4e)**
$(\mu\text{-XRX})_4(\mu\text{-X})_4\mathrm{M_4}$	0	0	8	0	**(4g)**
$(\mu_4\text{-XRX})_2(\mu\text{-XRX})_4\mathrm{M_4}$	0	2	4	0	**(4k)**
$(\mu\text{-X})_8\mathrm{M_4}$	0	0	8	0,4	4.4.1.9
$(\mu_4\text{-X})_2(\mu\text{-X})_4\mathrm{M_4Y_8}$	0	2	4	8	**(4n)**
M_4 Rectangle					
$(\mu\text{-XRX})_6(\mu\text{-X})_2\mathrm{M_4}$	0	0	8	0	**(4f)**
$(\mu\text{-X})_8\mathrm{M_4L_4}$	0	0	8	4	**(4l)**
$(\mu\text{-X})_4\mathrm{M_4Y_4L_4}$	0	0	4	8	**(4m)**
M_4 Rhomb					
$(\mu_3\text{-X})_2(\mu\text{-X})_4\mathrm{M_4Y_{10}}$	0	2	4	10	**(4p)**
M_4 Parallelogram					
$(\mu\text{-XRX})_4(\mu\text{-X})_4\mathrm{M_4}$	0	0	8	0	**(4h)**
$(\mu_3\text{-X})_2(\mu\text{-X})_2\mathrm{M_4L_4}$	0	2	2	4	**(4i)**
M_4 Butterfly					
$(\mu_3\text{-X})_2(\mu\text{-X})_5\mathrm{M_4Y_4}$	0	2	5	4	**(4q)**
$(\mu_3\text{-X})_2(\mu\text{-X})_4\mathrm{M_4Y_6}$	0	2	4	6	4.4.2.2
M_4 Disphenoid					
$(\mu\text{-X})_4\mathrm{M_4Y_8}$	0	0	4	8	**(4r)**
M_4 Trigonal pyramid					
$(\mu_3\text{-X})_3\mathrm{M_4L_7}$	0	3	0	7	4.4.2.5
M_4 Tetrahedron					
$(\mu\text{-X})_6\mathrm{M_4}$	0	0	6	0	**(4s)**
$(\mu\text{-X})_6\mathrm{M_4Y_4}$	0	0	6	4	**(4t)**
$(\mu\text{-X})_6\mathrm{M_4Y_{12}}$	0	0	6	12	4.4.3.3
$(\mu_4\text{-Z})(\mu\text{-X})_6\mathrm{M_4}$	1	0	6	0	**(4u)**
$(\mu_4\text{-Z})(\mu\text{-X})_6\mathrm{M_4L_4}$	1	0	6	4	**(4v)**
$(\mu_3\text{-X})_4\mathrm{M_4}$	0	4	0	0,4,12	**(4w)**, 4.4.4.4
M_5 Pentagon					
$(\mu_5\text{-X})_2(\mu\text{-X})_5\mathrm{M_5}$	0	2	5	0	**(5d)**
M_5 Trigonal bipyramid					
$(\mu\text{-X})_6\mathrm{M_5}$	0	0	6	0,7	**(5a)**,**(5b)**
$(\mu_3\text{-X})_6\mathrm{M_5L_5}$	0	6	0	5	**(5c)**
M_5 Square pyramid					
$(\mu_3\text{-X})_4(\mu\text{-X})_4\mathrm{M_5X_5}$	0	4	4	5	4.5.3
M_6 Hexagon					
$(\mu\text{-X})_6\mathrm{M_6}$	0	0	6	0	**(6a)**
$(\mu\text{-X})_{12}\mathrm{M_6}$	0	0	12	0,12	**(6b)**,**(6c)**
M_6 Concentric triangles					
	0	4	9	3	4.6.1.3
M_6 Bicapped tetrahedron					
$(\mu_4\text{-Z})(\mu_3\text{-X})_6\mathrm{M_6}$	1	6	0	0	**(6f)**
M_6 Edge-linked tetrahedra					
$\mathrm{M_6L_6}$	0	0	0	6	4.6.3.3
M_6 Pentagonal pyramid					
$(\mu_6\text{-X})(\mu_3\text{-X})_5(\mu\text{-X})_5\mathrm{M_6Y_6}$	1	5	5	6	**(6h)**

Table 2 *(continued)*

General formula	*Ligand positions*				*Structure/ section number*
		bridging			
	central	*face*	*edge*	*terminal*	
M_6 Trigonal prism					
$(\mu_6\text{-Z})(\mu\text{-X})_9M_6$	1	0	9	0	4.6.7.1
$(\mu_6\text{-Z})(\mu_3\text{-X})_2(\mu\text{-X})_9M_6$	1	2	9	6	4.6.7.2
M_6 Octahedron					
$(\mu_3\text{-X})_6M_6Y_6$	0	6	0	6	**(6j)**,**(6k)**,**(6n)**
$(\mu\text{-X})_{12}M_6$	0	0	12	0,6	**(6l)**
$(\mu_3\text{-X})_8M_6$	0	8	0	6	**(6m)**
M_7 Pentagonal bipyramid					
M_7L_7	0	0	0	7	4.7.1
M_7 Centred hexagon					
$(\mu_3\text{-X})_6(\mu\text{-X})_6M_7Y_{12}$	0	6	6	12	**(7a)**
M_7 Capped octahedron					
$(\mu_3\text{-X})_7M_7Y_7$	0	7	0	7	**(7d)**
M_8 Octagon					
$(\mu\text{-X})_{16}M_8$	0	0	16	0	**(8a)**
M_8 Hexagonal bipyramid					
$(\mu_3\text{-X})_2(\mu\text{-X})_{14}M_8Y_{14}$	0	2	14	14	**(8j)**
M_8 Cube					
$(\mu_4\text{-X})_6M_8Y_8$	0	6	0	8	**(8b)**
$(\mu\text{-XRX})_6M_8$	0	0	12	0	**(8c)**
$(\mu_8\text{-Z})(\mu\text{-X})_{12}M_8$	1	0	12	0,8	**(8d)**,**(8e)**
M_8 Tetracapped tetrahedron					
$(\mu_4\text{-Z})(\mu\text{-X})_{12}M_4$	1	0	12	4	**(8f)**
M_9 Confacial bioctahedron					
$(\mu_4\text{-X})_3(\mu\text{-X})_6M_9L_6$	0	6	3	6	**(9a)**
M_9 Tricapped trigonal prism					
M_9	0	0	0	0	4.9.3
M_9 Monocapped square antiprism					
M_9	0	0	0	0	4.9.3
M_9 Body-centred cube					
M_9L_8	0	0	0	8	**(9f)**
M_{10} Tetracapped octahedron					
$M_6M'_4L_{12}$	0	0	0	12	4.10.1.1
$(\mu_3\text{-X})_4M_6(\mu\text{-X})_{12}M_4Y_4$	0	4	12	4	**(10a)**
$(\mu_3\text{-X})_4(\mu_3\text{-X}')_4M_6(\mu\text{-X})_{12}M_4Y_4$	4	4	12	4	4.10.1.3
M_{10} Body-centred face-capped trigonal prism					
$M_{10}Y_3L_6$	0	0	0	9	**(10c)**
M_{12} Cuboctahedron					
$(\mu_3\text{-X})_8M_{12}$	0	8	0	0	**(12b)**

complexes where X is a bidentate ligand which bridges unsymmetrically p of the triangular faces of the metal polyhedron. These are structures **(4w)** and **(6n)**, symmetry D_{nd} where $n = p/2$ [the homologous structure with $p = 8$ occurs for (o-anisylcopper)$_8$[26]]. This topological interpretation has been extended by Hesse.[27,28]

4.2.3.3 MCp moieties

In the series of complexes $Cp_3M_3S_2$ (M = Co, Ni), $Cp_4Cr_4O_4$, $Cp_5V_5O_6$ and $Cp_6Ti_6O_8$ (Sections 4.3.4, 4.4.4.3, 4.5.1.2 and 4.6.8.2, respectively), the MCp moieties are arrayed as triangle, tetrahedron, trigonal bipyramid and octahedron respectively, with oxide or sulfide ions capping the triangular faces.

4.3.2.4 Metal polygons

Metal polygons with pairs of doubly-bridging ligands on each edge occur with three, four, six and eight metals (Sections 4.3.2, 4.4.1.9, 4.6.1.1 and 4.8.1, respectively).

4.2.3.5 *Expansion of copper and silver cages*

Polycyclic copper and silver cages with doubly-bridging thiolate ligands $[M_4(SR)_6]^{2-}$ (**4s**; Section 4.4.3.1), $[M_5(SR)_7]^{2-}$ (**5e**; Section 4.5.5) and $[M_6(SR)_8]^{2-}$ (**6e**; Section 4.6.3.1) are related by replacement of a μ-SR bridge by a linear (μ-SR)M(μ-SR) bridge.[29]

4.2.3.6 *Tetrahedral progressions*

A growth progression of tetrahedra of tetrahedra is:

$$\underset{}{MX_4} \longrightarrow \underset{\text{adamantanoid}}{M_4X_{10}} \longrightarrow \underset{\text{tetra-adamantanoid}}{M_{10}X_{20}} \longrightarrow \underset{\text{deca-adamantanoid}}{M_{20}X_{35}\ ?}$$

Each of these clusters is tetrahedral in overall shape, contains tetrahedral coordination for all metal atoms, and is a T_d fragment of the cubic ZnS lattice.[6]

4.2.3.7 *Concentric polygons and polyhedra*

Concentric metal polygons or concentric metal polyhedra occur: inner and outer triangles in Section 4.6.1.3; an octahedron outside a cube in Section 4.8.2.4; and inner and outer tetrahedra in Section 4.8.3.

4.3 TRIMETALLIC COMPLEXES[11]

The metal array in trimetallic complexes is only two-dimensional and with few exceptions an equilateral triangle, but there is variety in the ligand bridging modes which buttress the M_3 triangle. Bridging ligands may cap the M_3 triangle or doubly-bridge the triangle edges, with single-atom or three-atom connections, and the following classification is according to the types and combinations of ligand bridges. Triangular clusters maintained only by M—M bonds are not known in other than metal carbonyl or organometallic systems.

4.3.1 Three Single-atom Edge Bridges: $(\mu\text{-}X)_3M_3$ Core

Observable variables in this class are (i) the number of terminal ligands, (ii) the influence of direct M—M bonding and the M—(μ-X)—M angles, and (iii) the stereochemistry of the X_3M_3 cycle.

4.3.1.1 $(\mu\text{-}X)_3M_3L_3$

Single terminal ligands, trigonal coordination and no M—M bonding occur in complexes $(\mu\text{-SR})_3(CuCl)_3$, R = PMe_3 or $C(NH_2)Me$,[30] with S_3Cu_3 chair conformation. A variation with two terminal ligands and tetrahedral stereochemistry at one metal is $(\mu\text{-SPh})_3(CuPPh_3)_2Cu(PPh_3)_2$,[31] with S_3Cu_3 twist boat conformation.

When M—M bonds are present the $(\mu\text{-}X)_3M_3$ atoms and the terminal ligand donor atoms are virtually coplanar, as in low-oxidation state Pd and Pt complexes: $(\mu\text{-}SO_2)_3Pt_3(PPh_3)_3$,[32] $(\mu\text{-}PPh_2)_2(\mu\text{-}H)Pt_3(PPh_3)_3$,[33] $(\mu\text{-}Ph)(\mu\text{-}PPh_2)(\mu\text{-}SO_2)Pt_3(PPh_3)_3$,[34] $[(\mu\text{-}Cl)(\mu\text{-}PPh_2)_2Pd_3(PEt_3)_3]^+$ and variants.[35] M—M distances (2.7–2.9 Å) are related to the electronic properties of the bridging ligands.[36] Two Pt—Pt bonds (2.79 Å) only occur in $(\mu\text{-}PPh_2)_3Pt_3Ph(PPh_3)_2$ [formed by refluxing $Pt(PPh_3)_4$ in benzene] where the Pt—Pt edge opposite the terminal Ph ligand is 3.63 Å.[37]

4.3.1.2 $(\mu\text{-}X)_3M_3L_6$

These complexes are known with planar and non-planar M_3X_3 cores, and with tetrahedral or square-planar metal coordination. The X_3M_3 cycle in chair conformation and with tetrahedral metal coordination occurs in $(\mu\text{-SMe})_3B_3X_6$ (X = Cl, Br)[38] and is proposed in the form of $(\mu\text{-Scys})_3Cd_3(Scys)_6$ for one of the two clusters with cysteinate coordination in metallothionein proteins.[39] The twist-boat conformation occurs in $S_3Sn_3Me_6$[40] and probably in the related compounds $S_3M_3R_6$ (M = Ge, Sn, Pb; R = Me, Bu, Ph).[41] The same structural unit with distorted twist-boat stereochemistry occurs in the $(\mu\text{-S})_3Fe_3(Scys)_5L$ cluster recently discovered in several ferredoxins.[15,42]

A planar X_3M_3 cycle and tetrahedral metal coordination is known in $[(\mu\text{-SPh})_3Fe_3Cl_6]^{3-}$,[43] where remarkably[31] all atoms in the $(\mu\text{-SPh})_3Fe_3$ set are coplanar, and in $(\mu\text{-O})_3Zr_3Cp_6$.[44] In both of these compounds the M—X—M angles are singularly large, 140° and 143° respectively.

Square-planar metal coordination in $(\mu\text{-X})_3M_3L_6$ complexes occurs in $(\mu\text{-H})_3Rh_3(P(OMe)_3)_6$ with twist H_3Rh_3 conformation,[45] and in the chelated versions $(\mu\text{-SEt})_3Pd_3(S_2CSEt)_3$[46] and $(\mu\text{-SCH}_2CH_2SCH_2CH_2S)_3Pd_3$,[47] both with chair S_3Pd_3 conformation.

4.3.1.3 $(\mu\text{-X})_3M_3Y_6L_3$

Structure **(3a)** is now well known in trirhenium clusters, whose discovery in 1963 marked the renaissance of cluster chemistry. It is considered that Re—Re bonds of order 2 exist in the Re^{III} complexes such as $[Re_3Cl_{12}]^{3-}$ or $Re_3Br_9(PPh_3)_3$. When uncharged ligands are present they occupy the equatorial terminal positions L, which are the most labile. The less labile terminal positions marked Y on **(3a)** are invariably occupied by anionic ligands, while the bridging ligands X are inert.

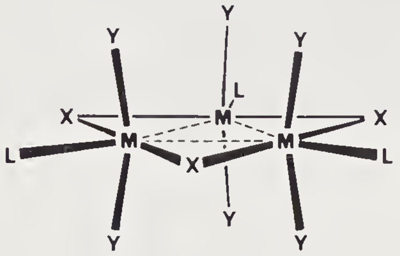

(3a)

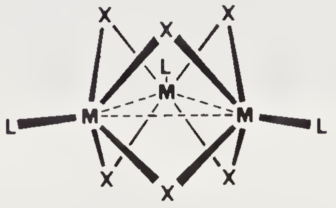

(3b)

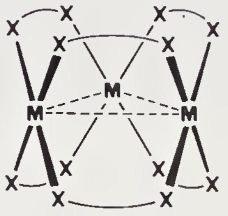

(3c)

4.3.2 Six Single-atom Bridges: $(\mu\text{-X})_6M_3$ Core

In the D_{3h} structure **(3b)** each metal atom lies outside a rectangular face of the $(\mu\text{-X})_6$ trigonal prism, and is coordinated to a terminal ligand L. Instances of this structure are $[(\mu\text{-Cl})_6Nb_3(\eta^6\text{-}C_6Me_6)_3]^+$ and its one-electron oxidation product,[48] and $(S_2C_{10}Cl_6)_3Ni_3(PPh_3)_3$ in which the dithiolate ligands chelate the three axial edges of the $(\mu\text{-X})_6$ trigonal prism.[49]

4.3.3 Six Multiple-atom Bridges: $(\mu\text{-XRX})_6M_3$ Core

Two- or three-atom bridges on the edges of the M_3 triangle allow closer approach to square-planar metal stereochemistry in structure **(3c)**. Examples are $Pd_3(OAc)_6$[50] with near D_{3h} symmetry and the M atoms inside their O_4 planes, and $Pd_3(OAc)_3(ONCMe_2)_3$[51] with two-atom acetoxime bridges on one side of the Pd_3 triangle and acetate bridges on the other.

4.3.4 Triple Bridges Only: $(\mu_3\text{-X})_2M_3$ Core

Cluster **(3d)** is held together predominantly if not solely by the triply-bridging ligands (S^{2-} or Se^{2-}). Two terminal ligands L usually complete square-planar coordination at each M, generating a structure that can be described as a $(\mu_3\text{-E})_2M_3$ (E = S, Se) trigonal bipyramid inside and coaxial with an L_6 trigonal prism, or as three *cis*-$L_2M_2E_2$ square planes sharing the E—E edge. Reaction of $H_2E(g)$ with Ni^{2+}/EtOH in the presence of excess PEt_3 generates the diamagnetic complexes $(\mu_3\text{-E})_2Ni_3(PEt_3)_6$[52] with pseudo-square-planar coordination of Ni. This stereoisomer of **(3d)**, with no direct M—M bonding, occurs also in $[(\mu_3\text{-S})_2\{Pt(PPh_3)_2\}_2Pd(dppe)]^{2+}$.[53] Partial M—M bonding in the **(3d)** core is present in complexes $(\mu_3\text{-S})_2Ni_3Cp_3$ and $[(\mu_3\text{-S})_2Co_3Cp_3]^z$ (z = 0, +1),[54] while in $[(\mu_3\text{-S})_2Fe_3\{(\mu\text{-S})_2WS_2\}_3]^{4-}$[55] the core of **(3d)** is chelated by three $[WS_4]^{2-}$ 'ligands', creating pseudo-tetrahedral stereochemistry at each Fe atom.

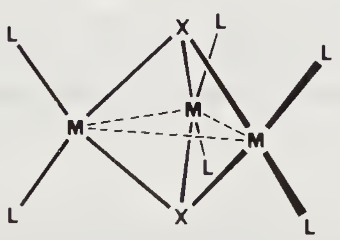

(3d)

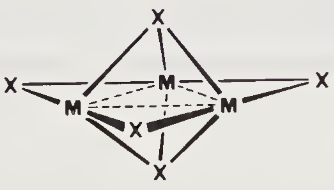

(3h)

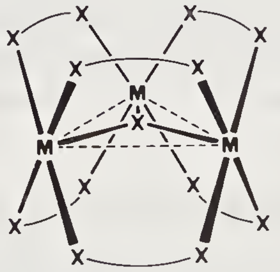

(3i)

4.3.5 The (μ_3-X)(μ-X)$_3$M$_3$ Core

The M_3X_4 core **(3e)** possesses one triply-bridging cap and three double bridges. It is known with variable numbers of terminal ligands, and is frequently encountered in the chemistry of Mo^{IV} and W^{IV}.

4.3.5.1 (μ_3-X)M$_3$(SRS)$_3$: four-coordinate M

The connectivity of **(3f)** occurs in a series of complexes (all formed by direct reaction) in which X is S or Se, M is Fe, Co or Ni, and the chelating dithiolate ligand SRS^{2-} is *o*-xylene-α,α′-dithiolate (S_2-*o*-xyl) or durene-α,α′-dithiolate (S_2-dur). In the paramagnetic but spin-coupled Fe and Co complexes $[SFe_3(S_2\text{-}o\text{-xyl})_3]^{2-}$, $[SeFe_3(S_2\text{-}o\text{-xyl})_3]^{2-}$, $[SFe_3(S_2\text{-dur})_3]^{2-}$ and $[SCo_3(S_2\text{-}o\text{-xyl})_3]^{2-}$ the metal coordination is pseudo-tetrahedral,[56,57] while in $[SNi_3(S_2\text{-}o\text{-xyl})_3]^{2-}$ the chelate ligand is configured to allow pseudo-square-planar coordination at each metal atom.[58]

Analysis of the FeS protein aconitase suggests that an Fe_3S_4 cluster is present.[59] A possible structure is the **(3e)** skeleton, which can be regarded as the Fe_4S_4 cubane **(4w)** with one Fe atom removed.

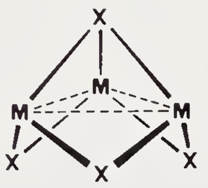

(3e)

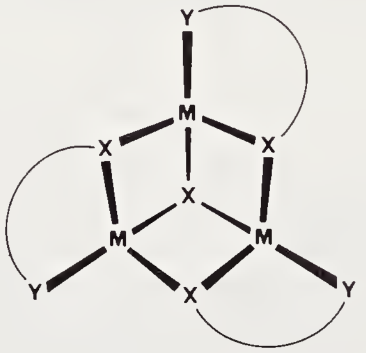

(3f)

(3g)

4.3.5.2 (μ_3-X)(μ-X)$_3$M$_3$Y$_9$: six-coordinate M

Examples of structure **(3g)** with distorted octahedral coordination at each metal are $[M_3O_4F_9]^{5-}$ (M = Mo,[60] W[61]), $[Mo_3S_4(CN)_9]^{5-}$,[62] $[Mo_3O_4(NCS)_8(OH_2)]^{4-}$,[63] $[Mo_3O_4(ox)_3(OH_2)_3]^{2-}$, [64] $[Mo_3O_4\{(O_2CCH_2)_2NMe\}_3]^{2-}$ [65] and $[Mo_3S_4Cp_3]^+$. Mo^{IV} complexes are precipitated directly from acidic aqueous Mo^{IV} solutions which probably contain analogous clusters such as $[Mo_3O_4(OH_2)_9]^{4+}$. [63,65] The M_3 core in these complexes contains six electrons with M—M distances in the range of 2.48–2.81 Å, representing three single M—M bonds.[66] Structure **(3g)** also occurs in $[(\mu_3\text{-OMe})(\mu\text{-OMe})_3Mo_3(CO)_6(NO)_3]^-$ [67] and in $[(\mu_3\text{-O})(\mu\text{-H})_3Rh_3(\eta^5\text{-}C_5Me_5)_3]^+$.[68]

4.3.5.3 Dissymmetric variants

Reaction of $Cp_2Er(Bu^t)(THF)$ in toluene with LiCl yields $[(\mu_3\text{-H})(\mu\text{-H})_2(\mu\text{-Cl})(ErCp_2)_3]^-$,[69] in which there are two terminal Cp ligands completing nine coordination at each Er atom. The central triply-bridging H ligand is only 0.06 Å from the Er_3 plane. In $(\mu\text{-NPh})_3V_3Cl_2(NBu^t)_3(PhNCONHBu^t)$[70] the O atom functions as the apical triply-bridging donor atom, chelated to a terminal position. Each V has highly distorted trigonal-bipyramidal coordination.

4.3.5.4 The (μ_3-S)(μ-S$_2$)$_3$Mo$_3$ core

Here the doubly-bridging positions of **(3e)** are occupied by η^2-S_2 ligands. One terminal η^2-S_2 ligand completes pseudo-tetrahedral coordination at each Mo atom in $[(\mu_3\text{-S})(\mu\text{-S}_2)_3Mo_3(S_2)_3]^{2-}$,[71] while one dithiophosphinate ligand is terminal at each Mo in $[(\mu_3\text{-S})(\mu\text{-S}_2)_3Mo_3(S_2PEt_2)_3]^+$.[72]

4.3.6 The (μ_3-X)$_2$(μ-X)$_3$M$_3$ Core

Core **(3h)**, with two terminal ligands and distorted octahedral coordination at each metal atom, occurs in $(\mu_3\text{-O})(\mu_3\text{-OR})(\mu\text{-OR})_3Mo_3(OR)_6$ ($R = CH_2CMe_3$),[73] formed in the reaction of $MoO(OR)_4$ with $Mo_2(OR)_6$. Again the $\{Mo^{IV}\}_3$ core contains three Mo—Mo single bonds at 2.53 Å.

4.3.7 The $(\mu_3\text{-X})(\mu\text{-XRX})_6\text{M}_3$ Core

Structure **(3i)** usually has D_{3h} symmetry, with O as the central triply-bridging ligand in the M_3 plane, and is the ligand-centred adaptation of **(3c)**. The three-atom bridges are carboxylates, and a terminal ligand L completes octahedral coordination at each metal. These aggregates are known in two oxidation states, $[OM_3(O_2CR)_6L_3]^+$ which contains three M^{III}, and $[OM_3(O_2CR)_6L_3]^0$, formally with M^{III}, M^{III} and M^{II}. Details and references are collected in references 21, 74 and 75. Instances of the first type are $[OCr_3(OAc)_6(OH_2)_3]^+$, $[OFe_3(O_2CCMe_3)_6(MeOH)_3]^+$, $[OFe_3(OAc)_6(OH_2)_3]^+$, $[OFe_3(O_2CCH_2NH_2)_6(OH_2)_3]^+$, $[OFe_3(O_2CCH_2NH_3Me)_6(OH_2)_3]^{7+}$, $[OV_3(OAc)_6(THF)(HOAc)_2]^+$ and $[ORu_3(OAc)_6(py)_3]^+$.[76] Examples of the reduced type are $[OV_3(O_2CCF_3)_6(THF)_3]$, $[OCr_3(O_2CCHF_2)_6(py)_3]$, $[OMn_3(OAc)_6(py)_3]$ and $[ORu_3(OAc)_6(PPh_3)_3]$, which have effectively threefold symmetry and no valence trapping of the M^{II} site, and $[OMn_3(OAc)_6(3Clpy)_3]$[77] in which the Mn^{II} site is clearly distinguished. Magnetic properties and electron transfer and substitution reactions of these complexes have been studied.[21,76,78] The unique cluster $[OW_3(OAc)_6(OH_2)_3]^{2+}$ has the triply-bridging O atom displaced from the W_3 plane.

4.3.8 The $(\mu_3\text{-X})_2(\mu\text{-XRX})_3\text{M}_3$ Core

Structure **(3j)**, with three-atom bridging ligands in the M_3 plane, two triply-bridging ligands, and distorted tetrahedral metal coordination, is found in $[Cl_2Cu_3(dppm)_3]^+$ and $[Br_2Ag_3(dppm)_3]^+$.[79] A related structure is $(\mu_3\text{-Cl})(\mu_3\text{-O}_3SO)(\mu\text{-O}_2CCF_3)_3Co_3$ $(MeOCH_2CH_2OCH_2CH_2OMe)_3$,[80] where a tripodal SO_4 group functions as one triple bridge and the chelating dimethoxyethane ligands complete pseudo-octahedral Co^{II} coordination.

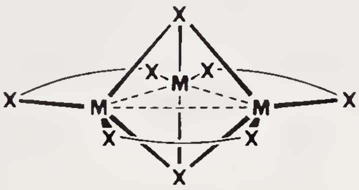

(3j)

(3k)

4.3.9 The $(\mu_3\text{-X})_2(\mu\text{-XRX})_6\text{M}_3$ Core

Compounds with this core invariably possess a terminal ligand at each seven-coordinate (neglecting M—M bonds) metal atom, *i.e.* **(3k)**. Examples[81] are $[O_2M_3(O_2CR)_6(OH_2)_3]^{2+}$ (M = Mo, W; R = Me, Et), all with M^{IV} and three M—M single bonds in the triangle. These compounds are formed in reactions of $M(CO)_6$ with acetic acid/acetic anhydride, and in the reduction of MoO_4^{2-} in acetic anhydride by Zn or $W(CO)_6$.[82] The cluster $[O_2Nb_3(SO_4)_6(OH_2)_3]^{5-}$, produced by electrochemical reduction of Nb^V in H_2SO_4, has the same D_{3h} structure but with only four electrons in M—M bonding orbitals.[83] Recent investigations of $Mo(CO)_6$ plus acetic acid/anhydride reactions have yielded additional compounds with one or two ethylidyne (CMe) ligands in the triply-bridging positions.[84,85] Clusters $[(\mu_3\text{-X})(\mu_3\text{-Y})Mo_3(OAc)_6(OH_2)_3]^z$ with X = O, Y = CMe, $z = +1$ have six M—M bonding electrons, with X = Y = CMe, $z = +1$ have five M—M bonding electrons, and with X = Y = CCH_3, $z = +2$ have four M—M electrons; the Mo—Mo distances increase accordingly.[84]

4.3.10 Non-threefold Clusters

These include $(\mu_3\text{-Cl})(\mu\text{-O})_3(\mu\text{-OAc})W_3Cl_4(PBu_3)_3$,[86] $(\mu_3\text{-S})(\mu\text{-S})_3(\mu\text{-S}_2PEt_2)Mo_3(S_2PEt_2)_3$,[87] $(\mu_3\text{-OEt})_2(\mu\text{-F})Mn_3(CO)_9$ and derivatives,[88] and $(\mu_3\text{-O})(\mu\text{-O})(\mu\text{-OSiMe}_3)Re_3O_3(NBu^t)_4(OSiMe_3)_2$.[89]

4.4 TETRAMETALLIC COMPLEXES

4.4.1 Planar Monocyclic M_4

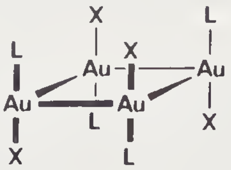

(4a)

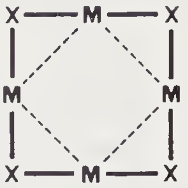

(4b)

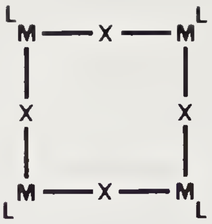

(4c)

4.4.1.1 No bridging ligands

$[ClAu(pip)]_4$, structure (**4a**), is simply an almost square association of parallel and antiparallel ClAu(pip) units (Cl—Au—N, 176°): Au—Au = 3.30 Å, Au ± 0.29 Å from the best plane.[90]

4.4.1.2 Single one-atom bridges

Two variants of the eight-membered ring of alternating metal and ligand atoms are known, one (**4b**) with near linear metal coordination, the other (**4c**) with near linear donor atom coordination. Structure (**4b**) occurs in Cu^I compounds with X = OBu^t, CH_2SiMe_3, NEt_2,[91] and with X the C_5H_4 ring of a substituted ferrocene. The (**4b**) type structure occurs also with M = Ag and X = SR in the compound $Ag_8(SCMeEt_2)_8(PPh_3)_2$, in which a $(\mu\text{-SR})_4Ag_4$ cycle is associated with a similar but di-ligated $(\mu\text{-SR})_4Ag_4(PPh_3)_2$ cycle by weak Ag···S secondary bonding. Both of these cycles [and also di-ligated $(\mu\text{-SBu}^t)_4Cu_4(PPh_3)_2$] are distorted from planarity.[92]

Structure (**4c**), with X = O, is known for ML = $Ti^{IV}\{(O_2CCH_2)_3N\}$,[93] $Ti(C_2O_4)_2$,[94] $ClTi(\eta^5\text{-Cp})$ and $W^{(V,VI)}O(NCS)_3$[95] and for the mixed iodo nitrosyl compound in which ML is IVCp (twice) and (NO)VCp (twice).[96] In all except the second compound the eight-membered rings are puckered, with M—O—M angles in the range 139–179°. Structure (**4c**; X = F) is adopted also by a large number of molecules M_4F_{20} in two structural variants with M—F—M angles of 180° or 132°.

4.4.1.3 Single three-atom bridges

Complexes with connectivity (**4d**) occur with M^I/X—X = Cu/O_2CCF_3, Cu/O_2CPh,[97] Cu/MeNNNMe,[98] Au/S_2CCH_3[99] and Cu/6-methyl-2-oxopyridine.[100] An M_4 square with idealized molecular symmetry D_{2d} does not occur, for reasons of inter-ligand interference on each side of the square, and (**4d**) contains a planar M_4 rhomb, virtually D_2, in all compounds except the last which has a puckered M_4 square. Both geometries cause separation of opposing ligands on the same side of M_4, but still these pairs of ligands are bent away from each other, with the consequence that X—M—X angles range from 162–180°. These angles and the M—M distances reflect only weak direct bonding between the electron excessive metal atoms that adopt this structure type.

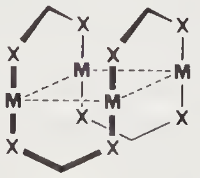

(4d)

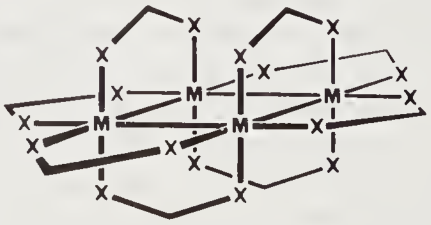

(4e)

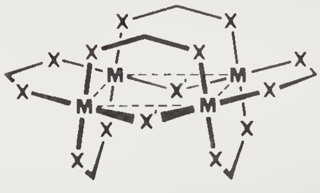

(4f)

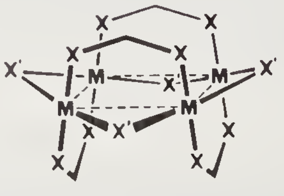

(4g)

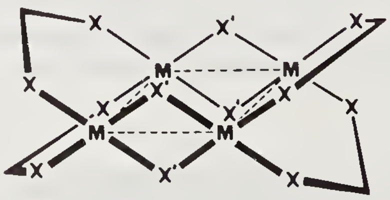

(4h)

4.4.1.4 *Double three-atom bridges*

Structure (**4e**), related to (**4d**) by addition of four equatorial three-atom bridges in the M_4 plane, occurs in two crystalline modifications of the industrial catalyst black platinum(II) acetate, $Pt_4(OAc)_8$,[101] prepared from silver acetate. This near D_{2d} structure is dominated by the Pt_4 quadrilateral, which is square and slightly puckered with short (2.49 Å) Pt—Pt bonds and octahedral Pt coordination.

4.4.1.5 *Mixed three-atom and single-atom bridges*

Structure (**4e**) is modified in three different ways by replacement of three-atom bridges with single-atom bridges in structures (**4f**, **4g** and **4h**). The metal coordination is essentially square-planar in each, with any metal–metal interactions as minor bonding influences. Reduction of Pt^{IV} in nitric acid/acetic acid produces black crystals of $Pt_4(OAc)_6(NO)_2 \cdot 2HOAc$ with structure (**4f**; X′ = NO[102]), in which the atoms of the Pt_4 rectangle (Pt—Pt = 2.94, 3.31 Å) are displaced ±0.14 Å from their best plane. Stable orange *t*-butylperoxopalladium(II) carboxylates are formed by reaction of the peroxide with $Pd(O_2CR)_2$:[103] the structure of $[(Bu^tO_2)Pd(O_2CCCl_3)]_4$ is (**4g**), with the terminal peroxide oxygen atom as X′, molecular symmetry exactly C_2, virtually D_{2d}, and with Pd—Pd = 2.92 Å. This structure can be regarded as an amalgamation of (**4d**) and (**4b**). When carboxylic acids or their mixtures with benzene are the solvents for the reaction of $Pd(O_2CR)_2$ with CO, yellow Pd^I carbonyl carboxylates can be prepared.[104] The structure of the acetate is (**4h**), with the two acetate bridges on each of the longer edges (2.91 Å) of the Pd_4 parallelogram, and two carbonyl bridges on each of the shorter (2.66 Å) edges.

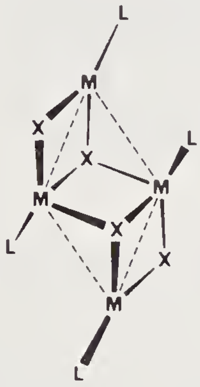

(**4i**)

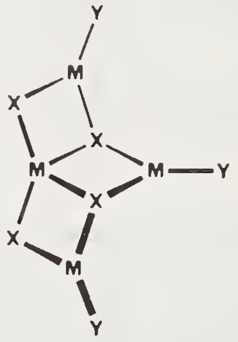

(**4j**)

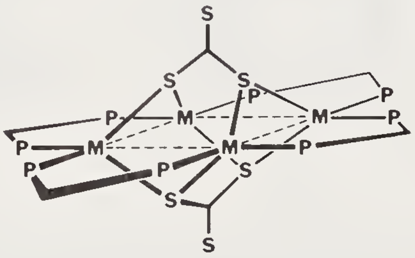

(**4k**)

4.4.1.6 $(\mu_3\text{-}X)_2(\mu\text{-}X)_2M_4L_4$ *'step' structure*

Structure (**4i**), described in terms of the constituent M_2X_2 rhombs which are arranged as a 'step', occurs in the compounds $(Ph_3P)_4Cu_4X_4$ (X = Br, I,[105] SPh[106]) and $(Ph_3P)_4Ag_4I_4$.[107] The latter crystallizes also with the cubane Ag_4I_4 skeleton. The three compounds $Cu_4X_4(dpm)_2$ (X = Cl, Br, I)[108,109] are also in this structural category, with the chelating diphosphine ligand dpm connecting the copper atoms not doubly-bridged by X. Structure (**4i**) is centrosymmetric with a strictly planar central M_2X_2 rhomb, and with variation in the M—M edge lengths of the M_4 parallelogram. $(2\text{-Mepy})_6Cu_4I_4$ possesses the same centrosymmetric type of structure, but with two terminal amine ligands at each non-central M atom.[110]

The $(\mu_3\text{-}X)_2(\mu\text{-}X)_2M_4Y_3$ 'corner step' structure (**4j**) also contains three M_2X_2 rhombs, and is obtained by reaction of MS_4 (M = Mo,[111] W[112]) with CuCl.

4.4.1.7 *Single-atom bridges of four metals*

The centrosymmetric complex $(dppa)_2Ag_4Br_4$ (dppa = bis(diphenylphosphino)methylamine)[113] has two bromine atoms quadruply-bridging an Ag_4 square to form a near octahedron with edges Ag—Ag = 2.96, 3.08 Å, Ag—Br = 2.83, 2.97 Å. Doubly-bridging Br atoms and three-atom bridges on the Ag_4 equator complete very distorted tetrahedral coordination at each Ag atom.

4.4.1.8 Three-atom bridges of four metals

The orange compound $Cu_4(dppm)_4(S_2CS)_2$, prepared by reaction of CS_2, *m*-tolylcopper and dppm in toluene, or by reaction of CuCl, K_2CS_3 and dppm in DMF,[114] has the molecular structure (**4k**) (exactly C_2, virtually D_{2d}) containing two trithiocarbonate ions each of which provides three-atom bridges to all four Cu atoms. At each Cu atom the coordination stereochemistry is tetrahedral, and the 3.31 Å Cu—Cu edges of the Cu_4 square do not contribute to the cage bonding.

4.4.1.9 Two single-atom bridges per M_4 edge

The complex $Ni_4(\mu\text{-}SR)_8$ (SR = 4-mercapto-*N*-methylpiperidine)[115] has two double-thiolate bridges outside each edge of an Ni_4 square to provide approximately square-planar coordination at each Ni atom. Two electronically equivalent instances of the rectangular structure (**4l**) with terminal ligands are $(\mu\text{-}SEt)_8Co_4(CO)_4$[116] (formed by reaction of $CoCl_2{\cdot}6H_2O$, NaOH, EtSH and CO in MeOH) and $(\mu\text{-}PPh_2)_4(\mu\text{-}Cl)_4Ru_4(NO)_4$.[117] The terminal ligands provide the apex of square-pyramidal metal coordination. The significant property of these complexes is the pronounced distortion from D_{4h} symmetry, as an inequivalence of the M—M edges corresponding to two M—M single bonds. The D_{2h} molecular symmetry is exact in the Ru complex and closely approximated in the $S_8Co_4(CO)_4$ core. A related but square structure (virtually D_{4h}) occurs in the electronically different compound $Mo_4Cl_4(OPr^i)_8$, formed from $Mo_2(OPr^i)_6$ and MeCOCl.[118] The Mo—Mo distance of 2.38 Å is consistent with delocalized Mo—Mo bonds of order 1.5, due to the 12 Mo_4 electrons in bonding MOs.

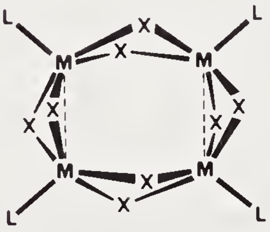

(**4l**)

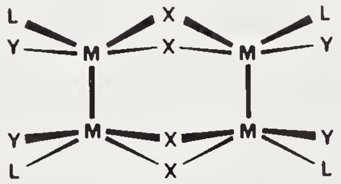

(**4m**)

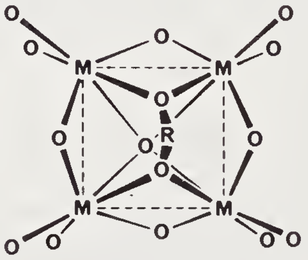

(**4n**)

4.4.1.10 $(\mu\text{-}X)_4M_4Y_4L_4$ with M—M multiple bonds (4m)

The composition and the planar rectangular array of metal atoms in this cluster are the same as those in Section 4.4.1.9, but the cluster bonding is very different. The structure is confirmed crystallographically for $Mo_4Cl_8(PEt_3)_4$[119] (*ca.* C_{2h}) and $W_4Cl_8(PBu^n{}_3)_4$[120] (D_{2d}), and probably exists in a series of related molecules.[120,121] Two edges of the M_4 rectangle are very short, 2.21 Å (Mo) and 2.309 Å (W), consistent with the presence of an M—M triple bond unsupported by bridging ligands. The longer edges, connecting doubly chloride-bridged metal atoms, are 2.901 Å (Mo) and 2.840 Å (W), interpreted as M—M single bonds.

Molybdenum complexes in this class are formed on dissolution of the Mo—Mo quadruply-bonded $Mo_2Cl_4L_2L'_2$ species, which dissociate ligands and undergo [2 + 2] cycloaddition:

$$2Mo_2Cl_4L_2L'_2 \longrightarrow Mo_4Cl_8L_4 + 4L'$$

Variations, using also $Mo_2Cl_8{}^{2-}$, $Mo_2Br_8{}^{2-}$ and $Mo_2(OAc)_4$ as quadruply-bonded precursors, and L substitution reactions,[121] yield related yellow-brown compounds $Mo_4X_8L_4$: X/L = Cl/MeOH; Cl/EtCN; Cl/THF; Cl/PPh_3; Cl/$PBu^n{}_3$; and Br/$PBu^n{}_3$. The tungsten compound is prepared by reductive condensation of $W_2Cl_6(THF)_2(PBu^n{}_3)_2$.[120]

4.4.1.11 $[(\mu_4\text{-}RO_2{}^-)(\mu_4\text{-}OH)(\mu\text{-}O)_4Mo_4O_8]^z$

Structure (**4n**) contains an Mo_4 square, with doubly-bridging oxide ions slightly out of plane and out-of-plane terminal oxide ions. The resulting Mo_4O_{12} cycle is quadruply-bridged on one face by OH^- and on the other by $RO_2{}^-$ where R is H_2C ($z = 3-$)[122] or R'_2As (R′ = Me, Et, Ph; $z = 2-$).[123] Acetal derivatives with R = R′HC can be similarly prepared by reaction of excess aldehyde with $Mo_2O_7{}^{2-}$ in aprotic solvents.[122]

4.4.1.12 $(\mu_3\text{-}X)_2(\mu\text{-}X)_4M_4Y_{10}$, *four fused octahedra*

The centrosymmetric cluster (**4p**) can be regarded as the condensate of two M_3X_{13} structures (**3g**), or as four edge-fused metal coordination octahedra. $Ti_4(OR)_{16}$ (R = Me, Et)[124] and $[W^{VI}{}_4O_{16}]^{8-}$[125] with no excess metal electrons and equivalent ligands are virtually C_{2h} (twofold axis M_a—M_a') with M···M distances 3.2–3.5 Å, while $W^{IV}{}_4(OEt)_{16}$ with eight metal electrons has (in symmetry C_i) M_a—M_b 2.65, M_a—M_b' 2.94, M_a—M_a' 2.76 Å.[126] Black $W_4(OMe)_{16}$ is rigid in solution,[126] while $Ti_4(OEt)_{16}$ dissociates.

Ligand positions are distinguished in three different ways (all C_i) in the complexes $Mo^V{}_4O_8(OPr^i)_4(py)_4$ (OPr = X_c, X_f; py = X_e, X_h),[127] $Mo^V{}_4O_6(OPr)_4Cl_4(HOPr)_2$ (OPr = X_b, X_c; Cl = X_e, X_f; HOPr = X_h)[128] and $Mo^V{}_4O_8(OEt)_2Cl_4(HOEt)_2$ (OEt = X_c; Cl = X_d, X_f; HOEt = X_h),[129] reformulated as in ref.128. All three possess four metal electrons and (in C_i) M_a—M_b = *ca.* 2.6 Å, other M—M = *ca.* 3.4 Å, X_b bridges the shorter of M_a—M_b and M_a—M_b' when they are unequal, and X_d, X_e on M_a (and X_g, X_h on M_b) may be differentiated (C_i) as *cis* and approximately *trans* to the shorter M—M distance, respectively.

For $[Mo_4O_{16}]^z$, $z=0$ (eight metal electrons) and $z=2-$ (10e) occur in the non-stoichiometric non-molecular crystal $Ba_{1.13}Mo_8O_{16}$,[120] but the apportionment of electrons is not unequivocal:[127,130] both have (in C_i) M_a—M_b ≈ M_a—M_a' ≈ 2.56 Å, and M_a—M_b' ≈ 2.85 Å (8e), 2.6 Å (10e). $[Bi_4Br_{16}]^{4-}$ (8e) possesses structure (**4p**).[131]

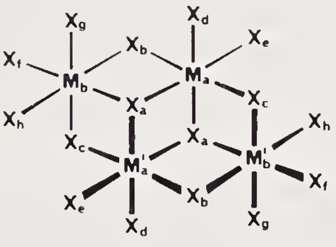

(**4p**)

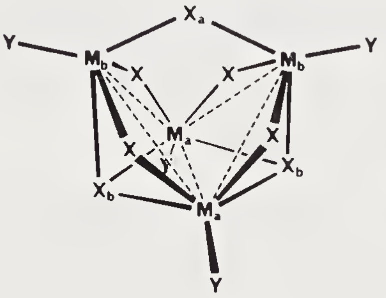

(**4q**)

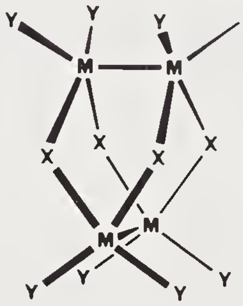

(**4r**)

4.4.2 M_4 'Butterfly', Disphenoid and Trigonal Pyramid

Known M_4 polyhedra intermediate between the planar array and the regular tetrahedron are the C_{2v} 'butterfly' in which one M···M distance is longer than the other five, the D_{2d} disphenoid with M···M distances in sets of four and two, and the trigonal pyramid with M···M distances in sets of three and three.

4.4.2.1 *The* $(\mu_3\text{-}X)_2(\mu\text{-}X)_5M_4X_4$ *'butterfly'*

The $(\mu_3\text{-}X)_2(\mu\text{-}X)_5M_4X_4$ 'butterfly' with linked wings (**4q**) occurs in the clusters $[Mo_4I_{11}]^{2-}$ (prepared by thermolysis of $[Mo(CO)_4I_3]^-$ in the presence of I_2)[132] and in $Rh_4(CO)_4(SO_2)_3\{P(OPh)_3\}_4$[133] where SO_2 functions as the unique bridging ligand X_a with Rh—S bonds only, and as the triply-bridging ligand X_b with Rh—S bonds and an Rh—O bond M_b—X_b. The first cluster has 15 Mo_4 electrons of which six pairs are postulated to be in bonding MOs, while in the second cluster five Rh—Rh bonds are proposed with 18e at each Rh atom. A variation on this butterfly structure occurs in the cluster $(\mu_4\text{-}S)(\mu_3\text{-}S)_2(\mu\text{-}S_2)_4Mo_4(S_2)(NO)_4$.[134] The S^{2-} ion at X_a is bonded equally to all four Mo atoms. The doubly-bridging ligands are unsymmetrically bonded (η^2,η^1) S_2 groups, and there is one terminal NO at each metal and an η^2-S_2 terminal at one metal atom.

4.4.2.2 *The* $(\mu_3\text{-}X)_2(\mu\text{-}X)_4M_4Y_6$ *'butterfly'*

In the $(\mu_3\text{-}X)_2(\mu\text{-}X)_4M_4Y_6$ butterfly structure the wings are released by replacement of the X_a bridge in (**4q**) by an extra terminal ligand on each M_b. This structure is known for $Mo_4Br_4(OPr^i)_8$ with terminal Br ligands, M_a—M_a = 2.48 Å, mean M_a—M_b = 2.51 Å, M_b···M_b = 3.29 Å, and 12 Mo_4 electrons available for Mo—Mo bonding.[118]

4.4.2.3 *The* $(\mu\text{-}X)_4M_4Y_8$ *disphenoid*

The $(\mu\text{-}X)_4M_4Y_8$ disphenoid (**4r**), with two short and four long M—M distances, is known in $(\mu\text{-}F)_4Mo_4(OBu^t)_8$ and $(\mu\text{-}F)_3(\mu\text{-}NMe_2)Mo_4(OBu^t)_8$,[135] and probably ($^1H$ NMR) in

$(\mu\text{-X})_3(\mu\text{-OPr}^i)Mo_4(OPr^i)_8$ (X = Cl, Br).[118] The Mo—Mo triple bonds (length 2.26 Å) in the two fluoro clusters are isolated from each other at Mo···Mo non-bonded distances of 3.75 Å.

4.4.2.4 Structural and chemical relationships

The planar structure of $Mo_4Cl_4(OPr^i)_8$ and the butterfly structures of $[Mo_4I_{11}]^{2-}$ (**4q**) and $Mo_4Br_4(OPr^i)_8$ are core fragments of the cubic $[M_6X_8]^{z+}$ structure (**6m**) for molybdenum, as shown in Figure 1.[118,132] Some intriguing questions arise when it is noted that the compounds $X_4Mo_4(OR)_8$ (X = F, Cl, Br) adopt three different structures,[118,135] and that the compounds $X_3Mo_4(OPr^i)_9$ (X = Cl, Br) are structurally different from both $Cl_4Mo_4(OPr^i)_8$ and $Br_4Mo_4(OPr^i)_8$.[118]

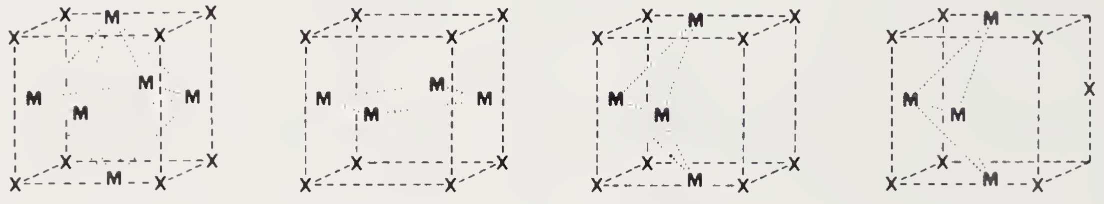

(a) (b) (c) (d)

Figure 1 Structural relationships between the cores of (a) $(\mu_3\text{-X})_8M_6$ core (**6m**), (b) $(\mu\text{-OPr}^i)_8Mo_4Cl_4$, (c) the $Mo_4Br_4(OPr^i)_8$ butterfly structure, and (d) the $[Mo_4I_{11}]^{2-}$ butterfly structure

4.4.2.5 The $(\mu_3\text{-}X)_3M_4L_7$ trigonal pyramid

The $(\mu_3\text{-X})_3M_4L_7$ trigonal pyramid occurs in Roussin's black cluster $[(\mu_3\text{-S})_3Fe_4(NO)_7]^-$. The S ligands bridge the isosceles faces of the Fe_4 trigonal pyramid (Fe_{basal}—Fe_{basal} 3.57 Å, Fe_{apical}—Fe_{basal} 2.70 Å) and all NO ligands are terminal, one at Fe_{apical} and two at each Fe_{basal}.[136]

4.4.3 Tetrahedral M_4

A very large number of clusters and cages contain four metal atoms arrayed as an exact or near tetrahedron. The major sub-category is that of the 'cubane' structure type with a $(\mu_3\text{-X})_4M_4$ core comprised of intersecting concentric M_4 and X_4 tetrahedra. Another sub-group contains the $(\mu\text{-X})_6M_4$ core, with an octahedral array of bridging ligands intersecting the M_4 tetrahedron. The M_4X_4 core contains triply-bridging ligands over M_4 faces and fused M_2X_2 cycles, while the M_4X_6 core contains doubly-bridging ligands over M_4 edges and fused M_3X_3 cycles. Variable numbers of terminal ligands occur in both of these main types, while the M_4X_6 core is known also with a central ligand quadruply bridging the M_4 set.

The following descriptions cover the miscellaneous and M_4X_6 based structures before summarizing the systematic knowledge of cubane structures.

4.4.3.1 Octahedro-*$(\mu\text{-}X)_6$*-tetrahedro-*M_4*

This high symmetry (T_d) cage (**4s**) with trigonal metal coordination occurs in $[Cu_4I_6]^{2-}$,[137] $[Cu_4(SMe)_6]^{2-}$ and $[Cu_4(SPh)_6]^{2-}$,[138] and $[Cu_4(tu)_6]^{4+}$.[139] The Cu atoms are slightly outside the faces of the X_6 octahedron, and the cage is held together by the bridging ligands, not appreciable Cu—Cu bonding. This structure type occurs also with the bidentate ligand $SP(Ph_2)N(Ph_2)PS$.

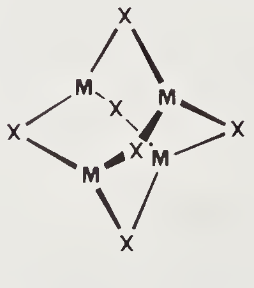

(**4s**)

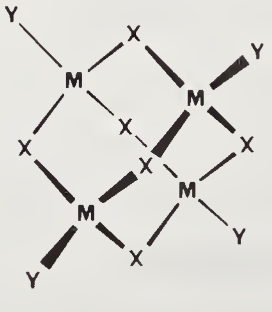

(**4t**)

4.4.3.2 Octahedro-*(μ-X)$_6$*-tetrahedro-*(MY)$_4$*

The high symmetry (T_d) 'adamantanoid' cage structure **(4t)**, with occurrence through all areas of chemistry, is derived from **(4s)** by addition of one terminal ligand to each metal atom which now caps a face of the X_6 octahedron and acquires tetrahedral coordination. The cage is also a molecular fragment of the non-molecular zinc blende (diamond) structure, and it is significant that most instances of the structure occur with closed shell metals and sulfur donor ligands: $[M_4(SPh)_{10}]^{2-}$ (M = Mn, Fe, Co, Zn, Cd),[140–143] $[Fe_4(SEt)_{10}]^{2-}$,[141] $[(\mu\text{-}SPh)_6M_4(SPh)_2Cl_2]^{2-}$ ((M = Co, Zn),[144] $[(\mu\text{-}SPh)_6Fe_4Cl_4]^{2-}$,[145] $[Cu_4(tu)_{10}]^{4+}$, and as the repeat unit in *catena*-(μ-SPh)-$[(\mu\text{-}SPh)_6Zn_4(SPh)(ROH)]$.[146] All except the last two complexes are formed in equilibrium mixtures of metal ions and thiolate ligands.

In these cages the metal atoms are separated by *ca.* 3.9 Å and not directly bonded, although metal atoms in the Fe and Co complexes are antiferromagnetically coupled. Cages $[M_4(SPh)_{10}]^{2-}$ in solution undergo rapid exchange of bridging and terminal thiolate ligands, and exchange of metal atoms.[142]

The complex $[Cu_4(tu)_9]^{4+}$ has one terminal ligand missing in structure **(4t)**.[139]

4.4.3.3 Octahedro-*(μ-X)$_6$*-tetrahedro-*(MY$_3$)$_4$*

Controlled hydrolysis of $[TaF_6]^-$ generates $[O_6Ta_4F_{12}]^{4-}$,[147] which has the adamantanoid $(\mu\text{-}O)_6Ta_4$ core but with three terminal ligands completing regular octahedral coordination at each Ta: Ta—O—Ta angles average 139°. Reaction of 1,4,7-triazacyclononane (triaza) with aqueous $MnCl_2$ and oxygen produces the black complex $[(\mu\text{-}O)_6Mn_4(triaza)_4]^{4+}$, in which octahedral spin-quartet $Mn^{IV}N_3O_3$ centres are separated by 3.2 Å with Mn—O—Mn angles of 129°.[148]

4.4.3.4 Centro-*(μ_4-Z)*-tetrahedro-*M$_4$*-octahedro-*(μ-X)$_6$* (4u)

Here the stereochemistry of metal four-coordination is variable according to the position of the metal atoms along the threefold axes. The one confirmed instance, $OPb_4(OSiPh_3)_6$, obtained from $PbCp_2$ and Ph_3SiOH,[149] has the Pb atoms outside the faces of the O_6 octahedron and outside their own coordination polyhedra, while tetrahedral metal coordination is proposed for $OCo_4(O_2CBu^t)_6$.[150]

4.4.3.5 Centro-*(μ_4-Z)*-octahedro-*(μ-X)$_6$*-tetrahedro-*(ML)$_4$*

Still in symmetry T_d, a terminal ligand is added to each metal in structure **(4u)** to achieve trigonal bipyramidal metal coordination **(4v)**. Crystallographically confirmed instances of this structure are: $OCl_6Cu_4L_4$ [L = $OPPh_3$, py; L_4 = $(nmp)_3(OH_2)$ (nmp = *N*-methyl-2-pyrrolidinone),[151] L_4 = (3-quinuclidinone)$_4$,[152] $[OCu_4Cl_{10}]^{4-}$,[153] and $OBr_6Mg_4(OEt_2)_4$, while a considerable number of other analogous Cu^{II} complexes $OX_6Cu_4L_4$ have been prepared and their intramolecular magnetic exchange investigated.[154,155] A novel cluster $[O(S_2)_6Mo_4(NO)_4]^{2-}$,[156] formed by reaction of MoO_4^{2-}, NH_2OH and H_2S, has a related structure with S_4 symmetry.

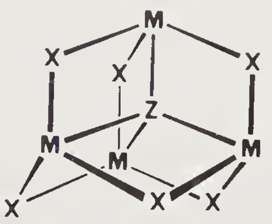

(4u)

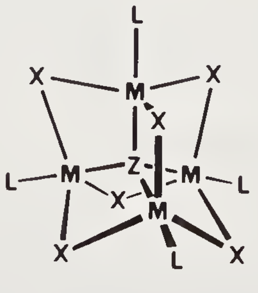

(4v)

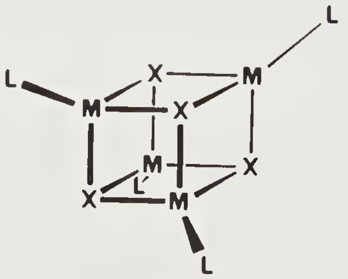

(4w)

4.4.4 $(\mu_3\text{-}X)_4M_4$ Based Cubane Structures

The class of cubane clusters **(4w)** is large and includes complexes of metals distributed throughout the Periodic Table, with diverse bridging ligands X and with 0–4 terminal ligands L. There is substantial variability of shape, symmetry and dimensions of the central core: apart from dissymmetry due to partial substitution of M, X or L, the concentric interpenetrating M_4 and X_4

polyhedra of the core can be regular or distorted tetrahedra, and the two polyhedra can have quite different dimensions. See ref. 157 for a full discussion of cubane cluster symmetry.

Separate studies have elucidated both the steric and electronic influences on the size and symmetry of $X_4M_4L_4$ clusters. When M is a pre- or post-transition metal there is no significant M—M bonding, and the relative sizes of M and X and the volume demands of L determine the cubane dimensions. In contrast, transition metal cubane clusters are known with a range of electron populations in cluster MOs which are M—M bonding, M—M non-bonding or M—M antibonding in character. Consequently there are varying degrees of M—M bonding, localized or delocalized, which can have pronounced influences on the size and symmetry of the cluster. For example, $S_4Fe_4(NO)_4$ has 12e in six M—M bonding MOs, and six Fe—Fe bonds, at 2.63 Å inside the S_4 tetrahedron of edge length 3.50 Å, whereas $S_4Co_4Cp_4$ has an additional 12e occupying antibonding MOs, separating the Co atoms at 3.30 Å outside the S_4 tetrahedron of edge length 2.99 Å.

Cubane clusters in the specialized subset $[S_4Fe_4(SR)_4]^{z-}$ are 10^8 years old in Nature, as the mediators of biological electron transfer, but are only 13 years old (born 1972) in the laboratory. Comprehensive and detailed knowledge of all facets of the chemistry of these complexes is now available, mainly due to Holm and his collaborators. Complete expositions are contained in recent reviews.[12–16]

4.4.4.1 MO bonding theory for cubanoid clusters

Figure 2 is a generalized and qualitative representation of the energies and predominant characters of the cluster MOs: more sophisticated versions are available.[157–160] The 16 MOs for the 16 M—X and M—L σ-bonds are at low energy with the unused X (lone-pair) orbitals, and are always filled with electrons equal in number to those provided by the ligands. Corresponding high-energy σ-antibonding MOs are always empty.

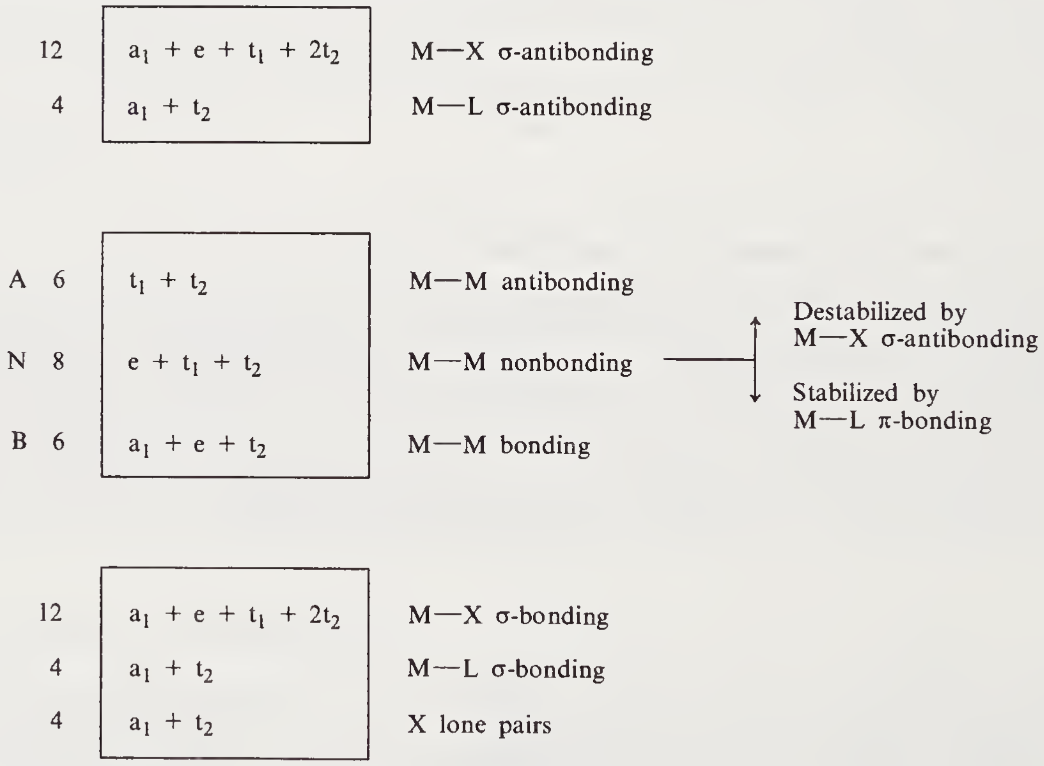

Figure 2 Simplified MO energy pattern for cubanoid $(\mu_3\text{-}X)_4M_4L_4$ clusters, emphasizing the key MOs B, N, A. The numerals give the number of MOs of each type, and the symmetry symbols are for point-group T_d

The key orbitals are those in the central blocks labelled B, N and A. There are six M_4 bonding (B) MOs, six M_4 antibonding (A) MOs, and eight MOs (N) which are essentially non-bonding with respect to M···M interactions, but are susceptible to the electronic structure of X and L. In pre-transition metal clusters, MOs B, N and A are completely empty, while in Cu^I, Ag^I, Zn^{II} and other d^{10} metal cubanes these orbitals (which can accommodate a total of 40e) are completely filled. The MOs N are slightly M—X σ-antibonding (and possibly at higher energy than A in Cu, Ag halide clusters[158]) but M—L π-bonding (and therefore at lower energy than B in complexes such as $S_4Fe_4(NO)_4$[160]). In more highly coordinated clusters $X_4M_4L_{12}$ and $X_4M_4Cp_4$ the eight N MOs are stabilized by the eight additional M—L and M—Cp σ interactions. Nevertheless, in all except two known transition metal cubanes the MOs N are filled with 16 electrons, and the M—M bonding MOs B contain 12 electrons. The variability is in the filling of the M—M antibonding MOs A, and the concomitant decrease in total M—M bond order from 6 to 0.

4.4.4.2 *Cubanes with* d^0, d^{10} *metals*

Al—N cubanes are prepared by reactions (1), (2) and (3):

$$4AlPh_3 + 4H_2NPh \longrightarrow [PhAlNPh]_4 + 8C_6H_6 \qquad (1)$$

$$4AlMe_3 + 4H_2NPr^i \longrightarrow [MeAlNPr^i]_4 + 8CH_4 \qquad (2)$$

$$4LiAlH_4 + 4H_2NPr^i \longrightarrow [HAlNPr^i]_4 + 4LiH + 8H_2 \qquad (3)$$

Tetrameric alkyl beryllium, zinc and cadmium alkoxides are formed by controlled alcoholysis of the metal dialkyls,[161,162] while cubanoid thallium alkoxides are obtained by reaction of the metal with refluxing ethanol, and alcohol metathesis.[163] Reaction (4) affords a tin phosphide cubane in low yield:[164]

$$4PhSnCl_3 + 4PH_3 + 12Et_3N \longrightarrow [PhSnP]_4 + 12Et_3NH^+Cl^- \qquad (4)$$

while the lead(II) species $[Pb_4(OH)_4]^{4+}$ is formed by reaction (5):[165,166]

$$4PbO + 4H^+ \longrightarrow [Pb_4(OH)_4]^{4+} \qquad (5)$$

Reactions of limited proportions of amine and phosphine Lewis bases with non-molecular copper and silver halides generate crystalline cubanes. Crystallographic determinations of molecular structure have been reported for at least 31 complexes with d^0 or d^{10} metal configurations, spanning the following types or homologous series of compounds. Compilations of data occur in references 157, 158 and 167.

(a) $(HAlNPr^i)_4$, $(MeAlNPr^i)_4$,[168] $(PhAlNPh)_4$
(b) $(XCuPEt_3)_4$ (X = Cl, Br, I)
(c) $(XAgPEt_3)_4$ (X = Cl, Br,[169] I)
(d) $(XAgPPh_3)_4$ (X = Cl,[158] Br, I[170])
(e) $(XCuPPh_3)_4$ (X = Cl, Br, I[171])
(f) $(ICuL)_4$ (L = PEt_3, $AsEt_3$, PPh_2Me,[172] PPh_3,[171] $AsPh_3$[173])
(g) $(XCuNEt_3)_4$ (X = Cl, Br[171])
(h) $(ICuL)_4$ (L = py, 2-Mepy,[110] 3-Mepy, *N*-pyridyl or *N,N*-diethylnicotinamide[174])
(i) $(IM\,piperidine)_4$ (M = Cu, Ag[175])
(j) $(IAgEEt_3)_4$ (E = N,[167] P)
(k) $(BrCuPR_3)_4$ (R = Et, Bu^t [176])
(l) $(MOMe)_4$ (M = MeZn, Tl),[163] $(EtZnOBu^t)_4$
(m) $[Pb_4(OH)_4]^{4+}$[166]

The M···M distances are too large for significant direct bonding between M atoms, consistent with the M electron counts. Therefore the geometrical patterns and structural principles that can be extracted from these data are independent of the interference from direct M—M interactions:

(i) The M_4X_4 core is essentially cubic (M···M = X···X) in the light element compounds (a), but in all other groups the X_4 and M_4 tetrahedra are different in size, without breaking the T_d molecular symmetry. Only in the complexes with oxygen as X is the M_4 tetrahedron larger than the X_4 tetrahedron.

(ii) In the X = halide cages the X···X distances are but slightly larger (0–0.3 Å) than the X···X van der Waals' separation, indicating that the X_4 tetrahedron is close to its minimum size in most cages.

(iii) The M_4 tetrahedron shrinks inside the halide X_4 tetrahedron, in order to maintain suitable M—X bond lengths. This effect is illustrated clearly by the mean X—X, M—M and M—X distances in the series (b) and (c):

		X···X	M···M	M—X
$X_4Cu_4(PEt_3)_4$	X = Cl	3.66	3.21	2.44
	Br	3.93	3.18	2.54
	I	4.38	2.93	2.68
$X_4Ag_4(PEt_3)_4$	X = Cl	3.93	3.54	2.65
	Br	4.20	3.48	2.74
	I	4.75	3.21	2.92

The size disparity is greatest in $I_4Cu_4L_4$ cubanes.

(iv) As M_4 shrinks inside X_4 the intramolecular steric interferences by the terminal ligands ($Ph_3E > Et_3E$; E = P, As) become more significant. $I_4Ag_4(PPh_3)_4$[170] and $X_4Cu_4(PPh_3)_4$ (X = Br, I)[171] crystallize with the step structure (**4i**) and the cubane structure.

$Br_4Cu_4(PBu^t_3)_4$, with the bulkiest phosphine, expands Cu_4 and thus $(PR_3)_4$ at the expense of Cu—Br bond strength in the solid state, but it dissociates in solution like its Cl and I homologues.[176]

4.4.4.3 *Complexes with partially filled M—M MOs*

A handsome collection of structural data is now available on complexes intermediate between the d^0 and d^{10} extremes of the previous section, that is with partial population of the M—M MOs. Listed according to the number of M—M bonding plus antibonding electrons (*i.e.* $b + a$ in the configuration $N^{16}B^bA^a$ of Figure 2), and with mean M—M bond lengths (sample size) they are:

10e:	$[S_4Mo_4(\eta^5\text{-}C_5H_4Pr^i)_4]^{2+}$[177]	2.86[6]
11e:	$[S_4Mo_4(\eta^5\text{-}C_5H_4Pr^i)_4]^{+}$[177]	2.89[6]
	$[(PhP)_4Co_4(PPh_3)_4]^{+}$[178]	2.57[6]
12e:	$[S_4Mo_4(\eta^5\text{-}C_5H_4Pr^i)_4]$[177]	2.90[6]
	$[S_4Fe_4(NO)_4]$[160]	2.63[6]
	$[(PhP)_4Co_4(PPh_3)_4]$[178]	2.58[6]
	$[S_2(NCBu^t)_2Fe_4(NO)_4$[179]	2.50[1], 2.56[4], 2.64[1]
	$[O_4Cr_4(\eta^5\text{-}Cp)_4]$[180,181]	2.71[2], 2.83[2], 2.90[2]
13e:	$[S_4Fe_4(NO)_4]^{-}$[160]	2.69[6]
	$[S_2(NCBu^t)_2Fe_4(NO)_4]^{-}$[179]	2.57[5], 2.70[1]
14e:	$[S_4Cr_3Fe(\eta^5\text{-}Cp)_3(O_2CBu)]$	2.76[3], 2.84[3]
16e:	$[(NCBu^t)_4Co_4(NO)_4]$[182]	2.47[2], 2.54[2], 2.71[2]
18e:	$[S_4Fe_4(S_2C_2(CF_3)_2)_4]^{2-}$[183]	2.73[4], 3.22[2]
	$[S_4Fe_4(\eta^5\text{-}Cp)_4]^{2+}$[159]	2.83[4], 3.25[2]
19e:	$[S_4Fe_4(\eta^5\text{-}Cp)_4]^{+}$[159]	2.65[2], 3.19[2], 3.32[2]
20e:	$[S_4Fe_4(\eta^5\text{-}Cp)_4]$[159]	2.65[2], 3.36[4]
	$[P_4Co_4(\eta^5\text{-}Cp)_4]$[184]	2.50[2], 2.63[4]
22e:	$[S_4Fe_4(SPh)_4]^{2-}$[14,15]	2.73[6]
	$[S_4Fe_4(SCH_2Ph)_4]^{2-}$	2.73[4], 2.78[2]
	$[S_4Fe_4(SCH_2CH_2CO_2)_4]^{6-}$	2.74[4], 2.78[2]
	$[S_4Fe_4(SCH_2CH_2OH)_4]^{2-}$	2.73[6]
	$[Se_4Fe_4(SPh)_4]^{2-}$	2.78[6]
	$[S_4Fe_4(OPh)_4]^{2-}$[185]	2.75[6]
	$[S_4Fe_4Cl_4]^{2-}$[186]	2.77[6]
23e:	$[S_4Fe_4(SPh)_4]^{3-}$[187]	2.74[6]
	$[S_4Co_4(\eta^5\text{-}Cp)_4]^{+}$[184]	3.17[4], 3.33[2]
	$[Te_4Fe_4Te_4]^{7-}$[188]	2.85[6]
24e:	$[S_4Co_4(\eta^5\text{-}Cp)_4]$[184]	3.30[6]
	$[(OH)_4Ru_4(\eta^6\text{-}C_6H_6)_4]^{4+}$[189]	3.29[6]
30e:	$[S_3ClCu_3MX(PPh_3)_3]$ (M = Mo, W; X = O, S)[190]	

Analyses of the correlations between geometrical structure, electronic structure, and other physical properties are given in references 157 and 160.

4.4.4.4 *Cubanoid $(\mu_3\text{-}X)_4(ML_3)_4$*

Here three terminal ligands complete octahedral coordination at each metal in the cubane core and the L_{12} array is cuboctahedral. Examples are: $[S_4Mo_4(CN)_{12}]^{8-}$,[191] $[S_4Mo_4(CN)_8(NO)_4]^{8-}$,[192] $[S_4Mo_4(NAr)_4(S_2P(OEt)_2)_4]$,[193] $[S_4Mo_4(edta)_4]^{3-}$,[194] $[S_4Re_4(CN)_{12}]^{4-}$,[195] $[Se_4Re_4(CN)_{12}]^{4-}$,[195] $[Re_4(SMe)_4(CO)_{12}]$,[196] $[O_4Os_4(CO)_{12}]$, $[Cl_4Pt_4R_{12}]$,[197] $[Pt_4(OH)_4Me_{12}]$ and $[S_4Mo_4Br_{12/3}]$.[198]

4.5 PENTAMETALLIC COMPLEXES

Symmetric M_5 arrays in pentametallic aggregates include the trigonal bipyramid, the centred tetrahedron, the square pyramid and the pentagon.

4.5.1 Trigonal Bipyramido-M_5

4.5.1.1 Six ligands bridging edges

Six ligands bridging the M^{ax}—M^{eq} edges of an M_5 trigonal bipyramid constitute a trigonal prism (cluster symmetry D_{3d}) and generate trigonal coordination at M^{ax} and digonal coordination at M^{eq}, *i.e.* **(5a)**. Contrary rotation of the trigonal planes about the threefold axis generates *octahedro*-(μ-X)$_6$-*trigonal bipyramido*-M_5 (symmetry D_3) without change in the metal coordination stereochemistry. The complexes $[M_5(SBu^t)_6]^-$ (M = Cu, Ag)[199] have this connectivity, with the S_6 polyhedron approximately midway between trigonal prism and octahedron and with the digonal atoms displaced slightly (*ca.* 0.2 Å) towards the cage centre. In $Pt_5H_8(PBu^t{}_2Ph)_5$ **(5b)** [prepared from $Pt(C_2H_4)_2(PBu^t{}_2Ph)$ with 300 atm H_2],[200] in addition to the six bridging H ligands, there are terminal phosphine ligands at each Pt atom, and one terminal H ligand at each axial Pt.

4.5.1.2 Six ligands bridging faces

Reaction of Cp_2V with N_2O yields black crystals of weakly paramagnetic $Cp_5V_5O_6$, with structure **(5c)**, terminated by Cp ligands at each metal.[180,181] All V—V edges are equal (2.75 Å), but the V^{ax}—O distances are appreciably shorter than the V^{eq}—O distances.

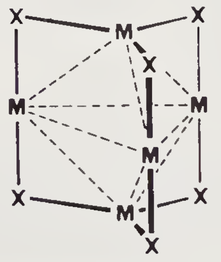

(5a)

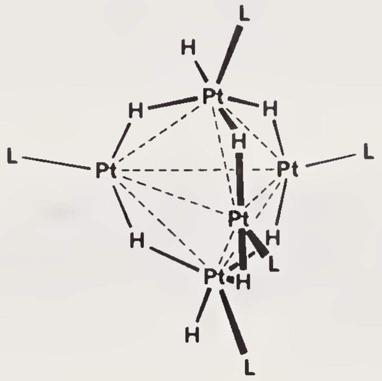

(5b)

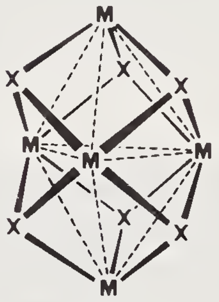

(5c)

4.5.2 *Centro*-M^i-*Tetrahedro*-$(M^o)_4$

The ion $[Cu_5Cl_{16}]^{11-}$ is *centro*-Cu-*tetrahedro*-((μ-Cl)$CuCl_3$)$_4$, in which T_d symmetry is disrupted only by the terminal ligands, and the Cl bridges are linear and asymmetric.[201] Cu_5(benzotriazolate)$_6$($CNBu^t$)$_4$ is a more complex cluster with central (octahedral) Cu^{II} and outer (tetrahedral) Cu^I.[202]

4.5.3 *Square Pyramido*-M_5

The anion $[Mo_5Cl_{13}]^{2-}$, formed in reactions which also generate $[Mo_6Cl_{14}]^{2-}$, has the $(\mu_3\text{-}Cl^i)_8(MoCl^o)_6$ structure **(6m)** of the latter but with one ($MoCl^o$) moiety removed.[203] $[Mo_5Cl_{13}]^{2-}$ is therefore $(\mu_3\text{-}Cl^i)_4(\mu\text{-}Cl^i)_4(MoCl^o)_5$, with double bridges below the basal edges and triple bridges on the triangular faces of the Mo_5 square pyramid.

4.5.4 *Pentagono*-M_5-*Pentagonal Bipyramido*-X_7

A Cu_5 pentagon, subject to some puckering disorder, occurs inside a pentagonal bipyramid of doubly- and quintuply-bridging I^- ligands in the ion $[Cu_5I_7]^{2-}$ **(5d)**.[204]

4.5.5 M Bridging One Edge of an M_4 Tetrahedron

This metal arrangement occurs in the ions $[(\mu\text{-}SPh)_7M_5]^{2-}$ (M = Cu, Ag).[205] The four metals of the tetrahedron are trigonally coordinated, and the fifth metal digonally coordinated, all by doubly-bridging thiolate ligands (structure **5e**).

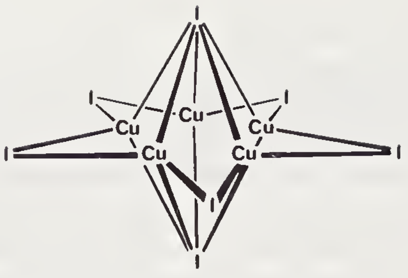

(5d)

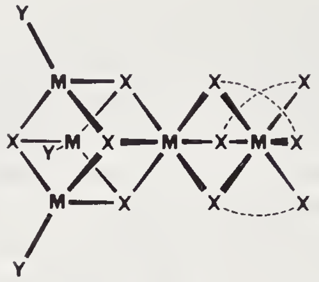

(5f)

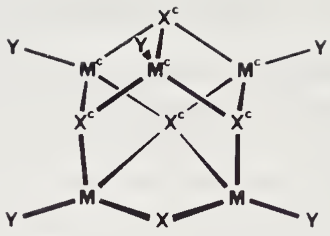

(5g)

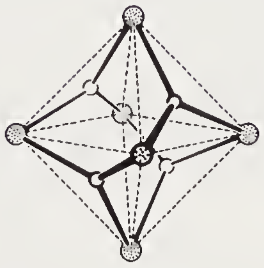

(4o)

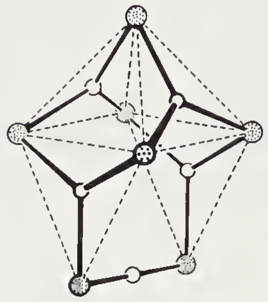

(5e)

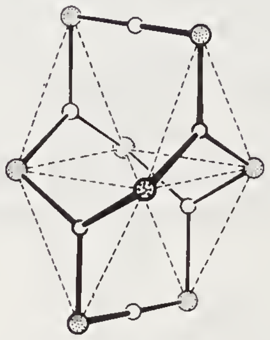

(6e)

4.5.6 M Extended from One Vertex of an M_4 Tetrahedron

$[(EtS)_3S_4Fe_3MoFe(catecholate)_3]^{3-}$ contains[206] the $S_4Fe_4(SR)_4$ type cubane, modified by replacement of one FeSR vertex by Mo, which then acquires six coordination by face sharing with six-coordinate $Fe(catecholate)_3$ **(5f)**.

4.5.7 Low Symmetry Arrays

Structure **(5g)**, with $X = SBu^t$ and $MY = ZnMe$, is adopted by $(MeZnSBu^t)_5$,[207] formed in the reaction $Me_2Zn + HSBu^t$. This cage can be regarded as an expanded cubane **(4w)** where the atoms marked M^c, X^c correspond to seven vertices of the cube, but in place of the last M triconnected to the $(X^c)_3$ tripod there is an M—X—M unit connected to two pairs of X^c.

4.6 HEXAMETALLIC COMPLEXES

In hexametallic clusters the metal atoms can be arranged as the regular polygon (hexagon), the regular polyhedron (octahedron), and the semi-regular trigonal prism. Aggregates are also known with M_6 as a planar edge-bridged square, a puckered hexagon, an edge-linked bitetrahedron, an edge-bridged tetrahedron, a face-capped tetrahedron and less regular arrays. The organization of the following sections progresses from regular hexagonal M_6 to octahedral M_6.

4.6.1 Planar M_6

4.6.1.1 Hexagono-M_6

Rhombohedral silver fulminate contains an almost planar regular hexagon of silver atoms, bridged by carbon atoms (C—Ag—C 163°). A planar hexagon of Cu atoms, bridged by in-plane Br atoms in stellar $(CuBr)_6$ motif, occurs as the equatorial plane of $(triphos)Co(P_3)(CuBr)_6(P_3)$-$Co(triphos)$[208] [triphos = 1,1,1-tris(diphenylphosphinomethyl)ethane, P_3 is *cyclo*-triphosphorus]. Two triangular P_3 ligands sandwich the Cu_6 hexagon such that the Cu_6P_6 atoms lie at the vertices of a cuboctahedron, as shown in **(6a)**. Each Cu is tetrahedrally coordinated.

The M_6 planar hexagon with pairs of doubly-bridging ligands on each edge, creating square-planar metal coordination **(6b)**, occurs in molecules $M_6(\mu\text{-}SR)_{12}$ (M/R = Pd/Pr, Ni/Et,[209] Ni/CH_2CH_2OH[210]). The β-modification of $MoCl_4$ has a disordered crystal structure containing layers of the cyclic molecules Mo_6Cl_{24}, structure **(6c)**, with regular $MoCl_6$ octahedra electronically coupled.[211]

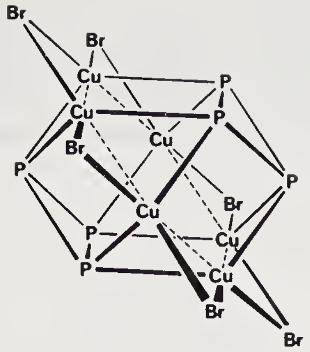

(6a)

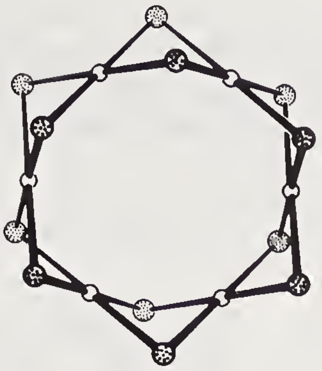

(6b)

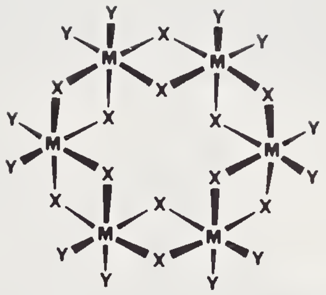

(6c)

4.6.1.2 *Square M_4 with two M edge bridges*

Four homologues $[Fe_6S_9(SR)_2]^{4-}$ (R = Et,[212] Bu^t,[213] SCH_2Ph,[214] Ph[213]) possess structure (**6d**) (virtually C_{2v}) in which the four metal atoms are arranged as a square with two (*trans*) coplanar (within 0.2 Å) equilateral triangles. Sulfide ions cap the M_4 square and the two M_3 triangles, and bridge the six edges of the M_6 polygon, and together with two terminal thiolate ligands provide pseudo-tetrahedral coordination at each metal. These complexes, formed in the diverse reactions [$Fe(SR)_3$ + Na_2S_2,[214] $FeCl_3$ + Li_2S + LiSR + LiOMe,[213] $[Fe(SR)_4]^{2-}$ + S,[212] $[Fe_3S_4(SEt)_4]^{3-}$ heated[212]], undergo reversible one-electron oxidation and terminal ligand substitution.

4.6.1.3 *Concentric M_3 triangles*

Reaction of $Cr(CO)_6$ and $W(CO)_6$ with Bu^tCO_2H leads eventually to $(\mu_3\text{-}OCH_2Bu^t)W_3(\mu_3\text{-}O)_3\text{-}Cr_3(O_2CBu^t)_{12}$.[215] The inner W_3 triangle, with some W—W bonding, is not coplanar with the outer Cr_3 triangle. Concentric and coplanar M_3 triangles occur in $[Ag_6(\text{imidazole})_{12}]^{6+}$ [216] and $[(\mu_3\text{-}S)_2Fe_3\{(\mu\text{-}S)_2WS_2\}_3]^{4-}$.[55]

4.6.2 Puckered Hexagon M_6

A puckered cyclic M_6 structure occurs in four related compounds $M_6(O_2CCH_2R)_{12}$, where R contains an uncharged donor atom X. The compounds are $M_6(O_2CCH_2CH_2PPh_2)_{12}$ (M = Co, Ni),[217] $Cu_6(O_2CCH_2OPh)_{12}$[218] and $Co_6(O_2CCH_2SPr^n)_{12}$,[219] with exact or approximate S_3 molecular symmetry.

4.6.3 Derivatives of *Tetrahedro*-M_6

A pattern among some M_6 aggregates is the presence of a pseudo-tetrahedral array of four, with two appendages.

4.6.3.1 *Edge-bridged tetrahedron*

The idealized structure of the $[Ag_6(SPh)_8]^{2-}$ cage is (**6e**) with the four central Ag atoms trigonally coordinated, and the two outer Ag atoms almost linearly coordinated.[29] The edge-bridged tetrahedron of metal atoms occurs in $[Au_6(Ph_2PCH_2CH_2CH_2PPh_2)_4]^{2+}$ but the loosely connected metal array is distorted due to the absence of Au—Au bonding.[220]

4.6.3.2 *Bicapped tetrahedron*

Basic aqueous solutions of Pb^{II} yield crystals containing the cluster $[OPb_6(OH)_6]^{4+}$ (**6f**)[221] with a centred $(\mu_4\text{-}O)Pb_4$ tetrahedron capped on two faces by $\{(\mu_3\text{-}OH)_3Pb\}$ units. There are three types of Pb coordination, and the Pb—O distances range from 2.2–3.0 Å.[221] X-ray scattering data, vibrational spectra and potentiometric titration data[222] indicate that this cluster also exists in solution.

4.6.3.3 *Edge-linked tetrahedra*

A pair of Au_4 tetrahedra sharing an edge occurs in $[Au_6(PPh_3)_6]^{2+}$.[223] The complicated structure of the aggregate $[Cu_6(S_4)_3(S_5)]^{2-}$ (prepared in methanol from $[Cu_4(SR)_6]^{2-}$ + S_8[224] or $Cu(acac)_2$ + S_x^{2-} [225]) can be simplified as edge-sharing metal tetrahedra with eight edges bridged by the terminal

S atoms of chelating S_4^{2-} ligands, and the other two edges bridged by the end S_2 moieties of the S_5^{2-} ligand. Two approximate Pt_2Ag_2 bisphenoids sharing an Ag—Ag edge occur in $[\{((Ph_3P)_2Pt)_2(\mu_3\text{-}S)_2\}_2Ag_2]^{2+}$,[226] which is held together only by four triply-bridging S^{2-} ligands: any Ag—Ag attraction (at 2.82 Å) is insufficient to bend the linear S—Ag—S coordination.

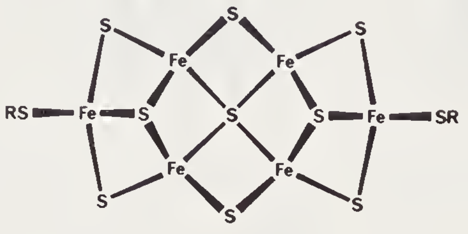

(6d)

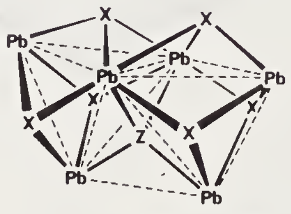

(6f)

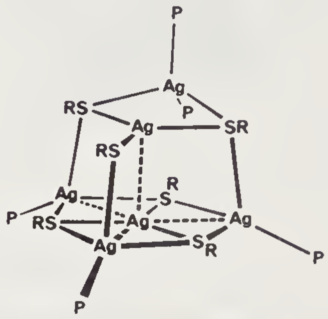

(6g)

4.6.4 Base-centred Trigonal Pyramid

Treatment of $(AgSC_6H_4Cl)$ with PPh_3 yields $Ag_6(SC_6H_4Cl)_6(PPh_3)_5$, which has an odd structure (**6g**) interpreted in terms of an $Ag(\mu_3\text{-}SR)_3(AgPPh_3)_3$ basal unit, an $Ag(SR)_3$ podant unit and an $Ag(PPh_3)_2^+$ appendage. Apart from the latter, the Ag_5 array is a base-centred trigonal pyramid.[227]

4.6.5 *Pentagonal Pyramido*-M_6: $(\mu_6\text{-}S)(\mu_3\text{-}S)_5(\mu\text{-}S)_5(MS)_6$

The ions $[M_6S_{17}]^{4-}$ (M = Nb, Ta) [prepared by $M(OEt)_5 + (Me_3Si)_2S]^{25}$ present the singular structure (**6h**), symmetry C_{5v}. The regular pentagonal pyramid of metal atoms is bridged by one S atom above each of the five triangular faces, and by one S atom below each of the edges of the M_5 pentagon. This creates 10 non-planar M_2S_2 rhombs fused as a crown-shaped M_6S_{10} cage. Each metal has one terminal S ligand. The 17th S is unique, being inside the cage, below the M_5 plane, in a position *trans* to the terminal S on all six metals, and completing pentagonal bipyramidal coordination for the apical M and tetragonal six coordination for the basal M atoms. The $(\mu_3\text{-}S)_5(\mu\text{-}S)_5M_6$ core of this structure is half of the hypothetical I_h stellated icosahedron $M_{12}S_{20}$ (**6i**), in which *icosahedro*-M_{12} is slightly inside *pentagonal dodecahedro*-S_{20}.

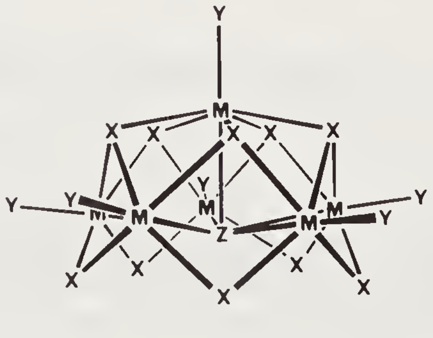

(6h)

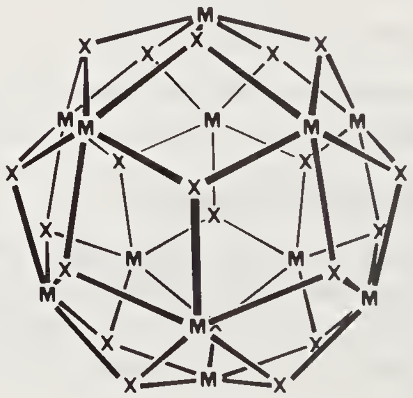

(6i)

4.6.6 M_6X_6 Hexagonal Prism and Derivatives

This type contains two M_3X_3 cycles and six M_2X_2 cycles, and is known in two forms, one in which the M_3X_3 cycles are planar and the M_6X_6 cage is an hexagonal prism, while the other has the M_3X_3 cycles in chair conformation.

4.6.6.1 *The* $(\mu_3\text{-}X)_6M_6$ *hexagonal prism*

The $(\mu_3\text{-}X)_6M_6$ hexagonal prism (**6j**) occurs with symmetry virtually D_{3d}, exactly S_3, in the hexa-(*N*-alkyliminoalanes): $(HAlNPr^i)_6$, $(HAlNPr^n)_6$, $(ClAlNPr^i)_6$ and $(MeAlNPr^i)_6$.[228,229]

4.6.6.2 (μ_3-X)$_6$M$_6$ parallel chairs

The two centrosymmetrically related M_3X_3 chairs are linked by six M—X bonds (axial) while terminal ligands (equatorial) are present on each metal atom (**6k**). The most symmetrical (D_{3d}) occurrence is in $[Fe_6S_6X_6]^{2-}$ [X = Cl,[230] I (prepared from the elements)[231]], while lower-symmetry examples[190] are formed by reaction of tetra- or tri-thiometallates, MS_4^{2-} or MOS_3^{2-} (M = Mo, W), with solutions containing a terminal ligand (phosphine) and copper or silver: $\{(\mu_3\text{-S})_6Mo_2Ag_4\}S_2(PPh_3)_4$, $\{(\mu_3\text{-S})_6W_2Ag_4\}S_2(PPh_3)_4$ and $\{(\mu_3\text{-S})_6W_2Cu_4\}O_2(PPh_3)_4$.

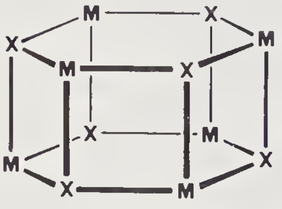

(6j)

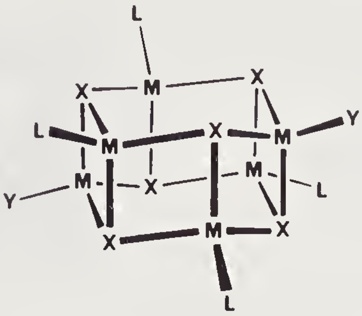

(6k)

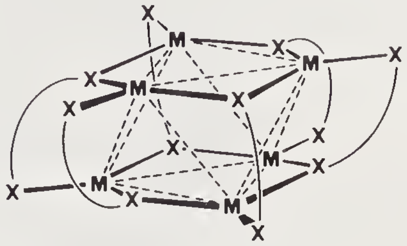

(6n)

4.6.7 Centred *Trigonal Prismo*-M$_6$

4.6.7.1 (μ_6-Z)M$_6$(μ-X)$_9$

One product of the reaction of magnesium with t-butylamine is $(\mu_6\text{-N})Mg_6(\mu\text{-NHBu}^t)_9$,[232] with the amide ligands bridging the nine edges of the regular trigonal prism.

4.6.7.2 (μ_6-Z)(μ_3-X)$_2$(μ-X)$_9$M$_6$X$_6$

Paramagnetic $ClNd_6(OPr^i)_{17}$, prepared by reaction of $NdCl_3$ with $NaOPr^i$ in $C_6H_6/HOPr^i$,[233] has propoxide ligands triply-bridging the two triangular faces, doubly-bridging the nine edges of the Cl-centred Nd_6 trigonal prism, and terminal.

4.6.8 *Octahedro*-M$_6$

Octahedro-$(ML)_6$ with terminal ligands only has been determined crystallographically for $[AuP(C_6H_4Me)_3]_6^{2+}$.[223,234]

4.6.8.1 Edge-bridging ligands: **cuboctahedro**-*(μ-X)$_{12}$*-**octahedro**-*M$_6$ and derivatives*

The M_6X_{12} core (**6l** without terminal ligands) occurs in β-Pd_6Cl_{12}[235] and β-Pt_6Cl_{12}. These unique molecules are soluble in aromatic hydrocarbons, which probably function as electron donors to the metal atoms on the surface of the cluster.[236] The same structure is proposed for the species $[Bi_6(OH)_{12}]^{6+}$ on the basis of X-ray scattering from concentrated solutions, and vibrational spectra.[237] The stoichiometry and the metal coordination stereochemistry are the same as those in the quite different cluster structure (**6b**).

Structure (**6l**), $(\mu\text{-X})_{12}(MY)_6$, has six terminal ligands Y completing the metal coordination. Some of the many complexes[238] of Nb and Ta with this structure are $M_6Cl_{14}\cdot 8H_2O$ [Y_6 = $Cl_2(OH_2)_4$],[239] $[M_6Cl_{18}]^{4-}$ (Y_6 = Cl_6)[240] and $M_6Cl_{14}L_4$ [Y_6 = Cl_2L_4 (L = DMSO, DMF, $OPPh_3$, PR_3[241])]. With Nb and Ta the $[M_6X_{12}]^{2+}$ core is known with all four halides as X,[238] and compounds containing these cores are susceptible to oxidation (electrochemical or by halogen, NO^+[241]) by one or two electrons. Series of compounds with structure (**6l**) maintained in three cluster oxidation states are: $[\{Ta_6X_{12}\}X_n(OH_2)_{6-n}]$ (n = 2, 3, 4),[242] $[\{M_6X_{12}\}X_6]^{z-}$ (z = 2, 3, 4; M = Nb, Ta; X = halide) and $[\{Ta_6Cl_{12}\}Cl_2(PR_3)_4]^{z+}$ (z = 0, 1, 2).[241] Eight M—M bonding MOs are calculated for the $\{M_6X_{12}\}$ core (Nb, Ta),[243] and are fully populated by 16 electrons in $[M_6X_{12}]^{2+}$ (Nb, Ta) and their derivatives, giving an average M—M bond order of 8/12. The EPR hyperfine coupling of $[Nb_6Cl_{12}]^{3+}$ shows that the MO involved is delocalized equally over the six metal atoms. Other cluster cores $\{M_6X_{12}\}^z$ of early transition metals contain 8–21 electrons in these (and higher energy non-bonding) MOs.

Examples of structure (**6l**) with Mo, W and Mo+Ta in the core are $\{W_6Cl_{12}\}Cl_6$ (18 W_6 e^-, $S=1$), $\{Mo_6Cl_{12}\}Cl_{6/2}$, $[\{Mo_6Cl_{12}\}Cl_6]^{3-}$ (21e$^-$, $S=1/2$),[244] $[\{Ta_5MoCl_{12}\}Cl_6]^{z-}$ [$z=3$ (16e$^-$), 2 (15e$^-$)] and $[\{Ta_4Mo_2Cl_{12}\}Cl_6]^{2-}$ (16e$^-$).[245]

A ligand-centred version of this structure occurs in the hexamolybdate ion $[Mo_6O_{19}]^{2-}$ and homologues.

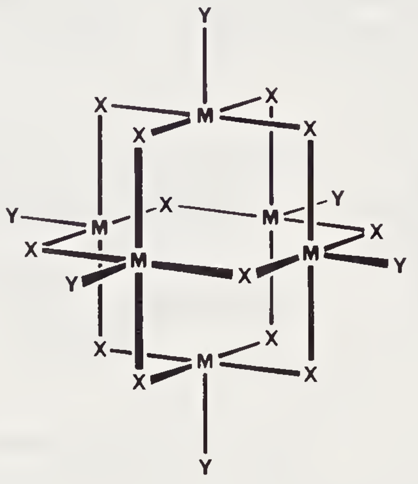

(6l)

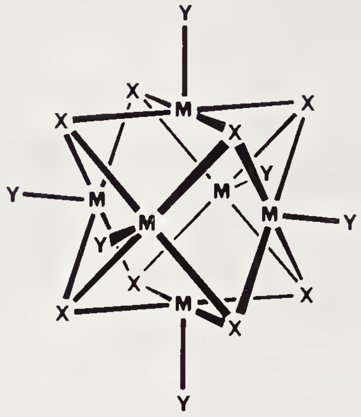

(6m)

4.6.8.2 *Face-bridging ligands:* **hexahedro-**$(\mu_3\text{-}X)_8$**-octahedro-**M_6

Many compounds contain this cluster core (**6m**), in which the eight triply-bridging ligands cap the faces of the M_6 octahedron. In all cases except $(\mu_3\text{-}O)_4(\mu_3\text{-}OMe)_4Sn_6$,[246] each metal is coordinated at the fifth centrifugal position. Only completely molecular complexes terminated by six outer ligands Y, $(\mu_3\text{-}X)_8(MY)_6$, can be described here: in other compounds outer ligands Y function as inter-cluster bridges, allowing one-, two- or three-dimensional non-molecularity, or the inner core ligands X function as inter-cluster bridges, occupying centrifugal positions on adjacent clusters.

Instances of molecular clusters $[(\mu_3\text{-}X)_8(MY)_6]^z$, listed with the number of e$^-$ in the M_6 MOs, are: $[\{Mo_6Cl_8\}Y_6]^{2-}$ (24e) [Y_6 = Cl_6, Br_6, $(OMe)_6$, $Cl_4(PPh_3)_2$, $Cl_4(PEt_3)_2$, $(DMSO)_6$, $(DMF)_6$], $[\{Mo_6Cl_7S\}Cl_6]^{3-}$ (24e),[247] $[\{Mo_6Br_8\}Br_4(OH_2)_2]$ (24e), $[\{Mo_6(OMe)_8\}(OMe)_6]^{2-}$(24e),[248] $[\{Mo_6Cl_8\}(PR_3)_6]^{2+}$ (26e),[249] $[\{Fe_6S_8\}(PEt_3)_6]^{2+}$ (30e),[250] $[\{Co_6S_8\}(PEt_3)_6]^+$ (37e),[251] $[\{Co_6S_8\}(PEt_3)_6]$ (38e),[252] $[\{Co_6S_8\}(CO)_6]$ (38e)[253] and $[\{Ti_6O_8\}(\eta^5\text{-}Cp)_6]$ (2e).[181,254] High (O_h) potential symmetry is virtually achieved (at least for M_6) despite the variation (2–38) in the number of electrons accommodated in the M_6 MOs. Twelve of these MOs are M—M bonding,[181,243,255] and therefore the 24e species have an average M—M bond order of one, consistent with the observed distances. The bond order decreases with increasing occupancy of M—M antibonding MOs.[255]

Replacement of terminal ligands is facile, while the bridging ligands are substituted slowly. In general the $[(\mu_3\text{-}X)_8M_6]$ cluster core is not known to survive redox reactions, but $[Mo_6Cl_8]Cl_6{}^{2-}$ and some homologues can be reduced at potentials separated by 3.1 V, and electrogenerated chemiluminescence from the relatively long-lived excited state of $[Mo_6Cl_8]Cl_6{}^{2-}$ has been observed.[256]

4.6.8.3 *Unsymmetrically bridged* **octahedro-**M_6

(i) $X_6M_6L_6$

Complexes $H_6Cu_6(PR_3)_6$ are prepared from $Cl_4Cu_4(PR_3)_4$ with $LiHBR'_3$, or from $(CuOBu^t)_4$ with PR_3 and H_2,[257,258] and release H_2 upon acidolysis. The hydride ligands were not detected by X-ray diffraction, and according to ^1H NMR are intramolecularly fluxional. The phosphine ligands are terminal from the Cu_6 octahedron, which is trigonally distorted with six Cu—Cu edges 0.11 Å longer than the other six, reflecting but not revealing the hydride bridges.[259]

(ii) $M_6(X\text{—}X)_6$

Four complexes of Cu^I or Ag^I with three-atom bridging ligands possess this structure (**6n**): $M_6(S_2CNPr_2)_6$ (M = Cu,[260] Ag[28]), $Ag_6(SOCNPr_2)_6$[261] and $[Ag_6(S_2CC(CN)_2)_6]^{6-}$.[262] The M_6 octahedron and the whole cage have approximate D_{3d} symmetry, with the six M—M edges of the polar triangular faces (normal to the S_3 axis) longer than the six edges that connect the two polar triangles. Each ligand spans an equatorial M_3 triangle, one donor atom being bonded to one M and the other bridging the long M—M edge. The atoms of the $M_6(\mu\text{-}X)_6$ set are approximately at the vertices of a hexagonal prism. Each metal has distorted trigonal coordination, and is 0.2–0.4 Å inside its X_3 coordination plane.

(iii) $(M^e)_4(R\text{—}L)_4(M^a)_2X_2$

There are two metal types, M^a axial and M^e equatorial, in this S_4 symmetry cluster. Four 2-dimethylaminophenyl ligands (R—L) span four of the $(M^e)_2M^a$ faces by bridging an M^e—M^a edge through C (three-centre–two electron) bonding, and chelating through N to the other M^e. Two X ligands bridge the M^e—M^e edges not spanned by R—L. Metal coordination is digonal M^aC_2, and trigonal M^eCNX. M^e is Cu or Ag; M^a is Cu, Ag or Au; X is Br, I, O_3SCF_3 or C_2Ar.[263,264]

4.7 HEPTAMETALLIC COMPLEXES

4.7.1 Pentagonal Bipyramid

Unique amongst Au clusters is $[Au_7(PPh_3)_7]^+$, which is *pentagonal-bipyramido*-Au_7-*pentagonal-bipyramido*-$(PPh_3)_7$, each Au—P bond being radial to the centre. The bipyramids are compressed, Au^{ax}—Au^{ax} = 2.58, Au^{ax}—Au^{eq} = 2.82, Au^{eq}—Au^{eq} = 2.95 Å.[265]

4.7.2 Centred Hexagon

Structure (**7a**), described variously as a fragment of close-packed O atoms with M atoms in octahedral holes, or six octahedra sharing edges around a central octahedron, or the Anderson–Evans 6-heteropoly structure,[266] is ideally D_{3d} with coplanar metal atoms. Examples are $[TeMo_6O_{24}]^{6-}$,[266] $[Cr(\mu_3\text{-}OH)_6Mo_6O_{24}]^{6-}$ and analogs with other central metals.[266]

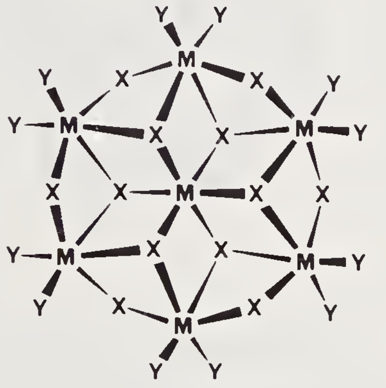

(**7a**)

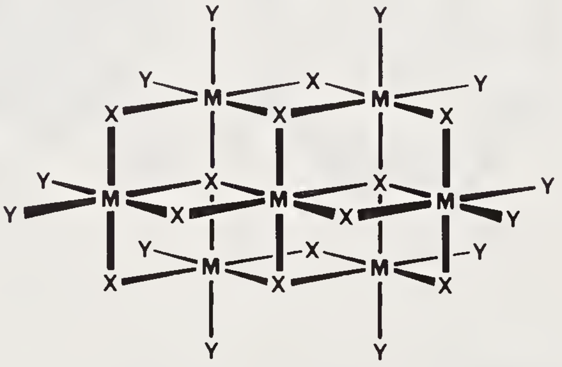

(**7b**)

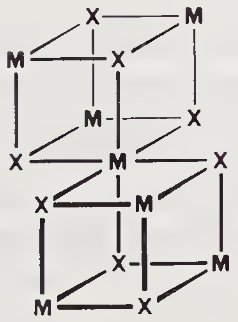

(**7c**)

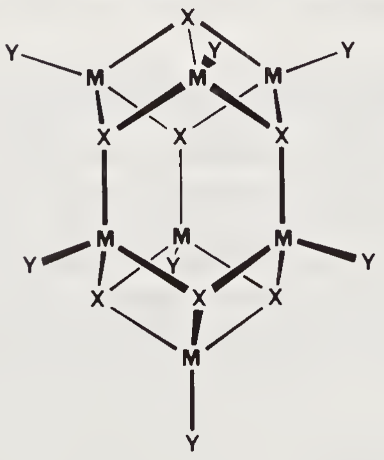

(**7d**)

4.7.3 $M_7(\mu_4\text{-}X)_2(\mu_3\text{-}X)_2(\mu\text{-}X)_8Y_{12}$, Paramolybdate $[Mo_7O_{24}]^{6-}$

Structure (**7b**), adopted by $[Mo_7O_{24}]^{6-}$ and a product, $Ti_7O_6(OEt)_{18}$ or $Ti_7O_5(OEt)_{19}$,[268] of partial hydrolysis of $Ti_4(OEt)_{16}$, contains two quadruply-bridging O ligands, and is related to (**7a**) by a shift of five parallel M—O connections.

4.7.4 Monocapped ZM_6X_{12}

This derivative of the $[OMo_6O_{18}]^{z-}$ structure (Section 4.6.8.1), by addition of an ML_3 cap on a triangular $(\mu\text{-}O)_3$ face of the $(\mu\text{-}O)_{12}$ cuboctahedron, is proposed[269] for $[(CO)_3ReNb_2W_4O_{19}]^{3-}$ (prepared by $[Nb_2W_4O_{19}]^{4-}$ + $[(CO)_3Re(MeCN)_3]^+$ in MeCN), which belongs to a class of mixed mode clusters amalgamating polyoxometallates and metal carbonyls.

4.7.5 Derivatives of Cubanoid $(RMXR')_4$

Structure **(7c)**, two cubanes sharing a metal vertex with $M(\mu_3\text{-}X)_6$ octahedral coordination, is confirmed for $Me_6Zn_7(OMe)_8$ and $Et_6Zn_7(OMe)_8$.[270] Structure **(7d)**, which occurs in $(\mu_3\text{-}NMe)_7\text{-}(AlMe)_7$[271] with virtual C_{3v} symmetry, is envisaged as two $(MeNAlMe)_4$ cubanes, one excised of an AlMe vertex and the other excised of an NMe vertex, and connected on the resulting triangular faces by three Al—N bonds.

4.8 OCTAMETALLIC COMPLEXES

4.8.1 Planar Octagonal M_8

The octagonal toroid $Ni_8(SCH_2CO_2Et)_{16}$[272] **(8a)** has pairs of doubly-bridging thiolate ligands connecting adjacent square-planar metal atoms.

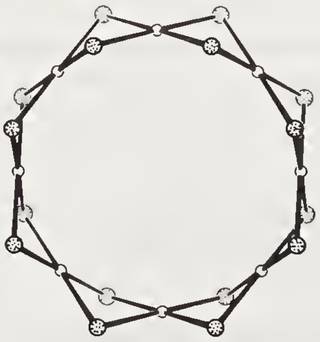

(8a)

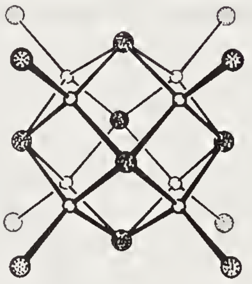

(8b)

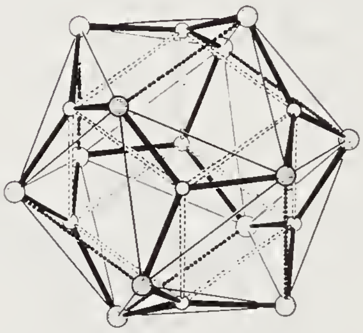

(8c)

4.8.2 *Hexahedro*-M_8

The main variables here are the capacity of the ligand to provide single- or multiple-atom bridging and the presence or absence of a monoatomic ligand at the centre of the cube. A central octuply-bridging ligand probably provides mechanical stability.

4.8.2.1 Octahedro-$(\mu_4\text{-}X)_6$-hexahedro-$(ML)_8$

This cluster **(8b)** has quadruply-bridging ligands over the faces of the cube, and maintains O_h idealized symmetry. Examples are $[(\mu_4\text{-}S)_6(CoSPh)_8]^{4-}$ (prepared by $[Co_4(SPh)_{10}]^{2-}$ + HS^-),[273] $(\mu_4\text{-}PPh)_6Ni_8Cl_4(PPh_3)_4$, $(\mu_4\text{-}PPh)_6Ni_8(CO)_4(PPh_3)_4$[178] and $(\mu_4\text{-}PPh)_6Ni_8(CO)_8$,[274] with 108, 116, 120 and 120 core electrons respectively. The cobalt cluster undergoes one-electron oxidation and reduction, and the Co atoms show evidence of electronic coupling and equivalence. The Co_8S_{14} array is congruent with a fragment of the non-molecular lattice of the mineral cobalt pentlandite, Co_9S_8.

4.8.2.2 $M_8(X—X)_6$

In the idealization of this structure **(8c)**, the 12 donor atoms of the six 1,3-bridging ligands (dotted connections) constitute an icosahedron which encompasses the cube of metal atoms (each with trigonal planar coordination), and the symmetry is T_h, the highest subgroup common to O_h and I_h. Variations in the cube size and the ligand bite size need not destroy this symmetry, but do substantially distort the X_{12} icosahedron and the planarity of the metal coordination. Examples, only with dianionic dithiolate chelating ligands, are $[M_8\{S_2C_2(CN)_2\}_6]^{4-}$ (M = Cu, Ag), $[Cu_8(S_2CC\{C(O)OR\}_2)_6]^{4-}$ and $[Cu_8(S_2C_4O_2)_6]^{4-}$.[275,276]

4.8.2.3 (μ_8-Z)M_8(μ-X)$_{12}$

The one known example of (**8d**), a centred cube of metal atoms intersecting an icosahedron of doubly-bridging ligands, is $[ICd_8(SCH_2CH_2OH)_{12}]^{3+}(I^-)_3$,[277] which is substantially dissymmetric and distorted. Five Cd atoms are terminally coordinated by exogenous I^-, while the other three are each coordinated by either three or one ligand alcohol function. The I—Cd distances are long, 3.17–3.86 Å.

4.8.2.4 (μ_8-Z)M_8(X_2M')$_6$

Structure (**8e**) combines features of (**8c**) and (**8d**), namely a central monatomic ligand, a cube of metal atoms and a pseudo-icosahedron of single-atom bridges X linked in pairs by an octahedral array of connections. The distinctive characteristic here is that the connections are the *cis*-square-planar bis-chelate (X—L) complexes of a set of six outer metal atoms M′. The central halide is necessary for formation of these complexes. In all characterized examples Z is Cl, M is Cu^I or Ag^I, M′ is Cu^{II}, Ni^{II} or Pd^{II}, and X—L is $SCMe_2CH(NH_2)CO_2$, $SCMe_2CH_2NH_2$ or $SCMe_2CO_2$.[278,279]

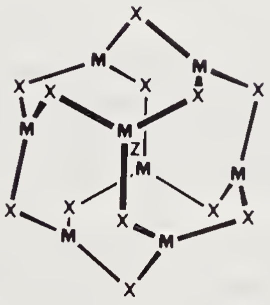

(**8d**)

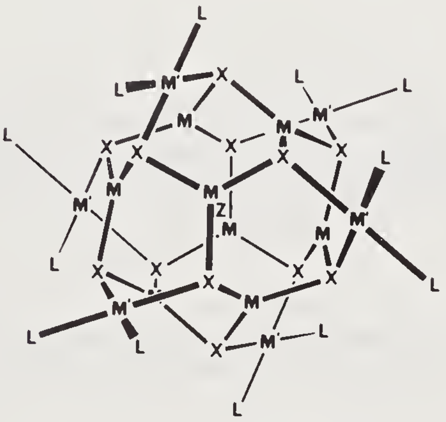

(**8e**)

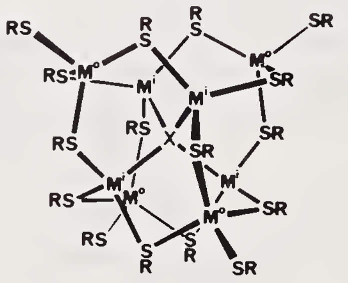

(**8f**)

4.8.3 *Tetracapped Tetrahedro*-M_8

Two very different clusters comprised of inner and outer M_4 tetrahedra are known.

4.8.3.1 *The* $[Pb_4O_4Pb_4]^{8+}$ *cluster*

The $[Pb_4O_4Pb_4]^{8+}$ cluster embedded in Br^- ions occurs in the compounds $TlPb_8O_4Br_9$ and $Pb_9O_4Br_{10}$.[280] It can be regarded as a tetracapped tetrahedron $(Pb_{inner})_4(Pb_{outer})_4$ with O atoms within the caps, or as cubanoid Pb_4O_4 with Pb atoms extended beyond O on the body diagonals.

4.8.3.2 Centro-*Cl*-tetrahedro-*Zn_4*-icosahedro-(μ-*SPh*)$_{12}$-tetrahedro-(*ZnSPh*)$_4$

The cage (**8f**), comprised of concentric Platonic polyhedra with virtual T_d symmetry if the ligand substituents are disregarded, occurs in $[ClZn_8(SPh)_{16}]^-$.[7] The inner and outer tetrahedra of Zn constitute a tetracapped tetrahedron, the edges of which are bridged by the S atoms of 12 thiolates. Regular tetrahedral coordination is completed at each Zn^i by the central Cl, and at Zn^o by the terminal thiolate ligands. Structure (**8f**) bears some relationship to (**8d**), with the difference that the metal atoms lie alternatively inside and outside the S_{12} icosahedron.

4.8.4 Dicubanes: $[(\mu\text{-}X)_3\{M'(\mu_3\text{-}S)_4(MY)_3\}_2]^z$

In (**8g**) two cubanes are linked by three doubly-bridging ligands, with the consequence that one metal atom M′ (Mo or W) in each cubane acquires six coordination. M is Fe, X is SR or OMe, Y is SR, Cl or Br, z = 3−.[281,282]

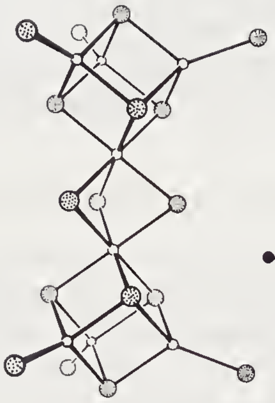

(8g)

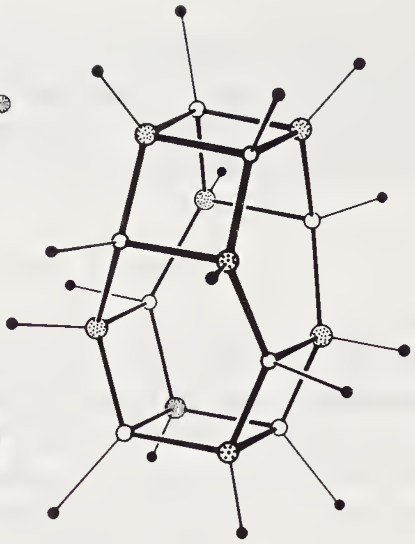

(8h)

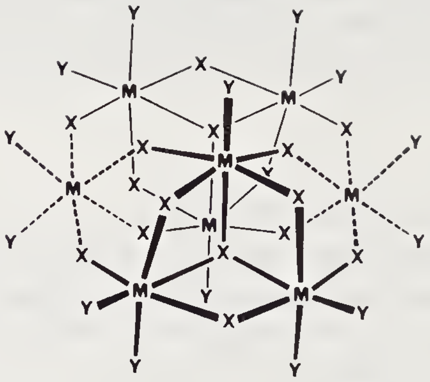

(8i)

4.8.5 $(MX)_8$ Cages

Two different uncharged cage structures are constructed with triply-bridging ligands. Structure (**8h**), $(RMXR')_8$, comprised of six M_2X_2 cycles and four non-planar M_3X_3 cycles, with tetrahedral stereochemistry at both M and triply-bridging X, occurs for $(HAlNPr^i)_8$,[228] $(MeZnSPr^i)_8$[283] and possibly (by NMR) $(MeAlNMe)_8$[284] and $(HAlNEt)_8$.[285] A late intermediate in the multistage elimination of methane from Me_3M and NH_2Me (M = Al or Ga) is $(MeMNMe)_6(Me_2MNHMe)_2$, [284] which contains two M_2X_2 cycles and six M_3X_3 cycles in boat conformation. Similar structures are proposed for $(HAlNEt)_6(H_2AlNHEt)_2$[285] and found for $(GaH)_6(GaH_2)_2(\mu_3\text{-}O)_2(\mu_3\text{-}NCH_2CH_2NMe_2)_4(\mu\text{-}NHCH_2CH_2NMe_2)_2$.[286]

4.8.6 $Nb_8O_{10}(OEt)_{20}$

Crystalline $Nb_8O_{10}(OEt)_{20}$, obtained by hydrolysis of $Nb(OEt)_5$, has structure (**8i**).[287] There are several analyses of this structure: one view has eight slightly distorted NbO_6 octahedra in two sets of three edge-sharing octahedra (see **3g**) linked by two bridging octahedra through vertex sharing. An alternative view sees the M_8 array as a distorted hexagonal bipyramid, with a vacant central cavity.

4.9 M_9 COMPLEXES

Nine-metal arrays in conventional coordination clusters are the confacial bioctahedron and two M_4 cubanes linked through a non-cluster metal atom: among naked metal clusters the M_9 polyhedron is the tricapped trigonal prism or the monocapped square antiprism, and in gold clusters the metal array is the centred cube, the centred crown, or a fragment of the centred icosahedron.

4.9.1 *Confacial Bioctahedro*-M_9: the $(\mu_4\text{-}X)_3(\mu_3\text{-}X)_6M_9$ Core

Two structures with different peripheries are based on a central confacial bioctahedral set of nine metal atoms in three parallel planes of staggered M_3 triangles. Nine bridging ligands, also in these planes, span each edge of the triangles, with the ligands of the central plane bridging also (quadruply) to the metal atoms in the outer planes, and the ligands in the outer planes bridging also (triply) to metal atoms in the central plane. $[S_9Ni_9(PEt_3)_6]^{2+}$,[52] with one additional terminal ligand on each metal atom of the outer layers (**9a**), is virtually D_{3h} and is held together more by the bridging S ligands than by direct Ni—Ni bonding. The end M_3 triangles of (**9a**) are capped by triply-bridging ligands in D_{3h} $\{Mo_9Se_{11}\}$ aggregates found in the solid state compound $In_3Mo_{15}Se_{19}$:[288] inter-cluster Mo—Se contacts complete the radial coordination at the six end Mo atoms.

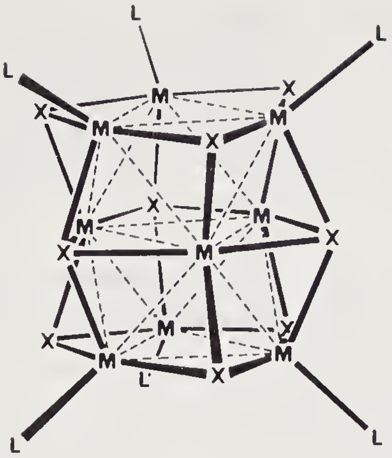

(9a)

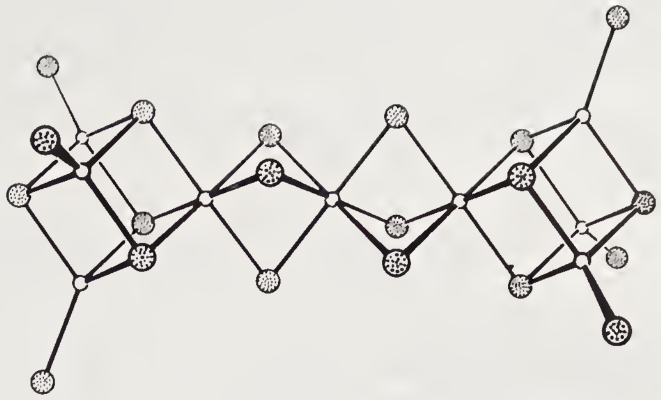

(9b)

4.9.2 Metal-linked Double Cubanes $[M\{(\mu\text{-}X')_3M'(\mu_3\text{-}X)_4(MY)_3\}_2]^{z-}$

Elongated complexes of structure (**9b**) are obtained in reactions very similar to those yielding the directly linked double cubanes (**8g**). All characterized complexes have M = Fe, M′ = Mo or W, X = S, X′ = Y = SR, and an overall charge of 3− or 4−:[289,290] $[M_2Fe_7S_8(SEt)_{12}]^{3-}$, $[W_2Fe_7S_8(SEt)_{12}]^{4-}$, $[M_2Fe_7S_8(SCH_2Ph)_{12}]^{4-}$. The central iron atom has slightly twisted trigonal antiprismatic stereochemistry and undergoes electron transfer at a potential more positive than the cubane electron transfer, between high-spin Fe^{II} ($z = 4-$) and low-spin Fe^{III} ($z = 3-$).

4.9.3 M_9^{z-}

Polymetallic anions, prepared by dissolution of alloys of the alkali and post-transition metals in amine solvents (often with a complexand for the alkali metal cation), have been characterized in crystalline and solution phases. Clusters $TlSn_8^{3-}$, Ge_9^{2-} (with 20 skeletal bonding electrons), Sn_9^{3-} (21 skeletal e) and Bi_9^{5+} (22 skeletal e) possess a tricapped trigonal prismatic structure, symmetry D_{3h}, with variations of dimensional detail which correlate with the electron population.[291,292] This structure is a *closo*-deltahedron, and with 20 ($2n + 2$) skeletal electrons can be construed to be three-dimensionally aromatic.[292] The 22e clusters M_9^{4-} (M = Ge, Sn, Pb) occur as the C_{4v} monocapped square antiprism, a *nido* polyhedron.

4.9.4 Au_9 Clusters

Four different structures are known for gold clusters containing nine metal atoms and eight terminal ligands: in all structures there is one central Au atom, with Au^c—Au^p (c, central; p, peripheral) bonding stronger than Au^p—Au^p bonding (Section 4.12.1). Diagrams (**9c**)–(**9f**) show only the $(Au^p)_8$ connections and the Au^c position. Two distinctly and intriguingly different structures have been determined for $[Au_9(PAr_3)_8]^{3+}$ in crystals: with Ar = Ph and anion PF_6^- the structure is a D_{2d} fragment (**9c**) of the centred icosahedron.[293,294] When Ar = 4-C_6H_4OMe, anion BF_4^-, the cluster is an Au centred octagonal crown (**9d**), virtually D_{4d}.[295] $Au_9(PCy_3)_5(SCN)_3$, with the same skeletal electron count, has the variation (**9e**) on structure (**9c**).[296] Both structures can be regarded as an Au^c centred $(Au^p)_6$ chair plus two Au^p vertices in icosahedral locations on the same (**9e**) or opposite (**9c**) sides of the chair. $[Au_9(PPh_3)_8]^+$, with two more skeletal electrons, has a body centred cubic arrangement of Au atoms (**9f**).[297]

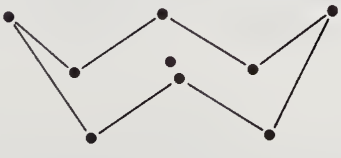

(9d)

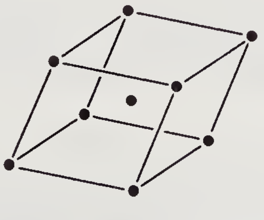

(9f)

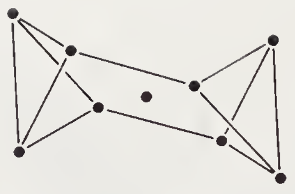

(9c)

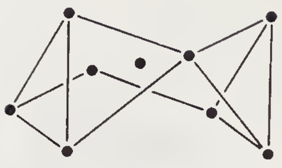

(9e)

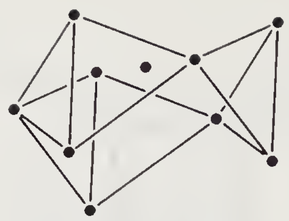

(10c)

4.10 M_{10} COMPLEXES

4.10.1 *Octahedro*-M_6-*tetrahedro*-M_4

The high-symmetry (T_d) framework in which four metal atoms cap four tetrahedrally arrayed faces of an M_6 octahedron is prevalent amongst M_{10} complexes.

4.10.1.1 Octahedro-*Hg_6*-tetrahedro-*$(Rh(PMe_3)_3)_4$*

In the remarkable compound $Hg_6Rh_4(PMe_3)_4$,[298] formed by Na/Hg reduction of $RhCl(PMe_3)_3$, the Hg_6 octahedron with four Rh face caps is maintained only by Hg—Hg and Hg—Rh bonds. The terminal phosphine ligands complete octahedral coordination at each Rh atom. Virtual T_d symmetry extends over the $Hg_6Rh_4P_{12}$ atom set.

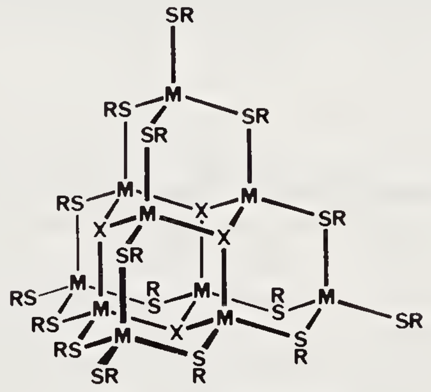

(10a)

(10b)

4.10.1.2 Tetra-adamantanoid supertetrahedron

Structure **(10a)** differs from the previous one by the introduction of 16 bridging ligands, which adhere to the T_d molecular symmetry and dispense with the need for M—M bonds. The structural framework can be described in various ways: (i) as four symmetrically fused adamantanoid **(4t)** cages; (ii) as an $(M^i)_6$ octahedron capped on four faces by triply bridging ligands and on the other four by podant $(\mu\text{-}X)_3M^oY$ groups, *i.e. octahedro*-$(M^i)_6$-*tetrahedro*-$(\mu_3\text{-}X)_4$-*truncated tetrahedro*-$(\mu\text{-}X)_{12}$-*tetrahedro*-$(M^o)_4$-*tetrahedro*-Y_4; (iii) as ten vertex-linked coordination tetrahedra; or (iv) as a symmetrical ten metal fragment of the cubic MX (sphalerite) lattice.

The last aggregate occurs in the four compounds $[(\mu_3\text{-}E)_4M_6(\mu\text{-}SPh)_{12}(MSPh)_4]^{4-}$ (E = S, Se; M = Zn, Cd), prepared by the reaction of $[M_4(SPh)_{10}]^{2-}$ with the chalcogen.[6] Three crystal-structure determinations have confirmed the molecular structure, and defined the small (< 0.2 Å) distortions of the $M_{10}S_{20}$ core, attributable to different arrays of phenyl substituents in two configurational isomers. In solution these complexes retain their integrity, as shown by the ^{113}Cd NMR which displays the two-bond $^{113}Cd-E-^{111}Cd$ isotope coupling between Cd^i atoms, and the two-bond Cd^i-Cd^o coupling.[299] In aprotic solvents at 80 °C the complexes do not degrade to metal chalcogenide. An analogous complex with a large-bite chelate ligand, $[S_4Zn_{10}(S_2\text{-}o\text{-}xyl)_8]^{4-}$, has been mentioned.[58]

The aggregate $[Cd_{10}(SCH_2CH_2OH)_{16}]^{4+}$ has a related structure but with thiolate S atoms in the triply-bridging positions of **(10a)** and not in the four terminal positions.[300] Each Cd^o is six coordinate, being chelated by the SCH_2CH_2OH ligands from the doubly-bridging positions of the core (partly shown in diagram **10b**). Four of the six Cd^i atoms are five coordinate by chelation through the OH functions of the triply-bridging thiolate ligands. Solution and solid phase ^{113}Cd NMR[301] distinguish the different types of Cd atoms. The equilibria for formation of $[Cd_{10}(SCH_2CH_2OH)_{16}]^{4+}$ in aqueous solution and its further reaction with thiolate to produce $Cd_{10}(SR)_{20}$ and $[Cd_{10}(SR)_{24}]^{4}$ have been studied.[302]

Aggregates (**10a**) linked one-dimensionally through vertices occur in the anion $\{(B_{10}S_{18})^{6-}\}_\infty$ of $Ag_3B_5S_9$.[20]

4.10.1.3 *Tetrahedro*-$(\mu_3\text{-}S)_4$-*tetrahedro*-$(\mu_3\text{-}O)_4$-*octahedro*-$(Sn^i)_6$-*truncated tetrahedro*-$(\mu\text{-}S)_{12}$-*tetrahedro*-$(Sn^o)_4$-*tetrahedro*-S_4

Reaction of CsOH, H_2S and SnS_2 in water yields the Cs^+ salt of $[Sn_{10}O_4S_{20}]^{8-}$.[303] In this cluster the $Sn_{10}S_{20}$ atoms are arrayed as in (**10a**), and the four O atoms are contained within the four adamantane cages, but closer to and bonded to the faces of the $(Sn^i)_6$ octahedron. The O atoms are not bonded to Sn^o. The Sn^i atoms have strongly distorted $(\mu_3\text{-}O)_3(\mu_3\text{-}S)_3$ octahedral coordination.

4.10.1.4 *Octahedro*-$(Pd^i)_6$-*disphenoidal*-$(Pd^o)_4$

This reduction in symmetry of the metal array occurs in $Pd_{10}(\mu_3\text{-}CO)_4(\mu\text{-}CO)_8(PBu_3)_6$,[304] where there is also a lower symmetry set of ligand connections. There is still a $(Pd^i)_6$ octahedron, capped by $(\mu_3\text{-}CO)$ on four tetrahedrally arrayed faces, but the Pd^o are located unsymmetrically over the remaining faces, being connected by doubly-bridging carbonyls to the equatorial Pd^i only. The Pd^o thereby constitute a disphenoid rather than a tetrahedron. Phosphine ligands terminate the Pd^o and the two axial Pd^i.

4.10.2 Two Edge-sharing M_6 Octahedra

This structure is best conceived as two $(\mu\text{-}X)_{12}M_6$ structures (**6l**), fused at a common M—M bond with elimination of six X ligands, resulting in $(\mu_3\text{-}X)_4(\mu\text{-}X)_{14}M_{10}$. The one example is in the quasi-molecular compound $Gd_{10}Cl_{18}(C_2)_2$, prepared by electrolysis of fused $GdCl_3$ in a graphite crucible at a Gd anode, or by reaction of Gd_2Cl_3, $GdCl_3$ and C.[305] The C_2 groups occupy the centres of the Gd_6 octahedra.

4.10.3 $[Au_{10}Cl_3(PR_3)_6]^+$

The only ten-atom gold cluster, $[Au_{10}Cl_3(PCy_2Ph)_6]^+$, has structure (**10c**) with approximate D_{3h} symmetry.[306] The structure is an Au-centred trigonal prism of Au atoms (each with one radial Au—P bond), with Au—Cl groups capping the prismatic faces. The Au-centred Au_6 chair of other gold clusters is present.

4.11 M_{11}, M_{12}, M_{13} AND M_{14} COMPLEXES

Complexes $(\mu_8\text{-}Z)M_8(X_2M')_6$ are described in Section 4.8.2.4, and Au_{11} and Au_{13} clusters are listed in Section 4.12.1. No Au_{12} clusters have been reported.

4.11.1 $(AgSR^{sec})_{12}$ Cycles

Ebullioscopic molecular weight measurements for $CHCl_3$ and C_6H_6 solutions indicate that uncharged compounds $(AgSR)_n$ have $n = 12$ when R is secondary. When R is cyclohexyl the crystal structure has been interpreted as containing cyclic $(AgSR)_{12}$ molecules (**12a**), with intra- and inter-molecular secondary Ag···S interactions.[307]

4.11.2 *Hexahedro*-$(\mu_3\text{-}X)_8$-*cuboctahedro*-M_{12}

Reaction of Li_2S with $CuCl_2$ in methanol yields $[Cu_{12}S_8]^{4-}$ (Ph_4P^+) with structure (**12b**).[308] The triangular faces of the cuboctahedron of Cu^+ atoms are capped by triply-bridging S^{2-} such that each Cu is slightly inside an edge of the S_8 cube.

4.11.3 $[(Cu^I)_{10}(Cu^{II})_2(N—S)_{12}(MeCN)_4]^{2+}$

A unique Cu^I–Cu^{II} cage compound containing the monoanionic 1,3-bidentate ligand mmi^- is formed when 1-methyl-2-mercaptoimidazole (mmiH) is mixed with $[Cu(MeCN)_4]^+$ and Cu^{II} acetate

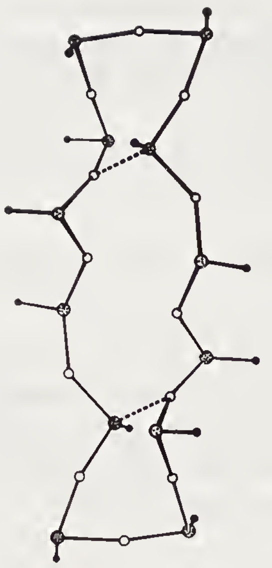

(12a)

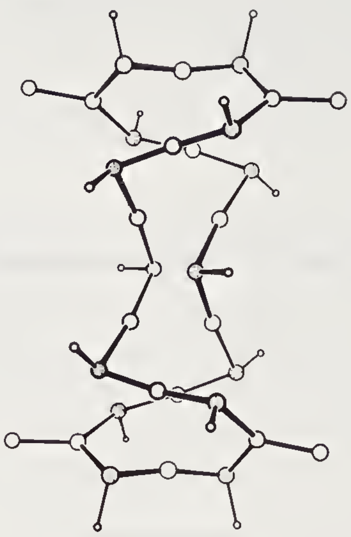

(14a)

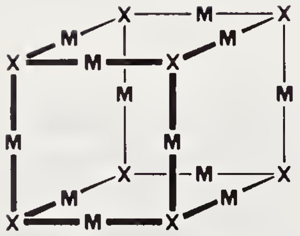

(12b)

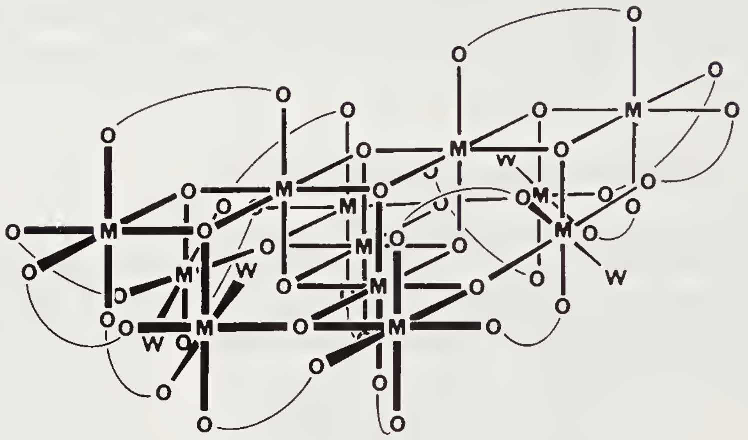

(12c)

in MeCN/MeOH.[309] The cage structure (exactly C_i, virtually C_{2h}) is comprised of a central cycle containing eight Cu^I atoms, bridged (triply and quadruply) by the sulfur atoms of 8 of the 12 ligands and two pairs of externally appended coordination units. In one pair, Cu^I atoms are each digonally coordinated between the N atoms of cycle-bridging ligands. In the other pair are the Cu^{II} atoms, each with distorted square pyramidal coordination and with the acetonitrile coordinated in apical position. None of the ligands is chelating, all connecting between one of the eight inner Cu atoms and one of the four outer Cu atoms. Despite the similarity of composition there is little structural relationship with the *hexahedro*-$(Cu^I)_8$ core of (**8e**).

The Cu^{II} atoms are well separated and are not coupled magnetically, but absorb intensely (3800 $l\ mol^{-1}\ cm^{-1}$ at 635 nm) in the visible region. This charge-transfer absorption is reversibly lost on electrochemical reduction and regained on reoxidation by O_2. These properties, together with $A_{\parallel}$ hyperfine coupling apparent in the ESR spectrum, are closely related to those of the distorted tetrahedral type-1 Cu site of blue Cu proteins,[310] despite the different Cu coordination stereochemistry in the cluster.

4.11.4 $(Co^{II})_{12}(OH)_6(OAc)_6(N—O)_{12}$

An unexpected product of the reaction of cobalt acetate with molten 6-methyl-2-hydroxypyridine (mhpH) is the aggregate $Co_{12}(\mu_3\text{-}OH)_6(OAc)_6(mhp)_{12}$.[311] With exact C_3 and approximate D_3 symmetry this compact and roughly spherical aggregate is described with geographical imagery. The cobalt atoms are: central Co^c, 'polar' (on the threefold axis) Co^a (×2), 'equatorial' Co^e (×3), and 'tropical' Co^t (×6). The $(Co^t)_3$ planes are 1.68 Å from the $(Co^e)_3$ plane, and rotated 20° from a $(Co^t)_6$ trigonal prism. The OH ligands triply-bridge Co^c, Co^e and Co^t, the acetate ligands bridge Co^e and Co^t, half of the mhp ligands bridge (μ-N, μ_3-O), Co^e, Co^t and Co^t, and the other half chelate Co^a with a bridge to Co^t. Each Co atom in this paramagnetic aggregate has distorted octahedral coordination.

4.11.5 $(Mn^{III})_8(Mn^{IV})_4O_{12}(O_2CMe)_{16}(OH_2)_4$

Reaction of Mn^{II} acetate with $KMnO_4$ in acetic acid yields red-black crystals of this complex.[312] The structure (**12c**), with exact S_4 symmetry, is built around a central $(\mu_3\text{-}O)_4(Mn^{IV})_4$ cubane unit. Eight O^{2-} ions which project equatorially from the central cube form triple bridges to the Mn^{III} atoms of the outer annulus. Sixteen acetate ions functioning as three-atom bridges between Mn atoms, together with the four terminal water molecules, complete octahedral coordination at each metal atom.

4.11.6 The $Mo_{12}S_{14}$ Cluster Unit

The compounds $K_2Mo_9S_{11}$ and $Tl_2Mo_9S_{11}$, prepared from the elements, contain (in addition to the Mo_6S_8 cluster unit (**6m**) the $Mo_{12}S_{14}$ cluster unit with four triangular M_3S_3 tiers.[313] Intercluster connections in the crystal provide additional exogenous coordination to the atoms in the end tiers. The $M_{12}S_{14}$ core is in fact the next member of the series M_6X_8 (Section 4.6.8.2), M_9X_{11} (Section 4.9.1) of elongated cores.

4.11.7 $(AgSBu^t)_{14}(PPh_3)_4$

Reaction of $AgSBu^t$ with limited PPh_3 yields $(AgSBu^t)_{14}(PPh_3)_4$, which contains a 28-membered ring of alternating Ag and S atoms, twisted into a compact molecule (**14a**). The phosphine ligands generate trigonal coordination at four Ag atoms in the more twisted regions towards the ends of the molecule.[92]

4.12 METAL–METAL BONDED CLUSTERS OF Rh, Pt, Ag, Au AND Hg

These heavy late- and post-transition metals in low positive oxidation states form clusters held together only by direct M—M bonds, with a relatively small number of terminal ligands. This cluster chemistry is distinctly different from that of all other aggregates (including the naked metal anions), and can be regarded as an expansion of the chemistry of Hg_2^{2+}: it is most developed for gold.

4.12.1 Gold Clusters[17,314]

Three preparative methods have been deployed for gold clusters: (i) reduction of R_3PAuX compounds with $NaBH_4$, B_2H_6 or $Ti(\eta\text{-toluene})_2$; (ii) evaporation of elemental gold into a solution of R_3PAuX and/or PR_3, and (iii) rearrangement (growth and fragmentation) of existing clusters. In method (i) the product depends on the anion present: coordinating anions produce $Au_{11}(PR_3)_7X_3$, while non-coordinating anions A^- produce $[Au_9(PR_3)_8]^{3+}(A)_3$ which is a valuable precursor for type (iii) preparations.

Characterized clusters are: $Au_4(PPh_3)_4(\mu\text{-}I)_2$ (A),[315] $(\mu_3\text{-}I)Au_3(dppm)_3AuI$ (B),[316] $[Au_5(dppm)_3(dppm\text{-}H)]^{2+}$ (C),[317] $[Au_6(PPh_3)_6]^{2+}$ (D),[318] $Au_6(PPh_3)_4\{Co(CO)_4\}2$ (E),[319,320] $[Au_6(dppp)_4]^{2+}$ (F),[321] $[Au_6(Ptol_3)_6]^{2+}$ (G),[322] $[Au_7(PPh_3)_7]^+$ (H),[265] $[Au_8(PPh_3)_7]^{2+}$ (I),[320,323] $[Au_8(PPh_3)_6I]^+$ (J),[265] $[Au_8(PPh_3)_8]^{2+}$ (K),[324] $[Au_9(PAr_3)_8]^{3+}(PF_6^-)$ (L),[293] $[Au_9(PAr_3)_8]^{3+}(BF_4^-)$ (M),[295] $[Au_9(PPh_3)_8]^+$ (N),[297] $[Au_9(PPh_3)_6(CNPr^i)_2]^{3+}$ (O),[325] $Au_9(PCy_3)_5(SCN)_3$ (P),[296] $[Au_{11}(PPhMe_2)_{10}]^{3+}$ (Q),[326] $[Au_{11}(dppp)_5]^{3+}$ (R),[327] $[Au_{11}(PPh_3)_8X_2]^+$ (S),[328] $Au_{11}(PPh_3)_7(SCN)_3$ (T),[329] $Au_{11}(PAr_3)_7I_3$ (U),[329-331] $[Au_{13}(dppm)_6]^{5+}$ (V),[317] $[Au_{13}(PPhMe_2)_{10}Cl_2]^{3+}$ (W),[326] $Au_{55}(PPh_3)_{12}Cl_6$ (X).[332]

To some extent the structures of the Au_n frameworks can be described in terms of deltahedra: (A)-(F) are derivatives of *tetrahedro*-Au_4; (G) contains *octahedro*-Au_6; the only Au_7 cluster (H) is also a *closo*-deltahedron (pentagonal bipyramid, see Section 4.7.1); and the Au_{13} framework of (V) and (W) is a centred icosahedron, the next regular deltahedron. Structures first reported for Au_8, Au_9 and Au_{11} clusters led to the generalization that Au_n clusters are *arachno* fragments of the centred icosahedron, which is regarded as a pair of Au_3 triangles either side of an Au-centred Au_6 chair because the latter central section can be recognized in many clusters. The structures of clusters (H), (I), (K), (L), (P), (T) and (U) can be analyzed in this fashion. However, recent structural results discredit this interpretation: (N) is an Au-centred Au_8 cube (**9f**), and (M) is an Au-centred octagonal Au_8 crown (**9d**), both geometrically unrelated to the icosahedron and to the chemically similar cluster (L). NMR (^{31}P) spectra for clusters in solution[333] do not reveal the inequivalences which occur in the solid state NMR[334] and the crystal structures, and indicate strongly that these clusters are intramolecularly fluxional.[17] EHMO calculations[295] support the conclusion that the potential energy surfaces for interconversion of alternative polyhedral arrays are very soft, particularly for Au_8, Au_9 and Au_{11} clusters.

An alternative porcupine imagery of Au_n clusters involves radial Au^p—L quills attached to a central Au^c atom (p, peripheral; c, central) with angular fluxionality. This view is supported by additional structural features: the radial Au^c—Au^p distances are always appreciably less than the tangential Au^p—Au^p distances, and Au^c—Au^p—L angles are close to 180° except where ligand chelation interferes. Linear P—Au—Au—P moieties are sometimes evident.

The electronic structures of Au_n clusters are unique.[295,335] The major bonding interactions involve the Au 6*s* orbitals, while the 5*d* orbitals have negligible overlap and influence. The participation of the higher energy 6*p* orbitals is enhanced by the coordination of the outer ligands, which improves the radial 6*s*–6*p* hybridization and forms strongly stabilized MOs which are Au^c—Au^p and Au^p—L bonding. The significant feature is the absence of strongly bonding MOs which are tangential to the polyhedral surface: the most stabilized MOs involve the central Au atom and are Au^c—Au^p bonding. These calculations are entirely consistent with the structural features, namely the retention of Au^c when Au^p polyhedron vertices are missing, the shorter Au^c—Au^p distances and the longer Au^p—Au^p distances. Mössbauer data[336] and X-ray photoelectron spectra[337] support this electronic structure model, the latter data giving no indication of broadening of Au 5*d* bands.

4.12.2 The $Au_{13}Ag_{12}$ Alloy Cluster

The metal atom array of the cluster $[Au_{13}Ag_{12}(PPh_3)_{12}Cl_6]^{m+}$ is shown as **(25)**,[338] without ligands and without bonds to the enclosed metal atoms. The idealized structure is a pair of icosahedra, each centred by an Au atom, with a common vertex (the central Au atom) and a common five-fold axis. About this axis the metal atom layers are Ag, Au_5, Au, Ag_5, Au, Ag_5, Au, Au_5, Ag, with successive M_5 pentagons staggered. The 12 phosphine ligands are terminal to the pentagonal-pyramidal Au_5Ag caps at either end of the molecule, while the Cl ligands doubly bridge 6 of the 10 edges of the Ag_{10} pentagonal antiprism around the equator of the cluster. The M—M distances range 2.5–3.3 Å, except for two of the Cl bridged edges of 3.5 Å.

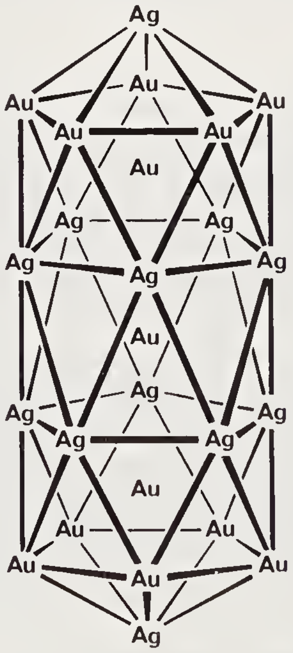

(25)

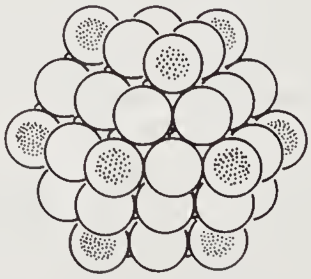

(55)

4.12.3 M_{55} Clusters

The compounds $Au_{55}(PPh_3)_{12}Cl_6$[332] and $Rh_{55}(PBu^t_3)_{12}Cl_{20}$[339] have been prepared by B_2H_6 reduction of conventional monometallic phosphine halide precursors and formulated by composition, molecular weight and Au Mössbauer data. A high-symmetry molecular structure is proposed, with an M_{13} core (centred icosahedron or cuboctahedron) enclosed within an M_{42} shell which is probably cuboctahedral as shown in **(55)**, but may be fluxional through an M_{42} icosahedron. The phosphine ligands are postulated to terminate at the 12 vertices of the outer polyhedron: in the Au cluster the Cl ligands are postulated to radiate from the metal atoms central to the six square faces of the cuboctahedron, while in the Rh cluster it is proposed that the 20 Cl atoms triply-bridge the eight triangular faces and occupy two interstices on each of the square faces.

4.13 SYNTHESIS

4.13.1 Reaction Types

The ligand/metal (L/M) ratios of clusters and cages are intermediate between the low values of non-molecular compounds (**I**) and the high values of monometallic complexes (**III**):

$$\begin{array}{ccccc} \text{Non-molecular compounds} & \longrightarrow & \text{Clusters and cages} & \longleftarrow & \text{Monometallic complexes} \\ \textbf{(I)} & & \textbf{(II)} & & \textbf{(III)} \\ \text{L/M low} & & & & \text{L/M high} \\ \text{(infinite ligand bridging)} & & & & \text{(no ligand bridging)} \end{array}$$

Accordingly, cluster formation reactions can be (a) (**I**) → (**II**) with L/M increase (usually by ligand addition) or (b) (**III**) → (**II**) with L/M decrease (by ligand removal or metal addition). The $Zn^{2+}/^{-}SPh$ and $Cu^{+}/^{-}SPh$ systems exemplify both directions of formation of molecular cages:

$$[(\mu\text{-SPh})\{(\mu\text{-SPh})_6Zn_4(SPh)(ROH)\}]_\infty \rightarrow [Zn_4(SPh)_{10}]^{2-} \leftrightarrow [Zn(SPh)_4]^{2-} \tag{6}$$

$$\{CuSPh\}_\infty \longrightarrow [Cu_5(SPh)_7]^{2-} \longleftrightarrow [Cu_4(SPh)_6]^{2-} \longleftarrow [Cu(SPh)_3]^{2-} \tag{7}$$

The (**I**) → (**II**) conversion involves replacement of some ligand-bridged connections with terminal ligands, resulting in isolation of a molecular fragment of the non-molecular precursor. Many examples are found in the formation of cubanoid clusters (equation 8; M = Cu, Ag; X = Cl, Br, I):

$$[MX]_\infty + 4L \longrightarrow [X_4M_4L_4] \tag{8}$$

Aggregation occurs in the (**III**) → (**II**) conversion because terminal ligands must bridge in order to satisfy metal coordination requirements. Innumerable instances of both types of conversion are known.

A second important factor in cluster formation reactions is the oxidation level, or possible change in oxidation level, of the metals or clusters. Under reducing conditions, direct interactions between metals can contribute to metal bonding, diminishing the requirement for bridging ligands. This type of cluster formation reactivity is seen in gold chemistry, in reactions such as (9),[320] but it occurs also at the other end of the transition series in reactions such as (10).[340]

$$Ph_3PAuNO_3 + BH_4^- \longrightarrow [Au_9(PPh_3)_8]^{3+}(NO_3^-) \tag{9}$$

$$Zr + ZrI_4 \longrightarrow Zr_6I_{12} \tag{10}$$

$\{Mo^{IV}Cl_4\}_6$, which contains a cyclic hexametallic cage without Mo—Mo bonds,[211] when reduced yields $Mo^{II}Cl_2$ containing the Mo—Mo bonded hexametallic cluster $[Mo_6Cl_8]^{4+}$.

More specialized reaction types are hydrocarbon elimination (Section 4.4.4.2) and condensation of species with M—M multiple bonds[121] (Section 4.4.1.10).

4.13.2 Solvent Influences

Bridging ligands are frequently anionic, and a fair proportion of clusters and their precursors are also anionic. The kinetic and thermodynamic characteristics of cluster formation reactions involving such anions are subject to the pronounced influences of solvent on anion activity. Amassed thermodynamic data (expressed as free energies of transfer of anions between solvents)[341] show the magnitude of the effects (for instance the activity of Cl^- in MeCN is almost 10^9 times larger than its activity in H_2O) and allow the generalization that anions are activated approximately in proportion to their charge density, and to the aproticity of the solvent.

These effects are particularly pertinent in type (**I**) → (**II**) reactions, where the high anion activity is required to overcome the lattice energy of the non-molecular precursor (**I**). Thus many non-molecular metal halides, sulfides and thiolates which are insoluble and unreactive in aqueous media will dissolve with anionic ligands in aprotic solvents, and clusters can be isolated from the resulting solutions. Anion activation by use of cation complexands to solubilize salts in hydrocarbon solvents is advantageous, as is the use of complexands in the isolation of polymetallate anions.[342]

4.13.3 Cluster Formation Equilibria in Solution

Designed syntheses of aggregates are aided by knowledge of solution equilibria. Equilibria involving polyoxo- and polyhydroxo-polymetallate complexes in aqueous solution have been studied for many metals by numerous methods.[222,302,343] Most of the classical methods depend on the fitting of models of the equilibria and species compositions to single properties (such as pH) of the mixture, sometimes with equivocal conclusions. Polymolybdates and polytungstates have been studied in great detail.[19] More recently, NMR measurements of metal[65,344,345] and ligand[346] nuclei provide responses from individual species and structural information.

The interconversions of the numerous aggregates in the Fe/S/SR systems have been successfully described from measurements of electronic spectra and ^1H NMR.[141,212] It is evident that some clusters such as $[Fe_4S_4(SR)_4]^{2-}$ have thermodynamic advantage; similarly, in the Cd/S/SPh system, $[S_4Cd_{10}(SPh)_{16}]^{4-}$ predominates, and $M^{2+} + H_2S + PEt_3$ reactions yield stable aggregates $[S_xM_m(PEt_3)_n]^{2+}$ instead of metal sulfides.[52,250]

4.13.4 Metal Complexes as Ligands

Heterometal aggregates can be formed using precursor complexes with exposed donor atoms which ligate another metal site. Thiometallates MS_4^{2-} and OMS_3^{2-} (M = Mo, W), which have been regarded as cluster 'synthons',[190,347,348] react with metal ions in the presence of terminal ligands to form cages **(4w)** and **(6k)** and other aggregates in reactions such as (11).

$$4AgNO_3 + 4PPh_3 + 2WS_4^{2-} \rightarrow (\mu_3\text{-}S)_6(WS)_2(AgPPh_3)_4 \tag{11}$$

Another reactant deployed for preparation of heterometallic aggregates is $(\mu\text{-}S)_2\{(Pt(PPh_3)_2\}_2$,[53,226] which is folded at the S—S bridge such that the S lone-pairs can chelate one metal in $[(\{(Ph_3P)_2Pt\}_2S_2)_2Pd]^{2+}$ or bridge two metals in $[(\{(Ph_3P)_2Pt\}_2S_2)_2Ag_2]^{2+}$.

4.14 REFERENCES

1. A. Simon, *Angew. Chem., Int. Ed. Engl.*, 1981, **20**, 1.
2. E. L. Muetterties, T. N. Rhodin, E. Band, C. F. Brucker and W. R. Pretzer, *Chem. Rev.*, 1979, **79**, 91.
3. E. L. Muetterties, *J. Organomet. Chem.*, 1980, **200**, 177.
4. E. L. Muetterties, *Chem. Eng. News*, 1982, **60** (35), 28.
5. E. L. Muetterties and M. J. Krause, *Angew. Chem., Int. Ed. Engl.*, 1983, **22**, 135.
6. I. G. Dance, A. Choy and M. L. Scudder, *J. Chem. Soc., Chem. Commun*, 1982, 1246; *J. Am. Chem. Soc.*, 1984, **106**, 6285.
7. I. G. Dance, *Aust. J. Chem.*, 1985, **38**, 1391.
8. F. A. Cotton, *Q. Rev., Chem. Soc.*, 1966, **20**, 389.
9. G. A. Clegg, J. E. Fitton, P. M. Harrison and A. Treffry, *Prog. Biophys. Mol. Biol.*, 1980, **36**, 56.
10. 'Transition Metal Clusters', ed. B. F. G. Johnson, Wiley, Chichester, 1980.
11. A. Muller, R. Jostes and F. A. Cotton, *Angew. Chem., Int. Ed. Engl.*, 1980, **19**, 875.
12. R. H. Holm, in 'Biological Aspects of Inorganic Chemistry', ed. A. W. Addison, W. R. Cullen, D. Dolphin and B. R. James, Wiley-Interscience, New York, 1977, chap. 3.
13. R. H. Holm, *Acc. Chem. Res.*, 1977, **10**, 427.
14. R. H. Holm, *Chem. Soc. Rev.*, 1981, **10**, 455.
15. J. M. Berg and R. H. Holm, in 'Iron-Sulfur Proteins', vol. 4, ed. T. G. Spiro, Wiley-Interscience, New York, 1982, chap. 1.
16. B. A. Averill, *Struct. Bonding (Berlin)*, 1983, **53**, 59.
17. J. J. Steggarda, J. J. Bour and J. W. A. van der Velden, *Recl. Trav. Chim. Pays-Bas*, 1982, **101**, 164.
18. T. J. R. Weakley, *Struct. Bonding (Berlin)*, 1974, **18**, 131.
19. K.-H. Tytko and O. Glemser, *Adv. Inorg. Chem. Radiochem.*, 1976, **19**, 239.
20. B. Krebs, *Angew. Chem., Int. Ed. Engl.*, 1983, **22**, 113.
21. J. Catterick and P. Thornton, *Adv. Inorg. Chem. Radiochem.*, 1977, **20**, 291.
22. P. Chini, *J. Organomet. Chem.*, 1980, **200**, 37.
23. B. F. G. Johnson and J. Lewis, *Adv. Inorg. Chem. Radiochem.*, 1981, **24**, 225.
24. G. A. Ozin and S. A. Mitchell, *Angew. Chem., Int. Ed. Engl.*, 1983, **22**, 674.
25. J. Sola, Y. Do, J. M. Berg and R. H. Holm, *J. Am. Chem. Soc.*, 1983, **105**, 7784.
26. A. Camus, N. Marsich, G. Nardin and L. Randaccio, *J. Organomet. Chem.*, 1979, **174**, 121.
27. H. Anacker-Eickhoff, R. Hesse, P. Jennische and A. Wahlberg, *Acta Chem. Scand., Ser. A*, 1982, **36**, 251.
28. R. Hesse and L. Nilson, *Acta Chem. Scand.*, 1969, **23**, 825.
29. I. G. Dance, *Inorg. Chem.*, 1981, **20**, 1487.
30. C. J. De Ranter and M. Rolies, *Cryst. Struct. Commun.*, 1977, **6**, 399.
31. I. G. Dance, L. J. Fitzpatrick and M. L. Scudder, *J. Chem. Soc., Chem. Commun.*, 1983, 546.
32. D. C. Moody and R. R. Ryan, *Inorg. Chem.*, 1977, **16**, 1052.
33. P. L. Bellon, A. Ceriotti, F. Demartin, G. Longoni and B. T. Heaton, *J. Chem. Soc., Dalton Trans.*, 1982, 1671.
34. S. J. Cartwright, K. R. Dixon and A. D. Rattray, *Inorg. Chem.*, 1980, **19**, 1120.
35. K. R. Dixon and A. D. Rattray, *Inorg. Chem.*, 1978, **17**, 1099.

36. D. G. Evans, G. R. Hughes, D. M. P. Mingos, J.-M. Bassett and A. J. Welch, *J. Chem. Soc., Chem. Commun.*, 1980, 1255.
37. N. J. Taylor, P. C. Chieh and A. J. Carty, *J. Chem. Soc., Chem. Commun.*, 1975, 448.
38. S. Pollitz, F. Zettler, D. Forst and H. Hess, *Z. Naturforsch., Teil B*, 1976, **31**, 897.
39. Y. Boulanger, C. M. Goodman, C. P. Forte, S. W. Fesik and I. M. Armitage, *Proc. Natl. Acad. Sci. USA*, 1983, **80**, 1501.
40. H.-J. Jacobsen and B. Krebs, *J. Organomet. Chem.*, 1977, **136**, 333.
41. H. Schumann, *Z. Anorg. Allg. Chem.*, 1967, **354**, 192.
42. D. Ghosh, S. O'Donnell, W. Furey Jr., A. H. Robbins and C. D. Stout, *J. Mol. Biol.*, 1982, **158**, 73.
43. K. S. Hagen and R. H. Holm, *J. Am. Chem. Soc.*, 1982, **104**, 5496.
44. G. Fachinetti, C. Floriani, A. Chiesi-Villa and C. Guastini, *J. Am. Chem. Soc.*, 1979, **101**, 1767.
45. R. K. Brown, J. M. Williams, A. J. Sivak and E. L. Muetteries, *Inorg. Chem.*, 1980, **19**, 370.
46. J. P. Fackler Jr. and W. J. Zegarski, *J. Am. Chem. Soc.*, 1973, **95**, 8566.
47. E. M. McPartlin and N. C. Stephenson, *Acta Crystallogr.*, 1969, **B25**, 1659.
48. F. Stollmaier and U. Thewalt, *J. Organomet. Chem.*, 1981, **222**, 227.
49. W. P. Bosman and H. G. M. van der Linden, *J. Chem. Soc., Chem. Commun.*, 1977, 714.
50. A. C. Skapski and M. L. Smart, *Chem. Commun.*, 1970, 658.
51. A. Mawby and G. E. Pringle, *J. Inorg. Nucl. Chem.*, 1971, **33**, 1989.
52. F. Cecconi, C. A. Ghilardi and S. Midollini, *Inorg. Chem.*, 1983, **22**, 3802.
53. C. E. Briant, T. S. A. Hor, N. D. Howells and D. M. P. Mingos, *J. Chem. Soc., Chem. Commun.*, 1983, 1118.
54. P. D. Frisch and L. F. Dahl, *J. Am. Chem. Soc.*, 1972, **94**, 5082.
55. A. Muller, W. Hellmann, H. Bogge, R. Jostes, M. Romer and U. Schimanski, *Angew. Chem. Suppl.*, 1982, 1757.
56. K. S. Hagen, G. Christou and R. H. Holm, *Inorg. Chem.*, 1983, **22**, 309.
57. G. Henkel, W. Tremel and B. Krebs, *Angew. Chem., Int. Ed. Engl.*, 1983, **22**, 318.
58. W. Tremel, B. Krebs and G. Henkel, *Inorg. Chim. Acta*, 1983, **80**, L31.
59. H. Beinert and A. J. Thomson, *Arch. Biochem. Biophys.*, 1983, **222**, 333.
60. A. Muller, A. Ruck, M. Dartmann and U. Reinsch-Vogell, *Angew. Chem., Int. Ed. Engl.*, 1981, **20**, 483.
61. K. Mennemann and R. Mattes, *Angew. Chem., Int. Ed. Engl.*, 1976, **15**, 118.
62. N. C. Howlader, G. P. Haight, T. W. Hambley, G. A. Lawrance, K. M. Rahmoeller and M. R. Snow, *Aust. J. Chem.*, 1983, **36**, 377.
63. R. K. Murmann and M. E. Shelton, *J. Am. Chem. Soc.*, 1980, **102**, 3984.
64. A. Bino, F. A. Cotton and Z. Dori, *J. Am. Chem. Soc.*, 1978, **100**, 5252.
65. S. F. Gheller, T. W. Hambley, R. T. C. Brownlee, M. J. O'Connor, M. R. Snow and A. G. Wedd, *J. Am. Chem. Soc.*, 1983, **105**, 1527.
66. B. E. Bursten, F. A. Cotton, M. B. Hall and R. C. Najjar, *Inorg. Chem.*, 1982, **21**, 302.
67. S. M. Kirtley, J. P. Chanton, R. A. Love, D. L. Tipton, T. N. Sorrell and R. Bau, *J. Am. Chem. Soc.*, 1980, **102**, 3451.
68. A. Nutton, P. M. Bailey, N. C. Braund, R. J. Goodfellow, R. S. Thompson and P. M. Maitlis, *J. Chem. Soc., Chem. Commun.*, 1980, 631.
69. W. J. Evans, J. H. Meadows, A. L. Wayda, W. E. Hunter and J. L. Atwood, *J. Am. Chem. Soc.*, 1982, **104**, 2015.
70. D. C. Bradley, M. B. Hursthouse, A. N. de M. Jelfs and R. L. Short, *Polyhedron*, 1983, **2**, 849.
71. A. Muller, R. Jostes, W. Jaegermann and R. G. Bhattacharyya, *Inorg. Chim. Acta*, 1980, **41**, 259.
72. H. Keck, W. Kuchen, J. Mathow, B. Meyer, D. Mootz and H. Wunderlich, *Angew. Chem., Int. Ed. Engl.*, 1981, **20**, 975.
73. M. H. Chisholm, K. Folting, J. C. Huffman and C. C. Kirkpatrick, *J. Am. Chem. Soc.*, 1981, **103**, 5967.
74. R. V. Thundathil, E. M. Holt, S. L. Holt and K. J. Watson, *J. Am. Chem. Soc.*, 1977, **99**, 1818.
75. F. A. Cotton, G. E. Lewis and G. N. Mott, *Inorg. Chem.*, 1982, **21**, 3316.
76. J. L. Walsh, J. A. Baumann and T. J. Meyer, *Inorg. Chem.*, 1980, **19**, 2145.
77. A. R. E. Baikie, M. B. Hursthouse, L. New, P. Thornton and R. G. White, *J. Chem. Soc., Chem. Commun.*, 1980, 684.
78. H. Lehmann and G. Wilkinson, *J. Chem. Soc., Dalton Trans.*, 1981, 191.
79. U. Schubert, D. Neugebauer and A. A. M. Aly, *Z. Anorg. Allg. Chem.*, 1980, **464**, 217.
80. J. Estienne and R. Weiss, *J. Chem. Soc., Chem. Commun.*, 1972, 862.
81. M. Ardon, A. Bino, F. A. Cotton, Z. Dori, M. Kaftory and G. Reisner, *Inorg. Chem.*, 1982, **21**, 1912.
82. A. Birnbaum, F. A. Cotton, Z. Dori, D. O. Marler, G. M. Reisner, W. Schwotzer and M. Shaia, *Inorg. Chem.*, 1983, **22**, 2723.
83. A. Bino, *Inorg. Chem.*, 1982, **21**, 1917.
84. A. Bino, F. A. Cotton and Z. Dori, *J. Am. Chem. Soc.*, 1981, **103**, 243.
85. A. Bino, F. A. Cotton, Z. Dori and B. W. S. Kolthammer, *J. Am. Chem. Soc.*, 1981, **103**, 5779.
86. F. A. Cotton, T. R. Felthouse and D. G. Lay, *Inorg. Chem.*, 1981, **20**, 2219.
87. H. Keck, W. Kuchen, J. Mathow and H. Wunderlich, *Angew. Chem., Int. Ed. Engl.*, 1982, **21**, 929.
88. E. W. Abel, I. D. H. Towle, T. S. Cameron and R. E. Cordes, *J. Chem. Soc., Dalton Trans.*, 1979, 1943.
89. W. A. Nugent and R. L. Harlow, *J. Chem. Soc., Chem. Commun.*, 1979, 1105.
90. J. J. Guy, P. G. Jones, M. J. Mays and G. M. Sheldrick, *J. Chem. Soc., Dalton Trans.*, 1977, 8.
91. H. Hope and P. P. Power, *Inorg. Chem.*, 1984, **23**, 936.
92. I. G. Dance, L. J. Fitzpatrick, M. L. Scudder and D. Craig, *J. Chem. Soc., Chem. Commun.*, 1984, 17.
93. K. Wieghardt, U. Quilitzsch, J. Weiss and B. Nuber, *Inorg. Chem.*, 1980, **19**, 2514.
94. G. M. H. van de Velde, S. Harkema and P. J. Gellings, *Inorg. Nucl. Chem. Lett.*, 1973, **9**, 1169.
95. J. P. Launay, Y. Jeannin and A. Nel, *Inorg. Chem.*, 1983, **22**, 277.
96. F. Bottomley, J. Darkwa and P. S. White, *J. Chem. Soc., Chem. Commun.*, 1982, 1039.
97. M. G. B. Drew, D. A. Edwards and R. Richards, *J. Chem. Soc., Dalton Trans.*, 1977, 299.
98. J. E. O'Connor, G. A. Janusonis and E. R. Corey, *Chem. Commun.*, 1968, 445.
99. O. Piovesana and P. F. Zanazzi, *Angew. Chem., Int. Ed. Engl.*, 1980, **19**, 561.
100. M. Berry, W. Clegg, C. D. Garner and I. H. Hiller, *Inorg. Chem.*, 1982, **21**, 1342.
101. M. A. Carrondo and A. C. Skapski, *Acta Crystallogr.*, 1978, **B34**, 3576.
102. P. de Meester and A. C. Skapski, *J. Chem. Soc., Dalton Trans.*, 1973, 1194.
103. H. Mimoun, R. Charpentier, A. Mitschler, J. Fischer and R. Weiss, *J. Am. Chem. Soc.*, 1980, **102**, 1047.

104. I. I. Moiseev, T. A. Stromnova, M. N. Vargaftig, G. J. Mazo, L. G. Kuz'mina and Y. T. Struchkov, *J. Chem. Soc., Chem. Commun.*, 1978, 27.
105. M. R. Churchill, B. G. DeBoer and D. J. Donovan, *Inorg. Chem.*, 1975, **14**, 617.
106. I. G. Dance, M. L. Scudder and L. J. Fitzpatrick, *Inorg. Chem.*, 1985, **24**, 2547.
107. B. K. Teo and J. C. Calabrese, *Inorg. Chem.*, 1976, **15**, 2474.
108. G. Nardin and L. Randaccio, *Acta Crystallogr.*, 1974, **B30**, 1377.
109. A. Camus, G. Nardin and L. Randaccio, *Inorg. Chim. Acta*, 1975, **12**, 23.
110. P. C. Healy, C. Pakawatchai, C. L. Raston, B. W. Skelton and A. H. White, *J. Chem. Soc., Dalton Trans.*, 1983, 1905.
111. W. Clegg, C. D. Garner, J. R. Nicholson and P. R. Raithby, *Acta Crystallogr.*, 1983, **C39**, 1007.
112 J.-M. Manoli, C. Potvin and F. Secheresse, *J. Chem. Soc., Chem. Commun.*, 1982, 1159.
113. U. Schubert, D. Neugebauer and A. A. M. Aly, *Z. Anorg. Allg. Chem.*, 1980, **464**, 217.
114. A. M. M. Lanfredi, A. Tiripicchio, A. Camus and N. Marsich, *J. Chem. Soc., Chem. Commun.*, 1983, 1126.
115. W. Gaete, J. Ros, X. Solans, M. Font-Altaba and J. L. Brianso, *Inorg. Chem.*, 1984, **23**, 39.
116. C. H. Wei, L. Marko, G. Bor and L. F. Dahl, *J. Am. Chem. Soc.*, 1973, **95**, 4840.
117. R. Eisenberg, A. P. Gaughan Jr., C. G. Pierpont, J. Reed and A. J. Schultz, *J. Am. Chem. Soc.*, 1972, **94**, 6240.
118. M. H. Chisholm, R. J. Errington, K. Folting and J. C. Huffman, *J. Am. Chem. Soc.*, 1982, **104**, 2025.
119. R. N. McGinnis, T. R. Ryan and R. E. McCarley, *J. Am. Chem. Soc.*, 1978, **100**, 7900.
120. R. E. McCarley, T. R. Ryan and C. C. Torardi, *ACS Symp. Ser.*, 1981, **155**, 41.
121. T. R. Ryan and R. E. McCarley, *Inorg. Chem.*, 1982, **21**, 2072.
122. V. W. Day, M. F. Fredrich, W. G. Klemperer and R. S. Liu, *J. Am. Chem. Soc.*, 1979, **101**, 491.
123. M. T. Pope, C. O. Quicksall, W. Kwak, L. M. Rajkovic, J. K. Stalick, K. M. Barkigia and T. F. Scully, *J. Less-Common Met.*, 1977, **54**, 129.
124. D. A. Wright and D. A. Williams, *Acta Crystallogr.*, 1968, **B24**, 1107.
125. P. M. Skarstad and S. Geller, *Mater. Res. Bull.*, 1975, **10**, 791.
126. M. H. Chisholm, J. C. Huffman and J. Leonelli, *J. Chem. Soc., Chem. Commun.*, 1981, 270.
127. M. H. Chisholm, J. C. Huffman, C. C. Kirkpatrick, J. Leonelli and K. Folting, *J. Am. Chem. Soc.*, 1981, **103**, 6093.
128. S. A. Koch and S. Lincoln, *Inorg. Chem.*, 1982, **21**, 2904.
129. M. F. Belicchi, G. G. Fava and C. Pelizzi, *J. Chem. Soc., Dalton Trans.*, 1983, 65.
130. F. A. Cotton and A. Fang, *J. Am. Chem. Soc.*, 1982, **104**, 113.
131. A. L. Rheingold, A. D. Uhler and A. G. Landers, *Inorg. Chem.*, 1983, **22**, 3255.
132. S. Stensvad, B. J. Helland, M. W. Babich, R. A. Jacobson and R. E. McCarley, *J. Am. Chem. Soc.*, 1978, **100**, 6257.
133. C. E. Briant, B. R. C. Theobald and D. M. P. Mingos, *J. Chem. Soc., Chem. Commun.*, 1981, 963.
134. A. Muller, W. Eltzner and N. Mohan, *Angew. Chem., Int. Ed. Engl.*, 1979, **18**, 168.
135. M. H. Chisholm, J. C. Huffman and R. L. Kelly, *J. Am. Chem. Soc.*, 1979, **101**, 7100.
136. C. T.-W. Chu and L. F. Dahl, *Inorg. Chem.*, 1977, **16**, 3245.
137. G. A. Bowmaker, G. R. Clark and D. K. P. Yuen, *J. Chem. Soc., Dalton Trans.*, 1976, 2329.
138. I. G. Dance, G. A. Bowmaker, G. R. Clark and J. K. Seadon, *Polyhedron*, 1983, **2**, 1031.
139. E. H. Griffith, G. W. Hunt and E. L. Amma, *J. Chem. Soc., Chem. Commun.*, 1976, 432.
140. I. G. Dance, *J. Am. Chem. Soc.*, 1979, **101**, 6264.
141. K. S. Hagen and R. H. Holm, *Inorg. Chem.*, 1984, **23**, 418.
142. K. S. Hagen, D. W. Stephan and R. H. Holm, *Inorg. Chem.*, 1982, **21**, 3928.
143. K. S. Hagen and R. H. Holm, *Inorg. Chem.*, 1983, **22**, 3171.
144. I. G. Dance, *Inorg. Chem.*, 1981, **20**, 2155.
145. D. Coucouvanis, M. Kanatzidis, E. Simhon and N. C. Baenziger, *J. Am. Chem. Soc.*, 1982, **104**, 1874.
146. I. G. Dance, *J. Am. Chem. Soc.*, 1980, **102**, 3445.
147. J. Sala-Pala, J. E. Guerchais and A. J. Edwards, *Angew. Chem., Int. Ed. Engl.*, 1982, **21**, 870.
148. K. Wieghardt, U. Bossek and W. Gebert, *Angew. Chem., Int. Ed. Engl.*, 1983, **22**, 328.
149. C. Gaffney, P. G. Harrison and T. J. King, *J. Chem. Soc., Chem. Commun.*, 1980, 1251.
150. A. B. Blake, *Chem. Commun.*, 1966, 569.
151. M. R. Churchill and F. J. Rotella, *Inorg. Chem.*, 1979, **18**, 853.
152. R. C. Dickinson, F. T. Helm, W. A. Baker Jr., T. D. Black and W. H. Watson Jr., *Inorg. Chem.*, 1977, **16**, 1530.
153. J. A. Bertrand and J. A. Kelly, *Inorg. Chem.*, 1969, **8**, 1982.
154. H. Wong, H. tom Dieck, C. J. O'Connor and E. Sinn, *J. Chem. Soc., Dalton Trans.*, 1980, 786.
155. M. E. Lines, A. P. Ginsberg, R. L. Martin and R. C. Sherwood, *J. Chem. Phys.*, 1972, **57**, 1.
156. A. Muller, W. Eltzner, H. Bogge and S. Sarkar, *Angew. Chem., Int. Ed. Engl.*, 1982, **21**, 535.
157. C. D. Garner, in 'Transition Metal Clusters', ed. B. F. G. Johnson, Wiley, Chichester, 1980, chap. 4, p. 265.
158. B. K. Teo and J. C. Calabrese, *Inorg. Chem.*, 1976, **15**, 2467.
159. T. Toan, B. K. Teo, J. A. Ferguson, T. J. Meyer and L. F. Dahl, *J. Am. Chem. Soc.*, 1977, **99**, 408.
160. C. T.-W. Chu, F. Y.-K. Lo and L. F. Dahl, *J. Am. Chem. Soc.*, 1982, **104**, 3409.
161. G. E. Coates and D. Ridley, *J. Chem. Soc.*, 1965, 1870.
162. G. E. Coates and A. Lauder, *J. Chem. Soc. (A)*, 1966, 264.
163. L. F. Dahl, G. L. Davies, D. L. Wampler and R. West, *J. Inorg. Nucl. Chem.*, 1962, **24**, 357.
164. H. Schumann and H. Benda, *Angew. Chem., Int. Ed. Engl.*, 1968, **7**, 813.
165. V. A. Maroni and T. Spiro, *J. Am. Chem. Soc.*, 1967, **89**, 45.
166. S.-H. Hong and A. Olin, *Acta Chem. Scand., Ser. A*, 1974, **28**, 233.
167. P. C. Healy, N. K. Mills and A. H. White, *Aust. J. Chem.*, 1983, **36**, 1851.
168. G. P. Del Piero, M. Cesari, G. Dozzi and A. Mazzei, *J. Organomet. Chem.*, 1977, **129**, 281.
169. M. R. Churchill, J. Donahue and F. J. Rotella, *Inorg. Chem.*, 1976, **15**, 2752.
170. B. K. Teo and J. C. Calabrese, *Inorg. Chem.*, 1976, **15**, 2474.
171. J. C. Dyason, P. C. Healy, L. M. Englehardt, C. Pakawatchai, V. A. Patrick, C. L. Raston and A. H. White, *J. Chem. Soc. Dalton Trans.*, 1985, 831.
172. M. R. Churchill and F. J. Rotella, *Inorg. Chem.*, 1977, **16**, 3267.
173. M. R. Churchill and W. J. Youngs, *Inorg. Chem.*, 1979, **18**, 1133.
174. M. R. Churchill, G. Davies, M. A. El-Sayed, J. P. Hutchinson and M. W. Rupich, *Inorg. Chem.*, 1982, **21**, 995.
175. V. Schramm, *Inorg. Chem.*, 1978, **17**, 714.
176. R. G. Goel and A. L. Beauchamp, *Inorg. Chem.*, 1983, **22**, 395.

177. J. A. Bandy, C. E. Davies, J. C. Green, M. L. H. Green, K. Prout and D. P. S. Rogers, *J. Chem. Soc., Chem. Commun.*, 1983, 1395.
178. D. Fenske, R. Basoglu, J. Hachgenei and F. Rogel, *Angew. Chem., Int. Ed. Engl.*, 1984, **23**, 160.
179. C. T.-W. Chu, R. S. Gall and L. F. Dahl, *J. Am. Chem. Soc.*, 1982, **104**, 737.
180. F. Bottomley, D. E. Paez and P. S. White, *J. Am. Chem. Soc.*, 1982, **104**, 5651.
181. F. Bottomley and F. Grein, *Inorg. Chem.*, 1982, **21**, 4170.
182. R. S. Gall, N. G. Connelly and L. F. Dahl, *J. Am. Chem. Soc.*, 1974, **96**, 4017.
183. T. H. Lemmen, J. A. Kocal, F. Y.-K. Lo, M. W. Chen and L. F. Dahl, *J. Am. Chem. Soc.*, 1981, **103**, 1932.
184. G. L. Simon and L. F. Dahl, *J. Am. Chem. Soc.*, 1973, **95**, 2175.
185. W. E. Cleland, D. A. Holtman, M. Sabat, J. A. Ibers, G. C. DeFotis and B. A. Averill, *J. Am. Chem. Soc.*, 1983, **105**, 6021.
186. M. A. Bobrik, K. O. Hodgson and R. H. Holm, *Inorg. Chem.*, 1977, **16**, 1851.
187. E. J. Laskowski, R. B. Frankel, W. O. Gillum, G. C. Papaefthymiou, J. Renaud, J. A. Ibers and R. H. Holm, *J. Am. Chem. Soc.*, 1978, **100**, 5322.
188. W. Bronger, M. Kimpel and D. Schmitz, *Angew. Chem., Int. Ed. Engl.*, 1982, **21**, 544.
189. R. O. Gould, C. L. Jones, D. R. Robertson and T. A. Stephenson, *J. Chem. Soc., Chem. Commun.*, 1977, 222.
190. A. Muller, H. Bogge and U. Shimanski, *Inorg. Chim. Acta*, 1983, **69**, 5.
191. A. Muller, W. Eltzner, H. Bogge and R. Jostes, *Angew. Chem., Int. Ed. Engl.*, 1982, **21**, 795.
192. A. Muller, W. Eltzner, W. Clegg and G. M. Sheldrick, *Angew. Chem., Int. Ed. Engl.*, 1982, **21**, 536.
193. A. W. Edelblut, K. Folting, J. C. Huffman and R. A. D. Wentworth, *J. Am. Chem. Soc.*, 1981, **103**, 1927.
194. T. Shibahara, H. Kuroya, K. Matsumoto and S. Ooi, *J. Am. Chem. Soc.*, 1984, **106**, 789.
195. M. Laing, P. M. Kiernan and W. P. Griffith, *J. Chem. Soc., Chem. Commun.*, 1977, 221.
196. W. Harrison, W. C. Marsh and J. Trotter, *J. Chem. Soc., Dalton Trans.*, 1972, 1009.
197. R. N. Hargreaves and M. R. Truter, *J. Chem. Soc. (A)*, 1971, 90.
198. C. Perrin, R. Chevrel and M. Sergent, *C.R. Hebd. Seances Acad. Sci., Ser. C*, 1975, **281**, 23.
199. G. A. Bowmaker, G. R. Clark, J. K. Seadon and I. G. Dance, *Polyhedron*, 1984, **3**, 535.
200. D. Gregson, J. A. K. Howard, M. Murray and J. L. Spencer, *J. Chem. Soc., Chem. Commun.*, 1981, 716.
201. P. Murray-Rust, P. Day and C. K. Prout, *Chem. Commun.*, 1966, 277.
202. G. E. Kokoszka, J. Baranowski, C. Goldstein, J. Orsini, A. D. Mighell, V. L. Himes and A. R. Siedle, *J. Am. Chem. Soc.*, 1983, **105**, 5627.
203. K. Jodden and H. Schafer, *Z. Anorg. Allg. Chem.*, 1977, **430**, 5.
204. H. Hartl and F. Mahdjour-Hassan-Abadi, *Angew. Chem., Int. Ed. Engl.*, 1984, **23**, 378.
205. I. G. Dance, *Aust. J. Chem.*, 1978, **31**, 2195.
206. T. E. Wolff, J. M. Berg and R. H. Holm, *Inorg. Chem.*, 1981, **20**, 174.
207. G. W. Adamson, N. A. Bell and H. M. M. Shearer, *Acta Crystallogr.*, 1982, **B38**, 462.
208. F. Cecconi, C. A. Ghilardi, S. Midollini and A. Orlandini, *J. Chem. Soc., Chem. Commun.*, 1982, 229.
209. P. Woodward, L. F. Dahl, E. W. Abel and B. C. Crosse, *J. Am. Chem. Soc.*, 1965, **87**, 5251.
210. R. O. Gould and M. M. Harding, *J. Chem. Soc. (A)*, 1970, 875.
211. U. Muller, *Angew. Chem., Int. Ed. Engl.*, 1981, **20**, 692.
212. K. S. Hagen, A. D. Watson and R. H. Holm, *J. Am. Chem. Soc.*, 1983, **105**, 3905.
213. G. Christou, M. Sabat, J. A. Ibers and R. H. Holm, *Inorg. Chem.*, 1982, **21**, 3518.
214. G. Henkel, H. Strasdeit and B. Krebs, *Angew. Chem., Int. Ed. Engl.*, 1982, **21**, 201.
215. V. Katovic, J. L. Templeton and R. E. McCarley, *J. Am. Chem. Soc.*, 1976, **98**, 5705.
216. G. W. Eastland, M. A. Mazid, D. R. Russell and M. C. R. Symons, *J. Chem. Soc., Dalton Trans.*, 1980, 1682.
217. G. E. Lewis and C. S. Kraihanzel, *Inorg. Chem.*, 1983, **22**, 2895.
218. J. R. Carruthers, K. Prout and F. J. C. Rossotti, *Acta Crystallogr.*, 1975, **B31**, 2044.
219. M. Shimoi, F. Ebina, A. Ouchi, Y. Yoshino and T. Takeuchi, *J. Chem. Soc., Chem. Commun.*, 1979, 1132.
220. J. W. A. van der Velden, J. J. Bour, J. J. Steggerda, P. T. Beurskens, M. Roseboom and J. H. Noordik, *Inorg. Chem.*, 1982, **21**, 4321.
221. A. Olin and R. Soderquist, *Acta Chem. Scand.*, 1972, **26**, 3505.
222. R. N. Sylva and P. L. Brown, *J. Chem. Soc., Dalton Trans.*, 1980, 1577.
223. C. E. Briant, K. P. Hall and D. M. P. Mingos, *J. Organomet. Chem.*, 1983, **254**, C18.
224. G. Henkel, P. Betz and B. Krebs, *J. Chem. Soc., Chem. Commun.*, 1984, 314.
225. A. Muller, M. Romer, H. Bogge, E. Krickemeyer and D. Bergmann, *J. Chem. Soc., Chem. Commun.*, 1984, 348.
226. C. E. Briant, T. S. A. Hor, N. D. Howells and D. M. P. Mingos, *J. Organomet. Chem.*, 1983, **256**, C15.
227. I. G. Dance, L. J. Fitzpatrick and M. L. Scudder, *Inorg. Chem.*, 1984, **23**, 2276.
228. G. Del Piero, M. Cesari, G. Perego, S. Cucinella and E. Cernia, *J. Organomet. Chem.*, 1977, **129**, 289.
229. G. Del Piero, G. Perego, S. Cucinella, M. Cesari and A. Mazzei, *J. Organomet. Chem.*, 1977, **136**, 13.
230. M. G. Kanatzidis, W. R. Dunham, W. R. Hagen and D. Coucouvanis, *J. Chem. Soc., Chem. Commun.*, 1984, 356.
231. W. Saak, G. Henkel and S. Pohl, *Angew. Chem., Int. Ed. Engl.*, 1984, **23**, 150.
232. G. Dozzi, G. Del Piero, M. Cesari and S. Cucinella, *J. Organomet. Chem.*, 1980, **190**, 229.
233. R. A. Andersen, D. H. Templeton and A. Zalkin, *Inorg. Chem.*, 1978, **17**, 1962.
234. P. Bellon, M. Manassero and M. Sansoni, *J. Chem. Soc., Dalton Trans.*, 1973, 2423.
235. A. Yatsimirski and R. Ugo, *Inorg. Chem.*, 1983, **22**, 1395.
236. M. F. Pilbrow, *J. Chem. Soc., Dalton Trans.*, 1975, 2432.
237. V. A. Maroni and T. G. Spiro, *Inorg. Chem.*, 1968, **7**, 183.
238. D. L. Kepert, 'The Early Transition Metals', Academic, London, 1972.
239. F. W. Koknat, J. A. Parsons and A. Vongvusharintra, *Inorg. Chem.*, 1974, **13**, 1699.
240. R. A. Field, D. L. Kepert, B. W. Robinson and A. H. White, *J. Chem. Soc., Dalton Trans.*, 1973, 1858.
241. D. D. Klendworth and R. A. Walton, *Inorg. Chem.*, 1981, **20**, 1151.
242. R. A. Walton, *Prog. Inorg. Chem.*, 1972, **16**, 1.
243. F. A. Cotton and G. G. Stanley, *Chem. Phys. Lett.*, 1978, **58**, 450.
244. D. L. Kepert, R. E. Marshall and D. Taylor, *J. Chem. Soc., Dalton Trans.*, 1974, 506.
245. J. L. Meyer and R. E. McCarley, *Inorg. Chem.*, 1978, **17**, 1867.
246. P. G. Harrison, B. J. Haylett and T. J. King, *J. Chem. Soc., Chem. Commun.*, 1978, 112.
247. J. B. Michel and R. E. McCarley, *Inorg. Chem.*, 1982, **21**, 1864.

248. M. H. Chisholm, J. A. Heppert and J. C. Huffman, *Polyhedron*, 1984, **3**, 475.
249. A. D. Hamer, T. J. Smith and R. A. Walton, *Inorg. Chem.*, 1976, **15**, 1014.
250. F. Cecconi, C. A. Ghilardi and S. Midollini, *J. Chem. Soc., Chem. Commun.*, 1981, 640.
251. F. Cecconi, C. A. Ghilardi and S. Midollini, *Inorg. Chim. Acta*, 1982, **64**, L47.
252. F. Cecconi, C. A. Ghilardi, S. Midollini and A. Orlandini, *Inorg. Chim. Acta*, 1983, **76**, L183.
253. G. Gervasio, R. Rossetti and P. L. Stanghellini, *Inorg. Chim. Acta*, 1984, **83**, L9.
254. J. C. Huffman, J. G. Stone, W. C. Krusell and K. G. Caulton, *J. Am. Chem. Soc.*, 1977, **99**, 5829.
255. T. Hughbanks and R. Hoffmann, *J. Am. Chem. Soc.*, 1983, **105**, 1150.
256. D. G. Nocera and H. B. Gray, *J. Am. Chem. Soc.*, 1984, **106**, 824.
257. M. R. Churchill, S. A. Bezman, J. A. Osborn and J. Wormald, *Inorg. Chem.*, 1972, **11**, 1818.
258. G. V. Goeden and K. G. Caulton, *J. Am. Chem. Soc.*, 1981, **103**, 7354.
259. D. M. Ho and R. Bau, *Inorg. Chim. Acta*, 1984, **84**, 213.
260. R. Hesse and U. Aava, *Acta Chem. Scand.*, 1970, **24**, 1355.
261. P. Jennische and R. Hesse, *Acta Chem. Scand.*, 1971, **25**, 423.
262. H. Dietrich, W. Storck and G. Manecke, *J. Chem. Soc., Chem. Commun.*, 1982, 1036.
263. G. van Koten, J. T. B. H. Jastrzebski and J. G. Noltes, *Inorg. Chem.*, 1977, **16**, 1782.
264. R. W. M. ten Hoedt, J. G. Noltes, G. van Koten and A. L. Spek, *J. Chem. Soc., Dalton Trans.*, 1978, 1800.
265. J. W. A. van der Velden, P. T. Beurskens, J. J. Bour, W. P. Bosman, J. H. Noordik, M. Kolenbrander and J. A. K. M. Buskes, *Inorg. Chem.*, 1984, **23**, 146.
266. H. T. Evans Jr., *Acta Crystallogr.*, 1974, **B30**, 2095.
267. A. Perloff, *Inorg. Chem.*, 1970, **9**, 2228.
268. K. Watenpaugh and C. N. Caughlan, *J. Chem. Soc., Chem. Commun.*, 1967, 76.
269. C. J. Besecker and W. G. Klemperer, *J. Am. Chem. Soc.*, 1980, **102**, 7598.
270. M. Ishimori, T. Hagiwara, T. Tsuruta, Y. Kai, N. Yasuoka and N. Kasai, *Bull. Chem. Soc. Jpn.*, 1976, **49**, 1165.
271. P. B. Hitchcock, J. D. Smith and K. M. Thomas, *J. Chem. Soc., Dalton Trans.*, 1976, 1433.
272. I. G. Dance, M. L. Scudder and R. Secomb, *Inorg. Chem.*, 1985, **24**, 1201.
273. G. Christou, K. S. Hagen, J. Bashkin and R. H. Holm, *Inorg. Chem.*, 1985, **24**, 1010.
274. L. D. Lower and L. F. Dahl, *J. Am. Chem. Soc.*, 1976, **98**, 5046.
275. P. J. M. W. L. Birker and G. C. Verschoor, *J. Chem. Soc., Chem. Commun.*, 1981, 322.
276. F. J. Hollander and D. Coucouvanis, *J. Am. Chem. Soc.*, 1977, **99**, 6268.
277. H. B. Burgi, H. Gehrer, P. Strickler and F. K. Winkler, *Helv. Chim. Acta*, 1976, **59**, 2558.
278. P. J. M. W. L. Birker, J. Reedijk and G. C. Verschoor, *Inorg. Chem.*, 1981, **20**, 2877.
279. P. J. M. W. L. Birker and H. C. Freeman, *J. Am. Chem. Soc.*, 1977, **99**, 6890.
280. H.-L. Keller, *Angew. Chem., Int. Ed. Engl.*, 1983, **22**, 324.
281. G. Christou and C. D. Garner, *J. Chem. Soc., Dalton Trans.*, 1980, 2354.
282. T. E. Wolff, J. M. Berg, K. O. Hodgson, R. B. Frankel and R. H. Holm, *J. Am. Chem. Soc.*, 1979, **101**, 4140.
283. G. W. Adamson and H. M. M. Shearer, *Chem. Commun.*, 1969, 897.
284. S. Amirkhalili, P. B. Hitchcock and J. D. Smith, *J. Chem. Soc., Dalton Trans.*, 1979, 1206.
285. H. Noth and P. Wolfgardt, *Z. Naturforsch., Teil B*, 1976, **31**, 697.
286. S. Rettig, A. Storr and J. Trotter, *Can. J. Chem.*, 1975, **53**, 753.
287. D. C. Bradley, M. B. Hursthouse and P. F. Rodesiler, *Chem. Commun.*, 1968, 1112.
288. A. Gruttner, K. Yvon, R. Chevrel, M. Potel, M. Sergent and B. Seeber, *Acta Crystallogr.*, 1979, **B35**, 285.
289. T. E. Wolff, P. P. Power, R. B. Frankel and R. H. Holm, *J. Am. Chem. Soc.*, 1980, **102**, 4694.
290. T. E. Wolff, J. M. Berg, P. P. Power, K. O. Hodgson and R. H. Holm, *Inorg. Chem.*, 1980, **19**, 430.
291. S. C. Critchlow and J. D. Corbett, *J. Am. Chem. Soc.*, 1983, **105**, 5715.
292. R. B. King, *Inorg. Chim. Acta*, 1982, **57**, 79.
293. J. M. M. Smits, P. T. Beurskens, J. J. Bour and F. A. Vollenbroek, *J. Cryst. Spect. Res.*, 1983, **13**, 365.
294. J. W. Diesveld, E. M. Menger, H. T. Edzes and W. S. Veeman, *J. Am. Chem. Soc.*, 1980, **102**, 7935.
295. K. P. Hall, B. R. C. Theobald, D. I. Gilmour, D. M. P. Mingos and A. J. Welch, *J. Chem. Soc., Chem. Commun.*, 1982, 528.
296. M. K. Cooper, G. R. Dennis, K. Henrick and M. McPartlin, *Inorg. Chim. Acta*, 1980, **45**, L151.
297. J. W. A. van der Velden, J. J. Bour, W. P. Bosman, J. H. Noordik, and P. T. Beurskens, *Recl. Trav. Chim. Pays-Bas*, 1984, **103**, 13.
298. R. A. Jones, F. M. Real, G. Wilkinson, A. M. R. Galas and M. B. Hursthouse, *J. Chem. Soc., Dalton Trans.*, 1981, 126.
299. I. G. Dance and J. K. Saunders, *Inorg. Chim. Acta*, 1985, **96**, L71.
300. P. Strickler, *Chem. Commun.*, 1969, 655.
301. P. M. DuBois Murphy, W. C. Stevens, T. T. P. Heung, S. Lacelle, B. C. Gerstein and D. M. Kurtz, Jr., *J. Am. Chem. Soc.*, 1981, **103**, 4400.
302. G. Schwarzenbach, K. Gautschi, J. Peter and K. Tunaboylu, *Trans. R. Inst. Technol. Stockholm*, 1972, **271**, 295.
303. W. Schiwy and B. Krebs, *Angew. Chem., Int. Ed. Engl.*, 1975, **14**, 436.
304. E. G. Mednikov, N. K. Eremenko, V. A. Mikhailov, S. P. Gubin, Y. L. Slovokhotov and Y. T. Struchkov, *J. Chem. Soc., Chem. Commun.*, 1981, 989.
305. A. Simon, E. Warkentin and R. Masse, *Angew. Chem., Int. Ed. Engl.*, 1981, **20**, 1013.
306. C. E. Briant, K. P. Hall, A. C. Wheeler and D. M. P. Mingos, *J. Chem. Soc., Chem. Commun.*, 1984, 248.
307. I. G. Dance, *Inorg. Chim. Acta*, 1977, **25**, L17.
308. P. Betz, B. Krebs and G. Henkel, *Angew. Chem., Int. Ed. Engl.*, 1984, **23**, 311.
309. Y. Agnus, R. Louis and R. Weiss, *J. Chem. Soc., Chem. Commun.*, 1980, 867.
310. E. I. Solomon, K. W. Penfield and D. E. Wilcox, *Struct. Bonding (Berlin)*, 1983, **53**, 1.
311. W. Clegg, C. D. Garner and M. H. Alsamman, *Inorg. Chem.*, 1983, **22**, 1534.
312. T. Lis, *Acta Crystallogr.*, 1980, **B36**, 2042.
313. R. Chevrel, M. Potel, M. Sergent, M. Decroux and O. Fischer, *J. Solid State Chem.*, 1980, **34**, 247.
314. D. M. P. Mingos, *Gold Bull.*, 1984, **17**, 5.
315. F. Demartin, M. Manassero, L. Naldini, R. Ruggeri and M. Sansoni, *J. Chem. Soc., Chem. Commun.*, 1981, 222.
316. J. W. A. van der Velden, J. J. Bour, R. Pet, W. P. Bosman and J. H. Noordik, *Inorg. Chem.*, 1983, **22**, 3112.

317. J. W. van der Velden, F. A. Vollenbroek, J. J. Bour, P. T. Beurskens, J. M. M. Smits and W. P. Bosman, *Recl. Trav. Chim. Pays-Bas*, 1981, **100**, 148.
318. C. E. Briant, K. P. Hall and D. M. P. Mingos, *J. Organomet. Chem.*, 1983, **254**, C18.
319. J. W. A. van der Velden, J. J. Bour, B. F. Otterloo, W. P. Bosman and J. H. Noordik, *J. Chem. Soc., Chem. Commun.*, 1981, 583.
320. J. W. A. van der Velden, J. J. Bour, W. P. Bosman and J. H. Noordik, *Inorg. Chem.*, 1983, **22**, 1913.
321. J. W. A. van der Velden, J. J. Bour, J. J. Steggerda, P. T. Beurskens, M. Rosenboom and J. H. Noordik, *Inorg. Chem.*, 1982, **21**, 4321.
322. P. Bellon, M. Manassero and M. Sansoni, *J. Chem. Soc., Dalton Trans.*, 1973, 2423.
323. J. W. A. van der Velden, J. J. Bour, W. P. Bosman and J. H. Noordik, *J. Chem. Soc., Chem. Commun.*, 1981, 1218.
324. F. A. Vollenbroek, W. P. Bosman, J. J. Bour, J. H. Noordik and P. T. Beurskens, *J. Chem. Soc., Chem. Commun.*, 1979, 387.
325. W. Bos, J. J. Bour, J. W. A. van der Velden, J. J. Steggerda, A. L. Casalnuovo and L. H. Pignolet, *J. Organomet. Chem.*, 1983, **253**, C64.
326. C. E. Briant, B. R. C. Theobald, J. W. White, L. K. Bell, D. M. P. Mingos and A. J. Welch, *J. Chem. Soc., Chem. Commun.*, 1981, 201.
327. J. M. M. Smits, J. J. Bour, F. A. Vollenbroek and P. T. Beurskens, *J. Cryst. Spect. Res.*, 1983, **13**, 355.
328. F. A. Vollenbroek, J. J. Bour and J. W. A. van der Velden, *Recl. Trav. Chem. Pays-Bas*, 1980, **99**, 137.
329. M. McPartlin, R. Mason and L. Malatesta, *Chem. Commun.*, 1969, 334.
330. J. M. M. Smits, P. T. Beurskens, J. W. A. van der Velden and J. J. Bour, *J. Cryst. Spect. Res.*, 1983, **13**, 373.
331. P. Bellon, M. Manassero and M. Sansoni, *J. Chem. Soc., Dalton Trans.*, 1972, 1481.
332. G. Schmid, R. Pfeil, R. Boese, F. Bandermann, S. Meyer, G. H. M. Calis and J. W. A. van der Velden, *Chem. Ber.*, 1981, **114**, 3634.
333. F. A. Vollenbroek, J. P. van den Berg, J. W. A. van der Velden and J. J. Bour, *Inorg. Chem.*, 1980, **19**, 2685.
334. J. W. Diesveld, E. M. Menger, H. T. Edzes and W. S. Veeman, *J. Am. Chem. Soc.*, 1980, **102**, 7935.
335. D. M. P. Mingos, *J. Chem. Soc., Dalton Trans.*, 1976, 1163.
336. F. A. Vollenbroek, P. C. P. Bouten, J. M. Trooster, J. P. van den Berg and J. J. Bour, *Inorg. Chem.*, 1978, **17**, 1345.
337. P. M. T. M. van Attekum, J. W. A. van der Velden and J. M. Trooster, *Inorg. Chem.*, 1980, **19**, 701.
338. B. K. Teo and K. Keating, *J. Am. Chem. Soc.*, 1984, **106**, 2224.
339. G. Schmid, U. Giebel, W. Huster and A. Schwenk, *Inorg. Chim. Acta*, 1984, **85**, 97.
340. D. H. Guthrie and J. D. Corbett, *Inorg. Chem.*, 1982, **21**, 3290.
341. R. Alexander, A. J. Parker, J. H. Sharp and W. E. Waghorne, *J. Am. Chem. Soc.*, 1972, **94**, 1148.
342. R. C. Burns and J. D. Corbett, *J. Am. Chem. Soc.*, 1982, **104**, 2804.
343. L. G. Sillen, in 'Coordination Chemistry', vol. 1, ed. A. E. Martell, ACS Monograph, 1971, **168**, 491.
344. C. Brevard, R. Schimpf, G. Tourne and C. M. Tourne, *J. Am. Chem. Soc.*, 1983, **105**, 7059.
345. S. F. Gheller, M. Sidney, A. F. Masters, R. T. C. Brownlee, M. J. O'Connor and A. G. Wedd, *Aust. J. Chem.*, 1984, **37**, 1825.
346. M. Fillowitz, R. K. C. Ho, W. G. Klemperer and W. Shum, *Inorg. Chem.*, 1979, **18**, 93.
347. A. Muller, E. Diemann, R. Jostes and H. Bogge, *Angew. Chem., Int. Ed. Engl.*, 1981, **20**, 934.
348. D. Coucouvanis, *Acc. Chem. Res.*, 1981, **14**, 201.

5

Isomerism in Coordination Chemistry

JACK MacB. HARROWFIELD
University of Western Australia, Perth, Australia
and
S. BRUCE WILD
Australian National University, Canberra, Australia

5.1 INTRODUCTION

5.1.1 General Considerations — Isomerism and Stereochemistry

Any given assemblage of atoms will interact with one another and, in principle, can exist in an infinite variety of configurations, all of which will have different energies. Atomic arrays that correspond to energy minima may be detected in many ways and the heat changes that occur in chemical reactions are, of course, evidence of the formation and breakdown of the relatively stable arrays that are termed 'molecules'. A chemical bond may be said to exist when at least 100 kJ per Avogadro's number of aggregates is required to disrupt a two-atom aggregate into isolated atoms. It is possible, nonetheless, for there to be different configurations and hence different energies for a given group of atoms regarded as constituting a molecule. Energy minima within this subset are then considered to define isomers of the molecule. The problem of identifying such energy minima is discussed elsewhere.[1] The present chapter is primarily concerned with classification and exemplification of the well-known and important forms of isomers found for coordination compounds. The field is important both because of its association with the development of the basic concepts of chemistry and because of its relevance to an understanding of complex chemical reactions in industry and biology.

The phenomenon of isomerism, that is the existence of isomers, may be simply defined as the fact that molecules of identical elemental composition may exist in forms with different chemical or physical properties. Given that identity of chemical composition includes the specification of identical molecular formulae, the most obvious possible cause of differences in properties is a difference between isomers in the relative spatial distribution of their component atoms. Thus, the study of stereochemistry originated from attempts to understand isomerism.[2]

The evidence for isomerism varies from the obvious, such as a difference in phase, to the subtle, such as the temperature dependence of an NMR spectrum. These instances illustrate an important point, namely, that the detection of isomerism is dependent upon the existence of an energy barrier between the different forms and upon a method of detection sensitive enough to observe the barrier. A compound that appears to be a single species on one time-scale may prove to be a mixture on another. The relationship between the lifetime of a particular molecular structure and the various physical methods for studying it has been discussed by Muetterties.[3] The essentially instantaneous method of X-ray diffraction (10^{-18} s) may be contrasted with NMR techniques (10^{-1}–10^{-9} s) and the time scale for the experimental separation of isomers ($>10^2$ s).

The earliest observations of isomerism depended upon the fact that the compounds involved interconverted only slowly, if at all. Although Wöhler's demonstration of the interconversion of ammonium cyanate and urea is perhaps the best known early work on isomerism,[4] Liebig and Gay-Lussac, for example, had previously noted the identical composition of the apparently non-interconvertible substances silver fulminate and silver cyanate.[5] Pasteur's notable contributions to the study of *optical isomerism* can be traced back to eighteenth century studies of crystal morphology[2,6,7] and the seminal postulate of the tetrahedral carbon atom by van't Hoff and Le Bel in 1874[8] was founded upon the by then extensive knowledge of stable, readily separable pairs of carbon compounds. Later development of an understanding of the stereochemistry of inorganic complex ions was similarly based on the ready separation of isomeric forms of inert complexes of metal ions such as Cr^{3+}, Co^{3+} and Pt^{2+}.[9] Nevertheless, the phenomenon of isomerism is of equal significance in labile systems, although its detection is then generally dependent upon the use of modern spectroscopic techniques. The degree of stereochemical rigidity of molecules in fact varies over an enormous range, though non-rigidity could be considered the normal situation, rigidity being a characteristic of but a few of the possible coordination geometries of complex ions.[1,10,11]

The consideration of isomerism as reflecting the existence of multiple local energy minima is, in relation to conventional usage, possibly unusually general. Thus, an electronically excited molecule is not normally termed an isomer of the ground state species, even though it may differ dramatically in its chemical properties. The distinction is, however, quite arbitrary and there are several instances of subtle molecular changes in addition to simple electronic excitation that should quite validly be considered as sources of isomerism. Thus, nuclear excitations,[12] spin-state changes[13] and isotopic substitutions[14,15] are all known to give rise to changes in physical and chemical properties just as significant as those typifying 'conventional' isomerism. They are, nonetheless, not factors of primary importance in any general classification of isomers and hence will be taken to be implicit refinements of the following considerations.

5.1.2 Classification of Isomers

Differing spatial distributions of atoms within a molecule may or may not be associated with significant differences in bonding interactions (bonding electron distributions). Thus, it is possible to differentiate isomer types on this basis and the simplest and most familiar isomer classification, common to all areas of chemistry, is that of constitutional and configurational isomerism.[16] Constitutional isomers differ with respect to the spatial distribution of the atoms *and* the bonding electrons in the molecule, that is they differ with respect to atom connectivity or bond sequence, as is simply illustrated by the isomeric ions fulminate, CNO^-, and cyanate, NCO^-. Configurational isomers or stereoisomers differ only with respect to the spatial distribution of the atoms and can be distinguished in terms of relative orientations of bonds, but not in terms of the atoms connected by those bonds. A simple illustration of configurational isomerism is found with the materials of composition $[PtCl_2(NH_3)_2]$, where two forms which differ in that the ClPtCl bond angle is close to either 90° or 180° are known.

It is obvious that this constitution/configuration dichotomy does not readily accommodate isomerism of the special types (*e.g.* spin isomers)[13] mentioned above but it does form a very convenient basis for the consideration of the most frequently encountered and most important forms of isomerism. Nonetheless, it is also true that constitutional isomerism is nearly always readily recognized and is not a reflection of subtle aspects of molecular structure, so that the subject of configurational isomerism is worthy of more detailed analysis and attention. The classification of stereoisomers into enantiomers (non-superimposable mirror-image molecules) and diastereomers (all other molecules of identical composition) reflects more closely this view of the significance of isomerism.[17] Both of these classification schemes will be considered presently, although the basic framework of the discussion will be in terms of the configurational/constitutional distinction.

It should be noted that the sub-classifications of configurational isomers shown in Figure 1 correspond to formal procedures for distinguishing between isomers and in most cases to the magnitude of the energy barriers between isomeric forms. Thus, conformational isomers are species interconvertible by rotation about single bonds; that is they may be distinguished in terms of particular dihedral angles, such as in the chair and skew-boat forms of metal ion pyrophosphate chelate rings (Figure 2). Because the energy barrier between conformational isomers is usually small and interconversion between them is rapid however, techniques such as NMR spectroscopy are required to detect such processes and to demonstrate that the various isomeric forms are present. However, in polycyclic systems in particular, barriers to rotation may become large and conformational isomers isolable as stable, separate species. Of course, even when interconversion is rapid, differences in reactivity can be important so long as interconversions and other reactions occur at competitive rates.[18]

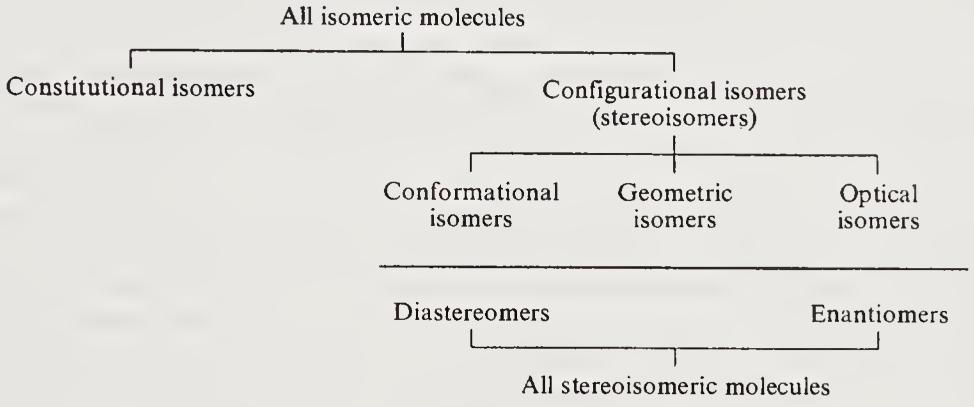

Figure 1 Two conventional isomer classification schemes

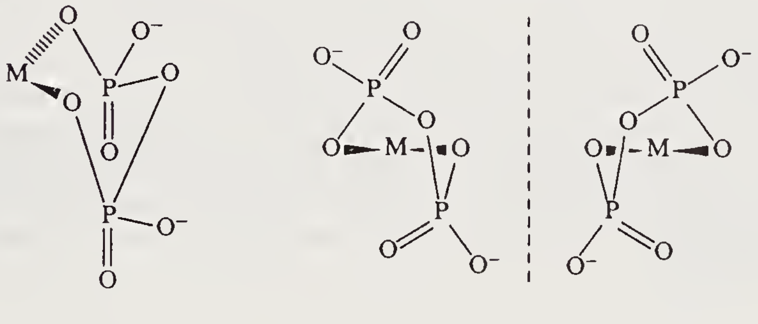

(a) (b)

Figure 2 (a) Chair and (b) enantiomorphic skew-boat conformations of the $[M(P_2O_7)]$ chelate ring

Geometric isomers may be distinguished in terms of the relative orientations of two bonds to a single atom, as described above in relation to $[PtCl_2(NH_3)_2]$. Here, it is common for the energy barrier between isomers to be large, a process involving bond cleavage and reformation being the most obvious pathway to interconversion, so that the separate forms may be readily isolated. Again, however, rates of interconversion vary widely and stereochemically non-rigid geometric isomer systems are well known, as, for example, with five-coordinate phosphorus(V).[19]

Optical isomerism is said to occur when a molecule and its mirror image are non-superimposable, that is when there is no rotation or translation of the mirror image which brings it into coincidence with the original. Molecules that can exist in optically isomeric forms are said to be chiral and the isomeric pair forms are termed enantiomers or catoptromers.[20] Chiral molecules may be dissymmetric or asymmetric, depending upon whether or not they have rotational symmetry (*vide infra*). The term chirality is to be preferred to optical isomerism since the latter derives simply from the earliest, but not the only, means of detecting this form of isomerism. However, it is important to note that the terms are not equivalent in that a chiral molecule is one that can exist in non-superimposable mirror-image forms, whereas an optical isomer is one of these forms, that is an enantiomer (catoptromer). The conventional designations of enantiomers are discussed below but it may be noted here that these are based upon a means of assigning alternative sequences to atoms distributed in space.

5.1.3 Isomerism and Molecular Structure

The classical use of isomer identification in coordination chemistry was to establish the geometry of the donor atom distribution about the metal ion. For example,[21] the fact that only two isomers, green and violet in colour, of $[CoCl_2(NH_3)_4]^+$ can be isolated suggests that the cobalt(III) ion must have a coordination environment that is octahedral rather than hexagonal planar. This method of structure determination is now rarely of importance because the structural problems to be solved are usually of greater subtlety than the determination of coordination geometry. Indeed, it is now usual to apply the vast contemporary knowledge concerning molecular structures to deduce which isomeric forms may be possible, and even what their relative energies might be in new complexes.[22,23] This process in part depends upon the recognition that the reaction of a ligand with a metal ion does not usually lead to drastic changes in bond angles and lengths or atom connectivity within the ligand, so that known properties of the ligand can be used to predict properties of the complex. Thus, the consideration of isomerism in complex ions rarely needs to begin from the point of knowing only atomic composition. When, for example, 1,2-ethanediamine forms a chelate ring by binding as a bidentate ligand to a metal ion, the C—C and C—N bonds remain of a length such that coordination sites farther than ~2.5 Å apart cannot be spanned, thus eliminating the possibility of *trans* coordination. Further, some degree of rotation about the C—C bond is retained and different conformations of the chelate ring are possible. In addition, both N and C atoms retain nearly tetrahedral geometries, so that the pairs of protons of the NH_2 and CH_2 groups of the complex are not in identical environments to one another.

The assembly of a complex ion by assuming retained features of the ligand and, indeed, the metal ion structure is essentially what is involved in the construction of a molecular model. This can be an extremely useful way of analyzing the stereochemistry, and hence isomerism, of a coordination compound. It is, however, usually based upon averaged or idealized structures for the component species and can be misleading when details of stereochemistry are considered. The 90° bond angles in an octahedral metal ion model, for example, make it almost impossible to attach a model of 1,8-diamino-3,6-diazaoctane (trien) with its nitrogen donor atoms in a planar array, even though such species are known. In the quantitative analysis of isomer equilibria, it is therefore essential to know the subtle distortions from 'ideality' that may result from the combination of metal ion and ligands and this, of course, can only be derived from a detailed study of known isomeric structures.

5.2 CONSTITUTIONAL ISOMERISM

Gross differences in physical and chemical properties usually characterize constitutional isomers of coordination compounds. Hence, where equilibrium can be attained, it may lie at a point where few, often only one, of all possible isomers can be detected. For both of these reasons, the study of constitutional isomerism is not of major importance, although it may not always be a simple task to establish the particular constitution of a given coordination compound. Crystallization of a solid incorporating a metal ion and a ligand does not guarantee that both interact *via* coordinate bonding and simple spectroscopic techniques may not readily indicate the situation that obtains. This is familiar in relation to hydrated metal salts (*vide infra*), but it is also a contemporary problem, as illustrated by the nature of materials incorporating the macrocyclic polyether, 18-crown-6,[24,25] and similar ligands.[26]

5.2.1 Ionization, Hydrate and Coordination Isomerism

Ionization, hydrate and coordination isomerism are classifications of constitutional isomerism that originated with Werner.[27,28] Ionization and hydrate isomerism (equation 1) apply to cases in which there is a ligand exchange between primary and outer coordination spheres, whereas coordination isomerism (equation 2) arises in systems containing at least two metal ions, so that alternative primary coordination spheres are available.

$$[ML_n]X_y \rightleftharpoons [ML_{n-x}X_x]L_xX_{y-x} \qquad (1)$$

$$[M_1(L_1)_n][M_2(L_2)_m] \rightleftharpoons [M_1(L_2)_m][M_2(L_1)_n] \qquad (2)$$

Ionization isomerism is best characteized in systems involving substitutionally inert metal ions where kinetic, rather than thermodynamic, factors control isomer formation. Numerous cases are known of cobalt(III) compounds in which exchange of a ligand between inner and outer coordination spheres results in a spectacular colour change. Thus, *trans*-$[CoCl_2(en)_2]NO_2$ (en = 1,2-ethanediamine) is green and *trans*-$[CoCl(NO_2)(en)_2]Cl$ is orange; *trans*-$[CoCl(NCS)(en)_2]NCS$ is blue and *trans*-$[Co(NCS)_2(en)_2]Cl$ is deep red.

When water is the ligand involved in the exchange, the phenomenon is known as hydrate isomerism. The hydrated chromium(III) chlorides of empirical formula $CrCl_3{\cdot}6H_2O$ are the best known examples of this isomer type. When CrO_3 is reduced with concentrated HCl, the major product is drak green *trans*-$[CrCl_2(OH_2)_4]Cl{\cdot}2H_2O$ (commercial 'hydrated chromic chlroide'), which by aquation for 24 h at room temperature is converted into light green $[CrCl(OH_2)_5]Cl_2{\cdot}H_2O$. When CrO_3 is reduced by H_2O_2 in the presence of HNO_3 or $HClO_4$, a solution of $[Cr(OH_2)_6]^{3+}$ is obtained and $[Cr(OH_2)_6]Cl_3$ may be precipitated from it with gaseous HCl.[29] It might have been anticipated that solvate isomerism would be a general phenomenon but, apart from limited work on dimethyl sulfoxide,[30] there does not appear to have been much investigation of the possibility.

Coordination isomerism is another relatively rare, though well-known, phenomenon, exemplified in the compounds $[Cr(NH_3)_6][Co(CN)_6]/[Cr(CN)_6][Co(NH_3)_6]$ and $[Cr(en)_2ox][Cr(ox)_2en]/[Cr(en)_3][Cr(ox)_3]$ (ox = $C_2O_4^{2-}$). It is related to the structural isomerism that might be expected to be encountered in polynuclear systems (Figure 3). Although examples of such isomer types are known, *e.g.* the chiral cobalt(III) 'hexol', $[Co\{Co(OH)_2(NH_3)_4\}_3]^{6+}$,[9,31,32] and the chromium(III) 'rhodoso' ion[33] with the alternative achiral structure shown in Figure 3, no isomeric pairs have been thoroughly characterized.

$[M_3(OH)_6(NH_3)_{12}]^{6+}$

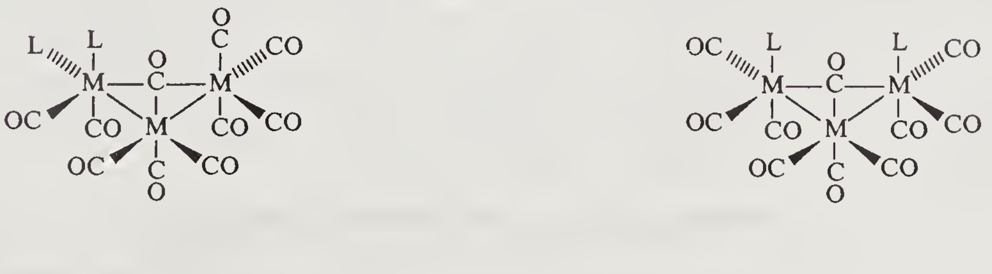

$[M_3(CO)_{10}L_2]$

Figure 3 Some stereoisomers of polynuclear complexes

5.2.2 Linkage Isomerism

Linkage isomerism is the most widely studied form of constitutional isomerism.[34-40] It may occur in complexes containing ligands with at least two inequivalent donor atoms where bonding, of the same denticity to the metal, can take place by different combinations of donor atoms. Ligands of this kind are relatively common, ranging from diatomic species such as cyanide ion to macromolecular proteins, and are generally referred to as *ambidentate* species. Some examples of particularly well-known alternative bonding arrangements of various ambidentate ligands are shown in Figure 4.

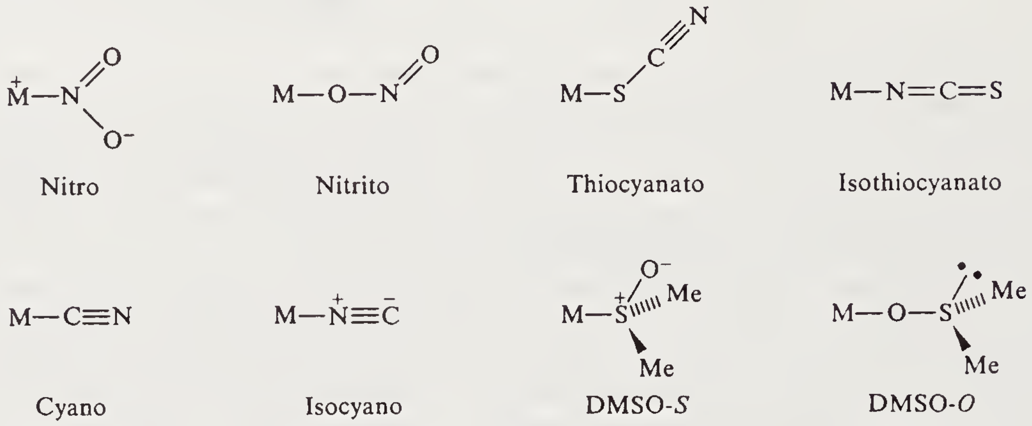

Figure 4 Alternative bonding modes of some ambidentate ligands

It has been possible to study both the kinetics and thermodynamics of the interconversion of many linkage isomers and a wide range of spectroscopic techniques has been applied to the identification of the separate forms, although X-ray crystallography remains the preferred method. The first linkage isomers to be well characterized were orange $[CoONO(NH_3)_5]Cl_2$ and yellow $[CoNO_2(NH_3)_5]Cl_2$[41] and numerous studies have since been made of the properties of these and many other nitrito (ONO, *O*-bound) and nitro (NO_2, *N*-bound) isomer pairs.[42] Usually, the nitro isomer is the more stable form, but with inert metal ions such as Co^{III}, Rh^{III}, Ir^{III} and Pt^{IV}, it is possible to use a non-substitutional method to rapidly convert the aquo to a nitrito ligand and to then observe the slow conversion of this species into the nitro compound either in the solid state or in solution.[43-52] This conversion, however, can be reversed photochemically.[43] With chromium(III) nitrito complexes on the other hand, there is no evidence of tendency towards rearrangement to the nitro form.[53,54]

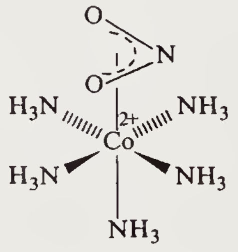

(1)

The conversion of $[CoONO(NH_3)_5]^{2+}$ into $[CoNO_2(NH_3)_5]^{2+}$ appears to typify linkage isomerization in that it occurs without ligand dissociation as an intermediate step; that is the process is intramolecular. This mechanistic conclusion is based upon isotope exchange and isomerization rate studies in water[50] and in liquid ammonia,[51] as well as on activation volume measurements.[52] It has been suggested that the activated complex may involve η^3-coordination of the nitrite ligand as in (**1**). This may also be the case for Ni^{II}-complex isomerizations,[42] although with this labile metal ion it has only been possible to demonstrate equilibrium (3), where there is a shift to the right (in chloroform solution) as the temperature is increased.[55-60]

$$[Ni(NO_2)_2(diamine)_2] \rightleftharpoons [Ni(ONO)_2(diamine)_2] \tag{3}$$

Thiocyanato (M—SCN) and isothiocyanato (M—NCS) complexes constitute another group of well-known linkage isomers and their properties are the subject of a detailed review by Burmeister.[61] Often the energy difference between the isomers is small and it is apparently dependent upon many subtle influences, such as the electronic and steric requirements of other ligands present and upon the nature of the solvent.[62] Considerable controversy, however, surrounds the interpretation of M—NCS/M—SCN isomerism in terms of steric and electronic factors.[63] A study of a variety of complexes of the type $[Pd(SCN)_2(diamine)]$ clearly demonstrated that increasing steric hindrance created by the diamines tended to promote *N*-bonding of the thiocyanate ligands. It is, of course, anticipated that linear M—NCS should be less sterically demanding than bent M—SCN. It was noted, however, that the actual bonding mode observed for a given complex depended upon kinetic factors and upon the nature of the solvents used in the preparation and the characterization of the complex.

In related tertiary phosphine complexes of the type $[Pd(SCN)_2(PR_3)_2]$, ^{31}P NMR spectroscopy has been used to identify linkage isomers. Thus, in an important study,[64] the distribution of linkage isomers of $[Pd(SCN)_2\{Ph_2P(CH_2)_nPPh_2\}]$ ($n = 1$-3), $[Pd(SCN)_2\{cis\text{-}Ph_2PCHCHPPh_2\}]$ and $[Pd(SCN)_2\{Ph_2PCH_2PPh_2\}]$ was investigated in a variety of solvents. Three linkage isomers can in principle exist for these square-planar complexes, *viz.* (**2a**)-(**2c**). For (**2a**) and (**2b**) different conformations of the bent Pd—SCN unit are also possible. At *ca.* 25 °C a single broad $^{31}P\{^1H\}$ signal due to time averaging over several environments was observed for each compound, but at −40 to −60 °C, well-defined resonances were found that could be assigned to the individual linkage isomers. The distribution of isomers was strongly influenced by the solvent, but for each complex detectable concentrations of all three linkage isomers were observed. Interestingly, similar complexes containing unidentate phosphines are more stable: the individual linkage isomers of *cis*- and *trans*-$[Pd(SCN)_2(PR_3)_2]$ can be distinguished by ^{31}P NMR studies at 25 °C.[65]

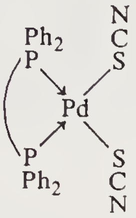

(**2a**)

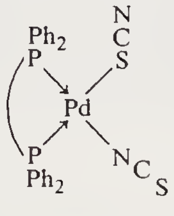

(**2b**)

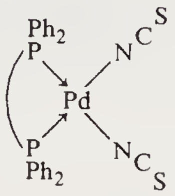

(**2c**)

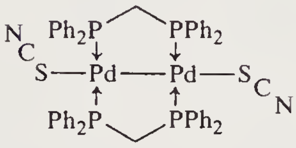

(**3a**)

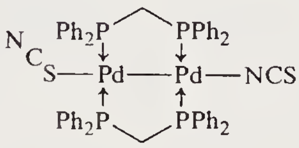

(**3b**)

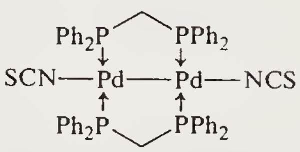

(**3c**)

Linkage isomerism also occurs in the dimeric palladium(I) complex $[Pd_2(SCN)_2\{Ph_2PCH_2PPh_2\}_2]$.[64,66] This complex can exist in the isomeric forms (**3a**)-(**3c**). Two different crystalline forms of the complex have been isolated. IR data for the solids suggested that these were the linkage isomesrs (**3a**) and (**3b**). In solution at room temperature, however, the complex exhibits a single ^{31}P NMR signal. Upon cooling the signal broadens and shifts, and at −35 °C the spectrum shows separate resonances due to (**3b**) (deceptively simple A_2B_2 pattern) and a singlet due to isomers (**3a**) and (**3c**). The variable temperature results are independent of concentration.

The kinetics of thiocyanato-isothiocyanato conversion have again been thoroughly studied using inert metal ion complexes for which the thermodynamically less stable form can be isolated *via* a catalyzed substitution process.[62] Thus, the base hydrolysis of $[Co(NO_3)(NH_3)_5]^{2+}$ in the presence of a large excess of thiocyanate ion gives an immediate mixture of $[Co(OH)(NH_3)_5]^{2+}$, $[Co(SCN)(NH_3)_5]^{2+}$ and $[Co(NCS)(NH_3)_5]^{2+}$. The less stable Co—SCN isomer predominates over the Co—NCS one and it isomerizes sufficiently slowly to be isolated by ion-exchange chromatography and to be purified by crystallization.[67] ($[Co(SCN)(NH_3)_5]_2\cdot 1.5H_2O$ is more soluble than orange $[Co(NCS)(NH_3)_5]Cl_2$.) The thiocyanato complex rearranges spontaneously by an intramolecular path to the more stable *N*-bonded isomer in neutral or dilute acid solutions, but the solid can be kept at 0 °C in the absence of light. At 80 °C the solid *S*-bonded isomer is rapidly converted into the *N*-bonded species. Other studies on solid $[CoSCN(NH_3)_5](N^{14}CS)_2$ have shown that at least 45% of the *N*-bonded isomerization product arises by an intermolecular dissociative mechanism.[68,69]

In contrast to these extensive studies of complexes of the triatomic ligands NO_2^- and NCS^-, little substantial information exists concerning linkage isomers of closely related ligands such as cyanate (NCO^-), fulminate (CNO^-) and selenocyanate ($NCSe^-$).[35-37] Some particular systems incorporating other small ligands have been well studied, an example being the conversion, *via* spontaneous and base-catalyzed pathways, of *O*- to *S*-bound thiosulfate in $[Co(S_2O_3)(NH_3)_5]^+$.[70] Also, *S* to *O* linkage isomerization has been observed when $[Ru(Me_2SO\text{-}S)(NH_3)_5]^{2+}$ is oxidized to the Ru^{III} species. The *O*-bound product is quite stable towards aquation and can be reduced to the *O*-bound Ru^{II} species, which then undergoes rapid *O* to *S* isomerization.[71] *N* to *N* isomerization, as in (**4a**) $\rightleftharpoons$ (**4b**), has been investigated in a Co^{III}-tetrazolate complex[72,73] and *N* to *C* isomerization has been observed for several cyanide ion complexes. Thus, by clever exploitation of the relative ease of water substitution in $[Co(CN)_5(H_2O)]^{2-}$, and the nucleophilicity of the cyanide nitrogen atoms in $[CoCN(NH_3)_5]^{2+}$, the novel dimers $[(NH_3)_5CoCNCo(CN)_5]$ and $[(NH_3)_5CoNCCo(CN)_5]$ were prepared for intramolecular electron transfer rate measurements.[74,75] In more recent work,[76] orange $[CoNC(dmgH)_2]$ ($dmgH_2$ = dimethylglyoxime), with ν_{CN} 2136 cm^{-1}, was isolated from the decomposition of $[Co(dmgH)_2(NH_3)_2][Ag(CN)_2]$ in boiling water. The *N*-bonded isomer isomerizes to the more stable *C*-bonded species (ν_{CN} 2186 cm^{-1}) when it is heated at 250–260 °C for 1 h, or when it is exposed to laser irradiation.

A variety of linkage isomer pairs have been produced from somewhat more complex ligands, such as substituted pyridines and benzoic acids, for example (**5a**) and (**5b**).[77,78] These complexes have been employed in detailed studies of inner-sphere electron transfer reactions in order to assess the importance of the nature and orientation of the bridge between redox centres on intramolecular electron transfer rates.[77-80]

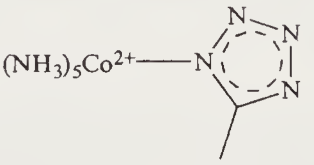

(4a)

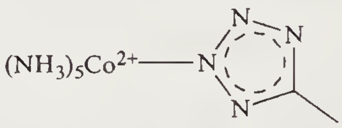

(4b)

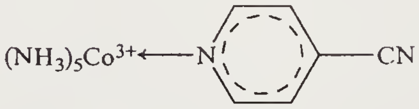

(5a)

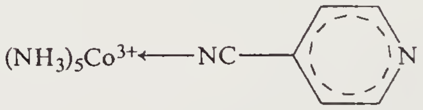

(5b)

Interest in linkage isomerism of complexes containing biologically important molecules such as amino acids, urea and its derivatives, purines, pyrimidines, polyphosphates, nucleosides and nucleotides has been substantial and is increasing.[38,39] As might be expected, different metal ions show quite different binding site preferences and hence can influence the properties of coordinated ligands in very different ways. Under acidic conditions, *N*-bound complexes of glycine and ethylglycinate with Ru^{III} undergo facile isomerization to *O*-bound forms,[81,82] but there is no evidence of a similar reaction for Co^{III} analogues.[83] A significant difference has also been found in the stability of urea derivatives of $[Co(NH_3)_5]^{3+}$ and $[Rh(NH_3)_5]^{3+}$. Whereas the reaction of urea with $[Co(OSO_2CF_3)(NH_3)_5](CF_3SO_3)_2$ gives only the *O*-bound isomer,[84] the corresponding rhodium complex reacts to produce a separable mixture of *N*- and *O*-bonded linkage isomers.[85] At pH 2.05 and 25 °C, the decomposition of the $[Rh(NH_2CONH_2)(NH_3)_5]^{3+}$ ion to $[Rh(NH_3)_6]^{3+}$ by way of $[Rh(NCO)(NH_3)_5]^{2+}$ proceeds *ca.* 30 000 times faster than the analogous reaction of urea under similar conditions.

5.2.3 Polymerization Isomerism

In conventional organic nomenclature, a polymer is not considered to be an isomer of the repeating molecular unit, because the molecular formulas formally differ. This is a somewhat arbitrary distinction, however, because it is never really an isolated, single molecule of monomer that is compared with the polymer. In an aggregate of monomer molecules, intermolecular forces exist and the constitutional difference from an aggregate of polymer molecules is simply that some intermolecular forces have been converted into 'true' chemical bonds. In any case, the term 'polymerization isomerism' has had a long-standing use in coordination chemistry. It may refer

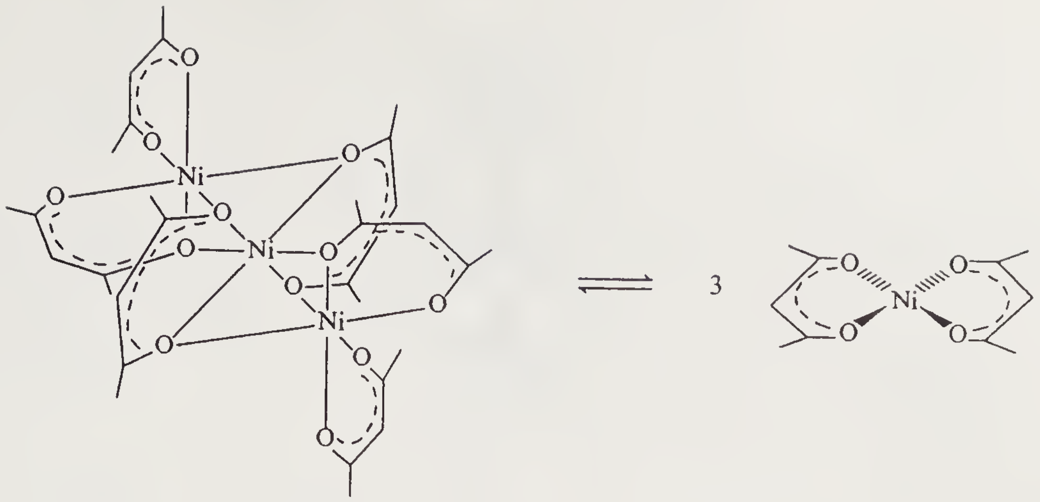

(6a) **(6b)**

to true polymerization, as seen in [Ni(acac)$_2$] (acac$^-$ = 2,4-pentanedionate), which is green and trimeric (**6a**) in non-coordinating solvents at low temperatures (80 °C), but is red and monomeric (**6b**) at high temperatures (200 °C).[86–89] Solid state oligomerization resulting from ligand bridging of this kind is very common[90,91] and in many simple solids, such as Zn(CN)$_2$ and PdCl$_2$,[92] for example, true polymerization can be considered to have occurred. It leads, of course, to an increase in the coordination number of the metal, although consequences of this, as in the case of the yellow β-isomer of [NiCl$_2$(2,9-dimethyl-10-phenanthroline)]·CHCl$_3$ (**7**), have not always been clearly recognized on the basis of simple spectroscopic measurements.[93,94]

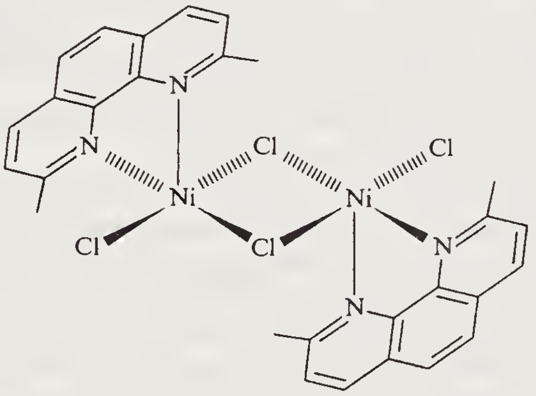

(**7**)

Usually, however, the term 'polymerization isomerism' is applied to a form of coordination isomerism that is possible when multiple units of a given metal ion–ligand aggregate are considered. Thus, $[Pt(NH_3)_4][PtCl_4]$ and $[PtCl(NH_3)_3][PtCl_3(NH_3)]$ are polymerization isomers of $[Pt(NH_3)_2Cl_2]$ (degree of polymerization = 2), as are $[Pt(NH_3)_4][PtCl_3(NH_3)]_2$ and $[PtCl_4][PtCl(NH_3)_3]_2$ (degree of polymerization = 3). Although few examples are known, this group of complexes can be considered important if only because of the nature of 'Magnus' Green Salt', $[Pt(NH_3)_4][PtCl_4]$.[95] The unusual deep green colour of this material (*cis*- and *trans*-$[Pt(NH_3)_2Cl_2]$ are both pale yellow, $[PtCl_4]^{2-}$ is brown, and $[Pt(NH_3)_4]^{2+}$ is white) is attributed to Pt—Pt interactions that occur in the columnar stacks of alternating planar anions and cations that make up the solid. A similar structure, associated again with intense colour and high (and anisotropic) conductivity, is found in many compounds that can be formally regarded as containing platinum in an oxidation state between +2 and +4, although they are better considered as mixed valence Pt^{II}/Pt^{IV} species.[96,97] The intense colour of these compounds is then associated with intervalence transitions,[98–102] corresponding to what might be termed electronic isomerism, $Pt^{II}\cdot Pt^{IV} \rightarrow \{Pt^{III}\}_2$. There is evidence that this mixed valence description may also be appropriate for some Ni^{III} compounds.[103–105]

The structure of one of the best known mixed valence platinum compounds, 'Wollfram's red salt', $[Pt(NH_2Et)_4][PtCl_2(NH_2Et)_4]Cl\cdot 4H_2O$, has a linear chain structure involving eclipsed ethanamine groups and unsymmetrically bridging chlorine atoms, (**8**).[106] A comprehensive listing

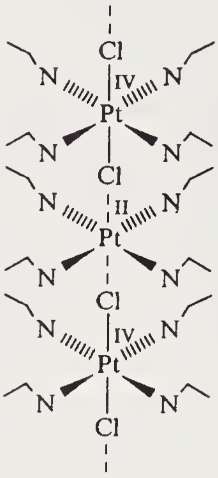

(8)

of similar complexes may be found in the review by Clark concerning Raman spectroscopy of such compounds.[107]

5.3 CONFIGURATIONAL ISOMERISM (STEREOISOMERISM)

At least three objectives may be taken to be paramount in the study of the stereochemistry of coordination compounds: (i) an attempt to gain a general understanding of the factors that determine the shapes of molecules;[1] (ii) the origins of specificity and/or selectivity of substitution and other processes occurring at or near metal centres;[22,23,62,108] and (iii) to suggest, on the basis of the analysis of relatively simple systems, the factors that may be operating in the highly complex and usually highly stereospecific reactions of living systems.[14,38,109] These objectives are not necessarily ends in themselves; one application, for example, is the design of chiral hydrogenation catalysts for α-amino acid and hence protein synthesis.[110]

The study of stereochemistry inevitably involves the isolation and identification of configurational isomers or, as they are generally known, stereoisomers, although emphasis on the former aspect is now less than in the past due to the diagnostic utility of NMR spectroscopy in solution studies. Nevertheless, the isolation of stereoisomers is fundamental to the study of stereochemistry and provides the basis for the resolution of chiral compounds. Thus, during the period 1893–1914 Werner established the octahedral geometry of six-coordinate compounds and the square-planar structure of four-coordinate complexes studied, by the isolation of isomeric complexes formed by a given transition metal with two different types of ligands, and by the optical resolution (separation of enantiomers) of metal chelates.[2,111–113]

5.3.1 Stereochemical Language

The terminology applied in the description of stereochemistry has been developed over a long period and continues to be frequently reviewed. Changes have derived both from the understanding of increasingly complex phenomena and from the significance attached to particular areas of study and have often led to confusion and inconsistency in the literature. Problems associated with introduction of the term diastereomer and abandonment of the term diastereoisomer and with the use of *E*/*Z* (*entgegen*/*zusammen*) in place of *cis*/*trans*, for example, have been discussed by Eliel.[114] More complex and general problems have also recently been discussed.[115,116]

As noted previously, the classification of stereoisomers preferred by contemporary organic chemists is the enantiomer–diastereomer dichotomy[17] and this may be quite conveniently applied to coordination compounds. Thus, complexes (**9a**) and (**9b**) are enantiomers, but (**9a**) and (**9c**), and (**9b**) and (**9c**), are diastereomers. Older terminology might have led to the description of A and B as optical antipodes and to (A+B) and C as geometrical isomers.

In principle, if not necessarily in practice, new coordination complexes are generated by substitution of particular ligands of an existing species. If the original complex contains two (or more) chemically identical groups and either one is replaced during a single substitution, then it is possible that enantiomeric or diastereomeric products may result. In the former situation, the

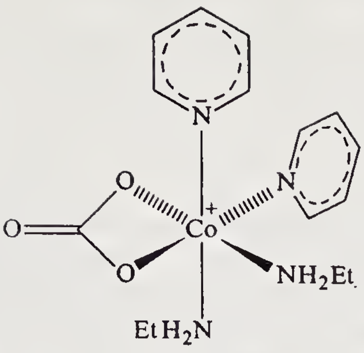

(9a)

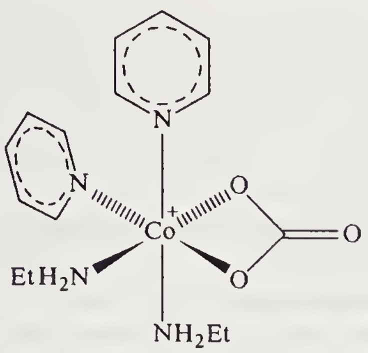

(9b)

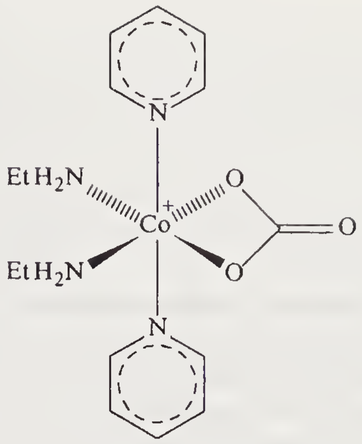

(9c)

original ligand sites are said to be enantiopic, and in the latter, diastereotopic. Thus, the sites C,C in (**10**) are enantiopic and in (**11**) they are diastereotopic (equations 4 and 5). If neither enantiomers nor diastereomers result, the sites are said to be homotopic, as indeed are the sites C,C of (**12**) (equation 6). Obviously homotopic and enantiotopic sites are both symmetry-related sites but for enantiotopism the symmetry cannot only be rotational.

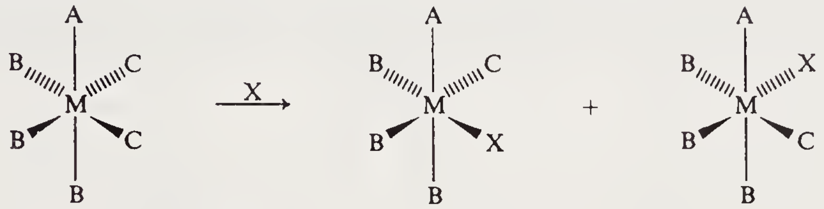

(4)

(10)

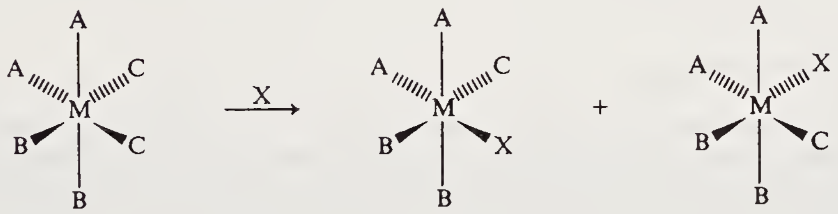

(5)

(11)

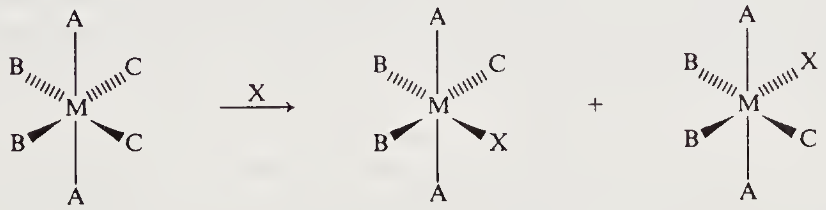

(6)

(12)

When equivalent components of a molecule can be altered in turn to produce stereoisomers, that component which may be associated with an atom or symmetry planes or axes is termed stereogenic.[117–119] A chemical process that is stereogenic can produce several stereoisomers, in which case it is said to be stereoselective if the products are not present in equimolar amounts, and stereospecific if only one stereoisomer is produced. A detailed mathematical model for the prediction of the extent of stereoselectivity in organic syntheses has been developed by Ruch and Ugi.[120]

In describing a stereoisomer, it is perhaps most important initially to define whether or not it is chiral. The origins of chirality (optical activity) in coordination compounds and important experimental results have been recently reviewed.[112,113,121,122] The classical example of chirality or enantiomerism in coordination chemistry is that of octahedral complexes of the type [M-(bidentate)$_3$]. These exist in the propeller-like,[123] non-superimposable, mirror-image forms (**13a**) and (**13b**). Synthesis of this type of complex from M and the bidentate ligand in an achiral environment such as water results in an equimolar mixture of the two stereoisomers. The product

(13a)

(13b)

is termed a racemate or racemic mixture of the stereoisomers and the process of resolution is required to obtain the separate enantiomers.[112,113] Provided the complex is stereochemically rigid, physical separation and storage of the enantiomers may be possible. In a chiral environment, it may also be possible to isolate one enantiomer of a stereochemically non-rigid species.[124,125] It should be noted that if an achiral molecule undergoes a stereogenic process to give a chiral species, the original molecule is described as prochiral.[117]

Defining a molecule to be chiral does not mean that it cannot also be described as a diastereomer. Diastereomers are non-mirror-image isomers of one another and a diastereomer of a given molecule (chiral or achiral) may itself be chiral or achiral. A very familiar illustration of this point is given by the stereoisomers of $[CoCl_2(en)_2]^+$ (en = 1,2-enthanediamine). The *cis* and *trans* geometric isomers of this material (**14a**) and (**14b**) are diastereomers with the *cis* isomer alone existing as an enantiomeric pair. (This simple description of isomerism for $[CoCl_2(en)_2]^+$ neglects conformational isomers, or conformers, but is nevertheless complete on the time scale of laboratory manipulations.)

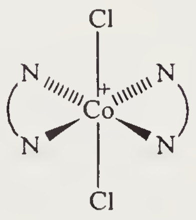

(14a) *trans*

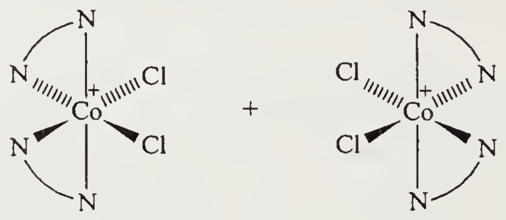

(14b) *cis*

5.3.2 Chirality and Symmetry

A molecule that lacks all symmetry and is therefore termed asymmetric belongs to the class of chiral compounds, but so also do molecules containing some symmetry elements, provided these do not include improper axes of rotation, S_n ($n \geqslant 1$). Thus, simple rotational axes of symmetry may be present and the class of chiral molecules retaining C_n or D_n symmetry is known as the dissymmetric group.[112,113,121,126,127] This includes a larger number of metal chelates, so that whereas a classic example of a chiral organic molecule is one such as alanine, $CH_3CH(NH_2)CO_2H$, which contains an asymmetric carbon atom, the classical example of a chiral inorganic molecule is Werner's 'hexol' (**15**), of D_3 symmetry.[9,21,31]

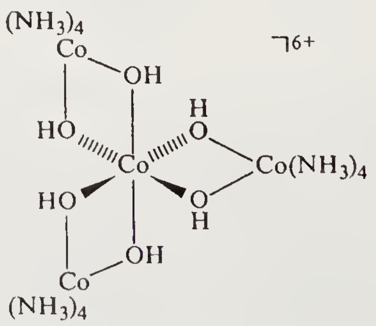

(15)

The interconversion of enantiomers can be viewed in general as requiring inversion at a particular atom or twisting about an axis of the molecule. Provided these processes are inhibited to some degree, the chirality of a molecule will be detectable so that any chiral species may be said to contain centres and/or axes and/or planes of chirality.[115,116,117,118] The precise meanings and utility of these concepts are, however, a matter of some debate,[115,116,129] and they have not been extensively applied to coordination compounds.

5.3.3 Stereochemical Nomenclature

It has become increasingly clear that the classification of inorganic stereoisomers with the use of descriptors such as *cis*, *trans*, *fac*(ial) and *mer*(idional) as codified by IUPAC[130] and as used, for a simple system, in previously describing the isomers of $[CoCl_2(en)_2]^+$, is inadequate. For example, four geometric arrangements are possible for octahedral complexes of the type $[MA_3BCD]$ (one *mer* and three *fac*) and for octahedral $[MA_2BCDE]$ there are nine possible diastereomers, six of which are chiral. In this context many other difficulties have been discussed by Saito.[131]

The *Chemical Abstracts* index names for organic molecules are[132] based on the Cahn–Ingold–Prelog (CIP) system, in which an *R* or *S* symbol is assigned to a three-dimensional valence-bond representation of the molecule on the basis of a ranking of ligands in accordance with a sequence rule.[133,134] The sequence rule provides an order of preference (or seniority) for ligands based on a series of sub-rules. Although a full discussion of the sequence rule is beyond the scope of the present brief account, it will be sufficient for the examples that follow to consider sub-rule 1 only, which states that atoms of higher atomic number are preferred to those of lower. The rule is applied to each of the ligands, working outwards atom by atom along the bonding sequence until all of the ligands are arranged in order. Free electron pairs are considered as ligands of atomic number zero. For example, in the tetrahedral molecule [MABCD], in which the order of preference of the ligands is $A_1 > B_2 > C_3 > D_4$ (where > denotes 'preferred to'),[135] an absolute descriptor can be assigned by viewing the model from the side remote to the least preferred ligand D and observing if the route A–B–C involves a right-handed (clockwise) or a left-handed (anticlockwise) turn. If right-handed, the enantiomer is said to be the *R*-form (*R* from Latin *rectus* = right) (**16a**), if left-handed, the enantiomer is the mirror-image *S*-form (*S* from Latin *sinister* = left) (**16b**).[133,134]

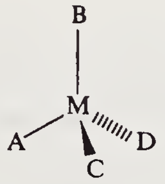

(**16a**) *R*

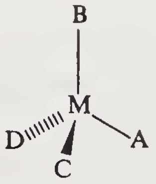

(**16b**) *S*

The stereochemistry of mononuclear coordination compounds[136] is expressed by special descriptors that consist of up to four parts: (a) a symmetry site term that identifies the gross symmetry of the metal site; (b) a configuration number that defines the geometry completely in achiral systems (for example, in simple square-planar complexes); (c) a chirality symbol that may be *R* or *S* if the central atom geometry is tetrahedral, Δ or Λ if the compound is a bis(bidentate) or tris(bidentate) octahedral complex, and *A* (anticlockwise) or *C* (clockwise) for other systems; and (d) a ligand segment that defines the stereochemistry of the ligand (if necessary). The symmetry site terms for coordination numbers four to six are the following: CN4, *T*-4 (tetrahedron), *SP*-4 (square-plane); CN5, *TP*-5 (trigonal bipyramid), *SP*-5 (square pyramid); CN6, *OC*-6 (octahedron), *TP*-6 (trigonal prism). As with all systems of stereochemical nomenclature, these descriptors can become unwieldy and obscure and are no substitute for a well-drawn structural formula.

For tetrahedral compounds (*T*-4) containing achiral ligands, only optical isomerism is possible. The two common situations that give rise to non-superimposable mirror-image structures are shown in Figure 5(a). The molecules [MABCD] are asymmetric and *R*- and *S*-forms can be readily identified by application of the sequence rule. The tetrahedral complexes $[M(AB)_2]$ are dissymetric with C_2 symmetry. In order to assign a sequence rule symbol *R* or *S* to molecules of this type it is necessary to differentiate the bidentates by priming, as shown in Figure 5(a). The primed donors are considered to be of lower priority. The sequence rule symbol is then determined by observing the handedness of the route A_1-B_2-A'_1-B'_2 when the structure is viewed down the twofold axis.

Square-planar structures are unambiguously identified by a single configuration number, in addition to the symmetry site term (*SP*-4). The configuration number is simply the priority number of the ligand *trans* to the ligand of highest priority as determined by the sequence rule. The well-known *cis–trans* prefixes cause difficulties in other than $[MA_2B_2]$ systems. The *E*/*Z* prefixes of modern organic nomenclature, similarly, are not generally applicable to four-coordinate square-planar complexes. Examples of assignments are given in Figure 5(b).

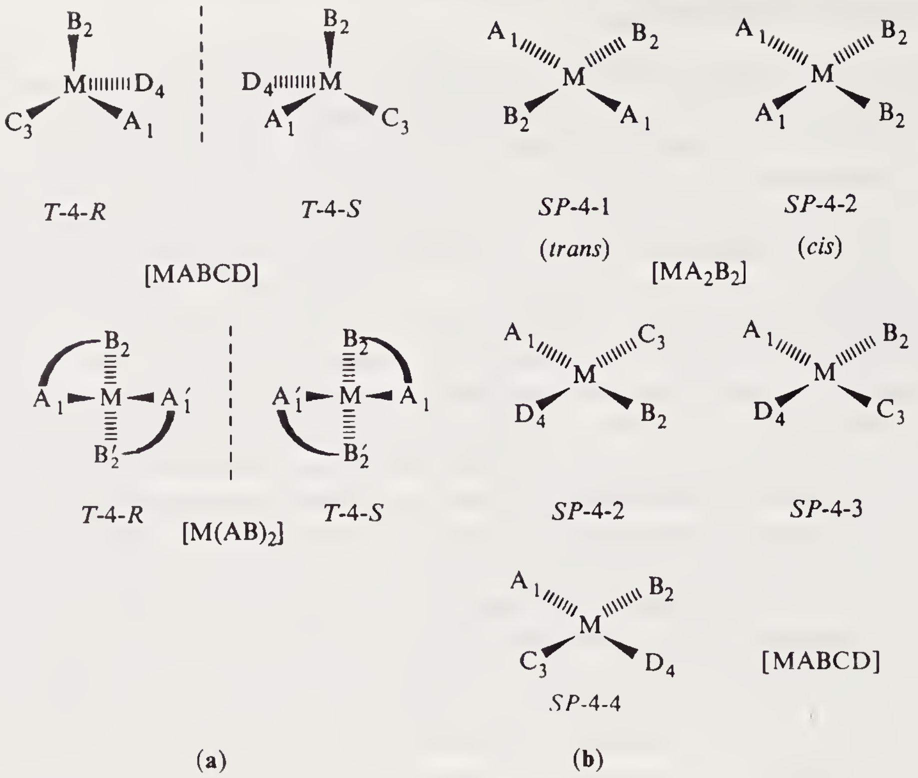

Figure 5 Stereochemical descriptors for (a) chiral tetrahedral compounds, and (b) square-planar complexes

Octahedral complexes (*OC*-6) require a two-digit configuration number that consists of the CIP priority numbers of the ligating atoms *trans* to the ligating atom of priority 1 (first digit) and *trans* to the most preferred atom in the plane perpendicular to the principal axis that contains the ligand of priority 1 (second digit). If two ligands are given priority 1 on the basis of the CIP rules, the preferred axis is the one that obeys the principle of maximum *trans* difference, that is 1,3 takes precedence over 1,2, *etc.* For octahedral compounds that contain only unidentate ligands, or no more than one bidentate, chirality is specified by the direction of the ordering of the ligands in the plane perpendicular to the principal axis, when viewed with the donor atom of lowest priority on the remote side. Donor atoms of *R* absolute configuration take precedence over those of *S* absolute configuration.[137] Some examples of the use of this versatile stereonotation system are given in Figure 6.

For octahedral complexes containing two bidentates in a *cis* arrangement, or three bidentates, the chirality is denoted by Δ for a right-handed and Λ for a left-handed helix, as specified by the IUPAC recommendations.[138,139] In Figure 7(i), line *aa* is the axis of the cylinder traced out by the helix, and *bb* is a tangent to the cylinder and is parallel to the helix. In (ii), the two non-orthogonal skew lines are shown, as seen when viewed down the perpendicular line *cc* that joins *aa* and *bb*. Since *aa* has to be moved to the left to be brought into coincidence with *bb*, then *aa* and *bb* uniquely define the left-handed helix. The opposite is true for the right-handed helix. It should be noted that the line representing the axis of the cylinder, *aa* in this case, must be placed behind the tangential line *bb* in order to define the helicity.

To define the configurational chirality (*vide infra*) of octahedral [M(bidentate)$_2$(unidentate)$_2$] and [M(bidentate)$_3$] complexes, their helicity is assigned by associating pairs of edges of the coordination sphere spanned by chelate rings with the helix axis and tangent described above. This system has the advantage over earlier, similar systems, such as the $P(C_3)$, $M(C_2)$ convention developed by Mason,[126] in that it is immaterial which edge is considered the axis and which the tangent. It is, however, only straightforwardly applied to bis- and tris-bidentate complexes because in the former there is only one pair of edges to be considered and in the latter all possible pairs must have the same helicity, so that it is only necessary to consider any one. Illustration of this method of determining chirality is given in Figure 8. For either type of complex, once axis *aa* is nominated, a skew line representing one other chelate ring determines the handedness of the helix. Note that it is the distribution of the chelate rings alone that determines the chirality. The geometrical relationship of the donor atoms with unsymmetrical bidentates is a matter of diastereomerism rather than chirality in these dissymetric systems. Ref. 138 should be consulted for a full discussion and for the application of the rules to complexes containing multidentates.

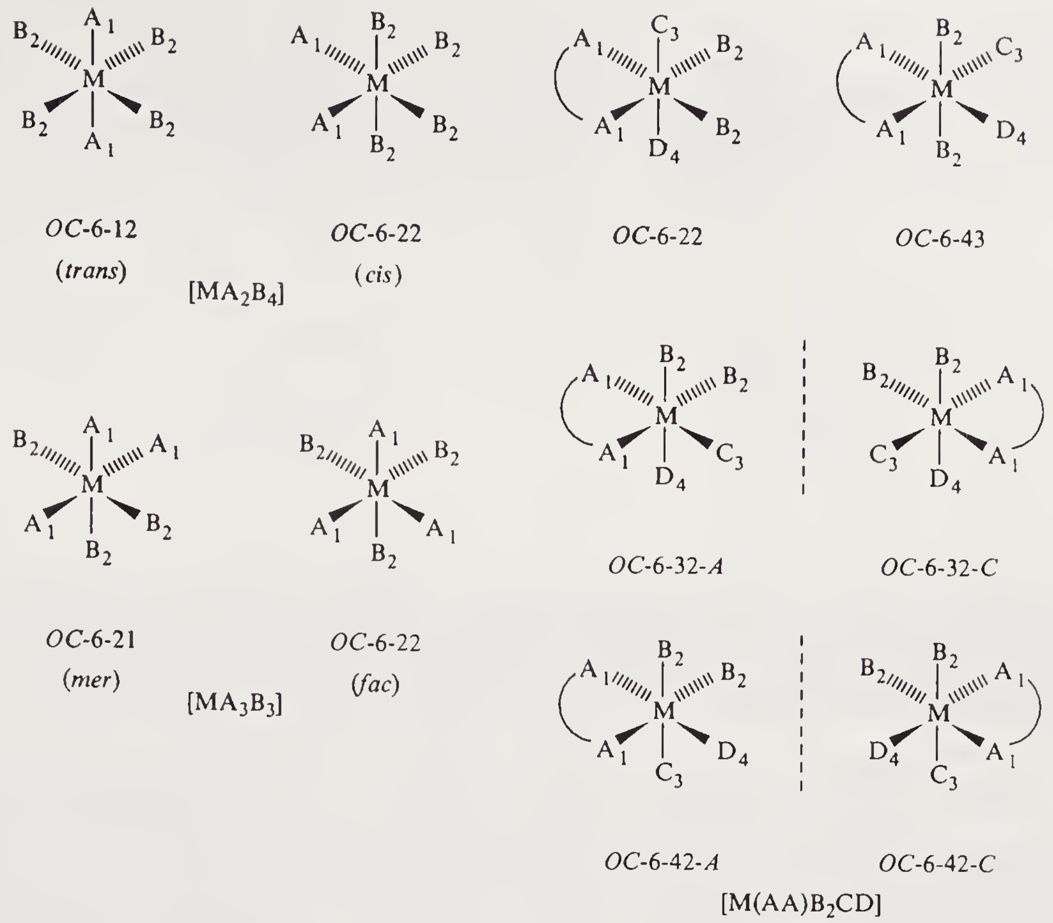

Figure 6 Stereochemical descriptors for some important types of octahedral complexes

An additional chiral reference system based on chiral pairs of oriented lines has recently been proposed.[140]

5.3.4 Sources of Chirality

In assessing the full possible complexity of stereoisomerism in coordination compounds it is convenient to consider that particular structural features may independently contribute to chirality.[22,121,122,141] Thus, the array of donor atoms and/or chelate ring spans, regardless of the

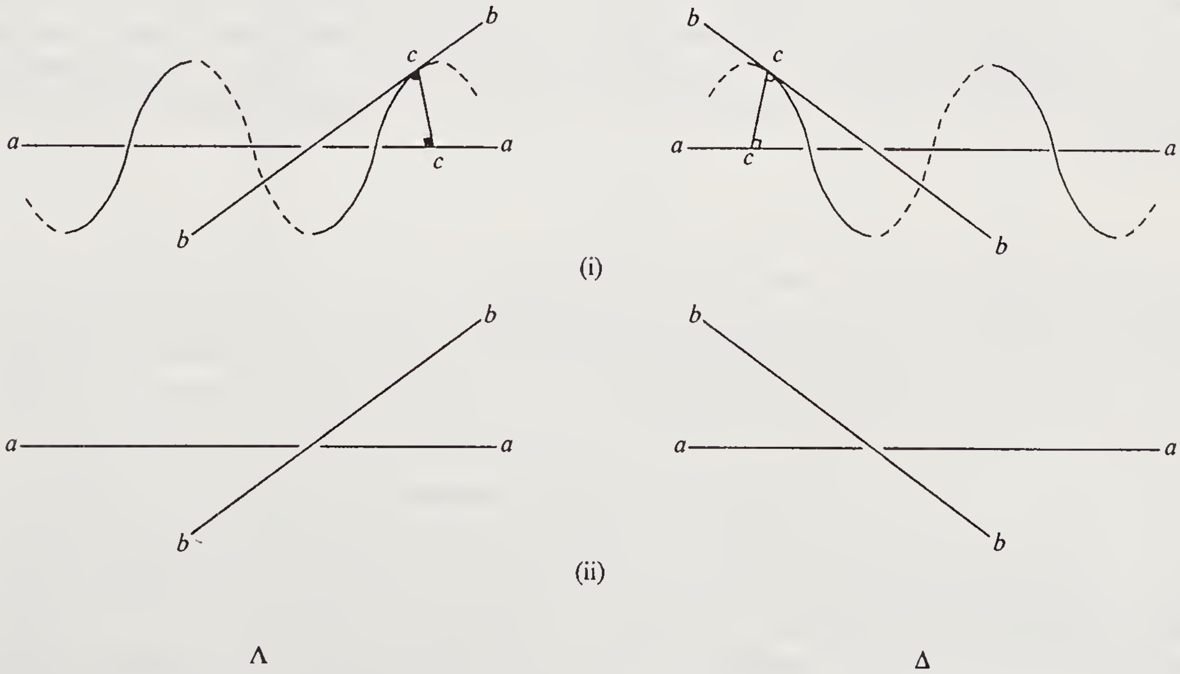

Figure 7 Specification of helicity in terms of skew lines representing axis and tangent

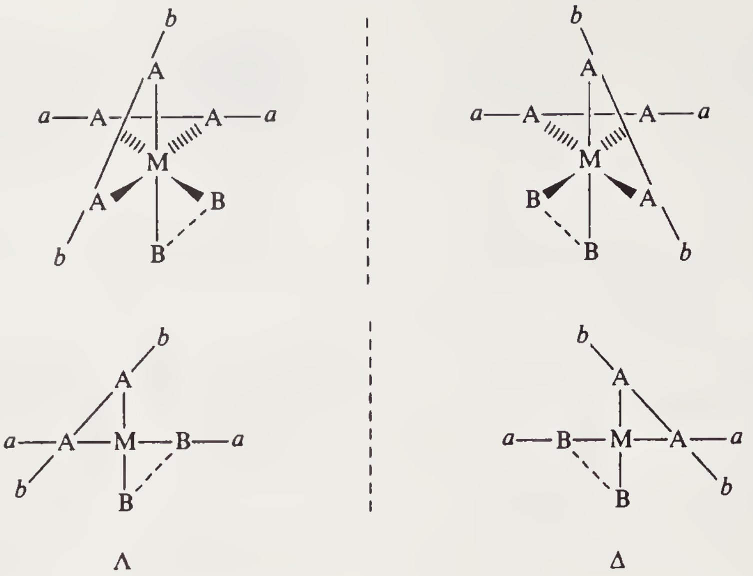

Figure 8 Schematic representation of the relationship of octahedral $[M(AA)_2B_2]$ or $[M(AA)_2(BB)]$ structures to left- and right-handed helices. Note that the line *aa* that represents the helix axis must be placed behind the tangential line *bb* in order to define the helicity. It should also be noted that it is immaterial which chelate-spanned edge is taken as the axis or the tangent and that in tris(bidentate) species it is only necessary to consider one pair of edges

actual form of the chelate ring, can be chiral and is then said to give rise to configurational chirality about the metal ion. If the chelate rings, considered in isolation, are able to adopt chiral conformations, a contribution to the overall structure from conformational chirality is possible. A third contribution, termed the vicinal effect, arises when either the donor atoms are asymmetric or the chelate rings incorporate asymmetric centres. These factors are not necessarily independent in that, for example, the dimensions or bite of a chelate ring may cause only a single set of asymmetric donor atom configurations to be compatible with a particular distribution of a multidentate ligand about the metal ion. Thus, in the complex (*OC*-6-22)-$[CoCl_2(trien)]^+$ (or *cis*-α-$[CoCl_2(trien)]^+$, where trien = 1,8-diamino-3,7-diazaoctane), the *C* configuration requires both secondary *N*-donor atoms to adopt the *R* configuration since, with normal bond lengths retained, the CH_2CH_2 chelate link will not span the donor atoms if either has or both have the *S* configuration.[142] Ignoring conformational factors, it is therefore expected that only two enantiomeric forms of this complex would exist. The actual structure, including ring conformations, of the *C* enantiomer is shown in (**17**). Analysis of some other systems will be given below, after a more detailed consideration of the separate factors. It should be emphasized, however, that it is purely a matter of convenience to apply the configuration–conformation–vicinal factorization of structure. Physical properties that reflect stereochemistry, such as the rotational strength of $d-d$ transitions in chiral complexes, have been shown to obey an approximate additivity with respect to these contributions, but theory does not demand an analysis in such terms.[141] It should also be noted that although configuration, conformation and vicinality have been introduced as factors contributing to chirality, it is common to find that various chiral units may combine to give an overall achiral structure and hence this analysis of stereochemistry is of quite general application.

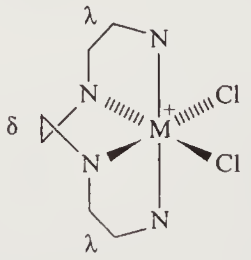

(**17**) *OC*-6-22-*C*-[*R*-(*R**,*R**)]-(λ,δ,λ)

5.3.4.1 Configurational elements

Chirality in a coordination complex can arise from the arrangements of unidentate ligands alone. Few examples of the resolution of such complexes are known, however, and unless species such as $[SP(^{16}O)(^{17}O)(^{18}O)]^{3-}$ are[143] considered as coordination complexes, the only cases are those of (OC-6-32)-$[MA_2B_2C_2]$ ('all *cis*' octahedral $[MA_2B_2C_2]$)[144–147] compounds. Thus the partial resolution of *cis,cis*-$[PtX_2(NO_2)_2(NH_3)_2]$ (X = Cl, Br) by preferential adsorption on chiral quartz crystals, was reported in 1965.[144] The enantiomers (**18a**) and (**18b**) did not racemize (directly convert to and from A and C forms), but slowly converted over 24 h at 25 °C into an achiral diastereomer.

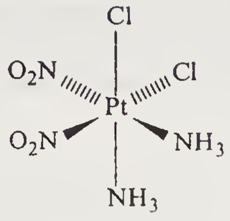

(**18a**) *OC*-6-32-*A*

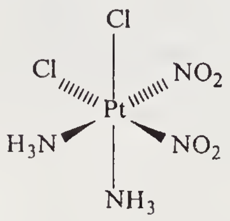

(**18b**) *OC*-6-32-*C*

Many more examples of configurationally chiral metal complexes are known when one,[22,147] two or three[112,113,121] bidentate ligands are present, although again they are limited (in the sense that resolutions have been performed) to octahedral species incorporating inert metal ions such as Co^{III}, Cr^{III}, Rh^{III}, $Ru^{III,II}$ and Pt^{IV}. Silicon(IV) in $[Si(acac)_3]^+$ is a well-known[148] but exceptional case involving a configurationally stable non-transition metal ion. To exhibit what would be regarded as 'pure' configurational chirality, the chelate rings in these complexes must be achiral and the simplest cases are those formed by planar, symmetrical, bidentate ligands such as the acetylacetonate or oxalate ions.

In the numerous octahedral bis- and tris-bidentate complexes of this type, the configurational chirality can be associated simply with the array of chelate-spanned edges, and is designated Δ or Λ, as in (**19a**) and (**19b**), as discussed previously. The nature of the donor atoms is immaterial in this regard, although their consideration is necessary in the analysis of diastereomers with unsymmetrical bidentate ligands and in the assessment of any quantitative measures of chirality, such as the rotational strengths of electronic transitions.[121,149]

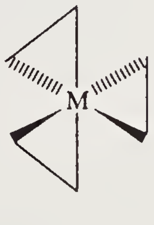

(**19a**) *OC*-6-Λ

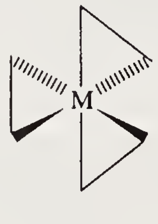

(**19b**) *OC*-6-Δ

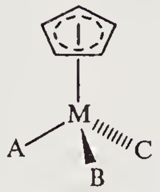

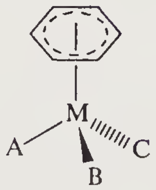

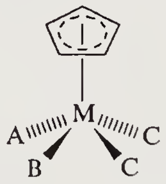

(**20**) (**21**) (**22**)

It is interesting to note that whereas four different unidentate ligands are required for asymmetry in a tetrahedral complex, only three are needed for the octahedron. An asymmetric or dissymmetric tetrahedral complex involving a transition metal ion has not yet been resolved (see, however, ref. 246). Enantiomers of so-called pseudo-asymmetric organometallic compounds (**20**)–(**22**), in which a coordination site on a tetrahedron or square pyramid is occupied by an η^5-cyclopentadienyl or η^6-arene ring (or similar π-donor ligands), have been well characterized however, due largely to the efforts of Brunner and coworkers.[150,151]

The absolute configurations of many coordination complexes showing purely configurational chirality have been included in comprehensive compilations of structural data.[131,152,153] In essentially all cases these absolute configurations have been determined by Bijvoet's anomalous dispersion X-ray technique.[154] Complexes of this type have also been thoroughly examined in relation to analysis of exciton coupling in their circular dichroism spectra as an alternative means of assigning absolute configuration.[149]

5.3.4.2 Conformational elements

Conventional Newman projections of a free 1,2-disubstituted ethane, such as 1,2-ethanediamine (the archetype of a vast number of bidentate ligands), suggest three conformational isomers are possible, *viz.* (**23a**)-(**23c**). Only the *gauche* forms, (**23a**) and (**23b**), will permit coordination of both amino groups to one metal ion (to form a chelate ring) and since they are non-superimposable mirror-image forms, an M(en) chelate is expected to have two puckered, enantiomeric forms,[155] usually represented as (**24a**) and (**24b**). The helicity of these conformations can be specified by associating the chelate edge spanned by the ligand and the C—C bond of the ligand with the axis and tangent to a helix (Figure 9). To distinguish chelate ring helicity from configurational helicity, the lower case symbols δ and λ are used.[138,156]

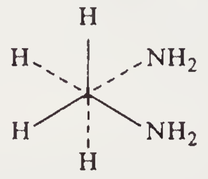

(23a)

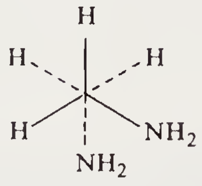

(23b)

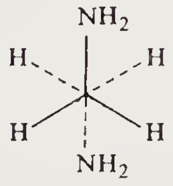

(23c)

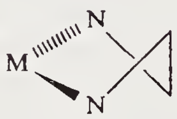

(24a)

(24b)

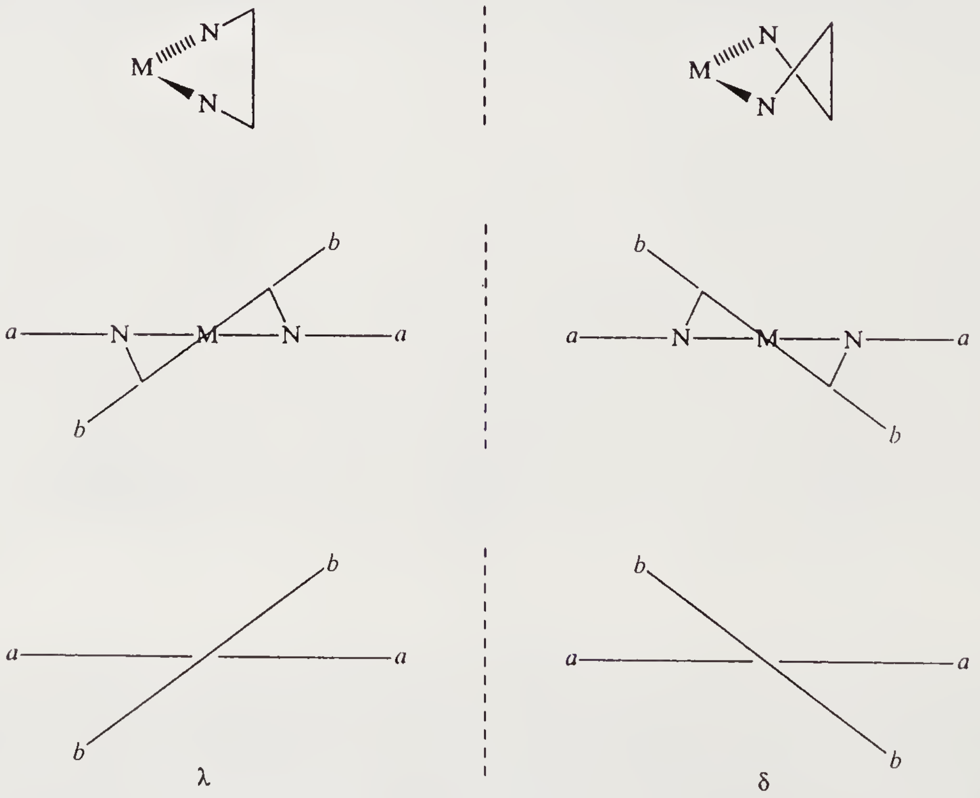

Figure 9 Specification of helicity in the five-membered (1,2-ethanediamine)metal ring

In principle, any non-planar chelate ring can adopt a chiral conformation and thereby endow chirality on the complex as a whole. In six-membered and larger rings, helicity may be specified in terms of a pair of skew lines associated with the chelated edge and an imaginary link between the ligand atoms bonded directly to the two donor atoms. The conformational behaviour of large chelate rings has not been as extensively studied as that of five-membered rings and it is possible that many chiral conformers of closely similar energy could be present.[22] The introduction of a substituent to the ring, however, can lead to conformational 'locking' by energetically favouring one particular form, usually that where the substituent adopts an equatorial disposition.[22] In octahedral complexes, for example, 1,2-propanediamine (pn) appears to be exclusively in this form.[157] This means that conformational and vicinal elements of chirality are interactive in such systems, since (*R*)-pn will give a chelate predominantly in the λ conformation and (*S*)-pn one in the δ conformation (Figure 10).

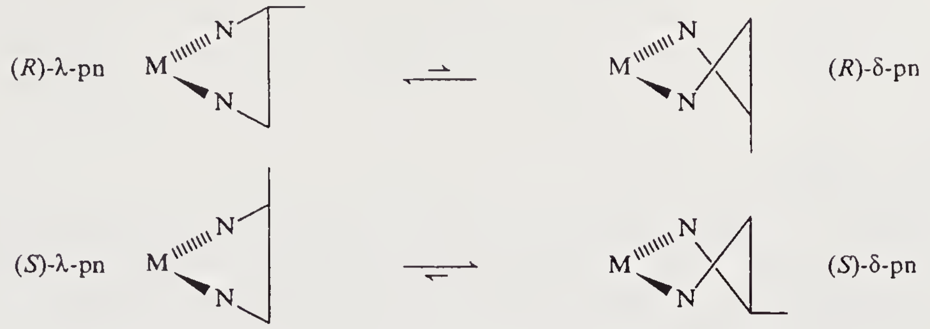

Figure 10 Conformations of the (1,2-propanediamine)metal ring

The study and calculation of the relative stability of conformations is known as conformational analysis and is an aspect of molecular mechanics.[158] NMR spectroscopy is an exceptionally useful tool for the experimental study of conformational interconversions and its application to five- and six-membered chelate rings has been reviewed by Hawkins and Palmer.[159] (Rings containing *As*-, *S*- and *Se*-, as well as *O*- and *N*-donors, have been considered.) A more recent review provides a comprehensive coverage of molecular mechanics applications in coordination chemistry and includes a discussion of complicated multidentate ligand systems.[160] The seminal paper on conformational analysis in coordination compounds was that of Corey and Bailar.[161] Their relatively crude calculations suggested that a significant energy difference existed between the dissymmetric C_2 $\lambda\lambda$ (or $\delta\delta$) conformer and the achiral C_{2h} $\delta\lambda$ conformer of (*OC*-6-12)-$[CoX_2(en)_2]^+$ (*trans*-$[CoX_2(en)_2]^+$) and structural evidence seems to indicate that this is so, although in the opposite sense to that calculated. More significantly, however, the Corey–Bailar calculations indicated quite large energy differences between the $\Lambda\lambda\lambda\lambda$ and $\Lambda\delta\delta\delta$ (or $\Delta\delta\delta\delta$ and $\Delta\lambda\lambda\lambda$) diastereomers of complexes such as $[Co(en)_3]^{3+}$ and the $\Lambda\delta\delta\delta$ structure found in $\{(+)_{589}$-$[Co(en)_3]Cl_3\}_2\cdot NaCl\cdot 6H_2O$ was that predicted to be the more stable.[162] In this diastereomer, the C—C bonds of the en ligands are approximately parallel to the C_3 axis in the complex, leading ultimately to its designation as the *lel*$_3$ isomer. In the $\Lambda\lambda\lambda\lambda$ (or $\Delta\delta\delta\delta$) form, the C—C bonds are obverse to this axis and the isomer is designated *ob*$_3$.[163,164] In solution, an equilibrium between all conformational diastereomers appears to exist, the *lel*$_2$*ob* forms ($\Lambda\delta\delta\lambda$ and/or $\Delta\delta\lambda\lambda$) being dominant[165] due to an entropic (statistical) factor that compensates for enthalpic differences (the quantities usually calculated by molecular mechanics).

In six-membered chelate rings such as those formed by 1,3-propanediamine (tn), at least two conformational energy minima, which correspond to an achiral chair structure (**23a**) and the chiral skew- or twist-boat forms (**25b**) and (**25c**),[166–168] occur and both have been observed in crystal structures.[169–176] The possible conformational isomerism in tn complexes is therefore even more involved than in en complexes.[177] In (*OC*-6-12)-$[CoCl_2(tn)_2]^+$ (*trans*-$[CoCl_2(tn)_2]^+$), for example, there are two achiral bis(chair) forms (**26a** and **26b**), two enantiomeric (chair, skew-boat) forms (**26c** and **26d**), one achiral form (**26e**) and two enantiomeric bis(skew-boat) forms (**26f** and **26g**). Several of these have been isolated in conformationally locked systems.[178–180]

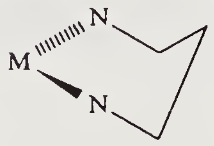

(25a)

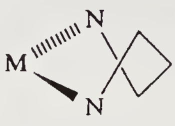

(25b)

(25c)

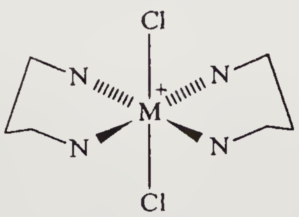

(26a)

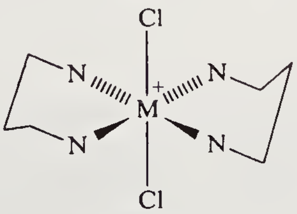

(26b)

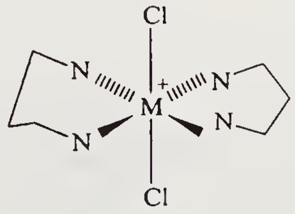

(26c)

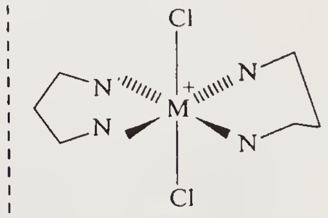

(26d)

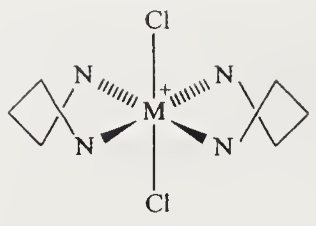

(26e)

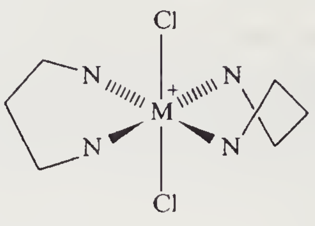

(26f)

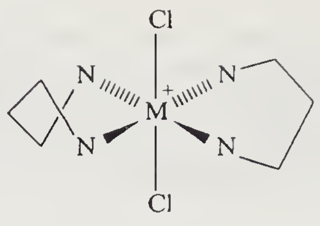

(26g)

5.3.4.3 Vicinal elements

The rather obscure term vicinal is used to denote ligand-based sources of chirality, other than those due to conformation.[181] These sources may be the donor atom itself (the free ligand may or may not be chiral), or the framework of the ligand, in which case central, axial or planar chirality may be involved.[16,115,116,129] As noted previously, vicinal and conformational effects are often interdependent, since the substitution of a ligand required to introduce chirality may simultaneously result in conformational locking.

(i) Asymmetric donor ligands

Asymmetrically substituted secondary and tertiary amines (**27**) are configurationally stable when irreversibly coordinated to metal ions, where they may be considered to be formally analogous to ammonium ions.

In the absence of a kinetically stable M—N bond the asymmetry is lost due to rapid pyramidal inversion of the free amine ($\Delta G < 25\ \mathrm{kJ\ mol^{-1}}$), unless the asymmetrically substituted nitrogen atom is part of a rigid organic ring system.[182] The simplest and earliest studied coordination compound incorporating an asymmetric coordinated secondary nitrogen as the sole source of chirality is $[\mathrm{Co(sarcosine)(NH_3)_4}]^{2+}$ (sarcosine = *N*-methylglycinate) (**28**).[183] Numerous reports of resolutions of coordinated secondary amines in chelates involving cobalt(III), palladium(II) and platinum(II) have appeared more recently.[62] In all cases, inversion at nitrogen (leading to enantiomerization) has been found to be 10^2–10^6 times slower than proton exchange, suggesting that even the deprotonated amine, when coordinated, has considerable pyramidal stability (Figure 11). An even stronger inhibition of inversion occurs in multidentate and macrocyclic systems, where multiple conformational changes may be concomitant. Thus, $[\mathrm{Ni(cyclam)}]^{2+}$ (cyclam = 1,4,8,11-tetraazacyclotetradecane) can be deprotonated and methylated at all four nitrogen atoms without isomerization, whereas reaction between tetra-*N*-methylcyclam and $\mathrm{Ni^{2+}}$ produces none of this particular product.[184]

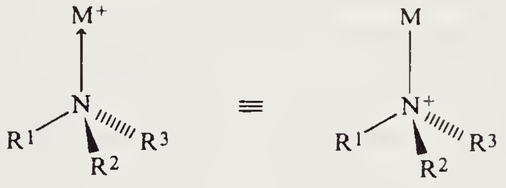

(27)

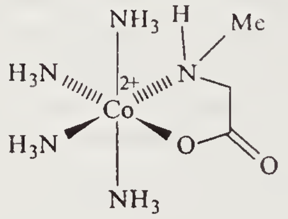

(28)

Unlike tertiary amines the inversion barriers of simple tertiary phosphines of the type PRMePh are high enough to allow isolation, if not distillation of pure enantiomers.[185] Determinations of

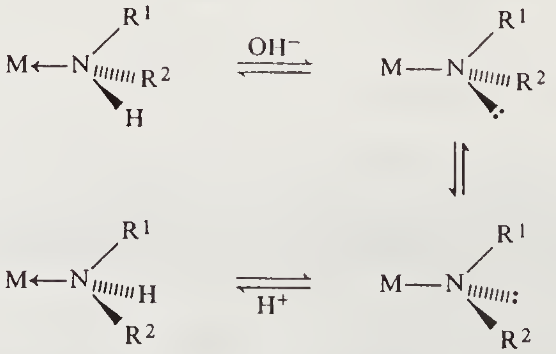

Figure 11 Inversion of a coordinated secondary nitrogen group

E_{inv} for (+)-PMePhPr^n by polarimetry have given values of 120–134 kJ mol^{-1};[186,187] the barriers are increased in certain ring compounds, and are reduced by electron-withdrawing substituents that tend to stabilize the planar transition state relative to the ground state, due to $(p-p)\pi$ conjugation. On the other hand, a thermal racemization study[188] of optically active (+)-AsEtMePh[189] gave an E_{inv} value of 180 kJ mol^{-1}, which corresponds to a $t_{1/2}$ of 740 h at 200 °C. A further important difference between tertiary arsines and phosphines lies in their markedly different sensitivity to mineral acids; optically active tertiary phosphines can be recovered unchanged from 10 M HCl,[190] whereas the corresponding arsines are racemized instantly by traces of this acid.[191,192] The racemization of the latter is believed to occur by pseudorotation of a five-coordinate species containing a weak H···As···X interaction. Quaternary salts of the type [AsR$_4$]X with X = Cl, Br or I racemize (I > Br > Cl) in solvents promoting ion pair formation under certain conditions,[193] and there is an example known of tertiary arsine centres coordinated to cobalt(III) behaving similarly in boiling acetonitrile in the presence of chloride ions.[194]

A wide range of bidentates containing one or more asymmetric phosphorus or arsenic donor atoms is now available due to the exploitation of a resolution technique involving the fractional crystallization of pairs of diastereomeric complexes formed by the chiral bidentates with palladium(II) complexes containing optically active dimethyl(α-methylbenzyl)amine or dimethyl(1-ethyl-α-naphthyl)amine. Indeed, in recent work the two enantiomer pairs of 1-(methylphenylarsino)-2-(methylphenylphosphino)benzene, (**29a**) and (**29b**), have been separated and isolated as optically pure air-stable crystalline solids with $[\alpha]_D^{20}$ values of ±79° (R^*, R^*) and ±15.5° (R^*, S^*).[195]

Unsymmetrically substituted sulfoxides R^{1}R^{2}SO are another ligand type readily separated into enantiomers;[146] the enantiomers are remarkably stable to heat, although they racemize in the presence of (LiCH$_3$)$_4$ or HCl.[197] Sulfoxides in general are excellent ligands and chelating disulfoxides can be readily produced as pure enantiomers by, for example, the oxidative coupling of optically active sulfinyl carbanions.[198] Significant chiral discrimination (stereoselectivity) has been observed in reactions involving both free and coordinated sulfoxides.[199,200]

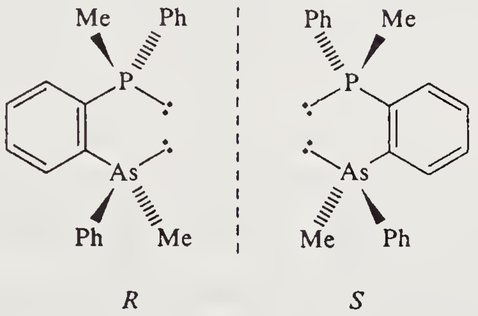

(**29a**) (R^*,R^*)

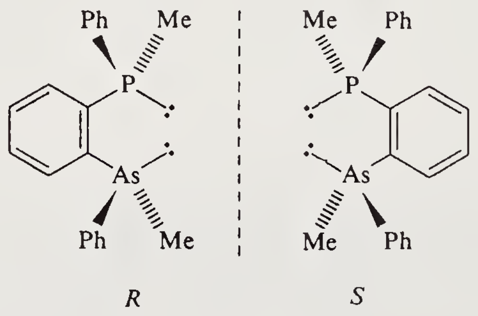

(**29b**) (R^*,S^*)

Thioethers and their selenium and tellurium analogues are also ligands that may be sources of chirality in complexes if they are unsymmetrically substituted (RSR′). The free ligands are, of course, achiral unless R or R′ is chiral and generally the rate of inversion at sulfur is still fast in the coordinated form,[62] so that physical separation of enantiomers is virtually impossible. However, in some thioether complexes of Re^I, Pd^{II}, Pt^{II}, Rh^{III}, Ir^{III} and Pt^{IV}, the existence of diastereomers associated with different configurations at sulfur is detectable by NMR spectroscopy[201,202] and the $\Delta G^{\ddagger}$ values for inversion of chiral sulfur bound to Pt^{IV} and Re^I lie in the range 51–56 kJ mol^{-1}. For inversion of chiral coordinated selenium, $\Delta G^{\ddagger}$ is ~25 kJ mol^{-1} greater. In cobalt(III) complexes of (R)-S-methylcysteine and S-methylcysteamine,[203] sulfur inversion is slow on the NMR time scale at room temperature ($k_i < 10$ s^{-1}), but is still too fast ($k_i > 0.1$ s^{-1}) for physical separation of the two forms.[204] Again, the incorporation of a thioether unit into a multidentate ligand in a particular coordination geometry can fix the C configuration, as in (OC-6-22-C)-[CoCl$_2$(tet)]$^+$ (tet = 1,10-diamino-4,7-dithiadecane) (**30**).[205]

(ii) Asymmetric skeletal atoms

The simplest ligands in this category contain a single asymmetric carbon atom (R or S) in the skeleton, as in the amino acid anions, H$_2$NCH(R)CO$_2$$^-$. Amino acids and other natural product enantiomers provide a wealth of potential for elaboration into useful chiral ligands of this type. There is a compendium available[206] of absolute configurations of 6000 selected compounds containing one asymmetric carbon atom and resolution procedures in organic chemistry are well established.[207,208] Numerous syntheses are already known for dissymmetric bidentate ligands

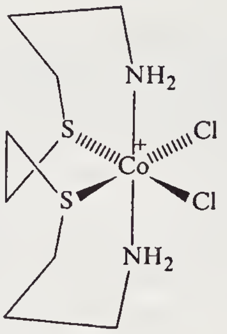

(**30**) *OC*-6-22-*C*-[*R*-(*R**,*R**)]

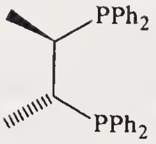

(**31**)

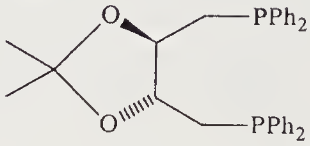

(**32**)

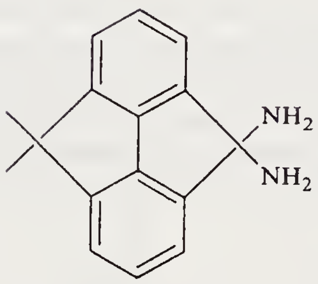

(**33**)

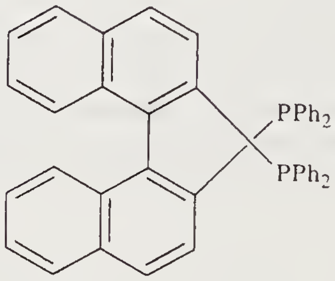

(**34**)

derived from natural products containing two directly bonded asymmetric carbons of the same absolute configuration. (*R*,*R*)-Chiraphos (**31**),[209] for example, is derived from (*S*,*S*)-2,3-butanediol and (*R*,*R*)-DIOP (**32**) from (*R*,*R*)-tartaric acid.[210]

Where barriers to rotation about single bonds are very large, as is the case in the biphenyl and binaphthyl compounds 6,6′-dimethyl-2,2′-diaminobiphenyl (**33**) and 2,2′-bis(diphenylphosphino)-1,1′-binaphthyl (**34**), chiral forms described as atropisomers may exist.[211] Atropisomers are said to exhibit axial chirality and any chromophoric unit such as the aromatic rings in (**33**) and (**34**) is usually of the type described as inherently dissymmetric. Both (**33**)[212] and (**34**)[213,214] are useful ligands that have been resolved. Recent studies have also been made of the racemic carbanionic analogues,[215] and in an exciting new development, 2,2′-dilithio-1,1′-binaphthyl has recently been stereospecifically generated from the corresponding optically pure 2,2′-dibromo compound.[216]

5.3.5 Considerations of Isomerism in Some Particular Systems

5.3.5.1 Quadridentate ligands on octahedral metal ions

Isomerism in cobalt(III) complexes of acyclic tetramines has been more thoroughly studied than in any other particular type of coordination compound.[22,23,178–180,217–219] Best characterized is the $[CoXY(trien)]^{n+}$ system (trien = 1,8-diamino-3,7-diazaoctane; X, Y = unidentate ligands or the donor atoms of a bidentate ligand), where essentially all possible stereoisomers have been identified.[23,220–224] A primary consideration is the donor atom topology and, given the impossibility of an $—NCH_2CH_2N—$ unit spanning other than adjacent positions in the coordination sphere of a metal ion, only three isomers are expected. These have been designated in various ways, although the '*cis*-α, *cis*-β and *trans*' nomenclature, as indicated in (**35a**)–(**35c**), originally due to Bailar,[225] has been most widely used. Sloan nomenclature requires that X and Y be identified and hence the trivial nomenclature will be used to cover the general situations that follow.

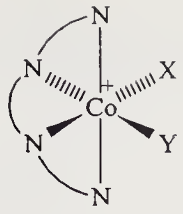

(**35a**) *cis*-α

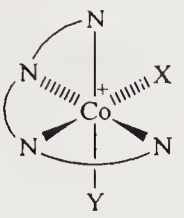

(**35b**) *cis*-β

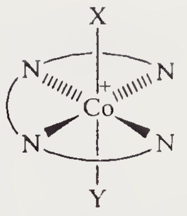

(**35c**) *trans*

For X = Y = Cl^-, it has been found that purple, mauve and green forms of $[CoCl_2(trien)]^+$ are readily prepared and these have been identified as the *cis-α*, *cis-β* and *trans* forms, respectively.[220-222] Of course, it will be noted that the α and β topologies are configurationally chiral and enantiometric forms of both *cis-α*- and *cis-β*-$[CoCl_2(trien)]^+$ have, indeed, been characterized. In addition, however, diastereomeric forms of *cis-β*-$[CoCl_2(trien)]^+$ are known[220-222] and this fact focuses attention on the asymmetric inner *N*-donor atoms of trien as sources of isomerism. Thus, each of these atoms may in principle adopt an *R* or an *S* configuration and in systems where the inner nitrogen atoms are topologically inequivalent, up to four forms (*R,R*, *S,S*, *R,S* and *S,R*) might be expected. Fortunately, the system is not quite so complicated in reality, since the inner donor atoms are only inequivalent in the *cis-β* form and the configurational and vicinal contributions to the isomerism of $[CoXY(trien)]^{n+}$ are not completely independent. The latter point has been noted previously in relation to *cis-α*-$[CoCl_2(trien)]^+$ but both simple model construction and conformational analysis calculations suggest that when an inner donor atom is part of a 'planar' CoN_3 unit, topology does not restrict the nitrogen configuration, so that in both *cis-β* and *trans* species greater isomeric complexities arise than with *cis-α*,[220-222] due to enantiomerism between (**36a**) and (**36b**). Hence, the diastereomeric forms of mauve *cis-β*-$[CoCl_2(trien)]^+$ are identified in that the inner nitrogen configurations are *R,R* (*S,S*) or *R,S* (and *S,R*), with these designations implying particular donor atom configurations (**37a**)-(**37d**). It is usual to consider the donor atom topology in complexes of this type in terms of that of the related unidentate ligand systems, such as $[CoCl_2(NH_3)_4]^+$. In this sense, if not in reality, *trans*-$[CoXY(trien)]^{n+}$ is configurationally achiral but, because it contains two 'planar' inner *N*-donors, it can be considered to show vicinal chirality. Thus, three isomers, with (*R,R*), (*S,S*) and (*R,S*) inner nitrogen configurations, are possible, the first and second being enantiomeric. The two chiral forms are also considered to show conformational chirality because each five-membered chelate ring may adopt a chiral conformation, with two taking λ (or δ) and one δ (or λ) forms. In the achiral (*R,S*) form it is assumed that the inner chelate ring adopts an achiral envelope conformation, with the outer rings taking mirror-image δ and λ conformations. Unfortunately X-ray structural data are not available for any *trans*-$[CoXY(trien)]^{n+}$ isomer, although the enantiomers of *trans*-(*R**,*R**)-$[CoCl_2(trien)]^+$, (**38a**) and (**38b**),[226] and the (*R**,*R**) and (*R**,*S**) forms of *trans*-$[Co(NH_3)_2(trien)]^{3+}$ (**39**)[224] have been spectroscopically characterized. The structures of some closely related complexes have been determined and extensive testing of empirical force-field, strain-energy minimization methods of calculating conformations has been based on studies of other Co^{III}/trien complexes.[23,222]

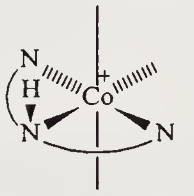

(**36a**)

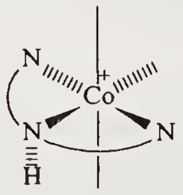

(**36b**)

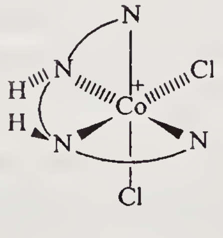

Δ-*R,R*-*cis*-β
OC-6-32-*C*-[*R*-(*R**,*R**)]
(**37a**)

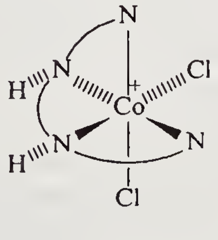

Δ-*R,S*-*cis*-β
OC-6-43-*C*-(*R**,*S**)
(**37b**)

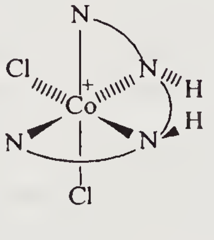

Λ-*S,S*-*cis*-β
OC-6-32-*A*-[*S*-(*R**,*R**)]
(**37c**)

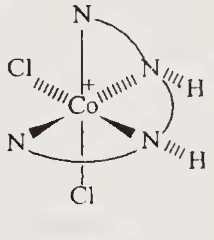

Λ-*S,R*-*cis*-β
OC-6-52-*A*-(*R**,*S**)
(**37d**)

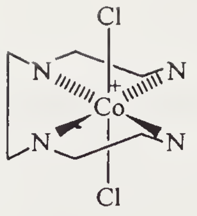

R,R-trans

OC-6-13-[*R*-(*R**,*R**)]-(λ,δ,λ)

(38a)

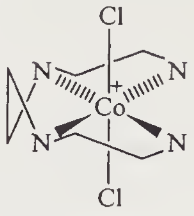

S,S-trans

OC-6-13-[*S*-(*R**,*R**)]-(δ,λ,δ)

(38b)

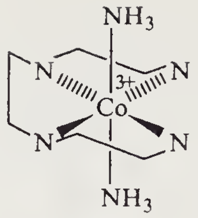

R,S-trans

OC-6-15-(*R**,*S**)-(λ,ε,δ)

(39)

Conformational subtleties in $[\mathrm{CoXY(trien)}]^{n+}$ complexes have been characterized in numerous crystal structures of *cis*-β complexes incorporating a bidentate X, Y ligand.[23] Thus, conformational diastereomers of *cis*-β-$[\mathrm{Cogly(trien)}]^{2+}$ (gly = glycinate anion, $\mathrm{NH_2CH_2CO_2^-}$) have been observed in the one crystal where, for a given donor atom topology and chirality, one terminal chelate ring is observed in both λ and δ conformations.[227] It should be noted, however, that this and many related structures show it to be somewhat misleading to describe conformations in multidentate ligand complexes in terms of idealized conformations of isolated chelate ring components, even though it does appear possible to predict the number and approximate structure of isomers in this way. Thus, the conformation of a given chelate ring is influenced by the number of connected chelate arms and the overall ligand topology, so that terms such as δ and λ should be at best considered as only qualitative designations of ring chirality.

Conformational analysis as applied to $[\mathrm{CoXY(trien)}]^{n+}$ complexes has involved consideration of a further aspect of stereoisomerism, arising from the fact that the sites X in both *cis*-β-$[\mathrm{CoX_2(trien)}]^{n+}$ and *trans*-(*R,S*)-$[\mathrm{CoX_2(trien)}]^{n+}$ are diastereotopic. Thus, in *cis*-β-$[\mathrm{Cogly(trien)}]^{2+}$ for example, two isomers exist, regardless of which inner donor atom configuration of trien is considered.[222] They may be distinguished in terms of whether the glycine *O*-donor atom is opposite (*trans*) to the secondary or the primary nitrogen donor atoms of the trien ligand, as in (**40a**) and (**40b**). Isomerism of this type has not yet been observed in *trans*-(*R,S*)-$[\mathrm{CoXY(trien)}]^{n+}$ systems, but has been for related complexes.[228]

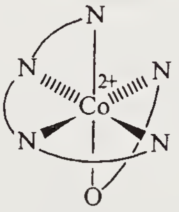

Δ-*cis*-β₂

OC-6-43-*A*-[*R*-(*R**,*R**)]

(40a)

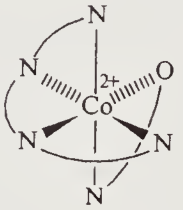

Δ-*cis*-β₁

OC-6-24-*C*-[*R*-(*R**,*R**)]

(40b)

5.3.5.2 Phosphate and polyphosphate complexes

Phosphate esters, particularly AMP, ADP and ATP, have vital biological functions and this fact has generated intense interest in their reaction mechanisms. Subtle stereochemical experiments, such as the use of isotopically chiral compounds, have been important and, since all biological phosphorylation reactions appear to involve metal ion catalysis, the stereochemistry of phosphate ion coordination has also been subject to much attention.[229,230] Apart from its biological significance, this work has revealed some interesting contrasts with the stereochemistry of ligand systems in which saturated carbon units link the donor atoms.

One of these is the apparently preferred conformation of pyrophosphate $[\mathrm{P_2O_7}]^{4-}$, when chelated to cobalt(III). In that all atoms in this ligand might be considered approximately tetrahedral, a parallel with the conformational properties of a 1,3-propanediamine chelate could be expected with two forms, chair and skew-boat, being produced, but with the former preferred.[23,166–168,177] However, the crystal structures of $[\mathrm{CoHP_2O_7(en)_2}]$ (**35**)[231] (phosphorus asymmetry due to proton attachment has been ignored) and $[\mathrm{CoHP_2O_7(NH_3)_4}]$ (**41**)[232,233] both show just the skew-boat conformer. No evidence of the linkage isomer 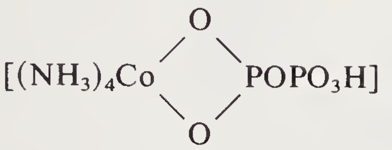 $[(NH_3)_4Co\genfrac{}{}{0pt}{}{O}{O}POPO_3H]$ was found, although this was perhaps not unexpected in view of the evidence of considerable ring strain in the structure of $[CoPO_4(en)_2]$.[234]

More surprising was the observation that substituents introduced into the chelate ring appeared to prefer the axial disposition. For a ligand such as ATP (**42**; R = adenosinyl) or any $[P_3O_{10}]^{5-}$ derivative, chelation through oxygen atoms of P^{β} and P^{γ} renders P^{β} asymmetric and, even if it is assumed that the chelate ring adopts the skew-boat conformation only, four stereoisomers could be expected in $[CoATP(NH_3)_4]^-$, *viz.* (**43a**)–(**43d**). (As represented, these appear to be two sets of enantiomers but in the case of ATP, since *R* is chiral, the four are diastereomers.) Of course, given rapid conformational interconversion, only two species (*R* and *S* at P^{β}) would be expected to be physically separable and in the case of the 'parent' ligand, $[H_2P_3O_{10}]^{3-}$, this has been achieved.[235–237] The conformation is, of course, fixed in the solid state and the surprising feature of the X-ray structure of $[CoH_2P_3O_{10}(NH_3)_4]\cdot H_2O$ is that it shows the conformation fixed in such a way that the PO_4 'substituent' group is axial, as represented by (**44**).[232,238]

The ligand $[H_2P_3O_{10}]^{3-}$ has also been found to form linkage isomers with cobalt(III) in that the eight-membered ring species (**45**) has been characterized as well as the enantiomers just described.[239] The formation of large rings of this type may prove to be an important aspect of phosphate coordination chemistry and the prospect of a form of polymerization isomerism is raised by the observation of a doubly bridged binuclear structure in $[Co(C_6H_5OPO_3)(en)_2]ClO_4$,[240] which contrasts with the mononuclear structure of $[CoPO_4(en)_2]$ that incorporates a four-membered phosphate chelate ring.[234]

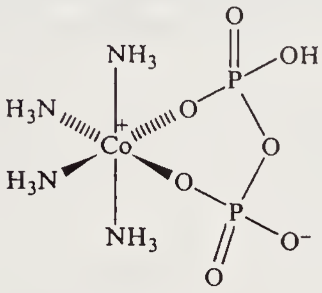

(**41**) *OC*-6-22-(λ)

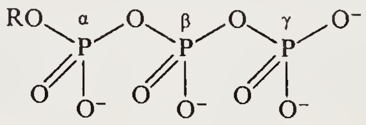

(**42**)

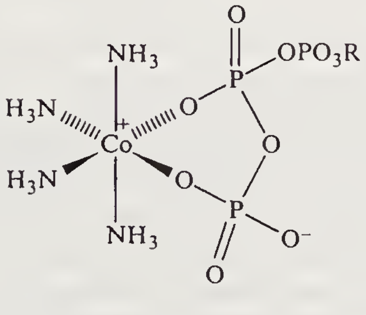

(**43a**) *OC*-6-22-(*R*,λ)

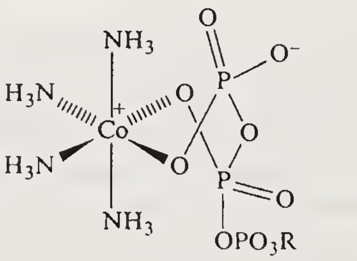

(**43b**) *OC*-6-22-(*R*,δ)

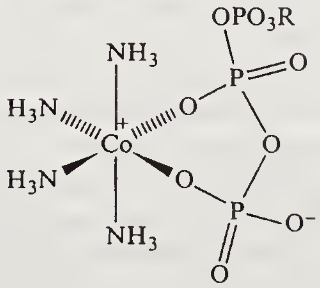

(**43c**) *OC*-6-22-(*S*,λ)

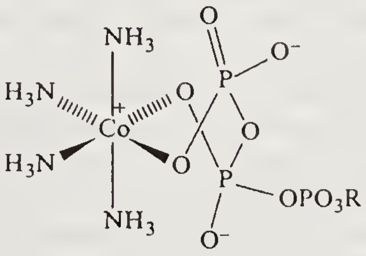

(**43d**) *OC*-6-22-(*S*,δ)

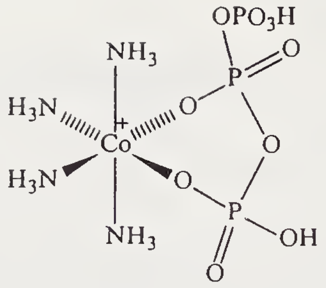

(**44**) *OC*-6-22-(*S*,λ)

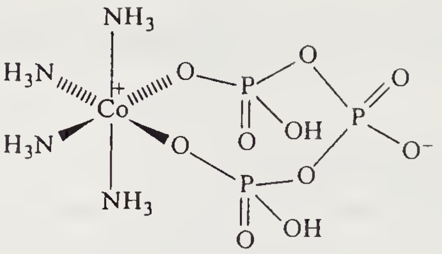

(**45**)

5.3.5.3 Square-planar complexes of quadridentate macrocyclic ligands

The coordination chemistry of macrocyclic ligands has been extensively studied and aspects of isomerism have been considered in numerous systems.[241] Methods whereby two diastereomers of complexes of tetra-*N*-methylcyclam may be isolated have been discussed previously.[184] This, however, is a relatively simple system and it is usually necessary to consider isomerism due to the presence of asymmetric atoms in the chelate arms, as well as that due to asymmetric donor atoms that may be rendered stable to inversion by coordination. An example of a system exhibiting this level of complexity is afforded by the nickel(II) complexes of the macrocyclic ligands generated by reduction of the readily prepared macrocycle (**46**).[242] These ligands contain two asymmetric carbon atoms and four asymmetric nitrogen atoms but, because *N*-inversion is rapid, it is conventional to consider that only three separable stereoisomers exist. There is an enantiomeric pair, (**47a**) and (**47b**), which constitutes the racemic isomer (*R**,*R**), and an achiral (*R**,*S**) diastereomer (**47c**), the *meso* isomer.

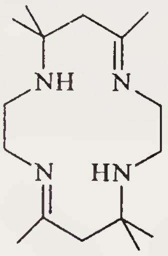

(**46**)

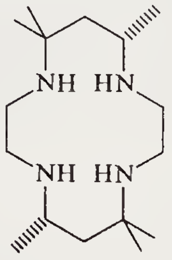

(**47a**) *S*-(*R**,*R**)

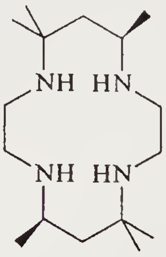

(**47b**) *R*-(*R**,*R**)

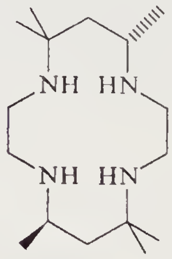

(**47c**) (*R**,*S**)

Reaction of $[Ni(OH_2)_6](ClO_4)_2$ with this mixture of ligands results in the formation of yellow, square-planar complexes.[243,244] The square-planar coordination geometry renders it necessary only to consider vicinal and conformational factors in analyzing possible isomerism, although the vicinal factors must now include the asymmetric donor atoms. Thus, from the racemic ligand forms shown above, 10 complex ion diastereomers arise as a result of alternative donor atom configurations and another 10 arise from the *meso* form. Six of the latter exist as enantiomer pairs, giving rise to a stereoisomer total of 36 for all three ligands. These stereoisomers can be represented in shorthand form as shown in Figure 12. These representations do not take into account conformations of the chelate rings and although the diastereomers shown in Figure 11 would be expected to differ in energy, it is only from consideration of conformations that it becomes apparent that some of the differences should be large. Thus, if it is assumed that the six-membered rings will adopt chair or skew-boat conformations with as many methyl substituents as possible (two, in fact) equatorial, then the preferred conformations for six-membered rings containing an asymmetric carbon of *R* absolute configuration would be those shown in Figure 13 of λ helicity. The preferred conformation for an isolated, unsubstituted five-membered ring is a δ or λ *gauche* arrangement and the only Ni^{II}-macrocycle complexes in which relatively low energy conformations of both the five-membered and six-membered rings can be attained are (**48a**), (*R**,*R**) ligand, and (**48b**), (*R**,*S**) ligand. Indeed, on the basis of spectroscopic measurements and considerations similar to those just described, these structures were assigned to two of the three isomers of the nickel(II) complex of racemic- and *meso*-5,5,7,12,12,14-hexamethyl-1,4,8,11-tetraazacyclotetradecane isolated by Warner and Busch.[243] The third diastereomer (containing the *C*-racemic ligand) was assigned the structure (**48c**). Warner and Busch advanced

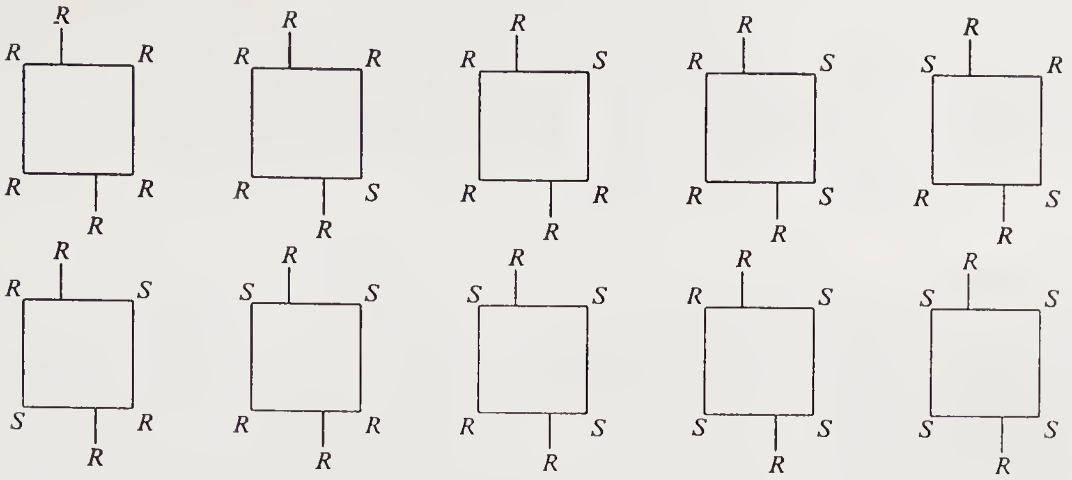

(R^*,R^*)-ligand

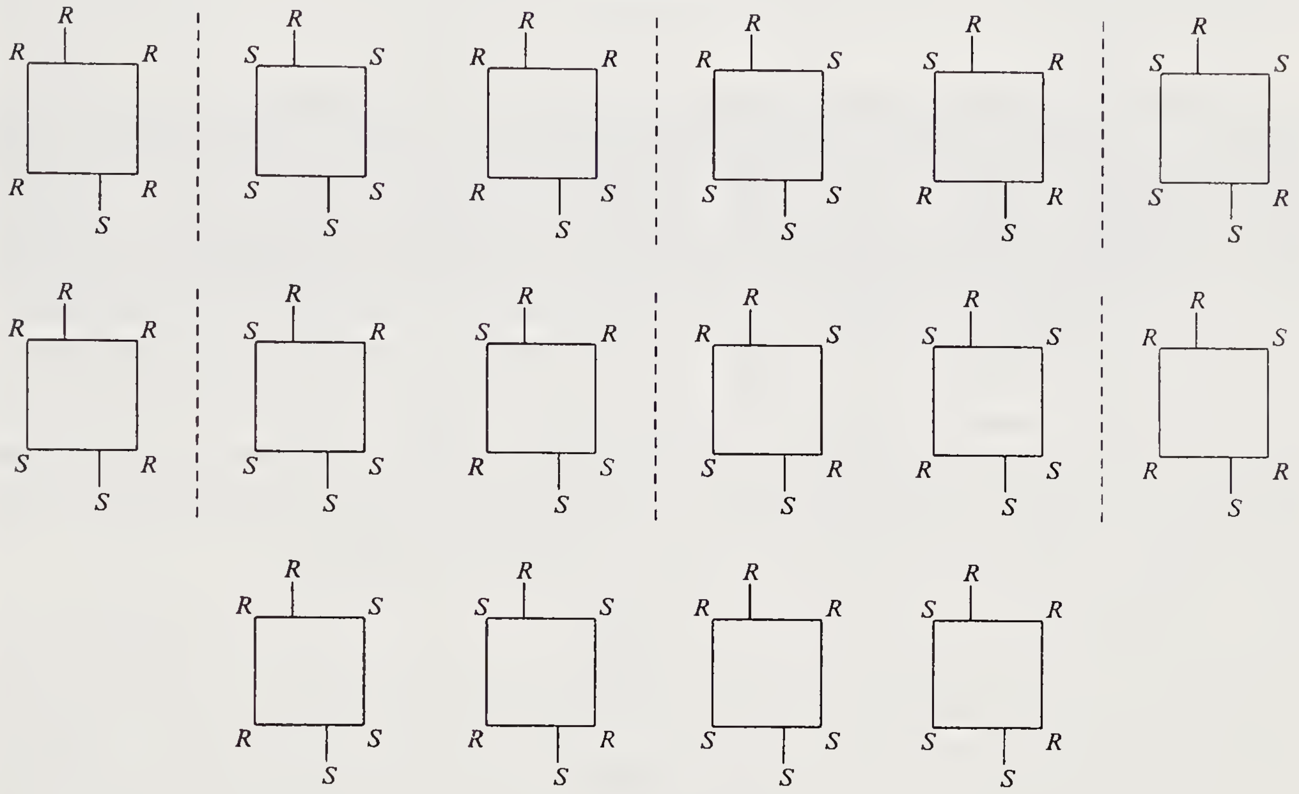

(R^*,S^*)-ligand

Figure 12 Representations of the stereoisomers of (R^*,R^*)- and (R^*,S^*)-[Ni(hexa-*C*-methylcyclam)]$^{2+}$ ([S-(R^*,R^*)]-ligand complexes not shown)

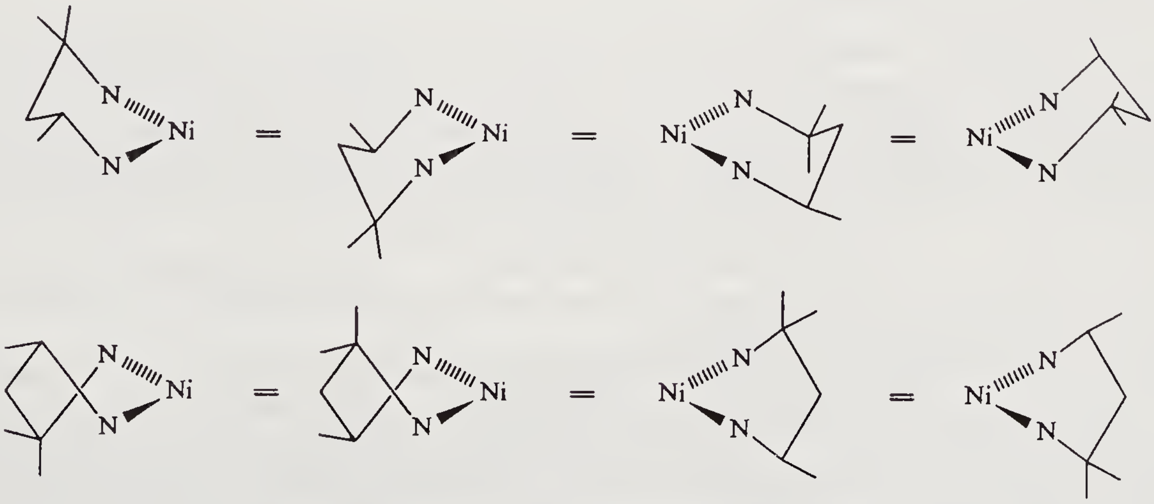

Figure 13 Preferred conformations of six-membered chelate rings containing an asymmetric carbon centre of (R) absolute configuration

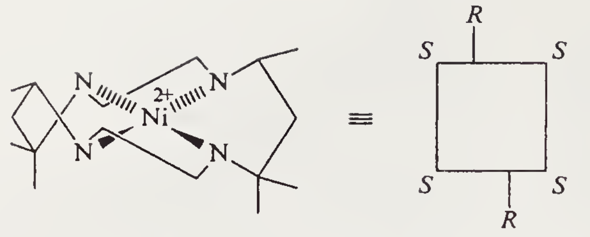

(48a)

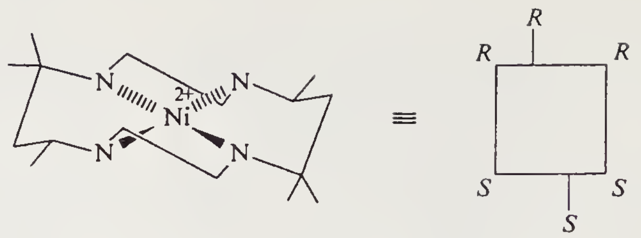

(48b)

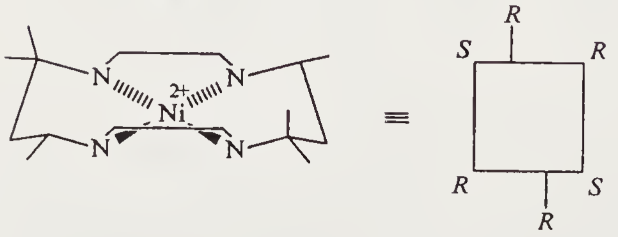

(48c)

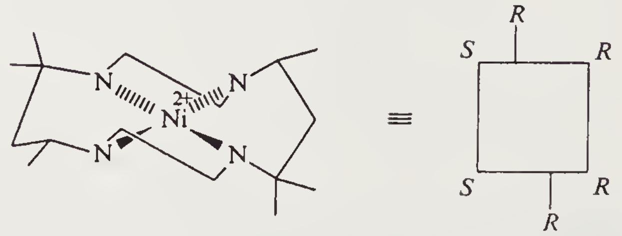

(48d)

evidence for the argument that the energy difference between five-membered ring conformations should be less than that for six-membered ring conformations, so that the attainment of a double chair arrangement of the six-membered rings would then more than compensate for the presence of the two eclipsed envelope five-membered rings. These assignments were confirmed by structural studies,[244] although a third diastereomer derived from the *C*-racemic ligand was shown to have structure (**48d**) in which one six-membered ring adopted an unsymmetrical skew-boat conformation. This crystallographic information and the procedures used to isolate the diastereomeric complexes suggest that rather subtle balances of factors may control the nature of isolated species. It is also true that conformations observed crystallographically are often considerably distorted from the idealized structures represented above. The five-membered rings described previously as being in an eclipsed envelope form, for example, in fact are twisted away from the truly eclipsed position. Nevertheless, this simple approach to conformational analysis is not misleading and has recently been usefully applied to the consideration of the five stereoisomers formed by coordination of nickel(II) to the (R^*,R^*)- and (R^*,S^*)-carbon diastereomers of (**49**).[245]

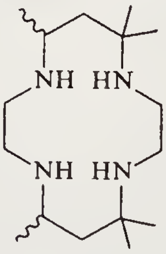

(49)

5.3.5.4 *Allogons and interallogons*

A form of isomerism essentially unknown in organic chemistry is one in whch the same donor atoms are attached to a metal ion in two (or possibly more) different coordination geometries. A simple example is afforded by $[Ni(CN)_5]^{3-}$, which is known in the trigonal-bipyramidal and square-pyramidal forms (**50a**) and (**50b**).[246] Five-coordination appears to be the best characterized system where energy minima for different configurations are comparable, as is exemplified in the very large number of phosphorus(V) compounds (phosphoranes) known to adopt trigonal-bipyramidal, square-pyramidal or intermediate structures.[247] Calculations suggest, however, that this situation may also apply commonly to seven- and higher coordination.[1] It is certainly well known for four-coordination (*vide infra*).[248]

The existence of isomers differing with respect to coordination geometry has been described as a form of conformational isomerism,[26,249] although the isomers are not interconvertible by simple rotation about a single bond and this appellation seems to have derived more from a consideration of the ease of interconversion of the isomers. Geomertric isomerism would be a more appropriate term but the special term *allogon* (Greek *allos* = other, *goma* = angle)[250] has been applied to these relatively rare species. Where two allogons coexist in the same crystal the

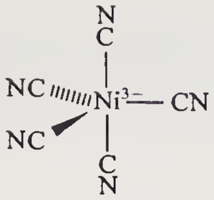

(50a)

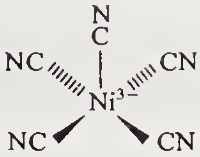

(50b)

compound is referred to as an *interallogon.* The compound $[Cr(en)_3][Ni(CN)_5]\cdot 1.5H_2O$ may accordingly be regarded as the archetypical interallogon.[246] The crystalline structure of this compound contains two crystallographically independent $[Ni(CN)_5]^{3-}$ ions; one is a regular square pyramid and the other is a distorted trigonal bipyramid of very nearly C_2 symmetry. The difference in energies of the individual allogons in this compound is exceedingly small. If the sesquihydrate is dehydrated, the Raman and IR bands due to the distorted trigonal-bipyramidal isomer disappear. Furthermore, if 1,3-propanediamine replaces en in the counterion, only square-pyramidal $[Ni(CN)_5]^{3-}$ is found in the crystal, as shown by an X-ray crystal structure determination.[251]

Allogonism has been observed most frequently in complexes of nickel(II), the structure of a given complex being primarily determined by the steric and electronc properties of the ligands, with secondary effects outside of the first coordination sphere often determining the actual structure.[94,252] Thus, square-planar and tetrahedral allogons of *N*-alkylsalicylaldimine chelates of nickel(II) (**51**) are known in the solid state, and a temperature controlled equilibrium exists between the diamagnetic square-planar and tetrahedral paramagnetic complexes in non-coordinating solvents, with the latter species predominating at elevated temperatures.[248,253]

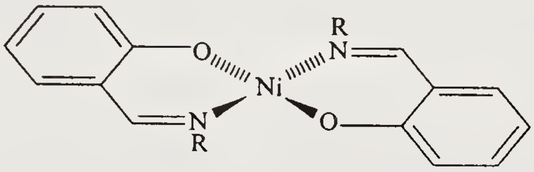

(51)

Venanzi and coworkers have shown in complexes of the type $[NiX_2(PR_3)_2]$ that arylphosphines and bromo and iodo ligands favour the high-spin tetrahedral allogon whereas alkylphosphines and chloro or thiocyanato ligands favour the low-spin square-planar state.[254] The compound $[NiBr_2(PBzPh_2)_2]$ exists in a red diamagnetic form and in a green paramagnetic form of moment 2.7 BM.[250] An X-ray crystal structure determination made on the green form revealed that the triclinic unit cell, space group $P\bar{1}$, contained three single molecules. One molecule has its nickel atom at the centre of symmetry and has the *trans* square-planar configuration. The other two are related by the centre of symmetry with tetrahedral coordination around the nickel. Recalculation of the magnetic moment on the basis of the crystal structure gave a value of approximately 3.3 BM, in agreement with the value expected for a purely tetrahedral nickel(II) compound of this type. The authors make the point that magnetic moments must be regarded with caution if there is a possibility of a substance being a crystalline molecular compound of different magnetic forms. This warning would naturally extend to the interpretation of other physical measurements made on compounds in the solid state.

Allogonic behaviour has also been observed in complexes of the type $[NiX_2(\text{amine})_2]$. For example, dark green diamagnetic $[NiI_2(\text{2-methylpyridine})_2]$ is considered to have a distorted square-planar structure in the solid state, but in dichloromethane it is tetrahedrally coordinated.[255]

5.4 CONCLUDING REMARKS

The present discussion of isomerism in coordination compounds is not, nor was it intended to be, comprehensive and exhaustive. The examples considered are an eclectic selection, and many important systems may have been neglected through ignorance. An obvious omission is any detailed consideration of polynuclear complexes[139,256-259] and it is, of course, a quite arbitrary decision not to include any consideration of organometallic species. Other neglected issues, such as the development of a truly comprehensive system of stereochemical nomenclature, are perhaps not yet capable of solution. Nevertheless, it is to be hoped that the principal factors to be considered in analyzing potential isomerism in a complex ion system have been clearly identified and that a logical procedure for assessing the interaction of these factors has been outlined. Isomerism is one of the more subtle, fascinating and important aspects of chemistry as a whole and, as expressed in the phenomenon of chirality, is one of the more singular features of life.[260]

5.5 REFERENCES

1. D. L. Kepert, 'Inorganic Stereochemistry', Springer-Verlag, Berlin, 1982 (Inorganic Chemistry Concepts, vol. 6). Also see this volume, p. 31.
2. S. F. Mason, *Top. Stereochem.*, 1976, **9**, 1.
3. E. L. Muetterties, *Acc. Chem. Res.*, 1970, **3**, 266.
4. J. R. Partington, 'A Short History of Chemistry', 3rd edn., Macmillan, London, 1957, chap. 10.
5. J. Liebig and J. L. Gay-Lussac, *Ann. Chim. (Paris)*, 1824, **25**, 285.
6. T. M. Lowry, 'Optical Rotatory Power', Longmans-Green, London, 1935.
7. E. L. Eliel, 'Stereochemistry of Carbon Compounds', McGraw-Hill, New York, 1962. See also refs. 17 and 119.
8. J. Gasteiger, P. Gillespie, D. Marquarding and I. Ugi, *Top. Curr. Chem.*, 1974, **48**, 1.
9. For a detailed historical review and, in particular, an assessment and description of the major contributions made by Alfred Werner, see G. B. Kauffman, 'Inorganic Coordination Compounds, Nobel Prize Topics in Chemistry', ed. J. W. van Spronsen, Heyden, London, 1981.
10. F. Valach, B. Koren, P. Sivy and M. Melnik, *Struct. Bonding (Berlin)*, 1983, **55**, 101.
11. L. H. Pignolet, *Top. Curr. Chem.*, 1975, **56**, 91 and references therein.
12. S. K. Shukla, G. B. Manni and C. Cipriani, *Inorg. Chim. Acta*, 1983, **79**, 286.
13. P. Gutlich, *Struct. Bonding (Berlin)*, 1981, **44**, 83.
14. J. A. Gerlt, J. A. Corderre and S. Mehdi, *Adv. Enzymol. Relat. Areas Mol. Biol.*, 1983, **55**, 291.
15. D. Arigoni and E. L. Eliel, *Top. Stereochem.*, 1969, **4**, 127.
16. R. S. Cahn and O. C. Dermer, 'Introduction to Chemical Nomenclature', 5th edn., Butterworths, London, 1979.
17. K. Mislow, 'Introduction to Stereochemistry', 2nd edn., Benjamin, Reading, MA, 1965, Note also ref. 117.
18. A. Oki, *Acc. Chem. Res.*, 1984, **17**, 154.
19. R. R. Holmes, 'Pentacoordinated Phosphorus', ACS Monograph 175, American Chemical Society, 1980, vol. 1, chaps. 1 and 4 in particular.
20. The latter term is a neologism that has received limited acceptance — see D. A. Buckingham and A. M. Sargeson, *Top. Stereochem.*, 1971, **6**, 219 (p. 220 in paticular).
21. This type of work was the essence of much of Werner's research (see ref. 9) and has been discussed numerous times in standard textbooks of inorganic chemistry. See, for example, J. C. Bailar, Jr. and D. H. Busch (eds.), 'The Chemistry of the Coordination Compounds', Reinhold, New York, 1956, chaps. 7 and 8 in particular.
22. C. J. Hawkins, 'Absolute Configuration of Metal Complexes', Wiley-Interscience, New York, 1971, chap. 3.
23. D. A. Buckingham and A. M. Sargeson, *Top. Stereochem.*, 1971, **6**, 219.
24. A. Navaza, F. Villain and P. Charpin, *Polyhedron*, 1984, **3**, 143.
25. H. M. Colquhoun, S. M. Doughty, J. F. Stoddart and D. J. Williams, *Angew. Chem., Int. Ed. Engl.*, 1984, **23**, 235 and references therein.
26. P. L. Ritger, J. H. Burns and G. Bombieri, *Inorg. Chim. Acta*, 1983, **77**, L217.
27. See ref. 9. For translations of Werner's works on particular topics, see G. B. Kauffman, *Coord. Chem. Rev.*, 1972, **9**, 339 (polynuclear coordination); 1973, **11**, 161 (structural isomerism); 1974, **12**, 105 (optical activity); 1975, **15**, 1 (geometrical isomerism).
28. A brief tabulation of these and some other isomer types recognized by Werner is given by F. Basolo and R. G. Pearson in 'Mechanisms of Inorganic Reactions', 2nd edn., Wiley, New York, 1967, p. 13. See also ref. 21.
29. The preparations of these isomers are described in G. Brauer, 'Handbook of Preparative Inorganic Chemistry', 2nd edn., Academic, New York, 1963, vol. 2, pp. 1348–1350. See also J. Barbier, C. Kappenstein and R. Hugel, *J. Chem. Educ.*, 1972, **49**, 204.
30. J. A. Davies, *Adv. Inorg. Chem. Radiochem.*, 1981, **24**, 115 (p. 135 in particular).
31. I. Sotofte and E. Bang, *Acta Chem. Scand.*, 1971, **25**, 1164.
32. U. Thewalt and J. Ernst, *Z. Naturforsch., Teil B*, 1975, **30**, 818.
33. E. Bang, *Acta Chem. Scand.*, 1968, **22**, 2671; E. Bang and T. Narasimhayya, *Acta Chem. Scand.*, 1970, **24**, 275.
34. J. L. Burmeister, *Coord. Chem. Rev.*, 1968, **3**, 225.
35. W. Beck and W. P. Fehlhammer, *MTP Int. Rev. Sci., Inorg. Chem. Series 1*, Butterworths, London, 1972, vol. 2, pp. 253–300.
36. A. H. Norbury, *Adv. Inorg. Chem. Radiochem.*, 1975, **17**, 231.
37. R. J. Balahura and N. A. Lewis, *Coord. Chem. Rev.*, 1976, **20**, 109.
38. H. Sigel (ed.), 'Metal Ions in Biological Systems', vol. 1, chap. 3; vol. 8, 'Nucleotides and their Derivatives: Their Ligating Ambivalency'; vol. 9, 'Amino Acids and their Derivatives as Ambivalent Ligands', Dekker, New York.
39. D. J. Hodgson, *Prog. Inorg. Chem.*, 1977, **23**, 211.
40. L. G. Marzilli, *Prog. Inorg. Chem.*, 1977, **23**, 255.
41. S. M. Jørgensen, *Z. Anorg. Allg. Chem.*, 1894, **5**, 147; 1898, **17**, 455.
42. M. A. Hitchman and G. L. Rowbottom, *Coord. Chem. Rev.*, 1982, **42**, 55.
43. B. Adell, *Z. Anorg. Allg. Chem.*, 1955, **279**, 220 and references cited therein.
44. B. Adell, *Acta Chem. Scand.*, 1947, **1**, 624 (with G. Thohn), 659; 1950, **4**, 1; 1951, **5**, 54, 941.
45. R. G. Pearson, P. M. Henry, J. G. Bergmann and F. Basolo, *J. Am. Chem. Soc.*, 1954, **76**, 5920.
46. R. K. Murmann and H. Taube, *J. Am. Chem. Soc.*, 1956, **78**, 4886.
47. F. Basolo and G. S. Hammaker, *Inorg. Chem.*, 1962, **1**, 1.
48. I. Grenthe and E. Nordin, *Inorg. Chem.*, 1979, **18**, 1109, 1869.

49. A. W. Zanella and A. F. Fucaloro, *Inorg. Nucl. Chem. Lett.*, 1980, **16**, 515.
50. For recent work in this area see: W. G. Jackson, G. A. Lawrance, P. A. Lay and A. M. Sargeson, *Inorg. Chem.*, 1980, **19**, 904; *J. Chem. Soc., Chem. Commun.*, 1982, 70; *J. Chem. Educ.*, 1981, **58**, 734.
51. S. Balt, H. J. A. M. Kuipers and W. E. Renkema, *J. Chem. Soc., Dalton Trans.*, 1983, 1739.
52. M. Mares, D. A. Palmer and H. Kelm, *Inorg. Chim. Acta*, 1978, **27**, 153.
53. W. W. Fee, C. S. Garner and J. MacB. Harrowfield, *Inorg. Chem.*, 1976, **6**, 87; 1971, **10**, 290 and references cited therein.
54. T. C. Matts and P. Moore, *J. Chem. Soc. (A)*, 1969, 219 and references cited therein.
55. D. M. L. Goodgame and M. A. Hitchman, *Inorg. Chem.*, 1966, **5**, 1303.
56. R. D. Alexander and P. N. Holper, *Inorg. Nucl. Chem. Lett.*, 1978, **14**, 309.
57. A. J. Finney, M. A. Hitchman, C. L. Raston, G. L. Rowbottom and A. H. White, *Aust. J. Chem.*, 1981, **34**, 2047, 2061, 2069.
58. A. L. Finney, M. A. Hitchman, C. L. Raston, G. L. Rowbottom, B. W. Skelton and A. H. White, *Aust. J. Chem.*, 1981, **34**, 2095.
59. A. J. Finney, M. A. Hitchman, D. L. Kepert, C. L. Raston, G. L. Rowbottom and A. H. White, *Aust. J. Chem.*, 1981, **34**, 2177.
60. M. A. Hitchman, R. Thomas, B. W. Skelton and A. H. White, *J. Chem. Soc., Dalton Trans.*, 1983, 2273.
61. J. L. Burmeister, in 'The Chemistry and Biochemistry of Thiocyanic Acid and its Derivatives', ed. A. A. Newman, Academic, London, 1975, p. 68. See also ref. 34.
62. W. G. Jackson and A. M. Sargeson, *Rearrangements in Ground and Excited States*, 1980, **2**, 273.
63. J. J. MacDougall, J. H. Nelson, W. C. Fultz, J. L. Burmeister, E. M. Holt and N. W. Alcock, *Inorg. Chim. Acta*, 1982, **63**, 75 and references cited therein.
64. C. T. Hunt and A. L. Balch. *Inorg. Chem.*, 1982, **21**, 1242.
65. J. J. MacDougall, A. W. Verstuyft, L. W. Cary and J. H. Nelson, *Inorg. Chem.*, 1980, **19**, 1036.
66. L. S. Benner and A. L. Balch, *J. Am. Chem. Soc.*, 1978, **100**, 6099.
67. D. A. Buckingham, I. I. Creaser and A. M. Sargeson, *Inorg. Chem.*, 1970, **9**, 655.
68. M. R. Snow and R. F. Boomsma, *Acta Crystallogr., Sect. B*, 1972, **28**, 1908.
69. M. R. Snow and R. J. Thomas, *Aust. J. Chem.*, 1974, **27**, 1391.
70. W. G. Jackson, D. P. Fairlie and M. L. Randall, *Inorg. Chim. Acta*, 1983, **70**, 197.
71. A. Yeh, N. Scott and H. Taube, *Inorg. Chem.*, 1982, **21**, 2542.
72. W. R. Ellis and W. L. Purcell, *Inorg. Chem.*, 1982, **21**, 834.
73. W. L. Purcell, *Inorg. Chem.*, 1983, **22**, 1205.
74. R. A. de Castello, C. P. Mac-Coll and A. Haim, *Inorg. Chem.*, 1971, **10**, 203.
75. A. Haim, *Acc. Chem. Res.*, 1975, **8**, 264.
76. S. Alvarez and C. Lopez, *Inorg. Chim. Acta*, 1982, **64**, L99.
77. R. J. Balahura, *Can. J. Chem.*, 1974, **52**, 1762.
78. R. J. Balahura, *J. Am. Chem. Soc.*, 1976, **98**, 1487.
79. A. P. Szecsy and A. Haim, *J. Am. Chem. Soc.*, 1982, **104**, 3063.
80. H. Taube, *Angew. Chem., Int. Ed. Engl.*, 1984, **23**, 329 and references cited therein.
81. S. E. Diamond and H. Taube, *J. Am. Chem. Soc.*, 1975, **97**, 5921.
82. A. Yeh and H. Taube, *J. Am. Chem. Soc.*, 1980, **102**, 4725.
83. D. A. Buckingham, D. M. Foster and A. M. Sargeson, *J. Am. Chem. Soc.*, 1969, **91**, 3451.
84. N. E. Dixon, W. G. Jackson, W. Marty and A. M. Sargeson, *Inorg. Chem.*, 1982, **21**, 688.
85. N. J. Curtis, N. E. Dixon and A. M. Sargeson, *J. Am. Chem. Soc.*, 1983, **105**, 5347.
86. J. P. Fackler and F. A. Cotton, *J. Am. Chem. Soc.*, 1961, **83**, 3775.
87. F. A. Cotton and J. J. Wise, *Inorg. Chem.*, 1966, **5**, 1200.
88. S. Shibata, *Bull. Chem. Soc. Jpn.*, 1957, **30**, 753.
89. D. P. Graddon, *Coord. Chem. Rev.*, 1969, **4**, 1.
90. E. Sinn and C. M. Harris, *Coord. Chem. Rev.*, 1969, **4**, 391.
91. J. C. Bailar, Jr., *Prep. Inorg. Reactions*, 1964, **1**, 1.
92. A. F. Wells, 'Structural Inorganic Chemistry', 4th edn., Clarendon Press, Oxford, 1975, pp. 351–352, 753.
93. H. S. Preston and C. H. L. Kennard, *J. Chem. Soc. (A)*, 1969, 2682.
94. E. Uhlig, *Coord. Chem. Rev.*, 1973, **10**, 227.
95. M. Atoji, J. W. Richardson and R. E. Rundle, *J. Am. Chem. Soc.*, 1957, **79**, 3017.
96. L. V. Interrante and R. P. Messmer, in 'Extended Interactions Between Metal Ions', ed. L. V. Interrante, ACS Symposium Series, no. 5, American Chemical Society, Washington, 1974, p. 382.
97. S. J. Lippard, *Science*, 1982, **218**, 1075.
98. M. B. Robin and P. Day, *Adv. Inorg. Chem. Radiochem.*, 1967, **10**, 247.
99. G. C. Allen and N. S. Hush, *Prog. Inorg. Chem.*, 1967, **8**, 357.
100. N. S. Hush, *Prog. Inorg. Chem.*, 1967, **8**, 391.
101. K. Y. Wong and P. N. Schatz, *Prog. Inorg. Chem.*, 1981, **28**, 369.
102. As well as Pt systems, mixed-valence Ru(II)–Ru(III) complexes have been very widely studied — see C. Creutz, *Prog. Inorg. Chem.*, 1983, **30**, 1.
103. M. Yamashita and I. Ito, *Inorg. Chim. Acta*, 1984, **87**, L5.
104. M. Yamashita, Y. Nonaka, S. Kida, Y. Hamaue and R. Aoki, *Inorg. Chim. Acta*, 1981, **52**, 43.
105. R. I. Haines and A. McAuley, *Coord. Chem. Rev.*, 1981, **39**, 77.
106. B. M. Craven and D. Hall, *Acta Crystallogr.*, 1961, **14**, 475.
107. R. J. H. Clark, *Adv. Infrared Raman Spectrosc.*, 1984, **11**, 95.
108. D. P. Craig and D. P. Mellor, *Top. Curr. Chem.*, 1976, **63**, 1.
109. C. F. Meares and T. G. Wensel, *Acc. Chem. Res.*, 1984, **17**, 202.
110. B. Bosnich and M. D. Fryzuk, *Top. Stereochem.*, 1981, **12**, 119.
111. D. P. Mellor, *Chem. Rev.* 1943, **33**, 137.
112. H. P. Jensen and F. Woldbye, *Coord. Chem. Rev.*, 1979, **29**, 213.
113. F. Woldbye, in 'Technique of Inorganic Chemistry', eds. H. B. Jonassen and A. Weissberger, Interscience, New York, 1965, vol. 4, p. 249.

114. E. L. Eliel, *J. Chem. Educ.*, 1971, **48**, 163.
115. H. Hirschmann and K. R. Hanson, *Top. Stereochem.*, 1983, **14**, 183.
116. V. Prelog and G. Helmchen, *Angew. Chem., Int. Ed. Engl.*, 1982, **21**, 567.
117. E. L. Eliel, *Top. Curr. Chem.*, 1982, **105**, 1.
118. G. E. McCasland, 'A New General System for the Naming of Stereoisomers', *Chem. Abstr.*, 1953, **47**, 2.
119. K. Mislow and J. Siegel, *J. Am. Chem. Soc.*, 1984, **106**, 3319 (for clarification of the meaning of much stereochemical nomenclature).
120. E. Ruch and I. Ugi, *Top. Stereochem.*, 1969, **4**, 99.
121. S. F. Mason, 'Molecular Optical Activity and the Chiral Discriminations', Cambridge University Press, Cambridge, 1982.
122. F. S. Richardson, *Inorg. Chem.*, 1972, **11**, 2366.
123. K. Mislow, D. Gust, P. Finocchiaro and R. J. Boettcher, *Top. Curr. Chem.*, 1974, **47**, 1.
124. F. P. Dwyer and E. C. Gyarfas, *Proc. R. Soc. New South Wales*, 1950, **83**, 263.
125. B. Bosnich, in 'Fundamental Aspects and Recent Developments in ORD and CD-NATO Advanced Study Institute, Pisa, 1971', eds. F. Ciardelli and P. Salvadori, Heyden, London, 1973, chap. 3.8 (p. 259 in particular). See also ref. 113.
126. S. F. Mason, *Q. Rev.*, 1963, **17**, 20.
127. S. F. Mason in ref. 125, chap. 2.1.
128. H. H. Jaffé and M. Orchin, 'Symmetry in Chemistry', Wiley, New York, 1965.
129. G. L. Lemiere and F. C. Alderweireldt, *J. Org. Chem.*, 1980, **45**, 4175.
130. 'IUPAC Nomenclature of Inorganic Chemistry, Definitive Rules 1970', 2nd edn., Butterworths, London, 1971, rules 7.5-7.6.
131. Y. Saito, *Top. Stereochem.*, 1978, **10**, 95.
132. *Chem. Abstr.*, Index Guide to vol. 76, 1972. *Ninth Collective Index*, 1972-1976, **76–85**, para. 203.
133. R. S. Cahn, C. K. Ingold and V. Prelog, *Angew. Chem., Int. Ed. Engl.*, 1966, **5**, 385.
134. R. S. Cahn, C. K. Ingold and V. Prelog, *J. Org. Chem.*, 1970, **35**, 2849. See also ref. 116.
135. Since the priority of ligands in stereochemical descriptors is indicated by numbers each ligand has also been given a priority number (shown here as subscript).
136. T. E. Sloan, *Top. Stereochem.*, 1981, **12**, 1.
138. 'IUPAC Nomenclature of Inorganic Chemistry, Definitive Rules 1970', 2nd edn., Butterworths, London, 1971, section 7.8; *Inorg. Chem.*, 1970, **9**, 1.
139. U. Thewalt, K. A. Jensen and C. E. Schäffer, *Inorg. Chem.*, 1972, **11**, 2129.
140. T. Damhus and C. E. Schäffer, *Inorg. Chem.*, 1983, **22**, 2406.
141. B. Bosnich and J. MacB. Harrowfield, *J. Am. Chem. Soc.*, 1972, **94**, 3425.
142. G. R. Brubaker, D. P. Schäffer, J. H. Worrell and J. I. Legg, *Coord. Chem. Rev.*, 1971, **7**, 161. See also refs. 205 and 220-222.
143. M. D. Tsai and T. T. Chang, *J. Am. Chem. Soc.*, 1980, **102**, 5416.
144. I. I. Chernyaev, L. S. Korablina and G. S. Muraveiskaya, *Russ. J. Inorg. Chem.* (*Engl. Transl.*), 1965, **10**, 567.
145. S. F. Mason, *Mol. Phys.*, 1979, **37**, 843.
146. S. F. Mason and R. H. Seal, *Mol. Phys.*, 1976, **31**, 755.
147. S. Fujinami, K. Tsuji, R. Musa and M. Shibata, *Bull. Chem. Soc. Jpn.*, 1982, **55**, 617; S. Fujinami, K. Tsuji and M. Shibata, *Bull. Chem. Soc. Jpn.*, 1981, **54**, 1531 and references cited therein.
148. E. Larsen, S. F. Mason and G. H. Searle, *Acta Chem. Scand.*, 1966, **20**, 191. See also G. Klebe and D. T. Qui, *Acta Crystallogr.*, 1984, **C40**, 476 for the structure of a chiral silicon complex with 8-hydroxyquinoline ligands.
149. B. Bosnich, *Acc. Chem. Res.*, 1969, **2**, 266.
150. H. Brunner, *Adv. Organomet. Chem.*, 1980, **18**, 151.
151. H. Brunner, *Top. Curr. Chem.*, 1975, **56**, 67.
152. Y. Saito, *Coord. Chem. Rev.*, 1974, **13**, 305.
153. Y. Saito, 'Inorganic Molecular Dissymmetry', Springer-Verlag, New York, 1979.
154. A. F. Peerdeman and J. M. Bijvoet, *Acta Crystallogr.*, 1957, **9**, 1012 (see also ref. 22, chap. 4). Note that the first application of this procedure in coordination chemistry was to the determination of the absolute configuration of Λ-[Co(en)$_3$]$^{3+}$ — see Y. Saito, K. Nakatsu, M. Shiro and H. Kuroya, *Acta Crystallogr.*, 1955, **8**, 729; *Bull. Chem. Soc. Jpn.*, 1957, **30**, 158.
155. W. Theilacker, *Z. Anorg. Allg. Chem.*, 1937, **234**, 161.
156. A. D. Liehr, *J. Phys. Chem.*, 1964, **68**, 3629.
157. In square-planar systems, however, the distinction between axial and equatorial substituent positions does not appear to be so marked — see B. Bosnich and E. A. Sullivan, *Inorg. Chem.*, 1975, **14**, 2768.
158. Numerous reviews and books on this topic exist. A recent article describing the development of the method for organic systems is E. Osawa and H. Musso, *Top. Stereochem.*, 1982, **13**, 117. For inorganic systems see ref. 160.
159. C. J. Hawkins and J. A. Palmer, *Coord. Chem. Rev.*, 1982, **44**, 1.
160. G. R. Brubaker and D. W. Johnson, *Coord. Chem. Rev.*, 1984, **53**, 1.
161. E. J. Corey and J. C. Bailar, Jr., *J. Am. Chem. Soc.*, 1959, **81**, 2620. Note Corey and Bailar used conformational designations k and k', where $k \equiv \lambda$ and $k' \equiv \delta$.
162. See ref. 154.
163. C. E. Schaffer, *Proc. R. Soc. London, Ser. A*, 1967, **297**, 96.
164. P. Anderson, F. Galsbøl and S. E. Harnung, *Acta Chem. Scand.*, 1969, **23**, 3027.
165. J. K. Beattie, *Acc. Chem. Res.*, 1971, **4**, 253.
166. Ref. 22, p. 86-94.
167. L. J. DeHayes and D. H. Busch, *Inorg. Chem.*, 1973, **12**, 1505.
168. S. R. Niketić and F. Woldbye, *Acta Chem. Scand.*, 1973, **27**, 621, 3811; *Acta Chem. Scand., Ser. A*, 1974, **28**, 248.
169. T. Nomura, F. Marumo and Y. Saito, *Bull. Chem. Soc. Jpn.*, 1969, **42**, 1016.
170. K. Matsumoto, M. Yonezawa, H. Kuroya, H. Kawaguchi and S. Kawaguchi, *Bull. Chem. Soc. Jpn.*, 1970, **43**, 1269.
171. E. Yasaki, I. Oonishi, H. Kawaguchi, S. Kawaguchi and Y. Komiyama, *Bull. Chem. Soc. Jpn.*, 1970, **43**, 1354.
172. K. Matsumoto, S. Ooi and H. Kuroya, *Bull. Chem. Soc. Jpn.*, 1970, **43**, 1903.

173. B. Morosin and J. Howatson, *Acta Crystallogr., Sect. B*, 1970, **26**, 2062 and references cited therein.
174. B. Bosnich and J. MacB. Harrowfield, *Inorg. Chem.*, 1975, **14**, 853.
175. R. J. Geue and M. R. Snow, *J. Chem. Soc. (A)*, 1971, 2981.
176. See refs. 178–180, 246 and 251.
177. J. R. Gollogly and C. J. Hawkins, *Inorg. Chem.*, 1972, **11**, 156.
178. H. Boucher and B. Bosnich, *Inorg. Chem.*, 1976, **15**, 1471, 2364.
179. F. Mizukami, H. Ito, J. Fujita and K. Saito, *Bull. Chem. Soc. Jpn.*, 1972, **45**, 2129.
180. M. Ajioka, S. Yano, M. Saburi and S. Yoshikawa, *Inorg. Chem.*, 1981, **20**, 884 and references cited therein.
181. Y. Shimura, *Bull. Chem. Soc. Jpn.*, 1958, **31**, 315.
182. J. B. Lambert, *Top. Stereochem.*, 1971, **6**, 19.
183. B. Halpern, A. M. Sargeson and K. R. Turnbull, *J. Am. Chem. Soc.*, 1966, **88**, 4630.
184. E. K. Barefield and F. Wagner, *Inorg. Chem.*, 1973, **12**, 2435; 1976, **15**, 408.
185. K. Mislow, *Trans. N.Y. Acad. Sci.*, 1973, **35**, 227.
186. L. Horner and H. Winkler, *Tetrahedron Lett.*, 1964, 461.
187. R. D. Baechler and K. Mislow, *J. Am. Chem. Soc.*, 1970, **92**, 3090.
188. G. H. Senkler and K. Mislow, *J. Am. Chem. Soc.*, 1972, **94**, 291.
189. B. Bosnich and S. B. Wild, *J. Am. Chem. Soc.*, 1970, **92**, 459.
190. N. K. Roberts and S. B. Wild, *J. Am. Chem. Soc.*, 1979, **101**, 6254.
191. L. Horner and W. Hofer, *Tetrahedron Lett.*, 1966, 3323.
192. N. K. Roberts and S. B. Wild, *J. Chem. Soc., Dalton Trans.*, 1979, 2015.
193. L. Horner and W. Hofer, *Tetrahedron Lett.*, 1965, 3281.
194. B. Bosnich, W. G. Jackson and S. B. Wild, *J. Am. Chem. Soc.*, 1973, **95**, 8269.
195. G. Salem and S. B. Wild, *Inorg. Chem.*, 1983, **22**, 4049 and references cited therein.
196. K. Mislow, M. M. Green, P. Laur, J. T. Mellillo, T. Simmons and A. L. Ternay, *J. Am. Chem. Soc.*, 1965, **87**, 1958.
197. R. Tang and K. Mislow, *J. Am. Chem. Soc.*, 1970, **92**, 2100.
198. C. A. Maryanoff, B. E. Maryanoff, R. Tang and K. Mislow, *J. Am. Chem. Soc.*, 1973, **95**, 5839.
199. H. Boucher and B. Bosnich, *Inorg. Chem.*, 1977, **16**, 717.
200. H. Boucher and B. Bosnich, *J. Am. Chem. Soc.*, 1977, **99**, 6253.
201. E. W. Abel, S. K. Bhargava, K. Kite, K. G. Orrell, V. Sik and B. L. Williams, *J. Chem. Soc., Dalton Trans.*, 1984, 365.
202. E. W. Abel, S. K. Bhargava and K. G. Orrell, *Prog. Inorg. Chem.*, 1984, **32**, 1.
203. W. G. Jackson and A. M. Sargeson, *Inorg. Chem.*, 1978, **17**, 2165.
204. Single diastereomers have, however, been isolated in related systems — see S. Ohba and Y. Saito, *Acta Crystallogr., Sect. C*, 1984, **40**, 398; J. D. Lydon, R. C. Elder and E. Deutsch, *Inorg. Chem.*, 1982, **21**, 3186.
205. B. Bosnich, W. R. Kneen and A. T. Philip, *Inorg. Chem.*, 1969, **8**, 2567.
206. J. Jacques, C. Gros and S. Boucier, in 'Stereochemistry', ed. H. B. Kagan, Thieme, Stuttgart, 1977, vol. 4.
207. S. H. Wilen, *Top. Stereochem.*, 1971, **6**, 107. See also J. Jacques, A. Collet and S. H. Wilen, 'Enantiomers, Racemates and Resolutions', Wiley-Interscience, New York, 1981.
208. P. Newman, 'Optical Resolution Procedures for Chemical Compounds', vols. I–IV, Optical Resolution Information Center, New York, 1978.
209. M. D. Fryzuk and B. Bosnich *J. Am. Chem. Soc.*, 1977, **99**, 6262.
210. H. B. Kagan and T. P. Dang, *J. Am. Chem. Soc.*, 1972, **94**, 6429.
211. Ref. 17, pp. 78–81.
212. F. A. McCrinn, A. K. Lazarus, M. Siegel, J. E. Ricci and K. Mislow, *J. Am. Chem. Soc.*, 1958, **80**, 476.
213. A. Miyashita, A. Yasuda, H. Takaya, K. Toriumi, T. Ito, T. Souchi and R. Noyori, *J. Am. Chem. Soc.*, 1980, **102**, 7932.
214. A. Miyashita, H. Takaya, T. Souchi and R. Noyori, *Tetrahedron*, 1984, **40**, 1245.
215. L. M. Engelhardt, W.-P. Leung, C. L. Raston, P. Twiss and A. H. White, *J. Chem. Soc., Dalton Trans.*, 1984, **321**, 331.
216. K. J. Brown, M. S. Berry, K. C. Waterman, D. Lingenfelter and J. R. Murdoch, *J. Am. Chem. Soc.*, 1984, **106**, 4717.
217. A. general review of metal complexes with amine ligands is given by D. A. House in Chapter 13.1 of Volume 2.
218. D. A. House, *Coord. Chem. Rev.*, 1977, **23**, 223.
219. Some more recent references that typify the range of studies made include G. H. Searle and M. E. Angley, *Inorg. Chim. Acta*, 1981, **49**, 185; M. Kojima and J. Fujita, *Bull. Chem. Soc. Jpn.*, 1982, **55**, 1454; G. H. Searle and T. W. Hambley, *Aust. J. Chem.*, 1982, **35**, 2399; G. R. Brubaker and D. W. Johnson, *Inorg. Chem.*, 1983, **22**, 1422; A. Watson, A. R. Gainsford and D. A. House, *Inorg. Chim. Acta*, 1984, **86**, L11; and M. F. Gargallo, R. E. Tapscott and E. N. Duesler, *Inorg. Chem.*, 1984, **23**, 918. See also ref. 160.
220. A. M. Sargeson and G. H. Searle, *Inorg. Chem.*, 1965, **4**, 45; 1967, **6**, 787; 1967, **6**, 2172.
221. D. A. Buckingham, P. A. Marzilli and A. M. Sargeson, *Inorg. Chem.*, 1967, **6**, 1032.
222. D. A. Buckingham, P. J. Cresswell, R. J. Dellaca, M. Dwyer, G. J. Gainsford, L. G. Marzilli, I. E. Maxwell, W. T. Robinson, A. M. Sargeson and K. R. Turnbull, *J. Am. Chem. Soc.*, 1974, **96**, 7113 and references cited therein.
223. R. K. Wismer and R. A. Jacobson, *Inorg. Chim. Acta*, 1973, **7**, 477.
224. S. Utsuno, Y. Sakai, S. Yoshikawa and H. Yamatera, *J. Am. Chem. Soc.*, 1980, **102**, 6903.
225. J. Selbin and J. C. Bailar, Jr., *J. Am. Chem. Soc.*, 1960, **82**, 1524.
226. See refs. 220–222. The enantiomers of *trans*-$[(\mathrm{CN})_2\mathrm{Co}(\mathrm{trien})]^+$ have also been described in ref. 220.
227. Conformational isomers of $[\mathrm{Cogly}(\mathrm{trien})]^{2+}$ are referred to in ref. 23, p. 258 (W. T. Robinson and V. Jansen, unpublished work). Two conformers in one crystal have also been observed in (*OC*-6-22)-$[\mathrm{Co}(\mathrm{dien})_2]$-$[\mathrm{Co}(\mathrm{CN})_6]\cdot 2\mathrm{H_2O}$ — M. Kabayashi, F. Marumo and Y. Saito, *Acta Crystallogr., Sect. B*, 1972, **28**, 470; M. Konne, F. Marumo and Y. Saito, *Acta Crystallogr., Sect. B*, 1973, **29**, 739.
228. These include *trans,trans*-$[\mathrm{CoCl}(\mathrm{NO_2})(\mathrm{Meen})_2]^+$ and *trans*-$[\mathrm{CoCl}(\mathrm{NO_2})(R,S\text{-tetars})]\mathrm{Cl}$ isomers — see D. A. Buckingham, L. G. Marzilli and A. M. Sargeson, *Inorg. Chem.*, 1968, 7, 915 and ref. 194.
229. W. W. Cleland and A. S. Mildvan, *Adv. Inorg. Chem. Biochem.*, 1979, **1**, 163.
230. F. Eckstein, *Acc. Chem. Res.*, 1979, **12**, 204.
231. G. J. Gainsford and A. M. Sargeson (Australian National University), unpublished work.
232. E. A. Merritt and M. Sundaralingam, *Acta Crystallogr., Sect. B*, 1980, **36**, 2576.
233. R. D. Cornelius, P. A. Hart and W. W. Cleland (*Inorg. Chem.*, 1977, **16**, 2799) discuss isomerism in cobalt(III)-polyphosphate complexes.

234. B. Anderson, R. M. Milburn, J. MacB. Harrowfield, G. B. Robertson and A. M. Sargeson, *J. Am. Chem. Soc.*, 1977, **99**, 2652.
235. R. D. Cornelius, *Inorg. Chem.*, 1980, **19**, 1286.
236. P. R. Norman and R. D. Cornelius, *J. Am. Chem. Soc.*, 1982, **104**, 2356.
237. For related studies on complexes of ATP and ADP, see R. D. Cornelius and W. W. Cleland, *Biochemistry*, 1978, **17**, 3279; D. Dunaway-Mariano and W. W. Cleland, *Biochemistry*, 1980, **19**, 1496, 1506; S. H. McClaugherty and C. M. Grisham, *Inorg. Chem.*, 1982, **21**, 4133 and references cited therein.
238. E. A. Merritt, M. Sundaralingam, R. D. Cornelius and W. W. Cleland, *Biochemistry*, 1978, **17**, 3274 (a refinement of the $[CoH_2P_3O_{10}(NH_3)_4]\cdot H_2O$ structure is reported in ref. 232).
239. R. D. Cornelius, E. A. Merritt and M. Sundaralingam, *J. Am. Chem. Soc.*, 1980, **102**, 6151.
240. D. R. Jones, L. F. Lindoy, A. M. Sargeson and M. R. Snow, *Inorg. Chem.*, 1982, **21**, 4155.
241. For reviews of the field with emphasis on transition metal complexes of ligands other than ethers, see G. A. Melson (ed.), 'Coordination Chemistry of Macrocyclic Compounds', Plenum, New York, 1979. For some particular considerations of this chemistry, see D. H. Busch, *Acc. Chem. Res.*, 1978, **11**, 392. There is an extensive literature on macrocyclic ethers but recent brief reviews covering aspects of their coordination chemistry are given in 'Host-Guest Complex Chemistry', ed. F. Vögtle, vols. I and II, *Top. Curr. Chem.*, nos. 98 (1981) and 101 (1982).
242. N. F. Curtis, *Coord. Chem. Rev.*, 1968, **3**, 3.
243. L. G. Warner and D. H. Busch, *J. Am. Chem. Soc.*, 1969, **91**, 4092.
244. N. F. Curtis, D. A. Swann and T. N. Waters, *J. Chem. Soc., Dalton Trans.*, 1973, 1963.
245. C. S. Lee, S. Y. Wu and C. S. Chung, *Inorg. Chem.*, 1984, **23**, 1298.
246. K. N. Raymond, P. W. R. Corfield and J. A. Ibers, *Inorg. Chem.*, 1968, **7**, 1362.
247. R. R. Holmes, *Acc. Chem. Res.*, 1979, **12**, 257 — for similar comments on Cu^{II} in 5-coordination, see D. Reinen and C. Friebel, *Inorg. Chem.*, 1984, **23**, 791.
248. R. H. Holm and M. J. O'Connor, *Prog. Inorg. Chem.*, 1971, **14**, 241.
249. N. N. Greenwood and A. Earnshaw, 'Chemistry of the Elements', Pergamon, Oxford, 1984, p. 1078.
250. B. T. Kilbourn, H. M. Powell and J. A. C. Derbyshire, *Proc. Chem. Soc. London*, 1963, 207.
251. A. Terzis, K. N. Raymond and T. G. Spiro, *Inorg. Chem.*, 1970, **9**, 2415.
252. S. Yamada and A. Takeuchi, *Coord. Chem. Rev.*, 1982, **43**, 187.
253. L. Sacconi, *Coord. Chem. Rev.*, 1966, **1**, 126.
254. C. R. C. Coussmaker, M. H. Hutchinson, J. R. Mellor, L. E. Sutton and L. M. Venanzi, *J. Chem. Soc.*, 1961, 2705.
255. L. M. Vallarino, W. E. Hill and J. V. Quagliano, *Inorg. Chem.*, 1965, **4**, 1598.
256. A. G. Sykes and J. A. Weil, *Prog. Inorg. Chem.*, 1970, **13**, 1.
257. K. Wade, *Adv. Inorg. Chem. Radiochem.*, 1976, **18**, 1.
258. K. H. Tytko and O. Glemser, *Adv. Inorg. Chem. Radiochem.*, 1976, **19**, 239.
259. J. Catterick and P. Thornton, *Adv. Inorg. Chem. Radiochem.*, 1977, **20**, 291.
260. D. C. Walker (ed.), 'Origins of Optical Activity in Nature', (Studies in Physical and Theoretical Chemistry, no. 7), Elsevier, Amsterdam, 1979.

6

Ligand Field Theory

BRIAN N. FIGGIS

University of Western Australia, Nedlands, Australia and *Brookhaven National Laboratory, Upton, NY, USA*

6.1 OVERVIEW

Ligand field theory may be taken to be the subject which attempts to rationalize and account for the physical properties of transition metal complexes in fairly simple-minded ways. It ranges from the simplest approach, crystal field theory, where ligands are represented by point charges, through to elementary forms of molecular orbital theory, where at least some attempt at a quantum mechanical treatment is involved. The aims of ligand field theory can be treated as essentially empirical in nature: *ab initio* and even approximate proper quantum mechanical treatments are not considered to be part of the subject, although the simpler empirical methods may be.

Numerous physical properties are studied with transition metal complexes as the subjects, and many of them involve the use of ligand field theory in their interpretation. They vary from those such as the spectra and magnetic properties, which are heavily dependent on ligand field theory, to others such as reaction kinetics where the application of the theory is rather peripheral.

Obviously, in a presentation such as this, there is not room to develop the basics of the various forms of ligand field theory in detail nor to describe applications to all the relevant physical properties. This chapter will set out to compare the major aspects of the different forms, will give an account of their use in the interpretation of spectra and magnetism of transition metal complexes, and will make some mention of other areas.

The major features of the energy level distribution in a complex of a *d*-electron or *f*-electron metal ion may be supposed to be reproduced by a Hamiltonian operator of the general form

$$H = H_{LF} + H_{ER} + H_{LS}$$

operating on the *d*-orbital or *f*-orbital manifold; H_{LF} is the ligand field term, H_{ER} the interelectronic repulsion term and H_{LS} the spin–orbit coupling term.

It is useful to recognize the relative importance of the forms in this Hamiltonian for different systems:

First and second transition series	$H_{LF} \approx H_{ER} > H_{LS}$
Third transition series	$H_{LF} \approx H_{ER} \approx H_{LS}$
Lanthanoids	$H_{ER} > H_{LS} > H_{LF}$
Actinoids	$H_{ER} \gtrsim H_{LS} \gtrsim H_{LF}$

H_{LF} will take into account the presence of the surrounding ligand molecules whether treated as point charges, as in the crystal field model, or as covalently bound entities, as in ligand field methods. It will be discussed first in some detail in Section 6.2, as it forms the whole strategy for the presentation of this chapter. H_{ER} takes into account the repulsions between the *d* or *f* electron sets, including the application of the constraints of the Pauli Exclusion Principle and electron spin. It consists of two components, the Coulomb repulsion and the exchange terms. This subject will be introduced, to the extent necessary for the application of the H_{LF} term to relevant physical properties, in Section 6.3. H_{LS} takes into account the formal coupling between the spin and angular momenta of the *d* or *f* electrons. In fact, it arises from the same basis as H_{ER}, and is treated along with that term for the same purposes in Section 6.3.

The use of the principles laid down in Sections 6.2 and 6.3 in accounting for the physical properties of complexes will proceed in Sections 6.4–6.7.

6.2 LIGAND FIELD THEORIES

A ligand field theory considers the interaction between a central transition metal atom and its ligands, in particular the part arising from the immediate donor atoms and their effects on the *d*-orbitals of the metal atom and the electrons which occupy them. Secondary considerations may also include more distant parts of the ligand molecules and the presence of orbitals other than *d* on the metal atom. It is in this way that the empirical nature of ligand field theories is emphasized. There is no doubt from proper quantum mechanical considerations that the energetics, and therewith major features of many physical properties, are determined by a number of attributes of a ligand molecule, particularly a polyatomic one, and by its interaction with all the valence electrons of a central metal atom — coordination chemistry is certainly well established outside the transition metals. A ligand field theory seeks to explain and rationalize as much as possible using only the facets specified in the first sentence of this section.

6.2.1 Crystal Field Theory (CFT)[1–11]

The oldest and simplest of the ligand field theories is the one which assumes that the transition metal atom is ionized according to its formal positive oxidation number, and that the effects of the ligands can be obtained by representing them as corresponding negative charges. The name arose because the initial application[1] was intended for the spectra of simple crystalline solids, where the model is probably not too far from reality. The bivalent transition metal oxides, MO, approximating M^{2+} and O^{2-} ions stacked in the simple cubic lattice of the NaCl structure with six anions in octahedral coordination about each cation, and *vice versa*, are examples. However, it was soon realized that the spectra and magnetic properties of the complexed transition metal ions in general, including those in solution, are often strongly related to those for an ionic crystal,[9,12–16] and the approach gained wide acceptance.

6.2.1.1 The crystal field potential (CFP)[1–3,5,6,8]

The calculation of the energy of a transition metal ion *d*-orbital in the presence of the electric field gradients produced by a regular array of the positive and negative charges of other cations and anions in, say, a simple cubic lattice is at first sight a straightforward, if rather tedious, exercise. The procedure is outlined in principle only here; detailed expositions are available elsewhere.

From elementary electrostatics a charge z, at point i, produces a potential $z_i/r_{ij} = z_i(1/r_{ij})$ at point j, a distance r_{ij} from the charge. It is convenient to express the $1/r_{ij}$ term in the potential as the standard expansion[17]

$$\frac{1}{r_{ij}} = \sum_{n=0}^{\infty} \sum_{m=-n}^{n} \frac{4\pi}{2n+1} \frac{r_<^{\,n}}{r_>^{\,n+1}} Y_{n_j}^{\;m} Y_{n_i}^{\;m*} \qquad (1)$$

Here $Y_{n_j}^{\;m}$ and $Y_{n_i}^{\;m}$ are spherical harmonics, functions of the angles θ and ϕ as set out in Figure 1, and $r_<$ and $r_>$ are respectively the lesser and the greater of the distances from the arbitrarily chosen origin and the points i and j.

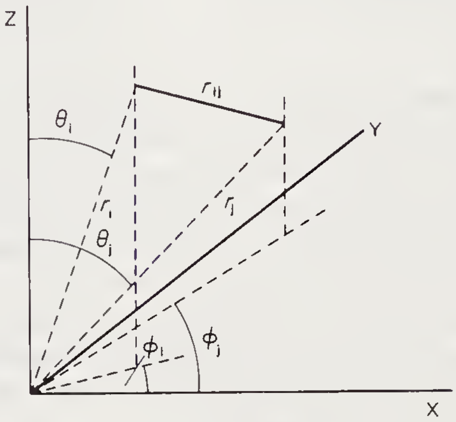

Figure 1 The angles θ and ϕ involved in the expansion of $1/r_{ij}$ (reproduced with permission from 'Introduction to Ligand Fields', Wiley-Interscience, 1966)

The evaluation of the crystal field potential at one of the transition metal ions in, say, a simple cubic lattice is simply a matter of choosing it as the origin for the spherical harmonics in the above expansion, and filling in values of i for the positions of the other ions in the lattice, with charges z_i. The calculation is considerably simplified because it can be shown that, for d-orbitals, no term in the expansion with $n > 4$ can affect the energy and, because of their inversion symmetry, neither can terms with n odd. Further, the spherical harmonics with $n = 0$ are simply the number $2^{-\frac{1}{2}}$, and so do not differentiate between the d-orbitals. Consequently, it is only necessary to use terms with $n = 2$ and 4. Nevertheless, the summation in principle is over an infinite number of lattice points, and in practice over a great many, since the term involving $r_>^{-3}$, for $n = 2$, does not decrease very rapidly with distance from the origin.

The crystal field potential obtained in this way will be of the general form

$$V_{(xyz)} = \sum_{i=0}^{m} b_n^{\,i} r^n Y_n^{\,i} \qquad n = 2, 4 \qquad (2)$$

with the $b_n^{\,i}$ a set of constants dependent upon the details of the particular lattice chosen, and with the terms in $n = 2$ greater than those in $n = 4$ because of the slower decrease with distance.

For the simple cubic lattice, the very high symmetry forces further simplifications

$$V_{\mathrm{NaCl}}(xyz) = C\left(\frac{ze\overline{r_d^{\,4}}}{a^5}\right)\left[Y_4^{\,0} + \left(\frac{5}{14}\right)^{1/2}(Y_4^{\,4} + Y_4^{\,-4})\right] \qquad (3)$$

with a the anion–cation separation. Other cubic lattices also have similarly simple forms of the crystal field potential. For the cation in a ZnS (wurtzite) lattice, where the coordination is tetrahedral, the potential is

$$V_{\mathrm{ZnS}} = \frac{-4}{9} V_{\mathrm{NaCl}} \frac{2\overline{r_{\mathrm{M}^{2+}}^{\,4}}\, a_{\mathrm{oct}}^{\,5}}{\overline{r_{\mathrm{M}^{+}}^{\,4}}\, a_{\mathrm{tet}}^{\,5}}$$

6.2.1.2 *The effects of the CFP*

The derivation of the crystal field potential V_{CF} at a transition metal ion site in a crystal is seen to be conceptually straightforward, and to obtain the relative effects such a potential should have on the energies of the *d*-orbital is, similarly, formally simple. We note that the *d*-orbitals are mathematical functions of the form

$$d_i = R_n{}^2 Y_2{}^i \qquad i = -2 \dots 2$$

where n is the principal quantum number of the orbitals. The required energies are roots of the 5×5 secular determinant

$$|H_{ij} - \lambda\delta(i, j)| = 0 \tag{4}$$

where, in the usual nomenclature,

$$H_{ij} = \langle d_i{}^* | V_{\mathrm{CF}} | d_j \rangle$$

For example, for the simple cubic lattice, the determinant takes the form

$$\begin{array}{c|ccccc|}
d_{-2} & C' - \lambda & . & . & . & 5C' \\
d_{-1} & . & -4C' - \lambda & . & . & . \\
d_0 & . & . & 6C' - \lambda & . & . \\
d_1 & . & . & . & -4C' - \lambda & . \\
d_2 & 5C' & . & . & . & C' - \lambda
\end{array}$$

where, for example

$$C' = \langle d_1{}^* | V_{\mathrm{NaCl}} | d_1 \rangle$$

is a constant which depends upon C in equation (3) and the standard result of the integration of three spherical harmonics[18]

$$C_2{}^{l,l} = \int Y_2{}^{l*} Y_4{}^0 \, Y_2{}^l \, \mathrm{d}\iota \tag{5}$$

The energies which result from the diagonalization of equation (5) are

$\lambda = 6C'$ twofold degenerate, and

$\lambda = -4C'$ threefold degenerate

Thus, for a transition metal ion in a simple cubic lattice, crystal field theory predicts that the *d*-orbitals are split into two types, one consisting of two members, henceforth referred to as the e_g set, of higher energy than the remaining three, which are also degenerate and referred to as the t_{2g} set. The labels e_g and t_{2g} are given because of their transformation properties in the group O_h which describes the site symmetry of an ion in a simple cubic lattice.[19]

Using the solutions for λ in the set of secular equations which corresponds to the secular determinant (equation 3) yields the linear combinations of the *d*-orbitals which belong to the two types in the crystal field. Using the coordinate system of Figure 2, where the origin is at a cation in the simple cubic lattice and the Cartesian axes are the cell axes, one obtains the well known result that

$$t_{2g} \equiv \begin{cases} d_{xz} \\ d_{yz} \\ d_{xy} \end{cases} \qquad e_g \equiv \begin{cases} d_{x^2-y^2} \\ d_{z^2} \end{cases}$$

In the simple cubic lattice, as has been pointed out, the terms in the crystal field potential with $n = 2$ cancel, and the remaining terms with $n = 4$ involve an r_d^{-5} distance dependence. As a first approximation, in this case, it is reasonable to consider only the nearest neighbours of the cation at the origin, that is the six anions in the octahedral positions shown in Figure 2. The deduction concerning the splitting of the *d*-orbitals is then confirmed qualitatively very readily. The $d_{x^2-y^2}$ and d_{z^2} orbital lobes are directed directly at the anion positions, and so the orbitals are raised in energy by repulsion by the negative charges. The d_{xz}, d_{yz} and d_{xy} orbital lobes are directed between the anions, and so these orbitals are raised less in energy. There is a splitting between the t_{2g} and e_g orbital sets, with the e_g set higher in energy.

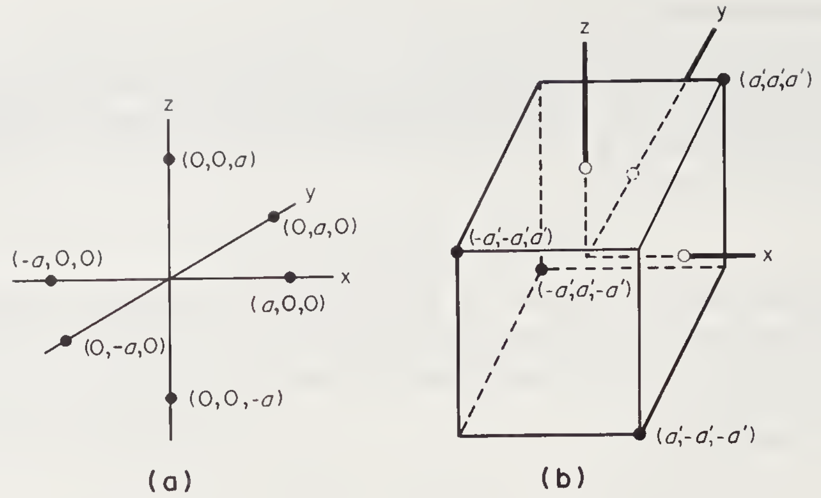

Figure 2 Octahedral (a) and tetrahedral (b) arrays of point charges. For equal origin–point distances, $a' = (8/3)^{1/2}a$. For a cube arrangement add points at $(\pm a', \pm a', -a')$, $(\pm a', \pm a', a')$

The form of equation (3) is most suitable for the evaluation of the effects of the CFP using d-orbital wave functions. However, it is possible to recast it in the form of equation (6), where functions of the Cartesian axes rather than the spherical harmonics are employed

$$V_{\mathrm{NaCl}} = D\,(x^4 + y^4 + z^4 - 3r^4/5) \tag{6}$$

The numbers involving the integrations over the d-orbitals with this potential can be absorbed into a constant q. Then the solutions to the secular determinant (equation 5) take the form

$$\lambda = 6Dq \quad \text{for the } e_g \text{ set}$$
$$\lambda = -4Dq \quad \text{for the } t_{2g} \text{ set}$$

and we get the familiar splitting pattern for the d-orbitals in an octahedral crystal field set out in Figure 3. The d-orbitals are seen to be separated so that their 'center of gravity' is maintained. The overall separation, $10Dq$, is often referred to by the symbol Δ. The fact that the 'center of gravity' of the d-orbitals is maintained in the presence of the crystal field potential is a result of the conventional procedure of omitting the terms in the potential with $n = 0$. In fact, there is an overall shift in the d-orbital energy, as illustrated in Figure 3, but as this is not distinguishable from other energy changes in the cation consequent upon its incorporation into the lattice, the convention is to ignore it.

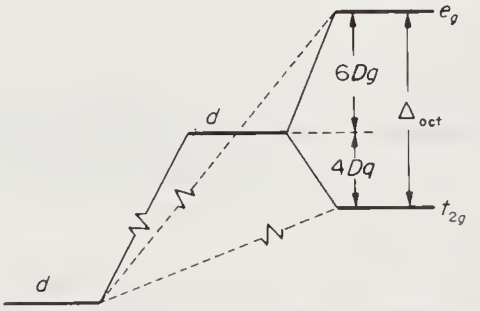

Figure 3 Effect of an octahedral ligand field on the d-orbitals

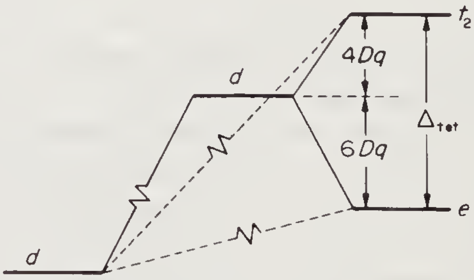

Figure 4 Effect of a tetrahedral ligand field on the d-orbitals

For the tetrahedron, the d_{z^2} and $d_{x^2-y^2}$ orbital (e) set is directed to avoid the anion positions (Figure 2b), while the d_{xy}, d_{yz} and d_{xz} set (t_2) is more directed towards them. For a cation in tetrahedral coordination by its nearest-neighbour anions the CFP is of opposite sign and of 4/9 times the magnitude of the octahedral nearest-neighbour case for given cation–anion separation and charges. The arguments used in connection with V_{NaCl} can be transferred along with V_{ZnS} to give the result that for regular tetrahedral coordination the crystal field splitting makes the t_2 orbital set higher in energy than the e set. Note that the g subscript has been dropped, as there is no center of symmetry for the tetrahedron, so that the inversion properties of the d-orbitals are not relevant. The d-orbital splitting resulting from V_{ZnS} is set out in Figure 4. We have the result that, for constant cation–anion separation and charge

$$Dq_{\mathrm{tet}} = -\frac{4}{9}Dq_{\mathrm{oct}}$$
$$\Delta_{\mathrm{tet}} = -\frac{4}{9}\Delta_{\mathrm{oct}}$$

Note also that a cube is composed of two tetrahedra, each of which occupies alternate cube corners. Consequently, we may write

$$V_{\mathrm{cube}} = 2V_{\mathrm{tet}}$$

$$Dq_{\mathrm{cube}} = -\frac{8}{9}Dq_{\mathrm{oct}} \ : \ \Delta_{\mathrm{cube}} = -\frac{8}{9}\Delta_{\mathrm{oct}}$$

6.2.1.3 Generality of the crystal field model

A prediction of crystal field theory as outlined in the preceding subsections is that the crystal field splitting parameter, Δ, should be rather critically dependent upon the details of the crystal lattice in which the transition metal ion is found, and that the splittings of the *d*-orbital energies should become larger and quite complicated in lattices of symmetry lower than cubic. The theory could not be expected to apply, for example, to the spectra of transition metal ions in solution.

In fact, the converse is observed. The main features of the spectra of transition metal ions in solution are very similar to those for crystal lattices where the same donor atom is present as an anion. Further, the spectra differ little between solids provided the nearest-neighbour atom is unchanged, even if it is part of a multi-atom species and even if the symmetry of the crystal structure is low. The spectra of the first transition series carbonates, for example, are not markedly different from those of their oxides, nor from those of the ions in aqueous solution. In each case the nearest-neighbour atom is oxygen and six of these surround the metal atom in approximately octahedral positions.

The obvious deduction from these observations is that the *d*-orbital energy splitting is not primarily of a simple electrostatic nature, but reflects rather the much shorter range effects to be expected of covalence in chemical bonding to the immediate donor atoms. The conclusion is reinforced by the fact that when the known interionic separations are used together with free ion 3*d*-orbital wave functions to evaluate Dq for first transition series ions in an MF_2 lattice, values too small by an order of magnitude are obtained.[6,20–22]

Although the physical basis of the crystal field model is seen to be unsound, the fact remains that, in summarizing the importance of the symmetry of the ligand environment, it *qualitatively* reproduces many of the features of the magnetic and spectral properties of transition metal complexes. This early qualitative success established its nomenclature in the fields of these properties. While we shall have little more to say about crystal field theory as such, much of the rest of this article will be couched in the language of the crystal field model, and for that reason some little trouble has been taken to outline its development.

One area where crystal field theory has been thought to provide some quantitative predictive power perhaps deserves mention. As will be mentioned later, the calculation of Δ on an absolute basis presents considerable difficulty for any theory dealing with the (transition metal)–ligand bond. The prediction of how Δ should vary with change in the length of that bond for a given metal–donor atom pair is correspondingly uncertain. Crystal field theory offers a direct answer here. *If* it is accepted that only the immediate donor atoms are important in determining the value of Δ, then for regular octahedral coordination the value of D in equation (6) can be written down quite readily as

$$D = 35ze/4a^5 \tag{7}$$

where a is the metal–donor atom distance. The prediction of CFT is that

$$\Delta \propto a^{-5}$$

For several systems, including those related to the MO lattices, it is indeed observed from experiments which change, for example, the M—O distance by applying pressure or changing the temperature that the value of Δ changes in a manner fairly consistent with the equation (7).[23,24] However, the result is probably largely fortuitous. If the metal–donor atom distance is changed by altering the nature of the bonding interaction between the two atoms then equation (7) fails.[25] For example, the —CH_3 group as ligand to Co^{III} gives rise to a Co—C bond length of 200 pm, the $C{\equiv}N^-$ ion to one of 189 pm, yet the value of Δ corresponding to these two systems is not very different, ~33000 and 33500 cm^{-1}.

At this point it is pertinent to mention other ways in which CFT has shown obvious limitations in dealing with the physical properties of transition metal complexes.

As will be elaborated later, to deal with the spectra of transition metal ions with more than one electron in the empty (or hole in the filled) d^{10} shell, it is necessary to take into account interelectronic repulsion energies within the *d* manifold. On the basis of CFT, of course, the parameters of such repulsion to be used should be those of the free transition metal ions, values of which are quite well known from atomic spectroscopy. In fact, one can determine the parameters for interelectronic repulsion for use in the interpretation of the spectra of the complexes, and they are found to be reduced, often considerably, from their free-ion magnitudes.[26,27] It is obvious that the *d*-orbitals, in their involvement in chemical bonding to the ligand donor atom, suffer appreciable effective changes.

Such effective changes are also manifest in connection with magnetic properties. On the basis of the orbital angular momentum of *d*-electrons, as will be examined in detail in due course, the magnetic behaviour of complexes is predicted by CFT to depart in a number of ways from that expected for the presence of electron spin alone. In fact, the magnetic properties of complexes are often rather close to the spin-only behaviour,[2,28,29] and it is seen that a free-ion description of the *d*-orbitals is not adequate.

6.2.1.4 Crystal fields of low symmetry

The above discussion has emphasized that the splitting of the energies of the *d*-orbitals is dominated by the effects of the formal octahedral or tetrahedral symmetry of the ligand donor atom environment. This dominance is also present for coordination stereochemistries approximating to these symmetries. However, the effects of departure from these cubic symmetries are not negligible, and may be dominant for stereochemistries which do not even approximate to one of the cubic ones, *e.g.* a square-planar coordination geometry.

Given a set of donor atom positions around a central ion it is fairly straightforward to derive a CFP of the form of equation (2). If all but the main terms arising from the donor atom formal charges are omitted, the potential is of the general form[30–33]

$$V_{\mathrm{CF}} = b_2{}^0 r^2 Y_2{}^0 + b_4{}^0 r^4 Y_4{}^0 + b_4{}^4 r^4 (Y_4{}^4 + Y_4{}^{-4}) \tag{8}$$

if the symmetry is at least approximately tetragonal, and

$$V_{\mathrm{CF}} = b_2{}^0 r^2 Y_2{}^0 + b_4{}^0 r^4 Y_4{}^0 + b_4{}^3 r^4 (Y_4{}^3 - Y_4{}^{-3}) \tag{9}$$

if it is at least approximately trigonal; $b_4{}^0$ is related to $b_4{}^3$ or $b_4{}^4$, so only two independent parameters are involved.

As indicated earlier, a difficulty immediately arises: the evaluation of the parts of the matrix elements (equation 4) involving terms containing *r* using free-ion *d* wave functions gives results which are obviously grossly in error. Consequently, there is not likely to be any relationship between the parameters such as developed in cubic symmetry: the low symmetry cases involve (at least) three parameters to describe the *d*-orbital splitting pattern.

The parameterization schemes of equation (8) or (9) are sometimes maintained, particularly when parameterization is the only goal. However, in many chemical applications a different scheme is used,[3,34] involving a correspondence to those of equations (8) or (9) such that *Ds* contains the effects of $b_2{}^0 r^2$ and *Dt* those of the difference between $b_4{}^0 r^4$ and the value it would have in an undistorted cubic stereochemistry. There results the *d*-orbital energy sequence

$$\left.\begin{array}{llll} a_{1g} & d_{z^2} & \text{at} & 6Dq - 2Ds - 6Dt \\ b_{1g} & d_{x^2-y^2} & \text{at} & 6Dq + 2Ds - Dt \end{array}\right] 4Ds + 5Dt \tag{10}$$

$$\left.\begin{array}{llll} b_{2g} & d_{xy} & \text{at} & -4Dq + 2Ds - Dt \\ e_g & d_{xy}, d_{yz} & \text{at} & -4Dq - Ds + 4Dt \end{array}\right] 3Ds - 5Dt$$

The symmetry labelling is that of the group D_{4h}.

Note that, of course, the cubic crystal field splitting d_{z^2}, $d_{x^2-y^2}$ (e_g) at $6Dq$ and d_{xz}, d_{yz}, d_{xy} at $-4Dq$ is reproduced if *Ds* and *Dt* are both zero. Note also that the 'centre of gravity' of neither of the e_g nor of the t_{2g} sets is maintained as the symmetry departs from cubic. This means that, in low symmetry, the concept of the 'cubic field splitting' is not clearly defined. For small departures from cubic symmetry the lack of definition is not serious in practice, but to maintain the concept in, say, a square-planar complex, as is sometimes done, requires care.

6.2.1.5 Crystal field calculations

In spite of the conceptual inadequacies of CFT outlined in Section 6.2.1.3, parameterization of spectral and other data within the crystal field framework has been widespread and continues to be so. The calculation of the CFT matrix of the type of equation (4) by the direct methods indicated in their preamble is tedious. Elegant and efficient procedures for performing the evaluation of these elements have been developed.[30–33,35–37] Briefly, these procedures are mostly based upon operator or operator-equivalent methods. For example, the CFP may be put in the form

$$V_{\mathrm{CF}} = \sum_{n=0}^{2l} \sum_{k=-n}^{n} B_n{}^k O_n{}^k \tag{11}$$

$$= \sum_{n=0}^{2l} \sum_{k=-n}^{n} A_n{}^k Q_n{}^k \tag{12}$$

The $O_n{}^k$ and $Q_n{}^k$ are operators which are respectively linear combinations of spherical harmonics and expansions in terms of Cartesian coordinates, $l = 2$ for d-orbitals, 3 for f-orbitals. The parameters $B_n{}^k$ and $A_n{}^k$ are, of course, specialized forms of the general form given in equation (2), but including the evaluation of the relevant radial integrals.

Entirely general analytical expressions for the matrix elements of equation (4) have been listed for the d-orbital case for an almost arbitrary assembly of charges surrounding a metal atom.[5,38] They are reproduced in Appendix 1. By implementing these expressions as a computer program the problem of calculating the d-orbital energies in the crystal field model for any ordinary stereochemistry is made trivial.

6.2.2 Ligand Field Theory as Extended CFT[2–6,9]

6.2.2.1 The identification of Δ in qualitative MO theory

In this section the consequences are given of relaxing the purely ionic basis of crystal field theory, but stopping short of a proper quantum mechanical treatment of the metal–donor atom bonding. The basis for proceeding is that the d-orbitals of a transition metal ion are differentiated in energy in a manner which obviously reflects most strongly the immediate donor atom symmetry of the ligand environment. No attempt will be made to relate the size of the differentiation to the details of metal–ligand bonding in a quantitative fashion, although some qualitative arguments will be introduced.

The obvious choice for taking into account the covalency in metal–donor atom bonding necessary to put into practice the intent of the previous paragraph is a *qualitative* molecular orbital diagram of the type set out in Figure 5 for an octahedral complex when σ-bonding only is considered. The ligand donor atom lone pair electrons are sufficient to fill the diagram up to the e_g MO and the metal d-electrons go into the essentially metal-centered $t_{2g}{}^n$ and $e_g{}^*$ orbitals.

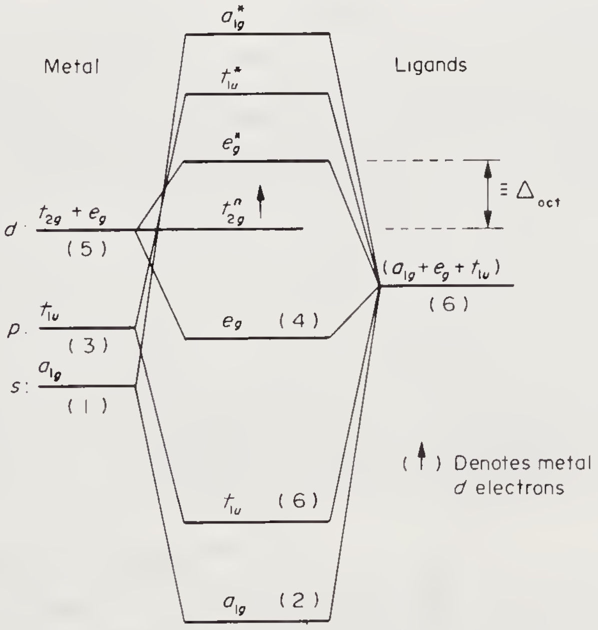

Figure 5 Simple MO treatment of an octahedral complex with σ-bonding only, and showing equivalance of Δ_{oct} to the $t_{2g}{}^t - e_g{}^*$ separation

In this description the quantity Δ_{oct} or $10Dq$(oct) of CFT is identified with the $t_{2g}{}^n - e_g{}^*$ MO separation. This is the basis of the ligand field theory (LFT) concept.

Figure 6 is a somewhat more complicated diagram of similar qualitative intent, but in which the possibility of π-bonding has been introduced. It is only illustrative in nature, as the relative ordering of some of the atomic and molecular orbitals can only be a matter of guesswork. However, an important point can be made: the significance to be attached to the quantity Δ_{oct} is dependent upon the type of ligand involved. If the donor atom has filled p_π atomic orbitals, as would be the case for a halide ion, then they fill the diagram up to the level of the $t_{1g}{}^n - t_{1u}{}^n - t_{2u}{}^n(\pi)$ MOs and the *d*-electrons from the metal atom will be accommodated in the $t_{2g}{}^*$ and $e_g{}^*$ essentially metal-centered MOs. In this case the quantity Δ_{oct} *is to be associated with the* $t_{2g}{}^*(\pi) - e_g{}^*(\sigma)$ *separation*, and this is likely to be reduced by the π-bonding relative to the σ-bonding-only situation.

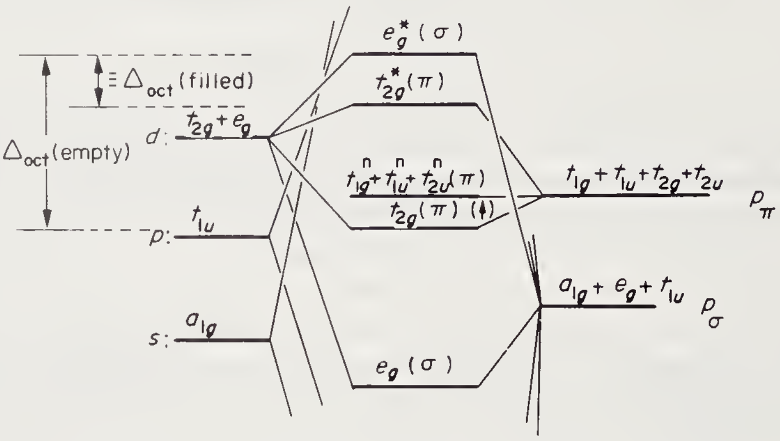

Figure 6 Simple MO treatment of an octahedral complex including π-bonding. The $a_{1g}(\sigma)$ and $t_{1u}(\sigma)$ orbitals of Figure 5 are omitted. The different definitions of Δ_{oct} for filled and for empty ligand p_π orbitals are indicated

On the other hand, for certain ligands such as CO and the CN^- ion it may be considered that the donor atom π-orbitals which overlap with the metal *d*-orbitals are the internal *antibonding* set, and are empty. In this case the MOs in Figure 6 would only be filled up to the $e_g(\sigma)$ orbitals, the donor atom electrons, and identification of Δ_{oct} would be with the $t_{2g}(\pi) - e_g{}^*(\sigma)$ separation, the former now being mainly metal-centered, but reduced in energy by the π-bonding. The separation is likely to be larger than for the only-σ-bonding case.

Using such an argument it is perhaps possible to rationalize the fact set out later, that halide ions create rather small ligand field splittings, the cyanide ion a very large one. The argument, of course, follows closely that used to describe enhanced stability and changes in ligand infrared band frequencies associated with ligands which are believed to be involved in π-backbonding.[39]

In a similar spirit of qualitative representation, Figure 7 sets out a possible scheme for a tetrahedral complex, considering σ-bonding only. The diagram is somewhat complicated by the fact that, in tetrahedral stereochemistry, both the *d* and the *p* orbitals of the central metal atom give rise to a set of t_2 symmetry, and any mixture of these can be used to combine with the ligand t_2 set. While it may be presumed that it is essentially the *d*-orbitals that are concerned with forming the MOs in which we are interested, the *p*-orbital impurity has important consequences which are dealt with later. The available ligand donor atom lone pairs fill the diagram up to the t_2 level and the metal *d*-electrons go into the essentially metal-based e^n and $t_2{}^*$ MOs. The quantity Δ_{tet} *is to be associated with the separation* $e^n - t_2{}^*$ *in tetrahedral stereochemistry.*

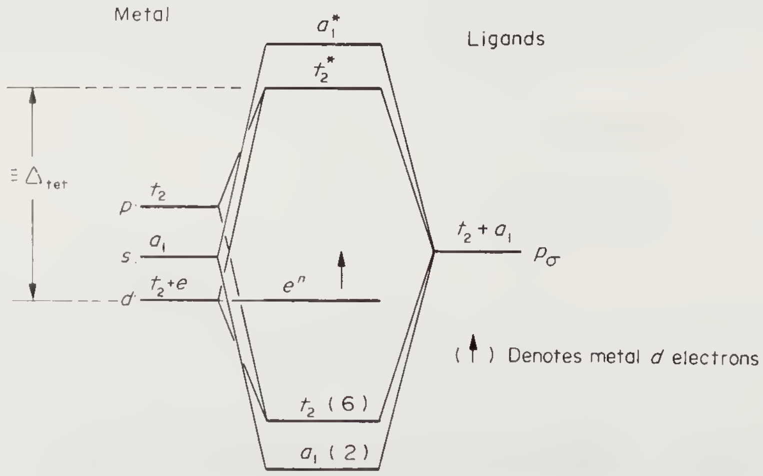

Figure 7 Simple MO treatment of a tetrahedral complex assuming π-bonding only, showing the equivalence of Δ_{tet} to the $e^n - t_2{}^*$ separation

6.2.2.2 *The concept of an 'effective'* d*-orbital set*[42–44]

As a result of the covalence in the metal–donor atom bonding it is obvious that the proper development of the description of the physical properties of transition metal complexes should proceed using appropriate mixtures of the metal *d*-orbitals and, presumably, donor atom *s–p* hybrid combinations. Of course, that is what is done in a treatment of the problem by the methods of theoretical chemistry.

The spirit of ligand field theory is to admit that the *d*-orbitals can no longer be 'pure' but, knowing from the results of more rigorous investigations that the degree of admixture of donor atom orbitals is small as the overlap is rather poor, to continue to use them as an effective set. It is expected, of course, that the properties of this effective *d*-orbital set must be changed from those of the free-ion set. The interelectronic repulsion parameters, for example, must certainly be expected to be lowered since the admixture of donor atom orbitals tends to spread the effective orbitals over a larger volume. The orbital angular momentum associated with the set must also be expected to be reduced as the admixed donor atom component may have little or any such momentum. However, most importantly, the symmetry properties of the MOs taken for the effective *d*-orbital set are the same as those seen to arise in crystal field theory.

The reason for proceeding with the ligand field approach is the belief that it is the symmetry properties of the *d*-orbitals which are their critical feature. The changes brought about by admixture of donor atom orbitals can be accommodated by changing the appropriate details of the wave function describing the effective *d*-orbital set, but the major features of behaviour will remain because the symmetry is maintained.

Of course, the effective *d*-orbital sets cannot be expected to be eigenfunctions of the proper quantum mechanical operators for various physical properties of the complex, including the energy. It is presumed that effective operators, related to the proper ones, can be set up, of which the effective *d*-orbitals are eigenvalues.

The parameters of ligand field theory then are entities which reproduce physically observable quantities as eigenvalues of these effective operators, operating on the effective *d*-orbital sets. For example, below in connection with the Angular Overlap Model we shall show that the energies observed in transition metal spectra of octahedral complexes can be rationalized in terms of an effective Hamiltonian for effective t_{2g} and e_g orbital sets and the corresponding parameters e_π and e_σ. Again, in dealing with magnetic properties it is conventional to use the operator mL_z in place of L_z for the component of orbital angular momentum in the z direction;[45,46] k is usually found to be < 1 in order to reproduce the data.

The physical significance to be attached to the meaning of ligand field parameters is, then, very limited. The extent to which k, for example, is truly connected with orbital angular momentum cannot be known. It will probably be the exception rather than the rule that ligand field parameter values determined from experiments of one type can be employed to help rationalize the results from those of other types.

6.2.2.3 Lower symmetries

In symmetries lower than cubic the *d*-orbitals mix with the donor atom $s{-}p$ hybrid orbitals to varying extents in molecular orbitals of appropriate symmetry. However, the mixing is believed to be small and the ligand field treatment of the problem proceeds upon the basis that the effective *d*-orbitals still follow the symmetry requirements as *d*-orbitals should. There will be separations between the MOs which can be reproduced using the formal parameters appropriate to free-ion *d*-orbitals. That is, the separations may be parameterized using the crystal field scheme. Of course, the values that appear for the parameters may be quite different to those expected for a free ion *d*-orbital set. Nevertheless, the formalism of the CFT approach can be used. For example, for axially distorted octahedral or tetrahedral complexes we expect to be able to parameterize the energies of the MOs which house the *d*-orbitals using the parameter set *Dq*, *Ds* and *Dt* as set out in Section 6.2.1.4 or perhaps one of the schemes defined in equations (11) and (12).

6.2.2.4 Transferability of ligand field parameters

It is highly desirable, of course, that a theory have predictive power as well as the ability to parameterize data. In the context of ligand field theory this means that one hopes that the parameter values obtained for some M—L bond system can at least be used sometimes where this system occurs again and that, more audaciously, there might be some attribute of M and of L that would allow the derivation of the parameter from a knowledge of M and of L.

Ligand field theory meets these hopes only to a rather limited extent, and that confined to at least formal cubic symmetry. In so far as the spectrum of a complex of the type MX_5Y, say, can be interpreted within the framework of a single *d*-orbital splitting parameter, one may investigate the existence of a 'law of average environment' in which the value of Δ_{oct} would be the weighted average of the values of Δ_{oct} for the two ligand types, *viz.*:

$$\Delta_{\text{oct}}(\text{MX}_5\text{Y}) = \frac{5}{6}\Delta_{\text{oct}}(\text{MX}_6) + \frac{1}{6}\Delta_{\text{oct}}(\text{MY}_6)$$

and more generally, for $\text{MX}_{6-p}\text{Y}_p$

$$\Delta_{\text{oct}}(\text{MX}_{6-p}\text{Y}_p) = \frac{6-p}{6}\Delta_{\text{oct}}(\text{MX}_6) + \frac{p}{6}\Delta_{\text{oct}}(\text{MY}_6) \tag{13}$$

In fact the relationships represented by equation (13) do hold fairly well in related systems: there is a reasonable degree of additivity in the contribution of M—L to the value of Δ_{oct}.[27] For example, the Co^{III}—N bond in Co(en)_3^{3+} is associated with a value of $\Delta_{\text{oct}}(\text{Co(en)}_3)$ of 23000 cm^{-1}, the Co^{III}—F bond in CoF_6^{3-} with a value of $\Delta_{\text{oct}}(\text{CoF}_6^{3-})$ of 13 000 cm^{-1}. One predicts, then

$$\begin{aligned}\Delta_{\text{oct}}(\text{Co(en)}_2\text{F}_2) &= \frac{1}{6}(4 \times 23\,000 + 2 \times 13\,000) \\ &= 20\,000\ \text{cm}^{-1}\end{aligned}$$

The value observed for both the *cis* and *trans* isomers is *ca.* 21000 cm^{-1}, there being some uncertainty in the interpretation because of band splitting caused by the lowered symmetry. However, the relationship fails completely if Co^{III} is replaced by Co^{II}, for example.

As will be elaborated later, it is possible to suppose

$$\Delta_{\text{oct}}(\text{M—L}) = f_{\text{M}} f_{\text{L}} \tag{14}$$

where f_{M} is a number characteristic of M irrespective of L, f_{L} of L irrespective of M. This relationship does seem to work as a first approximation.[27]

Thus with simple ligands, at any rate, LFT provides as much predictive power for the estimation of Δ_{oct} as could reasonably be hoped for, given the reservations that have been expressed about its basis. For complicated ligands involving extensive π-delocalized systems or strong steric constraints the laws implicit in equations (13) and (14) are likely to fail to a greater or lesser extent.

For complexes of symmetry lower than cubic no general relationships which connect the parameters describing departure from cubic symmetry, *Ds* and *Dt* say, with features of M and L or their combination appear. For example, it is difficult to obtain a coherent account even of the signs of the splittings of the cubic field spectral bands of $\text{Cr(en)}_2\text{X}_2^{+}$ ions using the parameters $\Delta_{\text{oct}}(\text{Cr(en)}_3^{3+})$ and $\Delta_{\text{oct}}(\text{CrX}_6^{3-})$. The predictive power of the LFT parameterization scheme does not seem to extend to symmetries lower than cubic.

6.2.2.5 f-Orbital systems[47–49]

For f^n systems, parameterization in the CFT scheme using the expansions and coefficients of equations (11) or (12) follows on directly from the application to d^n systems. The number of parameters rises, and even in cubic symmetry two parameters are necessary to describe the splittings of the f orbitals. These parameters involve respectively $\overline{r_f^4}$ and $\overline{r_f^6}$ terms. Using the same coordinate system and defining quantities equivalent to Dq for d-orbitals

$$Dq' = (7/66)(ze\overline{r_f^4}/a^5)$$

$$Fr = (99/1295648)2^{1/2}(ze\overline{r_f^6}/a^7)$$

the f-orbital splitting pattern is, in cubic symmetry, at

$$\begin{array}{lll} 6Dq' + 20Fr & [f_{z(5z^2-r^2)},\ f_{x(5x^2-r^2)},\ f_{y(5y^2-r^2)}] & t_{1u} \\ -2Dq' - 36Fr & [f_{z(x^2-y^2)},\ f_{x(y^2-z^2)},\ f_{y(z^2-x^2)}] & t_{2u} \\ -12Dq' + 48Fr & f_{xyz} & a_{2u} \end{array}$$

Because the f-orbitals are fairly well shielded from the valence effects it might appear that a relationship between the Dq' and Fr parameters could be calculated. However, it seems that the $4f$-orbital wave functions are not known sufficiently well for this purpose, and Dq' and Fr are to be treated as independent variables. This makes the interpretation of f-electron system properties, even in high symmetry, a much less straightforward business than for d-systems.

In fact, even approximate cubic symmetry seems to be rare for lanthanoid or actinoid element complexes.[50] In low symmetry the number of crystal field parameters necessary to account for the system can be quite large. On the other hand, the spectra of lanthanoid complexes contain many lines, usually quite narrow, so that a great deal of experimental data is available. It is not unknown for an interpretation to be made in terms of eight or ten of the crystal field parameters which appear in equation (11) or (12). However, the physical, and certainly the chemical, significance to be attached to the values of the individual parameters in such a set is obscure. The values are, as expected, an order of magnitude smaller than those for the *d*-electron systems because of the shielding from the valence effects.

For the actinoid element compounds the difficulties of the multiplicity of CFT parameters necessarily remains, but their values are larger because of less effective shielding from valence interactions and, the spectral bands being correspondingly broadened, the amount of spectral information available is reduced. The level at which actinoid crystal field parameterization can be discussed is limited. However, there are some series of complexes which approach cubic symmetry, and also it appears that the neglect of the parameters corresponding to terms in $\overline{r_f^6}$ is justified, at least as a starting point. In such cases the CFT parameterization scheme can be used with some success in dealing with physical properties. However, generalizations are difficult, and discussion will probably continue to proceed on an individual case basis.

6.2.3 The Angular Overlap Model (AOM)[6,41–43,51–54]

6.2.3.1 Introduction

Although essentially within the spirit of ligand field theory as enunciated in introductory remarks, there is an approach to dealing with the metal–ligand bonding which has developed into a field of its own, and deserves separate treatment. It is the so-called Angular Overlap Model (AOM). The choice of name arose from the early ways in which its procedures were applied, and is no longer particularly apt. Nevertheless the name persists and is likely to do so, and will be employed here. Some of the reasons for the initial choice of the name will become obvious as the subject is outlined.

In order to avoid the difficulties and tedium of a proper quantum mechanical treatment of all the nuclear–electron and electron–electron interactions in a molecule such as a transition metal complex, the processes of theoretical chemistry contain many levels of approximation and empiricism. Attempts have been made from time to time to develop a successful model which does not directly violate the laws of quantum mechanics and yet which is simple enough to apply generally to coordination transition metal ions. It was with such aims that the AOM was conceived.

It seems that, in its most widely used forms at any rate, the AOM involves such severe approximations and draws on empirical information to such an extent that it cannot be regarded as a proper implementation of quantum mechanics. Nevertheless, as a form of ligand field theory, it possesses distinct advantages and leads to a novel parameterization scheme which promises some degree of transferability of parameters with a metal–ligand bond. This last feature is entirely lacking, at least outside cubic symmetry, in crystal or ordinary ligand field treatments.

A careful examination of the concepts of the AOM suggest that it is possible to avoid making the assumptions that interfere with the rigour of quantum mechanics in the development and application of the AOM.[43,44] Used in this way the AOM ceases to be just another parameterization scheme and may relate directly to the nature of the bonding between the metal and each donor atom in some way. It has been used to try to draw together data on physical properties of more than one type to produce at least a semi-quantitative account of relative amounts of σ and π bonding character in a metal–ligand bond. It seems however that this very interesting approach carries the model beyond the area it is intended to cover in this article, more into the borderline with theoretical chemistry.

6.2.3.2 The roots of the AOM in quantum mechanics[6,42–44]

The simplest widely useful application of quantum mechanics in chemistry has been the Hückel method applied to π-conjugated systems in organic chemistry.[55] The Hückel method neglects bonding interaction except between neighbouring σ-bonded atoms and parameterizes the energy of a carbon atom and of the resonance integral between adjacent pairs as the variables. For a pair of carbon atoms the Hückel secular determinant might take the form

$$\begin{vmatrix} H_{CC} - E & \beta - S_{CC} \\ \beta - S_{CC} & H_{CC} - E \end{vmatrix} = 0 \qquad (15)$$

H_{CC} and β are the two variables mentioned, and S_{CC} the C—C π-bonding overlap integral.

In the same spirit, early treatments of transition metal complexes with a set of equivalent ligands were put in the form, for one of the MX bonds

$$\begin{vmatrix} H_{\mathrm{MM}} - E & H_{\mathrm{MX}} - S_{\mathrm{MX}} \\ H_{\mathrm{MX}} - S_{\mathrm{MX}} & H_{\mathrm{XX}} - E \end{vmatrix} = 0 \tag{16}$$

Here H_{MM} and H_{XX} might be estimated in various ways from the ionization potentials for M and X respectively. A difficulty arises because the off-diagonal form H_{MX} is less easy to assess than say β for the C—C π-bond. The Wolfsberg–Helmholtz treatment used the assumption

$$H_{\mathrm{MX}} = \tfrac{1}{2}F(H_{\mathrm{MM}} + H_{\mathrm{XX}})$$

with the F an adjustable constant. In practice F was found to be ≈ 2.

With the approximation $F = 2$ the determinant of equation (16) may be multiplied out and solved (assuming H_{MM} and H_{XX} are well separated and S_{MX} is small) to give the two roots

$$E_{\mathrm{B}} = H_{\mathrm{MM}} + H_{\mathrm{XX}}^2 S_{\mathrm{MX}}^2/(H_{\mathrm{MM}} - H_{\mathrm{XX}})$$

$$E_{\mathrm{A}} = H_{\mathrm{XX}} - H_{\mathrm{MM}}^2 S_{\mathrm{MX}}^2/(H_{\mathrm{MM}} - H_{\mathrm{XX}}) \tag{17}$$

In this approximation the energy of the antibonding MO corresponding to E_{A}, in particular, is raised by an amount proportional to the square of the metal–donor atom overlap integral.

Before proceeding further it is important to note that if X is monatomic, or is the donor atom in a linear ligand such as $\mathrm{CN^-}$, then the bonding between it and the metal atom can be conceived to be made up of components of three distinct symmetry types:

(a) σ if the overlap region is concentrated along the internuclear axis;
(b) π if the overlap region is concentrated to each side of the internuclear axis and the resultant charge density has twofold symmetry about that axis; and
(c) δ if the overlap density is concentrated off the internuclear axis and has cylindrical symmetry about that axis.

6.2.3.3 *Group overlap integrals*[6,42–44]

The introductory material of the previous subsection was couched in terms of a diatomic molecule and can be expanded with very little change to cover a complex with several equivalent M—X bonds. However, the intention of the AOM is to be more general than that. It seeks to cover the case of a metal atom with inequivalent ligands. In order to do this we introduce group overlap integrals — the integrals involving symmetry-adapted sets of orbitals on the metal atom on the one hand and on the set of ligand atoms on the other. Generally, we have

$$G_\mu = \int \psi_\mu \varphi_\mu \, \mathrm{d}t$$

where μ is a specified symmetry label, ψ is an appropriate set of metal orbitals of symmetry μ and φ is an equivalent set of ligand orbitals, taken from all the ligand donor atoms, of that symmetry. Specifically, for an octahedral complex for example, $\mu = A_{1g}$, E_g, T_{2g}, *etc.* The symmetry-adapted ligand orbital sets have been listed in detail by several sources.[3,5,6]

Using the concept of group overlap integrals, equation (15) can be rewritten for a multi-ligand complex, and for a specific symmetry, in the form

$$E_{\mathrm{B}}{}^{\mu} = H_{\mathrm{M}}{}^{\mu} + H_{\mathrm{L}}{}^2 G_\mu{}^2/(H_{\mathrm{M}} - H_{\mathrm{L}}) \tag{18}$$

$$E_{\mathrm{A}}{}^{\mu} = H_{\mathrm{L}}{}^{\mu} - H_{\mathrm{M}}{}^2 G_\mu{}^2/(H_{\mathrm{M}} - H_{\mathrm{L}})$$

Here the opportunity has been taken to abbreviate H_{MM} to H_{M} and H_{XX} to H_{L}. If the ligands are all equivalent there is no difficulty in identifying H_{L}, but if they are not equivalent then, presumably, H_{L} is the average

$$H_{\mathrm{L}} = \sum_{i=1}^{n} H_{\mathrm{L}_i}$$

6.2.3.4 *Angular and radial overlap integrals*[6,42–44]

The initial step in the development of the AOM is the supposition that the group overlap integrals may be factored

$$G_\mu = F_\mu R_\mu \tag{19}$$

where R_μ is an expression which depends only on the radial functions of the overlapping wave functions of the metal and the ligand donor atoms, and F_μ is an expression which contains only terms which depend upon the orientation of the ligand orbitals with respect to the metal orbitals. R_μ will be some average over the metal–donor atom radial integrals and will depend upon the metal–donor atom separations.

F_μ is simply a number composed of the trigonometric functions of the two angles which are necessary to relate two coordinate systems, one on the metal and one on the ligand, to each other. F_μ is made up of numbers arising from the summation over the set of metal–ligand orientations. F_μ is the angular overlap integral for the metal with its set of ligands.

The angular overlap integrals for a regular octahedron and a regular tetrahedron are set out in Table 1.

Table 1 The F_μ Coefficients of the AOM for the Octahedron and the Tetrahedron

μ	F_μ	*Metal orbital*	*Bond symmetry*	μ	F_μ	*Metal orbital*	*Bond symmetry*
A_{1g}	$6^{1/2}$	s	σ	A_1	2	s	σ
T_{1u}	$2^{1/2}$	p	σ	T_2	$2/3^{1/2}$	p	σ
T_{1u}	2	p	π	T_2	$-8^{1/2}/3^{1/2}$	p	π
E_g	$3^{1/2}$	d	σ	E	$8^{1/2}/3^{1/2}$	d	π
T_{2g}	2	d	π	T_2	$2/3^{1/2}$	d	σ
				T_2	$8^{1/2}/3$	d	π

6.2.3.5 *AOM: regular octahedron and tetrahedron*[6,42–44]

The material of the previous subsections may now be assembled into a useful result. If the energy zero for equation (18) is defined to be H_L then a simplification takes place: we may write, remembering $E_A{}^\mu$ was defined to be the antibonding orbital, simply

$$E_\mu{}^* = e_\mu F_\mu{}^2 \tag{20}$$

where

$$e_\mu = H_M R_\mu{}^2 \tag{21}$$

is the AOM parameter specifying the energy of the effective d-orbital set of symmetry μ.

Now the symmetries of the bonding orbital sets in an octahedral complex can be identified with the *local* symmetry of the overlap in an M—L bond in the following way

$$e_g \equiv \sigma \qquad\qquad t_{2g} \equiv \pi$$

Thus we write, from equation (17)

$$E_{e_g}^* = E_\sigma{}^* = e_{e_g} F_{e_g,\sigma}^2 \tag{22}$$

$$E_{t_{2g}}^* = E_\pi{}^* = e_{t_{2g}} F_{t_{2g},\pi}^2$$

Using F_μ of Table 1, we have

$$E_{e_g}^* = 3e_\sigma$$

$$E_{t_{2g}}^* = 4e_\pi \tag{23}$$

e_σ and e_π are the parameters of the AOM which reproduce the energies of the effective e_g and t_{2g} d-orbital sets in octahedral coordination.

In principle, the group radial overlap integrals R_μ can be calculated knowing the wave functions on the metal and the ligand donor atoms, and their separations. Then the ratio $f = e_\sigma/e_\pi$ is obtained, and the theory would reduce to one of a single parameter, e_σ say, to describe the raising of the energies of both d-orbital types. However, while that approach has indeed been used by some workers to reduce the level of parameterization required to use the AOM, it possesses obvious dangers, in connection with the transition metals in any case. It must be remembered that effective d-orbital sets have been assumed which are eigenvalues of an effective Hamiltonian. It is very doubtful that a proper comparison can be made between the radial integrals for the two symmetries when evaluated with such a background. Early work with the AOM was concerned with f-orbital systems, and was able to use the procedure with more confidence.[57,58] It is much more satisfactory to reduce the parameterization by appeal to chemical arguments, as outlined below for certain examples.

The formal correspondence between the crystal/ligand field parameter for *d*-orbital splitting and the AOM result is given by the difference between the antibonding t_{2g} and e_g orbitals, $E_{e_g}{}^* - E_{t_{2g}}{}^*$

$$\Delta_{\text{oct}} = 3e_\sigma - 4e_\pi \tag{24}$$

For a tetrahedral complex the position is somewhat complicated because the t_2 orbital set has *both* σ and π overlap with appropriate ligand orbital sets, the former dominating. The equivalent of equation (22) becomes

$$E_e{}^* = E_\pi{}^* = e_e F_{e,\pi}^2$$

$$E_{t_2}{}^* = E_\sigma{}^* = e_{t_2} F_{t_2,\sigma}^2 + e_{t_2} F_{t_2,\pi}^2 \tag{25}$$

With the aid of Table 1, the results

$$E_e{}^* = \frac{8}{3} e_\pi$$

$$E_{t_2}{}^* = \frac{4}{3} e_\sigma + \frac{8}{9} e_\pi \tag{26}$$

are obtained.

If the metal and donor atom wave functions and their separations are the same, the group radial integrals may be unchanged and we can note that the result for the difference between the t_2 and e antibonding *d*-orbital sets, $E_{t_2}{}^* - E_e{}^*$

$$\Delta_{\text{tet}} = \frac{16}{9} e_\pi - \frac{4}{3} e_\sigma \tag{27}$$

$$= -\frac{4}{9}(3e_\sigma - 4e_\pi)$$

The result seen for crystal field theory

$$\Delta_{\text{tet}} = -\frac{4}{9}\Delta_{\text{oct}}$$

for the same ligands at the same distances is reproduced in the AOM.

As is usual, the above expressions for the energies of the two *d*-orbital sets in the AOM have neglected the δ-bonding interaction which is allowed by symmetry. Its effects are assumed to be small. Expressions for the energies corrected for the δ-bonding by the inclusion of a parameter e_δ are given in Appendix 2.

6.2.3.6 *AOM* versus *CFT: cubic symmetry*

At the level of the regular octahedron or tetrahedron discussed in the previous subsection the AOM appears to be at a disadvantage relative to CFT or ordinary LFT as it is a two-parameter theory, whereas there is fundamentally only one piece of data experimentally accessible — the *d*-orbital splitting into $t_{2(g)}$ and $e_{(g)}$ sets. At best the AOM could be made a one-parameter theory by supposing that the ratio e_π/e_σ can be treated as a constant, not experimentally accessible. Then

$$\Delta_{\text{oct}} = e_\sigma(3 - 4f)$$

and $e_\sigma(3-4f)$ would be the 'parameter' of the AOM. No new insight would be gained by such a procedure.

Some progress is possible if an appeal to chemical experience is made. Suppose a metal hexa-ammine ion $M(NH_3)_6^{n+}$ is involved. The NH_3 molecule is known to be close to sp^3 hybridization on the N atom, with the lone pair occupying the 'fourth' position. Consequently, there are *no* orbitals of π symmetry available on the N atom. In this situation it can be proposed with some confidence the π-bonding involving the central atom is negligible and consequently the AOM parameter e_σ is zero.[59] Then

$$\Delta_{\text{oct}}(NH_3) = 3e_\sigma(NH_3)$$

That is, a measurement of $e_\sigma(NH_3)$ is available, as $\Delta_{\text{oct}}(NH_3)/3$.

From the information available, $\Delta_{\text{oct}}(NR_3)$ does not change much as R is changed successively from H to an alkyl group, so that $e_\sigma(NR_3)$ is likewise fairly independent of the details of what is bonded to the nitrogen atom. Viewed in the light of the roots of the AOM in empirical MO theory this is an unexpected result. There appear to be appreciable M—N bond length changes on the substitution of R for H in these amines, and simple considerations would have led to the belief that these, taken together with the changes of the N lone pair wave function, would have changed the group overlap integral R_{e_g} of equation (21) substantially, and e_σ with it. This emphasizes the role of the AOM as a ligand field theory: the energy parameters such as e_σ are the observables of effective operators operating on effective wave function sets, and as such do not necessarily conform to the expectations for the proper Hamiltonian operating on pure d-orbital functions.

6.2.3.7 **Lower symmetries: 'linear' ligands**[6,42–44]

The application of the AOM to complexes of symmetry lower than cubic is more straightforward than is that of CFT, particularly if the distortion from cubic symmetry involves changes in ligand type or in metal–ligand distance without changing the angle between the ligands. In the simplest the effect on the energy of any given d-orbital is the sum over the ligands of appropriate e_λ parameters multiplied by appropriate overlap integral terms, F_λ. Neglecting δ-bonding contributions as usual, we may write

$$E_\mu^* = \sum_{i=\text{ligands}} \left(e_\sigma^{\,i} F_\sigma^{\,\mu} + e_\pi^{\,i} F_\pi^{\,\mu}\right) \tag{28}$$

where, as before, μ represents a set of d-orbitals of symmetry μ. If no angular distortion is involved the functions F_σ^μ and F_π^μ are simple trigonometric functions related to the F_μ in Table 1. The procedure has been set out in detail in various sources. In some cases the position is a good deal more complicated than that outlined in equation (28), and it is necessary to take into account cross terms involving two d-orbitals, that is of the type $E_{d_{ij}}^*$, and to solve appropriate secular determinants. In principle, up to 15 AOM parameters could be required. Such complications are not considered here.

Consider first the tetragonally distorted octahedral complexes obtained by the substitution of MX_6, *viz.* MX_5Y and *trans*-MX_4Y_2, the interligand angles remaining at 90°. Further we restrict attention to ligands which are monatomic or axially symmetrical or have no π-bonding capability — sometimes referred to as 'linear ligators'. The complexes belong respectively to the groups C_{4v} and D_{4h}. The groups C_{4v} and D_4 are isomorphous, so that initially it is sufficient to use the symmetry labels of D_4 for the *trans*-MX_4Y_2 complex, and to add the required g subscript later. The d-orbitals in D_4 transform as a_1 (d_{z^2}), $b_1(d_{x^2-y^2})$, $b_2(d_{xy})$ and $e(d_{xy}, d_{yz})$. Application of equation (28) takes the form given in Table 2.

Table 2 d-Orbital Energies in MX_5Y and *trans*-MX_4Y_2 Tetragonally Distorted Complexes for 'Linear' Ligands Derived from the AOM[a]

		MX_5Y	trans-MX_4Y_2
$E_{a_1}^*$	=	$2e_\sigma^X + e_\sigma^Y$	$e_\sigma^X + 2e_\sigma^Y$
$E_{b_1}^*$	=	$3e_\sigma^X$	$3e_\sigma^X$
$E_{b_2}^*$	=	$4e_\pi^X$	$4e_\pi^X$
E_e^*	=	$3e_\pi^X + e_\pi^Y$	$2e_\pi^X + 2e_\pi^Y$

[a] For the MX_4Y_2 case, add the subscript g to the symmetry labels.

In this application the AOM is a four-parameter model, e_σ^X, e_σ^Y, e_π^X and e_π^Y being AOM parameters in each case. It is to be noted that the CFT/LFT parameterization of these complexes would also most usually be at the same level. Indeed, recalling equation (10), it is easy to write the correspondence between the two parameter sets, say for MX_5Y

$$E_{a_1}^* - E_{b_1}^* = -e_\sigma^X + e_\sigma^Y = -4Ds - 5Dt$$

$$E_{b_{2g}}^* - E_{e_g}^* = e_\pi^X - e_\pi^Y = 3Ds - 5Dt \tag{29}$$

Thus

$$Ds = \frac{1}{7}\left(e_\sigma^X + e_\pi^X - e_\sigma^Y - e_\pi^Y\right)$$

$$Dt = \frac{1}{35}\left(3e_\sigma^X - 4e_\pi^X - 3e_\sigma^Y + 4e_\pi^Y\right) \tag{30}$$

The spectra of MX_5Y and *trans*-MX_4Y_2 complexes, in principle, yield three pieces of information about d-orbital energies, say the energy separations of the a_1, b_1 and b_2 orbital energies relative to that of e. In the general case that is not sufficient to give values for all four parameters of one of the species. However, if the situation is simplified by making one of the ligands, X say, NH_3, so that $e_\pi^X = e_\pi^{NH_3} = 0$ as discussed in Section 6.2.3.6, the remaining parameters, $e_\sigma^{NH_3}$, e_σ^X and e_π^X, may be obtained.

The procedure outlined in the previous paragraph has been carried out for the series $Cr(NH_3)_5X^{2+}$ and $Cr(NH_3)_4X_2^+$, with X = halogen.[59] In this way values for $e_\sigma^{NH_3}$, e_π^X and e_σ^X were obtained for the ligands attached to Cr^{3+}. It was observed that the $e_\sigma^{NH_3}$ value was substantially the same for all the species involved, and further could be used fairly successfully to reproduce the observed value of Δ_{oct} in $Cr(NH_3)_6^{3+}$. The values of e_σ^X and e_π^X also were essentially the same in the $Cr(NH_3)_5X^+$ and the $Cr(NH_3)_4X_2^+$ species.

It seems that here the AOM offers a distinct advantage over the LFT parameterization scheme. While using the same number of parameters as the LFT scheme, indeed formal linear combinations of those parameters, it seems to account fairly well for the *d*-orbital energies not only in octahedral but also in environments of less than cubic symmetry. The LFT approach failed to do this, as discussed in Section 6.2.2.4. It is this ability to deal with low symmetry systems by the summation of the parameters for the individual ligands that is the strength of the AOM.

It is to be noted that the AOM parameters for an M—L system promise to be fairly independent of what other systems M is engaged in, as found for LFT parameters (Section 6.2.2.4). It follows from this that the 'law of average environment' for the cubic field *d*-orbital splitting parameter Δ_{oct}, say, discussed also in that section, is also a feature of the AOM.

The position is not always as simple and clean-cut as set out in the paragraphs above. The possibility of 'cross terms' of the type $E_{d_{ij}}^*$ has been mentioned. Also, in square-planar complexes for example, it has been found an advantage to assign formal AOM parameters to the 'vacant' axial sites in order better to reproduce spectral and magnetic properties.[44]

As well as departure from octahedral symmetry of the tetragonal type discussed above, angular distortions in which M—L bond lengths are preserved unchanged present a fairly obvious case for the application of the AOM. An octahedron 'squashed' or elongated in the C_3 axis is an example. In the resultant D_{3d} symmetry the *d*-orbitals are split into three sets, one of symmetry a_{1g} and two of symmetry e_g. In fact, the expressions for F_σ^μ and F_π^μ ($\mu = a_{1g}$ or e_g) in terms of the angle of distortion are not simple and the existence of two sets of the same symmetry label creates complications. However, it is readily shown that it is a two-parameter problem in the AOM, e_σ and e_π, the same level as for LFT (see equation 9). In principle, the two energy separations available should allow the evaluation of both parameters.

6.2.3.8 *Lower symmetries: 'non-linear' ligands*[6,42–44]

Many ligands do not conform with the 'linear ligator' requirements of the previous subsection; they have appreciable π-bonding capability and are not axially symmetric. Amongst the common ligand molecules pyridine (py) and water are examples. For these molecules the π-bonding interaction with the metal atom is anisotropic. For either of the molecules mentioned, the donor atom *p*-orbital perpendicular to the molecular plane gives obvious π-bonding capability, but within the molecular plane π-bonding to the metal atom is much less favourable.

If the procedures of the preceding subsection are applied to complexes containing such ligands then the parameter e_π derived will reflect the average of contributions from the two types of π-bonding. However, it is quite straightforward to extend the AOM to provide two π-bonding parameters, $e_{\pi_\parallel}$ and $e_{\pi_\perp}$, provided the orientations of the ligand molecular planes relative to the complex framework is known. The parameter $e_{\pi_\parallel}$ reflects the π-bonding interactions in the ligand molecular plane, $e_{\pi_\perp}$ that perpendicular to it. One expects for molecules like py and water that $e_{\pi_\perp} > e_{\pi_\parallel}$.

Of course, the additional parameterization of the AOM to include the separate $e_{\pi_\parallel}$ and $e_{\pi_\perp}$ subdivisions of e_π place a corresponding requirement on the amount of experimental information available. The amount of information on *d*-orbital splittings necessary to allow the evaluation of, say, e_σ, $e_{\pi_\parallel}$ and $e_{\pi_\perp}$ for two types of ligand in a complex, *i.e.* six pieces, cannot come from simple absorption spectroscopy. It requires, for example, the study of the polarized single crystal spectrum, possibly taken in conjunction with the single-crystal magnetic anisotropy and the ESR spectrum.[43] It is not proposed to examine matters in the depth required to cover such applications in this article. While some reference may be made to the differing values found for $e_{\pi_\parallel}$ and $e_{\pi_\perp}$ for certain ligands, reference to the original literature should be made in order to follow their derivation.

In a particularly simple example, where only one type of donor atom is involved, the planar molecule $Cu(acac)_2$ (acac = acetylacetone) has a spectrum in which three *d*-orbital separations are available, and may be used to deduce the three AOM parameters for the extended treatment.[60] In the case of the square plane the *d*-orbital energies are

$$\begin{aligned} E_{a_1}^* &= e_\sigma & E_{b_1}^* &= 3e_\sigma \\ E_{b_2}^* &= 4e_{\pi_\parallel} & E_e^* &= 2e_{\pi_\perp} + 2e_{\pi_\parallel} \end{aligned} \qquad (31)$$

Values of $e_\sigma = 7250$, $e_{\pi_\parallel} = 1350$ and $e_{\pi_\perp} = 1880\ \mathrm{cm}^{-1}$ have been derived. Here, as observed, the difference for $e_{\pi_\perp}$ and $e_{\pi_|}$ on the oxygen atoms is not very great as the departure of the C=O group from a 'linear ligator' occurs only at the atom removed from the donor atom, not as it is in py.

To the extent that the AOM parameterization scheme can be supported to give information connected with ligand molecule symmetry and bonding properties, it obviously presents a much more attractive alternative to the CFT/LFT scheme for chemical purposes.

6.2.3.9 f-*Orbital systems*[57,58]

In Section 6.2.2.5 the difficulties of the CFT parameterization scheme when applied to *f*-electron systems were outlined. It was in an effort to overcome these difficulties that the AOM was conceived. In the event, it has proved of relatively little help in this connection, in spite of its success in *d*-orbital applications.

In order to make facile progress in the treatment of *f*-orbital systems, in practice it is necessary to restrict consideration to the σ-bonding component. Of course, quite good justification can be given for assuming the contribution from π- let alone δ-bonding interactions are negligible, at least for the lanthanoids. Then we have a theory of one parameter only, e_σ, per ligand. In regular octahedral symmetry the *f*-orbital splitting (*cf.* Section 6.2.2.5) is:

$$E_{t_{1u}^*} = 2e_\sigma \qquad E_{t_{2u}^*} = E_{a_{2u}^*} = 0 \tag{32}$$

At this level of approximation the AOM is at an advantage over CFT which requires two parameters in cubic symmetry. This simple treatment is successful at the first level only in dealing with the rich spectra of lanthanoid ions in situations of mean cubic symmetry. However, as such it offers some measure of transferability not found amongst CFT parameters, and it may be possible to attach some relative chemical significance to the e_σ parameters for different ligands.

In lower symmetries the application of the AOM in *f*-electron systems becomes quite a complicated matter, and it is not established that it is as successful as CFT in accounting for fine details of lanthanoid spectra. Consequently, as the aim is often to parameterize the spectra rather than to seek the chemical basis for them, the AOM has not received wide usage in dealing with *f*-electron systems.

6.3 ATOMIC SPECTROSCOPY[2,3,5,17,18,61,62]

6.3.1 Introduction

In the previous section the perturbations of the *d*- and *f*-orbital energies caused by the presence of donor atoms around a central metal atom in a complex were examined. However, in spite of the impression that may have been given there, the perturbations are not of a single energy belonging to the *d*- or *f*-electrons. The repulsions between the electrons and the coupling of their spin and orbital angular momenta ensure that the degeneracy of their energies is at least partly removed. The ligand field splitting effects act in competition with these others. In this section we examine the energy level distribution in a formal gaseous metal ion of appropriate charge, unaffected by the presence of other atoms or ions — the so-called *free ion*.

The examination takes place in two stages, one corresponding to the formal 'interelectronic repulsion' component of the Hamiltonian $\boldsymbol{H}_{\mathrm{ER}}$ and the second to the 'spin–orbit' coupling term $\boldsymbol{H}_{\mathrm{LS}}$. As will be pointed out, in principle, and in certain cases in practice, it is not proper to separate the two components. However, the conventional procedure is to develop $\boldsymbol{H}_{\mathrm{LS}}$ as a perturbation following the application of $\boldsymbol{H}_{\mathrm{ER}}$. That suffices for most purposes, and simplifies the procedures. Any interaction between the *d*- or *f*-electron set and any other set is ignored. It is assumed that it is negligible or can be taken up within the concept of an 'effective' *d*-orbital set.

It is now necessary to define certain terms which will be used frequently from now on. *Configuration*: a specified number (n) of electrons occupying the specified orbital set; *term*: an energy level of the free ion which is an eigenvalue of $\boldsymbol{H}_{\mathrm{ER}}$. A term energy is specified by the orbital and spin angular momentum numbers, L and S; *state*: an energy level of the free ion which is an eigenvalue of $\boldsymbol{H}_{\mathrm{LS}}$. A state energy is specified by the *total* angular momentum quantum number, J. In general a configuration gives rise to a number of terms, each of which is split by spin–orbit coupling into a number of states. In common usage term and state are often used interchangeably, but here we make a clear distinction.

The procedures for finding the eigenvalues, and the corresponding eigenfunctions, of $\boldsymbol{H}_{\mathrm{ER}}$ and H_{LS} in a multi-electron *d* or *f* configuration can be very complex and tedious. Several formalisms of varying mathematical sophistication have been developed for the purpose. Only a brief summary of the results is presented here.

6.3.2 Free-ion Terms

The requirement that the term energies, E_{LS}, be eigenvalues of $\boldsymbol{H}_{\mathrm{ER}}$ can be shown to reduce to the requirement that they be simultaneously eigenvalues of the operators $\boldsymbol{S}^2$ and $\boldsymbol{L}^2$, where for *n* electrons,

$$S_x = \sum_{i=1}^{n} s_{x,i} \tag{33}$$

$$L_x = \sum_{i=1}^{m} l_{x,i}$$

with equivalent expressions for the *y* and *z* directions

$$\boldsymbol{S}^2 = S_x{}^2 + S_y{}^2 + S_z{}^2 \tag{34}$$

$$\boldsymbol{L}^2 = L_x{}^2 + L_y{}^2 + L_z{}^2$$

The procedures for finding these eigenvalues and their corresponding eigenfunctions are not investigated here.

Qualitatively, the result of the interelectronic repulsions are summed up in Hund's rules, which may be summarized: of the free-ion terms arising from a configuration, those specified by the highest values of *S* tend to lie lowest in energy; and of the terms with maximum *S*, that with highest *L* lies lowest.

Since maximum *S* arises from having the greatest possible number of electrons unpaired, *the free-ion ground term of a configuration is that with the highest value of L consistent with the maximum possible number of unpaired electrons.* The largest value of *L* is obtained as the maximum value of $\sum_{i=1}^{n} m_{l_i}$ consistent with the Pauli exclusion principle, where m_{l_i} is the quantum number for the orbital angular momentum of electron *i* in the *z* direction.

Quantitatively, E_{LS} is a complicated function of the quantum numbers *L* and *S*. Two parameterization schemes are in common usage. In that of Condon and Shortley

$$E_{\mathrm{LS}} = \sum_{k=0}^{m} a_k F_k$$

where *k* is even and $m = 4$ or 6 for *d*- or *f*-electrons, respectively; and in that of Racah

$$E_{\mathrm{LS}} = a_{\mathrm{A}}A + a_{\mathrm{B}}B + a_{\mathrm{C}}C + \cdots$$

where a_k and a_{X} are appropriate coefficients. The parameter sets are linear combinations of each other. In particular

$$B = F_2 - 5F_4 \qquad C = 35F_4$$

Each of these schemes has its merits in performing calculations involving atomic energy levels and is in common usage. The Racah scheme has the advantage for some purposes in that *terms of the same* ***S*** *involve only the parameter B.* In both schemes the leading term, F_0 or *A*, is unchanged for a given configuration, and consequently may be omitted for many purposes. For the treatment of atomic term energies of *d*-electron systems, then, in a ligand field context, the Condon and Shortley parameters are F_2 and F_4, the Racah parameters *B* and *C*. Values of the interelectron repulsion parameters *B* and *C* are given for some transition metal ions in Appendix 3, and for the lanthanoids and actinoids elsewhere.[47–49]

L is the quantum number specifying the total orbital angular momentum for the term, *S* the total spin angular momentum. Each of these momenta has components in any chosen direction, *z* say, which take on the integral values L_z, from *L* to $-L$, or S_z from *S* to $-S$, respectively. There are $2L + 1$ values of L_z, and $2S + 1$ values of S_z, each with appropriate wave functions. Consequently, a term specified by *L* and *S* is $(2L + 1)(2S + 1)$-fold degenerate.

Free-ion terms are labelled by a system which uses capital letters to encode the value of L in the same way as lower case letters do for electrons, together with a super-prefix known as the *multiplicity*, of value $(2S + 1)$. Thus we have the correspondence

value of quantum no., l or L	0	1	2	3	4	5	6
single electron type	s	p	d	f	g	h	i
free-ion term type	S	P	D	F	G	H	I

For example, the ground term of the d^2 configuration has, from Hund's Rules, $S=1$ and $L=3$. It is the ^3F term.

A particular result that will be of much use is that for the d^n configurations which give rise to F ground terms (d^2, d^3, d^7 and d^8), the separation to the higher-lying P term of the same multiplicity is $15B$ ($= 15F_2 - 75F_4$). In d^3 the ^4P term lies $15B$ above the ground ^4F term.

For shells more than half-full it can be noted that the resultant 'holes' in the filled shell formally repel each other in essentially the same manner as do the equivalent number of electrons in a less-than-half-filled shell. In this way the labour of evaluating L and S for a large configuration can be avoided: the terms which arise from a d^n ($n < 5$) configuration are repeated for the d^{10-n} configuration. Similarly those for an f^n ($n < 7$) configuration are repeated for the f^{14-n} configuration. This electron-hole equivalence also will be useful in another context presently.

Using the above material the ground terms of the various d^n and f^n configurations may be written down

d^n configurations:	d^1, d^9	d^2, d^8	d^3, d^7	d^4, d^6	d^5		
term	^2D	^3F	^4F	^5D	^6S		
f^n configurations:	f^1, f^{13}	f^2, f^{12}	f^3, f^{11}	f^4, f^{10}	f^5, f^9	f^6, f^8	f^7
term	^2F	^3H	^4I	^5I	^6H	^7F	^8S

The relative energies of the lower lying terms which arise from d^n configurations are given in Figure 8.

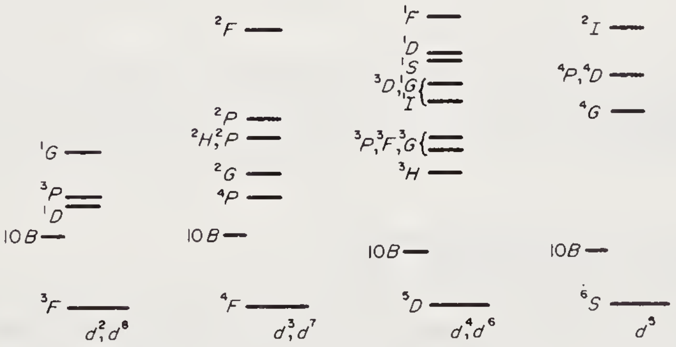

Figure 8 Relative energies of the lower lying terms from d^n configurations, assuming $C/B = 4.7$

6.3.3 Spin–Orbit Coupling: Russell–Saunders Case

The spin and the orbital angular momenta of electrons in a free-ion give them the properties of corresponding magnetic dipoles. This fact will obviously be of the greatest importance in discussing the magnetic and ESR properties of transition metal complexes. For the present purposes we can note that the formal interaction between such dipoles provides a mechanism for the coupling of the angular momenta.

In principle four types of coupling could be important:

(i) spin–spin: $s_i\,s_j$
(ii) orbit–orbit: $l_i\,l_j$
(iii) spin–orbit: $l_i\,s_i$
(iv) spin–other-orbit: $s_i\,l_j$

In practice, (i) is rather more important than (ii) and usually much greater than $\zeta_i s_i . l_i$, where ζ_i is the spin–orbit coupling coefficient for a single electron. The coupling (iv) is negligible. As seen in the previous section, the couplings (i) and (ii) are associated with the splitting of a configuration into terms. If the term $s_i\,l_i$ is much smaller than the separations between the free-ion terms then the effects of spin–orbit coupling can be treated as a perturbation on those terms by coupling between the total angular momenta L and S. The coupling is dipolar in nature and is of magnitude determined by a coefficient λ_{LS}; *viz.* for the term specified by L and S

$$H_{\mathrm{LS}} = \lambda_{\mathrm{LS}} LS \tag{35}$$

This is the *Russell–Saunders* coupling scheme: free-ion terms, set up as in the previous section, are perturbed by this Hamiltonian.

The perturbation of a free-ion term, specified by L and S, by spin–orbit coupling takes the form of a splitting into states, $2L + 1$ or $2S + 1$ in number, whichever is the less. Each state is specified by the total angular momentum quantum number J, and is $(2J + 1)$-fold degenerate. J takes on values from $|L-S|$ to $|L+S|$, and for a shell less than half-full the state with the lowest value of J lies lowest in energy. The energy separation between a state specified by J and that lying next above it, specified by $J + 1$, is

$$\Delta E_{J,J+1} = \lambda_{\mathrm{LS}}(J + 1) \tag{36}$$

The single electron spin–orbit coupling constant ζ_{nl} is fundamentally a positive quantity. The term coefficient λ_{LS} can be of either sign

$$\lambda_{\mathrm{LS}} = \pm \zeta_{nl}/2S \tag{37}$$

The positive sign in equation (37) holds for a shell less than half-full, the negative sign for one more than half-full. The negative sign in the latter case arises because of the hole-electron formalism mentioned earlier. It has the consequence that for more-than-half-full configurations the term splitting is inverted: the state with *highest* J lies lowest in energy.

Using the rules set out in the preceding paragraph, it is straightforward to write down the free-ion ground states of the various d^n and f^n configurations:

$$\begin{array}{llllll}
d^n \text{ configurations:} & d^1, d^9 & d^2, d^8 & d^3, d^7 & d^4, d^6 & d^5 \\
\text{ground state:} & {}^2D_{1\frac12,2\frac12} & {}^3F_{2,4} & {}^4F_{1\frac12,4\frac12} & {}^5D_{0,4} & {}^6S_{2\frac12}
\end{array} \tag{38}$$

$$\begin{array}{llllllll}
f^n \text{ configurations:} & f^1, f^{13} & f^2, f^{12} & f^3 f^{11} & f^4, f^{10} & f^5, f^9 & f^6, f^8 & f^7 \\
\text{ground state:} & {}^2F_{2\frac12,3\frac12} & {}^3H_{4,6} & {}^4I_{4\frac12,7\frac12} & {}^5I_{4,8} & {}^6H_{2\frac12,7\frac12} & {}^7F_{0,6} & {}^8S_{3\frac12}
\end{array}$$

Values for the spin–orbit coupling constants for ions of the transition, lanthanoid and actinoid series are listed in Appendix 3.

6.3.4 Spin–Orbit Coupling: *j–j* and Intermediate

For the heavier elements of the Periodic Table, say the third transition series and the actinoids, the approximation that spin–orbit coupling is so small it can be treated as a perturbation on free-ion terms fails. Spin–orbit coupling rises rapidly with nuclear charge while interelectronic repulsion terms decrease with the diffuseness of the valence electron density of larger atoms.

If the approximation is made that $\boldsymbol{H}_{\mathrm{LS}} \gg \boldsymbol{H}_{\mathrm{ER}}$, then we have the reverse of the Russell–Saunders coupling scheme. The individual electron total angular momenta, specified by $\boldsymbol{j}$, couple together to give the total angular momentum for the set of electrons. The equivalent of equation (33) becomes

$$\boldsymbol{J}_x = \sum_{i=1}^{n} \boldsymbol{j}_{x,i} \tag{39}$$

This is the basis of the so-called ***j–j*** coupling scheme. The interelectronic repulsions are then considered as a perturbation on the states determined by the scheme. Of course, for d^1, d^9, f^1 or f^{13}, where there are no interelectronic repulsions, the Russell–Saunders and the ***j–j*** coupling schemes are identical. For example, for the d^2 configuration there are two electrons each with $l = 2$, $s = \frac12$ and each giving possible $\boldsymbol{j}$ values of $|l \pm s|$, *viz.* $2\frac12$ and $1\frac12$. The states which arise under ***j–j*** coupling are $J = 5$, $J = 4$ and $J = 3$, with $J = 4$ occurring three times.

In fact, no atom has a value of ζ_d or ζ_f so large that the ***j–j*** coupling scheme is a good approximation. What has to be dealt with is an *intermediate* coupling scheme in which the effects of $\boldsymbol{H}_{\mathrm{ER}}$ and $\boldsymbol{H}_{\mathrm{LS}}$ are of comparable magnitude. The calculation of the energies of the resultant states are then not straightforward, and simple expressions involving L, S, and J are not available. The configurations have to be examined case by case.

6.4 FREE-ION TERMS IN LIGAND FIELDS[2–5,8–16,62]

6.4.1 Introduction

We now examine what happens to the energy levels of a free-ion when it is subject to the effects of the surrounding ligands. The treatment will use the terminology of CFT for convenience. However, the results are presented in forms suitable for discussion in any form of LFT including the AOM. The discussion of the ligand field concept of effective operators operating on effective orbital sets as set out in Section 6.2.2.2 should be constantly kept in mind.

6.4.2 Weak-field Case

We first consider what happens to a free-ion term when perturbed by a CFP small compared with the separation between free-ion terms, so that its action can be considered within that term without reference to other terms. In this approximation the 'centre of gravity' of each term will be maintained unchanged in spite of splittings it may undergo.

The CFP contains no term that relates to electron spin, so its effect can only be to lift orbital degeneracy. The multiplicity of a term is not affected. An immediate deduction is that S terms ($L = 0$) are not affected by the CFP. For terms that are orbitally degenerate ($L > 0$) we can note that the symmetries of the orbital components into which the term is split must conform to the group to which the CFP belongs. Qualitatively, then, predictions about the splittings caused by the CFP of the stereochemistries we have considered may be made with the aid of standard methods for the decomposition of angular momenta in spherical symmetry to cubic symmetry, as given in Table 3. The orbital degeneracies of A, B, E and T are respectively 1, 1, 2 and 3.

Table 3 The Terms Arising from Free-ion Terms in Cubic Symmetries

Term	S	P	D	F	G	H	I
O_h	A_{1g}	T_{1g}	$T_{2g} + E_g$	$T_{1g} + T_{2g} + A_{2g}$	$T_{1g} + T_{2g} + E_g + A_{1g}$	$2T_{1g} + T_{2g} + E_g$	$2T_{1g} + T_{2g} + E_g + A_{2g} + A_{1g}$
T_d	A_1	T_1	$T_2 + E$	$T_1 + T_2 + A_2$	$T_1 + T_2 + E + A_1$	$2T_1 + T_2 + E$	$2T_1 + T_2 + E + A_2 + A_1$

The evaluation of the quantitative aspects of the splitting involves calculations which become quite involved for the terms of higher L value from multi-electron configurations. We only present the results for the ground terms of the d configurations. The splitting patterns of these are set out in Figure 9.

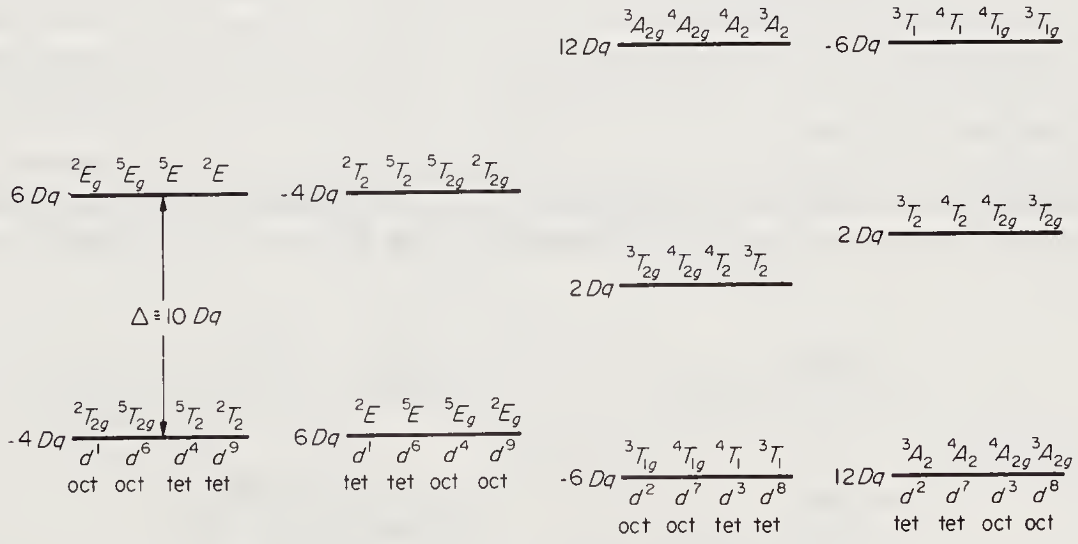

Figure 9 Splitting of free-ion D and F ground terms by cubic ligand fields

In the lower symmetries that were considered in Section 6.2 the D and F ground terms gave components as follows:

$$D_{4(h)} \qquad \begin{array}{l} D \rightarrow A_{1(g)} + B_{1(g)} + B_{2(g)} + E_{(g)} \\ F \rightarrow A_{2(g)} + B_{1(g)} + B_{2(g)} + 2E_{(g)} \end{array}$$

The quantitative aspects of the splitting in low symmetry cannot be generalized; they depend strongly on the effective CFP of the model employed.

6.4.3 Strong-field Case

It is instructive to investigate the assumption that the ligand field splitting is much larger than the effects of H_{ER}, that is, than the separation between free-ion terms. We restrict ourselves to cubic symmetry. Under such conditions the starting point is the ligand field configuration rather than the d^n configuration. Presuming octahedral symmetry the first three configurations in each case are

n	1	2	3	4	5	6	7	8	9
$2\Delta_{\mathrm{oct}}$		e_g^2	$t_{2g}^1 e_g^2$	$t_{2g}^2 e_g^2$	$t_{2g}^3 e_g^2$	$t_{2g}^4 e_g^2$	$t_{2g}^4 e_g^3$	$t_{2g}^4 e_g^4$	
Δ_{oct}	e_g^1	$t_{2g}^1 e_g^1$	$t_{2g}^2 e_g^1$	$t_{2g}^3 e_g^1$	$t_{2g}^4 e_g^1$	$t_{2g}^5 e_g^1$	$t_{2g}^5 e_g^2$	$t_{2g}^5 e_g^3$	$t_{2g}^5 e_g^4$
O	t_{2g}^1	t_{2g}^2	t_{2g}^3	t_{2g}^4	t_{2g}^5	t_{2g}^6	$t_{2g}^6 e_g^1$	$t_{2g}^6 e_g^2$	$t_{2g}^6 e_g^3$

Each of these configurations, except d^1 and d^9, will give rise to terms under the action of H_{ER} as a perturbation. The terms, of course, bear the labels of the cubic group, here O_h. The terms which arise are determined qualitatively by the decomposition of the group theoretical direct product of the electrons (or holes) involved into irreducible representations of the cubic groups. A t_{2g} or e_g orbital set more than half-full is treated as the equivalent number of holes, and a filled one is ignored. Then, for instance

$$\begin{aligned} t_{2g}^2 &\rightarrow T_{2g} \times T_{2g} = T_{2g} + T_{1g} + E_g + A_{1g} \\ t_{2g}^1 e_g^3 &\rightarrow T_{2g} \times E_g = T_{2g} + T_{1g} \\ t_{2g}^3 &\rightarrow T_{2g} \times T_{2g} \times T_{2g} = 4T_{2g} + 3T_{1g} + 2E_g + A_{2g} + A_{1g} \end{aligned}$$

Only the term labels are obtained in this way. The multiplicities to be attached to each label as well as quantitative aspects of their energies must be obtained by other more sophisticated means. For example, the t_{2g}^2 configuration gives the terms $^3T_{1g}$, $^1T_{1g}$, ^1E_g and $^1A_{1g}$. However, even the symmetry labels can be valuable in tracing the origin of terms.

6.4.4 Intermediate Ligand Field Strengths

6.4.4.1 Qualitative features: correlation diagrams[2-5]

There are some situations which correspond fairly well to the weak-field classification of Section 6.4.2; for example, the tetrahedral complexes of weakly coordinating ligands such as Cl^-, as in the $CoCl_4^{2-}$ ion. No system has a ligand field strength so great and interelectronic repulsions so small that the strong-field case applies well. In most cases the ligand field perturbations of the free-ion terms are so great that it is not sufficient to consider them in isolation; there is appreciable mixing of terms of the same symmetry label and multiplicity by the ligand field. The ligand field strength is of 'intermediate' magnitude.

The weak-field and strong-field limits discussed in the two previous sections provide the basis for the construction of qualitative diagrams which illustrate behaviour of the term energy levels in the intermediate strength region. These diagrams are given in Figure 10: in the centre representa-

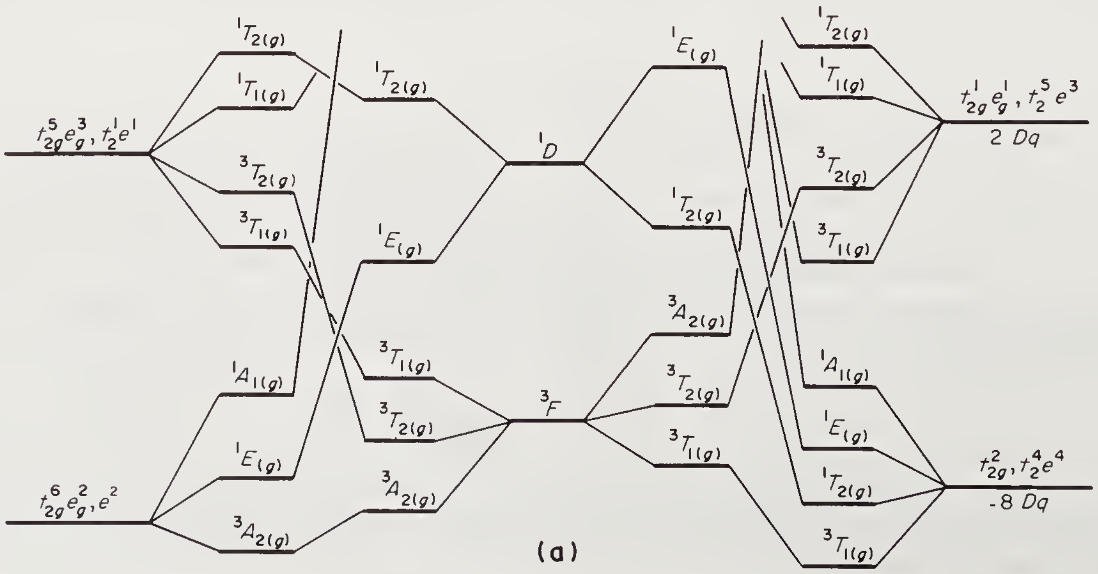

(a)

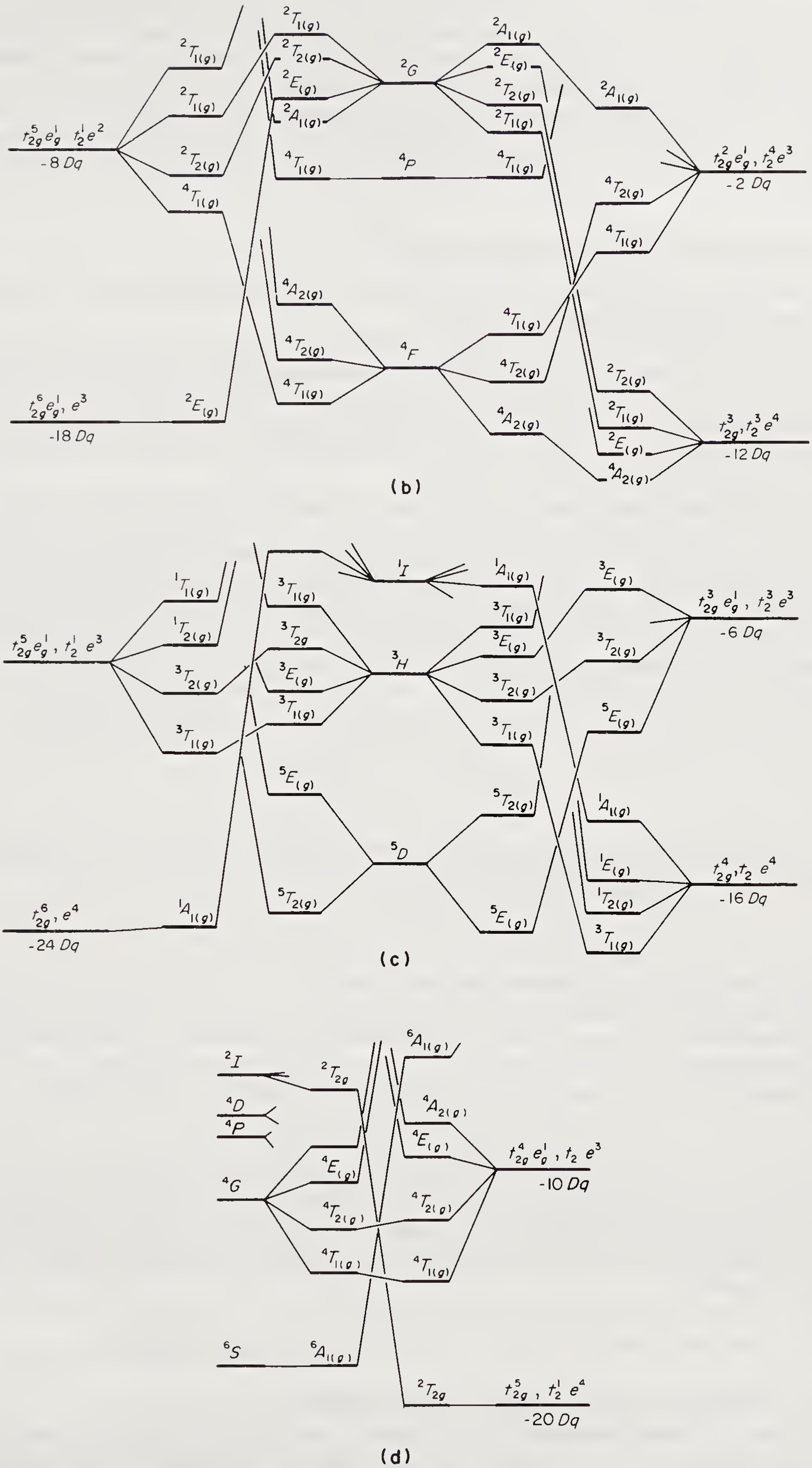

Figure 10 Free-ion term–strong-field configuration correlation diagrams for octahedral and tetrahedral stereochemistries: (a) d^2 and d^8, (b) d^3 and d^7, (c) d^4 and d^6 and (d) d^5

tive free-ion term energies are in units of the interelectronic repulsion parameter B; on the left- and right-hand sides the $t_{2g}-e_g$ configuration energies are in units of $Dq_{(\text{oct or tet})}$.

These diagrams demonstrate immediately the fact that for some configurations, *viz.* d^1, d^2, d^3, d^8 and d^9, there is no change of ground term no matter how large the ligand field splitting of the d-orbitals. For the remaining configurations, d^4, d^5, d^6 and d^7, there is a change of ground term, always to one of lower multiplicity, when the ligand field strength is sufficiently great. Complexes where the d-orbital splitting forces a ground term of multiplicity lower than that of the free-ion ground term are referred to as 'low spin', 'spin-paired' or 'strong-field'. Complexes of those configurations but where the multiplicity is that of the free-ion ground term are 'high-spin' or 'weak-field'.

6.4.4.2 *Quantitative treatment:* d^n *ground terms*[3–5,63–66]

The calculation of the splitting of the ground terms of d^n configurations can be performed to at least the first approximation fairly directly.

In the case of the free-ion D ground terms, ^2D of d^1,d^9 and ^5D of d^4,d^6, it can be noted from Figure 8 that there is no other term of the same, highest, multiplicity. The splitting of the D term in each case arises from the promotion of a t_{2g} to an e_g orbital. Consequently in all the cases the splitting is simply $\Delta_{oct} = 10Dq_{oct}$ or $\Delta_{tet} = 10Dq_{tet}$ as appropriate. The spin-allowed spectra of complexes giving $^2E_{(g)}$, $^2T_{2(g)}$, $^5E_{(g)}$ or $^5T_{2(g)}$ ground terms can be immediately identified with the appropriate ligand field parameter, Δ_{oct} or Δ_{tet}.

For the F free-ion ground terms the position is a little more complex. The F terms in cubic symmetry give corresponding $T_{1(g)}$, $T_{2(g)}$ and $A_{2(g)}$ terms of the same multiplicity. From Figure 8 it is seen that a P term of the same multiplicity lies higher at $15B$, and Table 3 shows that this also leads to a $T_{1(g)}$ term. The two terms $T_{1(g)}\,(F)$ and $T_{1(g)}(P)$ mix under the influence of the ligand field. The amount of mixing can be determined quite readily by observing their energies at the weak- and strong-field limits. In the weak-field limit (Section 6.4.2), defining $E_F = 0$ for octahedral symmetry, $E_{T_{1g}(F)} = -6Dq_{oct}$ and $E_{T_{1g}(P)} = 15B$. In the strong-field limit (Section 6.4.3), defining for example $E_{T^2_{2g}} = -8Dq_{oct}$ as in Figure 10a, $E_{T_{1g}(F)} = 2Dq_{oct}$ and $E_{T_{1g}(P)} = 2Dq_{oct}$.

The interaction between the two terms can be expressed by the secular determinant

$$\begin{array}{cc} T_{1g}\,(F) & T_{1g}\,(P) \\ \left|\begin{array}{c} -6Dq_{oct} - E \\ X \end{array}\right. & \left.\begin{array}{c} X \\ 15B - E \end{array}\right| \end{array} = 0 \tag{40}$$

where X has to be such as to reproduce the term energies at the weak- and strong-field limits. Multiplying the determinant out gives the equation

$$E^2 + (6Dq_{oct} - 15B)E - 90Dq_{oct}\,B - X^2 = 0$$

whose roots only satisfy the requirements if $X = 4Dq_{oct}$.

Examination of the appropriate figures shows that the same equation arises, with the same solution meeting the requirements, for all the F ground term cases in both octahedral and tetrahedral ligand fields.

The energies of the two $T_{1(g)}$ terms are then given by the roots of equation (41):

$$E^2 + (6Dq - 15B)E - 90DqB - 16D^2q^2 = 0 \tag{41}$$

Using this result, and the energies of the other components of the F ground term in the weak-field limit (Figure 9), it is possible to draw a diagram which shows the variation of the energies of all the terms of highest multiplicity for the F ground state configurations. It holds for both octahedral and tetrahedral symmetries, by employing the fact that Dq_{tet} has the opposite sign from Dq_{oct}. It is given as Figure 11.

Figure 11 allows, amongst other things, a straightforward interpretation of the spin-allowed spectra of complexes giving rise to $^3T_{1(g)}$, $^3A_{2(g)}$, $^4T_{1(g)}$ or $^4A_{2(g)}$ ground terms.

6.4.4.3 *Quantitative treatment: Tanabe–Sugano diagrams*[63–65]

The treatment of the previous section is limited to the terms of the same multiplicity as the free-ion ground term, and the mixing between them caused by the ligand field. Many other terms with lower multiplicity arise in most configurations, and in some one may become the ground term in a strong ligand field. For the treatment of the absorption spectra of complexes at all but the simplest level it is necessary to deal with at least all the lower lying terms of a configuration and the mixing between them caused by the ligand field.

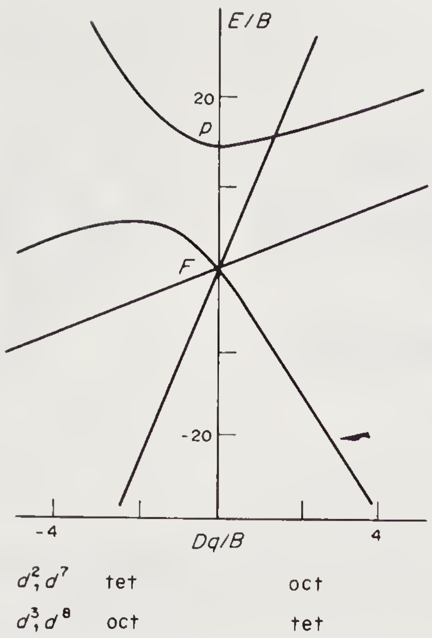

Figure 11 Splitting of free-ion F ground terms and mixing with P terms in cubic ligand fields

The calculation of all the term energies which arise from a d^n configuration may start from either the free-ion term energies with H_{LF} as a perturbation, or from the strong-field configurations with H_{ER} as the perturbation. If it is required to include the effects of spin–orbit coupling in the calculation then it is much better to use the former route, as the free-ion term wave functions can be operated on by the operator H_{LS} in a straightforward fashion. However, if spin–orbit coupling is not to be considered properly in the calculation, commencing with strong-field configurations presents computational advantages.

The terms which arise from all the strong cubic-field configurations of d^n systems have been listed together with the matrix elements of the operator H_{ER} which occur between them.[62] This permits the setting up of secular equations based upon all the terms of given symmetry label and multiplicity whose solutions give these term energies. The solution of the determinants is straightforward with the use of computer methods, although quite time consuming in the case of d^4 and d^5. In this way all the term energies arising from any d^n configuration in octahedral symmetry, say, can be obtained as a function of the parameters Dq_{oct}, B and C.

For a given ratio C/B it is then possible to present the term energies as a function of the ligand field strength, measured in units of Dq. Diagrams in which the term energies in units of B are presented as a function Dq are referred to as Tanabe–Sugano diagrams. A separate one will, in general, be needed for each ion, as the ratio C/B is peculiar to each ion. However, the ratio C/B does not vary very greatly from one closely related ion of a series to another,[67] so that one of these diagrams using a representative ratio C/B can give the main features to be expected for the spectra of ions giving rise to a given configuration, although not the detail. By noting that the free-ion term structure is the same for d^{10-n} as $d^n(n < 5)$ and by extending the diagrams to the left to include negative values of Dq, the number of such diagrams required can be reduced to five, and simultaneously they include tetrahedral ligand fields as well as octahedral.

Tanabe–Sugano diagrams with representative values of C/B are given in Figures 12–15 for the lower lying terms of each of the d^n configurations, $n = 1$–5. They can be used to deduce the principal features to be expected of the spectra of complexes of all the first transition metal ions in approximate octahedral or tetrahedral stereochemistry.

6.4.4.4 Quantitative treatment: low symmetry

The calculation of the energies which arise when H_{LF} corresponds to symmetry lower than cubic becomes an involved process which cannot be dealt with here, and which tends to proceed on an individual basis for each complex. However, an extensive compilation of results is available in which the departure from cubic symmetry is parameterized using Ds and Dt, and various ratios of C/B are employed. The compilation is in the form of a series of diagrams of the Tanabe–Sugano type, but with many for each configuration.[176] By examining such diagrams it may be possible to fit the experimental spectrum of a low symmetry complex and obtain at least approximate values for some or all of the parameters Dq, Ds, Dt, B and C which constitute a ligand field treatment.

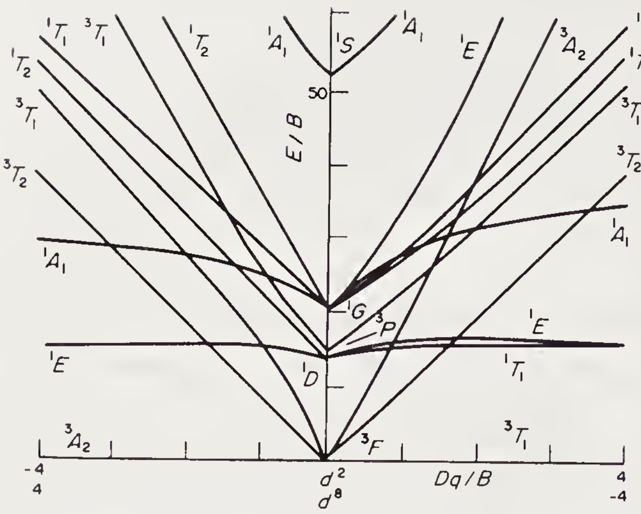

Figure 12 Tanabe–Sugano diagram for d^2 and d^3 for $C/B = 4.71$

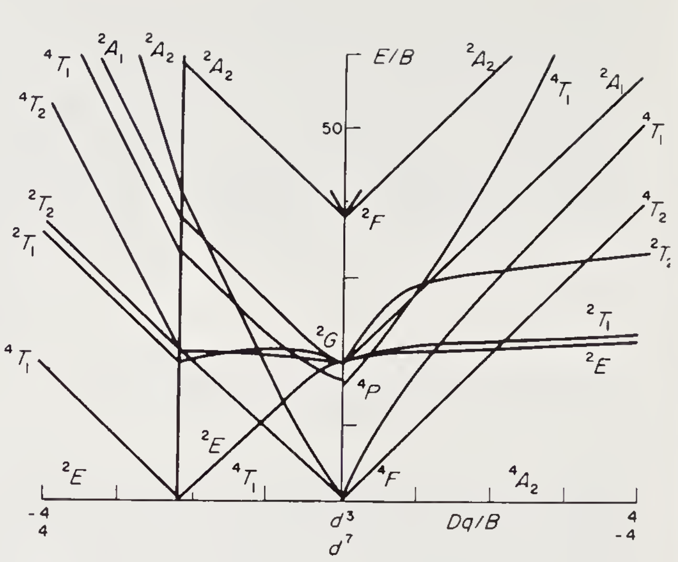

Figure 13 Tanabe–Sugano diagram for d^3 and d^7 for $C/B = 4.50$

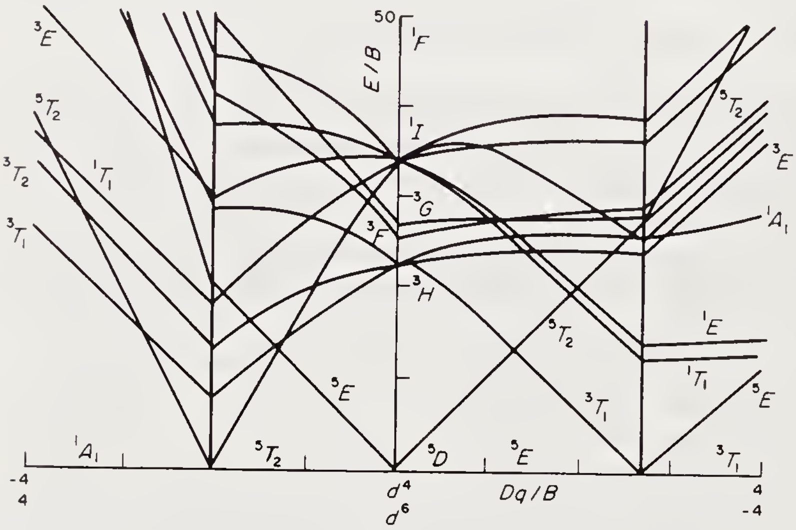

Figure 14 Tanabe–Sugano diagram for d^4 and d^6 for $C/B = 4.60$

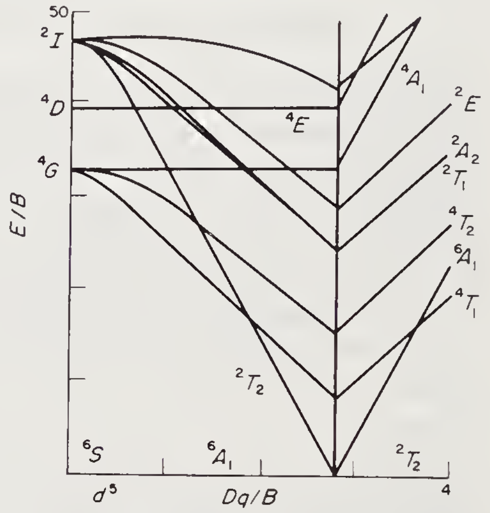

Figure 15 Tanabe-Sugano diagram for d^5 for $C/B = 4.48$

6.4.4.5 Spin–orbit coupling: cubic symmetry

Applications of ligand field theory to magnetic and ESR properties of complexes, in particular, often require a fairly detailed knowledge of the effects of spin–orbit coupling amongst the lower lying terms. The resolution of spin–orbit coupling splittings of terms is comparatively rare in the absorption spectroscopy of complexes, but at times some knowledge of the splittings of both the ground and excited terms is required.

The calculation of the spin–orbit splittings of the ground terms which arise from *d* configurations in ligand field strengths from weak to strong in cubic symmetry has been performed.[68,69] The results are summarized in Figure 16, where some other quantities relevant to magnetic properties are also included. The calculations leading to Figure 16 include all terms with the same multiplicity as the ground term, if that is the same as the free-ion. The mixing of the $T_{1(g)}(P)$ and $T_{1(g)}(F)$ terms (Section 6.4.4.2) is included *via* the parameter A which is defined as[70]

$$A = (1.5 - C^2)/(1 + C)^2 \tag{42}$$

where

$$\begin{aligned} \Psi_{T_{1(g)}} &= (1 + C)^{-\frac{1}{2}}\left[\Psi_{T_{1(g)}(F)} + C\Psi_{T_{1(g)}(P)}\right] \\ C &= (6Dq + E)/4Dq \end{aligned} \tag{43}$$

E is the lower root of equation (41). Spin-orbit coupling also mixes terms of different multiplicity, but the mixing is small unless the terms lie quite close together in energy. The calculations probably provide a good level of approximation in this situation, and the limitations will be taken up in the values derived for the parameter λ, remembering that spin–orbit coupling, like any other operator, will be an effective one in the ligand field context.

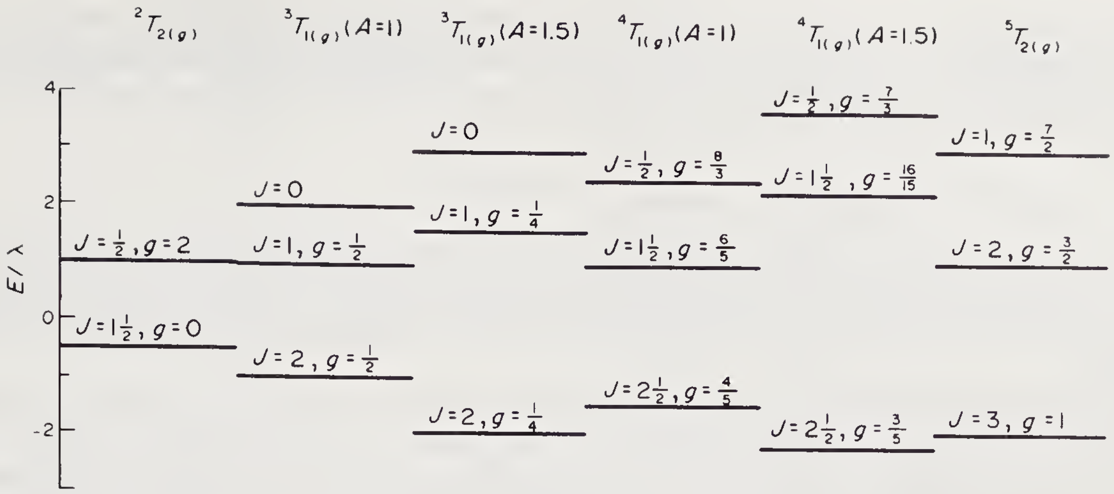

Figure 16 Splitting of cubic-field T ground terms by spin–orbit coupling

For cases where the ligand field has forced a term of multiplicity lower than the free ion as the ground term, the calculations of spin–orbit coupling splitting neglect many excited terms of the same multiplicity as the ground term. The neglect may show up as larger deviations of λ from the free-ion value than are likely to be observed in the situation described in the previous paragraph. These calculations are facilitated by the observation of an equivalence that the splitting patterns for the T terms arising from $t_{2g}{}^n$ configurations are inverted relative to those of p^n, an inversion formally obtained by reversing the sign of λ, with e_g electrons making no contribution.[62]

Calculation of excited term spin–orbit coupling splittings are available for the configurations $d^2(d^8)$, $d^4(d^6)$ and d^5, with $d^3(d^7)$ and $d^1(d^9)$ being trivial cases.[67,71–82]

For the lanthanoid element compounds the ligand field effects are a good deal smaller than those of spin–orbit coupling, and may be treated as perturbations on the state energies.[36,47–49,83] This introduces considerable simplification into the problem, but the complication of two cubic field parameters, one involving r^{-4} and one r^{-6} (Section 6.2.2.5) is present. Calculation of state splittings by cubic ligand fields have been performed using the operator methods mentioned in Section 6.2.1.5 for all the states which arise from f^n configurations. The results are presented as a set of diagrams in which the energies of the various components which arise are given as a function of the ratio of the contribution arising from $\overline{r^{-4}}$ to that arising from $\overline{r^{-6}}$ components of the potential.[84] One such diagram is given in Figure 17, for the $J=4$ state, which is the ground state of f^3. In that diagram the coefficient W is related to the r^4 terms, x to the r^6/r^4 terms, in the CFP. Note that, because spin–orbit coupling mixes the spin and orbital angular momenta, the labelling of the energy levels uses a different nomenclature ($\Gamma_1 \dots \Gamma_n$) suitable for the groups within which spin–orbit coupling must be treated.

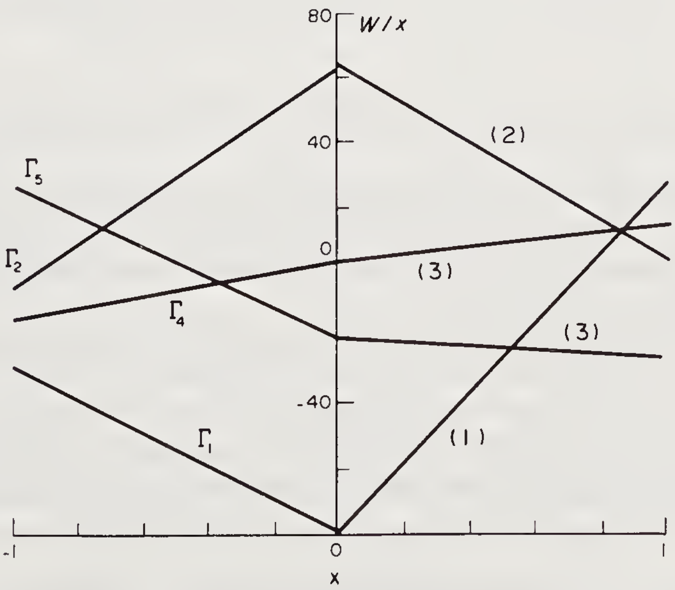

Figure 17 The splitting of the $^3H_4$ state by cubic ligand fields, as a function of $\overline{r^6}/\overline{r^4}$; $x = f(B_4{}^0/B_6{}^0)$ of equation (11) and $W \propto B_4{}^0$

For the actinoid complexes the approximation that the ligand field splittings are small compared with the spin–orbit coupling splittings of the free-ion terms is probably not very good. A proper treatment would involve the simultaneous operation by $\boldsymbol{H}_{\mathrm{ER}}$, $\boldsymbol{H}_{\mathrm{LF}}$ and $\boldsymbol{H}_{\mathrm{IS}}$ on the f^n configurations.

However, there does not seem to be sufficient experimental data of sufficient accuracy to have made that elaborate procedure worthwhile. It has proved possible to use the diagrams published for the lanthanoid ion case with some success for treating the magnetic properties of actinoid complexes in at least some cases.[49,85]

6.4.4.6 Spin–orbit coupling: lower symmetry

The calculation of spin–orbit coupling effects in d^n configurations in the presence of ligand fields of lower than cubic symmetry becomes a rather involved exercise. This occurs to a large extent because second-order terms become of importance, particularly in the interpretation of magnetic properties.

To the extent that the lower symmetry may be considered an axial deformation of the main cubic ligand field one may write the Hamiltonian for the system in the form $\boldsymbol{H}_{\mathrm{CLF}} + \boldsymbol{H}_{\mathrm{ER}} + (\boldsymbol{H}_{\mathrm{LS}} + \boldsymbol{H}_{\mathrm{AX}})$ where $\boldsymbol{H}_{\mathrm{AX}}$ is the axial ligand field component and might be parameterized, for example, in terms of Ds and Dt. The last two terms, in brackets, may be examined as a perturbation on the cubic intermediate ligand field strength terms set up by the first two terms. In that way it is possible to give expressions for the energies which arise, in particular, from the ground term in closed form.[70,86,87] For example, in D_{4h} or D_{3d} symmetry a $^2T_2$ ground term can be defined to be split by $\boldsymbol{H}_{\mathrm{AX}}$ into a $^2B_{2g}$ and a ^2E_g term with separation Δ_{AX},[87] which will be a function of Ds and Dt dependent upon the configuration which gave rise to the $^2T_{2g}$ term. The energies in the presence of spin–orbit coupling are $\Delta_{\mathrm{AX}}/3 - \lambda/2$ and $-\Delta_{\mathrm{AX}}/6 + \lambda/4 \pm (\Delta_{\mathrm{AX}}^2 + \Delta_{\mathrm{AX}}\lambda + 9\lambda^2/4)^{1/2}$.

However, the simplification inherent in the last paragraph, that only the ground term need be considered, is often not justified in detail. For example, the $^3A_{2g}$ ground term of the d^8 configuration in octahedral stereochemistry cannot be split in first order by spin-orbit coupling or by a low-symmetry ligand field component.[13,88] However, it is split in second order by interaction with the $^3T_{2g}$ term lying higher, itself split by the low-symmetry component, say by an amount $\Delta_{\mathrm{AX}}(T_{2g})$. The situation is illustrated qualitatively in Figure 18. The splitting, δ, is of the order of

$$\lambda^2\left(\frac{1}{\Delta_{\parallel}} - \frac{1}{\Delta_{\perp}}\right)$$

In fact, it cannot be calculated by reference to the $^3T_{2g}$ term alone; it requires consideration of the entire $d^8(d^2)$ manifold to obtain even fair agreement between theory and observation for δ.[71]

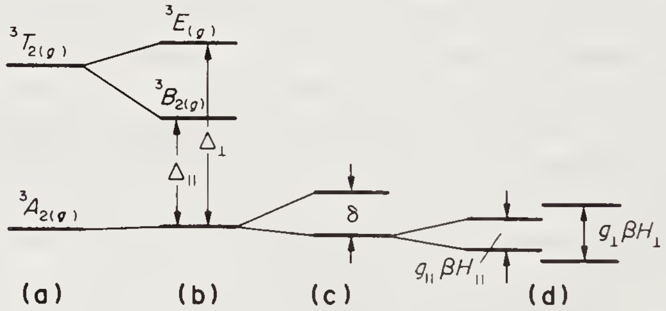

Figure 18 Splitting of a $^3A_{2(g)}$ ground term by (a) cubic ligand field, (b) tetragonal ligand field component, (c) spin–orbit coupling in second order and (d) magnetic fields parallel and perpendicular to the tetragonal component axis

Obviously, δ is a small quantity if the ligand field does not depart much from cubic symmetry. It may well be < 1 cm^{-1}. However, as magnetic properties are often studied at very low temperatures when kT is not $\gg \delta$, even such small energy separations in the ground terms may be important.

Although second-order spin–orbit splittings are present in most ground terms, they assume particular importance in those which are orbitally non-degenerate, *viz.* A and B types, with $S > 1/2$. Although approximation to axial symmetry is usually sufficient, the ESR experiment can respond well to even lower symmetry, and in the general case it is necessary to take that into account. The second-order spin–orbit coupling splitting of an A or B ground term of spin S is given by the formula

$$E_{M_S} = D\left(S_z^2 - S(S+1)/3\right) + E\left(S_x^2 - S_y^2\right) \qquad (44)$$

where M_S is the quantum number specifying the z component of spin angular momentum for the ground term; D is a parameter which accounts for the splitting in the approximation of axial symmetry and E the effects of still lower symmetry, for example rhombic; $E = 0$ for axial symmetry. The reference energy is that of the unperturbed ground term. The splittings for $S = 1$ to $S = 2\frac{1}{2}$ are given in Figure 19 under the assumption that $E = 0$. For $S = 2\frac{1}{2}$, extra terms occur which may make equation (44) inadequate.[32]

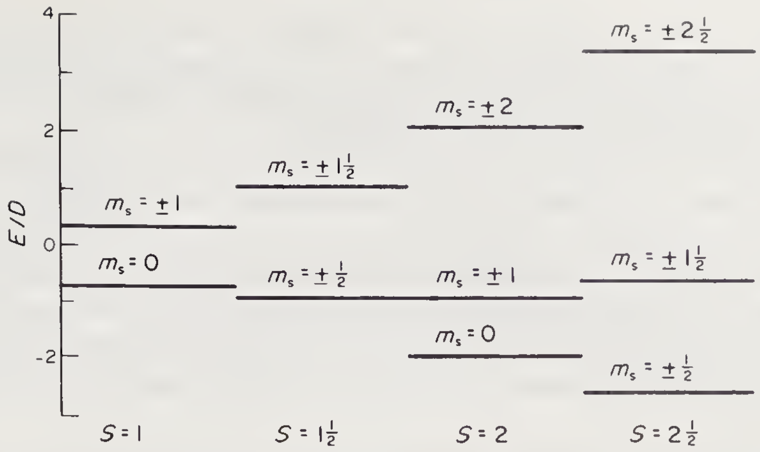

Figure 19 Zero-field splitting of terms $S = 1$ to $S = 2\frac{1}{2}$, assuming $E=0$

Both D and E are usually treated as parameters required to reproduce the data. They cannot, it seems, be related to the crystal field parameters by a treatment of the ground terms alone, nor even of all the terms of the same multiplicity as the ground term. However, there are indications that a calculation involving the whole manifold of the d^n configuration concerned may reproduce them in at least a semi-quantitative fashion.[89,90]

As pointed out above, for approximately cubic symmetry D is likely to be quite small. This arises partly because the separations between adjacent terms are fairly large. In lower symmetries it is not uncommon for terms to be brought close together by the ligand field. Then the denominators represented in Figure 18 may be small and the quantities of the type $\lambda^2\{(1/\Delta_{\parallel})-(1/\Delta_{\perp})\}$ correspondingly large. In this situation D (and E) may become quite large: values of up to perhaps 100 cm^{-1} occur in square-planar complexes. Then the second-order spin–orbit coupling may be the dominant feature of magnetic properties and may even play a role in the analysis of spectra.

The analysis of low-symmetry ligand field splittings in the terms of d^n configuration is complex because the cubic ligand field effects are comparable to those of $\boldsymbol{H}_{\mathrm{ER}}$ and the low-symmetry components to $\boldsymbol{H}_{\mathrm{LS}}$. The analysis of low-symmetry ligand field effects on the spectra of lanthanoid complexes, using the CFT parameterization scheme, is a well-developed field involving tedious rather than exceedingly complex calculations.[36,47–49,83] However, as the interpretation of the parameters is a rare exception[92] connected to the coordination chemistry of the complex containing the lanthanoid ion, the subject is not followed at depth in this article.

In the actinoid elements the approximation of cubic symmetry is probably sufficient to deal with the available experimental data, with some exceptions.[85,93] In the chemistry of certain of the actinoid ions the linear O═M═O unit can play an important role, as exemplified by the unit UO_2 in complexes of the uranyl type, *e.g.* $UO_2(OAc)_4{}^{2-}$. This unit introduces a very strong axial component into the ligand field which may be even more important than the cubic one.[49,85] However, information on the absolute magnitudes of such components seems difficult to obtain.

6.5 UV–VISIBLE SPECTRA OF COMPLEXES[3,27,38,47–49,67,83,94–100]

6.5.1 Selection Rules[3,27,67,98–103]

For transition metal complexes, light is absorbed essentially by the electric dipole mechanism. The interaction of the magnetic vector of the radiation can be of some importance but it does not seem necessary to discuss it here.[67] If ψ is a ground-state wave function of the complex and ψ' one for an excited state, and electromagnetic radiation of frequency corresponding to the energy difference between the two states is incident, then absorption takes place to a degree given by the *transition moment*

$$Q = \langle \psi | r | \psi' \rangle \tag{45}$$

where r is the radius vector, and which has the symmetry of an electric dipole. If the radiation is polarized the absorption is in general anisotropic, and Q has components, for example

$$Q_z = \langle \psi | z | \psi' \rangle$$

Ignoring for the present purposes rotational and translational phenomena, the wave functions may be expanded in the general form

$$\psi = \psi_{\mathrm{orbital}}\, \psi_{\mathrm{spin}}\, \psi_{\mathrm{vibrational}} \tag{46}$$

Now the spin functions are not related to the Cartesian coordinate system, so that

$$\langle \psi_{\text{spin}} | r | \psi'_{\text{spin}} \rangle = \delta(\psi_{\text{spin}}, \psi'_{\text{spin}})$$

Hence $Q = 0$ unless $\psi_{\text{spin}} = \psi'_{\text{spin}}$. We have, then, the selection rule $\Delta S = 0$. Transitions between states of different spin quantum number are forbidden.

The orbital and vibrational components of the wave functions as expanded in equation (46) are functions of the Cartesian coordinates. They can generally be classified as being symmetric to inversion through the origin (g) or antisymmetric to this operation (u). The integration implicit in equation (45), from $-\infty$ to $+\infty$, yields two qualitatively different results on the basis of such a classification. As r has the u classification it gives a zero value if ψ and ψ' have the same classification (both g or both u) but, possibly, a finite value if they differ in classification (one g, one u). We have then a further selection rule: only transition between functions of opposite parity are allowed.

Transitions of the type $g \leftarrow g$ and $u \leftarrow u$ are forbidden. In particular $d \leftarrow d$ and $f \leftarrow f$ inter-orbital transitions are forbidden. Transitions involving the same fundamental vibrational mode in the ground and excited states are forbidden.

The orbital and vibrational matrix elements may now be examined for symmetry requirements other than g and u. The requirement may best be expressed as the group-theoretical condition

$$\Gamma_{\psi_{\text{orbital}}} \times \Gamma_r \times \Gamma_{\psi'_{\text{orbital}}} \in A_1 \, (\text{or } \Gamma_1) \qquad (47)$$

where the $\times$ signifies the direct product and A_1 (or Γ_1) is the totally symmetric irreducible representation of the group to which the molecule belongs. An expression exactly analogous to equation (47) holds with $\psi^{(1)}{}_{\text{vibrational}}$ replacing $\psi^{(1)}{}_{\text{orbital}}$.

Consider the spin-allowed transitions possible from the $^3T_{1g}(F)$ ground term of an octahedral d^2 complex, ignoring the $g \leftarrow g$ selection rule and vibrational complications. The candidates are the $^3T_{1g}(P)$, $^3T_{2g}(F)$ and $^3A_{2g}(F)$ excited terms. We note that r transforms as T_{1u} in O_h. In the Group O

$$T_1 \times T_1 \times T_1 = 3T_2 + 4T_1 + 2E + A_2 + A_1 \in A_1$$
$$T_1 \times T_1 \times T_2 = 4T_2 + 3T_1 + 2E + A_2 + A_1 \in A_1$$
$$T_1 \times T_1 \times A_2 = T_2 + T_1 + E + A_2 \notin A_1$$

On these grounds, then, the transitions to the $^3T_{1g}(P)$ and $^3T_{2g}(F)$ terms are not forbidden, but that to the $^3A_{2g}(F)$ is.

6.5.2 Relaxation of Selection Rules: Band Intensities[3,27,67,98–103]

6.5.2.1 *The need for relaxation*

On the basis of the preceding section, it would appear that there should be almost no more spectroscopy for transition metal complexes than for non-transition metal complexes. All the transitions within the d or f shells are forbidden, and it should be only transitions from these to excited states of the same multiplicity involving other orbital sets that should contribute anything new. Such transitions would be few in number and lie at high energies. In fact, of course, quite the converse is known to be the case. The spectra of transition and lanthanoid element compounds are rich and lie at low energies.

Obviously, the selection rules enunciated do not hold rigorously. In this section we examine the mechanisms for overcoming the restrictions placed by the symmetry-based selection rules.

In this connection it is necessary to have a quantity which is a convenient measure of the intensity of a spectral band, that is, of the degree to which it is allowed. The conventional measure of intensity is the *oscillator strength*

$$f = 1.096 \times 10^{11} \nu Q^2$$

where ν is the frequency at the band centre and Q the transition moment of the band. The experimental value of f is obtained from the absorption spectrum by integrating the molar extinction coefficient over the band, stretching from ν_1 to ν_2, say. If ν is measured in cm^{-1}

$$f = 4.32 \times 10^{-9} g \int_{\nu_1}^{\nu_2} \varepsilon \, d\nu$$

where g is a factor which takes into account degeneracy in either or both of the ground and excited states involved. For approximate purposes the integration may be replaced by taking the product $\varepsilon_{\max} \times$ (width at half-height) as the measure of band intensity.

For a fully-allowed transition in the visible region of the spectrum, $f \approx 0.1$. Bands of such intensity occur, for example, in charge transfer spectra where an electron may be excited from a closed-shell configuration MO on the metal atom to another similar MO on the ligand. Such spectra are not confined to the transition metals and are responsible for the strong colours of some complexes of heavy non-transition metals. The colours are the consequence of very intense UV bands with 'tails' tending into the visible part of the spectrum.

6.5.2.2 The spin selection rule

All other considerations aside, transition metal complex spectra should contain only bands of the same multiplicity as that of the ground term. In practice, certainly the dominant bands in the spectra are of that type, but bands of intensity some 10^2 or 10^3 times lower are present, usually restricted to those corresponding to $\Delta S = \pm 1$ relative to the ground term, in the first transition series complexes.

The spin selection rule is relaxed by spin-orbit coupling. The operator involved, $\lambda L \cdot S$, can be expanded and rearranged:

$$\begin{aligned} L \cdot S &= L_zS_z + L_xS_x + L_yS_y \\ &= L_zS_z + \tfrac{1}{2}(L_+S_+ + L_-S_-) \end{aligned} \tag{48}$$

where $L_\pm$ and $S_\pm$ are the 'ladder' angular momentum operators.[17] These latter change the value of L or S respectively, by one unit. Consequently, perturbation by spin–orbit coupling can mix into the ground term small quantities of excited terms differing from the ground term by $\Delta S = 1$ or $\Delta L = 1$. The amount of mixing will be proportional to the value of the spin–orbit coupling constant, λ, and inversely proportional to the separation between the ground and excited term energies. Typically, for a first transition series element, $\lambda \approx 100\ \text{cm}^{-1}$ and $\Delta E_{\text{ground,excited}} \geqslant 10\,000\ \text{cm}^{-1}$, so that admixtures of terms with multiplicity different from that of the pure ground term are expected to be $\geqslant 10^{-4}$ if several excited terms contribute. It is to about this extent that the spin selection rule is seen to be relaxed. The expected greater relaxation of the rule for heavier elements where λ is larger is observed experimentally, and indeed for the actinide elements the spin selection rule may have little influence.[38,47–49,85]

6.5.2.3 Orbital/vibrational selection rules

Although the ψ_{orbital} and $\psi_{\text{vibrational}}$ components of the wave function were separated for discussion in Section 6.5.2.1, as far as considering the allowed character of transition metal spectra is concerned, they are better taken together. The vibrations associated with $\psi_{\text{vibrational}}$ can be taken to modulate the ligand field as they cause changes in the donor atom positions. This modulation can cause a mixing of the electronic wave functions. If it is taken that both ψ_{orbital} and ψ'_{orbital} are of g parity then u-type vibrations will cause the mixing of u-type electronic wave functions. Then

$$\begin{aligned} \psi_{\text{orbital}} &= \psi^0_{\text{orbital}}(g) + \sum^{u\ \text{vibrations}} C_i \psi^i_{\text{orbital}}(u) \\ \psi'_{\text{orbital}} &= \psi^{0'}_{\text{orbital}}(g) + \sum^{u\ \text{vibrations}} C'_i \psi'_{\text{orbital}}(u) \end{aligned} \tag{49}$$

where the C_i and C'_i are small numbers.

Using ψ_{orbital} and ψ'_{orbital} in this form, the integrals implicit in equation (45) are likely to be of the order of the values of C_i or C'_i, and the band oscillator strengths of the order of their squares. The orbital symmetry selection rule discussed at the end of Section 6.5.1 will have some effect in determining band intensities, but even orbitally forbidden transitions can be expected to appear with finite intensity.

For all complexes, at ambient temperatures at any rate, sufficient vibrational modes are available that it is certain that some of the appropriate symmetries will be coupled to the ground and excited electronic terms to at least a minor degree, and so provide a relaxation of the $d \nleftarrow d$ $(g \nleftarrow g)$ selection rule for the transition metals or the $f \nleftarrow f$ $(u \nleftarrow u)$ rule for the lanthanoids.

It is in this way that the $d \leftarrow d$ or $f \leftarrow f$ spectra of the transition metals and the lanthanoids become such a feature of their respective compounds. Without a very detailed knowledge of the vibrational spectrum, and the mechanism of its coupling to the electronic terms, it is not possible to quantify the degree of relaxation of the parity selection rule and that contained in equation (49). For some very simple cases, such as MX_6 or MX_4 units (X = halogen) in high-symmetry lattices at low temperatures where the vibrational structure is simplified, such an analysis has been performed and at least semi-quantitative agreement between calculated and observed oscillator strengths obtained.[104–108] For most purposes only qualitative information is to be obtained from a knowledge of the values of f. For example, for multi-atom ligands the number of vibrational modes is larger than for monatomic or simple diatomic ligands and, as observed, band intensities are larger. Typically $f \approx 10^{-4}$ for the spectral bands of transition metal complexes. In non-centrosymmetric complexes the role of the orbital symmetry selection rule in determining relative band intensities is more important than in centrosymmetric ones.

The coefficients C_i and C'_i in equation (49), which represent the coupling between electronic wave functions brought about by the vibrations, are not subject to quantitative assessment except in the simplest cases. The expressions for them, however, in general contain the inverse of the energy separation between the wave functions mixed. The excited u-functions mixed may include ones which are of the same energy as those which correspond to very intense, highly allowed bands. Then the mixing coefficients C_i or C'_i become rather larger, and the corresponding bands more intense. The phenomenon is known as 'intensity stealing': as $d \leftarrow d$ bands lie closer to very intense bands, say of charge-transfer origin, they become more intense, perhaps by a factor of up to 10.

If the complex does not possess a centre of symmetry, an even more powerful mechanism is present for the relaxing of the $g \nleftarrow g$ or $u \nleftarrow u$ selection rule. In such symmetries the distinction between the d and p orbitals for bonding purposes is not as clear as it is in centrosymmetric complexes. In particular, for the tetrahedron it is well known that the conventional $(sp^3)_\sigma$ hybridization cannot, as far as symmetry is concerned, be distinguished from an $(sd^3)_\sigma$ hybrid set. The d-orbitals which are the basis of the ligand field formalism are certain to be contaminated by some admixture of p character. For the purposes of dealing with spectral bands the p admixture has the effect of reducing the 'purity' of the g-parity of the d-orbitals. It is difficult to predict quantitatively the degrees of $p-d$ mixing in a tetrahedral transition metal complex: that requires a high-level MO treatment. However, the observation that the spectral bands of tetrahedral complexes have $f \approx 10^{-4}-10^{-3}$, some 50 times greater than for octahedral complexes with the same ligands, indicates that the mixing is not negligible.

Another qualitative prediction which may be made on the above grounds is that the intensity of transition metal spectral bands should decrease with temperature, as the degree of excitation of vibrational modes decreases. This issue is developed in more detail in Section 6.5.4.2.

The intensities of the $f \leftarrow f$ transitions of the tripositive lanthanoid element spectral bands are a good deal lower than those of the transition metals, presumably because the coupling between the electronic and vibrational wave functions is smaller on account of the shielding from the valence electrons. Value of f in the order of 10^{-7} are observed.[47–49,109] However, certain of the elements in the divalent state show $d \leftarrow f$ transitions which, as expected, are much more intense and blanket the $f \leftarrow f$ bands.[47–49]

At this point it is suitable to summarize the discussion by tabulating the intensities found for bands of different types. This is done in Table 4. In principle, the molar extinction coefficient, ε, is not a good measure of band intensity. However, for transition metal compounds at any rate, the band widths for spin-allowed bands at ambient temperatures are mostly of the order of 2000 cm^{-1}. With this fact in mind, it has become the custom to use ε as a rough measure of band intensity, and to facilitate comparisons of that type the values of ε associated with the varying types of transition are included in Table 4.

Table 4 Representative Values for the Oscillator Strengths and Molar Extinction Coefficients Found in Transition Metal Complexes

	Type of transition	*Approx. f*	*Approx. ε*
(i)	Spin-allowed, parity-allowed	10^{-1}	20 000
(ii)	Spin-allowed, parity-forbidden	10^{-4}	10
(iii)	As (ii) but with $p-d$ mixing	10^{-2}	1000
(iv)	As (ii) but with 'intensity stealing'	10^{-2}	1000
(v)	Spin-forbidden, parity-forbidden	10^{-7}	0.1
(vi)	$f \leftarrow f$	10^{-7}	1

6.5.3 Band Widths

For the lanthanoid elements the spectra often consist of many bands corresponding to the transitions between the states of the free-ion terms, each state perturbed by small ligand field effects to give several components. The bands are quite sharp, perhaps only a few cm^{-1} wide. The sharpness arises because of the small interaction of the f-electrons with the valence electrons.

For the transition metal complexes the position is much different. Each cubic-field term, say, may be split into components by spin–orbit coupling and departure from cubic symmetry and in addition is overlaid by closely coupled vibrations. The result is that for only the simplest ions and at very low temperatures it is likely that resolution of transitions between individual energy levels is possible. For the great majority of compounds, particularly at ambient temperatures, only the envelope of series of levels arising from a term is seen and that is fairly symmetrical. If the symmetry departs appreciably from cubic then the terms involved may be those of the low symmetry, corresponding to resolution of the ligand field splitting of the cubic field terms. For bands lying at low energy, or for heavy transition metals, where the spin–orbit coupling is an appreciable fraction of the transition energy, some signs of structure due to spin–orbit coupling may appear.[104,110]

It is valuable to consider the role of the vibrational structure further. Figure 20 illustrates a typical situation. The excited term potential well minimum is shifted slightly along the internuclear separation axis and has different vibrational structure relative to the ground term. According to the Franck–Condon principle, the spectral bands observed must correspond to vertical transitions on this diagram, as the electronic structure is able to rearrange to adjust to changed nuclear positions in a time short compared with the period of vibration.

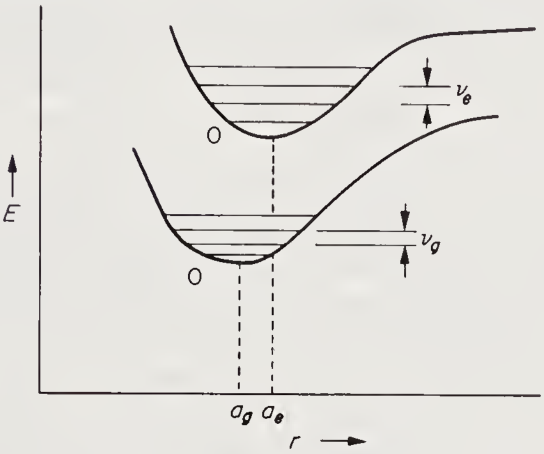

Figure 20 Potential wells and vibrational levels for the ground and an excited term of a complex

The first vibrational progression would start with the energy $\Delta E_0 + \nu_e$ and have components with intensities which might not have a simple monotonic decrease with vibrational quantum number, as overlap of the region along r as well as excitation energy would be involved. The second vibrational progression would be the 'hot band' starting with $\Delta E_0 - \nu_g - \nu_e$ and again with non-simple intensity distribution.

From the preceding discussion, and given that for a complex with polyatomic ligands a number of vibrational modes may be involved simultaneously, simple generalization about the structures of bands is unlikely. As a matter of observation, however, unless there is obvious splitting due to low symmetry or spin–orbit coupling, $d \leftarrow d$ spectral bands are fairly symmetrical and of width of the order of 2000 cm^{-1}, which presumably arises from the excitation of an average number of vibrational quanta of average vibrational frequency by the thermal energy available.

The *Jahn–Teller* theorem requires that any orbitally degenerate ground term become distorted so as to remove the orbital degeneracy and leave an orbitally non-degenerate ground term.[111,112] Space does not permit the development of the basis nor of many of the important consequences of this theorem.[113–117] The theorem does not give simple predictions about the magnitude of the energy separations involved in lifting the degeneracy of the ground term. They can only be obtained after detailed consideration of a number of pieces of data. For the present purposes we can note that the theorem can apply in two qualitatively different forms. Figure 21 should be consulted.

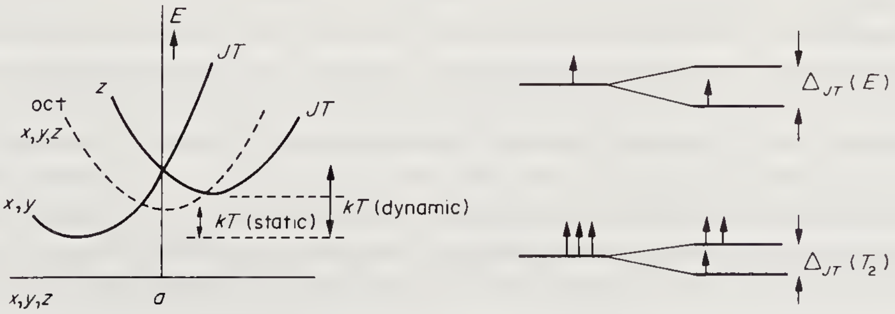

Figure 21 Qualitative representation of the origin of the Jahn–Teller splitting of orbitally degenerate ground terms. On the right the net lowering of energy is $\frac{1}{2}\Delta_{JT}(E)$

The 'static' Jahn–Teller distortions appear as structural changes which may be associated with the origin of low symmetry terms in the ligand field potential. Here, the separation of the orbital degeneracy appears to be greater than the vibrational energies available. Static Jahn–Teller distortions, if sufficiently large in energy, are an obvious cause of low-symmetry splitting of, say, the bands of what otherwise might be expected to be cubic symmetry. Large static Jahn–Teller distortions are associated particularly with the occurrence of one or three e_g electron configurations, for example in d^9, $t_{2g}^6e_g^3$, because the e_g electrons are directly engaged in bonding. They may be responsible for donor atom shifts of ~10 pm and spectral band splittings of several thousands of cm^{-1}.

The 'dynamic' Jahn–Teller distortions do not appear as structural changes at ambient temperatures, although they may 'freeze-in' at low temperatures. Here the orbital degeneracy appears to be lifted by an amount less than the vibrational energy available although, on account of the existence of zero-point motions, that is a very oversimplified statement. The dynamic Jahn–Teller effects are likely to appear in spectra as the broadening of spectral bands rather than their separation into components, at least at ambient temperature, and a reduction in the effects of spin–orbit coupling, and in k.[118,119] Dynamic Jahn-Teller systems tend to arise from t_{2g}^n $(n = 1, 2, 4, 5)$ systems, as the t_{2g} electrons are not so directly concerned in bonding.

The coupling mechanism given above for mixing excited u terms into g electronic terms through vibrational modulation of the ligand field is likely to be less efficient if terms of different spin are involved. In accordance with this, it is observed that spin-forbidden bands are a good deal narrower than are the spin-allowed ones dealt with above, corresponding to reduced overlap of available vibrational structure. Half-widths of a few hundred to one thousand cm^{-1} seem to be involved.

An exception to the foregoing discussion on vibrational coupling *via* modulation of the ligand field arises where the ground and excited terms have the same strong-field configuration and differ only in interelectronic repulsion effects. Such excited terms are obvious in Tanabe–Sugano type diagrams (Figures 12–15) as belonging to horizontal lines: their energy is *not* dependent on the ligand field strength. Coupling by modulation of the ligand field strength affects the ground and excited terms to the same extent, and in a diagram of the type of Figure 20 the potential minima lie directly above each other. The transitions available in such a situation are quite lacking in vibrational structure. The corresponding spectral bands are quite narrow, perhaps only 100–200 cm^{-1} even at ambient temperature.

6.5.4 Temperature Effects[67,100,105,106,120,121]

6.5.4.1 Band maxima and widths

The energy at which the maximum extinction coefficient for the transition between two terms occurs can vary with temperature from two main causes. Firstly, there may be a change in atom positions. If this change lengthens the average metal–donor atom separations then the ligand field suffered by the central atom would be expected to decrease, with consequent changes in the energies of its term separations. Secondly, the vibrational structure of the ground and excited terms will become simpler as the temperature is reduced. As pointed out earlier, the occupation of vibrational levels of a term may not be a monotonic function of the vibrational quantum number. As the vibrational occupation scheme becomes simpler it is possible that as well as narrowing the band, shifts in the centre-of-gravity of the occupation of higher vibrational levels may take place, changing the band maximum position.

In fact the two mechanisms outlined in the previous paragraph are not entirely independent unless the vibrational spectrum is purely harmonic. As anharmonicity is known to occur with the occupation of higher vibrational levels, an increase in average metal–donor atom bond length may well accompany an increase in temperature. It seems that provided no appreciable structural changes accompany the temperature change, the shifts in band maxima positions accompanying a change of 80–300 K, say, are usually quite small, and perhaps correspond to a change in the effective value of Δ of a few percent at most. In some cases, however, quite significant structural changes do accompany a change in temperature. This occurs, for example, when a dynamic Jahn–Teller system 'freezes' into a static system at low temperature. Then quite substantial changes to band maxima can take place, corresponding to the new ligand field from the altered environment. Band position shifts of 10% or more of their energy are not unknown.

If the transition involved were between two orbitally non-degenerate terms the effect of temperature would be to cause broadening as it is raised, consequent on the occupation of higher vibrational levels. However, such a simple situation does not arise for any d^n configuration. In the presence of orbital degeneracy the ground or excited term, or both, are split by spin–orbit coupling or a low-symmetry ligand field component, or both. No generalization about their competition with excited vibrational levels in responsibility for the width of the band envelope is possible. In particularly simple systems and at very low temperatures it may be possible to resolve the individual components, as discussed in Section 6.5.5.

6.5.4.2 *Band intensities*

The oscillator strengths of parity allowed ($g \longleftrightarrow u$) transitions are expected to be essentially independent of temperature, and this is observed experimentally in connection with charge transfer spectra.[38] It also seems that in complexes lacking a centre of symmetry the resulting mixing of u functions into the d-orbitals is sufficient to make the source of intensity largely independent of the vibrational coupling considerations dealt with in the next paragraph.[100] For tetrahedral complexes, for example, the $d \leftarrow d$ spectral bands undergo only relatively small intensity changes as temperature falls from ambient to 80 K or below.

For centrosymmetric complexes the intensities of the parity-forbidden $d \leftarrow d$ bands arise through vibronic interactions and consequently show substantial temperature dependence. It can be shown that for the ideal case of a single harmonic vibration of frequency γ coupled to the electronic system the intensity of a band should be given by[105,106]

$$f_T = f_0 \coth(\gamma/2kT) \tag{50}$$

Note that if γ is high enough, as may occur for light, tightly bound atoms, essentially only the ground level is occupied and the $\coth^{-1}$ term is close to unity.

In fact, although derived for an idealized situation, equation (50) holds in first approximation for the intensities of the bands of many $d \leftarrow d$ spectra.[67,100] Presumably γ is then an average over the various frequencies excited and the occupations assumed in deriving equation (50) are averages over the populations for the various modes. Of course, significant exceptions do occur. For example, in the presence of a dynamic Jahn–Teller effect a considerable distortion of the vibrational occupation scheme is likely to occur, particularly if it ‘freezes’ into a static situation. However, the indications given by equation (50) are sufficiently reliable that for a complex with a multi-atom ligand system, absence of temperature dependence of the intensity of strong bands can be taken as support that a centre of symmetry is absent. The absence of temperature dependence for one band amongst others with temperature dependence may indicate it is a weak intraligand transition rather than of $d \leftarrow d$ origin.[100]

6.5.5 Single Crystal Polarized Light Spectra[67,100,122]

With single crystals of complexes at very low temperatures using polarized light, for suitable systems with the right crystal packing and with simple ligands, it is possible that individual electronic and vibrational components can be resolved and identified by their symmetry properties with relationship to the plane of polarization of the light. Then, identification of low-symmetry ligand field components and even assessment of spin–orbit coupling effects may be made. The investigation of the role of dynamic Jahn–Teller effects can yield information about modes of deformation in the complex and vibration structure.

Experimental techniques and the methods of treating the data in this field have been under review, the latter particularly in reference to application of the AOM of ligand field effects.[100] Earlier reviews have covered various aspects of the results.[67,122–129]

6.5.6 Fitting of Spectra

Given the spectrum of a transition metal or lanthanoid complex, the process of determining what values of ligand field parameters best reproduce it varies from trivial to very sophisticated, according to the nature and extent of the data on the one hand and of the model to be used on the other. For, say, the single band of $\mathrm{Ti(H_2O)_6}^{3+}$ (d^1) in aqueous solution the identification of the band maximum, or perhaps center-of-gravity, with Δ_{oct} $e_g \leftarrow t_{2g}$, is the only step to be made. For the polarized single crystal spectrum of a multi-electron ion taken at very low temperature, the fitting may require repetitive diagonalization of large energy matrices so that least-squares procedures may be used to take advantage of the over-determination available (*i.e.* a data/parameter ratio >1).

All intermediate levels of parameter determination are likely to arise. Perhaps the most common situation is that a model is set up with as many parameters as there are independent pieces of data available. This has been discussed in connection with the use of the AOM (Section 6.2.3).[42–44] If only two parameters are to be evaluated, say Dq and B for fitting the ${}^4T_{2g} \leftarrow {}^4A_{2g}$ and ${}^4T_{1g} \leftarrow {}^4A_{2g}$ spin-allowed transitions of a d^3 complex, then simple inspection of Figure 11 to find the required ratio of energy separations may be the easiest thing to do.[2] Alternatively, solution of equation (41) by hand for the ratio Dq/B may give a little more accuracy. For more than two parameters, some form of least-squares fitting which does not seek to evaluate errors or information about the goodness-of-fit is convenient. Some idea of errors probable in the parameters may be obtained by repeating the fitting with the band energies changed by as much as the experimental data make reasonable.

For multi-parameter over-determined situations a least-squares fitting procedure is the method of choice provided the calculation of the energy levels is not too time-consuming. The energies may be non-linear functions of the parameters when, unless a non-linear program is employed, a low damping factor may be necessary to achieve convergence. The weighting of observations and the assessment of the meaning of the errors associated with the parameters need to be given very careful consideration. If the repetitive calculation of the energies in the least-squares process is too time-consuming, various other parameter fitting procedures of the grid-search, steepest-in-descent or 'Simplex' types are available and may be adapted for individual applications.[134]

6.5.7 Spectra of Typical Transition Metal Species[2,38,67,94–103,122–129]

6.5.7.1 *Introduction*

Obviously, it is not possible to give here a full account of the vast experimental data available on the spectra of transition metal complexes. The treatment will be restricted to examining the principal features shown by the most common ions of each configuration of the transition series. Species involving much charge transfer are not mentioned. Fuller accounts of the spectra are available at a fairly simple level.[2,38] More detailed accounts including articles treating single-crystal polarized spectra are available.[67,100,122] Comprehensive accounts of lanthanoid spectra are available.[47–49] In the following discussion, ε values are in l cm^{-1} mol^{-1}.

Table 5 lists representative values of Δ_{oct} and Δ_{tet} for some common ligands coordinating to some transition metal ions, from analysis of the absorption spectra.[27] Table 6 gives a list of parameters which reproduce Δ_{oct} and Δ_{tet} values and also the ratio B/B_0, at least approximately, as a product of a metal-ion and of a ligand quantity. The material in Table 6 should be used as a guide rather than in any quantitative fashion.

Table 5 Values of Δ_{oct} for Various Ligands and of Δ_{tet}(4Cl) Created with Some Common Transition Metal Ions[a]

d^m	Ion	6F	6Cl	6Br	$6H_2O$	3(ox)	3(acac)	6(urea)	$6NH_3$	3(en)	6CN	4Cl
1	Ti^{3+}	18.9	13.0		20.1		16.9	17.5	(17)		22	7
	V^{4+}	20.1	(15)									8
2	V^{3+}	16.1	12		20.0	18		17.4	(18)		24	6
3	V^{2+}		8		12.4		(14)					
	Cr^{3+}	14.5	13	13	17.0	17.4		16.0	21.5	22.0	26.0	
	Mo^{3+}		19.2	14.5			(14)	16				
4	Cr^{2+}	(14)	10		13					18		
	Mn^{3+}	22	17.5		20	20					31	
5	Mn^{2+}	7.8	7.5	7.0	8.5						33	
	Fe^{3+}	14			14	(14)					35	5
6	Fe^{2+}	10			10						32	4.05
	Co^{3+}	13			20.8	18.0			22.9	23.2	32.0	
	Ru^{2+}				19.8				28.1			
	Rh^{3+}		20.4	19.0	27.0	26.0			34	35		
	Ir^{3+}		25.0	23.0					41	41		
	Pt^{4+}	33	29	25								
7	Co^{2+}	8.3	7.65	6.5	9.3	11			10.2	11		2.65
8	Ni^{2+}	7.25	7.2	6.8	8.5				10.8	11.5		4.09
9	Cu^{2+}				12				15	16		

[a] Values are expressed in cm^{-1} × 10^3.

6.5.7.2 d^1

(i) Ti^{3+}

Formally octahedral complexes show an absorption band corresponding to the $^2E_g(e_g)\leftarrow{}^2T_{2g}(t_{2g})$ excitation as expected, often with a lower energy shoulder due to Jahn–Teller splitting in ML_6 cases and to low symmetry for inequivalent ligand compounds.[38,67,135] The shoulder is mostly 500–1000 cm^{-1} lower in energy, whether for equivalent or inequivalent ligands. The band is of low intensity ($\varepsilon \approx 10$) and very broad—perhaps 8000 cm^{-1} at half height. Curiously,

Table 6 Parameters for the Estimation of Δ and B for Various Combinations of Metal Ions and Ligands[a]

Metal ion	*g*	*k*	*Ligand*	*f*	*h*
Co^{2+}	9.3	0.15	3(acac)	1.0	—
Co^{3+}	20.8	0.35	6Br	0.75	2.0
Cr^{2+}	13	—	6OAc	0.96	—
Cr^{3+}	17.0	0.17	4Cl	−0.38	2.0
Cu^{2+}	12	—	6Cl	0.76	1.5
Fe^{2+}	10	—	6CN	1.5	2.0
Fe^{3+}	14	0.24	6NCS	1.03	—
Ir^{3+}	32	—	2(den)	1.28	—
Mn^{2+}	8.5	0.30	enta	1.2	—
Mn^{3+}	20	—	3(dtp)	0.86	2.4
Mn^{4+}	23	—	3(bipy)	1.4	2.0
Mo^{3+}	19	0.15	3(en)	1.27	1.4
Ni^{2+}	8.5	0.12	6F	0.88	0.8
Pt^{4+}	38	—	3(glycine)	1.2	—
Re^{4+}	35	—	$6H_2O$	1.00	—
Rh^{3+}	27	—	$6NH_3$	1.2	1.2
Ti^{3+}	20.1	—	$6NO_2$	1.4	—
V^{2+}	12.4	0.08	6OH	0.94	—
V^{3+}	20.0	0.29	3(ox)	0.98	1.5
V^{4+}	23	—	3(σ-phen)	1.4	2.0
			6(py)	1.25	—
			6(urea)	0.91	1.2

[a] $\Delta = fg\,(\text{cm}^{-1} \times 1000)$, $B = B_0(1-hk)$. Much of the information in this table is only very approximate in nature, particularly that pertaining to B.

the splitting is quite small (150 cm^{-1}) in Ti^{3+}/Al_2O_3 solid solution,[136] but very large (~3000 cm^{-1}) in $Ti(acac)_3$ where the intensity is very high ($\varepsilon \approx 1500$).[137] Dq varies from 1300 (6Cl) through 2010 ($6H_2O$) to 2230 cm^{-1} (6CN).

(ii) V^{4+}

Most tetravalent vanadium complexes contain the VO^{2+} unit which leads to a strong low-symmetry ligand field component. Three ligand field bands with $\varepsilon \approx 20$ commonly occur, one ~13000 cm^{-1}, one ~17000 and one 25000–30000 cm^{-1}, in VOL_4 units, but their classification in formal C_{4v} symmetry is not clear, in spite of the availability of polarized light results.[38,138,139] However, the ground term is accepted to be $^2B_2$.

Formally octahedral VL_6 complexes give a band rather like that of TiL_6 ones, but the splitting is rather larger (2000–6000 cm^{-1}).[38] Tetrahedral VCl_4 gives a very broad band ($\varepsilon \approx 100$) at ~9000 cm^{-1}, which has a structure which may arise from Jahn–Teller splitting.[140] The band is of course $^2T_2(t_2) \leftarrow {}^2E(e)$, with $Dq \approx -900$ cm^{-1}.

(iii) Cr^{5+}, Mo^{5+}

A number of compounds contain MOL_5 units, particularly with L = halogen, and the spectra seem to resemble those of VO^{2+} complexes in some respects[38,141] — there is a band at ~14 000 cm^{-1} ($\varepsilon < 100$) and another at 18000–23000 cm^{-1}. In the $Mo(CN)_8{}^{3-}$ ion the 'dodecahedral' symmetry is in fact rather low and splits the *d*-orbitals completely so that four bands are possible and the spectrum, which consists of absorption between 24000 and 42000 cm^{-1} with ε rising from ~1000 to ~3000, has been decomposed into such components.

6.5.7.3 d^2

(i) V^{3+}

Octahedral complexes in solution[38,67] give two broad (~4000 cm^{-1}), weak ($\varepsilon \approx 5$) spin-allowed bands, $^3T_{2g} \leftarrow {}^3T_{1g}$ (11000–22000 cm^{-1}) with $^3T_{1g}(P) \leftarrow {}^3T_{1g}$ (18000–29000 cm^{-1}) lying higher (Figures 9, 10a, 12). These can be interpreted in terms of Dq and B/B_0, giving respective values from 1200 and 0.68 (6Cl) through 1900 and 0.71 ($6H_2O$) to 2400 and 0.64 (6CN). In the solid state (V^{3+}/Al_2O_3), the transition $^3A_{2g} \leftarrow {}^3T_{1g}$ (38 000 cm^{-1}) may be observed if charge transfer bands are pushed to higher energies.[136] There, very weak narrow bands at ~9000 and at ~22 000 cm^{-1} are attributed to spin-forbidden transitions to the $^1T_{2g}$, ^1E_g and $^1A_{1g}$ terms.

The tetrahedral anion $VCl_4{}^-$ is present in certain solid solutions and gives a complex band at ~9500 cm^{-1}, presumably $^3T_2 \leftarrow {}^3A_2$ split by spin–orbit coupling and low symmetry, and a band at 15000 cm^{-1} about 1500 cm^{-1} wide, which is interpreted as arising from $^3T_1 \leftarrow {}^3A_2$ with possibly $^3T_1(P) \leftarrow {}^3A_2$ superimposed and $Dq \approx -600$ cm^{-1}, $B/B_0 \approx 0.69$.

Some of the features of V^{3+} spectra are set out in Figure 22.

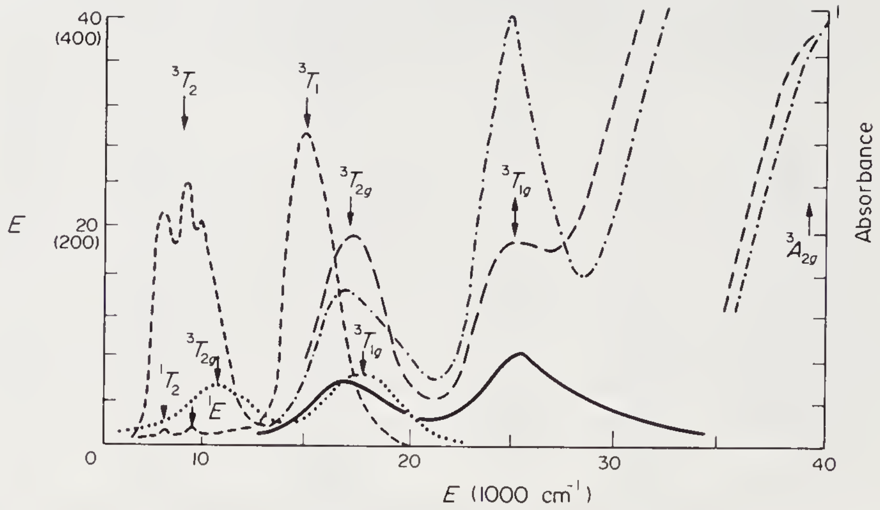

Figure 22 Absorption spectra of some V^{III} species: —, $V(H_2O)_6^{3+}$ in aqueous solution; ·····, VCl_6^{3-}, and ----, VCl_4^-, in solid solution; — · — · and — — —, V^{3+}/Al_2O_3 single crystal at 77 K, ∥ and ⊥, respectively, to the C_3 axis. The vertical axis labelling in parentheses applies to VCl_4^-

(ii) Mo^{4+}

Some Mo^{IV} complexes of the type $MoCl_4{\cdot}2L$, including L = Cl, show rather intense bands at ~20000 and ~26000 cm^{-1} which have tentatively been assigned as ${}^3T_{2g}\leftarrow{}^3T_{1g}$ and ${}^3T_{1g}(P)\leftarrow{}^3T_{1g}$ in octahedral symmetry. The $Mo(CN)_8^{4-}$ ion shows rising absorption from 18000 ($\varepsilon \approx 1$) to 38000 cm^{-1} ($\varepsilon \approx 1000$) with structure which has been assigned to the four transitions between the *d*-orbitals split by the 'dodecahedral' stereochemistry.[142]

6.5.7.4 d^3

(i) V^{2+}, Cr^{3+}

Octahedral V^{II} complexes in solution show the three weak bands ($\varepsilon \approx 10$, ~4000 cm^{-1} wide) expected for spin-allowed transitions from the ${}^4A_{2g}$ ground term (Figures 10b, 13).[38,67,146] For $6H_2O$ ligands the positions are ${}^4T_{2g}\leftarrow{}^4A_{2g}$ (12400), ${}^4T_{1g}\leftarrow{}^4A_{2g}$ (18500) and ${}^4T_{1g}(P)\leftarrow{}^4A_{2g}$ (27900 cm^{-1}), corresponding to $Dq = 1230$, $B/B_0 \approx 0.89$. For Cr^{III} the highest band may be lost in the charge transfer background, but a range of complexes show features very similar to those of V^{II} except that the values for Dq are higher: $Dq(6H_2O) = 1700$, $B/B_0 = 0.67$. For Cr^{3+}/Al_2O_3 (ruby) the spin-forbidden bands at ~15000 cm^{-1} (${}^2T_{1g},{}^2E_g\leftarrow{}^4A_{2g}$) and at ~ 22000 cm^{-1} (${}^2T_{2g}\leftarrow{}^4A_{2g}$) and their luminescence properties have been much studied.[136] The polarized absorption spectrum of Cr^{3+}/Al_2O_3 is illustrated in Figure 22, where symmetry labels corresponding to the trigonally distorted octahedral site symmetry are used. The ${}^4T_{2g}$, ${}^4T_{1g}$ and ${}^4T_{1g}(P)$ bands appear to be split by 450, 800 and 400 cm^{-1} respectively by the lower site symmetry. Some complexes of the type CrN_5X and CrN_4X_2, where N represents a nitrogen-based donor center, show splittings of the octahedral ${}^4T_{2g}$ level into ${}^4E_g$ and ${}^4B_{2g}$ components in the lower symmetry of up to 5000 cm^{-1}, which have been interpreted in terms of CFT[3,143-145], MO[135,136] and AOM[59] models.

(ii) Mo^{3+}, Re^{4+}

The spectra of a number of octahedral Mo^{III} complexes contain the spin-allowed ${}^4T_{2g}\leftarrow{}^4A_{2g}$ (16000–26000 cm^{-1}) and ${}^4T_{1g}\leftarrow{}^4A_{2g}$ (20000–31000 cm^{-1}) transitions and, in addition, much more prominent than for the Cr^{3+} case ($\varepsilon \approx 5$), presumably because of the higher spin–orbit coupling, the ${}^2E_g,{}^2T_{2g}\leftarrow{}^4A_{2g}$ (~9000 cm^{-1}) and ${}^2T_{1g}\leftarrow{}^4A_{2g}$ (~15000 cm^{-1}) spin-forbidden bands.[38,115] $Dq(6Cl)$ is 1920 cm^{-1}. The spectra of ReX_6^{2-} ions show the expected importance of high spin-orbit coupling.[147]

6.5.7.5 d^4

(i) Cr^{2+}, Mn^{3+}

The d^4 configuration gives in octahedral stereochemistry both high-spin (${}^5E_g$) and low-spin (${}^3T_{1g}$) ground term complexes (Figure 10c). The spectral properties of the low-spin case have scarcely been studied. The high-spin complexes at first sight are expected to give the ${}^5T_{2g}\leftarrow{}^5E_g$ transition as the principal feature of the spectrum, the only other bands being spin-forbidden. In fact the position is more complicated because the configuration seems to be unusually sensitive to low symmetry splitting, whether of Jahn–Teller or physical distortion origin.[38,67] The ${}^5D$ free-ion term can be split by a tetragonal distortion to yield, as shown in Figure 23, a group of three fairly close excited terms if the ${}^5T_{2g}$ term is much less affected than the ${}^5E_g$ term.

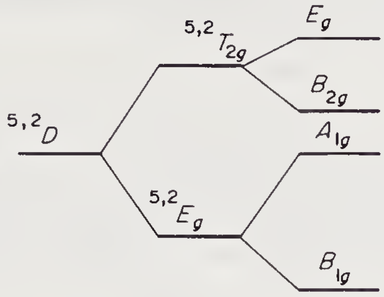

Figure 23 Splitting of a ${}^5D$ or ${}^2D$ term by an octahedral ligand field with a large tetragonal component, as from an e_g-based Jahn–Teller effect

The position illustrated in Figure 23 seems to hold for a number of Cr^{II} complexes. The very broad band (6000 cm^{-1}, $\varepsilon = 5$) for $Cr(H_2O)_6^{2+}$ in aqueous solution at ~14000 cm^{-1} has in fact been suggested to be composed of no less than four components, corresponding presumably to symmetry even lower than tetragonal. In these circumstances, interpretation in terms of octahedral ligand field parameters is probably not useful. Nevertheless, a value of Dq of ~1400 cm^{-1} has been put forward for the ion with help from other sources.[148] The remarks made for Cr^{II} appear to hold also for Mn^{III} to some extent, although the splittings of the octahedral terms may be relatively less. The overall splitting of the free-ion ${}^5D$ term is of course larger because of the higher metal atom formal charge. For $Mn(H_2O)_6^{3+}$, Dq has been assigned as 2100 cm^{-1}. For both ions, in the solid state at any rate, the presence of spin-forbidden bands is obvious, although analysis of them does not seem to be common.[67]

6.5.7.6 d^5

(i) Mn^{2+}, Fe^{3+}

For the d^5 configuration in octahedral stereochemistry the high-spin ${}^6A_{1g}$ and the low-spin ${}^2T_{2g}$ terms occur. Analysis of the ligand field bands of the low-spin cases is scarcely possible. Tetrahedral stereochemistry yields the ${}^6A_1$ ground term. As there is no higher-lying sextet term, all the transitions observed are spin-forbidden. It can be noted that in Figure 15, for lower values of Dq/B at any rate, many of the excited terms run at least approximately parallel to the ground ${}^6A_{1(g)}$ term. This leads to the fact that the resulting transitions are largely of the 'ligand-field-independent' type, and consequently are relatively narrower (Section 6.5.4.1). A number of excited quartet terms lie relatively closely spaced, but some distance above the ground term.

As a consequence of these points, the spectra of octahedral Mn^{II} high-spin and of tetrahedral iron complexes consist of a number of bands of width ~500 cm^{-1} with $\varepsilon \approx 0.1$ lying at fairly high energies [those for $Mn(H_2O)_6^{2+}$ commence at 18000 cm^{-1}] and whose positions are not very sensitive to the details of the ligands.[67,138] Probably because the chemical species present are not well defined in solution, the spectra for octahedral Fe^{III} complexes are diffuse and rarely interpretable. Because a number of bands are present for the other cases, it may be possible to deduce several of the ligand field and interelectronic repulsion parameters and even λ, although the uncertainty in Dq may be substantial.

6.5.7.7 d^6

(i) Fe^{2+}, Co^{3+}

Octahedral complexes of the d^6 configuration give rise to the high-spin ${}^5T_{2g}$ and the low-spin ${}^1A_{1g}$ ground terms.[38,67] In the former case the spectrum would be expected to be dominated by the only spin-allowed transition ${}^5E_{2g} \leftarrow {}^5T_{2g} \equiv 10Dq$. To some extent that is the situation, but as with the converse transition for d^4, there is substantial band splitting by low-symmetry and/or Jahn–Teller effects. In the example of $Fe(H_2O)_6^{2+}$ the very weak band at ~10000 cm^{-1} ($\varepsilon \approx 1$) is wide (~4000 cm^{-1}) and is clearly split into two components. Most low-spin Fe^{II} complexes show the band split by 2000–3000 cm^{-1}. The main example of low-spin Co^{III}, the CoF_6^{3-} ion, behaves similarly. Spin-forbidden transitions are not observed.

In contrast to the previously-treated configurations, the spectra arising from the low-spin ground term are well defined and can be interpreted, sometimes in detail. Referring to Figure 14, it is seen that the next singlet terms above ${}^1A_{1g}$ are ${}^1T_{1g}$ and ${}^1T_{2g}$, at fairly high energy, with the ${}^3T_{1g}$ and ${}^3T_{2g}$ forms intermediate. Some low-spin octahedral Fe^{II} complexes are known to show the features anticipated on these grounds, for example $Fe(CN)_6^{4-}$: ${}^1T_{1g} \leftarrow {}^1A_{1g}$, 31000 cm^{-1}, $\varepsilon \approx 350$; ${}^1T_{2g} \leftarrow {}^1A_{1g}$, 37000 cm^{-1}, $\varepsilon \approx 2000$; and ${}^3T_{1g} \leftarrow {}^1A_{1g}$, 24000 cm^{-1}, $\varepsilon \approx 2$. The high values of ε are probably associated with the covalent nature of bonding concerning the CN^- ion and the fact that charge transfer bands lie just above the transition to ${}^1T_{2g}$.

For Co^{III} the low-spin ground term is usual and, owing to the vast number of complexes available, the spectra have been much studied. The two bands corresponding to the ${}^1T_{1g}$ and ${}^1T_{2g}$ terms are regularly observed, the former lying between 15000 and 32000 (6CN) cm^{-1} and the latter 6000–8000 cm^{-1} higher, ε being ~100. Band widths are variable above 2000 cm^{-1}, and may show splitting due to low-symmetry environments. The spin-forbidden bands corresponding to ${}^3T_{1g}$ and ${}^3T_{2g}$ may sometimes be observed, with $\varepsilon \approx 1$. Analysis of the ${}^1T_{1g}$ and ${}^1T_{2g}$ band energies readily yields values for Dq and B.

For Co^{III} more than for other cases the splittings of the ligand field bands even in solution can be related directly to the departure of the ligand environment from octahedral symmetry. Figure 24 shows the absorption spectra of the *cis*- and *trans*-$[(H_2O)F(en)_2Co]^{2+}$ ion. Simple arguments show that the ${}^1T_{2g}$ band should be little affected in each compound, and also the ${}^1T_{1g}$ band for the *cis* compound. The ${}^1T_{1g}$ term is expected to be markedly affected in the *trans* compound. The diagram supports the arguments. Study of the ${}^1T_{1g}$ and ${}^1T_{2g}$ band splitting for complexes of the type CoN_xX_y, where N represents a nitrogen based ligand and $x + y = 6$, has enabled the evaluation of Ds and Dt, on the angular overlap model parameters, for a variety of systems.[3,59,135,136,143–145]

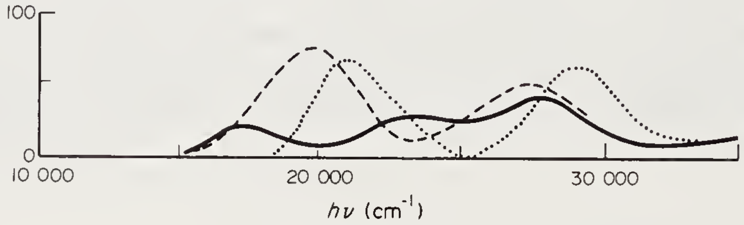

Figure 24 Solution absorption spectrum of: —, *trans*-$[Co(en)_2F_2]^+$; ----, *cis*-$[Co(en)_2F_2]^+$; and ······, $[Co(en)_3]^{3+}$

Tetrahedral stereochemistry is well known for Fe^{III} and gives rise to the ${}^5T_2 \leftarrow {}^5E$ transition at ~4500 cm^{-1}, $\varepsilon \approx 100$, which is nearer the lower values found for octahedral complexes in other systems. In some solids, strong Jahn–Teller effects are present.[114,117]

(ii) Ru^{2+}, Rh^{3+}, Ir^{3+}, Pd^{4+}, Pt^{4+}

The octahedral complexes of these ions are, of course, all of the spin-paired type.[38] The values of Dq are higher than for, say Co^{III}, so that usually only the ${}^1T_{1g}$ band is observed below the charge transfer bands. The spin-forbidden transitions to the ${}^3T_{1g}$ and ${}^3T_{2g}$ terms can be quite intense ($\varepsilon \approx 10$), presumably because of the very large spin–orbit coupling in some of these ions. Square-planar complexes have been studied.[149]

6.5.7.8 d^7

(i) Co^{2+}

Octahedral Co^{II} complexes possess either the high-spin ${}^4T_{1g}$ or the low-spin ${}^2E_g$ ground terms. The spectra of the latter have not been successfully treated. The high-spin complexes show absorption at ~8000–10000 cm^{-1} and again in the region of 20000 cm^{-1}. The lower band ($\varepsilon \approx 5$) is clearly the ${}^4T_{2g} \leftarrow {}^4T_{1g}$ transition (Figures 10b, 13), but the interpretation of the more complex absorption in the visible is not certain, in spite of the large number of complexes which have been studied.[38,67] There may be several unresolved components, with a maximum $\varepsilon \approx 10$. Certainly some of this absorption arises from the transition ${}^4T_{1g}(P) \leftarrow {}^4T_{1g}$, probably split by low-symmetry effects, but superimposed upon it may be the ${}^4A_{2g} \leftarrow {}^4T_{1g}$ band and spin-forbidden transitions to doublet terms. Spectra of solids at low temperature remove some, but not necessarily all, of the ambiguity. Nevertheless, values of Dq may be extracted fairly reliably. Values span the range 650–10200 cm^{-1}, with B/B_0 0.80–0.91.[38]

Tetrahedral Co^{II} complexes give the ${}^4A_2$ ground term. There is a band at ~5000 cm^{-1}, $\varepsilon \approx 200$, often with signs of structure, and complex absorption from ~12000 to 18000 cm^{-1} with maximum $\varepsilon \approx 1000$. The lower band is clearly ${}^4T_1 \leftarrow {}^4A_2$ with the structure due to spin–orbit coupling and/or low symmetry effects. The higher energy absorption probably all arises from the ${}^4T_1(P) \leftarrow {}^4A_2$ transition, but with strong perturbation by low-symmetry, spin–orbit coupling and vibrational effects in combination.[67,149] Dq varies from −265 (4I) to −470 cm^{-1} (4CNSe), with B/B_0 for these, 0.68 and 0.67, quite typical.[38]

Unlike the position for most of the preceding configurations, the spectra of some Co^{II} complexes of low symmetry are fairly well defined and can be interpreted in terms of transitions between the *d*-orbitals.[38] A number of square-planar and square pyramidal complexes have been the subject of detailed study.[150–156] However, there is often a lack of agreement between the interpretations of different workers.

6.5.7.9 d^8

(i) Ni^{2+}

Octahedral Ni^{II} complexes give the three spin-allowed transitions from the $^3A_{2g}$ ground term expected on the basis of Figures 10a and 12. $^3T_{2g} \leftarrow {}^3A_{2g}$ lies between $\sim$7000 and $\sim$13000 cm^{-1}, $^3T_{1g} \leftarrow {}^3A_{2g}$ between $\sim$11000 and $\sim$20000 cm^{-1}, and $^3T_{1g}(P) \leftarrow {}^3A_{2g}$ between $\sim$19000 and $\sim$27000 cm^{-1}, all with $\varepsilon \approx 10$ and some signs of structure.[38,67,157] The spin-forbidden transitions to singlet terms may be observed with $\varepsilon \leqslant 0.5$, relatively strong because of the high spin–orbit coupling. The spectra are readily interpreted in terms of *Dq* and *B*, and possibly a low-symmetry parameter. Different values of *B* for the t_{2g} and e_g electrons have often been considered. *Dq* varies from 680 (6Br) through 850 (6H_2O) to 1270 cm^{-1} (3bipy), with corresponding values of $B/B_0 \approx 0.7$, 0.88 and 0.70 respectively. Complexes of the type NiN_4X_2 show splitting of the $^3T_{2g} \leftarrow {}^3A_{2g}$ band which has been rationalized in terms of ligand field parameters characteristic of N and of X.[157]

Tetrahedral Ni^{II} complexes are well established. There is a band in the near IR which arises from $^3A_2 \leftarrow {}^3T_1$ ($\varepsilon \approx 20$) which is usually simple, and another, often more complex, in the visible at $\sim$15000 cm^{-1} ($\varepsilon \approx 100$) which is assigned to $^3T_1(P) \leftarrow {}^3T_1$.[38,67] The lowest-energy band, $^3T_2 \leftarrow {}^3T_1$, is rarely observed. The value of -410 cm^{-1} for *Dq* in $NiCl_4^{2-}$ is typical, as is the value of B/B_0 $\sim$0.75. The transitions to singlet terms may be quite strong, $\varepsilon \approx 1$.

Square-planar Ni^{II} complexes often show quite well-resolved spectral bands, and some progress has been made towards assignment.[149,157] A band at $\sim$20000 cm^{-1} ($\varepsilon \approx 100$) is often assigned as $b_{2g} \leftarrow b_{1g}$ in terms of orbital occupations, and the band, responsible for the characteristic red color, at $\sim$25000 cm^{-1} ($\varepsilon \approx 1000$) as $a_{1g} \leftarrow b_{1g}$, using the nomenclature for D_{4h}, but there is some controversy over such assignments. The position for five-coordinate Ni^{II} is complex as both $S = 0$ and $S = 1$ ground terms occur associated with both square-pyramidal and trigonal-bipyramidal stereochemistry, and fairly well-resolved spectral bands are present.[155,157] While assignments of these have been made on reasonable grounds, space prevents discussion here.

(ii) Pd^{2+}, Pt^{2+}, Au^{3+}

These ions are mainly associated with square-planar stereochemistry. Fairly well-resolved spectral bands are often observed, but their interpretation in terms of *d*-orbital separations, if indeed that is possible in view of strong charge transfer, is not simple and is not pursued here.[38]

6.5.7.10 d^9

(i) Cu^{2+}

Octahedral complexes of Cu^{II} are Jahn–Teller unstable, so that the formal E_g and T_{2g} terms are split. The spectra do not usually correspond to the simple $^2T_{2g}(t_{2g}) \leftarrow {}^2E_g(e_g)$ excitation,[38,67,100] but rather to one based upon Figure 23. The $Cu(H_2O)_6^{2+}$ ion is almost an exception: the band at 12000 cm^{-1} ($\varepsilon \approx 10$) is broadened to $\sim$6000 cm^{-1} but structure is not resolved. Often the splitting is considerable: $Cu(bipy)_3^{2+}$, for example, shows bands at 15000 and at 6000 cm^{-1}, which must be interpreted with the aid of a diagram of the type of Figure 23, but for trigonal symmetry, as $^2A_1 \leftarrow {}^2E$ and $^2E \leftarrow {}^2E$.

Four-coordinate Cu^{II} complexes are common, but the strict tetrahedral or square-planar stereochemistries are rare. Rather, some intermediate stereochemistry of approximate D_{2d} symmetry is more usual, and four transitions between the *d*-orbitals may be available.[38,67] The spectra of such complexes often show two or three more or less resolved bands below about 20000 cm^{-1}, $\varepsilon \approx 50$. The polarization properties of these bands have been studied in some detail in certain cases,[100,122] assisting in the assignments of the transitions involved. Figure 25 shows the polarized spectrum of a $CuCl_4^{2-}$ salt at different temperatures. Figure 26 shows how the intensities of these bands as a function of temperature relate to the expression of equation (50).

6.5.8 Excited States and Photochemistry

Reviews have covered applications of ligand field theory to excited states and the photochemistry of complexes, especially those of Cr^{III}.[130–133]

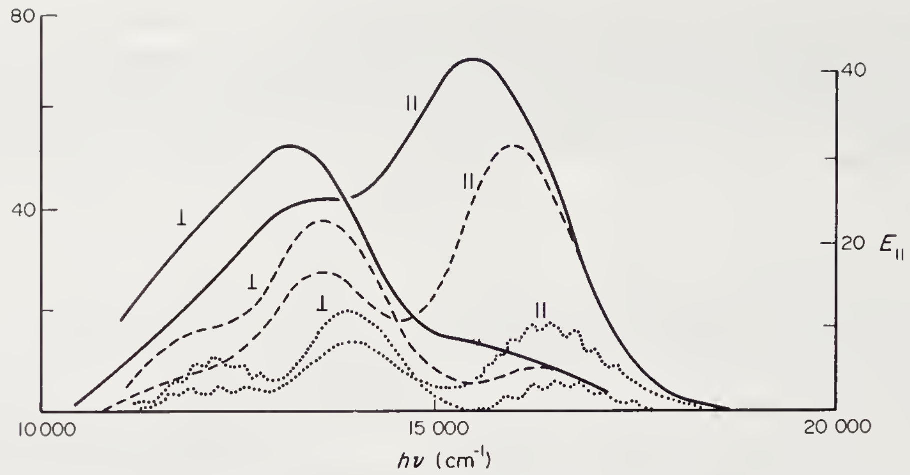

Figure 25 Single crystal absorption spectrum of $(\text{methadonium})_2\text{CuCl}_4$ with the electric vector (i) parallel and (ii) perpendicular to the (100) face at: —, *ca.*300 K; ----, *ca.*100 K; and ·····, *ca.*10 K

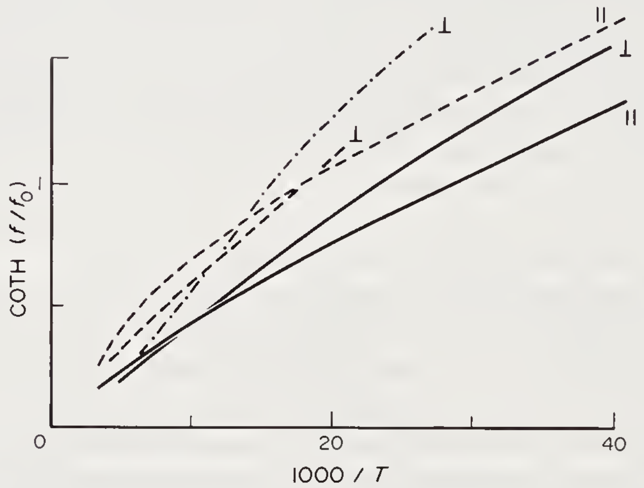

Figure 26 Intensity of some of the bands of $(\text{methadonium})_2\text{CuCl}_4$ as a function of temperature, compared with equation (50) (solid lines)

6.6 MAGNETIC PROPERTIES OF COMPLEXES

6.6.1 Types of Magnetic Behaviour

6.6.1.1 Fundamentals[158–161]

If a magnetic field, H, is applied to a substance the value of the field inside it, B, in general differs from that external to it. We write

$$B = H + I \tag{51}$$

where I is the *intensity of magnetization* of the substance. For many substances I is colinear with H and proportional to it. Then B/H is a constant and may be expressed in the SI system as

$$\begin{aligned} B/H &= 1 + I/H \\ &= 1 + \chi \end{aligned} \tag{52}$$

χ, the 'volume susceptibility', is also a constant, usually of rather small value. It measures how susceptible the substance is to magnetization by the applied field. If χ is negative the substance is said to be diamagnetic; if positive, paramagnetic or perhaps ferro- or antiferro-magnetic.

For some purposes, an alternative but equivalent definition of χ is preferable. In general, the energy of the substance is altered by the presence of the field. If, for unit volume, the energy is W, we write

$$\chi = \frac{-\langle\mu\rangle}{H} \; \frac{\mathrm{d}W}{\mathrm{d}H} \tag{53}$$

where $\langle\mu\rangle$ is the 'magnetic moment'. In most cases the change in W is proportional to H^2, and again χ is a constant.

The interaction of an electron, as a charged particle, with an applied magnetic field causes a precession of its orbital motion which acts to cancel the field so that I, and hence χ in equation (52), is negative. The effect is small but omnipresent. The spin and angular momenta of an electron confer upon it the properties of a magnetic dipole, which tends to be oriented by the applied field, lowering the energy and making χ positive (equation 53). This effect is larger than that due to electron charge, so the paramagnetism of an atom is larger than its diamagnetism. Net spin and angular momenta appear only for partly filled electron shells, and so paramagnetism is essentially a phenomenon of the transition, lanthanide and actinide elements.

The charge–magnetic field interaction is independent of temperature, so that diamagnetism is essentially independent of temperature. The energy of orientation of the atomic dipole by the magnetic field is usually less than the thermal energy available to the substance, so that its effects are temperature dependent. Paramagnetism is usually a temperature-dependent phenomenon. An ideal paramagnet obeys the *Curie law*

$$\chi = \frac{C}{T} \tag{54}$$

where C is the Curie constant. Since diamagnetism is omnipresent, this equation, in practice, must be modified to

$$\chi = \frac{C}{T} + \chi_{\mathrm{diam}} \tag{55}$$

Few substances behave as ideal paramagnetics, even with allowance for the diamagnetic contribution of the second term in equation (55). It is found that a more practical expression for dealing with most paramagnets is a variation of the *Curie–Weiss Law*

$$\chi = \frac{C}{T-\theta} + \chi_{\mathrm{TIP}} + \chi_{\mathrm{diam}} \tag{56}$$

Here, θ is the Weiss constant and χ_{TIP} is a temperature-independent paramagnetic contribution, often neglected as it may be even smaller than χ_{diam}.

For some purposes it is more convenient to deal with magnetic properties per unit mass rather than per unit volume. We define

$$\chi_{\mathrm{m}} = \chi/\rho$$

where ρ is the density. Equations (53)–(56) all may be written replacing χ by χ_{m}. The units of χ and χ_{m} in the SI system are respectively m^3 and $\mathrm{m}^3\ \mathrm{kg}^{-1}$. In the c.g.s. system the quantities are related to the SI values by[154]

$$\begin{aligned} \chi(\text{c.g.s.}) &= (4\pi)^{-1} \times 10^6\,\chi \quad (\text{c.g.s.})\ \text{unit cm}^3 \\ \chi_{\mathrm{m}}(\text{c.g.s.}) &= (4\pi)^{-1} \times 10^3\chi_{\mathrm{m}} \quad (\text{c.g.s.})\ \text{unit cm}^3\ \text{g}^{-1} \end{aligned}$$

Diamagnetic susceptibilities are approximately $\chi_{\mathrm{m}_{\mathrm{diam}}} = -0.5 \times 10^{-8}\ \mathrm{m}^3\ \mathrm{kg}^{-1}$; paramagnetic susceptibilities vary from zero to the order of $10^{-5}\ \mathrm{m}^3\ \mathrm{kg}^{-1}$.

6.6.1.2 *Magnetic exchange/dilution*

In many substances, particularly transition metal complexes, the atom which possesses the partially filled electron shell is associated with many others with filled shells. We have, then, the paramagnetic centers separated by intervening diamagnetic atoms. To a first approximation the diamagnetic and paramagnetic origins of susceptibility are independent, so that in such a substance the paramagnetic centers are independent of each other, except for the through-space coupling between their effective magnetic dipoles, a coupling which can be shown to be very small for separations corresponding to more than, say, two atom diameters.

Substances in which the paramagnetic atoms are independent are *magnetically dilute*; those in which the atoms are coupled so that their magnetic dipoles — that is, angular momenta — are not independent are *magnetically concentrated*. The effect such coupling has on the paramagnetic properties depends upon how it affects the orienting effects of the magnetic field, and consequently upon its relationship to temperature. Magnetic concentration is, then, relative to the temperature being considered; at sufficiently low temperature even the smallest coupling is important and almost all substances have to be considered magnetically concentrated. At ambient temperatures most coordination complexes can be considered as magnetically dilute.

For the most part this article will be restricted to magnetically dilute systems, but some outline of the features which appear with magnetic concentration is called for. The cooperative effects which are the result of coupling between the angular momenta of paramagnetic atoms are loosely referred to as magnetic exchange. The coupling between two atoms, i and j, is parameterized by the exchange integral, J_{ij}.[28]

For our purposes we distinguish two types of magnetic exchange system. One is the more common situation where a single paramagnetic atom is coupled to several other paramagnetic atoms, and these in turn to further such atoms. This we call intermolecular exchange. In certain cases a very small number of paramagnetic atoms are coupled to each other, but effectively not to other sets of paramagnetic atoms. This we refer to as intramolecular exchange. The two situations present distinctly different problems and will be dealt with separately.

The cooperative effects associated with magnetic exchange fall into two opposite, but related, categories.[163] If the exchange is such that the nearest neighbours of any given paramagnetic atom tend to have their magnetic dipoles — loosely referred to as 'spins' — aligned parallel to its spin we have the phenomenon of ferromagnetism. If the exchange is such that the nearest neighbour spins tend to be anti-parallel to the initial spin we have antiferromagnetism. In ferromagnetism J_{ij} is positive for nearest neighbours, in antiferromagnetism it is negative.

The orienting effects of the magnetic exchange on the directions of neighbouring spins compete with the disordering effects of temperature.[164] Below a certain temperature the exchange dominates and the substance is said to become magnetically ordered. If the exchange is ferromagnetic the transition temperature is called the *Curie temperature*, T_C. If the exchange is antiferromagnetic we have the Néel temperature, T_N. In high-symmetry systems the transition from the paramagnetic region above T_C or T_N to the ordered region below can be very sharp, involving fractions of 1 K, and be accompanied by dramatic changes in magnetic properties and behaviour. In the more widespread case of low symmetry the ordering temperature may be rather ill-defined and order accompanied by only a gradual change of magnetic behaviour with temperature. Fe and MnO are respective ferro- and antiferro-magnets showing sharp transition temperatures, T_C and T_N.

Below the ordering temperature the magnetic behaviour, particularly of ferromagnets, is likely to be complicated. The susceptibility may become very large for ferromagnets, very small for antiferromagnets, and may depend strongly on the magnetic field strength. We do not further consider substances in the ordered region.

Above the ordering temperature a substance showing magnetic exchange is in the paramagnetic region: χ_m is independent of magnetic field strength, although the behaviour may be well away from that of the equivalent system of independent atoms. Substances with ferromagnetic exchange interactions show susceptibilities enhanced above that of the independent atom system; substances with antiferromagnetic exchange show reduced susceptibilities.

If the equivalent magnetically dilute system is taken to obey the Curie law (equation 54), then the presence of ferromagnetic exchange is characterized by a positive value of the Weiss constant, θ, in equation (56). Antiferromagnetic exchange correspondingly gives a negative value for θ.

In so far as θ in the Curie–Weiss law expression arises only from the effects of magnetic exchange it can, in simple systems, be related to the magnitude of the exchange integrals between a paramagnetic atom and its various neighbours, nearest and otherwise.[163,164] The relationships are not simple, but we can note that θ is usually of the order of the nearest neighbour (J_{NN}) perhaps next-nearest-neighbour (J_{NNN}) exchange integrals, according to the symmetry.

Detailed description of magnetic behaviour of magnetically concentrated substances in the paramagnetic region is difficult, and rarely proceeds beyond the so-called *mean-field model*, in which each paramagnetic atom is treated as being subject to an average magnetic field generated by the presence of all the other paramagnetic atoms in the crystal. This average field is called the Weiss field. In its simpler forms, relating to lower magnetic fields and temperatures well above the ordering temperature, the mean-field model leads to the Curie–Weiss law, and a linear relationship between θ and J_{ij}.

6.6.1.3 High magnetic fields[158,164]

The linearity of I in equation (52) with H, which gives χ as constant in the case of paramagnetics, only holds so long as the orienting effects of the magnetic field on the atomic dipoles is very much less than the disordering effects of temperature. If the magnetic field is strong enough, or the temperature low enough, χ becomes field dependent. The relationship $g\beta H \gg kT$ is necessary for linearity in equation (52), where β is the Bohr magneton and k the Boltzmann constant; g is a number defined in Figure 27. If magnetic exchange is present its orienting effects must also be considered. For $g = 2$, a common situation, and $H = 1$ T, $g\beta H \equiv 1.44$ K.

For an ideal paramagnet which obeys the Curie law at low magnetic field strengths the solution of the problem at $g\beta H \approx kT$ is available in closed form. It is convenient to formulate the situation in terms of the *magnetization*, $M = \chi_m H$, rather than of χ. Then

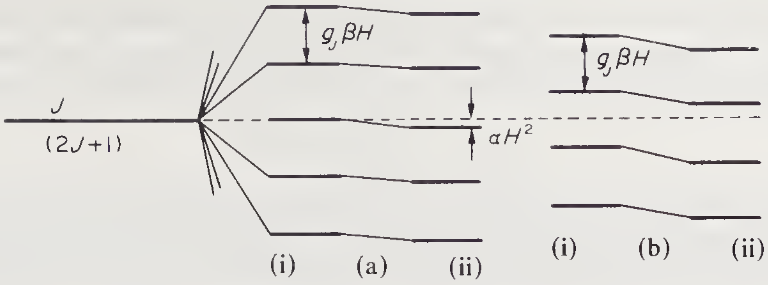

Figure 27 Splitting of a free-ion state into $2J+1$ components by a magnetic field (a) for J even, (b) for J odd: (i) for the first-order Zeeman effect; (ii) including the second-order Zeeman effect

$$\begin{aligned} M &= g\beta S B(S,a) \\ &= g\beta S\left[\frac{2S+1}{2S}\coth\left(\frac{2S+1}{2S}a\right) + \frac{1}{2S}\coth\left(\frac{a}{2S}\right)\right] \end{aligned} \tag{57}$$

with S the spin quantum number from the paramagnetic atom, $a = g\beta SH/kT$ and $B(S,a)$ is the Brillouin function.[165]

In the presence of magnetic exchange a treatment by the mean-field method gives an implicit expression similar to equation (57):

$$M = g\beta SB\left(S, a + \frac{2S\sum J_{ij}}{Ng\beta kT}M\right) \tag{58}$$

where $\sum J_{ij}$ is the sum of the exchange integrals for the system. If the system has ferromagnetic exchange its effect is to increase the field-strength dependence of the susceptibility, while antiferromagnetic exchange tends to make it more constant with field change.

6.6.1.4 Quantities for chemical applications[158]

The measurement χ or χ_m, or perhaps M, is the one usually carried out. For chemical applications it is usual to relate these to more relevant quantities. *The molar susceptibility*, χ_M, is

$$\chi_M = \chi(MV) = \chi_m(MW)$$

where MV and MW are the molecular volume and mass respectively. Further, in most applications only the paramagnetism of a single atom amongst many diamagnetic atoms is of interest. A correction for the diamagnetism of other atoms is made to give the atomic paramagnetism of the transition metal, lanthanoid or actinoid atom:

$$\chi_A = \chi_M - \sum_{i = \text{other atoms}}^{\text{molecule}} \chi_{A_i} \tag{59}$$

where χ_{A_i} is the atomic diamagnetism, including covalent bonding contributions, of the ligands and counterions, if present.

Atomic diamagnetic susceptibilities are of the order of $2 \times 10^{-10}\ \text{m}^3\ \text{mol}^{-1}$; atomic paramagnetic susceptibilities, at ambient temperature, range up to $3 \times 10^{-7}\ \text{m}^3\ \text{mol}^{-1}$. A list of some diamagnetic susceptibilities for common atoms and ions is given, for example, in references 166 and 167.

It is convenient for many purposes to have a quantity which summarizes magnetic properties and which is, ideally at least, independent of temperature. We define the 'magnetic moment', in units of the Bohr magneton:

$$\begin{aligned} \mu_{\text{eff}} &= \left(\frac{3k}{N\beta^2}\right)^{1/2}(\chi_A T)^{1/2} \\ &= 797.5(\chi_A T)^{1/2} \end{aligned} \tag{60}$$

If the Curie law is obeyed, μ_{eff} is not dependent on the temperature. If χ_A is expressed in c.g.s. units the number in equation (59) is 2.84 rather than 797.5.

Mostly, of course, the Curie law is not obeyed accurately. A form of equation (56) is usually sufficient to describe magnetic behaviour except at the lowest of temperatures or if the magnetic exchange is strong:

$$\chi_A = \frac{C}{T-\theta} + \chi_A(TIP) \tag{61}$$

In such a case μ_{eff} does depend upon temperature although the change is small unless θ is large, usually indicating strong magnetic exchange, or $\chi_A(TIP)$ is large, a rare situation. If it is known that θ arises mainly from magnetic exchange it may be useful to derive, ignoring the $\chi_A(TIP)$:

$$\mu'_{\text{eff}} = 797.5\,[\chi_A(T-\theta)]^{1/2} \tag{62}$$

which will be less dependent on temperature and may be properly related to the value of μ_{eff} for the system in the absence of magnetic exchange. However, if θ arises from causes other than magnetic exchange, this procedure will be misleading and will obscure important facets of magnetic behaviour.[2]

6.6.2 Magnetic Properties of Atomic Systems

6.6.2.1 The Van Vleck equation[2,28,160,168]

The ground term of a free atom or ion is $(2L + 1)(2S + 1)$-fold degenerate. This degeneracy is lifted in various ways, including by the action of spin–orbit coupling (Section 6.3.3) and ligand fields (Section 6.4). The energy corresponding to each component of the term is also a function of the applied magnetic field. If we write for the ith wave function of the atom

$$W_i = W_i^{0} + W_i^{\text{I}} H + W_i^{\text{II}} H^2 + \cdots \tag{63}$$

it can be shown that for laboratory scale fields terms after $W^{\text{II}}H^2$ are negligibly small, and further that $W_i^{\text{I}}H$ and $W_i^{\text{II}}H^2$ are $\ll kT$ in magnitude except at very low temperatures. Then the average energy for the atom is obtained as the partition function

$$\bar{W} = \sum_i W_i \exp(W_i/kT) \Big/ \sum_i \exp(W_i/kT) \tag{64}$$

The 'magnetic moment' $\langle\mu\rangle$ in equation (53) for a state i may be identified with the matrix element $\langle\psi_i|L_j + 2S_j|\psi_i\rangle$, where $j = x$, y or z. With the use of equation (53) and the simplification of the exponentials because $W_i^{\text{I}}/kT \ll 1$ and $W_i^{\text{II}}/kT \ll 1$, neglecting diamagnetism and multiplying by Avogadro's number, the result

$$\chi_A = N \sum_i [W_i^{\text{I}^2}/kT - 2W_i^{\text{II}}] \exp(W^0/kT) \Big/ \sum_i \exp(W^0/kT) \tag{65}$$

is obtained. This is the Van Vleck equation and is the basis of the calculation of the magnetic properties of atomic systems in ordinary circumstances.

The first- and second-order Zeeman effect coefficients in the expansion of equation (62) are defined by the quantum numbers which specify the atomic energy level. They are in general a function of the direction of the magnetic field with respect to the axis of quantization of the wave functions. They are obtained by the use of the *magnetic moment operator* for the appropriate direction, $q = x, y$ or z:

$$W_i^{\text{I}}(q) = \langle\psi_i|\boldsymbol{L}_q + 2\boldsymbol{S}_q|\psi_i\rangle\beta$$
$$W_i^{\text{II}}(q) = \sum_j [\langle\psi_i|\boldsymbol{L}_q + 2\boldsymbol{S}_q|\psi_j\rangle^2\beta^2/(W_i^0 - W_j^0)] \tag{66}$$

Of course, χ_A is correspondingly also a function of the direction of the magnetic field.

Most usually, the atomic wave functions are specified by the quantum number set L, M_L, S, M_S and are thus eigenfunctions of $\boldsymbol{L}_z$ and $\boldsymbol{S}_z$, making the evaluation of the matrix elements and then of the susceptibility in that direction facile.

6.6.2.2 Free-atom states and terms[2,28,168]

If a free-atom state (Section 6.3.3) is subject to a magnetic field the $(2J + 1)$-fold degeneracy is lifted so that, as shown in Figure 27, each level specified by the quantum number M_J is separated from its neighbour by the amount $g_J\beta H$, where g_J is the *spectroscopic splitting factor*. The value of g can be calculated from a knowledge of the term from which the state arose.

$$g_J = 1 + [S(S+1) - L(L+1) + J(J+1)]\,/\,2J(J+1) \tag{67}$$

Note that if $L = 0$ in equation (67) then $J = S$ and $g = 2$, the 'spin-only-value'. The energy pattern of Figure 27 is linear in H: there is no second-order Zeeman effect unless other states are considered. Application of equation (64) to this system is fairly straightforward since it yields

$$\chi_A = \frac{N\beta^2}{3kT} g_J^{\,2} J(J+1) \tag{68}$$

and hence

$$\mu_{\text{eff}} = g_J[J(J+1)]^{½} \tag{69}$$

Equations (68) and (69) apply quite well to the majority of the lanthanoid element compounds, where the approximation to an isolated ground state is good. Table 7 exemplifies this.

Table 7 The Magnetic Properties of Some Lanthanoid Element Compounds

No. of f *electrons*	*Ground state*	*Ion*	*Compound*	$\mu_{eff}^{300\,K}$ *(expt)*	$g[J(J+1)]^{½}$
1	$^2F_{2½}$	Ce^{3+}	$Ce_2Mg_3(NO_3)_6{\cdot}24H_2O$	2.28 BM	2.54 BM
2	$^3H_4$	Pr^{3+}	$Pr_2(SO_4)_3{\cdot}8H_2O$	3.40	3.58
3	$^4I_{4½}$	Nd^{3+}	$Nd_2(SO_4)_3{\cdot}8H_2O$	3.50	3.62
4	$^5I_4$	Pm^{3+}			
5	$^6H_{2½}$	Sm^{3+}	$Sm_2(SO_4)_3{\cdot}8H_2O$	1.58	1.6[a]
6	$^7F_0$	Eu^{3+}	$Eu_2(SO_4)_3{\cdot}8H_2O$	3.42	3.61[a]
		Sm^{2+}	$SmBr_2$	3.57	3.61[a]
7	$^8S_{3½}$	Gd^{3+}	$Gd_2(SO_4)_3{\cdot}8H_2O$	7.91	7.94
		Eu^{2+}	$EuCl_2$	7.91	7.94
8	$^7F_6$	Tb^{3+}	$Tb_2(SO_4)_3{\cdot}8H_2O$	9.50	9.72
9	$^6J_{7½}$	Dy^{3+}	$Dy_2(SO_4)_3{\cdot}8H_2O$	10.4	10.63
10	$^5I_8$	Ho^{3+}	$Ho_2(SO_4)_3{\cdot}8H_2O$	10.4	10.60
11	$^4I_{7½}$	Er^{3+}	$Er_2(SO_4)_3{\cdot}8H_2O$	9.4	9.57
12	$^3H_6$	Tm^{3+}	$Tm_2(SO_4)_3{\cdot}8H_2O$	7.1	7.63
13	$^2F_{3½}$	Yb^{3+}	$Yb_2(SO_4)_3{\cdot}8H_2O$	4.86	4.50

[a] These values are not $g_J[J(J+1)]^{½}$; they are values calculated as outlined in Section 6.6.2.2.

If $L = 0$ then equations (68) and (69) reduce to the spin-only expressions $\chi_A = 4(N\beta^2/3kT)S(S+1)$ and $\mu_{\text{eff}} = 2[S(S+1)]^{½}$, but it is more useful to regard these as special cases of equations (70) and (71) where g is close to, but not necessarily equal to, the spin-only value.

$$\chi_A = \frac{N\beta^2}{3kT} g^2 S(S+1) \tag{70}$$

$$\mu_{\text{eff}} = g[S(S+1)]^{½} \tag{71}$$

For a state showing only the first-order Zeeman effect the magnetization as a function of field strength is given by the Brillouin function (equation 57).

For two of the lanthanoid M^{3+} ions, equations (68) and (69) do not hold. They are Eu^{3+}, $f^6(^7F_0)$, and Sm^{3+}, $f^5(^6H_{2½})$, where another state lies fairly close above the ground state which then cannot be considered in isolation. For the $^7F_0$ state, $J = 0$ and χ_{Eu} and μ_{eff} are predicted to be zero. In fact, $\chi_{Eu} \approx 100\ \text{mm}^3\ \text{mol}^{-1}$ independent of temperature. This effect arises because the $^7F_1$ state, a few hundred cm^{-1} higher, interacts with the ground state to give substantial second-order Zeeman effect terms $W_i^{\text{II}}H^2$ in equations (64) and (65) and, as there is no first-order term and the higher state lies $\ll kT$, it is seen that equation (64) tends to a temperature independent susceptibility. For Sm^{3+} the position is more complicated as the ground $^6H_{2½}$ state has a first-order Zeeman term as well as a second-order one from the $^6H_{3½}$ state a few hundred cm^{-1} higher. Here, for temperatures such that the $^6H_{3½}$ state lies $\ll kT$,

$$\chi_{Sm} = \frac{N\beta^2}{3kT} g_{3½}^2\,\frac{5}{2}\,\frac{7}{2} + N\alpha$$

where $N\alpha$ is a temperature independent paramagnetic term (TIP). This is a specialized form of equation (72), which has some general applicability:

$$\chi_A = \frac{N\beta^2}{3kT} g^2 S(S+1) + N\alpha \tag{72}$$

and is a form of equation (56) with $C = N\beta^2 g^2 S(S+1)/3kT$ and $\theta = 0$.

Although there is no ion for which spin–orbit coupling is so small that all states of the ground term lie $\ll kT$ above the ground state, it is instructive to develop the expression for such a condition. The application of equation (65) gives

$$\mu_{\text{eff}} = [4S(S+1) + L(L+1)]^{½}$$

putting $L = 0$ which gives the spin-only result of equation (71) again.

For state separations of the order of kT the first- and second-order Zeeman effect coefficients for equation (65) are both important and the exponents vary with temperature; there results complicated expressions for the magnetic behaviour for which a general expression has been developed.[2,28]

6.6.2.3 *Zero-field splitting (ZFS)*

Spin-orbit coupling in second order (Section 6.4.4.6) raises the degeneracy of orbitally non-degenerate ground terms by amounts of up to a few cm^{-1}, occasionally more. For temperatures of the order of D and E, the magnetic susceptibility is a complicated function of temperature and varies strongly with direction, as the various levels for equation (65) become occupied to different extents.[169] At temperatures much smaller than D and E, the susceptibility usually becomes independent of temperature but highly dependent on direction.

At temperatures much higher than D, the susceptibility becomes much more isotropic and the average may approximate well to the Curie law, or more generally to the relationship of equation (57) with θ small. However, anisotropy usually remains, and the susceptibilities in individual directions are of the form of equation (57) but θ is of the order of, and linearly related to, D. For the ${}^4A_{2g}$ ground term, in axial symmetry where E is zero, we have the parallel direction defined as Z and obtain $\theta_{\parallel} = -4D/5k$ and $\theta_{\perp} = 2D/5k$.

6.6.3 Quenching of Orbital Angular Momentum[2,28,168]

When a free ion is subject to a ligand field there is generally a restriction of the number of orbitals of the same energy available to an electron without changing its spin. For example, the single electron of d^1 in the free ion can occupy any of the five d-orbitals of a transition metal, but in the presence of an octahedral ligand field has only the planes of three of the t_{2g} set available. This restriction manifests itself as a reduction in the orbital angular momentum associated with the system. In place of $L = 2$ for a free ion d-electron it can have an effective angular momentum $L' = 1$ in a $t_{2(g)}$ orbital set, and none in an $e_{(g)}$ set ($L' = 0$). The orbital angular momentum is said to be quenched by the ligand field. For a filled or half-filled $t_{2(g)}$ subshell the net value of L is zero, just as it is for d^{10} or d^5 in the free ion.

Using the above arguments it is possible to derive for what strong-field configurations orbital angular momentum is partially or, nominally at any rate, fully quenched. The results are set out in Table 8, assuming cubic symmetry. As a generalization, it is seen that orbital angular momentum is quenched ($L = 0$) for transition metal ions giving A or E ground terms, and partially quenched ($L = 1$) for those giving T ground terms.

Table 8 Strong-field d^n Configurations and Corresponding Terms for which Orbital Angular Momentum should be Quenched, Assuming Cubic Stereochemistry

No. d-*electrons*	*1*	*2*	*3*	*4*	*5*	*6*		*7*		*8*	*9*
Stereochemistry	tet	tet	oct	oct	oct/tet	tet	oct	tet	oct	oct	oct
Strong-field configuration	e^1	e^2	$t_{2g}{}^3$	$t_{2g}{}^3e_g{}^1$	$t_{2(g)}{}^3e_{(g)}{}^2$	$e^3t_2{}^3$	$t_{2g}{}^6$	$e^4t_2{}^3$	$t_{2g}{}^6e_g{}^1$	$t_{2g}{}^6e_g{}^2$	$t_{2g}{}^6e_g{}^3$
Ground term	${}^2E$	${}^3A_2$	${}^4A_{2g}$	${}^5E_g$	${}^6A_{1(g)}$	${}^5E$	${}^1A_{1g}$	${}^4A_2$	${}^2E_g$	${}^3A_{2g}$	${}^2E_g$
$\mu_{\text{eff}}{}^{\text{SO}}$ (BM)	1.73	2.83	3.87	4.90	5.92	4.90	0.0	3.87	1.73	2.83	1.73

In practice, because of spin–orbit coupling, the quenching is not as complete as indicated by Table 8. Spin–orbit coupling acts to mix in higher configurations with orbital angular momentum into the ground term. The effect takes two different forms according to the type of ground term. For the $A_{2(g)}$ and $E_{(g)}$ ground terms, L remains zero but the g-value is changed from the spin-only value by an amount which decreases with increasing ligand field magnitude as follows:

$$\begin{aligned} A_{2(g)} \quad & g = 2(1 - 4\lambda/\Delta) \\ E_{(g)} \quad & g = 2(1 - 2\lambda/\Delta) \end{aligned} \tag{73}$$

For $A_{1(g)}$ ground terms, which arise only from d^5, g remains at 2.00 as there is no higher term of the same multiplicity.

The spin-orbit coupling mixing of $T_{1(g)}$ terms acts to increase the effective value of L, L', from 1 to as much as 1.5, depending on the relationship between the magnitudes of the ligand field and of the interelectronic repulsions. The relationship is conveniently taken from equation (41). The quantity A defined in equation (43) is required. In the present application, A has the meaning that, for example

$$\left\langle \psi_{T_{1(g)}} \middle| L_z \middle| \psi_{T_{1(g)}} \right\rangle \quad = \quad A \ \ (h/2\pi \text{ units})$$

$A = 1$ in the strong ligand field limit, 1.5 in the weak field case. For $T_{2(g)}$ terms, L' remains at unity.

For the lanthanoid elements, ligand field splittings are so small that quenching of orbital angular momentum is not important. This probability also applies in the actinoid elements.

6.6.4 Magnetic Properties of Cubic Field Systems[2,68,168]

6.6.4.1 A *and* E *ground terms*

As well as changing the g-value, spin–orbit coupling mixing introduces a component in the susceptibility, due to the higher-lying terms, which is independent of temperature. The amount of this contribution again decreases with increasing ligand field magnitude. The net result for the two types of term is, if $\lambda/\Delta \ll 1$

$$\begin{aligned} A_{2(g)}: \chi_{\mathrm{A}} &= \frac{4N\beta^2}{3kT}\left(1-\frac{8\lambda}{\Delta}\right)S(S+1)+\frac{8N\beta^2\boldsymbol{k}^2}{\Delta} \\ E_{(g)}: \chi_{\mathrm{A}} &= \frac{4N\beta^2}{3kT}\left(1-\frac{4\lambda}{\Delta}\right)S(S+1)+\frac{4N\beta^2\boldsymbol{k}^2}{\Delta} \end{aligned} \tag{74}$$

Here, the factor $\boldsymbol{k}$ has been introduced to accommodate the fact that $\boldsymbol{L}$ is an effective operator in the ligand field model, and in the same sense λ for use in these equations may not have a direct relationship to its use in the interpretation of spectra, say; $\boldsymbol{k}$ is generally expected to be somewhat less than unity. There is no similar TIP contribution for $A_{1(g)}$ ground terms as there is no higher-lying term of the same multiplicity.

The TIP terms in equation (73) are often fairly small compared with the Curie law component, and to the extent that they may be neglected

$$\mu_{\mathrm{eff}} \quad = \quad g[S(S+1)] \quad = \quad g\mu_{\mathrm{eff}}{}^{\mathrm{SO}} \tag{75}$$

with g defined in equation (73), and $\mu_{\mathrm{eff}}{}^{\mathrm{SO}}$ the 'spin-only' magnetic moment.

The ${}^6A_{1g}$ ground term of d^5 is notable for the simplicity of its behaviour; $g = 2.00$ and no TIP; equation (75) holds with $S = 2\frac{1}{2}$.

6.6.4.2 T *ground terms*

For $T_{1(g)}$ and $T_{2(g)}$ ground terms the residual orbital angular momentum allows that spin–orbit coupling split them into states. For the transition metals, spin–orbit coupling constants are of the order of kT at ambient temperature, so that the states may all be thermally occupied and second-order Zeeman effect contributions between them substantial. The susceptibilities to be expected are thus complicated functions of temperature, and with them the effective magnetic moments, μ_{eff}. Expressions which give μ_{eff} as a function of the parameter kT/λ have been developed for all the $T_{1(g)}$ and $T_{2(g)}$ ground terms which arise from d^n configurations. The formulation of these expressions is facilitated by noting that there is a formal relationship between a $t_{2(g)}{}^n$ and a free-ion p^{6-n} configuration which allows the calculation to be made using the well developed free-ion formalism.[62] It is found to be necessary to introduce the effective nature of the orbital angular momentum operator, $\boldsymbol{L}$, by means of the separate parameter, $\boldsymbol{k}$, having the same significance as for A and E terms.

The magnetic moments calculated for the various T ground terms are given in Table 9 as a function of the parameter kT/λ with $\boldsymbol{k}=1$ and $\boldsymbol{k}=0.7$. For the $T_{1(g)}$ terms only the extremes of ligand field strength, $A = 1$ (strong) and $A = 1.5$ (weak), are listed. Roughly, a linear interpolation between these extremes may be made.

6.6.4.3 Lanthanoids and actinoids[83,85,92,93]

The effects of ligand field splittings on the magnetic properties of lanthanoid complexes is minor except at quite low temperatures. The splitting patterns for the various ground states are available but as they depend on the relationship between the fourth- and sixth-order crystal field parameters the development of generally applicable formulae has not proceeded. Some generalizations from these patterns may be available, for example when a non-degenerate (Γ_1) level lies lowest the susceptibility will be of the TIP type at low temperatures, while if a degenerate level is lowest with others a good deal higher, approximation to Curie law behaviour should follow. However, the magnitudes of the TIP or Curie constant need to be evaluated for each system as a function of λ and the crystal field parameters.

Table 9 μ_{eff} Calculated for Cubic-field T Ground Terms as a Function of Temperature[a]

		λ (kJ mol^{-1})															
Term	k	*A*	*0.1*	*0.2*	*0.3*	*0.5*	*0.75*	*1.0*	*1.5*	*2.0*	*−0.1*	*−0.2*	*−0.3*	*−0.5*	*−0.75*	*−1.0*	*−1.5*	*−2.0*
$^2T_{2(g)}$	1.0	—	0.63	0.90	1.10	1.39	1.62	1.76	1.92	2.00	1.95	2.14	2.31	2.49	2.54	2.52	2.47	2.43
	0.7	—	0.69	0.89	1.06	1.30	1.50	1.61	1.75	1.80	1.60	1.79	1.95	2.13	2.21	2.20	2.18	2.14
$^5T_{2(g)}$	1.0	—	3.52	3.58	3.63	3.74	3.87	4.00	4.21	4.38	5.08	5.22	5.34	5.54	5.67	5.72	5.70	5.64
	0.7	—	3.85	3.90	3.94	4.02	4.12	4.21	4.36	4.48	4.85	4.96	5.07	5.24	5.36	5.41	5.42	5.38
$^3T_{1(g)}$	1.0	1.5	0.89	1.09	1.27	1.56	1.85	2.09	2.44	2.68	1.83	2.55	3.10	3.74	4.05	4.16	4.17	4.11
		1.0	1.40	1.55	1.69	1.93	2.17	2.35	2.59	2.72	1.90	2.66	3.11	3.49	3.61	3.62	3.56	3.50
	0.6	1.5	1.45	1.54	1.63	1.79	1.97	2.13	2.36	2.52	1.50	2.12	2.57	3.11	3.38	3.48	3.52	3.49
		1.0	1.81	1.90	1.99	2.15	2.30	2.42	2.58	2.67	1.65	2.30	2.71	3.06	3.18	3.21	3.19	3.16
$^4T_{1(g)}$	1.0	1.5	1.88	1.98	2.08	2.26	2.47	2.66	2.98	3.24	3.99	4.21	4.42	4.75	5.03	5.16	5.21	5.18
		1.0	2.46	2.54	2.63	2.79	2.97	3.12	3.36	3.52	3.74	4.00	4.22	4.49	4.64	4.68	4.65	4.58
	0.6	1.5	2.54	2.59	2.64	2.74	2.86	2.97	3.16	3.32	3.58	3.75	3.92	4.18	4.40	4.51	4.57	4.56
		1.0	2.90	2.95	3.01	3.11	3.23	3.33	3.48	3.59	3.46	3.67	3.85	4.09	4.22	4.27	4.27	4.24

[a] See text for definition of k, A and λ. The terms arise from the strong-field configurations:
$t_{2g}{}^1$, $t_{2g}{}^5$, $e^4t_2{}^5 \rightarrow {}^2T_{2(g)}$
$t_{2g}{}^2$, $t_{2g}{}^4$, $e^4t_2{}^4 \rightarrow {}^3T_{1(g)}$
$t_{2g}{}^4e_g{}^2$, $e^2t_2{}^2 \rightarrow {}^5T_{2(g)}$
$t_{2g}{}^5e_g{}^2$, $e^2t_2 \rightarrow {}^4T_{1(g)}$

For the actinoid elements, ligand field splittings and spin–orbit coupling are both a good deal larger than for the lanthanoids. The effects of the splittings on the magnetic behaviour become evident at higher temperatures, but the remarks about the lack of generality of treatment hold equally well.

6.6.5 Magnetic Properties in Lower Symmetry[168–175]

6.6.5.1 Introduction

As with spectra, the derivation of magnetic behaviour in low-symmetry complexes in detail is a complicated matter, which needs to be treated on an individual basis. Only some general features will be outlined here. The problem can be divided into two categories: firstly, small departures from cubic symmetry and, secondly, truly low-symmetry complexes, such as those of square planar stereochemistry.

6.6.5.2 Near cubic symmetry: A *and* E *terms*

In symmetry lower than cubic, E ground terms are likely to be split to give an orbitally non-degenerate ground term. Also the excited terms which are mixed by spin–orbit coupling into the ground term are split, and their components contribute differently to the ground term because of differing energy separations. The g values of equation (73) become functions of direction. The position is further complicated because, except for the orbitally non-degenerate $S=\frac{1}{2}$ case (Kramers doublet), spin–orbit coupling in second order raises the spin degeneracy of the ground term — the zero field splitting (ZFS). The situation is set out in Figure 28 for the ^5E_g ground term of d^4.

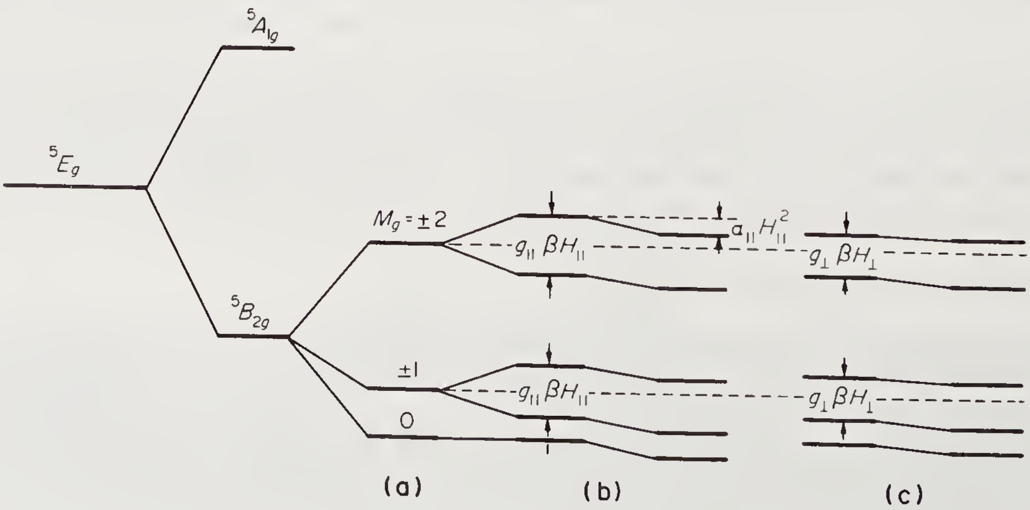

Figure 28 Splitting of the ground term arising from ^5E_g with a tetragonal ligand field component, showing the effects of (a) the zero-field splitting, and a magnetic field (b) parallel to the tetragonal axis, or (c) perpendicular to that axis

The general results of low symmetry on A and E term magnetic susceptibilities can, in the light of the previous paragraph, be summarized as follows. At higher temperatures the susceptibility is of the form of equation (74) and slightly anisotropic. Restricting consideration to axial distortion from cubic symmetry, those equations become

$$A_{2(g)} \quad : \quad \chi_{\mathrm{A}_{\parallel,\perp}} = \frac{4N\beta^2}{3kT}\left(1-\frac{8\lambda}{\Delta_{\parallel,\perp}}\right)S(S+1)+\frac{8N\beta^2k^2}{\Delta_{\parallel,\perp}} \tag{76a}$$

$E_{(g)}$: B component lowest:

$$\chi_{\mathrm{A}_{\parallel,\perp}} = \frac{4N\beta^2}{3kT}\left(1-\frac{4\lambda}{\Delta_{\parallel,\perp}}\right)+\frac{4N\beta^2k^2}{\Delta_{\parallel,\perp}} \tag{76b}$$

A component lowest:

$$\chi_{\mathrm{A}_{\parallel,\perp}} = \frac{4N\beta^2}{3kT}\left(1-\left(\frac{0.6}{\Delta_{\parallel,\perp}}\right)\lambda\right)+\frac{4N\beta^2}{\Delta_{\parallel,\perp}} \tag{76c}$$

At low temperatures the effects of the ZFS become of dominating importance, and the susceptibility consequently highly anisotropic and temperature dependent.

In principle, it is possible to relate the excited term splittings Δ_e, the ground term splitting Δ_g, and to express the ZFS value of D in terms of Δ and Δ_e. For example, for tetragonal symmetry one can deduce $\Delta_e = 3\Delta_g/4$ and $D = 4\lambda^2(\Delta_\perp^{-1} - \Delta_\parallel^{-1})$, where $\Delta_\perp = \Delta + \frac{1}{2}\Delta_g - \frac{1}{3}\Delta_e$ and $\Delta_\parallel = \Delta + \frac{1}{2}\Delta_g + \frac{2}{3}\Delta_e$. However, in practice, as is known from spectral studies, these relationships do not hold well, particularly for the calculation of D, to which many excited terms including those of different multiplicity contribute. To evaluate D with any accuracy from the ligand field parameters it appears to be necessary to use the entire relevant d^n manifold.[89,90]

6.6.5.3 *Near cubic symmetry:* T *terms*

The calculation of the magnetic properties which arise when the degeneracy of a T ground term is lifted simultaneously by spin–orbit coupling and a low-symmetry ligand field component is of some complexity. The calculations have been carried out for all the T terms arising from $t_{2(g)}{}^n e_{(g)}{}^m$ configurations assuming axial symmetry, and the results compiled as tables of μ_{eff} corresponding to the parameters kT/λ, Δ_T/λ, k and, where applicable, A; Δ_T is the splitting of the T term by the axial ligand field component, which is restricted to be a good deal less than Δ.

The fitting of μ_{eff} *versus* T magnetic data to these tabulations to obtain values of the parameters Δ_T, λ and k may be a rather tedious process. It may be helped by using some form of least-squares process. In many cases the variation of μ_{eff} with one or more of the parameters is small, so that that parameter is ill-defined or there is strong correlation between pairs. If data on the anisotropy of the susceptibility corresponding to T ground terms is available, the magnetic moment corresponding to the different directions may be fitted to calculations of the same type as those listed for the average. This usually allows much better definition of the parameters and the breaking of correlations between them. If available, g-values from the ESR experiment can be used to help fix parameter values. However, the procedures involved lie outside the scope of this article.

6.6.5.4 *The orbital-reduction parameter,* k[45,46]

The effective reduction of orbital angular momentum introduced by using, for example, the operator kL_z in place of L_z in the magnetic moment operator kL_z+2S_z, or the spin-orbit coupling operator $k\lambda L_zS_z$, for the z-direction was first associated with the concept of d-electron delocalization away from the central metal atom on to the ligands. However, its significance is more complex and less clearly defined than that. It may include the effects of delocalization around ligand ring systems and of configuration interaction on the central atom. In many applications it has little more significance than as a 'fudge factor' which allows the fitting of magnetic data to theories of magnetic behaviour using other parameters.

In connection with the Jahn–Teller effect the role of k may be well defined. It has been shown that if a dynamic Jahn–Teller effect is operative, very substantial quenching of orbital angular momentum may take place — the Ham effect. In the case of T ground terms, if the dynamic Jahn-Teller frequencies bear the right relationship to spin-orbit coupling and temperature, k may be reduced to values well below 0.5.[113–119]

6.6.5.5 Low-symmetry stereochemistry

In complexes of stereochemistry far removed from cubic, the *d*-orbital splittings are expected to be large and to remove most if not all of their degeneracy. Spin pairing results, with cases of $S > \frac{1}{2}$ rare. In such a case the general prediction may be made that the susceptibility will be of the type set out in equation (76) but with $\Delta_{\parallel}$ and $\Delta_{\perp}$ defined in terms of the *d*-orbital splitting pattern and not necessarily related to a cubic-field Δ, and replaced by Δ_1, Δ_2 and Δ_3, say, if the symmetry is less than axial. $\Delta_{\parallel}$ and $\Delta_{\perp}$, for example, might be quite different in magnitude so that considerable anisotropy may arise. Zero-field splitting may become quite large — many cm^{-1} — so that its effects are manifest in more complicated directional and temperature dependence of the susceptibility at higher temperatures than for cubic or near-cubic cases. Apart from these generalizations, however, each situation is likely to require individual consideration.

There are exceptions to the above generalizations. In particular, in a number of square-planar complexes it seems that the *d*-orbital splitting pattern is such that d_{xz}, d_{yz} and d_{z^2} remain quite close in energy. Here the spin-pairing is often only partial. In the case of Co^{II} it seems that the near-degeneracy is especially marked, and some of the features of the presence of orbital angular momentum develop, as demonstrated by departure from spin-only behaviour and by high magnetic anisotropy.[156,174]

6.6.6 Spin Pairing

6.6.6.1 Low-spin complexes

For the configurations d^4 to d^7, if a cubic ligand field is sufficiently large relative to interelectronic repulsions it forces the occupation of one type of *d*-orbital to the exclusion of the other. Since no tetrahedral ligand field is of sufficient magnitude to be relevant, we deal with octahedral complexes only. The t_{2g} orbital set is occupied in preference to the e_g set. The relative strength of the ligand field can be assessed, at least approximately (*i.e.* for fixed C/B), by reference to Figures 11–15. The results are summarized in Table 10 where, for simplicity, the high-spin state is described by a strong-field configuration, although a mixture may be more properly required.

Table 10a High- and Low-spin Complexes in Octahedral Stereochemistry, Giving the Approximate Value of Dq/B for Spin Equilibrium

	High-spin		*Low-spin*		Dq/B
d^4	$t_{2g}{}^3e_g{}^1$	^5E_g	$t_{2g}{}^4$	$^3T_{1g}$	2.7
d^5	$t_{2g}{}^3e_g{}^2$	$^6A_{1g}$	$t_{2g}{}^5$	$^2T_{2g}$	2.8
d^6	$t_{2g}{}^4e_g{}^2$	$^5T_{2g}$	$t_{2g}{}^6$	$^1A_{1g}$	2.0
d^7	$t_{2g}{}^5e_g{}^2$	$^4T_{1g}$	$t_{2g}{}^6e_g{}^1$	^2E_g	2.2

Table 10b Spin-pairing Energies (Π) and Spin-crossover Ligand Field Strengths $(Dq/B)^*$ for d^n Configurations[a]

	d^2	d^3	d^4	d^5	d^6	d^7	d^8
$\overline{S(S+1)}$	4/3	7/4	2	25/12	2	7/4	4/3
$(Dq/B)^*$	—	—	2.7	2.8	2.0	2.2	—

[a] $\Pi = \alpha[\overline{S(S+1)} - S(S+1)]B$; $(Dq/B)^*$ is evaluated for $C/B \approx 4.5$ when $\alpha \approx 7$.[38]

In symmetry lower than cubic a number of possibilities for spin-pairing arise. These can mostly be categorized as giving $S = 0$ for even *d*-electron systems and $S = \frac{1}{2}$ for odd *d*-electron systems, provided the *d*-orbital splitting is large and degeneracy does not remain. However, if degeneracy remains, as it does in particular for square-planar complexes in the e (d_{xz}, d_{yz}) set, intermediate degrees of spin-pairing arise if the relationship between the *d*-orbital splittings and the interelectronic repulsions is suitable. The conditions can be obtained from the diagram of the energy levels of d configurations given as functions of the crystal field parameters Dq, Ds and Dt.[176] Of particular interest are the cases of d^5 and d^6 where terms respectively with $S = 1\frac{1}{2}$ and $S = 1$ arise.

Most generally, the orbital angular momentum is further quenched by the lowering of the symmetry from cubic and the consequent greater differentiation between *d*-orbitals. Then the magnetic susceptibility is likely to be of the type of equation (76), with the riders outlined in Section 6.6.5.5. However, accidental near-degeneracy of the *d*-orbitals can arise with consequent restoration of orbital angular momentum and magnetic behaviour, which must be investigated on an individual basis.[177]

6.6.6.2 *Spin equilibria*[178–180]

If the relationship between the ligand field splittings and the interelectronic repulsions is of the critical value then the energy of the term of lower spin may be the same as that of the higher spin.[177–179] Provided the equality is met within a few times the thermal energy available to the system, the energy levels corresponding to both terms will be occupied and the magnetic properties will contain contributions from each. In the simplest case of two states specified by S_1 and S_2 and separated by an energy ΔE_S one may write as a first approximation

$$\chi_A = \frac{(2S_1+1)\chi_A(S_1)+(2S_2+1)\chi_A(S_2)\exp(-\Delta E_S/kT)}{(2S_1+1)+(2S_2+1)\exp(-\Delta E_S/kT)} \tag{77}$$

However, each term may in fact cover a range of energies, corresponding to spin–orbit coupling, low-symmetry ligand field splitting and vibrational coupling, so that expressions a good deal more complex than equation (77) are required in practical situations.

Further, the two spin states may not be independent. They may be coupled through the lattice, in that the occupation of the low-spin configuration usually corresponds to shorter metal–ligand bond lengths. Coupling of this type can result in cooperative phenomena, in which the occupation factors for the terms involved may change sharply with temperature rather than smoothly as required by thermal equilibrium. Again, the two terms may be connected by a matrix element of the spin–orbit coupling operator. Then, as they approach equality in energy, the concept of individual spin quantum numbers is no longer valid and the system is said to be in a mixed-spin state.[183] The consideration of the magnetic behaviour of equilibrium systems in detail is a matter for individual attention, and cannot be elaborated further here.

6.6.7 Magnetic Exchange[28,158–160,169]

6.6.7.1 *The exchange Hamiltonian*

Some of the phenomenological aspects of magnetic exchange have been mentioned in Sections 6.6.1.2/3. At the atomic level it is usually introduced by adding a term to the Hamiltonian for the ith atom

$$H_{ex} = -2\sum_J J_{ij} S_i S_j \tag{78}$$

where the summation j is over all other paramagnetic atoms, but in practice can be limited to those nearest or next-nearest to atom i. In high site-symmetry situations J_{ij} has a single value, say J_{nn}, corresponding to nearest neighbours or perhaps two values, one for nearest and one for next-nearest neighbours, J_{nnn}. In low symmetry there may be several values for J_{ij}.

If each of the atoms j is coupled to a set of neighbours, as in a metal oxide or halide crystal, the evaluation of the effects of the Hamiltonian of equation (78) rapidly becomes exceedingly complex, although simplification is available in high-symmetry crystals, particularly above the ordering temperature.

The Hamiltonian of equation (78) corresponds to so-called Heisenberg exchange. In some systems, particularly chains of atoms, it seems that the coupling is restricted to one direction, z. Then the $\boldsymbol{H}_{ex}$ becomes

$$H_{Is} = -2\sum_J J_{ij} S_{zi} S_{zj} \tag{79}$$

which describes the Ising model for exchange. In a chain J_{ij} has a single value, J_{nn}. The application of the Ising Hamiltonian is usually more tractable than that of equation (77).

6.6.7.2 *Intramolecular exchange*[169,174]

Where the exchange is intramolecular amongst a few paramagnetic atoms in a group isolated from other groups, closed expressions for the energies of the application of the Hamiltonians of equations (78) and (79) may be derived. However, for even a few atoms they are quite cumbersome for $S > ½$, particularly as J_{ij} may take on several values. The energies of the system are $E_{S'}$ where the subscript specifies the net spin of the energy level. In general, S' can take on values from $S_{tot} = \sum_1^n S_i$, n being the number of atoms in the cluster, down to 0 (S_{tot} integral) or $\frac{1}{2}$ (S_{tot} half-integral), and a value of S' ($\neq S_{\text{tot}}$, ½ or 0) may occur repeatedly. The resultant susceptibilities are obtained by applying the Van Vleck equation (equation 65) in a straightforward although often cumbersome manner.

The simplest case, a pair of atoms of $S = ½$ coupled, is of some importance. The energies are readily shown to be $E_1 = -J/2$ and $E_0 = 3J/2$. The susceptibility is obtained as

$$\chi_A = \frac{N\beta^2}{3kT} g^2 [3\exp(2J/kT)]/[3\exp(2J/kT) + 1] + \chi_{\text{TIP}} \tag{80}$$

The susceptibility calculated for this system as a function of temperature is given in Figure 29.[184]

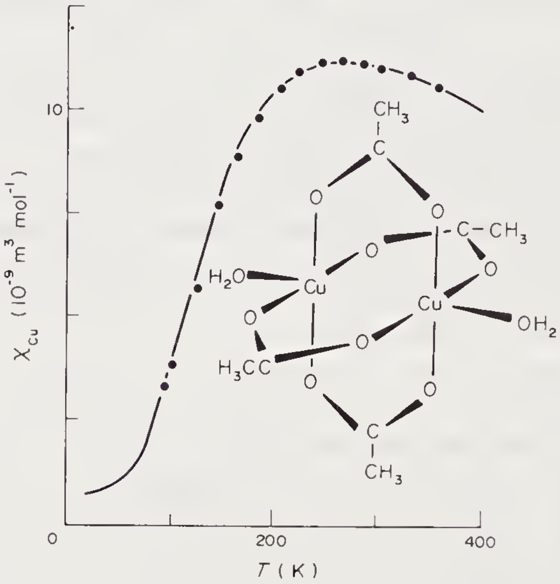

Figure 29 The magnetic susceptibility of $Cu_2(OAc)_4 \cdot 2H_2O$ as a function of temperature (°C) and the best fit (—) of equation (80) ($J = -160$ cm^{-1}, $\chi_{\text{TIP}} = 0.81 \times 10^9$ m^3 mol^{-1})

6.6.7.3 *Superexchange*[158–160,185,186]

The separations between the transition metal atoms in complexes are such that direct through-space coupling of their spins is not significant except, of course, for direct metal–metal bonding. Rather, the coupling of the spins occurs by polarization of intervening diamagnetic atoms. Systems such as

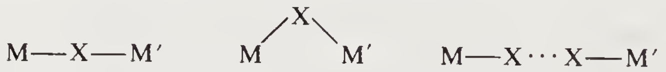

$$\text{M—X—M}' \qquad \text{M}\overset{\text{X}}{\wedge}\text{M}' \qquad \text{M—X}\cdots\text{X—M}'$$

where the X ··· X unit can indicate several sorts of chemical bonding interaction, including ionic contact in a crystal, an intervening carbon or other atom and even hydrogen bonding, are involved. The term superexchange is used to cover all such indirect exchange, whatever its detailed nature. X is commonly O, S or a halogen atom.

The mechanism of superexchange has received much attention.[163,185,186] Rationalization of the sign and magnitude of the values of $J_{MM'}$, which arise from different pathways, is sometimes available. The M—X—M′ angle and the available orbitals on M and M′ (empty, half-filled or filled) are important considerations. Mostly $J_{MM'}$ is negative, corresponding to antiferromagnetic exchange, but positive values arise, particularly for the single bridging atom case. Of course the magnitude of $J_{MM'}$ decreases with the length of the X···X pathway, although it may not be entirely negligible even for path lengths as great as 1 nm. An M—O—M system may give $|J_{MM}|$ as great as 200 cm^{-1} or more. However, it is exceedingly difficult to calculate absolute magnitudes of exchange integrals, even of J_{nn}, resulting from superexchange.

The simplest types of superexchange coupling are shown in Figure 30. The σ-type of Figure 30a might on simple grounds be expected to be larger in magnitude than the π-type of Figure 30b, but in practice this is not necessarily observed. Unpaired spin in the appropriate M atom *d*-orbital polarizes the spin of the filled *p*-orbital of the central diamagnetic atom, X, which in turn polarizes the spin in the *d*-orbital of M′. In the case of Figure 30c, internal spin coupling within the central atom very efficiently allows that the M—X—M′ angle need not be 180°, but say 90°, giving the 'right angle exchange' pathway often observed. M—X—M′ angles intermediate between 90 and 180° may be considered to possess an exchange component corresponding to each of these angles to give the net value for $J_{MM'}$. Of course, in the presence of superexchange coupling pathways of this, and even greater complexity, the definition of 'nearest-neighbour' and 'next-nearest-neighbour' for magnetic purposes may not correspond with their physical locations in the crystal. The description of the more complex pathways and even of the variations of coupling schemes which arise from the M—X—M′ arrangement are beyond the scope of this article.

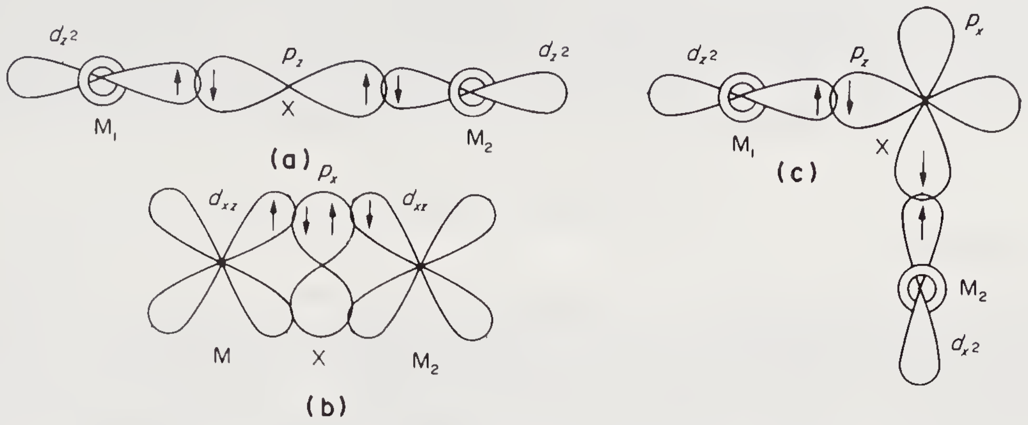

Figure 30 Superexchange mechanisms: (a) 180° – σ; (b) 180° – π; and (c) 90°

6.6.8 Magnetism in the AOM[42–44,160]

The preceding discussion of the magnetic properties of *d*-electron systems has proceeded in the context of a simple ligand field model, with the paramagnetism taken to be a property of the central metal atom of a complex. In a treatment of the electronic structure of a complex at the MO theory level this simplification cannot properly be made — the magnetic properties are a function of the whole metal–ligand system. In practice, attempts to calculate paramagnetic susceptibilities arising from the wave functions derived on the basis of *ab initio* MO calculations for complexes have very rarely been made. However, it has been pointed out that the AOM provides a basis for the treatment of magnetic properties as arising from metal-ligand bonding interactions.[42–44,160] There seems to be the possibility of deducing information about those interactions in the spirit of the effective orbital sets and operators of the ligand field concept. The approach cannot be followed further here.

6.6.9 Electron Spin Resonance (ESR)[128,187–192]

6.6.9.1 Introduction

In the ESR experiment, microwave radiation is used to probe the energy level distribution represented by, for example, the lowest right-hand section of Figure 27. The experiment can be a very complicated one, for very small energy level splittings due to nuclear-spin–electron-spin coupling occur, and the effects of magnetic exchange can be marked and complex. The interpretation of the experiment is correspondingly complex and can yield information about a number of features of the interaction of the metal ion with its ligand environment, including covalency in chemical bonding. For the present purposes we restrict consideration to those features directly connected to simple ligand field theory. They are the *g*-value, giving the first-order Zeeman effect, and the zero-field splitting of the lowest lying level.

Ignoring the other perturbations which determine the energy level structure of the ground state, and hence details of the ESR experiment, the results of the experiment for the present purposes are conventionally summarized by the *spin Hamiltonian* formalism. In simplest form we have

$$H_{S'} = \sum_{q} g_q \beta H_q S'_q + D\left(S'^{2}_{q} - S'(S'+1)\right) \tag{81}$$

where $q = x, y, z$. S' is the *fictitious spin* quantum number, such that $2S'+1$ is the number of levels to be considered, and may or may not be the same as the real spin of the system. For the z direction this Hamiltonian gives the first-order Zeeman energies as $g_z\beta H_z M_{S'_z}$, where $M_{S'_z} = S', S'-1, \ldots -S'$.

For technical reasons the ESR experiment cannot be performed usefully on all systems. In many cases, configurations with an even number of electrons (S integral) give a non-degenerate level lying lowest of all, and consequently no splitting by the magnetic field takes place. Even a small amount of magnetic exchange can profoundly affect the ESR experiment, so that it is usually performed on a system in which the paramagnetic ion is diluted by making a solid solution of the complex in an isomorphous one containing a diamagnetic metal. For these reasons the values of the g and ZFS parameters obtained from ESR are not always directly comparable with those relevant for magnetic susceptibility. However, the two experiments are quite complementary.

In the ESR experiment it may be difficult to separate the effects of the magnetic field and the ZFS in determining the energy level structure of the lowest levels unless more than one microwave frequency is used. It is not unusual that ESR results are present as 'g-values' which represent energy level separations which simply correspond to the microwave energy, but which may arise from some combination of magnetic field and ZFS. The discussion below is based on the availability of 'true' g-values and ZFS and care should be used in making sure that literature g-values have such a correct meaning.

6.6.9.2 The g*-value*

In suitable systems the g-value can be measured with great accuracy. Also, the ESR experiment is such that each paramagnetic ion contributes separately to the spectrum, and in principle the contributions can be obtained separately. This is in contrast to the magnetic susceptibility, where the experiment reflects only the average of the contributions of individual ions in a crystal.

The g-value is, then, often a very sensitive probe of the ligand field experienced by the transition metal ion. It acts in this way because the amount of orbital angular momentum associated with the lowest level is determined by the ligand field. In the absence of orbital angular momentum g has the value of 2.0023, which arises from the effects of electron spin alone. Departure from this value is direct evidence of the incomplete quenching of orbital angular momentum by the ligand field. Complete, or virtually complete, quenching is only seen for the $^6A_{1g}$ of d^5, for which the result $g = 2.00$ is well known, along with the 'spin-only' magnetic moment, $\mu_{\text{eff}} = 5.92$ BM. It is convenient to divide the results for other ground levels into a near spin-only and a highly anisotropic category, arising respectively from non-orbitally degenerate and orbitally degenerate ground terms.

Mean-spin-only g-values arise essentially from either the A or E ground terms of cubic or near-cubic symmetry, or the A or B ground terms which arise in low-symmetry complexes. They are associated with magnetic susceptibility behaviour of the type expressed in equation (76). In those equations the terms in parentheses are, as is obvious by reference to equation (73), approximations to $g/2$. However, ESR determines g much more accurately than does magnetic susceptibility, and more elaborate expressions for g, involving say terms in λ^2/Δ_i^2, are often required to use the experimental information completely. Here i may refer to more than one excited energy level, and of course different sets are involved for different directions to reproduce the anisotropy in g. As pointed out in connection with the magnetic susceptibility for these situations, the anisotropy in g is not large. For A or B terms arising in low symmetry the anisotropy in g may reach as high as perhaps 20%.

Highly anisotropic g-values are associated with orbitally degenerate ground terms with a relatively small splitting by low-symmetry ligand field components. In fact, in order that appreciable orbital angular momentum remain it is necessary that such a splitting be not much larger in magnitude than the spin–orbit coupling constant. On the other hand, although in a cubic symmetry the g-value may in principle be quite different from 2, it is required to be isotropic. Highly anisotropic g-values are then associated with the splitting of orbitally degenerate terms, most usually cubic field T terms, by low-symmetry ligand field components by an amount rather less than, but comparable with, the spin–orbit coupling constant. The details of the calculation of g in certain such situations have been set out.[32,191] It can be noted that ESR almost certainly cannot be observed in such systems unless S is half-integral, when the level must be a Kramer's doublet. Owing to spin–lattice coupling introduced by the presence of levels $\approx kT$, ESR in complexes with T ground terms is usually only observable at very low temperatures.

There remains the possibility of g-values which depart substantially from 2.00 but are isotropic because of cubic symmetry. In practice such conditions are rare for transition metal complexes, as the Jahn–Teller theorem ensures departure from cubic symmetry in the electronic structure. However, for the lanthanoid and actinoid elements, where the spin–orbit coupling constant is very much larger than kT, the Jahn–Teller theorem may not be relevant and effective cubic symmetry certain. For the lanthanoids, g-values often depart considerably from 2.00, although some anisotropy arising from ligand field splittings is common. For the actinoids, direct observation of ESR is less common but there is evidence of a similar situation.

6.6.9.3 Zero-field splitting

The ZFS representation in the spin Hamiltonian of equation (81) is that for axial symmetry. The parameter D arises (Section 6.4.4.6) from the action of spin–orbit coupling in second order.

Its origin is strongly concerned with the details of the ligand field splittings of excited terms, but simple calculations do not reproduce its magnitude at all well. In rhombic symmetry, D is supplemented by a second parameter E. More generally still, D is a second-rank tensor the magnitude of whose principal values and the directions of whose axes are determined by the ligand field splittings of the excited states.[32] There is some evidence that calculations using a ligand field model but encompassing all the terms arising from the d manifold can reproduce the D tensor with some success,[89,90] but such calculations are quite rare.

6.7 MAGNETIC BEHAVIOUR OF SOME COMPLEXES

6.7.1 Introduction

Exhaustive compilations of magnetic properties of transition metal complexes are available.[166,192–194] The following sections describe very briefly the magnetic behaviour of a selection of complexes or groups of complexes, from the various electronic configurations which arise for the transition metals. They are intended to be illustrative of the points made in the earlier sections; no attempt at completeness of coverage is made. More detailed and intensive accounts of magnetic properties of transition metal complexes are available.[99,166–169,174,175,186,195–197] No mention is made of results for lanthanoid and actinoid elements, nor of ESR g-values.

6.7.2 d^1

(i) Ti^{3+}

Compounds with close to octahedral stereochemistry, *e.g.* TiX_6^{3-}, including some with a mixture of ligands, have $\mu_{eff}(300) \approx 1.8$ BM decreasing to ~ 1.5 BM at 80 K in a manner conforming to the $^2T_{2g}$ term with a low-symmetry ligand field component (Δ_T), although a unique determination of k, Δ and λ is often not possible. Although others have formal octahedral stereochemistry $[Ti(H_2O)_6^{3+}]$, the electronic structure seems to correspond to low symmetry; $\mu_{eff}(300) \approx 1.7$ BM, $\mu_{eff}(80) \approx 1.6$ BM.

(ii) V^{4+}

Compounds of octahedral stereochemistry, *e.g.* VCl_6^{2-}, have $\mu_{eff}(300) \approx 1.8$ BM decreasing to ~ 1.3 at 80 K, corresponding to the $^2T_{2g}$ term with small Δ_T, but much more common are the derivatives of the VO^{2+} ion, *e.g.* $VO(H_2O)_4^{2+}$, where the high distortion leads to $\mu_{eff} \approx 1.7$, corresponding to behaviour of the type of equation (75). $VO(OAc)_2$ has the dimeric structure of $Cu(OAc)_2$ (see Section 6.7.10) and shows similar intramolecular magnetic exchange.

(iii) Cr^{5+}

The examples of this valence state with known magnetic properties have distorted octahedral structures of the type $CrOX_5^{2-}$ and show $\mu_{eff} \approx 1.9$ BM, corresponding to behaviour of the type of equation (75).

(iv) Nb^{4+}, Mo^{5+}, W^{5+}, Re^{6+}

Nb^{IV} and Mo^{V} compounds of octahedral stereochemistry ($NbCl_6^{2-}$, MoX_6^{-}) show respectively $\mu_{eff} \approx 1.2$ BM and $\mu_{eff}(300) \approx 1.6$ decreasing to 1.0 BM at 80 K, corresponding to the $^2T_{2g}$ term with a high value of λ and moderate Δ_T. Compounds of the type $MoOX_5^{2-}$ and WOX_5^{2-} show $\mu_{eff} \approx 1.7$ and 1.4 respectively, corresponding to the presence of both large λ and large Δ_T. Presumably because of the low symmetry, some eight-coordinate Nb^{IV} complexes have $\mu_{eff} \approx 1.8$ BM. The magnetic behaviour for Re^{VI} seems more varied: some complexes with CN^- have $\mu_{eff} \approx 1.5-2.0$ BM, but others are diamagnetic.

6.7.3 d^2

(i) V^{3+}

A number of fairly regular octahedral complexes show $\mu_{eff}(300) \approx 2.9$ decreasing to ~ 2.3 BM at 80 K, but others of less symmetric nature have $\mu_{eff}(300) \approx 2.7$ decreasing only to ~ 2.6 BM [*e.g.* $V(acac)_3$], corresponding to the $^3T_{1g}$ ground term with smaller or larger Δ_T relative to λ. The tetrahedral molecule VCl_4 shows the properties expected of the $^3A_2$ ground term, $\mu_{eff} = 2.6$ BM. In V_2Cl_9 intramolecular dimer exchange is present.

(ii) Mn^{5+}

The tetrahedral Mn^{5+} ion gives $\mu_{eff} = 2.8$ BM, as expected for the ${}^3A_2$ ground term.

(iii) Mo^{4+}, W^{4+}, Re^{5+}, Os^{6+}

Octahedral Mo^{IV} complexes have $\mu_{eff}(300) \approx 2.4$ decreasing to ~ 1.5 at 80 K, while those of W^{IV} have $\mu_{eff} \approx 1.6$ BM; these results are as expected for the ${}^3T_{1g}$ term with increasing λ. The eight-coordinate cyanide complexes have $\mu_{eff} \approx 0$, due to spin-pairing following the reduction in symmetry. The $[Cl_5W{-}O{-}WCl_5]^{2+}$ system shows intermolecular dimer antiferromagnetic exchange transmitted by a classical superexchange pathway. The magnetic properties of Re^V compounds seem more varied, and do not correspond well to the ${}^3T_{1g}$ term with large λ; μ_{eff} lies between 2.1 and 1.0 BM, not much dependent on T. Os^{VI} complexes show spin-pairing consequent upon low symmetry, to give $\mu_{eff} \approx 0$.

6.7.4 d^3

(i) V^{2+}, Cr^{3+}, Mn^{4+}

The formally octahedral complexes of these ions all show the behaviour expected for the ${}^4A_{2g}$ ground term with λ fairly small, according to equation (73), *i.e.* $\mu_{eff} \approx 3.8$ BM. Cr^{III} shows intramolecular antiferromagnetic magnetic exchange *via* superexchange in compounds such as $[Cr(OAc)_6O]^+$, $[Cr_2(OH)_2(en)_4]^{4+}$ and $[Cr_4(OH)_6(en)_6]^{6+}$ as well as a more intermolecular type in many compounds of polymeric nature, where $\mu_{eff} = 3.3-3.7$ is common, falling with decreasing temperatures with θ values of a few degrees.

(ii) Mo^{3+}, Tc^{4+}, Re^{4+}, Os^{5+}

Octahedral complexes of these ions show magnetic moments somewhat lower than the spin-only value for the ${}^4A_{2g}$ term as expected from equation (73), the decrease being the greater as the value of λ rises. For the ions listed, $\mu_{eff} \approx 3.7$, 3.7, 3.7−3.0 and 3.2 BM. For the very high values of λ, equation (73) ceases to be adequate.

6.7.5 d^4

(i) V^+, Cr^{2+}, Mn^{3+}, Fe^{4+}

Most octahedral complexes of Cr^{II} and Mn^{III} show the magnetic properties expected for the high-spin ${}^5E_g$ ground term, *viz.* $\mu_{eff} \approx 4.9$ BM. However, with high ligand field strengths, spin-pairing is forced and the ground term is ${}^3T_{1g}$ with $\mu_{eff}(300) \approx 3.00$ BM (Cr) and 3.5 BM (Mn), in the latter case falling to 2.5 BM at 80 K, which is consistent with the presence of $\Delta_T \approx \lambda$. Some V^I complexes, including $(C_5H_5)^-$ derivatives as well as some Fe^{IV} compounds, have at least pseudo-octahedral symmetry and correspond to the low-spin ${}^3T_{1g}$ term with $\mu_{eff} \approx 2.9$ BM. Cr(phthalocyanine), for example, seems to be an example of $S = 1$, arising from the square-planar stereochemistry, $\mu_{eff} \approx 3.0$ BM. $Cr(OAc)_2$ shows intramolecular antiferromagnetic exchange as in the copper compound of the same dimeric structure, but of such large extent that $\mu_{eff} \approx 0$.

(ii) Re^{3+}, Ru^{4+}, Os^{4+}

For the formally octahedral complexes of these ions the large spin–orbit coupling dominates the behaviour of the ${}^3T_{1g}$ low-spin ground term. The magnetic susceptibility is of the TIP type, giving $\mu_{eff}(300) \approx 1.4$, 2.9 and 1.6 BM respectively which, in the first and third cases at any rate, decrease $\propto T^{1/2}$.

6.7.6 d^5

(i) V^0, Cr^+, Co^{4+}

Some compounds of these ions with formal octahedral or pseudo-octahedral stereochemistries have $\mu_{eff} \approx 1.8$ BM, corresponding to the low-spin ${}^2T_{2g}$ ground term, with the presence of Δ_T of some magnitude.

(ii) Mn^{2+}, Fe^{3+}

Both octahedral and tetrahedral high-spin complexes are common and give the expected magnetic moment of 5.92 BM for the ${}^1A_{1(g)}$ term with good accuracy; for example, $Mn(H_2O)_6{}^{2+}$, $Fe(H_2O)_6{}^{3+}$, $MnCl_4{}^{2-}$ and $FeCl_4{}^-$. In octahedral stereochemistry with high-field ligands each also gives low-spin, $S = 1/2$, complexes $[Mn(CN)_6{}^{4-}$, $Fe(CN)_6{}^{3-}]$ with $\mu_{eff}(300) \approx 2.4$ BM, $\mu_{eff}(80) \approx$

2.0 BM, corresponding to the $^2T_{2g}$ ground term with moderately small values of λ and comparable Δ_T. Square-planar [*e.g.* Mn(phthalocyanine)] or square pyramidal [*e.g.* $Fe(S_2CNEt_2)_2Cl$] complexes may give the intermediate-spin case, $S = {}^3/_2$, with $\mu_{eff} \approx 4.0$ BM.

A number of Fe^{III} complexes lie at the borderline of the high- and low-spin region of ligand field strengths, and several spin-equilibrium systems are known, including the $Fe(S_2CNR_2)$ series where the position of the equilibrium depends upon R.[178] Some compounds in the haemoglobin series are involved here, and may also involve the intermediate spin state.

Magnetic exchange transmitted by superexchange coupling is common amongst Fe^{III} complexes, and examples of intramolecular exchange are $[Fe_3(OAc)_6O]^+$, $Fe_2Cl_9{}^{3-}$ and $[\{Fe(phen)_2\}_2O]^{4+}$. Also there are many examples of distributed exchange in polymeric systems, accompanied by values of θ of a few degrees.

(iii) Re^{2+}, Ru^{3+}, Os^{3+}, Rh^{4+}, Ir^{4+}

The formal octahedral complexes of these ions correspond to the $^2T_{2g}$ term with large to very large spin–orbit coupling and the presence of a Δ_T term. $\mu_{eff}(300)$ is respectively ~1.7, 1.9–2.2, 1.7, 1.8 and 1.9 BM, falling little as T decreases except perhaps for Ru^{III}, where $\mu_{eff}(80) \approx 1.7$–$1.9$ BM.

6.7.7 d^6

(i) Cr^0, Mn^+

The octahedral complexes of these ions correspond to the low-spin case, $^1A_{1g}$, with $\mu_{eff} \approx 0$.

(ii) Fe^{2+}, Co^{3+}

High-spin Fe^{II} complexes are known in both octahedral, $^5T_{2g}$, and tetrahedral, ^5E, stereochemistries. In the former, $Fe(H_2O)_6{}^{2+}$ for example, $\mu_{eff}(300) \approx 5.0$–$5.7$ BM falling to ~4.5 BM at 80 K, corresponding to the fairly small value of λ with a comparable one of Δ_T. In the latter, $FeCl_4{}^{2-}$ for example, $\mu_{eff} \approx 5.4$ BM, corresponding to behaviour of the type of equation (73). For Co^{III}, essentially the octahedral stereochemistry only is available and the high-spin condition is rare. It occurs in the $CoF_6{}^{3-}$ ion, for which $\mu_{eff}(300) \approx 5.0$ BM.

Low-spin complexes of the $^1A_{1g}$ ground term are known for Fe^{II}, *e.g.* $Fe(CN)_6{}^{4-}$, and are by far the most usual for Co^{III}, *e.g.* $Co(NH_3)_6{}^{3+}$. The magnetic moments are low, but not zero as ideal for the $^1A_{1g}$ term, particularly for Co^{III} compounds. The values of $\mu_{eff}(300)$ are commonly ~0.4 BM and arise from a TIP contribution of the form of the second term in equation (73), and with $S = 0$ in the first term. For Fe^{II} a number of $^5T_{2g} - {}^1A_{1g}$ spin-equilibrium or pseudo-equilibrium systems occur, particularly series based upon Fe(bipy, phen)X_2, whereby magnetic moments between ~1.0 and 5.0 BM can be obtained by changing temperature.[179,180]

Square-planar complexes of Fe^{II} are well established and can lead to the intermediate spin case of $S = 1$. This situation, exemplified by Fe(phthalocyanine), $\mu_{eff} = 3.8$ BM, is often accompanied by remarkably large ZFS of the triplet ground state, such that TIP is observed below say 20 K. Complexes of other lower symmetries may also lead to $S = 1$.

(iii) Mo^0, W^0, Re^+, Ru^{2+}, Rh^{3+}, Ir^{3+}, Pd^{4+}, Pt^{4+}

All these ions are characterized by the low-spin $^1A_{1g}$ ground term, with $\mu_{eff} \approx 0$, but often with some TIP as for Co^{III}.

6.7.8 d^7

(i) Co^{2+}, Ni^{3+}

Octahedral high-spin Co^{II}, and possibly some Ni^{III}, complexes have the $^4T_{1g}$ ground term and show $\mu_{eff}(300) \approx 4.7$–$5.5$ BM, falling to ~4.0–4.5 BM at 80 K, as expected for the moderately small value of λ and the presence of Δ_T. An example is $(NH_4)_2Co(SO_4)_2 \cdot 6H_2O$, where $\mu_{eff}(300) = 5.1$, $\mu_{eff}(80) = 4.6$ BM. Tetrahedral high-spin complexes, as in $CoX_4{}^{2-}$, have $\mu_{eff} \approx 4.5$ BM, arising from the $^4A_2$ ground term and behaviour conforming with equation (73). This position also seems to apply to certain five-coordinate complexes.

Octahedral low-spin complexes of Co^{II} and Ni^{II} have the ^2E_g ground term and consequently $\mu_{eff} \approx 1.8$ BM and behaviour characteristic of equation (73). An example is the $Co(NO_2)_6{}^{4-}$ ion. Several spin-equilibria systems are known for Co^{II} complexes, particularly with nitrogen heterocycle ligands; an example is the $[Co(terpyridyl)_2]X_2 \cdot xH_2O$ series, where the 300 K and 80 K populations of the $^4T_{1g}$ and ^2E_g terms depend on X and also on the degree of hydration, in a complicated fashion.

Square-planar $\mathrm{Co^{II}}$ complexes also give an $S = ½$ ground term but, apparently because of low-lying excited *d*-orbitals, give magnetic moments well above the spin-only value, with behaviour corresponding to equation (75). μ_{eff} is commonly ~2.2 BM, but Co(phthalocyanine) is an extreme example, with $\mu_{\mathrm{eff}} = 2.8$ BM.

6.7.9 d^8

(i) Fe^0, Co^+, Ni^{2+}, Cu^{3+}

For octahedral stereochemistry the ground term is $^3A_{2g}$ and behaviour dictated by equation (73) is expected. Respectively, $\mu_{\mathrm{eff}} \approx 2.7$, 2.8, and 3.2 BM is found for the first three members, *e.g.* $\mathrm{Ni(NH_3)_6}^{2+}$, 3.20 BM. $\mathrm{Ni(C_5H_5)_2}$ is pseudo-octahedral, giving an $S = 1$ ground term, but with a remarkably large ZFS. Tetrahedral stereochemistry, found only in the $\mathrm{Ni^{2+}}$ case, gives the $^3T_1$ ground term with more complicated behaviour. For example in $\mathrm{NiCl_4}^{2-}$, $\mu_{\mathrm{eff}}(300) = 3.9$ BM, decreasing to 3.25 BM at 80 K, and consistent with the term perturbed by moderately small spin–orbit coupling combined with similar Δ_T.

In square-planar or other lower symmetry these ions give rise to an $S = 0$ ground term, with consequent values of $\mu_{\mathrm{eff}} \approx 0$, and compounds of these types are found for all the members; for example, Ni(dimethylglyoxime)$_2$. Nickel(II) shows a form of spin-equilibrium associated with the stereochemistry interchanges

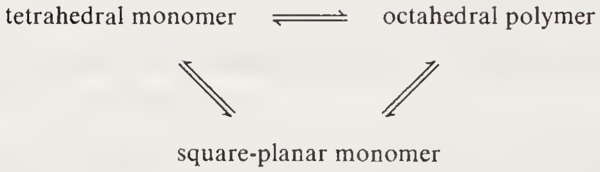

These occur particularly in solution, but in the solid state also coexistence of the different stereochemistries is possible; in either case, complicated magnetic behaviours as functions of concentration, preparative details and temperature arise. Complexes of β-diketones, substituted alkylenediamines and salicylaldiamines are characteristic sources of these phenomena.

(ii) Rh^+, Ir^+, Pd^{2+}, Pt^{2+}, Cu^{3+}, Ag^{3+}

These ions almost always lead to complexes of square-planar or other low symmetry, with the result that electron pairing takes place and $\mu_{\mathrm{eff}} \approx 0$.

6.7.10 d^9

(i) Ni^+, Cu^{2+}

Complexes of near octahedral stereochemistry have $\mu_{\mathrm{eff}} \approx 1.9$ BM and correspond to equation (73). The behaviour of $\mathrm{CuSO_4 \cdot 5H_2O}$ can be taken as typical: $\mu_{\mathrm{eff}}(300\ \mathrm{K}) = 1.88$ BM, obeying the Curie–Weiss law with $|\theta| < 1\ ^\circ\mathrm{C}$ and a small TIP contribution. In lower stereochemistries, such as approximate square-planar, the average magnetic susceptibility behaviour is similar, but there can be quite substantial anisotropy, conforming to the requirements of equation (75).

A few tetrahedral examples of $\mathrm{Cu^{II}}$ complexes are found and here the $^2T_2$ ground term brings temperature variation, although the effect is not large, in spite of the substantial size of λ, because of large Δ_T.

A wide variety of $\mathrm{Cu^{II}}$ compounds form dimeric or polymeric structures,[193,194] with $\mathrm{Cu_2(OAc)_4 \cdot 2H_2O}$ as the archetype. Here the copper atoms are bridged by four

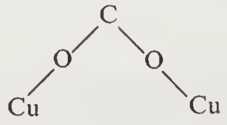

linkages, and antiferromagnetic superexchange with $J_{\mathrm{CuCu}} \approx -100$ Hz results. The magnetic susceptibility is given by the fairly simple relationship of equation (79). Other bridging systems, particularly $\mathrm{OH^-}$, given similar dimers but with differing values, including positive (ferromagnetic) ones. Behaviour of the form of equation (80) is characteristic.

(ii) Ag^{2+}

$\mathrm{Ag^{II}}$ complexes of the known stereochemistries, presumably formally octahedral or square-planar, give $\mu_{\mathrm{eff}} \approx 1.8$ BM and, as for $\mathrm{Cu^{II}}$ compounds, behaviour corresponding to equations (73) or (75). The larger spin–orbit coupling constant for $\mathrm{Ag^{2+}}$ does not seem to lead to higher values of μ_{eff}, for reasons which are not immediately obvious.

6.8 APPENDIXES

6.8.1 APPENDIX 1 A Method for Obtaining the *d*-Orbital Energies for an Arbitrary Array of Ligand Charges

V_{cf} is the general crystal field potential arising from n ligands of charge q_i at effective distances a_i from the central metal atom, and with positions specified by the angles θ_i and ϕ_i as defined in Figure 1 (z must be an axis of at least twofold symmetry). Let

$$a_i^{\,n} = q_i \overline{r_2^{\,n}} \,/\, a_i^{\,n+1}$$

$$D^{lm} = \sum_{i=1}^{n} D_i^{lm}$$

$$G^{lm} = \sum_{i=1}^{n} G_i^{lm}$$

We use the abbreviation, for example

$$H_{xy,xz} = \int d_{xy}^{*} \, V_{\mathrm{cf}} \, d_{xz} \, \mathrm{d}\tau$$

Then

$$\begin{aligned}
H_{z^2,z^2} &= -D^{20}/7 + 3D^{40}/28 \\
H_{x^2-y^2,x^2-y^2} &= -D^{20}/7 + D^{40}/56 + 5D^{44}/24 \\
H_{xy,xy} &= -D^{20}/7 + D^{40}/56 - 5D^{44}/24 \\
H_{xz,xz} &= D^{20}/14 - D^{40}/14 + 3D^{22}/14 + 5D^{42}/42 \\
H_{yz,yz} &= D^{20}/14 - D^{40}/14 - 3D^{22}/14 - 5D^{42}/42 \\
H_{z^2,x^2-y^2} &= -3^{1/2}D^{22}/7 + 75D^{42}/84 \\
H_{z^2,xy} &= -3^{1/2}G^{22}/7 + 75^{1/2}G^{42}/84 \\
H_{z^2,xz} &= -3^{1/2}D^{21}/7 + 75^{1/2}D^{41}/14 \\
H_{z^2,yz} &= 3^{1/2}G^{21}/7 + 75^{1/2}G^{41}/14 \\
H_{x^2-y^2,xy} &= 5G^{44}/24 \\
H_{x^2-y^2,xz} &= 3D^{21}/7 - 5D^{41}/28 + 5D^{43}/12 \\
H_{x^2-y^2,yz} &= -3G^{21}/7 + 5G^{41}/28 + 5G^{43}/12 \\
H_{xy,xz} &= 3G^{21}/7 - 5G^{41}/28 + 5G^{43}/12 \\
H_{xy,yz} &= 3D^{21}/7 - 5D^{41}/28 - 5D^{43}/12 \\
H_{xz,yz} &= 3G^{22}/14 + 5G^{42}/42
\end{aligned}$$

where

$$\begin{aligned}
D_i^{20} &= (3\cos^2\theta_i - 1)a_i^2 \\
D_i^{21} &= \sin\theta_i\cos\theta_i\cos\phi_i a_i^2 \\
D_i^{22} &= \sin^2\theta_i\cos2\phi_i a_i^2 \\
D_i^{40} &= (35\cos^4\theta_i - 30\cos^2\theta_i + 3)a_i^4/3 \\
D_i^{41} &= \sin\theta_i\cos\theta_i(7\cos^2\theta_i - 3)\cos\phi_i a_i^4/3 \\
D_i^{42} &= \sin^2\theta_i(7\cos^2\theta_i - 1)\cos2\phi_i a_i^4 \\
D_i^{43} &= \sin^3\theta_i\cos\theta_i\cos3\phi_i\, a_i^4 \\
D_i^{44} &= \sin^4\theta_i\cos4\phi_i a_i^4
\end{aligned}$$

$$\begin{aligned}
G_i^{21} &= \sin\theta_i\cos\theta_i\sin\phi_i a_i^2 \\
G_i^{22} &= \sin^2\theta_i\sin2\phi_i a_i^2 \\
G_i^{41} &= \sin\theta_i\cos\theta_i(7\cos^2\theta_i - 3)\sin\phi_i a_i^4/3 \\
G_i^{42} &= \sin^2\theta_i(7\cos^2\theta_i - 1)\sin2\phi_i a_i^4 \\
G_i^{43} &= \sin^3\theta_i\cos\theta_i\sin3\phi_i a_i^4 \\
G_i^{44} &= \sin^4\theta_i a_i^4
\end{aligned}$$

The energies of the *d*-orbitals for the system E_i, $i = 1-5$, are then obtained by diagonalization of the real symmetrical matrix H_{ij}, $i = d_{z^2} \ldots d_{yz}$. The real *d*-orbital linear combinations which correspond to these energies are then obtained by substituting the solutions, E_i, into the sets of simultaneous equations derived from the secular determinant.

6.8.2 APPENDIX 2 AOM Expressions Including δ Symmetry for the Octahedron and Tetrahedron

$e_\delta = H_{\mathrm{M}}R^2$

Octahedron

$$\left.\begin{aligned}
E_{e_g}^{*} &= 3e_\sigma + 3e_\delta \\
E_{t_{2g}}^{*} &= 4e_\pi + 2e_\delta
\end{aligned}\right\}\Delta_{\mathrm{oct}} = 3e_\sigma - 4e_\pi + e_\delta$$

Tetrahedron

$$\left.\begin{aligned}
E_{t_2}^{*} &= (4/3)e_\sigma + (8/9)e_\pi + (16/9)e_\delta \\
E_{e}^{*} &= (8/3)e_\pi + (4/3)e_\delta
\end{aligned}\right\}\Delta_{\mathrm{tet}} = (4/3)e_\sigma - (16/9)e_\pi + (4/9)e_\delta$$

6.8.3 APPENDIX 3 Racah Electron Repulsion Parameters and Spin–Orbit Coupling Constants

(a) Racah Electron Repulsion Parameters and Spin–Orbit Coupling Constants for the Transition Metals

		Ti	*Zr*	*Hf*	*V*	*Nb*	*Ta*	*Cr*	*Mo*	*W*	*Mn*	*Tc*	*Re*	*Fe*	*Ru*	*Os*	*Co*	*Rh*	*Ir*	*Ni*	*Pd*	*Pt*	*Cu*	*Ag*	*Au*
	B	560	250	280	580	300	350	790	455	370	720		850	805			800	600		1025					
0	C	1840	1980		2270	2390	1290	2520	1770	1900	3090		1190	3510			4170	3240		4230					
	ζ_{nd}	110	335	1310	160	475	1660	220	550	2090	240	650	2290	390	880		520	970		600	1410	4050	820		4900
	B	680	450	440	660	260	480	710	440		870			870	470		880	670		1040			1220		
1+	C	2480	1770	1530	2420	1990	1840	2790	1990		3130			3640	1810		3830	2310		4310			4750		
	ζ_{nd}	88	340		136	490		222	670		254	660		356	890		456	1210		603	1320	3370	828	1830	5090
	B	720	540		770	530		.830			960			1060			1120	620		1080	830	600	1240		
2+	C	2630	1640		2860	2100		3430			3330			3900			4370	4000		4830	2620		4660		
	ζ_{nd}	121			167			230			347			410			533			649			829	1840	
	B				860	600		1030	610		1140						1100	720	660						
3+	C				4170	1370		3850			3680														
	ζ_{nd}	154	500		209	670		273	820		352			460			580			705			890		

	B	Cr^{4+} 1040; Fe^{4+} 1140; Mn^{4+} 1060; Mo^{4+} 680; Re^{4+} 650; Os^{4+} 700; Pt^{4+} 720; Os^{6+} 780; Ir^{6+} 810
Other	C	Cr^{4+} 4240; Fe^{4+} 4460
	ζ_{nd}	V^{4+} 250; Cr^{4+} 330; Mn^{4+} 400; Fe^{4+} 510; Nb^{4+} 750; Mo^{4+} 890

(b) Spin–Orbit Coupling Constants for the Lanthanoid Tripositive Ions

	Ce	*Pr*	*Nd*	*Pm*	*Sm*	*Eu*	*Gd*	*Tb*	*Dy*	*Ho*	*Er*	*Tm*	*Yb*
ζ_{4f}	644	730	844	1070	1200	1320	1583	1705	1900	2163	2393	2656	2883

(c) Spin–Orbit Coupling Constants for Some Actinoid Ions; ζ_{5f}

$5f^2$	$5f^3$		$5f^4$			$5f^6$	
U^{4+}	U^{3+}	Np^{4+}	Np^{3+}	Pu^{3+}	Am^{4+}	Am^{3+}	Cm^{4+}
1640	1670	2100	2000	2300	2820	2550	3040

6.9 REFERENCES

1. H. A. Bethe, *Ann. Phys. (Leipzig)*, 1929, **3**, 133 (English translation: Consultants Bureau, New York, 1955).
2. B. N. Figgis, 'Introduction to Ligand Fields', Wiley-Interscience, New York, 1966.
3. C. J. Ballhausen, 'Introduction to Ligand Field Theory', McGraw Hill, New York, 1962.
4. L. E. Orgel, 'Introduction to Transition Metal Chemistry, Ligand Field Theory', Methuen, London, 1960.
5. H. L. Schlafer and G. Gliemann, 'Basic Principles of Ligand Field Theory', Wiley-Interscience, New York, 1969.
6. M. Gerloch and R. C. Slade, 'Ligand Field Parameters', Cambridge University Press, Cambridge, 1973.
7. T. M. Dunn, D. S. McClure and R. G. Pearson, 'Some Aspects of Ligand Field Theory', Harper, New York, 1965.
8. A. L. Companion and M. A. Komarynsky, *J. Chem. Educ.*, 1964, **41**, 257.
9. J. H. Van Vleck, *J. Chem. Phys.*, 1935, **3**, 803, 807.
10. P. George and D. S. McClure, *Prog. Inorg. Chem.*, 1959, **1**, 381.
11. W. Moffitt and C. J. Ballhausen, *Ann. Rev. Phys. Chem.*, 1956, **7**, 107.
12. J. H. Van Vleck, *J. Phys. Chem.*, 1937, **41**, 67.
13. J. H. Van Vleck, *J. Chem. Phys.*, 1939, **7**, 61, 72.
14. W. G. Penney and R. Schlapp, *Phys. Rev.*, 1932, **41**, 194.
15. R. Schlapp and W. G. Penney, *Phys. Rev.*, 1932, **42**, 666.
16. W. G. Penney and G. J. Kynch, *Proc. Roy. Soc. (London)*, 1939, **A170**, 112.
17. H. Eyring, J. Walter and G. E. Kimball, 'Quantum Chemistry', Wiley, New York, 1944.
18. E. U. Condon and G. H. Shortley, 'Theory of Atomic Spectra', Cambidge University Press, Cambridge, 1957.
19. F. A. Cotton, 'Chemical Applications of Group Theory', Interscience, New York, 1963.
20. J. Hubbard, D. E. Rimmer and F. R. A. Hopgood, *Proc. Phys. Soc. (London)*, 1966, **88**, 13.
21. A. A. Misetich and R. E. Watson, *Phys. Rev.*, 1966, **143**, 335.
22. A. Aizman and D. A. Case, *Inorg. Chem.*, 1981, **20**, 528.
23. H. G. Drickamer and J. C. Zahner, *Adv. Chem. Phys.*, 1962, **4**, 161.
24. J. C. Zahner and H. G. Drickhamer, *J. Chem. Phys.*, 1961, **35**, 1483.
25. B. N. Figgis, E. S. Kucharski, J. M. Patrick and A. H. White, *Aust. J. Chem.*, 1984, **37**, 265.
26. C. E. Schaffer and C. K. Jorgensen, *J. Inorg. Nucl. Chem.*, 1958, **8**, 143.
27. C. K. Jørgensen, 'Absorption Spectra and Chemical Bonding in Complexes', Pergamon Press, Oxford, 1962.
28. J. H. Van Vleck, 'Theory of Electric and Magnetic Susceptibilities', Oxford University Press, Oxford, 1932.
29. R. S. Nyholm, *Quart. Rev. Chem. Soc.*, 1953, **7**, 377.
30. K. W. H. Stevens, *Proc. Phys. Soc. (London)*, 1952, **A65**, 209.
31. B. Bleaney and K. W. H. Stevens, *Repts. Prog. Phys.*, 1953, **16**, 108.
32. A. Abragam and B. Bleaney, 'Electron Paramagnetic Resonance of Transition Ions', Clarendon Press, Oxford, 1970.
33. E. Koenig and S. Kremer, *Int. J. Quantum Chem.*, 1977, **12**, 1017.

34. C. J. Ballhausen, 'Introduction to Ligand Field Theory', McGraw Hill, New York, 1962, p. 35.
35. H. Watanabe, 'Operator Methods in Ligand Field Theory', Prentice-Hall, New Jersey, 1966.
36. B. R. Judd, 'Operator Techniques in Atomic Spectroscopy', McGraw Hill, New York, 1963.
37. J. C. Donini, B. R. Hollebone and A. B. P. Lever, *Prog. Inorg. Chem.*, 1977, **22**, 225.
38. A. B. P. Lever, 'Inorganic Electronic Spectroscopy', Elsevier, Amsterdam, 1984.
39. F. A. Cotton and G. Wilkinson, 'Advanced Inorganic Chemistry: A Comprehensive Text', 4th edn., Wiley, New York, 1980.
40. G. E. Kimball, *J. Chem. Phys.*, 1940, **8**, 188.
41. C. J. Ballhausen and A. D. Liehr, *J. Mol. Spectrosc.*, 1958, **2**, 342.
42. M. Gerloch, *Prog. Inorg. Chem.*, 1979, **26**, 1.
43. M. Gerloch, J. H. Harding and R. G. Woolley, *Struct. Bonding (Berlin)*, 1981, **46**, 1.
44. M. Gerloch and R. G. Woolley, *Prog. Inorg. Chem.*, 1984, **31**, 371.
45. K. W. H. Stevens, *Proc. Roy. Soc. (London)*, 1953, **A219**, 542.
46. M. Gerloch and J. R. Miller, *Prog. Inorg. Chem.*, 1968, **10**, 1.
47. B. G. Wybourne, 'Spectroscopic Properties of Rare Earths', Interscience, New York, 1965.
48. S. Hufner, 'Optical Spectra of Transparent Rare Earth Compounds', Academic, New York, 1978.
49. S.-K. Chan and D. J. Lam, 'The Actinides, Electronic Structures and Related Properties', ed. A. J. Freeman and J. B. Darby, Academic, New York, 1974, vol. 1.
50. D. L. Kepert, 'Inorganic Stereochemistry', Springer-Verlag, Berlin, 1982.
51. K. F. Purcell and J. C. Kotz, 'Inorganic Chemistry', Saunders, Philadelphia, 1977.
52. D. W. Smith, *Struct. Bonding (Berlin)*, 1978, **35**, 87.
53. C. K. Jørgensen, R. Pappalardo and H.-H. Schmidte, *J. Chem. Phys.*, 1963, **39**, 1422.
54. J. K. Burdett, 'Molecular Shapes: Theoretical Models of Inorganic Stereochemistry', Wiley, New York, 1980.
55. K. Yates, 'Hückel Molecular Orbital Theory', Academic, New York, 1978.
56. M. Wolfsberg and L. Helmholtz, *J. Chem. Phys.*, 1952, **20**, 837.
57. C. K. Jorgensen, 'Modern Aspects of Ligand Field Theory', North Holland, Amsterdam, 1971.
58. C. E. Schaffer, *Struct. Bonding (Berlin)*, 1968, **5**, 68.
59. J. Glerup, O. Monsted and C. E. Schaffer, *Inorg. Chem.*, 1976, **15**, 1399.
60. M. A. Hitchman, *Inorg. Chem.*, 1974, **13**, 2218.
61. W. Kauzmann, 'Quantum Chemistry', Academic, New York, 1957.
62. J. S. Griffith, 'Theory of Transition Metal Ions', Cambridge University Press, Cambridge, 1961.
63. Y. Tanabe and S. Sugano, *J. Phys. Soc. Jpn.*, 1954, **9**, 753.
64. Y. Tanabe and S. Sugano, *J. Phys. Soc. Jpn.*, 1954, **9**, 766.
65. S. Sugano, Y. Tanabe and H. Kamimura, 'Multiplets of Transition Metal Ions in Crystals', Academic, New York, 1970.
66. L. E. Orgel, *J. Chem. Phys.*, 1955, **23**, 1004.
67. J. Ferguson, *Prog. Inorg. Chem.*, 1970, **12**, 159.
68. B. N. Figgis, *Nature (London)*, 1958, **182**, 1568.
69. M. Kotani, *J. Phys. Soc. Jpn.*, 1949, **4**, 293.
70. B. N. Figgis, J. Lewis, F. E. Mabbs and G. A. Webb, *J. Chem. Soc. (A)*, 1966, 1411.
71. A. D. Liehr and C. J. Ballhausen, *Ann. Phys. (New York)*, 1959, **2**, 134.
72. R. Finkelstein and J. H. Van Vleck, *J. Chem. Phys.*, 1940, **8**, 790.
73. T. M. Dunn and W.-K. Li, *J. Chem. Phys.*, 1967, **47**, 3783.
74. J. Ferguson, H. J. Guggenheim and E. R. Krausz, *Aust. J. Chem.*, 1969, **22**, 1809.
75. J. W. Stout, *J. Chem. Phys.*, 1959, **31**, 709.
76. J. C. Eisenstein, *J. Chem. Phys.*, 1961, **34**, 1628.
77. W. A. Runciman and K. A. Schroeder, *Proc. Roy. Soc. (London)*, 1961, **A265**, 489.
78. Y. Tanabe and H. Kamimura, *J. Phys. Soc. Jpn.*, 1958, **13**, 394.
79. J. S. Griffith, *Trans. Faraday Soc.*, 1958, **54**, 1109.
80. J. S. Griffith, *Trans. Faraday Soc.*, 1960, **56**, 193.
81. A. D. Liehr, *J. Phys. Chem.*, 1960, **64**, 43.
82. K. A. Schroeder, *J. Chem. Phys.*, 1962, **37**, 1587.
83. G. H. Dieke, 'Spectral Energy Levels in Rare Earth Ions in Crystals', ed. H. M. Crosswhite and H. Crosswhite, Interscience, New York, 1968.
84. K. R. Lea, M. J. M. Leask and W. P. Wolf, *J. Phys. Chem. Solids*, 1962, **23**, 1381.
85. D. J. Lam and A. T. Aldred, 'The Actinides: Electronic Structure and Related Properties', ed. A. J. Freeman and J. B. Darby, Academic, New York, 1974.
86. F. E. Mabbs and D. J. Machin, 'Magnetism and Transition Metal Complexes', Chapman and Hall, London, 1973.
87. B. N. Figgis, *Trans. Faraday Soc.*, 1961, **57**, 198.
88. P. H. E. Meijer and H. J. Gerritsen, *Phys. Rev.*, 1955, **100**, 742.
89. E. Koenig and R. Schnakig, *Phys. Status Solidi B*, 1976, **77**, 857.
90. E. Koenig, R. Schnakig, S. Kremer, B. Kanellanopulos and R. Klenze, *Chem. Phys.*, 1978, **27**, 331.
91. B. W. Dale, R. J. P. Williams, C. E. Johnson and T. L. Thorp, *J. Chem. Phys.*, 1968, **49**, 3441.
92. T. J. Marks, *Prog. Inorg. Chem.*, 1978, **24**, 51.
93. T. J. Marks, *Prog. Inorg. Chem.*, 1979, **25**, 223.
94. J. Ferguson, 'Electronic States of Inorganic Compounds: New Experimental Techniques', ed. P. Day, Reidel, Boston, 1975.
95. A. B. P. Lever, *Coord. Chem. Rev.*, 1968, **3**, 119.
96. A. B. P. Lever, *Coord. Chem. Rev.*, 1982, **43**, 63.
97. B. J. Hathaway, *Struct. Bonding (Berlin)*, 1973, **14**, 49.
98. C. J. Ballhausen, 'Molecular Electronic Structure of Transition Metal Complexes', McGraw Hill, New York, 1979.
99. P. Day (ed.), 'Electronic Structure and Magnetism of Inorganic Compounds', Specialist Reports, Royal Society of Chemistry, vol. 1, London, 1970.
100. M. A. Hitchman, *Transition Met. Chem.*, 1984, **9**, 1.
101. P. J. Stevens, 'Electronic States of Inorganic Compounds: New Experimental Techniques', ed. P. Day, Reidel, Boston, 1975.
102. C. D. Flint, *Coord. Chem. Rev.*, 1974, **14**, 47.
103. M. Cieslak-Golonka, A. Bartecki and S. P. Sinha, *Coord. Chem. Rev.*, 1980, **31**, 251.
104. J. Ferguson and H. J. Guggenheim, *J. Chem. Phys.*, 1966, **44**, 1095.
105. A. D. Liehr and C. J. Ballhausen, *Phys. Rev.*, 1957, **106**, 1161.
106. A. D. Liehr and C. J. Ballhausen, *Ann. Phys. (New York)*, 1958, **3**, 304.

107. S. Koide and M. H. L. Pryce, *Philos. Mag.*, 1958, **3**, 607.
108. S. Koide, *Philos. Mag.*, 1959, **4**, 243.
109. D. E. Henrie, R. L. Fellows and G. R. Choppin, *Coord. Chem. Rev.*, 1976, **18**, 199.
110. W. Moffitt, G. L. Goodman, M. Fred and B. Weinstock, *Mol. Phys.*, 1959, **2**, 109.
111. H. A. Jahn and E. Teller, *Proc. Roy. Soc. (London)*, 1937, **A161**, 220.
112. H. A. Jahn, *Proc. Roy. Soc. (London)*, 1938, **A164**, 117.
113. R. Englman, 'The Jahn–Teller Effect in Molecules and Crystals', Wiley-Interscience, New York, 1976.
114. E. Koenig, *Struct. Bonding (Berlin)*, 1971, **9**, 175.
115. M. D. Sturge, *Solid State Phys.*, 1967, **20**, 91.
116. N. S. Ham, *Spectrochim. Acta*, 1962, **18**, 775.
117. I. B. Bersuker, *Coord. Chem. Rev.*, 1975, **14**, 357.
118. W. C. Scott and M. D. Sturge, *Phys. Rev.*, 1966, **146**, 262.
119. G. A. Slack, F. S. Ham and R. M. Chrenko, *Phys. Rev.*, 1966, **152**, 376.
120. R. Englman, *Mol. Phys.*, 1960, **3**, 23, 48.
121. L. L. Lohr, *J. Chem. Phys.*, 1969, **50**, 4596.
122. N. S. Hush and R. J. M. Hobbs, *Prog. Inorg. Chem.*, 1968, **10**, 259.
123. D. M. Gruen, *Prog. Inorg. Chem.*, 1971, **14**, 119.
124. G. C. Allen and K. D. Warren, *Coord. Chem. Rev.*, 1975, **16**, 227.
125. D. R. Rosseinsky and I. A. Dorrity, *Coord. Chem. Rev.*, 1978, **25**, 31.
126. C. N. R. Rao and J. R. Ferraro (eds.), 'Spectroscopy in Inorganic Chemistry', Academic, New York, 1970.
127. C. J. Ballhausen and A. E. Hansen, *Annu. Rev. Phys. Chem.*, 1972, **23**, 15.
128. A. E. Martell (ed.), 'Coordination Chemistry', Van Nostrand, New York, 1971, vol. 1.
129. L. Banci, A. Bencini, C. Benelli, D. Gatteschi and C. Zanchini, *Struct. Bonding (Berlin)*, 1982, **52**, 37.
130. P. D. Fleischauer, A. W. Adamson and G. Sartori, *Prog. Inorg. Chem.*, 1972, **17**, 1; 'Concepts of Inorganic Photochemistry', Interscience, New York, 1975.
131. M. A. Jamieson, N. Serpone and M. Z. Hoffman, *Coord. Chem. Rev.*, 1981, **39**, 121.
132. L. G. Vanquickenborne and A. Ceulemans, *Coord. Chem. Rev.*, 1983, **48**, 157.
133. A. D. Kirk, *Coord. Chem. Rev.*, 1981, **39**, 225.
134. P. Gans, *Coord. Chem. Rev.*, 1976, **19**, 99.
135. I. M. Walker and R. L. Carlin, *J. Chem. Phys.*, 1967, **46**, 3931.
136. D. S. McClure, *J. Chem. Phys.*, 1962, **36**, 2757.
137. D. W. Barnum, *J. Inorg. Nucl. Chem.*, 1961, **21**, 221.
138. J. Selbin, *Chem. Rev.*, 1965, **65**, 153.
139. J. Selbin, *Coord. Chem. Rev.*, 1966, **1**, 293.
140. F. A. Blankenship and R. L. Belford, *J. Chem. Phys.*, 1962, **36**, 633.
141. P. C. H. Mitchell, *Quart. Rev. Chem. Soc.*, 1966, **20**, 103.
142. J. R. Perumareddi, A. D. Liehr and A. W. Adamson, *J. Am. Chem. Soc.*, 1963, **85**, 249.
143. C. J. Ballhausen and W. Moffitt, *J. Inorg. Nucl. Chem.*, 1956, **3**, 178.
144. R. A. D. Wentworth and T. S. Piper, *Inorg. Chem.*, 1965, **4**, 709.
145. H. Yamatera, *Bull. Chem. Soc. Jpn.*, 1958, **31**, 95.
146. D. S. McClure, 'Advances in the Chemistry of Coordination Compounds', ed. S. Kirschner, MacMillan, New York, 1961.
147. P. B. Dorain, *Transition Met. Chem.*, 1968, **4**, 1.
148. J. P. Fackler and D. G. Holah, *Inorg. Chem.*, 1965, **4**, 954, 1112, 1721.
149. H. A. Weakliem, *J. Chem. Phys.*, 1962, **36**, 2117.
150. H. B. Gray, *Transition Met. Chem.*, 1965, **1**, 239.
151. M. Nicolini, C. Pecile and A. Turco, *Coord. Chem. Rev.*, 1966, **1**, 133.
152. M. Campolini, N. Nardi and G. P. Serponi, *Coord. Chem. Rev.*, 1966, **1**, 222.
153. L. Sacconi, *Coord. Chem. Rev.*, 1966, **1**, 192.
154. J. S. Wood, *Prog. Inorg. Chem.*, 1972, **16**, 227.
155. R. Morassi, I. Bertini and L. Sacconi, *Coord. Chem. Rev.*, 1973, **11**, 343.
156. Y. Nishida and S. Kida, *Coord. Chem. Rev.*, 1979, **27**, 275.
157. L. Sacconi, *Transition Met. Chem.*, 1968, **4**, 199.
158. L. F. Bates, 'Modern Magnetism', Cambridge University Press, Cambridge, 1961.
159. H. Zijlstra, 'Experimental Methods in Magnetism', Selected Topics in Solid State Physics IX, ed. P. Wolfath, Elsevier, New York, 1967, vol. 2.
160. M. Gerloch, 'Magnetism and Ligand Field Analysis', Cambridge University Press, Cambridge, 1983.
161. A. S. Chakravarty, 'Introduction to the Magnetic Properties of Solids', Wiley-Interscience, New York, 1970.
162. T. I. Quickenden and R. C. Marshall, *J. Chem. Educ.*, 1972, **49**, 114.
163. J. B. Goodenough, 'Magnetism and the Chemical Bond', Interscience, New York, 1963.
164. A. B. Lidiard, *Repts. Prog. Phys.*, 1954, **17**, 201.
165. L. Brillouin, *J. Phys. Radium*, 1927, **8**, 74.
166. E. Koenig, *Landolt-Bornstein*, Springer-Verlag, Berlin, 1966, Group II, vol. 2.
167. L. N. Mulay and E. A. Boudreaux (eds.), 'Theory and Applications of Molecular Dimagnetism', Wiley-Interscience, New York, 1976.
168. F. E. Mabbs and D. J. Machin, 'Magnetism and Transition Metal Complexes', Chapman and Hall, London, 1973.
169. C. J. O'Connor, *Prog. Inorg. Chem.*, 1982, **29**, 203.
170. B. N. Figgis, *Trans. Faraday Soc.*, 1960, **56**, 1553.
171. B. N. Figgis, M. Gerloch and R. Mason, *Proc. Roy. Soc. (London)*, 1964, **A279**, 210.
172. B. N. Figgis, J. Lewis, F. E. Mabbs and G. A. Webb, *J. Chem. Soc. (A)*, 1967, 442.
173. B. N. Figgis, M. Gerloch, J. Lewis, F. E. Mabbs and G. A. Webb, *J. Chem. Soc. (A)*, 1968, 2086.
174. S. Mitra, *Prog. Inorg. Chem.*, 1977, **22**, 309.
175. W. deW. Horrocks, *Coord. Chem. Rev.*, 1971, **6**, 147.
176. E. Koenig and S. Kremer, 'Ligand Field Energy Diagrams', Plenum Press, New York, 1977.
177. E. Koenig and S. Kremer, 'Magnetism Diagrams for Transition Metal Ions', Plenum Press, New York, 1979.
178. R. L. Martin and A. H. White, *Transition Met. Chem.*, 1968, **4**, 113.
179. H. A. Goodwin, *Coord. Chem. Rev.*, 1976, **18**, 293.
180. P. Gutlich, *Struct. Bonding (Berlin)*, 1981, **44**, 83.
181. E. Koenig and S. Kremer, *Theor. Chim. Acta*, 1971, **23**, 12.
182. L. G. Vanquickenborne and L. Haspeslagh, *Inorg. Chem.*, 1982, **21**, 2448.
183. G. Harris, *Theor. Chim. Acta*, 1968, **10**, 119, 155.

184. B. N. Figgis and R. L. Martin, *J. Chem. Soc.*, 1956, 3837.
185. A. P. Ginsberg, *Inorg. Chim. Acta Rev.*, 1971, **5**, 45.
186. E. A. Boudreaux and L. N. Mulay, 'Theory and Applications of Molecular Paramagnetism', Wiley-Interscience, New York, 1976.
187. G. E. Pake and T. M. Estle, 'The Physical Principles of Paramagnetic Resonance', Benjamin, New York, 1976.
188. C. P. Slicher, 'Principles of Magnetic Resonance', Harper, New York, 1963.
189. W. Low, 'Paramagnetic Resonance in Solids', Academic, New York, 1960.
190. B. R. McGarvey, *Transition Met. Chem.*, 1966, **3**, 89.
191. B. R. Bencini and D. Gatteschi, *Transition Met. Chem.*, 1982, **8**, 1.
192. E. Koenig and G. Koenig, *Landolt-Bornstein*, Springer-Verlag, Berlin, 1976, Group II, vol. 8.
193. E. Koenig and G. Koenig, *Landolt-Bornstein*, Springer-Verlag, Berlin, 1979, Group II, vol. 10.
194. E. Koenig and G. Koenig, *Landolt-Bornstein*, Springer-Verlag, Berlin, 1980, Group II, vol. 11, 1983, vol. 12a, 1984, vol. 12b.
195. B. A. Goodman and J. B. Raynor, *Adv. Inorg. Chem. Radiochem.*, 1970, **13**, 135.
196. M. Melnik, *Coord. Chem. Rev.*, 1982, **42**, 259.
197. D. J. Hodgson, *Prog. Inorg. Chem.*, 1975, **19**, 173.

7.1

Substitution Reactions

MARTIN L. TOBE
University College London, UK

7.1.1 INTRODUCTION AND DEFINITIONS

7.1.1.1 Introduction

Although the detailed study of the mechanisms of inorganic reactions was not undertaken until the foundations of organic reaction mechanisms were laid, and even now it only attracts the interest of a small number of people (relative to the hordes that have been involved with the organic systems), a comprehensive account of one aspect, namely substitution reactions, would be supported by many thousands of references. Fortunately, the field has been reviewed extensively and all references worth considering up to 1966 can be found in the yet unsurpassed classic of Basolo and Pearson.[1] The *Specialist Periodical Reports* of the Chemical Society[2] provide a comprehensive coverage of the literature from 1969 to 1979, when they were unaccountably withdrawn, but fortunately they have reappeared thanks to Martyn Twigg and Plenum Press.[3] The gap between 1966 and 1969 is partly filled by the *MTP International Review of Science* series.[4] In addition, there are many textbooks[5–11] which cover the subject at various levels and multiauthor volumes containing selections of review articles, some or all of which are relevant to ligand substitution.[12–17] There are many other specialist reviews which will be referred to at appropriate places in the text. The point has been reached where no self-respecting general textbook on inorganic chemistry can be without its chapters on inorganic reaction mechanisms.[18–20] Courses of 10 or more lectures on the subject are a common feature of advanced inorganic chemistry courses for undergraduates in the universities of Great Britain and North America.

7.1.1.2 Substitution Reactions

In terms of coordination chemistry, a substitution reaction can be defined as a process whereby a ligand in a complex is replaced by another ligand from outside. This definition can be applied to any system provided one can identify a reaction centre and an entering and leaving group, but it remains ambiguous until it is specified whether it relates to observations on matter in bulk (*i.e.* the relationship between reagents and products in a preparative reaction) or to a specific set of acts at the molecular level. Many preparative substitution reactions, on close examination, appear to involve passage through an intermediate whose oxidation state differs from that of the substrate and the product, and the act of ligand substitution arises from a general or specific high lability in this intermediate, or is a direct consequence of the redox processes involved in its formation or consumption. Although of considerable importance and interest, both practically and theoretically, such processes have not yet been studied systematically and in depth. Because of shortness of space such reactions have not been included in this chapter but a review of some aspects is available.[21]

The term *substitution reaction* will therefore be restricted to those processes where the act of ligand substitution involves a temporary change in the coordination number of the reaction centre and nothing more. In the reactions of classical coordination complexes, the Lewis acid–Lewis base relationship between the metal and the ligand ensures that the process is *nucleophilic*, *i.e.* the leaving group departs with its pair of electrons and the entering group arrives with its pair of electrons. As a consequence the number of non-bonding electrons on the reaction centre does not change and its oxidation state remains constant. This is not true for *electrophilic* or *homolytic* substitution where, irrespective of the molecularity, there is, albeit momentarily, a change in the number of non-bonding electrons at the reaction centre and hence in its oxidation state. Initiation of substitution will only lead to substitution if the intermediate generated undergoes a subsequent reaction that mirrors the mode of its formation. Thus, the two-electron oxidation that is the formal result of adding an electrophile to the reaction centre can be reversed when the electrofuge departs leaving a pair of electrons behind and results in an act of electrophilic substitution. However, the oxidation may be 'frozen' when the adduct (now possibly coordinatively unsaturated) stabilizes itself by adding a ligand (nucleophile) from its environment. Such a mechanism is one of those associated with the highly important *oxidative addition* reaction (Scheme 1). A similar process involving shifting one electron from a non-bonding to a bonding situation could represent homolytic substitution and one-electron oxidative addition. Dissociative electrophilic and homolytic substitution could be diverted to analogous two-electron and one-electron reduction processes.

7.1.1.3 Molecularity

In discussing the molecularity of substitution reactions the Langford–Gray nomenclature will be used throughout.[6] This defines a STOICHIOMETRIC mechanism, which distinguishes processes

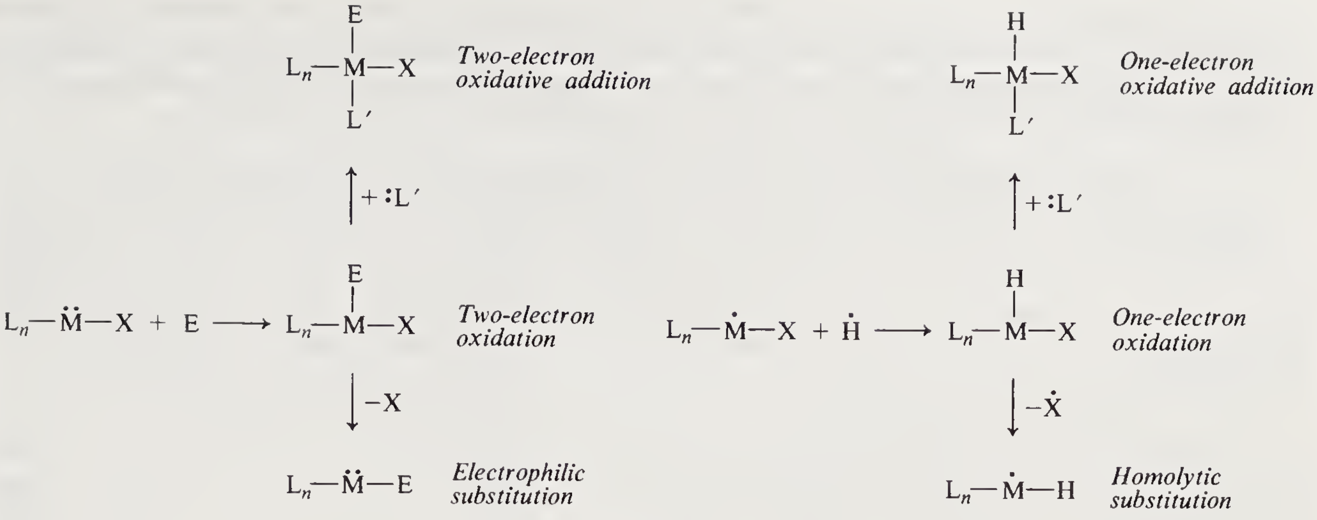

Scheme 1

where independently reacting intermediates can be detected by kinetic, stereochemical or product distribution studies, from those where none can be seen. The latter are termed INTERCHANGE processes and labelled *I*, while the former are termed ASSOCIATIVE, *A*, if the intermediate has a higher coordination number than the substrate, or DISSOCIATIVE, *D*, if it has a lower coordination number. The interchange process requires further subdivision according to its INTIMATE mechanism. If the rate of interchange is sensitive to the nature of the entering group it is assumed that there is bonding between it and the reaction centre in the rate determining transition state and the process is said to be ASSOCIATIVELY ACTIVATED and labelled with the subscript 'a'. If the rate of interchange is independent of the nature of the entering group it is assumed to be DISSOCIATIVELY ACTIVATED and labelled with subscript 'd'. The interchange process is therefore subdivided into I_a and I_d processes. Assignment of an intimate mechanism to a *D* process is redundant, and it is difficult to see how an *A* process can have a d intimate mechanism. However, since the formation of an intermediate of higher coordination number is associated with a bond making *and* a bond breaking stage, it is important to know which of the two processes has the higher energy transition state.[22,23] The Langford–Gray nomenclature has proved to be very useful in the past but it now appears that *D* mechanisms are rarer than was once thought and that a major part of substitution takes place with interchange mechanisms. This is not too surprising when the solvent is water, or water like, and where, in order to compete with the solvent, other nucleophiles must be in position before the act of substitution is initiated. Considerable interest is being aroused regarding the questions of the lifetimes of the postulated intermediates and this will be disscussed in the appropriate places in the review. Some doubt is now arising as to whether the Langford–Gray system of mechanistic labelling with its operational definitions is as big an advance over the old S_N1, S_N2 nomenclature as was thought. A penetrating critique has recently been published[24] and similar questions have concerned organic reaction mechanists.[25,26]

7.1.2 KINETICS AND MECHANISM OF SOLVENT EXCHANGE

Conceptually, the simplest substitution reaction of a coordination complex is the exchange between the coordinated solvent molecules of a solvated metal ion and free molecules of solvent S:

$$[\mathrm{M(S)}_N]^{n+} + {}^*\mathrm{S} \rightleftharpoons [\mathrm{M(S)}_{N-1}{}^*\mathrm{S}]^{n+} + \mathrm{S}, \ etc.$$

It allows a detailed examination of the way in which the rate and mechanism depend upon the parameters of the metal ion, *e.g.* size, charge, electronic configuration, coordination number, and those of the solvent, *e.g.* size, dipole moment, nature of the donor atom. It can be applied to both labile and inert systems provided the solvated cations can exist in the conditions under which the measurements are made. For inert complexes it is possible to exchange a smaller number of ligands (ideally one) with the solvent and to extend the number of parameters that can be examined independently. The isotopic dilution technique, which requires that the time of sampling is short compared to the half-life of the exchange, has only been used in a limited number of cases.[27,28] The quenched-flow method used to determine the solvation number of Al^{3+},[29] was not used to follow the exchange kinetics. Although isotopic exchange techniques are still being used,[30] the major part of the published work is based on NMR line broadening and other relaxation techniques. Stopped-flow NMR has also been used when exchange nalf-times are long on the NMR timescale.[31] The line broadening technique became available towards the end of the 1950s and many of the references date between 1960 and 1966. There has been a recent revival of interest as a result of the extra information that can be obtained from the dependence of rate upon pressure. The whole area has been reviewed extensively and on many occasions.[11,25,32–35] A selection of rate constants, enthalpies, entropies and volumes of activation are collected in Table 1.

Table 1 Rate Constants and Activation Parameters[a] for the Exchange of Water with $[M(H_2O)_6]^{n+}$

Configuration	$3d^0$	$3d^1$	$3d^2$	$3d^3$	$3d^4$	$3d^5$	$3d^6$	$3d^7$	$3d^8$	$3d^9$	$3d^{10}$
M	Ca^{2+}	—	—	V^{2+}	Cr^{2+}	Mn^{2+}	Fe^{2+}	Co^{2+}	Ni^{2+}	Cu^{2+}	Zn^{2+}
log *k*	8.4[32]	—	—	1.9[36]	> 8.5[37]	7.32[38]	6.64[38]	6.51[38]	4.50[38]	9.9[39]	7.5[32]
$\Delta H^{\ddagger}$/kJ mol^{-1}	—	—	—	61.9	—	33.0	41.0	46.8	56.9	23.0	—
$\Delta S^{\ddagger}$/J K^{-1} mol^{-1}	—	—	—	0	—	5.9	20.9	36.8	32.2	25.1	—
$\Delta V^{\ddagger}$/cm^3 mol^{-1}	—	—	—	−4.1	—	−5.4	+3.8	+6.1	+7.2	—	—
M	—	Ti^{3+}	V^{3+}	Cr^{3+}	—	Fe^{3+}	—	—	—	—	Ga^{3+} [b]
log *k*	—	5.26[40]	2.69[59]	−5.5[27]	—	2.20[42]	—	—	—	—	2.60[40]
$\Delta H^{\ddagger}$/kJ mol^{-1}	—	43.5	49.3	109.9	—	64.0	—	—	—	—	66.9
$\Delta S^{\ddagger}$/J K^{-1} mol^{-1}	—	1.3	−27.6	15.9	—	12.1	—	—	—	—	30.1
$\Delta V^{\ddagger}$/cm^3 mol^{-1}	—	−12.1	−8.9	−9.3[41]	—	−5.4[43]	—	—	—	—	+5.0

[a] At 25 °C, although some of the $\Delta V^{\ddagger}$ values were determined at lower temperatures.
[b] An earlier study of this system[44] did not take sufficient account of the acid hydrolysis of this ion.

The utilization of these data is mainly twofold. Firstly they provide a means of studying quantitatively the relationship between lability and parameters such as electron configuration, frontier orbital symmetry, charge and size, and, secondly, in combination with the data for ligand substitution in these solvated ions, they allow an assignment of mechanism to these reactions, assuming of course that the replacement of a coordinated solvent molecule by another ligand would be mechanistically similar to the replacement of one solvent molecule by another. More recently, application of volumes of activation has allowed a direct assignment of molecularity to the exchange reaction. The validity of this application and the general significance of $\Delta V^{\ddagger}$ has been reviewed in great depth[34,45,46] and although the nature of the corrections to be applied in reactions where there is a significant development or cancellation of charge on going from the ground state to the transition state, *i.e.* when there is a considerable solvation change of activation, may be open to some debate,[47] its application to solvent exchange rests on firm ground. The main contribution to the $\Delta V^{\ddagger}$ value in such a process is the loosening in I_d, or the release in D of a coordinated solvent molecule and the expansion that accompanies it, or the capture and subsequent constriction of a solvent molecule in the I_a or A mechanism. Attention has been paid to the possibility of geometric change in the transition state. For example, the activation parameters for water exchange[48,49] in *trans*-$[Co(en)_2(H_2O)_2]^{3+}$ are different from those of the slower accompanying *trans* → *cis* isomerization.[48,50] In particular, the great increase in $\Delta V^{\ddagger}$ on going from the water exchange (+5.9 cm^3 mol^{-1}),[49] which is stereoretentive and thought to be I_d with a square pyramidal intermediate, to the isomerization (+14.3 cm^3 mol^{-1}),[50] which is thought to be D with a trigonal bipyramidal intermediate, is ascribed to the releasing of solvating water that accompanies the opening of the square pyramid to form the trigonal bipyramid.

The water exchange rate for bivalent, high-spin transition metal ions demonstrates the wide range of lability that can be encountered. The minima at $3d^3$ (V^{2+} and Cr^{3+}) and $3d^8$ (Ni^{2+}) were predicted long ago on the basis of the amount of crystal field stabilization energy lost on going from the ground state to the transition state[51] and later by somewhat more sophisticated arguments.[52] The high reactivity of $3d^4$ (Cr^{2+}) and $3d^9$ (Cu^{2+}) is a consequence of the Jahn–Teller distortions expected in the ground states of these configurations. Exchange at the weakly bound tetragonally extended sites is almost diffusion controlled and a facile vibration allows rapid exchange of the six coordination sites. For the first-row divalent aquo ions $[M(H_2O)_6]^{2+}$, the volumes of activation indicate a change from associative activation for V^{2+} and Mn^{2+} to dissociative activation for the rest (Fe^{2+}, Co^{2+} and Ni^{2+}) and it has been suggested that in these relatively electrovalent complexes, the size of the ion, and hence its ability to increase its coordination number temporarily if large enough, plays the major part in determining the mode of activation.[36,38] The number of tervalent $[M(H_2O)_6]^{3+}$ first-row transition metal ion systems that has been examined in depth is far less but the negative $\Delta V^{\ddagger}$ values indicate that the associative mode of activation is still found for the d^2, d^3 and d^5 configurations in spite of the smaller size of the 3+ cation.[34,41,43] The mechanistic conclusions drawn from the volumes of activation are partially borne out by the studies of the kinetics of complex formation and the extent to which the interchange process can discriminate between the different nucleophiles. However, the lack of discrimination in the interchange reactions of Mn^{2+} contradicts the negative $\Delta V^{\ddagger}$ values. It has been suggested that the lack of discrimination does not necessarily indicate a dissociative mechanism in an essentially electrostatic system.[38,41] Langford[53] has tried to relate the change in the sign of $\Delta V^{\neq}$ to the way in which the non-bonding *d*-electrons affect the extent to which the non-exchanging ligands can mitigate the changes caused by ligand loss or ligand gain, but there are strong counter arguments.[54,55]

Studies of ligand exchange in non-aqueous solvent systems have increased enormously in recent years. In general, the results parallel those obtained in water but frequently the reactions are slower. A selection of rate constants and activation data can be found in ref. 34. Once again, examples are found of associative activation and others of dissociative activation and the main controlling features seem to be ion size and ligand size. Coordination numbers may be different from those found in aqueous solution, especially for ions where orbital symmetry and directional covalence do not require a fixed coordination number and geometry. Changes in the dominant coordination number can be observed on changing the temperature, *e.g.* $[Ga(MeOH)_6]^{3+}$ changes to $[Ga(MeOH)_7]^{3+}$ below −45°C,[56] or on changing the pressure, *e.g.* $[Nd(DMF)_8]^{3+}$ changes to $[Nd(DMF)_9]^{3+}$ on increasing the pressure.[57] Studies of this sort give the clue as to the mode of activation. Systematic studies on the solvated lanthanide ions $[Ln(DMF)_8]^{3+}$ exchanging with solvent in DMF indicate that the mode of activation changes from associative to dissociative as the size of the Ln^{3+} ion decreases on going along the group, the dissociative mode of activation changing from I_d for Ln = Tb, Dy, Ho and Er to *D* for Ln = Tm and Yb.[57] In these ions, eight coordination dominates but of course when eight and nine coordination are in equilibrium, the complexes are extremely labile with respect to exchange, and nine-coordinate systems of necessity exchange dissociatively while eight-coordinate systems exchange associatively.

The classification of solvent exchange reactions has been extended by Merbach[34] to include reactions where a neutral ligand is exchanged with a similar species which is in dilute solution in a non-interfering solvent. Here, of course, we have the ideal systems for mechanistic assignment from rate laws as well as volumes of activation. For example, the mechanistic pattern for the exchange of DMF reported above is maintained when the reaction mixture is diluted with nitromethane and the kinetics are totally consistent with the assignment of the I_d mechanism (k_{obs} dependent upon [DMF] until a limiting value is reached) for Ln = Tb, and a *D* mechanism (k_{obs} independent of [DMF]) for Ln = Tm. However, from the point of view of general discussion it is convenient to consider these reactions under a separate heading and to include not only these 'solvato complexes' $[MS_N]^{n+}$, removed from their parent solvent, but any form of ligand exchange that can be carried out under these conditions.

7.1.3 SUBSTITUTION REACTIONS IN NON-INTERFERING SOLVENTS

7.1.3.1 General Remarks

When interest first developed in the study of inorganic substitution reaction mechanisms, the substrates used, usually classical Werner complexes, were not particularly soluble in non-aqueous solvents. It was soon clear that water was a strongly interfering solvent and became deeply involved in the act of substitution either as an entering group or a leaving group. When such studies were extended to other solvent systems, it soon became apparent that the absence of directly observable amounts of the solvento complex did not guarantee that the solvent was not involved in the same way as water and the preparation and study of many such species was necessary to show whether or not 'cryptosolvolysis' (solvent mediated substitution where no measurable amounts of the solvento intermediate were generated) dominated the act of ligand substitution.[58–61] This has proved to be particularly important in the substitution reactions of four-coordinate planar d^8 complexes and is discussed in Section 7.1.7.

The systematic study of substitution reactions in non-participating solvents is now well advanced and involves charged, as well as uncharged, reagents. In general, non-interfering solvents are non-coordinating and frequently non-polar so that ionogenic reactions are less favoured because the solvation cannot assist the separation of charge, but they certainly cannot be ruled out altogether. Reactions involving the exchange of neutral ligands can give the most direct kinetic evidence of the mechanism of activation because they do not require the correction for ion association between the substrate and the reagent, nor between the reagent (and/or the substrate) and its counter ion. Volumes of activation need no correction for electrostriction effects.

7.1.3.2 Exchange Reactions of Solvato Ions

Studies of the exchange reactions indicated by equation (1) have been considered in Section 7.1.2. Since dissolving $[M(S)_N](ClO_4)_n$ (or the salt with any other anion that coordinated much more poorly than S) in a non-coordinating solvent and examining the way in which the rate of exchange depends upon the concentration of added S is in no way different from taking a solution of $[M(S)_N](ClO_4)_n$ in solvent S and seeing how the rate of exchange is affected by diluting it with another, inert, solvent, many of these reactions have been examined in conjunction with the solvent exchange and are still classified as solvent exchange. A selection of published data is collected in Table 2, where the rate laws, volumes of activation (where known) and the proposed mechanisms are considered.

Table 2 Kinetic Rate Laws, Volumes of Activation and Assigned Mechanisms for Reactions of the Type $[MS_N]^{n+} + {}^*S \rightarrow [MS_{N-1}{}^*S]^{n+} + S$ in Inert Solvents

Complex	S^b	*Solvent*	*Dependence on [S]*			$\Delta V^{\ddagger}$	*Refs.*
			Independent	*Linear*	*Curved*	(cm^3 mol^{-1})	
			D	I_a, A	I_d		
$[BeS_4]^{2+}$	TMP	CD_2Cl_2	√	—	—	—	62
$[BeS_4]^{2+}$	TMP	CD_3NO_2	—	√	—	—	63
$[BeS_4]^{2+}$	DMMP	CD_3NO_2	—	√	—	—	63
$[MgS_6]^{2+}$	TMP	CD_2Cl_2	√	—	—	—	64
$[MgS_6]^{2+}$	TMP	$(CD_3)_2CO$	√	—	—	—	64
$[AlS_6]^{3+}$	TMP	CD_3NO_2	√	—	—	—	65
$[AlS_6]^{3+}$	DMMP	CD_3NO_2	√	—	—	—	65
$[AlS_6]^{3+}$	DMSO	CD_3NO_2	√	—	—	+15.6	66,67
$[AlS_6]^{3+}$	DMF	CD_3NO_2	√	—	—	+13.7	66
$[AlS_6]^{3+}$	DMMP	CD_3NO_2	√	—	—	—	65
$[AlS_6]^{3+}$	TMP	CD_3NO_2	√	—	—	+22.5	68,69
$[AlS_4]^{3+}$	HMPA	CD_3NO_2	—	√	—	—	65
$[GaS_6]^{3+}$	DMSO	CD_3NO_2	√	—	—	+13.1	66,67
$[GaS_6]^{3+}$	DMF	CD_3NO_2	√	—	—	+7.9	66
$[GaS_6]^{3+}$	TMP	CD_3NO_2	√	—	—	+20.7	68,69
$[InS_6]^{3+}$	TMP	CD_3NO_2	—	√	—	−22.9	68,69
$[ScS_6]^{3+}$	TMP	CD_3CN	√	√	—	—	70
$[ScS_6]^{3+}$	TMP	$C_2D_2Cl_4$	√	√	—	—	70
$[ScS_6]^{3+}$	TMP	CD_3NO_2	—	√	—	—	70
$[ScS_6]^{3+}$	DMMP	CD_3CN	√	√	—	—	71
$[ScS_6]^{3+}$	DMMP	CD_3NO_2	—	√	—	—	71
$[ScS_6]^{3+}$	NMA	CD_3CN	√	√	—	—	72
$[ScS_6]^{3+}$	DMA	CD_3NO_2	√	√	—	—	72
$[ScS_6]^{3+}$	DMA	CD_3CN	√	√	—	—	72
$[ScS_6]^{3+}$	DEA	CD_3NO_2	√	√	—	—	72
$[ScS_6]^{3+}$	DEA	CD_3CN	√	√	—	—	72
$[ScS_6]^{3+}$	TMU	CD_3NO_2	√	—	—	—	73
$[ScS_6]^{3+}$	TMP	CD_3NO_2	—	√	—	−18.7	34
$[ZnS_4]^{2+}$	TMTU	CD_2Cl_2	√	—	—	—	74
$[ZnS_4]^{2+}$	HMPA	CD_2Cl_2	—	√	—	—	75
$[ErS_8]^{3+}$	DMF	CD_3NO_2	√	—	√	+5.4[a]	76
$[TbS_8]^{3+}$	DMF	CD_3NO_2	—	—	√	+5.7[a]	57
$[TmS_8]^{3+}$	DMF	CD_3NO_2	√	—	—	+7.4[a]	57

[a] Values for exchange in DMF (= $HC(O)NMe_2$).
[b] TMP = $(MeO)_3PO$; DMMP = $(MeO)_2(Me)PO$; NMA = $MeC(O)NHMe$; DMA = $MeC(O)NMe_2$; DEA = $MeC(O)NEt_2$; TMU = $OC(NMe_2)_2$; DMSO = Me_2SO; HMPA = $(Me_2N)_3PO$; TMTU = $SC(NMe_2)_2$.

The rate laws that are observed are (i) zero order with respect to [S], usually attributed to a D mechanism, although an I_d mechanism with strong preferential outer-sphere association by S might have reached this saturation limit at the lowest [S] employed; (ii) first order with respect to [S] suggesting either an A mechanism or I_a (or even I_d with unfavoured solvation); (iii) a mixed zero- and first-order dependence on [S] which has been interpreted as a duality of mechanism, *i.e.* parallel dissociatively and associatively activated pathways; and (iv) a non-linear dependence on [S] that is fully consistent with the approach to saturation that is associated with an interchange process. Even under the ideal conditions of having an inert solvent, the rate law does not allow an unambiguous assignment of mechanism and $\Delta V^{\ddagger}$ values are now frequently measured to help resolve the problem. The two-term rate laws found in the reactions of $[ScS_6]^{3+}$ present problems of interpretation similar to those in the substitutions of four-coordinate planar d^8 complexes (section 7.1.7.2), *i.e.* do they represent parallel dissociative and associative pathways or is the zero-order term the result of associative solvolysis? Each case must be treated on its own merits, but the very marked solvent dependence of the zero-order term in the cases where L = DMMP and TMP in CD_3CN (a significant zero-order term)[70] and in CD_3NO_2 (no zero-order term)[71] does suggest that acetonitrile is not as inert as supposed; however, the fact that the two-term rate law is also found[70] in $C_2D_2Cl_4$ makes this alternative unlikely. The change in mechanism in the Al^{III} system on going from dissociative substitution for the six-coordinate species to associative substitution for the four-coordinated species[65] is consistent with the importance of size and coordination unsaturation in determining the mode of activation. It is also interesting to note the change from 'd' to 'a' activation on going from S = $(Me_2N)_2CS$ to S = $(Me_2N)_3PO$ in the exchange of $[ZnS_4]^{2+}$;[74,75] it is suggested that the congestion caused by the larger sulfur donor disfavours the associative mechanism. This is in spite of the fact that zinc is on the 'hard–soft' borderline and might be expected to favour sulfur donor nucleophiles. The change from dissociative to associative exchange on going from $[Al(TMP)_6]^{3+}$ and $[Ga(TMP)_6]^{3+}$, on the one hand, to $[In(TMP)_6]^{3+}$, on the other, is consistent with the increase in the radius of the central atom.[68,69]

All systems studied in this way until now have a spherical distribution of the non-bonding electrons, so no account need be taken of the symmetry relationships between the ground state and the possible transition states. Consequently, the size of the reaction centre, the coordination number and the effective size and packability of the ligands determine whether the mode of activation is associative or dissociative. There is, as yet, no suitable evidence to decide whether the nucleophilicity of the entering group plays a significant part in deciding the mode of activation.

7.1.3.3 Exchange of Neutral Ligands with Neutral Complexes

A considerable body of information has been collected on reactions of this sort. The use of NMR line broadening has allowed a wide range of rates to be examined. A selection of the systems studied is collected in Table 3. A particularly interesting group of studies involves the pentahalide derivative of the type $[MX_5(R_2Y)]$, which are uncharged octahedral complexes, exchanging with free R_2Y in a non-coordinating solvent such as CD_2Cl_2 or $CDCl_3$ (M = Nb, Ta, Sb; X = Cl, Br; Y = O, S, Se, Te; and R = Me, Et). The exchanges of R_2S, R_2Se and R_2Te have clean second-order kinetics, the rate constants are much reduced on going from R = Me to Et, and the entropies and volumes of activation are negative. All of this is consistent with an associative mode of activation. On the other hand, the reactions with R_2O are zero-order with respect to $[R_2O]$, they are not retarded by increased steric hindrance and have positive $\Delta S^{\ddagger}$ and $\Delta V^{\ddagger}$ values, all of which is consistent with dissociative activation. Above 300 K, the exchange of $[TaBr_5(Me_2S)]$ with Me_2S has a two-term rate law, suggesting a mechanistic crossover point. What is lacking is the study of nucleophilic discrimination, k_2 values for the exchange of Me_2S, Me_2Se and Me_2Te being suspiciously similar.

Table 3 Rate Constants and Activation Parameters for the Exchange of the Neutral Ligand, L, in the Reaction[a] $[MX_5L] + {}^*L \rightarrow [MX_5{}^*L] + L$

M	*X*	*L*	k_1 (s^{-1})	k_2 $(M^{-1}\,s^{-1})$	$\Delta H^{\ddagger}$ $(kJ\,mol^{-1})$	$\Delta S^{\ddagger}$ $(J\,K^{-1}\,mol^{-1})$	$\Delta V^{\ddagger}$ $(cm^3\,mol^{-1})$	*Refs.*
Nb	Cl	Me_2O	80[b]	—	76.9	+64.8	+28.7	77,78
		MeCN	0.43[b,c]	—	71.1	+51.0	+19.5	77,79
		Me_3CCN	0.21[b,c]	—	71.5	+41.8	+15.2	77,79
		$(MeO)Cl_2PO$	25[a]	—	64.0	+16.7	+20.5	77,80
		$(Me_2N)_3PS$	1.8[b]	—	58.5	−25.1	+17.7	77,80
Nb	Br	Me_2O	3200	—	66.5	+66.9	—	78
Ta	Cl	Me_2O	1.6[c]	—	70.2	+18.0	—	78
		Me_2O	0.7	—	83.2	+58.5	+27.8	77,78
		Et_2O	4.5	—	—	—	—	78
Ta	Br	Me_2O	54	—	74.4	+62.7	+30.5	77,78
Sb	Cl	MeCN	—	—	66.9	+83.6	+24.7	34
		Me_3CCN	—	—	66.0	+71.1	+18.2	34
		Me_2O	—	—	74.8	+71.1	+27.2	34
		Et_2O[b]	—	—	95.7	+158.8	+30.0	34
		Me_2CO	—	—	70.6	+58.5	+28.1	34
		$(Me_2N)Cl_2PO$	—	—	71.1	+41.8	+20.4	34
Nb	Cl	Me_2S	—	15000	15.9	−104.5	—	78
Nb	Br	Me_2S	—	2600	17.6	−100.3	−12.1	77,78
Ta	Cl	Me_2S	—	1000	21.7	−108.7	−19.8	77,78
		Et_2S	—	46[d]	—	—	—	78
		Me_2Se	—	1200	23.8	−96.1	−18.8	77,78
		Me_2Te	—	1400	24.7	−96.1	−10.7	77,78
Ta	Br	Me_2S	[e]	90	28.8	−100.3	−12.6	77,78
		Me_2Se	—	340	33.0	−75.2	−13.5	77,78
		Me_2Te	—	570	31.8	−75.2	−16.4	77,78

[a] In CD_2Cl_2 at 0 °C.
[b] In $CDCl_3$.
[c] At −33 °C.
[d] At −23 °C.
[e] A first-order term appears above 300 K.

However, a drawback of symmetrical substitution reactions of this sort is that it is not possible to vary the entering group and leaving group independently. The change in mechanism on going from the 'hard' oxygen donor to the 'soft' S, Se, and Te donors shows that size is no longer playing the dominant role and that it must be the stronger nucleophilicity of the latter that determines the change to associative activation. The exchange of the halide ligand seems to be considerably slower than that of the neutral ligand and so the alternative pathway need not be considered.

However, in the case of the exchange between free and coordinated Me_2S in *trans*-$[Pt(Me_2S)_2Cl_2]$ in a non-coordinating solvent, it is necessary to decide whether the process is a single-stage symmetrical displacement of Me_2S by Me_2S or whether it goes by way of the ionic intermediate $[Pt(Me_2S)_3Cl]^+$.[81] Comparison of the corresponding Pd^{II} system[82] with one necessarily involving charge separation[47]

$$\textit{trans}\text{-}[Pt(py)_2(NO_2)Cl] + py \longrightarrow [Pt(py)_3(NO_2)]^+ + Cl^-$$

has shown that the $\Delta V^{\neq}$ values for the former reaction are much more consistent with a symmetrical transition state and the act of Me_2S exchange is thought to be direct. Problems of this sort have been considered in other contexts where it is necessary to decide whether the substitution is direct or multistage in the replacement from Pt^{II} complexes of thioethers and sulfoxides by amines in dimethoxyethane solution.[23,83,84]

7.1.3.4 Exchange and Substitution of Carbon Monoxide in Carbonyl and Substituted Carbonyl Complexes

Because of its relevance to the mechanisms of catalytic processes of organometallic reagents, interest in the substitution mechanisms of carbonyl complexes has been considerable since the first work of Basolo in 1961.[85] The subject has been generally and specifically reviewed from time to time[86–93] and has experienced a recent resurgence of interest. Because it is impossible to discuss this area without moving rapidly outside the scope of this chapter, only the simplest systems will be considered.

The highly covalent nature of transition metal carbonyls and their derivatives leads to the 18-electron rule being closely followed. The mononuclear species $Ni(CO)_4$, $Fe(CO)_5$, $Ru(CO)_5$, $Os(CO)_5$, $Cr(CO)_6$, $Mo(CO)_6$ and $W(CO)_6$ obey this well and, if the formalized rules of electron counting are applied, so do the metal–metal bonded and carbonyl bridged species. Such compounds are therefore coordinately saturated and the normal (but by no means unique) mode of substitution is dissociative (a 16-electron valence shell being less difficult to achieve than one with 20 electrons).[94]

The early work on $Ni(CO)_4$ + *CO, using radioactive ^{14}CO, demonstrated[85] the zero-order dependence on [CO] but suggested, because of differences in the activation parameters, that the replacement of CO by PPh_3 was mechanistically distinct from its replacement by *CO in spite of the lack of dependence of rate upon $[PPh_3]$. Elaborate mechanisms were proposed but it was later shown that the discrepancy was an artefact due to facile exchange between the reagents in the gas phase.[95] Apart from $Ni(CO)_4$ the simple mononuclear carbonyls with 18-electron valence shells are substitutionally inert, the degree of inertness increasing dramatically with the coordination number. At 25 °C, in hydrocarbon solvents, d^{10} $Ni(CO)_4$ ($t_{1/2}$ = 1 min) $\gg$ d^8 $Fe(CO)_5$ ($t_{1/2}$ = 4 years) $\gg$ d^6 $Cr(CO)_6$ ($t_{1/2} = 2.5 \times 10^5$ years, a value extrapolated from data obtained between 100 and 130 °C).[95–98] Although the [CO] dependence of the exchange in the Cr(0) system is probably zero order, the reaction with PPh_3 and other strong nucleophiles has a mixed zero- and first-order dependence on $[PPh_3]$.[98] The reactivity sequence is consistent with the increasing tendency to tolerate coordination unsaturation as the number of non-bonding electrons increases. At one time considerable disquiet was expressed because, although the CO exchanges were dissociative, the most labile species, $Ni(CO)_4$, had the highest average bond strength but it was eventually realized that average M—C bond strengths are totally irrelevant. It has been suggested that $Ni(CO)_4$ owes its relatively high reactivity to the absence of crystal-field effects in the spherically symmetrical d^{10} configuration.[99]

In contrast to the 18-electron systems, the 17-electron $V(CO)_6$ is substitutionally labile. It is one of the few 17-electron systems that can be studied under non-transient conditions but there is considerable evidence that the conclusions drawn from the study of this system can be applied to transient 17-electron species such as $\cdot Mn(CO)_5$. Data from a published study of CO exchange with $V(CO)_6$ are absent but there is much anecdotal reporting. For example, a $t_{1/2}$ value of 7 h for the reaction in heptane at 10 °C under 2 atm of CO is quoted.[97] The substitution reactions of $V(CO)_6$ are associatively activated (k_2 for the reaction between $V(CO)_6$ and PPh_3 in hexane at 25 °C =

0.253 mol $^{-1}$ dm^3 s^{-1}).[100] Displacement of a second CO by phosphine, phosphite or an arsine (= L) is very much slower and complicated by a displacement of L by L. When L is a 'hard' Lewis base, the complex disproportionates to $[V(L)_6]^{2+}$ + $[V(CO)_6]^-$ + CO.[101] The rate law is the same as for ligand substitution and a common initiation step, namely the formation of $[V(CO)_5L]$, is proposed in both cases. It is surprising that no comment has been made on the observation that, although the rate constant is very sensitive to the nature of L, k_2 for PMe_3, which leads only to simple substitution (1.22 mol^{-1} dm^3 s^{-1} at 25 °C),[100] is very similar to that for pyridine (0.70 mol^{-1} dm^3 s^{-1} at 25 °C),[101] which leads to disproportionation. In other systems where only the substitution reaction is observed, the nucleophilicity of nitrogen donors can be very much less (many orders of magnitude difference in the rate constants) than that of phosphines and other P donors. Is it possible that the site of nucleophilic attack changes from the metal to the carbonyl carbon? Mechanisms which involve a preliminary disproportionation of the 17-electron species, *i.e.* $2[V(CO)_6] \rightleftharpoons [V(CO)_6]^+ + [V(CO)_6]^-$,[102] can be ruled out because they are inconsistent with the experimental evidence.[100, 101] The rate law is wrong and the 18-electron $[V(CO)_6]^-$ is, not surprisingly, substitutionally inert.[101] The 16-electron $[V(CO)_6]^+$, which can be generated electrochemically, undergoes general decomposition.

Lability can be reasonably high in some M—M bonded and CO bridged polynuclear carbonyl complexes and their derivatives, even though formal electron counting indicates that they obey the 18-electron rule. Exchange of CO with $[Co_2(CO)_8]$ is relatively fast[85] and, owing to the fluxional nature of the complex, all eight CO ligands are equivalent in this respect. It has been suggested that the exchange takes place in the thermodynamically disfavoured form $[(OC)_4Co—Co(CO)_4]$.[103] Not all M—M bonded and CO bridged species are substitutionally labile and the $[M_2(CO)_{10}]$ species (M = Mn, Tc, Re, and 0.5 TcRe), held together by a single M—M bond, exchange their CO as slowly as $Fe(CO)_5$. The controversy about the mechanism of these reactions is as fresh now as it has ever been. Arguments have been presented in favour of a simple dissociative mechanism, $[M_2(CO)_{10}] \rightleftharpoons [M_2(CO)_9] + CO$, with retention of the M—M bond throughout the substitution[104] and others have been presented to support the idea that homolytic fission produces the substitutionally labile $[\cdot M(CO)_5]$ species.[105] Such 17-electron complexes can be generated by non-thermal modes of activation, *e.g.* photochemically, and they have been shown to be labile, undergoing substitution with an associatively activated mechanism[106] in the same way as $V(CO)_6$. However, in view of the lack of scrambling and disproportionation in the appropriate substrates, it is thought to be unlikely that this pathway plays a major role in the thermally activated reactions. Even the halogenation of $M_2(CO)_{10}$ does not generate the $\cdot M(CO)_5$ 'radical' but rather resembles the heterolytic bromination of alkenes.[107]

The catalogue of substrates can be extended, either by replacing CO by other neutral ligands, thereby maintaining the same central atom, *e.g.* $[Ni(CO)_4]$ and $[Ni(CO)_3PPh_3]$, or by anionic ligands, thereby retaining the coordination number and geometry relevant to the electronic configuration of the now changed central atom, *e.g.* $[Cr(CO)_6]$ and $[Mn(CO)_5Br]$, both with a d^6 bonding configuration. The mechanistic pattern is retained although the reactivity may be greatly altered. In other cases, where 'non-innocent' ligands are present, there may be a dramatic change of mechanism.

The d^{10} system, dominated by $Ni(CO)_4$, sticks closely to the rule that substitution is dissociative. Very little had been done since the early days[85,95,108] apart from the reaction between, *inter alia*, $Ni(CO)_4$ and bidentate ligands where the interest was in the mechanism of chelation,[109] and a volume of activation study[110] that confirmed the assignment of mechanism. With ligands other than CO it is possible to include Pd(0) and Pt(0) reaction centres. $M(PF_3)_4$ (M = Ni, Pt)[111] and $M[P(OEt_3)]_4$[112] undergo dissociatively activated substitution.

The octahedral d^6 carbonyl and substituted carbonyl complexes have been studied extensively and a number of reviews have been published.[90,91,93] With neutral ligands L (or bidentate L—L, or multidentate ligands), neutral complexes of Cr(0), Mo(0) and W(0) of the type $[M(CO)_5L]$, $[M(CO)_4(L)_2]$, *etc.* have been examined with respect to displacement of CO, displacement of L, and even isomerization. Details can be found in the review articles. In many cases, the rate law for the displacement of L or CO takes the form rate = $(k_1 + k_2[L'])$[complex] (where L′ is the entering group), with the k_1 pathway consistent with the dissociative mechanism predicted from the simple electron counting arguments recounted above. The alternative associatively activated solvolytic mechanism is unlikely in view of the non-coordinating nature of the solvents used. Darensbourg, in his recent excellent review,[91] has implied that the k_2 pathway arises from an I_d mechanism (presumably because of his reluctance to accept a 20-electron valence shell even in the transition state) but the dependence of k_2 upon the nature of L′ would suggest associative activation. In these cases, which bear a strong conceptual resemblance to reactions of tetrahedral carbon, the reluctance to undergo the predicted dissociative rate-determining step leaves the possibility of an I_a mechanism (analogous to the S_N2 mechanism) where the extra two electrons in the higher coordinate transition state are in a molecular orbital that is located mainly on the entering and leaving groups.

The reaction $[M(CO)_5X] + L \rightarrow [M(CO)_4(X)L] + CO$ (M = Mn(I), Re(I)) and others involving $[M(CO)_4(X)L]$, *etc.* allow a wider choice of ligand for the acido monodentate species X, and permit studies of the way in which the nature and position of X affects the reactivity. The first study showed that the rate of exchange of *CO with $[Mn(CO)_5X]$ was independent of [CO], but very sensitive to the nature of X, Cl (200) > Br (8) > I (1) (relative rate constants in parentheses),[113] and indicated that one CO, presumably the one *trans* to X, exchanged more slowly than the rest. Although this indicated a dissociative mechanism, it should be remembered that CO is a poor nucleophile and frequently does not bring out the ligand dependent pathway when other ligands that are stronger nucleophiles do. The special *cis* effect was questioned[114,115] but, in a group of penetrating papers,[116-118] Atwood and Brown have addressed themselves to this problem and shown that substitution in $[Mn(CO)_5Br]$ is dissociative, the rate constant for the dissociation of the CO *cis* to Br is at least 10 times greater than that for the *trans* CO and the five-coordinate intermediate is fluxional and able to rearrange during its lifetime.[116] Extensions to other compounds of the type $[M(CO)_5X]$ and $[M(CO)_4(L)X]$[117] have indicated that this is a *cis* labilizing effect produced not by ground state bond weakening but by stabilization of the five-coordinate intermediate.[118] This reference also offers a very useful and well documented review of the problem.

Although coordinately saturated carbonyl complexes are frequently inert and undergo substitution by dissociative or borderline dissociative/associative activation, there is a group of substituted carbonyl complexes that, although apparently coordinately saturated, undergo substitution with clearly associatively activated mechanisms. This was first observed when $[Co(NO)(CO)_3]$ was compared with the formally isoelectronic $[Ni(CO)_4]$. The reaction $[Co(NO)(CO)_3] + L \rightarrow [Co(NO)(CO)_2L] + CO$ obeys a typical two-term rate law, rate = $(k_1 + k_2[L])[Co(NO)(CO)_3]$,[119] with k_1 much smaller than that observed for $[Ni(CO)_4]$ and k_2 very dependent upon the nature of L, with $PR_3 > P(OR)_3 \approx AsR_3 \approx$ pyridine $\gg$ CO (indeed no second-order term is observed for the weakly nucleophilic CO). $[Fe(CO)_2(NO)_2]$,[120] $[Mn(CO)(NO)_3]$,[121] the five coordinate $[Mn(NO)(CO)_4]$[121] and octahedral $[V(NO)(CO)_5]$[122] behave in a similar fashion. It was suggested that, in the associative transition state, a pair of non-bonding electrons was transferred from the metal to the NO ligand, formally oxidizing the former by two units and converting the latter to NO^- (Scheme 2)

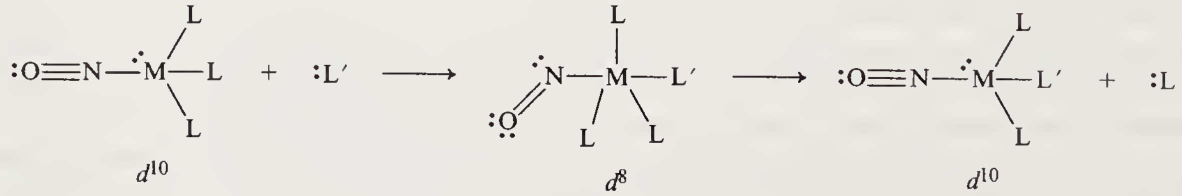

Scheme 2

This explanation can be applied to a wide range of compounds that obey the 18-electron rule but which undergo substitution with associative activation, for example $(\eta^5\text{-}C_5H_5)Co(CO)_2$ which can undergo substitution by way of the trihapto intermediate $\eta^3\text{-}(C_5H_5)Co(CO)_2L$,[123] $(\eta^6\text{-arene})\text{-}Cr(CO)_3$,[124] and $Fe(CO)_3(N_4Me_2)$.[125] Basolo has generalized this observation in the statement *'substitution reactions by 18-electron transition metal organometallic compounds may proceed by an associative mechanism provided the metal complex can delocalize a pair of electrons on to one of its ligands'*.[125] This type of reaction brings us into areas that rapidly move outside the scope of this chapter, and, if one sticks rigidly to the definition of simple substitution discussed in the introduction, these processes, with their temporary change in the number of non-bonding electrons on the reaction centre and hence its oxidation state, should be treated as redox mediated reactions.

7.1.4 THE SOLVOLYTIC REACTION

7.1.4.1 General Remarks

The substitution reaction in which a molecule of solvent replaces one of the ligands represents one of the most commonly and conveniently studied processes in coordination chemistry. In labile systems, analysis of the relaxation kinetics in the complex formation studies will, of course, give the rate constants for the solvolysis as well as those for the complex formation. In inert systems the variables can be separated and the solvolysis studied under virtually irreversible conditions. Thus the effect of (i) the nature of the reaction centre, (ii) the nature of the leaving group, and (iii) the nature and position of the other ligands in the complex upon the rates, activation parameters and the steric course of the solvolytic process can be studied readily. The price that has to be paid is that the mechanism of the reaction, *i.e.* the mode of activation, cannot be deduced from the kinetic form which remains first order throughout, nor can the variation of entering group be examined since this cannot be separated from solvation effects. The substrate will be solvated by an environment of solvent molecules which make up the outer-sphere aggregate, some of which are ideally arranged for an interchange process. Virtually all solvolytic processes are interchanges and, in order to compete with this solvolysis, a potential entering ligand, other than a solvent molecule, must compete with the solvent molecules for a place in the outer-sphere (the inner solvation shell) of the substrate, and its entry, likewise must be an interchange process. It is possible that the only way to get an extreme D mechanism is to carry out the reaction in a poorly solvating and strictly non-coordinating solvent.

7.1.4.2 Aquation

Solvolysis in aqueous solution is by far the most commonly studied of the solvolytic reactions. With relatively weak ligands, such as NO_3^-, Cl^- or Br^-, the substrates are readily made and the reactions generally go to completion in dilute solution. The reaction can be complicated by the fact that, when coordinated, water has acidic properties and the loss of a proton can be accompanied by rapid polymerization through OH or O bridges. In general, solvolytic aquation is studied in the presence of added acid ($10^{-1}-10^{-3}$ mol dm^{-3}) and the term *acid hydrolysis* is synonymous with *aquation*. This sometimes leads to labelling confusion when the solvolysis of ligands subject to acid catalysis, *e.g.* F^- or RCO_2^-, is being studied.

A major compilation of solvolytic data for octahedral complexes up to 1976 can be found in the review by Edwards *et al.*[126] and an extensive review by House[127] covers the acido–pentaamine complexes of Co(III) and Cr(III). Both are limited to substitutionally inert complexes and this section of the chapter will also be so restricted in order to allow an independent examination of the variables, in so far as they can be conveniently separated.

7.1.4.2.1 The nature of the leaving group

The problem of assigning mechanism to a solvolytic process has already been mentioned. It is not possible to know the way in which the rate depends upon the concentration of the solvent because this cannot be varied, nor is it possible to know how the rate varies with the nature of the entering group. The two most prominent approaches to this problem have been (1) through the linear relationships between the free energies of activation and the overall free energy change of the process, and (2), more recently, volumes of activation. The problems associated with the interpretation of $\Delta V^{\ddagger}$ values when there is extensive solvent electrostriction, because of charge separation in the transition state, have already been discussed.

Langford and Gray[6] took up and extended a proposal by Leffler and Grunwald[128] that a plot of the logarithm of the rate constant against that of the equilibrium constant should be linear and that the slope of this line should indicate the extent to which the transition state resembled the reagents or the products. This approach has since been used extensively, modified, reinterpreted, misunderstood and generally been the subject of much discussion.[45,129,130] The most extensive set of data relates to the aquations of the complexes $[Co(NH_3)_5X]^{n+}$ where the only restrictions imposed upon the nature of X (other than problems of making the complexes) are the following. (1) X must not be less labile than ammonia. (2) Unless the complex can be generated *in situ* by a reaction that converts a less labile ligand at a rate that is fast compared with that of the subsequent aquation, it must not react more rapidly than it dissolves. A common dodge has been to add the complex as a small amount of a concentrated solution in a water miscible solvent with which it does not react. The limit is a rate constant of about 0.1 s^{-1} ($t_{1/2} \approx 7$ s). (3) Fission must take place at the metal–ligand bond. There are a number of examples, particularly of oxygen donor ligands, *e.g.* $[Co(NH_3)_5(OMoO_3)]^+$,[131] where fission takes place elsewhere. A selection of rate constants for this reaction is presented in Table 4, together with those for other $[M(NH_3)_5X]^{n+}$ species, where M is a tervalent metal ion. The relative scarcity of systematic data for systems other than Co^{III} is readily seen.

The plot of $\log k_{aq}$ against $\log K$ for the process

$$[Co(NH_3)_5X]^{n+} + H_2O \rightleftharpoons [Co(NH_3)_5(H_2O)]^{3+} + X^{(3-n)-}$$

Table 4 The Dependence of the Rate Constants for the Aquation[a] of $[M(NH_3)_5X]^{n+}$ upon the Nature of the Leaving Group, X, and upon the Central Metal Atom, M

X			*M*		
	Co^{III}	*Cr*^{III}	*Ru*^{III}	*Rh*^{III}	*Ir*^{III}
ClO_4^-	810000[132]	—	—	—	—
$CF_3SO_3^-$	270000[133]	—	—	—	—
p-$NO_2C_6H_4SO_3^-$	6300[133]	—	—	—	—
$(MeO)_3PO$	2500[134]	—	—	—	—
$MeSO_3^-$	2000[133]	—	—	—	—
$(Me)_2Se$	—	—	1590[135]	—	—
$(NH_2)_2CO$	510[136]	—	—	—	—
NO_3^-	241[127]	24000[137]	—	123[138]	0.69[138]
$(Me)_2SO$	180[136]	—	—	—	—
$(Me)_2S$	—	—	2.6[135]	—	—
I^-	83[139]	10000[140]	2.5[141]	0.062[142]	0.0019[143]
H_2O	59[144]	520[145]	—	107[146]	0.65[147]
Br^-	39[148]	950[145]	9.8[149]	0.34[142]	0.011[150]
Cl^-	18[127]	95[145]	7.1[141]	0.48[151]	0.011[150]
SO_4^{2-}	8.9[152]	12[153]	—	16[152]	—
$CCl_3CO_2^-$	5.8[154]	41[155]	4900[b,156]	—	—
$CF_3CO_2^-$	1.7[157]	87[158]	1000[b,156]	2.0[157]	0.051[157]
$CHCl_2CO_2^-$	1.5[154]	—[c]	1910[b,156]	—	—
F^-	0.86[176]	2.5[159]	—	—	—
$CH_2ClCO_2^-$	—	—[c]	750[b,156]	—	—
$MeCO_2^-$	0.27[157]	—[c]	—	—	—
HCO_2^-	0.026[160]	—	—	—	—
N_3^-	0.021[161]	0.36[162]	—	—	—
NCS^-	0.0037[163]	0.92[163]	—	—	—
PO_4^{3-}	0.0033[164]	—	—	—	—
NH_3	0.000058[165]	—	—	—	—

[a] Values are $10^7 k_{aq}$ (s^{-1}) at 25 °C.
[b] At 60 °C.
[c] Ammonia is displaced first.

gives a straight line for complexes of the same charge type and a set of parallel lines for substrates of different charge type. If the ion association between $X^{(3-n)-}$ and $[Co(NH_3)_5(H_2O)]^{3+}$ is taken into account, the points lie on a common line. Within experimental error, the slope of these lines is 1.0 and an I_d mechanism has been assigned not only to the aquation process but also to the reverse (anation, or complex formation) process.[129] This is in accord with the positive (+1.2 $cm^3\ mol^{-1}$) volume of activation for water exchange in $[Co(NH_3)_5(H_2O)]^{3+}$,[144] although it might be argued that the value of $\Delta V^{\neq}$ indicates that bond breaking is not greatly developed in the rate determining transition state. The corresponding Cr^{III} system, using far fewer data points, gives a slope that varies between 0.7[166] and 0.9[167] depending upon the value assigned to the equilibrium constant for the bromo complex. Attempts to resolve the discrepancy by adding more data points are being made,[168,169] but chromium(III) is a very difficult reaction centre.

Fission away from the metal–ligand bond is more common, *e.g.* the case of $[Cr(NH_3)_5SeO_4]^+$,[170] and many bifunctional ligands with a 'bite' that is too small for stable chelation, *e.g.* —ONO^-,[171] —ONO_2^-,[137] —OSO_3^{2-},[172] —OSO_2^{2-},[172] —OCO_2^{2-},[173] and carboxylates[155,174] have the ability to labilize the ligands (whether NH_3 or H_2O) *cis* to themselves, possibly by some intramolecular 'cartwheeling' type of substitution mechanism. A volume of activation of −5.8 $cm^3\ mol^{-1}$ for the exchange of water with $[Cr(NH_3)_5(H_2O)]^{3+}$ strongly suggests[145] associative activation which, unless water exchange is mechanistically different, requires that the complex formation reactions and, to conserve microscopic reversibility, the aquation reactions of the chromium–pentaamine complexes are also associative. The $[Cr(H_2O)_5X]^{n+}$ system gives[175] a slope of 0.56 and $\Delta V^{\neq}$ for water exchange with the $[Cr(H_2O)_6]^{3+}$ ion is −9.3 $cm^3\ mol^{-1}$.[41] Many similar treatments have been made over a much narrower range of reactivity, for example a slope of 1.0 for the plot for complexes of the type $[Ru(NH_3)_5(O_2CR)]^{2+}$ has been taken to indicate a dissociative mechanism.[156] It has been suggested that there is a correlation between the slope of this type of linear free energy plot and $\Delta V^{\neq}$ for the exchange of water with the appropriate aquo complex,[166] but it should be recognized that, if indeed such linear relationships have any reality, the accuracies with which the slopes are determined are considerably less than those involved in the $\Delta V^{\neq}$ determinations. A valuable critique of this type of approach can be found in Swaddle's recent review.[24] Irrespective of such problems of interpretation, it is abundantly clear that the reactivity of complexes of this sort is very sensitive to the nature of the leaving group and parallels the 'instability' of the complex.

The data from Table 4 can also be used to examine the ways in which reactivity depends upon the nature of the metal. There is no consistent pattern, although for the isoelectronic, isovalent sequence $Co^{III} \geqslant Rh^{III} \gg Ir^{III}$. This matches the $Ni^{II} \geqslant Pd^{II} \gg Pt^{II}$ sequence found for the low-spin square planar complexes undergoing associative substitution (Section 7.1.7). The relative nucleofugicities of the halides found for Co^{III} and Cr^{III}, $F < Cl < Br < I$ (F^- displacement may be complicated by competing ammonia release[159,176]), changes towards $I < Br < Cl$ for Ir^{III}, thus illustrating the change from class a (hard) to class b (soft) character on going down a group from the first-row to the third element. In the $[Co(CN)_5X]^{3-}$ ion, which is made strongly class b by the synergic effect of the cyanide ligands, the sequence $I < Br < Cl \ll F$ is observed (the high lability of the fluoro complex being inferred from the fact that the complex has not yet been synthesized).[177] Because the role of the metal appears to be strongly related to the nature and the position of the other ligands in the complex (including the leaving group) it will not be considered as a separate section.

7.1.4.2.2 The nature of the other ligands in the complex: general discussion

A number of unconnected effects are grouped together in this section. The electron displacement properties of the other ligands may have a profound effect upon the reactivity that depends upon their position with respect to the leaving group and the nature of the metal. Steric effects are also of considerable importance, not only in their more usual role, namely the change in congestion on going from the ground state to the transition state, but also in the more subtle and frequently more important role of restricting or promoting the stereochemical changes involved in going from the ground state to the transition state. By far the bulk of the systematic experimental data refer to octahedral complexes (substitution in four-coordinate planar complexes warranting a major section of its own) and, until recently, the major part of these data related to cobalt(III) reaction centres. For a long time it was thought that the behaviour pattern of these cobalt(III) complexes was typical of octahedral systems. As Langford has pointed out,[178] this is far from correct. The special properties of Co^{III} systems will therefore be discussed first and, in so far as the information is available, the extent to which the other reaction centres conform or differ will be discussed separately.

7.1.4.2.3 The dependence of reactivity of cobalt(III) complexes upon the nature of the other ligands

In octahedral systems, a convenient starting point can be found among the complexes of the type $[Co(en)_2AX]^{n+}$, (en = 1,2-diaminoethane) bequeathed by Alfred Werner, where the effect of the nature and position of ligand A upon the rate constant for the aquation of the labile ligand X (frequently Cl^-, Br^- or NO_3^-) and the steric course of the reaction has been studied for many years. This presents a series of complexes of 'minimum complication' and while over the years there has been a steady addition to the number of 'non-participating groups', the extent to which the systematic study has been extended to ligands other than diaminoethane and reaction centres other than Co^{III} is still rather limited. The main drawback is that complexes where A is a strong σ-donor, *e.g.* H, Me or PR_3, have not yet been prepared. To study the effect of these it is necessary to consider complexes of the type $[Co(dmg)_2(A)X]$ (dmg = dimethylglyoximate), which will be done below. Unfortunately, this system, while providing a greater variety of 'non-participating groups', is restricted to *trans* complexes and the positional relationships and steric courses are not available. The relevant data for the diaminoethane system are collected in Table 5. Because of a revival of interest in the precise determination of steric course and the relationship between stereochemistry and the nature of the leaving group, many of the reactions have been re-examined by modern techniques and equipment. The most recent data are quoted. As might be expected from the relative labilities of the complexes of the type $[Co(NH_3)_5X]^{n+}$, there are a number of complexes of the type *trans*-$[Co(en)_2(A)Cl]^{2+}$, notably where A = H_2O,[180] MeOH[61] or Me_2SO,[201] in which A is displaced by water in preference to Cl^-.

Two types of effect can be observed. In the case of A = OH, Cl, Br or NCS, the *cis* isomer is more labile than the *trans* (a study of the *cis* isomers of the $[Co(en)_2(RCO_2)Cl]^+$ would tell us whether carboxylates could also be included in this group). In the case of NO_2, CN and especially SO_3, the activation is greatest from the *trans* position. Although only the *trans* isomer of $[Co(en)_2(SO_3)Cl]$ has yet been prepared and examined, and the value of the rate constant can only be estimated because the process is said to be too fast for stopped-flow kinetics,[200] the *trans* specificity of this labilizing effect has been demonstrated in the ammonia exchange and substitution reactions of $[Co(NH_3)_5SO_3]^+$ and *cis*-$[Co(NH_3)_4(SO_3)_2]^-$, where the kinetics are consistent with a *D* mechanism and only the ammonias *trans* to SO_3 are exchanged over a long period.[202] There is extensive crystallographic evidence for bond lengthening *trans* to SO_3 in many octahedral complexes [203,204] and also, to a lesser extent, *trans* to CN.[205] It has been suggested that the *trans* specific

Table 5 Rate Constants, Activation Parameters and Steric Courses for the Spontaneous Aquation of *cis*- and *trans*-$[Co(en)_2(A)Cl]^{n+}$ at 25 °C

A			*CIS*						*TRANS*			
	$10^4\ k_{aq}$ (s^{-1})	$\Delta H^{\ddagger}$ ($kJ\ mol^{-1}$)	$\Delta S^{\ddagger}$ ($J\ K^{-1}\ mol^{-1}$)	% *cis*	% *trans*	*Refs.*	$10^4\ k_{aq}$ (s^{-1})	$\Delta H^{\ddagger}$ ($kJ\ mol^{-1}$)	$\Delta S^{\ddagger}$ ($J\ K^{-1}\ mol^{-1}$)	% *trans*	% *cis*	*Refs.*
OH	120	94.1	+33.0	84	16	179,180	16	107.0	+61.0	25	75	180
Cl	2.4	115.0	+71.5	76	24	179	0.42	109.1	+36.0[a]	74	26	182,183
Br	1.4	94.1	−2.9	>95	<5	184	0.45	102.8	+17.1	50	50	184
$MeCO_2$	—	—	—	—	—		0.031	112.0	+28.0	75	25	185
$PhCO_2$	—	—	—	—	—		0.012	122.5	+55.2	75	25	185
—NCS	0.11	84.4	−56.4	100	0	186	0.00045	124.6	+30.1	40	60	186
CO_3	—	—	—	—	—		1.0	130.0	+97.4	0	100	187
N_3	2.4	89.0	−16.7	86	14	179,188	2.48	86.6	−25.1	91	9	188,189
NH_3	0.0050	102.4	−24.7	100	0	190,191	0.0034	97.0	−46.0	100	0	190,191
$MeNH_2$[b]	0.023	102.0	−29.3	100	0	192,193	—	—	—	—	—	
NH_2OH	0.050	82.4	−69.8	—	—	194	—	—	—	—	—	
CN	0.0062	102.8	−12.5	100	0	195	0.82	94.1	−8.4	100	0	196
NO_2	1.1	91.1	−12.5	100	0	197,198	9.8	87.4	−8.4	100	0	197,198
S_2O_3	—	—	—	—	—		40	—	—	100	0	199
SO_3	—	—	—	—	—		130000[c]	66.5	+0.8	100	0	200

[a] A wide range of values can be found in the literature: see ref. 126; data from ref. 182 as recalculated in ref. 126 are used; see also Table 6.

[b] A large number of complexes of the type *cis*-$[Co(en)_2(am)Cl]^{2+}$ have been prepared and shown to have similar reactivities; see ref. 127.

[c] Rate constant for the dissociation of water from *trans*-$[Co(en)_2(SO_3)(H_2O)]^{+}$; data for the aquation of the chloro complex not yet available.

labilization arises from bond weakening in the ground state (*trans* influence) in which a strong σ-donor will strengthen its bond to the metal at the expense of the ligand that is *trans* to it.[206] This effect is encountered in most of the transition metal reaction centres and has been very closely examined in reactions at four-coordinate planar reaction centres (Section 7.1.7.4.2). The *cis* preferred labilization effect is associated with ligands that can function as π-donors and seems to be a peculiarity of cobalt(III) (although it can be found occasionally in the labilizing role of coordinated OH at Cr^{III}, Fe^{III} and other reaction centres that seem to favour a dissociative mode of substitution). It is suggested that the π-donation serves to stabilize the five-coordinate intermediate,[207] which would appear to have a trigonal bipyramidal geometry because such complexes with potential π-donors do appear to undergo aquation with stereochemical change.

At one stage there was disquiet that only the *trans* isomers appeared to behave in this way (even though stereochemical change was common in reactions of such *cis* complexes carried out in non-aqueous solvents)[58,208,209] but *cis*-$[Co(en)_2Br_2]^{+}$[210] and *cis*-$[Co(en)_2(N_3)Cl]^{+}$[188] were shown to form some *trans* product on aquation and recent re-examination of the complexes where A = *cis*-Cl and *cis*-OH[179] has shown that there is some steric change. In all of these cases it is of interest to note that the *cis* part of the product has the same enantiomeric configuration as the *cis* starting material. There has been continuous interest in the factors that decide whether or not there is stereochemical change on substitution. The observation that many aquations accompanied by such changes had considerably higher entropies of activation than those that occurred with complete retention of configuration indicated that the geometry of the intermediate has been decided by the time that the transition state for aquation is reached and did not require any subsequent act of activation.[211] Although exceptions to this empirical rule are uncovered from time to time, it remains a useful guide. It has recently been pointed out that there is a relationship between the extent of stereochemical change and the effect of ligand A upon the height of the barrier for the square pyramid to trigonal bipyramid conversion in the five-coordinate intermediate $[Co(en)_2A]^{n+}$ and an attempt is made[212] to show how this explains the differences in the entropies of activation.

On changing the amine from diaminoethane to any other four-amine nitrogen donor system there can be considerable change in the reactivity and stereochemistry of the aquation process. This can be seen most readily and systematically in the reactions of complexes of the type *trans*-$[Co(L_4)Cl_2]^{+}$, where L_4 is a combination of amine nitrogen donors (Table 6). A number of effects are in operation and the published explanations almost outnumber the facts. It is likely that electronic effects play only a minor part, except where the ligand system becomes conjugated. Poon attempted to relate the reactivity to the 'nephelauxetic effect' of the ligands[227,228] and Basolo and Pearson talked in terms of the extent of alkylation,[214,215] but steric arguments now dominate. Busch tried to relate reactivity to the calculated ring strain in the macrocyclic systems[223] and steric repulsions between the leaving group and alkyl side groups have been invoked on a number of occasions.[222,224,229] The calculated decrease in the strain energy when $[Co(L_5)Cl]^{2+}$ (L_5 is a combination of five nitrogen donors) or *trans*-$[Co(L_4)Cl_2]^+$ loses a chloride to become five coordinate is said to parallel the solvolytic reactivity.[230] However, one should beware of these global explanations. For example, the profound effect of increasing ring size, seen in the 10^3-fold increase in reactivity on going from *trans*-$[Co(en)_2Cl_2]^+$[180] to *trans*-$[Co(tn)_2Cl_2]^+$,[216] is not general for all the non-participating groups A in $[Co(tn)_2(A)Cl]^{n+}$ (Table 7). Although there is considerable rate enhancement for *cis* complexes of the type $[Co(tn)_2(am)Cl]^{2+}$ (where am is a primary amine and somewhat bulky), this enhancement is considerably less when am = NH_3 and also in the complexes *trans*-$[Co(tn)_2(NO_2)Cl]^+$ and *trans*-$[Co(tn)_2(SO_3)X]$. All of these results are consistent with the suggestion of House[234] that the crowding arising from the two six-membered rings, possibly in twisted boat conformations,[235] is much more relieved on going to the trigonal bipyramid (as it would in the case of the dichloro complex) than it would on going to the square pyramid (which would be the fate of the nitrosulfito, and *cis*-amine species).

Table 6 Rate Constants and Activation Parameters for the Aquation of *trans*-Dichloro(tetraamine)cobalt(III) Cations, *trans*-$[Co(L_4)Cl_2]^+$, in dilute acid at 25 °C

L_4	$10^5\,k_{aq}$ (s^{-1})	$\Delta H^{\ddagger}$ (kJ mol^{-1})	$\Delta S^{\ddagger}$ (J K^{-1} mol^{-1})	$\Delta V^{\ddagger}$ (cm^3 mol^{-1})	*Refs.*
$(NH_3)_4$	224	92.4	+43.9	−1.3	213
$(NH_3)_2$; $H_2NCH_2CH_2NH_2$	2.3	—	—	—	214
$(H_2NCH_2CH_2NH_2)_2$	3.2	111.6	+43.9	−1.1	213
NH_3; $H_2NCH_2CH_2NHCH_2CH_2NH_2$	52.1	96.6	+7.9	—	226
$(H_2NCH_2CH(Me)NH_2)_2$	6.2	—	—	—	215
(±)-$(H_2NCH(Me)CH(Me)NH_2)_2$	15	—	—	—	215
(*meso*-$H_2NCH(Me)CH(Me)NH_2)_2$	42	—	—	—	215
$(H_2NCH_2C(Me)_2NH_2)_2$	22	—	—	—	215
$(H_2NCH_2CH_2CH_2NH_2)_2$	5330	86.5	+29.3	—	216
$H_2NCH_2CH_2NH_2$; $H_2NCH_2CH_2CH_2NH_2$	40	98.7	+21.3	—	217
$(H_2NCH_2C(Me)_2CH_2NH_2)_2$	300	—	—	—	215
RSSR-cyclam[a,b]	0.11	102.8	−12.5	−2.0	213,218
RRRR-cyclam	175	101.2	+41.8	—	219
SS-2,2,2-tet[c]	350	106.6	+66.9	—	220
RS-2,3,2-tet[d]	1.5	101.6	+4.18	−0.8	213,221
RR-2,3,2-tet	29	108.3	+50.2	+1.0	213,221
tet-a[f]	9.3	107.0	+54.3	—	222
tet-b[g]	420[h]	118.3	+104.5	—	222
tet-b[g]	34[h]	165.1	+242.4	—	222
13-ane$[N]_4$[i]	67.6	81.5	−29.3	—	223
15-ane$[N]_4$[j]	116	72.3	−58.5	—	223
15-ane$[N]_4$[k]	992	61.5	−75.2	—	223
16-ane$[N]_4$[l]	257000	—	—	—	223
N-meso-trans-(14)-diene[m]	3600	97.0	+51.4	—	224
N-(±)-*trans*-(14)-diene[n]	7300	—	—	—	224
14-ane$[N]_4$-1,3-diene[o]	23	—	—	—	225
14-ane$[N]_4$-1,3,8,10-tetraene[p]	2100	—	—	—	225

[a] cyclam = 1,4,8,11-tetraazacyclotetradecane.
[b] *R* and *S* indicate the chirality of the coordinated nitrogen.
[c] 2,2,2-tet = 1,8-diamino-3,6-diazaoctane.
[d] 2,3,2-tet = 1,9-diamino-3,7-diazanonane.
[e] 3,2,3-tet = 1,10-diamino-4,7-diazadecane.
[f] tet-a = *meso*-5,7,7,12,14,14-hexamethyl-1,4,8,11-tetraazacyclotetradecane.
[g] tet-c = *rac*-5,7,7,12,14,14-hexamethyl-1,4,8,11-tetraazacyclotetradecane.
[h] The two chlorides in this complex are non-equivalent, the two rate constants are deduced from the chloride exchange data.
[i] 13-ane$[N]_4$ = 1,4,8,11-tetraazacyclotridecane.
[j] 15-ane$[N]_4$ = 1,4,8,12-tetraazacyclopentadecane.
[k] There are two isomers of this complex.
[l] 16-ane$[N]_4$ = 1,5,9,13-tetraazacyclohexadecane.
[m] *trans*-(14)-diene = 5,7,7,12,14,14-hexamethyl-1,4,8,11-tetraazacyclotetradeca-4,11-diene.
[n] The isomerism arises from the chirality of the secondary nitrogen.
[o] 14-ane$[N]_4$-1,3-diene = 2,3-dimethyl-1,4,8,11-tetraazacyclotetradeca-1,3-diene.
[p] 14-ane$[N]_4$-1,3,8,10-tetraene = 2,3,9,10-tetramethyl-1,4,8,11-tetraazacyclotetradeca-1,3,8,10-tetraene.

The systematic work that has been carried out in order to see how the effects of the variation of the nature and position of ligand A vary with the nature of the amine ligands is patchy. Apart from the change from en to tn, which is still being examined, the only other major study concerns *trans*-$[Co(L_4)ACl]^{n+}$ (L_4 = $(NH_3)_4$, cyclam, tet-a, tet-b, *trans*-(14)-diene and other macrocycles of varying degrees of unsaturation; A = NO_2, NCS, N_3, CN, Cl, Br; X = Cl, Br). Apart from the general observation that reactivity increases with increasing unsaturation of the tetraamine ligand[225,236] (which is ascribed to the greater ability of the unsaturated macrocycle to stabilize the five-coordinate intermediate), it is found that the relative labilizing effects of A remain constant.

Table 7 Rate Constants for the Aquation of $[Co(tn)_2(A)Cl]^{n+}$: The Effect of Ring Size[a]

A	*X*	$10^3\,k_{aq}$ (s^{-1})	k_{tn}/k_{en}[b]	*Refs.*
trans-Cl	Cl	53	1500	216
trans-NO_2	Cl	27	28	231
trans-SO_3	N_3	6750	12	232
trans-SO_3	NO_2	810	9.8	232
trans-SO_3	NCS	1000	25	232
cis-NH_3	Cl	0.0065	15.4	233
cis-NH_2Me	Cl	0.0435	272	233
cis-NH_2Et	Cl	0.0443	211	233
cis-NH_2Pr^n	Cl	0.0367	118	233
cis-NH_2Bu^n	Cl	0.0428	92	233
cis-NH_2Bu^i	Cl	0.0390	87	233
cis-NH_2Bz	Cl	0.0290	207	233

[a] In acid aqueous solution at 25 °C.
[b] Data for $[Co(en)_2(A)Cl]^{n+}$ from Table 5.

Plots of $\log(k_A/k_{Cl})$ (where k_A and k_{Cl} are the aquation rate constants for A = A and A = Cl respectively, for a constant X) for one L_4 combination against the same function for another are frequently linear,[237] from which it has been concluded that the labilizing effects arising from the electronic properties of A act independently of those arising from the steric and electronic properties of L_4. This is of interest because the initial motivation for the study of complexes of the type $[Co(cyclam)(A)Cl]^{n+}$ was to see the extent to which the reactivity pattern was affected by replacing the flexible diamine with the stereoretentive cyclam. It was hoped that this would indicate the importance of the trigonal bipyramidal form for π-donor labilizing ligands.[218] The conclusion is at variance with that drawn from the incomplete and more ambiguous study of the tn_2 complexes and does not take account of the large difference in lability of the *RSSR* (which cannot fold)[218] and *RRRR* (which can fold)[219] isomers of *trans*-$[Co(cyclam)Cl_2]^+$ cation. Clearly the extended set of *trans*-[Co(*RRRR*-cyclam)(A)Cl]$^{n+}$ substrates ought to be prepared and examined. The observation that *trans*-$[Co(cyclam)(OH)Cl]^+$ is more labile than the corresponding en_2 species, while all the other members of the series are less reactive, has been ascribed to an internal conjugate base mechanism (see Section 7.1.4.3) in which the OH ligand, being in a favourable position, takes a proton from an adjacent NH to generate a labile amido species.[237] The isomer studied is known to have the *RSSR* configuration and so the alternative explanation can be ruled out. Palmer[213] supports the view of House[238] that the linear relationship between log k_{aq} and the frequency of the in-plane δ_{N-Co-N} deformation mode indicates that the lability of the dichloro complexes reflects the flexibility of the molecule as it approaches the trigonal bipyramidal intermediate but he points out that the wide range of rates is not reflected in the $\Delta V^{\ddagger}$ values (see Table 6) whose variation from one another is less than the experimental error.

The diligando(tetraamine) complexes, at present, have the disadvantage of only offering a restricted range of 'non-participating' ligands; complexes with very strong *trans* effect ligands containing P, As, H and σ-bonded C (other then CN) are not yet available and the range of S donors is limited. Co^{III} complexes with planar macrocyclic anionic ligands (which may or may not be conjugated) offer a wider range of *trans* ligands to study, but the relative *trans* to *cis* effectiveness of a particular non-participating group cannot be assessed because either the ligand will not fold or the act of folding changes its characteristics. There is an enormous literature associated with the chemistry and reactions of such complexes, particularly of those where Co—C bonds can be formed and studied. In addition, Co^I becomes a readily accessible oxidation state. Unfortunately, this falls well outside the scope of this chapter and will not be discussed further. Complexes of the type *trans*-$[Co(dmg)_2(A)X]^{n+/-}$ are particularly well represented and, while dimethylglyoximate is formally a bidentate ligand, the hydrogen bonding interactions between the oxime oxygens gives the two molecules the properties of a macrocycle. It has been suggested that the complexes of this type, where A is a σ-bonded alkyl group, can serve as models for coenzyme B_{12}.[239] Classic studies of aquation when X = Cl have been carried out[240–243] but, generally through interest, convenience or necessity, the kinetics of the complex formation reactions of the solvento complexes (X = H_2O, MeOH, *etc.*) have been studied. When these are examined under reversible conditions, the solvolytic rate constants for X = Cl can be extracted.[244]

With strong *trans* effect ligands, the high lability of the substrates requires that the kinetics are followed by relaxation techniques and ligands much more tightly bound than chloride have to be used in order to ensure effective competition with the solvent.[245] The bulk of the strong *trans* effect data relates to the dissociation rate constant for the solvento species (these processes having a *D* mechanism) but in order to avoid unnecessary repetition later, they will be discussed here. The *trans* effect sequence, A = Me^- (1 000 000) $\gg$ SO_3^{2-} (50 000) $\gg$ $MeC_6H_4SO_2^-$ (950) > $MeSO_2^-$ (750) $\gg$ I^- (1.8) > NO_2^- (1.0) (where the values in parentheses are the limiting anation rate constants for the reactions of the MeOH complex relative to that of the nitro complex), is collated and discussed in a well referenced paper by Deutsch,[246] who later augments the sequence to give Me^- (900) > $C_6H_6^-$ (300) > SO_3^{2-} (100) > $(MeO)_2PO^-$ (50) $\gg$ *p*-$MeC_6H_4SO_2^-$ (1)[247] (values in parentheses are relative to the *p*-$MeC_6H_4SO_2^-$ complex). The data are all consistent with a ground state bond weakening associated with the strong *trans* influence of a strong σ-donor, but the evidence that points to the anation reactions of these complexes (see below) having a limiting *D* mechanism suggests that there might be a stabilization of the five-coordinate intermediate sufficient to increase its lifetime.

A systematic examination of cooperative or antagonistic electronic effects from pairs of 'non-participating' groups (the work on the effect of changing the amine ligands notwithstanding) has not yet been carried out. Complexes of the type $[Co(L_3)(A^1)(A^2)X]^{n+/-}$ would be useful in this context.

7.1.4.2.4 *The dependence of reactivity of chromium(III) complexes upon the nature of the other ligands*

A comprehensive review of the literature relating to all aspects of chromium(III) amine complex chemistry, including their substitution reactions, was published in 1970.[248] Although the first aquation studies of *cis*-$[Cr(en)_2Cl_2]^+$ suggested[249] that Cr^{III} was similar in its kinetic behavior to Co^{III} (a belief that continued rather longer than necessary),[250] it was soon shown that whereas aquation might be similar, the base-catalyzed aquation (see below) certainly was not.[251] Even the simple aquation was shown to be complicated in many cases by parallel loss of the chelating amine (and reversible ring opening too might offer new pathways for substitution and isomerization).[252] The preparation, purification and isolation of the $[Cr(en)_2(A)X]^{n+}$ complexes proved to be much more difficult than that of their Co^{III} analogues and, for all these reasons, the examination of the electronic effects of the non-participating ligand A is restricted to a few examples, collected together in Table 8. It is thus not possible to say with any certainty just how much Cr^{III} and Co^{III} differ in their response to the electronic effects of A and its position with respect to the leaving group. The labilizing order OH > Cl > NCS is repeated in the *cis* complexes (the *trans* chloro–isothiocyanato complex has not yet been studied and the other *trans* complexes lose diaminoethane at least as easily as chloride), but while Cl labilizes a chloride *cis* to itself much better than one *trans*, hydroxide is a better labilizer from the *trans* position (the same is found when X = Br).[257] The isomers with A = —NO_2 are unknown, only the —ONO complex being described. While no quantitative data are available, it is stated [258] that *cis*-$[Cr(en)_2(ONO)Cl]^+$ loses chloride much more rapidly than does *cis*-$[Cr(en)_2(NCS)Cl]^+$.[256] This high *cis* effect is ascribed to the 'cartwheeling effect'[127] mentioned above (see Scheme 3).

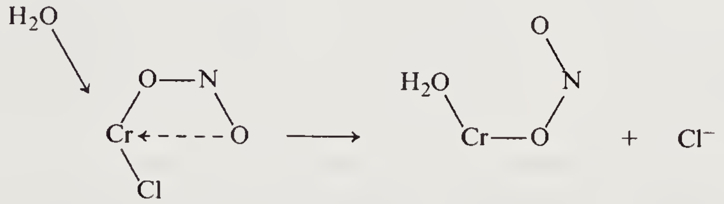

Scheme 3

Table 8 Rate Constants and Activation Parameters[a] for the Aquation of Complexes of the Type $[Cr(en)_2(A)Cl]^{n+}$

	cis				*trans*			
A	$10^5 k_{aq}$ (s^{-1})	$\Delta H^{\ddagger}$ (kJ mol^{-1})	$\Delta S^{\ddagger}$ (J K^{-1} mol^{-1})	*Refs.*	$10^5 k_{aq}$ (s^{-1})	$\Delta H^{\ddagger}$ (kJ mol^{-1})	$\Delta S^{\ddagger}$ (J K^{-1} mol^{-1})	*Refs.*
—OH	330	—	—	253	460	—	—	253
—F	—	—	—	—	6.2	75.2	−58.5	254,255
—Cl	33	88.2	−23.8	249	2.2	94.9	−20.9	250
—NCS	8.1	81.9	−48.1	256	—	—	—	—
—OH_2	2.8	—	—	249	—	—	—	—

[a] In acid aqueous solution at 25 °C.

Much more information is available about the effect of changing the nature of the amine ligands (Table 9), and it is here that Cr^{III} differs greatly from Co^{III} in its response to steric effects. Most of the *trans*-$[Cr(L_4)Cl_2]^+$ complexes have very similar rate constants, bearing in mind that in some of the cases there may be a parallel reversible or even irreversible breakage of the Cr—N bonds, and the *cis*-dichloro complexes also have similar reactivities although the rate constants are generally some 10 times greater than those of the *trans* isomers. The exceptions to this generalization are worth further consideration; for example, *trans*-$[Cr(cyclam)Cl_2]^+$ is considerably less labile than the other *trans*-dichloro species and the change of L_4 from $(en)_2$ to cyclam has much the same effect on the lability in the Cr^{III} and Co^{III} series. The *cis*-$[Cr(cyclam)Cl_2]^+$ complex, which is known to have the same configuration as the analogous Co^{III} species,[270] is, on the other hand, the more reactive. All of these results seem to strengthen the view that the driving force for the aquation of the Co^{III} dichloro complexes, thought to be the accessibility of the trigonal bipyramidal geometry for the five-coordinate intermediate, is absent in the Cr^{III} system. However, the high reactivity of $[Cr(tren)Cl_2]^+$[269] and *β-cis*-$[Cr(2,2,2\text{-tet})Cl_2]^+$[268] (especially when compared to that of the α-*cis* isomer[267]) indicates that there is at least one more parameter. The explanation of Adamson,[268] that the water approaches from the rear in an associatively activated process, would account for the much lower reactivity of the α-isomer (approach blocked) when compared to that of the β-form (approach clear), but we are really looking for an explanation as to why the β-2,2,2-tet and the tren complexes are unusually reactive. The *cis*-$[Cr(2,3,2\text{-tet})Cl_2]^+$ complex, thought to be the β-isomer, behaves normally.[262] Clearly, much more work needs to be done on the Cr^{III} system.

Table 9 Rate Constants and Activation Parameters for the Aquation of $[Cr(L_4)Cl_2]^+$ Complexes[a]

L_4	$10^5 k_{aq}$ (s^{-1})	$\Delta H^{\ddagger}$ (kJ mol^{-1})	$\Delta S^{\ddagger}$ (J K^{-1} mol^{-1})	*Refs.*
trans isomers				
$(NH_3)_4$	4.0	90.3	−25.1	259
$(H_2NCH_2CH_2NH_2)_2$	2.3	97.0	−16.7	250
$(H_2NCH_2CH(Me)NH_2)_2$	11.6[b]	—	—	260
$(H_2NCH_2CH_2CH_2NH_2)_2$	2.1	102.4	0	234
$H_2NCH_2CH_2NH_2$; $H_2NCH_2CH_2CH_2NH_2$	1.9	97.8	−16.7	217
2,3,2-tet[c]	0.33	103.7	+4.2	261
3,2,3-tet[c]	0.106	91.7	−50.2	262
cyclam[c]	0.002	112.9	−8.4	263
cis isomers				
$(H_2NCH_2CH_2NH_2)_2$	33	85.7	−25.1	249
$(H_2NCH_2CH(CH_2)NH_2)_2$	35	—	—	264
$(H_2NCH_2C(Me)_2NH_2)_2$	15.7	—	—	265
(*meso*-$H_2NCH(Me)CH(Me)NH_2)_2$	32.1	—	—	265
$(\pm\text{-}H_2NCH(Me)CH(Me)NH_2)_2$	41.0	—	—	265
(*o*-$C_6H_4(NH_2)_2)_2$	17.1	—	—	266
α-2,2,2-tet	19	86.5	−25.1	267
β-2,2,2-tet	3000[d,e]	—	—	268
β-2,2,2-tet	500[d]	—	—	268
β-2,3,2-tet	—	—	—	262
tren[f]	5180	51.4	−96.1	269
β-3,2,3-tet	10.2	86.1	−33.4	262
RRRR-cyclam	2.5	93.6	−20.9	263

[a] In dilute acid at 25 °C.
[b] At 35 °C.
[c] Configurations uncertain; possibly the same as their Co^{III} analogues.
[d] At 0 °C.
[e] The two rate constants are for two separate isomers, probably *RR* and *RS*, but it is not known which is which.
[f] tren = tris(2-aminoethyl)amine.

7.1.4.2.5 The dependence of the reactivity of rhodium(III) and iridium(III) complexes upon the nature of the other ligands

One of the first differences to be noted about the Rh^{III} acido–amine complexes is that the chloro complexes are frequently much more stable with respect to solvolysis than their Co^{III} and Cr^{III} analogues and solvolytic equilibrium is reached when very little of the chloro complex has aquated, even in dilute solution and in the absence of added chloride ions. This is, to some extent, the consequence of the move away from 'class a' character already mentioned above. As a result, the rate constants for aquation are obtained from ligand substitution reactions (including chloride exchange) which first have to be shown to be mediated by a rate determining aquation. More recently, data have been obtained from a study of the solvolysis in basic solution. This serves to trap the aquo product as the inert hydroxo species and the base-catalyzed solvolysis is never strong enough to dominate the reaction (as it would be the case of the analogous Co^{III} complexes). A small nucleophile dependent contribution to the rate of substitution has been reported for the entry of Cl^- and Br^-.[271] The rate constants for the two nucleophiles are similar and only about ¼ of the magnitude of that measured for OH^-. Although a number of complexes of the type *cis*- and *trans*-$[Rh(en)_2(A)Cl]^{n+}$ have been described,[272] those studied kinetically are few in number. This is partly because a number of the reactions are either autocatalytic or else subject to catalysis by traces of reducing agents[273–277] and need to be studied under conditions where such pathways are eliminated. Some of the odd results that appear from time to time could be explained in this way. Much interest has developed in the photochemistry of Rh^{III} complexes and this has diverted attention away from the study of the thermally activated processes.

Within the limits of the published data it appears that the lability of Rh^{III} complexes is sensitive to the nature of the ligand *trans* to the leaving group. For complexes of the type *trans*-$[Rh(en)_2(A)Cl]^+$, the *trans* effect increases along the sequence Cl (1.49) < Br (3.94) ≪ I (825)[278] (values in parentheses are $10^6 k_{aq}$, s^{-1} at 50 °C). A = NO_2 is also said to have a strong labilizing effect[279] and the inability to push the reaction between *trans*-$[Rh(en)_2Cl_2]^+$ and NCS^- beyond the formation of *trans*-$[Rh(en)_2(NCS)Cl]^+$ is taken as evidence for a very poor *trans* labilizing effect of NCS.[272] The rate constant for the displacement of I^- from *trans*-$[Rh(en)_2I_2]^+$ is some 10 times greater than that for *trans*-$[Rh(en)_2(OH)I]^+$ and suggests the sequence I < OH < Cl. Arguing on the basis of the enthalpies of activation, Pöe[280] suggests a *trans* effect sequence, $OH \leqslant Cl < NH_3 < Br < I$. In the aquation of *trans*-$[Rh(dmg)_2(L)Cl]^-$, the complex where L = SO_3H[281] is only about twice as reactive as that with L = NO_2.[282] However, the difference in the published activation energies is so great (66.0 and 133.8 kJ mol^{-1} respectively) that a relatively small change in temperature could reverse the reactivity sequence.

Very little can be said about *cis* effects in the Rh^{III} system owing to lack of systematic data. *cis*-$[Rh(en)_2Cl_2]^+$ is some 10 times more labile than the *trans* isomer at 80 °C,[283,284] but how does one distinguish the *cis* effect of Cl from the *trans* effect of $—CH_2NH_2$? The displacement of Cl^- from α-*cis*-$[Rh(trien)Cl_2]^+$ by other nucleophiles X takes place in two stereoretentive stages, the rate limiting step of each being the aquation. Assuming that the second stage corresponds to the rate determining solvolysis of α-*cis*-$[Rh(trien)(X)Cl]^+$, the *cis* effect sequence becomes Cl (8) > N_3 (4) > I (2.5) ≈ Br (2.5) ≫ NCS (no reaction observed) (numbers in parentheses = $10^4\,k\,s^{-1}$ at 70 °C).[285] Apart from the case of thiocyanate, the *cis* effect in this sequence is rather small.

Although a number of complexes of the general type *cis*- and *trans*-$[Rh(L_4)Cl_2]^+$ have been characterized, aquation data are limited for the reasons already given. Unlike their Co^{III} analogues, the dependence of reactivity upon the nature of the L_4 system seems to be very small if the data are compared at 80 °C (the very crowded *N,N,N′,N′*-tetramethyldiaminoethane being the exception). These values are reported in Table 10, where an attempt has also been made to extrapolate data to 25 °C in order to make comparisons with other systems. However, such extrapolations are frequently long and the uncertainty is often greater than the reactivity differences between the complexes. The small dependence of lability on the geometric requirements of the L_4 system (which resembles that encountered in the Cr^{III} system) strengthens the suspicion that it is Co^{III} that is exceptional and that the effect arises from the need for the Co^{III} to develop a trigonal bipyramid during the aquation of its dichlorotetraamine complexes.

Table 10 Rate Constants and Activation Parameters for the Aquation of *trans*- $[Rh(L_4)Cl_2]^+$ Complexes[a]

L_4	$10^9\,k_{aq}$ *at 25 °C* (s^{-1})	$10^5\,k_{aq}$ *at 80 °C* (s^{-1})	$\Delta H^{\ddagger}$ (kJ mol^{-1})	$\Delta S^{\ddagger}$ (J K^{-1} mol^{-1})	*Refs.*
$(NH_3)_4$	155	8.7	95.3	−55.2	286
$(MeNH_2)_4$	9.1	3.5	128.7	33.4	288
$(MeCH_2NH_2)_4$	44	2.6	99.1	−53.1	288
$(MeCH_2CH_2NH_2)_4$	107	8.1	102.8	−33.0	288
$(H_2NCH_2CH_2NH_2)_2$	28	4.9	116.2	0.8	284
$(Me_2NCH_2CH_2NH_2)_2$	14	2.5	117.0	−2.9	284
$(Me_2NCH_2CH_2NMe_2)_2$	720	70	106.6	−5.0	284
$(H_2NCH_2CH_2CH_2NH_2)_2$	33	3.1	106.2	−32.6	287

[a] Values at 80 °C are interpolated using data provided while those at 25 °C are extrapolated using the activation parameters provided.

Although the reactivity of Rh^{III} complexes is generally much less than that of the corresponding Co^{III} species, there are examples where reactivity is similar, *e.g.* the anations of $[Rh(NH_3)_5H_2O]^{3+}$[289] and $[Co(NH_3)_5H_2O]^{3+}$.[144] The observation that the reaction[290] *trans*-$[Rh(dmg)_2(Me)(H_2O)] + SC(NH_2)_2 \rightarrow$ *trans*-$[Rh(dmg)_2(Me)\{SC(NH_2)_2\}] + H_2O$ is some 10^2 times faster than that of the corresponding Co^{III} complex,[291] and has a much lower activation energy, is an indication that these Rh^{III} systems respond much more than those of Co^{III} to the *trans* effect of strong σ-donors.

Little can be said about the way in which the non-participating ligands affect the lability of octahedral Ir^{III} complexes. Their very low labilities require study at temperatures in excess of 100 °C over long periods of time. What is known suggests that the systems resemble Rh^{III} in the relative behaviour pattern.[292]

7.1.4.2.6 The dependence of the reactivity of ruthenium(III) and ruthenium(II) complexes upon the nature of the other ligands

Apart from a comparison of the *cis* and *trans* dichloro complexes and a comparison of dichloro with chloroaquo species, little has been done to study the effect of the non-amine, monodentate non-participating ligands upon the lability of Ru^{III} complexes. Where studied, *cis*-dichlorotetra(amine) complexes are considerably more labile than their *trans* isomers but there are insufficient data at this time to say whether there is any great sensitivity of lability to the nature of the tetraamine ligand in such systems. The extremely low reactivity of *trans*-$[Ru(cyclam)Cl_2]^+$ (the rate constant for Cl^- exchange is reported[293] to be $3 \times 10^{-7} s^{-1}$ at 102 °C) seems to be an exception that is, as yet, unexplained. Some relevant data are collected in Table 11.

Table 11 Rate Constants and Activation Parameters for the Aquation of Complexes of the Type *cis*- and *trans*-$Ru(L_4)Cl_2^+$

L_4	$10^6 k_{aq}$ (s^{-1} 25 °C)	$\Delta H^{\ddagger}$ ($kJ\ mol^{-1}$)	$\Delta S^{\ddagger}$ ($J\ K^{-1}\ mol^{-1}$)	*Refs.*
trans isomers				
$(NH_3)_4$	1.7	91.1	−50.2	293
$(en)_2$	4.2	97.4	−20.9	293
RS-2,3,2-tet	0.48	102.8	−20.1	293
cyclam (*RSSR*?)	0.3[a]	—	—	293
cis isomers				
$(NH_3)_4$	88	91.1	−36.8	141
$(en)_2$	370	83.6	−48.9	141
α-trien	580	76.1	−51.8	293[b]

[a] Rate constant for chloride exchange at 102 °C.
[b] Recalculated from data in ref. 141.

It might be convenient to point out in this section that, in common with Cr^{III} and Os^{III}, the anation of the anionic $[M(edta)(H_2O)]^-$ complex [M = Ru^{III}, Cr^{III}][294,295] is many orders of magnitude faster than the analogous reactions of the tetraamine and pentaamine complexes. It has been suggested that this is due to the associative nature of the substitution in the d^5 and d^3 ions. In comparison, the corresponding reactions of the Co^{III}, Rh^{III} and Ru^{II} $[M(edta)(H_2O)]^{n-}$ species (n = 1 or 2) are only about 10^2 times faster than those of the amine species. It was thought that all of these d^6 systems reacted dissociatively. One consequence is that whereas Ru^{II} substrates are usually many orders of magnitude more labile than those of Ru^{III}, the anation of $[Ru(edta)(H_2O)]^{2-}$ is catalyzed by traces of Ru^{III}.[294]

Although the systems might be classified as labile, it has been possible to examine the analogous d^6 Ru^{II} *trans*-dichloro(tetraamine) complexes by cyclic voltammetry, using the Ru^{III} species as primary reagents. The data, reported in Table 12, suggest that, apart from the cyclam complex *trans*-$[Ru(cyclam)Cl_2]$, which is not unusually inert, the Ru^{II} species parallel those of Ru^{III} in their comparative lability but are some 10^5–10^6 times more reactive.

7.1.5 BASE CATALYZED SOLVOLYSIS AND SUBSTITUTION

7.1.5.1 General Remarks

Certain octahedral complexes, particularly the acido–amine complexes of cobalt(III), undergo substitution in protonic solvents at rates that are proportional to the concentration of the conjugate base of the solvent (*e.g.* OH^- in water) or inversely proportional to the concentration of the conjugate acid of the solvent (*e.g.* retardation by H_3O^+ in water or NH_4^+ in liquid ammonia). Such reactions have received considerable attention since systematic studies of ligand substitution commenced, and figured amongst the earliest kinetic studies in the field.[298] The subject has been

Table 12 Rate Constants and Activation Parameters for the Aquation of *cis*- and *trans*-$[Ru(L_4)Cl_2]$

L_4	k_{aq} (s^{-1} 25 °C)	$\Delta H^{\ddagger}$ (kJ mol^{-1})	$\Delta S^{\ddagger}$ (J K^{-1} mol^{-1})	*Refs.*
trans isomers				
$(NH_3)_4$	1.0	71.9	−2.9	296
$(en)_2$	0.35	72.7	−9.2	296
$(tn)_2$	0.53	72.7	−5.9	297
$(MeNHCH_2CH_2NHMe)_2$	0.068	70.2	−38.9	297
RR-3,2,3-tet	0.059	74.8	−18.8	297
RS-2,3,2-tet	0.066	78.6	−4.2	296
3,3,3-tet	0.25	67.3	−30.9	297
RSSR-cyclam	0.023	78.2	−13.8	296
15-ane$[N_4]$	0.074	78.6	−4.2	297
tet-a	5.0	—	—	297
cis isomers				
$(NH_3)_4$	50	—	—	296
$(en)_2$	38	—	—	296

extensively reviewed[299–301] and the most recent[301] should be consulted for a more detailed discussion and extensive compilation of references.

The kinetics of the reaction, established only for the catalyzed solvolysis

$$[M(L_4)(HNR_2)X]^{n+} + S^- \longrightarrow [M(L_4)(HNR_2)S]^{n+} + X^-$$

(where HS is the protonic solvent) (if the pH of the study is low enough the product may well be $[M(L_4)(HNR_2)(HS)]^{(n+1)+}$) usually take the form

$$-d[M(L_4)(HNR_2)X^{n+}]/dt = (k_{solv} + k_S[S^-])[M(L_4)(HNR_2)X^{n+}]$$

(where k_{solv} is the rate constant for the uncatalyzed solvolysis). The bulk of the studies has been carried out in aqueous solution where HS is H_2O and S^- is OH^-. In cases where the catalysis is sufficiently strong compared with the uncatalyzed reaction and can be observed in acid solution, the rate law can be rewritten as

$$-d[M(L_4)(HNR_2)X^{n+}]/dt = (k_{solv} + k_H[H_2S^+]^{-1})[M(L_4)(HNR_2)X^{n+}]$$

(where H_2S^+ is the protonated solvent). This form is relatively uncommon in aqueous solution where it is seen as an acid retarded aquation ($H_2S^+ = H_3O^+$),[302–305] but it is the normal behaviour in liquid ammonia ($H_2S^+ = NH_4^+$).[306–312]

7.1.5.2 The Mechanism

The need for the presence of at least one amine proton in the substrate and a wealth of experimental evidence support a mechanism in which the lyate ion (or even the solvent itself) acts as a base to remove a proton from a suitably placed amine group, thereby generating a substitutionally labile amido species. There is strong evidence to support the idea that the mode of activation of this species (at least in the case of the Co^{III} species) is dissociative, but there is still disagreement as to whether the stoichiometric mechanism is dissociative (*D*) or interchange (I_d). The distinction between these mechanisms rests upon the presence or absence of an identifiable five-coordinate intermediate that has lost all memory of its origins.

The reaction pathways involved can be formulated as

$$[M(L_4)(NHR_2)X]^{n+} + S^- \underset{k_{-1}}{\overset{k_1}{\rightleftharpoons}} [M(L_4)(NR_2)X]^{(n-1)+} + HS \tag{1}$$

$$[M(L_4)(NR_2)X]^{(n-1)+} \xrightarrow{k_2} [M(L_4)(NR_2)]^{n+} + X^- \tag{2}$$

$$[M(L_4)(NR_2)]^{n+} + HS \xrightarrow{\text{fast}} [M(L_4)(NR_2)(HS)]^{n+} \rightleftharpoons [M(L_4)(HNR_2)S]^{n+} \tag{3}$$

$$[M(L_4)(NR_2)]^{n+} + Y^- \xrightarrow{\text{fast}} [M(L_4)(NR_2)Y]^{(n-1)+} \xrightarrow{+HS} [M(L_4)(HNR_2)Y]^{n+} + S^- \tag{4}$$

The mechanism provides (in equation 1) a pathway for proton exchange in amine complexes. (In fact, it was the observation that proton exchange in $[Co(NH_3)_6]^{3+}$[313] and the base hydrolysis of $[Co(NH_3)_5Br]^{2+}$[298] had the same kinetic form that led Garrick to propose this mechanism in 1937.[314]) The pathway for base catalyzed solvolysis is made up of (1) + (2) + (3) and the pathway for base catalyzed substitution is (1) + (2) + (4). It was the observation of base catalyzed ligand substitution that provided the first strong evidence for the dissociative nature of the process.[315]

Although the generally accepted current theology is that the labilizing role of the amido group comes from its ability to act as a π-donor and thereby stabilize the transition state leading to the five-coordinate intermediate,[316] there are some reservations that this may not be strong enough to account for some of the extremely large increases in lability following the removal of a proton from certain cobalt(III) amine complexes.

Analysis of the reaction sequence (1)–(3) under stationary state conditions (*i.e.* only $[M(L_4)(HNR_2)X]^{n+}$ and $[M(L_4)(HNR_2)S]^{n+}$ are present in any significant quantity during the reaction) gives the observed rate law with $k_S = k_1k_2/(k_{-1} + k_2)$. In substrate in which there are n equivalent protons, *e.g.* *trans*-$[Co(NH_3)_4Cl_2]^+$, in which $n = 12$, this changes to $k_S = nk_1k_2/(k_{-1} + k_2)$. If, as is often the case, the complex contains a number of sets of non-equivalent amine protons each capable of generating a labile amido complex, the single rate constant will be made up of contributions from all the participating pathways, and $k_s = \Sigma\, n^ik_1{}^ik_2{}^i/(k_{-1}{}^i + k_2{}^i)$.

7.1.5.3 The Limiting Cases

7.1.5.3.1 The 'normal' limit

It was originally thought that the high basicity of the amido complex would make the reprotonation a diffusion controlled process so that k_{-1} was always much greater than k_2. This is indeed true for the majority of Co^{III} systems examined and for all studied cases of Cr^{III}, Ru^{III}, Rh^{III} and Ir^{III} complexes. Under these conditions, the expression for the rate constant reduced to $k_S = \Sigma\, n^ik_1{}^ik_2{}^i/k_{-1}{}^i$ or $\Sigma\, K^ik_2{}^i$ where K^i is the equilibrium constant for the proton transfer process (1). With proton transfer as a rapid preequilibrium, such systems exhibit specific base catalysis.

7.1.5.3.2 Rate limiting deprotonation

Until the early 1960s it was assumed that proton transfer would always be much faster than the overall base hydrolysis. However, in 1968 it was shown that, at 0 °C, proton exchange and base hydrolysis of *trans*-[Co(*RSSR*-cyclam)$Cl_2]^+$ had similar rates.[317] Under these circumstances, $k_{-1} \approx k_2$, and, in the limit when $k_2 \gg k_{-1}$, the expression reduces to $k_S = \Sigma\, n^ik_1{}^i$ so that deprotonation becomes rate limiting. Such a system will exhibit general base catalysis. A detailed study of the base hydrolysis[318] and proton exchange[319] of three isomers of $[Co(cyclam)Cl_2]^+$ (the *RSSR-trans*, the *RRRR(SSSS)-trans* and the *RRRR(SSSS)-cis*) has recently been published. The *cis* isomer behaves normally. The *RS*[320] and *RR(SS)*[321] isomers of *trans*-$[Co(2,3,2\text{-}tet)Cl_2]^+$ have $k_2 > 10k_{-1}$ at 0 °C and because the activation energy for the dissociation (k_2) step is greater than that for the reprotonation (k_{-1}) step, the *trans-RSSR*-cylam complex[319] and even *trans*-$[Co(en)_2Cl_2]^+$[322] approach these limits at higher temperatures. Apart from these *trans*-dichlorotetraaminecobalt(III) complexes, rate-limiting deprotonation is rare and has so far only been claimed for the reactions of the *trans*-[Co(*trans*-14-diene)(A)X]$^+$ cations (A = Cl, N_3, NCS, CN; X = Cl, Br; *trans*-14-diene = 5,7,7,12,12,12-hexamethyl-1,4,8,11-tetraazacyclotetradeca-4,11-diene),[323] where the increase in the dissociative lability due to a combination of the unsaturation of the macrocycle and the steric effects of the methyl groups increases k_2 sufficiently to make deprotonation rate limiting. This conclusion is based mainly on the fact that k_{OH} is not very sensitive to the natures of A and X.

The systems where $k_2 \gg k_{-1}$ offer a direct demonstration of the conjugate base mechanism. In the reactions of the *trans-RS*[320] and *trans-RR(SS)*[321] isomers of the $[Co(2,3,2\text{-}tet)Cl_2]^+$ complex, examination of the reaction product showed that the act of base hydrolysis was accompanied by the exchange of one secondary amine proton. All other exchange was shown to take place after this product was formed. Comparison of the amount of proton exchange in recovered unreacted *trans*-$[Co(en)_2Cl_2]^+$ with that in the recovered reaction product likewise indicated that an act of base hydrolysis required the removal of one amine proton.

7.1.5.3.3 The changeover from 'normal' behaviour to rate-limiting deprotonation

In all cases so far studied in aqueous solution the reprotonation is effected by H_2O and so variation in the ratio $k_{-1}:k_2$ cannot be achieved by changing the pH of the solution. However, the enthalpies of activation of the k_{-1} and k_2 processes can differ sufficiently for the change from one limit to the other to be achieved by changing the temperature sufficiently. Since, at the normal limit ($k_{OH} = nk_1k_2/k_{-1}$) $\Delta H_{OH}^{\ddagger} = \Delta H_1^{\ddagger} + \Delta H_2^{\ddagger} - \Delta H_{-1}^{\ddagger}$ and, at the rate determining deprotonation limit ($k_{OH} = nk_1$), $\Delta H_{OH}^{\ddagger} = \Delta H_1^{\ddagger}$, there will be a region of curvature in the Eyring plot [$\ln(k_{OH}/T)$ *vs.* T^{-1}] on passing through the region where $k_{-1} \approx k_2$ and the extent of the curvature will depend upon the magnitude of $|\Delta H_{-1}^{\ddagger} - \Delta H_2^{\ddagger}|$. This has now been well established in the cases of *trans*-[Co(*RSSR*-cyclam)Cl$_2$]$^+$ [319] and *trans*-[Co(en)$_2$Cl$_2$]$^+$.[322]

In liquid ammonia, where the solvent is a much stronger base than water, the rate limiting deprotonation reactions can lead to some unusual rate laws. Because the solvent itself can act as a base, it is necessary to introduce an extra step in the reaction sequence discussed above, *i.e.*

$$[\mathrm{M(L_4)(HNR_2)X}]^{n+} + \mathrm{NH_3} \underset{k'_{-1}}{\overset{k'_1}{\rightleftharpoons}} [\mathrm{M(L_4)(NR_2)X}]^{(n-1)+} + \mathrm{NH_4^+} \qquad (5)$$

for $SH = NH_3$, and the expression for the rate constant for base hydrolysis in liquid ammonia, k_{NH_2} must be modified to $k_{NH_2} = (k_1[NH_2^-] + k'_1)k_2/(k_{-1} + k'_{-1}[NH_4^+] + k_2)$. When proton transfers are fast and reversible, specific base catalysis ensures that this reduces to the usual form $k_{NH_2} = Kk_2[NH_2^-]$ or, since the reaction occurs in acid solution, $k_{NH_2} = KK_Ak_2[NH_4^+]^{-1}$, where K_A is the ionic product of ammonia. However, when $k_2 \gg (k'_{-1}[NH_4^+] + k_{-1})$, general base catalysis is observed and the expression reduces to a new limit, $k_{NH_2} = k'_1 + k'_1K_A[NH_4^+]^{-1}$. Since the reprotonation is dominated by the $k'_{-1}[NH_4^+]$ term in sufficiently acidic solution, it might be possible to change the relative importance of the reprotonation and dissociation and change from deprotonation rate limiting base hydrolysis at low $[NH_4^+]$ to the 'normal' mechanism simply by increasing $[NH_4^+]$. This has been achieved in a very thorough study of the reaction of *trans*-[Co(NH$_3$)$_4$Cl$_2$]$^+$ in liquid ammonia.[311] The data also appear to indicate a temperature dependence of the crossover.

7.1.5.4 The *E*2 Mechanism

In order to account for the observation that the rate constants for the base hydrolysis of *cis*-[Co(cyclen)X$_2$]$^+$ depend on the nature of the leaving group (k_{OH} for X = Br is about $10k_{OH}$ for X = Cl) even though the observation of general base catalysis indicated rate limiting deprotonation, Hay[324,325] has suggested a synchronous deprotonation dissociation process (Scheme 4). Because there is some resemblance between the formation of the five-coordinate intermediate and the bimolecular elimination reaction at carbon, this has been labelled the *E*2 mechanism, and there was some suggestion that the reactions in which it seemed that $k_2 \gg k_{-1}$ might fit into this category. The problem is that with two *cis* X ligands in the system it is likely that the deprotonation rate constant k_1, which is strongly dependent upon the nature of the *trans* ligand, has also been affected. However, recent studies of the proton exchange behaviour of the *syn,anti* isomer (the labels refer to the orientation of the N—H bonds with respect to the Co—X bonds), which is almost certainly the one studied by Hay, have shown clearly that this is not a rate limiting deprotonation system and that for the protons on the nitrogens *trans* to X (the only ones that are exchanged during the reaction), $k_{-1} \gg k_2$.[326]

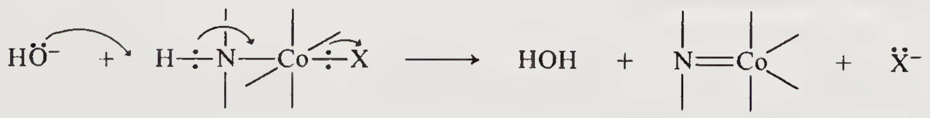

Scheme 4

7.1.5.5 Departures from the Simple Rate Law

There are a number of ways in which the rate law for base hydrolysis can depart from the simple second-order rate law discussed above in addition to the special cases in liquid ammonia already referred to.

7.1.5.5.1 *When a significant amount of the substrate exists in the form of the amido conjugate base*

Provided the proton transfer is rapid and reversible, the proton transfer process can be treated as a pre-equilibrium. At a constant [OH$^-$] the system will still possess first-order kinetics even when the amount of substrate in the form of the conjugate base is large and the stationary state condition is not required. The rate constant k_{obs} takes on the dependence. $k_{obs} = k_2K_{hy}[OH^-]/(1 + K_{hy}[OH^-])$

(in aqueous solution, where $K_{hy} = K_a/K_w$). When $K_{hy}[OH^-] \ll 1$ (*i.e.* the equilibrium amount of conjugate base is very small) this approaches the usual first-order dependence upon $[OH^-]$ and when $K_{hy}[OH^-] \gg 1$ (the complex being almost entirely in the form of the conjugate base) the rate becomes independent of $[OH^-]$($k_{obs} = k_2$). Contributions from a rate law of this sort have been found[327] for *cis*-$[Co(en)_2(imidazole)Cl]^{2+}$ where deprotonation occurs at the coordinated imidazole. Such departures are not observed[328] in the corresponding reactions of the *cis*-$[Co(en)_2(C_6H_5NH_2)Cl]^{2+}$ even though the coordinated aniline is thought to be sufficiently acidic to produce the effect.

7.1.5.5.2 *Blind alley deprotonation*

Although the hydroxide ion dependence can reflect distribution of the substrate between species of widely differing lability and might even be demonstrated using non-labile analogues,[327,329] all of the species studied have other sets of amine protons (*e.g.* on the diaminoethane) whose removal can lead to considerable labilization. Consequently, the rate law will not, in itself, distinguish between a pathway in which the major deprotonated species is highly reactive and undergoes reaction with rate constant k_2 (as depicted in Section 7.1.5.5.1) and one in which the deprotonated species is unreactive and the original substrate undergoes substitution that is first order in $[OH^-]$ using a different and far less acidic amine proton. The base catalyzed displacement of urea from $[Co(NH_3)_5\{OC(NH_2)_2\}]^{3+}$ shows such a departure from the first-order dependence on $[OH^-]$ at high enough concentrations[136] but, since the deprotonation occurs at the leaving group and thereby generates a much more tightly bound ligand, it must be concluded that the reaction involves the un-deprotonated substrate.

Other systems are ambiguous and require a careful consideration of the magnitudes of the derived rate constants before a conclusion can be drawn. An extreme case can be found in the pH dependence of the solvolysis of *cis*-$[Co(en)_2(H_2O)Cl]^{2+}$.[330] The rate is independent of pH in the range 7–9, where the complex is almost entirely in the form of *cis*-$[Co(en)_2(OH)Cl]^+$ and it is usually, and probably correctly, assumed that the pH independent rate constant is that for the uncatalyzed aquation of this species.[180] However, consideration ought to be given to the possibility that the observed process is the base catalyzed hydrolysis of the aquo complex in which a primary amine proton is removed. Problems of this sort are discussed in ref. 301, p.84.

7.1.5.5.3 *Ion association*

If instead of pre-equilibrium deprotonation the hydroxide ion was associated with the cationic substrate and thereby generated a more labile species, the rate law discussed above would also apply. Such a mechanism was originally suggested by Chan to account for the departures from the first-order $[OH^-]$ dependence that he observed in the base hydrolysis of $[Co(NH_3)_5Cl]^{2+}$,[331] but this was later shown to be an artefact.[332] The mechanism has been reinvoked recently to account for similar departures for the simple rate law for the loss of Me_2SO from $[Co(tren)(NH_3)(Me_2SO)]^{3+}$ (Me_2SO *trans* to the tertiary nitrogen[333]).

7.1.5.5.4 *Alternative reaction pathways*

The contribution from a second-order $[OH^-]$ dependence in the base hydrolysis of $[Co(NH_3)_5(OCOCF_3)]^{2+}$ is associated with C—O bond fission and comes from a pathway in which the first hydroxide adds to the carbonyl carbon and the second deprotonates it.[334]

7.1.5.5.5 *Double deprotonation*

A recent paper by Jackson[335] has thrown light on a puzzle first encountered many years ago,[336] namely that, under certain conditions, now known to be high concentrations of hydroxide,[337] Λ-*cis*-$[Co(en)_2Cl_2]^+$ gives as product $[Co(en)_2(OH)_2]^+$ in which there is net inversion. The usual behaviour encountered in the base hydrolysis of chiral *cis* complexes of this sort (and which is found for the *cis*-dichloro complex at lower OH^-) is that there is more retention than inversion. It was confirmed that, as has been suggested previously,[338,339] the new pathway with $[OH^-]$ dependence greater than one led directly to the dihydroxo complex without passing through the chlorohydroxo species with predominant *cis* inverted stereochemistry (70% Δ-*cis*; 18%-*trans*; 12% Λ-*cis*). It is inferred that double deprotonation generates a species that labilizes two sites rather than one. Up till now the *cis*-dichlorobis(diaminoethane) cobalt(III) cation presents the only example of this mechanism and until others are found it is not clear just what are the special requirements.

7.1.5.6 The Dissociative Nature of the Process

The base catalyzed solvolysis and substitution reactions of cobalt(III) complexes has provided some of the most fertile ground for the study of dissociatively activated processes and the attempts to distinguish between I_d and D mechanisms in terms of the lifetime of the intermediate species. The dissociative intimate mechanism has been demonstrated by a variety of trapping, competition and stereochemical studies. The base catalyzed substitutions of $[Co(NH_3)_5X]^{n+}$, in which addition of small amounts of OH^- in the presence of excess Y^- leads to a mixture of $[Co(NH_3)_5Y]^{2+}$ and $[Co(NH_3)_5OH]^{2+}$, are all consistent with a dissociatively activated process in which there is competition between Y^- and H_2O for the place vacated by $X^{(3-n)-}$. At the first approximation, the ratio $[Co(NH_3)_5Y^{2+}]/[Co(NH_3)_5OH^{2+}]$ increases linearly with $[Y^-]$ and is independent of $[OH^-]$[315] (indicating that it is H_2O and not OH^- that captures the intermediate, a conclusion reached many years ago from the isotopic fractionation studies).[340] The competition ratios are not independent of the nature of the leaving group but vary somewhat with its charge.[133,136,319,341,342]

A more subtle form of competition is found in the trapping of ambidentate ligands where the ratio of the concentrations of the two linkage isomers has to be determined with particular care and correction made for the subsequent reactions in order to avoid some of the mistakes made in some of the earlier work. It is now clear that in reactions of $[Co(NH_3)_5X]^{n+}$ the ratio is independent of the nature of the leaving group, which varies in charge from 0 to 2−, for Y = NCS^- (S:N = 2.0),[343] $S_2O_3^{2-}$ (S:O = 2.3),[344] and NO_2^- (O:N = 2.0).[345] These ratios do not reflect the thermodynamic stabilities of the isomers. It has been concluded that all of these reactions go by way of a '*common, short-lived intermediate* $[Co(NH_3)_4(NH_2)]^{2+}$ *which captures competing nucleophiles from an ion-atmosphere inherited from the conjugate-base complex,* $[Co(NH_3)_4(NH_2)X]^{(n-1)+}$'.[343] This, to some extent, overcomes the problem of distinguishing the role of the leaving group before the act of reaction (determining the charge on the complex and hence the consequent pre-equilibrium development of the ionic and solvation environment that might be inherited by a sufficiently short lived intermediate) from its role after bond breaking (when its continued presence in the vicinity will affect the processes that consume the intermediate).

The pentaammine system does not offer a convenient signpost for stereochemical studies (although the use of $^{15}NH_3$ to label the *trans* position, as in *trans*-$[Co(NH_3)_4(^{15}NH_3)Cl]^{2+}$, creates a signpost that does not introduce any steric, polar or other electron displacement effect to disturb the simple symmetry of the pentaammine system.[346,347] The most extensively used system of signposting is found in the *cis*- and *trans*-$[Co(en)_2(A)X]^{n+}$ series where there is not only the geometric isomerism but also the chirality of the *cis* complex. Base hydrolysis proceeds with extensive rearrangement in these Co^{III} systems, as might be expected if the role of the amido group is to stabilize the transition state leading to the trigonal bipyramidal intermediate. Careful and precise studies of the steric course of base hydrolysis show that *cis* and *trans* substrates rarely give the same product composition, indicating that any five-coordinate intermediates formed do not have time to rearrange by some form of pseudorotation. For a long time it has been believed that the *cis:trans* product ratio was independent of the nature of the leaving group,[335,348–350] but it is now clear that the distribution of chiral product of the base hydrolysis of a chiral *cis* substrate between the Δ and Λ forms is dependent upon the nature of X.[350] In a recent paper, Jackson[351] has shown that there is indeed a small dependence of the *cis:trans* product ratio upon the nature of X in the reactions of *cis*- and *trans*-$[Co(en)_2(A)X]^{n+}$ (A = NCS, N_3). For example, the percentages of *cis* product from *cis*-$[Co(en)_2(NCS)X]^{n+}$ are 82, 75 and 72 respectively for X = Cl^-, Br^- and Me_2SO. The implications are discussed in depth and it is concluded that the intermediate does not live long enough to equilibrate its environment and that the leaving group, therefore, may remain in its vicinity long enough to influence the subsequent behaviour.

7.1.5.7 The Labilizing Power of the Amido Group

In the absence of pK_a data for the individual amine protons in these substitutionally labile complexes it is not possible to evaluate k_2 and thereby measure precisely the amount by which deprotonation increases the lability of the complex. Even if such data were available it would be difficult, in complexes containing more than one type of amine proton, to be sure whether the two quantities related to the same proton. In spite of this major drawback it is possible to estimate orders of magnitude. The evidence suggests that in Co^{III} complexes the amido conjugate base can be between 10^5 and 10^{13} times more labile than the amine complex from which it was derived.[301] The effect is far less marked in equivalent complexes of Cr^{III}, Ru^{III} and Rh^{III}[352,353] and, so far, there have not been enough systematic studies to see whether the behaviour patterns resemble those established for Co^{III}.

Basolo and Pearson[207] suggested that the labilizing ability of the amido group stemmed from its ability to act as a π-donor and thereby facilitate the bond-breaking process (Scheme 5) and to stabilize the resultant five-coordinate intermediate. It was looked upon as more effective addition to the sequence of π-donors that had already been established, Cl— < HO— < H_2N—. It is possible to test this hypothesis by examining the factors that affect the labilizing power of the amido group; indeed it is of great interest to account for the wide varation of labilizing effects. Care must be taken to ensure that, in the absence of any example of complexes with only one removable amine proton, the labilizing nitrogen is correctly identified. There is considerable circumstantial evidence that an amido group *cis* to the leaving group will be far more labilizing than one *trans*,[354,355] although there is at least one exception to this rule.[225]

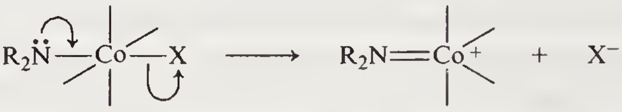

Scheme 5

The π-donor mechanism has fairly stringent stereochemical requirements. Clearly, the amido nitrogen should be planar in the transition state and it has been suggested that, in a d^6 system at least, best overlap is achieved when the metal has trigonal bipyramidal geometry and the nitrogen lies in the trigonal plane with its own coordination plane lying perpendicular.[356] The trigonal bipyramidal geometry of the intermediate has been well demonstrated in the Co^{III} system where the act of base hydrolysis is frequently accompanied by stereochemical change;[357] but this is almost unique to Co^{III}, the corresponding d^6 Rh^{III} systems always undergo substitution with retention of configuration. Even the d^3 Cr^{III} and low-spin d^5 Ru^{III} complexes undergo base hydrolysis without stereochemical change. There is almost certainly a very close connection between the ability to undergo substitution with stereochemical change and the sensitivity towards base hydrolysis but, as yet, no satisfactory explanation has been offered.

Studies of the stereochemical changes that occur at the amido nitrogen during the course of base hydrolysis have been made with varying success. Sargeson's pioneer work with *sym*-$[Co(trenen)Cl]^{2+}$ [358] (trenen = 1,8-diamino-3-(2′-aminoethyl)-3,6-diazaoctane), which claimed to disprove the π-donor mechanism, did not provide convincing evidence that the stereochemically labelled nitrogen (the secondary amine, *trans* to the chloride) was the labilizing π-donor. Other studies have demonstrated that the labilizing group did indeed become planar in the act of base hydrolysis.[321,359]

The very great difference in reactivity between α-*cis* on the one hand, and β-*cis* and *trans* isomers, on the other, of $[Co(L_4)Cl_2]^+$, where L_4 is a linear quadridentate ligand of the type $YCH_2NH(CH_2)_nNHCH_2Y$ (Y = 2-pyridyl, CO_2^-, NH_2CH_2—; $n = 2$ or 3) has been ascribed to the inability of the secondary amine nitrogen of the α-*cis* isomer, which is the site of the labilizing nitrogen, to arrange its coordination plane perpendicular to that of the cobalt in the five-coordinate intermediate.[355] This proves to be a fairly general observation and suggests the rule that '*the presence of a "flat" nitrogen* (i.e., *the central atom in a group of three linked donors occupying meridional sites*) cis *to the leaving group leads to high sensitivity towards base hydrolysis in cobalt(III) complexes*'.[360] As one might expect, there are a number of exceptions to this rule.[361,362]

Although the π-donation explanation for the labilizing power of the amido group is the one most commonly accepted, there has been, from time to time, a certain amount of disquiet arising from the lack of any obvious reason as to why only Co^{III} is so sensitive to the presence of a suitably oriented and positioned amido group and why complexes of the type *trans*-$[Co(L_4)Cl_2]^+$ are so particularly labile. The accessibility of the lower oxidation state has attracted some comment.[363] Since low-spin d^7 Co^{II} would be expected to be five-coordinate (or labile at one of its six octahedral sites), the k_2 step might in some way involve the transfer of a single electron to Co. The analogous reduction of d^3 Cr^{III} to high-spin d^4 Cr^{II} is known to increase substitutional lability by some 14 orders of magnitude in the case of the hexaaquo complex (see Table 1). It has been suggested that the difference in the sensitivity of analogous Co^{III} and Cr^{III} complexes towards base hydrolysis is related to the difference in the accessibility of the lower oxidation state.[364] Gillard suggested that the single-electron transfer came directly from the hydroxide ion in a preformed outer sphere complex,[365] but the energetics of the process will not allow this.[255] However, the analogous single-electron transfer from the bound amido group might provide the required reduction and offers an alternative explanation of the labilizing role of the amido group, possibly as an additional contribution found in the especially sensitive Co^{III} complexes. This suggestion, made in passing,[366] has never been properly followed up and, while there is as yet no established evidence for its occurrence anywhere in Co^{III} chemistry, it has been invoked in certain base catalyzed amine ligand oxidations involving complexes of Ni^{III},[367,368] Fe^{III} [369,370] and, in particular, Ru^{III}.[371,372]

It is tempting to suggest that the synchronous loss of *two* chlorides from the *cis*-$[Co(en)_2Cl_2]^+$ cation at high $[OH^-]$, where double deprotonation has been indicated,[335] arises from the formation of a *four-coordinate* intermediate produced as a consequence to *two* electron transfers, one from each amido group, forming a d^8 square-planar Co^I intermediate.

7.1.6 COMPLEX FORMATION AND ANATION

7.1.6.1 Introduction

Studies of labile systems involving metal ions and ligands in coordinating solvents will yield, through a study of their relaxation kinetics, the rates and rate laws for the solvolysis of the complex together with those for the reverse reaction, the replacement of coordinated solvent by another ligand. This second process has been termed *complex formation*. In inert systems, the displacement of the coordinated solvent can be studied under non-reversible conditions, starting with the appropriate solvento complex. In many cases, *e.g.* $[Co(NH_3)_5(H_2O)]^{3+}$ in water, it is possible to study the displacement of a single ligand. Such a reaction has termed an *anation* because the early work dealt almost entirely with the entry of anionic reagents, but the process applies to all entering ligands, irrespective of charge. The terms *complex formation* and *anation* are therefore synonymous in their mechanistic connotation.

This area has attracted a great deal of interest and many reviews have been published.[17,373–379] The most recent, and probably the largest, [17] deals primarily with labile systems and should provide an excellent source of references for that area. The literature up to and including 1975 is covered and so this review is too early to include the important contributions of Merbach and coworkers which are discussed in Section 7.1.2.

For a considerable time the complex formation reaction was the most direct way of using kinetics to establish the mechanisms of substitutions of labile metal complexes. For those inert systems in which ligand substitution occurred only by way of a solvolysis–anation sequence, the anation reaction provided the only means of using kinetics to assign mechanism. Although the solvolytic reaction might be mechanistically evaluated through the use of structure–reactivity arguments of the sort recounted in previous sections, it was usual to assign a molecularity to the anation reaction and then plead the Law of Microscopic Reversibility. In recent years, more and more substitutions have been studied in non-interfering solvents and their mechanisms established from their kinetics. In addition, the development of techniques to measure the volumes of activation of solvent exchange has allowed a direct assignment of mechanism to such processes. This has been discussed in Sections 7.1.2 and 7.1.3.

The arguments in favour of treating complex formation/anation processes as mechanistically separate phenomena have therefore lost some of their force as the subject has developed in recent years and, for this reason, only certain aspects will be discussed in this section.

7.1.6.2 The Rate Laws and Mechanisms

The fact that the leaving group is chemically identical to the solvent leads to further complications in the relationship between the kinetics and the mechanism of these reactions. All mechanistic types, *i.e.* A, D, I_a and I_d, can give rise to the same rate law and the interest lies in the criteria that are needed to make the distinction and, eventually, in the significance of the distinctions that are made.

In aqueous solution, the general rate law for complex formation represented by:

$$[M(L)_n S] + L' = [M(L)_n L'] + S$$

(where L may also be the solvent, S, and charges are omitted for the sake of simplicity) takes the simple second-order form

$$-d[M(L)_n S]/dt = k'[M(L)_n S][L']$$

(the exceptions to this will be discussed separately). Frequently in coordinating non-aqueous solvents, the rate law becomes more complex, often taking the form[61,380,381]

$$-d[M(L)_n S]/dt = kK[M(L)_n S][L']/(1 + K[L'])$$

This expression reduces to the simple second-order rate law when $K[L'] \ll 1$ (and to a simple first-order rate law, $-d[M(L)_nS]/dt = k[M(L)_nS]$, when $K[L'] \gg 1$).

Interchange mechanisms (I_a or I_d), which take place within a preformed outer-sphere complex, will generate the observed rate laws

$$\begin{aligned} &[M(L)_nS] + L' \rightleftharpoons [M(L)_nS]\ldots L', && K_{os} \\ &[M(L)_nS]\ldots L' \longrightarrow [M(L)_nL']\ldots S, && k_i \end{aligned}$$

with $K = K_{os}$ and $k = k_i$. If outer-sphere complexes containing more than one L′ have different interchange lability or lead to different products, the rate law might be even more complicated.[382] The rate law will not distinguish associative from dissociative interchange.

The dissociative (D) mechanism, in which the intermediate of lower coordination number lives long enough to equilibrate its environment and hence be consumed in a way that is independent of its mode of formation

$$\begin{aligned} &[M(L)_nS] \rightleftharpoons [M(L)_n] + S, && k_1, k_{-1} \\ &[M(L)_n] + L' \longrightarrow [M(L)_nL'], && k_2 \end{aligned}$$

will, because of the mass-law retardation by the solvent whose concentration remains unchanged, give the required rate law with $k = k_1$ and $K = k_2/k_{-1}[S]$.

A truely associative (A) mechanism will give a simple second-order rate law as long as the concentration of the intermediate of higher coordination number remains small.

$$\begin{aligned} &[M(L)_nS] + L' \rightleftharpoons [M(L)_nS(L')], && k_a, k_{-a} \\ &[M(L)_nS(L')] \longrightarrow [M(L)_nL'] + S, && k_b \end{aligned}$$

whence $-d[M(L)_nS]/dt = [k_ak_b/(k_{-a} + k_b)][M(L)_nS][L']$.

7.1.6.3 Assignment of Mechanism

The most commonly used criteria for the assignment are collected together in Table 13. It is quite obvious from this that the key to assigning mechanism is the ability to detect and measure K.

Table 13 Distinction between D, I_d, I_a and A Mechanisms for Solvent Displacement Reactions: General Rate Law, $k_{obs} = ab[L']/(1 + b[L'])$

	D	I_d	I_a	A
The significance of the quantity a	k_1[a]	k_i	k_i	$\frac{k_ak_b}{k_{-a} + k_b}K_{os}^{-1}$
The magnitude of a	Independent of nature of L′	Not very dependent on L′	Dependent on nature of L′	Strongly dependent on nature of L′
Relationship of a to k_{exch}	$a = k_{exch}$	$a < k_{exch}$	No relationship	No relationship
The significance of the quantity b	$k_2/k_{-1}[S]$	K_{os}	K_{os}	K_{os}
The magnitude of b	Depends on chemical nature of L′	Depends upon the size and charge of the substrate and L′ and the solvent dielectric constant. May be enhanced by hydrogen bonding.		

[a] Rate constants are defined in the text.

When conditions are such that $K[L']$ is always much less than 1, the rate law alone is a very poor guide to mechanism. In aqueous solution, where K_{os} is usually small, considerable problems present themselves when high concentrations of L′ are used, especially when this is a charged reagent. The meaning of *constant ionic strength* (which must be maintained in order to cancel primary salt effects) is not unambiguous and specific ion effects, ion-association by non-coordinating anions, such as ClO_4^-, and the general problems of replacing one ion by another, may cause departures from a simple second-order rate law that are not the result of distributing the substrate between reactive and unreactive forms. Consequently errors appear in the determination of K (and hence k_i in an interchange process). Even more serious is the absence of a departure from first-order dependence on [L′] even when an independent, non-kinetic determination of K_{os} would predict one. The reaction

$$[Co(NH_3)_5(H_2O)]^{3+} + SO_4^{2-} \rightleftharpoons [Co(NH_3)_5(SO_4)]^+ + H_2O$$

presents such an example since K_{os}, determined non-kinetically, $= 11\ dm^3\ mol^{-1}$ at 25 °C (μ = 1.0),[383] and yet there is no significant departure from first-order dependence on $[SO_4]^{2-}$ at 0.60 mol dm^{-3} (μ = 2.0).[384] Possible explanations are discussed in this paper which also contains a very comprehensive list of references. The question is also discussed by Swaddle.[25] The deceptively simple reaction

$$[Co(NH_3)_5(H_2O)]^{3+} + Cl^- \rightleftharpoons [Co(NH_3)_5Cl]^{2+} + H_2O$$

has been examined by at least four groups[384–387] who are by no means unanimous in their conclusions. Because of a variety of problems, *e.g.* reversibility, small absorbance change, *etc.*, such systems frequently do not yield data of sufficient precision or reproducibility to allow the mechanistic distinctions to be made and present a minefield for the inexperienced or the unwary.

In many cases, K_{os} is calculated using the Fuoss–Eigen equation[388] or some other electrostatic model based on charge, size and dielectric constant. Although not an obvious complication in aqueous solution where solvation of amine protons by water is strong, there is extensive evidence that hydrogen bonding between suitabily oriented amine protons and anionic nucleophiles can greatly increase K_{os}.[382,389,410]

7.1.6.4 The Interchange Mechanism

According to the definitions of Langford and Gray,[6] the distinction between the I_a and I_d mechanism should rest upon the extent to which the interchange rate constant k_i depends upon the nature of the entering group L′. An associatively activated process should demonstrate a considerable nucleophilic discrimination and if all systems behaved as well as the four-coordinate planar complexes of d^8 metal ions, (see 7.1.7 below), there would be little room left for argument. However, the main problem encountered is that many systems exhibit what might be looked upon as borderline behaviour. For a long time it was thought that all complex formation and anation reactions had the Eigen–Wilkins mechanism,[373] which was the standard I_d mechanism (k_i being independent of the nature of the entering group) but predated the introduction of the latter nomenclature in the Langford–Gray book.[6] The $[Co(NH_3)_5(H_2O)]^{3+}$ system showed this behaviour with k_i independent of the nature of L′ and about 20% of the magnitude of the rate constant for water exchange, k_{exch}. It was suggested that this fraction represented the statistical chance of L′ in the outer sphere competing with the water molecules that were also there.[385] The volume of activation and slope of the plot of log K against log k_{aq} are all consistent with an I_d mechanism (see Section 7.1.4.2.1).

The criterion that k_i cannot be greater than k_{exch} in an I_d process is based on the assumption that, in the absence of competing nucleophiles, every act of ligand dissociation in the solvento complex results in solvent exchange. Even assuming that the proper statistical treatment has been applied to the exchange data when there is more than one solvent molecule in the coordination shell,[67,390] there is always the possibility that many of the acts of bond dissociation are followed by the undetectable recapture of the same solvent molecule that had dissociated. This is most likely when the solvent molecule is large and the availability of others, suitably placed for exchange, is consequently reduced. For example, whereas $[Co(NH_3)_5(H_2O)]^{3+}$ obeys all the rules for the I_d mechanism, k_{exch} for $[Co(NH_3)_5S]^{3+}$ is less than k_i when $S = Me_2SO$[391] and dimethylformamide[392] even though the other criteria firmly indicate dissociative activation.

The assignment of an I_a mechanism to the anation of $[Rh(NH_3)_5(H_2O)]^{3+}$ by Cl^-, based on the observation[146,393] that $k_i > k_{exch}$, is weakened by the results of a detailed study of the effect of varying the ionic strength on the rate of anation.[394] Using these data to guide the extrapolation it is found that, at zero ionic strength, k_{exch} is no longer less than k_i. Even so, the volume of activation for water exchange (-4.1 cm^3 mol^{-1})[145] is fully consistent with an I_a mechanism. There is now considerable evidence that strong nucleophilic discrimination is not a necessary requirement for a mode of activation that is indicated as associative by the possession of a negative $\Delta V^{\ddagger}$ value and that the behaviour pattern of $[Mn(H_2O)_6]^{2+}$ (negative $\Delta V^{\ddagger}$ for water exchange, k_i insensitive to the nature of the entering group)[38] is not an isolated example.

Many cases exist where the nucleophilic discrimination may be quite significant. Of the d^3 ions, $[Cr(H_2O)_6]^{3+}$ exerts considerable nucleophilic discrimination[395,396] and the volume of activation for water exchange is negative, and $[Mo(H_2O)_6]^{3+}$, with much fewer nucleophiles studied, is also strongly discriminating.[397] The much greater reactivity of the Mo^{III} system compared with Cr^{III} is consistent with its greater size and hence its greater ability to expand its coordination shell. The d^2 $[V(H_2O)_6]^{3+}$ [398,399] and even the high-spin d^5 $[Fe(H_2O)_6]^{3+}$ [32,400] also exhibit considerable nucleophilic discrimination that is consistent with the negative $\Delta V^{\ddagger}$ values for water exchange.[43]

7.1.6.5 The Dissociative (D) Mechanism

A proper D mechanism requires that k_1 be identical to the rate constant for the exchange of solvent (due account being taken of any statistical correction when more than one solvent molecule is present) and the value of k_2 (in reality the term $k_2/k_{-1}[\mathrm{S}]$ is used because the constants cannot be separated) should be sensitive to the chemical nature of L′ rather than its size and charge (factors that control K_{os} in an interchange mechanism). The most convincing demonstration of a D mechanism would be found in cases where $k_2/k_{-1}[\mathrm{S}]$ is much larger than any value expected for an outer-sphere complex formation constant, but this is not a necessary requirement for the mechanism.

The first published example was thought to be the anation of $[\mathrm{Co(CN)_5(H_2O)}]^{2-}$, it being argued that the interactions between the negatively charged substrate and anionic reagents would make K_{os} very small. Departures from a simple first-order dependence on [L′] were found at concentrations low enough to avoid the ambiguities that arise in attempts to maintain a constant ionic strength.[177,401–403] No value has yet been produced for water exchange and a recent reexamination of the kinetics of the reaction with $\mathrm{N_3}^-$ has indicated that the departure from a first-order dependence is a great deal less than originally thought,[404] or even non-existent.[405] Volumes of activation are said to be consistent with a D mechanism.[406] The complex *trans*-$[\mathrm{Co(CN)_4(SO_3)(H_2O)}]^{3-}$, with the greater negative charge and the strong *trans* labilizing sulfito group, provides a less debatable example[407] and many complexes containing other very strong *trans* labilizing ligands demonstrate the mechanism very well indeed.[291,408,409]

7.1.6.6 The Associative Mechanism

Although the conceptual distinction between an I_{a} and an A mechanism is that in the latter case there can be direct reaction between the substrate and the entering nucleophile, the rate law for the A mechanism can still be affected by outer sphere complex formation. If the substrate is in equilibrium with its outer sphere complex then, if the reaction is carried out under pseudo first-order conditions

$$k_{\mathrm{obs}} = (k_{\mathrm{a}}k_{\mathrm{b}} + K_{\mathrm{os}}k_{\mathrm{i}})[\mathrm{L'}]/\{(k_{-\mathrm{a}} + k_{\mathrm{b}} + k_{-\mathrm{i}})(1 + K_{\mathrm{os}}[\mathrm{L'}])\}$$

(where the symbols are as defined in Section 7.1.6.2 and $k_{-\mathrm{i}}$ is the rate constant for the dissociation of the intermediate of higher coordination number to give the outer sphere complex). Thus, even if the interchange process represented a 'blind alley', *i.e.* $k_{\mathrm{i}} = 0$, the reaction will still obey saturation kinetics. If it is possible to achieve a situation where $K_{\mathrm{os}}[\mathrm{L'}] \gg 1$ and there is still no significant departure from a first-order dependence on [L′], it must be assumed either that the outer-sphere complex can react with a second L′ with a rate constant very close to that of the free substrate or that the assumption that the formation of the outer-sphere complex is a rapid pre-equilibrium process is wrong.

When $K_{\mathrm{os}}[\mathrm{L'}] \ll 1$, the usual second-order kinetic rate law will arise and any distinction between A and I_{a} will be arbitrary and based upon imposed criteria such as the extent of nucleophilic discrimination and the magnitude of the volume of activation. Because the dominant pathway for substitution in four-coordinate planar d^8 metal ion complexes is associative (Section 7.1.7), the complex formation reactions of $[\mathrm{Pd(H_2O)_4}]^{2+}$[411] and $[\mathrm{Pt(H_2O)_4}]^{2+}$[412,413] ought to provide a model for the A process. The kinetics do not depart from the simple second-order rate law over the range of concentration of L′ examined, even when this nucleophile is anionic. The rate constants are very sensitive to the nature of the entering group and many reactions are much faster than water exchange[414] in keeping with the nucleophilic preferences of these reaction centres. It was suggested that the similarity of the rate constants for the entry of some of the weaker nucleophiles, including water, indicated an $I_{\mathrm{d}}/I_{\mathrm{a}}$ crossover,[414] but the volumes of activation of the water exchange in $[\mathrm{M(H_2O)_4}]^{2+}$ ($-2.2\ \mathrm{cm^3\ mol^{-1}}$ for M = $\mathrm{Pd^{II}}$ [415] and $-4.6\ \mathrm{cm^3\ mol^{-1}}$ for M = $\mathrm{Pt^{II}}$)[416] clearly indicate associative activation.

The replacement of a single coordinated solvent molecule in four-coordinate planar complexes of the type $[\mathrm{M(L_3)S}]$ is a well studied phenomenon for a wide variety of charged and uncharged substrates and is best considered in Section 7.1.7 below. $[\mathrm{Pt(dien)(H_2O)}]^{2+} + \mathrm{L'}^- \rightleftharpoons [\mathrm{Pt(dien)L'}]^+ + \mathrm{H_2O}$ has been studied in great depth.[417,418] The reactivities of the various nucleophiles follow the appropriate nucleophilicity scale for other dicationic substrates[419] and the substrate is reasonably discriminating. The rate law is strictly second order (the observation that $k_{\mathrm{obs}} = k_1 + k_2[\mathrm{L'}]$ observed by Gray and Olcott[417] has since been shown to be an artefact).[420]

7.1.7 SUBSTITUTION IN FOUR-COORDINATE PLANAR d^8 METAL COMPLEXES

7.1.7.1 Introduction

It is convenient to consider these substitution reactions separately because they constitute a group with very characteristic mechanistic features. Many involve inert complexes (although reactions can be fast once the reagents are mixed) and are therefore capable of study in great depth. Since the first systematic work was published in 1957 [421] there has been a steady stream of papers and many reviews[422–432] have appeared.

The d^8 configuration is represented by a group of very stable oxidation states. Of those that favour four-coordinate planar coordination, platinum(II) stands out because the level of reactivity places its complexes within the range of rates conveniently studied by conventional, classical techniques and because the stability of the oxidation state is high. Oxidation state (II) is even more stable for palladium but the 10^5 fold greater reactivity tends to restrict the scope of any study. Complexes of gold(III) are generally more labile than those of Pt^{II} but can conveniently be studied by classical techniques; however, they can be reduced to Au^I by many of the 'soft' nucleophiles. Closer examination has shown that, as a rule, the reduction follows, rather than accompanies, the act of substitution[433–435] and much more should be done in this area. There are cases when the reduction is direct, *e.g.*[436]

$$[AuCl_4]^- + I^- \longrightarrow [AuCl_2]^- + Cl^- + ICl$$

Ag^{III} is a very strongly oxidizing state and any detailed and extensive study is ruled out because of the lack of a large range of substrates. However, it has been shown that the rate determining step in certain redox reactions of $[Ag(OH)_4]^-$ is ligand substitution, the kinetics of which are consistent with those of the other d^8 systems.[437] Rhodium(I) and iridium(I) species, on the other hand, are susceptible to oxidation and, although their reactions have been widely examined the thrust of interest has been towards oxidative addition processes. In the +I and lower oxidation states there is an increasing tendency towards stable five-coordination and/or metal–metal bonding and the four-coordinate form is very rare in the chemistry of Co^I, Fe^0, Ru^0, Os^0, Mn^{-I}, Tc^{-I}, Re^{-I}, *etc.*.[438] Although there is an extensive four-coordinate planar chemistry of nickel(II), it is necessary to have strong field ligands to achieve this. Even then, the availability of the tetrahedral geometry and the various forms of five and six coordination and the high lability makes the system potentially very complicated.

7.1.7.2 The Rate Laws

The dominant feature of substitution reactions in four-coordinate planar systems is that, with very few exceptions, they are associatively activated, the rates of reaction often being extremely sensitive to the nature of the entering nucleophile. When the reaction is studied under irreversible conditions the observed rate law is

$$-d[L_3MX]/dt = \left\{\frac{k_1k_y[Y]}{k_x[X] + k_y[Y]} + k_2[Y]\right\}[L_3MX]$$

or one of its limiting forms. The processes are usually studied under conditions where $[Y] \gg$ [complex] in order to ensure first-order conditions in any one kinetic run, so that the relationship can be written in terms of the observed first-order rate constant,

$$k_{obs} = \frac{k_1k_y[Y]}{k_x[X] + k_y[Y]} + k_2[Y]$$

Frequently, another consequence of this condition is that $k_y[Y] \gg k_x[X]$ and the expression reduces to the familiar

$$k_{obs} = k_1 + k_2[Y]$$

Often it is necessary to add a considerable excess of X to the reaction mixture, perhaps to suppress solvolysis of the substrate, and then the more general form of the rate law is observed.[439,440] In extreme cases, where $k_x[X] \gg k_y[Y]$, the expression should reduce to

$$k_{obs} = \left\{\frac{k_1k_y}{k_x[X]} + k_2\right\}[Y]$$

but, unless the contribution from the k_2 pathway is negligible, it is obvious that the observed form will be $k_{obs} = k_2[Y]$. When it is possible to study the reactions under conditions where the two-term rate law applies it is found that k_1 is independent of the nature of Y while k_2 is very dependent upon it. Frequently when k_1 appears to be sensitive to the nature of Y it can be shown that the data fit the more complicated expression.

The rate law is consistent with a two-path mechanism in which the first term arises from the reversible solvolysis in which X and Y compete for some labile intermediate and the second arises from the direct reaction between Y and the substrate $[L_3MX]$ (Scheme 6). If the concentration of the labile solvento intermediate remains small enough for the stationary state approximation to be valid, the observed rate law is obtained. It is possible to use the more detailed description of the *A* mechanism (see Section 7.1.6.2) with k_a as the rate constant for the formation of the five-coordinate intermediate and k_{-a} and k_b its rate constants for dissociation, then $k_2 = k_a k_b/(k_{-a}+k_b)$. When no advantage is to be gained in separating the bond making and breaking aspects of the process, the simple description, *i.e.* k_2, will be used.

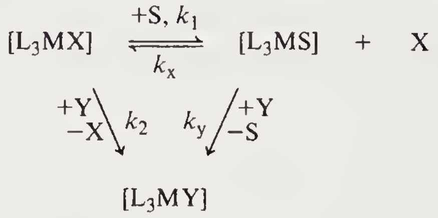

Scheme 6

Occasionally the amount of solvento complex present is too great for the stationary state approximation to be valid and the analysis of the rate constants will be more complicated.[441] A rapidly established equilibrium between the substrate and the solvento complex is not uncommon in labile systems with low concentrations of the nucleophile and leads to a rate law of the type

$$k_{obs} = \left\{\frac{k_y K + k_2[X]}{[X] + K}\right\}[Y]$$

where K is the solvolytic equilibrium constant ($= k_1/k_y$).[442,443]

Unusual rate laws involving higher orders are known, *e.g.* $k_{obs} = (a + b[H^+])[Br^-] + c\,[H^+][Br^-]^3$ for the displacement of bipyridine from $[Au(bipy)Br_2]^+$ by Br^- in acid aqueous solution,[444] and are frequently associated with the displacement of a multidentate ligand. However, the $k_{obs} = k_1{}^0 + k_a[OH^-] + k_b[OH^-]^2$ rate law observed in the displacement of NH_3 from *cis*-$[Pt(NH_3)_2(Me_2S)_2]^+$ by hydroxide[445] offers no such explanation.

Although the evidence for the direct attack on the substrate by the nucleophile is overwhelming it was necessary to examine the k_1 pathway in depth to decide whether it represented a parallel dissociative process or associative solvolysis. Trapping,[417] $\Delta V^{\ddagger}$ measurements[446] and the general observation that k_1 and k_2 respond in a similar fashion to electronic and steric variations in the other ligands in the substrate suggest that both pathways possess the same mode of activation. The possibility of dissociative activation in d^8 planar complexes is discussed separately below (Section 7.1.7.6) and further consideration of this question is best reserved until then.

7.1.7.3 Nucleophilicity Scales in Four-coordinate Planar Substitution

When an associative mode of activation is indicated it is instructive to examine the ways in which reactivity, as measured by the second-order rate constant k_2, depends upon the nature of the nucleophile and if a large number of substrates show the same pattern of preference it is useful to consider scales of nucleophilicity. A systematic study of the substitution reactions of *trans*-$[Pt(py)_2Cl_2]$ (it appears that pyridine and piperidine were used interchangeably) in methanol at 30 °C (displacement of chloride) led to the establishment of an n_{Pt} scale, $n_{Pt} \overset{\mathrm{def}}{=} \log_{10}(k_2/k_1)$ for the standard reaction,[447] and later the more dimensionally correct $n_{Pt}{}^0$ scale[448,449] ($n_{Pt}{}^0 \overset{\mathrm{def}}{=} \log_{10}(h_2/k_1)[MeOH]$) so that $n_{Pt}{}^0 = n_{Pt} + 1.41$ (unfortunately this distinction has not been strictly adhered to in the literature).[449] A collection of $n_{Pt}{}^0$ values will be found in Table 14.

In general, the nucleophilicity pattern is in accord with the 'soft' or Class b requirements of platinum(II). Ligands with light element donors, N, O and F, are considerably less effective than their second-row equivalents. Thus, $F^- \ll Cl^- < Br^- < I^-$; $R_2O \ll R_2S < R_2Se$; and $R_3N \ll R_3P > R_3As$. Carbon donors, *e.g.* CNR and CN^-, are good nucleophiles towards Pt^{II}. The extent to which the nucleophilicity is modified by the substituents attached to the donor has not yet been evaluated thoroughly. Probably the most extensive set of data refers to sulfur donors, the values

Table 14 A Selection of $n_{Pt}{}^0$ Values[a] Listed According to Donor Atoms

Carbon		*Nitrogen*					
$C_6H_{11}NC$	6.34	NH_3	3.07	C_5H_5N	3.19	N_3^-	3.48
CN^-	7.14	$C_5H_{10}NH$	3.13	NO_2^-	3.22	NH_2OH	3.85
		$PhNH_2$	3.16	imididazole	3.44	NH_2NH_2	3.86
Oxygen		*Halogens*		*Phosphorus*			
MeOH	0.00	F^-	$<2.2^{b}$	$(Et_2N)_3P$	4.57	Ph_3P	8.93
MeO^-	$<2.4^{b}$	Cl^-	3.04	$(MeO)_2PO^-$	5.01	$Bu_3{}^nP$	8.96
OH^-	$<2.4^{b}$	Br^-	4.18	$(MeO)_3P$	7.23	Et_3P	8.99
$MeCO_2^-$	$<2.4^{b}$	I^-	5.46				
Sulfur							
Me_2SO	2.56^{c}	$(4\text{-}MeOC_6H_4)PhS$	3.64^{e}	$(4\text{-}MeOC_6H_4)MeS$	4.55^{d}	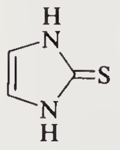	6.39^{c}
$(4\text{-}MeC_6H_4)MeSO$	2.60^{d}	$(4\text{-}MeC_6H_4)_2S$	3.68^{e}	Me_2S	4.87		
$(Ph)MeSO$	2.90^{d}	$(4\text{-}MeOC_6H_4)_2S$	3.73^{e}	$(CH_2)_5S$	5.02		
$(4\text{-}MeOC_6H_4)MeSO$	3.16^{d}	$(4\text{-}HOC_6H_4)_2S$	3.85^{e}	$(CH_2)_4S$	5.14	$(NH_2)_2CS$	7.17
$(4\text{-}ClC_6H_4)_2S$	3.21^{e}	PhMeS	3.99^{d}	SCN^-	5.75	PhS^-	7.17
Ph_2S	3.22^{e}	$(4\text{-}ClC_6H_4)MeS$	4.04^{d}	SO_3^{2-}	5.79	$S_2O_3^{2-}$	7.34
$(4\text{-}ClC_6H_4)PhS$	3.25^{e}	PhSH	4.15	$(Me_2N)_2CS$	5.83^{c}		
$(4\text{-}FC_6H_4)_2S$	3.30^{e}	$(4\text{-}MeC_6H_4)MeS$	4.24^{d}				
$(4\text{-}NH_2C_6H_4)(4\text{-}NO_2C_6H_4)S$	3.31^{e}	$(4\text{-}H_2NC_6H_4)_2S$	4.27^{e}	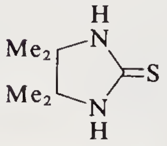	6.07^{c}		
$(PhCH_2)_2S$	3.43	Et_2S	4.52				
Arsenic		*Selenium*		*Tin*		*Antimony*	
Ph_3As	6.89	$(PhCH_2)_2Se$	5.53	$SnCl_3^-$	5.44	Ph_3Sb	6.79
Et_3As	7.68	Me_2Se	5.70				
		$SeCN^-$	7.11				

[a] Data from ref. 449 except where stated.
[b] No k_2 term could be observed.
[c] Data from ref. 452.
[d] Data from ref. 451.
[e] Data from ref. 450.

of $n_{Pt}{}^0$ ranging from 2.56 for Me_2SO to 7.34 for $S_2O_3{}^{2-}$. For a series of related species such as thioethers, RR′S,[451,452] and sulfoxides, RR′S(O)[450,451] (bonding finally through S although it is possible that the initial attack is made through the oxygen, hence the low $n_{Pt}{}^0$ value), there are reasonably good linear relationships between $n_{Pt}{}^0$ and $\Sigma\sigma$ (the sum of the Hammett functions relating to the inductive effects of the substituents) suggesting that displacement of charge towards the sulfur is a major factor controlling its nucleophilicity. Variation of the substituent at nitrogen, on the other hand, seems to have a far smaller effect on $n_{Pt}{}^0$. Within the range of amines studied, the $n_{Pt}{}^0$ values have little dependence on the proton basicity of the ligand. Although strictly speaking they refer to nucleophilic discrimination it is convenient here to draw attention to the many studies of the way in which the rate of entry of amines into a wide range of d^8 substrates depends upon the proton basicity of the amine. In many cases, but not always, [453] there is a linear dependence of the type $\log k_2 = \alpha(pK_a) + b$ (where pK_a refers to that of amH^+ in water at 25 °C). Some of these α values are collected in Table 15 together with those for Pd^{II} and Au^{III} systems. Although far less common in Pt^{II} substrates than elsewhere, large values of α are frequently observed. In some cases,[440,441,453,456] α for the entry of heterocyclic nitrogen bases is negative, *i.e.* the least basic nucleophiles have the greatest reactivity, and it has been suggested that back donation from filled orbitals on the metal into empty antibonding orbitals on the ligand can assist the early stages of bond formation.

When the platinum nucleophilicity scale was first proposed[447] it was implied that one $n_{Pt}{}^0$ scale was applicable to all substrates and that plots of $\log k_2{}^Y$ against $n_{Pt}{}^0(Y)$ were linear, taking the form $\log_{10} k_2{}^Y = Sn_{Pt}{}^0(Y) + C$, where S is termed the nucleophilic discrimination factor of the substrate and C its intrinsic reactivity. Discussions of mechanism based on a comparison of nucleophilic discrimination factors are frequently encountered.[463–466] Nucleophiles that do not retain their positions in the nucleophilicity scale, *e.g.* NO_2^-, $SeCN^-$ and $SC(NH_2)_2$, were termed *biphilic* by Cattalini[463] since their behaviour could be explained by their π-acceptor properties. When the Pt^{II} reaction centre had a greater π-basicity than the standard complex (for example a smaller effective nuclear charge) the substrate was more reactive than predicted and *vice versa*. This concept had been deduced some years earlier by Bosnich[467] from his work with octahedral Ru^{II} complexes

Table 15 Dependence of the Second-order Rate Constants for the Entry of Heterocyclic Nitrogen Bases of their Proton Basicity[a]

Substrate	*Leaving group*	*Solvent*	α	*Refs.*
$[\mathrm{Pt(bipy)Cl_2}]$	$\mathrm{Cl^-}$	MeOH	0.06	454
trans-$[\mathrm{Pt(py)_2Cl_2}]$	$\mathrm{Cl^-}$	MeOH	0.05	428
cis-$[\mathrm{Pt(Me_2S)_2Cl_2}]$	$\mathrm{Me_2S}$	dme[b]	0.18	24
trans-$[\mathrm{Pt(Me_2S)_2Cl_2}]$	$\mathrm{Me_2S}$	dme	0.18	24
trans-$[\mathrm{Pt(Pr_2{}^iS)_2Cl_2}]$	$\mathrm{Pr_2{}^iS}$	dme	0.14	455
cis-$[\mathrm{Pt(Me_2SO)_2Cl_2}]$	$\mathrm{Me_2SO}$	dme	0.41	84
meso-$[\mathrm{Pt(SOSO)Cl_2}]$[c]	SOSO ring opening	dme	0.58	83
rac-$[\mathrm{Pt(SOSO)Cl_2}]$[c]	SOSO ring opening	dme	0.58	83
$[\mathrm{Pt(Me_2SO)Cl_3}]^-$	*trans*-$\mathrm{Cl^-}$	MeOH	−0.07	453
$[\mathrm{Pt(Me_2S)Cl_3}]^-$	*trans*-$\mathrm{Cl^-}$	MeOH	−0.10	440
$[\mathrm{Pt(Et_2S)Cl_3}]^-$	*trans*-$\mathrm{Cl^-}$	MeOH	−0.12	456
$[\mathrm{Pt\{P(OMe)_3\}Cl_3}]^-$	*trans*-$\mathrm{Cl^-}$	MeOH	−0.11	441
$[\mathrm{Pt(PPh_3)Cl_3}]^-$	*trans*-$\mathrm{Cl^-}$	MeOH	−0.16	441
$[\mathrm{Pt(PEt_3)Cl_3}]^-$	*trans*-$\mathrm{Cl^-}$	MeOH	−0.19	441
$[\mathrm{Pt\{(Bu^n)_3P\}Cl_3}]^-$	*trans*-$\mathrm{Cl^-}$	MeOH	−0.20	441
$[\mathrm{Pt(PMe_3)Cl_3}]^-$	*trans*-$\mathrm{Cl^-}$	MeOH	−0.22	441
$[\mathrm{Pt(AsEt_3)Cl_3}]^-$	*trans*-$\mathrm{Cl^-}$	MeOH	−0.18	441
$[\mathrm{PdCl_4}]^{2-}$	$\mathrm{Cl^-}$	$\mathrm{H_2O}$	0.24	457
$[\mathrm{Pd(dien)X}]^{+}$[d]	$\mathrm{X^-}$	$\mathrm{H_2O}$	0.00	458
$[\mathrm{Pd(SS)Cl_2}]$[e]	SS	dme	0.22	459
trans-$[\mathrm{Pd(Pr_2{}^iS)_2Cl_2}]$	$\mathrm{Pr_2{}^iS}$	dme	0.13	455
trans-$[\mathrm{Pd(4\text{-}Cl\text{-}py)_2Cl_2}]$	4-Cl-py	dme	0.08	460
trans-$[\mathrm{Pd(4\text{-}Cl\text{-}py)_2Br_2}]$	4-Cl-py	dme	0.24	460
trans-$[\mathrm{Pd(4\text{-}Cl\text{-}py)_2I_2}]$	4-Cl-py	dme	0.34	460
$[\mathrm{AuCl_4}]^-$	$\mathrm{Cl^-}$	acetone	0.15	461
$[\mathrm{Au(phen)Cl_2}]^+$	$\mathrm{Cl^-}$	acetone	0.22	462
$[\mathrm{Au(bipy)Cl_2}]^+$	$\mathrm{Cl^-}$	acetone	0.46	462
$[\mathrm{Au(5\text{-}NO_2\text{-}phen)Cl_2}]^+$	$\mathrm{Cl^-}$	acetone	0.89	462
$[\mathrm{Au(tmen)Cl_2}]^{+}$[f]	$\mathrm{Cl^-}$	acetone	0.14	428

[a] Rate constants obey the relationship $\log_{10}k_2 = \alpha(\mathrm{p}K_a \text{ of amH}^+) + b$.

[b] dme = dimethoxyethane.

[c] SOSO = 1,2-bis(phenylsulfinyl)ethane.

[d] X = I, $\mathrm{NO_2}$, NCS, $\mathrm{N_3}$.

[e] SS = 1,2-bis(phenylthio)ethane.

[f] tmen = *N,N,N′,N′*-tetramethyl-1,2-diaminoethane.

and was termed by him *amphiphilicity*. Many more exceptions have since sprung to light and it seems now that a single nucleophilicity scale will not serve for all $\mathrm{Pt^{II}}$ containing substrates and that it might be useful to consider a scale for each charge type. The +2[418,419,468] and +1[468,469] cationic scales have already been examined. In general, electrostatic considerations play a greater part than was originally thought.[421]

A quantitative study of n_{Pd} using the equivalent substrate *trans*-$[\mathrm{Pd(py)_2Cl_2}]$ has not yet been carried out, presumably because of the much greater lability of $\mathrm{Pd^{II}}$ species. However, using a less labile leaving group and bulky *cis* ligands, a scale based on *trans*-$[\mathrm{Pd(Pr_3{}^iP)_2(NO_2)_2}]$ has been established.[470] Since the values for $n_{\mathrm{Pd}}{}^0$ obtained in this way are virtually identical to the $n_{\mathrm{Pt}}{}^0$ values of the same nucleophiles and yet the discrimination of the standard is considerably greater than that of *trans*-$[\mathrm{Pd(piperidine)_2(NO_2)_2}]$, which ought to be much more comparable with a bis(pyridine) standard, one might conclude that $\mathrm{Pd^{II}}$ nucleophilicities are less spread than those of $\mathrm{Pt^{II}}$.

Although a large number of $\mathrm{Au^{III}}$ systems have been studied, there has been no serious attempt to establish a set of nucleophilicity scales for gold. Reactions of a variety of $\mathrm{Au^{III}}$ complexes with amines and heterocyclic nitrogen bases indicate a dependence on proton basicity that is frequently greater than that observed for $\mathrm{Pt^{II}}$ (Table 15). A number of rate constants for the reactions involving $[\mathrm{AuCl_4}]^-$ are collected in Table 16. Reactions of anions with $[\mathrm{AuCl_4}]^-$ and similar anionic

Table 16 Rate Constants for the Reaction[a] $[\mathrm{AuCl_4}]^- + \mathrm{X}^{n-} \rightarrow [\mathrm{AuCl_3X}]^{n-} + \mathrm{Cl^-}$

X	k_2 ($\mathrm{dm^3\ mol^{-1}\ s^{-1}}$)	$\log k_2/k_1{}^0$	*Refs.*
$\mathrm{Cl^-}$	1.5	3.58	471
$\mathrm{C_5H_5N}$[b]	1.6	4.90	461
$\mathrm{Br^-}$	63	5.20	472
$\mathrm{SCN^-}$	13000	7.53	435
$\mathrm{I^-}$[c]	85000	8.33	436

[a] In water at 25 °C. $k_1 = 2.2 \times 10^{-2}\ \mathrm{s^{-1}}$.[473] $[\mathrm{H_2O}] = 55.5\ \mathrm{mol\ dm^{-3}}$.

[b] In methanol at 25 °C. $k_1 = 5.0 \times 10^{-4}\ \mathrm{s^{-1}}$. $[\mathrm{MeOH}] = 25.7\ \mathrm{mol\ dm^{-3}}$.[477]

[c] Probably the rate constant for reduction.

species are very much faster than those with analogous $[PtX_4]^{2-}$ species but the solvolytic (k_1) pathway is less important.[472,473,474] The main difficulty in setting up n_{Au} scales (apart from the possible interference from redox processes) is that minor variation in the nature of the substrate may affect the nucleophilicity sequence, as for example in the reaction $[AuCl_3am] + X^- \rightarrow [AuCl_3X]^- + am$, where the position of the N-donor ligands in the group $X = Cl^-, Br^-, N_3^-, NO_2^-$ depends upon the basicity of am.[475,476] The general conclusion at the moment is that the five-coordinate intermediate in Au^{III} substitutions is less stable than that in Pd^{II} and Pt^{II} reactions so that the bond making and breaking processes are much more closely interrelated.[477,478]

7.1.7.4 The Effect of the Non-participating Ligands on the Reactivity

7.1.7.4.1 General remarks

Although this problem has been discussed in some detail in Section 7.1.4.2, this has been a major preoccupation of workers in the field of square planar substitution and since the mechanism is unambiguously associative the features are, in a number of respects, quite different from those of the dissociative reactions of Co^{III}. Because the *trans* ligand and the two *cis* ligands (with respect to the leaving group in the substrate) usually retain their T-shaped relationship throughout the act of substitution, not only does this occur with retention of configuration but the relationship between the reactivity and the nature of the groups *cis* to the leaving group is completely different from that between reactivity and the nature of the *trans* ligand.

7.1.7.4.2 The trans *effect*

Since it presents the inorganic chemist with one of the few opportunities for planned synthesis, the *trans* effect has received much attention since it was first conceived by Werner[479] and developed by Chernayev and his colleagues.[480] Defined now as *'the effect of a coordinated group on the rate of substitution reactions of ligands* trans *to itself'*,[422] it clearly requires a kinetic and hence a mechanistic explanation. The *trans* effect can be applied to any system in which the geometry allows a pair of mutually *trans* ligands AND where the unique site of the *trans* ligand is retained in the rate determining transition state, *e.g.* dissociatively activated octahedral substitution with the *trans* ligand occupying the apical site in the square pyramidal transition state, as well as the associatively activated square planar substitution where the *trans* ligand occupies a site in the trigonal plane of the trigonal bipyramidal transition state together with the entering and leaving groups.

A number of general reviews have been written but none recently.[432,481,482,483] The qualitative sequence of *trans* effect is usually written as: $H_2O \approx OH^- < NH_3 \approx$ amines $\approx$ pyridine $< Cl^- \approx Br^- <$ —$SCN^- \approx I^- \approx$ —$NO_2^- \approx$ —$SC(NH_2)_2 < PR_3 \approx AsR_3 < C_2H_4 \approx CO \approx CN^-$. Such a sequence is based on information from preparative chemistry, but this technique is far too crude to allow any quantitative evaluation. A kinetic quantification would require a large series of substrates differing from one another only in the nature of the ligand *trans* to the leaving group. Several such series exist, for example *trans*-$[Pt(L)(am)Cl_2]$ (displacement of am) and $[Pt(L)Cl_3]^-$ in which the neutral ligand L is varied (Table 17), and neutral complexes of the type *trans*-$[Pt(PEt_3)_2(R)Cl]$ in which the displacement of Cl^- under the *trans* effect of anionic R has been studied (Table 18). Many other limited series have been evaluated. For example, Elding,[412] as a result of his studies of the reactions of complexes of the type $[PtX_n(H_2O)_{4-n}]^{(2-x)+}$ has produced the quantitative relative sequence H_2O (1) $< Cl^-$ (300) $< Br^-$ (3300) $<$ —SCN^- (40000) $< I^-$ (100000) $< Me_2SO$ (2000000) $< C_2H_4$ (*ca.*10^{11}).

No attempt has yet been made to develop a numerical parameter representing *trans* effectiveness as has been done for nucleophilicity. Not only does the magnitude of the effect depend upon the nature of the reaction being studied but, as is obvious from the data in Table 17, the sequence can also be strongly dependent upon the nature of the entering group. The weak nucleophile MeOH produces a sequence different from that of thiourea. Belluco has suggested that the *trans* effect might be better quantified in terms of the nucleophilic discrimination of the substrate with the highest *trans* effect ligand generating the least discriminating substrate.[489]

There are at least two factors contributing to *trans* labilization. The *trans* specific bond weakening effects, in which a strong σ-donor will strengthen its bond at the expense of the ligand *trans* to itself, is a widespread phenomenon and has already been mentioned in Section 7.1.4.2.3. It was first postulated in purely electrostatic terms[493] as a mutual polarization effect but, after losing ground to the π-acceptor stabilization models (see below), it regained its position in its new form to account for the high *trans* effect of purely σ-binding ligands such as —H and —CH_3.[494]

Table 17 The Kinetic *trans* Effect of Neutral Ligands

(A) Rate constants for the reaction:[a]
trans-$[Pt(L)(am)Cl_2] + MeOH \rightarrow$ *trans*-$[Pt(L)(MeOH)Cl_2] + am$

L	10^3k (s^{-1}) *am = pyridine*	 *am = 3-Cl-pyridine*	*Refs.*
C_2H_4	6800[b]	—	484
CO	1210[b]	—	484
$P(OMe)_3$	365	5240	441
PPh_3	27	335	441
PEt_3	26	495	441
PBu^n_3	23	380	441
PMe_3	15	275	441
$AsEt_3$	1.7	39	441
Me_2SO	0.11	2.8	453
Et_2S		0.13	456
Me_2S		0.039	440

(B) Rate constants for the solvolytic reaction:
$[Pt(L)Cl_3]^- + S \rightarrow$ *trans*-$[Pt(L)(S)Cl_2] + Cl^-$

L	k (s^{-1}) *S = H_2O*[c]	 *S = MeOH*[a]	*Refs.*
C_2H_4	10000	—	485
$P(OMe)_3$	—	10.7	441
PEt_3	—	6.6	441
PBu^n_3	—	5.2	441
PMe_3	—	4.8	441
PPh_3	—	3.1	441
$AsEt_3$	—	0.67	441
Me_2SO	0.098	0.0081	453, 485
Et_2S	—	0.0024	456
Me_2S	—	0.0014	440
Br^-	0.000084	—	485
Cl^-	0.0000092	—	485
NH_3	0.0000063	—	486
H_2O	0.000000028	—	487

[a] In methanol at 30 °C.
[b] In 95:5 methanol:water at 25 °C.
[c] In water at 25 °C.

Table 18 The *trans* Effect of Anionic Ligands

Rate constants for the reaction:[a]

trans-$[Pt(PEt_3)_2(R)Cl] + L \rightarrow$ *trans*-$[Pt(PEt_3)_2(R)(L)]^+ + Cl^-$

L *R*	*MeOH* 10^3k_1 (s^{-1})	*$(NH_2)_2CS$* k_2 ($dm^3\ mol^{-1}\ s^{-1}$)	*Refs.*
H	560	6310	488
Et	48	15.5	488
Me	40[b]	$\geqslant$1.5[b]	489
Ph	10.2[b]	6.3[b]	489, 490
4-FC_6H_4	5.0[b]	5.9[b]	491
3-FC_6H_4	4.0[b]	4.0[b]	491
3-$CF_3C_6H_4$	3.0	3.2	488
2-MeC_6H_4	2.0[b]	0.65[b]	490, 492
2,4,6-$Me_3C_6H_2$	0.44[b]	0.049[b]	490, 492
C_6F_5	0.020	0.35	488
Cl	0.00015[b,c]	47[b]	447, 463

[a] In methanol at 25 °C.
[b] In methanol at 30 °C.
[c] Reported too small to measure in ref. 447; value quoted is that estimated in ref. 463.

Calculation of overlap between the appropriate donor orbitals and the Pt $6p\sigma$ orbitals led to the sequence[6,495] $H^- > PR_3 > —SCN^- > I^- \approx CH_3^- \approx CO \approx CN^- > Br^- > Cl^- > NH_3 > H_2O$ Since this effect occurs in the substrate, it should be observable also as a non-kinetic effect and, indeed, studies of the *trans* influence (ground state *trans* bond weakening) considerably outnumber those of the kinetic *trans* effect. The topic has been extensively reviewed.[206,496,497] Bond lengths are generally assumed to relate most directly to bond weakening,[206,498] although when ground state π-acceptor properties accompany the σ-donation (*e.g.* CO) the two effects may compete.[499] Vibrational frequencies and force constants[500] have also been used and various aspects of NMR, such as coupling constants, [495,501] and nuclear quadrupole coupling[502] have also been applied to the problem. While it is obvious that ground state bond weakening will lead to enhanced reactivity in a dissociatively activated process, it may work in either direction when the activation is associative. To enhance reactivity, the destabilizing effect must be greatly diminished in the transition state. The p_z-orbital on the metal, which remains orthogonal to any σ-orbital on the *trans* ligand throughout the act of substitution, becomes involved in bonding both the entering group and leaving group in the transition state and relieves some of the competition that destabilized the ground state.[6]

The *trans* bond weakening effect is clearly inadequate to account for the behaviour of those ligands, *e.g.* C_2H_4, CO, Me_2SO, whose *trans* effect is high but whose *trans* influence is negligible. A transition state stabilization effect was first proposed by Chatt[503] and Orgel[504] in which a π-acceptor *trans* to the leaving group will facilitate bond formation and stabilize the five-coordinate transition state. Labilization through the stabilization of a transition state has already been encountered in the π-donor mechanism for the labilization of dissociative substitution in Co^{III} by an amido group (see Section 7.1.5.7). This predicts a labilizing sequence, according to Langford and Gray,[6] of $C_2H_4 > CO > CN^- > NO_2^- > —SCN^- > I^- > Br^- > Cl^- > OH_2$.

The two effects are not mutually exclusive and both may contribute to the labilizing power. There has been some interest in trying to find ways of assessing the separate contributions and it seems generally agreed that a bond weakening *trans* effect ligand generates a substrate of low nucleophilic discrimination.[441,488] It also seems reasonable to expect that a labilizing effect that depends upon a lowering of the energy of the transition state should be very sensitive to the nature of the entering group which is also bound in the transition state, so that strong nucleophilic discrimination will be observed.[441] Since ethylene is the paradigm for a π-acceptor *trans* effect ligand (and indeed leads to the detection of significant amounts of five-coordinate species such as $[Pt(C_2H_4)(C_5H_5N)_2Cl_2]$[505] or even stable isolable species such as $[Pt(C_2H_4)(L—L)Cl_2]$ where L—L is the diimine butane-2,3-dionebisphenylhydrazone[506]), it would be of interest to know whether ethylene containing complexes, such as $[Pt(C_2H_4)Cl_3]^-$ and *trans*-$[Pt(C_2H_4)(am)Cl_2]$, do in fact exert high nucleophilic discrimination. Unfortunately the very high reactivity precludes a study of all but the weakest nucleophiles and care must be taken to avoid alternative pathways where the nucleophile adds to the ethylene, leading to a β-substituted σ-bound ethyl substituted species. For the displacement of pyridine from *trans*-$[Pt(L)(C_5H_5N)Cl_2]$ by chloride in methanol the ratio of the direct and solvolytic rate constants, k_2^{Cl}/k_1^{MeOH}, decreases along the sequence L = C_2H_4 (300) ≫ CO (2.4) > Me_2SO (1.0) ≫ PMe_3 (0.04).[484]. Although it is risky to use the ratio of two rate constants as a measure of nucleophilic discrimination, it does seem that ethylene is outstanding at one extreme while PMe_3, the only ligand of the series to exert a marked *trans* influence, is at the other.

It has been suggested that when the *trans* ligand is a strong σ-donor with no π-acidity the role of transition state stabilization is taken up by any biphilic species, such as thiourea.[488] Such potential π-acceptors seem to be more capable than others in making use of the direct substitution pathway.

In contrast to the sensitivity of the *trans* effect to the electron displacement properties of the ligand, the presence of bulky substituents does not lead to any marked steric hindrance effects. The retardation due to progressive *ortho* methylation in aryl groups R in the complex *trans*-$[Pt(PEt_3)_2(R)Cl]$ is small: R = Ph(1.0; 1.0) > 2-MeC_6H_4 (0.20; 0.048) > 2,4,6-$Me_3C_6H_2$ (0.04; 0.0012), the first number in parentheses referring to the solvolytic rate constant in methanol[490] and the second to the second-order rate constant for the entry of CN^- in 2-propanol,[507] both relative to Ph = 1.This is consistent with the view that since the main source of non-bonding repulsion, which is between the methyl groups and the bulky PEt_3 ligand, does not change on going from the ground state to the transition state, there will be little effect upon reactivity.

7.1.7.4.3 *The* cis *effect*

In contrast to the very strong dependence of reactivity on the electron displacement properties of the *trans* ligand, there is small response to such variations in the *cis* ligand. There are no obvious ground state effects (*cis* influences) and it must be concluded that the effect , such as it is, relates to transition state stabilization. This is borne out by the fact that the effect is more marked the stronger the entering nucleophile, a manifestation of the change in the nucleophilic discrimination. In a series of complexes of the type $[Pt(en)(L)Cl]^+$, $\log k_2$ for the replacement of Cl *cis* to L plotted against $\log k_2$ for the similar reaction when L = NH_3 (a +1 charge nucleophilicity scale) gives a linear relationship, the slope of which increases as the *trans* effect of L becomes greater. This effect is not large, the slopes increasing L = NH_3 (1.0)[508] < Me_2S (1.14)[469] < Me_2SO (1.26)[508] ≈ PMe_3 (1.24),[509] and is only seen with the stronger nucleophiles; the solvolytic rate constants are virtually identical. Similar effects have been observed with substrates of the type *trans*-$[Pt(L)_2Cl_2]$ (displacement of Cl^-).[447] It is of interest to note that the *cis* effect of amines can be quite significant, the least basic being the most labilizing.[510,511]

The reactivity is extremely sensitive to the bulkiness of the *cis* ligand, even to the replacement of PMe_3 by PEt_3.[509] A much more dramatic effect is seen in the effect of *ortho* methylation in aryl complexes of the type *cis*-$[Pt(PEt_3)_2(R)Br]$ where the reduction in reactivity is large, R = Ph (1.0; 1.0), 2-MeC_6H_4 (0.0091; 0.0013), 2,4,6-$Me_3C_6H_2$ (0.000032; 0.000015), the numbers in parentheses indicating the relative rate constants for the solvolysis[512] and cyanide substitution[507] respectively. Non-bonding repulsions from these substituents increase enormously when the entering group develops its bond to the metal in the transition state. A similar effect is observed when the protons in the terminal amine groups of the terdentate ligand 1,5-diamino-3-azapentane (dien) are replaced by bulky ethyl groups.[513,514] These steric effects will be discussed in more detail in connection with the search for dissociative activation in d^8 chemistry.

7.1.7.5 Stereochemical Change in Four-coordinate Planar d^8 Metal Complexes

The act of substitution by way of a trigonal bipyramidal transition state, in which the entering group, the leaving group and the *trans* ligand occupy the sites in the trigonal plane, predicts that the substitution will take place with complete retention of configuration. The occurrence of stereochemical change in square planar d^8 systems is, therefore, always a source of some interest. The subject has been well reviewed recently and this review should be consulted for a more detailed presentation.[515]

As Drew pointed out as long ago as 1934,[516] it is possible to cause isomerization by a sequence of successive substitutions. One of the earliest examples of this mechanism, adequately investigated, was the *cis* to *trans* isomerization of $[Pd(am)_2Cl_2]$ which is catalyzed by free amine,am (Scheme 7).[517]

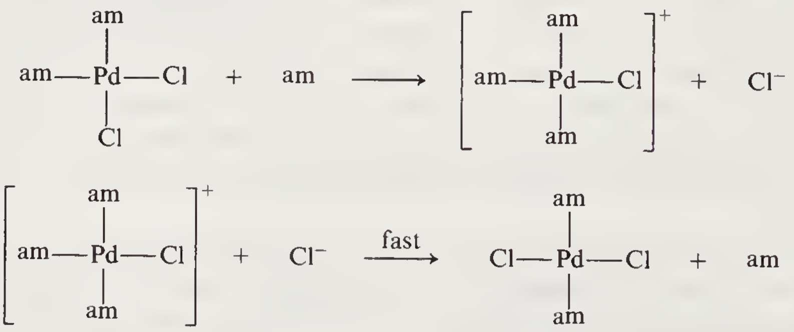

Scheme 7 The Successive Displacement Mechanism for Isomerization

If the concentration of the intermediate remained small the process would be catalyzed by one of the ligands, the amine in the above case, with the same rate law as that of the substitution, *i.e.* rate = $(k_1 + k_2[\text{am}])[\text{complex}]$. This mechanism has also been demonstrated for the Me_2S catalyzed isomerization of *cis*- and *trans*-$[Pt(Me_2S)_2Cl_2]$, where the formation of $[Pt(Me_2S)_3Cl]^+$ is demonstrated in the presence of a chloride scavenger, *e.g.* Ag^+, at a rate that is the same as that for the isomerization in its absence.[81] The displacement of Me_2S from the complex is fast and gives the *cis* isomer. The isolation of such an intermediate is not, in itself, evidence for or against the mechanism but when the kinetics of its formation and decomposition are consistent with those for the isomerization, the case is compelling. The species $[Pt(PMe_3)_3Cl]Cl$ has been isolated from solutions containing $[Pt(PMe_3)_2Cl_2]$ and PMe_3 and shown to be the four-coordinate salt rather than a five-coordinate species. This, together with other reasonably compelling evidence, has been presented to show that the phosphine catalyzed *cis–trans* isomerizations of $[Pt(PR_3)_2Cl_2]$, first observed by Chatt and Wilkins,[518] fall into this category.[519] Although there is no evidence for the formation of $[Pt(Me_2SO)_3Cl]^+$ as an intermediate in the Me_2SO catalyzed isomerization of *trans*-$[Pt(Me_2SO)_2Cl_2]$, it is still suggested that the successive displacement mechanism operates.[520]

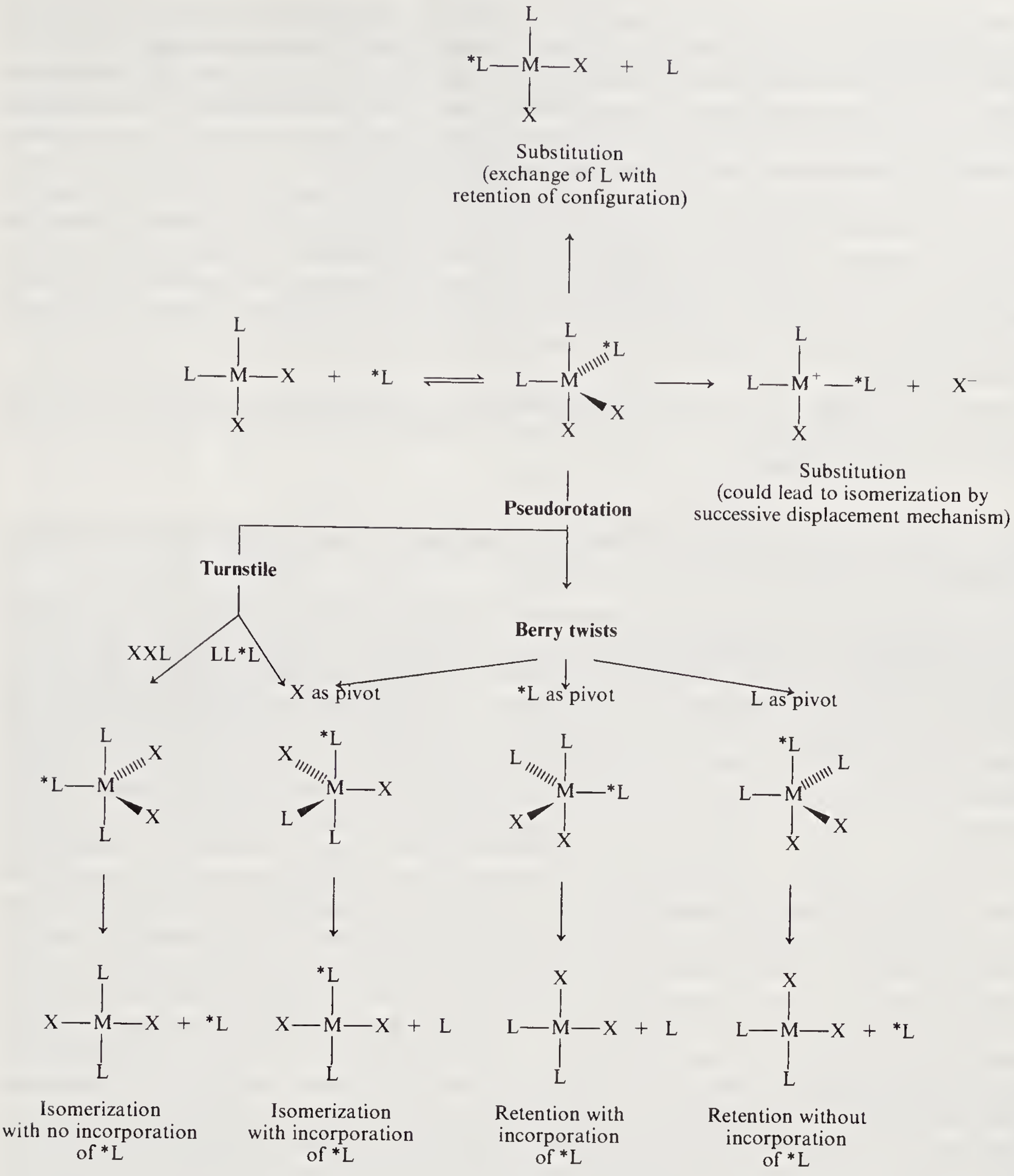

Berry twist: an axial pair exchanges with an equatorial pair, the third equatorial ligand acting as the pivot[521]
Turnstile: a facial set of three ligands rotates, thereby exchanging one equatorial with one axial ligand (the sequence in the trigonal plane is inverted)

Scheme 8 Consequences of Possible Pseudorotation of Five-coordinate Species $[M(L)_2{}^*L(X)_2]$

If a five-coordinate species could be formed in sufficient concentration with sufficient lifetime and fluxionality to undergo pseudorotation, it could lead to substitution with stereochemical change or ligand catalyzed isomerization. This mechanism was first suggested to account for the fact that the phosphine catalyzed isomerization of $[Pt(PBu_3)_2Cl_2]$, which was first order in $[PBu_3]$ in cyclohexane, was much retarded on the addition of polar solvents,[522] it being argued that this should favour the formation of the ionic intermediate required in the successive displacement mechanism. It was also observed that there was no ligand scrambling when the catalyzing phosphine was different from that in the phosphine.[523] Much of the evidence produced in support of the pseudorotation mechanism could equally well support the successive displacement. The whole question is discussed very critically by Anderson and Cross,[515] who suggest that the two schemes are the limits of a whole spectrum of processes initiated by the partial binding of the catalyzing ligand.

A detailed study of the reaction between $[Pt(N—O)Cl_2]^-$ and Me_2SO (where N—O is one of a number of amino acid anions) and the exchange of Me_2SO and Cl^- with the product $[Pt(N—O)(Me_2SO)Cl]$, and their catalysis of its isomerization, has led to the suggestion that the pseudorotation of a long-enough lived five-coordinate intermediate was involved.[524] The mutual labilization of a *cis* pair of sulfoxides has been explained, in part, in terms of a long-enough lived five-coordinate intermediate that can undergo pseudorotation.[419]

In principle, site exchange in a four-coordinate planar complex might be achieved by passage through a tetrahedral transition state or intermediate. Orbital symmetry arguments suggest that the barrier to thermal activation for Pd^{II} and Pt^{II} species would be large;[525] indeed a change in spin multiplicity would be required. The pathway is accessible to photochemical activation and many examples exist. Irradiation of *cis*-$[Pt(Me_2SO)_2Cl_2]$ generates a considerable amount of the *trans* isomer, which is the more stable form in the electronically excited state. The *cis* form dominates the ground state.[526]

Isomerization though a three-coordinate intermediate is so closely related to the occurrence of a dissociative mechanism in d^8 four-coordinate planar systems that it is best considered in the next section, where this is discussed.

7.1.7.6 Dissociative Activation in the Substitution Reactions of Four-coordinate, Planar d^8 Metal Complexes

It has always been of some interest to examine the extent to which associative activation dominates the mechanism of substitution of four-coordinate planar d^8 metal complexes. The coordination unsaturation of these formally 16-electron valence shell complexes predicts that a substitution pathway with increased coordination number (18-electron valence shell) will be favoured over one with a reduced coordination number (14 electrons). This was well understood by workers in the field[438] long before Tolman[94] published his rules. The first attempt to force a dissociative mechanism was made by Basolo and Baddley[513,514] who reasoned that since the steric requirements of associative substitution (rates reduced by steric hindrance from the *cis* position) were opposite to those of a dissociative mechanism (rates increased or unchanged by increased steric hindrance), sufficient congestion in the substrate should reduce the rate of the associative process to the point where dissociative activation took over. If this did not produce a change in mechanism it could at least indicate a lower limit to the difference of the two modes of activation.

Taking $[Pt(dien)X]^+$, which behaves as a normal associatively activated substrate,[527] and replacing the terminal nitrogen protons by the bulky ethyl groups in $[Pt(Et_4dien)X]^+$, the reactivity was reduced by many orders of magnitude, so much so that rather than work at 80 °C the subsequent studies were made on the analogous Pd^{II} complex. The absence of a nucleophile dependent contribution was interpreted as a change to a dissociative mechanism.[514] Hydroxide behaved anomalously with a first-order dependence (not then seen elsewhere in square planar substitution), which was assigned to a base catalyzed solvolysis through the labilizing effect of the amido nitrogen (*cf.* Section 7.1.5) because it was absent from the reactions of $[Pd(Et_4Medien)X]^+$ where the proton on the secondary nitrogen had been replaced by CH_3.[513] Later studies showed that strong nucleophiles, such as $S_2O_3^{2-}$ entered by a concentration dependent pathway[528,529] and the negative entropies of activation[530] and the negative volumes of activation of the solvolytic process, which are not greatly affected by the extent of alkyl substitution, suggested a common, and hence associative, mode of activation.[446,531,532] The steric hindrance therefore also reduces the nucleophilic discrimination to the point where the solvent, by virtue of its high concentration relative to that of the other nucleophiles, dominates the substitution which remains associative. Reactions of the analogous Au^{III} complexes are associative[533,534,535] and some take place with ring-opening of the terdentate system.[536]

In the first studies of the reactions of *trans*-$[Pt(PEt_3)_2(R)X]$ (R = H, Me, Ph, 2-MeC_6H_4 and 2,4,6-$Me_3C_6H_2$; X = Cl, Br, I) the weak nucleophile pyridine seemed to generate a marked concentration dependent term,[494] but subsequent work[490,507] has shown an error in the interpretation of the kinetics and here too the nucleophilic discrimination is low and only strong nucleophiles of biphilic species make a significant concentration dependent contribution to the rate.[488,492,537] Steric hindrance by *ortho* methylation in the phenyl group reduces the discrimination even further. In the corresponding *cis* isomers the discrimination is very low and very strong nucleophiles, such as CN^-, must be used to obtain a concentration dependent rate.[507] The *cis* complexes are much more labile, since X is *trans* to PEt_3, and they are much more sensitive to steric hindrance. They also undergo spontaneous isomerization to the *trans* isomer.[538] This isomerization is suppressed by addition of excess X^- and is usually much slower than the displacement of X by another nucleophile, a process which takes place with complete retention of configuration. Whereas the substitution reaction is extremely sensitive to steric hindrance, the isomerization is not and, when R = 2,4,6-$Me_3C_6H_2$, isomerization and substitution take place at the same rate. The isomerization is said to take place by way of a dissociation to a three-coordinate species which retains memory of the starting material configuration (T-shaped) and then rearranges in competition with its recapture to a species which holds the *trans* configuration (Scheme 9).[512,538]

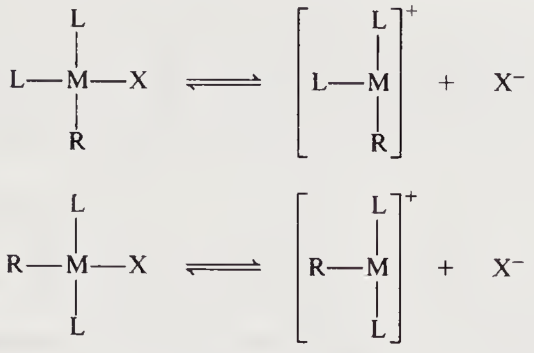

Scheme 9 A Dissociative Mechanism for Isomerization

The rate constant for isomerization is sensitive to inductive effects of non-hindering substituents as required by the dissociative nature of the activation.[539,540] Solvent effects,[541] positive entropies of activation[540] and positive volumes of activation[542,543,544] are all consistent with a dissociative activation. The substitution reactions, on the other hand, have negative $\Delta S^{\neq}$ and $\Delta V^{\neq}$ values. Suggestions that substitution in the 2,4,6-$Me_3C_6H_2$ complex, which occurs at the same rate as isomerization, is also dissociative have led to some controversy[545,546] because $\Delta S^{\neq}$ [540] and $\Delta V^{\neq}$ [547] are negative and consistent with an associative process. It is possible that, in this case, the isomerization takes place through the solvento complex that is formed in a rate-determining associative process. Although ligand substitution accompanying isomerization is probably dissociatively activated, it appears that, in all of the cases studied, there is a more facile associative pathway. A similar dissociative mechanism has been suggested for the isomerization of *cis*-$[Au(Et)(Me)_2(PPh_3)]$.[548]

It was suggested that, although the kinetics of the substitution reactions of $[Pt(H_2O)_4]^{2+}$ are first order in nucleophile concentration, the similarity of the second-order rate constants for the entry of Me_2SO, $HgCl^+$ and H_2O indicated a dissociative activation[414] and since other nucleophiles have second-order rate constants that are strongly dependent upon their nature, an I_d–I_a crossover was suggested.[412,549] This mechanistic duality is not supported by the $\Delta V^{\neq}$ for water exchange, which is fully consistent with associative activation.[416]

A recent study has shown that the displacement of Me_2SO from *cis*-$[Pt(R)_2(Me_2SO)_2]$ by Me_2SO and bidentate ligands (2,2′-bipyridyl, 1,10-phenanthroline and 1,2-bis(diphenylphosphinoethane); R = Ph, 4-MeC_6H_4) in non-coordinating solvents such as benzene and chloroform proceeds mainly, or even entirely, through the 14-electron intermediate, $[Pt(R)_2(Me_2SO)]$.[550] It was suggested that interaction between the oxygen of the sulfoxide and the platinum might stabilize the three-coordinate intermediate but it is now known that the analogous Me_2S species reacts in a similar way.[551] These are relatively reactive systems and the substrate does not experience, nor need, strong steric hindrance to suppress what elsewhere is the overwhelming associative alternative pathway. A similar dissociative loss of Me_2S has been postulated as the initial step in the methyl for halogen exchange between *cis*-$[Pt(Me)_2(Me_2S)_2]$ and *cis*-$[Pt(Me_2S)_2Cl_2]$.[552]

7.1.7.7 Five-coordinate d^8 Metal Complexes

With five-coordinate d^8 metal complexes the mechanistic pattern is, not surprisingly, reversed. Although the associative mechanism for substitution of X^- in $[Ni(PMe_3)_4X]^+$ involves a 20-electron transition state,[553] it is more likely that a 16-electron four-coordinate transition state/intermediate will be favoured. Since this will be planar for Pd^{II} and Pt^{II} the dissociative mechanism will have strict steric requirements. For example, substitution of an axial monodentate ligand in a square pyramidal five-coordinate species is dissociative and facile because the square planar intermediate is easily formed.[554,555] However, when the leaving group is not in an axial position and when the rest of the complex is prevented from assuming a square planar form, other mechanisms apply. Thus in the substitution reactions of $[Pt(Qas)Cl]^+$, which has a trigonal bipyramidal geometry with the tripod ligand (Qas = tris(2-dimethylarsinophenyl)arsine) forcing the chloride into the axial position, dissociation of this chloride cannot lead to a square planar arrangement of the four arsenic atoms. The observed pathway requires that one of the three terminal arsenic atoms dissociates in a rapid pre-equilibrium and the square planar species thus formed undergoes associative substitution in the usual way.[556] A similar mechanism has been proposed for the substitution reactions of $[Ni(QAS)X]^+$ (QAS = tris(2-diphenylarsinophenyl)arsine).[557] An alternative ion-pair pre-equilibrium mechanism seems unduly complicated.[558]

7.1.8 REFERENCES

1. F. Basolo and R. G. Pearson, 'Mechanisms of Inorganic Reactions', 2nd edn., Wiley, New York, 1967.
2. 'Inorganic Reaction Mechanisms, Specialist Periodical Reports', The Chemical Society, London, vol. 1, 1971; vol. 2, 1972; vol. 3, 1974; vol. 4, 1976; vol. 5, 1977; vol. 6, 1979; vol. 7, 1981.
3. M. V. Twigg (ed.), 'Mechanisms of Inorganic and Organometallic Reactions', Plenum, New York, vol. 1, 1983; vol. 2, 1984; vol. 3, 1985.
4. M. L. Tobe (ed.), *MTP Int. Rev. Sci., Inorg. Chem. Ser. 1,* vol. 9, 'Reaction Mechanisms in Inorganic Chemistry', Butterworths, London, 1972; *Ser. 2*, 1973.
5. J. O. Edwards, 'Inorganic Reaction Mechanisms', Benjamin, New York, 1964.
6. C. H. Langford and H. B. Gray, 'Ligand Substitution Processes', Benjamin, New York, 1965.
7. A. G. Sykes, 'Kinetics of Inorganic Reactions', Pergamon, Oxford, 1966.
8. D. Benson, 'Mechanisms of Inorganic Reactions in Solution', McGraw-Hill, London, 1968.
9. M. L. Tobe, 'Inorganic Reaction Mechanisms', Nelson, London, 1972.
10. R. G. Wilkins, 'The Study of Kinetics and Mechanism of Reactions of Transition Metal Complexes', Allyn & Bacon, New York, 1974.
11. J. Burgess, 'Metal Ions in Solution', Ellis Horwood, Chichester, 1978, chaps. 11 and 12.
12. J. O. Edwards (ed.), *Prog. Inorg. Chem.*, 1970, **13**.
13. J. O. Edwards (ed.), *Prog. Inorg. Chem.*, 1972, **17**.
14. S. J. Lippard (ed.), *Prog. Inorg. Chem.*, 1983, **30**.
15. A. G. Sykes, 'Advances in the Mechanisms of Inorganic and Bioinorganic Mechanisms', Academic, London, vol. 1, 1982; vol. 2, 1983; vol. 3, 1985; vol. 4, 1986.
16. 'Mechanisms of Inorganic Reactions', ACS Monograph 49, American Chemical Society, Washington, 1965.
17. D. W. Margerum, G. R. Caley, D. C. Weatherburn and G. K. Pagenkopf, 'Kinetics and Mechanisms of Complex Formation and Ligand Exchange', in 'Co-ordination Chemistry', vol. 2, ACS Monograph 174, ed. A. E. Martell, American Chemical Society, Washington, 1978.
18. F. A. Cotton and G. Wilkinson, 'Advanced Inorganic Chemistry', 4th edn., Wiley-Interscience, New York, 1980, chap. 28.
19. K. F. Purcell and J. C. Kotz, 'Inorganic Chemistry', Saunders, Philadelphia, 1977, chap. 13.
20. W. W. Porterfield, 'Inorganic Chemistry', Addison-Wesley, London, 1984, chap. 12.
21. M. Chanon and M. L. Tobe, *Angew. Chem., Int. Ed. Engl.*, 1982, **21**, 1.
22. F. Basolo and R. G. Pearson, 'Mechanisms of Inorganic Reactions', 2nd edn., Wiley, New York, 1967, p. 379.
23. L. Canovese, L. Cattalini, G. Marangoni, G. Michelon and M. L. Tobe, *Inorg. Chem.*, 1981, **20**, 4166.
24. T. W. Swaddle, 'Advances in Inorganic and Bioinorganic Mechanisms', ed. A. G. Sykes, vol. 2., Academic, London, 1983, p. 95.
25. W. W. Reenstra and W. P. Jencks, *J. Am. Chem. Soc.*, 1979, **101**, 5780.
26. W. P. Jencks, *Acc. Chem. Res.*, 1980, **13**, 161.
27. J. P. Hunt and R. A. Plane, *J. Am. Chem. Soc.*, 1954, **76**, 5960.
28. W. Plumb and G. M. Harris, *Inorg. Chem.*, 1964, **3**, 542.
29. H. H. Baldwin and H. Taube, *J. Chem. Phys.*, 1960, **33**, 206.
30. H. Gamsjager and R. K. Murmann, 'Advances in Inorganic and Bioinorganic Mechanisms', ed. A. G. Sykes, vol. 2, Academic, London, 1983, p. 317.
31. A. J. Brown, D. A. Couch, O. W. Howarth and P. Moore, *J. Magn. Reson.*, 1976, **21**, 503.
32. M. Eigen, *Pure Appl. Chem.*, 1963, **6**, 97.
33. A. Fratiello, *Prog. Inorg. Chem.*, 1972, **17**, 57.
34. A. E. Merbach, *Pure Appl. Chem.*, 1982, **54**, 1479.
35. J. P. Hunt and H. L. Friedman, *Prog. Inorg. Chem.*, 1983, **30**, 359.
36. Y. Ducommun, D. Zbinden, and A. E. Merbach, *Helv. Chim. Acta*, 1982, **65**, 1385.
37. H. P. Bennetto and E. F. Caldin, *J. Chem. Soc.(A)*, 1971, 2198.
38. Y. Ducommun, K. E. Newman and A. E. Merbach, *Inorg. Chem.*, 1980, **19**, 3696.
39. R. Poupko and Z. Luz, *J. Phys. Chem.*, 1972, **57**, 3311.
40. A. Hugi, D. Hugi, L. Helm and A. E. Merbach, Poster XXIII, ICCC, Boulder, 1984.
41. D. R. Stranks and T. W. Swaddle, *J. Am. Chem. Soc.*, 1971, **93**, 2783.
42. M. Grant and R. B. Jordan, *Inorg. Chem.*, 1981, **20**, 55.
43. T. W. Swaddle and A. E. Merbach, *Inorg. Chem.*, 1981, **20**, 4212.
44. D. N. Fiat and R. E. Connick, *J. Am. Chem. Soc.*, 1968, **90**, 608.
45. T. W. Swaddle, *Coord. Chem. Rev.*, 1974, **14**, 217.
46. G. A. Lawrance and D. R. Stranks, *Acc. Chem. Res.*, 1979, **12**, 403.
47. M. Kotowski, D. A. Palmer and H. Kelm, *Inorg. Chem.*, 1979, **18**, 2555.
48. W. Kruse and H. Taube, *J. Am. Chem. Soc.*, 1961, **83**, 1280.
49. S. B. Tong, H. R. Krouse and T. W. Swaddle, *Inorg. Chem.*, 1976, **15**, 2643.
50. D. R. Stranks and N. Vanderhoek, *Inorg. Chem.*, 1976, **15**, 2639.
51. F. Basolo and R. G. Pearson, 'Mechanisms of Inorganic Reactions', 2nd edn., Wiley, New York, 1967, p. 145.
52. J. K. Burdett, *J. Chem. Soc., Dalton Trans.*, 1976, 1725.
53. C. H. Langford, *Inorg. Chem.*, 1979, **18**, 3288.
54. T. W. Swaddle, *Inorg. Chem.*, 1980, **19**, 3203.
55. K. E. Newman and A. E. Merbach, *Inorg. Chem.*, 1980, **19**, 2481.
56. D. Richardson and T. D. Alger, *J. Phys. Chem.*, 1975, **79**, 1733.

57. D. Pisanello, L. Helm, P. Meier and A. E. Merbach, *J. Am. Chem. Soc.*, 1983, **105**, 4528.
58. M. L. Tobe and D. W. Watts, *J. Chem. Soc.*, 1964, 2991.
59. M. L. Tobe, *Adv. Chem.*, 1966, **47**, 7.
60. M. L. Tobe, *Rec. Chem. Prog.*, 1966, **27**, 79.
61. B. Bosnich, J. Ferguson and M. L. Tobe, *J. Chem. Soc. (A)*, 1966, 1634.
62. J. Crea and S. F. Lincoln, *J. Chem. Soc., Dalton Trans.*, 1973, 2075.
63. J. J. Delpuech, A. A. Peguy, P. Rubini and J. Steinmetz, *Nouv. J. Chim.*, 1976, **1**, 133.
64. D. L. Pisanello, S. F. Lincoln and E. H. Williams, *Inorg. Chim. Acta*, 1978, **31**, 237.
65. J. J. Delpuech, M. R. Khaddar, A. A. Peguy and P. R. Rubini, *J. Am. Chem. Soc.*, 1975, **97**, 3373.
66. C. Ammann, P. Moore, A. E. Merbach and C. H. McAteer, *Helv. Chim. Acta*, 1980, **63**, 268.
67. A. E. Merbach, P. Moore, O. W. Howarth and C. H. McAteer, *Inorg. Chim. Acta*, 1980, **39**, 129.
68. L. Rodehuser, P. R. Rubini and J. J. Delpuech, *Inorg. Chim. Acta*, 1977, **16**, 2837.
69. C. Ammann and A. E. Merbach, *Inorg. Chim. Acta*, 1980, **40**, X98.
70. D. L. Pisanello, S. F. Lincoln and E. H. Williams, *J. Chem. Soc., Dalton Trans.*, 1979, 1473.
71. D. L. Pisanello and S. F. Lincoln, *Inorg. Chim. Acta*, 1979, **36**, 85.
72. D. L. Pisanello and S. F. Lincoln, *Inorg. Chem.*, 1981, **20**, 3689.
73. D. L. Pisanello and S. F. Lincoln, *J. Chem. Soc., Dalton Trans.*, 1980, 699.
74. M. N. Tkaczuk and S. F. Lincoln, *Aust. J. Chem.*, 1979, **32**, 1915.
75. M. N. Tkaczuk and S. F. Lincoln, *Aust. J. Chem.*, 1980, **33**, 2621.
76. D. L. Pisanello, L. Helm, D. Zbinden and A. E. Merbach, *Helv. Chim. Acta*, 1983, **66**, 1872.
77. H. Vanni and A. E. Merbach, *Inorg. Chem.*, 1979, **18**, 2758.
78. R. Good and A. E. Merbach, *Inorg. Chem.*, 1975, **14**, 1030.
79. A. E. Merbach and J. C. Bunzli, *Helv. Chim. Acta*, 1972, **55**, 1903.
80. C. M. P. Favez and A. E. Merbach, *Inorg. Chim. Acta*, 1977, **60**, 2695.
81. R. Roulet and C. Barbey, *Helv. Chim. Acta*, 1973, **56**, 2179.
82. M. Tubino and A. E. Merbach, *Inorg. Chim. Acta*, 1983, **71**, 149.
83. L. Cattalini, G. Marangoni, G. Michelon, G. Paolucci and M. L. Tobe, *Inorg. Chem.*, 1981, **20**, 71.
84. M. Bonivento, L. Canovese, L. Cattalini, G. Marangoni, G. Michelon and M. L. Tobe, *Inorg. Chem.*, 1981, **20**, 1493.
85. F. Basolo and A. Wojcicki, *J. Am. Chem. Soc.*, 1961, **83**, 520.
86. F. Basolo and R. G. Pearson, 'Mechanisms of Inorganic Reactions', 2nd edn., Wiley, New York, 1967, p. 540.
87. F. Basolo, *Inorg. Chim. Acta*, 1981, **50**, 65.
88. F. Basolo, *Coord. Chem. Rev.*, 1982, **43**, 7.
89. E. W. Abel and F. G. A. Stone, *Quart. Rev.*, 1970, **24**, 498.
90. G. R. Dobson, *Acc. Chem. Res.*, 1976, **9**, 300.
91. D. J. Darensbourg, *Adv. Organomet. Chem.*, 1982, **21**, 113.
92. R. J. Angelici, *Organomet. Chem. Rev.*, 1968, **3**, 173.
93. H. Werner, *J. Organomet. Chem.*, 1975, **94**, 285.
94. C. A. Tolman, *Chem. Soc. Rev.*, 1972, **1**, 337.
95. J. P. Day, R. G. Pearson and F. Basolo, *J. Am. Chem. Soc.*, 1968, **90**, 6927.
96. D. F. Keeley and R. E. Johnson, *J. Inorg. Nucl. Chem.*, 1959, **11**, 33.
97. Q.-Z. Shi, T. G. Richmond, W. C. Trogler and F. Basolo, *J. Am. Chem. Soc.*, 1982, **104**, 4032.
98. J. R. Graham and R. J. Angelici, *Inorg. Chem.*, 1967, **6**, 2082.
99. S. P. Modi and J. D. Atwood, *Inorg. Chem.*, 1983, **22**, 26.
100. Q.-Z. Shi, T. G. Richmond, W. C. Trogler and F. Basolo, *J. Am. Chem. Soc.*, 1984, **106**, 71.
101. T. G. Richmond, Q.-Z. Shi, W. C. Trogler and F. Basolo, *J. Am. Chem. Soc.*, 1984, **106**, 76.
102. G. F. Holland, M. C. Manning, D. E. Ellis and W. C. Trogler, *J. Am. Chem. Soc.*, 1983, **105**, 2308.
103. K. Noack, *Helv. Chim. Acta*, 1964, **47**, 1064.
104. S. S. Schmidt, W. C. Trogler and F. Basolo, *Inorg. Chem.*, 1982, **21**, 1698 and references therein.
105. A. Pöe, *Inorg. Chem.*, 1981, **20**, 4029 and references therein.
106. H. Yesaka, T. Kobayashi, K. Yasufuku and S. Nagakura, *J. Am. Chem. Soc.*, 1983, **105**, 6249.
107. S. P. Schmidt, W. C. Taylor and F. Basolo, *J. Am. Chem. Soc.*, 1984, **106**, 1308.
108. L. S. Meriwether and M. L. Fiene, *J. Am. Chem. Soc.*, 1959, **81**, 4200.
109. B. J. Plankey and J. V. Rund, *Inorg. Chem.*, 1979, **18**, 957.
110. K. R. Brower and T.-S. Chen, *Inorg. Chem.*, 1973, **12**, 2198.
111. R. D. Johnson, F. Basolo and R. G. Pearson, *Inorg. Chem.*, 1971, **10**, 247.
112. M. Meier, F. Basolo and R. G. Pearson, *Inorg. Chem.*, 1969, **8**, 795.
113. F. Basolo and A. Wojcicki, *J. Am. Chem. Soc.*, 1961, **83**, 525.
114. B. F. G. Johnson, J. Lewis, J. R. Miller, P. W. Robinson and A. Wojcicki, *Chem. Commun.*, 1967, 379.
115. B. F. G. Johnson, J. Lewis, J. R. Miller, B. H. Robinson, P. W. Robinson and A. Wojcicki, *J. Chem. Soc. (A)*, 1968, 522.
116. J. D. Atwood and T. L. Brown, *J. Am. Chem. Soc.*, 1975, **97**, 3155.
117. J. D. Atwood and T. L. Brown, *J. Am. Chem. Soc.*, 1975, **97**, 3380.
118. J. D. Atwood and T. L. Brown, *J. Am. Chem. Soc.*, 1976, **98**, 3160.
119. E. M. Thorsteinson and F. Basolo, *J. Am. Chem. Soc.*, 1966, **88**, 3929.
120. D. E. Morris and F. Basolo, *J. Am. Chem. Soc.*, 1968, **90**, 2531.
121. H. Wawersik and F. Basolo, *J. Am. Chem. Soc.*, 1967, **89**, 4626.
122. Q.-Z. Shi, T. G. Richmond, W. C. Trogler and F. Basolo, *Inorg. Chem.*, 1984, **23**, 957.
123. H. G. Schuster-Wolden and F. Basolo, *J. Am. Chem. Soc.*, 1966, **88**, 1657.
124. F. Zingales, A. Chiesa and F. Basolo, *J. Am. Chem. Soc.*, 1966, **88**, 2707.
125. C.-Y. Cheng, C. E. Johnson, T. G. Richmond, Y.-T. Chen, W. C. Trogler and F. Basolo, *Inorg. Chem.*, 1981, **20**, 3167.
126. J. O. Edwards, F. Monacelli and G. Ortaggi, *Inorg. Chim. Acta*, 1974, **11**, 47.
127. D. A. House, *Coord. Chem. Rev.*, 1977, **23**, 223.
128. J. E. Leffler and E. Grunwald, 'Rates and Equilibria of Organic Reactions', Wiley, New York, 1963, p. 156.
129. C. H. Langford, *Inorg. Chem.*, 1965, **4**, 265.
130. A. Haim, *Inorg. Chem.*, 1970, **9**, 426.

131. E. Lenz and R. K. Murmann, *Inorg. Chem.*, 1968, **7**, 1880.
132. J. McB. Harrowfield, A. M. Sargeson, B. Singh and J. C. Sullivan, *Inorg. Chem.*, 1975, **14**, 2864.
133. D. A. Buckingham, P. J. Cresswell, W. G. Jackson and A. M. Sargeson, *Inorg. Chem.*, 1981, **20**, 1647.
134. W. Schmidt and H. Taube, *Inorg. Chem.*, 1963, **2**, 698.
135. C. A. Stein and H. Taube, *Inorg. Chem.*, 1979, **18**, 1168.
136. N. E. Dixon, W. G. Jackson, W. Marty and A. M. Sargeson, *Inorg. Chem.*, 1982, **21**, 688.
137. G. Guastalla and T. W. Swaddle, *Can. J. Chem.*, 1974, **52**, 527.
138. F. Monacelli and S. Viticoli, *Inorg. Chim. Acta*, 1973, **7**, 231.
139. R. G. Yalman, *Inorg. Chem.*, 1967, **1**, 16.
140. G. Guastalla and T. W. Swaddle, *Can. J. Chem.*, 1973, **51**, 821.
141. J. A. Broomhead and L. Kane-Maguire, *Inorg. Chem.*, 1968, **7**, 2519.
142. A. J. Pöe, K. Shaw and M. J. Wendt, *Inorg. Chim. Acta*, 1967, **1**, 371.
143. G. B. Schmidt, *Z. Phys. Chem. (Frankfurt am Main)*, 1966, **50**, 222.
144. H. R. Hunt and H. Taube, *J. Am. Chem. Soc.*, 1958, **80**, 2642.
145. T. W. Swaddle and D. R. Stranks, *J. Am. Chem. Soc.*, 1972, **94**, 8357.
146. F. Monacelli and E. Viel, *Inorg. Chim. Acta*, 1967, **1**, 467.
147. E. Borghi and F. Monacelli, *Inorg. Chim. Acta*, 1971, **5**, 211.
148. W. L. Reynolds, I. Murati and S. As̃perger, *J. Chem. Soc., Dalton Trans.*, 1974, 719.
149. T. Eliades, R. O. Harris and P. Reinsalu, *Can. J. Chem.*, 1969, **47**, 3823.
150. G. B. Schmidt, ‘Exchange Reactions’, Proc. Symp., Upton, N. Y., 1965, p. 219.
151. G. C. Lalor and G. W. Bushnell, *J. Chem. Soc. (A)*, 1968, 2520.
152. F. Monacelli, *Inorg. Chim. Acta*, 1973, **7**, 65.
153. B. Adell, *Z. Anorg. Allg. Chem.*, 1942, **249**, 251.
154. N. S. Angerman and R. B. Jordan, *Inorg. Chem.*, 1967, **6**, 379.
155. E. Zinato, C. Furlani, G. Lanna and P. Riccieri, *Inorg. Chem.*, 1972, **11**, 1746.
156. A. Ohyoshi, S. Shida, S. Izuchi, F. Kitigawa and K. Ohkubo, *Bull. Chem. Soc. Jpn.*, 1973, **46**, 2431.
157. F. Monacelli, F. Basolo and R. G. Pearson, *J. Inorg. Nucl. Chem.*, 1962, **24**, 1241.
158. R. Davies, G. B. Evans and R. B. Jordan, *Inorg. Chem.*, 1969, **8**, 2025.
159. T. P. Jones and J. K. Phillips, *J. Chem. Soc. (A)*, 1968, 674.
160. W. E. Jones, R. B. Jordan and T. W. Swaddle, *Inorg. Chem.*, 1969, **8**, 2504.
161. G. C. Lalor and E. A. Moelwyn-Hughes, *J. Chem. Soc.*, 1963, 1560.
162. C. Chatterjee and P. Chaudhuri, *Indian J. Chem.*, 1971, **9**, 1132.
163. D. L. Gay and G. C. Lalor, *J. Chem. Soc. (A)*, 1966, 1179.
164. S. F. Lincoln, J. Jayne and J. P. Hunt, *Inorg. Chem.*, 1969, **8**, 2267.
165. A. M. Newton and T. W. Swaddle, *Can. J. Chem.*, 1974, **52**, 5751.
166. L. Mønsted, *Acta Chem. Scand.*, 1978, **32**, 377.
167. T. Ramasami and A. G. Sykes, *Inorg. Chem.*, 1976, **15**, 2885.
168. M. Ferrer and A. G. Sykes, *Inorg. Chem.*, 1979, **18**, 3345.
169. S. Castillo-Blum and A. G. Sykes, *Inorg. Chem.*, 1984, **23**, 1049.
170. A. Creix and M. Ferrer, *Inorg. Chim. Acta*, 1982, **59**, 177.
171. T. C. Matts and P. Moore, *J. Chem. Soc. (A)*, 1969, 219.
172. T. Ramasami, R. K. Wharton and A. G. Sykes, *Inorg. Chem.*, 1975, **14**, 359.
173. J. E. Earley and W. Alexander, *J. Am. Chem. Soc.*, 1970, **92**, 2294.
174. T. Ramasami, R. S. Taylor and A. G. Sykes, *Inorg. Chem.*, 1976, **15**, 2318.
175. T. W. Swaddle and G. Guastalla, *Inorg. Chem.*, 1968, **7**, 1915.
176. T. W. Swaddle and W. E. Jones, *Can. J. Chem.*, 1970, **48**, 1054.
177. R. Grassi, A. Haim and W. K. Wilmarth, *Inorg. Chem.*, 1967, **6**, 237.
178. C. H. Langford and V. S. Sastri, *MTP Int. Rev. Sci., Inorg. Chem. Ser. 1*, vol. 9, ed. M. L. Tobe, Butterworths, London, 1972, p. 203.
179. W. G. Jackson and A. M. Sargeson, *Inorg. Chem.*, 1978, **17**, 1 348.
180. M. E. Baldwin, S. C. Chan and M. L. Tobe, *J. Chem. Soc.*, 1961, 4637.
181. W. G. Jackson and C. M. Begbie, *Inorg. Chim. Acta*, 1982, **61**, 167.
182. S. C. Chan, *Aust. J. Chem.*, 1967, **20**, 595.
183. W. D. Panasayuk, V. P. Solomko and L. G. Reiter, *Zh. Neorg. Khim.*, 1961, **6**, 2091.
184. S. C. Chan and M. L. Tobe, *J. Chem. Soc.*, 1963, 5700.
185. T. P. Dasgupta, W. Fitzgerald and M. L. Tobe, *Inorg. Chem.*, 1972, **11**, 2046.
186. M. E. Baldwin and M. L. Tobe, *J. Chem. Soc.*, 1960, 4275.
187. T. Inoue and G. M. Harris, *Inorg. Chem.*, 1980, **19**, 1091.
188. V. Ricevuto and M. L. Tobe, *Inorg. Chem.*, 1970, **9**, 1785.
189. W. G. Jackson and C. M. Begbie, *Inorg. Chim. Acta*, 1982, **60**, 115.
190. R. S. Nyholm and M. L. Tobe, *J. Chem. Soc.*, 1956, 1707.
191. M. L. Tobe, *J. Chem. Soc.*, 1959, 3776.
192. S. C. Chan and F. Leh, *J. Chem. Soc. (A)*, 1966, 129.
193. I. J. Kindred and D. A. House, *Inorg. Chim. Acta*, 1975, **14**, 185.
194. S. C. Chan and F. Leh, *J. Chem. Soc.(A)*, 1967, 573.
195. M. L. Tobe and C. K. Williams, *Inorg. Chem.*, 1976, **15**, 918.
196. S. C. Chan and M. L. Tobe, *J. Chem. Soc.*, 1963, 514.
197. S. As̃perger and C. K. Ingold, *J. Chem. Soc.*, 1956, 2862.
198. W. Rindermann and R. van Eldik, *Inorg. Chim. Acta*, 1982, **64**, L203.
199. J. N. Cooper, J. G. Bentson, T. M. Handel, K. M. Strohmaier, W. A. Porter, B. C. Johnson, A. M. Carr, D. A. Farnath and S. L. Appleton, *Inorg. Chem.*, 1983, **22**, 3060.
200. D. Stranks and Y. Yandell, *Inorg. Chem.*, 1970, **9**, 751.
201. W. G. Jackson, *Inorg. Chim. Acta*, 1981, **47**, 159.
202. L. Richards and J. Halpern, *Inorg. Chem.*, 1976, **15**, 2571.
203. R. C. Elder and M. Trkula, *J. Am. Chem. Soc.*, 1974, **96**, 2635.
204. R. C. Elder, M. J. Heeg, M. D. Payne, M. Trkula and E. Deutsch, *Inorg. Chem.*, 1978, **17**, 431.

205. W. Ozbirn and R. A. Jacobson, *Inorg. Chim. Acta*, 1970, **4**, 377.
206. R. McWeeny, R. Mason and A. D. C. Towl, *Discuss. Faraday Soc.*, 1969, **47**, 20.
207. R. G. Pearson and F. Basolo, *J. Am. Chem. Soc.*, 1956, **78**, 4878.
208. M. L. Tobe and D. W. Watts, *J. Chem. Soc.*, 1962, 4614.
209. B. Bosnich, Sir Christopher Ingold and M. L. Tobe, *J. Chem. Soc.*, 1965, 4074.
210. C. G. Barraclough, R. W. Boschen, W. W. Fee, W. G. Jackson and P. T. McTigue, *Inorg. Chem.*, 1971, **10**, 1994.
211. M. L. Tobe, *Inorg. Chem.*, 1968, **7**, 1260.
212. L. G. Vanquickenborne and K. Pierloot, *Inorg. Chem.*, 1984, **23**, 1471.
213. G. Daffner, D. A. Palmer and H. Kelm, *Inorg. Chim. Acta*, 1982, **61**, 57.
214. R. G. Pearson, C. R. Boston and F. Basolo, *J. Phys. Chem.*, 1955, **59**, 304.
215. R. G. Pearson, C. R. Boston and F. Basolo, *J. Am. Chem. Soc.*, 1953, **75**, 3089.
216. I. R. Jonassen, R. S. Murray, D. R. Stranks and Y. K. Yandell, in 'Proc. 12th Int. Conf. Coord. Chem.', 1969, p. 32.
217. M. C. Couldwell, D. A. House and H. K. J. Powell, *Inorg. Chem.*, 1973, **12**, 627.
218. C. K. Poon and M. L. Tobe, *J. Chem. Soc.(A)*, 1967, 2069.
219. C. J. Cooksey and M. L. Tobe, *Inorg. Chem.*, 1978, **17**, 1558.
220. A. M. Sargeson and G. H. Searle, *Inorg. Chem.*, 1967, **6**, 2172.
221. R. Niththyananthan and M. L. Tobe, *Inorg. Chem.*, 1969, **8**, 1589.
222. W. K. Chau and C. K. Poon, *J. Chem. Soc. (A)*, 1971, 3087.
223. Y. Hung and D. H. Busch, *J. Am. Chem. Soc.*, 1977, **99**, 4977.
224. J. A. Kernohan and J. F. Endicott, *Inorg. Chem.*, 1970, **9**, 1604.
225. D. P. Rillema, J. F. Endicott and J. R. Barber, *J. Am. Chem. Soc.*, 1973, **95**, 6987.
226. M. C. Couldwell and D. A. House, *Inorg. Chem.*, 1974, **13**, 2949.
227. C. K. Poon, *J. Am. Chem. Soc.*, 1970, **92**, 4467.
228. C. K. Poon, *Inorg. Chim. Acta Rev.*, 1970, **4**, 123.
229. M. D. Alexander, *Inorg. Chem.*, 1966, **5**, 2084.
230. D. A. House and R. G. A. R. Maclagan, *Aust. J. Chem.*, 1984, **37**, 239.
231. Y. Scullion and M. L. Tobe, unpublished results, 1984.
232. Y. Ito, A. Terada and S. Kawaguchi, *Bull. Chem. Soc., Jpn.*, 1978, **51**, 2898.
233. B. M. Oulaghan and D. A. House, *Inorg. Chem.*, 1978, **17**, 2197.
234. M. C. Couldwell and D. A. House, *Inorg. Chem.*, 1972, **11**, 2024.
235. P. G. Beddoe, M. J. Harding, S. F. Mason and B. J. Peart, *Chem. Commun.*, 1971, 1283.
236. C. K. Poon, *Coord. Chem. Rev.*, 1973, **10**, 1.
237. W. K. Lee and C. K. Poon, *Inorg. Chem.*, 1974, **13**, 2526.
238. L. M. Eade, G. A. Rodley and D. A. House, *J. Inorg. Nucl. Chem.*, 1975, **37**, 1049.
239. G. N. Schrauzer, *Acc. Chem. Res.*, 1968, **1**, 97.
240. A. V. Ablov and A. Y. Sychev, *Russ. J. Inorg. Chem.*, 1959, **4**, 1153.
241. A. Y. Sychev, A. V. Ablov and V. A. Zarinskii, *Russ. J. Inorg. Chem.*, 1961, **6**, 421.
242. A. Y. Sychev and A. V. Ablov, *Russ. J. Inorg. Chem.*, 1961, **6**, 1163.
243. A. V. Ablov and D. M. Palade, *Dokl. Akad. Nauk SSSR*, 1962, **144**, 414.
244. D. N. Hague and J. Halpern, *Inorg. Chem.*, 1967, **6**, 2059.
245. H. G. Tsiang and W. Wilmarth, *Inorg. Chem.*, 1968, **7**, 2535.
246. J. M. Palmer and E. Deutsch, *Inorg. Chem.*, 1975, **14**, 17.
247. L. Seibles and E. Deutsch, *Inorg. Chem.*, 1977, **16**, 2273.
248. C. S. Garner and D. A. House, *Transition Met. Chem.*, 1970, **6**, 59.
249. J. Selbin and J. C. Bailar, Jr. *J. Am. Chem. Soc.*, 1957, **79**, 4285.
250. D. J. McDonald and C. S. Garner, *J. Inorg. Nucl. Chem.*, 1961, **18**, 219.
251. R. G. Pearson, R. A. Munson and F. Basolo, *J. Am. Chem. Soc.*, 1958, **80**, 504.
252. D. J. McDonald and C. S. Garner, *J. Am. Chem. Soc.*, 1961, **83**, 4152.
253. D. C. Olsen and C. S. Garner, *Inorg. Chem.*, 1963, **2**, 558.
254. G. Wirth and R. G. Linck, *J. Am. Chem. Soc.*, 1973, **95**, 5913.
255. J. M. DeJovine, W. R. Mason and J. W. Vaughn, *Inorg. Chem.*, 1974, **13**, 66.
256. J. M. Veigel and C. S. Garner, *Inorg. Chem.*, 1965, **4**, 1569.
257. L. Randolph and R. G. Linck, *Inorg. Chem.*, 1977, **16**, 2653.
258. W. W. Fee, J. MacB. Harrowfield and C. S. Garner, *Inorg. Chem.*, 1971, **10**, 290.
259. D. W. Hoppenjans, J. B. Hunt and R. Gregoire, *Inorg. Chem.*, 1968, **7**, 2506.
260. R. R. Barona and J. A. McLean, Jr., *Inorg. Chem.*, 1971, **10**, 286.
261. C. Kutal and A. W. Adamson, *Inorg. Chem.*, 1973, **12**, 1990.
262. D. Yang and D. A. House, *Inorg. Chem.*, 1982, **21**, 2999.
263. E. Campi, J. Ferguson and M. L. Tobe, *Inorg. Chem.*, 1970, **9**, 1781.
264. M. Esparza and C. S. Garner, *J. Inorg. Nucl. Chem.*, 1967, **29**, 2377.
265. C. P. Madhusudhan and J. A. McLean, Jr., *Inorg. Chem.*, 1975, **14**, 82.
266. J. C. Chang, *J. Inorg. Nucl. Chem.*, 1976, **38**, 1390.
267. C.-Y. Hsu and C. S. Garner, *Inorg. Chim. Acta*, 1967, **1**, 17.
268. W. A. Fordyce, P. S. Sheridan, E. Zinato, P. Riccieri and A. W. Adamson, *Inorg. Chem.*, 1977, **16**, 1154.
269. S. G. Zipp and S. K. Madan, *Inorg. Chem.*, 1976, **15**, 587.
270. D. A. House and V. McKee, *Inorg. Chem.*, 1984, **23**, 4237.
271. A. Pöe and C. P. J. Vuik, *Inorg. Chem.*, 1980, **19**, 1771.
272. S. A. Johnson and F. Basolo, *Inorg. Chem.*, 1962, **1**, 925.
273. F. Basolo, E. J. Bounsall and A. J. Pöe, *Proc. Chem. Soc.*, 1963, 366.
274. J. V. Rund, F. Basolo and R. G. Pearson, *Inorg. Chem.*, 1964, **3**, 658.
275. R. D. Gillard, J. A. Osborn and G. Wilkinson, *J. Chem. Soc.*, 1965, 1951.
276. R. D. Gillard, B. T. Heaton and D. H. Vaughan, *Chem. Commun.*, 1969, 974.
277. H. W. Munro, D. M. Stevenson and D. H. Vaughan, *J. Chem. Soc., Dalton Trans.*, 1983, 1029.
278. H. L. Bott, E. J. Bounsall and A. J. Pöe, *J. Chem. Soc. (A)*, 1966, 1275.
279. F. Basolo and R. G. Pearson, 'Mechanisms of Inorganic Reactions', 2nd edn., Wiley, New York, 1967, p. 176.
280. A. J. Pöe and C. P. J. Vuik, *J. Chem. Soc., Dalton Trans.*, 1972, 2250.

281. G. P. Syrtsova and T. S. Bolgar, *Russ. J. Inorg. Chem.*, 1971, **16**, 1322.
282. G. P. Syrtsova and T. S. Bolgar, *Russ. J. Inorg. Chem.*, 1972, **17**, 1585.
283. S. A. Johnson. F. Basolo and R. G. Pearson, *J. Am. Chem. Soc.*, 1963, **85**, 1741.
284. M. P. Hancock, B. T. Heaton and D. H. Vaughan, *J. Chem. Soc., Dalton Trans.*, 1971, 761.
285. P. M. Gidney, R. D. Gillard, B. T. Heaton, P. S. Sheridan and D. H. Vaughan, *J. Chem. Soc., Dalton Trans.*, 1973, 1462.
286. A. J. Pöe and M. V. Twigg, *Can. J. Chem.*, 1972, **50**, 1089.
287. A. J. Thirst and D. H. Vaughan, *J. Inorg. Nucl. Chem.*, 1981, **43**, 2889.
288. J. McGilly and D. H. Vaughan, *J. Chem. Soc., Dalton Trans.*, 1984, 1117.
289. F. Monacelli, *Inorg. Chim. Acta*, 1968, **2**, 263.
290. R. D. Garlatti, G. Tauzher, M. Blaschich and G. Costa, *Inorg. Chim. Acta*, 1984, **86**, L63.
291. A. L. Crumblis and W. K. Wilmarth, *J. Am. Chem. Soc.*, 1970, **92**, 2593.
292. R. A. Bauer and F. Basolo, *Inorg. Chem.*, 1969, **8**, 2237.
293. C. K. Poon and D. A. Isabirye, *J. Chem. Soc., Dalton Trans.*, 1977, 2115.
294. T. Matsubara and C. Creutz, *Inorg. Chem.*, 1979, **18**, 1956.
295. G. A. K. Thompson and A. G. Sykes, *Inorg. Chem.*, 1979, **18**, 2025.
296. C. K. Poon, C.-M. Che and Y.-P. Kan, *J. Chem. Soc., Dalton Trans.*, 1980, 128.
297. C. K. Poon, T. C. Lan, C. L. Wong and Y. P. Kan, *J. Chem. Soc., Dalton Trans.*, 1983, 1641.
298. J. N. Bronsted and R. Livingston, *J. Am. Chem. Soc.*, 1927, **49**, 435.
299. F. Basolo and R. G. Pearson, 'Mechanisms of Inorganic Reactions', 2nd edn., Wiley, New York, 1967, p. 177.
300. M. L. Tobe, *Acc. Chem. Res.*, 1970, **3**, 377.
301. M. L. Tobe, *Adv. Inorg. Bioinorg. Mech.*, 1983, **2**, 1.
302. R. K. Nanda and R. N. Nanda, *Inorg. Chem.*, 1969, **8**, 104.
303. B. S. Rao, R. Nanda and K. K. Tripathy, *Transition Met. Chem.*, 1981, **6**, 97.
304. A. C. Dash and S. K. Mohapatra, *J. Chem. Soc., Dalton Trans.*, 1977, 246.
305. A. C. Dash and S. K. Mohapatra, *J. Inorg. Nucl. Chem.*, 1978, **40**, 1596.
306. S. Balt and G. F. Pothoff, *J. Coord. Chem.*, 1975, **4**, 167.
307. S. Balt, *Inorg. Chem.*, 1979, **18**, 133.
308. S. Balt, J. Breman and W. de Neviet, *J. Inorg. Nucl. Chem.*, 1979, **41**, 331.
309. S. Balt and A. Jesma, *Inorg. Chem.*, 1981, **20**, 733.
310. S. Balt, W. E. Renkema and P. C. M. van Zijl, *Inorg. Chim. Acta*, 1980, **45**, L241.
311. S. Balt, H. J. Gamelkoorn, H. J. A. M. Kuipers and W. Renkema, *Inorg. Chem.*, 1983, **22**, 3072.
312. S. Balt. H. J. Gamelkoorn and W. E. Renkema. *J. Chem. Soc., Dalton Trans.*. 1983. 2415.
313. J. S. Anderson, F. W. James and H. V. A. Briscoe, *Nature (London)*, 1937, **139**, 109.
314. F. J. Garrick, *Nature (London)*, 1937, **139**, 507.
315. D. A. Buckingham, I. I. Olsen and A. M. Sargeson, *J. Am. Chem. Soc.*, 1966, **88**, 5443.
316. F. Basolo and R. G. Pearson, *J. Am. Chem. Soc.*, 1956, **78**, 4878.
317. C. K. Poon and M. L. Tobe, *Chem. Commun.*, 1968, 156.
318. J. Lichtig and M. L. Tobe, *Inorg. Chem.*, 1978, **17**, 2442.
319. J. Lichtig, M. E. Sosa and M. L. Tobe, *J. Chem. Soc., Dalton Trans.*, 1984, 581.
320. G. Marangoni, M. Panayotou and M. L. Tobe, *J. Chem. Soc., Dalton Trans.*, 1973, 1989.
321. E. Ahmed and M. L. Tobe, *Inorg. Chem.*, 1974, **13**, 2956.
322. C. Blakeley and M. L. Tobe, unpublished results.
323. C. K. Poon and P. W. Mak, *J. Chem. Soc., Dalton Trans.*, 1978, 216.
324. R. W. Hay and P. R. Norman, *J. Chem. Soc., Chem. Commun.*, 1980, 734.
325. R. W. Hay. *Inorg. Chim. Acta.*, 1980, **45**, 83.
326. M. E. Sosa and M. L. Tobe, *J. Chem. Soc., Dalton Trans.*, 1985, 475.
327. R. W. Hay, M. Tajik and P. R. Norman, *J. Chem. Soc., Dalton Trans.*, 1979, 636.
328. S. C. Chan and O. W. Lau, *Aust. J. Chem.*, 1969, **22**. 1851.
329. J. MacB. Harrowfield, V. Norris and A. M. Sargeson, *J. Am. Chem. Soc.*, 1976, **98**, 7282.
330. S. C. Chan, *J. Chem. Soc.*, 1963, 5137.
331. S. C. Chan, *J. Chem. Soc. (A)*, 1966, 1124.
332. D. A. Buckingham, I. I. Olsen and A. M. Sargeson, *Inorg. Chem.*, 1968, **7**, 147.
333. D. A. Buckingham, C. R. Clark and W. S. Webley, *Aust. J. Chem.*, 1980, **33**, 263.
334. R. B. Jordan and H. Taube, *J. Am. Chem. Soc.*, 1966, **88**, 4406.
335. W. G. Jackson and C. M. Begbie, *Inorg. Chem.*, 1983, **22**, 1190.
336. J. C. Bailar, Jr. and W. Auten, *J. Am. Chem. Soc.*, 1934, **56**, 774.
337. L. J. Boucher, E. Kyuno and J. C. Bailar, Jr., *J. Am. Chem. Soc.*, 1964, **86**, 3656.
338. E. A. Dittmar and R. D. Archer, *J. Am. Chem. Soc.*, 1968, **90**, 1468.
339. W. S. Kwak and R. D. Archer, *Inorg. Chem.*, 1976, **15**, 986.
340. M. Green and H. Taube, *Inorg. Chem.*, 1963, **2**, 948.
341. D. A. Buckingham, I. I. Creaser and A. M. Sargeson, *Inorg. Chem.*, 1970, **9**, 655.
342. W. G. Jackson and C. M. Begbie, *Inorg. Chem.*, 1981, **20**, 1654.
343. W. G. Jackson and C. N. Hookey, *Inorg. Chem.*, 1984, **23**, 668.
344. W. G. Jackson, D. P. Fairlie and M. L. Randall, *Inorg. Chim. Acta*, 1983, **70**, 197.
345. W. G. Jackson, M. L. Randall, A. M. Sargeson and W. Marty, *Inorg. Chem.*, 1983, **22**, 1013.
346. D. A. Buckingham, I. I. Olsen and A. M. Sargeson, *J. Am. Chem. Soc.*, 1968, **90**, 6539.
347. S. Balt and H. J. Gamelkoorn, *J. Chem. Soc., Dalton Trans.*, 1985, 659.
348. R. B. Jordan and A. M. Sargeson, *Inorg. Chem.*, 1965, **4**, 433.
349. D. A. Buckingham, I. I. Olsen and A. M. Sargeson, *J. Am. Chem. Soc.*, 1968, **90**, 6654.
350. D. A. Buckingham, C. R. Clark and T. W. Lewis, *Inorg. Chem.*, 1979, **18**, 1985.
351. W. G. Jackson and C. M. Begbie, *Inorg. Chem.*, 1984, **23**, 659.
352. D. A. House and O. Nor, *Inorg. Chim. Acta*, 1983, **70**. 13.
353. M. E. Sosa and M. L. Tobe, *J. Chem. Soc., Dalton Trans.*, 1986, 427.
354. F. Nordmeyer, *Inorg. Chem.*, 1969, **8**, 2780.
355. R. A. Henderson and M. L. Tobe, *Inorg. Chem.*, 1977, **16**, 2576.

356. R. Hoffmann and A. R. Rossi, *Inorg. Chem.*, 1975, **14**, 365.
357. M. L. Tobe, *Adv. Inorg. Bioinorg. Mech.*, 1983, **2**, 68.
358. D. A. Buckingham, P. A. Marzilli and A. M. Sargeson, *Inorg. Chem.*, 1969, **8**, 1595.
359. P. Comba and W. Marty, *Helv. Chim. Acta*, 1980, **63**, 693.
360. M. L. Tobe, *Adv. Inorg. Bioinorg. Mech.*, 1983, **2**, 24.
361. L. R. Graham, G. A. Lawrence and A. M. Sargeson, *Aust. J. Chem.*, 1982, **35**, 1119.
362. U. Tinner and W. Marty, *Inorg. Chem.*, 1981, **20**, 3750.
363. J. A. Broomhead, F. Basolo and R. G. Pearson, *Inorg. Chem.*, 1964, **3**, 826.
364. M. Green, communication to author of ref. 1, p. 125.
365. R. D. Gillard, *J. Chem. Soc. (A)*, 1967, 917.
366. D. A. Buckingham, W. Marty and A. M. Sargeson, *Helv. Chim. Acta*, 1978, **61**, 2223.
367. E. K. Barefield, F. V. Lovecchio, N. E. Tokel, E. Ochiai and D. H. Busch, *Inorg. Chem.*, 1972, **11**, 283.
368. E. K. Barefield and M. T. Mocella, *J. Am. Chem. Soc.*, 1975, **97**, 4238.
369. V. L. Goedken and D. H. Busch, *J. Am. Chem. Soc.*, 1972, **94**, 7355.
370. A. M. daC. Ferreira and H. E. Toma, *J. Chem. Soc., Dalton Trans.*, 1983, 2051.
371. S. E. Diamond and H. Taube, *J. Am. Chem. Soc.*, 1975, **97**, 2661.
372. C. K. Poon and C. M. Che, *J. Chem. Soc., Dalton Trans.*, 1981, 1019.
373. M. G. Eigen and R. G. Wilkins, *Adv. Chem. Ser.*, 1965, **49**, 55.
374. A. McAuley and J. Hill, *Q. Rev., Chem. Soc.*, 1969, **23**, 18.
375. D. J. Hewkin and R. H. Prince, *Coord. Chem. Rev.*, 1970, **5**, 45.
376. K. Kustin and J. Swineheart, *Prog. Inorg. Chem.*, 1970, **13**, 107.
377. R. G. Wilkins, *Acc. Chem. Res.*, 1970, **3**, 408.
378. R. Winkler, *Struct. Bonding (Berlin)*, 1972, **10**, 1.
379. J. Burgess, 'Metal Ions in Solution', Ellis Horwood, Chichester, 1978, chap. 12.
380. M. N. Hughes and M. L. Tobe, *J. Chem. Soc.*, 1965, 1204.
381. I. R. Lantzke and D. W. Watts, *Aust. J. Chem.*, 1966, **19**, 949.
382. D. W. Watts, *Rec. Chem. Prog.*, 1968, **29**, 131.
383. F. A. Posey and H. Taube, *J. Am. Chem. Soc.*, 1956, **78**, 15.
384. R. Van Eldik, D. Palmer and H. Kelm, *Inorg. Chem.*, 1979, **18**, 1520.
385. C. H. Langford and W. R. Muir, *J. Am. Chem. Soc.*, 1967, **89**, 3141.
386. M. G. Burnett, *J. Chem. Soc. (A)*, 1970, 2486.
387. E. C. Barber and W. L. Reynolds, *Inorg. Chem.*, 1973, **12**, 951.
388. R. G. Wilkins, 'The Study of Kinetics and Mechanism of Reactions of Transition Metal Complexes', Allyn and Bacon, New York, 1974, p. 185.
389. I. R. Lantzke and D. W. Watts, *Aust. J. Chem.*, 1966, **19**, 969.
390. L. Mønsted and O. Mønsted, *Acta Chem. Scand., Ser. A*, 1980, **34**, 259.
391. S. T. D. Lo, E. M. Oudeman, J. C. Hansen and T. W. Swaddle, *Can. J. Chem.*, 1976, **54**, 3685.
392. S. T. D. Lo, M. J. Sisley and T. W. Swaddle, *Can. J. Chem.*, 1978, **56**, 2609.
393. A. L. Bott, A. J. Pöe and K. Shaw, *J. Chem. Soc. (A)*, 1970, 1745.
394. M. J. Pavelich, S. M. Maxey and C. Pfaff, *Inorg. Chem.*, 1978, **17**, 564.
395. J. H. Espenson, *Inorg. Chem.*, 1969, **8**, 1554.
396. D. Thusius, *Inorg. Chem.*, 1971, **10**, 1106.
397. Y. Sasaki and A. G. Sykes, *J. Chem. Soc., Dalton Trans.*, 1975, 1048.
398. B. R. Baker, N. Sutin and T. J. Welch, *Inorg. Chem.*, 1967, **6**, 1948.
399. J. H. Espenson and J. R. Pladziewicz, *Inorg. Chem.*, 1970, **9**, 1380.
400. E. Mentasti, F. Secco and M. Venturi, *Inorg. Chem.*, 1982, **21**, 2314.
401. A. Haim and W. K. Wilmarth, *Inorg. Chem.*, 1962, **1**, 573.
402. A. Haim and W. K. Wilmarth, *Inorg. Chem.*, 1962, **1**, 583.
403. R. Barca, J. Ellis, M. S. Tsao and W. K. Wilmarth, *Inorg. Chem.*, 1967, **6**, 243.
404. A. Haim, *Inorg. Chem.*, 1982, **21**, 2887.
405. M. G. Burnett and M. W. Gilfillan, *J. Chem. Soc., Dalton Trans.*, 1981, 1578.
406. D. A. Palmer and H. Kelm, *Z. Anorg. Allg. Chem.*, 1979, **450**, 50.
407. W. K. Wilmarth, J. E. Byrd and H. N. Po, *Coord. Chem. Rev.*, 1983, **51**, 209.
408. H. C. Chiang and W. K. Wilmarth, *Inorg. Chem.*, 1968, **7**, 2535.
409. J. E. Byrd and W. K. Wilmarth, *Inorg. Chim. Acta Rev.*, 1971, **5**, 7.
410. D. A. Palmer and D. W. Watts, *Inorg. Chem.*, 1971, **10**, 281.
411. L. I. Elding, *Inorg. Chim. Acta*, 1972, **6**, 683.
412. L. I. Elding, *Inorg. Chim. Acta*, 1978, **28**, 255.
413. L. I. Elding and A. B. Gröning, *Inorg. Chim. Acta*, 1978, **31**, 243.
414. Ö. Gröning, T. Drakensberg and L. I. Elding, *Inorg. Chem.*, 1982, **21**, 1820.
415. L. Helm, L. I. Elding and A. E. Merbach, *Helv. Chim. Acta*, 1984, **67**, 1453.
416. L. Helm, L. I. Elding and A. E. Merbach, *Inorg. Chem.*, 1985, **24**, 1719.
417. H. B. Gray and R. J. Olcott, *Inorg. Chem.*, 1962, **1**, 481.
418. R. Romeo and M. Cusumano, *Inorg. Chim. Acta*, 1981, **49**, 167.
419. S. Lanza, D. Minniti, R. Romeo and M. L. Tobe, *Inorg. Chem.*, 1983, **22**, 2006.
420. M. Kotowski, D. A. Palmer and H. Kelm, *Inorg. Chim. Acta*, 1980, **44**, L113.
421. D. Banerjea, F. Basolo and R. G. Pearson, *J. Am. Chem. Soc.*, 1957, **79**, 4055.
422. F. Basolo and R. G. Pearson, *Prog. Inorg. Chem.*, 1962, **4**, 381.
423. F. Basolo, *Adv. Chem. Ser*, 1965, **49**, 81.
424. U. Belluco, *Coord. Chem. Rev.*, 1966, **1**, 111.
425. D. S. Martin, *Inorg. Chim. Acta Rev.*, 1967, **1**, 87.
426. L. Cattalini, *Prog. Inorg. Chem.*, 1971, **13**, 263.
427. F. R. Hartley, *Chem. Soc. Rev.*, 1973, **2**, 163.
428. L. Cattalini, *MTP Int. Rev. Sci., Inorg. Chem. Ser. 1*, vol. 9, ed. M. L. Tobe, Butterworths, London, 1973, p. 269.
429. J. S. Coe, *MTP Int. Rev. Sci., Inorg. Chem. Ser. 2*, vol. 9, ed. M. L. Tobe, Butterworths, London, 1974, p. 45.
430. J. K. Burdett, *Inorg. Chem.*, 1977, **16**, 3013.

431. R. J. Mureinik, *Rev. Inorg. Chem.*, 1979, **1**, 1.
432. F. R. Hartley, 'The Chemistry of Platinum and Palladium', Applied Science, London, 1973, chapter 11.
433. G. Natile, E. Bordignon and L. Cattalini, *Inorg. Chem.*, 1976, **15**, 246.
434. R. Roulet, N. Quang Lan, W. R. Mason and G. P. Fenske, Jr., *Helv. Chim. Acta*, 1973, **56**, 2405.
435. L. I. Elding, A. B. Gröning and Ö. Gröning, *J. Chem. Soc., Dalton Trans.*, 1981, 1093.
436. L. I. Elding and L. F. Olsson, *Inorg. Chem.*, 1982, **21**, 779.
437. E. T. Borish and L. J. Kirschenbaum, *Inorg. Chem.*, 1984, **23**, 2355.
438. R. S. Nyholm and M. L. Tobe, 'Essays in Coordination Chemistry', Exp. Suppl. IX, Birkhauser Verlag, Basel, 1964, p. 112.
439. R. Pietropaulo, P. Uguagliati, M. Graziani and U. Belluco, *Inorg. Chim. Acta*, 1970, **4**, 637.
440. B. P. Kennedy, R. Gosling and M. L. Tobe, *Inorg. Chem.*, 1977, **16**, 1744.
441. R. Gosling and M. L. Tobe, *Inorg. Chem.*, 1983, **22**, 1235.
442. P. Van Z. Bekker, W. J. Louw and W. Robb, *Inorg. Chim. Acta*, 1972, **6**, 564.
443. C. Carturan, P. Uguagliati and U. Belluco, *Inorg. Chem.*, 1974, **13**, 542.
444. G. Annibale, L. Cattalini, A. A. El-Awady and G. Natile, *J. Chem. Soc., Dalton Trans.*, 1974, 802.
445. G. Annibale, M. Bonivento, L. Cattalini, G. Michelon and M. L. Tobe, *Inorg. Chem.*, 1984, **23**, 2829.
446. D. A. Palmer and H. Kelm, *Inorg. Chim. Acta*, 1976, **19**, 117.
447. U. Belluco, L. Cattalini, F. Basolo, R. G. Pearson and A. Turco, *J. Am. Chem. Soc.*, 1965, **87**, 241.
448. U. Belluco, M. Martelli and A. Orio, *Inorg. Chem.*, 1966, **5**, 582.
449. R. G. Pearson, H. Sobel and J. Songstad, *J. Am. Chem. Soc.*, 1968, **90**, 319.
450. J. R. Gaylor and C. V. Senoff, *Can. J. Chem.*, 1971, **49**, 2390.
451. T. Hoover and P. Zipp, *Inorg. Chim. Acta*, 1982, **63**, 9.
452. A. T. Treadgold, Ph.D. Thesis, London, 1986.
453. R. Romeo and M. L. Tobe, *Inorg. Chem.*, 1974, **13**, 1991.
454. L. Cattalini, A. Orio and A. Doni, *Inorg. Chem.*, 1966, **5**, 1517.
455. G. Marangoni, M. Martelli and L. Cattalini, *Gazz. Chim. Ital.*, 1968, **98**, 1038.
456. R. Gosling and M. L. Tobe, *Inorg. Chim. Acta*, 1980, **42**, 223.
457. L. Cattalini, A. Orio and M. Martelli, *Chem. Ind. (Milan)*, 1967, **49**, 625.
458. A. Orio, V. Ricevuto and L. Cattalini, *Chem. Ind. (Milan)*, 1967, **49**, 1337.
459. L. Cattalini, M. Martelli and G. Marangoni, *Inorg. Chim. Acta*, 1968, **2**, 405.
460. L. Cattalini, G. Marangoni and M. Martelli, '3rd Coord. Chem. Conf., Debrecen, Hungary', 1970, p. 347.
461. L. Cattalini, M. Nicolini and A. Orio, *Inorg. Chem.*, 1966, **5**, 1674.
462. L. Cattalini, A. Doni and A. Orio, *Inorg. Chem.*, 1967, **6**, 280.
463. L. Cattalini, A. Orio and M. Nicolini, *J. Am. Chem.Soc.*, 1966, **88**, 5734.
464. U. Belluco, R. Ettore, F. Basolo, R. G. Pearson and A. Turco, *Inorg. Chem.*, 1966, **5**, 59.
465. L. Cattalini and M. Martelli, *Inorg. Chim. Acta*, 1967, **1**, 189.
466. L. Cattalini and M. Martelli, *Gazz. Chim. Ital.*, 1967 **97**, 488.
467. B. Bosnich, *Nature (London)*, 1962, **196**, 1196.
468. G. Annibale, L. Canovese, L. Cattalini, G. Marangoni, G. Michelon and M.L. Tobe, *Inorg. Chem.*, 1981, **20**, 2428.
469. M. Bonivento, L. Canovese, L. Cattalini, G. Marangoni, G. Michelon and M. L. Tobe, *Inorg. Chem.*, 1981, **20**, 3728.
470. M. Cusumano, G. Faraone, V. Ricevuto, R. Romeo and M. Trozzi, *J. Chem. Soc., Dalton Trans.*, 1974, 490.
471. R. L. Rich and H. Taube, *J. Phys. Chem.*, 1954, **58**, 57.
472. L. I. Elding and A. B. Gröning, *Acta Chem. Scand., Ser. A* ., 1978, **32**, 867.
473. W. Robb, *Inorg. Chem.*, 1967, **6**, 382.
474. W. J. Louw and W. Robb, *Inorg. Chim. Acta*, 1974, **9**, 33.
475. L. Cattalini and M. L. Tobe, *Inorg. Chem.*, 1966, **5**, 1145.
476. L. Cattalini, A. Orio and M. L. Tobe, *Inorg. Chem.*, 1967, **6**, 75.
477. L. Cattalini, A. Orio and M. L. Tobe, *J. Am. Chem.Soc.*, 1967, **89**, 3130.
478. K. M. Ibne-Rasa, J. O. Edwards and J. L. Rogers, *J. Solution Chem.*, 1975, **4**, 609.
479. A. Werner, *Z. Anorg. Chem.*, 1893, **3**, 267.
480. I. I. Chernyaev, *Ann. Inst. Platine USSR*, 1926, **4**, 246, 261.
481. J. V. Quagliano and L. Schubert, *Chem. Rev.*, 1952, **50**, 201.
482. A. A. Grinberg, 'The Chemistry of Complex Compounds', 2nd edn., translated by J. R. Leach, Pergamon, Oxford, 1962, p. 218 *et seq.*
483. Yu. N. Kukushkin, *Russ. Chem. Rev.*, 1974, **43**, 805.
484. L. Canovese, M. L. Tobe and L. Cattalini, *J. Chem. Soc., Dalton Trans.*, 1985, 27.
485 L. I. Elding and Ö. Gröning, *Inorg. Chem.*, 1978, **17**, 1872.
486. M. A. Tucker, C. B. Colvin and D. S. Martin, Jr., *Inorg. Chem.*, 1964, **3**, 1373.
487. L. I. Elding, *Acta Chem. Scand.*, 1970, **24**, 1527.
488. M. Cusumano, P. Marricchi, R. Romeo, V. Ricevuto and U. Belluco, *Inorg. Chim. Acta*, 1979, **34**, 169.
489. U. Belluco, M. Graziani and P. Rigo, *Inorg. Chem.*, 1966, **5**, 1123.
490. V. Ricevuto, R. Romeo and M. Trozzi, *J. Chem. Soc., Dalton Trans.*, 1972, 1857.
491. U. Belluco, P. Rigo, M. Graziani and R. Ettore, *Inorg. Chem.*, 1966, **5**, 1125.
492. G. Faraone, V. Ricevuto, R. Romeo and M. Trozzi, *Inorg. Chem.*, 1970, **9**, 1525.
493. A. A. Grinberg, *Ann. Inst. Platine, USSR*, 1927, **5**, 107.
494. F. Basolo, J. Chatt, H. B. Gray, R. G. Pearson and B. L. Shaw, *J. Chem. Soc.*, 1961, 2207.
495. S. S. Zumdahl and R. S. Drago, *J. Am. Chem. Soc.*, 1968, **90**, 6669.
496. A. Pidcock, R. E. Richards and L. M. Venanzi, *J. Chem. Soc. (A)*, 1966, 1707.
497. T. G. Appleton, H. C. Clark and L. E. Manzer, *Coord. Chem. Rev.*, 1973, **10**, 335.
498. L. J. Manojlovic-Muir and K. W. Muir, *Inorg. Chim. Acta*, 1974, **10**, 47.
499. D. R. Russell, P. A. Tucker and S. Wilson, *J. Organomet. Chem.*, 1976, **104**, 387.
500. R. J. Goodfellow, R. L. Goggin and D. A. Duddell, *J. Chem. Soc. (A)*, 1968, 504.
501. T. G. Appleton and M. A. Bennett, *Inorg. Chem.*, 1978, **17**, 738.
502. C. W. Fryer and J. A. S. Smith, *J. Chem. Soc. (A)*, 1970, 1029.
503. J. Chatt, L. Duncanson and L. M. Venanzi, *J. Chem. Soc.*, 1955, 4456.
504. L. E. Orgel, *J. Inorg. Nucl. Chem.*, 1956, **2**, 137.

505. G. Natile, L. Maresca and L. Cattalini, *J. Chem. Soc., Dalton Trans.*, 1977, 651.
506. L. Maresca, G. Natile, M. Calligaris, P. Delise and L. Randaccio, *J. Chem. Soc., Dalton Trans.*, 1976, 2386.
507. G. Faraone, V. Ricevuto and R. Romeo, *J. Chem. Soc., Dalton Trans.*, 1974, 1377.
508. M. Bonivento, L. Cattalini, G. Marangoni, G. Michelon, A. P. Schwab and M. L. Tobe, *Inorg. Chem.*, 1980, **19**, 1743.
509. G. Annibale, L. Canovese, L. Cattalini, G. Marangoni, G. Michelon and M. L. Tobe, *J. Chem. Soc., Dalton Trans.*, 1983, 775.
510. L. Cattalini, G. Marangoni and A. Cassol, *Inorg. Chim. Acta*, 1969, **3**, 74.
511. P. D. Braddock, R. Romeo and M. L. Tobe, *Inorg. Chem.*, 1974, **13**, 1170.
512. R. Romeo, D. Minniti and M. Trozzi, *Inorg. Chem.*, 1976, **15**, 1134.
513. W. H. Baddley and F. Basolo, *J. Am. Chem. Soc.*, 1964, **86**, 2075.
514. W. H. Baddley and F. Basolo, *J. Am. Chem. Soc.*, 1966, **88**, 2944.
515. G. K. Anderson and R. J. Cross, *Chem. Soc. Rev.*, 1980, **9**, 185.
516. H. D. K. Drew and G. H. Wyatt, *J. Chem. Soc.*, 1934, 56.
517. L. Cattalini and M. Martelli, *J. Am. Chem. Soc.*, 1969, **91**, 312.
518. J. Chatt and R. W. Wilkins, *J. Chem. Soc.*, 1956, 525.
519. R. Favez, R. Roulet, A. A. Pinkerton and D. Schwartzenbach, *Inorg. Chem.*, 1980, **19**, 1356.
520. G. Annibale, M. Bonivento, L. Canovese, L. Cattalini, G. Michelon and M. L. Tobe, *Inorg. Chem.*, 1985, **24**, 797.
521. R. S. Berry, *J. Chem. Phys.*, 1960, **32**, 933.
522. P. Haake and R. M. Pfeiffer, *J. Am. Chem. Soc.*, 1970, **92**, 5243.
523. P. Haake and R. M. Pfeiffer, *J. Am. Chem. Soc.*, 1970, **92**, 4996.
524. L. E. Erickson, T. A. Ferrett and L. F. Buhse, *Inorg. Chem.*, 1983 , **22**, 1461.
525. T. W. Whitesides, *J. Am. Chem. Soc.*, 1969, **91**, 2395.
526. J. H. Price, J. P. Birk and B. B. Wayland, *Inorg. Chem.*, 1978, **17**, 2245.
527. F. Basolo, H. B. Gray and R. G. Pearson, *J. Am. Chem. Soc.*, 1960, **82**, 4200.
528. J. B. Goddard and F. Basolo, *Inorg. Chem.*, 1968, **7**, 936.
529. D. A. Palmer and H. Kelm, *Inorg. Chim. Acta*, 1975, **14**, L27.
530. R. Roulet and H. B. Gray, *Inorg. Chem.*, 1972, **11**, 2101.
531. D. A. Palmer and H. Kelm, *Aust. J. Chem.*, 1979, **32**, 1415.
532. D. A. Palmer and H. Kelm, *Inorg. Chim. Acta*, 1980, **39**, 275.
533. C. F. Weik and F. Basolo, *Inorg. Chem.*, 1966, **5**, 576.
534. M. J. Blandamer, J. Burgess, S. J. Hampshire and P. Wellings, *Transition Met. Chem.*, 1979, **4**, 161.
535. R. D. Alexander and P. N. Holper, *Transition Met. Chem.*, 1980, **5**, 108.
536. D. L. Fant and C. F. Weick, *Inorg. Chem.*, 1973, **12**, 1864.
537. G. Faraone, V. Ricevuto, R. Romeo and M. Trozzi, *Inorg. Chem.*, 1969, **8**, 2207.
538. G. Faraone, V. Ricevuto, R. Romeo and M. Trozzi, *J. Chem. Soc.* (*A*), 1971, 1877.
539. R. Romeo, D. Minniti and M. Trozzi, *Inorg. Chim. Acta*, 1975, **14**, L15.
540. R. Romeo, D. Minniti and S. Lanza, *Inorg. Chem.*, 1979, **18**, 2362.
541. M. J. Blandamer, J. Burgess, D. Minniti and R. Romeo, *Inorg. Chim. Acta*, 1985, **96**, 129.
542. H. Kelm, W. J. Louw and D. A. Palmer, *Inorg. Chem.*, 1980, **19**, 843.
543. W. J. Louw, R. Van Eldik and H. Kelm, *Inorg. Chem.*, 1980, **19**, 2878.
544. R. Van Eldik, D. A. Palmer, H. Kelm and W. J. Louw, *Inorg. Chem.*, 1980, **19**, 3551.
545. W. J. Louw, *Inorg. Chem.*, 1977, **16**, 2147.
546. R. Romeo, *Inorg. Chem.*, 1978, **17**, 2040.
547. R. Van Eldik, D. A. Palmer and H. Kelm, *Inorg. Chem.*, 1979, **18**, 572.
548. S. Komiya, T. A. Albright, R. Hoffmann and J. K. Kochi, *J. Am. Chem. Soc.*, 1976, **98**, 7255.
549. L. I. Elding and A. B. Gröning, *Inorg. Chim. Acta*, 1980, **38**, 59.
550. S. Lanza, D. Minniti, P. Moore, J. Sachinidis, R. Romeo and M. L. Tobe, *Inorg. Chem.*, 1984, **23**, 4428.
551. S. G. Alibrandi, G. Bruno, S. Lanza, D. Minniti, R. Romeo and M. L. Tobe, *Inorg. Chem.*, in press.
552. J. D. Scott and R. J. Puddephatt, *Organometallics*, 1983, **2**, 1643.
553. P. F. Meier, A. E. Merbach, M. Dartiguenave and Y. Dartiguenave, *Inorg. Chem.*, 1979, **18**, 610.
554. T. Ramasami and J. H. Espenson, *Inorg. Chem.*, 1980, **19**, 1523.
555. R. Favez and R. Roulet, *Inorg. Chem.*, 1981, **20**, 1598.
556. T. D. B. Morgan and M. L. Tobe, *Inorg. Chim. Acta*, 1971, **5**, 563.
557. H. L. Collier and E. Grimley, *Inorg. Chem.*, 1980, **19**, 511.
558. R. G. Pearson, M. M. Muir and L. M. Venanzi, *J. Chem. Soc.*, 1965, 5221.
559. A. D. Hugi, L. Helm and A. E. Mirbach, *Helv. Chim. Acta*, 1985, **68**, 508.

7.2

Electron Transfer Reactions

THOMAS J. MEYER
University of North Carolina, Chapel Hill, NC, USA
and
HENRY TAUBE
Stanford University, Stanford, CA, USA

7.2.1 INTRODUCTION

The mechanism of an oxidation–reduction reaction can be simple, as illustrated by the ferrocene–ferricenium self-exchange in equation (1) where only electron transfer need occur.[1] In other cases the mechanistic demands imposed by the net reaction are far greater. An example is shown in reaction (2) where, in the net sense, two protons and two electrons must be transferred from isopropanol, which is the reducing agent, to the $\mathrm{Ru^{IV}}$ oxidizing agent.[2]

$$\mathrm{Fe(\eta^5\text{-}C_5H_5)_2^+ + Fe(\eta^5\text{-}C_5H_5)_2 \rightarrow Fe(\eta^5\text{-}C_5H_5)_2 + Fe(\eta^5\text{-}C_5H_5)_2^+} \qquad (1)$$

$$(bipy)_2(py)Ru^{IV}{=}O^{2+} + HCMe_2OH \rightarrow (bipy)_2(py)Ru^{II}{-}OH_2^{2+} + Me_2C{=}O \tag{2}$$

(bipy is 2,2′-bipyridyl ; py is pyridine)

In general, any of several possibile mechanisms may be operative for complex reactions. For example, in the oxidation of isopropanol by Ru^{IV} the key redox step could involve initial outer-sphere electron transfer, initial H-atom transfer, or even two-electron hydride transfer. The hydride mechanism, which has been proposed to be the actual low-energy pathway in water at 25 °C, is illustrated in reaction (3).[2]

$$\begin{aligned} &(bipy)_2(py)Ru^{IV}{=}O^{2+} + HCMe_2OH \longrightarrow (bipy)_2(py)Ru^{II}{-}OH^{2+} + Me_2C{=}OH^+ \\ &(bipy)_2(py)Ru^{II}{-}OH^+ + Me_2C{=}OH^+ \xrightarrow{\text{fast}} (bipy)_2(py)Ru^{II}{-}OH_2^{2+} + Me_2C{=}O \end{aligned} \tag{3}$$

Electron transfer is only one of many pathways by which redox reactions can occur. Nonetheless, the importance of electron transfer in transition metal redox chemistry has long been recognized and more recently it has become increasingly obvious that many reactions in organic chemistry once thought to be concerted in nature also occur *via* sequential one-electron steps.[3]

It is sometimes possible to establish the intimate details of how electron transfer reactions occur based on isotopic labelling or product appearance studies for reactants and products having appropriate substitutional properties.[4–7] The earliest examples of this kind came from the work of Taube and coworkers based on the reduction of substitutionally inert ammine complexes of Co^{III} by substitutionally labile $Cr(H_2O)_6^{2+}$ (equation 4).[8,9] From the appearance of Cl^- in the inert Cr^{III} product it was deduced that when electron transfer occurred, both metal centers must have been bound simultaneously to Cl^- as a bridging ligand (equation 4a). Co^{III} is substitutionally inert and unwilling to give up Cl^- until it has gained an electron; the contents of the coordination sphere around the Cr^{II} ion are frozen once an electron has been removed to give Cr^{III}.

$$Cr(H_2O)_6^{2+} + Co(NH_3)_5Cl^{2+} + 5H^+ + 5H_2O \rightarrow Cr(H_2O)_5Cl^{2+} + Co(H_2O)_6^{2+} + 5NH_4^+ \tag{4}$$

$$(H_2O)_5Cr^{II}ClCo^{III}(NH_3)_5^{4+} \rightarrow (H_2O)_5Cr^{III}ClCo^{II}(NH_3)_5^{4+} \tag{4a}$$

A related example of ‘inner-sphere’ reaction is shown in reaction (5), where an additional mechanistic subtlety appears.[10] As shown by the products, inner-sphere electron transfer also occurs but now by ‘remote attack’ in which the sites of bridging ligand binding to the reductant and oxidant are at different atoms on the bridging ligand.

$$(H_2O)_5FeNCS^{2+} + Cr(H_2O)_6^{2+} \rightarrow Fe(H_2O)_6^{2+} + (H_2O)_5CrSCN^{2+} \tag{5}$$

In ‘outer-sphere’ reactions, electron transfer occurs without the utilization of a bridging ligand. The existence of such pathways is suggested for reactants which have no readily available coordination sites for forming a chemical bridge, as in equation (1), and where at least one of the reactants undergoes slow ligand substitution on the timescale for electron transfer, *e.g.* reaction (6).

$$Fe(H_2O)_6^{2+} + Ru(bipy)_3^{3+} \rightarrow Fe(H_2O)_6^{3+} + Ru(bipy)_3^{2+} \tag{6}$$

Often the substitutional characteristics of the reactants are such that they do not allow for an unequivocal determination of mechanism. An example is $Fe(H_2O)_6^{3+/2+}$ self-exchange, where the half-lives for water exchange, $Fe^{2+}(t_{1/2}(25\ °C) = 2\times10^{-7}\ s)$ and $Fe^{3+}(t_{1/2}(25\ °C) = 2\times10^{-4}\ s)$, are short compared with the timescale for electron transfer ($k(25\ °C,\ I = 0.55\ M) = 4\ M^{-1}\ s^{-1}$).[11] The mechanism could be either inner sphere using a bridging water molecule (equation 6a) or outer sphere. It should be noted that the question remains open as to whether or not a water molecule can function as a bridging ligand,[6] and detailed calculations have been carried out on $Fe(H_2O)_6^{3+/2+}$ self-exchange assuming that it occurs by an outer-sphere mechanism.[12]

$$(H_2O)_5Fe^{II}(H_2O)Fe^{III}(H_2O)_5^{5+} \rightarrow (H_2O)_5Fe^{III}(H_2O)Fe^{II}(H_2O)_5^{5+} \tag{6a}$$

The series of elementary steps which constitute the overall electron transfer mechanisms for outer-sphere and inner-sphere reactions are illustrated in Schemes 1 and 2.

$$\begin{aligned} &Fe(H_2O)_6^{2+} + Ru(bipy)_3^{3+} \rightleftharpoons Fe(H_2O)_6^{2+},\ Ru(bipy)_3^{3+}:\ K_A \\ &Fe(H_2O)_6^{2+},\ Ru(bipy)_3^{3+} \longrightarrow Fe(H_2O)_6^{3+},\ Ru(bipy)_3^{2+}:\ k_{et} \\ &Fe(H_2O)_6^{3+},\ Ru(bipy)_3^{2+} \longrightarrow Fe(H_2O)_6^{3+} + Ru(bipy)_3^{2+} \end{aligned}$$

Scheme 1

For outer-sphere reactions, electron transfer can occur over a range of distances between reactants but it is believed that the major contribution comes from reactants in relatively close contact.

$$Cr(H_2O)_6^{2+} + Co(NH_3)_5Cl^{2+} \rightleftharpoons Cr(H_2O)_6^{2+},\ Co(NH_3)_5Cl^{2+}$$

$$Cr(H_2O)_6^{2+},\ Co(NH_3)_5Cl^{2+} \rightleftharpoons (H_2O)_5Cr^{II}ClCo^{III}(NH_3)_5^{4+} + H_2O$$

$$(H_2O)_5Cr^{II}ClCo^{III}(NH_3)_5^{4+} \xrightarrow{k_{et}} (H_2O)_5Cr^{III}ClCo^{II}(NH_3)_5^{4+}$$

$$(H_2O)_5Cr^{III}ClCo^{II}(NH_3)_5^{4+} \rightarrow\ \rightarrow\ \rightarrow Cr(H_2O)_5Cl^{2+} + Co(H_2O)_6^{2+} + 5NH_4^{+}$$

Scheme 2

As discussed in later sections, at close contact the contribution to the barrier to electron transfer arising from the solvent is minimized and, more importantly, electronic coupling is maximized. At experimentally accessible ionic strengths, even for like-charged reactants, a significant fraction of the reactants are in close contact as defined by the association constant $K_A = [D, A]/[D][A]$, where D and A refer to the electron transfer donor and acceptor, respectively. As long as the reaction rate constant, k_{obs}, is well below the diffusion-controlled limit, it is related to the constants in Scheme 1 by $k_{obs} = K_A k_{et}$.

For an inner-sphere reaction there are necessarily more steps since both association and substitution must precede electron transfer. Intermediates like $(H_2O)_5Cr^{II}ClCo^{III}(NH_3)_5^{4+}$ and $(H_2O)_5Cr^{III}ClCo^{II}(NH_3)_5^{4+}$ shown in Scheme 2 are often referred to as the 'precursor' and 'successor' complexes since they precede or follow the electron transfer step.

In principle, any of the steps in Scheme 2 can be rate limiting from the diffusion controlled formation of the association complex to the substitutional breakup of the successor complex. Because of the multiplicity of steps, a detailed interpretation of an experimentally observed rate constant can be extremely difficult. However, in some cases it has been possible to obtain direct or indirect information about the electron transfer step in an inner-sphere reaction using chemically prepared, ligand-bridged dimeric complexes. For example, reduction of the $Co^{III}-Ru^{III}$ precursor to the product shown in equation (7) by $Ru(NH_3)_6^{2+}$ or Eu^{2+} occurs selectively at the Ru^{III} site. The initial reduction to give Ru^{II} is followed by intramolecular electron transfer from Ru^{II} to Co^{III} which is irreversible since the Co^{II} site is rapidly lost by aquation.[13]

(7)

Indirect evidence concerning intramolecular electron transfer has also been obtained by the observation of low-energy charge transfer absorption bands in mixed-valence complexes (reaction 8)[14] even for outer-sphere electron transfer within ion pairs (reaction 9).[15] The theoretical work of Hush makes it possible to use the energies and integrated intensities of such bands to estimate rates of intramolecular electron transfer.[16]

(8)

$$Ru(NH_3)_5py^{3+},\ Fe(CN)_6^{4-} \xrightarrow{h\nu} Ru(NH_3)_5py^{2+},\ Fe(CN)_6^{3-} \qquad (9)$$

In the absence of complicating features, outer-sphere electron transfer is expected to provide the more facile pathway because mechanistic demands are minimal. They include approach and electronic coupling between reactants and, perhaps most importantly, are not subject to rate limitations imposed by substitution. However, if the intrinsic barriers to electron transfer are too high or the net reaction too demanding in terms of molecular complexity, the relative simplicity of the outer-sphere pathway may lead to its undoing as a facile competitor. For example, the outer-sphere reduction of $Co(NH_3)_6^{3+}$ by $Cr(H_2O)_6^{2+}$ is extremely slow, because significant structural differences between the $Co^{III/II}$ and $Cr^{III/II}$ forms of the two couples lead to a large barrier to electron transfer. By contrast, the related inner-sphere reaction in equation (4) is more rapid by $\sim 10^{11}$.[17,18] Substitution on Cr^{II} is extremely facile and there is no inherent reason why, once an inner-sphere intermediate is formed, this rate of reaction cannot be greatly enhanced.

The reduction of MeI by $Co(CN)_5^{3-}$, which occurs by the mechanism represented by reaction (10),[19] is offered as a second example of a facile inner-sphere process. The outer sphere alternative, reaction (11), has a very high energy barrier because of the formation of the five-coordinate intermediate $Co^{III}(CN)_5^{2-}$. Spin-paired complexes of Co^{III} have a strong preference to be six-coordinate and the sizeable energies of activation for dissociative ligand loss to give intermediates like $Co(CN)_5^{3-}$ are large.[20]

$$\begin{aligned} &Co^{II}(CN)_5^{3-} + MeI \rightarrow (CN)_5Co^{III}I^{3-} + Me \\ &Co^{II}(CN)_5^{3-} + Me \rightarrow (CN)_5Co^{III}{-}Me^{3-} \quad \text{(fast)} \end{aligned} \tag{10}$$

$$Co^{II}(CN)_5^{3-} + MeI \rightarrow Co^{III}(CN)_5^{2-} + Me + I^- \tag{11}$$

In a third case, the comproportionation of Ru^{IV} and Ru^{II}, as in reaction (12), has a k_{H_2O}/k_{D_2O} kinetic isotope effect of 16 at 25 °C.[21] It has been suggested that the origin of the dramatic isotope effect is in a pathway in which a proton-coupled electron transfer occurs from $Ru^{II}{-}OH_2^{2+}$ to $Ru^{IV}{=}O^{2+}$ to give 2 $Ru^{III}{-}OH^{2+}$ in a single step.

$$(bipy)_2(py)Ru^{IV}{=}O^{2+} + (bipy)_2(py)Ru^{II}{-}OH_2^{2+} \rightarrow 2(bipy)_2(py)Ru^{III}{-}OH^{2+} \tag{12}$$

A mechanism involving initial outer-sphere electron transfer, although accessible, suffers energetically from the necessity of forming the two Ru^{III} ions initially in non-equilibrium states with regard to proton composition (equation 12a).[22]

$$\begin{aligned} &(bipy)_2(py)Ru^{IV}{=}O^{2+} + (bipy)_2(py)Ru^{II}{-}OH_2^{2+} \longrightarrow (bipy)_2(py)Ru^{III}{-}O^{+} + (bipy)_2(py)Ru^{III}{-}OH_2^{2+} \\ &(bipy)_2(py)Ru^{III}{-}O^{+} + (bipy)_2(py)Ru^{III}{-}OH_2^{2+} \xrightarrow{\text{fast}} 2(bipy)_2(py)Ru^{III}{-}OH^{2+} \end{aligned} \tag{12a}$$

It is important to realize that for the inner-sphere or 'atom transfer' pathways in reactions (4), (10) or (12) to appear at the expense of accessible outer-sphere pathways, there are heightened mechanistic demands on the reactants which must be met. For the cases cited there is a necessity for the substitutional lability of Cr^{II} in reaction (4), the existence of an open coordination site in $Co^{II}(CN)_5^{3-}$ in reaction (10), or the availability of the $Ru^{IV}{=}O$ group to act as an electron–proton acceptor in reaction (12).

The theme here is electron transfer, in inner- and outer-sphere reactions and, to a lesser degree, in related processes like optically induced charge transfer or excited state decay. Three books have been written on electron transfer, by Reynolds and Lumry,[23] Cannon[24] and Ulstrup,[25] the last of which emphasizes theoretical aspects. In addition, a series of theoretical and experimental articles appear in the book 'Tunneling in Biological Systems', edited by Chance *et al.*,[26] and in volume 74 (1982) of the *Faraday Discussions of the Chemical Society*. A number of reviews have appeared, dealing both with general aspects[5,7,27] and more specialized themes, and many will be referred to in the sections that follow.

7.2.1.1 Organization of the Chapter

In the broader context of chemical reactivity a feature that makes electron transfer reactions distinctive is the close interplay between theory and experiment that has been applied to their study. This interplay has led to rapid advances and a clear insight into how electron transfer occurs. To a large degree, it has also dictated how the contents of a chapter are organized.

The first topic to be presented is experimental, a listing of representative rate constants for self-exchange reactions. Self-exchange reactions are a good place to begin since $\Delta G = 0$ and rate constants and rate constant variations are a direct measure of intrinsic reactivity toward electron transfer. Once presented, the outer-sphere self-exchange data provide a basis for discussing the factors at the molecular level that determine electron transfer rate constants, first outer sphere then inner sphere. With a microscopic model in place it is possible to understand the bases for theories of electron transfer. For outer-sphere electron transfer the theories include the classical approach of Marcus and Hush, the quantum mechanical approach based on time dependent perturbation theory, and such concepts as 'tunneling'. Although the electron transfer theories give explicit equations for the electron transfer rate constant in terms of the molecular properties of the reactants, complete rate constant expressions, which can be compared with experimental values, must also take into account: (1) the distance dependence of electron transfer, (2) diffusional effects as the rates of electron transfer approach the diffusion-controlled limit, (3) the different time scales for the molecular motions involved, *i.e.* solvent dipole reorientations, transitions between intramolecular vibrational levels, the rate of electron hopping, and (4) the role that the time scale plays in determining the proper 'frequency factor' or pre-exponential term in equations that define the electron transfer rate constant. A consideration of timescales, and whether the timescales for electron hopping or solvent/vibrational changes are shorter, leads to the concept of 'adiabatic' and 'non-adiabatic' electron transfer.

With the results of the electron transfer theories in place it is possible to return to the listing of outer-sphere self-exchange rate constants and explain many of the trends that appear in the data. The most striking conclusion is that it is possible to use the theoretical results to calculate experimental rate constants for outer-sphere electron transfer to a high degree of accuracy. In addition it is possible to discuss in a general way how the magnitudes of outer-sphere self-exchange rate constants depend on pre-association between reactants, electronic coupling between reactants, the surrounding solvent, and structural variations between oxidation states in the reactants.

The theoretical results obtained for outer-sphere electron transfer based on self-exchange reactions provide the essential background for discussing the interplay between theory and experiment in a variety of electron transfer processes. The next topic considered is outer-sphere electron transfer for net reactions where $\Delta G \neq 0$ and application of the Marcus 'cross reaction equation' for correlating experimental data. A consideration of reactions for which ΔG is highly favorable leads to some peculiar features and the concept of electron transfer in the 'inverted region' and, also, excited state decay.

In general, inner-sphere reactions are more difficult to treat theoretically since they are more complex and involve bond-making and bond-breaking steps (compare Schemes 1 and 2). However, in appropriately designed, ligand-bridged dimeric systems, intramolecular electron transfer can be followed by direct measurement or, in mixed-valence dimers, indirectly by observing absorption bands which arise from charge transfer between the donor and acceptor redox sites. A very difficult problem to deal with theoretically in mixed-valence ions and in inner-sphere electron transfer is the incorporation of electronic coupling when electronic interactions between redox sites becomes appreciable.

In a final section the experimental facts concerning inner-sphere electron transfer are presented, and an attempt is made to understand, at least in a qualitative way, how the rates depend on the properties of the reaction partners.

7.2.2 SELF-EXCHANGE REACTIONS

As noted above, 'self-exchange' reactions like the ferrocene/ferricenium exchange in reaction (1) are a good place to begin a discussion of electron transfer since $\Delta G = 0$ and rate constants for electron transfer depend on the intrinsic properties of the reactants toward electron transfer. Since there is no net chemical change, special experimental techniques are needed to obtain self-exchange rate constant data. The most commonly used techniques have been: (1) isotopic tracers for relatively slow reactions where the distribution of a radioactive label is observed between the two different oxidation states as a function of time, *e.g.* as applied to $\mathrm{Fe(H_2O)_6}^{2+/3+}$;[11] (2) NMR or EPR techniques based on pulsed or line broadening experiments as used, for example, for reaction (1); (3) pseudo self-exchange measurements where there is a net chemical change but for which $\Delta G^\circ \approx 0$ and the net reaction, as in equation (13), involved a measureable change in some property, commonly light absorptivity (phen is 1,10-phenanthroline).

$$\mathrm{Ru(bipy)_3}^{2+} + \mathrm{Ru(phen)_3}^{3+} \rightarrow \mathrm{Ru(bipy)_3}^{3+} + \mathrm{Ru(phen)_3}^{2+} \qquad (13)$$

In Table 1 are summarized representative examples of self-exchange rate constant data for a variety of different types of redox couples based on metal complexes, organometallic compounds, organics and clusters. Where available the results of temperature dependence studies are also cited. For convenience, data obtained from temperature dependence studies are presented as enthalpies and entropies of activation as calculated from the reaction rate theory expression in equation (14).

$$k_{\mathrm{obs}} = (k_{\mathrm{B}}T/h)\exp(-\Delta G^{\ddagger}/RT) = (k_{\mathrm{B}}T/h)\exp(-\Delta H^{\ddagger}/kT)\exp(\Delta S^{\ddagger}/R) \qquad (14)$$

Some comments need to be made concerning the data in Table 1. For some couples an extensive set of additional data are available in a variety of media, *e.g.* $\mathrm{Fe}^{3+/2+}$. For others, data are available for a series of structurally related analogs, *e.g.* $\mathrm{Fe(C_5H_5)_2}^{+/0}$. For couples like $\mathrm{Cr(bipy)_3}^{+/0}$ (5, Table 1) the electron transfer process is ligand π^*(bipy) rather than metal based and in clusters like those in couples 19 and 26 (Table 1) the redox levels are almost surely delocalized over the cluster unit. The inclusion of some of the entries listed as inner-sphere cases is not based on product studies but, rather, mechanistic details have been inferred from rate comparisons, as illustrated in a later section of the chapter.

Table 1 Representative Self-exchange Rate Constants[a]

Couple	*Medium*	k (M^{-1} s^{-1}) (°C)	ΔH^{+} (kJ mol^{-1})	ΔS^{+} (J mol^{-1} deg^{-1})	*Ref.*
1. $V(H_2O)_6^{3+/2+}$	$\mu = 2.0$ M;1.0 M $HClO_4$	1.0×10^{-2} (25)	52.7	−105	206
2. $Cr(H_2O)_6^{3+/2+}$	1.0 M $NaClO_4$	$\leqslant 2 \times 19^{-5}$ (24.5)	88	−33	207
3. $Cr(edta)^{2-/-}$	pH 4.5−6.5	3.0×10^{3} (25)	20.9	−107	208
4. $Cr(C_6H_6)_2^{+/0}$	DMSO	6.0×10^{7} (22)	14.2	−47.7	209
5. $Cr(bipy)_3^{+/0}$	DMF	$(1.5 \pm 0.4) \times 10^{9}$ (25)	—	—	210
6. $Mo(CN)_8^{3-/4-}$	H_2O	3×10^{4} (25)	—	—	211
7. $W(CN)_8^{3-/4-}$	H_2O	$\leqslant 4 \times 10^{8}$ (~25)	—	—	212
8. $CoO_4W_{12}O_{36}^{5-/6-}$	0.21 M LiCl	3.1×10^{-1} (12.6)	18.4 ± 2.1	−184 ± 8	213
9. $MnO_4^{-/2-}$	$\mu = 0.16$ M, Na^{+}	$(7.1 \pm 0.3) \times 10^{2}$ (0)	41.8 ± 4.2	−38	214
10. $Mn(EtNC)_6^{2+/+}$	MeCN	$(6.4 \pm 0.6) \times 10^{5}$ (7)	7.3 ± 0.3	−110.8 ± 8	215
11. $Fe(H_2O)_6^{3+/2+}$	$\mu = 0.55$ M, $NaClO_4$, $HClO_4$	3.3 (21.6)	38.9	−105	216
12. $Fe(CN)_6^{3-/4-}$	0.01 M KOH	$(2.26 \pm 0.03) \times 10^{2}$ (0.1)	23.0 ± 0.8	−117	217
13. $Fe(phen)_3^{3+/2+}$	CD_3CN, 0.048 M PF_6^-	$(6.0 \pm 0.6) \times 10^{6}$ (25)	8.8 ± 4.2	−88±13	218
14. $Fe(bipy)_3^{3+/2+}$	CD_3CN, 0.068 M PF_6^-	$(3.7 \pm 0.8) \times 10^{6}$ (25)	8.8 ± 12.5	−92±42	218
15. $Fe(edta)^{-/2-}$	pH = 4.5−6.5, $\mu = 0.1$ M	3.0×10^{4} (25)	16.7	−105	218
16. $Fe(S_2CNMe_2)_3^{+/0}$	CD_2Cl_2	2.5 ± 0.2 (−32)	8.8 ± 1.7	−46±17	219
17. $Fe^{II/III}$(cyt-*c*)[b]	H_2O, $\mu = 1.0$ M	1.2×10^{3} (40)	29.3	−71	220
18. $Fe(C_5H_5)_2^{+/0}$	MeCN, $\mu \leqslant 0.1$ M	$(5.7 \pm 1.0) \times 10^{6}$ (25)	18.4 ± 4.2	−54	221
19. $Fe_4S_4(S\text{-}p\text{-}C_6H_4Me)_4^{2-/3-}$	MeCN	$(2.8 \pm 0.3) \times 10^{6}$ (28)	15.1	−71	222
20. $Ru(NH_3)_6^{3+/2+}$	D_2O, $\mu = 0.013$ M, CF_3CO_2D	$(8.2 \pm 1.0) \times 10^{2}$ (25)	43.1 ± 4.2	−46±13	223
21. $Ru(NH_3)_5py^{3+/2+}$	1.0 M CF_3SO_3H	4.75×10^{5} (25)	12.1	−92	224
22. $Ru(NH_3)_4(bipy)^{3+/2+}$	1.0 M CF_3SO_3H	3.25×10^{6} (25)	11.7 ± 2.1	−79 ± 13	225
23. $Ru(bipy)_3^{3+/2+}$	CD_3CN, 0.048 M PF_6^-	$(8.3 \pm 1.6) \times 10^{6}$ (25)	15.4 ± 12.5	−6.3 ± 4.2	218
24. $Ru(bipy)_3^{3+/2+}$	0.1 M $HClO_4$	$(4.2 \pm 0.8) \times 10^{8}$ (25)	32.2 ± 6.3	−27.6	226
25. $Ru(bipy)_2(py)Cl^{2+/+}$	MeCN	$(4.9 \pm 0.3) \times 10^{7}$ (25)	13.8 ± 2.5	−50 ± 8	227
26. $Ru_3O(OAc)_6(py)_3^{+/0}$	CH_2Cl_2	$(1.15 \pm 0.10) \times 10^{8}$ (24)	15.9	−35.5	228
27. $Ru(hexafluoroacac)_3^{0/-}$	MeCN, $NBu^{n}{}_4^{+}$	$(5.0 \pm 0.5) \times 10^{6}$ (25)	16.7	−59	229
28. $RuO_4^{-/2-}$	0.1 M OH^-	$> 3.3 \times 10^{4}$ (0)	—	—	230
29. $Os(bipy)_3^{3+/2+}$	CD_3CN, 0.034 M PF_6^-	$(2.2 \pm 1.0) \times 10^{7}$ (31)	—	—	218
30. $Co(H_2O)_6^{3+/2+}$	1.0 M $NaClO_4/HClO_4$	2.50 ± 0.20 (20)	52.7 ± 2.1	−59 ± 8	231
31. $Co(NH_3)_6^{3+/2+}$	$\mu = 2.5$ M, $CF_3SO_3^-$	$(8 \pm 1) \times 10^{-6}$	—	—	232
32. $Co(en)_3^{3+/2+}$	1 M KCl	7.7×10^{-5} (25)	56.4 ± 0.8	−134	233
33. $Co(sep)^{3+/2+}$	$\mu = 0.2$ M	5.1 ± 0.3 (25)	41.8	−95.7	234
34. $Co(phen)_3^{3+/2+}$	0.1 M KNO_3	4.0×10^{-2} (0)	21.3	−142	235
35. $Co(edta)^{-/2-}$	pH = 2, $\mu = 0.2$ M	1.53×10^{-4} (85)	84.9	−64.4	236
36. $Co(Me_4[14]\text{-}tetraeneN_4)(H_2O)_2^{3+/2+}$ [c]	$\mu = 0.1$ M, pH 2	9×10^{-1} (35)	—	—	237
37. $IrCl_6^{2-/3-}$	H_2O, $\mu = 0.10$ M	2.3×10^{5} (25)	—	—	238
38. $Cu^{2+/+}$	MeCN	$\geqslant 0.3$ (~25)	—	—	239
39. $Cu^{III/II}(H_{-2}Aibu_3)^{0/-}$ [d]	H_2O	5.5×10^{4} (25)	29.3	−54	240
40. $Ag^{2+/+}$	5.87 M $HClO_4$	< 0.1(0)	—	—	241
41. $Tl^{3+/+}$	3 M $NaClO_4/HClO_4$	7.0×10^{-5} (25)	70.2	−88	242
42. $Ce^{4+/3+}$	0.8 N H_2SO_4	4.2 ± 0.1 (0)	—	—	243
43. $U^{VI/V}$	1.0 M $HClO_4$	$\geqslant 5.2 \times 10^{1}$ (25)	—	—	244
44. $NpO_2^{2+/+}$	3.0 M $NaClO_4$	7.35×10^{1} (4.5)	48.1	−38±105	245
45. $Eu^{3+/2+}$	2.0 M $NaClO_4$	$< 1 \times 10^{-4}$ (25)	—	—	246
46. $Ni([14]aneN_4)^{3+/2+}$ [e]	1.5 M $HClO_4$	$(6.42 \pm 0.94) \times 10^{2}$ (25)	—	—	247
	Organics				
47. $Benzophenone^{0/-}$	DME, Na^{+}	$(1.10 \pm 0.04) \times 10^{8}$ (12)	23.8 ± 0.8	−10.9	248
48. $Benzoquinone^{0/-}$	DMF	$(3.7 \pm 0.1) \times 10^{8}$ (~25)	—	—	249
49. $Anthracene^{0/-}$	DME	$(1.8 \pm 0.2) \times 10^{9}$ (25)	8.8 ± 1.3	−38.0	250
50. $Naphthalene^{0/-}$	DME, Na^{+}	3.4×10^{8} (−30)	13.0	−25.5	251
51. $Biphenyl^{0/-}$	DME, Na^{+}	$\sim 1 \times 10^{8}$ (23)	7.1	—	249
52. $Benzene^{0/-}$	DME, K^{+}	$(3.6 \pm 0.6) \times 10^{7}$ (18)	24.2 ± 4.2	−13.8	252
53. $2,2'\text{-}Bipy^{0/-}$	DME, K^{+}	3.4×10^{6} (20)	41.8	21	253
54. $PhNO_2^{0/-}$	DMF, 0.01M $(NEt_4)ClO_4$	$(3.0 \pm 0.2) \times 10^{7}$ (25)	—	—	249
55. $Phenothiazine^{+/0}$	MeCN, 0.1M $(NEt_4)ClO_4$	$(6.7 \pm 0.4) \times 10^{9}$ (23)	—	—	254
56. $N(C_6H_4Me)_3^{+/0}$	$CHCl_3$/MeCN (2:1), $\mu = 0.04$ M $(NEt_4)ClO_4$	$(8.7 \pm 5.0) \times 10^{8}$ (18)	1.3 ± 2.1	—	255
57. $PhCN^{0/-}$	DMF, $\mu = 0.1$ M	$(5.6 \pm 0.3) \times 10^{8}$ (23)	—	—	254
58. $TCNE^{0/-}$	DME, $N(Bu^{n})_4^{+}$	1.3×10^{8} (20)	24.7 ± 2.5	15.1	256
	Inner-sphere				
59. VOH^{2+}/V^{2+}	$\mu = 2.0$ M	3.5×10^{-3}	—	—	257
60. $CrOH^{2+}/Cr^{2+}$	$\mu = 1.0$ M	0.66(24.5)	9.2	50	258
61. $CrCl^{2+}/Cr^{2+}$	$\mu = 1.0$ M	11(0)	—	—	259
62. $CrO_2(CCH{=}CHCO_2H)^{2+}/Cr^{2+}$	$\mu = 1.0$ M	1.1(0.5)	—	—	260

Table 1 *(continued)*

Couple	Medium	k (M^{-1} s^{-1})(°C)	$\Delta H^{\ddagger}$ (kJ mol^{-1})[b]	$\Delta S^{\ddagger}$ (J mol^{-1} deg^{-1})[b]	*Ref.*
63. $FeOH^{2+}/Fe^{2+}$	μ = 0.55 M	1×10^3(0)	30.9	−75	216
64. $FeCl^{2+}/Fe^{2+}$	μ = 0.55 M	9.7(0)	36.8	−100	216
65. $Co(Me_4[14]tetraeneN_4)(H_2O)Cl^{2+}$ $Co(Me_4[14]tetraeneN_4)(H_2O)_2^{2+}$	μ = 1.0 M	5.0×10^4 (25)	—	—	261
66. $Pt(en)_2Cl_2^{2+}/Pt(en)_2^{2+}/Cl^-$	μ = 0.008–0.018 M	12±1.4 (25)	42.2	−84	262
67. $Ru(C_5H_5)_2I^+/Ru(C_5H_5)_2$	CD_3NO_2	2×10^6 (25)	34.7	−8	263
	Intramolecular				
68. 4,4′-Dinitrobiphenyl$^{0/-}$	MeCN	$\geqslant 10^8$ (~25)	—	—	264
69. $(p\text{-}C_6H_4NO_2)_2O^{0/-}$	MeCN	1×10^6(~25)	—	—	264
70. [2.2]Paracyclophane$^{0/-}$	DME	$> 10^8$(−70)	—	—	265

[a] The references for Table 1 are collected and cited at the end of the chapter in Section 7.4. The citations are based on the numbers assigned to the couples in Table 1.

[b] Cytochrome c–$Fe^{II/III}$ exchange.

[c] $Me_4[14]tetraeneN_4$ =

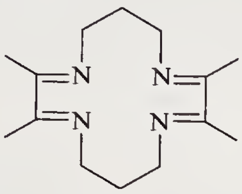

[d] $H_{-2}Aibu_3$ =

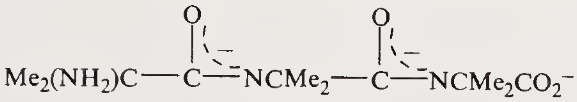

$Me_2(NH_2)C-\overset{O}{C}\cdots NCMe_2-\overset{O}{C}\cdots NCMe_2CO_2^-$.

[e] $[14]aneN_4$ =

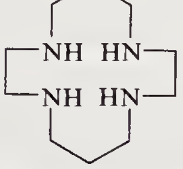

7.2.3 FACTORS AFFECTING OUTER-SPHERE REACTIVITY

With the compilation of data in Table 1 available, it is possible to begin to assess the factors at the molecular level which determine rates of electron transfer, first outer-sphere because of its relative simplicity and then inner-sphere. Because of the absence of bond-making or bond-breaking steps, outer-sphere electron transfer is far easier to treat theoretically than inner-sphere.

A point of note in the data in Table 1 is the extraordinary range in electron-transfer reactivity that can exist even for outer-sphere reactions among what appear to be closely related reactions. For example, the self-exchange rate constants for $Co(NH_3)_6^{3+/2+}$ and $Ru(bipy)_3^{3+/2+}$ differ in magnitude by $\sim 10^{14}$.

For an outer-sphere reaction there are three factors which play a role in determining the rate of electron transfer. The first is the approach of the reactants to be in sufficiently close proximity to create an electronic interaction which provides a basis for the 'delocalization' of the exchanging electron. The second is a barrier to electron transfer that is created by the equilibrium structural differences between reactants and products. The third is an additional barrier that is created in the surrounding solvent by the change in charge distribution associated with the electron transfer act.

7.2.3.1 Intramolecular Vibrational Trapping: Structural Changes

A commonly used example for illustrating intramolecular 'vibrational trapping' induced by structural changes is $Fe(H_2O)_6^{3+/2+}$ self-exchange. X-ray crystallographic[28,29] and EXAFS studies in solution[30] show that the most significant structural difference between the aquated Fe^{II} and Fe^{III} ions is a symmetrical decrease in the Fe—OH_2 bond distance upon oxidation. From EXAFS studies, Fe—O changes from 2.10 to 1.97 Å in aqueous solution. Electron transfer is accompanied by net structural changes at each redox site since both change their electron content during the reaction. For example, the site labelled B in equation (15) will have the equilibrium structure of Fe^{II} before electron transfer and the equilibrium structure of Fe^{III} after electron transfer.

$$\underset{(A)}{Fe(H_2O)_6^{3+}},\ \underset{(B)}{Fe(H_2O)_6^{2+}} \rightarrow \underset{(A)}{Fe(H_2O)_6^{2+}},\ \underset{(B)}{Fe(H_2O)_6^{3+}} \qquad (15)$$

The changes in structure that must occur create a barrier to electron transfer. In order to understand the origin of the barrier and to treat it quantitatively, it is necessary to recall that the structural changes at each reactant can be resolved into a linear combination of its normal vibrational modes. The normal modes constitute a complete, orthonormal set of molecular motions into which any change in intramolecular structure can be resolved.

From the essentially symmetrical decrease in all six Fe—O bonds between Fe^{II} and Fe^{III}, it can be concluded that the only significant normal mode contributing to the structural change between Fe^{II} and Fe^{III} is the totally symmetric $\nu_{a_{1g}}$(Fe—O) iron-oxygen breathing mode.

In Figure 1 are shown potential energy-normal coordinate curves for the $\nu_{a_{1g}}$ mode for site A as Fe^{III} in the reactants (R) and Fe^{II} in the products (P). The coordinate is a normal coordinate of the molecule composed of an equally weighted linear combination of the displacement coordinates (q) for the six Fe—O local coordinates, $Q = 1/\sqrt{6}[q(\text{Fe—O})_1 + q(\text{Fe—O})_2 + \ldots + q(\text{Fe—O})_6] = \sqrt{6}[q(\text{Fe—O})]$. It has no connection with an 'electron transfer distance' nor with the intersite separation between reactants.

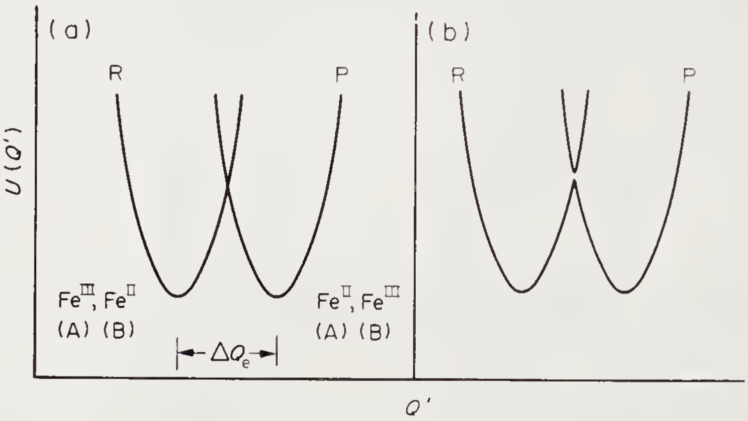

Figure 1. (a) Potential energy-coordinate diagram for the $\nu_{a_{1g}}$ (Fe—O) trapping mode at the site labelled A; it is Fe^{III} in the reactants (R) and Fe^{II} in the products (P). $\Delta Q_e = 0.13$ Å is the change in average Fe—O bond length upon reducing Fe^{III} to Fe^{II}. (b) The same figure as in (a) but including electronic coupling between Fe^{II} and Fe^{III}

A second, equivalent set of curves exists for the $\nu_{a_{1g}}$ mode at site B. In Figure 1 it is assumed that the energy of the molecule varies with the normal coordinate Q' as for a harmonic oscillator. The equation for the harmonic oscillator can be written as $U - U_e = \frac{1}{2}k_jQ_j^2$, where k_j is the force constant and $Q_j = (Q'_j - Q_e)$, the displacement coordinate for normal mode j. U_e is the total energy of the system, including both sites A and B, when the normal modes are at their equilibrium coordinates, Q_{ej}, and U is the total energy of the system including the vibrational energy. The two curves are offset (by $\Delta Q_e = 0.13$ Å) in Figure 1 because of the change in equilibrium bond distances when Fe^{III} is reduced to Fe^{II}. Although drawn symmetrically, the potential curves for $\nu_{a_{1g}}$ at Fe^{III} and Fe^{II} are, in fact, not exactly symmetrical because the frequencies (490 and 390 cm^{-1}) and force constants decrease upon reduction.[31]

The basis for the 'vibrational' or 'reorganizational' barrier to electron transfer arising from structural changes is inherent in the potential curves in Figure 1. As in any chemical process, electron transfer between Fe^{II} and Fe^{III} must occur with the conservation of energy. In the classical limit, vibrational quantum spacings ($h\nu = \hbar\omega$) are small compared with the background thermal energy in solution, $h\nu < k_BT$ (~200 cm^{-1} at 25 °C). In this limit the only value of the normal coordinate where electron transfer can occur with the conservation of energy is at the intersection point between the potential curves. This value, Q_{int}, can be derived by: (1) expressing the product potential curve as a function of Q through $U^P - U^P_e = \frac{1}{2}k(Q - \Delta Q_e)^2$; (2) equating U^P and U^R at the intersection point $\frac{1}{2}kQ^2_{\text{int}} = \frac{1}{2}k(Q_{\text{int}} - \Delta Q_e)^2$ to give $Q_{\text{int}} = \frac{1}{2}\Delta Q_e$. For a self-exchange reaction it follows that the energy from the minimum of potential curve R to the intersection is given by $\frac{1}{2}(\Delta Q_e/2)^2$. This quantity corresponds to the contribution from the $\nu_{a_{1g}}$ (Fe—O) mode at site A to the classical energy of activation for electron transfer and equation (16) gives the total contribution from both $\nu_{a_{1g}}$ (Fe—O) modes. In equation (16), $\Delta Q_e = \sqrt{6}(\Delta q_e)$ and $\Delta q_e = 0.13$ Å is the difference in Fe—O bond distance between Fe^{II} and Fe^{III}. When the difference in force constants between the two oxidation states (k_2 and k_3) is taken into account, equation (16a) results.

$$E_{a(\nu_{a_{1g}})} = 2\left[\tfrac{1}{2}k(\Delta Q_e/2)^2\right] = 3/2k(\Delta q_e)^2 \tag{16}$$

$$E_{a(\nu_{a_{1g}})} = 3k_2k_3(\Delta q_e)^2/\,(k_2 + k_3) \tag{16a}$$

The form of equation (16a) is a consequence of the fact that for two or more trapping vibrations only total energy need be conserved when electron transfer occurs. The condition imposed by energy conservation can be met, for example, by combinations of the two modes, one in a vibrational level below its intersection point and the other in a level above its intersection point. The expression in equation (16a) gives the minimum contribution to the energy of activation when both vibrations are considered. It can be derived by: (1) constructing total potential energy functions for the products and reactants which include the contribution from the $\nu_{a_{1g}}$ modes at both $\mathrm{Fe^{II}}$ and $\mathrm{Fe^{III}}$, *e.g.* $U^R - U^R_e = \frac{1}{2}k_{III}Q_{III}^2 + \frac{1}{2}k_{II}(Q_{II} + \Delta Q)^2$ where the subscripts label the sites; (2) equating U^R and U^P in order to establish the relationship between Q_{II} and Q_{III} consistent with energy conservation, $Q_{II} = Q_{III} = Q^*$; and (3) minimizing the expression for U^R written in terms of Q^* in order to find the minimum value of the displacement coordinate required for electron transfer to occur with energy conservation.[31,37]

The $\mathrm{Fe^{III/II}}$ case is particularly simple. For electron transfer reactions in general, several normal modes may contribute to the trapping of the exchanging electron at a particular site. In addition, intramolecular vibrational modes are of relatively high frequency, 200–4000 $\mathrm{cm^{-1}}$, and at room temperature the classical approximation is not valid since only the $\nu = 0$ level is appreciably populated. In order to treat the problem more generally, it is necessary to turn to the quantum mechanical results in a later section.

7.2.3.2 Solvent Trapping

The solvent plays a role in trapping the exchanging electron on one site similar to that of intramolecular structural changes. An ion can be thought of as creating a polarization field in the surrounding solvent. At the molecular level there are three ways that the solvent molecules respond to the electrostatic field of the ion: (1) orientation of permanent solvent dipoles, (2) electrostatically induced structural distortions within the molecule, and (3) induced electrostatic polarization of electronic clouds including bonding and nonbonding electron density. The strength of the ion-solvent interaction depends on the charge on the ion. When electron transfer occurs, changes must also occur in the orientation of the surrounding solvent dipoles since in the electron transfer act the polarization fields at the reactants are interchanged.

The necessary reorientation or reorganization of solvent dipoles also creates a barrier to electron transfer. An attempt is made to illustrate the point schematically in Figure 2. Rather than try to show individual solvent molecules and their dipole orientations, the decrease in ion-solvent interaction between a +3 and a +2 ion is illustrated by the more tightly drawn circle around the +3 ion. The circles are a schematic attempt to illustrate the interactions between the surrounding solvent 'sheath' and the ionic charges.

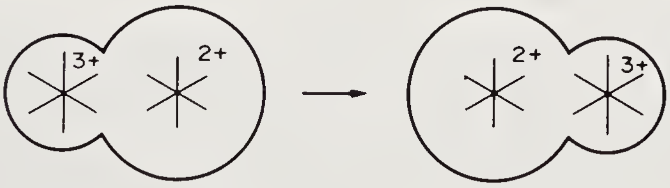

Figure 2 Schematic illustration of the change in solvent polarization interactions for electron transfer between octahedral +3 and +2 ions

For intramolecular vibrations, each site was considered independently. However, the 'reorganizations' in the surrounding solvent are necessarily properties of *both* sites since some of the solvent molecules involved are shared between reactants. The critical motions in the solvent are reorientations of the solvent dipoles. These motions are closely related to rotations of molecules in the gas phase but are necessarily collective in nature because of molecule–molecule interactions in the condensed phase of the solution. They have been treated theoretically as vibrations by analogy with lattice vibrations of 'phonons' which occur in the solid state.[32,33]

From frequency dependent dielectric loss measurements, the transitions associated with solvent dipole reorientations occur on a timescale of $10^{-11} - 10^{-13}$ s. By contrast, the time response of the electronic contribution to the solvent polarization is much more rapid since it involves a readjustment in 'electron clouds'. The difference in timescales for the two types of polarization is of paramount importance in deciding what properties of the solvent play a role in electron transfer. The electronic component of the polarization adjusts rapidly and remains in equilibrium with the charge distribution while electron transfer occurs. The orientational component arising from solvent dipoles must adopt a non-equilibrium distribution before electron transfer can occur. The reorientation of solvent dipoles contributes to the energy of activation and, as noted in a later section, through the timescale for dipole reorientations, can also contribute to the pre-exponential or 'frequency factor' for electron transfer.

The energy spacings between levels associated with solvent dipole reorientations are small, 1–10 cm^{-1}. Since the spacings are well below k_BT at room temperature (~200 cm^{-1}), the contribution of the solvent to the energy of activation for electron transfer can be treated classically. The results of classical treatments, where the solvent is modelled as a structureless dielectric continuum, will be discussed in later sections.

7.2.3.3 Electronic Coupling

For electron transfer to occur between reactants, an electronic interaction must exist which tends to 'delocalize' the exchanging electron between sites. Neglecting overlap, the magnitude of the interaction is given by V (equation 17), where ϕ_A and ϕ_D are the electronic wavefunctions for the acceptor and donor orbitals and $\hat{V}$ is an electrostatic operator that describes the electronic perturbation between the electron donor and acceptor and causes electron transfer to occur.

$$V = \langle \phi'_D | \hat{V} | \phi_A \rangle \tag{17}$$

The electronic interaction leads to two new electronic states, an upper state and a lower state, as shown in Figure 1b. V is of the form of a resonance integral and the situation is analogous to the combination of two atomic orbitals to give bonding and antibonding molecular orbitals. If overlap between ϕ_D and ϕ_A is negligible, the energies of the two new states, including the electronic interaction but neglecting the vibrational energies, are given by $U_e + V$ and $U_e - V$ where $U_e = U^P{}_e = U^R{}_e$ for a self-exchange reaction.

The existence of vibrational trapping creates an unusual situation compared with other molecular orbital-type problems. If electronic coupling between the two sites is weak, the effect of vibrational trapping will be to localize the exchanging electron either on the electron donor site *or* on the acceptor site. The delocalization of the exchanging electron is, in fact, the electron transfer process itself. If electronic coupling is weak, electron transfer becomes an occasional event that can only occur at an appreciable rate from electron donors and acceptors having the non-equilibrium vibrational distributions and solvent dipole orientations appropriate for maximizing the electron transfer rate.

With the inclusion of electronic coupling as in Figure 1b, *electron transfer between* Fe^{II} *and* Fe^{III} *becomes a 'redistribution' of electron density within the ground electronic state from* Fe^{II} *to* Fe^{III} and not a transition between different states.

7.2.4 THEORIES OF ELECTRON TRANSFER

The discussion in the previous section was helpful in identifying the factors at the molecular level which are involved when electron transfer occurs. Two different theoretical approaches have been developed which incorporate these features and attempt to account for electron transfer rate constants quantitatively. The first, by Marcus[34] and Hush,[35] is classical in nature, and the second is based on quantum mechanics and time dependent perturbation theory. The theoretical aspects of electron transfer in chemical[36–38] and biological systems[39] have been discussed in a series of reviews.

7.2.4.1 Marcus–Hush Theory

Marcus attempted to calculate the minimum energy 'reaction coordinate' or 'reaction trajectory' needed for electron transfer to occur. The reaction coordinate includes contributions from *all* of the trapping vibrations of the system including the solvent and is not simply the normal coordinate illustrated in Figure 1. In general, the reaction coordinate is a complex function of the coordinates of the series of normal modes that are involved in electron trapping. In this approach to the theory of electron transfer the rate constant for outer-sphere electron transfer is given by equation (18).

$$k_{obs} = Z\kappa \exp\left[-(w_R/RT)\right] \exp\left[-(\Delta G^*/RT)\right] \tag{18}$$

In equation (18) the rate constant is written as a product of four factors. (1) Z is the collision frequency between two neutral molecules in solution. It is not the diffusion limited rate constant since it also includes encounters between reactants in a solvent cage. For water at 25 °C, $Z \approx 10^{11}$ $\mathrm{M}^{-1}\ \mathrm{s}^{-1}$. (2) κ is the transmission coefficient. As discussed in a later section, it is related to the probability that electron transfer will occur once the intersection region in Figure 1b is reached. For most simple outer-sphere electron transfer reactions, κ appears to be near 1. (3) w_R is defined in equation (19).[37] It is the free energy change associated with bringing together the reactants and is unfavorable for like charged reactants and favorable for unlike charged reactants. In equation (19), Z_D and Z_A are the charges on the ions, e the unit electron charge, r the internuclear separation and D_s the static dielectric constant of the solvent. In the ionic strength term, μ is the ionic strength, β is the Debye–Hückel length $(8\pi Ne^2/1000D_sRT)^{1/2}$, and σ_D and σ_A are the ionic radii (a_A or a_D) plus the radius of the main ion of opposite charge in the ion atmosphere. When $r = a_A + a_D$ and the radii of all of the ions are equal, equation (19) becomes equation (20). (4) ΔG^* is the minimum free energy increase above the background thermal energy, RT, required in the vibrational and solvent trapping modes in order for electron transfer to occur with energy conservation. ΔG^* is related to the inner-sphere (vibrational) and outer-sphere (solvent) reorganizational energies for self-exchange reactions as shown in equation (21).

$$w_R = \frac{Z_D Z_A e^2}{2D_s r}\left[\frac{\exp(\beta\sigma_A\sqrt{\mu})}{1+\beta\sigma_A\sqrt{\mu}} + \frac{\exp(\beta\sigma_D\sqrt{\mu})}{1+\beta\sigma_D\sqrt{\mu}}\right]\exp(-\beta r\sqrt{\mu}) \tag{19}$$

$$w_R = \frac{Z_A Z_D e^2}{D_s r(1+\beta r\sqrt{\mu})} \tag{20}$$

$$4\Delta G^* = \lambda_i + \lambda_0 = \lambda \tag{21}$$

For the normal modes that contribute to vibrational trapping, $\Delta Q_e \neq 0$. If there is a series of such modes, λ_i is given by equation (22) where the summation is over all of the trapping vibrations. For the general case of unequal force constants, the contribution of the intramolecular vibrations to ΔG^* is not given by λ_i but rather by a more complex expression arising from the energy minimization procedure described in the derivation of equation (16a).

$$\lambda_i = \sum_j \tfrac{1}{2}k_j(\Delta Q_{e,j})^2 \tag{22}$$

An expression has been derived by Marcus[34] and Hush[35] for λ_0 assuming the solvent to be a structureless dielectric continuum characterized by the macroscopic dielectric constants D_{op} and D_s. D_{op} and D_s are the optical and static dielectric constants, respectively, and $D_{op} = n^2$ where n is the index of refraction in the visible spectral region. In the limit that the reactants can be treated as two non-interpenetrating spheres, λ_0 is given by equation (23).

$$\lambda_0 = e^2\left(\frac{1}{D_{op}} - \frac{1}{D_s}\right)\left(\frac{1}{2a_1} + \frac{1}{2a_2} - \frac{1}{r}\right) \tag{23}$$

In equation (23), a_1 and a_2 are the molecular radii of the reactants and r the internuclear separation between them. For a self-exchange reaction where there is no change in coordination number, $a_1 \approx a_2 = a$, and if it is assumed that electron transfer occurs between the reactants in close contact, $a_1 + a_2 = r$ which leads to equation (24). Equations (23) and (24) neglect specific contributions from individual solvent molecules such as hydrogen bonding and, also, possible 'dielectric saturation' effects that may arise because of restricted rotations of solvent dipoles in the near vicinity of the electrostatic fields of the ions.

$$\lambda_0 = e^2\left(\frac{1}{D_{op}} - \frac{1}{D_s}\right)\left(\frac{1}{2a}\right) \tag{24}$$

As derived, λ_0 is a free energy change and so it includes entropic contributions which may arise, for example, from changes in the number of solvent orientational states before and after electron transfer occurs. In the dielectric continuum approximation, entropic effects are included through the temperature dependencies of the macroscopic dielectric quantities D_{op} and D_s.

As discussed in a later section, the expression for λ_0 was derived using a thermodynamic approach. The key to the derivation is the calculation of the difference in the energy of interaction of the solvent with the reactants when: (1) the solvent is at equilibrium with the charge distribution of the reactants, and (2) the solvent assumes the dipole orientations appropriate for electron transfer to occur.

The expression for λ_0 in equation (23) gives the free energy difference between the reactants (D, A) and products (D^+, A^-) with the orientational part of the solvent polarization field remaining that appropriate for the charge distribution of the reactants. Because of the difference in timescales involved, the electronic part of the solvent polarization is assumed to remain in equilibrium with the change in charge distribution associated with the electron transfer. In fact as an energy quantity

λ_0, or rather the internal energy part of λ_0, gives the solvent contribution to the energy of the optical transition,

$$\mathrm{D}, \mathrm{A} \xrightarrow{h\nu} \mathrm{D}^+, \mathrm{A}^- \qquad \text{(note for example equations 8 and 9)}$$

Because of the short timescale for the optical transition, solvent dipole orientations in the initially formed excited state are the same as in the ground state and there is no entropic change. For a self-exchange reaction, the contribution to ΔG^* is $\lambda_0/4$ as noted above.

7.2.4.2 Quantum Mechanics: Time Dependent Perturbation Theory

A more complete accounting of electron transfer is available from quantum mechanics and time dependent perturbation theory.[25,32b,36–43] A beginning to the insight that quantum mechanics brings to the role of the trapping vibrations can be gleaned from Figure 3. Figure 3 is taken from Figure 1 but also includes the vibrational energy levels and wavefunctions for the trapping vibration as well as the potential functions. The vibrational wavefunctions χ_v and $\chi_{v'}$ are complex functions of Q, the vibrational frequency ν, the reduced mass M, and the vibrational quantum number v.[44] Integrals of the type $\langle \chi_v | \chi_{v'} \rangle = \int \chi_v \chi_{v'} \mathrm{d}Q'$, where the integration is over the normal coordinate Q', give the probability distribution of the nuclear coordinates in a given vibrational level v. The probability distributions become more nearly classical for high values of v since then the squares of the amplitudes of the vibrational wavefunctions approach the sides of the potential curve.

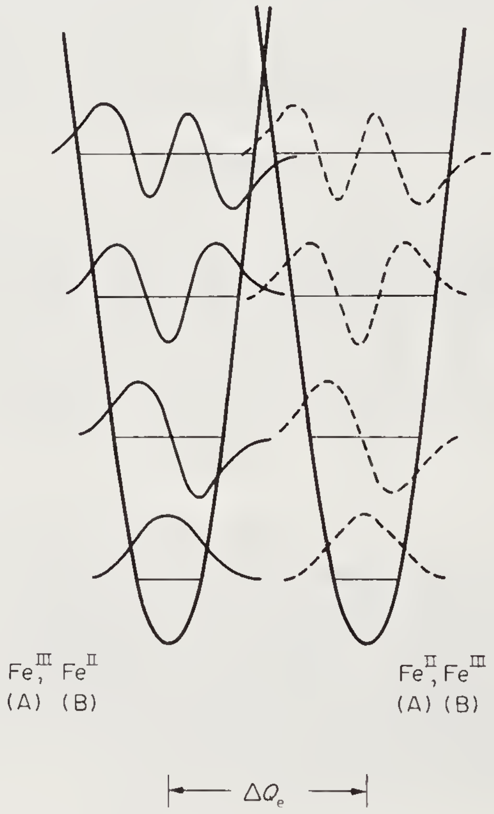

Figure 3. Potential energy-coordinate curve as in Figure 1 but illustrating vibrational energy levels and wavefunctions, χ_v

In one quantum mechanical approach based on the 'diabatic approximation', the electron is assumed to be confined initially at one of the reactant sites and electron transfer is treated as a transition between the vibrational levels of the reactants to those of the products. The quantum mechanical treatment begins with the time dependent Schrödinger equation, $H\psi = -i\hbar\delta\psi|\delta t$, where the wavefunction ψ is written as a sum of the initial (reactant) and final (product) states. In the limit that the Born–Oppenheimer approximation for the separation of electronic and nuclear motion is valid, the time dependent Schrödinger equation eventually leads to the 'Golden Rule' result in equation (25).

$$k_{j\to k} = \frac{2\pi V^2}{\hbar} \langle X_j{}^{\mathrm{R}} | X_k{}^{\mathrm{P}} \rangle^2 \rho_{jk} \tag{25}$$

Equation (25) gives the rate constant for electron transfer between a pair of reactants for which the levels of the various normal modes occupied are specified by $\mathrm{X}_j{}^{\mathrm{R}} = \chi_{v_1}\chi_{v_2}\ldots$ to give products having the distribution $\mathrm{X}_k{}^{\mathrm{P}} = \chi_{v'_1 v'_2}\ldots$; v_1 specifies the quantum level occupied in normal mode

1 in the vibrational distribution of the reactants, v'_1 the level occupied in the distribution of the products and so on.

The magnitude of the rate constant is determined by the product of three factors. The first contains the electronic coupling term V. The second is the product of a series of vibrational overlap integrals, $\langle \chi_{v_1} | \chi_{v_1'} \rangle \langle \chi_{v_2} | \chi_{v_2'} \rangle \ldots$, where the integrations are over the normal coordinates $Q_1, Q_2, \ldots$. The third, ρ_{jk}, is the number of vibrational levels in X_k at the same energy as X_j. ρ_{jk} includes energy conservation since $\rho_{jk} = 0$ unless the total energy of the system is the same before and after electron transfer, $E_j = (v_1 + \frac{1}{2})h\nu_1 + (v_2 + \frac{1}{2})h\nu_2 + \ldots = E_k = (v_1' + \frac{1}{2})h\nu_1 + (v_2' + \frac{1}{2})h\nu_2 + \ldots$. Statistical effects are also included in ρ_{jk} if there are degeneracies in X_k.

The vibrational overlap integrals play a key role in electron transfer. A region of vibrational overlap defines values of the normal coordinate where a finite probability exists for finding coordinates appropriate for both reactants and products. The greater the overlap, the greater the transition rate. The vibrational overlap integrals can be evaluated explicitly for harmonic oscillator wavefunctions. An example is shown in equation (26) for the overlap between an initial level with vibrational quantum number $v = 0$ to a level $v = v'$ where the frequency (and force constant) are taken to be the same before and after electron transfer.

$$\langle \chi_0 | \chi_{v'} \rangle = e^{-S/2} \left(\frac{S^{v'}}{v'!} \right)^{1/2} \tag{26}$$

Introduced in equation (26) is a new parameter S which is related to the reduced mass M, the angular frequency ($\omega = 2\pi\nu$), and the change in equilibrium normal coordinate between reactants and products by $S = \frac{1}{2}(M\omega/\hbar)(\Delta Q_e)^2$. In the solid state physics literature, S is often called the 'electron–phonon' coupling constant since it is a measure of the degree of the structural change induced by the change in electron content at the different redox sites. Other useful relationships include $S\hbar\omega = \frac{1}{2}k(\Delta Q_e)^2$ and $k = M\omega^2$, where k is the force constant for the vibration.

Returning to equation (25), evaluation of the total vibrational overlap integral, $\langle X_i | X_j \rangle$, is less formidable than it appears. The vibrational wavefunctions are a complete orthonormal set for which $\langle \chi_v | \chi_{v'} \rangle = \delta_{vv'}$, where δ is the Kronecker delta. For the vast majority of normal modes, S (and $\Delta Q_e) = 0$. For these modes the vibrational overlap integrals become $\langle \chi_v | \chi_{v'} \rangle = 1$ if $v = v'$, and $\langle \chi_v | \chi_{v'} \rangle = 0$ if $v \neq v'$. Except for the requirement that the vibrational quantum number must be the same before and after electron transfer, these modes play no role in electron transfer and can be neglected. The only significant contributions to the electron transfer rate constant come from the 'trapping vibrations' for which S (and $\Delta Q_e) \neq 0$. (Contributions also exist from modes for which there is a change in vibrational frequency, $v \neq v'$, even when $S = 0$, but these contributions are usually negligible.)[44,45]

Note that a temperature dependence for electron transfer is predicted from equation (25) and Figure 3. At higher temperatures a greater population in levels of trapping modes near the intersection region should exist and, from Figure 3, vibrational overlaps increase as the intersection region is approached. On the other hand, there are finite vibrational overlaps even for levels low in the potential curves. This leads the quantum mechanical treatment to predict that electron transfer can occur even at very low temperatures where the population of levels near the intersection region is essentially zero even though electron transfer is forbidden by energy conservation in the classical limit. As noted in a later section, contributions to electron transfer from vibrational levels below the intersection region are often referred to as 'nuclear tunneling' in the electron transfer literature.

The expression in equation (25) gives the rate constant for electron transfer from a particular vibrational distribution of the reactants to a particular distribution of the products. In order to calculate the *total* electron transfer rate constant it is necessary to include two additional features. One is all possible transitions from a particular vibrational distribution of the reactants to all of the possible vibrational distributions of the products. In addition, it is necessary to recognize that a statistical distribution exists in solution amongst the various vibrational distributions of the reactants. The total transition rate will include contributions from each distribution of the reactants to all distributions of the products.

The contribution to the total electron transfer rate from a single vibrational distribution of the reactants, j, is given by: (1) summing over the transition rates from j to each of the product vibrational distributions k, $\Sigma_k k_{jk}$, and (2) multiplying $\Sigma_k k_{jk}$ by the fraction of reactant pairs which are actually in distribution j, p_j. The result is $p_j \Sigma_k k_{kj}$, which is the fraction of total electron transfer events that occur through distribution j. Recall that for a harmonic oscillator normal mode the fractional population in a specific vibrational level j is given as a function of temperature by equation (27). The sum in the denominator of equation (27) is the partition function for the vibration.

$$p_j = \frac{\exp-(v_1+\frac{1}{2})\hbar\nu/k_BT}{\sum\limits_j \exp-(v_1+\frac{1}{2})\hbar\nu/k_BT} = \sum \frac{\exp-(v_1 h\nu/k_BT)}{1-\exp-(h\nu/k_BT)} \tag{27}$$

In order to complete the calculation and obtain the total rate constant, k_{et}, it is necessary to sum over all of the contributions from all of the vibrational distributions of the reactants *j*. The final result is shown in equation (28).

$$k_{et} = \sum_j p_j \sum_k k_{j\rightarrow k} \tag{28}$$

Although mathematically overwhelming in its full glory, there are some redeeming features to equation (28): (1) only the trapping vibrations are included in the sums; (2) except for V, from the mathematical form of the vibrational overlap integrals, *e.g.* equation (26), k_{et} is calculable from structural changes (S) and the properties of the vibrations (M, ν) that interconvert them; (3) computer-based calculations make the evaluation of the overlap integrals relatively straightforward; (4) reasonably accurate, closed form expressions have been derived to take the place of the summations — an example is shown in equation (28a) which gives the contribution to intramolecular trapping by a single trapping vibration;[36] and (5) perhaps best of all, in many cases the significant trapping vibrations are low-frequency skeletal modes as in $Fe(H_2O)_6^{3+/2+}$ self-exchange. Calculations show that at or near room temperature and if S is large, the contribution to electron transfer by low frequency modes is dominated by vibrational levels near the intersection region. Even the approximate, classical equations, *e.g.* equations (16) and (16a), give nearly the right answer.[31]

$$S\hbar\omega\left(\frac{4k_BT}{\hbar\omega}\right)\tanh\left(\frac{\hbar\omega}{4k_BT}\right) \tag{28a}$$

In the classical limit, the equation for k_{et} takes on the relatively simple form shown in equation (29). In equation (29), both intramolecular (λ_i) and solvent (λ_0) contributions are included. λ_i was defined in equation (22) and λ_0 in equation (23) in the dielectric continuum limit.

$$k_{et} = \frac{2\pi V^2}{h}\left[\frac{\pi}{(\lambda_i+\lambda_0)RT}\right]^{1/2} \exp-\left[(\lambda_i+\lambda_0)/4RT\right] \tag{29}$$

The expressions for k_{et} in equations (29) and (30) are the products of two factors: (1) an exponential term which, assuming a common force constant, gives the fractional population of reactants at temperature T with vibrational distributions at the intersection regions for each of the trapping vibrations, and (2) a pre-exponential term ν_e, the 'electron transfer frequency'; ν_e is defined in equation (31).

$$k_{et} = \nu_e \exp-(\lambda/4RT) \tag{30}$$

$$\nu_e = \frac{2\pi V^2}{h}\left(\frac{\pi}{\lambda RT}\right)^{1/2} \tag{31}$$

The expression for k_{et} in equation (29) is still not a complete expression for the total electron transfer rate constant. Both the electronic coupling term V and λ_0 are dependent upon the inter-reactant separation distance r, and, therefore, so is k_{et} in equation (29). The dependence of λ_0 on r is shown in equation (23) in the dielectric continuum limit. The magnitude of V depends upon the extent of donor–acceptor electronic orbital overlap (equation 17) and the electronic wavefunctions fall off exponentially from the centers of the reactants. In order to make comparisons between k_{et} and experimental values of electron transfer rate constants, it is necessary to include the dependence of k_{et} on r as discussed in a later section.

In principle, solvent trapping is also included in the vibrational overlap intergral in equation (25). As noted above, the solvent dipole reorientational motions associated with solvent trapping can be treated as a series of collective vibrations of the medium using approaches devised for treating the collective vibrations of ions or atoms that occur in a crystalline lattice.[32,33] However, the problem is mathematically intractable because of the many solvent molecules involved which lead to many 'normal modes' and the existence of a near continuum of energy levels. In addition, there is an absence of well-defined structural information concerning the fluid state. In practice, the contribution from solvent is usually treated as a single, averaged normal mode and, using a series of approximations, an expression can be obtained for λ_0 which is very similar to the dielectric continuum result in equation (23).[32]

7.2.4.3 Tunneling

Tunneling is a term often associated with electron transfer. It arises from the wave–particle duality inherent in quantum mechanics. For example, solution of the Schrödinger equation for a crystal of N atoms using the harmonic oscillator approximation gives rise to a series of $3N$ normal coordinates each with its characteristic frequency $\nu_1, \nu_2, \ldots \nu_{3N}$. The total accessible vibrational energy levels in the crystal are given by $E = 3N\Sigma_j(v_j + \frac{1}{2})h\nu_j$. Alternatively, E can be interpreted as the energy of a system of independent particles of energies $h\nu_1, h\nu_2, \ldots h\nu_{3N}$. The particles or 'phonons' are essentially quanta of lattice vibrations just as 'photons' are quanta of electromagnetic radiation. In the solid state physics literature, rather than treating vibrations as waves and being concerned with the overlap of wavefunctions, the particle description is adopted and calculations made for the *rate of 'tunneling' of a vibrational particle or phonon between two potential curves.* Although the two different approaches give mathematically equivalent results,[47] the underlying physical descriptions are quite different.

By the same token, electron transfer involves transfer of a particle between electronically coupled chemical sites and can be described as a tunneling process. In that sense, every electron transfer process involves electron tunneling with a tunneling frequency given, in the classical limit, by equation (31).

In the electron transfer literature it has become common to describe electron transfer reactions that occur through vibrational distributions below the intersection as having occurred by 'nuclear tunneling' and the actual electron hopping event as 'electron tunneling'.

7.2.5 RATE CONSTANT EXPRESSIONS FOR ELECTRON TRANSFER

The rate constant expression in equation (18) derived by Marcus is complete in the sense that it includes a pre-association between reactants, a time dependence arising from the frequency with which the reactants collide, and the thermal activation required for electron transfer to occur. On the other hand, the quantum mechanically derived expressions for k_{et} are dependent upon the interreactant separation, and the dependence on V must be included explicitly.

7.2.5.1 Distance Dependence

As noted above, inherent in the expressions derived for k_{et} in the previous section is the assumption that the internuclear separation between reactants, r, is fixed. In fact, k_{et} has a dependence on r, $k_{et} = k_{et}(r)$, arising from solvent trapping (equation 23), and a much stronger dependence on r through the electronic coupling integral V.

For an outer-sphere reaction, given the translation mobility of the reactants, electron transfer may occur over a range of distances. The problem can be treated in a general way since from statistical mechanics the equilibrium distribution of internuclear separations can be calculated based on pairwise distribution functions. Integration of the product of the distribution function and $k_{et}(r)$ over all space gives the total rate constant k_{et}.[32b,48]

In fact, given the distance dependencies of λ_0 and V, electron transfer is expected to be dominated by reactants in close contact. In that limit the experimentally observed rate constant is related to k_{et} and the association constant between reactants, K_A, as in equation (32). K_A can be estimated for spherical reactants, using the Eigen–Fuoss result in equation (33). The electrostatic term, w_R, was defined in equations (19) and (20).

$$k_{obs} = K_A k_{et} \tag{32}$$

$$K_A = \frac{4\pi N r^3}{3000} \exp -(w_R/RT) \tag{33}$$

Equation (33) is only an approximation for real molecules in that it assumes both a single value for r and structureless, spherical reactants. In fact, it has been suggested for $Fe(H_2O)_6^{3+/2+}$ self-exchange that a significant feature of the reaction may be the interpenetration of the coordination spheres in order to enhance electronic orbital overlap.[12] In addition, for low-symmetry cases, electronic coupling can have an angular dependence if rotational correlation times within the association complex are long compared with the average lifetime of an average complex. Such effects may be important in metalloprotein reactions, *e.g.* in cytochrome *c* self-exchange where electron transfer appears to occur predominantly within a relatively small surface area of 'active site'.[27] For such cases a steric factor needs to be included in equation (32) in order to account for the orientational demands imposed by orbital overlap within the association complex.

7.2.5.2 The Diffusion Controlled Limit

If electron transfer is dominated in fluid solution by reactants in close contact, those in close contact are quickly depleted and their statistical population is brought back to the equilibrium level by diffusion together of the reactants. As long as the timescale for the diffusional process is short compared with that for electron transfer, the equilibrium statistical distribution is maintained, equation (32) is valid, and the electron transfer rate constant is the product of k_{et} and K_A or, as defined by Marcus, is given by equation (18). However, if the electron transfer process is sufficiently rapid, statistical equilibrium is not reached and the experimentally observed rate constant will include a contribution from the diffusion together of the reactants. When that situation exists, the experimentally observed rate constant k_{obs} is given by equation (34) where k_D is the diffusion limited rate constant,[49–51] and k_{act} is either $K_A k_{et}$ or given by equation (18).[49]

$$\frac{1}{k_{obs}} = \frac{1}{k_D} + \frac{1}{k_{act}} \tag{34}$$

Diffusion controlled rate constants for spherical reactants can be calculated from the Debye–Smoluchowski equation (35), in which η is the viscosity of the solvent, a_D and a_A are the radii of the reactants and w was defined in equations (19) and (20). To put numbers into perspective, using equation (35) and assuming that $a_D = a_A = 6$ Å for +1 and +2 charged reactants, $k_D = 2 \times 10^{10}$ M^{-1} s^{-1} in pure acetonitrile and 5×10^9 M^{-1} s^{-1} in an acetonitrile solution with $\mu = 0.1$ M.

$$k_D = \left(\frac{2RT}{3000\eta}\right)\left(2 + \frac{a_D}{a_A} + \frac{a_A}{a_D}\right)\frac{w/RT}{e^{w/RT}-1} \tag{35}$$

7.2.5.3 Time Dependence: Frequency Factors

The derivation of equations like (29) and (30) for k_{et} relies on the use of equilibrium statistical mechanics to calculate statistical populations amongst various vibrational distributions. Electron transfer is assumed to be a slow process on the timescale for vibrational equilibration. In that limit, electron transfer occurs occasionally from a vibrational distribution of the reactants to a vibrational distribution of the products and the population of the initial distribution is rapidly re-established. However, for vibrational levels near the intersection region, this assumption may not be valid and, in general, it may not be valid for any case where electronic coupling is significant.

Timescales for transitions between vibrational levels in solution can be estimated from the band widths of IR bands if it is assumed that the origin of the broadening is by deactivation of the vibrational excited state by collisions with surrounding solvent molecules. For IR band widths in the range $1-10\ \mathrm{cm}^{-1}$, τ is in the range 0.5–5 ps ($0.5-5\times10^{-12}$ s). Estimates of 0.1–10 ps for the transitions between different orientations of solvent dipoles in solution can also be be made, for example, from frequency dependent dielectric loss measurements.[52] From equations (30) and (31) the electron transfer rate for vibrational distributions at the intersection region is given by $\nu_e = (2\pi V^2/h)(\pi/\lambda RT)^{1/2}$. If V is appreciable and/or λ relatively small, the timescale for electron hopping, τ_e ($=1/\nu_e$), may approach and even become shorter than the timescale for the nuclear motions associated with vibrational and solvent trapping, τ_n.

In order to explore this point, it is necessary to have estimates for the magnitude of V. One approach to estimating V is based on the integrated intensity of absorption bands for optically induced electron transfer as for the transition illustrated in equation (9).[16] From this type of analysis $V \approx 120\ \mathrm{cm}^{-1}$ for the particular case shown in equation (9).[15] A second approach to estimating V, which is purely theoretical and based on orbital overlap calculations, typically gives values in the range 100–200 cm^{-1} for outer-sphere reactions.[12,36,37]

Using $V = 100\ \mathrm{cm}^{-1}$ (0.012 eV) and $\lambda = 1$ eV, which are reasonable parameters for a moderately rapid self-exchange reaction, $\tau_e = 1/\nu_e = 6\times10^{-14}$ s (0.06 ps). ν_{et} was calculated using the pre-exponential term in equation (30). This calculation suggests that for reactions at room temperature which are dominated by transitions near the intersection region, $\tau_e < \tau_n$ and the assumption that $\tau_e \gg \tau_n$ is not justified.

Equation (36), which attempts to include both τ_n and τ_e, has been proposed as a more general expression for k_{et}.[48] Note that in the limit, when $\tau_e \ll \tau_n$, the expression for the electron transfer rate constant (equation 37) no longer depends on the extent of electronic coupling since $\nu_{et} \gg \nu_n$. In this limit the rate constant for electron transfer for a vibrational distribution near the intersection region is dictated by rates of repopulation of those intramolecular and/or solvent modes which cause the trapping of the exchanging electron.

$$k_{et} = \frac{\exp(-\lambda/4RT)}{2(\tau_e + \tau_n)} = \nu_{et} \exp -(\lambda/4RT) \tag{36}$$

$$k_{et} = \nu_n \exp -(\lambda/4RT) \tag{37}$$

7.2.5.4 Adiabatic and Non-adiabatic Electron Transfer

There is an alternate approach to introducing the time dependence into electron transfer which is based on the adiabatic approximation. In the adiabatic approximation the effect of electronic coupling on the potential curves (Figure 1b) is included from the beginning. The emphasis is on calculating the time dependence of the redistribution of electron density within the ground state, $\mathrm{D{-}A \rightleftharpoons D^+{-}A^-}$, rather than calculating the transition rate between weakly perturbed but isolated chemical sites D and A. Returning to the particle description for the trapping vibrations, but in the classical limit, the time dependence enters as the velocity with which a vibrational 'particle' or phonon approaches the intersection region. As the particle approaches the intersection region in Figure 1b it can continue on to the upper potential curve of the higher state or cross the barrier to achieve electron transfer. The probability of barrier crossing is related to the 'electronic transmission coefficient', κ_e, through the velocity of the nuclear motion, the slopes of the intersecting potential curves, and the splitting between potential curves. Based on some rather severe approximations,[31] κ_e is given by equation (38) and ν_{et} by equation (39). In the two equations ν_n is the frequency of a trapping vibration or solvent reorientation or an averaged frequency for all of the contributors to trapping.[31,36,37]

$$\kappa_e = \frac{2[1 - \exp(-\nu_e/2\nu_n)]}{2 - \exp(-\nu_e/2\nu_n)} \tag{38}$$

$$\nu_{et} = \nu_n \kappa_e \tag{39}$$

The expression for κ_e includes a rather elaborate correction for reversibility. It takes into account the fact that in the intersection region, there is no vibrational trapping. Electron transfer can occur back and forth between redox sites until vibrational redistribution removes the system from the intersection region.

Reversibility is not a problem in the limit that $\nu_e \ll \nu_n$. If the electron transfer frequency is slow relative to the rate of vibrational redistribution, the vibrational distribution at the intersection region will change *before* back electron transfer can occur.

Returning to equation (38), in the limit that $\nu_e \gg \nu_n$, $\kappa_e = 1$ and $\nu_{et} = \nu_n$. Electron transfer reactions that fall into this domain where the probability of electron transfer is unity in the intersection region have been called 'adiabatic' by Marcus. Reactions for which $\kappa_{el} < 1$, have been called 'non-adiabatic'. In the limit that $\nu_e \ll 2\nu_n$ and $\kappa_e = \nu_e/\nu_n$, the pre-exponential term for electron transfer is given by $\nu_{et} = \nu_e$. This was the limit assumed in the quantum mechanical treatment using time dependent perturbation theory.

The use of the terms adiabatic and non-adiabatic in this way leads to a source of confusion. Normally, in describing surface-crossing processes, a process which remains on the same potential curve is called adiabatic and in that sense every *net* electron transfer reaction is an adiabatic process. Processes which involve a transition between different states as between the two different potential curves in Figure 1b are usually called non-adiabatic. Such processes have some special features and will be returned to in a later section dealing with the 'inverted region' and excited state decay.

7.2.6 ACCOUNTING FOR SELF-EXCHANGE RATE CONSTANTS

The results of the theoretical analysis outlined above provide a deep and intuitively satisfying view of the electron transfer process and provide a quantitative basis for accounting for the magnitudes of electron transfer rate constants. Before applying the results to the experimental data in Table 1, it is necessary to remind ourselves of the limitations and approximations upon which the theory was based and to consider how comparisons between theory and experiment are to be made.

First, with regard to approximations and limitations: (1) it is difficult to obtain the magnitude of the electronic coupling term V especially in low-symmetry cases where electronic steric effects may exist; (2) the pre-exponential term ν_{et} is not well defined in the domain $\tau_e \approx \tau_n$; (3) the dielectric continuum model for the solvent neglects such specific interactions as hydrogen bonding or non-classical, relatively high-frequency collective modes; and (4) the approximate equations which assume the classical limit will not apply if there are high-frequency trapping vibrations nor will they apply at low temperatures where transitions from vibrational distributions well below the intersection region are important.

The equation for k_{obs} derived by Marcus (equation 18) is essentially equivalent to the quantum mechanical result in the classical limit (equation 30). If equation (23) is used for λ_0 assuming a dielectric continuum, the quantum mechanical result is given by equation (40) where $4\Delta G^* = \lambda_i + \lambda_0$.

$$k_{obs} = \nu_{et} K_A \exp -(\lambda/4RT) = \nu_{et} K_A \exp -(\Delta G^*/RT) \tag{40}$$

The difference between the two results is in the pre-exponential term. In the quantum mechanical treatments either $\nu_{et} = \nu_n \kappa_e$ or $\nu_{et} = 0.5(\tau_n + \tau_e)^{-1}$ depending on the model adopted. In the Marcus equation the pre-exponential term is $Z\kappa_e \exp(-w_R/RT)$ and the time dependence is introduced through the collision frequency, Z. In any case, in the non-adiabatic limit, $\nu_e < \nu_n$, and k_{obs} is given by equation (41). In the adiabatic limit, $\nu_e > \nu_n$ and k_{obs} is given by equation (42), with ν_n in the range $10^{11}-10^{13}$ s^{-1}.

$$k_{obs} = \nu_e K_A \exp -(\Delta G^*/RT) \tag{41}$$

$$k_{obs} = \nu_n K_A \exp -(\Delta G^*/RT) \tag{42}$$

The quantum mechanical result predicts a complex temperature dependence for k_{obs} arising from the statistical population factors in equation (28). However, in the limit that the classical approximation works reasonably well, and assuming that the temperature dependence of ν_{et} is negligible, k_{obs} is predicted to vary with T as shown in equation (43).

$$k_{obs} = \nu_{et} \exp -(\Delta H_A/RT) \exp (\Delta S_A/R) \exp - (\Delta H^*/RT) \exp (\Delta S^*/R) \tag{43}$$

Equation (43) includes temperature dependent contributions from both K_A and k_{et}. ΔH_A and ΔS_A are the enthalpy and entropy changes associated with the pre-association step and ΔH^* and ΔS^* are the enthalpic and entropic components of ΔG^*.

The experimentally observable kinetic quantities $\Delta H_{obs}{}^*$ and $\Delta S_{obs}{}^*$ obtained from the slopes and intercepts of plots of k_{obs} *vs.* $1/T$ are related to the microscopic quantities in equation (43) as shown in equation (44). Similarly, the enthalpies and entropies of activation from reaction rate theory are related to the experimental quantities as shown in equation (45).

$$\begin{aligned} \Delta H^*_{obs} &\fallingdotseq \Delta H_A + \Delta H^* \\ \Delta S^*_{obs} &= (\Delta S_A + \Delta S^*) + \ln \nu_{et} \end{aligned} \tag{44}$$

$$\Delta H^{\ddagger} = \Delta H_A + \Delta H^* - RT = \Delta H^*_{obs} - RT$$

$$\Delta G^{\ddagger} = \Delta G_A + \Delta G^* + RT \ln (k_B T/h\nu_{et}) = \Delta G^*_{obs} + RT \ln (k_B T/h\nu_{et}) \tag{45}$$

7.2.6.1 Calculation of Rate Constants

Table 2 Calculated[a] and Observed Electron Transfer Rate Constants in Water at 25 °C

Reaction	r (Å)	ΔQ_e (Å)	κ_e	$\nu_n K_A$ (M^{-1} s^{-1})	κ_n	k_{calc} (M^{-1} s^{-1})	k_{obs} (M^{-1} s^{-1})
$Fe(H_2O)_6{}^{3+/2+}$	6.5	0.14	10^{-2}	2×10^{11}	2×10^{-11}	3×10^{-2}	4.2
	5.25	0.14	0.2[b]	4×10^{10}	3×10^{-10}	2[b]	—
$Ru(NH_3)_6{}^{3+/2+}$	6.7	0.04	0.2	3×10^{10}	4×10^{-6}	2×10^{4}	3×10^{3}
$Ru(bipy)_3{}^{3+/2+}$	13.6	~0	~1	3×10^{11}	4×10^{-3}	1×10^{9}	4×10^{8}
$Co(NH_3)_6{}^{3+/2+}$	6.6	0.22	$\geqslant 10^{-3}$	3×10^{11}	1×10^{-17}	4×10^{-9}	$\geqslant 10^{-7}$
$Co(bipy)_3{}^{3+/2+}$	13.6	0.19	$\geqslant 10^{-2}$	3×10^{12}	4×10^{-12}	0.2	18

[a] $k_{calc} = (\nu_n \kappa_e) K_A \kappa_n$. The various terms are described in the text. κ_n includes contributions from both solvent and vibrational trapping vibrations using equation (23) for λ_0 and the quantum mechanical result in equation (29) for the metal–ligand stretching modes.

[b] Calculated assuming interpenetration of the inner coordination spheres to r = 5.25 Å past the spherical close contact distance of 6.5 Å.

The most striking application of electron transfer theory has been to the direct calculation of electron transfer rate constants for a series of metal complex couples.[36,37,46] The results of several such calculations taken from ref. 37b are summarized in Table 2. The calculations were made based on internuclear separations appropriate to the reactants in close contact except for the second entry for $Fe(H_2O)_6^{3+/2+}$, where at $r = 5.25$ Å there is significant interpenetration of the inner coordination spheres. The κ_e values are based on *ab initio* calculations of the extent of electronic coupling. κ_n includes the total contributions to electron transfer from solvent and the trapping vibrations using the dielectric continuum result for λ_0, the quantum mechanical result for intramolecular vibrations, and known bond distance changes from measurements in the solid state or in solution.

7.2.6.2 Comparisons

The agreement between the calculated and observed results in Table 2 is quite remarkable and provides strong confirmatory evidence for the validity of the overall theoretical approach. In addition, the quantitative partitioning of the rate constant into its various components is most revealing as to the factors that dictate rates of electron transfer and leads to a basis for discussing the variations in self-exchange rate constants in Table 1.

7.2.6.2.1 Rate constant variations: diffusional effects

Contributions to k_{obs} from diffusional effects are only numerically significant for reactions which approach within a factor of ~10 of the diffusion-controlled limit. From the data in Table 1, only a few self-exchange cases, *e.g.* $Ru(bipy)_3^{3+/2+}$ and some of the organic couples, approach this limit although it is a common feature for net reactions where ΔG is highly favorable and λ small.

7.2.6.2.2 Preassociation

From equations (19) and (33), the magnitude of K_A depends on the sizes and charges of the reactants and on the static dielectric constant and ionic strength of the surrounding medium. Variations in k_{obs} of more than an order of magnitude can arise through K_A in comparing small, highly charged ions with ions of larger molecular dimensions. Note the $\nu_n K_A$ values in Table 2. For net reactions involving ions of different charge types, K_A can make a sizeable contribution to k_{obs}. For example, for the reaction $Ru(NH_3)_5py^{3+} + Fe(CN)_6^{4-} \rightarrow Ru(NH_3)_5py^{2+} + Fe(CN)_6^{3-}$, $K_A = 2.4 \times 10^3$ and $k_{obs} = 4.3 \times 10^6$ M^{-1} s^{-1} at 25 °C.[55]

7.2.6.2.3 Electronic coupling

The lack of structural definition inherent in an outer-sphere reaction makes the problem of calculating or measuring V difficult. However, electronic coupling is expected to be relatively weak since it must occur through space and not by orbital mixing through a bridging ligand. This point has been studied in detail by *ab initio* calculations for $Fe(H_2O)_6^{3+/2+}$ exchange.[12] If close contact between the ions is assumed, $\nu_e \ll \nu_n$ ($\kappa_e = 10^{-2}$) and the reaction is non-adiabatic. However, if interpenetration of the inner coordination spheres to 5.25 Å is considered, κ_e increases to 0.2.

The $Ru(bipy)_3^{3+/2+}$ self-exchange reaction with $\kappa_e \approx 1$ illustrates an important point with regard to the orbital composition of the donor and acceptor orbitals involved in the electron transfer process. Electron transfer occurs between Ru^{II} and Ru^{III} having the nominal electronic configurations $(4d\pi)^6$ and $(4d\pi)^5$. Given the large internuclear separation, $r = 13-14$ Å, direct orbital overlap between pure $4d\pi$ orbitals is very small. However, the actual orbitals involved in electron transfer are molecular orbitals which are significantly mixed with low-lying π and/or π^* orbitals of the bipyridyl ligands. The effect of metal–ligand mixing is to carry the radial character of the redox orbitals to the periphery of the complexes where overlap is greatly enhanced. Such metal–ligand delocalization effects may be small and $\kappa_e < 1$ for classical complexes of the first transition series and the lanthanides where metal-ligand mixing is small. However, for organometallics, clusters, or organic couples, delocalization is expected to lead to extensive orbital redox character on the peripheries of the reactants and $\kappa_e \approx 1$.

For $Co(NH_3)_6^{3+/2+}$ self-exchange (equation 46), κ_e is small and the reaction non-adiabatic. The major contributor to the decreased magnitude for κ_e is the fact that changes in oxidation state at cobalt not only cause significant changes in molecular structure but also a change in spin state from high-spin Co^{II} ($t_{2g}{}^5 e_g{}^2$) to low-spin Co^{III} ($t_{2g}{}^6$).

$$\underset{{}^1A_{1g}(t_{2g}{}^6)}{\overset{\text{A}}{\text{Co(NH}_3)_6{}^{3+}}} + \underset{{}^4T_{1g}(t_{2g}{}^5e_g{}^2)}{\overset{\text{B}}{\text{Co(NH}_3)_6{}^{2+}}} \longrightarrow \underset{{}^4T_{1g}(t_{2g}{}^5e_g{}^2)}{\overset{\text{A}}{\text{Co(NH}_3)_6{}^{2+}}} + \underset{{}^1A_{1g}(t_{2g}{}^6)}{\overset{\text{B}}{\text{Co(NH}_3)_6{}^{3+}}} \qquad (46)$$

Spin effects have their origin in V. If it is assumed that there is no coupling between orbital and spin character, the wavefunctions that appear in equation (17) for V become simple products of orbital and spin components $\psi = \psi_{\text{el}}\psi_{\text{spin}}$. Recall, for example, that the spin wave function for a doubly occupied orbital is $(1/\sqrt{2})[\alpha(1)\beta(2) - \beta(1)\alpha(2)]$ where α and β refer to upwards or downwards spin, the labels are with respect to the two electrons, and $1/\sqrt{2}$ is a normalization constant.

Since the operator $\hat{V}$ does not include spin coordinates, V is given by equation (47) where ψ and ψ' refer to the reactants and products, respectively.

$$V = \langle\psi_{\text{el}}|\hat{V}|\psi'_{\text{el}}\rangle\langle\psi_{\text{spin}}|\psi'_{\text{spin}}\rangle \qquad (47)$$

In order for V to be nonzero, it is necessary that the integration over spin contains at least one nonzero component. Without elaborating on the details, this will only be the case if the change in spin at each redox site is $\Delta S = \pm\frac{1}{2}$ as would be the case, for example, for $\text{Ru(NH}_3)_6{}^{3+/2+}$ self-exchange (equation 47a).

$$\underset{(t_{2g}{}^5)}{\text{Ru(NH}_3)_6{}^{3+}} + \underset{(t_{2g}{}^6)}{\text{Ru(NH}_3)_6{}^{2+}} \rightarrow \underset{(t_{2g}{}^6)}{\text{Ru(NH}_3)_6{}^{2+}} + \underset{(t_{2g}{}^5)}{\text{Ru(NH}_3)_6{}^{3+}} \qquad (47a)$$

A possibility that has been suggested for the $\text{Co(NH}_3)_6{}^{3+/2+}$ reaction is that it could occur *via* initial thermal population of electronic excited states (equation 48a) followed by electron transfer between e_g orbitals on Co^{II} and Co^{III} (equation 48b) followed by decay of $\text{Co(NH}_3)_6{}^{2+*}$ $({}^2E_g)$ to the ground state.

$$\text{Co(NH}_3)_6{}^{2+}\ {}^4T_{1g}(t_{2g}{}^5e_g{}^2) \rightarrow \text{Co(NH}_3)_6{}^{2+*}\ {}^2E_g(t_{2g}{}^6e_g{}^1) \qquad (48a)$$

$$\underset{(t_{2g}{}^6)}{\text{Co(NH}_3)_6^{3+}} + \underset{(t_{2g}{}^6e_g{}^1)}{\text{Co(NH}_3)_6{}^{2+*}} \rightarrow \underset{(t_{2g}{}^6e_g{}^1)}{\text{Co(NH}_3)_6{}^{2+*}} + \underset{(t_{2g}{}^6)}{\text{Co(NH}_3)_6{}^{3+}} \qquad (48b)$$

However, it is not necessary to invoke such pathways when spin–orbit coupling is included. The separation of spin and orbital character is only an approximation. When the effects of spin–orbit coupling are included, more appropriate wavefunctions of combined spin and orbital character can be constructed by mixing into the ground states some excited states of different spin character. As shown in equation (49), the mixing coefficients for an excited state ψ_{i}, c_{i}, depend on the magnitude of the spin-orbit coupling integral and the energy difference between the excited and ground states.

$$c_{\text{i}} = \frac{\langle\psi_{\text{i}}|\hat{H}_{\text{SO}}|\psi_{\text{g}}\rangle}{(E_{\text{i}}-E_{\text{g}})} \qquad (49)$$

For Co^{II} an important low-lying state in this regard is ${}^2E_g$ $(t_{2g}{}^6e_g{}^1)$. The magnitude of the contribution to V when the E_g state is mixed into the ${}^4T_{1g}$ ground state of Co^{II} is shown in equation (50a) where c is the mixing coefficient. In equation (50a) the superscripts A and B label the sites in equation (46).

$$\langle\psi^{\text{A}}_{A_{1g}}(\psi^{\text{B}}_{{}^4T_{1g}} + \text{C}\psi^{\text{B}}_{{}^2E_g})|\hat{V}|(\psi^{\text{A}}_{{}^4T_{1g}} + \text{C}\psi^{\text{A}}_{{}^2E_g})\psi^{\text{B}}_{{}^1A_{1g}}\rangle = c^2\langle\psi^{\text{B}}_{{}^2E_g}|\hat{V}|\psi^{\text{A}}_{{}^2E_g}\rangle \qquad (50a)$$

$$c^2\langle\psi^{\text{B}}_{{}^2E_g}|\hat{V}|\psi^{\text{A}}_{{}^2E_g}\rangle = c^2\langle d^{\text{B}}_{\sigma*}|\hat{V}|d^{\text{A}}_{\sigma*}\rangle \qquad (50b)$$

Writing the state wavefunctions in equation (50a) as products of one-electron orbitals, *e.g.* $\psi({}^2E_g) = d\pi_1{}^2d\pi_2{}^2d\pi_3{}^2d\sigma^*$, leads to equation (50b). Equation (50b) is written in terms of the actual redox orbitals involved in electron transfer and is, therefore, in the same form as equation (17) for V. The result shown in equation (50b) gives only the contribution to V from mixing ${}^2E_g$ character into the Co^{II} ground state. Important contributions to V arising from mixing into the ground states of excited states on Co^{III} and of other excited states on Co^{II} also exist.[46]

An important feature to emerge from the comparisons in Table 2 is that variations in the electronic coupling term play a relatively small role in dictating the magnitudes of self-exchange rate constants for outer-sphere reactions, at least for transition metal complexes. Even for reactions involving a spin change, spin–orbit coupling can lead to appreciable electronic coupling. For the lighter elements, where spin-orbit coupling is small, spin effects can play a far larger role.

At the other end of the scale, even relatively small values of V lead to the limit where $\nu_e > \nu_n$ and ν_{et} is dictated solely by dynamic processes associated with solvent and/or trapping vibrations.

However, in a polymer or in a biological membrane, the spatial distribution of redox sites may be relatively fixed, resulting in a loss of translational mobility. In such milieux the redox sites may be trapped at relatively long separation distances where small overlap between the donor and acceptor electronic wavefunctions is imposed even when electronic mixing with the surrounding medium or intervening chemical bridges is included. For such cases the magnitude of k_{obs} may be determined largely by the small magnitude of V or, if available, by intermolecular motions which have the effect of decreasing the internuclear separation. Given the exponential decrease with distance from the nucleus for electronic wavefunctions, V is predicted to vary with r as shown in equation (51).[56] In equation (51), V^0 is the value of V at the close contact separation distance, r_0, and B is a constant which depends on the nature of the electronic coupling.

$$V = V^0 \exp[B(r-r_0)/2] \tag{51}$$

Electron transfer over long distances has been studied using a variety of approaches. The most common has been the use of pulse radiolysis or flash photolysis to create high-energy redox distributions in frozen solutions in order to inhibit translational mobility. Following the initial light or energy pulse, 'relaxation' of the system by intra- or inter-molecular electron transfer is observed. Examples include: (1) pulse radiolytic generation of anion radicals or trapped electrons in frozen solutions containing suitable acceptors;[57,58] and (2) time resolved quenching of the metal to ligand charge transfer (MLCT) excited state of $Ru[Me_4(phen)]_3^{2+}$ by the pyridinium ion $Me^+NC_5H_4C_5H_4N^+Me$ (methyl viologen) in glycerol.[59] The results of a series of experiments of this kind suggest that the constant B in equation (51) is in the range 1.0–2.0 $Å^{-1}$.

7.2.6.2.4 *Solvent*

The solvent plays a role in determining the magnitudes of electron transfer rate constants in three ways: (1) for ionic reactants, through K_A (equation 33); (2) in general, by solvent trapping; and (3) in introducing a time dependence through the dynamics of changes in solvent dipole orientations as they appear in ν_n.

As noted in a later section, perhaps the clearest experimental confirmation of the dielectric continuum prediction for λ_0 has come from measurements on the solvent dependence of charge transfer band energies for mixed valence ions. For outer-sphere electron transfer involving charged ions the fact that both K_A and λ_0 depend on solvent make experimental tests somewhat difficult. However, for self-exchange reactions involving a neutral and a charged ion, for example $Fe(\eta^5\text{-}C_5H_5)_2^{+/0}$, there is no electrostatic contribution to K_A and k_{obs} (and λ_0) should vary with $1/D_{op} - 1/D_s$ as predicted by equation (23). This point has been tested experimentally and agreement has been found in some cases, *e.g.* $Cr(arene)_2^{+/0}$ (arene = C_6H_6, . . .)[60] and $Ru(hfac)_3^{-/0}$[61] (hfac = hexafluoroacetylacetonate), while for others, *e.g.* $Fe(\eta^5\text{-}C_5H_5)_2^{+/0}$, the solvent dependence is more complex.[61,62] For the ferrocene–ferricenium case the predicted dependence on $1/D_{op} - 1/D_s$ *is* observed for optically induced electron transfer in the dimer $[(\eta^5\text{-}C_5H_5)Fe(C_5H_4C_5H_4)Fe^+(\eta^5\text{-}C_5H_5)]^+$[63] and the possibility exists that the outer-sphere reaction is adiabatic ($\nu_{et} > \nu_n$) with ν_n dictated by the dynamics of solvent reorientation. This was the conclusion reached in an electrochemical rate study based on a series of couples of the type $Fe(C_5Me_5)_2^{+/0}$, $Cr(C_6H_6)_2^{+/0}$ . . ., where the role of solvent was included both through λ_0 and, by including solvent dynamics, in ν_n through the longitudinal solvent dipole relaxation time τ_L.[64] τ_L is related to the Debye relaxation time, τ_D, obtained from dielectric loss measurements, by $\tau_L = (D_\infty/D_s)\tau_D$, where D_∞ and D_s are the high-frequency and static dielectric constants of the medium.[65]

From the experimental point of view, significant variations in k_{obs} can be induced by changes in solvent and/or molecular size. For example, there are relatively small contributions to λ_i for the self-exchange reactions for the $Ru(NH_3)_6^{3+/2+}$ and $Ru(bipy)_3^{3+/2+}$ couples in Table 1 and the effects of the differences in molecular radii on K_A and λ_0 are sufficient to account for the difference in self-exchange rate constants of $\sim 10^6$.

λ_0 varies with $(1/D_{op} - 1/D_s)$ and for polar solvents $D_{op} \ll D_s$, *e.g.* D_{op} = 2.028 and D_s = 8.9 for dichloromethane. As a consequence, dielectric continuum theory predicts electron transfer rates to be enhanced in solvents like CH_2Cl_2 which are electronically relatively highly polarizable.

7.2.6.2.5 Stuctural changes

The influence on k_{obs} of structural changes between oxidation states has already been considered quantitatively. The keys are the linear combination of normal modes into which the structural change can be resolved and the properties of the individual modes (ΔQ_e or S, k, ν).

For simple transition metal ions the molecular orbitals which act as redox levels are largely metal d in character and the structural changes which occur between oxidation states are confined largely to the metal–ligand framework. For a case like $Fe(H_2O)_6^{3+/2+}$, nearly O_h symmetry is maintained in both oxidation states and the only metal–ligand skeletal mode for which ΔQ_e is significantly greater than 0 is the $\nu_{a_{1g}}$ (Fe—O) symmetrical breathing mode as noted earlier. The normal modes arising from the Fe—O framework can be constructed from linear combinations of the six Fe—O local coordinates. The non-A_{1g} modes necessarily involve compression along some of the Fe—O coordinates and elongation along others. The reason why they do not contribute to $Fe(H_2O)_6^{3+/2+}$ exchange is that the combination of compressions and elongations along the local Fe—O axes do not lead to the symmetrical change in structure associated with the change in oxidation state. When the differences in local equilibrium coordinates, Δq_e, are added together, $\Delta Q_e = 0$ for the non-A_{1g} modes.

In general, in the absence of electronic degeneracies, the same overall structure will be maintained between oxidation states. Changes in electron content may lead to an overall lengthening or shortening of bonds, but the changes will be symmetrical and the symmetry of the molecule maintained. For such cases, *the only normal modes which can act as trapping vibrations are those which belong to the totally symmetrical irreducible representation of the molecule.* They are the modes into which the structural changes can be resolved.

Other normal vibrations of the molecules may also be affected by the change in oxidation state but still not make a significant contribution to vibrational trapping. For example, for $Fe(CN)_6^{3-/4-}$ exchange in water there is a shift in $\nu_{a_{1g}}$ (C—N) from 2094 cm^{-1} for $Fe(CN_6)^{4-}$ to 2132 cm^{-1} for $Fe(CN)_6^{2-}$; yet average C—N bond distances between the two oxidation states are the same within experimental error, 1.138(19) Å for $Fe(CN)_6^{4-}$ and 1.148(5) Å for $Fe(CN)_6^{3-}$.[66] It is important to recall that the magnitude of the contribution of a particular mode depends both on ΔQ_e and $h\nu$. For high-frequency modes, even small changes in S can lead to significant contributions to k_{obs}. In fact, based on rate comparisons between H_2O and D_2O as solvents, it has been suggested that for $Fe(H_2O)_6^{3+/2+}$ exchange, high-frequency (~3600 cm^{-1}) ν(O—H) modes do play a role even though ΔQ_e may be small.[67]

For organic self-exchange reactions like $TCNQ^{-/0}$, changes in electron content frequently lead to symmetrical changes in the skeletal structure. For TCNQ there are 54 normal modes but because of the symmetry restriction only those nine normal modes having a_g symmetry have $S \neq 0$.[68] The structural changes that occur upon oxidation of $TCNQ^-$ to TCNQ and two of the most important normal mode contributors to the change are illustrated in Figure 4.[68,69] It is important that even though there are several contributors to λ_i, the change in electron content between 'oxidation states' is spread amongst several atoms in delocalized molecular orbitals. As a result, there are only slight changes in structure, S is small, and the self-exchange reaction occurs near the diffusion controlled limit.

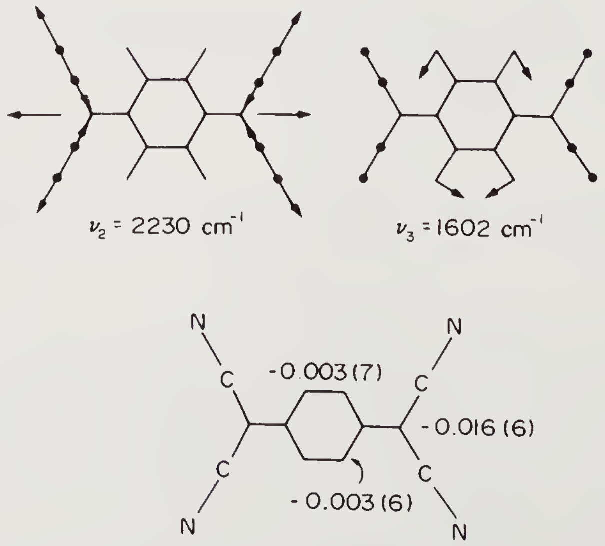

Figure 4. Structural changes[69] upon oxidation of $TCNQ^-$ to TCNQ in Å, also illustrating two of the most important normal mode contributors to the interconversion between structures[68]

The structures of transition metal complexes are more or less predictable based on *d*-electron content and the nature of the ligands. As a consequence, it is possible to develop a basis for understanding how changes in electronic structure between oxidation states lead to changes in molecular structure and through them help to dictate relative magnitudes of $k_{\text{obs.}}$. (1) For first-row transition metal complexes where the bonding is largely ionic, significant bond distance changes may accompany changes in occupation of $d\pi$ orbitals. For the high-spin complexes $\text{Fe(H}_2\text{O)}_6^{2+}$ ($t_{2g}^4e_g^2$) and $\text{Fe(H}_2\text{O)}_6^{3+}$ ($t_{2g}^3e_g^2$), the t_{2g} redox orbitals are slightly antibonding with respect to the *p*-electrons of the aqua ligands, leading to a lengthening of the Fe—O bonds in the lower oxidation state.[28,29] (2) Large differences in metal–ligand bond lengths occur when a change in electron occupation of the $d\sigma^*$ (e_g) orbitals occurs since they are antibonding with regard to the metal–ligand interaction. A dramatic example occurs in $\text{Co(NH}_3)_6^{3+/2+}$ self-exchange where the electronic configurations are t_{2g}^6 and $t_{2g}^5e_g^2$ and the change in average Co—N bond lengths is 0.18 Å. (3) For complexes where there are ligands having low-lying, vacant orbitals of π-type symmetry, for example π^* in CO or pyridine or $d\pi$ in PR_3, mixing between filled, metal-based $d\pi$ orbitals and ligand orbitals leads to delocalization and pseudo-oxidation of the lower oxidation state. The result is a decrease in ΔQ_e for the largely metal–ligand skeletal modes. An example is Fe(phen)_3^{2+} and Fe(phen)_3^{3+} where there is no difference in Fe—N bond distances within experimental error.[70] (4) The same arguments may also apply, but in reverse, to high oxidation state couples where the higher oxidation states are stabilized by good π-donor ligands like O^{2-} or NR_2^-. (5) The analysis presented here is inadequate to deal with cases where there is a change in coordination number between oxidation states such as Cu^{I} (tetrahedral) and Cu^{II} (axially distorted octahedron) because of the change in coordination number which accompanies electron transfer. As a rule, where there is a change in coordination number between oxidation states, self-exchange rates are expected to be relatively slow. A detailed analysis of the self-exchange would have to include both the structural reorganization that occurs at the two sites and the incipient changes in bonding at the Cu^{I} and Cu^{II} sites.

7.2.7 OUTER-SPHERE ELECTRON TRANSFER REACTIONS WITH $\Delta G \neq 0$: CROSS REACTIONS

Self-exchange reactions are an isolated and special case of electron transfer, but they provide a useful starting point for understanding electron transfer processes in general. This is certainly expected to be true for outer-sphere electron transfer where, in contrast to most chemical reactions, electronic interactions between reactants are weak and the internal electronic and molecular structures of the reactants are maintained throughout the course of the reaction with only slight perturbations. The reactants bring to an outer-sphere reaction their characteristic properties toward electron transfer and they are the same properties which were of importance in self-exchange. The new feature to consider is how non-zero changes in ΔG or ΔE influence k_{obs}.

7.2.7.1 Intramolecular Vibrations

In Figure 5 are illustrated potential energy curves for a trapping vibration for a case where $\Delta E \neq 0$. Assuming the harmonic oscillator approximation to be valid, the equation for the potential curve associated with a trapping normal mode at the reactants is $U^{\text{R}} = \frac{1}{2}kQ_{\text{R}}^2 + U^{\text{R}}_{\text{e}}$, where Q is the displacement coordinate and U^{R}_{e} is the potential energy at $Q = 0$. The displacement coordinate for a normal mode in the products can be related to the same mode in the reactants through ΔQ_{e} by $\Delta Q_{\text{e}} = Q_{\text{e,R}} - Q_{\text{e,P}}$, which gives $U^{\text{P}} = \frac{1}{2}k(Q_{\text{R}} - \Delta Q_{\text{e}})^2 + U^{\text{P}}_{\text{e}}$. The latter equation assumes that the force constant and, therefore, the vibrational spacings for the trapping vibration illustrated in Figure 5 are the same in reactants and products. As was the case for self-exchange, in order to meet the requirement of energy conservation in the classical limit, electron transfer can only occur through those vibrational levels which are at the intersection point between the reactant and product potential curves. At the intersection point $U^{\text{P}} = U^{\text{R}}$ and using the expressions above for U^{P} and U^{R}, Q_{int} is given by equation (52).

$$Q_{\text{int}} = \frac{\Delta Q_{\text{e}}}{2}\left(1 + \frac{\Delta E}{\frac{1}{2}k(\Delta Q_{\text{e}})^2}\right) \tag{52}$$

Note that strictly speaking the difference $U^{\text{P}}_{\text{e}} - U^{\text{R}}_{\text{e}}$ is equal to the internal energy difference ΔE only if the vibrational frequencies (ν) and, therefore, zero point energies ($\frac{1}{2}h\nu$) are the same in the reactants and products.

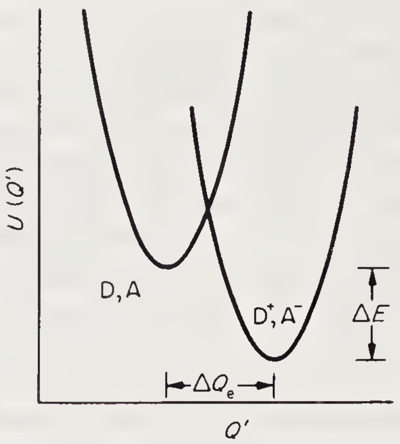

Figure 5 Potential energy–coordinate diagram as in Figure 1 but with $\Delta E \neq 0$

The contribution to the classical energy of activation by the normal mode in Figure 5, $\tfrac{1}{2}kQ^2_{\text{int}}$, is the energy difference between the minimum in the potential energy curve of the reactants and the intersection point. It is given by equation (53). When contributions from all of the trapping vibrations, j, are included, λ_{i} is given by equation (22) or a more complex expression like equation (16a) when the force constants differ considerably.

$$E_{\text{a},j} = \frac{\left[\tfrac{1}{2}k_j(\Delta Q_{\text{e},j})^2 + \Delta E\right]^2}{4\left[\tfrac{1}{2}k_j(\Delta Q_{\text{e},j})^2\right]} = \frac{(\lambda_j + \Delta E)^2}{4\lambda_j} = \frac{(S_j\hbar w_j + \Delta E)^2}{4S_j\hbar w_j} \tag{53}$$

For high-frequency vibrations at room temperature or, in general, at low temperatures, it is necessary to turn to the quantum mechanical description where transition rates are calculated for the series of possible vibrational distributions of the reactants. As for self-exchange reactions, the total rate is calculated by considering transitions from each vibrational distribution of the reactants to all of the levels of the products and then summing over each of the distributions of the reactants. The calculation differs from the self-exchange case in the fact that $\Delta E \neq 0$ must be included when energy conservation is taken into account. The general result in the classical limit is shown in equation (54) for E_{a} and equation (55) for k_{et}. As before, λ includes contributions from all sources of electron trapping, intramolecular and solvent, $\lambda = \lambda_i + \lambda_0$.

$$E_{\text{a}} = \frac{(\lambda + \Delta E)^2}{4\lambda} \tag{54}$$

$$k_{\text{et}} = \frac{2\pi V^2}{h}\left(\frac{\pi}{\lambda RT}\right)^{1/2} \exp -\left[\frac{(\lambda + \Delta E)^2}{4\lambda RT}\right] \tag{55}$$

ΔE is the internal energy change associated with the electron transfer act. If it is assumed that electron transfer occurs at the close contact distance of the association complex, ΔE is the internal energy change for the process, D,A → D^+, A^-, and not the internal energy change for the net reaction, $D + A \rightarrow D^+ + A^-$.

7.2.7.2 Solvent

Marcus and Hush calculate the contribution from solvent to k_{et} using a thermodynamic approach.[34,35] In this approach the key is the derivation of an expression for the energy difference between (1) the interaction between reactants and solvent when the reactants are at equilibrium with the polarization field arising from the surrounding solvent dipoles, and (2) the non-equilibrium case where the surrounding solvent molecules are in the dipole orientations appropriate for electron transfer to occur. To carry out the calculation, Marcus uses a two-step charging process in which (1) the charges on the reactants e_1 and e_2 are changed to e_1' and e_2', where the new charges are those required to produce the changes in the orientational polarization of the solvent molecules needed for electron transfer to occur, and (2) in order to account for the fact that the electronic component of the solvent polarization is very rapid and remains in equilibrium with the transferring electron, the charges on the two reactants are returned from e_1' and e_2' to e_1 and e_2 but the orientational component of the solvent polarization is left where it was at the end of stage one. Using this procedure, Marcus obtains equation (56) where $\Delta e_1 = e_1' - e_1$, $\Delta e_2 = e_2' - e_2$, a_1 and a_2 are the molecular radii assuming spherical reactants, and r is the interreactant separation distance.

$$\Delta G_s^* = \left(\frac{\Delta e_1{}^2}{2a_1} + \frac{\Delta e_2{}^2}{2a_2} + \frac{\Delta e_1 \Delta e_2}{r}\right)\left(\frac{1}{D_{op}} - \frac{1}{D_s}\right) \tag{56}$$

Equation (56) is based on a classical interaction between the ions, and the surrounding solvent is treated as a dielectric continuum. The terms that appear are free energies rather than internal energies. Entropic effects are included with the assumption of the solvent as a dielectric continuum through the temperature dependencies of the macroscopic quantities D_{op} and D_s which are the optical and static dielectric constants.

In order to obtain the minimum value for ΔG_s^*, which is the solvent contribution to the analog of the 'free energy of activation' of Reaction Rate Theory, (1) free energy must be conserved in the electron transfer process which means that $\Delta G_s^*(\text{forward}) = \Delta G_s^*(\text{reverse}) + \Delta G_{et}{}^{\circ\prime}$. The ΔG^* terms refer to the forward and reverse electron transfer steps and $\Delta G_{et}{}^{\circ\prime}$ is the free energy change associated with the electron transfer step, (2) equation (56) is next minimized with regard to e_1' and e_2'. Using this procedure, Marcus derives the expression $\Delta G_s^* = m^2\lambda_0$. For the case of only solvent trapping, $m = -\tfrac{1}{2}(1 + \Delta G_{et}{}^{\circ\prime}/\lambda_0) = -\tfrac{1}{2}[(\lambda_0 + \Delta G_{et}{}^{\circ\prime})/\lambda_0]$, and ΔG^* is given by equation (57). More generally, $\lambda = \lambda_i + \lambda_0$, $m = -\tfrac{1}{2}[(\lambda + \Delta G_{et}{}^{\circ\prime})/\lambda]$ and equation (57) becomes equation (58).

$$\Delta G_s^* = m^2\lambda_0 = \frac{(\lambda_0 + \Delta G_{et}{}^{\circ\prime})^2}{4\lambda_0} \tag{57}$$

$$\Delta G^* = \frac{(\lambda + \Delta G_{et}{}^{\circ\prime})^2}{4\lambda} \tag{58}$$

There is obviously a close similarity between the quantum mechanically derived result for E_a in equation (54) and the thermodynamically derived result for ΔG^* in equations (57) and (58). In the classical limit of the quantum mechanical result, the characteristic quadratic dependence on ΔE arose from energy conservation based on the intersection between potential curves. The dependence on ΔG in equation (57) arose from differences in ion–solvent interactions and the multiplier m is essentially the extent of electron transfer in the 'activated complex' for electron transfer.

7.2.7.3 Experimental Tests: The Marcus Cross-reaction Equation

From the expression for k_{et} in equation (55), assuming the appropriateness of the dielectric continuum approximation so the ΔE can be replaced by $\Delta G_{et}{}^{\circ\prime}$, the rate constant for electron transfer in the classical limit is given by equation (59).

$$k_{obs} = k_{et}K_A = \nu_{et}K_A \exp -\left[\frac{(\lambda + \Delta G_{et}{}^{\circ\prime})^2}{4\lambda RT}\right] \tag{59}$$

One way of testing equation (59) experimentally is to obtain rate constant data for a series of closely related reactions like $Fe(H_2O)_6^{2+} + M(phen)_3^{3+} \rightarrow Fe(H_2O)_6^{3+} + M(phen)_3^{2+}$ (M = Fe, Ru, Os), where charge types and molecular radii are constant, thus ensuring a constancy in λ_0 and K_A. In addition, the similarity in molecular structures ensures the λ_i remains relatively constant through the series, and the only remaining variable is $\Delta G_{et}{}^{\circ\prime}$, which for the series shown varies by ~0.5 V. For purposes of analysis, equation (59) can be rearranged to give equation (60) where $k(0)$ is the hypothetical member of the series of reactions for which $\Delta G_{et}{}^{\circ\prime} = 0$.

$$\begin{aligned} \ln k_{obs} &= \ln k(0) - \frac{\Delta G_{et}{}^{\circ\prime}}{2RT}\left(1 + \frac{\Delta G_{et}{}^{\circ\prime}}{2\lambda}\right) \\ \ln k(0) &= \ln \nu_{et}K_A - \frac{\lambda}{4RT} \end{aligned} \tag{60}$$

There are some caveats associated with the use of equation (60). (1) $\Delta G_{et}{}^{\circ\prime}$ is the free energy change for electron transfer between the reactants in the association complex. It is related to the overall free energy change for the reaction in the prevailing medium, $\Delta G^{\circ\prime}$, by $\Delta G_{et}{}^{\circ\prime} = \Delta G^{\circ\prime} - w_R + w_P$ where w_R and w_P are the electrostatic free energy changes associated with bringing together the reactants and products. $\Delta G^{\circ\prime}$ is related to the potential difference between the two redox couples as shown in equation (61). (2) From the definition of $\ln k(0)$, $\ln k(0) = \ln \nu_{et}K_A - \lambda/4RT$, in comparing a series of reactions it is necessary that both λ and the product $\nu_{et}K_A$ remain relatively constant if the dependence on ΔG is to be tested. The assumption that $\nu_{et}K_A$ remains constant may not be valid if there is an appreciable 'non-adiabatic' component to the reactions. In that case, k_{obs} depends on V and therefore on the specific nature of the electronic coupling between reactants for each individual reaction.

$$\Delta G^{\circ\prime}(\mathrm{eV}) = (E^{\circ\prime}(A^{\circ}/A^{-}) - E^{\circ\prime}(D^{+}/D)) \tag{61}$$

Equation (60) or equations like it have been tested with regard to the predicted dependence of k_{obs} on ΔG for a number of reactions including such cases as $\mathrm{Fe(H_2O)_6^{2+} + FeL_3^{3+} \rightarrow Fe(H_2O)_6^{3+} + FeL_3^{2+}}$ and $\mathrm{Ce^{IV} + FeL_3^{2+} \rightarrow Ce^{III} + FeL_3^{3+}}$[71] (L is 2,2′-bipyridyl, 1,10-phenanthroline or their substituted derivatives); note Table 6.2 in ref. 24. In a somewhat novel application, it has also been applied to the electron transfer quenching of excited states and in particular to the quenching of the metal-to-ligand charge transfer (MLCT) excited state of $\mathrm{Ru(bipy)_3^{2+}}$, $\mathrm{(bipy)_2Ru^{III}(bipy^{\overset{\cdot}{-}})^{2+*}}$, by both oxidative and reductive quenchers, for example equation (62).[72]

$$\mathrm{Ru(bipy)_3^{2+*}} + p\text{-}\mathrm{Me_2NC_6H_4Me} \longrightarrow \mathrm{Ru(bipy)_3^{+}} + p\text{-}\mathrm{Me_2NC_6H_4Me^{+}} \tag{62}$$

The second and far more common approach to testing the predicted dependence of k_{obs} on ΔG has been based on the so-called Marcus 'cross-reaction' equation. The cross-reaction equation interrelates the rate constant for a net reaction, $\mathrm{D+A \rightarrow D^{+}+A^{-}}(k_{12})$, with the equilibrium constant (K_{12}) and self-exchange rate constants for the two-component self-exchange reactions $\mathrm{D^{+/0}}$ (k_{11}) and $\mathrm{A^{0/-}}$ (k_{22}). Its derivation is based on the assumption that the contributions to vibrational and solvent trapping for the net reaction from the individual reactants are simply additive (equation 63). The factors of one-half appear because only one of the two components of the self-exchange reactions is involved in the net reaction. The expression for λ_0 in equation (63) is an approximation. Note from equation (23) that λ_0 is a *collective* property of both reactants and the approximation in equation (63) is valid only if the reactants have similar radii.

$$\lambda_{12} = \frac{\lambda_{11}}{2} + \frac{\lambda_{22}}{2}\,;\; \lambda_{\mathrm{i},12} = \frac{\lambda_{\mathrm{i},11}}{2} + \frac{\lambda_{\mathrm{i},22}}{2}\,;\; \lambda_{0,12} = \frac{\lambda_{0,11}}{2} + \frac{\lambda_{0,22}}{2} \tag{63}$$

The derivation of the cross-reaction equation follows by: (1) solving equation (63) for λ for each individual self-exchange reaction, *e.g.* $\lambda_{11} = 4RT(\ln(\nu_{\mathrm{et}}K_{\mathrm{A}})_{11}/k_{11})$; (2) inserting the expressions for λ_{11} and λ_{22} into equation (63) for λ_{12}; (3) incorporating this expression for λ_{12} into the rate constant expression in equation (59), assuming that $(\nu_{\mathrm{et}}K_{\mathrm{A}})_{12} = [(\nu_{\mathrm{et}}K_{\mathrm{A}})_{11}(\nu_{\mathrm{et}}K_{\mathrm{A}})_{22}]^{1/2}$. The final result is shown in equation (64).

$$k_{12} = (k_{11}k_{22}K_{12}f_{12})^{0.5}W_{12} \tag{64}$$

In the expression for $\ln f_{12}$ in equation (65), $\ln K_{12} = -\Delta G_{12}^{\circ\prime}/RT$ is related to the free energy change that occurs upon electron transfer within the association complex by $\Delta G_{12}^{\circ\prime} = \Delta G_{\mathrm{et}}^{\circ\prime} + w_{12} - w_{21}$ where $w_{12} = w_{\mathrm{R}}$ and $w_{21} = w_{\mathrm{P}}$ are the electrostatic free energy changes associated with formation of the products and reactants, respectively. The electrostatic term W_{12} (equation 66) is 1 for reactants and products of the same charge type and molecular size but otherwise must be taken into account in calculations involving equation (64).

$$\ln f_{12} = \frac{\left[\ln K_{12} + (w_{12}-w_{21})/RT\right]^2}{4\left\{\ln\left[k_{11}k_{22}/(\nu_{\mathrm{et}}K_{\mathrm{A}})_{11}(\nu_{\mathrm{et}}K_{\mathrm{A}})_{22}\right] + (w_{11} + w_{22})/RT\right\}} \tag{65}$$

$$W_{12} = \exp -\left[\frac{w_{12} + w_{21} - w_{11} - w_{22}}{2RT}\right] \tag{66}$$

Although a number of approximations are involved in the derivation of the cross-reaction equation, it has proved to be remarkably successful in accounting for electron transfer rate constants to within at least a few orders of magnitude and, as such, represents an important verification of the underlying theory. The results of a sampling of calculations of this kind are shown in Table 3. The agreement between calculated and observed values is generally good although the calculated values for k_{12} tend to be larger than the experimental values and there are exceptions. In fact, equation (64) is frequently used to estimate otherwise unknown kinetic parameters such as an

Table 3 Comparisons between Calculated and Observed Rate Constants at 25 °C in Water[a]

Reaction	$\log K_{12}$	k_{12}^{calc} ($\mathrm{M^{-1}\,s^{-1}}$)	k_{12}^{obs} ($\mathrm{M^{-1}\,s^{-1}}$)
$\mathrm{Ru(NH_3)_6^{2+} + Fe^{III}}$cytochrome *c* →	3.54	1.2×10^{5}	3.8×10^{4}
$\mathrm{V^{2+} + Co(en)_3^{3+}}$ →	5.19	7.2×10^{-4}	5.8×10^{-4}
$\mathrm{V^{2+} + Fe^{3+}}$ →	16.90	1.7×10^{6}	1.8×10^{4}
$\mathrm{Fe^{2+} + Ru(bipy)_3^{3+}}$ →	8.81	3.6×10^{8}	7.2×10^{5}
$\mathrm{Co(phen)_3^{2+} + Fe^{3+}}$ →	6.27	4.2×10^{3}	5.3×10^{2}

[a] Taken from M. Chou, C. Creutz and N. Sutin, *J. Am. Chem. Soc.*, 1977, **99**, 5615.

unmeasured self-exchange rate constant, and provides a powerful, near-quantitative basis for predicting electron transfer reactivity.

7.2.8 THE INVERTED REGION: EXCITED STATE DECAY

As illustrated in Figure 5 and shown quantitatively in equations like (59), an increasingly favorable energy change enhances the rate constant for electron transfer. The basis for the enhancement is an increase in relative populations of vibrational levels near the intersection region where vibrational overlaps are high. The trend of an increase in k_{obs} with $-\Delta G$ continues to the point where $-\Delta G = \lambda$, at which point the exponential term in equation (59) goes to zero. It follows from equation (59) that when $-\Delta G = \lambda$, $k_{\text{et}} = \nu_{\text{et}}K_{\text{A}}$ and, as shown in Figure 6a, the statistical distribution at the intersection region coincides with RT and there is no need for thermal activation.

Normally, it is not possible to explore this domain experimentally using bimolecular electron transfer reactions. In the absence of an activational requirement, electron transfer becomes sufficiently facile that the reactions are partly or wholly diffusion-limited and $k_{\text{obs}} \approx k_{\text{D}}$. The exception is for reactions which have a large non-adiabatic contribution so that $k_{\text{et}} = \nu_{\text{e}}K_{\text{A}}$ and if ν_{e} is sufficiently small, $k_{\text{obs}} = \nu_{\text{e}}K_{\text{A}}$.[73]

Figures 6b and 6c illustrate the situation when ΔG becomes even more favorable and $-\Delta G > \lambda$. In this domain, two remarkable things happen. (1) As in Figure 1b, the effect of electronic coupling is to produce two new states. However, now the upper potential curve is *imbedded* in the lower curve and electron transfer becomes a *non-adiabatic* process involving a transition between different electronic states rather than a redistribution of electron density within a single state. (2) As illustrated in Figure 6 and as can be seen from equation (59), it is predicted by the classical result that in this domain as ΔG becomes more favorable k_{et} should *decrease with increasing* $-\Delta G$. This seemingly counterintuitive result is a straightforward consequence of the necessity to reach the intersection region for purposes of energy conservation. Because of the inversion in the predicted dependence of k_{obs} on ΔG, the $-\Delta G > \lambda$ domain has been termed 'the inverted region' by Marcus.[34a]

The 'imbedded' nature of the potential curves in Figure 6 for electron transfer in the inverted region is a feature shared with the nonradiative decay of molecular excited states. In fact, in the inverted region another channel for the transition between states is by emission, $\text{D,A} \rightarrow \text{D}^+\text{,A}^- + h\nu$, which can be observed, for example, from organic exciplexes,[74] chemiluminescent reactions,[75] or from intramolecular charge transfer excited states, *e.g.* $(\text{bipy})_2\text{Ru}^{\text{III}}(\text{bipy}^{\cdot-})^{2+*} \rightarrow (\text{bipy})_2\text{Ru}^{\text{II}}(\text{bipy})^{2+} + h\nu$.

In order to deal with electron transfer in the inverted region it is necessary to understand the significance of the imbedded nature of the reactant and product potential curves. In this domain, vibrational overlaps are far higher than in the normal region (note Figures 3 and 6c) and there is no longer a clear advantage to thermal activation to the intersection region to enhance vibrational overlap. If high-frequency vibrations exist for which $\Delta Q_{\text{e}} \neq 0$, nonradiative transitions involving vibrational levels well below the intersection region will dominate the electron transfer process just as they would at low temperatures for normal electron transfer. Such processes are decidedly 'nonclassical'.

As for electron transfer in the normal region, based on the results of time dependent perturbation theory, electron transfer in the inverted or excited state decay region is also determined by the

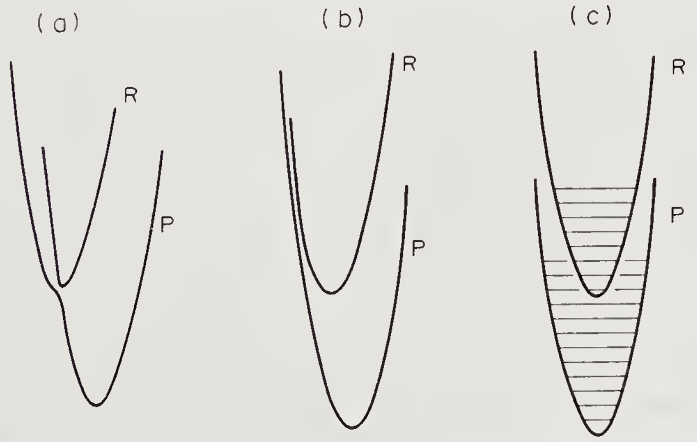

Figure 6. Potential energy-coordinate diagrams showing the effect of increasingly favorable ΔG or ΔE. Case (a), $-\Delta G = \lambda$; case (b), $-\Delta G > \lambda$; case (c), excited state decay in the limit $\lambda = S\hbar\omega \ll |\Delta E|$ showing the vibrational levels in the excited and ground states

product of electronic coupling and vibrational overlap terms.[76,77] However, since a transition occurs between different electronic states, electronic coupling is induced by a 'promoting' vibrational mode or modes. The symmetry properties of the promoting mode or modes are such that, when activated, the electronic distribution of the excited state is perturbed so as to cause a mixing between the excited and ground states. The necessity for vibrationally induced electronic coupling arises from the fact that solutions of the same Hamiltonian for the ground and excited states are orthogonal, at least at the fixed equilibrium nuclear coordinates. In the absence of the vibrationally induced electronic perturbation, the states cannot mix.

As for normal electron transfer, the vibrational overlap integral for excited state decay contains contributions from those normal modes for which $\Delta Q_e \neq 0$, but the changes in bond distances are now between the excited and ground states.

In excited state decay, the magnitude of the vibrational overlap integral depends upon the extent of overlap between the excited and ground state vibrational wavefunctions. The vibrations involved are sometimes called the 'acceptor' vibrations since the loss in electronic energy associated with the electron transfer act, *e.g.* $(\text{bipy})_2\text{Ru}^{\text{III}}(\text{bipy}^{\cdot-})^{2+*} \rightarrow (\text{bipy})_2\text{Ru}^{\text{II}}(\text{bipy})^{2+}$, appears in the acceptor vibrations by the population of excited vibrational levels in the ground state. Vibrational overlaps are enhanced when: (1) the distortion between the excited and ground state (ΔQ_e) is large, (2) the quantum spacing, $h\nu$, for the acceptor vibrations is large, and (3) the excited state energy difference between the ground and excited state, ΔE, becomes smaller.

In the limit that $|\Delta E| < S\hbar\omega$ (ΔQ_e relatively small) and $h\nu \gg k_BT$ (large quantum spacings for the acceptor modes), direct mathematical evaluation of the vibrational overlap integral leads to equation (67).

$$\ln k_{et} = \ln k_{nr} = \ln \beta - S - \frac{\gamma E}{\hbar\omega} + \frac{\chi_0}{\hbar\omega}\left[\frac{k_BT}{\hbar\omega}(\gamma+1)^2\right] \tag{67}$$

$$\gamma = \ln\frac{E}{S\hbar\omega} - 1 \tag{68}$$

The result in equation (67) is appropriate for the case where nonradiative decay (k_{nr}) is dominated by a single, relatively high frequency acceptor vibration. The contribution from solvent is included in the term containing χ_0. The promoting mode induced electronic coupling integral is β and S and ($h\nu$) are the electron–vibrational coupling constant and quantum spacing for the acceptor vibration. The quantity E is approximately equal to the emission energy, E_{em}, which is experimentally available from emission spectral measurements if the excited state emits. The result in equation (67) has been generalized to include both low and high frequency acceptor modes and the case where the two modes are an average of several contributors.[76,78] The latter is an important point since, for example, it has been concluded from the results of resonance Raman and low-temperature emission spectral fitting experiments that decay of the MLCT state for Ru(bipy)_3^{2+*} includes contributions from seven ν(bipy) ring stretching modes in the region ~1000 to 1600 cm^{-1} and a series of other vibrations as well.[79]

A notable feature of equation (67) is a prediction of how k_{et} (k_{nr}) should vary with ΔE. Recall that the classical prediction was that $\ln k_{et} \propto -[(\lambda + \Delta G)^2/4\lambda RT]$, while from equation (67), $\ln k_{et} \propto -\gamma E_{em}/h\nu \approx -\gamma|\Delta E|/h\nu$. In either case it is predicted that k_{et} *should decrease as* ΔE *or* ΔG *become more favorable.* Because of the dependence of $\ln k$ on $|\Delta E|$, equations of the form of equation (67) are often referred to as the 'energy gap law'.[76,77]

Experimental tests of electron transfer in the inverted region have come mainly from studies on nonradiative decay processes of excited states based on transient absorption or emission measurements. The studies have been based on a series of aromatic π–π^* excited states,[77b] and more recently on a series of MLCT excited states based on polypyridyl complexes of Os$^{\text{II}}$ and Ru$^{\text{II}}$, *e.g.* Ru(bipy)_3^{2+}.[78] From the latter work, a number of interesting observations have been made.[78] (1) The energy gap law result in equation (67) was shown to account for the variation of k_{nr} with E_{em} through the series $(\text{AA}^{\cdot-})\text{Os}^{\text{III}}\text{L}_4^{2+*}$ (AA = 2,2′-bipyridyl or 1,10-phenanthroline; L = pyridine, PR_3, ½bipy, MeCN, ...). The key to the experiment is that variations in the nonchromophoric ligands lead to systematic changes in ΔE between the ground state, $(\text{AA})\text{Os}^{\text{II}}(\text{L})_4^{2+}$, and the excited state, $(\text{AA}^{\cdot-})\text{Os}^{\text{III}}(\text{L})_4^{2+*}$. (2) The energy gap law was also shown to hold when the variations in emission energy were induced by ion pairing or variations in the solvent. (3) Vibrational progressions are observed in low-temperature emission spectra from which values for S, $h\nu$ and χ_0 can be obtained by emission spectral fitting.[79]

Tests of the inverted region for bimolecular electron transfer have proven to be more elusive. As mentioned above, a major difficulty is that, for many bimolecular reactions, $\nu_{et}K_A > k_D$ and a large portion of the free energy region of experimental interest is lost because the rate constants of note are at or near the diffusion controlled limit.[80] An additional complication associated with the large driving forces in the inverted region is that additional reaction channels may be available to the system such as energy transfer to low-lying excited states of one of the reactants, *e.g.* $D^{+}+A^{-} \rightarrow D^{*}+A$.

Pulse radiolysis studies on unsymmetrical, chemically linked organic systems have shown the expected fall off in rate constant as ΔG becomes more favorable.[81] In these experiments, advantage is taken of the fact that capture of electrons produced by pulse radiolysis is relatively indiscriminate and in some of the pulse events an electron is captured by the component in the dimeric systems which is the weaker oxidant. Following such an event, the experimental observation made is of the system 'relaxing' by intramolecular electron transfer to the stable redox configuration, as shown for **(1)** → **(2)** where A is one of a series of polyaromatic or quinone electron acceptors.[81]

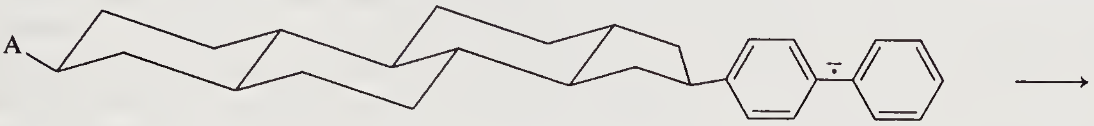

(1)

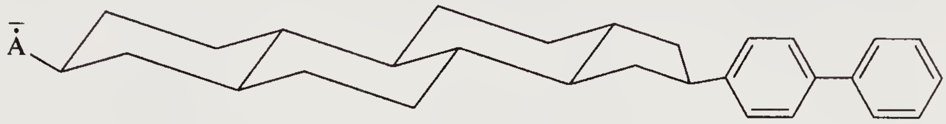

(2)

7.2.9 INNER-SPHERE REACTIONS

In contrast to outer-sphere reactions, the simple observation that a reaction occurs by an inner-sphere mechanism necessarily introduces an element of structural definition. The relative dispositions of the oxidizing and reducing agents are immediately established and, except for structurally flexible bridging ligands such as $NC_5H_4(CH_2)_nC_5H_4N$, the internuclear separation between redox sites can be inferred from known bond distances. Even so, bimolecular inner-sphere reactions necessarily occur by a sequence of elementary steps (Scheme 2) and the observed rate constant may include contributions from any of the series of steps.

Two separate but somewhat interwoven themes have emerged from the study of inner-sphere reactions. The first is the use of product and rate studies to establish the existence of inner-sphere pathways and then the exploitation of appropriate systems to demonstrate such special features as 'remote attack'. In the second theme the goal has been to assemble the reactants through a chemical bridge and then to study intramolecular electron transfer directly following oxidation or reduction of the resulting dimer (note equation 7). It is convenient to turn first to chemically prepared, intramolecular systems since many of the theoretical ideas and experimental results for outer-sphere reactions can be carried over directly as an initial basis for understanding the experimental observations.

7.2.9.1 Intramolecular Electron Transfer

7.2.9.1.1 Optical electron transfer in mixed-valence ions

There is by now an extensive chemistry of mixed-valence compounds where the distinguishing feature is the existence, at least in a formal sense, of different oxidation states within the same compound.[82–84] The first deliberate synthesis of a discrete metal-based mixed-valence ion was the Creutz and Taube ion, $(NH_3)_5Ru(pz)Ru(NH_3)_5^{5+}$ (pz is pyrazine).[85] A number of examples of this type are known based on metal complexes and organometallics, *e.g.* $[(C_5H_5)Fe(C_5H_4C_5H_4)Fe(C_5H_5)]^{+}$ [86] or chemically linked organics such as **(3)**,[87] especially for d^5-d^6 cases involving Ru^{III} and Ru^{II}.[83,84]

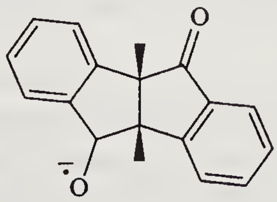

(3)

Characteristically, mixed-valence ions are prepared with the two redox sites in the same formal oxidation state, for example as in reaction (69), and the mixed-valence character is introduced subsequently by one-electron chemical or electrochemical oxidation or reduction.

(69)

Although mixed-valence ions are prime candidates for the direct investigation of electron transfer free of the complications of competing reactions, with the exception of some of the organic examples in Table 1, the direct measurement of intramolecular electron transfer rate constants has proved to be difficult. The problem lies in part with the choice of systems. For d^5–d^6 $\mathrm{Ru^{III}}$–$\mathrm{Ru^{II}}$ dimers the vibrational barriers to electron transfer are relatively low and rate constants high, which necessitates the utilization of techniques such as EPR line broadening which, unfortunately, are not always applicable. However, optically induced electron transfer is an allowed process (for example, equation 8) and metal-to-metal charge transfer (MMCT) bands can often be observed at relatively low energies in the absorption spectra of mixed-valence complexes. This type of transition has been termed intervalence transfer (IT) by Hush[16] and is illustrated using the potential energy diagram in Figure 7.

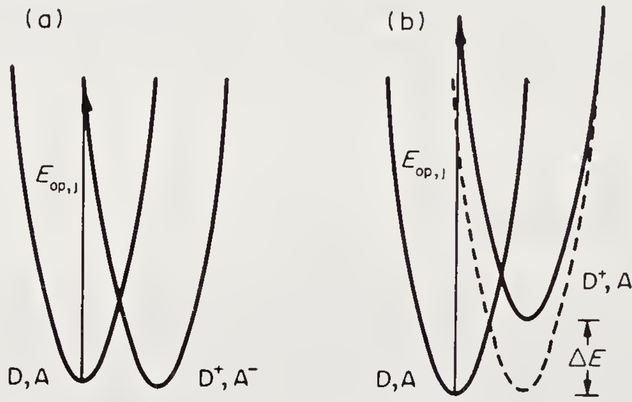

Figure 7 Potential energy curves illustrating the contribution from an intramolecular trapping vibration j to the energy of an IT band for (a) $\Delta E = 0$, (b) $\Delta E \neq 0$

In principle, a great deal of information concerning intramolecular electron transfer is available from IT absorption band measurements. Optical electron transfer is rapid on the vibrational timescale and, as illustrated in Figure 7, the optical transition is a vertical process in the Franck–Condon sense.

The absorption band shape is necessarily dictated by those same intramolecular trapping and solvent vibrations which determine the rate of thermal electron transfer since the change in electronic distribution is the same for the two processes. The band shape depends on the product of two terms. The first is the transition moment $\boldsymbol{M} = \langle \psi_e | \boldsymbol{\mu} | \psi_g \rangle$, the square of which determines the total integrated band intensity; ψ_e and ψ_g are the excited and ground state electronic wave functions and $\boldsymbol{\mu}$ is the dipole moment vector operator associated with the perturbation imposed by the incident electromagnetic radiation. The second term is the product of the series of Franck–Condon or vibrational overlap integrals, $\langle \chi_e | \chi_g \rangle^2$, for those normal modes for which $\Delta Q_e \neq 0$ for electron transfer. The vibrational overlap term determines the band shape.[44,45] Since the same sets of vibrations are involved for the optical and thermal electron transfer processes, in principle it is possible to use absorption band shapes to extract those parameters (S, $h\nu$, λ_0) which are needed to calculate electron transfer rate constants. In practice, IT bands are broad and featureless and if several trapping vibrations are involved, extraction of the needed structural and vibrational parameters is not practical.

However, in the classical limit the absorption band energy (E_{op}) is directly related to λ_i, λ_0 and ΔE as shown in equation (70) for a symmetrical case and in equation (71) for an unsymmetrical case where $\Delta E \neq 0$.[16]

$$E_{op} = \lambda_0 + \lambda_i = 4E_a \tag{70}$$

$$E_{op} = \lambda + \Delta E \tag{71}$$

Equations (70) and (71) are derived assuming that the splitting between potential curves induced by electronic coupling is negligible. It follows directly from the optical transition illustrated in Figure 7a if the contribution to E_{op} from a single trapping vibration j is given by $k(\Delta Q_{e,j})^2 = S_j\hbar\omega_j$. If there is a series of trapping vibrations, $\lambda_i = \Sigma_j S_j \hbar\omega_j$, where the summation is over all the trapping modes. If the solvent is assumed to be a dielectric continuum, its contribution to E_{op}, λ_0, follows directly from equation (23) as discussed in a previous section.

The energy of activation for thermal electron transfer is related to λ and ΔE in equation (54). Equations (70) and (71) relate E_{op} to the same variables. It follows that, in the classical limit, the energy of activation for thermal electron transfer can be calculated from E_{op} using equation (70) for a symmetrical case or equation (72) for an unsymmetrical case.

$$E_a = \frac{E_{op}^{\ 2}}{4(E_{op}-\Delta E)} \tag{72}$$

This is a striking result since it suggests that simple absorption band measurements can be used to calculate E_a for thermal electron transfer. Note that for unsymmetrical cases where $\Delta E \neq 0$, both E_{op} and ΔE must be known; ΔE can sometimes be estimated from temperature dependent redox potential measurements.

The use of the IT absorption band can be taken one step further. The acceptor site causes an electrostatic perturbation at the donor. Because of the perturbation a more appropriate set of electronic wavefunctions can be constructed from a linear combination of the unperturbed wavefunctions of the donor, ψ_D, and acceptor, ψ_A. Including the effect of the perturbation, the wavefunctions ϕ_D and ϕ_A in the expression for V in equation (17) can be written as $\phi_D = \psi_D + \alpha\psi_A$ and $\phi_A = \psi_A - \alpha\psi_D$, if overlap is neglected and the mixing coefficient, α, is small. From first-order perturbation theory, $\alpha = V/(E_D-E_A) = V/E_{op}$. If the dipole moment operator is written as $\mu = er$, where r is the interreactant separation distance and e the unit electron charge, α is also related to the transition moment through $|M| = \langle\phi_D|\mu|\phi_A\rangle \approx \alpha er$. From the two relationships it follows that $V = E_{op}|M|/er$. From the known relationship between the integrated band intensity and $|M|$ for a Gaussian shaped band, V can be calculated from the properties of the absorption band, as shown in equation (73).[16]

$$V = \frac{\left(4.2 \times 10^{-4}\varepsilon_{max}\bar{\nu}_{1/2}E_{op}\right)^{1/2}}{r^2} \tag{73}$$

From equation (73) it is possible to calculate V from the molar extinction coefficient at the absorption maximum (ε_{max}), the band width at half maximum ($\bar{\nu}_{1/2}$) and E_{op} if the interreactant separation is known.

With V in hand from the integrated intensity of the absorption band and E_a from the band maximum, all of the quantities that appear in equation (30) which are needed to calculate k_{et} in the classical limit are available from the properties of an IT band. Of course, this remarkable conclusion must be tempered by the fact that if V is appreciable, ν_{et} may be dictated by timescales arising from the trapping vibrations or solvent motions and not by V.[65b] As noted below, there are additional complicating features that may limit the validity of equations like (70) and (72).

Nonetheless, in Table 4 are summarized the results of a series of rate constant comparisons between calculated values using optical absorption data and experimental values.[83] The experimental data are derived from self-exchange rate constants for couples which are structurally related to the mixed-valence dimers shown in the table. The experimental values cited are calculated values for electron transfer within the association complex between reactants as estimated from $k_{et} = k_{obs}/K_A$. K_A values were calculated using equation (33) and it was assumed in the calculations that $\nu_{et} = 5 \times 10^{12}\ s^{-1}$. Calculations of this kind have been extended to unsymmetrical dimers like $(NH_3)_5Ru^{III}(pz)Ru^{II}Cl(bipy)_2^{4+}$ [83] and even to outer-sphere ion-pairs like (4).[88]

(4)

For unsymmetrical cases, the calculations are rather intricate since they require that an experimental value be obtained for ΔE and difficulties can arise from the fact that entropic effects are not included in the absorption band measurements.

The apparent ability of simple absorption band measurements to provide direct information about kinetic barriers to electron transfer constitutes a significant demonstration of the predicted relationship between optical and thermal electron transfer. Turning the argument around, it is possible to use variations in E_{op} with solvent, which are easily measured, to gain insight into solvent effects in thermal electron transfer. For example, equation (70) in the form of equation (74) has provided a convenient basis for the systematic exploration of solvent and molecular geometry in determining the magnitude of E_{op} and through it E_a.

$$E_{op} = \lambda_i + e^2\left(\frac{1}{2a_1} + \frac{1}{2a_2} - \frac{1}{d}\right)\left(\frac{1}{D_{op}} - \frac{1}{D_s}\right) \tag{74}$$

Table 4 Comparisons between Self-exchange Rate Constants and Intramolecular Rate Constants Calculated from IT Band Energies

Dimer[a]	k_{calc} (s^{-1})[b]	*Self-exchange couple*	k_{et} (s^{-1})[c]
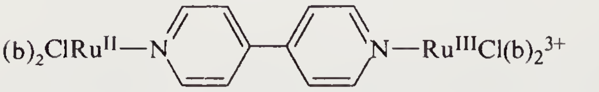	1×10^8	$Ru(b)_2(py)Cl^{2+/+}$	1×10^9
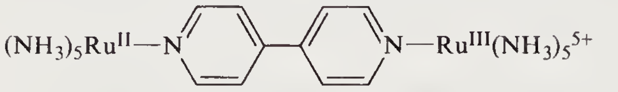	5×10^8	$Ru(NH_3)_5py^{3+/2+}$	2×10^7
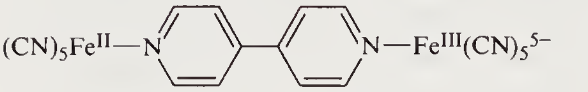	2×10^9	$Fe(CN)_5py^{3-/2-}$	1×10^9

[a] b is 2,2′-bipyridyl.

[b] Calculated using $\nu_{et} = 5 \times 10^{12}\ s^{-1}$ and $k_{calc} = \nu_{et}\exp[-(E_{op}/4RT)]$.

[c] Calculated from $k_{et} = k_{obs}/K_A$ where k_{obs} is the experimentally observed self-exchange rate constant and K_A is given by equation (33).

In one type of study, for mixed-valence ions of the type $[(C_5H_5)Fe^{II}(C_5H_4C_5H_4)Fe^{III}(C_5H_5)]^+$[63] or $[(NH_3)_5Ru^{II}(4,4'\text{-bipy})Ru^{III}(NH_3)_5]^{5+}$ the dependence on the dielectric properties of the medium predicted by equation (74) has been tested by observing the variation in E_{op} with $1/D_{op} - 1/D_s$.[14] In principle, this can be a remarkably revealing experiment. From equation (74) the intercept of a plot of E_{op} *vs.* $1/D_{op} - 1/D_s$ is predicted to give λ_i which provides an experimental basis for partitioning λ between its intramolecular (λ_i) and solvent (λ_0) contributions. In a second type of experiment the implied dependence of E_{op} on the interreactant separation r suggested by equation (74) was tested using a series of mixed-valence dimers. In the experiment the distance between redox sites was varied by varying the length of the bridging ligand in the series $[(bipy)_2ClRu^{II}(L)Ru^{III}Cl(bipy)_2]^{3+}$,[89] where

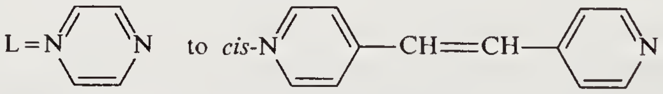

The use of optical charge transfer measurements to obtain kinetic parameters for thermal electron transfer is clearly promising, but further work is needed in this area and it is important to realize that there are a number of limitations. (1) The equations used in the calculations are only relevant in the classical limit. (2) The equations are valid only if electronic coupling is weak. (3) The use of dielectric continuum theory for λ_0 may be inappropriate if specific interactions like hydrogen bonding exist between the mixed-valence dimer and the solvent. In addition, in many cases, more realistic geometrical models than simple non-interpenetrating spheres, which was one of the assumptions used in deriving equations (23) and (74), are required.[24,90] (4) The use of solvent dependence studies to obtain λ_i may mask other effects whose origins are electronic in nature, especially for low-symmetry cases and/or for second- and third-row transition metals where spin–orbit coupling is large. For example, it has been concluded that the apparent 'IT' band for mixed-valence dimers like $(bipy)_2ClRu^{II}(pz)Ru^{III}Cl(bipy)_2^{3+}$ is actually a superposition of three different transitions. The three bands arise because optical excitation from Ru^{II} to Ru^{III} can occur from any of three different orbitals leading to three different spin–orbit states at the optically produced Ru^{III} site.[91] As a consequence, the observed absorption band 'maximum' represents an average of the contribution from three transitions. It gives too high an estimate for the energy of the optical transition for the lowest spin–orbit state. Electronic coupling between Ru^{II} and the lowest spin–orbit state at Ru^{III} is expected to dominate thermal electron transfer because of the relatively low statistical populations of the higher spin–orbit states at room temperatures.

7.2.9.1.2 *Electronic coupling*

For the $Ru^{III/II}$ or $Fe^{III/II}$ mixed-valence dimers of the previous section, the metal ion sites are sufficiently separated spatially for direct overlap between pure metal-based *d*-orbitals to be minimal. However, if there are low-lying π or π^* orbitals in the bridging ligand, $d\pi(\mathrm{Ru^{II}}) \rightarrow \pi^*$ or $d\pi(\mathrm{Ru^{III}}) \leftarrow \pi$ mixing can provide a basis for significant electronic coupling between sites by imparting bridging ligand character into the redox orbitals. The types of orbital interactions involved and the experimental consequences of electronic coupling have been explored in some detail both theoretically and experimentally.[92,93]

Variations in electronic coupling can lead to profound changes in properties, as illustrated by the series $(\mathrm{bipy})_2\mathrm{ClRu(pz)RuCl(bipy)}_2{}^{3+}$, $(\mathrm{NH_3})_5\mathrm{Ru(pz)Ru(NH_3)}_5{}^{5+}$ and $(\mathrm{bipy})_2\mathrm{ClRuORuCl}$-$(\mathrm{bipy})_2{}^{3+}$. In the first case there is clear evidence for localization of the excess electron on the vibrational timescale, in the last case the excess electron appears to be delocalized over both metal sites, and in the intermediate case, the Creutz and Taube ion, the system appears to be poised between the localized and delocalized limits.[94]

Incorporating the effects of significant electronic coupling into the calculation of electron transfer rate constants is an imposing problem. Qualitatively, the factors involved can be discussed using concepts developed earlier. As electronic coupling increases, to be properly written the wavefunctions ϕ_D and ϕ_A must be constructed using a greater admixture of the unperturbed ψ_D and ψ_A wavefunctions. The net result is a partial oxidation of the reduced site and a partial reduction of the oxidized site which (1) decreases ΔQ_e and the extent of intramolecular vibrational trapping, and (2) decreases the effective internuclear separation and, therefore, λ_0.

The effects of enhanced electronic coupling are illustrated in Figure 8. Note that in addition to a decrease in ΔQ_e, the effect of an increase in electronic coupling is to increase the splitting between potential curves for the upper and lower states. If electronic coupling is sufficient in magnitude, there is no longer a basis for vibrational trapping and the excess electron is delocalized over both donor and acceptor sites on the vibrational timescale.

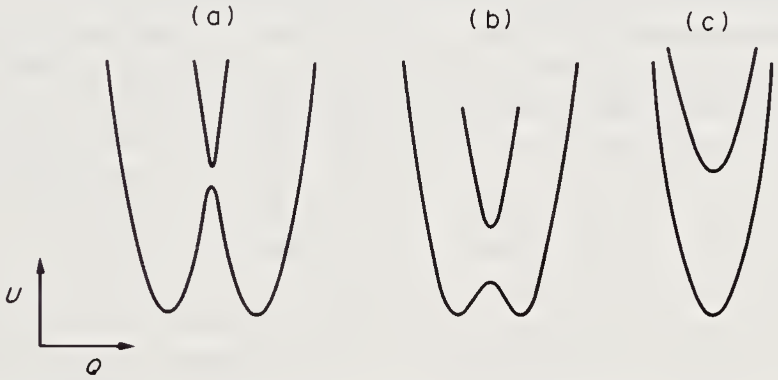

Figure 8. Potential energy-coordinate diagrams for a trapping vibration showing the effect of increasing electronic coupling between the electron donor and acceptor sites for a symmetrical mixed-valence dimer with ΔG, $\Delta E = 0$. (a) Weak electronic coupling compared with the extent of vibrational trapping. (b) Intermediate electronic coupling. (c) Strong electronic coupling leading to a delocalized ground state

The theoretical difficulties that arise in describing electron transfer in strongly coupled systems have several sources. (1) If electronic coupling is extensive, vibrational and structural information on the isolated reactants may not be relevant to the intramolecular process. (2) Vibrational levels well below the intersection region may play an increasingly more important role in dictating electron transfer rates. (3) If the rate of electron transfer from a vibrational distribution exceeds the rate of vibrational equilibration, vibrational populations cannot be calculated using equilibrium statistical mechanics. (4) In general, it is not possible to treat electronic and nuclear motions separately based on the Born–Oppenheimer approximation. (5) Increasingly subtle questions concerning timescale arise, *e.g.* what is the effect on solvent trapping as the rate of intramolecular electron transfer approaches the timescale for solvent dipole reorientation?

Electronic coupling has been incorporated by Piepho, Krausz, Schatz and coworkers for the case of a single trapping vibration assuming that electronic delocalization is rapid on the vibrational timescale.[95] In this model the wavefunction for the exchanging electron is a function of both Q and V and the Born–Oppenheimer approximation is no longer appropriate. Rather than the electron being *either* on the electron donor or acceptor sites, the extent of electron transfer is viewed as occurring synchronously with nuclear coordinate changes as the intersection region is approached. Based on the assumptions described above, Schatz and coworkers have incorporated electronic delocalization and derived expressions for the resulting energy levels, potential functions and wavefunctions, all of which depend on both V and Q.[95] The treatment of Piepho *et al.* is clearly of great value in incorporating electronic delocalization but, in applications to electron transfer, questions still remain concerning timescales and the incorporation of solvent and other trapping vibrations.

From the analysis outlined above, for inner-sphere reactions, electronic coupling within the precursor complex obviously can play a profound role on electron transfer rates by decreasing the vibrational barrier to electron transfer. The problem of treating electronic delocalization in inner-sphere reactions is even more complex than in mixed-valence dimers since the ligand-bridged intermediate of interest is transient and, in general, not observable experimentally. However, a great deal of kinetics data is available on systems which are closely related chemically, which allows some useful conclusions to be reached based on relative rate comparisons. From an analysis of the available data it has been concluded that a critical feature in inner-sphere electron transfer is the electron occupancy of the orbitals in the electron transfer donor and acceptor with regard to the orbitals that they have available for mixing with the bridging ligand.[96,97]

For example, it has been found that there is a significant rate advantage for inner-sphere electron transfer over outer-sphere electron transfer for a number of different metal ion reductant/oxidant combinations, notable examples occurring for reactions involving the $Co^{III/II}$ and $Cr^{III/II}$ couples. An explanation for the role of the electronic configurations at the donor and acceptor sites has been developed by considering a reference state where the transferring bridging ligand is equidistant between oxidant and reductant and nonbonding, for example $Cr^{III}—X—Cr^{II} \rightarrow Cr^{II},X,Cr^{II}$.[96] The role of electronic coupling during the electron transfer act can then be considered in terms of the extent of electronic stabilization arising from the three-center interaction between oxidant, bridging ligand and reductant. For example, for the macrocyclic $Co^{III/II}$ self-exchange in Table 1 (couple 65), an orbital basis for strong electronic coupling exists *via* a three-center three-electron interaction based on $d_{z^2}(Co^{III})-Cl-d_{z^2}(Co^{II})$ mixing.

7.2.9.1.3 *Direct measurement of intramolecular electron transfer rates*

In order to measure intramolecular rate constants directly, a number of approaches have been taken which rely on judicious applications of synthetic chemistry or by taking advantage of the substitutional and/or binding properties of the reactants involved.[98] Reaction (7) is an example of a system in which a direct measurement of intramolecular electron transfer has been made. The keys to the success of the experiment were the preparation of the initial $Ru^{III}-Co^{III}$ species, the kinetically preferred reduction at the Ru^{III} site to give $Ru^{II}-Co^{III}$, and the irreversibility of the net reaction: once formed, the Co^{II} moiety is rapidly lost by aquation. An example of a more straightforward case experimentally is shown in equation (75), where the combination of relatively facile substitution at the reducing agent and a low intramolecular electron transfer rate constant leads to the direct observation of intramolecular electron transfer by conventional spectroscopic techniques.[99]

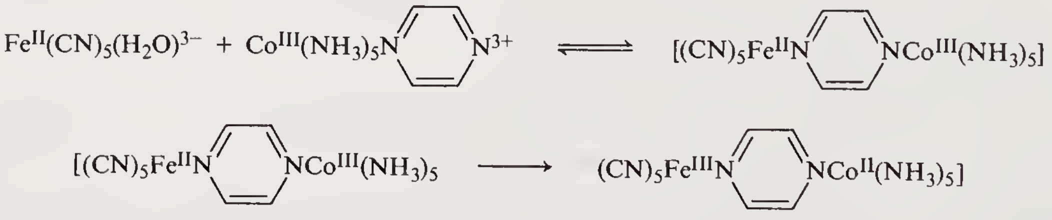

(75)

k (25 °C) = 5.5×10^{-2} s^{-1}

In an entirely different experimental approach the unsymmetrical mixed-valence ion shown in equation (76) was subjected to laser flash photolysis.[100] Excitation was carried out into the MLCT absorption band of the $Ru^{II} \rightarrow \pi^*(pz)$ chromophore. Following excitation, one of the deactivation channels leads to the 'unstable' mixed-valence isomer and its subsequent relaxation to the final, stable oxidation state distribution was observed directly using picosecond laser techniques.

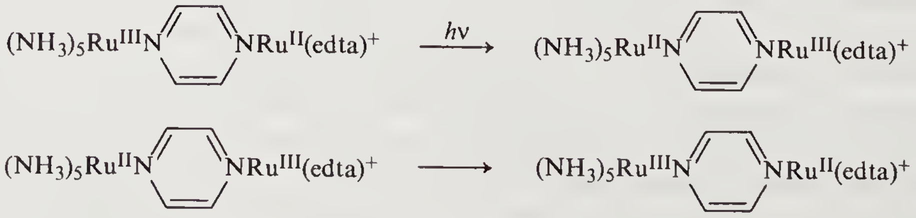

(76)

k (25 °C) = 8×10^9 s^{-1}

A number of results are available for directly measured rates of intramolecular electron transfer in bridging systems based on $(NH_3)_5Co^{III}$ dimers with $-Ru^{II}(NH_3)_5^{2+}$,$-Fe^{II}(CN)_5^{3-}$ or $-Ru^{II}(edta)^{2-}$ as the second redox partner.[98] The ligand systems chosen for study have characteristically been the diazene ligands used in mixed-valence studies such as 4,4′-bipyridyl or pyrazine. In these systems there is relatively weak electronic coupling between sites and only small variations in k_{obs} occur as the bridging ligand is varied. Nonetheless, some important results have emerged from such studies. One of them was an exploration of the role of internuclear separation using a series of diazene ligands of differing lengths. Experimentally, it was found that $\Delta G^{\ddagger}$ varies with $1/r$ as predicted from the $1/r$ dependence for λ_0 predicted by equation (23).[98]

The experimental approaches developed for the direct study of intramolecular electron transfer, as well as the chemical systems themselves, have found application in some very interesting studies. For example, reduction of the $\mathrm{Ru^{III}}$ site to $\mathrm{Ru^{II}}$ in the $\mathrm{Ru^{III}{-}Co^{III}}$ species (**5**) is followed by intramolecular electron transfer from $\mathrm{Ru^{II}}$ to $\mathrm{Co^{III}}$.[101]

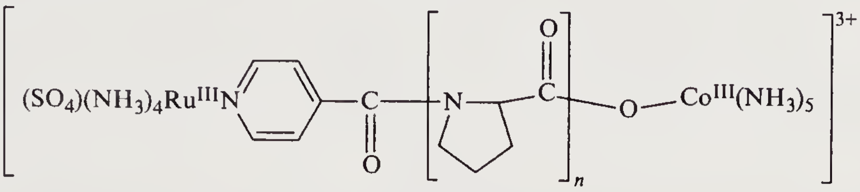

(**5**) $n = 0, 1, 2, 3, 4$

The variation in electron transfer rates through the series exceeds a factor of 2000. The rate constant falls initially as n is increased from 0 to 2. At $n = 3, 4$ the rate begins to increase again, apparently because conformational changes at the intervening proline chemical links occur which allow the two redox sites to come into close proximity.

The same type of thinking has led to experiments designed to test the role of long-range electron transfer in biological systems. In particular, complexes have been prepared between cytochrome *c* derivatives in the $\mathrm{Fe^{III}}$ state and a chemically attached $\mathrm{{-}Ru^{III}(NH_3)_5}$ group bound to a histidine residue (His-33). In the modified cytochrome the Ru site is held at an intersite distance of 14–16 Å. Preferential reduction at $\mathrm{Ru^{III}}$ either using pulse radiolysis and intermediate radicals like $\mathrm{CO_2^-}$ or $\mathrm{Me_2\dot{C}OH}$, or using the $\mathrm{Ru^{III}}$ site as quencher for an excited state, leads to reduction of $\mathrm{Ru^{III}}$ to $\mathrm{Ru^{II}}$ on a sufficiently rapid timescale that the rate constant for intramolecular electron transfer can be observed directly.[102,103]

$$\mathrm{Ru^{III}} - \mathrm{cyt}\ c^{\mathrm{III}} \xrightarrow{\text{rapid}} \mathrm{Ru^{II}} - \mathrm{cyct}\ c^{\mathrm{III}} \xrightarrow{k_{\mathrm{et}}} \mathrm{Ru^{III}} - \mathrm{cyct}\ c^{\mathrm{II}} \qquad (77)$$

7.2.9.2 Intermolecular Electron Transfer

7.2.9.2.1 Experimental criteria

When $\mathrm{Ru(NH_3)_5py^{3+}}$ oxidizes $\mathrm{Ru(NH_3)_6^{2+}}$, the redox change is much more rapid than is substitution at either metal center, and there is no disruption of either coordination sphere in the course of the reaction. In a case such as this, we feel confident that the activated complex for the reaction is of the outer-sphere type. Even if one reaction partner undergoes substitution readily, if a 'suitable' bridging ligand is lacking, the activated complex is again expected to be of the outer-sphere type. A system which meets this description is $\mathrm{Co(NH_3)_6^{3+}}$ and $\mathrm{Cr^{2+}(aq)}$ (in acid medium), where in a slow reaction, $\mathrm{Cr(H_2O)_6^{3+}}$, $\mathrm{Co^{2+}(aq)}$ and $\mathrm{NH_4^+}$ are formed as products. In this system, without evidence as to the identity of the products, we could by no means be certain that the reaction is of the outer-sphere class. In principle, $\mathrm{NH_3}$ could be transferred from the oxidant to the reductant, a possibility which must be entertained because of the documented[104,105] cases of methyl transfer in analogous situations. Ammonia transfer has in no case been reported, and it is commonly assumed that $\mathrm{NH_3}$ is not a 'suitable' bridging group, though the possibility of such transfer has not always been exhaustively explored.

The criteria which have been introduced serve to identify certain reactions as of the outer-sphere type. Other criteria, now to be introduced and illustrated, just as definitely serve to identify certain reactions as of the inner-sphere type.

Perhaps the criteria which lead most directly to a conclusion are those which were applied in the first unambiguous demonstration of this kind of mechanism for reactions between metal ion complexes.[8,106] When $\mathrm{Co(NH_3)_5Cl^{2+}}$ reacts with $\mathrm{Cr^{2+}(aq)}$ in acidic solution, the products are $\mathrm{Co^{2+}(aq)}$, $\mathrm{NH_4^+}$ and $\mathrm{Cr(H_2O)_5Cl^{2+}}$, the latter being formed virtually quantitatively. In the absence of further information, the identification of products would by no means provide proof of mechanism. The additional information which is pertinent to the issue follows: (a) the oxidizing agent, $\mathrm{Co(NH_3)_5Cl^{2+}}$, undergoes aquation much less rapidly than it does reduction by $\mathrm{Cr^{2+}(aq)}$;

(b) $Cr(H_2O)_5Cl^{2+}$ also aquates very slowly and moreover is known to be thermodynamically unstable relative to $[Cr(H_2O)_6^{3+} + Cl^-]$ under the experimental conditions. Thus it can be concluded that the bond between Cl^- and the chromium center is established before the latter is oxidized (the aqua chromium(II) species is know to undergo substitution readily). The possibility of the sequence of outer-sphere reactions in Scheme 3 needs to be considered, but is fully discounted by the observation that when the reaction takes place in the presence of free radioactive chloride, virtually none is incorporated into the product $Cr(H_2O)_5Cl^{2+}$. Moreover, this alternative reaction scheme implies that the reaction is strongly autocatalytic, and thus this particular outer-sphere formulation could also be eliminated by a kinetic study. The tracer experiment, however, is more direct and decisive.

$$5H^+ + Cr(H_2O)_6^{2+} + Co(NH_3)_5Cl^{2+} \longrightarrow Cr(H_2O)_6^{3+} + Co(H_2O)_6^{2+} + 5NH_4^+ + Cl^-$$

$$Cr(H_2O)_6^{2+} + Cl^- \rightleftharpoons Cr(H_2O)_5Cl^+ + H_2O$$

$$5H^+ + Cr(H_2O)_5Cl^+ + Co(NH_3)_5Cl^{2+} \longrightarrow Cr(H_2O)_5Cl^{2+} + Co(H_2O)_6^{2+} + 5NH_4^+ + Cl^-$$

Scheme 3

For there to be net transfer of a ligand requires that several conditions be met, not all of which were explicitly mentioned in the foregoing. One partner must be substitution inert and the other labile, and after reaction the metal centers reverse roles with respect to substitution rates. The electronic structures of the partners in the example offered, πd^6 for Co^{III} and $\pi d^3\sigma^1$ for Cr^{II}, ensure that the substitution pattern called for is realized. On being oxidized, Cr^{II} loses its sole antibonding electron, while the cobalt center on being reduced assumes its first antibonding electron (there is eventually a rearrangement of Co^{II} to the high spin state). It is also essential to the success of this kind of experiment that the primary products of the reaction are not reorganized during its course. This is always a concern when Cr^{II} is a reactant because Cr^{II} can reduce Cr^{III} complexes readily. Thus, were $Cr(H_2O)_4Cl_2^+$ a primary reaction product, unless the oxidant in the particular system under study consumes Cr^{II} very rapidly, we would need to take into account the secondary process (equation 78). The reaction (equation 79) which can occur by an outer-sphere path, or by an inner-sphere with OH^- as bridging ligand, and which might have vitiated the $Co(NH_3)_5Cl^{2+}$ + Cr^{2+}(aq) experiment, is fortunately very slow in acidic solution.[107]

$$Cr(H_2O)_4Cl_2^+ + Cr(H_2O)_6^{2+} \longrightarrow Cr(H_2O)_6^{2+} + Cl^- + Cr(H_2O)_5Cl^{2+} \tag{78}$$

$$Cr(H_2O)_5Cl^{2+} + Cr(H_2O)_6^{2+} \longrightarrow Cr(H_2O)_6^{2+} + Cl^- + Cr(H_2O)_6^{3+} \tag{79}$$

In the $Co(NH_3)_5Cl^{2+} + Cr(H_2O)_6^{2+}$ system, the Co^{III} reactant and Cr^{III} products undergo substitution so slowly that quite ordinary procedures can be used for reagent handling and product identification. Such procedures have sufficed to demonstrate the inner-sphere mechanism also for complexes of Cr^{III},[106,107,110–112] Ru^{III},[113,114] Rh^{III}[115] and Pt^{IV}[116,117] and undoubtedly also for others. When organometallic complexes are considered, the list can be expanded greatly.[118] Most of the potential oxidizing agents of this kind conform to the $18e^-$ rule, so that when an electron is adopted, it is antibonding in character and will labilize a ligand. Often there is the additional complication that to reach the stable state of lower oxidation number, a second electron must be added so that were $Cr(H_2O)_6^{2+}$ used as reductant, only one of every two Cr^{III} products would bear the bridging ligand. Just this situation is realized in the reduction of $Pt(NH_3)_5Cl^{3+}$ by $Cr(H_2O)_6^{2+}$ where $Cr(H_2O)_5Cl^{2+}$ and $Cr(H_2O)_6^{3+}$ are formed in equal amounts.[116]

The reducing agents $Co(CN)_5^{3-}$ and Co(dimethylglyoximate)$_2$(H_2O)$_2$ are both low-spin d^7 systems, and thus, as is true also of $Cr(H_2O)_6^{2+}$, one electron is antibonding (note that $Co(CN)_5^{3-}$ has a reduced coordination number because of the antibonding effect of one of the seven electrons). Each of these exhibits the capture properties of Cr^{2+}(aq), and an inner-sphere activated complex provides the reaction path for many oxidation reactions of these species.[119,120] Even when the electron given up by the reducing agent is not antibonding, there is usually a marked decrease in lability when the metal center is oxidized. Thus, the rate of aquation of $[Ru(NH_3)_5Cl]$ decreases[121,122] by a factor of about 10^6 when ruthenium is oxidized from the 2+ to the 3+ state. Advantage has been taken of this general tendency in demonstrating an inner-sphere mechanism for the oxidation of $Fe(CN)_5(OH_2)^{3-}$ by $Co(NH_3)_5$(4,4′-bipy)$^{3+}$.[123]

An inner-sphere mechanism has to date not been demonstrated for $Ru(NH_3)_5(OH_2)^{2+}$ as reducing agent. As has already been noted for Cl^-, all saturated ligands (but not all unsaturated ones) are displaced much more slowly when $Ru^{II}(NH_3)_5L$ is oxidized, so a system in which $Ru(NH_3)_5(OH_2)^{2+}$ is oxidized by an inner-sphere mechanism can undoubtedly be devised. (There is, however, a limitation on the choice of system. If the oxidizing agent can accept an electron in a πd orbital, the dominant reaction path will almost invariably be of the outer-sphere type.) There is no real incentive to search for such a case because the demonstration that $Ru(NH_3)_5Cl^{2+}$ reacts with $Cr(H_2O)_6^{2+}$ to produce $Ru(NH_3)_5(OH_2)^{2+}$ and $Cr(H_2O)_5Cl^{2+}$ as the major eventual products demonstrates an inner-sphere path for the forward reaction, and this of course requires that the reverse reaction takes place by the same kind of path.

The timescale on which the observations can be made has been much shortened by resorting to rapid mixing techniques and resorting also to techniques capable of detecting transient intermediate products, so that metal centers ordinarily considered to be labile have been added to the roster of those known to react by inner-sphere mechanisms. Some examples follow. In the presence of $Cr(H_2O)_6^{2+}$ at reasonable concentrations, the half-life of any of the Fe^{III} species present in a mixture of $Fe(H_2O)_6^{3+}$ and $FeCl^{2+}(aq)$ is so short that there is little reorganization of the Fe^{III} species during reaction. Thus, the rate at which $Cr(H_2O)_6^{2+}$ is consumed in such a mixture depends on whether the $Fe^{III}-Cl^-$ mixture has been given time to equilibrate before mixing with $Cr(H_2O)_6^{2+}$, and the product distribution $[Cr(H_2O)_6^{3+}$ *vs.* $Cr(H_2O)_5Cl^{2+}]$ is also sensitive to this variable. Advantage has been taken of this to identify four reaction paths in this system: $k_1[FeCl^{2+}][Cr^{2+}]$; $k_2[Fe^{3+}][Cr^{2+}]$; $k_3[FeOH^{2+}][Cr^{2+}]$; and $k_4[Fe^{3+}][Cr^{2+}][Cl^-]$. At 25 °C and $\mu = 1.00$ M, $k_1 = 2 \times 10^7$ $M^{-1}\,s^{-1}$; $k_2 = 2.3 \times 10^3\ M^{-1}\,s^{-1}$; $k_3 = 3.3 \times 10^6\ M^{-1}\,s^{-1}$; and $k_4 = 2.2 \times 10^4\ M^{-2}\,s^{-1}$.[124] Allowance can also be made in non-equilibrated mixtures of $Fe(H_2O)_6^{3+}$ and Cl^- for the path $k_5[Fe^{3+}][Cl^-]$ by using the known value[125] of the rate formation of $FeCl^{2+}(aq)$ from $Fe(H_2O)_6^{3+}$ [note that $FeCl^{2+}(aq)$ is scavenged very rapidly by $Cr(H_2O)_6^{2+}$; hence the form of the rate law]. The reaction of $FeCl^{2+}(aq)$ with $Cr(H_2O)_6^{2+}$ produces $Cr(H_2O)_5Cl^{2+}$ almost quantitatively, but the chloro complex is produced also by the k_4 path. We can conclude that the k_1 path involves an inner-sphere activated complex, and leave open the issue of the mechanism for the k_2, k_3 and k_4 paths.

In another early example, net ligand transfer was demonstrated,[126] but now to a quite labile oxidized product. The reaction of $V(H_2O)_6^{2+}$ with *cis*-$Co(en)_2(N_3)_2^+$ is rapid enough so that the formation of $V(H_2O)_5(N_3)^{2+}$ could be observed as well as its subsequent aquation to $V(H_2O)_6^{3+}$ + N_3^-.

In all of the examples which have been discussed, ligand transfer takes place from the oxidizing to the reducing agent. It was early recognized[106] that this is not an essential concomitant of an inner sphere reaction path but rather is a consequence of the pattern of substitution labilities of the reactants and products. In principle, ligand transfer from reducing agent to oxidizing agent can also be realized but the experimental demonstration requires that the oxidized member of each of the two couples be more labile than the reduced. Such an inversion of labilities should be encountered for a one-electron couple in which the oxidized member has the electronic structure πd^2. In fact, at 25 °C the rate of oxygen exchange between water and $V(H_2O)_6^{3+}$ is about tenfold greater[127,128] than between $V(H_2O)_6^{2+}$ and water.[129] However, a serious problem is that because of the high lability, characterization of the immediate reduced product would be difficult for any metal ion with a $(d\pi)^3$ electronic structure when the oxidation state is 2+ or lower.

There does, however, seen to be a high possibility that ligand transfer from reducing agent to the oxidant does take place in the oxidation of isopropanol by Cr^{VI}. It should be noted that $R_2C{=}O/RCH(OH)R$ is an example of a couple in which the oxidized member is more labile than the reduced (C—O bond cleavage). The first step of the redox change is taken to result in a complex of Cr^{IV} and Me_2CO from the ester as an intermediate.[130] In the aquation of this complex it is quite likely that oxygen originating in the alcohol remains on Cr^{IV}. Were Mn^{2+}, which is known to reduce Cr^{IV} rapidly, added to the reaction system, it is likely that the alcohol-oxygen would be found in the product $Cr(H_2O)_6^{3+}$.

An unambiguous demonstration of an inner-sphere mechanism, even in the absence of net ligand transfer, is possible in the following general reaction scheme (Scheme 4). A clearcut example is afforded[114] by the system $Cr(H_2O)_6^{2+}$ + $[Ru(NH_3)_5isn]^{3+}$ (where the heteroligand isonicotinamide is N-bound). On mixing the two reagents, a rapid reaction ensues, producing a highly colored species which on a much longer timescale reacts to form $[Ru(NH_3)_5isn]^{2+}$ and $Cr(H_2O)_6^{3+}$. There is no net transfer of ligand from oxidant to reductant, but it is clear from the evidence that an isonicotinamide-to-chromium bond is established in the course of the reaction. The chemistry of this system differs from those with Cr^{III} or Co^{III} as oxidants in two respects: (i) in the profiles of potential energy plotted against reaction coordinate (see Figure 9); (ii) in that when the successor complex aquates (dissociates), the bridging ligand is released from the oxidized, rather than from the reduced, metal center. These differences in no way affect the electron transfer act itself. In both (a) and (b) of Figure 9 the precursor complex is in labile equilibrium with the reactants, and if the rate is defined in terms of consumption of reactants rather than formation of final products, in each case $k_{redox} = K_r k_{et}$, where K_r is the equilibrium quotient for the formation of the precursor complex and k_{et} is the specific rate at which the precursor is converted to the successor complex.

Reactants $\rightleftharpoons$ Precursor complex $\longrightarrow$ Activated complex $\longrightarrow$ Successor complex $\longrightarrow$ Products

Scheme 4

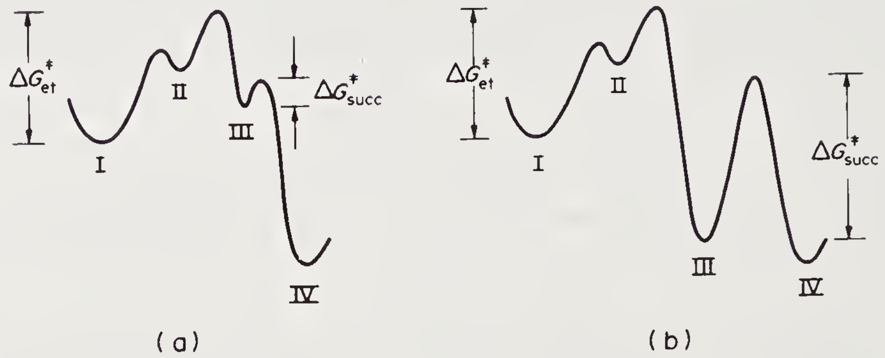

Figure 9 I, II, III and IV represent reactants, precursor complex, successor complex and products, respectively. In (a), ΔG^{+}_{succ}, the activation free energy for the successor complex changing to products, is much less than ΔG^{+}_{et}, the activation enthalpy for the relocation of charge. In (b) the reverse is true

Implicit in the foregoing is the assumption that the oxidation states can be assigned with certainty in the binuclear intermediate, and this issue will now be considered explicitly. In the present case, a strong item of evidence is that the $\pi^* \leftarrow \pi d$ absorption, characteristic of the Ru^{II}–heterocycle, is observed in the successor complex; an Ru^{III}–heterocycle shows no absorption in the same region of the spectrum. The *d–d* absorption characteristic of Cr^{III} in an oxygen environment is also observed. Finally, the rate of aquation at the chromium center is characteristic of the Cr^{III} state.

In the majority of the cases in which successor complexes have been identified, the reducing agent contains a single antibonding (σ) electron, and the oxidizing center has no antibonding electrons and has the πd levels not quite fully occupied. This provides for slow substitution at each center following electron transfer. Moreover, the symmetry mismatch in the metal donor and acceptor orbitals ensures that in the product there will be little electron delocalization between the metal centers so that the assignment of oxidation state is unambiguous.

It needs to be borne in mind, however, that the subsequent chemistry of the successor complex can be complicated by the operation of the equilibrium shown in equation (80). In the present instance the Ru^{II}–Cr^{III} state is favored so strongly that the rate of aquation of the Cr^{III}—$L'\cdots$ bond is characteristic of Cr^{III}, and there is no need to invoke a path through the $Cr^{II}L'\cdots$ state. For the aquation path through the Ru^{III}–Cr^{II} excited state to compete with aquation at Cr^{III} in the ground state, it is of course necessary that $Cr(H_2O)_6^{2+}$ react with the Cr^{III} complex at least in small part by an outer-sphere mechanism. This will of course be true in general though this fraction may be extremely small. The rate of the outer sphere reaction can be assessed by modifying the heteroligand just enough so that it loses the capacity to serve as a bridge. For the systems studied by Gaunder *et al.*[114] the inner sphere rate is about 150 times the outer sphere.

$$Ru^{II}L\cdots L'Cr^{III} \qquad Ru^{III}L\cdots L'Cr^{II} \tag{80}$$

Successor complexes are expected to be difficult to observe when the oxidant is a σ-electron acceptor, regardless of whether the reducing agent gives up a σ- or π-electron, because of the great lability of the reduced metal center–bridging ligand bond. Also, for the π-donor–π-acceptor case they will be encountered very infrequently because of the tendency such systems have to react by outer-sphere mechanisms. For any species of the latter type which might be formed, the problem of unique assignment of oxidation states is more difficult than it is for the σ-donor–π-acceptor case. Species of this kind which have been prepared not by electron transfer but by indirect means have in fact been studied in considerable detail[83] under the rubric 'mixed valence molecules' and a central issue for each such system,[131,16] where donor and acceptor orbitals have the same symmetry, is to discover whether the molecule is valence trapped or fully delocalized.

In view of the discussion just previous, it is natural to inquire into the circumstances under which the investigation of precursor complexes might lead to an assignment of inner-sphere *vs.* outer-sphere mechanism. The issue is not independent of the previous discussion because the successor complex for the forward reaction is the precursor complex for the reverse. If the reaction mechanism has been defined for the forward direction, it is defined also for that portion of the reverse reaction which makes use of the same path. But in terms of the experimental criteria which are applicable, basing evidence on precursor complexes is different from basing it on successor complexes.

When the precursor complex is in labile equilibrium with the reactants and, as is usual, is present in low concentrations, it is difficult to demonstrate its intervention by any direct means. In some cases, the earliest example[132] of which involves the reduction by $Fe(H_2O)_6^{2+}$ of $(NH_3)_5Co^{III}\{O_2CCH_2N(CH_2CO_2)_2\}$, there is strong complexing of the reducing agent by the Co^{III} complex. In this system the rate of reaction becomes independent of $[Fe^{2+}]$ as this concentration is raised at constant $[Co^{III}]$, behaviour which can reasonably be ascribed to the rapid conversion of all of the Co^{III} to the complex with Fe^{2+}. In general, if the complex is in labile equilibrium with the reactants, the possibility that the precursor complex has a quite different structure from the dominant form must be considered — the kinetic data do not distinguish between the rate formulation $k[Co^{III}L{\cdot}Fe^{II}]$ and $k'[Co^{III}L][Fe^{II}]$, where the latter can be taken to imply outer-sphere attack by Fe^{2+} on the oxidant. In systems such as these, a convincing conclusion can still be reached by arguments based on suitable blank experiments. In the present case, the rate of reaction cannot be accounted for unless, in the activated complex, advantage is taken of the great stabilization by the chelating function of Fe^{III} over Fe^{II}, thus increasing the driving force for the reaction. An experimental strategy which can be brought to bear is to modify the complexing ligand slightly, but enough to destroy its complexing power, then to investigate the rate corresponding to the k' path. The data thus generated together with the equilibrium quotient for complex formation can answer the question of whether the kinetically equivalent outer-sphere path can account for the rate. This strategy has also been used in the investigation of the $Ru(NH_3)_5(NC_5H_5CH{=}CH_2)^{3+} + Cu^+$ system,[133] where Cu^+ is known to be bound strongly to the double bond, and where the totality of the evidence strongly supports the conclusion that this complex is, in effect, the precursor to electron transfer.

When the formation of the precursor complex involves substitution at one of the centers, the possibility arises that the formation of the precursor is the slow step in the general sequence. It is believed that just this situation has been encountered in many reactions in which $V(H_2O)_6^{2+}$ is the reducing agent, and the evidence in support is so powerful as to be convincing. For the reactions in question, rates vary but little as the oxidizing agent is changed. Moreover, the kinetic parameters, $k \approx 2 \times 10\ M^{-1}\ s^{-1}$, $\Delta H^{\neq} = 50 \pm 4\ kJ\ mol^{-1}$, $-\Delta S^{\neq} = 59 \pm 17\ J\ deg^{-1}\ mol^{-1}$, conform to those for substitution on $V(H_2O)_6^{2+}$, and not to those observed when electron transfer is also partly rate determining. In particular, for reactants of the charge type under consideration, $\Delta S^{\neq}$ in the latter case tends to be more negative by *ca.* 42 J $deg^{-1}\ mol^{-1}$.[134]

In the examples just considered with $V(H_2O)_6^{2+}$ as reductant, the conclusion that the major reaction path in each of the systems is of the inner-sphere type rests solely on kinetic arguments. There are a number of additional situations,[98] a few of which will be considered, in which arguments of this kind suffice to the same end. It should be acknowledged that they seldom lead to conclusions that are as refined as is possible when ligand transfer is observed. In the general case, parallel inner- and outer-sphere paths must be considered, and when the more direct criteria are used, the relative contributions can frequently be quantified. For example, when $Co(NH_3)_5\{NC_5H_5C(NH_2){=}O\}^{3+}$ reacts with $Cr(H_2O)_6^{2+}$, ligand transfer is virtually complete, but when the *meta* isomer is used, only 70% of the ligand released by the cobalt complex is transferred to chromium, and it can therefore reasonably be assumed that the remainder reflects reaction by an inner-sphere path.[135] To be scrupulous in appraising the work which has been cited, the possibility that the ligand released in the outer-sphere path is reincorporated into the Cr^{III} product by the other path must be taken into account. This would not affect the general conclusions, only the quantitative assignment of reaction paths based on product analysis. Although this possibility was not considered by the authors, it can be discounted because the kinetics do not admit of this kind of complication.

To continue with arguments based on kinetics: the rate law for the reaction[136,137] of $Cr^{2+}(aq)$ with $V(H_2O)_6^{3+}$ is equation (81). A simple interpretation of this form of the rate law is that one of the reaction partners undergoes proton dissociation, and in this case b would be identified with the dissociation constant. This interpretation of the rate law can be dismissed because the value of b is too large to answer even for K_D of the more acidic partner. The alternative general interpretation is that the reaction involves two activated complexes of different compositions, and though the order in which they appear in the reaction sequence is not specified by the rate law (an important point recognized by Haim, and dealt with him by him in detail[138]) this particular issue does not affect the validity of the conclusions which will be reached on the matter of whether an inner- or outer-sphere path operates. Each mechanism requires an intermediate to be formed which contains one V, one Cr, less one proton and which has a charge of 4+. The values of the specific rates and specific rates ratios which follow from the experimental rate law are quite unrealistic if the intermediate involves simple outer-sphere association of the reaction partners, but are compatible with an inner-sphere mechanism. A second, but somewhat less cogent, argument is that on the basis of an outer-sphere mechanism it is difficult to justify an inverse dependence of the rate on $[H^+]$. Generally, in an outer-sphere mechanism a reducing agent reacts more rapidly with the intact form of an aquo oxidant than with the deprotonated form in equilibrium with it, due to the difference in driving force.

$$d[V(H_2O)_6^{2+}]/dt = \frac{a}{b+[H^+]}[V(H_2O)_6^{3+}][Cr^{2+}] \tag{81}$$

Perhaps the most generally applicable of the less direct methods for classifying mechanisms is based on establishing rate patterns for reactions in which mechanisms can be assigned without ambiguity, and then bringing this knowledge to bear on systems which are not amenable to the application of direct criteria. Many and varied tests of this kind have been made, and have proven to be instructive. The subject is reviewed thoroughly by Pennington[7] and here only a few examples will be introduced by way of illustration.

One such approach has already been mentioned, namely to compare the rate at which a reducing agent acts on an oxidizing agent with the rate at which it acts on the deprotonated form. As an extreme case of the rate difference, we may compare the rate for $Cr(H_2O)_6^{2+}$ on $Cr(H_2O)_5OH^{2+}$ ($0.7\ M^{-1}\ s^{-1}$)[139,140] with that on $Cr(H_2O)_6^{3+}$ ($\sim 5 \times 10^{-10}\ M^{-1}\ s^{-1}$)[141] where the great advantage of OH^- over H_2O as a bridging group is revealed (factor exceeds 10^9). By contrast, in the oxidation of $Ru(NH_3)_6^{2+}$, which, because of the substitution inertia of the complex, is constrained to an outer-sphere path, invariably the reaction with the intact form of an oxidant is more rapid than with the deprotonated, *e.g.* $4.2 \times 10^5\ M^{-1}\ s^{-1}$ and $5 \times 10^4\ M^{-1}\ s^{-1}$ (25 °C, $\mu = 0.10$ M) with $Fe(H_2O)_6^{3+}$ and $Fe(H_2O)_5OH^{2+}$ respectively.[142] The ready qualitative interpretation of the rate comparison in this system is that the driving force for the latter process is less than that for the former, and this alone can account for the rate difference. A more detailed analysis requires that account also be taken of the differences in self-exchange rates for the two couples and for the differences in the work terms. Furthermore, if the reducing agent were $Ru(NH_3)_5(H_2O)^{2+}$, the rate law $k[Fe(H_2O)_6^{3+}]$-$[Ru(NH_3)_5OH^+]$ which is kinetically equivalent to $k'[Fe(H_2O)_5OH^{2+}][Ru(NH_3)_5(OH_2)^{2+}]$ would need to be taken into account. Note that the driving force for the k path is greater than for the k' path as well as for the path $k''[Fe(H_2O)_6^{3+}][Ru(NH_3)_5(OH_2)^{2+}]$. It should be noted that the k and k' paths can be taken to imply different activated complexes because in one case $Fe(H_2O)_6^{2+}$ + $Ru(NH_3)_5OH^{2+}$ are the immediate products of the electron transfer act, and in the other, $Fe(H_2O)_5OH^+$ + $Ru(NH_3)_5(OH_2)^{3+}$. Because in general only a fraction of any change in driving force is reflected in the rate, the k' path, which has the higher concentration product, fully reflecting the difference in ground state stability, will be favored.

The above is a single example of a large number of comparisons which can be made of ligands which in an inner-sphere mechanism play a bridging role but which in an outer-sphere mechanism play a quite different role. Other possibilities for defining rate patterns when mechanisms can unambiguously be assigned are: (a) varying the non-bridging ligands for substitution-inert oxidants; (b) studying the rates of reduction of substitution-inert oxidants by labile reductants in the presence of complexing ligands (here again experiments using a reducing agent such as $Cr(H_2O)_6^{2+}$ which has 'capture' properties can be particularly revealing); and (c) using robust reducing agents such as $Ru(NH_3)_6^{2+}$ in reaction with labile oxidants in the presence of complexing agents. To get the most of the studies under (b) and (c) it is important to distinguish the effects exerted by the ligands when they are directly bound to reacting centers from those exerted in an outer-sphere mode. Two situations come to mind in which such a separation of the effects is possible. When the reducing agent has the 'capture' property already referred to, the product distribution can be used to ascertain whether the inner-sphere path accounts for the full rate participation of the potential complexing ligands. When both reaction partners are substitution inert, the free ligand effects are perforce of the outer-sphere type.

In concluding this section it is proper to ask whether the effort devoted to the simple classification of mechanism is worthwhile. The question answers itself: to the extent that observations lead to a distinction of mechanism, that distinction is obviously significant. The different types of mechanisms imply different kinetic patterns and, moreover, have associated with them different types of chemistry. That encountered in the inner-sphere mechanisms is particularly rich. It has been only partially developed in the foregoing, and will be further elaborated on somewhat later.

It is important to bear in mind that the central issue is always that of defining the nature of the activated complex, and the exercise which has been gone through on the simple classification of mechanism carries us part way to the goal, and then only in certain cases. No matter what definition of inner-sphere *vs.* outer-sphere is adopted, it is highly unlikely that each activated complex will fit neatly into one of the alternative categories. Consider for example the definition of an inner-sphere activated complex as one in which each metal center makes a bond to a common bridging group. There is no difficulty with this definition in the case of $Cr(H_2O)_6^{2+}$ as the reducing agent, if the coordination number of Cr^{II} is taken to be six, *i.e.* the axial ligands are regarded as being bound to Cr^{II} even though they lie at a much greater distance than do the equatorial ligands. In effect, we have defined, perhaps arbitrarily, what we mean by a bond. But suppose $Cr(H_2O)_6^{2+}$ were actually a square planar molecule. The question of 'bound' ligands in the axial positions is now much more difficult to deal with. Still, even in this case, were ligand transfer from oxidant observed in the oxidation reaction, one would argue that since the fifth and sixth ligands become bound in the course of the overall change, a partial bond is established in the activated complex.

Now let us carry the kind of issue raised here over to cases involving oxidation of octahedrally coordinated reducing agents, and choose the examples of $V(H_2O)_6^{2+}$ and $Ru(H_2O)_6^{2+}$. When $V(H_2O)_6^{2+}$ is acted on by a 1e⁻ oxidant, a possible mechanism for reaction is attack at the face of an octahedron, and in principle an electron removed in the act of oxidation can be replaced by a ligand, leading to an intermediate of coordination number seven. The issue of whether the bridging group on the oxidant makes a bond to the vanadium in the activated complex is analogous to that raised earlier for a square planar 1e⁻ reductant. Suppose a similar mechanism obtains for the 1e⁻ oxidation of $Ru(H_2O)_6^{2+}$. In this case an electron is still left in an orbital which is antibonding to the entry of a polar group derived from the oxidant, and it is quite unlikely that an intermediate of coordination number seven would ever be observed. In this case it is idle to argue about whether the mechanism should be classified as inner-sphere or outer-sphere, in particular because if the intimate details of the geometry of the activated complex for many of the outer-sphere reactions were known, they might well conform to the description which has been given of the 1e⁻ oxidation of $Ru(NH_3)_6^{2+}$. Whether the reaction is classified as inner-sphere or outer-sphere would depend on an arbitrary definition of what could be considered to be a bond.

A further caveat on the use of the inner-sphere/outer-sphere classification needs to be introduced. It has been tacitly assumed in the foregoing that the bridging group plays a specific role in the act of electron transfer, that is in providing electronic coupling between the metal centers. In work now in progress on intramolecular electron transfer, numerous examples have been encountered[143–145] in which the bridging group serves only to keep the reagents in proximity. To illustrate with a contrived example, consider electron transfer in the species $[(TEPA)Co^{III}-NH_2(CH_2)_4NH_2-Ru^{II}(TEPA)]^{5+}$ where TEPA is tetraethylenepentaammine. We can be rather certain in this case that the bridging group serves only to enhance the probability of encounter in a mode which would unambiguously be described as outer sphere were the two centers free to move independently of one another.

7.2.9.2.2 *Detailed description of a selected system*

As has already been acknowledged, classifying a reaction mechanism as inner sphere only advances us part way to the goal of defining the nature of the activated complex. In this section the most thoroughly studied reaction of the inner-sphere class is chosen for description and discussion so as to indicate some of the additional issues which can profitably be addressed.

The net change to be considered is shown in equation (82). Unfortunately, the early history of research on this reaction is marred by two serious errors, one in interpretation of evidence, the other in quality of evidence. As to the first error, the dominant term in the rate law was correctly identified as $k[Co(NH_3)_5(H_2O)^{3+}][Cr^{2+}]/[H^+]$ in the early work, but a contribution by the path $k'[Co(NH_3)_5(H_2O)^{3+}][Cr^{2+}]$ was also claimed.[146] In view of the oxygen tracer experiments which showed that oxygen transfer[147,148] from Co^{III} to Cr^{II} is virtually complete, participation by the k' path to the extent claimed would have been proof that water does act as a bridging ligand. Later work[149] showed that the k' path is an artifact arising from the changes in activity coefficients in mixtures at constant ionic strength as $NaClO_4$ is replaced by $HClO_4$; or at any rate, it showed that the putative k' path disappears when $LiClO_4$ is used to replace $HClO_4$ at constant ionic strength. Thus all the claims in the earlier literature bearing on the properties of the k' path are to be disregarded.

$$5H_2O + Co(NH_3)_5H_2O^{3+} + Cr(H_2O)_6^{2+} + 5H^+ \rightleftharpoons Co(H_2O)_6^{2+} + Cr(H_2O)_6^{3+} + NH_4^+ \qquad (82)$$

The form of the rate law for the major path for the reaction shows that the activated complex has one less proton than $[Co(NH_3)_5(H_2O)^{3+}\cdot Cr(H_2O)_6^{2+}]$, and in view of the demonstrated[149] inefficiency of H_2O as a bridging group, the most reasonable assumption is that the proton is lost from the water molecule in Co^{III}, *i.e.* OH^- serves as the bridging group. That transfer is complete[148] provides support for, but not proof of, the view that in making a bond to the bridging OH^-, a normal coordination position on Cr^{II} is being engaged. Were attack taking place at an octahedral face, an intermediate product of formula $Cr(H_2O)_6{}^{3+}$ might be expected, with loss of some labeled oxygen to the solvent when the final product is formed.

Kinetic isotopic effects also help in defining the activated complex for reaction. The kinetic isotopic effect $d\ln(H_2{}^{16}O)/d\ln(H_2{}^{18}O)$ for the oxygen bound to Co^{III} has been determined[147] as 1.043, and as 1.056 in a later study.[150] There is a contribution to the overall isotope effect from the proton dissociation equilibrium. The dissociation quotient for $H_2{}^{16}O$ as a ligand on Co^{III} compared with $H_2{}^{18}O$ has been measured[151] as 1.009, which then leaves the kinetic isotopic effect for breaking the Co^{III}—OH^- bond as $\geqslant 1.034$. Considering that the Co^{III}—OH^- frequencies are low, this is a large such effect, and the result demonstrates that stretching the Co^{III}—OH^- bond is an important feature of the activation process. By contrast, the nitrogen kinetic isotopic effect is small, $d\ln(N^{14})/d\ln(N^{15}) \approx 1.004 \pm 0.001$, irrespective of whether nitrogen is in positions *cis* or *trans* to the bridging group.[152] It appears to be even smaller for the reduction of $Co(NH_3)_5Cl^{2+}$, and the small values suggest that there are only small dislocations of the pentaammine moiety when $Co(NH_3)_5OH^{2+}$ or $Co(NH_3)_5Cl^{2+}$ is being reduced by Cr^{2+}. This cannot be taken as applying in all cases, and in fact isotopic fractionation studies on the reduction of some Cr^{III} complexes show a significant *trans* effect; thus $d\ln(^{16}O)/d\ln(^{18}O)$ for the reduction of *trans*-$Cr(NH_3)_4(H_2O)Cl^{2+}$ is reported as 1.017 while for the *cis* isomer a value of 1.007 is recorded.[153]

Since kinetic isotope effects, important though they are for defining the nature of activated complexes, are not considered in detail elsewhere, it seems worthwhile to deal with them further, even if this is a digression from the present theme. The kinetic isotope effect, $d\ln(^{16}O)/d\ln(^{18})O$, for $Ru(NH_3)_6{}^{2+}$ (which perforce acts as an outer-sphere reducing agent) acting on $Co(NH_3)_5OH^{2+}$ is 1.019, much lower than for $Cr(H_2O)_6{}^{2+}$. For $Ru(NH_3)_6{}^{2+}$, V^{2+} and Eu^{2+} acting on $Co(NH_3)_5(OH_2)^{3+}$ (acid independent paths), it is reported[150] as 1.021, 1.020 and 1.019, results which suggest that all three reducing agents act by a common mechanism, taken to be outer sphere because $Ru(NH_3)_6{}^{2+}$ is among the reducing agents.

An interest in H–D kinetic isotope effects for the diagnosis of mechanism dates back to the work of Hudis and Dodson,[154] who recorded a rate decrease by a factor of *ca.* 2.0 for the $Fe(H_2O)_6{}^{3+}/Fe(H_2O)_6{}^{2+}$ self-exchange when D_2O is substituted for H_2O as solvent. This factor is composite and includes effects contributed in the first coordination spheres of both partners by the solvent and, if the reaction is inner sphere, by H_2O acting as a bridging group. Zwickel and Taube[146] reported that the rate of reduction of aquapentaamminecobalt(III) by $Cr(H_2O)_6{}^{2+}$ decreases by a factor of 3.8 when D_2O replaces H_2O as solvent. It should be noted that in these experiments the ammine ligands remain protonated (a single experiment was done with deuterated amminecobalt(III) in D_2O, for which no significant effect was reported). The factor of 3.8 includes the isotope effect on the proton dissociation equilibrium, the effect of replacing H_2O by D_2O on Cr^{II}, and a general solvent isotope effect as well as the kinetic isotopic effect for OD^- replacing OH^- as a bridging group. The dissociation constant of the oxidant decreases[155] by a factor of 3.0 when D_2O rather than H_2O is the reactive medium. This leaves a factor of 1.3 as attributable to all other effects, including the change in bridging group from OH^- to OD^-. It is rather astonishing that this factor is no greater than that reported for the reaction of $Cr(NH_3)_5Cl^{2+}$ with Cr^{2+} in which Cl^- is now the bridging group.[110] The H–D isotope effect attending replacing the ammine protons in the oxidant by deuterons was measured by Itzkowitz and Nordmeyer[156] as a rate decrease of 1.54, in apparent conflict with the result reported by Zwickel and Taube.[146] It must be kept in mind that the earlier experiment by Zwickel and Taube was done using deuterated solvent, while Itzkowitz and Nordmeyer used ordinary water. The possibility remains that replacing H_2O by D_2O in the first coordination sphere of Cr^{2+} causes a rate increase by a factor of about 1.5, through it does seem more likely that the single result given in ref. 146 is simply in error.

Despite the errors which were made in the isotopic work described, taken as a whole it illustrates the power of kinetic isotope effects in defining the bond-breaking pattern in the activated complex for reaction. The central role played in the activation of the oxidant by Co^{III}—OH^- bond breaking is demonstrated, as is the lesser involvement of the auxiliary ligands, taken individually (though with five involved, the cumulative effect can be significant). Less well defined is the role of bond making at the reducing agent and of specific interest in this connection is the involvement of that molecule of water on Cr^{II} which is *trans* to the bridging group in the precursor complex. The kinetic isotopic results of DeChant and Hunt[153] on the reduction of Cr^{III} complexes suggest that this is an important feature when Cr^{2+} acts as a reducing agent, the *trans* ligand moving in toward the chromium center.

7.2.9.2.3 *Mechanism of electron transfer through bridging groups*

We have dealt thus far mainly with bridging ligands which involve electron transfer through a single atom. The possibility in redox reactions of electron transfer over extended bridging groups was a point of interest in this subject from early in its history, and was perhaps first encountered in experiments in which the self-exchange process (equation 83) was demonstrated.[157] In the light of later experience the only reasonable mechanism for the reaction appears to be an activated complex of geometry shown in (**6**). The first experiments with conjugated organic ligands were reported in 1955, where the possibility of electron transfer through the extended bond system, for example of the maleate group, was suggested.[158] Despite continuing interest in this kind of possibility, an unambiguous demonstration of this kind of mechanism was not offered until the reaction of pentaammineisonicotinamidecobalt(III) [note, the pyridine nitrogen is attached to cobalt(III)] with $Cr(H_2O)_6^{2+}$ was studied.[135,159] Though historically the motivation for this and much related research was to demonstrate electron transfer over large distances, whatever importance the results have or had derives more from the light they shed on the mechanism of electron transfer taken in another sense.

$$cis\text{-}Cr(H_2O)_4(N_3)_2^{+} + {}^*Cr(H_2O)_6^{2+} \rightleftharpoons Cr(H_2O)_6^{2+} + cis\text{-}{}^*Cr(H_2O)_4(N_3)_2^{+} \tag{83}$$

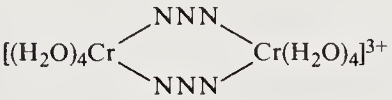

(**6**)

In trying to understand the differences in rates as the nature of the bridging group is changed, it is clearly important to distinguish between a so-called chemical mechanism in which electron transfer takes place stepwise (reaction 84 or 85) and resonance transfer in which electron transfer takes place directly from Cr^{II} to Co^{III} by a tunneling mechanism. For purposes of concrete illustration, we have chosen the redox system which has figured most prominently in the work in this area, work which did lead to the conclusion that the rapid rates observed for some systems in which L is a bifunctional conjugated organic molecule can be understood by invoking mechanism (84). Though in principle mechanism (85) is also possible, it has not yet been implicated in the $(NH_3)_5CoL^{2+}{-}Cr^{2+}$ reaction systems. The reason why is not difficult to find. Chromium(II) is a powerful reducing agent, powerful enough to reduce many conjugated organic molecules by a $1e^-$ change. On the other hand, $(NH_3)_5Co^{III}$ is a relatively weak oxidizing agent and has the capacity to oxidize but few organic ligands. In fact a demonstration of the inner-sphere mechanism as represented by equation (85) would be fraught with difficulty: were the ligand L easily oxidizable, the complex $(NH_3)_5Co^{III}L$ would itself likely be unstable.

$$(NH_3)_5Co^{III}\cdot L\cdot Cr^{II} \longrightarrow (NH_3)_5Co^{III}L^{-}\cdot Cr^{III} \longrightarrow Co^{II} + Cr^{III}L \tag{84}$$

$$(NH_3)_5Co^{III}\cdot L\cdot Cr^{II} \longrightarrow (NH_3)_5Co^{II}\cdot L^{+}\cdot Cr^{II} \longrightarrow Co^{II} + Cr^{III}L \tag{85}$$

Diverse lines of evidence support the conclusion that a chemical mechanism is operative in certain reactions of the type under consideration. In certain systems this evidence is quite direct.[160] Thus, when Cr^{2+} reacts with pentaammine-*O*-(pyrazinecarbonylato)cobalt(III), the first very rapid reaction phase ($k > 10^6$ M^{-1} s^{-1}) leads to a green intermediate which in a slower first-order process ($k = 4.5 \times 10^2$ s^{-1}) produces Co^{2+}(aq) and a Cr^{III} chelate of the new ligand. ESR measurements on the reaction mixture in a rapid flow apparatus show that the green intermediate is a radical cation.[161]

If, in the reduction of $(NH_3)_5Co^{III}L$, electron transfer to the ligand is rate determining, it is expected that the ligand, but with Co^{III} replaced by H^+, will be reduced at much the same rate. This test of mechanism has been applied[162] for *N*-bound isonicotinamide with Eu^{2+} as the reducing agent. The rates of reduction of $(NH_3)_5CoL^{3+}$ and HL^+ were found to be 0.83 ± 0.2 and 1.8 M^{-1}s^{-1} respectively, fully bearing out expectations based on a radical ion mechanism. The values of $E°$ for the Eu^{3+}/Eu^{2+} and HL^+/L couples are −0.43 and *ca.* −0.9 V respectively. The reduction of the radical product of the reaction of Eu^{2+} with HL^+ is apparently very rapid so that the first step, which is rate determining and catalyzed by $Cr(H_2O)_6^{2+}$, can also be followed,[135] whereupon the striking result emerges that the rate of reaction of Cr^{2+} with species (**7**) is only about tenfold faster than with the corresponding Cr^{III} complex (**8**) (the values of k are 17 M^{-1} s^{-1} and 1.8 M^{-1} s^{-1} respectively); with nonreducible bridging ligands such as OH^-, Cl^- or $MeCO_2^-$ the rate ratios are in excess of 10^4. A simple explanation for the insensitivity of the rate to the properties of the acceptor center is provided by the stepwise mechanism shown in Scheme 5. If k_2 is much greater than k_{-1}, k_{obs} reduces to k_1. Implicit in this interpretation is the assumption that for various tripositive ions of the same electronic structure type (as we shall see, this is an important caveat), k_1 will be constant, and in the limit when $k_2 \geqslant k_{-1}$, the rate will be independent of the nature of the reducing agent.

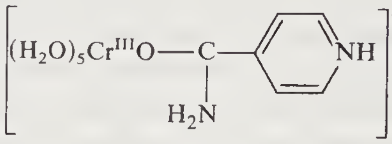

(7)

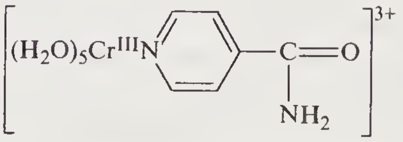

(8)

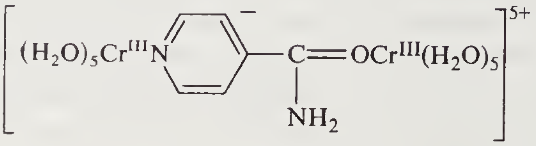

(9)

$$\text{Co}^{\text{III}}\cdot \text{L} + \text{Cr}^{2+} \underset{k_{-1}}{\overset{k_1}{\rightleftharpoons}} \text{Co}^{\text{III}}\text{L}^{-}\cdot \text{Cr}^{\text{III}}$$

$$k_{\text{obs}} = \frac{k_1 k_2}{k_{-1} + k_2}$$

$$\text{Co}^{\text{III}}\text{L}^{-}\cdot \text{Cr}^{\text{III}} \xrightarrow{k_2} \text{Products}$$

Scheme 5

Since the rate of reduction of the Cr^{III} complex is significantly slower than that of the Co^{III}, in the former case at least, the condition $k_2 \geqslant k_{-1}$ is not fulfilled. If we assume that k_1 is in fact the same for both systems, we calculate that in the intermediate **(9)** reduction by the radical ion of oxygen-bound Cr^{III} is ninefold faster than of nitrogen-bound. This is an altogether reasonable result because the ring nitrogen of isonicotinamide is more basic than the ammide oxygen and should provide for more stabilization of Cr^{III} over Cr^{II}.

The considerations of the last two paragraphs suggest a test of the radical-ion mechanism which has not yet been successfully applied. We will choose a symmetrical bridging ligand and will compare the rate of reduction by $Cr(H_2O)_6^{2+}$ of the complex with $(NH_3)_5Co^{3+}$ and with $(H_2O)_5Cr^{3+}$. If in the reduction of the cobalt complex the k_1 step is rate determining, we would expect the rate of reaction of $Cr(H_2O)_6^{2+}$ with the Cr^{III} complex to be one-half the rate with the Co^{III} complex to a degree of exactness determined by the constancy of k_1 in the two reactions. The rate of reaction of $(H_2O)_5Cr(O_2CHC{=}CCO_2H)^{2+}$ with $Cr(H_2O)_6^{2+}$ has in fact been measured (note that this is a self-exchange process), and the value of k is found[163] to be greater than it is for the reduction[164] of $(NH_3)_5Co(O_2CCH{=}CHCO_2H)$ by Cr^{2+}: *ca.* 3 $M^{-1}\,s^{-1}$ compared with 1.3. This surprising result can be understood if, as is suggested by other evidence, the major path for attack by Cr^{2+} is on the *endo* rather than *exo* carbonyl. This being so, the oxidizing and reducing centers are brought close together, and since the coordination spheres of Co^{II} and Cr^{III} are different, k_1 is not expected to be the same for the two cases. This complication would be avoided were a molecule such as 4,4′-bipyridyl the bridging group.

The evidence supporting the conclusion that the major reaction path for the reduction of $(NH_3)_5Co(O_2CCH{=}CHCO_2H)^{2+}$ by $Cr(H_2O)_6^{2+}$ involves attack at the *endo* rather than at the *exo* carboxyl[165] is that the rate is rather insensitive to modification of the remote end, being much the same for C(OH)O replaced by $C(NH_2)O$ or by C(OMe)O. If a radical-ion mechanism operates, the relative rates by the rival paths will be governed mainly by the relative concentration of the precursor complex, and while remote attack is favored on purely electrostatic grounds, the effect is not great at high ionic strength and may be more than compensated for by the greater basicity of the *endo* carboxyl – note that H^+ has a much stronger inductive effect than $(NH_3)_5Co^{3+}$. (There is in fact evidence that remote attack constitutes a significant though minor reaction path.[164]) The somewhat enhanced rate of reduction of $[(NH_3)_5Co(O_2CCH{=}CHCO_2H)]^{2+}$ compared with $[(NH_3)_5Co(O_2CMe)]^{2+}$ (1.3 *vs.* 0.35 $M^{-1}\,s^{-1}$)[165] therefore is a manifestation of what has been called the 'pendant group' effect.[166] An early, more straightforward example is afforded by the comparison of the rate of reduction by Cr^{2+} of $[(NH_3)_5Co(O_2CPh)]^{2+}$ and $[(NH_3)_5Co(O_2CC_5H_5NMe)]^{3+}$, where the latter is reduced eightfold more rapidly, despite the unfavorable electrostatic charge.[167] The 'pendant group' effect loses its air of mystery if a radical ion mechanism obtains. The higher rate for the *N*-methylpyridine derivative is simply a reflection of the fact that it is rather readily reduced.

In studies already referred to,[135,159] the rate of reduction by Cr^{2+} of the nicotinamide analog of the isonicotinamide complex of pentaamminecobalt(III) (species 7) referred to earlier was also measured. In contrast to the isonicotinamide case, a substantial fraction of the reaction now proceeds by a path producing $Cr(H_2O)_6^{3+}$ as product, and it is inferred that this represents outer-sphere reduction. The specific rates (25 °C, $\mu = 1.0$ M) for outer sphere (no ligand capture) and inner sphere (ligand capture) are 1.4×10^{-2} and 3.3×10^{-2} M^{-1} s^{-1} respectively. The latter rate, it should be noted, is about 500-fold slower than that observed for the isonicotinamide complex. A decision about the mechanism of electron transfer — whether by a resonance or stepwise process — is essential if the rate difference between the *para* and *meta* isomers is to be correctly interpreted. Since intermolecular rates are at issue, the relative concentrations of the precursor complexes will be a factor in determining the rates. It is unlikely that the difference arising from this cause will be large: probably no more than a factor of 5. If reaction is by resonance transfer, we would be bound to conclude that at least the slower reaction is not adiabatic, and the rate difference would be ascribed to a difference in electronic coupling between 1:4 and 1:3 positions, a not unreasonable position to take. The large difference noted here is at variance with that recorded for other cases where it is certain that a resonance mechanism operates.[168] If, as we believe, electron transfer is stepwise, we ascribe the rate difference mainly to a difference in ease of reduction of the two ligands. This is also a reasonable point of view because the π^* orbital will lie lower for the 1:4 than for the 1:3 isomer.

Also in this context, kinetic isotopic experiments have proved to be illuminating. A series of experiments was done[156] in which the rates of reduction of $(NH_3)_5Co^{III}L$ and $(ND_3)_5Co^{III}L$ were compared. For nonreducible ligands (pyridine, OH^-, CN^-, NCS^-, $MeCO_2^-$) the values of k_H/k_D lie in the range 1.34–1.5. For isonicotinamide and for 4-pyridinecarboxylate they are 1.1 ± 0.1 and 1.1 ± 0.02 respectively. In a stepwise mechanism and if k_1 (Scheme 5) is rate determining, the value of k_H/k_D is expected to be 1.0; if, on the other hand, electron transfer to the oxidizing center is direct, a difference in rate between the deuterated and isotopically normal complexes is not unexpected because the oxidizing center must prepare to accept the incoming electron. With fumarate as ligand, k_H/k_D is 1.26. This is quite in line with conclusions which have been reached earlier because a dual mechanism is expected here, a portion of the reaction proceeding by the same mechanism as observed for acetate, *i.e.* resonance transfer, and the remainder by the radical-ion mechanism. The kinetic isotope effects thus provide strong additional support for the two-stage mechanism.

What is the rate advantage of the two-step mechanism over direct reduction of the oxidant by Cr^{2+}? It probably derives from high self-exchange rates for the L/L^- couples. Any such couple, if it has a suitable value of $E°$ relative to the metal ion couples, can produce catalysis when, as is true in the present case, the self-exchange rates for the metal ion couples are low. In the direct reaction the intrinsic kinetic barriers for the two metal ion couples are compounded to make up the activation energy. In the catalyzed reaction the two barriers appear serially, and if the intrinsic barrier for the catalyst is very low, the resulting rate enhancement can be large. Gould and coworkers have shown that many organic radicals generated by metal reducing agents such as Cr^{2+} reduce Co^{III} very rapidly, and have demonstrated, for many systems, catalysis by external organic molecules of the reduction of cobalt complexes by metal reducing agents.[169,170]

$$Cr^{II} + L \rightarrow Cr^{III} + L^- \qquad Co^{III} + L^- \rightarrow Co^{II} + L$$

Scheme 6

In the present instance, where the donor and acceptor orbitals have σ symmetry and the carrier orbital on the ligand has π symmetry, the barrier for resonance transfer by way of the bridging ligand can be particularly high. Resonance transfer would require the symmetry restrictions at each center, as well as Franck–Condon restrictions at each center to be met simultaneously. It is to be expected then that if the oxidizing agent has a vacancy in the πd level, so that the orbital containing it can mix with the π^* orbital on the ligand, even though there is still a symmetry restriction at the (reducing agent)–(ligand) junction, once this restriction is overcome by a suitable distortion, resonance transfer from Cr^{2+} to the oxidizing agent can take place. This expectation has been tested with isonicotinamide as ligand by using $(NH_3)_5Ru^{3+}$ in place of $(NH_3)_5Co^{3+}$: a suitable choice also because the ruthenium complex is only slightly more oxidizing than the cobalt complex and the rate of reduction by Cr^{2+} is found to be approximately 2×10^4 more rapid than it is for the corresponding Co^{III} complex.[114] Thus when the bisisonicotinamide complex of Ru^{III} is reduced, the rate again increases, now by a factor of about 10. In direct transfer an increase is expected because of the greater driving force for the reduction of the bis complex.

To understand the stepwise mechanism more thoroughly, experiments on the reduction of the ligands themselves by Cr^{2+} and similar reagents are of obvious interest and value. It is probably advantageous for Cr^{2+} to react by an inner-sphere mechanism whenever there is a suitable polar group, but just how advantageous in a quantitative sense is not known in many cases. A program devoted to the study of the reduction by metal ion reducing agents of organic molecules that can function as bridging groups is under way,[171] but even more research activity in this subject area is needed.

7.2.9.2.4 Descriptive topics

(i) Adjacent vs. *remote attack*

The issue of adjacent *vs.* remote attack was raised in connection with the reduction of $[(NH_3)_5Co(OCOCH{=}CHCOOH)]^{2+}$ by $Cr(H_2O)_6{}^{2+}$, the conclusion being that the major portion of the reaction takes place at the *endo* carboxyl.[164] This still leaves open the question of whether the carboxyl oxygen or that joined to Co^{III} provides the site for attack by Cr^{2+}. The question has not been answered by direct experiments, such as might be done with isotopically labeled oxygen, but observations by Sykes and coworkers[172] strongly implicate the carbonyl oxygen as the site for attack. Earlier workers showed that when $(NH_3)_5Co(OCOH)^{2+}$ is reduced by Cr^{2+}, the dominant reaction path is inner sphere.[165] However, when μ-amido-μ-formatobis(tetraamminecobalt(III)) is reduced by Cr^{2+}, the major reaction path appears to be outer sphere.[172] It is unlikely that the difference in driving force is responsible for the change in mechanism, and the more likely cause is the obvious one, that in the binuclear case a carbonyl group is no longer available as a site for attack by Cr^{2+}.

Some basic issues are raised by studies which have been done with NCS^- as the bridging ligand. When $(NH_3)_5CoNCS^{2+}$ is reduced either by $Cr(H_2O)_6{}^{2+}$ [173] or $Co(CN)_5{}^{3-}$,[174,175] attack is quantitatively at the remote position. However, when $(NH_3)_5CoSCN^{2+}$ is reduced by Cr^{2+},[173] both $(H_2O)_5CrSCN^{2+}$ and $(H_2O)_5CoNCS^{2+}$ are formed as primary products; in the case of $Co(CN)_5{}^{3-}$, attack is restricted to the adjacent site.[175,176] There is an important difference between the two ends of SCN^-. When S is bound to the oxidizing center a lone pair of electrons is still available to provide a site for the reducing agent, but this is not the case for the N-bound isomer.

The quantitative aspects of the reactions with Cr^{2+} are particularly interesting. In reaction with Cr^{2+}, remote attack on $(NH_3)_5CoSCN^{2+}$ is favored by a factor of only 2.4, despite the greater steric interference encountered in adjacent attack, and the fact that the N-bound Cr^{III} product is more stable (by a factor of 3×10^5)[177] than the S-bound. If it is assumed that half of $\Delta G°$ for reduction is reflected in the activation process, the N-bound isomer is expected to be favored by a factor of at least 500. The remarkable facility of S to mediate in electron transfer is often referred to,[178,179] but is not understood. One factor contributing to its effectiveness may be that reaction by remote attack on $[{-}SCN^-]$ is not adiabatic, but it seems more likely that the major reason is that, in electron transfer through a single sulfur, electronic coupling in the transition state is so great as materially to lower the activation energy for reduction. This suggestion touches on the 'permeability' of a bridging atom to electron transfer, an issue to be discussed later. To understand why $Co(CN)_5{}^{3-}$ shows a much greater preference than does Cr^{II} for attack on sulfur rather than nitrogen, we need only take note of the fact that in the oxidized states the affinity ratio S to N is much greater for the former metal center.

(ii) The role of intermediates

A general and extremely important point was raised by Haim and coworkers[180] in a re-examination of the reaction of $Fe(CN)_6{}^{3-}$ with $Coedta^{2-}$. These species react rapidly to form a binuclear intermediate, which is diamagnetic, and is therefore to be formulated as $[(NC)_5Fe^{II}CNCo^{III}edta]^{5-}$, and which on the timescale of minutes decays to $Fe(CN)_6{}^{4-} + Coedta^-$. The earlier authors[181–183] had made the reasonable assumption that the intermediate in question is the successor complex in the overall reaction, *i.e.* that the slow reaction is as shown in equation (86). Haim and coworkers pointed out that the observed kinetics (these were thoroughly explored by the earlier workers) are compatible also with Scheme 7, *i.e.* the reaction to form the final products is in fact outer sphere, and the intermediate, rather than being on the path to final products, is really a 'dead-end'. The reinterpretation of the rate data by Haim and coworkers is convincing. The system is featured prominently here because it illustrates an important kinetic principle. When in a bimolecular process involving A and B, an intermediate $A\cdot B$ is detected, it is often assumed that $A\cdot B$ is on the way to products. If the concentration of $A\cdot B$ is small compared with that of the limiting reagent, whether it is a dead-end or not, it does not affect the overall rate, though if its structure is determined and it is really a dead-end, it can mislead the investigator about the true reaction course. However, when the formation of the dead-end intermediate depletes the limiting reagent, far from facilitating the overall reaction, the intervention of the intermediate impedes it.

$$[(NC)_5FeCNCo(edta)]^{5-} \longrightarrow Fe(CN)_6^{4-} + Co(edta)^- \qquad (86)$$

$$(CN)_5Fe^{II}CNCo^{III}(edta)^{5-} \rightarrow Fe(CN)_6^{3-} + Co(edta)^{2-}$$

$$Fe(CN)_6^{3-} + Co(edta)^{2-} \rightarrow Fe(CN)_6^{4-} + Co(edta)^-$$

Scheme 7

(iii) Applications

A number of applications of the special chemistry which an inner-sphere mechanism can involve have already been mentioned, though not with application the goal. Prominent among these is the preparation of unstable linkage isomers, *e.g.* the S-bound complex of Cr^{III} or the N-bound complexes of CN^-, both of which are unstable with respect to the alternative forms. Such systems should be regarded in another light — as a means of storing energy derived from electron transfer in a different form, here as a substitutionally metastable form. It is conceivable that applications can be based on this feature.

The essential point in the foregoing description is less the fact that we are dealing with unstable linkage isomers than that the inner-sphere mechanism can lead to product complexes which are not easily produced by direct substitution. An interesting example is the formation of the aldehyde complex[184] of $(H_2O)_5Cr^{3+}$ by the reaction of pentaammineparaformylbenzoatocobalt(III) with Cr^{2+}. As might be expected, the product complex aquates rapidly, presumably by C—O rather than Cr^{III}—O bond scission.

Observations[185] on the reaction of ethylmalonatopentaamminecobalt(III) with $Cr(H_2O)_6^{3+}$ introduce a new element of interest. The chromium(III) products are the chelated malonate (67%) with a corresponding amount of free alcohol and the monodentate ester complex (33%). Since ester hydrolysis in the latter species is slow, we conclude that hydrogen results from the ester in the chelate form. Again, since ring closure of the monodentate product complex is slow, chelation must have occurred before Cr^{II} is oxidized to Cr^{III}. It is possible that formation of the chelate as primary product is complete, and that this product reacts in part to yield the monodentate product before hydrolysis occurs. Activation based on electron transfer to trap a function which is sensitive to a substitution-inert metal ion acting as a Lewis acid could presumably be extended to other more interesting situations.

The foregoing example, in which two groups present on the bridging ligand are incorporated into the oxidized product, introduces the subject of multiply substituted complexes formed by electron transfer. Such species can be produced by two additional mechanisms: multiple bridges as in the example of the bis(azido)chromium(III)/(II) self-exchange process,[186] and by a combination of bridging and nonbridging ligand effects. As to the former, some systems which feature net changes, rather than virtual changes as in the Snellgrove and King case, and which lead to multiple substitution, as *cis*-$[Co(NH_3)_4(N_3)_2]^+$,[186] *cis*-$[Co(en)_2(HCO_2)_2]^+$ [187] and $Cr(C_2O_4)_3^{3-}$,[188] each in reaction with $Cr(H_2O)_6^{2+}$. As to the latter, an early example is the incorporation of both Cl^- and $P_2O_7^{4-}$ into the coordination sphere of Cr^{2+} when it reacts with $(NH_3)_5CoCl^{2+}$ in the presence of $H_2P_2O_7^{2-}$.[158] Numerous other instances have been encountered by Earley and co-workers in much more extensive studies of nonbridging ligand effects.[189]

The formation of binuclear successor complexes was described in discussing criteria for distinguishing inner- and outer-sphere mechanisms. This kind of phenomenon takes on a new interest if it is viewed as a method of preparation of such complexes. Examples are particularly numerous when a reducing agent with capture capability reacts with an oxidizing agent having the πd^5 electronic configuration. In certain instances, especially when a single atom separates the metal centers, the resulting species are useful in illuminating the issue of how much the rate of aquation of the ligand is affected by it being bound to a second metal ion. Thus the specific rate for the aquation of $(NH_3)_5RuCl^+$ is 4.7 s^{-1},[121] but when Cl^- is also bound to $(H_2O)_5Cr^{3+}$, the specific rate increases to 4.6×10^2 s^{-1}.[190] A similar comparison can be made for aquation of $(NH_3)_5RuO_2CH^+$ ($k = 1.3$ s^{-1}) and of the complex with $(H_2O)_5Cr^{3+}$ also bound to the formate ($k = 2.4$ s^{-1}).[191] The enhancement of rate in the latter case is remarkably small and supports the conclusion, reached also on the grounds[191] that Cr^{2+} attacks the carbonyl group in reducing $(NH_3)_5RuO_2CH^{2+}$.

Binuclear complexes can also be produced by another route, namely by the reaction with a binuclear or polynuclear oxidant of a reducing agent competent in trapping. This outcome was not realized in an early study[192] of this kind devoted to the reduction of bis-μ-hydroxo-octaamminedicobalt(III) by Cr^{2+} (and other reducing agents). Direct reduction is slow, and is preceded by opening of one of the bridges. Reduction of the resulting product is relatively rapid, but attack apparently takes place at a nonbridging OH^- (formed by dissociation of H^+ from coordinated H_2O) rather than at the remaining OH^- bridge. However, a number of examples of binuclear chromium(II) products have been reported by Sykes and coworkers in cases where a bridging group is attacked, for example μ-sulfatodichromium(III)[193] and μ-oxalatodichromium(III).[194] In each system a Co^{III}—Cr^{III} species bridged by the anion is implicated as an intermediate.

7.2.9.2.5 *Reaction systematics*

The principles embodied in the Marcus—Hush rate correlation have frequently been applied in comparing rates of inner-sphere reactions, for example as was done just previously in discussing, following Haim, a rate comparison with SCN^- as a bridging group. With single-atom bridging groups it is possible, perhaps even likely, that significant rate effects arise from the stabilization of the activated complex for electron transfer by electron delocalization, *i.e.* the systems do not conform to the weak interaction limit for which the correlation was first developed. Marcus has pointed out that a correlation does not necessarily fail even when electronic interaction in the activated complex is substantial. Moreover, for resonance transfer through bridging groups[195] such as RCO_2^-, N_3^- or NCS^-, it is highly unlikely that the interaction is at all great enough to invalidate the correlation. Despite the incentive there would be to extend the correlation to inner-sphere processes, only a small amount of systematic work along this line has been done. Haim and Sutin[196] have used the correlation in a relative sense and have shown that, given the specific rate of reduction of $(NH_3)_5Co^{III}L$ by Fe^{2+} (k_{13}), the Cr^{2+} rate (k_{12}) can be calculated, in reasonable agreement with experiment, from the relation $k_{12} = k_{13}\sqrt{(k_{22}K_{12}/k_{33}K_{13})}$. In this equation, k_{22} and k_{33} are the self-exchange specific rates for the $(H_2O)_5CrOH^{2+}/Cr^{2+}(aq)$ and $FeOH^{2+}(aq)/Fe^{2+}(aq)$ couples, and K_{12} and K_{13} are the equilibrium quotients for the reactions of $Cr^{2+}(aq)$ and $Fe^{2+}(aq)$ with the respective Co^{III} complexes. The ligands Cl^-, F^- and N_3^- are known to act as bridging groups in the reactions of $Cr(H_2O)_6{}^{2+}$ and are reasonably assumed to play the same role in the reactions of $Fe(H_2O)_6{}^{2+}$. The applicability of the Marcus-Hush correlation to inner-sphere reactions involving OH^- as a bridging group was also considered and discussed by Daugherty and Newton.[197] The most convincing test of the correlation as applied to inner-sphere reactions is that of Endicott and coworkers,[198] who studied reactions of the Co^{III}/Co^{II} couple as macrocyclic complexes. Ligands of this type have the enormous advantage that they remain bound also in the 2+ state, with the result that the redox potentials can now be determined. It is clear from all of the foregoing that the Marcus-Hush correlation is useful also for inner-sphere reactions, and the range of its applicability merits as much systematic study as has been given to outer-sphere reactions.

The relative efficiencies of the halide ions acting as bridging groups in electron transfer reactions has been a matter of interest from the very birth of this subject. In fact, it was commented[199] on even before the experiments were done which demonstrated that reaction actually does occur by this kind of mechanism. In the early discussions of relative efficiencies, the differences in driving forces were frequently overlooked, even though it was widely appreciated that rates can be responsive to changes in stability. An additional point is that for labile systems a rate law such as $[Fe^{3+}][FeX^+]$ is as valid a representation of the kinetic behavior as is the more commonly adopted form $[FeX^{2+}][Fe^{2+}]$ (in reporting, the second is preferable because of the desirability of expressing rate law in terms of the concentrations of the dominant forms) and the relative efficiencies in a series X^- would in general be altered in changing the reference basis law. Haim[200] has pointed out that the effect of driving force within a series is eliminated by referring the rates to the basis $[ox][red][X^-]$. The element of arbitrariness referred to is thereby also eliminated. The recommended formulation has the advantage that within a series in which only X^- changes, the overall reaction, and thus the driving force, remains the same (see equation 87). When the metal ions are changed the driving force can of course change, and this can of itself affect the relative efficiencies in a series such as $X = F \ldots I$.[201] The specific rate can of course be converted to an equilibrium quotient for reaction so that the relative affinities of the activated complexes for the different bridging ligands can be compared. These affinities will have an orthodox component, of the kind considered in trying to understand relative affinities in a purely equilibrium sense. Thus $[Cr^{2.5+}Cr^{2.5+}]$ might be expected to favor F^- over I^-, but since the activated complex is a rate construct, there will in all likelihood be a kinetic component as well. The component left after orthodox stability has been allowed for has been called 'permeability'. It may reflect differences in the reorganization energies required to reach the activated complexes, *i.e.* stretching and compression of X^- metal bonds, and may well have a component ascribable to differences in the degrees of electronic coupling in the activated complexes, a point already referred to in commenting on the efficiency of sulfur in mediating electron transfer.

$$\mathrm{Fe(H_2O)_6^{3+} + X^- + V(H_2O)_6^{2+} = Fe(H_2O)_6^{2+} + X^- + V(H_2O)_6^{3+}} \qquad (87)$$

$$[\mathrm{oxid}][\mathrm{red}][\mathrm{X^-}] = [\mathrm{oxid{\cdot}X^-{\cdot}red}]^+ \qquad (88)$$

The important issue of whether and which processes are adiabatic has not been dealt with systematically as applied to inner-sphere reactions, though it has on occasion (see above) been referred to. This situation applied not only to this article but to much of the literature on inner-sphere mechanisms. When single atoms separate the reaction partners, it is usually assumed that the reactions are adiabatic, and the possibility is in fact entertained that the reactions lie in the strong overlap region. However, what is the situation for formate, which we believe acts as a three-atom bridging group? (Formate is chosen over the other carboxylates because steric effects are minimal, thus making comparisons to other three-atom bridging groups more meaningful.) In considering this question we will introduce data for reactions of the class $(NH_3)_5Co^{III}L + Cr^{2+}$, where L in every case acts, highly probably, as a three-atom group, and in the usual case presents oxygens to the metal ions. Thus in the usual case it is unlikely that differences in driving force are responsible for the effects to be exposed, and even when $L = N_3$ is included it is highly unlikely that the enormous rate differences encountered owe much to change in $\Delta G°$.

The data to be considered follow. The specific rates ($M^{-1}\ s^{-1}$) governing the reactions of Cr^{2+}(aq) with $(NH_3)_5Co^{III}L$ when $L = HCO_2^-$,[165] NO_3^-,[202] SO_4^{2-},[202] $—SSO_3^{2-}$,[203] $—ONO^-$[204] and N_3^-,[202] are 7, ~90, 18, 0.18, $\geqslant 3 \times 10^2$ and $\sim 3 \times 10^5$ respectively. The interesting point is the much greater rates observed when $L = N_3^-$ or NO_2^- than when it is HCO_2^-, NO_3^- or SO_4^{2-}. One possibility is to ascribe the differences to orthodox conjugation in the cases of the two rapid reactions but this is tantamount to saying that the less rapid reactions of the class are non-adiabatic. In view of the fact that the rates within the slower group are so nearly alike, this is highly unlikely. Even the rate for $L = —SSO_3^{2-}$ would probably fall in the range of the slower group if allowance were made for the high affinity of Co^{III} for $—SSO_3^{2-}$. In addition, a rough indication of the rate for $L = PO_4H_2^-$ was obtained by Schmidt *et al.*,[205] and it also falls in the same range as those in the slower class. A more reasonable interpretation is that the reactions for the slower class are themselves adiabatic, the small differences being ascribable to differences in precursor stability and reorganization terms. How then are the more rapid rates to be understood? Both N_3^- and NO_2^- are reducible by Cr^{2+}, and we therefore advocate stepwise mechanisms in these cases. The fact that the rates are much slower for the complexes with $(H_2O)_5Cr^{3+}$ (*known* to be the case only for $L = N_3^-$) is not an argument against this interpretation. If the radical generated is a weak reducing agent, as could well be the case when the reaction with Cr^{2+} is very rapid, a great deal of discrimination between reduction of $(NH_3)_5Co^{3+}$ and $(H_2O)_5Cr^{3+}$ might be expected. It should be noted that when the rate of reduction of the $(NH_3)_5Co^{3+}$ complex is small, as is the case for L = fumarate, the rates for the Co^{III} and Cr^{III} complexes are much more nearly alike. This is the behavior expected if the fumarate radical ion is strongly reducing, which is in line with the slow rate of production as measured in the reaction $[(NH_3)_5Co\ \text{fumarate}\ H]^{2+} + Cr^{2+}$(aq). If in fact ONO^- functions by first being reduced to NO_2^{2-}, it is interesting that N—O bond cleavage does not occur before the extra electron is passed on. The reason may simply be that such cleavage would lead to O^{2-} coordinated to a metal center, and this is a highly unstable state. Reduction of $(H^+ + HNO_2)$ probably requires both protons to be on a single oxygen.

ACKNOWLEDGMENTS

The authors would like to acknowledge Dr. Jeffrey Nagle for collecting the self-exchange rate constant data and Dr. D. Geselowitz for suggestions. Professor Thomas J. Meyer acknowledges Dr. Kenneth Goldsby for his assistance in preparing the first part of the chapter, the Departments of Chemistry, Université Louis Pasteur, Strasbourg and CENG, Grenoble for their support and hospitality during a research leave, and the Guggenheim Foundation and the Pogue Research Leave Program of the University of North Carolina for sabbatical leave support.

7.2.10 REFERENCES

1. E. S. Yang, M.-S. Chan and A. C. Wahl, *J. Phys. Chem.*, 1975, **79**, 2049.
2. M. S. Thompson and T. J. Meyer, *J. Am. Chem. Soc.*, 1982, **104**, 4106.
3. (a) R. A. Sheldon and J. K. Kochi, 'Metal-Catalyzed Oxidations of Organic Compounds', Academic, New York, 1981; (b) M. Chanon and M. L. Tobe, *Angew. Chem., Int. Ed. Engl.*, 1981, **21**, 1.
4. H. Taube, 'Electron Transfer Reactions of Complex Ions in Solution', Academic, New York, 1970.
5. R. G. Linck, *M.T.P. Int. Rev. Sci. Inorg. Chem. Ser. 1*, 1972, **9**, 303; *Inorg. Chem. Ser. 2*, 1974, **9**, 173.
6. A. Haim, *Prog. Inorg. Chem.*, 1983, **30**, 273.
7. D. E. Pennington, in 'Coordination Chemistry', ed. A. E. Martell, ACS Monograph, No. 174, 1970, **2**, 476.
8. H. Taube, H. Myers and R. L. Rich, *J. Am. Chem. Soc.*, 1953, **75**, 4118.
9. H. Taube, *Can. J. Chem.*, 1959, **37**, 129.
10. A. Haim and N. Sutin, *J. Am. Chem. Soc.*, 1965, **87**, 4210; 1966, **80**, 434.
11. J. Silverman and R. W. Dodson, *J. Phys. Chem.*, 1952, **56**, 846.
12. (a) H. L. Friedman and M. D. Newton, *Faraday Discuss. Chem. Soc.*, 1982, **24**, 73; (b) J. Logan and M. D. Newton, *J. Chem. Phys.*, 1983, **78**, 4006.
13. S. S. Isied and H. Taube, *J. Am. Chem. Soc.*, 1973, **95**, 8198.
14. C. Creutz, *Inorg. Chem.*, 1978, **17**, 3723; G. M. Tom, C. Creutz and H. Taube, *J. Am. Chem. Soc.*, 1974, **96**, 7827.
15. J. C. Curtis and T. J. Meyer, *Inorg. Chem.*, 1982, **21**, 1562.
16. N. S. Hush, *Prog. Inorg. Chem.*, 1967, **8**, 391; *Electrochim. Acta*, 1968, **13**, 1005.
17. A. Zwickel and H. Taube, *J. Am. Chem. Soc.*, 1961, **83**, 793.
18. J. P. Candlin and J. Halpern, *Inorg. Chem.*, 1965, **4**, 766.
19. J. Halpern and J. P. Maher, *J. Am. Chem. Soc.*, 1964, **86**, 2311; 1965, **87**, 5381.
20. R. Grassi, A. Haim and W. K. Wilmarth, *Inorg. Chem.*, 1967, **6**, 237.
21. R. A. Binstead, B. A. Moyer, G. J. Samuels and T. J. Meyer, *J. Am. Chem. Soc.*, 1981, **103**, 2897.
22. B. A. Moyer and T. J. Meyer, *Inorg. Chem.*, 1981, **20**, 436.
23. W. L. Reynolds and R. W. Lumry, 'Mechanisms of Electron Transfer', Ronald Press, New York, 1966.
24. R. D. Cannon, 'Electron Transfer Reactions', Butterworths, London, 1980.
25. J. Ulstrup, 'Charge Transfer Processes in Condensed Media', Springer Verlag, Berlin, 1979.
26. B. Chance *et al.* (eds.), 'Tunneling in Biological Systems', Academic, New York, 1979.
27. N. Sutin, in 'Inorganic Biochemistry', ed. G. L. Eichhorn, Elsevier, New York, 1973, p. 611.
28. N. J. Hair and J. K. Beattie, *Inorg. Chem.*, 1977, **16**, 245.
29. J. K. Beattie, S. P. Best, B. W. Skelton and A. H. White, *J. Chem. Soc., Dalton Trans.*, 1981, 2105.
30. B. S. Brunschwig, C. Creutz, D. H. McCartney, T.-K. Sham and N. Sutin, *Faraday Discuss. Chem. Soc.*, 1982, **74**, 113.
31. B. S. Brunschwig, J. Logan, M. D. Newton and N. Sutin, *J. Am. Chem. Soc.*, 1980, **102**, 5798.
32. (a) V. G. Levich, *Adv. Electrochem. Electrochem. Eng.*, 1966, **4**, 249; (b) N. R. Kestner, J. Logan and J. Jortner, *J. Phys. Chem.*, 1974, **78**, 2148.
33. E. D. German and A. M. Kuznetsov, *Electrochim. Acta*, 1981, **25**, 1595.
34. (a) R. A. Marcus, *Annu. Rev. Phys. Chem.*, 1964, **15**, 155; (b) R. A. Marcus, *J. Chem. Phys.*, 1965, **43**, 679.
35. N. S. Hush, *Trans. Faraday Soc.*, 1961, **57**, 557.
36. M. D. Newton and N. Sutin, *Annu. Rev. Phys. Chem.*, 1984, **35**, 437.
37. (a) N. Sutin, *Acc. Chem. Res.*, 1982, **15**, 275; (b) N. Sutin, *Prog. Inorg. Chem.*, 1983, **30**, 441.
38. T. Guarr and G. McLendon, *Coord. Chem. Rev.*, 1985, **68**, 1.
39. D. DeVault, *Q. Rev. Biophys.*, 1980, **13**, 387.
40. (a) R. Kubo and Y. Toyozawa, *Prog. Theor. Phys. (Osaka)*, 1955, **13**, 161; (b) M. Lax, *J. Chem. Phys.*, 1952, **20**, 1752; (c) K. Huang and A. Rhys, *Proc. Phys. Soc., Ser. A*, 1951, **204**, 413.
41. (a) J. Ulstrup and J. Jortner, *J. Chem. Phys.*, 1975, **63**, 4358; (b) S. Efrima and M. Bixon, *Chem. Phys.*, 1976, **13**, 447; (c) R. P. Van Duyne and S. F. Fischer, *Chem. Phys.*, 1974, **5**, 183.
42. T. Holstein, *Philos. Mag.*, 1978, **37**, 49; *Ann. Phys. (Leipzig)*, 1959, **8**, 343.
43. J. J. Hopfield, *Proc. Natl. Acad. Sci. USA*, 1974, **71**, 3640.
44. I. R. Levine, 'Molecular Spectroscopy', Wiley-Interscience, New York, 1975, chap. 6.
45. C. J. Ballhausen, 'Molecular Electronic Structures of Transition Metal Complexes', McGraw-Hill, New York, 1979.
46. E. Buhks, M. Bixon, J. Jortner and G. Navon, *Inorg. Chem.*, 1979, **18**, 2014.
47. J. Jortner and J. Ulstrup, *Chem. Phys. Lett.*, 1979, **63**, 236.
48. B. L. Tembe, H. L. Friedman and M. D. Newton, *J. Chem. Phys.*, 1982, **76**, 1490.
49. C. H. Bamford and C. F. H. Tipper (eds.), 'Comprehensive Chemical Kinetics', Elsevier, New York, 1964.
50. R. M. Noyes, *Prog. React. Kinet.*, 1961, **1**, 129.
51. A. M. North, 'The Collision Theory of Chemical Reactions in Liquids', Wiley, New York, 1964.
52. (a) H. Frolich, 'Theory of Dielectrics', Oxford University Press, New York, 1949; (b) J. B. Hubbard, *J. Chem. Phys.*, 1982, **76**, 2993; (c) N. E. Hill, W. E. Vaughn, A. H. Price and M. Davies, 'Dielectric Properties and Molecular Behavior', Van Nostrand Reinhold, London, 1969.
53. J. Ulstrup, 'Charge Transfer Processes in Condensed Media', Springer Verlag, Berlin, 1979, chap. 5.
54. (a) L. Landau, *Phys. Z. Sowjetunion*, 1932, **2**, 46; (b) C. Zener, *Proc. R. Soc. London, Ser. A*, 1932, **137**, 696; 1933, **140**, 660.
55. A. J. Miralles, R. E. Armstrong and A. Haim, *J. Am. Chem. Soc.*, 1977, **99**, 1416.
56. D. N. Beratan and J. J. Hopfield, *J. Am. Chem. Soc.*, 1984, **106**, 1584.
57. J. R. Miller and J. V. Beitz, *J. Chem. Phys.*, 1981, **74**, 6746.
58. R. K. Huddleston and J. R. Miller, *J. Chem. Phys.*, 1983, **79**, 5337.
59. S. Straugh, G. McLendon, M. McGuire and T. Guarr, *J. Phys. Chem.*, 1983, **87**, 3579.
60. T. T. Tomi, M. J. Weaver and C. H. Brubaker, Jr., *J. Am. Chem. Soc.*, 1982, **104**, 2381.
61. M.-S. Chan and A. C. Wahl, *J. Phys. Chem.*, 1982, **86**, 126.
62. D. Borchardt and S. Wherland, *Inorg. Chem.*, 1984, **23**, 2537.
63. M. J. Powers and T. J. Meyer, *J. Am. Chem. Soc.*, 1978, **100**, 4393.
64. M. J. Weaver and T. Gennett, *Chem. Phys. Lett.*, 1985, **113**, 213.

65. (a) D. F. Calef and P. G. Wolynes, *J. Chem. Phys.*, 1983, **78**, 470; (b) D. F. Calef and P. G. Wolynes, *J. Phys. Chem.*, 1983, **87**, 3387; (c) L. D. Zusinan, *Chem. Phys.*, 1980, **49**, 295; (d) I. V. Aleksandrov, *Chem. Phys.*, 1980, **51**, 449.
66. B. I. Swanson, and J. J. Rafalko, *Inorg. Chem.*, 1976, **19**, 249.
67. T. Guarr, E. Buhks and E. G. McLendon, *J. Am. Chem. Soc.*, 1983, **105**, 3763.
68. N. O. Lipari, M. J. Rice, C. B. Duke, R. Bozio, A. Girlando and C. Pecile, *Int. J. Quant. Chem., Quant. Chem. Symp.*, 1977, **11**, 583.
69. (a) C. J. Fritchie, Jr., *Acta Crystallogr.*, 1966, **20**, 842; (b) R. E. Lons, R. A. Sperks and K. N. Trueblood, *Acta Crystallogr.*, 1965, **18**, 932.
70. (a) A. Zalkin, D. H. Templeton and T. Ueki, *Inorg. Chem.*, 1973, **12**, 1641; (b) J. Baker, L. M. Engelhardt, B. N. Figgis and A. N. White, *J. Chem. Soc., Dalton Trans.*, 1975, 530.
71. R. J. Campion, N. Purdie and N. Sutin, *Inorg. Chem.*, 1964, **3**, 1091.
72. (a) C. R. Bock, J. A. Conner, A. R. Gutierrez, T. J. Meyer, D. G. Whitten, B. P. Sullivan and J. K. Nagle, *J. Am. Chem. Soc.*, 1979, **101**, 4815; *Chem. Phys. Lett.*, 1979, **61**, 522; (b) R. Ballardini, G. Varani, M. T. Indelli, F. Scandola and V. Balzani, *J. Am. Chem. Soc.*, 1978, **100**, 7219.
73. C.-Y. Mok, A. W. Zanella, C. Creutz and N. Sutin, *Inorg. Chem.*, 1984, **23**, 2891.
74. M. Gordon (ed.), 'The Exciplex', Academic, New York, 1975.
75. (a) D. M. Hercules, *Acc. Chem. Res.*, 1979, **2**, 301; (b) E. H. White, J. D. Miano, C. J. Watkins and E. J. Breaux, *Angew. Chem., Int. Ed. Engl.*, 1974, **13**, 229.
76. (a) R. Englman and J. Jortner, *Mol. Phys.*, 1970, **18**, 145; (b) K. F. Freed and J. Jortner, *J. Chem. Phys.*, 1970, **52**, 6272.
77. (a) G. W. Robinson and R. P. Frosch, *J. Chem. Phys.*, 1963, **38**, 1187; (b) B. R. Henry and W. Siebrand, in 'Organic Molecular Photophysics', ed. J. B. Birks, Wiley, New York, 1973, vol. 1; (c) F. K. Fong, 'Theory of Molecular Relaxation', Wiley, New York, 1975.
78. T. J. Meyer, *Prog. Inorg. Chem.*, 1983, **30**, 389.
79. J. V. Caspar, T. D. Westmoreland, G. H. Allen, P. G. Bradley, T. J. Meyer and W. H. Woodruff, *J. Am. Chem. Soc.*, 1984, **106**, 3492.
80. (a) N. Sutin and C. Creutz, *Pure Appl. Chem.*, 1980, **52**, 2717; (b) N. Sutin, *J. Photochem.*, 1979, **10**, 19.
81. J. R. Miller, L. T. Calcaterra and G. L. Closs, *J. Am. Chem. Soc.*, 1984, **106**, 3047.
82. D. M. Brown (ed.), 'Mixed-Valence Compounds', Reidel, Dordrecht, 1980.
83. C. Creutz, *Prog. Inorg. Chem.*, 1983, **30**, 1.
84. (a) H. Taube, *Ann. N.Y. Acad. Sci.*, 1978, **313**, 481; (b) T. J. Meyer, *Acc. Chem. Res.*, 1978, **11**, 94; (c) T. J. Meyer, *Ann. N.Y. Acad. Sci.*, 1978, **313**, 497.
85. C. Creutz and H. Taube, *J. Am. Chem. Soc.*, 1973, **95**, 1086.
86. D. O. Cowan, C. LeVanda, J. Park and F. Kaufman, *Acc. Chem. Res.*, 1973, **6**, 1.
87. A. K. Schroeder and S. Mazur, *J. Am. Chem. Soc.*, 1978, **98**, 6713.
88. J. C. Curtis, B. P. Sullivan and T. J. Meyer, *Inorg. Chem.*, 1980, **19**, 3833.
89. M. J. Powers and T. J. Meyer, *J. Am. Chem. Soc.*, 1980, **102**, 1289.
90. R. D. Cannon, *Adv. Inorg. Chem. Radiochem.*, 1978, **21**, 179.
91. E. M. Kober, K. A. Goldsby, D. N. S. Narayana and T. J. Meyer, *J. Am. Chem. Soc.*, 1983, **105**, 4303.
92. D. E. Richardson and H. Taube, *Coord. Chem. Rev.*, 1984, **60**, 107.
93. P. Day, *Int. Rev. Phys. Chem.*, 1981, **1**, 149.
94. U. Fürholz, H.-B. Bürgi, F. E. Wagner, A. Stebler, J. H. Ammeter, E. Krausz, R. J. H. Clark, M. J. Stead and A. Ludi, *J. Am. Chem. Soc.*, 1984, **106**, 121.
95. K. Y. Wong and P. N. Schatz, *Prog. Inorg. Chem.*, 1981, **28**, 369.
96. J. F. Endicott, K. Kumar, T. Ramaswami and F. P. Rotzinger, *Prog. Inorg. Chem.*, 1983, **30**, 141.
97. J. K. Burdett, *Inorg. Chem.*, 1978, **17**, 2537.
98. A. Haim, *Prog. Inorg. Chem.*, 1983, **30**, 273.
99. A. Szecsy and A. Haim, *J. Am. Chem. Soc.*, 1981, **103**, 1679.
100. C. Creutz, P. Kroger, T. Matsubara, T. L. Netzel and N. Sutin, *J. Am. Chem. Soc.*, 1979, **101**, 5442.
101. S. S. Isied and A. Vassilian, *J. Am. Chem. Soc.*, 1984, **106**, 1732.
102. S. S. Isied, C. Kuehn and G. Worosila, *J. Am. Chem. Soc.*, 1984, **106**, 1722.
103. (a) J. R. Winkler, D. G. Nocera, K. M. Yokem, E. Brodignion and H. B. Gray, *J. Am. Chem. Soc.*, 1982, **104**, 5798; (b) S. S. Isied, G. Worosila and S. J. Atherton, *J. Am. Chem. Soc.*, 1982, **104**, 7659.
104. A. van den Bergen and B. O. West, *Chem. Commun.*, 1971, 52.
105. J. H. Espenson and J. S. Shveima, *J. Am. Chem. Soc.*, 1973, **95**, 4468.
106. H. Taube and H. Myers, *J. Am. Chem. Soc.*, 1954, **76**, 2103.
107. H. Taube and E. L. King, *J. Am. Chem. Soc.*, 1954, **76**, 4053.
108. D. E. Pennington and A. Haim, *J. Am. Chem. Soc.*, 1966, **88**, 3450.
109. A. Adin and A. G. Sykes, *J. Chem. Soc. (A)*, 1966, 1518.
110. A. E. Ogard and H. Taube, *J. Am. Chem. Soc.*, 1958, **80**, 1084.
111. D. E. Pennington and A. Haim, *Inorg. Chem.*, 1966, **5**, 1887.
112. J. H. Espenson and S. G. Slocum, *Inorg. Chem.*, 1967, **6**, 1906.
113. (a) J. F. Endicott and H. Taube, *J. Am. Chem. Soc.*, 1962, **84**, 4984; (b) J. F. Endicott and H. Taube, *Inorg. Chem.*, 1965, **4**, 437.
114. R. G. Gaunder and H. Taube, *Inorg. Chem.*, 1970, **9**, 2627.
115. F. Maspero and H. Taube, *J. Am. Chem. Soc.*, 1968, **90**, 7361.
116. J. K. Beattie and F. Basolo, *Inorg. Chem.*, 1971, **10**, 486.
117. J. K. Beattie and J. Starink, *Inorg. Chem.*, 1975, **14**, 996.
118. When $Cr(H_2O)_6^{2+}$ reacts with Cp_2RuBr^+, $Cr(H_2O)_5Br^{2+}$ is among the Cr^{III} products; T. Smith, unpublished observations.
119. J. P. Candlin, J. Halpern and S. Nakamura, *J. Am. Chem. Soc.*, 1963, **85**, 2517.
120. A. Adin and J. H. Espenson, *Inorg. Chem.*, 1972, **11**, 686.
121. H. S. Lim, D. J. Barclay and F. C. Anson, *Inorg. Chem.*, 1972, **11**, 1460.
122. J. A. Broomhead, F. Basolo and R. G. Pearson, *Inorg. Chem.*, 1964, **3**, 826.
123. D. G. Gaswick and A. Haim, *J. Am. Chem. Soc.*, 1974, **96**, 7845.

124. G. Dulz and N. Sutin, *J. Am. Chem. Soc.*, 1964, **86**, 829.
125. M. J. M. Woods, Sr., P. K. Gallagher and E. L. King, *Inorg. Chem.*, 1962, **1**, 55 (K_{eq}); R. E. Connick and C. P. Coppel, *J. Am. Chem. Soc.*, 1959, **81**, 6389 (rate data).
126. J. H. Espenson, *J. Am. Chem. Soc.*, 1967, **89**, 1276.
127. For a solution 0.1 M $VCl_3 + 0.85$ M *p*-toluenesulfonic acid, k_4 has been measured as 1.3×10^3 (25 °C), ΔH as 33.0 kJ mol^{-1} and ΔS as -75 J mol^{-1} deg^{-1} (D. L. Donham, M. S. Thesis, Stanford University, 1969).
128. J. P. Hunt and H. L. Friedman, *Prog. Inorg. Chem.*, 1983, **30**, 379 quote 1.5×10^3 s^{-1}, 33 kJ mol^{-1}, -67 J mol^{-1} deg^{-1} for a Br^- containing medium, using data obtained by A. M. Chmilnick and D. Fiat (1972), and of A. E. Merbach.
129. M. V. Olson, Y. Kanazawa and H. Taube, *J. Chem. Phys.*, 1969, **51**, 289.
130. F. H. Westheimer, *Chem. Rev.*, 1949, **45**, 419.
131. M. B. Robin and P. Day, *Adv. Inorg. Chem. Radiochem.*, 1967, **10**, 247.
132. R. D. Cannon and J. Gardner, *Inorg. Chem.*, 1974, **13**, 390.
133. J. K. Hurst, *J. Am. Chem. Soc.*, 1976, **98**, 4401.
134. This aspect of the subject is treated in detail in ref. 5.
135. F. R. Nordmeyer and H. Taube, *J. Am. Chem. Soc.*, 1968, **90**, 1162.
136. (a) J. H. Espenson, *Inorg. Chem.*, 1965, **4**, 1025; (b) J. H. Espenson and D. W. Carlyle, *Inorg. Chem.*, 1966, **5**, 586.
137. (a) A. G. Sykes and A. Adin, *J. Chem. Soc. (A)*, 1968, 351; (b) A. G. Sykes, *Chem. Commun.*, 1965, 442.
138. A. Haim, *Inorg. Chem.*, 1968, **5**, 2081.
139. A. Anderson and N. A. Bonner, *J. Am. Chem. Soc.*, 1954, **76**, 3826.
140. E. Deutsch and H. Taube, *Inorg. Chem.*, 1968, **7**, 1532.
141. W. S. Melvin and A. Haim, *Inorg. Chem.*, 1977, **16**, 2016.
142. T. J. Meyer and H. Taube, *Inorg. Chem.*, 1968, **7**, 2369.
143. H. Fisher and H. Taube, *J. Am. Chem. Soc.*, 1976, **98**, 5512.
144. S. S. Isied and A. Vassilian, *J. Am. Chem. Soc.*, 1984, **106**, 1726.
145. S. S. Isied and A. Vassilian, *J. Am. Chem. Soc.*, 1984, **106**, 1732.
146. A. M. Zwickel and H. Taube, *J. Am. Chem. Soc.*, 1959, **81**,1288.
147. R. K. Murmann, F. A. Posey and H. Taube, *J. Am. Chem. Soc.*, 1957, **79**, 262.
148. W. Kruse and H. Taube, *J. Am. Chem. Soc.*, 1960, **82**, 256.
149. D. L. Toppen and R. G. Linck, *Inorg. Chem.*, 1971, **10**, 2638.
150. H. Diebler, P. H. Dodel and H. Taube, *Inorg. Chem.*, 1966, **5**, 1688.
151. H. R. Hunt and H. Taube, *J. Phys. Chem.*, 1959, **63**, 124.
152. M. Green, K. Schug and H. Taube, *Inorg. Chem.*, 1965, **4**, 1184.
153. M. J. DeChant and J. B. Hunt, *J. Am. Chem. Soc.*, 1968, **90**, 3695.
154. J. Hudis and R. W. Dodson, *J. Am. Chem. Soc.*, 1956, **78**, 911.
155. R. C. Splinter, J. J. Harns and R. S. Tobias, *Inorg. Chem.*, 1968, **7**, 897; these measurements correct a value of 1.5 which appeared much earlier as a footnote (unpublished work of J. D. Bearcroft under the supervision of H. Taube) in ref. 146, and which was used in the evaluation of the results of that paper.
156. M. M. Itzkowitz and F. R. Nordmeyer, *Inorg. Chem.*, 1975, **14**, 2124.
157. R. Snellgrove and E. L. King, *J. Am. Chem. Soc.*, 1962, **84**, 4609.
158. H. Taube, *J. Am. Chem. Soc.*, 1955, **77**, 4481.
159. F. R. Nordmeyer and H. Taube, *J. Am. Chem. Soc.*, 1966, **88**, 4295.
160. E. S. Gould, *J. Am. Chem. Soc.*, 1972, **94**, 4360.
161. H. Spiecker and K. Wieghardt, *Inorg. Chem.*, 1977, **16**, 1290.
162. C. R. Norris and F. R. Nordmeyer, *J. Am. Chem. Soc.*, 1971, **93**, 4044.
163. H. Diaz and H. Taube, *Inorg. Chem.*, 1970, **9**, 1304.
164. J. K. Hurst and H. Taube, *J. Am. Chem. Soc.*, 1968, **90**, 1178.
165. M. B. Barrett, J. H. Swinehart and H. Taube, *Inorg. Chem.*, 1971, **10**, 1983.
166. H. Taube and E. S. Gould, *Acc. Chem. Res.*, 1969, **2**, 321.
167. E. S. Gould and H. Taube, *J. Am. Chem. Soc.*, 1964, **86**, 1318.
168. S. K. S. Zawacky and H. Taube, *J. Am. Chem. Soc.*, 1981, **103**, 3379.
169. E. S. Gould, *Acc. Chem. Res.*, 1985, **18**, 22.
170. J. R. Barber, Jr. and E. S. Gould, *J. Am. Chem. Soc.*, 1971, **93**, 4045.
171. J. Konstantatos, E. Vrachnou-Astra and D. Katakis, *Inorg. Chim. Acta*, 1984, **85**, 41, and earlier papers by V.-A.
172. K. L. Scott and A. G. Sykes, *J. Chem. Soc., Dalton Trans.*, 1972, 1832.
173. C. Shea and A. Haim, *J. Am. Chem. Soc.*, 1971, **93**, 3055.
174. J. L. Burmeister, *Inorg. Chem.*, 1964, **3**, 915.
175. J. P. Candlin, J. Halpern and S. Nakamura, *J. Am. Chem. Soc.*, 1963, **85**, 2517.
176. C. Shea and A. Haim, *Inorg. Chem.*, 1973, **12**, 3013.
177. A. Haim and N. Sutin, *J. Am. Chem. Soc.*, 1965, **87**, 4210.
178. R. H. Lane and L. E. Bennett, *J. Am. Chem. Soc.*, 1970, **92**, 1081.
179. C. Wechsler and E. Deutsch, *Inorg. Chem.*, 1976, **15**, 139.
180. L. Rosenhein, D. Spencer and A. Haim, *Inorg. Chem.*, 1974, **13**, 1571.
181. A. W. Adamson and E. Gonick, *Inorg. Chem.*, 1963, **2**, 129.
182. D. H. Huchital and R. G. Wilkins, *Inorg. Chem.*, 1967, **6**, 1022.
183. D. H. Huchital and R. H. Hodges, *Inorg. Chem.*, 1973, **12**, 998.
184. A. Zanella and H. Taube, *J. Am. Chem. Soc.*, 1972, **94**, 6403.
185. D. A. Huchital and H. Taube, *J. Am. Chem. Soc.*, 1965, **87**, 5271.
186. A. Haim, *J. Am. Chem. Soc.*, 1966, **88**, 2324.
187. J. R. Ward and A. Haim, *J. Am. Chem. Soc.*, 1970, **92**, 475.
188. D. H. Huchital, *Inorg. Chem.*, 1970, **9**, 486.
189. J. E. Earley, *Prog. Inorg. Chem.*, 1970, **13**, 243.
190. W. G. Morris and R. G. Linck, *J. Am. Chem. Soc.*, 1970, **92**, 5394.
191. J. A. Stritar and H. Taube, *Inorg. Chem.*, 1963, **8**, 2281.
192. A. B. Hoffman and H. Taube, *Inorg. Chem.*, 1968, **7**, 903.
193. R. S. Taylor, M. Green and A. G. Sykes, *J. Chem. Soc. (A)*, 1977, 277.
194. K. L. Scott, M. Green and A. G. Sykes, *J. Chem. Soc. (A)*, 1977, 3657.

195. R. A. Marcus, *J. Phys. Chem.*, 1968, **72**, 891.
196. A. Haim and N. Sutin, *J. Am. Chem. Soc.*, 1966, **88**, 434.
197. T. W. Newton and N. A. Daugherty, *J. Phys. Chem.*, 1967, **71**, 3768.
198. B. Durham, J. F. Endicott, C.-L. Wong and P. D. Rillema, *J. Am. Chem. Soc.*, 1979, **101**, 847.
199. H. C. Brown, discussion following *J. Phys. Chem.*, 1952, **56**, 846.
200. A. Haim, *Acc. Chem. Res.*, 1975, **8**, 264.
201. When the driving force for the reaction is great, the activated complexes resemble reactants more than products. Thus in the reaction of $Fe(H_2O)_6^{3+}$ with Cr^{2+}, the orthodox component of the affinities (*vide infra* in text) will be closer to that expected for Fe^{3+}/Cr^{2+} than Fe^{2+}/Cr^{3+}.
202. J. P. Candlin, J. Halpern and D. L. Trimm, *J. Am. Chem. Soc.*, 1969, **86**, 1019.
203. D. E. Peters and R. T. M. Fraser, *J. Am. Chem. Soc.*, 1965, **87**, 2759.
204. R. T. M. Fraser, *J. Chem. Soc.*, 1965, 3641. The rate for $(NH_3)_5CoONO^{2+}$ was not measured but it was shown to be much greater than that for $(H_2O)_5CrONO^{2+}$ or 3×10^2 M^{-1} s^{-1}. It should be noted that the rate for $(NH_3)_5CoN_3^{2+}$ is 5×10^4 that for $(H_2O)_5CrN_3^{2+}$.
205. W. Schmidt and H. Taube, *Inorg. Chem.*, 1963, **2**, 698.
206. K. V. Krishnamurty and A. C. Wahl, *J. Am. Chem. Soc.*, 1958, **80**, 5921.
207. A. Anderson and N. A. Bonner, *J. Am. Chem. Soc.*, 1954, **76**, 3826.
208. R. G. Wilkins and R. E. Yelin, *Inorg. Chem.*, 1968, **7**, 2667.
209. T. T.-T. Li and C. H. Brubaker, Jr., *J. Organomet. Chem.*, 1981, **216**, 223; T. T.-T. Li, M. J. Weaver and C. H. Brubaker, Jr., *J. Am. Chem. Soc.*, 1982, **104**, 2381.
210. T. Saji and S. Aoyagui, *Bull. Chem. Soc. Jpn.*, 1973, **46**, 2101.
211. R. J. Campion, unpublished observations reported in R. J. Campion, N. Purdie and N. Sutin, *Inorg. Chem.*, 1964, **3**, 1091.
212. E. L. Goodenow and C. S. Garner, *J. Am. Chem. Soc.*, 1955, **77**, 5272.
213. P. G. Rasmussen and C. H. Brubaker, Jr., *Inorg. Chem.*, 1964, **3**, 977.
214. J. C. Sheppard and A. C. Wahl, *J. Am. Chem. Soc.*, 1957, **79**, 1020.
215. D. S. Matteson and R. A. Bailey, *J. Am. Chem. Soc.*, 1969, **91**, 1975.
216. J. Silverman and R. W. Dodson, *J. Phys. Chem.*, 1952, **56**, 846.
217. R. J. Campion, C. F. Deck, P. King, Jr. and A. C. Wahl, *Inorg. Chem.*, 1967, **6**, 672.
218. M.-S. Chan and A. C. Wahl, *J. Phys. Chem.*, 1978, **82**, 2542.
219. M. C. Palazzotto and L. H. Pignolet, *Inorg. Chem.*, 1974, **13**, 1781.
220. (a) R. K. Gupta, *Biochim. Biophys. Acta*, 1973, **292**, 291; (b) R. K. Gupta, S. H. Koenig and A. G. Redfield, *J. Magn. Reson.*, 1972, **7**, 66.
221. E. S. Yang, M.-S. Chan and A. C. Wahl, *J. Phys. Chem.*, 1975, **79**, 2049.
222. J. G. Reynolds, C. L. Coyle and R. H. Holm, *J. Am. Chem. Soc.*, 1980, **102**, 4350.
223. T. J. Meyer and H. Taube, *Inorg. Chem.*, 1968, **7**, 2369.
224. H. Taube, *Adv. Chem. Ser.*, 1977, **162**, 127; G. M. Brown, H. J. Krentzian, M. Abe and H. Taube, *Inorg. Chem.*, 1979, **18**, 3374.
225. G. M. Brown and N. Sutin, *J. Am. Chem. Soc.*, 1979, **101**, 883.
226. R. C. Young, F. R. Keen and T. J. Meyer, *J. Am. Chem. Soc.*, 1977, **99**, 2468.
227. R. W. Callahan, F. R. Keene, T. J. Meyer and D. J. Salmon, *J. Am. Chem. Soc.*, 1977, **99**, 1064.
228. J. Walsh, J. A. Baumann and T. J. Meyer, *Inorg. Chem.*, 1980, **19**, 2145.
229. J.-S. Chan and A. C. Wahl, *J. Phys. Chem.*, 1982, **86**, 126.
230. E. V. Luoma and C. H. Brubaker, Jr., *Inorg. Chem.*, 1966, **5**, 1618.
231. J. Shankar and B. C. deSouza, *J. Inorg. Nucl. Chem.*, 1962, **24**, 693; H. S. Habib and J. P. Hunt, *J. Am. Chem. Soc.*, 1966, **88**, 1668.
232. A. Hammershi, D. Geselowitz and H. Taube, *Inorg. Chem.*, 1984, **23**, 979.
233. F. P. Dwyer and A. M. Sargeson, *J. Phys. Chem.*, 1961, **65**, 1892.
234. I. I. Greaser, J. MacB. Harrowfield, A. M. Sargeson, A. J. Herlt and J. Springborg, *J. Am. Chem. Soc.*, 1977, **99**, 3181.
235. R. Farina and R. G. Wilkins, *Inorg. Chem.*, 1968, **7**, 514.
236. Y. A. Im and D. H. Busch, *J. Am. Chem. Soc.*, 1961, **83**, 3357.
237. D. P. Rillema, J. F. Endicott and N. A. P. Kane-Maguire, *J. Chem. Soc., Chem. Commun.*, 1972, 495.
238. P. Hurwitz and K. Kustin, *Trans. Faraday Soc.*, 1964, **62**, 427.
239. S. E. Manahan, *Can. J. Chem.*, 1967, **45**, 2451.
240. C. A. Koval and D. W. Margerum, *Inorg. Chem.*, 1981, **20**, 2311.
241. B. M. Gordon and A. C. Wahl, *J. Am. Chem. Soc.*, 1958, **80**, 273.
242. E. Roig and R. W. Dodson, *J. Phys. Chem.*, 1961, **65**, 2175.
243. P. B. Sigler and B. J. Masters, *J. Am. Chem. Soc.*, 1957, **79**, 6353.
244. G. Gordon and H. Taube, *J. Inorg. Nucl. Chem.*, 1961, **16**, 272.
245. J. C. Sullivan, D. Cohen and J. C. Hindman, *J. Am. Chem. Soc.*, 1957, **79**, 3672.
246. D. J. Meier and C. S. Garner, *J. Phys. Chem.*, 1952, **56**, 853.
247. J. C. Bradovitch and A. McAuley, *Inorg. Chem.*, 1981, **20**, 1667.
248. (a) N. Hirota and S. I. Weissman, *J. Am. Chem. Soc.*, 1964, **86**, 2537; (b) N. Hirota, in 'Radical Ions', ed. E. T. Kaiser and L. Kevan, Wiley Interscience, New York, 1968, chap. 2, p. 80.
249. T. Layoff, T. Miller, R. N. Adams, H. Fah, A. Horsfield and W. Proctor, *Nature (London)*, 1965, **205**, 382.
250. K. Serga and S. Aoyagui, *Bull. Chem. Soc. Jpn.*, 1973, **46**, 755.
251. N. Hirota, R. Carraway and W. Schook, *J. Am. Chem. Soc.*, 1968, **90**, 3611.
252. G. Malinoski and W. H. Bruning, *J. Am. Chem. Soc.*, 1967, **89**, 5063.
253. W. L. Reynolds, *J. Phys. Chem.*, 1963, **67**, 2866.
254. B. A. Kowert, L. Marcoux and A. J. Bard, *J. Am. Chem. Soc.*, 1972, **94**, 5538.
255. S. P. Sorensen and W. H. Bruning, *J. Am. Chem. Soc.*, 1973, **95**, 2445.
256. M. Ogasawara, H. Takaoka and K. Hayaski, *Bull. Chem. Soc. Jpn.*, 1973, **46**, 35.
257. K. W. Krishnamurty and A. C. Wahl, *J. Am. Chem. Soc.*, 1958, **80**, 5921.
258. (a) A. Anderson and N. A. Bonner, *J. Am. Chem. Soc.*, 1954, **76**, 3826; (b) E. Deutsch and H. Taube, *Inorg. Chem.*, 1968, **7**, 1532.

259. (a) E. L. King and H. Taube, *J. Am. Chem. Soc.*, 1954, **76**, 4053; (b) D. L. Ball and E. L. King, *J. Am. Chem. Soc.*, 1958, **80**, 1091.
260. H. Diaz and H. Taube, *Inorg. Chem.*, 1970, **9**, 1309.
261. B. Durham, J. F. Endicott, C.-L. Wong and D. P. Rillema, *J. Am. Chem. Soc.*, 1979, **101**, 847.
262. L. T. Cox, S. G. Collins and D. S. Martin, Jr., *J. Inorg. Nucl. Chem.*, 1961, **17**, 383.
263. T. Smith, D. Iverson and H. Taube, in preparation.
264. J. E. Harriman and A. H. Maki, *J. Chem. Phys.*, 1963, **39**, 778.
265. D. J. Williams, J. M. Pearson and M. Levy, *J. Am. Chem. Soc.*, 1971, **93**, 5483.

7.3

Photochemical Processes

CHARLES KUTAL
University of Georgia, Athens, GA, USA
and
ARTHUR W. ADAMSON
University of Southern California, Los Angeles, CA, USA

7.3.1 INTRODUCTION

Inorganic photochemistry has progressed through several stages. We begin with a period of scattered observations extending to the early 1950s. Examples are Eder's reaction,[1] that is, the photoredox decomposition of $HgCl_2$ in the presence of oxalate ions, uranyl oxalate actinometry (ref. 2, for instance), and the classic blueprinting process in which the photoreduction of ferric citrate to Fe^{II} in the presence of ferricyanide ion leads to the formation of Turnbull's blue. Photoredox decompositions of Co^{III} complexes were studied by Vranek,[3] Schwarz and Tede,[4] and Linhard and Weigel.[5] There are also early observations of ligand photosubstitutions, as in the case of $PtCl_6^{2-}$.[6]

The foundations of the contemporary period were laid in the early 1960s with increasingly systematic studies of ammine complexes of Co^{III} and especially of Cr^{III}. In the latter case, these led to rules predictive as to which ligand would undergo photosubstitution in a mixed ligand complex.[7] Reference 8 reviews the photochemistry of this period.

The field matured rapidly during the 1970s, and in several directions. New phenomenology was discovered such as the photosensitization of Co^{III} ammine complexes,[9] and emission from Cr^{III} complexes in room temperature, fluid solution.[10] This last observation made emission quenching studies possible,[11] and from then on increasingly detailed and sophisticated investigations of excited state processes appear in the literature. Excited state electron transfer was observed,[12] with much stimulation of interest in the possibility of solar energy conversion through the solar splitting of water and like processes. The photochemistry of new families of Werner-type complexes was explored, such as those of Rh^{III}, Ir^{III} and Ru^{II}. Complexes with polypyridine-type ligands became of much interest. Systems involving coordinated sulfur and phosphorus were probed, as were new types of macrocyclic complexes, including those with biological relevance such as cobalamins and metalloporphyrins. Finally, the whole area of organometallic compounds received increasing attention.

Reviews that cover the field up to the middle 1970s are references 13–16. A useful contemporary series of review-type articles, intended for the more general reader, appeared in the October 1983 issue of the *Journal of Chemical Education*.

A qualitative profile of the current status of inorganic photochemistry is attempted in Table 1. Metals are grouped according to Periodic Table families, and ligands are differentiated according to whether they are of the traditional type (*e.g.* ammonia, saturated amines, pseudo-halogens), delocalized chelate/macrocyclic (*e.g.* 2,2′-bipyridine, porphyrin) or predominantly π-acid in character (*e.g.* carbonyl, alkene). In addition, the type of investigation performed is indicated. The best studied complexes are those of Cr^{III}, Co^{III} and the polypyridine complexes of Ru^{II}, while knowledge of the photobehavior of several elements is still rather primitive.

Table 1 Survey of Photochemistry and Photophysics of Coordination Compounds[a]

Metal	*Type of ligand*			*Type of study*			
	Ammine, cyano, etc.	*Delocalized chelate/macrocyclic*	*π-Acid*	*Photochemical*	*Photophysical*	*Mechanistic*	*Theoretical*
V	*	—	*	*	—	—	—
Nb	—	—	*	*	—	—	—
Ta	—	—	*	*	—	—	—
Cr	***	**	**	***	***	***	***
Mo	*	—	**	**	*	*	—
W	*	—	**	**	**	**	*
Mn	*	*	**	**	—	—	—
Tc	—	—	—	—	—	—	—
Re	—	—	*	*	*	—	—
Fe	**	**	**	**	*	*	*
Ru	*	***	**	***	***	***	***
Os	*	**	*	**	**	*	*
Co	***	**	**	***	*	***	***
Rh	**	*	**	**	**	**	**
Ir	*	*	*	*	*	*	*
Ni	*	*	*	*	—	—	—
Pd	*	*	*	*	—	—	—
Pt	**	*	—	**	**	**	**
Cu	**	**	—	**	—	*	*
Ag	***	—	—	***	—	*	—
Au	*	*	—	*	—	—	—
Zn	*	—	—	*	—	*	—
Cd	*	—	—	*	—	*	—
Hg	*	*	—	*	—	*	—
Actinides, lanthanides	**	*	—	**	*	*	*

[a] Asterisks denote extent of coverage: heavy (***), moderate (**) or light (*).

The plan of this article is as follows. In Section 7.3.2 we discuss the general physical chemistry of excited states and excited state processes. Section 7.3.3 surveys the characteristic reactivities of the various types of excited states found in *d* and *f* transition metal complexes (excluding organometallic compounds). Section 7.3.4 provides a brief account of some applications of transition metal photochemistry.

7.3.2 EXCITED STATES AND EXCITED STATE PROCESSES

7.3.2.1 Types of Excited States

Experimental information about excited states comes primarily from absorption spectra, and a fairly typical one for a transition metal ammine is shown in Figure 1, namely that of $[Cr(NCS)(NH_3)_5]^{2+}$ in aqueous solution. Transitions are characterized first of all by the energy, E, corresponding to the absorption band maximum. The Einstein relationship is given in equation (1), where h is Planck's constant, ν is the frequency at the band maximum, and $\bar{\nu}$ the corresponding wavenumber. Very commonly, band maxima positions are given in terms of their wavelength, λ. The second important quantity is the absorptivity, A (or optical density, D), defined by equation (2), where I_0 and I are the incident and emergent intensity of light in a beam passing through depth l of a solution of concentration C. The quantity ε is known as the extinction coefficient when expressed in M^{-1} cm^{-1} units (M denoting mol $liter^{-1}$); in SI units, it is called the molar absorptivity. Equation (2) is known as the Beer–Lambert Law.

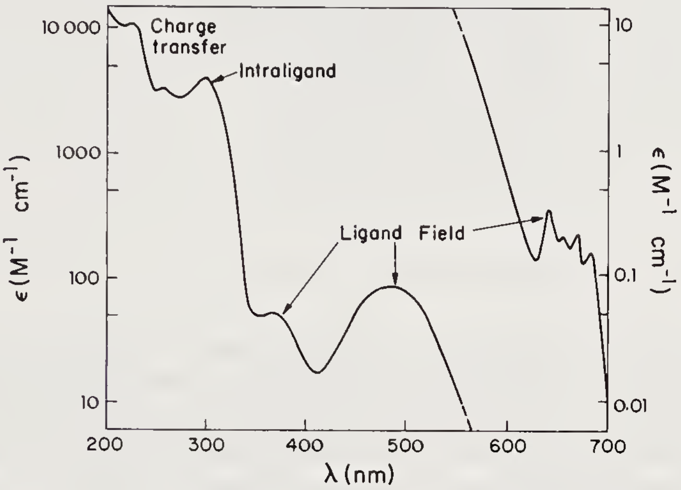

Figure 1 Electronic absorption spectrum of aqueous $[Cr(NCS)(NH_3)_5]^{2+}$ (after Figure 1 in *J. Am. Chem. Soc.*, 1969, **91**, 1076)

$$E = h\nu\ ;\ \nu = c/\lambda = c\bar{\nu} \tag{1}$$

$$A = \log(I_0/I) = \varepsilon l C \tag{2}$$

$$f = 4.33 \times 10^{-9}\int \varepsilon(\bar{\nu})\mathrm{d}(\bar{\nu}) \approx 4.6 \times 10^{-9}\varepsilon_{\max}\,\bar{\nu}_{1/2} \tag{3}$$

As suggested by Figure 1, the typical absorption band is fairly broad in the case of coordination compounds, and the total transition probability must be obtained by an integration over the whole band. A useful relationship is equation (3),[14] where f is called the transition probability, $\varepsilon_{\max}$ is the extinction coefficient at the band maximum, and $\bar{\nu}_{1/2}$ is the band width at half-maximum. Values of f range from about 10^8 for a fully allowed transition to a millionfold or so less for a highly forbidden one.

7.3.2.1.1 Ligand field states

Ligand field theory is covered in Chapter 6, and only especially relevant, simple aspects are summarized here. Much of inorganic photochemistry deals with d^3 or d^6 complexes and these two classes will serve as specific examples. The qualitative situation is that the spectroscopic free ion states are split by the electrostatic field of the ligands (the 'ligand field') as illustrated for the d^3 and d^6 cases in Figure 2. Both the one-electron orbital populations and the state designations based on orbital symmetry are shown. Thus for an octahedral (O_h) d^3 complex, the ground state is $^4A_{2g}$, A_2 denoting the orbital symmetry of three unpaired electrons in the t_{2g} (d_{xy}, d_{xz}, d_{yz}) set of orbitals; g indicates that the symmetry is *gerade*, and the left superscript is the spin multiplicity, $m+1$, where m is the number of unpaired electrons. Transitions to the low-lying states $^4T_{2g}$ and $^4T_{1g}$ correspond to the first two broad bands in Figure 1 (assuming effective O_h symmetry) and the weak, highly structured band in the figure corresponds to the transition to ^2E_g.

In the case of an octahedral d^6 complex, the ground state is $^1A_{1g}$ (strong ligand field case), and the first absorption band usually corresponds to the transition to the $^1T_{1g}$ state. There are, in addition, triplet and quintet states which may be low-lying, especially in less symmetric complexes.

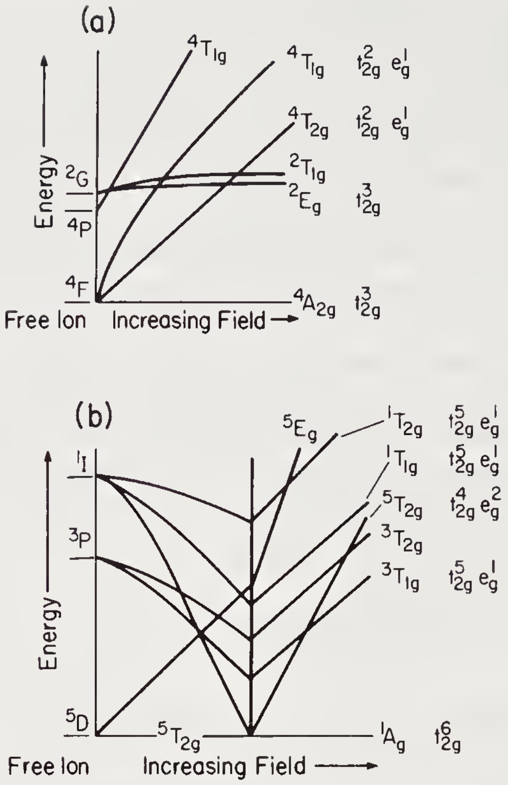

Figure 2 Qualitative energy-level diagrams for (a) d^3 and (b) d^6 transition metals in an octahedral ligand field

Note that the usual, spin-allowed *d–d* transition places an electron in an $e_g(d_{x^2-y^2}$ or $d_{z^2})$ orbital, which is antibonding. There is a special situation in the d^3 case in that the $^4A_{2g} \rightarrow {}^2E_g$ transition merely rearranges spins in the t_{2g} set of orbitals, which are essentially nonbonding.

In the case of less symmetric complexes, the above states may be split into further ones (except *A* states), although the basic electron population and the spin designation remain. To avoid dealing with a multitude of term symbols, some authors adopt the practice of designating states as *S*, *D*, *Q*, *etc.*, for singlet, doublet and quartet, with subscripts to be explained in Section 7.3.2.2.1.

7.3.2.1.2 Charge transfer states

Ligand field transitions involve what is essentially an angular rearrangement of electrons. In a molecular orbital diagram, however, one sees that it is possible to move an electron from a metal-centered *d* orbital to one that is more ligand centered, that is, to make a *radial* change in the electron distribution. We speak of such transitions as charge transfer, CT, with the sub-categories of CTTM for ligand-to-metal, CTTL for metal-to-ligand, CTTS for charge transfer to solvent and LLCT for ligand-to-ligand charge transfer. In the CTTS case, the electron may be ejected into adjacent solvent. Generally speaking, CTTM transitions vary in energy according to the ease of oxidation of the most easily oxidized ligand, while CTTL and CTTS transitions tend to be especially sensitive to the nature of the solvent medium. See ref. 17 for a case of an LLCT transition. CT transitions are often *g* to *u* and are relatively allowed (unless there is a spin change); accordingly, $\varepsilon_{\max}$ values may be several thousand $M^{-1}\ cm^{-1}$, as in the short wavelength band in Figure 1.

7.3.2.1.3 Intraligand states

A free, that is, uncoordinated ligand will have its own absorption spectrum, of course, and features of this spectrum may be seen when the ligand is coordinated, usually red-shifted. In Figure 1, the transition around 305 nm is thought to be primarily an internal thiocyanate transition. Polypyridine and related ligands will often show features derived from the free ligand, as another example.

7.3.2.1.4 Delocalized states

In chelate and macrocyclic complexes, electronic states may exist which are of a delocalized nature; they pertain to the *system* of metal and ligands. Such states are not simply derived from metal *d–d* states or from free ligand states and transitions involving delocalized states are often quite intense.

7.3.2.1.5 Metal–metal states

Complexes having a direct metal–metal bond will show a corresponding, usually low-energy, absorption band. If metals are connected by bridging ligands, there can be charge transfer excitations, especially if the two metals are in different oxidation states, corresponding roughly to transfer of an electron from one metal to the other.

7.3.2.2 Thexi States and DOSENCO States

7.3.2.2.1 Thexi states

The above discussion has been in relatively spectroscopic terms, the word 'state' implying some specific quantum mechanical designation. An important complication must now be described. Consider first the case of a diatomic molecule in which the internuclear distance is greater in the excited state than in the ground state. As shown in Figure 3, the most probable transition will be from the lowest vibrational level of the ground state, and will be 'vertical'. That is, one accepts the Franck–Condon principle that nuclei do not move appreciably during an electronic transition. The consequence is that the transition will most probably terminate on a high vibrational level of the excited state; we will call this a Franck–Condon (FC) state. The transition energy at the band maximum thus includes a certain amount of vibrational excitation.

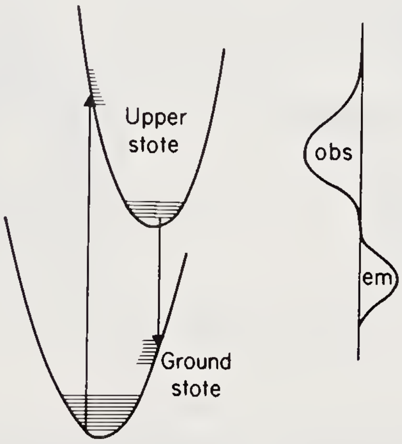

Figure 3 Illustration of vertical transitions during absorption (abs) and emission (em) in a diatomic molecule

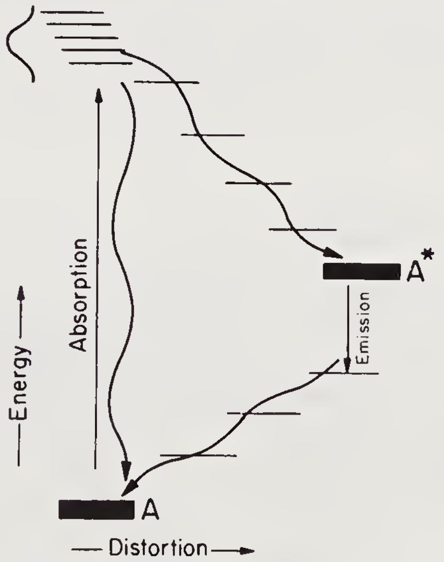

Figure 4 Energy *vs*. distortion diagram (reproduced with permission from *J. Chem. Educ.*, 1983, **60**, 797)

The same situation applies to coordination compounds. It is now impractical to show nuclear coordinates, and in Figure 4 we use the abscissa to denote distortion in a qualitative sense; this may now include bond angle as well as bond length changes. As was noted, the usual *d*–*d* transition places an electron in an antibonding orbital, and some geometry change is to be expected. The radial redistribution in a CT transition can likewise distort the excited state potential surface relative to the ground state. Excited state distortion may not be trivial in the case of coordination compounds. Thus, in the case of square-planar ones, such as $PtCl_4^{2-}$, the excited state is thought to have a distorted tetrahedral geometry.[18]

In solution, the excess vibrational energy following an FC transition is lost very quickly — there are indications that only a few picoseconds are needed for the complex to come to thermal equilibrium with the medium with respect to vibrational excitation.[19] We speak of the *thermally equilibrated excited* state, or, as an abbreviation, of the *thexi* state. Photochemical and photophysical processes very often involve thexi states.

The term 'state' is now being used in a different sense than before. Because of thermal equilibration, we have an electronically excited species that is in thermodynamic equilibrium with its surroundings with respect to vibration (and rotation). We are really talking about an ensemble of species having a Boltzmann distribution of vibrational energy and hence a valid partition function. In brief, a thexi state is a thermodynamic state. It will have an equilibrium structure, a definite absorption spectrum (both UV-visible and IR), well-defined free energy and entropy as well as energy, and well-defined chemistry. It is, in effect, an isomer of the ground state, just as, say, square-planar and tetrahedral forms of a Ni^{II} complex are isomers.

The thermal equilibration of an FC state, while rapid, probably takes place in stages. In solution, a complex is solvated and in a solvent cage. As illustrated in Figure 5, solvent molecules must move to allow the change in geometry to the thexi state. The thin lines of Figure 4 are intended to indicate successive stages of solvent shifting. At each stage, the complex is in a nonequilibrium solvent cage but might have loosely defined vibrational states.

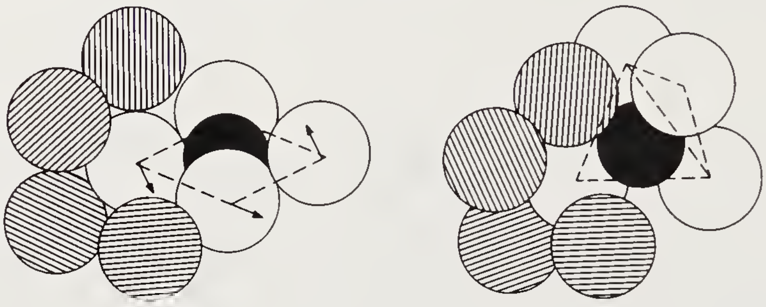

Figure 5 Illustration of solvent cage effect in delaying excited state thermal equilibration (reproduced with permission from *J. Chem. Educ.*, 1983, **60**, 797)

The symmetry-based term symbols used in Section 7.3.2.1.1 are now seen to be potentially misleading; the thexi state geometry may not be that of the ground state. This is the second reason why the nonspecific designations *S*, *D*, *Q*, *etc.* are sometimes used. For a d^3 complex, the ground state becomes Q°_{0}, the superscript denoting thermal equilibration. The state arrived at following light absorption would be Q_{FC}, and the thermally equilibrated first excited quartet state is Q°_{1}. The distortion diagram for a d^3 system is depicted in Figure 6. Note that the D°_{1} thexi state is shown as little distorted from Q°_{0}; this is because the electrons have remained in the t_{2g} set of orbitals. Direct evidence for this conclusion will be noted further below.

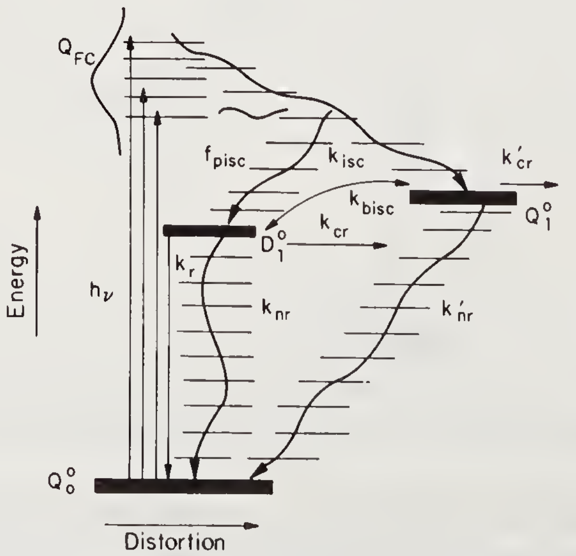

Figure 6 Energy *vs.* distortion diagram for d^3 systems (reproduced with permission from *J. Chem. Educ.*, 1983, **60**, 797)

A final point is that the energy of a thexi state will be less than that of the preceding FC state. The former has been difficult to estimate, but it can be seen from Figures 4 and 6 that it should correspond roughly to the long wavelength tail of the absorption band. A rule of thumb is to take the wavelength at which ε has dropped to 5% of its maximum value.[20]

7.3.2.2.2 DOSENCO states

There is a possibility that an FC state will react before complete thermal equilibration. In the case of diatomic molecules, the process is usually known as predissociation — a dissociative state crosses the excited state potential surface. The situation is more complicated in the case of a coordination compound, but one can imagine an FC state relaxing along some nuclear coordinate leading to bond breaking. A state capable of such a process has been called a DOSENCO state, an acronym for 'Decay On SElected Nuclear COordinates'.[21] The same authors use the term DERCOS (DEcay *via* Random COordinate Selection) for a thexi state.

7.3.2.3 Kinetics of Excited State Processes

The central process in photochemistry is that of chemical reaction, ordinarily from a thexi state. The quantum yield, ϕ, is defined by equation (4), where n denotes the moles of reaction (corrected for any ground state or thermal reaction) and $\mathscr{E}$ is the einsteins, that is, moles of light quanta absorbed.

The rate processes that must be considered are given by equations (5)–(8). The rate of the process in equation (5) is just that of light absorption by A, I_a. The other three are first order. There may, in addition, be second order processes, of the type given by equation (9), where Q, for quencher, denotes some species that can deactivate A*. Since the concentration of Q, [Q], is usually much larger than [A*], such reactions are pseudo first order.

$$n = \mathscr{E}\phi \tag{4}$$

$$\mathrm{A} \xrightarrow{h\nu} \mathrm{A}^* \tag{5}$$

$$\mathrm{A}^* \xrightarrow{k_{\mathrm{cr}}} \mathrm{P} \quad \text{(where P is the photoproduct)} \tag{6}$$

$$\mathrm{A}^* \xrightarrow{k_{\mathrm{nr}}} \mathrm{A} \quad \text{(nonradiative return to ground state)} \tag{7}$$

$$\mathrm{A}^* \xrightarrow{k_{\mathrm{r}}} \mathrm{A} \quad \text{(return } via \text{ emission of radiation)} \tag{8}$$

$$\mathrm{A}^* + \mathrm{Q} \xrightarrow{k_{\mathrm{q}}} \mathrm{A} + \mathrm{Q}\ (\text{or } \mathrm{Q}^*) \tag{9}$$

If A* is a thexi state, its reactions should obey conventional chemical kinetics, and we can examine several simple, important cases. Suppose firstly that A* is produced by a flash or laser pulse technique in a time short compared to the time scale of the other processes. The produced A* will disappear with a rate constant k which is the sum of the rate constants for all applicable processes. In the absence of quencher, we write $k^\circ = k_{\mathrm{nr}} + k_{\mathrm{r}} + k_{\mathrm{cr}}$; the time for [A*] to decrease by a factor of e, τ°, is just $1/k^\circ$. With quencher present, we have $k = k_{\mathrm{nr}} + k_{\mathrm{r}} + k_{\mathrm{cr}} + k_{\mathrm{q}}[\mathrm{Q}]$ and $\tau = 1/k$. The ratio of lifetimes in the absence and presence of quencher is given by equation (10). A plot of τ°/τ *versus* [Q] should thus be linear, with slope $k_{\mathrm{q}}\tau^\circ$; this product is often designated as K_{SV} and called the Stern–Volmer constant.

$$\tau^\circ/\tau = \frac{k_{\mathrm{nr}} + k_{\mathrm{r}} + k_{\mathrm{cr}} + k_{\mathrm{q}}[\mathrm{Q}]}{k_{\mathrm{nr}} + k_{\mathrm{r}} + k_{\mathrm{cr}}} = 1 + k_{\mathrm{q}}\tau^\circ[\mathrm{Q}] \tag{10}$$

$$\phi^\circ/\phi = \tau^\circ/\tau = 1 + k_{\mathrm{q}}\tau^\circ[\mathrm{Q}] \tag{11}$$

Since the quantum yield for reaction is simply k_{cr} divided by k° or by k, if Q is present, we also have the relationship in equation (11). Thus the quencher inhibits photochemistry to just the same degree as it reduces the A* lifetime. Since the intensity of emission, I_{e}, is given by $k_{\mathrm{r}}[\mathrm{A}^*]$, it also follows that I°_{e} and I_{e} decay with the lifetimes τ° and τ, and that the ratio $I^\circ_{\mathrm{e}}/I_{\mathrm{e}}$ obeys equation (11).

Consider next the case of a system under steady irradiation, with I_a einsteins of light absorbed per liter per second. We now have the relationship in equation (12). Under steady state conditions, $d[A^*]/dt = 0$, and we can solve equation (12) for $[A^*]$ to give equation (13). The rate of product formation, $d[P]/dt$, is ϕI_a by definition, but is also given by $k_{cr}[A^*]$. These relationships give rise to equation (14). Rearrangement, and taking ϕ° to be the yield in the absence of quencher, gives a result identical to equation (11). The intensity of emitted light is defined as $I_e = \phi_e I_a$ but is also given by $k_r[A^*]$. On combining these statements with equation (11), we obtain equation (15) which is again the Stern–Volmer relationship.

$$d[A^*]/dt = I_a - (k_{nr} + k_r + k_{cr})[A^*] - k_q[Q][A^*] \tag{12}$$

$$[A^*] = \frac{I_a}{(k_{nr} + k_r + k_{cr}) + k_q[Q]} \tag{13}$$

$$d[P]/dt = \phi I_a = \frac{k_{cr} I_a}{(k_{nr} + k_r + k_{cr}) + k_q[Q]} \tag{14}$$

$$I^\circ_e/I_e = \phi^\circ_e/\phi_e = 1 + k_q\tau^\circ[Q] \tag{15}$$

One further case should be examined. Suppose that in equation (9), Q^* is formed and is chemically reactive, going to product P' with a rate constant k'_{cr}. In addition, Q^* will have rate constants k'_{nr} and k'_r for nonradiative and radiative relaxation, respectively. The situation is now that light is absorbed by A, but we measure the formation of product P'. We speak of such a process as one of *sensitization*, that is, the formation of P' is photosensitized by A.

We now ask how the sensitization yield, ϕ_s, varies with [Q], where $d[P']/dt = \phi_s I_a$, and is also given by $k'_{cr}[Q^*]$. For steady-state conditions, the concentration of Q^* is given by equation (16). From the definition of ϕ_s and with the use of equation (13), equation (17) is obtained where ϕ_s^∞ is $k'_{cr}/(k'_{nr} + k'_r + k'_{cr})$ and is the yield of P' at infinite [Q]. From equation (17), a plot of $1/\phi_s$ *versus* $1/[Q]$ should be linear, the intercept and slope allowing calculation of ϕ_s^∞ and K_{SV}.

$$[Q^*] = \frac{k_q[Q][A^*]}{k'_{nr} + k'_r + k'_{cr}} \tag{16}$$

$$1/\phi_s = 1/\phi_s^\infty + \frac{1}{\phi_s^\infty K_{SV}}\,\frac{1}{[Q]} \tag{17}$$

Processes of the type given by equation (9) are often 'diffusion controlled'. That is, the rate is that at which A^* and Q can make diffusional encounters in solution. For room temperature aqueous solution, a typical k_q is in the range 10^9–10^{10} M^{-1} s^{-1}.

Note that in all of these situations, one can begin to unravel the excited state rate constants if measurements of τ° and of τ can be made. There are several ways in which this can be done. The most common one is from the decay of the emission from A^*, following pulse excitation. Alternatively, it has been possible in several cases to observe the UV-visible absorption spectrum of A^*, and the decay of this absorption again gives τ° or τ (see, for examples, refs. 22–26). In rare cases, it has been possible to observe the rate at which the primary photoproduct P grows in, again following a pulse excitation; it should do this with the lifetime of A^*.[27]

There are some additional, useful relationships. Since $\phi^\circ = k_{cr}/(k_{nr} + k_r + k_{cr})$, equations (18) and (19) follow straightforwardly. Thus measurement of τ° and of these yields allows calculation of k_{cr} and of k_r. Radiative relaxation is usually taken to be an intramolecular process whose rate is essentially independent of temperature. If k_r is constant, the relation in equation (20) holds. A common application of this relation is the following. Suppose that I°_e and τ° can be measured at some low temperature, but that at room temperature the k_{nr} and/or k_{cr} processes have become so rapid that τ° is too short to measure. It is sometimes possible, however, to measure I°_e at room temperature in such cases, and, since I°_e and ϕ°_e are proportional, it follows from equation (20) that the expression in equation (21) holds, thus affording an indirect measurement of a lifetime.

$$\phi^\circ = k_{cr}\tau^\circ \tag{18}$$

$$\phi^\circ_e = k_r\tau^\circ \tag{19}$$

$$(\phi^\circ_e/\tau^\circ)_{T_1} = (\phi^\circ_e/\tau^\circ)_{T_2} \tag{20}$$

$$\tau^\circ_{T_2} = (I^\circ_e)_{T_2}(\tau^\circ/I^\circ_e)_{T_1} \tag{21}$$

$$D^\circ_1 \underset{k_{\mathrm{isc}}}{\overset{k_{\mathrm{bisc}}}{\rightleftarrows}} Q^\circ_1 \tag{22}$$

To conclude this section, many systems are complicated by the presence of two (or more) low lying states (as in Figure 6). If these states can intercommunicate, one must add to the kinetic scheme various intersystem crossing processes. Thus for the Cr^{III} case, one may need to consider the processes in equation (22), where k_{isc} and k_{bisc} are the rate constants for intersystem crossing and for back intersystem crossing, respectively. The kinetic analysis at this point can become rather complex.[27,28]

7.3.2.4 Electron Distribution and Chemical Reactivity

We turn now to some more detailed considerations of the nature of the various rate processes, beginning with that of chemical reaction of A*. We consider only primary photochemical processes, that is, reactions undergone by A* directly, either uni- or bi-molecularly. The primary photoproduct or products may react further to give the final, observed product but such secondary reactions, while of great importance to the photochemist, are not a principal concern here.

As suggested in the Introduction, the type of excited state A* and the nature of its chemical reactivity often correlate. Thus if A* is a ligand field thexi state, one expects its reactivity to be primarily one of ligand substitution. If A* is a charge transfer state of the CTTM type, one generally observes at least a component of redox decomposition. An example is that of Co^{III} ammine complexes where irradiation in the visible region, where the absorption is of the *d*–*d* type, leads to ligand substitution, while irradiation in the UV, where CTTM absorption sets in, leads in part to Co^{II} and oxidized ligand.[13,14] If the absorption is into a CTTL band, a number of reactions can occur and, if into a CTTS band, actual free electron production may be observed. Absorption into an intraligand band is apt to result in ligand-centered chemistry. A thorough treatment of these generalizations is presented in Section 7.3.3.

7.3.2.4.1 Cage mechanism

An early as well as currently useful picture invokes the solvent cage (illustrated in Figure 5).[29,30] If the primary photochemical reaction is one of either homolytic or heterolytic bond fission, the geminal products will tend to remain in the same solvent cage for a few vibrational periods. There will be the possibility of back reaction, either to annul the primary reaction or to allow linkage isomerization.[31] If homolytic bond fission occurs, as with $[CoBr(NH_3)_5]^{2+}$, the Br radical may accept an electron from the Co^{II} moiety before escaping, leading to aquation as the net reaction. If heterolytic bond fission occurs, cage scavenging of the pentacoordinated intermediate would again lead to aquation (or solvation, if in a nonaqueous solvent).

7.3.2.4.2 Photolysis rules and ligand field theory

An early empirical observation with Cr^{III} complexes was that the following rules were obeyed.[7]

(1) Consider the six ligands to lie in pairs at the ends of three mutually perpendicular axes. That axis having the weakest average ligand field strength will be the one labilized, and the total quantum yield will be about that for an O_h complex of the same average ligand field.

(2) If the labilized axis contains two different ligands, then the ligand of greater field strength preferentially aquates. This may be a type of *trans* effect.

As an example, the photochemistry of $[CrCl(NH_3)_5]^{2+}$ is primarily one of ammonia aquation, labelling studies showing that the *trans* ammonia is indeed the one substituted.[32] The photoreaction is *antithermal*; the thermal reaction is entirely one of chloride aquation. The case of $[CrCN(NH_3)_5]^{2+}$ is interesting in that the acido group is a stronger field than ammonia; as predicted by the rules, the photoreaction is one of ammonia aquation, presumably of a *cis* ammonia.[33] While exceptions do exist (*e.g.* *trans*-$[CrF_2(en)_2]^+$),[34] the photolysis rules are qualitatively consistent with the behavior of a large number of mixed-ligand Cr^{III} complexes.

The rules have been accounted for in terms of ligand field theory, taking Q°_1 (see Figure 6) to be the reactive state.[35,36] Figure 7 illustrates the energy level orderings of the one-electron *d*-orbitals and the electronic states for $[CrX(NH_3)_5]^{2+}$ complexes of effective C_{4v} symmetry. The lowest quartet excited state is ${}^4E(\mathrm{a})$, a component of the ${}^4T_{2g}$ state in O_h symmetry. Excitation of the complex to ${}^4E(\mathrm{a})$ places an electron in a strongly σ-antibonding orbital which is mainly d_{z^2} in character. At the same time a π-antibonding electron has left the t_{2g} set. For purely σ-bonding ligands, such as NH_3, the net effect is to labilize that ligand on the z-axis; the X group is not labilized since it has some π-bonding ability, and thus any σ-bond-weakening effect is partially offset by π-bonding.

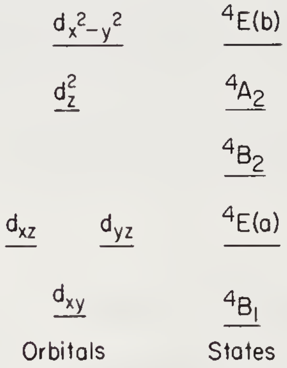

Figure 7 Energy orderings of the orbitals and states of some $[CrX(NH_3)_5]^{2+}$ complexes (X is Cl, Br, NCS) (from ref. 35)

The ligand field treatment has been extended by means of angular overlap calculations and ensuing correlation diagrams.[37] A similar treatment has been made for d^6 complexes, such as those of Co^{III} and Rh^{III}.[38,39] The photolysis rules, incidentally, are not as strongly obeyed with such complexes.

7.3.2.4.3 Environmental effects on photoreactivity

Quantum yields are generally somewhat temperature dependent, but not highly so. Apparent activation energies, E_{act}, in the 8–17 kJ mol^{-1} range are fairly common. Small E_{act} values are not surprising, partly because ϕ is determined by a ratio of rate constants (as in equation 18), and partly on the ground that since excited state lifetimes are short, an A* species will not have time to acquire any large energy of activation before disappearing by some other process. Cases of higher E_{act} values, in the 28–42 kJ mol^{-1} range, have in some cases been attributed to thermally activated intersystem crossing or internal conversion from an unreactive excited state to a higher lying reactive state.[40]

The wavelength dependence of quantum yields tends to be small over the region of absorption to a given type of excited state. Both quantum yield and reaction mode may change considerably, however, if a different type of absorption band is irradiated. The general conclusion is that crossing, particularly between d–d and CT states, is relatively inefficient.

Solvent effects on quantum yields have been studied to some extent. Yields for substitution fall precipitously and the nature of the reaction may change if the medium consists of a noncoordinating solvent. Thus *trans*-$[Cr(NCS)_4(NH_3)_2]^-$ shows a ϕ of about 0.3 in aqueous media (for thiocyanate aquation), but is photoinert in nitromethane. In a mixed solvent study, it was concluded that the photochemical behavior of this complex depended on the solvent composition of the solvation shell rather than on the stoichiometric composition.[41,42]

Some observations have been made on the effect of pressure on quantum yields, using pressures in the 1–2 kbar range.[43–45] Apparent volumes of activation range from about −10 cm^3 mol^{-1} to small positive values for Cr^{III} and Rh^{III} complexes.

7.3.2.4.4 Bimolecular thexi state reactions

There are several categories of reactions of the type represented by equation (9). That of excitation energy transfer has already been noted. Alternatively, the process may be one of electron transfer as in equation (23), with photoexcited $[Ru(bipy)_3]^{2+}$ being the prototypal example of A* and Q being a Co^{III} ammine in the first observed case,[12] but now any of a number of species (see ref. 46 for examples). There has been some success in fitting k_q values to the Marcus treatment of electron transfer rates.[46,47] The reverse of equation (23), that is, excited state reduction, has also been observed. In general, a complex is likely to show excited state electron transfer behavior if it has any accessible one-electron oxidized or reduced forms. The excitation energy of an A* species is usually two or more volts, and this is sufficient to drive a redox reaction that would be highly unfavorable for ground state A.

$$A^* + Q \xrightarrow{k_q} A^+ + Q^- \tag{23}$$

$$AH^* + Q \xrightarrow{k_q} A + QH \tag{24}$$

A third type of bimolecular reaction, summarized by equation (24), is that of excited state proton transfer where Q is now a proton acceptor. This type of process was proposed in the case of the OH^- and CO_3^{2-} quenching of emission from $[RhCl(NH_3)_5]^{2+}$.[48]

Finally, of course, process (9) may not involve any net reaction. In this case the encounter between A* and Q merely results in deactivation of A* to A. The general explanation is along the line that weak interactions during an encounter, especially if Q contains a metal or other heavy atom, can compromise the selection rules that make an A* → A deactivation relatively forbidden.

7.3.2.5 Photophysical Processes

Photophysical processes, that is, ones not involving any change in composition of an A*, have become of much interest to the inorganic photochemist, particularly in terms of excited state kinetic schemes. A brief discussion of the phenomenology and theory of radiative and nonradiative deactivations follows.

7.3.2.5.1 Radiative transitions

The process represented by equation (8), emission from an excited state, is generally called fluorescence if no spin change is deemed to occur, and phosphorescence if there is a spin change. Spin designations can be ambiguous in the case of second and third row transition metal complexes because of the importance of spin–orbit coupling.[49] Most authors retain them, however, as a matter of convention and convenience. A classic case is that shown in Figure 8, for $[Cr(urea)_6]^{3+}$.[50] The broad, long wavelength emission shows a mirror-image spectrum relative to that of the first spin-allowed absorption band, and is taken to correspond to the $Q^\circ_1 \rightarrow Q_{0,\,FC}$ transition ($^4T_{2g} \rightarrow {}^4A_{2g}$ in O_h symmetry), and is termed a fluorescence. Note the considerable Stokes' shift (red shift of fluorescence relative to absorption), indicating that there is significant excited state distortion. The shorter wavelength emission shown in the figure is narrow, and has vibrational structure. It is centered nearly over the doublet absorption band, and is taken to be due to the $D^\circ_1 \rightarrow Q_{0,\,FC}$ transition ($^2E_g \rightarrow {}^4A_{2g}$ in O_h symmetry), and is called a phosphorescence.

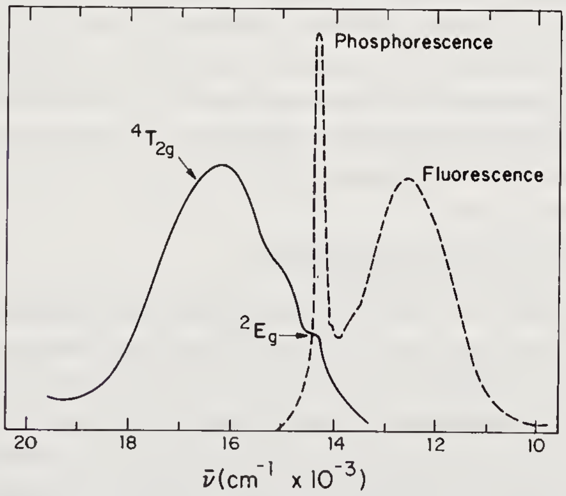

Figure 8 Absorption (—, 298 K) and emission (---, 77 K) spectra of $[Cr(urea)_6]^{3+}$ (after Figure 1 in ref. 50)

Emission from the lowest doublet state is fairly common with Cr^{III} complexes, and often is observable, although weak, in room temperature solution. Typically, τ° values are in the ms range at 77 K and decrease to ns or μs values at room temperature. The low temperature limit is just $1/k_r$; at intermediate low temperatures k_{nr} probably controls τ°, while at room temperature, other processes such as k_{cr} and k_{bisc} are probably controlling. It is this last situation that interests the inorganic photochemist, that is, the behavior of τ° under photochemical conditions. The apparent activation energy may now range up to 40 kJ mol^{-1}, and probably reflects the E_{act} for either the k_{cr} or the k_{bisc} path.

Empirical emission rules for Cr^{III} complexes are the following.[51]

(1) For complexes with six equivalent Cr—L bonds, the emission lifetime in room temperature aqueous solution decreases with decreasing ligand field strength.

(2) If two different kinds of ligand are coordinated, the emission lifetime will be relatively short if that ligand which is preferentially substituted in the *thermal* reaction lies on the weak field axis of the complex. A recent illustration of the application of these rules is with $[CrCN(NH_3)_5]^{2+}$, for which the emission lifetime of 22 μs is indeed relatively long.[52]

Room temperature emission has been observed for a number of transition metal complexes. Examples include Rh^{III} ammines,[53] $[Pt(CN)_4]^{2-}$,[54] and some Cu^I phosphine complexes.[55] An important class is that of the polypyridine complexes of Ru^{II} and related species.[56] This last emission, probably from a ^3CT state, is quite strong and its occurrence has made possible a number of detailed studies of electron transfer quenching reactions.

Values of the radiative rate constant k_r can be estimated from the transition probability. A suggested relationship[14,57] is given in equation (25), where n_i is the index of refraction of the medium, $\langle \nu_f^{-3} \rangle$ is the mean of the cube of the reciprocal of the emission frequency, and g_l/g_u is the ratio of the degeneracies in the lower and upper states. It is assumed that the absorption and emission spectra are mirror-image-like and that excited state distortion is small. The basic theory is based on a field wave mechanical model whereby emission is stimulated by the dipole field of the molecule itself. Theory, however, has not so far been of much predictive or diagnostic value.

$$k_r = 2.88 \times 10^{-9} n_i^2 \left\langle \nu_f^{-3} \right\rangle^{-1} \int \frac{\varepsilon(\bar{\nu})d\bar{\nu}}{\bar{\nu}} \frac{g_l}{g_u} \tag{25}$$

7.3.2.5.2 Nonradiative transitions

The rate of a nonradiative relaxation such as the k_{nr} process of equation (7) can be estimated from $\tau°$ values measured at a sufficiently low temperature such that k_{cr} and k_{bisc} are likely to be unimportant because of their higher activation energy. Under such a condition, $1/\tau° = (k_r + k_{nr})$, and k_r can be estimated from the low temperature limit to $\tau°$, or from equation (25). For coordination compounds, k_{nr} is usually not very temperature dependent, E_{act} typically being 8–12 kJ mol^{-1}.

The process has been treated theoretically in terms of simplified models.[14,58] The quantum mechanics is one of formulating the probability of crossing from an excited to a ground state, summed over all vibrational levels. For coordination compounds, the 'weak' coupling limit is presumably the important approximation. Here, the transition is from low lying vibrational levels of the excited state to very high vibrational levels of the ground state.

The treatment of intersystem crossing, that is, of the k_{isc} and k_{bisc} paths in equation (22), is in principle similar to that for k_{nr}.There is an added spin–orbit coupling term in the evaluation of the electronic factor in the treatment of the crossing probability. Although theory has provided a useful framework for discussing nonradiative processes, it has not so far been of much diagnostic or predictive value in the case of coordination compounds.

7.3.2.6 Chemiluminescence and Triboluminescence

Some mention should be made of ways of producing excited states other than by absorption of light or by excitation energy transfer. A chemiluminescent reaction may be formulated as in equation (26). Since the energy difference between C* and C will be 160 kJ mol^{-1} or more, the corresponding ground state reaction, given by equation (27), must be highly exoergic. As might be expected, the principal examples so far of chemiluminescent reactions involving coordination compounds have been redox ones. An example is presented in equation (28).[59] Both products have emissive excited states, and it is interesting that the actual excited state product is the lower energy one. With other reductants, $[Ru(bipy)_3]^{2+*}$ is formed,[59,60] the reaction with alkaline borohydride providing an excellent lecture demonstration.[61]

$$A + B \rightarrow C^* + D \tag{26}$$

$$A + B \rightarrow C + D \tag{27}$$

$$[Ru(bipy)_3]^{3+} + [Cr(bipy)_3]^{2+} \longrightarrow [Ru(bipy)_3]^{2+} + [Cr(bipy)_3]^{3+*} \tag{28}$$

In triboluminescence, light is produced by grinding or cleaving a solid. Most examples involve organic compounds, but one case of interest here is that of $Ba[Pt(CN)_4]$.[62] A laser-produced shock wave in the solid resulted in population of the emitting excited state.

An important point is that where it has been measured, the emission spectrum produced by either a chemiluminescent reaction or by triboluminescence is the same as that found in the conventional method of photoexcitation. This is a confirmation that thexi states indeed have thermodynamic status in that their properties are independent of the method of their preparation.

7.3.3 PHOTOCHEMICAL REACTIONS OF COORDINATION COMPOUNDS

The preceding discussion has emphasized that an electronic excited state of a coordination compound is an energy-rich species whose structure, electronic distribution and reactivity can differ substantially from the corresponding properties of the ground state. In this section the reactions of the various types of excited states are considered in detail. Most attention will be given to six-coordinate complexes of metals having a d^3 or low-spin d^6 electronic configuration, since the majority of mechanistic studies reported to date are concerned with these systems. Complexes of other *d* transition elements, the lanthanides and the actinides will also be treated, but the coverage here will necessarily be brief.

7.3.3.1 Ligand Field Excited States

To a first approximation, the ligand field excited states of coordination compounds arise from electronic transitions between valence *d*-orbitals localized on the metal. While such transitions result in an angular rearrangement of metal electron density, they do not alter the net charge distribution between the metal and its ligands. Consequently, ligand field excited states are not expected to undergo intramolecular oxidation–reduction processes such as homolytic fission of a metal–ligand bond. Angular changes in electron density can, however, lead to enhanced reactivity toward ligand substitution and isomerization processes. This theme will be developed in detail below for a number of well-studied transition metal systems.

7.3.3.1.1 Chromium(III) complexes

The low-lying electronic states of six-coordinate Cr^{III} complexes in octahedral (O_h) symmetry are shown in Figure 2a. The $^4A_{2g}$ ground state corresponds, in the strong-field limit, to the $t_{2g}{}^3$ electronic configuration whereas the $^4T_{2g}$ and $^4T_{1g}(F)$ ligand field excited states correlate with $t_{2g}{}^2e_g{}^1$. Consequently, transitions to these latter states occur with the promotion of an electron to the strongly σ-antibonding e_g orbitals. This redistribution of electron density weakens metal–ligand bonding and can cause considerable distortion of the complex from its original octahedral framework (see Figure 6). Moreover, the vacated t_{2g} orbital is available for bonding to an incoming ligand. These characteristics of the $^4T_{2g}$ and $^4T_{1g}(F)$ excited states make them particularly susceptible to ligand substitution reactions.[35,36] In contrast, the lowest doublet excited state, ^2E_g, arises from a spin-pairing of two electrons within the t_{2g} orbitals. Since these orbitals are nonbonding (except with respect to π-donor or acceptor ligands), this change in electronic distribution should not cause major alterations in metal–ligand bond strength or overall geometry. A recent theoretical study shows, however, that the activation barrier to associative attack by an incoming nucleophile should be lower in ^2E_g than in the ground state.[63] Thus, the lowest doublet state in Cr^{III} complexes must also be considered as potentially reactive toward ligand substitution.

In accord with these expectations, the vast majority of Cr^{III} complexes undergo ligand substitution when irradiated in their ligand field absorption bands.[40] Generally, the leaving ligand is replaced by solvent, although anation may occur at high anion concentration. Complexes having six equivalent metal–ligand bonds, such as $[Cr(NH_3)_6]^{3+}$, undergo initial photosubstitution of a single ligand (equation 29). The analogous process for $[Cr(en)_3]^{3+}$ (equation 30) results in the detachment and protonation of one end of an ethylenediamine ligand (denoted as enH). Thermal cleavage of the second Cr—N bond then yields a mixture of *cis*- and *trans*-$[Cr(en)_2(OH_2)_2]^{3+}$.

$$[Cr(NH_3)_6]^{3+} \xrightarrow[H_3O^+]{h\nu} [Cr(NH_3)_5(OH_2)]^{3+} + NH_4^+ \tag{29}$$

$$[Cr(en)_3]^{3+} \xrightarrow[H_3O^+]{h\nu} [Cr(en)_2(enH)(OH_2)]^{4+} \tag{30}$$

A pulsed-laser photolysis study of $[Cr(en)_3]^{3+}$ illustrates quite dramatically the enhancement in reactivity that can result upon populating a ligand field excited state.[26] Thus a significant fraction of the primary photoproduct, $[Cr(en)_2(enH)(OH_2)]^{4+}$, is formed within the 20 ns duration of the laser pulse and is thought to arise from reaction of the lowest excited quartet state, Q°_1 (see Figure 6). This observation establishes that the pseudo-first-order rate constant for this excited state process is $\geqslant 10^8\ s^{-1}$. By comparison, the rate constant for the corresponding ground-state thermal reaction is $8 \times 10^{-7}\ s^{-1}$ at 25 °C. Thus the promotion of a single electron from the t_{2g} to the e_g orbitals leads, in this case, to a 10^{14} acceleration in the rate of ligand substitution.

Mixed-ligand Cr^{III} complexes have a particularly rich substitutional photochemistry in that two (or more) reaction modes are normally observed. Data for the well-studied class of acidoamine complexes are presented in Table 2. The dominant photochemical reaction for $[CrX(NH_3)_5]^{2+}$ complexes in aqueous solution is NH_3 aquation, with X^- aquation occurring to a lesser extent (equation 31). In contrast, the latter pathway is the favored thermal reaction of these compounds. Such behavior again illustrates that the reactivity of ligand field excited states can differ sharply from that of the ground state.

Table 2 Photochemistry of Mixed-ligand Chromium(III) Complexes upon Irradiation into the Lowest Quartet Ligand Field Band

Complex	$\phi_{NH_3\,(\text{or amine})}$	ϕ_{X^-}	*Major product*	*Ref.*
$[CrCl(NH_3)_5]^{2+}$	0.36	0.005	*cis*-$[CrCl(NH_3)_4(OH_2)]^{2+}$	64
$[CrBr(NH_3)_5]^{2+}$	0.34	0.009	*cis*-$[CrBr(NH_3)_4(OH_2)]^{2+}$	65
$[Cr(NCS)(NH_3)_5]^{2+}$	0.47	0.02	*cis*-$[Cr(NCS)(NH_3)_4(OH_2)]^{2+}$	66
trans-$[CrF_2(en)_2]^+$	0.35	$\leqslant 0.08$	$[CrF_2(en)(enH)(OH_2)]^{2+}$	67
trans-$[CrCl_2(NH_3)_4]^+$	0.003	0.44	*cis*-$[CrCl(NH_3)_4(OH_2)]^{2+}$	68
trans-$[CrCl_2(en)_2]^+$	$< 10^{-3}$	0.32	*cis*-$[CrCl(en)_2(OH_2)]^{2+}$	69
trans-$[CrCl_2(2,3,2\text{-tet})]^{+a}$	$< 7 \times 10^{-3}$	0.06	*cis*-$[CrCl(2,3,2\text{-tet})(OH_2)]^{2+}$	70
trans-$[CrCl_2(cyclam)]^{+a}$	$< 2 \times 10^{-4}$	3.3×10^{-4}	*trans*-$[CrCl(cyclam)(OH_2)]^{2+}$	70

[a] 2,3,2-tet is 1,4,8,11-tetraazaundecane; cyclam is 1,4,8,11-tetraazacyclotetradecane.

$$[CrX(NH_3)_5]^{2+} \xrightarrow[H_2O]{h\nu} \begin{cases} cis\text{-}[CrX(NH_3)_4(OH_2)]^{2+} + NH_3 \\ [Cr(NH_3)_5(OH_2)]^{3+} + X^- \end{cases} \qquad (31)$$

One of the most controversial questions encountered in studies of Cr^{III} photochemistry concerns the identity of the reactive excited state(s).[71] As illustrated in Figure 6, uncertainty can arise because the Franck–Condon state initially populated during irradiation in the quartet absorption bands generally undergoes rapid equilibration to the lowest thexi quartet state, Q°_1, and/or intersystem crossing to the lowest doublet, D°_1. Reaction from either or both of the latter states must therefore be considered.

In a very important study of the quartet–doublet reactivity question,[72] it was found that ligand-field irradiation of $[Cr(CN)_6]^{3-}$ in degassed dimethylformamide results in both phosphorescence from the doublet and substitution of cyanide. In air-saturated solution, however, phosphorescence is quenched completely while the photoreaction is unaffected. The two processes appear to be uncoupled and thus originate from different excited states. The most straightforward conclusion is that the lowest quartet excited state in $[Cr(CN)_6]^{3-}$ is the sole precursor to photoreaction.

Studies of the photochemistry and photophysics of $[Cr(bipy)_3]^{3+}$, $[Cr(phen)_3]^{3+}$ and various substituted analogues have revealed behavior quite different from that just described.[73] In the prototypal case of $[Cr(bipy)_3]^{3+}$, ligand-field irradiation of the complex in neutral or basic aqueous solution results in phosphorescence and loss of one bipyridine ligand. Intersystem crossing from the lowest quartet state to the luminescent doublet occurs with near unit efficiency, while back-intersystem crossing is too endothermic to be of importance. Addition of 0.1 M iodide ion quenches >99.9% of the phosphorescence and ~98% of the photochemistry. This parallel behavior of the two processes strongly suggests that the quenchable portion of the reaction originates from the doublet.

The issue of quartet *versus* doublet reactivity becomes considerably more complicated for most other Cr^{III} complexes such as $[Cr(en)_3]^{3+}$, *trans*-$[Cr(NCS)_4(NH_3)_2]^-$ and *trans*-$[Cr(NCS)_2(en)_2]^+$. Both phosphorescence and photochemistry can be quenched in these systems, with the former process being affected to a greater degree. While the unquenchable portion of the photochemistry most likely involves prompt reaction from the lowest excited quartet state, the quenchable component could result from either (i) delayed reaction from the quartet following back-intersystem crossing from the doublet, or (ii) reaction from the doublet state itself. Despite a rather extensive series of investigations, the question as to which pathway (i or ii) dominates is still contentious.[40,71]

At present, then, the situation with regard to the identity of the reactive excited state(s) in Cr^{III} substitutional photochemistry can be summarized as follows. The lowest quartet excited state is the sole reactive state in $[Cr(CN)_6]^{3-}$ and is at least partly responsible for the photochemistry of several other Cr^{III} complexes. The lowest doublet state appears to be the predominant reactive state in $[Cr(bipy)_3]^{3+}$ and similar tris(polypyridyl)chromium(III) complexes and may also be reactive in a number of other complexes. Quite clearly, this aspect of Cr^{III} photochemistry requires additional study.

The photochemical and thermal substitution reactions of Cr^{III} complexes can follow quite different stereochemical courses. The behavior described by equation (32) is typical: thermal aquation of *trans*-$[CrCl_2(en)_2]^+$ proceeds with retention of configuration, whereas photoaquation is accompanied by a highly stereospecific ($\geq 99\%$ *cis* product) rearrangement.[69] With very few exceptions, it has been found that stereochemical mobility is a general feature of Cr^{III} photosubstitution reactions.

$$\textit{trans}\text{-}[CrCl_2(en)_2]^+ \xrightarrow{H_2O} \begin{cases} \textit{trans}\text{-}[CrCl(en)_2(OH_2)]^{2+} + Cl^- \\ \textit{cis}\text{-}[CrCl(en)_2(OH_2)]^{2+} + Cl^- \quad (h\nu) \end{cases} \qquad (32)$$

An interesting correlation between the ease of stereomobility during photolysis and the efficiency of photosubstitution has been observed for complexes of the type *trans*-$[CrCl_2N_4]^+$ (Table 2; N_4 is $4NH_3$, 2en, 2,3,2-tet or cyclam).[70] While the overall ligand field strength is approximately constant within the series, the quantum yield for chloride aquation drops by 10^3 as the amine is varied from NH_3 to cyclam. This decrease parallels the increasing chelation about the metal atom. The cyclam complex, in which the metal is completely surrounded by the macrocyclic tetradentate ligand, is remarkably photoinert. Significantly, it is also the only member of the series which cannot undergo stereochemical rearrangement and thus yields the *trans*-chloroaquo complex as the major photoproduct. Though the data base is limited, these results suggest that stereomobility is a necessary condition for efficient substitutional photochemistry in Cr^{III} complexes.

An angular overlap analysis of stereomobility in Cr^{III} photosubstitution reactions has been presented by Vanquickenborne and Ceulemans.[37] In this treatment, the overall reaction is formally dissected into three steps: (1) dissociative loss of a ligand from the lowest quartet excited state of the complex, (2) symmetry-controlled rearrangement of the resulting electronically excited square pyramid to a trigonal bipyramid, (3) symmetry-controlled attack of the incoming ligand on the trigonal bipyramid to yield the final product. Each of these steps is illustrated in Figure 9 for the case of $[CrCl(NH_3)_5]^{2+}$.

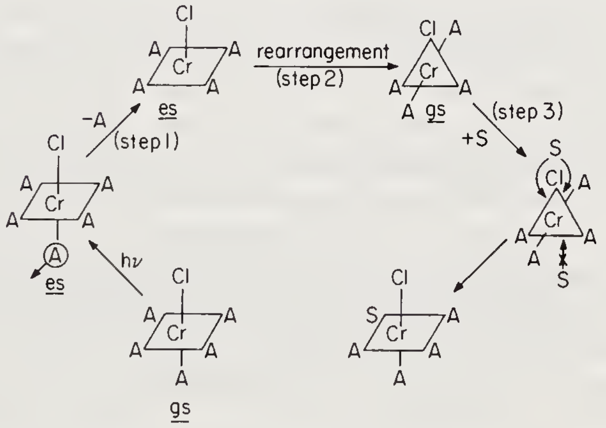

Figure 9 Vanquickenborne–Ceulemans model (see ref. 37) for photosubstitution in $[CrCl(NH_3)_5]^{2+}$; A is NH_3, S is solvent, *gs* and *es* denote ground state and excited state, respectively, and charges are omitted

Extensive comparisons between the stereochemical predictions of this theory and experiment have been presented and, in general, the agreement is satisfactory. Nevertheless, the assumption of dissociative ligand loss (*i.e.* step 1 in Figure 9) is not entirely compatible with other evidence. For example, the quantum yields for anation of $[Cr(DMSO)_6]^{3+}$ by azide are larger than those for anation by thiocyanate at all concentrations, including those that approach limits imposed by ion pairing.[74] This dependence on entering ligand, coupled with the observation that photoanation proceeds more efficiently than photoinduced solvent exchange, is indicative of an associative reaction pathway. In another study,[43] the pressure dependence of photoaquation was determined for $[CrX(NH_3)_5]^{2+}$ (X is Cl, Br or NCS) and $[Cr(NH_3)_6]^{3+}$. The negative volumes of activation found for both NH_3 and X^- loss were interpreted in terms of an I_a (associative interchange) mechanism. The extent of dissociative *versus* associative behavior in Cr^{III} photosubstitution reactions is an interesting and important question that will undoubtedly receive more attention in the future.

Thus far the discussion has focused on the reactivity of the lowest excited states of a given spin multiplicity (*e.g.* ${}^4T_{2g}$ or ${}^2E_g$ in O_h symmetry) since, as noted earlier, higher lying states generally undergo rapid deactivation by intersystem crossing and/or internal conversion. In some complexes, however, it appears that reaction from upper ligand field thexi states may be competitive with these latter processes. The behavior of *trans*-$[CrF(NCS)(en)_2]^+$ is illustrative in this regard.[75,76] The complex undergoes photosubstitution of both thiocyanate and ethylenediamine with a quantum yield ratio, ϕ_{NCS^-}/ϕ_{en}, that varies with the wavelength of irradiation. This wavelength dependence requires the existence of two reactive excited states, and it was proposed that the $^4E(a)$ and $^4B_2$ states in this nominally C_{4v} complex (see Figure 7) are involved. The $^4E(a)$ state gives rise to both en and NCS^- labilization whereas the higher energy $^4B_2$ state favors en loss. Extension of the Vanquickenborne–Ceulemans photochemical theory[37] to include the reactivity of higher-lying quartet excited states leads to predictions of reactivity which are in accord with the observed behavior.

There are now several reports of a small wavelength dependence of photochemical and emission quantum yields on irradiation into the red edge (long-wavelength portion) of the lowest quartet ligand field absorption band.[77,78] Such behavior has been attributed to prompt intersystem crossing and/or reaction occurring from vibronic levels at or near the Franck–Condon state initially populated during light absorption (see Figure 6). These processes must be extremely rapid (*i.e.* picosecond time scale) to be able to compete successfully with vibrational relaxation to the thexi state. A theoretical treatment of prompt photoreactions has recently been presented.[21]

Finally, it should be noted that the relatively long-lived doublet excited state in Cr^{III} complexes can undergo bimolecular processes of the type mentioned in Section 7.3.2.4.4. Energy transfer is a well-documented[79] pathway for this state and, more recently, electron transfer reactions have also been observed. In the example given by equation (33), the lowest doublet of $[Cr(bipy)_3]^{3+}$ undegoes reductive quenching by $[Ru(bipy)_3]^{2+}$.[80] While this redox process is energetically unfavorable when both reactants are in their ground electronic states, the higher energy of the doublet state provides the necessary driving force to accomplish the reaction photochemically. Additional examples of bimolecular excited state electron transfer processes are presented in Section 7.3.3.2.2.

$$(^2E)[Cr(bipy)_3]^{3+*} + [Ru(bipy)_3]^{2+} \longrightarrow [Cr(bipy)_3]^{2+} + [Ru(bipy)_3]^{3+} \qquad (33)$$

7.3.3.1.2 Cobalt(III), rhodium(III) and iridium(III) complexes

The energy level diagram for the six-coordinate complexes of Co^{III}, Rh^{III} and Ir^{III} in O_h symmetry is shown in Figure 2b. The $^1A_{1g}$ ground state derives from the $t_{2g}{}^6$ electronic configuration, while the low-lying ligand field excited states $^3T_{1g}$, $^3T_{2g}$, $^1T_{1g}$ and $^1T_{2g}$ correlate with the $t_{2g}{}^5e_g{}^1$ configuration. There is, in addition, a $^5T_{2g}$ state which arises from the $t_{2g}{}^4e_g{}^2$ configuration and whose energy is very sensitive to the ligand field strength. It is generally agreed that the quintet state lies above the $^3T_{1g}$ state in Rh^{III} and Ir^{III} ammine complexes as well as the strong-field complexes of Co^{III} such as $[Co(CN)_6]^{3-}$, whereas the relative positions of these states may be reversed for complexes of lower field strength such as $[Co(NH_3)_6]^{3+}$. This change in the nature of the lowest excited state may account for the different emission properties of the two types of complexes. Thus Rh^{III} and Ir^{III} ammine and Co^{III} cyanide complexes typically exhibit a broad phosphorescence assigned as $^3T_{1g} \rightarrow {}^1A_{1g}$, while Co^{III} ammines are nonemissive even at low temperature.[20]

Table 3 Photosubstitution Quantum Yields for some d^6 Complexes

Complex	λ_{irr}	*Assignment*	ϕ_{NH_3} (or amine)	ϕ_{X^-}	*Ref.*
$[Co(NH_3)_6]^{3+}$	365	$^1A_{1g} \rightarrow {}^1T_{2g}$	5.4×10^{-3}	—	82
	460	$^1A_{1g} \rightarrow {}^1T_{1g}$	5.2×10^{-4}	—	
$[Co(CN)_6]^{3-}$	365	$^1A_{1g} \rightarrow {}^1T_{1g}$	—	0.31	83
	405	$^1A_{1g} \rightarrow {}^3T_{1g}$	—	0.29	
$[Rh(NH_3)_6]^{3+}$	254	$^1A_{1g} \rightarrow {}^1T_{2g}$	0.07	—	84
	313	$^1A_{1g} \rightarrow {}^1T_{1g}$	0.075	—	
$[Ir(NH_3)_6]^{3+}$	254	$^1A_{1g} \rightarrow {}^1T_{1g}$	0.083	—	85
	313	$^1A_{1g} \rightarrow {}^3T_{1g}$	0.090	—	
$[RhCl(NH_3)_5]^{2+}$	380	$^1A_1 \rightarrow {}^1T_1$	$< 10^{-3}$	0.14	86, 87
$[RhBr(NH_3)_5]^{2+}$	420	$^1A_1 \rightarrow {}^1E$	0.17	0.019	86, 87
$[RhI(NH_3)_5]^{2+}$	420	$^1A_1 \rightarrow {}^1E$	0.87	0.01	86, 87
trans-$[RhCl_2(NH_3)_4]^+$	407	a	$< 2 \times 10^{-3}$	0.13	88
trans-$[RhCl_2(en)_2]^+$	407	a	$< 3 \times 10^{-3}$	0.057	88
trans-$[RhCl_2(cyclam)]^+$	407	a	$< 10^{-4}$	0.011	88

[a] Irradiation into first spin-allowed ligand field absorption band.

Table 3 summarizes the photochemistry of several Co^{III}, Rh^{III} and Ir^{III} complexes upon ligand-field excitation.[81] Ligand substitution is the sole reaction mode and, as shown by equation (34), more than one photoproduct may result for mixed-ligand complexes such as $[RhX(NH_3)_5]^{2+}$ (X is Cl, Br or I). The data reveal an interesting dichotomy between the photoreactivities of Rh^{III} and Ir^{III} ammines and Co^{III} cyanides on the one hand and Co^{III} ammines on the other. The former complexes undergo reasonably efficient substitution and, in most cases, the quantum yields are independent of the irradiation wavelength (λ_{irr}) even in the region corresponding to direct population of the lowest excited triplet state ($^3T_{1g}$ in Figure 2b). Such behavior indicates that photoexcitation is followed by efficient internal conversion/intersystem crossing to a common excited state, logically assigned as the lowest ligand field triplet, and that this state and those in thermal equilibrium with it are mainly responsible for the substitutional chemistry. This conclusion is reinforced by the finding[86] that triplet-state sensitizers drive the reactions in equation (34) with limiting quantum yields that closely match those obtained upon direct photolysis.

$$[RhX(NH_3)_5]^{2+} \xrightarrow[H_2O]{h\nu} \begin{cases} [Rh(NH_3)_5(OH_2)]^{3+} + X^- \\ trans\text{-}[RhX(NH_3)_4(OH_2)]^{2+} + NH_3 \end{cases} \tag{34}$$

In sharp contrast, Co^{III} ammines undergo photosubstitution with extremely low and wavelength-dependent quantum yields. Since ϕ values increase with higher-energy excitation, it can be concluded that much of the observed substitutional chemistry arises from higher-lying ligand field excited states. The small photosensitivity of Co^{III} ammines, particularly the lowest-energy excited state, has been attributed to the weak ligand field in these complexes.[20,81] As noted earlier, at sufficiently low field strength the energy of the quintet state, $^5T_{2g}$, falls below that of $^3T_{1g}$. In such cases configurational mixing between $^5T_{2g}$ and the ground state enhances radiationless decay and thus chemical processes (as well as luminescence) will be strongly diminished.[89]

The photosubstitution reactions of Co^{III} and Rh^{III} complexes can occur with a high degree of stereochemical change; some representative examples are presented in equations (35)–(37). Stereomobility during photolysis is not universal, however, as evidenced by the behavior within the series of *trans*-$[RhCl_2N_4]^+$ complexes (Table 3; N_4 is $4NH_3$, 2en or cyclam). Photosubstitution of chloride occurs with complete retention of configuration (equation 38) and, significantly, the quantum yields for this process show much less sensitivity to increasing chelation about the metal than was found for the corresponding Cr^{III} complexes (Table 2). Results such as these demonstrate that stereomobility is not a requirement for efficient photosubstitution in d^6 systems.

$$cis\text{- or } trans\text{-}[CoCl_2(en)_2]^+ \xrightarrow[H_2O]{h\nu} \underset{30\%\ cis + 70\%\ trans}{[CoCl(en)_2(OH_2)]^{2+}} + Cl^- \tag{35}$$

$$cis\text{-}[RhCl_2(NH_3)_4]^+ \xrightarrow[H_2O]{h\nu} trans\text{-}[RhCl(NH_3)_4(OH_2)]^{2+} + Cl^- \tag{36}$$

$$cis\text{- or } trans\text{-}[RhCl(OH)(NH_3)_4]^+ \xrightarrow[OH^-]{h\nu} cis\text{-}[Rh(OH)_2(NH_3)_4]^+ + Cl^- \tag{37}$$

$$trans\text{-}[RhCl_2N_4]^+ \xrightarrow[H_2O]{h\nu} trans\text{-}[RhClN_4(OH_2)]^{2+} + Cl^- \tag{38}$$

The photochemical model developed by Vanquickenborne and Ceulemans[39] provides a convenient theoretical framework for discussing the photosubstitutional behavior of d^6 complexes. In this treatment it is assumed that reaction occurs from the lowest triplet state of the complex and that any stereochemical change takes place subsequent to ligand loss. These features are illustrated in Figure 10 for the case of *cis*- and *trans*-$[RhCl_2(NH_3)_4]^+$. For both complexes, angular overlap considerations lead to the conclusion that relative bond strengths lie in the order Rh—N > Rh—Cl. Loss of Cl^- from the triplet state, ^{3}*cis*, of the *cis* isomer produces an electronically excited square-pyramidal intermediate, ^3SP_a, in which the remaining Cl^- lies in the basal plane. Similarly, loss of Cl^- from the triplet state of the *trans* isomer generates ^3SP_b, which contains a Cl^- ligand in the apical position. The square pyramidal intermediates can (i) interconvert along a reaction coordinate that passes through a trigonal bipyramidal transition state of triplet spin multiplicity, ^3TBP, or (ii) relax to their respective ground states and add a molecule of solvent. The identity of the final product therefore depends upon the competition between these two pathways. Calculation of relative energies indicates that the ^3SP intermediate of lowest energy will be the one having the weaker σ-donor ligand in the apical site and that the barrier for interconversion, ΔE, becomes larger with increasing ligand field strength. Thus in the example shown in Figure 10, ^3SP_a is predicted to be less stable than ^3SP_b. Isomerization of the former to the latter, followed by deactivation to ^1SP_b and rapid trapping by solvent, would give rise to the observed *trans* product in equation (36). Apparently, ^3SP_b faces too high a barrier (ΔE_T) for conversion to ^3SP_a and, as a result, aquation of the *trans* complex in equation (38) occurs with retention of configuration. High barriers would also account for the observation that most Ir^{III} complexes undergo photosubstitution with stereoretention. The identical product mixtures formed by *cis*- and *trans*-$[CoCl_2(en)_2]^+$ in equation (35), on the other hand, would require that the barriers for interconversion are sufficiently low (because of the smaller ligand field strengths of Co^{III} *versus* Rh^{III} or Ir^{III} complexes) to allow the same steady-state ratio of ^3SP_a and ^3SP_b to be reached by both isomers prior to deactivation and trapping by solvent.

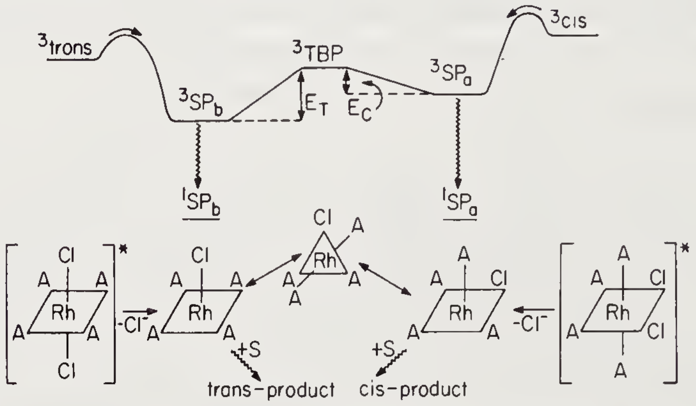

Figure 10. Vanquickenborne-Ceulemans model (see ref. 39) for photosubstitution in *cis*- and *trans*-$[RhCl_2(NH_3)_4]^+$; A is NH_3, S is solvent, and the remaining symbols are defined in the text. Charges on various species have been omitted

While ligand field considerations of the type discussed above usually lead to reliable predictions of photosubstitutional behavior, it is important to note that they are not the only determinant of excited state reactivity. Environmental factors can also play an important role, especially in cases where ligand field effects do not strongly favor one reaction pathway over another. The behavior of $[RhCl(NH_3)_5]^{2+}$ in different solvents illustrates this point;[90] the predominant photoreaction changes from Cl^- loss in water or formamide to NH_3 loss in dimethyl sulfoxide, methanol or dimethylformamide. Measurements of the excited-state rate constants, k_{Cl^-} and k_{NH_3}, for these two processes provide some useful insight about the intimate mechanism of ligand substitution. Thus k_{Cl^-} is found to be much more sensitive than is k_{NH_3} to changes in solvent. Moreover, while neither rate constant correlates with the donor properties of the solvent, k_{Cl^-} qualitatively parallels the solvation energy of the chloride ion. These observations are best interpreted in terms of a dissociative mechanism in which a considerable degree of charge separation develops in the transition state for Rh—Cl bond breaking and the overall energy for this process is influenced by the ability of the solvent to stabilize the developing charge. Other evidence, summarized elsewhere,[81] supports the view that ligand field excited states of d^6 complexes generally undergo ligand substitution *via* a dissociative process.

7.3.3.2 Charge Transfer Excited States

The various categories of CT transitions in coordination compounds were defined in Section 7.3.2.1.2. Such transitions occur with a radial redistribution of electron density and thus cause changes in the oxidation states of the species (metal, ligands, solvent) involved. This property of CT transitions leads to the expectation that the resulting excited states will be particularly susceptible to oxidation–reduction reactions.[91,92] Ligand substitution pathways also may become important, especially in systems where charge transfer creates a substitutionally labile metal center. Likewise, changes in the charge distribution about a coordinated ligand can enhance its reactivity toward processes such as protonation, electrophilic attack and isomerization.

In the acidoammine complexes of Cr^{III}, Co^{III} and Rh^{III}, CT states generally are higher in energy than other types of excited states. This situation is illustrated in Figure 1 for the case of $[Cr(NCS)(NH_3)_5]^{2+}$, where the NCS → Cr CT state is seen to lie above intraligand and ligand field states. Since the CT state reached in absorption can, in principle, relax to any lower energy state, it is often difficult to assign the excited state responsible for a particular reaction. The occurrence of ligand substitution in $[Cr(NCS)(NH_3)_5]^{2+}$ following irradiation of the CT band, for example, could result from reaction of the CT state and/or a lower-lying ligand field state. Another factor that can complicate the interpretation of CT photochemistry is the highly reactive nature of the primary photoproducts. CT excited states normally react to produce radicals which can undergo secondary reactions with each other, the original complex or the solvent.[91,92] Thus the final products observed may not be a reliable indicator of the nature or the efficiency of the primary photochemical step. Fast-reaction techniques such as laser flash photolysis and pulse radiolysis have been extremely useful in helping to unravel the complex sequence of reactions that can occur in these systems.

7.3.3.2.1 *Ligand-to-metal charge transfer states*

Most of the available information about the reactivity of CTTM excited states comes from studies of Co^{III} acidoammines.[91,92] Typically, irradiation of a CTTM absorption band in these systems leads to efficient redox decomposition accompanied, in many cases, by ligand substitution or linkage isomerization. The behavior of a representative complex, $[CoCl(NH_3)_5]^{2+}$, is summarized in equation (39).[93] A common observation in these systems is that photoredox quantum yields increase at shorter excitation wavelengths and decrease with increasing solvent viscosity.[91,92]

$$(\mathrm{CTTM})[\mathrm{CoCl(NH_3)_5}]^{2+*} \xrightarrow[\mathrm{H_2O}]{} \begin{cases} \mathrm{Co^{2+}_{(aq)} + 5NH_3 + Cl^{\bullet}} \\ \mathrm{[Co(NH_3)_5(OH_2)]^{3+} + Cl^-} \end{cases} \qquad (39)$$

The photochemistry of Co^{III} acidoammines upon CTTM excitation can be understood in terms of a mechanism in which homolytic fission of a metal–ligand bond is the primary reaction.[20,92,94] This process, which produces a solvent-caged or primary radical pair, is shown in equation (40) for the case of $[CoX(NH_3)_5]^{2+}$ (X is Cl, Br, NO_2, NCS). The quantity Δ represents the amount of absorbed light energy in excess of that required for electron transfer, and it determines to a large extent the magnitudes of the kinetic energies of the radical fragments. When Δ is small, recombination of the cage partners is favorable (equation 41a), while for large Δ the radicals are more likely to diffuse apart to form a solvent-separated (S denotes solvent) or secondary radical pair (equation 41b). The secondary radical pair, in turn, can recombine to yield the original complex (or perhaps an isomer; equation 42a), or diffuse apart with or without transfer of an electron back to X (equations 42b and 42c, respectively). The $[Co(NH_3)_5]^{2+}$ fragment produced in equation (42c) is substitutionally labile and rapidly undergoes NH_3 loss to give aquated Co^{2+}.[93] According to this mechanism, photoredox quantum yields increase at shorter excitation wavelengths because of the increasing value of Δ and, hence, the greater likelihood of forming secondary radical pairs. Moreover, a drop in quantum yield with increasing solvent viscosity is expected, since the rates of the processes in equations (41b) and (42c) should decrease in viscous solutions.

$$(\mathrm{CTTM})[(\mathrm{NH_3})_5\mathrm{Co^{III}X}]^{2+*} \longrightarrow \{(\mathrm{NH_3})_5\mathrm{Co^{II}, X\cdot}\}^{2+}_{\text{solvent cage}} + \Delta \qquad (40)$$

$$\{(\mathrm{NH_3})_5\mathrm{Co^{II}, X\cdot}\}^{2+} \rightleftarrows \begin{cases} [(\mathrm{NH_3})_5\mathrm{Co^{III}X}]^{2+} & (41a) \\ [(\mathrm{NH_3})_5\mathrm{Co^{II}S}]^{2+}, \mathrm{X}\bullet & (41b) \end{cases}$$

$$[(\mathrm{NH_3})_5\mathrm{Co^{II}S}]^{2+}, \mathrm{X}\bullet \longrightarrow \begin{cases} [(\mathrm{NH_3})_5\mathrm{Co^{III}X}]^{2+} + \mathrm{S} & (42a) \\ [(\mathrm{NH_3})_5\mathrm{Co^{III}S}]^{3+} + \mathrm{X}^- & (42b) \\ [(\mathrm{NH_3})_5\mathrm{Co^{II}}]^{2+} + \mathrm{S} + \mathrm{X}\bullet & (42c) \end{cases}$$

The mechanism summarized in equations (40)–(42) is applicable, with some modifications,[92,94] to the CTTM photochemistry of Cr^{III} and Rh^{III} acidoammine complexes. Thus the primary photochemical step is formation of a substitutionally labile reduced metal species and an oxidized ligand radical. In most systems, however, no permanent redox chemistry occurs owing to the facile reoxidation of the metal. The only net photoprocess observed in these cases is substitution of one or more ligands.[70,95]

Bimolecular reactions of CTTM excited states are rare, presumably because of the rapid formation of the primary radical pair in equation (40). In principle, however, it should be possible to intercept the excited state by a reactive species present at sufficiently high concentration in solution. Some evidence for this type of process comes from a study[96] of the photochemistry of $[Mo_2Cl_8]^{4-}$, a complex containing a quadruple metal–metal bond. In strongly acid solution, population of an excited state thought to be CTTM in character results in production of $[Mo_2Cl_8H]^{3-}$. The proposal was made that the increased electron density at the metal centers in this excited state facilitates Mo—H bond formation. Further studies are needed to test the validity of this interesting suggestion.

7.3.3.2.2 *Metal-to-ligand charge transfer states*

Detailed studies of the reactivity of CTTL excited states are of rather recent vintage and have tended to focus on complexes of d^6 metals. This type of state formally contains an oxidized metal center and a reduced ligand radical. In $[Ru(NH_3)_5py]^{2+}$, for example, the low energy Ru → py CT state can be formulated as $[(NH_3)_5Ru^{III}(py^-)]^{2+}$.[97] Several possible reactions can be envisioned for such a species. An intramolecular redox process leading to photooxidation of the metal is one potential pathway, but no net production of Ru^{III} results upon direct CTTL excitation. Another possibility is electrophilic attack by solvent on the reduced pyridine ligand. In acidic D_2O solution, electrophilic H/D exchange of pyridine protons does occur but with a rather small quantum yield ($\sim 10^{-3}$). The only significant photochemical reaction observed in this system is ligand substitution as described by equation (43). It appears unlikely, however, that this pathway originates from the Ru → py CT excited state, since low-spin Ru^{III} complexes (recall the $Ru^{III}(py^-)$ formulation) are known to be relatively substitution inert. Instead, it has been suggested that reaction originates from a ligand field excited state formed by interconversion from the initially populated CTTL state.[97] The situation is depicted schematically in Figure 11.

$$(\mathrm{CTTL})[Ru(NH_3)_5py]^{2+*} \xrightarrow[H_2O]{} \begin{cases} [Ru(NH_3)_5(OH_2)]^{2+} + py \\ cis\text{- or } trans\text{-}[Ru(NH_3)_4py(OH_2)]^{2+} + NH_3 \end{cases} \qquad (43)$$

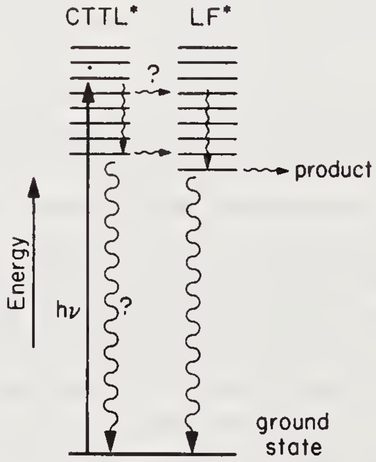

Figure 11 Relative disposition of the metal-to-ligand charge transfer (CTTL) and ligand field (LF) excited state manifolds in $[Ru(NH_3)_5\,py]^{2+}$ (after Figure 3 in ref. 98)

Support for this assignment was obtained from a study of the photosubstitutional chemistry of a series of $[Ru(NH_3)_5(pyX)]^{2+}$ complexes, where pyX is a substituted pyridine or related aromatic heterocycle.[98] Systematic variations in the electron withdrawing properties of pyX or, for a given ligand, the solvent polarity were used to 'tune' the energy of the CTTL state relative to the lowest ligand field excited state. When the CTTL state lies above the reactive ligand field state (as in Figure 11), efficient intersystem crossing/internal conversion of the former to the latter results in a relatively high quantum yield for substitution. If the energies of the two states are reversed, however, deactivation leads to population of the unreactive CTTL excited state and the observed quantum yields are low. Similar behavior has been reported for a series of $[Fe(CN)_5L]^{n-}$ complexes (n = 2, 3), where L is an aromatic nitrogen heterocycle.[99]

While intramolecular photoredox reactions of CTTL excited states appear to be relatively unimportant, there is considerable evidence that these states can undergo bimolecular electron transfer with high quantum efficiency.[100–102] Examples of this type of process are given in equations (44) and (45) for the paradigm case, $[Ru(bipy)_3]^{2+}$, a complex possessing a long-lived Ru → bipy CT excited state. The presence of an electron in a high energy π-antibonding orbital of a bipy ligand enhances the reducing ability of this state, while a vacancy (hole) in the t_{2g} metal orbitals increases its oxidizing ability. Thus the excited complex is both a stronger reductant and a stronger oxidant than the corresponding ground state by the excitation energy of 2.1 eV. This behavior is reflected in the reduction potential data shown in Figure 12. Several other transition metal complexes containing long-lived CTTL excited states undergo bimolecular electron transfer processes. The thermodynamic and kinetic aspects of these reactions and their potential applications in energy conversion schemes have been reviewed.[100–102]

$$[Ru(bipy)_3]^{2+*} + Eu^{2+}_{(aq)} \longrightarrow [Ru(bipy)_3]^{+} + Eu^{3+}_{(aq)} \qquad (44)$$

$$[\mathrm{Ru(bipy)_3}]^{2+*} + \mathrm{Fe}^{3+}_{(aq)} \longrightarrow [\mathrm{Ru(bipy)_3}]^{3+} + \mathrm{Fe}^{2+}_{(aq)} \tag{45}$$

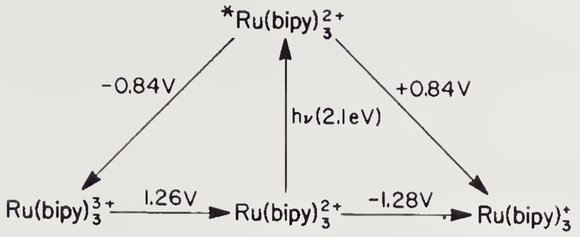

Figure 12 Reduction potentials for various reactions of ground and excited state $[\mathrm{Ru(bipy)_3}]^{2+}$ (in H_2O *vs.* NHE)

There are also numerous examples of bimolecular energy transfer processes involving CTTL excited states. The Ru → bipy CT state in $[\mathrm{Ru(bipy)_3}]^{2+}$, for example, photosensitizes the reactions of a number of organic and inorganic substrates by this pathway.[103]

Finally, it is conceivable that a CTTL excited state can eject an electron into the solution medium. In systems where this process has been observed, however, it has proved difficult to decide whether the reactive state is CTTL or CTTS in character. A discussion of photoelectron production is presented in the following section.

7.3.3.2.3 Charge-transfer-to-solvent states

CTTS transitions in coordination compounds result in a radial movement of electron density from the metal to the surrounding solution medium. The energies of these transitions generally are very sensitive to environmental parameters such as solvent polarity, temperature and the presence of salts.[104] This sensitivity has been used in a diagnostic sense to identify CTTS bands in the spectra of anionic cyanide complexes[105] and 1,2-dithiolene complexes of Ni, Pd and Pt.[106] Hydrated cations such as $\mathrm{Cr}^{2+}{}_{(aq)}$ and $\mathrm{Fe}^{2+}{}_{(aq)}$ exhibit absorption bands that are sometimes referred to as CTTS in character. Since the solvent occupies the first coordination sphere of the metal, however, the distinction between CTTS and CTTL transitions in these systems becomes obscured.

A characteristic reaction of CTTS excited states is photoelectron production with concomitant oxidation of the metal center.[107] In the example given in equation (46),[108] electrostatic repulsion of the primary photoproducts facilitates their separation and allows direct observation of the solvated electron. In other systems, photoelectron production has been inferred from the products observed in the presence of an electron scavenger such as N_2O or $CHCl_3$.[109]

$$(\mathrm{CTTS})[\mathrm{Ru(CN)_6}]^{4-*} \xrightarrow[H_2O]{} [\mathrm{Ru(CN)_6}]^{3-} + e^-_{(aq)} \tag{46}$$

$$\mathrm{M}^{n+}{}_{(aq)} + \mathrm{H}^+ \xrightarrow{h\nu} \mathrm{M}^{(n+1)+}_{(aq)} + \tfrac{1}{2}\mathrm{H}_2 \tag{47}$$

UV irradiation of low-valent cations (*e.g.* V^{2+}, Cr^{2+}, Fe^{2+}) in acidic aqueous solution leads to photooxidation of the metal and evolution of H_2.[110] This reaction, described by equation (47), is thought to involve the formation of the oxidized metal and an electron in the primary photochemical act. Immediate scavenging of the photoelectrons by protons yields hydrogen atoms which then combine to produce H_2. Some interest has been shown in this type of system as a component of a photochemical water-splitting cycle.[110,111]

7.3.3.3 Intraligand Excited States

Intraligand (IL) excited states of coordination compounds arise from electronic transitions between molecular orbitals primarily localized on a coordinated ligand. It is difficult, *a priori*, to predict the reactivity of this type of state. While it is logical to expect ligand-centered reactions, the influence of the metal on such processes can be substantial and result in net photochemistry which differs from that of the free ligand. A few examples should serve to illustrate the range of IL photoreactions reported to date.

The complex $[\mathrm{Co(TSC)(NH_3)_5}]^{2+}$, where TSC^- denotes *trans*-stilbenecarboxylate, exhibits an absorption band which is virtually identical to the spin-allowed $\pi-\pi^*$ band of free TCS^- and thus is straightforwardly assigned as IL in character.[112] The primary photoreaction upon irradiation into this IL band is redox decomposition to yield aquated Co^{2+} and the radical resulting from oxidation of TSC^-.[112,113] Photolysis of free TSC^-, on the other hand, results in *trans–cis* isomerization. One possible explanation for this disparate behavior is that the initially populated singlet IL excited state of $[Co(TSC)(NH_3)_5]^{2+}$ undergoes efficient intersystem crossing to a triplet CTTM excited state, from which redox decomposition then occurs. Alternatively, direct transfer of an electron from the locally excited TSC^- ligand to Co^{III} may be occurring. Regardless of the exact details of the mechanism, it is clear that the presence of the metal has a pronounced influence on the reactivity of the IL state.

Metal perturbation of IL photochemistry appears to be less important in $[Ru(bipy)_2(\textit{trans}\text{-4-stilbazole})_2]^{2+}$ and $[Ru(bipy)_2(\textit{cis}\text{-4-stilbazole})_2]^{2+}$. Both complexes undergo wavelength-dependent isomerization of the coordinated stilbazole ligands as the only important photoreaction.[114] This wavelength dependence has been attributed to the presence of two different types of reactive excited states, a Ru → stilbazole CT state which favors formation of the *trans* isomer and a higher energy IL state localized on stilbazole which decays with nearly equal probability to the two isomers. The latter pathway is qualitatively similar to the isomerization process that obtains upon direct photolysis of the free ligand. Thus coordination to Ru has not altered the characteristic photoreaction mode of the stilbazole molecule.

Photolysis of aqueous solutions of $[RhN_3(NH_3)_5]^{2+}$ and $[IrN_3(NH_3)_5]^{2+}$ results in the evolution of N_2 and the formation of a coordinated nitrene (M—NH) intermediate.[115,116] This cleavage of the $N—N_2$ bond originates primarily from an IL excited state localized on the azide ligand.[115–117] The metal is thought to play an important chemical role in the excited state reaction by stabilizing the incipient nitrene through a d_π–p_π backbonding interaction.

7.3.3.4 Survey of the Photoreactions of *d* and *f* Transition Metal Complexes

The preceding discussion of the relationships between excited state electronic structure and photochemical reactivity focused primarily upon coordination compounds containing d^3 or low-spin d^6 transition metals. These relationships are generally applicable, however, to complexes of other *d* transition elements, the lanthanides and the actinides. A brief survey of the photochemical reactions of these latter systems is presented below.

7.3.3.4.1 Complexes of d *transition elements*

Several coordination compounds in which the central metal possesses a high oxidation state and a d^0 electronic configuration have been reported to undergo photoinduced homolytic cleavage of a metal–ligand bond, presumably the result of populating a CTTM excited state. UV or visible irradiation of $TiCl_4$, for example, causes homolysis of a Ti—Cl bond with the resulting formation of $TiCl_3$ and Cl_2.[118] Vanadium complexes of general formula $VOQ_2(OR)$, where Q is the 8-quinolyloxo ligand and R is an alkyl group, undergo cleavage of the V—OR bond upon UV photolysis.[119] This reaction occurs for a wide selection of R groups and thus provides a convenient, general route to alkoxy radicals.

The eight-coordinate d^2 complexes $[Mo(CN)_8]^{4-}$ and $[W(CN)_8]^{4-}$ undergo two wavelength-dependent photoreactions. Photolysis in the short-wavelength (254 nm) region leads to efficient photoelectron production from an excited state assigned as CTTS in character.[107,108,120] Irradiation into the longer-wavelength (365 nm) ligand field bands, on the other hand, favors ligand substitution.[121–123] As described by equation (48), the primary substituted photoproduct in basic media is the hydroxo complex which, in a series of thermal reactions, undergoes additional release of cyanide.

$$[M(CN)_8]^{4-} \xrightarrow[OH^-]{h\nu} [M(CN)_7(OH)]^{4-} + CN^- \qquad (48)$$

In the dinuclear complex $[Re_2Cl_8]^{2-}$, the d^4 metal centers are linked by a quadruple bond. The lowest-lying singlet excited state in the complex arises from the δ–δ^* transition of the Re_2 unit.[124] This state has been found to undergo bimolecular electron transfer with a variety of substrates in acetonitrile solution, functioning either as a strong oxidant or a moderately good reductant.[125] Population of higher-energy excited states results in cleavage of the Re—Re bond and formation of monomeric $[ReCl_4(MeCN)_2]^-$.[126] In the absence of evidence for direct photodissociation of the quadruple bond, it was proposed that this reaction proceeds by way of an intermediate in which a chloride ligand bridges the two metal atoms. Since this type of structure leaves one of the Re atoms quite exposed to the environment, nucleophilic attack by solvent can assist the Re—Re bond rupture process.

Low-spin d^5 complexes possess a CTTM excited state that arises from the transfer of a ligand electron to a metal orbital having predominantly nonbonding (t_{2g}) character. In $[RuCl(NH_3)_5]^{2+}$, for example, the Cl → Ru CT state can be conceptualized as a Ru^{II} complex containing a bound ligand radical. Since the substitutional lability of Ru^{II} complexes is not especially great, this state might be expected to undergo internal back-electron transfer to regenerate the original complex faster than it decomposes to redox products. This expectation is borne out by the observation that CTTM excitation of $[RuCl(NH_3)_5]^{2+}$ leads to relatively inefficient ($\phi = 0.02$–0.04) loss of NH_3 as the only net photoprocess.[127] Similar considerations account for the lack of CTTM photochemistry for $[IrCl_6]^{2-}$.[128] Ligand field excitation of d^5 complexes generally results in ligand substitution and/or isomerization processes. As summarized in equation (49), photolysis of *cis*- or *trans*-$[RuCl_2(en)_2]^+$ leads to an isomeric mixture of the chloroaquo products but, interestingly, the isomer distribution differs for the two starting complexes.[129] This behavior has been analyzed in terms of the angular overlap model of ligand field photochemistry.[130]

$$\begin{tikzcd} & \mathit{cis}\text{-}[RuCl(en)_2(OH_2)]^{2+} & \\ \mathit{cis}\text{-}[RuCl_2(en)_2]^+ \arrow[ur, "h\nu\ 84\%"] \arrow[dr, "H_2O\ 16\%"'] & & \mathit{trans}\text{-}[RuCl_2(en)_2]^+ \arrow[ul, "66\%\ h\nu"'] \arrow[dl, "34\%\ H_2O"] \\ & \mathit{trans}\text{-}[RuCl(en)_2(OH_2)]^{2+} & \end{tikzcd} \qquad (49)$$

While four-coordinate d^8 complexes of Pt^{II} are square planar in their ground electronic states, spectroscopic[131,132] and theoretical studies[133] suggest that the low-lying ligand field excited states are significantly distorted and may even approach tetrahedral geometry. Minimally, such distortion provides a ready pathway for isomerization, and can also result in labilization of specific metal–ligand bonds. Consider the example of Zeise's anion, $[PtCl_3(C_2H_4)]^-$, which in the ground state undergoes rapid aquation of the chloride *trans* to ethylene. Ligand field excitation results in substitution of both *cis*-chloride and ethylene (the extent of *trans*-chloride photoaquation could not be determined).[18] The photolability of ethylene was attributed to the distortion of ligand field excited states toward a tetrahedron, since in this geometry π-backbonding from Pt to C_2H_4 is weakened relative to that in the square planar ground state. Several Pt^{II} complexes undergo *cis–trans* isomerization when irradiated in their ligand field absorption bands,[134] specific examples being $[PtCl_2(PEt_3)_2]$,[135] $[Pt(gly)_2]$ (gly is glycinate)[136] and $[Pt(py)_2Cl_2]$.[137] The first two systems are thought to isomerize *via* an intramolecular twisting mechanism, whereas a combination of intramolecular twisting and intermolecular ligand substitution pathways is responsible for the rearrangement of the last complex.

In solution the d^8 complexes of Ni^{II} are characterized by several rapid equilibria between species having different coordination numbers and/or geometries. Upon irradiation, these equilibria are perturbed and can be studied by relaxation techniques. A number of photoinduced changes have been investigated in this manner including square planar/tetrahedral, four-coordinate/five-coordinate and four-coordinate/six-coordinate interconversions.[138]

The photochemistry of d^9 Cu^{II} and d^{10} Cu^I complexes is dominated by redox processes.[139] Halide complexes of general formula $[CuCl_x]^{(2-x)-}$ or $[CuBr_x]^{(2-x)-}$ ($x = 1$–4), for example, undergo intramolecular electron transfer of the CTTM type to form a reduced metal species and a free halogen atom.[140,141] CTTM photochemistry has also been observed for Cu^{II} complexes containing amines, carboxylates, β-diketonates or polypyridines.[139] Copper(I) halide complexes such as $[CuCl_3]^{2-}$ undergo photoelectron production, presumably the result of populating a CTTS excited state.[142,143] In acidic aqueous media, scavenging of the electron by H^+ results in evolution of H_2. Irradiation of $[Cu(dmp)_2]^+$ (dmp is 2,9-dimethyl-1,10-phenanthroline) populates a low-lying CTTL excited state which can undergo bimolecular electron transfer to various Co^{III} complexes.[144] Photoinduced intramolecular electron transfer from Cu^I to Co^{III} in a mixed-metal dimer has also been reported.[145] Finally, $[Cu(prophos)BH_4]$ (prophos is 1,3-bis(diphenylphosphino)propane) has been shown to undergo bimolecular energy transfer to organic substrates in solution from an IL excited state localized on the prophos ligand.[146]

7.3.3.4.2 *Complexes of the lanthanide and actinide elements*

Most of the reported photochemical reactions of lanthanide complexes involve some type of redox behavior.[147] Photolysis (254–405 nm) of Eu^{2+} in acidic aqueous solution, for example, results in photooxidation of the metal and generation of H_2 (equation 50).[148] While the excited states responsible for this reaction nominally arise from $4f \rightarrow 5d$ transitions localized on the metal, strong mixing of the $5d$-orbital with ligand orbitals endows these states with appreciable CTTL character. Photoreduction of aquated Eu^{3+} can also be driven with UV ($\leqslant 254$ nm) light[149] and forms the basis of a photochemical separation of europium from other trivalent lanthanide elements.[150] The primary photoreaction, summarized in equation (51), is consistent with the population of a CTTM state. Several photoredox processes involving the Ce^{4+}/Ce^{3+} couple have been reported. Examples include bimolecular electron transfer from the *4f* → *5d* excited state of Ce^{3+} to Cu^{2+} in aqueous solution[151] and the Ce^{4+}-mediated oxidation of organic substrates such as alcohols, acids, aldehydes and ketones.[152]

$$Eu^{2+}_{(aq)} + H^+ \xrightarrow{h\nu} Eu^{3+}_{(aq)} + \tfrac{1}{2}H_2 \tag{50}$$

$$Eu^{3+}_{(aq)} + H_2O \xrightarrow{h\nu} Eu^{2+}_{(aq)} + H^+ + \cdot OH \tag{51}$$

A few observations of photosubstitution in lanthanide complexes have been reported. Irradiation into the *f–f* bands of $[Pr(thd)_3]$, $[Eu(thd)_3]$ and $[Ho(thd)_3]$ (thd is the anion of 2,2,6,6-tetramethyl-3,5-heptanedione) results in substitution of thd by solvent.[153] The proposed mechanism involves intramolecular energy transfer from an *f–f* excited state to a reactive IL excited state which is responsible for the observed ligand loss. Photosubstitution has also been observed upon direct excitation into the ligand absorption bands of $[Tb(thd)_3]$.[154]

Knowledge of actinide photochemistry is limited mainly to the complexes of uranium,[155] especially those containing the uranyl ion, UO_2^{2+}.[100,156,157] The lowest excited state of this ion is associated with a transition from essentially nonbonding π-orbitals to empty *5f*-orbitals on the U atom.[158] This state has been found to undergo a variety of bimolecular reactions. Upon irradiation in aqueous solutions of primary and secondary alcohols, for example, UO_2^{2+} abstracts a hydrogen atom from the α-carbon atom of the alcohol (equation 52).[159-161] The resulting U^V species deprotonates and then undergoes disproportionation to UO_2^{2+} and U^{4+}. Bimolecular electron transfer to photoexcited UO_2^{2+} from a variety of electron donors is now well documented,[162-164] and a few examples of bimolecular energy transfer have also been reported.[165,166] Complexes of UO_2^{2+} with several carboxylic acids or their conjugate bases possess reactive CTTM excited states which lead to reduction of the metal and oxidation of the organic moiety. The best known example is UO_2^{2+} oxalate,[167] since this system has found use as a chemical actinometer.[168]

$$UO^{2+}_{2(aq)} + R^1R^2CH(OH) \xrightarrow{h\nu} UO_2H^{2+}_{(aq)} + R^1R^2\dot{C}(OH) \tag{52}$$

Interest in the reprocessing of spent nuclear fuels has prompted studies of the solution photochemistries of Np and Pu. A recent review summarizes the photoredox behavior of the various oxidation states of these elements.[169]

7.3.4 APPLICATIONS OF PHOTOCHEMICAL REACTIONS OF COORDINATION COMPOUNDS

In this final section we turn our attention to some applications of inorganic photochemical reactions. One obvious and immensely important example, treated in Chapter 59, is the use of metal-based (particularly silver) systems in photographic processes. Additional applications occur in the area of solar energy conversion and storage. As discussed in Chapter 61.5, a variety of schemes for photochemical water-splitting make use of transition metal photoredox reactions. Other energy storage processes such as the production of highly strained organic molecules, the photoreduction of carbon dioxide and the generation of electricity in photogalvanic or photoelectrochemical cells also incorporate inorganic photochemical steps.[170-173] Several applications of inorganic photoreactions that are not treated elsewhere in this compendium are described below.

7.3.4.1 Synthesis and Catalysis

Photochemical reactions have been exploited to yield coordination compounds that are otherwise difficult to prepare. For example, mixed-ligand complexes of general formula *trans*-$[MClX(en)_2]^+$ (M is Rh or Ir; X is Br or I) can be obtained in high yields by initial photochemical conversion of aqueous *trans*-$[MCl_2(en)_2]^+$ to the corresponding chloroaquo complex as described in equation (53).[174] Precipitation of free Cl^- with Ag^+ followed by heating with one equivalent of X^- then yields the desired product. Thermal routes to these complexes are less desirable because of the propensity to form disubstituted products and the need for extended reaction times at high temperatures. Photosubstitution reactions are also employed in the syntheses of a large number of $[RuX(bipy)_2L]^+$ and $[RuX_2(bipy)]$ complexes, where L is an uncharged ligand such as py or CH_3CN and X^- is an anion such as ClO_4^-, NO_3^-, Br^- or Cl^-.[175] Additional examples of synthetic applications of inorganic photochemistry have been described.[176]

$$trans\text{-}[MCl_2(en)_2]^+ \xrightarrow{h\nu} trans\text{-}[MCl(en)_2(OH_2)]^{2+} + Cl^- \tag{53}$$

$$O \xrightarrow[M]{h\nu} O' \tag{54}$$

Organic molecules can undergo an assortment of fundamentally interesting and synthetically useful transformations when irradiated in the presence of coordination compounds. The generic process is represented by equation (54) where O and O′ denote the original and transformed organic substrate, respectively, and M symbolizes a transition metal compound normally present in catalytic amount. Among the classes of organic substrates reported to engage in this type of process are alkenes, aldehydes, ketones, acids, ethers, epoxides, alcohols, nitriles and various aromatics. Reaction types include isomerization, cycloaddition, polymerization, hydrogenation and oxidation.

The transformation shown in equation (54) retains many of the features of ordinary photochemical and transition-metal-catalyzed thermal reactions of organic compounds, but displays some unique characteristics as well. In cases where irradiation serves only to accelerate the rate of the expected thermal process, higher chemical yields of product can result, reaction rates are subject to greater control through regulation of light intensity, and thermally sensitive products are isolated more readily since elevated reaction temperatures can be avoided. Alternatively, the function of M may be to facilitate known photochemical reactions of O or perhaps introduce new reaction channels not observed upon irradiation of O alone. A detailed discussion of the mechanisms and synthetic applications of these processes has been presented.[177]

7.3.4.2 Chemical Actinometry

The accurate determination of incident light intensity is of pivotal importance in any quantitative photochemical experiment. While various physical devices are available for making absolute intensity measurements,[168] these devices can be difficult to calibrate and usually are rather expensive. A much simpler approach involves the use of a chemical actinometer. This type of system is based upon a photochemical reaction for which product quantum yields are reasonably insensitive to variations in reactant concentration, temperature, light intensity and excitation wavelength. Once the quantum yield is calibrated by an absolute method, a chemical actinometer becomes a rapid, inexpensive and highly accurate secondary standard for light intensity measurements.

Most solution-phase actinometers in use today are based upon the photochemical reactions of coordination compounds. The redox decomposition of acidic solutions of $[Fe(C_2O_4)_3]^{3-}$, for example, is very sensitive to light in the range 254–500 nm.[168] A very good actinometer for longer wavelengths (316–750 nm) involves the photoaquation of *trans*-$[Cr(NCS)_4(NH_3)_2]^-$ (the anion of Reinecke's salt).[178] The extent of reaction in these systems is determined spectrally following the addition of a reagent which forms a highly absorbing complex with one of the photoproducts.

A chemical actinometer especially designed for intensity measurements on high power lasers in the 330–520 nm range has been described.[179] It consists of a closed O_2-filled system containing methanolic $[Ru(bipy)_3]^{2+}$ and tetramethylethylene (TME). Photoexcited $[Ru(bipy)_3]^{2+}$ is quenched efficiently by dissolved O_2 to generate singlet oxygen which then reacts with TME to form a non-volatile hydroperoxide. The laser intensity is determined from the rate of O_2 consumption monitored on a gas buret.

Finally, the photoredox decomposition of $K_3[Mn(C_2O_4)_3]\cdot 3H_2O$ has been proposed for use as an actinometer for solid state photochemical studies.[180] Upon UV irradiation, the crystals of this complex change from deep red to white and the extent of reaction can be measured easily by reflectance spectroscopy.

7.3.4.3 Photochromism

Photochromism may be defined as the reversible light-induced interconversion of a system between two forms having distinguishably different absorption spectra.[181] The generalized process is outlined in equation (55) where ϕ represents the quantum yield for photochemical reaction and

k denotes the rate constant for the corresponding thermal process. When the combined (photochemical + thermal) rate of the back reaction equals that of the forward process, the system attains a photostationary state. In the case where $\phi_A \gg \phi_B$ and $k_B \gg k_A$, only the photochemical forward reaction and thermal reversion need to be considered and the system is termed singly photochromic.

$$A \underset{\phi_B, k_B}{\overset{\phi_A, k_A}{\rightleftharpoons}} B \tag{55}$$

The typical response of a singly photochromic system to light is depicted in Figure 13.[182] Initially, only form A is present, but upon exposure of the system to irradiation at time t_1, the photochemical conversion of A to B ensues. The B/A ratio thus increases until it attains the equilibrium value of the photostationary state. Upon removal of the light source at time t_2, the photoreaction ceases and B reverts to A at a rate characteristic of the thermal back reaction. The potential commercial and military applications of such reversible light-sensitive materials have provided much of the impetus for research on photochromic behavior. A partial listing of applications includes chemical switches, data displays, information storage, radiation intensity control (*e.g.* sunglasses) and camouflage.[183]

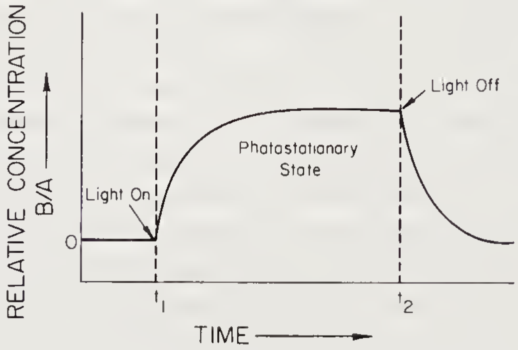

Figure 13 Response of a singly photochromic system to light; irradiation commences at time t_1 and ends at t_2

The majority of inorganic systems reported to exhibit photochromism are solids, examples being alkali and alkaline earth halides and oxides, titanates, mercuric chloride and silver halides.[184,185] The coloration is generally believed to result from the trapping of electrons or holes by crystal lattice defects. Alternatively, if the sample crystal is doped with an impurity capable of existing in variable oxidation states (*i.e.* iron or molybdenum), an electron transfer mechanism is possible.

In solution the photochromism of coordination compounds can result from photoinduced isomerization (*e.g.* metal dithizonates[186–188]), substitution (*e.g.* iron(II) phthalocyanine in the presence of benzyl isocyanide[189]) and oxidation–reduction (*e.g.* tris(diethyldithiocarbamato)-nickel(IV) bromide[190]).

7.3.4.4 Photocalorimetry

Photocalorimetry is a technique for determining the ordinary enthalpy (ΔH) of a reaction but, unlike conventional calorimetry, the reaction is light induced.[191] Essentially, the procedure involves measuring the rates of heat production in two irradiated solutions, one containing an absorbing but unreactive substance and the other containing the photosensitive compound. The difference between these rates, per mole of reaction, gives the ΔH for the photochemical process.

Photocalorimetry offers a convenient alternative to other methods of ΔH determination and, in some instances, may be the only practical method. The ligand substitution reactions of robust Werner-type complexes are a case in point. Conventional thermochemical measurements are complicated by the slowness of the substitution process and/or by competing reactions. Some of these same complexes, however, undergo clean photosubstitutions with high quantum yields and thus are excellent candidates for photocalorimetry. Examples include $[Cr(NH_3)_6]^{3+}$, $[Cr(CN)_6]^{3-}$ and $[Co(CN)_6]^{3-}$.[192] Photocalorimetric measurements of ΔH have also been obtained for isomerization and redox reactions of coordination compounds.[193,194]

7.3.5 ADDENDUM

The field of inorganic photochemistry continues to grow at a rapid pace. Summarized below are several interesting articles that have appeared since the original submission of this chapter.

Additional studies addressing the issue of doublet *vs.* quartet state reactivity in Cr^{III} complexes have been reported.[195–197] Factors affecting the nature and lifetime of the phosphorescent state in Cr^{III} ammines have been discussed.[198,199] The macrocyclic complex *trans*-$[Cr(CN)_2(cyclam)]^+$ was found to be photoinert and to possess a long-lived and relatively temperature independent phosphorescence;[200] these characteristics make it an attractive candidate for studies of bimolecular electron transfer and energy transfer processes.

Efforts continue to elucidate the excited-state dynamics and ligand substitutional reactivities of d^6 transition metal complexes.[201–203] Fluorescence from incompletely relaxed ligand field singlet states has been detected for some haloamminerhodium(III) complexes.[204]

Evidence continues to mount in support of the view that the optically excited electron in the metal-to-ligand charge transfer excited state of $[Ru(bipy)_3]^{2+}$ and related complexes resides on a single ligand ring.[205–208] Reviews dealing with bimolecular excited-state electron transfer reactions of d^6 metal–polypyridyl complexes have appeared.[209,210] Orthometallated Ir^{III} complexes containing one or more metal–carbon bonds possess some interesting properties including the ability to act as powerful excited-state reductants.[211,212] The excited-state redox properties of binuclear[213–215] and polynuclear[216] complexes containing metal–metal bonds have been investigated.

Studies of inorganic photochemistry in unusual environments has attracted considerable attention. Photochemical studies conducted in organized assemblies such as micelles, microemulsions and vesicles,[217] on surfaces such as porous Vycor glass,[218] in a lamellar solid,[219] and in the gas phase have been reported.[220]

Finally, two reviews have appeared describing the applications of inorganic photochemistry in the sensitization and/or catalysis of organic reactions.[221,222]

7.3.6 REFERENCES

1. J. Eder, *Ber.*, 1880, **13**, 166.
2. W. G. Leighton and G. S. Forbes, *J. Am. Chem. Soc.*, 1930, **52**, 3139.
3. J. Vranek, *Z. Elektrochem.*, 1917, **23**, 336.
4. R. Schwartz and K. Tede, *Ber.*, 1925, **58B**, 746.
5. M. Linhard and M. Weigel, *Z. Anorg. Allg. Chem.*, 1951, **266**, 49.
6. E. H. Archibald, *J. Chem. Soc.*, 1920, 1104.
7. A. W. Adamson, *J. Phys. Chem.*, 1967, **71**, 798.
8. A. W. Adamson, W. L. Waltz, E. Zinato, D. W. Watts, P. D. Fleischauer and R. D. Lindholm, *Chem. Rev.*, 1968, **68** 541.
9. A. Vogler and A. W. Adamson, *J. Am. Chem. Soc.*, 1968, **90**, 5943.
10. N. A. P. Kane-Maguire and C. H. Langford, *Chem. Commun.*, 1971, 895.
11. S. Chen and G. B. Porter, *Chem. Phys. Lett.*, 1970, **8**, 41.
12. H. D. Gafney and A. W. Adamson, *J. Am. Chem. Soc.*, 1972, **94**, 8238.
13. V. Balzani and V. Carassiti, ‘Photochemistry of Coordination Compounds’, Academic, New York, 1970.
14. A. W. Adamson and P. D. Fleischauer (eds.), ‘Concepts of Inorganic Photochemistry’, Wiley, New York, 1975.
15. M. Wrighton, *Chem. Rev.*, 1974, **74**, 401.
16. G. L. Geoffroy and M. S. Wrighton, ‘Organometallic Photochemistry’, Academic, New York, 1979.
17. A. Vogler and H. Kunkely, *J. Am. Chem. Soc.*, 1981, **103**, 1559.
18. P. Natarajan and A. W. Adamson, *J. Am. Chem. Soc.*, 1971, **93**, 5599.
19. A. D. Kirk, P. E. Hoggard, G. B. Porter, M. G. Rockley and M. W. Windsor, *Chem. Phys. Lett.*, 1976, **37**, 199.
20. P. D. Fleischauer, A. W. Adamson and G. Sartori, *Prog. Inorg. Chem.*, 1972, **17**, 1.
21. B. R. Hollebone, C. H. Langford and N. Serpone, *Coord. Chem. Rev.*, 1981, **39**, 181.
22. A. R. Gutierrez and A. W. Adamson, *J. Phys. Chem.*, 1978, **82**, 902.
23. M. Larsen, H. Macke, R. C. Rumfeldt and A. W. Adamson, *Inorg. Chim. Acta*, 1982, **57**, 229.
24. T. Ohno and S. Kato, *Bull. Chem. Soc. Jpn.*, 1973, **46**, 1602.
25. R. Bensasson, C. Salet and V. Balzani, *J. Am. Chem. Soc.*, 1976, **98**, 3722.
26. R. Fukuda. R. T. Walters, H. Macke and A. W. Adamson, *J. Phys. Chem.*, 1979, **83**, 2097.
27. A. W. Adamson, R. C. Fukuda and R. T. Walters, *J. Phys. Chem.*, 1981, **85**, 3206.
28. N. A. P. Kane-Maguire, C. G. Toney, B. Swiger, A. W. Adamson and R. E. Wright, *Inorg. Chim. Acta*, 1977, **22**, L11.
29. A. W. Adamson, *Discuss. Faraday Soc.*, 1960, **29**, 163.
30. K. Angermann, R. Schmidt, R. van Eldik, H. Kelm and F. Wasgestian, *Inorg. Chem.*, 1982, **21**, 1175.
31. F. Scandola, C. Bartocci and M. A. Scandola, *J. Am. Chem. Soc.*, 1973, **95**, 7988.
32. E. Zinato, P. Riccieri and A. W. Adamson, *J. Am. Chem. Soc.*, 1974, **96**, 375.
33. P. Riccieri and E. Zinato, *Inorg. Chem.*, 1980, **19**, 3279.
34. S. C. Pyke and R. G. Linck, *J. Am. Chem. Soc.*, 1971, **93**, 5281.
35. J. I. Zink, *J. Am. Chem. Soc.*, 1972, **94**, 8039.
36. M. Wrighton, H. B. Gray and G. S. Hammond, *Mol. Photochem.*, 1973, **5**, 165.
37. L. G. Vanquickenborne and A. Ceulemans, *J. Am. Chem. Soc.*, 1977, **99**, 2208; 1978, **100**, 475.
38. J. I. Zink, *Inorg. Chem.*, 1973, **12**, 1018.
39. L. G. Vanquickenborne and A. Ceulemans, *Inorg. Chem.*, 1978, **17**, 2730.
40. A. D. Kirk, *Coord. Chem. Rev.*, 1981, **39**, 225.
41. S. Behrendt, C. H. Langford and L. S. Frankel, *J. Am. Chem. Soc.*, 1969, **91**, 2236.
42. V. S. Sastri, R. W. Henwood, S. Behrendt and C.H. Langford, *J. Am. Chem. Soc.*, 1972, **94**, 753.
43. K. Angermann, R. van Eldik, H. Kelm and F. Wasgestian, *Inorg. Chem.*, 1981, **20**, 955.
44. K. Angermann, R. van Eldik, H. Kelm and F. Wasgestian, *Inorg. Chim. Acta*, 1981, **49**, 247.

45. W. Weber, R. van Eldik, H. Kelm, J. Dibenedetto, Y. Ducommun, H. Offen and P. C. Ford, *Inorg. Chem.*, 1983, **22**, 623.
46. N. Sutin and C. Creutz, *J. Chem. Educ.*, 1983, **60**, 809.
47. R. A. Marcus, *Int. J. Chem. Kinet.*, 1981, **13**, 865.
48. A. W. Adamson, R. C. Fukuda, M. Larson, H. Macke and J. P. Puaux, *Inorg. Chim. Acta*, 1980, **44**, L13.
49. G. A. Crosby, K. W. Hipps and W. H. Elfring, Jr., *J. Am. Chem. Soc.*, 1974, **96**, 629.
50. G. B. Porter and H. L. Schlafer, *Z. Phys. Chem. (Frankfurt am Main)*, 1963, **37**, 109.
51. R. T. Walters and A. W. Adamson, *Acta Chem. Scand., Ser. A*, 1979, **33**, 53.
52. E. Zinato, A. W. Adamson, J. L. Reed, J. P. Puaux and P. Riccieri, *Inorg. Chem.*, 1984, **23**, 1138.
53. P. C. Ford, *J. Chem. Educ.*, 1983, **60**, 829.
54. J. W. Schindler and A. W. Adamson, *Inorg. Chem.*, 1982, **21**, 4236.
55. P. A. Grutsch and C. Kutal, *J. Am. Chem. Soc.*, 1979, **101**, 4228.
56. J. N. Demas, *J. Chem. Educ.*, 1983, **60**, 803.
57. S. J. Strickler and R. A. Berg, *J. Chem. Phys.*, 1962, **37**, 814.
58. R. Englman and J. Jortner; *Mol. Phys.*, 1970, **18**, 145.
59. A. Vogler, L. El-Sayed, R. G. Jones, J. Namnath and A. W. Adamson, *Inorg. Chim. Acta*, 1981, **53**, L35.
60. F. Bolletta, A. Rossi and V. Balzani, *Inorg. Chim. Acta*, 1981, **53**, L23.
61. H. D. Gafney and A. W. Adamson, *J. Chem. Educ.*, 1975, **52**, 480.
62. G. E. Hardy, B. P. Chandra, J. I. Zink, A. W. Adamson, R. C. Fukuda and R. T. Walters, *J. Am. Chem. Soc.*, 1979, **101**, 2787.
63. A. Ceulemans, D. Beyens and L. G. Vanquickenborne, *J. Am. Chem. Soc.*, 1982, **104**, 2988.
64. H. F. Wasgestian and H. L. Schläfer, *Z. Phys. Chem. (Frankfurt am Main)*, 1968, **57**, 282; 1968, **62**, 127.
65. P. Riccieri and H. L. Schläfer, *Inorg. Chem.*, 1970, **9**, 727.
66. E. Zinato, R. D. Lindholm and A. W. Adamson, *J. Am. Chem. Soc.*, 1969, **91**, 1076.
67. S. C. Pyke and R. G. Linck, *Inorg. Chem.*, 1980, **19**, 2468.
68. P. Riccieri and E. Zinato, *J. Am. Chem. Soc.*, 1975, **97**, 6071.
69. A. D. Kirk, K. C. Moss and J. G. Valentin, *Can. J. Chem.*, 1971, **49**, 1524.
70. C. Kutal and A. W. Adamson, *Inorg. Chem.*, 1973, **12**, 1990.
71. A. W. Adamson, *Comments Inorg. Chem.*, 1981, **1**, 33.
72. H. F. Wasgestian, *J. Phys. Chem.*, 1972, **76**, 1947.
73. M. A. Jamieson, N. Serpone and M. Z. Hoffman, *Coord. Chem. Rev.*, 1981, **39**, 121.
74. C. H. Langford and J. P. K. Tong, *J. Chem. Soc., Chem. Commun.*, 1977, 138.
75. A. D. Kirk and C. F. C. Wong, *Inorg. Chem.*, 1979, **18**, 593.
76. A. D. Kirk, L. A. Frederick and S. G. Glover, *J. Am. Chem. Soc.*, 1980, **102**, 7120.
77. R. L. P. Sasseville and C. H. Langford, *J. Am. Chem. Soc.*, 1979, **101**, 5834.
78. R. L. P. Sasseville and C. H. Langford, *Inorg. Chem.*, 1980, **19**, 2850.
79. V. Balzani, L. Moggi, M. F. Manfrin, F. Bolletta and G. S. Laurence, *Coord. Chem. Rev.*, 1975, **15**, 321.
80. R. Ballardini, G. Varani, F. Scandola and V. Balzani, *J. Am. Chem. Soc.*, 1976, **98**, 7432.
81. P. C. Ford, *Coord. Chem. Rev.*, 1982, **44**, 61.
82. M. F. Manfrin, G. Varani, L. Moggi and V. Balzani, *Mol. Photochem.*, 1969, **1**, 387.
83. M. Nishazawa and P. C. Ford, *Inorg. Chem.*, 1981, **20**, 294.
84. J. D. Petersen and P. C. Ford, *J. Phys. Chem.*, 1974, **78**, 1144.
85. M. Talebinasab-Sarvari, A. Zanella and P. C. Ford, *Inorg. Chem.*, 1980, **19**, 1835.
86. T. L. Kelly and J. F. Endicott, *J. Phys. Chem.*, 1972, **76**, 1937.
87. M. A. Bergkamp, J. Brannon, D. Magde, R. J. Watts and P. C. Ford, *J. Am. Chem. Soc.*, 1979, **101**, 4549.
88. C. Kutal and A. W. Adamson, *Inorg. Chem.*, 1973, **12**, 1454.
89. R. B. Wilson and E. I. Solomon, *J. Am. Chem. Soc.*, 1980, **102**, 4085.
90. M. A. Bergkamp, R. J. Watts and P. C. Ford, *J. Am. Chem. Soc.*, 1980, **102**, 2627.
91. J. F. Endicott, *Isr. J. Chem.*, 1970, **8**, 209.
92. J. F. Endicott, in 'Concepts of Inorganic Photochemistry', ed. A. W. Adamson and P. D. Fleischauer, Wiley, New York, 1975, chap. 3.
93. J. Lilie, *J. Am. Chem. Soc.*, 1979, **101**, 4417.
94. J. F. Endicott, G. J. Ferraudi and J. R. Barber, *J. Phys. Chem.*, 1975, **79**, 630.
95. T. L. Kelly and J. F. Endicott, *J. Am. Chem. Soc.*, 1972, **94**, 1797.
96. W. C. Trogler, D. K. Erwin, G. L. Geoffroy and H. B. Gray, *J. Am. Chem. Soc.*, 1978, **100**, 1160.
97. D. A. Chaisson, R. E. Hintze, D. H. Stuermer, J. D. Petersen, D. P. McDonald and P. C. Ford, *J. Am. Chem. Soc.*, 1972, **94**, 6665.
98. G. Malouf and P. C. Ford, *J. Am. Chem. Soc.*, 1977, **99**, 7213.
99. J. E. Figard and J. D. Petersen, *Inorg. Chem.*, 1978, **17**, 1059.
100. V. Balzani, F. Bolletta, M. T. Gandolfi and M. Maestri, *Top. Curr. Chem.*, 1978, **75**, 1.
101. N. Sutin, *J. Photochem.*, 1979, **10**, 19.
102. N. Sutin and C. Creutz, *Pure Appl. Chem.*, 1980, **52**, 2717.
103. K. Kalyanasundaram, *Coord. Chem. Rev.*, 1982, **46**, 159.
104. M. Fox, in 'Concepts of Inorganic Photochemistry', ed. A. W. Adamson and P. D. Fleischauer, Wiley, New York, 1975, chap. 8.
105. C. Guttel and M. Shirom, *J. Photochem.*, 1973, **1**, 197.
106. A. Vogler and H. Kunkely, *Inorg. Chem.*, 1982, **21**, 1172.
107. W. L. Waltz and A. W. Adamson, *J. Phys. Chem.*, 1969, **73**, 4250.
108. O. Kalisky and M. Shirom, *J. Photochem.*, 1977, **7**, 215.
109. A. Vogler, W. Losse and H. Kunkely, *J. Chem. Soc., Chem. Commun.*, 1979, 187.
110. D. D. Davis, G. K. King, K. L. Stevenson, E. R. Birnbaum and J. H. Hageman, *J. Solid State Chem.*, 1977, **22**, 63.
111. A. W. Maverick and H. B. Gray, *Pure Appl. Chem.*, 1980, **52**, 2339.
112. A. W. Adamson, A. Vogler and I. Lantzke, *J. Phys. Chem.*, 1969, **73**, 4183.
113. A. Vogler and A. Kern, *Z. Naturforsch., Teil B.*, 1979, **34**, 271.

P. P. Zarnegar, C. R. Bock and D. G. Whitten, *J. Am. Chem. Soc.*, 1973, **95**, 4367.

115. H. D. Gafney, J. L. Reed and F. Basolo, *J. Am. Chem. Soc.*, 1973, **95**, 7998.

116. J. L. Reed, H. D. Gafney and F. Basolo, *J. Am. Chem. Soc.*, 1974, **96**, 1363.
117. J. I. Zink, *Inorg. Chem.*, 1975, **14**, 446.
118. T. Diem and J. P. Kennedy, *J. Macromol. Sci. Chem.*, 1978, **A12**, 1359.
119. S. M. Aliwi and C. H. Bamford, *J. Chem. Soc., Faraday Trans. 1*, 1977, **73**, 776.
120. M. Shirom and Y. Siderer. *J. Chem. Phys.*, 1972, **57**, 1013.
121. V. Balzani, M. F. Manfrin and L. Moggi, *Inorg. Chem.*, 1969, **8**, 47.
122. R. P. Mitra, B. K. Sharma and H. Mohan, *Aust. J. Chem.*, 1972, **25**, 499.
123. B. Sieklucka and A. Samotus, *J. Inorg. Nucl. Chem.*, 1980, **42**, 1003.
124. V. M. Miskowski, R. A. Goldbeck, D. S. Kliger and H. B. Gray, *Inorg. Chem.*, 1979, **18**, 86.
125. D. G. Nocera and H. B. Gray, *J. Am. Chem. Soc.*, 1981, **103**, 7349.
126. R. H. Fleming, G. L. Geoffroy, H. B. Gray, A. Gupta, G. S. Hammond, D. S. Kliger and V. M. Miskowski, *J. Am. Chem. Soc.*, 1976, **98**, 48.
127. W. L. Wells and J. F. Endicott, *J. Phys. Chem.*, 1971, **75**, 3075.
128. L. Moggi, G. Varani, M. F. Manfrin and V. Balzani, *Inorg. Chim. Acta*, 1970, **4**, 335.
129. M. E. Rerek and P. S. Sheridan, *Inorg. Chem.*, 1980, **19**, 2646.
130. A. Ceulemans, D. Beyens and L. G. Vanquickenborne, *Inorg. Chem.*, 1983, **22**, 1113.
131. D. S. Martin, Jr., M. A. Tucker and A. J. Kassman, *Inorg. Chem.*, 1966, **5**, 1298.
132. D. L. Webb and L. A. Rossiello, *Inorg. Chem.*, 1970, **9**, 2622.
133. F. S. Richardson, D. D. Shillady and A. Waldrop, *Inorg. Chim. Acta*, 1971, **5**, 279.
134. F. Scandola, *Org. Chem. (N.Y.)*, 1980, **42**, 549.
135. S. H. Goh and C. Y. Mok, *J. Inorg. Nucl. Chem.*, 1977, **39**, 531.
136. F. Bolletta, M. Gleria and V. Balzani, *Mol. Photochem.*, 1972, **4**, 205.
137. L. Moggi, G. Varani, N. Sabbatini and V. Balzani, *Mol. Photochem.*, 1971, **3**, 141.
138. L. G. Vanquickenborne, A. Ceulemans, D. Beyens and J. J. McGarvey, *J. Phys. Chem.*, 1982, **86**, 494.
139. G. Ferraudi and S. Muralidharan, *Coord. Chem. Rev.*, 1981, **36**, 45.
140. J. K. Kochi, *J. Am. Chem. Soc.*, 1962, **84**, 2121.
141. E. Cervone, F. D. Camassei, I. Giannini and J. Sykora, *J. Photochem.*, 1979, **11**, 321.
142. D. D. Davis, K. L. Stevenson and C. R. Davis, *J. Am. Chem. Soc.*, 1978, **100**, 5344.
143. G. Ferraudi, *Inorg. Chem.*, 1978, **17**, 1370.
144. B. T. Ahn and D. R. McMillin, *Inorg. Chem.*, 1978, **17**, 2253; 1981, **20**, 1427.
145. J. K. Hurst and R. H. Lane, *J. Am. Chem. Soc.*, 1973, **95**, 1703.
146. S. W. Orchard and C. Kutal, *Inorg. Chim. Acta*, 1982, **64**, L95.
147. P. C. Ford, R. E. Hintze and J. D. Petersen, in 'Concepts of Inorganic Photochemistry' , ed. A. W. Adamson and P. D. Fleischauer, Wiley, New York, 1975, chap. 5.
148. D. D. Davis, K. L. Stevenson and G. K. King, *Inorg. Chem.*, 1977, **16**, 670.
149. M. Brandys and G. Stein, *J. Phys. Chem.*, 1978, **82**, 852.
150. T. Donohue, *J. Chem. Phys.*, 1977, **67**, 5402.
151. R. P. Asbury, G. S. Hammond, P. H. P. Lee and A. T. Poulos, *Inorg. Chem.*, 1980, **19**, 3461.
152. D. Greatorex and T. J. Kemp, *Trans. Faraday Soc.*, 1971, **67**, 56; 1971, **67**, 1576; 1972, **68**, 121.
153. T. Donohue, *J. Am. Chem. Soc.*, 1978, **100**, 7411.
154. H. G. Brittain, *J. Phys. Chem.*, 1980, **84**, 840.
155. R. T. Paine and M. S. Kite, *ACS Symp. Ser.*, 1980, **131**, 369.
156. E. Rabinowitch and R. L. Belford, 'Spectroscopy and Photochemistry of Uranyl Compounds', Pergamon, Oxford, 1964.
157. H. D. Burrows and T. J. Kemp, *Chem. Soc. Rev.*, 1974, **3**, 139.
158. C. K. Jorgensen, *J. Lumin.*, 1979, **18/19**, 63.
159. R. Matsushima, *J. Am. Chem. Soc.*, 1972, **94**, 6010.
160. D. Greatorex, R. J. Hill, T. J. Kemp and T. J. Stone, *J. Chem. Soc., Faraday Trans. 1*, 1972, **68**, 2059.
161. H. D. Burrows and S. J. Formosinho, *J. Chem. Soc., Faraday Trans. 2*, 1977, **73**, 201.
162. H. D. Burrows, S. J. Formosinho, M. da Graca Miguel and F. Pinto Coelho, *J. Chem. Soc., Faraday Trans, 2*, 1976, **72**, 163.
163. O. Traverso, R. Rossi, L. Magon, A. Cinquantini and T. J. Kemp, *J. Chem. Soc., Dalton Trans.*, 1978, 569.
164. S. Sostero, O. Traverso, P. DiBernardo and T. J. Kemp, *J. Chem. Soc., Dalton Trans.*, 1979, 658.
165. J. L. Kropp, *J. Chem. Phys.*, 1967, **46**, 843.
166. R. Matsushima, T. Kishimoto and M. Suzuki, *Bull. Chem. Soc. Jpn.*, 1975, **48**, 3028.
167. A. G. Brits, R. van Eldik and J. A. van der Berg, *J. Inorg. Nucl. Chem.*, 1977, **39**, 1195.
168. J. G. Calvert and J. N. Pitts, Jr., 'Photochemistry', Wiley, New York, 1966, chap. 7.
169. L. M. Toth, J. T. Bell and H. A. Friedman, *ACS Symp. Ser.*, 1980, **177**, 253.
170. J. R. Bolton (ed.), 'Solar Power and Fuels', Academic, New York, 1977.
171. R. R. Hautala, R. B. King and C. Kutal (eds.), 'Solar Energy: Chemical Conversion and Storage', Humana Press, Clifton, NJ, 1979.
172. J. S. Connolly (ed.), 'Photochemical Conversion and Storage of Solar Energy', Academic, New York, 1981.
173. C. Kutal, *J. Chem. Educ.*, 1983, **60**, 882.
174. R. A. Bauer and F. Basolo, *J. Am. Chem. Soc.*, 1968, **90**, 2437.
175. B. Durham, J. L. Walsh, C. L. Carter and T. J. Meyer, *Inorg. Chem.*, 1980, **19**, 860.
176. J. R. Wasson, *Annu. Rep. Inorg. Gen. Synth.*, 1975, **3**, 309.
177. R. G. Salomon, *Tetrahedron*, 1983, **39**, 485.
178. E. E. Wegner and A. W. Adamson, *J. Am. Chem. Soc.*, 1966, **88**, 394.
179. J. N. Demas, R. P. McBride and E. W. Harris, *J. Phys. Chem.*, 1976, **80**, 2248.
180. E. L. Simmons and W. W. Wendlandt, *Coord. Chem. Rev.*, 1971, **7**, 11.
181. A. W. Adamson, in 'Concepts of Inorganic Photochemistry', ed. A. W. Adamson and P. D. Fleischauer, Wiley, New York, 1975, chap. 10.
182. G. H. Brown, in 'Techniques of Chemistry', ed. G. H. Brown, Wiley, New York, 1971, vol. 3, chap. 1.
183. R. C. Bertelson, in 'Techniques of Chemistry', ed. G. H. Brown, Wiley, New York, 1971, vol. 3, chap. 10.
184. S. D. Cohen and G. A. Newman, *J. Photogr. Sci.*, 1967, **15**, 290.
185. S. K. Deb and L. J. Forrestal, in 'Techniques of Chemistry', ed. G. H. Brown, Wiley, New York, 1971, vol. 3, chap. 7.

186. L. S. Meriwether, E. C. Breitner and C. L. Sloan, *J. Am. Chem. Soc.*, 1965, **87**, 4441.
187. L. S. Meriwether, E. C. Breitner and N. B. Colthup, *J. Am. Chem. Soc.*, 1965, **87**, 4448.
188. C. Geosling, A. W. Adamson and A. R. Gutierrez, *Inorg. Chim. Acta*, 1978, **29**, 279.
189. D. V. Stynes, *J. Am. Chem. Soc.*, 1974, **96**, 5942.
190. D. P. Schwendiman and J. I. Zink, *J. Am. Chem. Soc.*, 1976, **98**, 1248.
191. J. Olmsted, III, *Rev. Sci. Instrum.*, 1979, **50**, 1256.
192. M. Nakashima and A. W. Adamson, *J. Phys. Chem.*, 1982, **86**, 2910.
193. A. Cooper and C. A. Converse, *Biochemistry*, 1976, **15**, 2970.
194. A. W. Adamson, A. Vogler, H. Kunkely and R. Wachter, *J. Am. Chem. Soc.*, 1978, **100**, 1298.
195. T. Ramasami, J. F. Endicott and G. R. Brubaker, *J. Phys. Chem.*, 1983, **87**, 5057.
196. W. L. Waltz, J. Lilie and S. H. Lee, *Inorg. Chem.*, 1984, **23**, 1786.
197. J. F. Endicott, *Comments Inorg. Chem.*, 1985, **3**, 349.
198. L. S. Forster, J. V. Rund and A. F. Fucaloro, *J. Phys. Chem.*, 1984, **88**, 5012.
199. L. S. Forster, J. V. Rund, A. F. Fucaloro and S. H. Lin, *J. Phys. Chem.*, 1984, **88**, 5020.
200. N. A. P. Kane-Maguire, W. S. Crippen and P. K. Miller, *Inorg. Chem.*, 1983, **22**, 696.
201. P. C. Ford, D. Wink and J. Dibenedetto, *Prog. Inorg. Chem.*, 1983, **30**, 213.
202. L. H. Skibsted, M. P. Hancock, D. Magde and D. A. Sexton, *Inorg. Chem.*, 1984, **23**, 3735.
203. L. H. Skibsted, *Coord. Chem. Rev.*, 1985, **64**, 343.
204. D. A. Sexton, P. C. Ford and D. Magde, *J. Phys. Chem.*, 1983, **87**, 197.
205. P. S. Braterman, A. Harriman, G. A. Heath and C. J. Yellowlees, *J. Chem. Soc., Dalton Trans.*, 1983, 1801.
206. S. M. Angel, M. K. DeArmond, R. J. Donohoe, K. W. Hanck and D. W. Wertz, *J. Am. Chem. Soc.*, 1984, **106**, 3688.
207. E. M. Kober, B. P. Sullivan and T. J. Meyer, *Inorg. Chem.*, 1984, **23**, 2098.
208. S. F. McClanahan, R. F. Dallinger, F. J. Holler and J. R. Kincaid, *J. Am. Chem. Soc.*, 1985, **107**, 4835.
209. T. J. Meyer, *Prog. Inorg. Chem.*, 1983, **30**, 389.
210. V. Balzani and F. Scandola, in 'Energy Resources through Photochemistry and Catalysis', ed. M. Grätzel, Academic, New York, 1983, pp. 1–48.
211. K. A. King, M. F. Finlayson, P. J. Spellane and R. J. Watts, *Sci. Papers Inst. Phys. Chem. Res.*, 1984, **78**, 97.
212. K. A. King, P. J. Spellane and R. J. Watts, *J. Am. Chem. Soc.*, 1985, **107**, 1431.
213. S. A. Bryan, M. K. Dickson and D. M. Roundhill, *J. Am. Chem. Soc.*, 1984, **106**, 1882.
214. J. L. Marshall, S. R. Stobart and H. B. Gray, *J. Am. Chem. Soc.*, 1984, **106**, 3027.
215. J. V. Caspar and H. B. Gray, *J. Am. Chem. Soc.*, **106**, 3029.
216. A. W. Maverick, J. S. Najdzionek, D. MacKenzie, D. G. Nocera and H. B. Gray, *J. Am. Chem. Soc.*, 1983, **105**, 1878.
217. P. P. Infelta, in 'Energy Resources through Photochemistry and Catalysis', ed. M. Grätzel, Academic, New York, 1983, pp. 49–70.
218. W. Shi, S. Wolfgang, T. C. Strekas and H. D. Gafney, *J. Phys. Chem.*, 1985, **89**, 974.
219. M. M. Olken and A. B. Ellis, *J. Am. Chem. Soc.*, 1984, **106**, 7468.
220. X. Yang and C. Kutal, *J. Am. Chem. Soc.*, 1983, **105**, 6038.
221. H. Hennig, D. Rehorek and R. D. Archer, *Coord. Chem. Rev.*, 1985, **61**, 1.
222. C. Kutal, *Coord. Chem. Rev.*, 1985, **64**, 191.

7.4

Reactions of Coordinated Ligands

DAVID St C. BLACK
University of New South Wales, Kensington, NSW, Australia

7.4.1 INTRODUCTION

Traditionally, the study of coordination compounds has centred on the behaviour of the metal ions rather than the attached ligands. It has always been obvious that the properties of ligands could be modified by coordination to metals, but this feature of coordination chemistry has only been developed in recent years. Metal coordination plays important roles in biological processes involving metal–enzyme systems, but these are not yet understood in most cases. The course of certain organic reactions of a simpler type can be controlled to some extent by ligand coordination to metal ions. A wide variety of reaction types has been demonstrated, but the field is only in its infancy. Many important industrial processes involve reactions of coordinated ligands of the organometallic variety, such as alkene polymerization and carbon monoxide insertions, but these are outside the scope of this book.

Here the discussion will be limited to heterometallic systems in which the metal is linked to nitrogen, oxygen, sulfur and phosphorus donor atoms predominantly. Ligand reactions range from some very simple and almost trivial examples to complicated and sophisticated processes involving many steps. The coverage in this essay will be selective and will depend upon the type of reaction mechanisms either known to occur or reasonably supposed to take place.

Some reactions take place in close proximity to the metal ion and require direct involvement of one or more donor atoms. Other reactions occur at the periphery of a ligand and consequently owe little or nothing to the coordination of the ligand to a metal. Although a wide selection of examples will be included in this discussion, emphasis will centre on those reactions in which the metal ion plays at least a reasonably central role.

Metal ions can influence ligand reactions in various ways. They can act as 'super acids' and cause polarization of ligands by virtue of an electron-withdrawing effect. This phenomenon can then result in increased acidity of the ligand either directly at the donor atom or *via* conjugation to another part of the ligand. The nucleophilic character of a ligand can be modified by metal coordination, even to the point where an ambident nucleophile will undergo attack of an electrophile at a different position. Metal coordination enhances the attack of nucleophiles and this particular feature of coordination chemistry has been demonstrated over and over again in the case of nucleophilic addition to coordinated carbonyl groups.

The most dramatic reactions of coordinated ligands occur in complexes of transition metals, because of the inherent stability of these complexes and also the relatively high charge on the metal ion. The overall charge on cationic complexes is dispersed onto the ligands, which are consequently more greatly affected by relatively higher charges. Electrophilic attack is then retarded or repelled by the dispersed charge on cationic complexes, while nucleophilic attack is encouraged.

Metal ions can enhance reactions by stabilization of a transition state or a product by appropriate coordination. They can also retard reactions by coordination to a starting material and in this way can provide a protecting influence.

Probably the most important effect contributed by metal coordination to ligands is stereochemical in nature. Because of the rather strict coordination geometry imposed by metal ions, ligands can be held in suitable juxtaposition for reactions to take place between them. This phenomenon is the hallmark of metal template reactions and is also a crucial feature of metal enzyme reactions, where high specificity occurs.

The mechanistic aspects of the reactions of coordinated ligands could be discussed on the basis of several different organizational frameworks. It is not practical to subdivide a discussion according to a specific role of the metal ion because, in most examples, more than one role would be relevant. For instance, many reactions of nucleophilic addition to a coordinated carbonyl group occur in cases where a stereochemical influence is crucial. The following discussion has been somewhat arbitrarily divided into ligand reactions which do not give rise to the formation of chelate rings and those which do. Here, the stereochemical influence is critical. Within these subdivisions, a further distinction is made between reactions of donor atoms and non-donor atoms. The treatment will of necessity be selective and examples are chosen so that they best illustrate the mechanistic types of reactions. Emphasis will be on more recent work following earlier reviews of certain aspects of this subject.[1–5]

7.4.2 NON-CHELATE RING-FORMING REACTIONS

7.4.2.1 Reactions of Donor Atoms

7.4.2.1.1 Halogenation of coordinated nitrogen atoms

Direct chlorination of some platinum ammine complexes (**1**) leads ultimately to the corresponding chloro complexes (**3**) with retention of configuration (equation 1).[6] The reaction proceeds *via* the intermediate dichloroamino compounds (**2**) which are thermally unstable. Although coordinated amines are effectively quaternary and therefore lack nucleophilic properties, the above reaction presumably proceeds *via* initial deprotonation followed by nucleophilic attack of the nitrogen non-bonded pair of electrons on the chlorine molecule. Selectivity of chlorination is observed, with ammonia ligands *trans* to halogen being activated. Coordinated primary amines such as methylamine and 1,2-diaminoethane can also be chlorinated and nitrosated.[7]

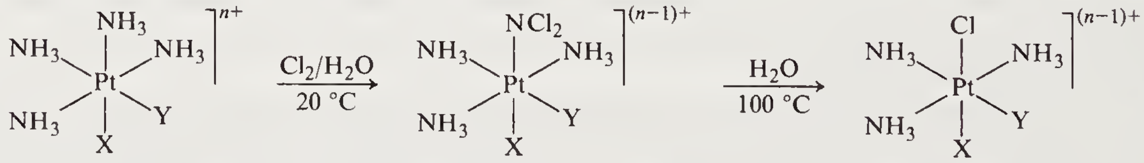

(**1**) (**2**) (**3**) (1)

$X = Cl$, $Y = NO_2$, $n = 2$
$X = Br$, $Y = NH_3$, $n = 3$

N-Bromination is almost certainly the initial step in a process which results in the overall arene bromination of some macrocyclic complexes of the arylamino type (*e.g.* equation 2).[8] In this reaction the arylamino nitrogen atoms still bear their pairs of non-bonded electrons and are capable of nucleophilic behaviour. Rearrangement of the *N*-bromo compound to the *p*-bromo isomer would then yield the observed product.

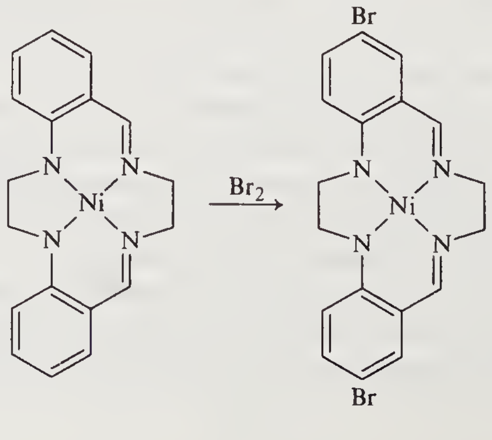

(2)

7.4.2.1.2 *Alkylation of coordinated sulfur and nitrogen atoms*

In 1959, the coordinated mercaptide ion in the gold(III) complex (**4**) was found to undergo rapid alkylation with methyl iodide and ethyl bromide (*e.g.* equation 3).[9] The reaction has since been used to great effect particularly in nickel(II) β-mercaptoamine complexes.[10,11] It has been demonstrated by kinetic studies that alkylation occurs without dissociation of the sulfur atom from nickel. The binuclear nickel complex (**5**) underwent stepwise alkylation with methyl iodide, benzyl bromide and substituted benzyl chlorides in second order reactions (equation 4). Bridging sulfur atoms were unreactive, as would be expected. Relative rate data were consistent with S_N2 attack of sulfur at the saturated carbon atoms of the alkyl halide. The mononuclear complex (**6**) yielded octahedral complexes on alkylation (equation 5), but the reaction was complicated by the independent reversible formation of the trinuclear complex (**7**). Further reactions of this type have been used to form new chelate rings (see Section 7.4.3.1).

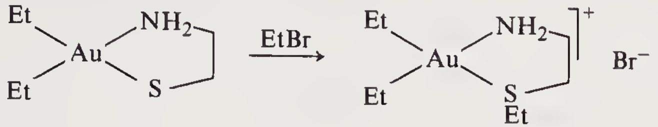

(**4**)

(3)

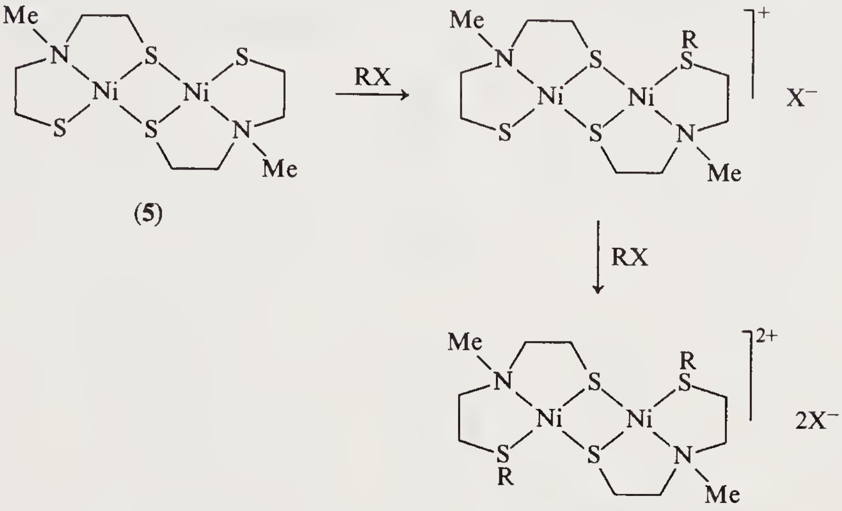

(**5**)

(4)

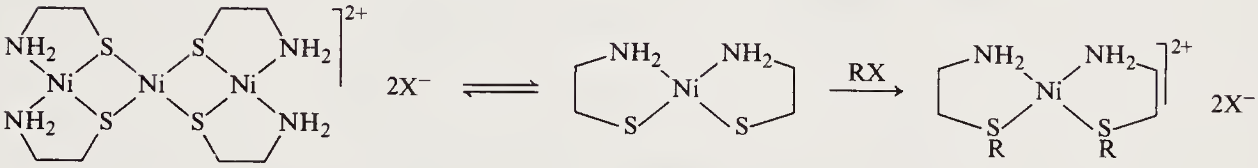

(**7**) (**6**)

(5)

Coordinated secondary amines can also be alkylated, but only after deprotonation by a strong base generates a suitable nucleophile. Work on rhodium(III) complexes of ethylenediamine[12] has been extended to nickel(II) complexes of various fully saturated macrocycles such as cyclam (Scheme 1).[13,14] The methylated cyclam complex is kinetically inert, unlike the isomer with all four methyl groups on the same side of the ring, which is obtained on reaction of the preformed tetramethyl cyclam with nickel ions.

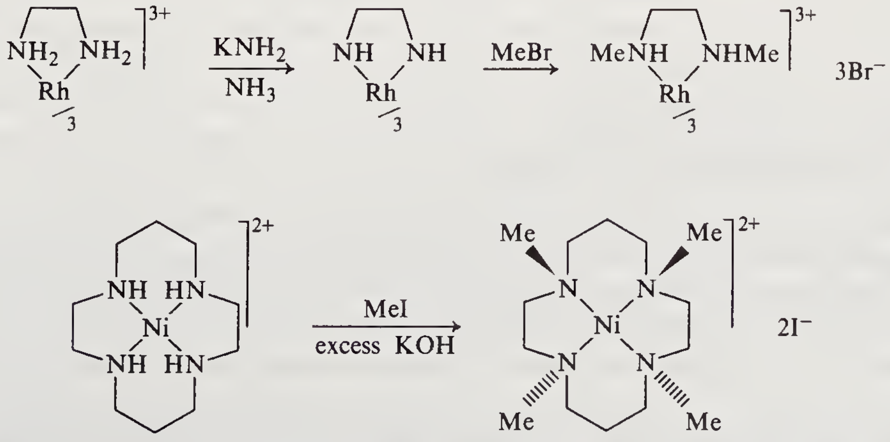

Scheme 1

7.4.2.1.3 Solvolysis of coordinated phosphorus atoms

Platinum(II)[15] and palladium(II)[16] complexes of phosphorus trichloride undergo solvolysis in water and alcohols to form complexes with orthophosphorous acid or orthophosphite ligands (equation 6). Similar reactions occur between the palladium(II) phenyldichlorophosphine complex (**8**) and the diols ethyleneglycol and catechol, but new chelate rings are not formed (Scheme 2). Solvolysis also occurs with attack of diphenylphosphinic acid or a similar diphenylchlorophosphine complex (**9**) (equation 7). The palladium complexes (**8**) and (**9**) are unstable to excess methanol, water or base and undergo reduction. Similarly, the phosphorus trichloride gold(I) complex (**10**) is reduced by water, but forms stable products on reaction with alcohols (equation 8).[15] During the above reactions, the phosphorus–metal bond remains intact and the overall process is one of substitution at phosphorus.

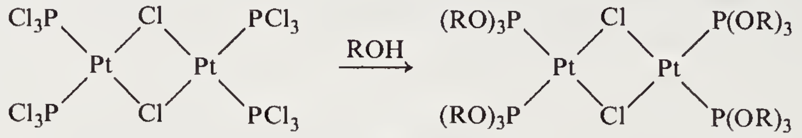

(6)

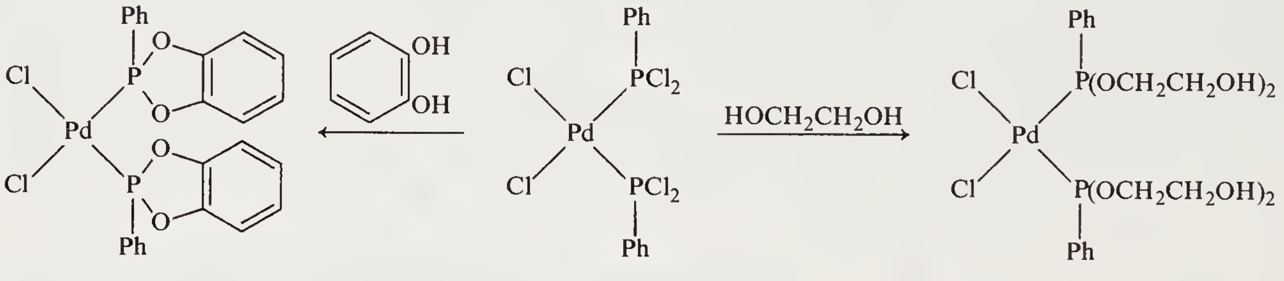

(**8**)

Scheme 2

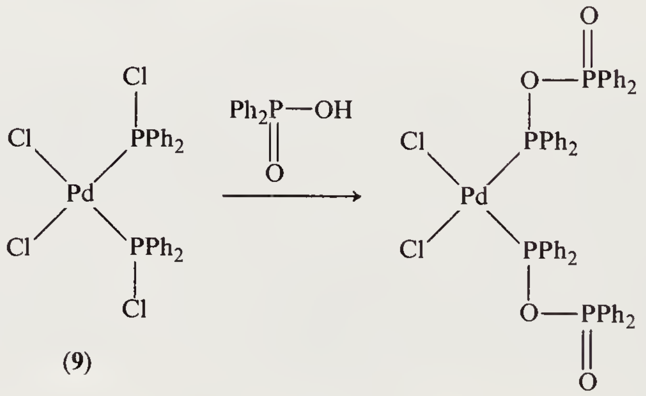

(**9**)

(7)

$$\mathrm{Cl{-}Au{-}PCl_3} \xrightarrow{\mathrm{ROH}} \mathrm{Cl{-}Au{-}P(OR)_3} \qquad (8)$$

(**10**)

Fluorophosphinenickel(0) complexes can be formed by reaction of the corresponding chlorophosphine complexes with potassium fluorosulfinate (equations 9 and 10).[17,18] The metal inhibits oxidation of the ligand to the phosphinic fluoride, a reaction that occurs readily to the free ligand.

$$\mathrm{Ni(PCl_3)_4} \xrightarrow{\mathrm{KSO_2F}} \mathrm{Ni(PF_3)_4} \qquad (9)$$

$$\mathrm{Ni(PhPCl_2)_4} \xrightarrow{\mathrm{KSO_2F}} \mathrm{Ni(PhPF_2)_4} \qquad (10)$$

7.4.2.2 Reactions of Non-donor Atoms

7.4.2.2.1 Nucleophilic behaviour of the ligand

In the previous section (7.4.2.1.1) an example was given of arene bromination as a result of intermediate *N*-bromination. Halogenation of various metal complexes of 8-hydroxyquinoline has been studied deliberately in order to identify any specific influence arising from metal coordination.[19] For example, bromination of the copper complex gave the dibromo-substituted product (equation 11). However, no significant effect of the metal was found. Rate retardation has been observed in the iodination of related 8-hydroxyquinoline 5-sulfonic acid complexes in comparison with reaction of the free ligand.[20] In these cases the phenolate anion is still an effective nucleophilic driving force for electrophilic substitution to occur. Bromination of trichlorotrisanilinechromium(III), effectively a quaternary anilinium salt, also yields the normal bromination product of aniline, without any noticeable rate enhancement (equation 12).[21]

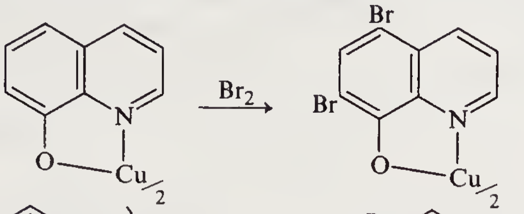

(11)

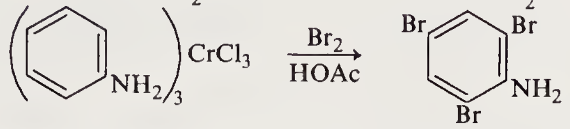

(12)

Reaction at part of a ligand quite remote from the metal can be influenced by the charge on a complex. The neutral copper(II) and nickel(II) imine complexes (**11**) undergo ready methylation of the quinoline nitrogen atom, whereas the related cationic complexes (**12**) are unreactive under similar conditions as a result of charge repulsion (Scheme 3).[2] Similarly, acylation of the uncoordinated hydroxyl group of the cationic cobalt(III) complex (**13**) cannot be achieved.[22] In contrast, both the free hydroxyl groups in the complex (**14**)[23] and the oxime hydroxyl groups in complex (**15**)[24] can be acetylated with acetic anhydride.

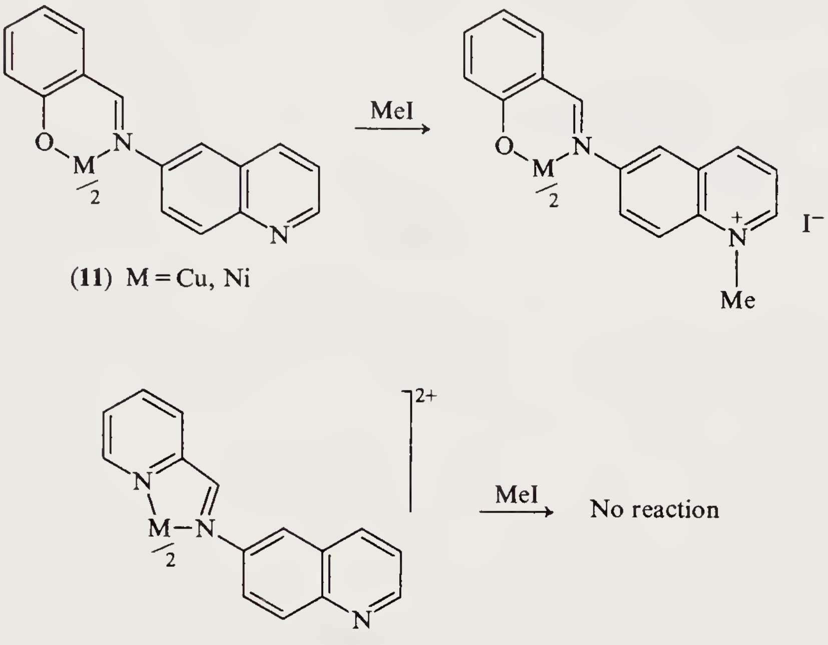

(**11**) M = Cu, Ni

(**12**) M = Cu, Ni

Scheme 3

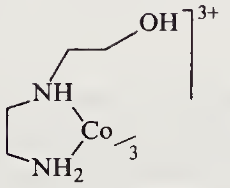

(**13**)

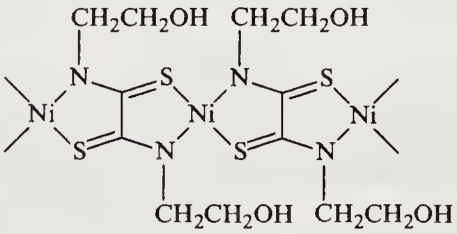

(**14**)

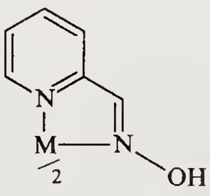

(**15**) M = Pd, Pt

Formation of copper(II) complexes of ornithine and lysine has enabled reactions to take place at the terminal amino group, while the α-amino acid moiety has been protected. For example, ornithine can be converted to citrulline by this technique (Scheme 4).[25,26]

The coordination of a carbonyl or imine group to a metal results in higher acidity of methylene protons adjacent to such a group. For instance, the diketo form of acetylacetone is deprotonated more readily in the case of a metal complex compared with the free ligand. The order of effectiveness for transition metal ions is Co > Ni > Zn > Mn > Cd. This phenomenon holds for β-keto esters as well. It has long been known that the rate of bromination of ethyl acetoacetate and ethylcyclopentanecarboxylate can be accelerated by copper(II) ions,[27,28] though it appears that the role of the metal is predominantly in the formation of the enolate anion rather than in the bromination step (Scheme 5).

The increase in acidity of methylene protons adjacent to coordinated carbonyl and imine groups is further reflected in the rapid deuterium exchange of such protons compared with rates of

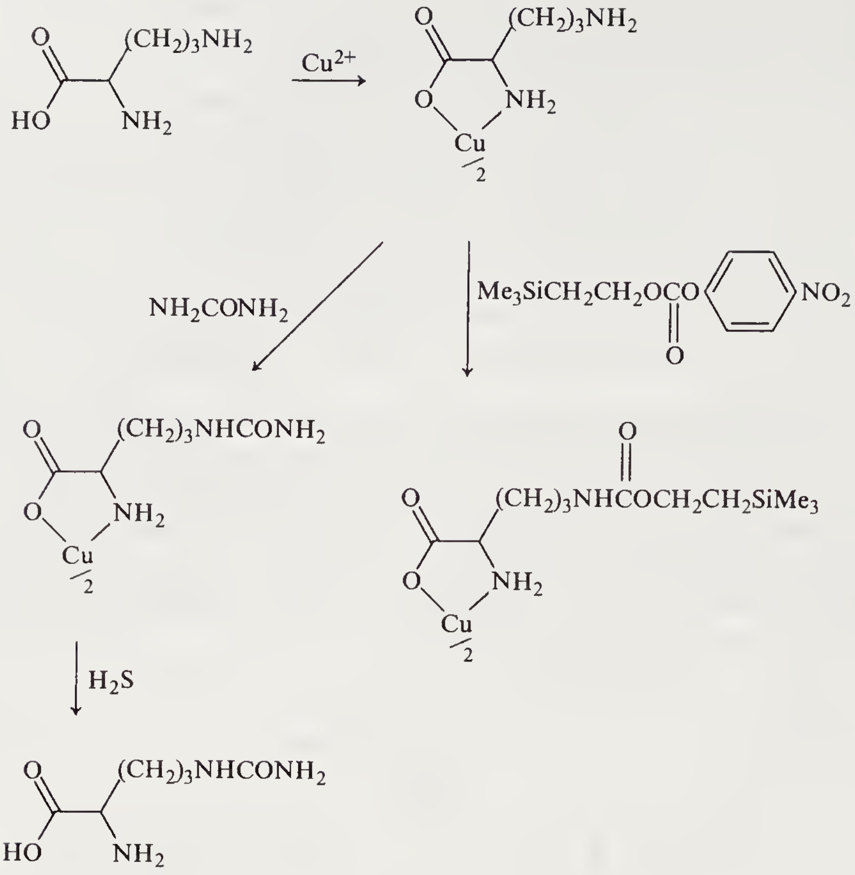

Scheme 4

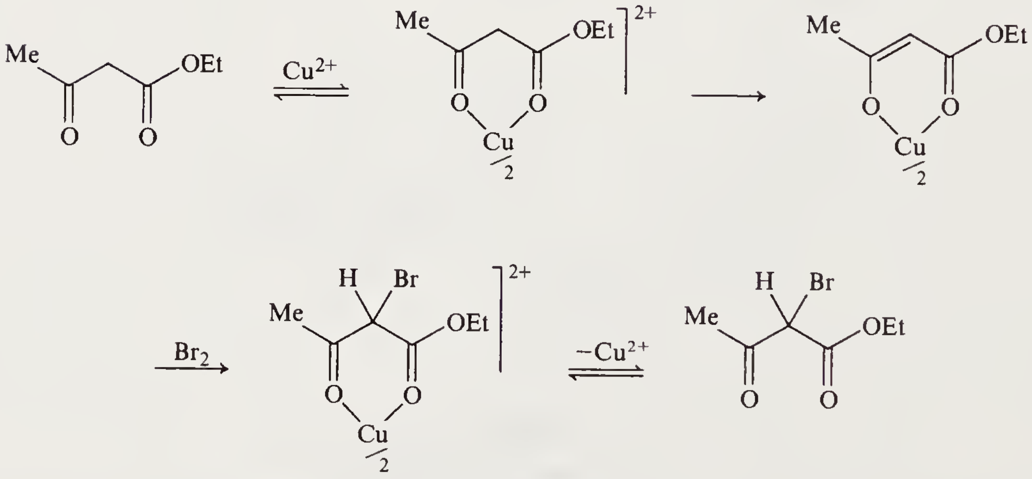

Scheme 5

exchange for the free ligands. Examples are afforded by the acetyl methyl protons of complexes (**16**) and (**17**), the imine methyl and methylene protons of complex (**18**) and the α-methylene protons of the amino acid complex (**19**). Indeed, in the last example, this phenomenon leads to rapid racemization of enantiomeric complexes. The bromination and iodination of pyruvic acid is similarly catalyzed by metal ions, which increase the rate of formation of the appropriate carbanion (Scheme 6).

In the above examples, the nucleophilic role of the metal complex only comes after the formation of a suitable complex as a consequence of the electron-withdrawing effect of the metal. Perhaps the most impressive series of examples of nucleophilic behaviour of complexes is demonstrated by the β-diketone metal complexes. Such complexes undergo many reactions typical of the electrophilic substitution reactions of aromatic compounds. As a result of the lability of these complexes towards acids, care is required when selecting reaction conditions. Despite this restriction, a wide variety of reactions has been shown to occur with numerous β-diketone complexes, especially of chromium(III), cobalt(III) and rhodium(III), but also in certain cases with complexes of beryllium(II), copper(II), iron(III), aluminum(III) and europium(III). Most work has been carried out by Collman and his coworkers and the results have been reviewed.[4,29] A brief summary of results is relevant here and the essential reaction is shown in equation (13). It has been clearly demonstrated that reaction does not involve any dissociation, by bromination of the chromium(III) complex in the presence of radioactive acetylacetone. Furthermore, reactions of optically active

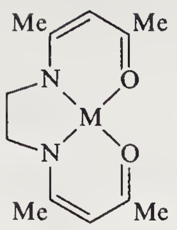

(16)

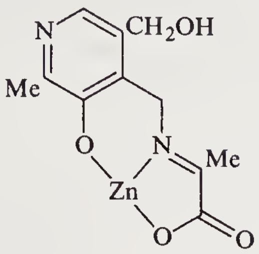

(17)

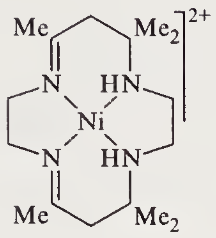

(18)

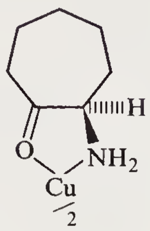

(19)

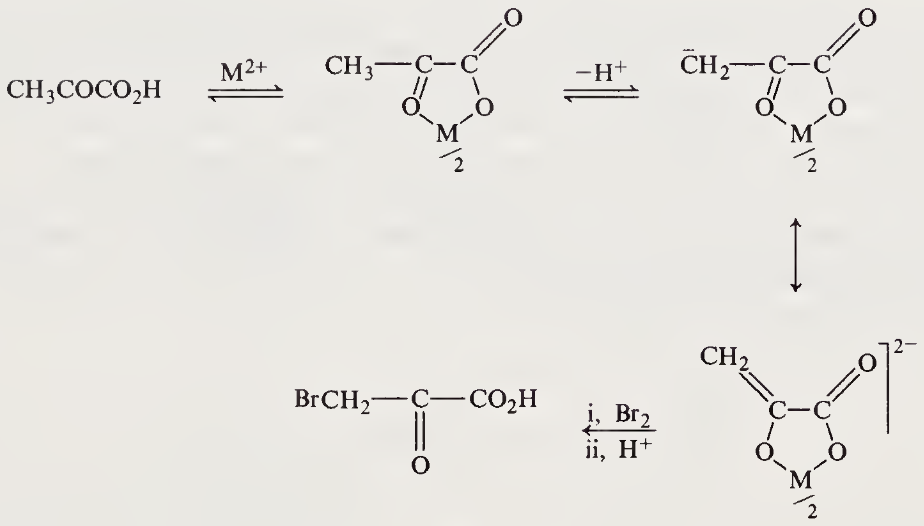

Scheme 6

complexes do not lead to any racemization. Halogenation can best be effected by use of *N*-halosuccinimides and is a stepwise process. Consequently, mixed ligand chelate complexes can be obtained. A combination of copper(II) nitrate and acetic anhydride has been used for nitration, either of the parent or iodo-substituted complexes. The nitro group can be hydrogenated catalytically to the amino group, which can be diazotized and modified by the Sandmeyer reaction. Halogeno groups can be removed by hydrogenolysis to give the unsubstituted complexes, but are inert to lithium and magnesium metal and do not usually undergo nucleophilic displacement; thiols are an exception.[30]

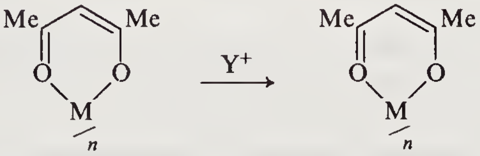

(13)

M = Cr, Co, Rh, Be, Cu, Fe, Al, Eu
Y = I, Br, Cl, SCN, SAr, NO_2, CH_2NMe_2, CHO, COR, D

Friedel–Crafts acetylation can be achieved, but the introduction of one acetyl group deactivates the remaining chelate rings so that mixtures of mono-, di- and tri-acetyl products are formed in the case of chromium(III) and cobalt(III) complexes, but only mono- and di-acetyl products from rhodium(III) acetylacetonate.

Introduction of larger acyl groups is made more difficult by the steric influence of the methyl groups adjacent to the position of attack. Formylation using phosphoryl chloride and dimethylformamide can be achieved but the reactivity of the introduced formyl group is rather low. The application of a modified Mannich reaction allows the introduction of dimethylaminomethyl groups which can be transformed by quaternization of the amino groups and nucleophilic displacement of trimethylamine (*e.g.* Scheme 7).

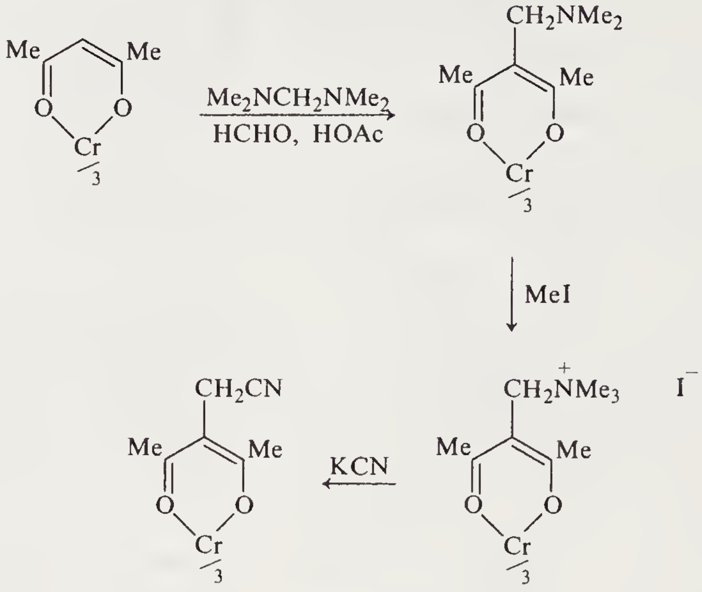

Scheme 7

Although the methyl groups in acetylacetonate complexes retard some reactions by steric hindrance, they provide some electronic enhancement in reactions with electrophiles and furthermore protect the donor oxygen atoms from electrophilic attack. These properties have been discerned by a comparison of the numerous reactions of acetylacetone complexes with the relatively few successful reactions of complexes of formylacetone and malondialdehyde.

The electrophilic substitution of β-diketonate complexes appears to occur as for arenes, and a process involving initial coordination of the electrophile, followed by an intramolecular group transfer, has not been observed, although it has been postulated for the reaction of copper(II) acetylacetonate with thioacetals (equation 14).[31]

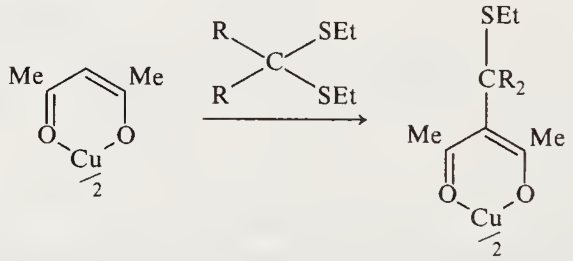

(14)

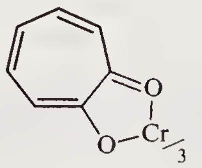

(20)

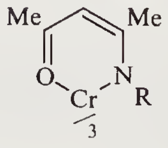

(21)

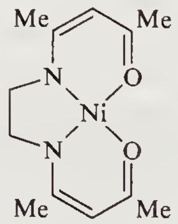

(22)

Tropolone complexes (**20**) also undergo electrophilic substitution, but the numerous positions for reaction give rise to mixtures of products. The β-keto imine complexes (**21**) and (**22**)[32] have been brominated successfully using *N*-bromosuccinimide.

In a mechanistically similar process, the neutral palladium(II) dipyridylamine complex (**24**), obtained by deprotonation of complex (**23**), underwent reaction with benzoyl chloride to give the substituted complex (**25**) together with some free ligand (Scheme 8).[33] This particular reaction sequence could not be generalized because of the relative instability of other metal complexes related to compound (**24**). However, a more extensive series of electrophilic substitutions could be carried out on the neutral complex (**26**), which displayed ambident nucleophilic behaviour by reaction with benzyl chloride and benzoyl chloride at nitrogen and reaction with benzenediazonium fluoroborate at carbon (Scheme 9).

Several series of macrocyclic β-diimine complexes have been shown to undergo reactions similar to those of the β-diketonates. Reversible protonation of the complexes (**27**) (equation 15) has been

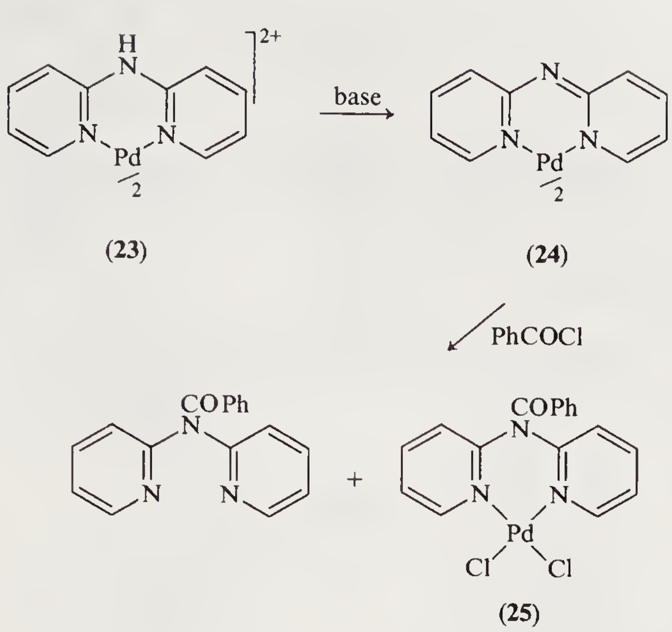

Scheme 8

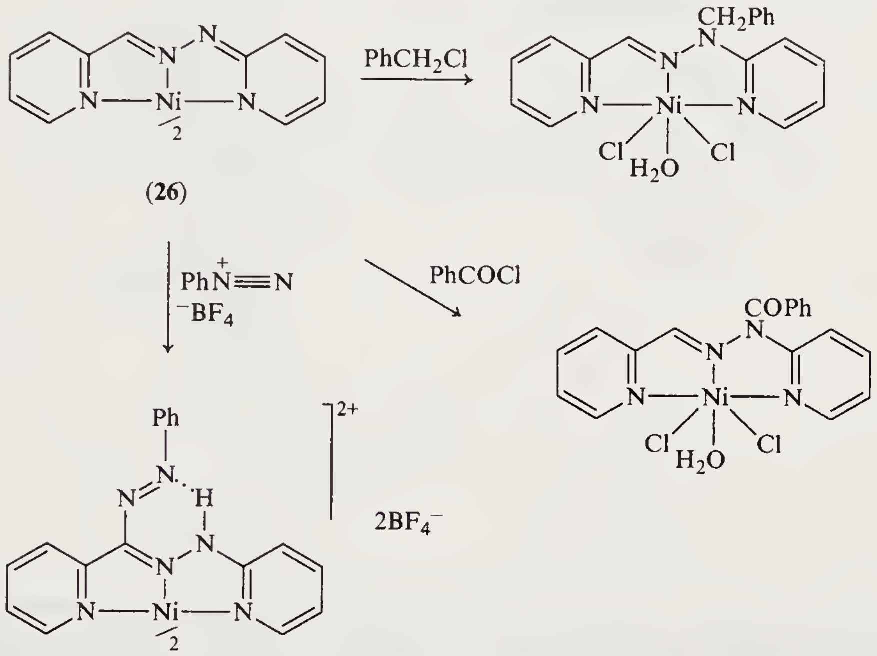

Scheme 9

found to depend upon the particular metal ion and the macrocyclic ring size.[34,35] For 14-membered macrocycles, the pK_a for the nickel complex is 6.45 and that for the copper complex is 9.3.

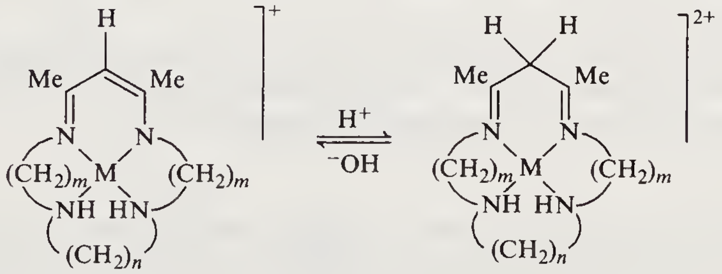

(15)

(**27**) M = Ni, Cu; m, n = 2, 3

It was found that the 15-membered macrocyclic complexes were significantly less acidic. Similar reversible protonations have been shown to occur in related macrocyclic complexes[36,37] and this work has been developed by Busch into a major study of ligand reactions,[38] which are summarized in equations (16)–(19). It is significant that these reactions include not only typical substitution reactions such as acylation and nitration (equations 16 and 19), but also nucleophilic addition to isocyanates (equation 17) and to α,β-unsaturated esters (equation 18).

The acetyl-substituted complexes, initially prepared by Jäger[36] by direct synthesis, have served as the basis for all of the work in this area. It has been shown that the acetyl group can be replaced by substitution, especially nitration, where reaction conditions are rather vigorous.[39] The acetyl-substituted complexes are not only nucleophilic at carbon, a property exhibited in the above reaction, but they are also nucleophilic at oxygen, being vinylogous amides, and undergo

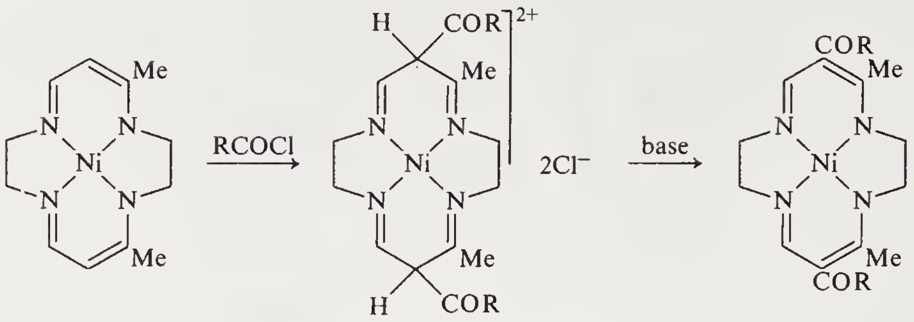

(16)

R = Me, Ph, *p*-MePh, *p*-NO_2Ph, $MeO_2C(CH_2)_2$

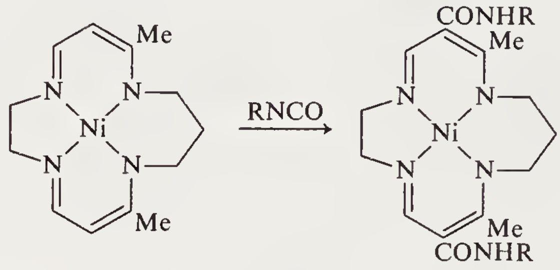

(17)

R = Et, α-naphthyl

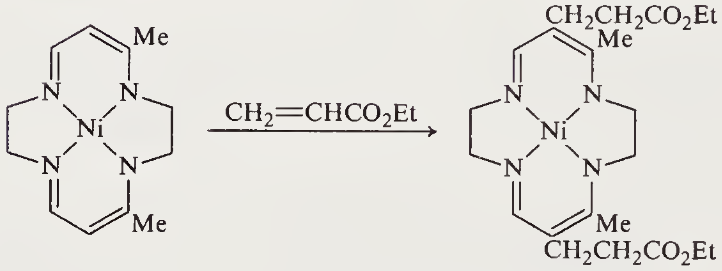

(18)

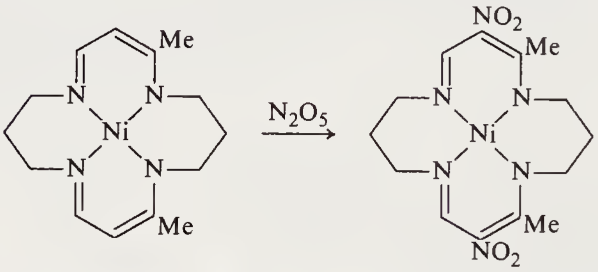

(19)

methylation to give imidate complexes (**28**).[40] The related amidine complexes (**29**), derived by amine attack on the imidate complexes (**28**), can themselves act as nucleophiles at nitrogen.[40,41] These reactions are summarized in Scheme 10. The amidine complexes (**29**) have more recently been alkylated by a range of dihalides to produce macrobicyclic complexes.[42,43] This work complements the addition of long-chain diamines to the imidate complexes (**28**) to yield similar macrobicyclic complexes.

The iron(II) diimine complex (**30**) displays unusual stability towards acids, alkali, reducing and oxidizing agents and has been termed 'quasi-aromatic'.[44] Complex (**30**) undergoes bromination in acetic acid to give the dibromo analogue (**31**) (equation 20).[45]

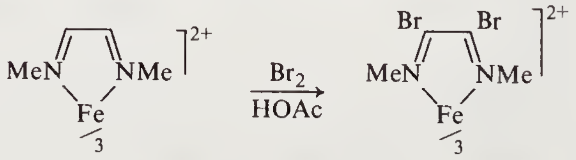

(20)

(**30**) (**31**)

The methylene group of α-amino acid metal complexes such as the copper(II) glycinato complex is activated to some extent by the polarizing influence of the metal.[46,47] Consequently, carbanion-type reactions can be carried out at this position, while the amino and carboxyl groups are protected by coordination. These reactions cannot be performed on either the free ligand or the conjugate base.

Not only can the α-methylene carbanion be produced and stabilized, but it can also undergo base-catalyzed aldol-type reactions without decomposition of the chelate ring. The most-studied reactions involve carbanion additions to acetaldehyde to produce threonine and allothreonine. This can be achieved for bis(glycinato)copper(II),[48,49] tris(glycinato)cobalt(III)[50,51] or glycinatobis(1,2-diaminoethane)cobalt(III),[52] with the best yield being obtained in the last case, where the

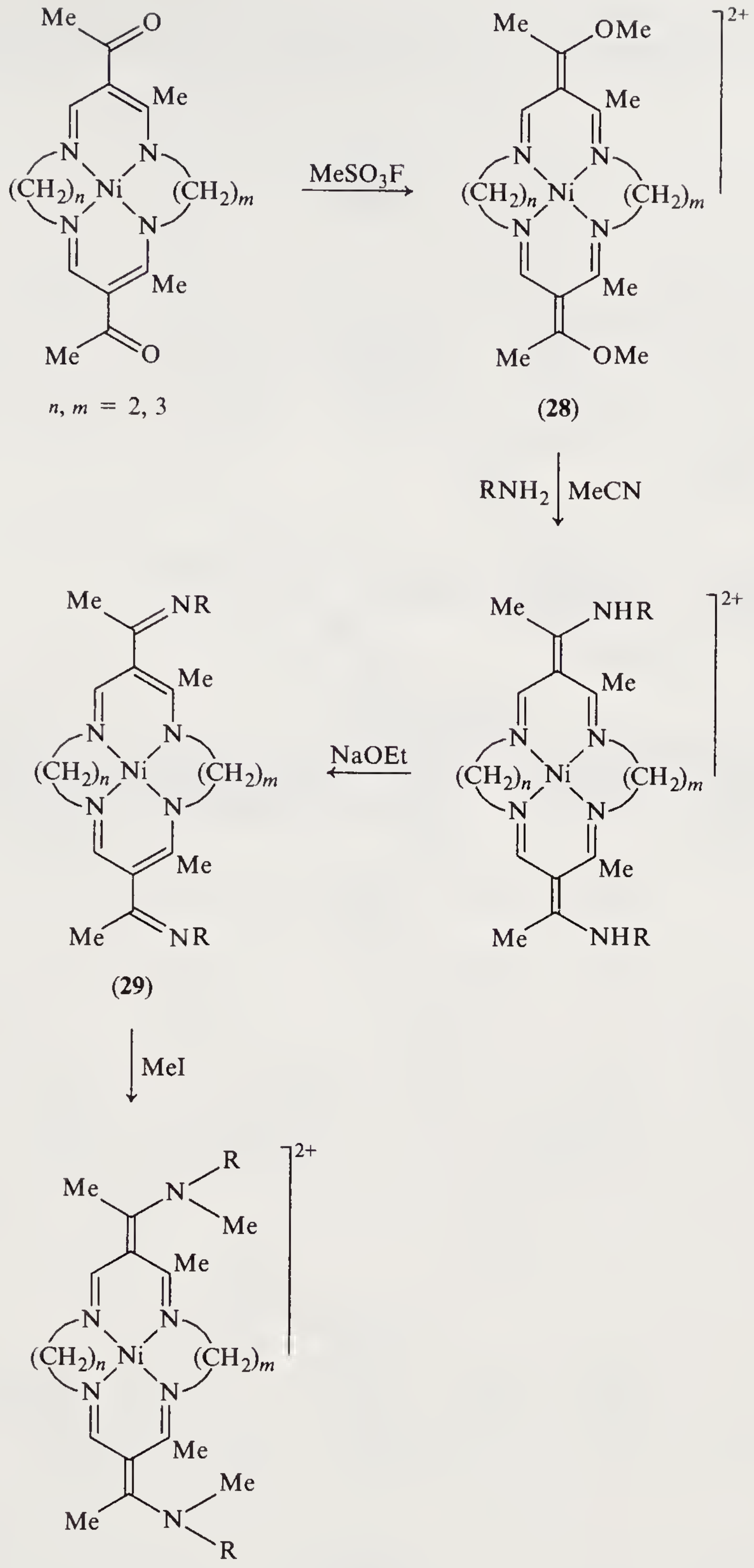

Scheme 10

reaction seems to be assisted by the positive charge on the cationic complex (Scheme 11). Similar reaction with formaldehyde instead of acetaldehyde can proceed to further substitution and cyclization as exemplified by the formation of a bicyclic product (Scheme 12).[53]

The use of chiral complexes gives rise to enantioselectivity of carbon–carbon bond formation and this phenomenon has also been applied to resolution[54] and enantioselective deuteration[55,56] of amino acids. Both the kinetic acidity of the α-methylene protons and the enantioselectivity of bond formation are greatly enhanced by the formation of chiral complexes (**32**) and (**33**) of imines derived from the amino acid and salicylaldehyde or pyridoxal respectively.[57–59] Similar use has been made of imine complexes (**34**) derived from pyruvic acid and the amino acid.[60,61] Very recently, an asymmetric synthesis of threonine has been achieved using the chiral imine complex (**35**).[62]

Amino acid complexes are also nucleophilic towards the Vilsmeier reagent. The cobalt(II) glycine complex (**36**) gives rise initially to an unusually stable iminium complex,[63] which can be hydrolyzed with concentrated sulfuric acid to the complex of formylglycine (Scheme 13). The formyl group is quite reactive and undergoes the usual additions of nucleophiles such as water, alcohols and hydride ion.[64] The synthetic utility of the above reactions will be considered again in Chapter 61.1.

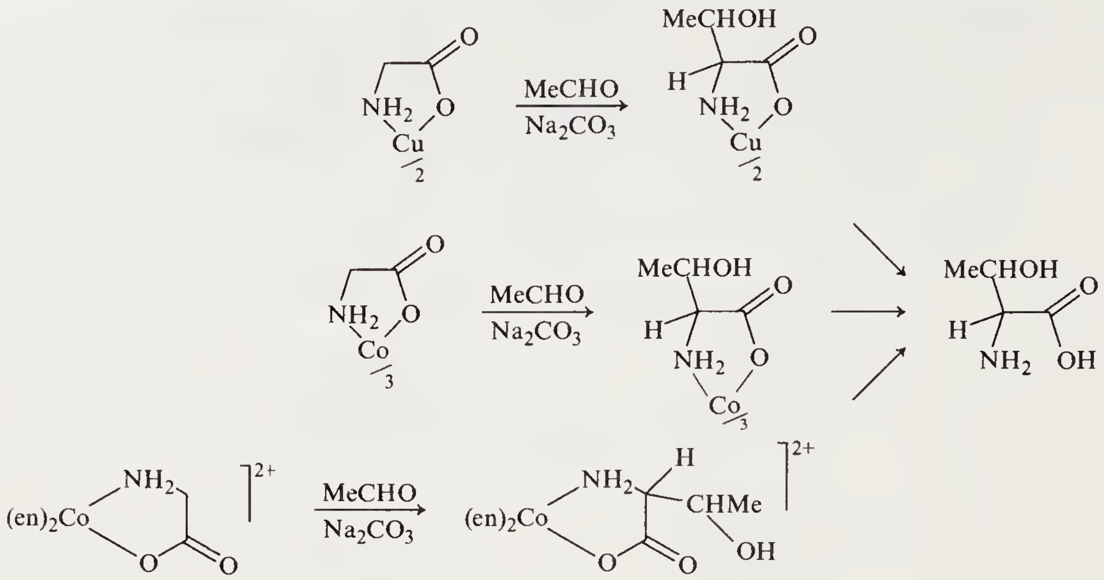

Scheme 11

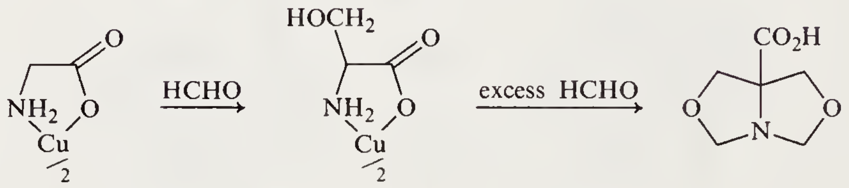

Scheme 12

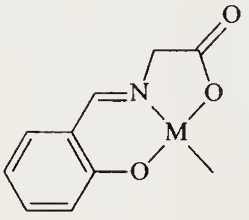

(32)

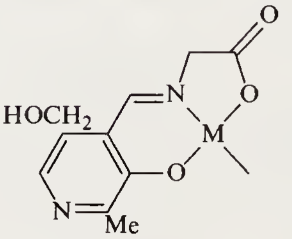

(33)

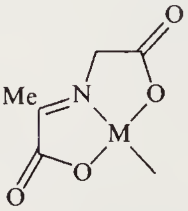

(34)

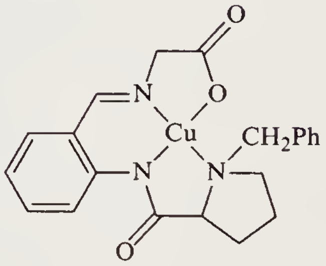

(35)

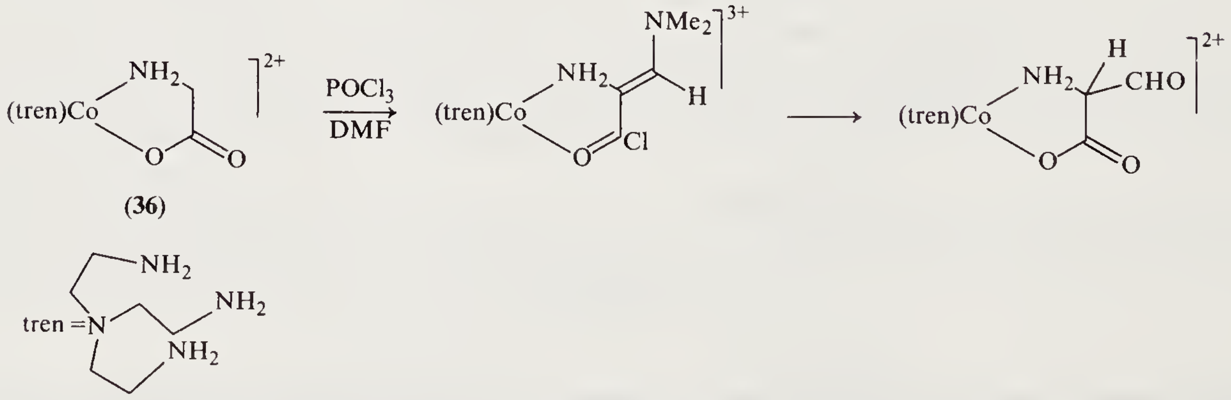

Scheme 13

In the case of peptide complexes (*e.g.* **37**), only the protons on carbon adjacent to the terminal carboxylate group are acidic enough to allow carbanion formation and to undergo deuterium exchange.[65]

In a series of reactions similar to those described for amino acid complexes, pyruvic acid undergoes metal-catalyzed condensation with aldehydes and also halogenation (Scheme 14). Again, the metal ion presumably functions by accelerating the formation of the methylene carbanion.

7.4.2.2.2 Electrophilic behaviour of the ligand

The coordination of a ligand to a metal ion results in polarization of the ligand such that its electrophilic character is enhanced. This facet of reactivity has already been mentioned in the previous section, with respect to deprotonation of a coordinated ligand to produce a good nu-

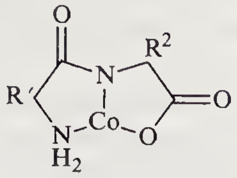

(37)

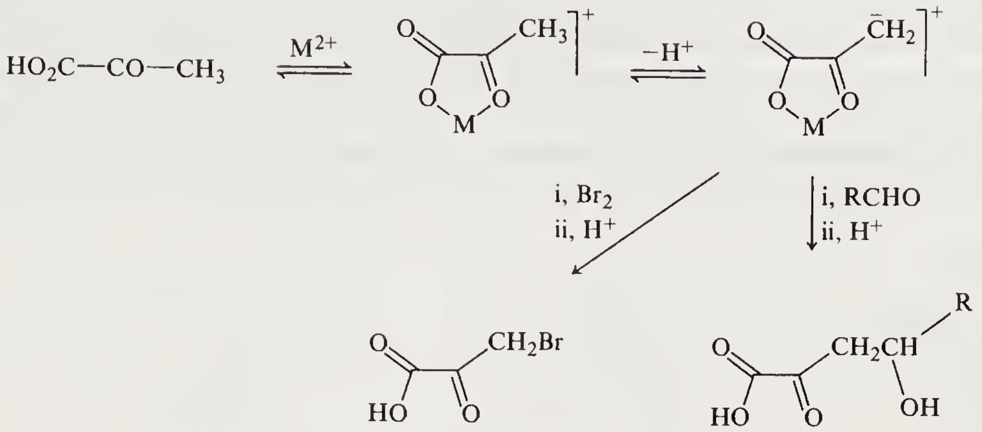

Scheme 14

cleophile. However, numerous catalytic and stoichiometric processes are known, in which the ligand behaves as an electrophile. Catalytic reactions are considered in detail in Chapter 61.4, but a brief summary of mechanistic types is included here.

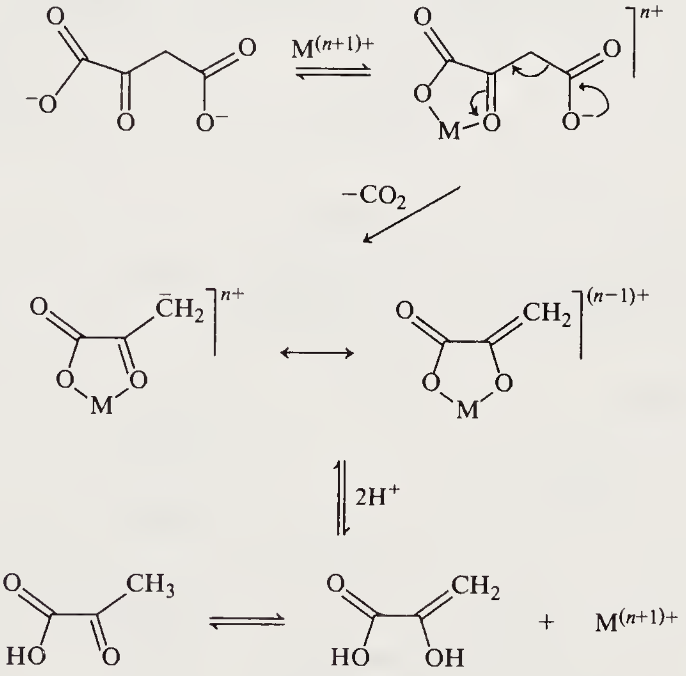

Scheme 15

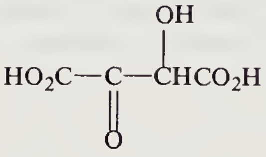

$HO_2C-\underset{\underset{O}{\|}}{C}-\overset{OH}{\overset{|}{C}}HCO_2H$

(38)

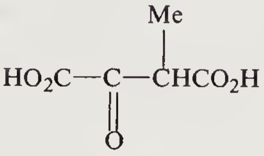

$HO_2C-\underset{\underset{O}{\|}}{C}-\overset{Me}{\overset{|}{C}}HCO_2H$

(39)

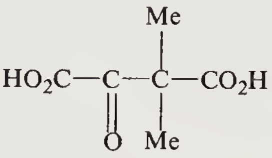

$HO_2C-\underset{\underset{O}{\|}}{C}-\overset{Me}{\overset{|}{\underset{\underset{Me}{|}}{C}}}-CO_2H$

(40)

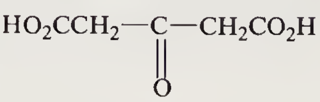

$HO_2CCH_2-\underset{\underset{O}{\|}}{C}-CH_2CO_2H$

(41)

Catalytic decarboxylation processes occur in aliphatic keto acids in which the keto group is in an α-position to one carboxyl group and in a β-relationship to another. Thus, the normal decarboxylation of a β-keto acid is facilitated by metal coordination to the α-keto acid moiety. The most-studied example is oxaloacetic acid and it has been shown that its decarboxylation is catalyzed by many metals following the general order $Ca^{2+} < Mn^{2+} < Co^{2+} < Zn^{2+} < Ni^{2+} < Cu^{2+} < Fe^{3+} < Al^{3+}$.[66,67] The overall rate constants can be correlated with the stability constants of 1:1 complexes of oxalic acid rather than oxaloacetic acid, as the uncoordinated carboxylate anion is essential for the decarboxylation. The generally accepted mechanism is shown in Scheme 15. Catalysis can be increased by the introduction of π-bonding ligands, which not only increase the effective positive charge on the metal ion, but also stabilize the coordinated anion. Metal-ion-catalyzed decarboxylation has also been studied for the related acids **(38)**,[68] **(39)**,[69] **(40)**[70] and **(41)**.[71]

Metal ions have a pronounced catalytic effect on the hydrolysis of α-amino acid esters as a consequence of metal coordination to the ester carbonyl oxygen atom, supported by the amino donor atom (Scheme 16).[72,73] Similar additions of alcohols, leading to ester exchange, and amines, leading to amide and peptide formation, are also metal catalyzed,[74,75] as are equivalent reactions of small peptide esters.[76,77] Initially, uncoordinated ester groups in complexes **(42)**[78] and **(43)**[79] undergo intermediate coordination prior to hydrolysis or similar reactions (Schemes 17 and 18). However, such coordination is not essential for the observation of a rate increase as the presence of a positively charged metal ion in the vicinity of the reaction can encourage the approach of a nucleophile. This phenomenon can be enhanced if the metal ion is firmly held in the reaction environment by a strongly coordinating group as in complexes **(44)**,[78] **(45)**,[80] **(46)**,[81] **(47)**[82] and **(48)**.[83]

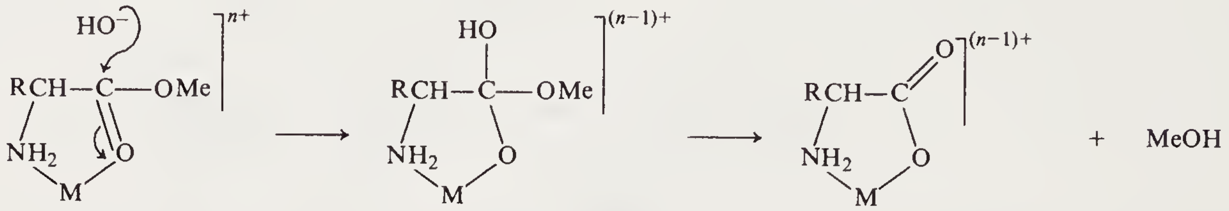

Scheme 16

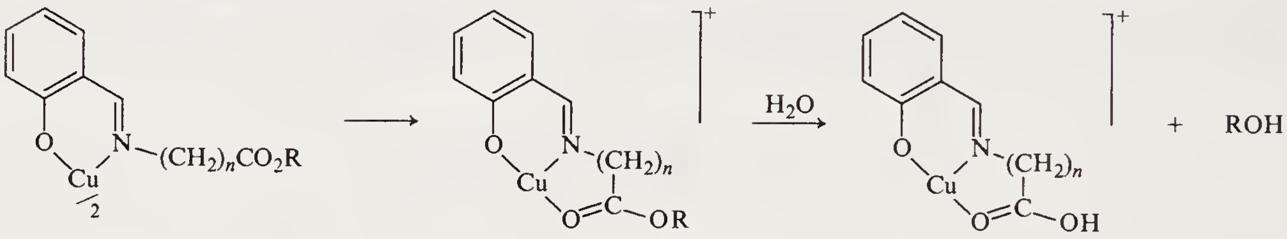

(42)

Scheme 17

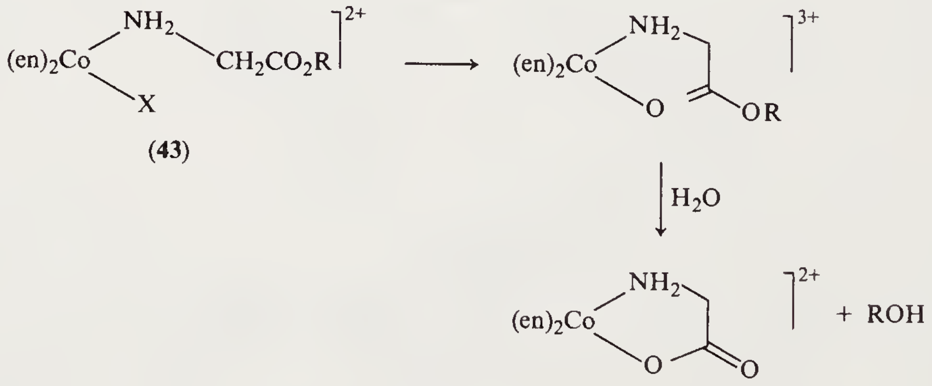

(43)

Scheme 18

Hydrolysis of peptides,[84] amides,[85] phosphate esters,[86] sulfonate esters[87] and acetals[88] can also be metal catalyzed. The hydrolysis of a phosphate ester coordinated to cobalt(III) also occurs at an increased rate (Scheme 19).[89] A rather similar reaction occurs in the amine exchange of coordinated dithiocarbamates (equation 21).[90] The conversion of imidates to amidines has been mentioned previously and is a similar type of reaction (see Section 7.4.2.2.1).

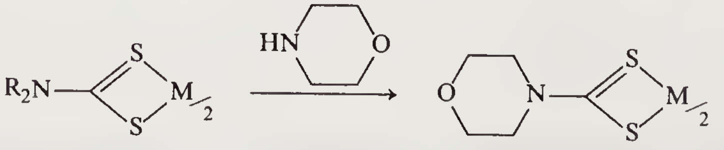

(21)

As well as the above addition and elimination sequences, metal-catalyzed nucleophilic addition can occur. Examples include the zinc(II)-catalyzed hydride ion addition in the reduction of the formyl group of the phenanthroline aldehyde **(49)**[91] and the copper(II)-catalyzed ring opening of 2-pyridyloxirane **(50)**[92] (equations 22 and 23).

Examples of carbanion additions to cobalt-coordinated imines will be considered in the next section (7.4.3.2) as chelate ring formation is a consequence in some cases.

One of the earliest reported reactions of coordinated ligands involves the hydrolysis of acetonitrile coordinated to platinum(II) and the formation of acetamide.[93] Such hydration is general

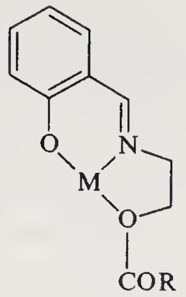

(44) R = Me, Ph

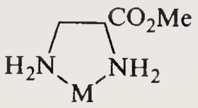

(45)

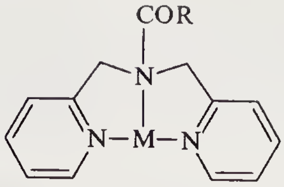

(46)

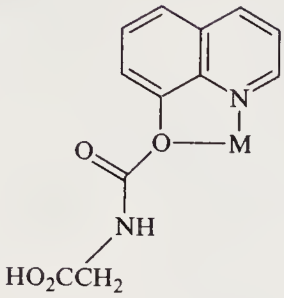

(47)

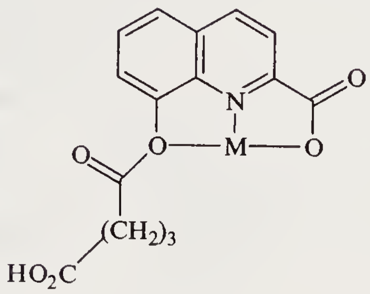

(48)

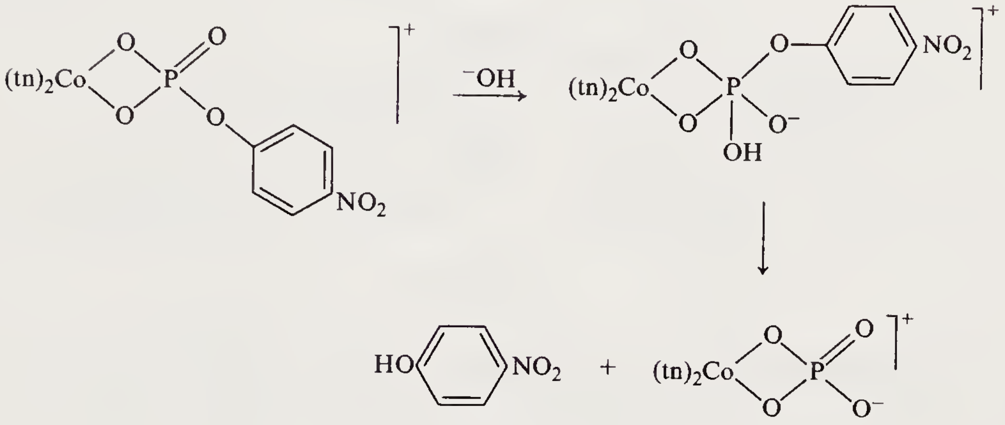

Scheme 19

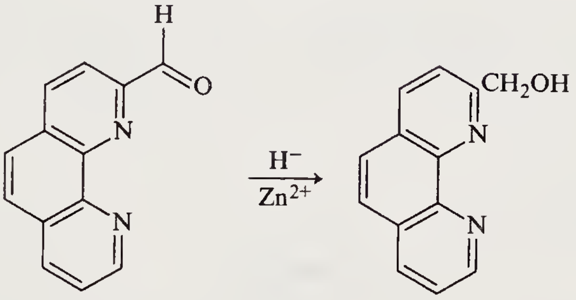

(49)

(22)

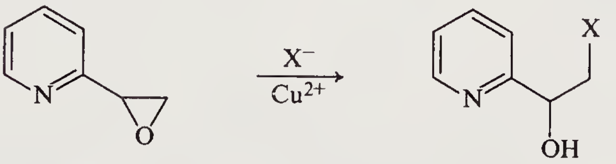

(23)

(50) X = OH, OMe, Cl, Br

for coordinated nitriles, as is the addition of amines to give amidine complexes and the addition of alcohols and thiols to give imidate and thiomidate complexes (Scheme 20).[94,95] Metal-ion catalysis also occurs in the hydration of 2-cyanophenanthroline (equation 24) and the mechanism is similar to that discussed above for the related esters. Coordinated nitriles are also susceptible to attack of hydride ion, and even carbanions have been added with great ease to the terminal carbon atom of coordinated acrylonitrile (Scheme 21).[96]

Addition of water to coordinated isocyanato groups has been suggested[97] as an intermediate step in the conversion of a pentammine rhodium(III) urea complex to the related hexammine complex (Scheme 22) and also in the nickel(II)-promoted hydrolysis of a pyridylurea (Scheme 23). The isocyanato intermediate has been observed in the first example but not the second.

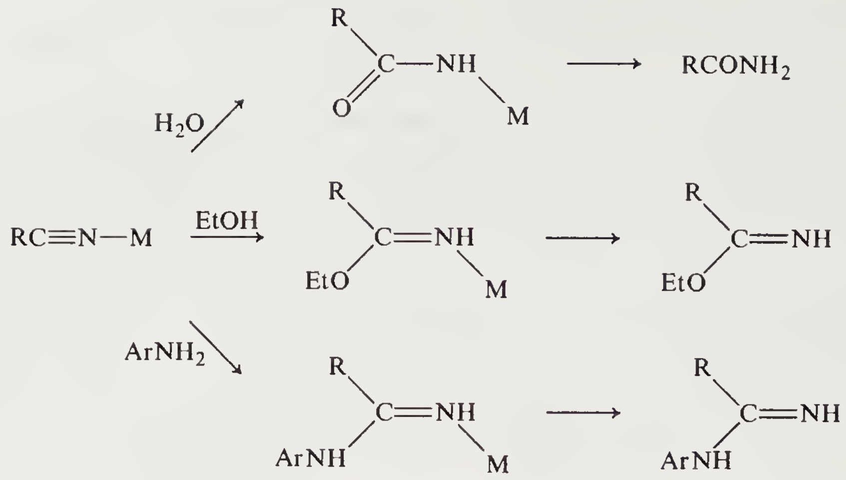

Scheme 20

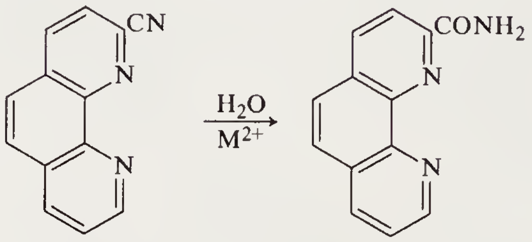

(24)

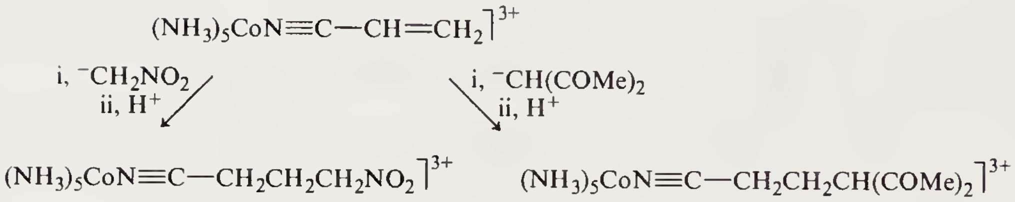

Scheme 21

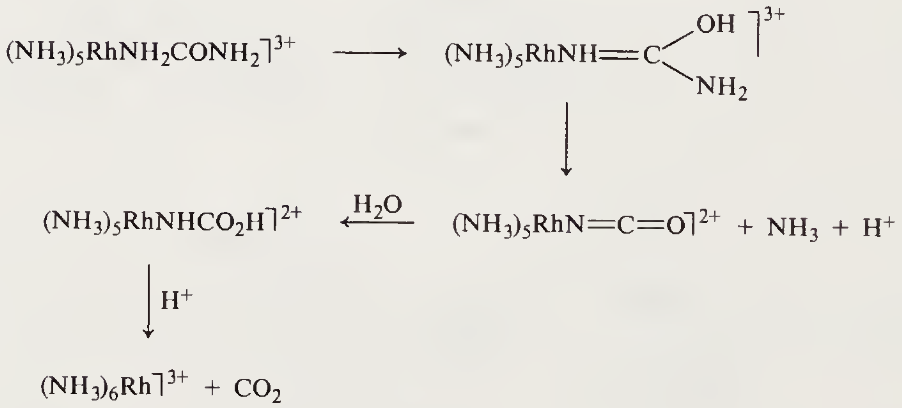

Scheme 22

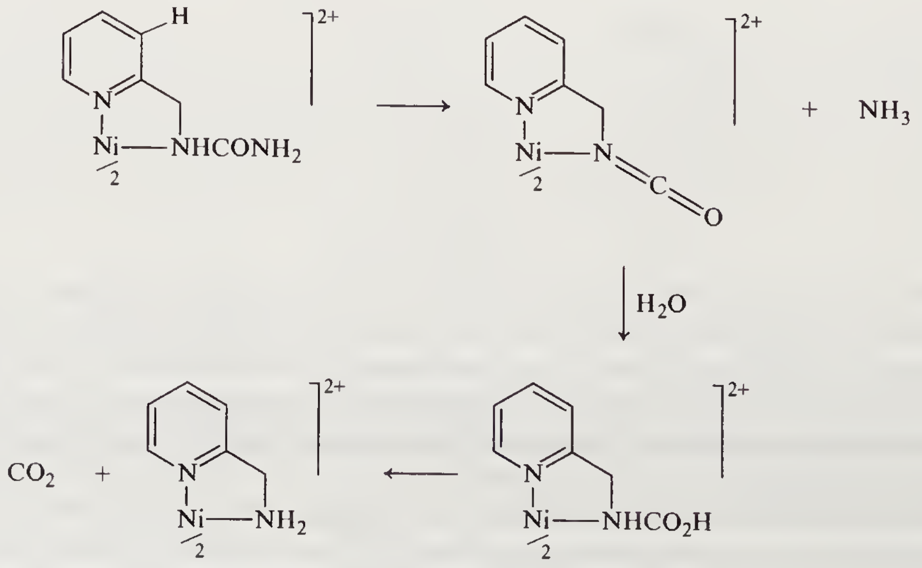

Scheme 23

The covalent hydration of coordinated heterocycles such as pyridine or phenanthroline has been postulated to account for a variety of anomalous results in hydrolysis reactions. The concept is sufficiently general to encompass attack of nucleophiles other than water (equation 25).[98] Reactions of this type have been reviewed very recently and the validity of the covalent hydration concept has come under attack.[99]

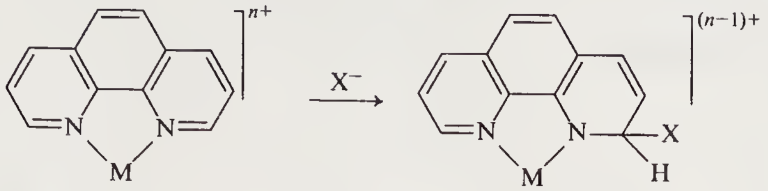

(25)

X = OH, OR, CN

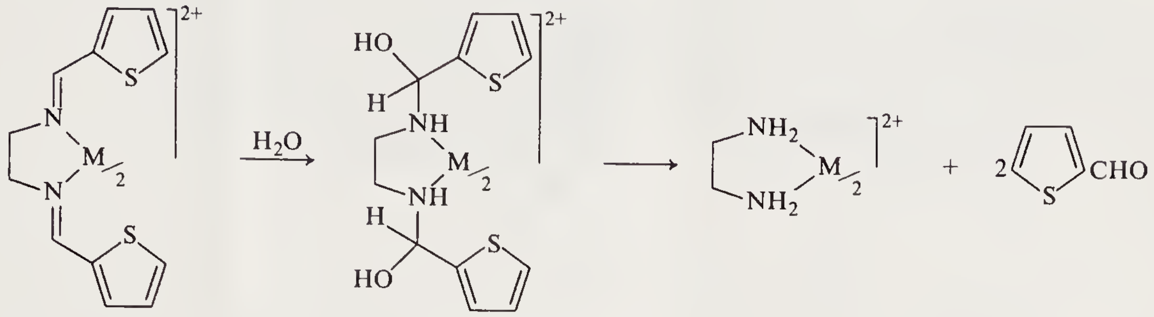

Scheme 24

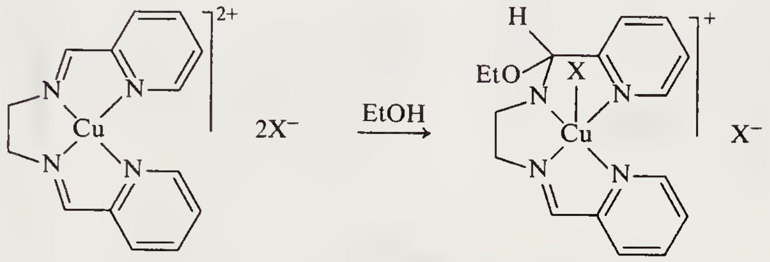

(26)

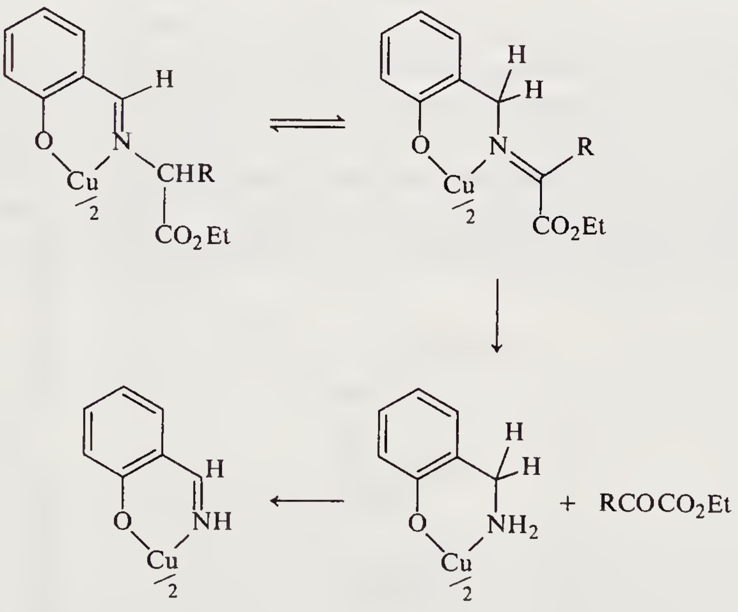

Scheme 25

In some cases where steric strain occurs, coordinated imines are susceptible to unusually ready hydrolysis. The most widely studied examples are those involving the bis-imine derived from thiophene-2-aldehyde and 1,2-diaminoethane. Hydrolysis of this imine is accelerated by metal ions and the isolated imine complexes also undergo rapid hydrolysis (Scheme 24).[100] The corresponding bis-imine from pyridine 2-aldehyde forms a copper(II) complex which undergoes addition of one equivalent of solvent ethanol to yield a thermally stable adduct (equation 26).[101] In an analogous situation, attempts to prepare copper(II) complexes of di(2-pyridyl) ketone in aqueous solution yield salts in which the ligand is hydrated, presumably in order to provide relief of chelate ring strain. Copper(II) complexes of imines derived from α-amino esters and salicylaldehyde have been observed to undergo isomerization, hydrolysis and oxidation as shown in Scheme 25.[102] In a rather curious reaction the magnesium(II) complex of a similar ligand affords 3-aminocoumarin on heating in dry methanol: the proposed reaction mechanism involves intramolecular addition of a carbanion on an unsaturated carbonyl ligand (Scheme 26).[103]

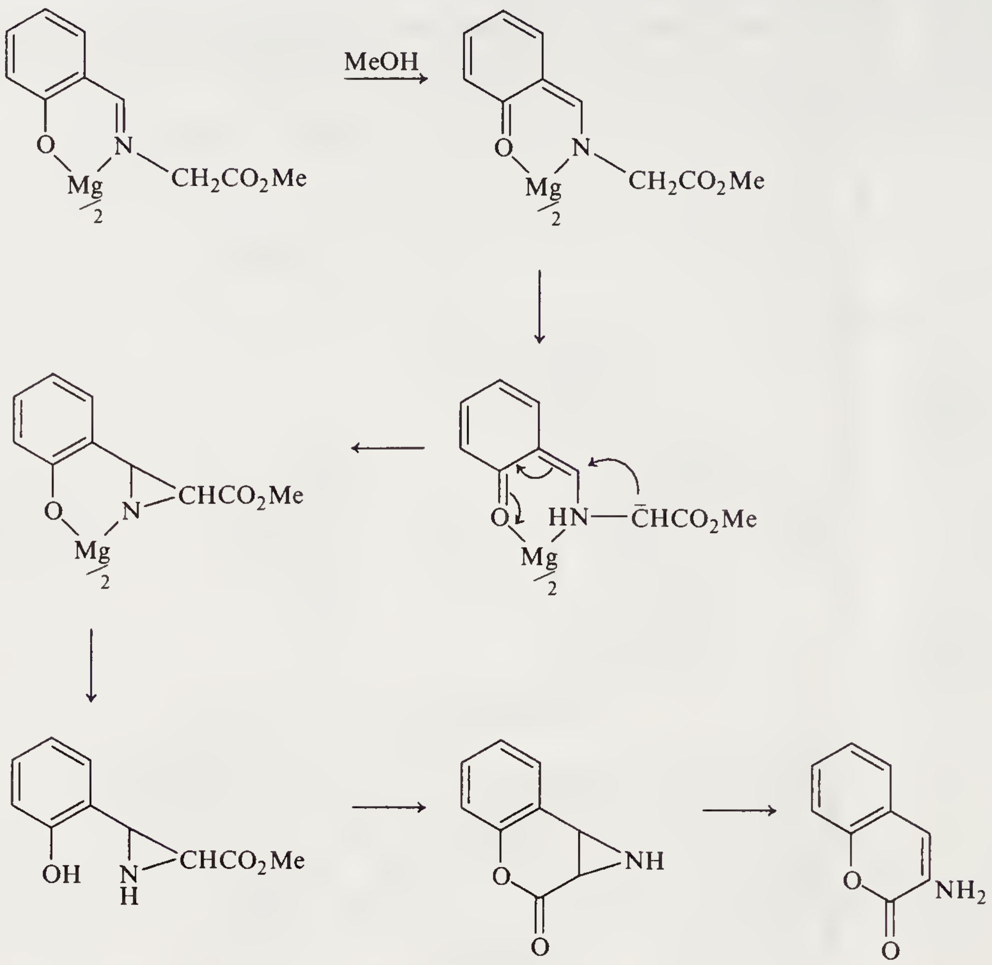

Scheme 26

The above reactions in this section have been examples of addition alone or addition followed by elimination. Ligand reactions involving nucleophilic substitution are also known and these are of the dealkylation type. Lewis acids such as aluminum chloride or tin(IV) chloride have been used for many years in the selective demethylation of aromatic methyl ethers, where chelation is involved (Scheme 27). Similar cleavage of thioethers, specially using mercury(II) salts, is commonly used to remove thioacetal functions masking ketones (equation 27).[104] In some cases, reactions of metal ions with thioether ligands result in isolation of complexes of the dealkylated organic moiety (equations 28 and 29).[105–107]

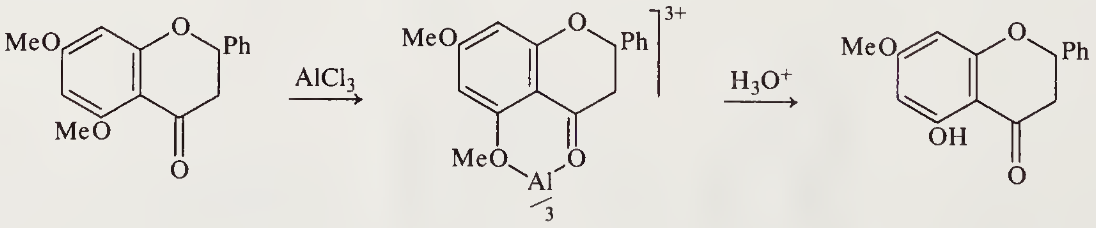

Scheme 27

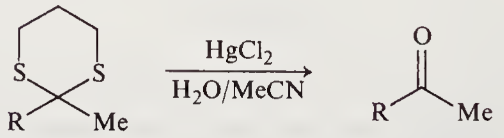

(27)

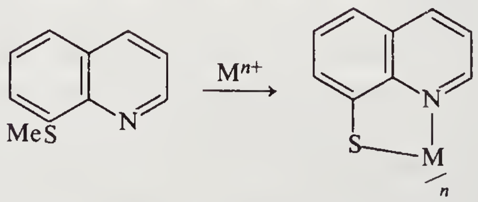

(28)

In an unusual sequence of reaction steps, nucleophilic attack of cyanide ion on a ligand results in cleavage of a sulfur–nitrogen bond.[108] The resulting product then undergoes nucleophilic attack on the intermediate isothiocyanate in a reaction typical of the previous section. The sequence is summarized in Scheme 28.

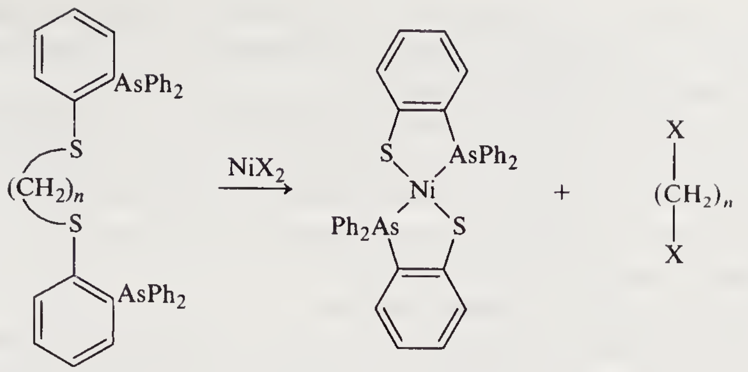

(29)

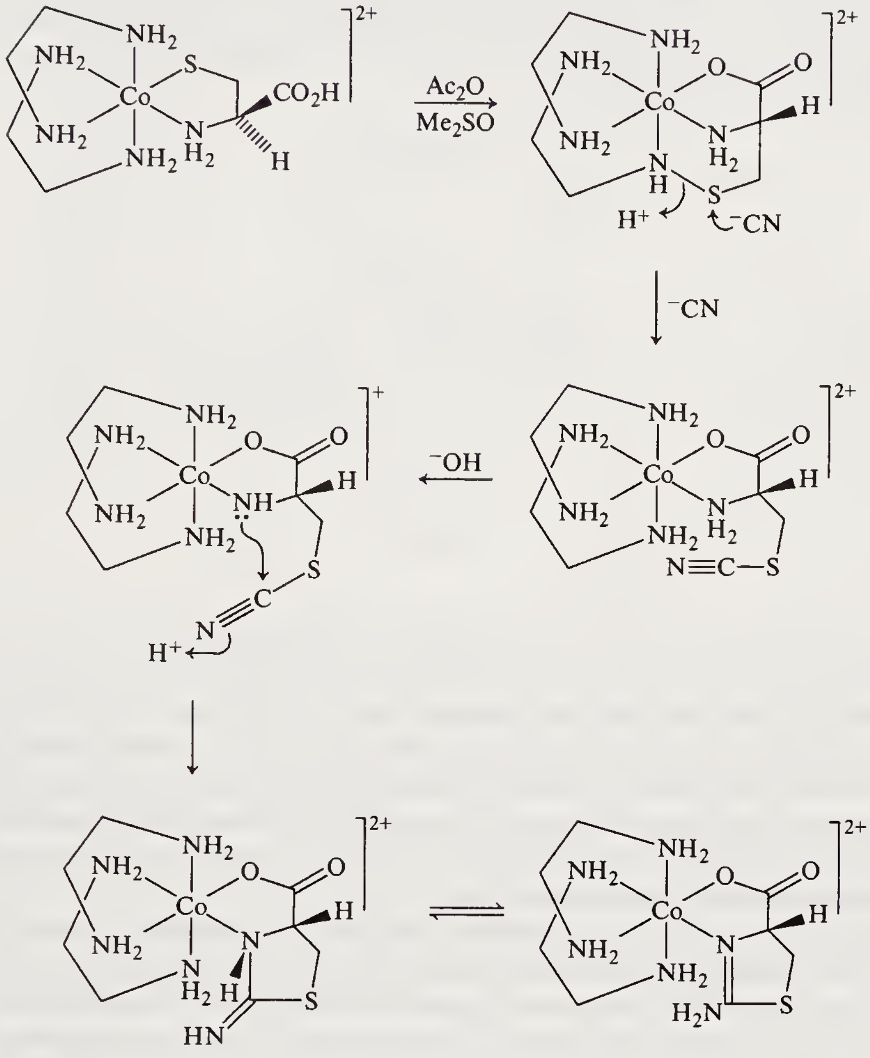

Scheme 28

7.4.3 CHELATE RING-FORMING REACTIONS

In the reactions discussed so far, the metal ion has played an electronic role in modifying ligand reactivity. However, no geometrical influence was evident. This section considers reactions in which the geometry of metal coordination plays a vital part and as a result new chelate rings are formed. Thus, the reaction types will be similar mechanistically to those already discussed but geometrical effects will present an added dimension. These reactions illustrate more dramatically the synthetic capacity of metal ions in directing the organic chemical reactivity around them. Consequently, this section will concentrate on mechanistic reaction types and synthetic aspects will be developed in more detail in Chapter 61.1.

Ligand reactions involving the formation of new chelate rings have become known as template reactions. The term 'template effect' was introduced by Busch in the early 1960s to describe reactions in which the 'metal ion serves as a slightly flexible template within which the coordination positions are in juxtaposition to the functional groups of the protracted ligand molecule'.[109] The same term was used slightly later, also by Busch, to describe processes in which the 'metal ion serves as a template to hold reaction groups in proper position for sterically highly selective multistep reactions'.[110] A still later and slightly broader definition of metal template reactions is 'ligand reactions which are dependent on, or can be significantly enhanced by, a particular geometrical orientation imposed by metal coordination'.[3,111] It is perhaps worth clarifying here that one of the definitions of 'template' in the *Oxford English Dictionary* is 'an instrument used as a guide in bringing any piece of work to the desired shape.'

Template reactions are now widely claimed but seldom proved. Detailed mechanistic work has not been carried out on many of the more complicated processes, largely because of the level of complexity and the number of steps involved. However, the concept has proved to be useful, especially as a stimulus for the synthesis of very complex, polyfunctional molecules. This aspect of synthetic utility will be covered in Chapter 61.1.

The 'template effect' has been recognized to show two or three aspects. The thermodynamic template effect involves the removal of a product from an equilibrium by stabilization of its metal complex (Scheme 29). This phenomenon has also been termed the equilibrium template effect,[112] but some authors[5] draw a distinction between these two types of effects. They reserve the equilibrium template effect for reactions which result in the formation of different products in the metal-assisted and metal-free reactions.

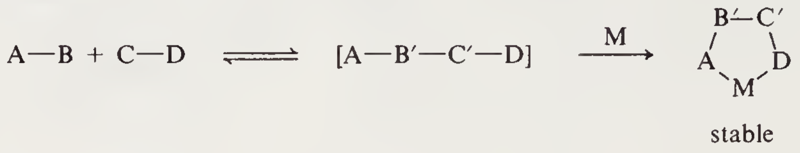

Scheme 29

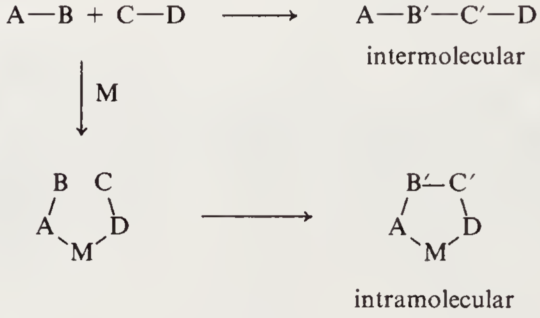

Scheme 30

The kinetic template effect is observed in reactions in which the metal ion acts by coordinating the reactants. This effect has also been described as a coordination template effect. A more direct description of a kinetic template reaction is one which involves *C*ombination of two *L*igands *A*ttached to the same *M*etal ion. Such a description leads to the useful acronym 'CLAM reaction', which graphically portrays the key reaction step. The process can be generalized and compared with the non-template reaction in Scheme 30.

An essential feature of template reactions of both the thermodynamic and kinetic type is the formation of a new chelate ring. One of the main difficulties in a discussion of mechanistic aspects of template reactions is the inevitable mixture and overlap of mechanistic effects. Those reactions which clearly exhibit a kinetic template effect could also depend to some extent on a thermodynamic one. Also, in some multistep macrocyclization processes, for example, both effects could be involved. Despite the inherent difficulties, the following discussion in this section will be subdivided into two, to cope predominantly with the thermodynamic and kinetic template effects. A further subdivision of thermodynamic and equilibrium effects will not be made.

7.4.3.1 Reactions Predominantly Involving Thermodynamic Template Effects

The most important reaction of this type is the formation of imine bonds and Schiff bases. For example, salicylaldehyde and a variety of primary amines undergo reaction to yield the related imines, which can be used as ligands in the formation of metal complexes. However, it is often more desirable to prepare such metal complexes directly by reaction of the amine and the aldehyde in the presence of the metal ion, rather than preform the imine.[113] As shown in Scheme 31, imine formation is a reversible process and isolation of the metal complex results from its stability, which in turn controls the equilibrium. It is possible, and quite likely, that prior coordination of the salicylaldehyde to the metal ion results in activation of the carbonyl carbon to amine nucleophilic attack. But it would be impossible for a precoordinated amine to act as a nucleophile and consequently no kinetic template effect could be involved. Numerous macrocyclic chelate systems have been prepared by means of imine bond formation (see Section 61.1.2.1). In mechanistic terms, the whole multistep process could occur without any geometrical influence on the part of the metal ion, which could merely act to stabilize the macrocycle in complex formation. On the other hand,

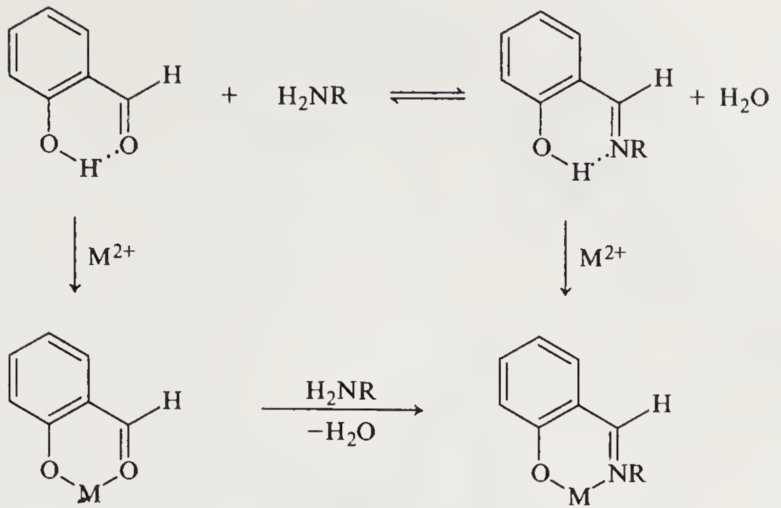

Scheme 31

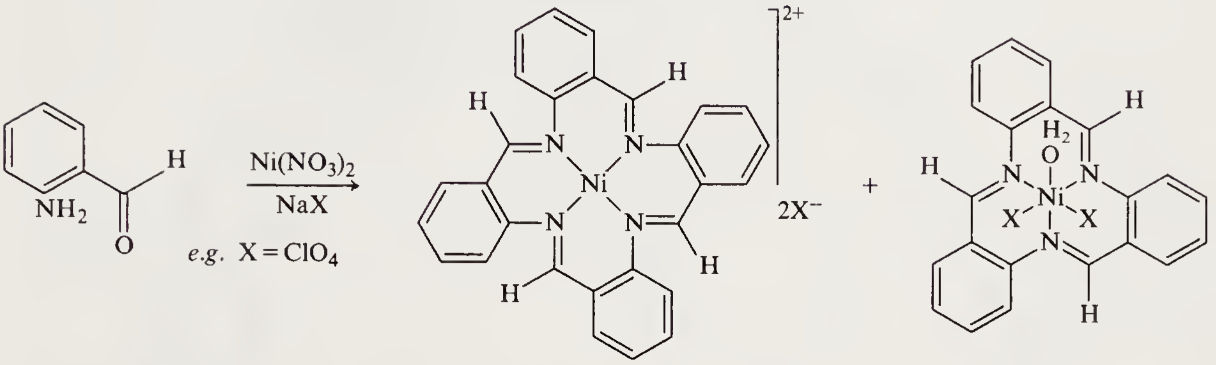

(30)

it is possible that the final cyclization could indeed involve a kinetic template effect, but there is no evidence for or against such a suggestion. One of the most dramatic and best studied template reactions is the formation of complexes of the 2-aminobenzaldehyde tetramer (TAAB) and the related trimer (equation 30).[114,115] A consideration of possible reaction steps in the multistep pathway is relevant here and is detailed in Scheme 32. One pathway depicts stepwise imine formation, in which thermodynamic template effects would operate in all steps, but only the final step could be influenced by a kinetic template effect. An alternative pathway could involve the combination of two dimers in a kinetically controlled macrocyclization. A further possibility is that the metal ion stabilizes the macrocyclic structure, which is in tautomeric equilibrium with the polycyclic salt (**51**), which in turn is produced from 2-aminobenzaldehyde by the action of strong acids (Scheme 33). Reaction of the salt (**51**) with numerous metal ions affords the TAAB complexes but not the related complexes of the macrocyclic trimer.[116] Furthermore, the anhydro trimer (**52**) can be converted to TAAB complexes. In the case of platinum(II), the intermediate complex (**53**) can be isolated.[117] The formyl group of this complex has also been shown to undergo dissociation from the platinum ion at the expense of dimethyl sulfoxide or acetonitrile.[118] Such dissociation would be essential for a dimerization pathway to the TAAB complex, as shown in Scheme 32, but there is no evidence for such a pathway. Various attempts to achieve similar metal-ion-promoted dimerizations have been unsuccessful.[119,120] Despite these observations, the amino carbonyl compounds (**55**) have been implicated as intermediates in the conversion of benzodiazepines (**54**) into the macrocyclic nickel(II) complexes (**56**),[121,122] which can be prepared more readily from 1,2-diaminobenzene and the β-dicarbonyl compounds (Scheme 34).[123,124] A dihydrodiazepine can also serve as a source of a related macrocycle presumably *via* the amino aldehyde (**57**) (Scheme 35).[125] It therefore seems possible that the role of the nickel ions in the formation of complexes (**56**) could be merely the stabilization of a preformed macrocyclic structure.

The hexahydropyrimidine (**58**), formed from 1-phenylpropane-1,2-dione and propane-1,3-diamine, is an excellent precursor for the α-diimine macrocyclic complexes (**60**), presumably *via* the amino ketone (**59**) (Scheme 36).[126] In this case, intramolecular cyclization of (**59**) to (**58**) is reversible, so that the metal ion can exert a thermodynamic template effect in formation of the complex (**60**). This represents a further example of a long-known phenomenon in which a metal ion can stabilize an α-diimine structure by virtue of the formation of stable five-membered chelate rings. Many 2-hydroxy- or 2-mercapto-amines undergo reaction with α-dicarbonyl compounds to yield heterocyclic compounds rather than α-diimines. However, in the presence of suitable metal

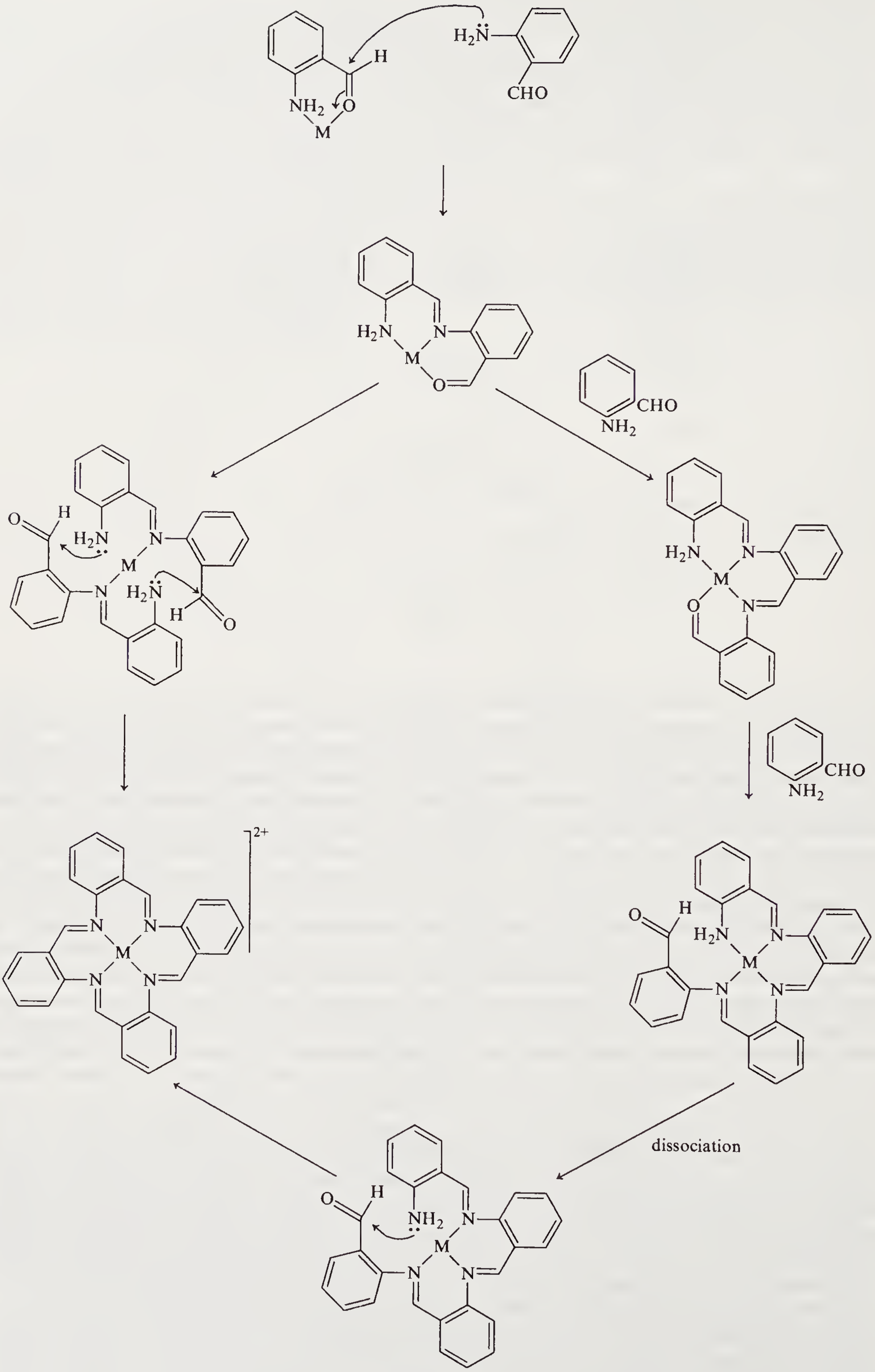

Scheme 32

ions the tautomeric α-diimine structure is stabilized by chelation (Scheme 37).[111,113] (see Section 61.1.2.2 for further examples.)

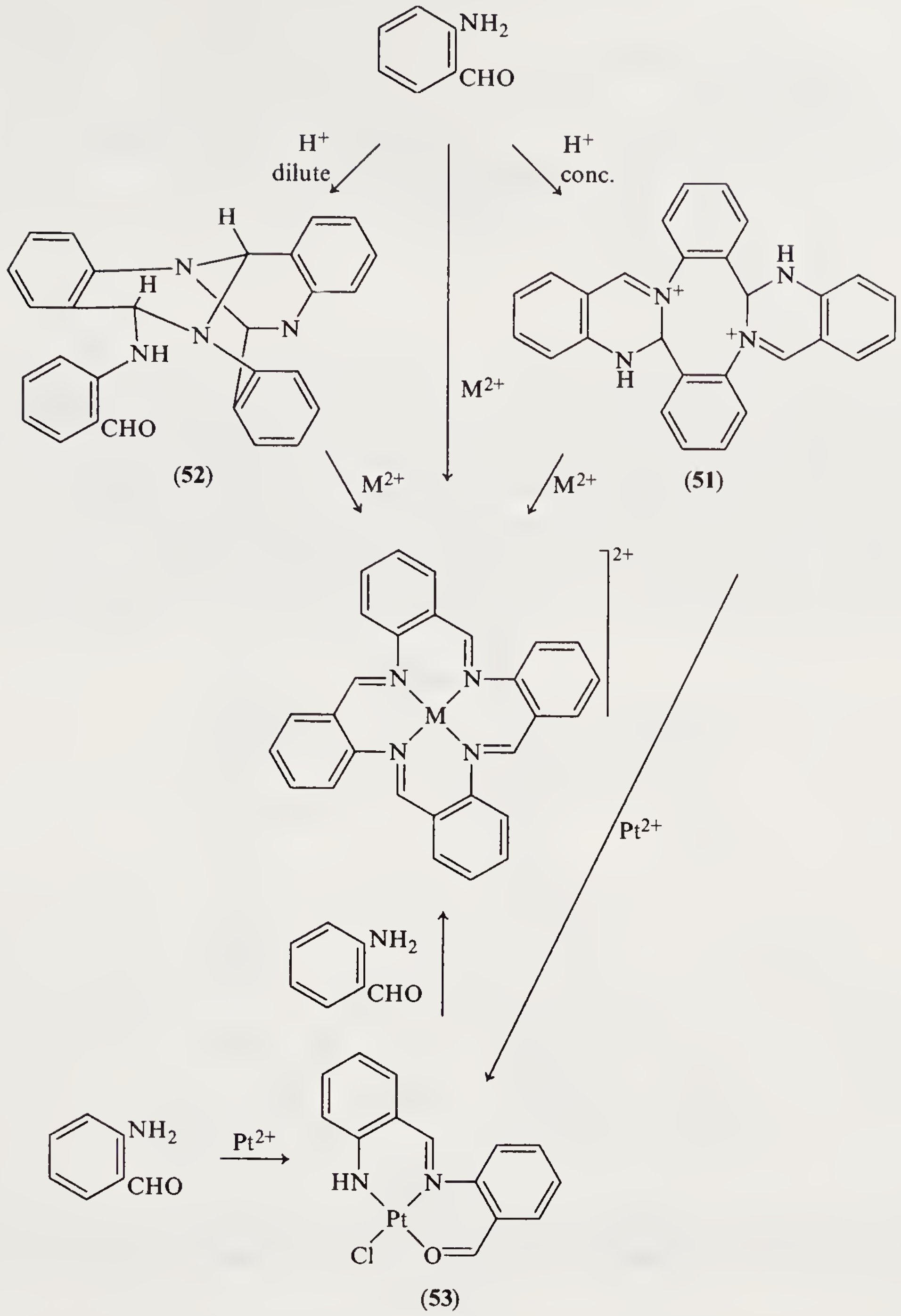

Scheme 33

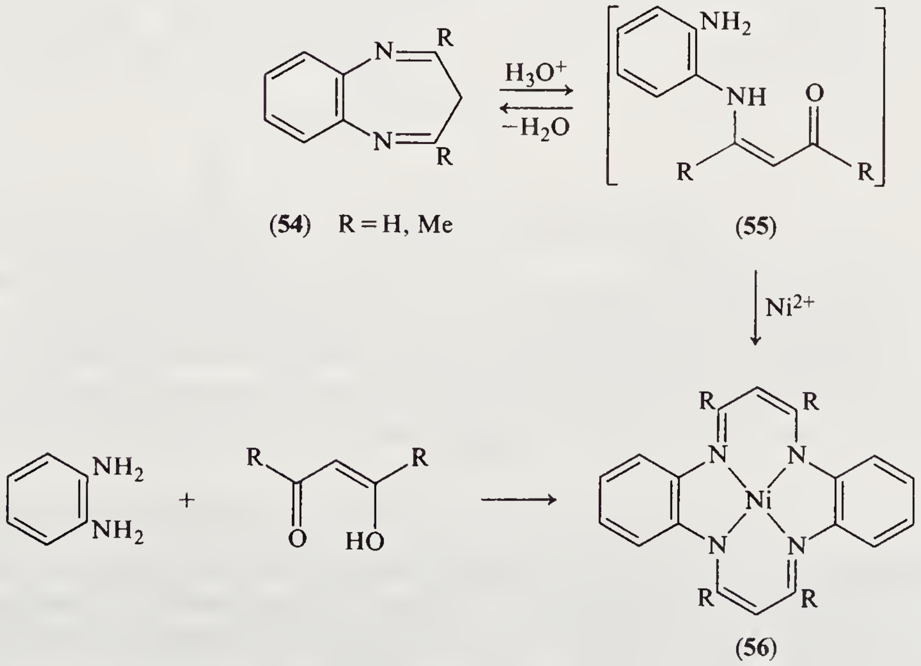

Scheme 34

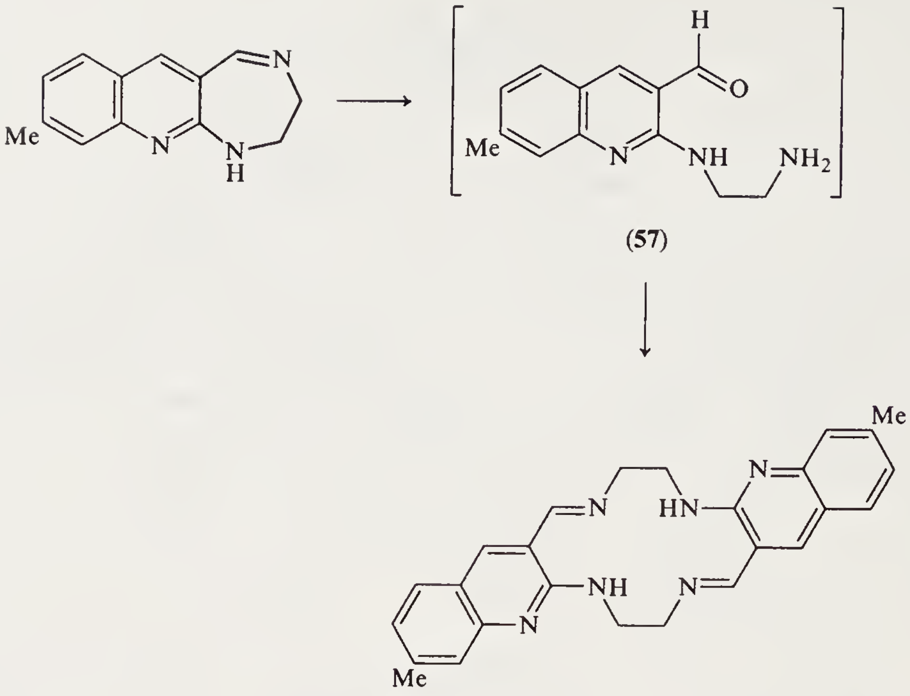

(57)

Scheme 35

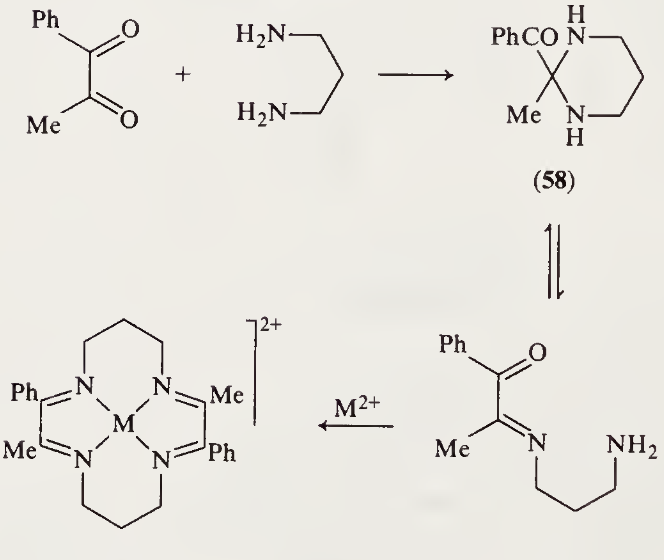

(58)

(59)

(60)

Scheme 36

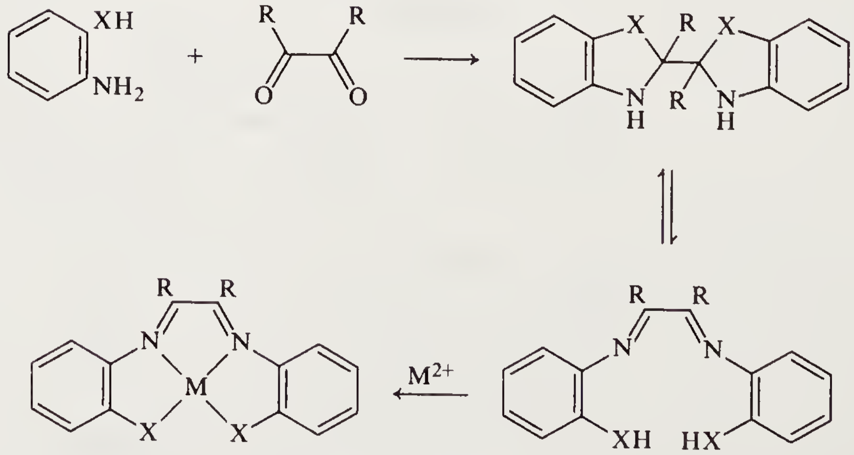

Scheme 37

New chelate rings can be formed by the nucleophilic addition of alcohols to imine complexes. For example, the nickel(II) TAAB complex is susceptible to attack by bis-alkoxides (equation 31).[127] It is not clear whether or not a kinetic template effect operates by prior coordination of the central oxygen or sulfur atom. However, such an effect is not necessary, as simple alkoxides undergo a similar addition reaction.[128]

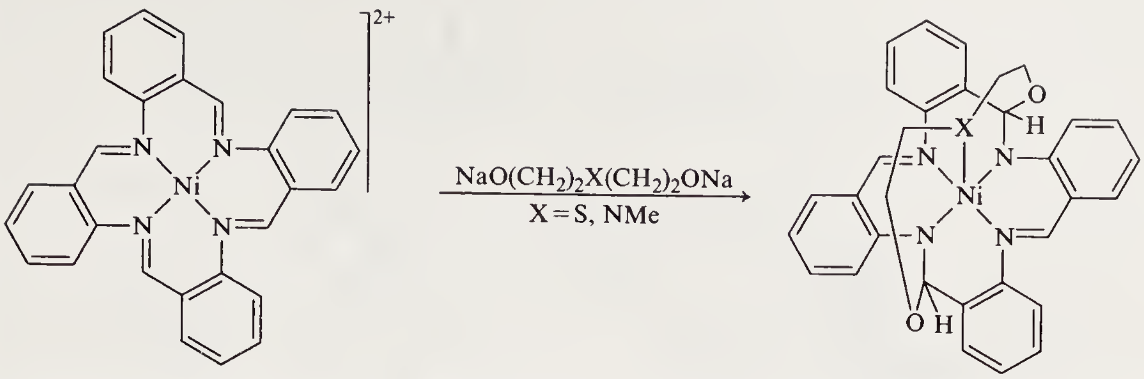

(31)

The addition of alcohols to suitable nitriles can give rise to the formation of new chelate rings containing imidate groups (equation 32).[129,130] In this situation it is unlikely that prior coordination of the nitrile occurs and the metal ion probably acts as a 'super acid' to stabilize the new chelate ring. Addition of an amino alcohol to 2-cyanopyridine is catalyzed by nickel(II) and copper(II) ions, probably on the basis of coordination of the transition state imidate complex (**61**), on the way to the isoxazoline product (Scheme 38).[131] Here again, a kinetic template effect is possible, but not required. Examples of nucleophilic addition to coordinated nitriles resulting in new chelate ring formation will be discussed in Section 7.4.3.2.

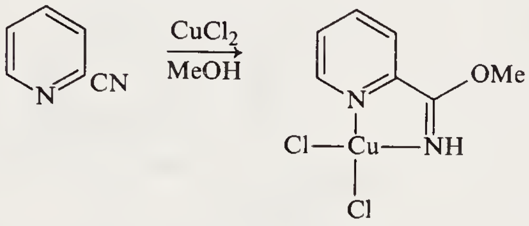

(32)

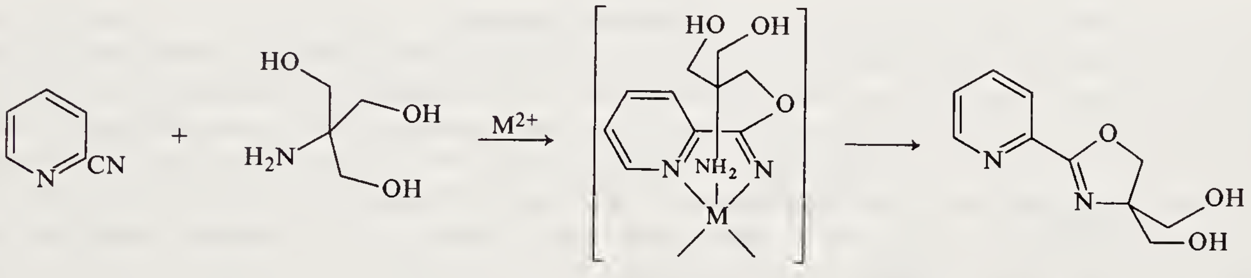

(61)

Scheme 38

The stabilization of an amino acetal by nickel ions has been reported very recently and although no mechanistic information is available, a thermodynamic template effect is likely (equation 33).[132]

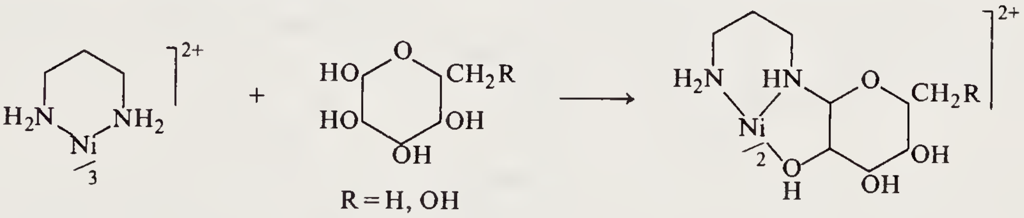

(33)

7.4.3.2 Reactions Predominantly Involving Kinetic Template Effects

Many reactions in this section probably owe a thermodynamic template effect for part of their success, but it is the kinetic effect which is most clearly illustrated. Reactions have been chosen to display a range of geometrical features and also various types of bond formation. The coverage will be selective and many topics will be developed more fully in Chapter 61.1 The present section will be subdivided according to the involvement or otherwise of donor atoms.

7.4.3.2.1 Reaction between one donor atom and one non-donor atom

This reaction process is depicted in general terms in equation (34), and includes the category generalized in equation (35). The earliest example of this type of reaction appears to be the ready transesterification of uncomplexed ester groups shown in Scheme 39,[133,134] in which intramolecular participation forms a new chelate ring in the transition state. Since this discovery, numerous studies have been made on the intramolecular catalysis of ester hydrolysis by metal-complexed hydroxide

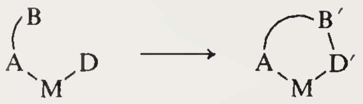

(34)

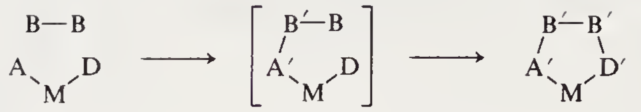

(35)

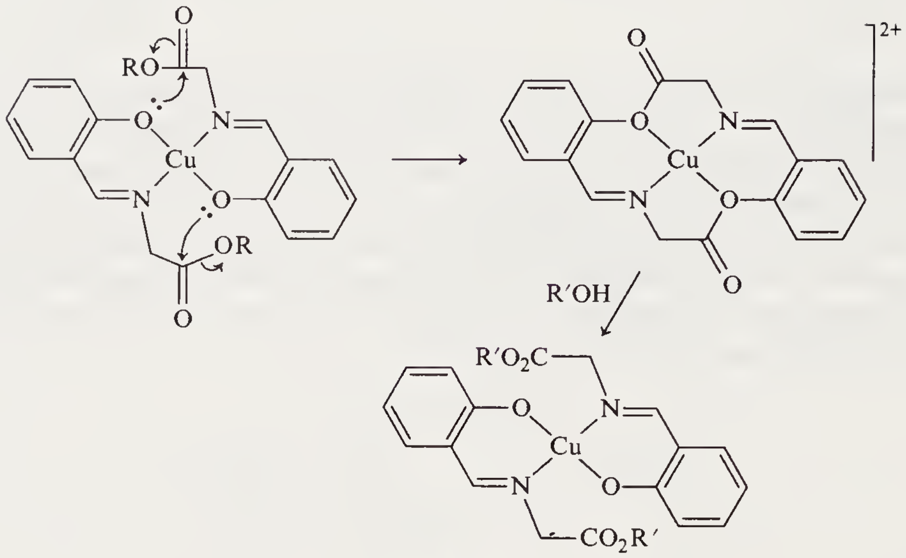

Scheme 39

ion.[135] Most studies have centred on coordination of ligands to cobalt(III), but copper(II) and zinc(II) have also been investigated. In the case of cobalt(III) a wide range of amino ester, amino amide and peptide hydrolyses can be summarized as shown in Scheme 40. Rate enhancements of the order of 10^7 to 10^{11} over intermolecular hydrolysis are observed. This technique is particularly suitable for a mild hydrolysis of N-terminal peptide bonds.[136,137] Zinc(II) ions have been shown to catalyze transesterification in 2-pyridinecarboxylic esters (Scheme 41)[138] and copper(II) ions promote ester hydrolysis in 2-pyridylcarbaldoxime esters (Scheme 42).[139] Related intramolecular mechanisms have been proposed for the conversion of 2-pyridylcarboxylic esters to amides using magnesium derivatives (Scheme 43),[140] for the hydrolysis of a pyridyl-substituted amide (equation 36)[141] and for the zinc(II)-catalyzed hydrolysis of an anhydride (equation 37).[142] Cobalt(III) hydroxide promoted hydrolysis of propionic anhydride has also been studied.[143]

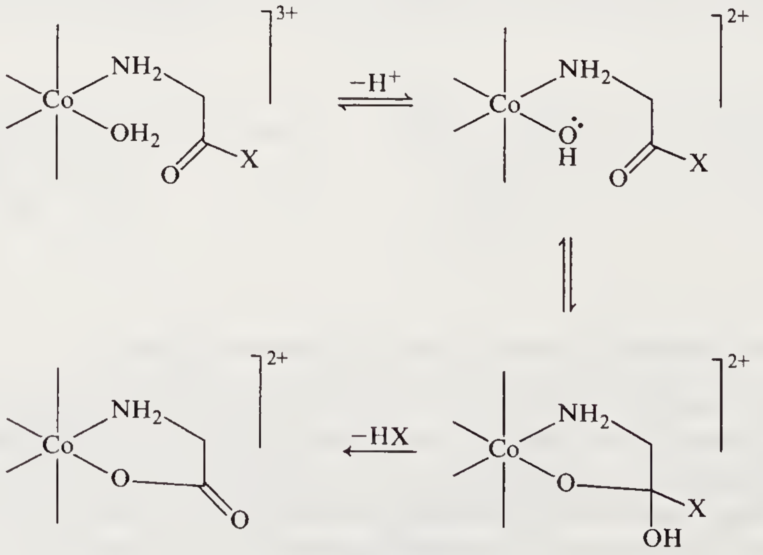

Scheme 40

Intramolecular lactonization has been studied on cobalt(III) complexes (Scheme 44).[144] The reaction is catalyzed by general acid and the attack of coordinated water occurs at a greater rate than that of coordinated hydroxide ion. Presumably, the relatively non-nucleophilic water is assisted by hydrogen bonding to the carboxyl group to become a ‘pseudo-hydroxide’ ion.

Sargeson and his coworkers have reported numerous examples of the intramolecular attack of cobalt(III)-coordinated amide anions to a variety of carbonyl groups, including those of α-keto

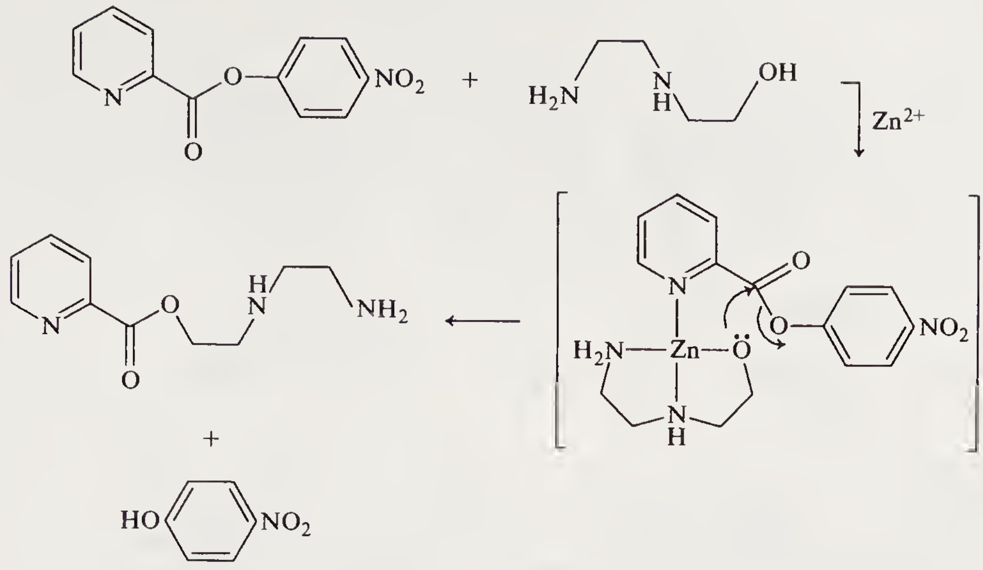

Scheme 41

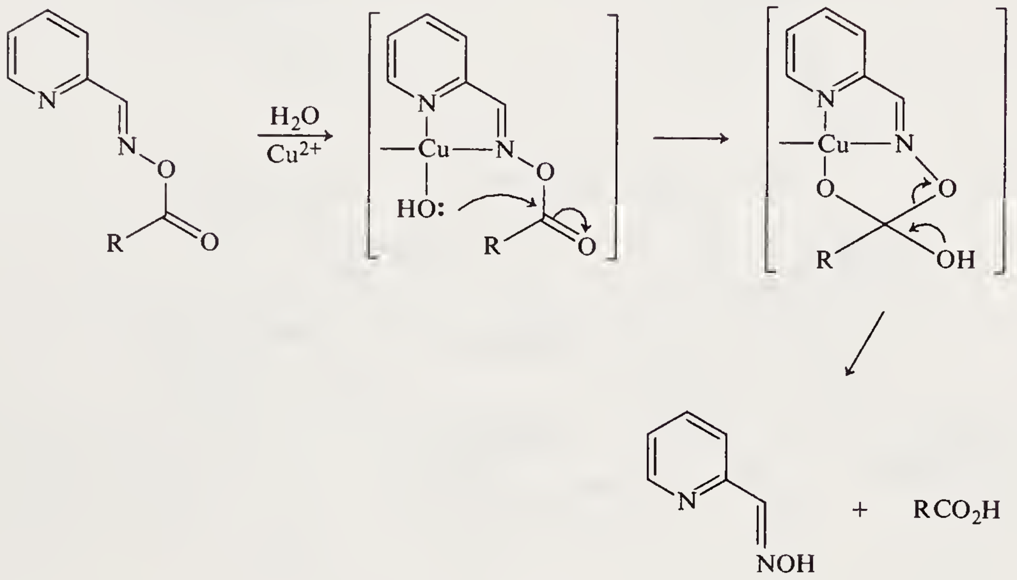

Scheme 42

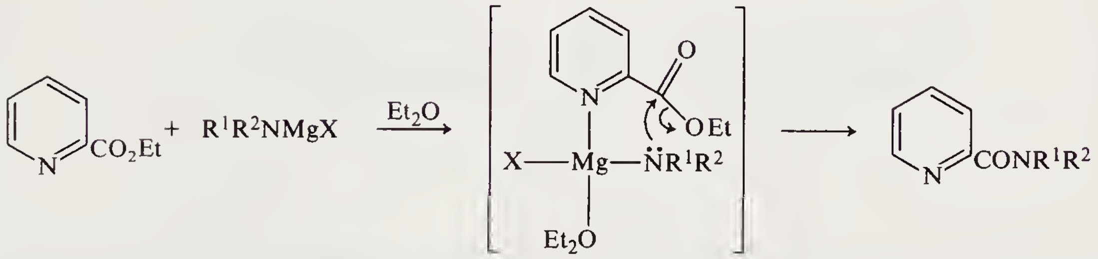

Scheme 43

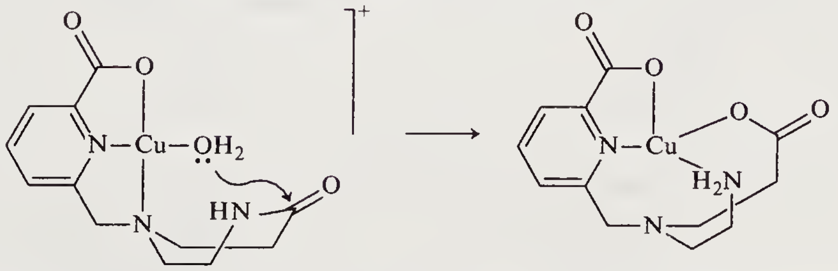

(36)

carboxylates (Scheme 45)[145,146] and α-amino carbonyl compounds (Scheme 46).[147] These reactions have been put to considerable synthetic use and will be considered in more detail in Chapter 61.1.

Cobalt-coordinated amide nucleophiles have also been observed to attack coordinated phosphate esters (equation 38),[148] disulfides (Scheme 47)[149,150] and nitriles (Scheme 48).[151,152] Chelated amides can also be formed by intramolecular attack of cobalt hydroxides.[153]

Kinetic template effects have been involved in the formation of crown ethers, with respect to the cyclization step involving a nucleophilic displacement of halide or tosylate by alkoxide ions. It has been proposed that cyclization of the linear bifunctional precursor is enhanced by a cyclic conformation in which the alkoxide cation brings the two ends of the molecule into close proximity

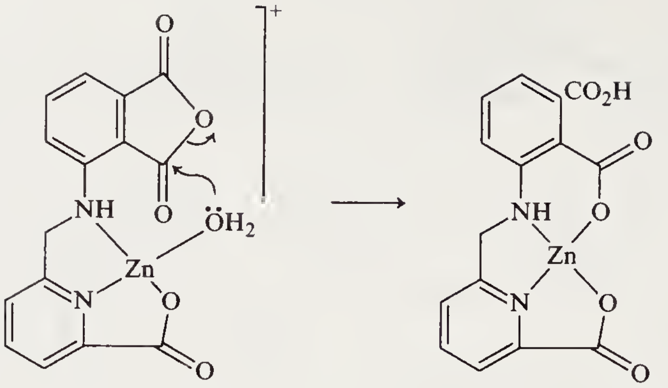

(37)

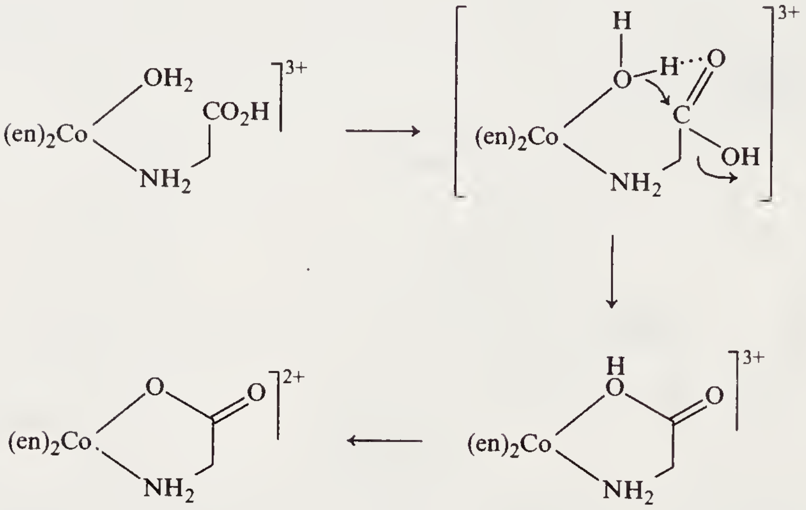

Scheme 44

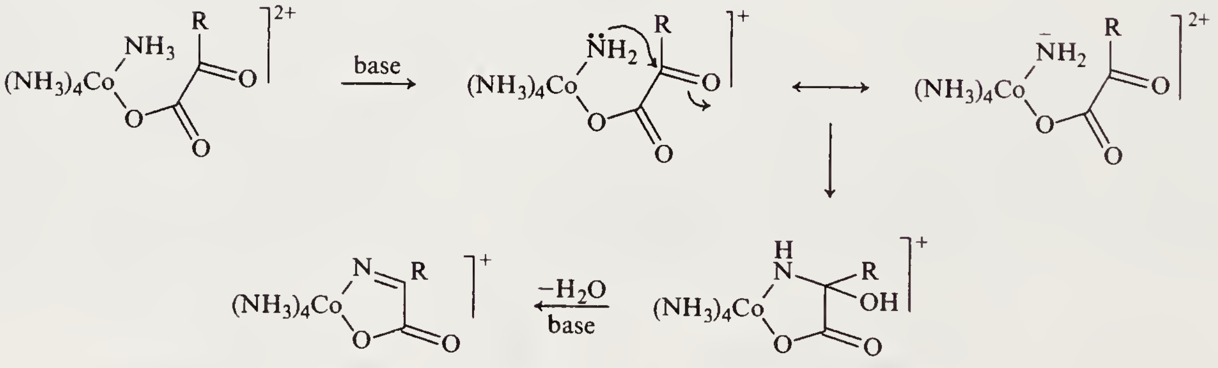

Scheme 45

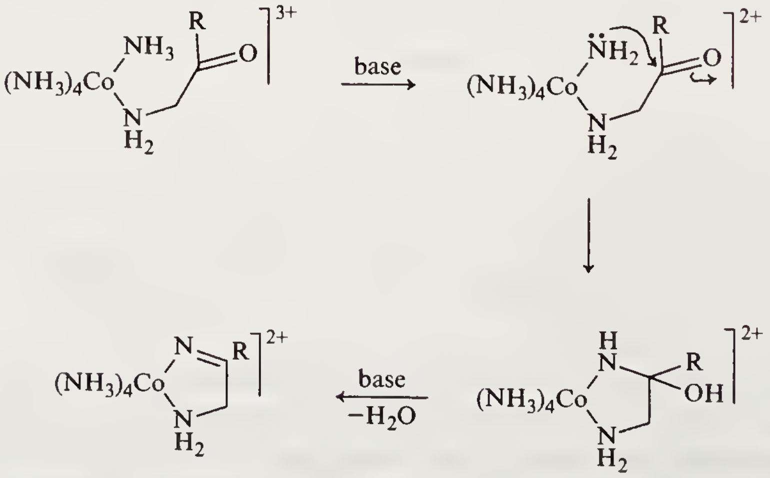

Scheme 46

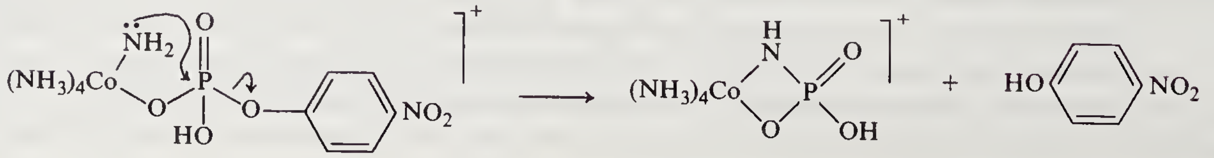

(38)

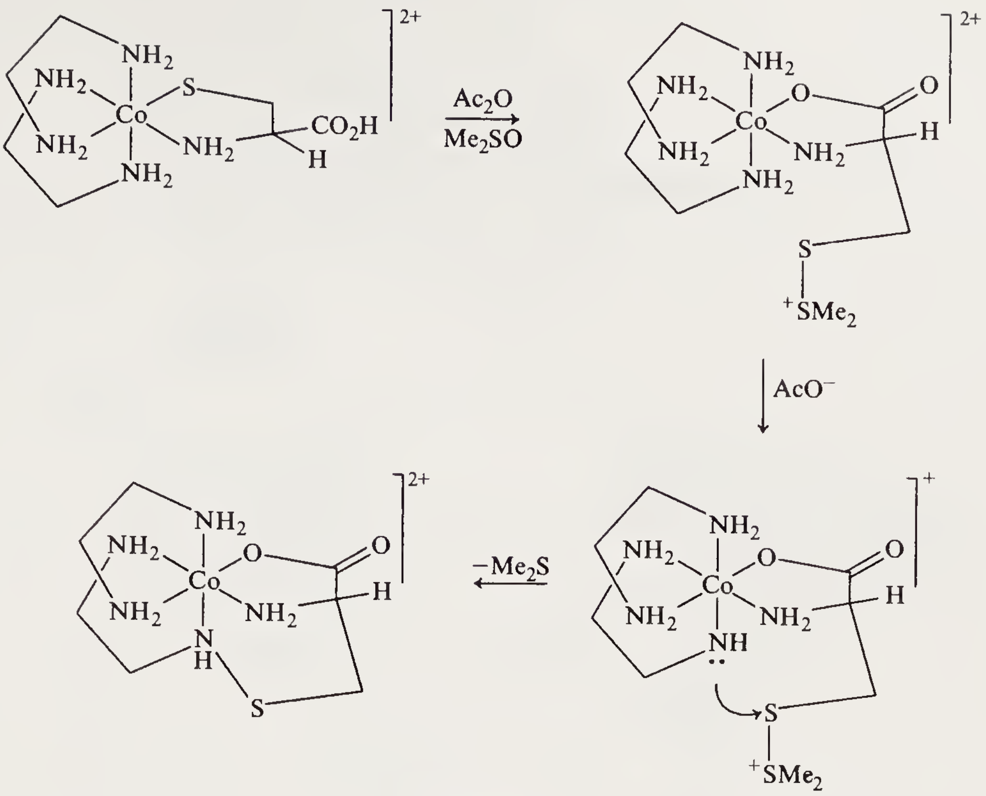

Scheme 47

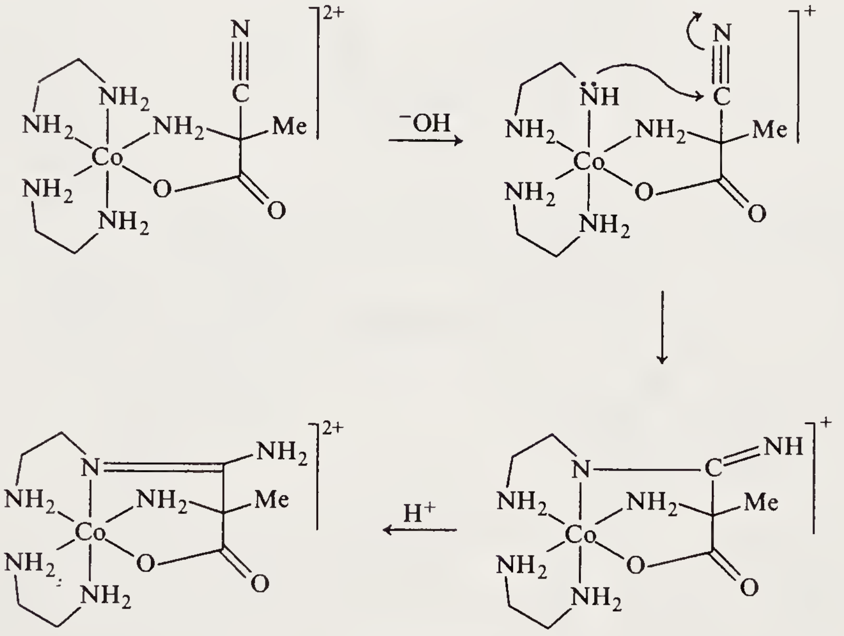

Scheme 48

(*e.g.* Scheme 49).[154–156] Although the proximity effect leads to rate enhancement there is also a rate retardation factor because of reduced nucleophilicity of the alkoxide ion resulting from its interaction with the metal ion. In the case of 18-crown-6 macrocycles, potassium ions can provide a template in contrast to sodium and other ions which are ineffective.[157,158] One possible mode of formation is shown in Scheme 50.[157] The yields of crown ethers can be increased in many cases by the judicious use of metal ions, but the mechanistic nature of the improvement is unclear. For instance, it has been observed that the addition of lithium salts improves the yield of the macrocycle (**62**) formed from furan and acetone,[159] but a recent study indicates that the improvement is a result of a pH rather than a template effect.[160]

While the precise role of metal coordination in the formation of cyclic ethers is open to some doubt, such is not the case where there is good supporting coordination from nitrogen donor atoms. This is illustrated by the macrocyclization on a salicylaldimine complex (equation 39).[161]

The situation is even more clear cut in the formation of thioethers by alkylation of thiolate complexes. Such reactions have been described in Section 7.4.2.1.2, but in those examples new chelate rings were not formed. The reaction which led Busch to propose the kinetic template effect is a thiolate complex alkylation, which does indeed produce a new chelate ring (equation 40).[110,162,163] This reaction is an example of the general type shown in equation (35) and it has been established clearly that the sulfur atoms remain coordinated to the metal ion throughout the

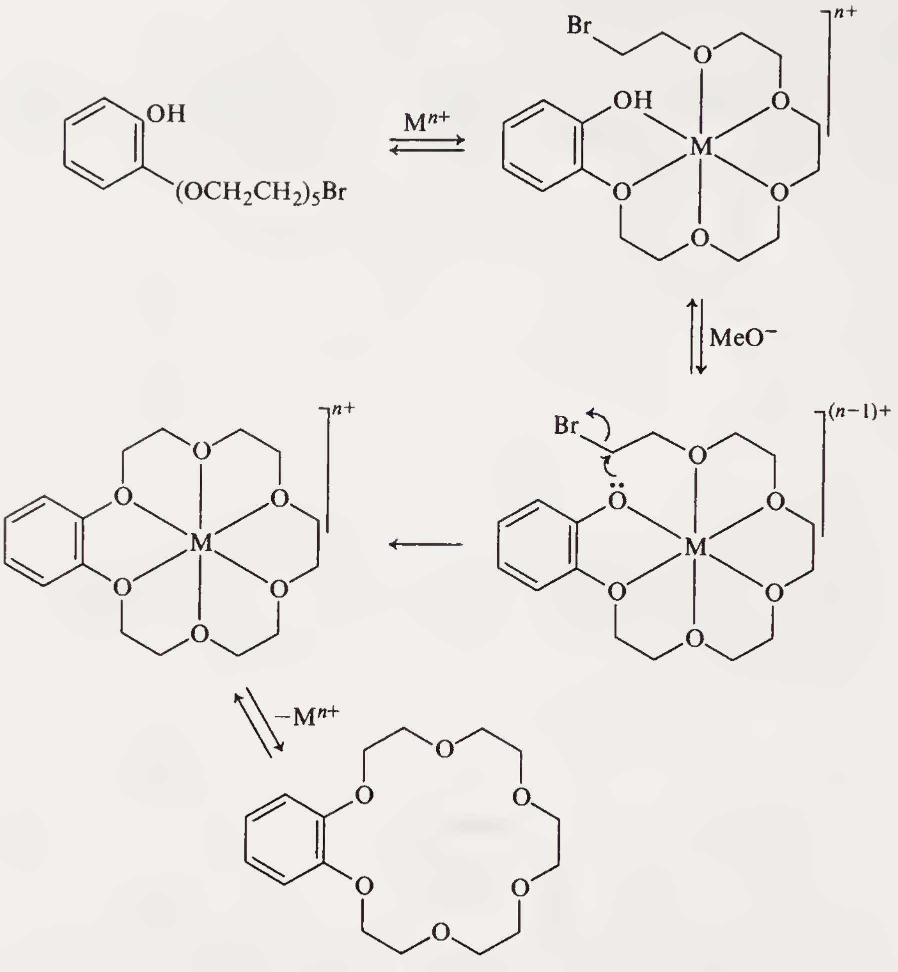

Scheme 49

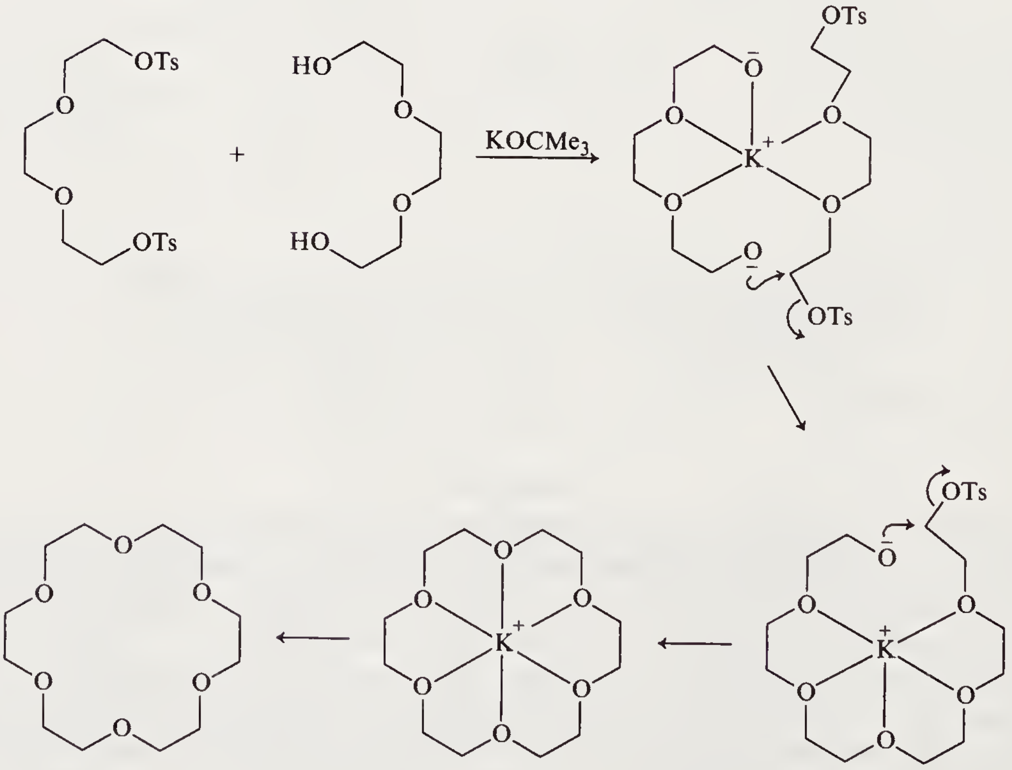

Scheme 50

process. A similar alkylation of coordinated sulfur by chloroacetate has been reported (equation 41).[164]

The chelate ring closure described in equation (42)[165,166] would be represented by a more concerted version of the general type shown by equation (35). The final product (**63**) has also been treated with α,α′-dibromo-*o*-xylene to produce the related macrocycle, *via* its complex.[165]

Alkylation of coordinated nitrogen atoms has also given rise to new chelate rings and coincidentally to macrocyclic structures (equations 43 and 44).[167,168] More recently, the alkylation technique has been extended to phosphorus (equation 45).[169] A more recent novel free radical cyclization

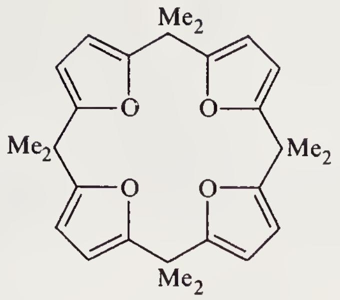

(62)

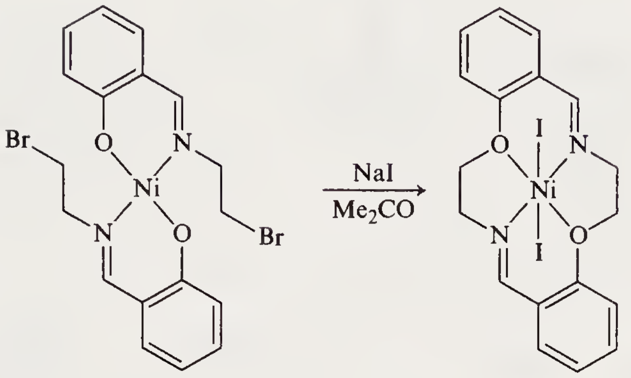

(39)

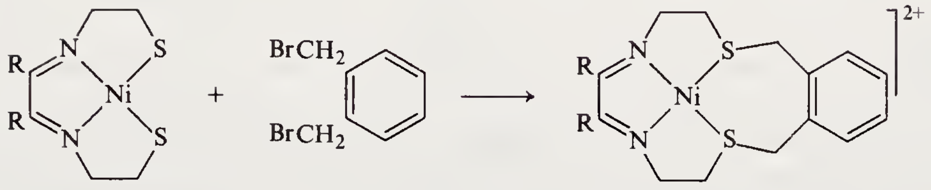

(40)

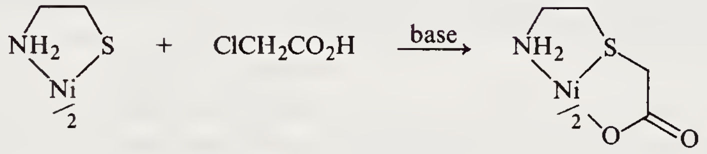

(41)

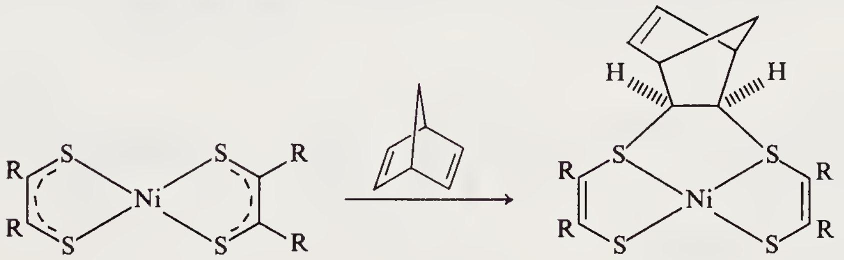

(42)

R = Ph, CF_3 **(63)**

technique involving phosphines coordinated to a molybdenum carbonyl provides a useful future strategy for macrocycle formation (Scheme 51).[170]

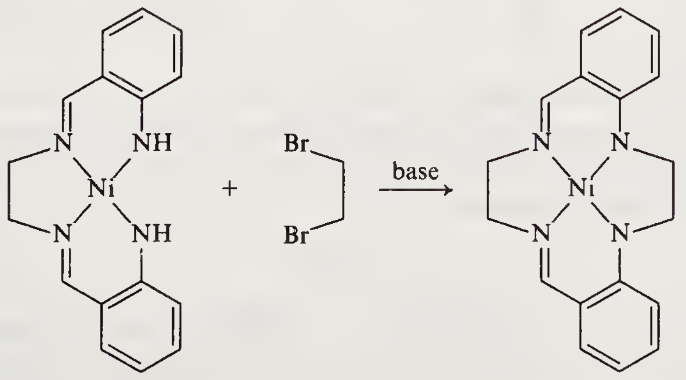

(43)

Coordinated nitrogen donor atoms can be involved in chelate-forming template reactions by virtue of nucleophilic addition to carbonyl compounds. An early and rather specific example does not allow the possibility of elimination following the addition step (equation 46).[171] More recent work on ruthenium(III) and osmium(III) results in the formation of α-diimine chelate rings

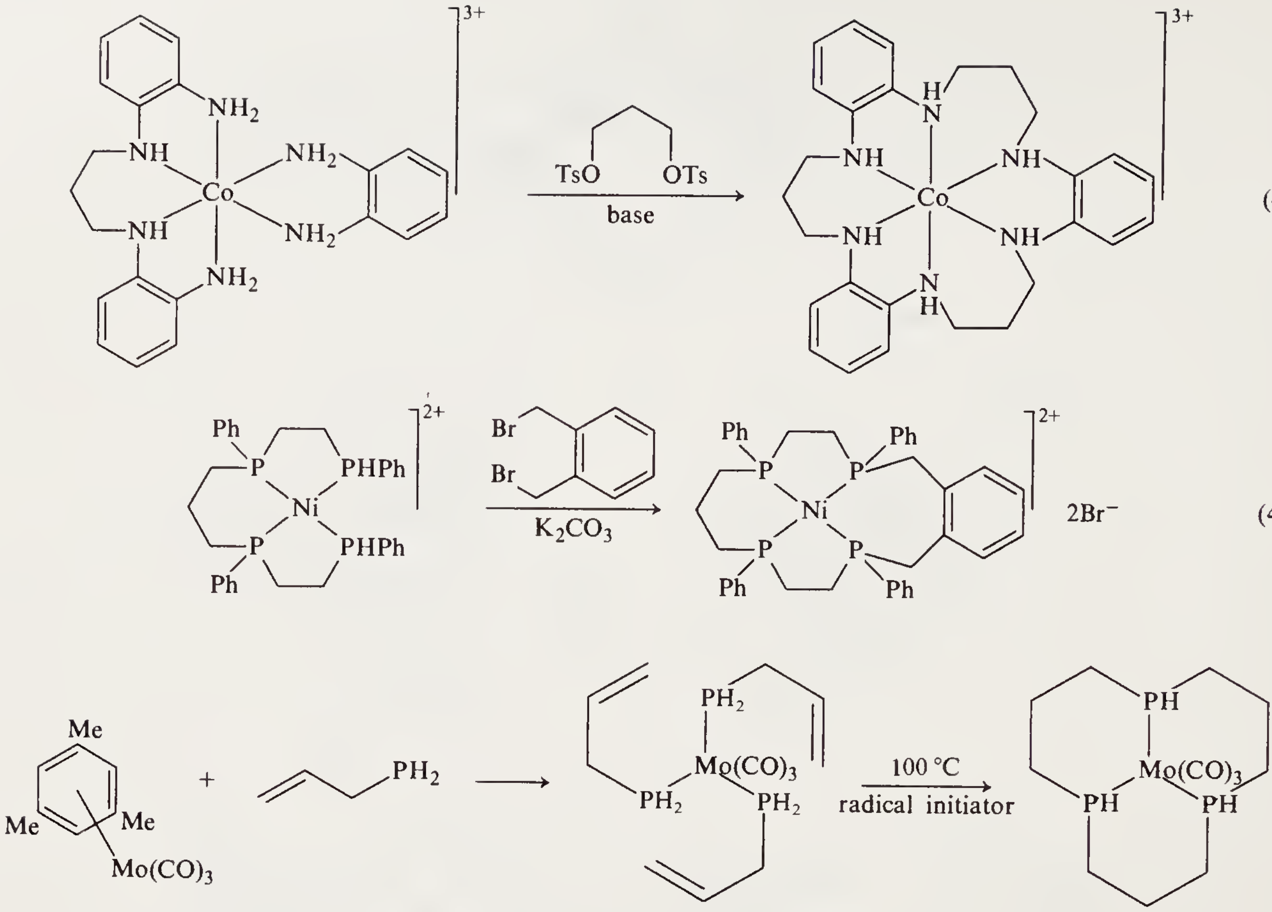

(44)

(45)

Scheme 51

(equations 47 and 48).[172] It is noteworthy that reduction occurs to ruthenium(II) and osmium(II) as a consequence of the properties of the α-diimine ligand.

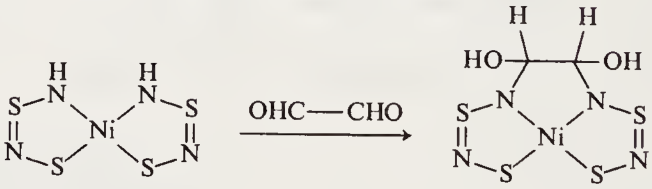

(46)

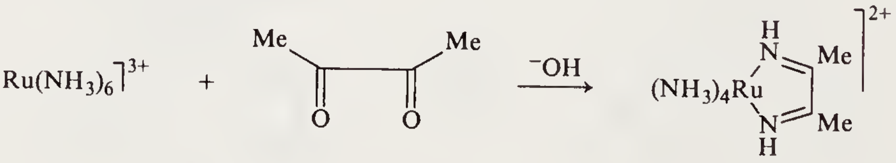

(47)

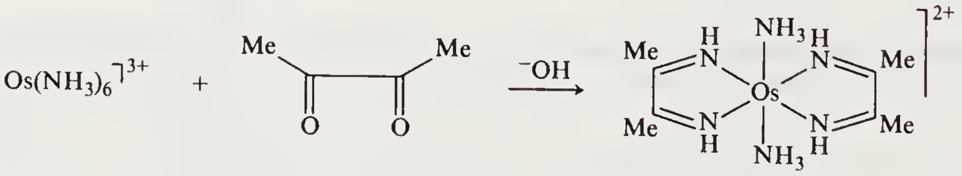

(48)

Hexaammineplatinum(IV) salts also undergo imine-forming reactions with acetylacetone (equation 49).[172] A cobalt(III) acetylacetone complex can be formed as a result of intramolecular addition of cobalt-bound hydroxide ion to acetylacetone. The cobalt-bound oxygen atoms are retained in the new chelate ring (equation 50).[173]

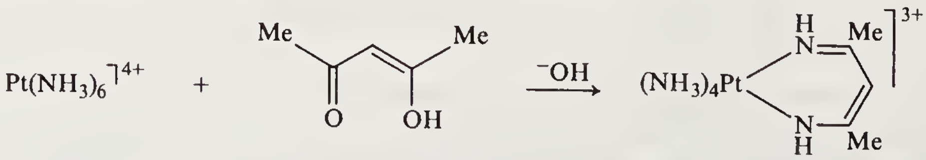

(49)

Dziomko and coworkers have utilized the nucleophilic aromatic substitution of aryl amines to chloropyrazoles or chloropyridines in the template step of their macrocycle syntheses.[174,175] The nature of the template process is unclear and it could simply be thermodynamic. However, a kinetic effect is a distinct possibility and would require attack of a coordinated aryl amine (Scheme 52).

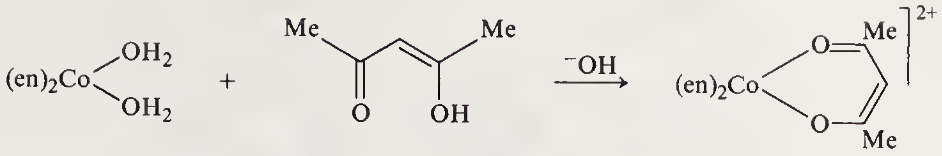

(50)

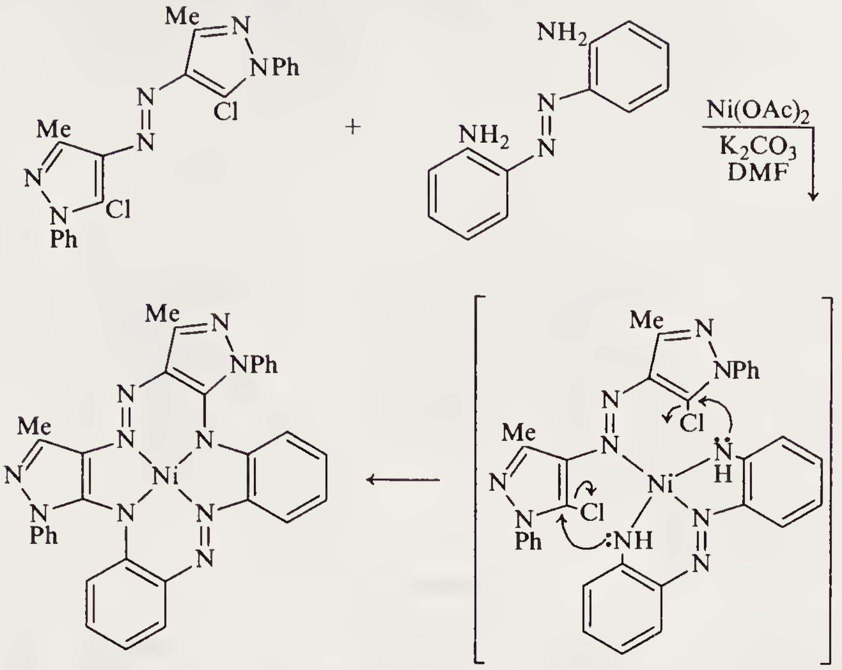

Scheme 52

An even more speculative area of template reactions is that in which a group migrates from the metal ion on to an adjacent ligand. In such a situation the transition state would contain a new chelate ring structure. This class of reactions is common in organometallic chemistry and includes the polymerization of alkenes. In heterometallic chemistry some very disparate examples have been observed. Some of these are briefly considered in this section. The conversion of aldehydes directly to esters under the influence of magnesium alkoxides probably involves migration of donor oxygen to the activated adjacent ligand (Scheme 53).[176] A very recently described reaction could also involve migration of coordinated oxygen, but in this case the chelate ring remains intact (Scheme 54).[177] A similar reaction had been described earlier in which phosphorus migrates, but this time the organic product is isolated (Scheme 55).[178]

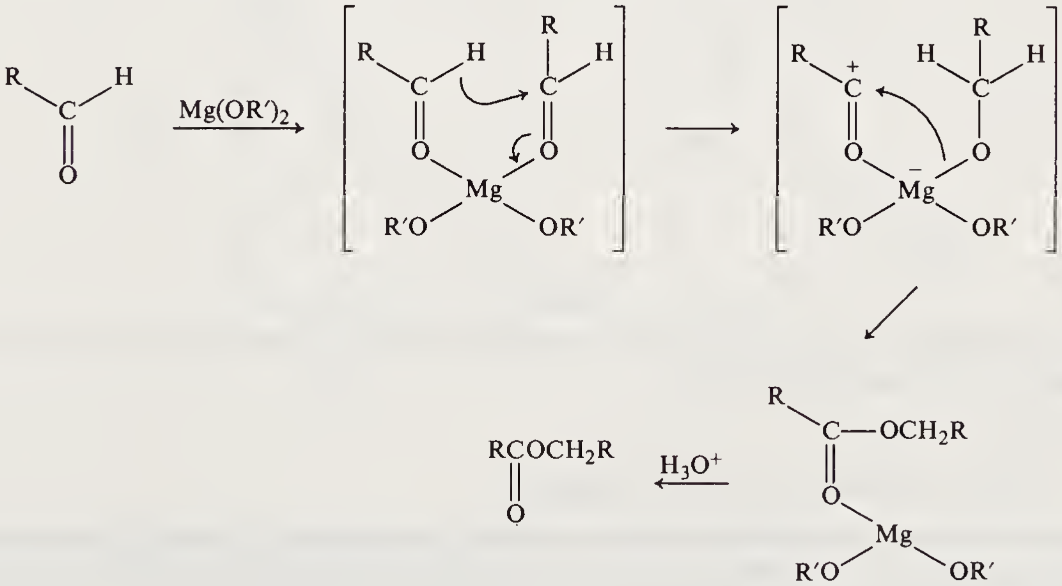

Scheme 53

Several alkylcobaloximes have been degraded by acetic anhydride in pyridine to an imidazopyridine, and a key step in a complicated sequence is the migration of pyridine from cobalt to an activated ligand (Scheme 56).[179]

Many reactions of organolithium or organomagnesium compounds depend upon the migration of the alkyl or aryl group from the metal on to the adjacent ligand. Such reactions are not clearly within the scope of this chapter as the reactions are organometallic in nature and the mechanisms

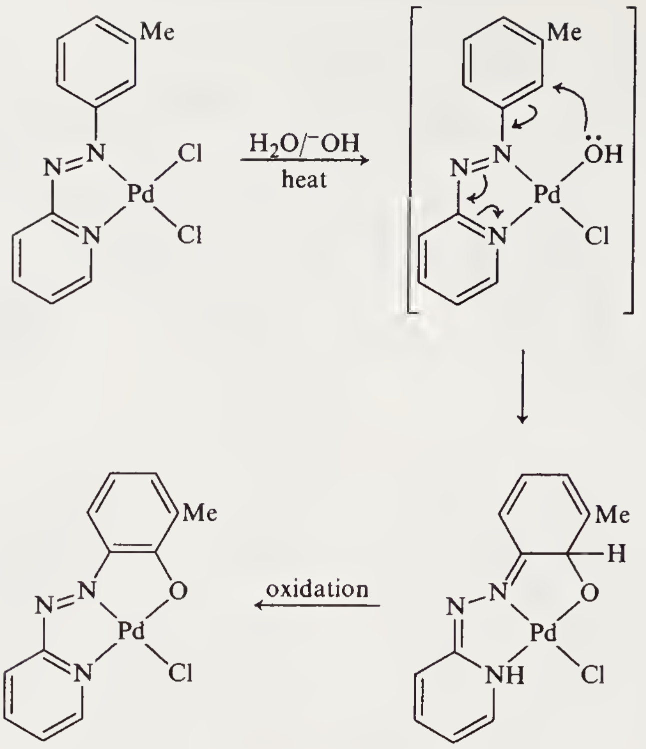

Scheme 54

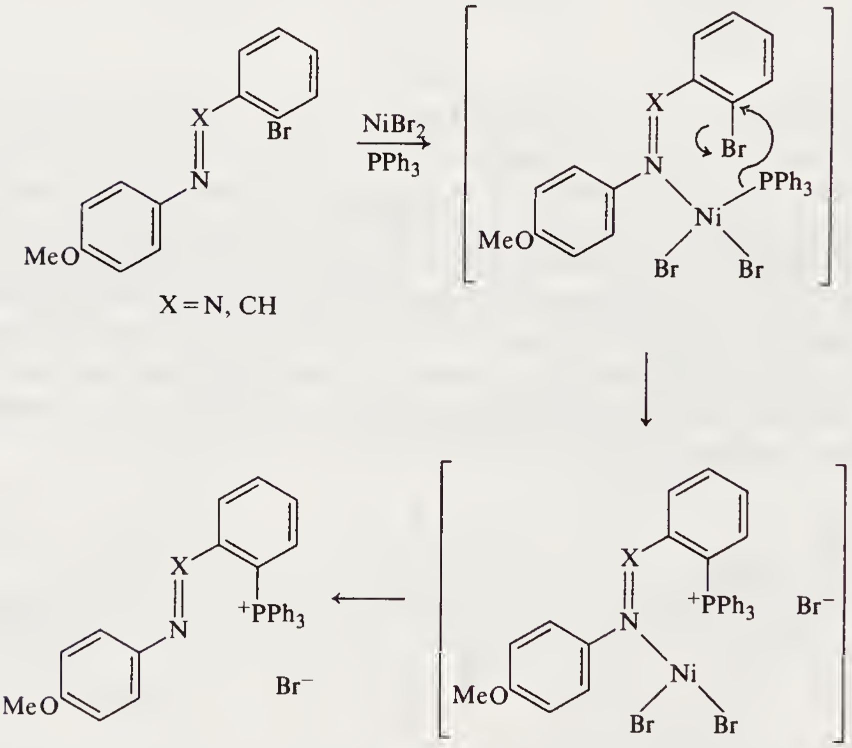

Scheme 55

are often speculative. One specific example is shown in Scheme 57[180] and a good entry into reactions of this type is *via* a recent review.[181]

7.4.3.2.2 Reaction between two non-donor atoms

This reaction process is depicted in general terms in equations (51) and (52). It includes the majority of reactions which exhibit a kinetic template effect. A selection of reactions will be given but many areas will be developed further in Chapter 61.1.

(51)

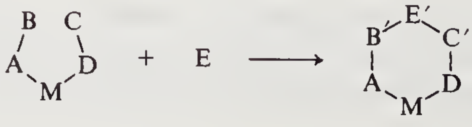

(52)

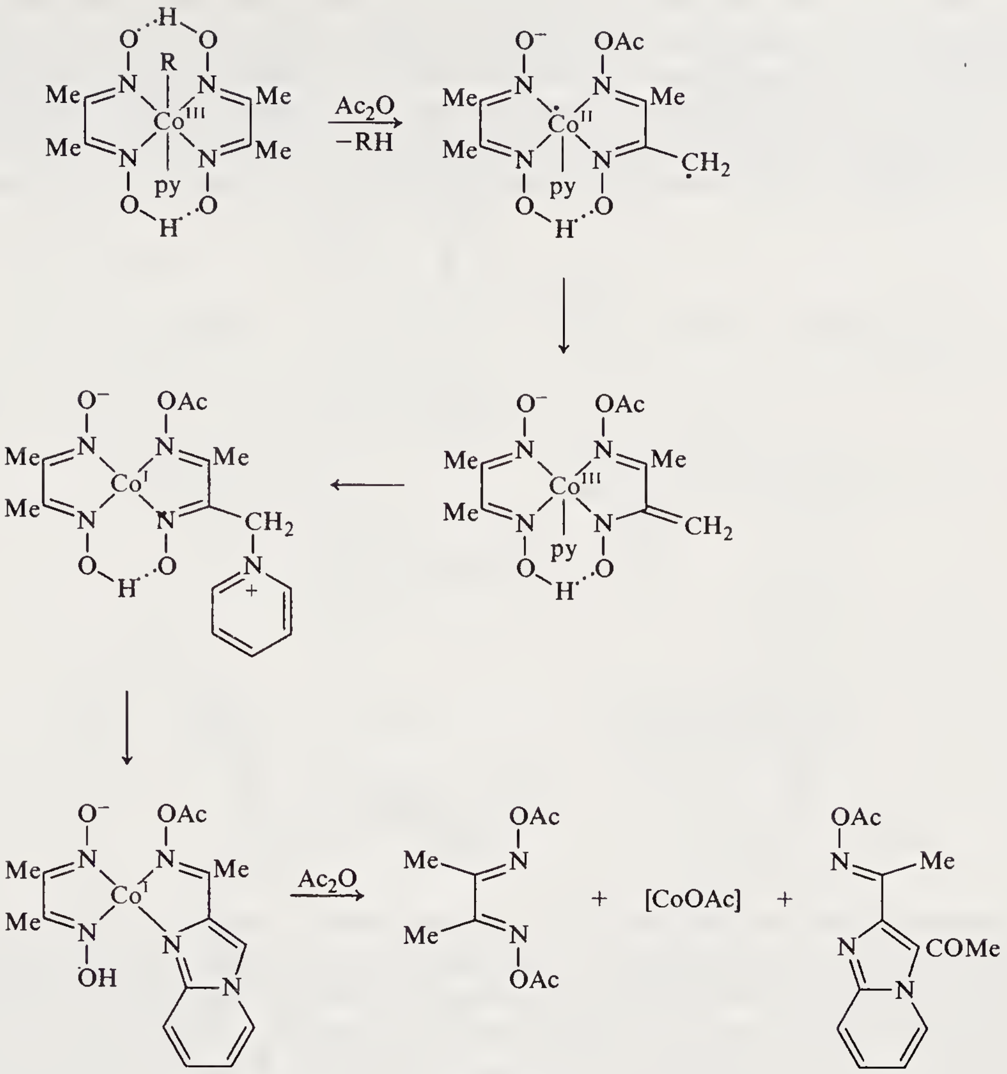

Scheme 56

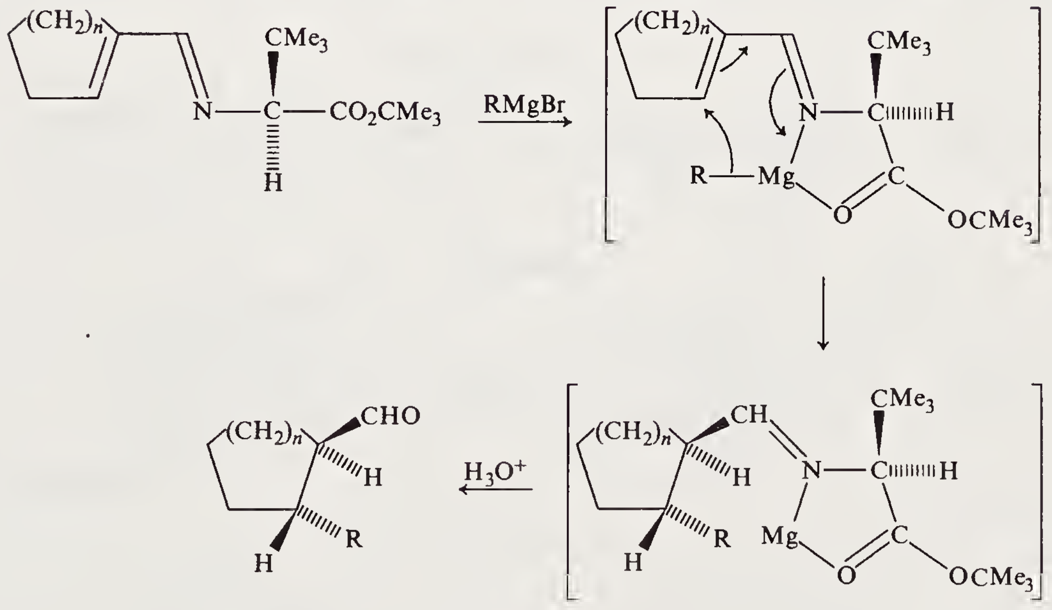

Scheme 57

One of the most spectacular and useful template reactions is the 'Curtis reaction', in which a new chelate ring is formed as the result of an aldol condensation between a methylene ketone or imine and an imine salt. The initial example of this reaction was the formation of a macrocyclic nickel(II) complex from tris(1,2-diaminoethane)nickel(II) perchlorate and acetone (equation 53).[182] The reaction has been developed by Curtis and numerous other workers and has been reviewed.[183] In mechanistic terms there is some circumstantial evidence to suggest that the nucleophile is an uncoordinated acetonyl carbanion which adds to a coordinated imine to yield a coordinated amino ketone (equation 54). If such a mechanism operates then the template effect is largely, if not wholly, thermodynamic in nature, as described for imine formation. Such a view is supported by the fact that the free macrocycle salts can be produced by acid catalysis alone. However, this fact does not mean that in metal-promoted reactions the metal only acts as a 'super acid' and loses its powerful coordinating facility. It is entirely reasonable that, at least in some cases, a kinetic template effect can be contributed by the capacity of the metal ion to bind both nucleophile and electrophile (equation 55). The definitive experiment to check such a mechanistic hypothesis has yet to be done, but the Curtis reaction is placed deliberately in this section for the purposes of stimulating such an investigation. The wide synthetic ramifications of this reaction are considered in Section 61.1.2.3.

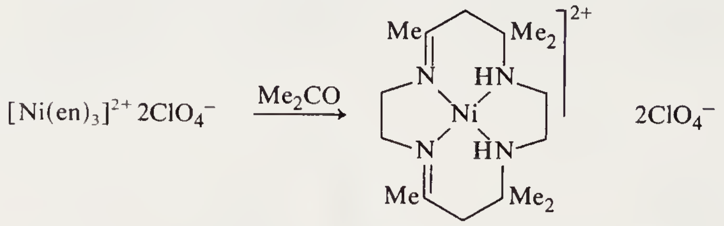

(53)

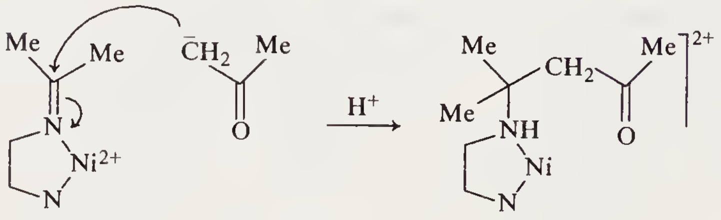

(54)

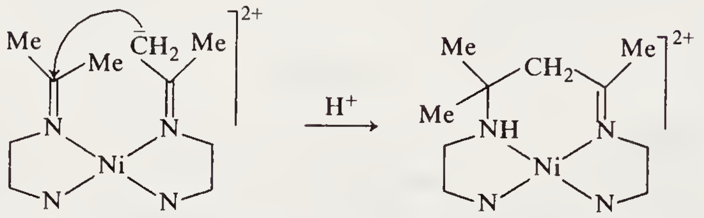

(55)

Kinetic template effects have been postulated in more typical organic aldol condensations, where metals such as lithium and zinc are likely to coordinate both the enolate or enamine nucleophile and the aldehyde in the transition state. The examples shown in Schemes 58[184] and 59[185] are illustrative of these reactions and the degree of selectivity obtained. The carboxylation of ketones and nitroalkanes by methyl magnesium carbonate to produce β-keto acids and α-nitro acids respectively provides early examples of similar reactions (Scheme 60).[186,187] See also Section 61.1.4.4.

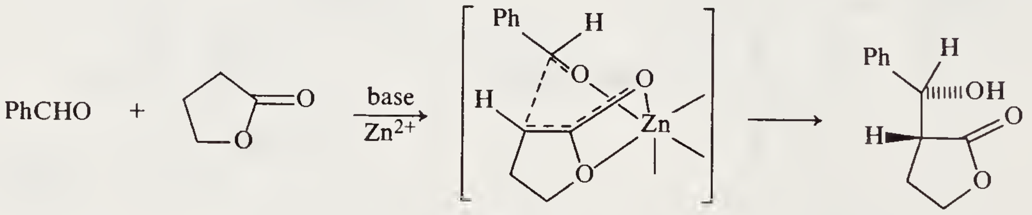

Scheme 58

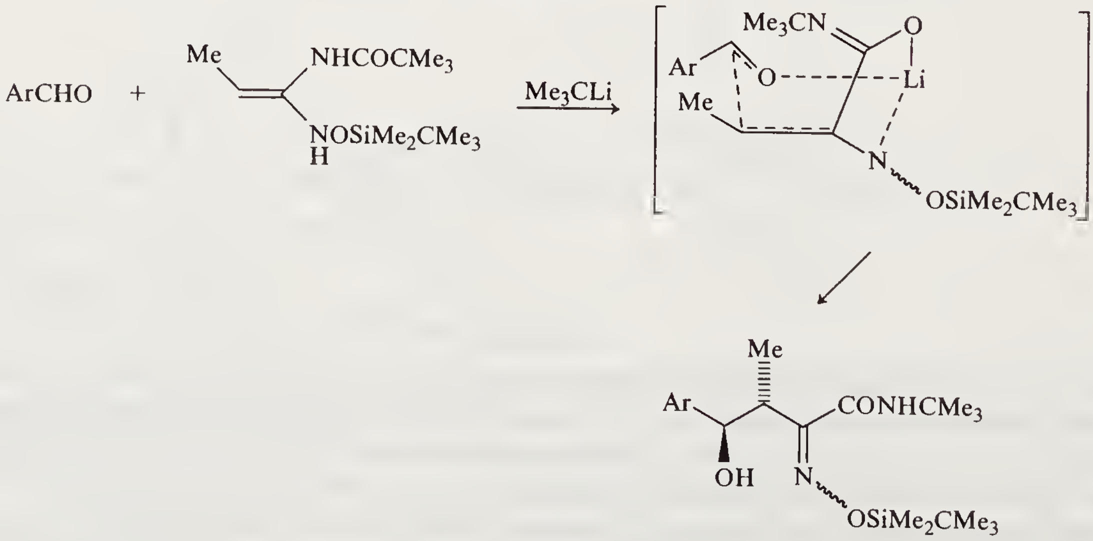

Scheme 59

New chelate rings have been formed by the nucleophilic attack of carbanions and nitriles, with both groups being coordinated throughout the reaction to either iron(II) or cobalt(III) (Scheme 61[188,189] and equation 56).[190]

Carbanion attack on an alkyne is responsible for cyclization in a palladium(II) diphosphine complex (Scheme 62).[191]

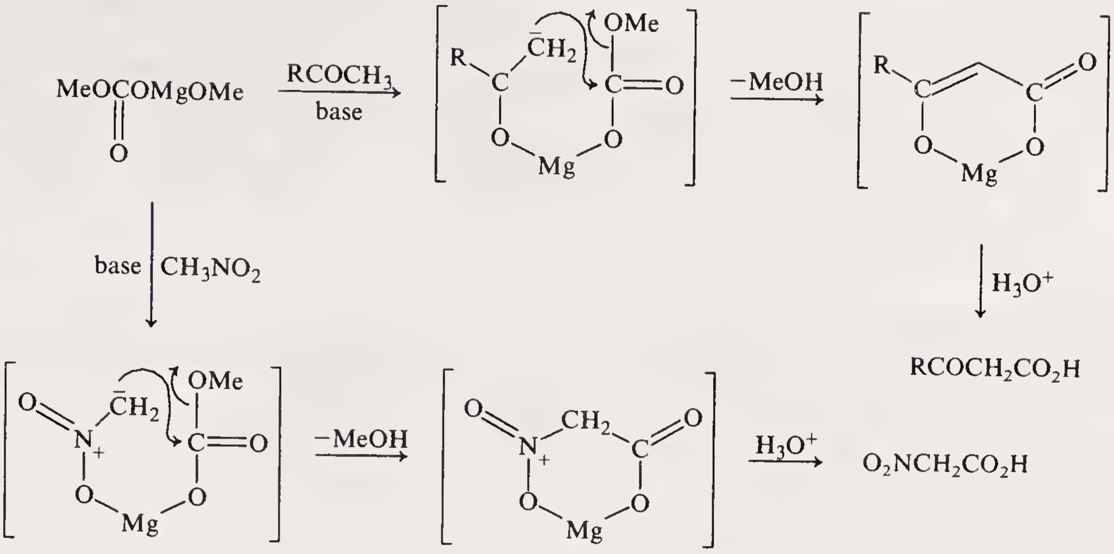

Scheme 60

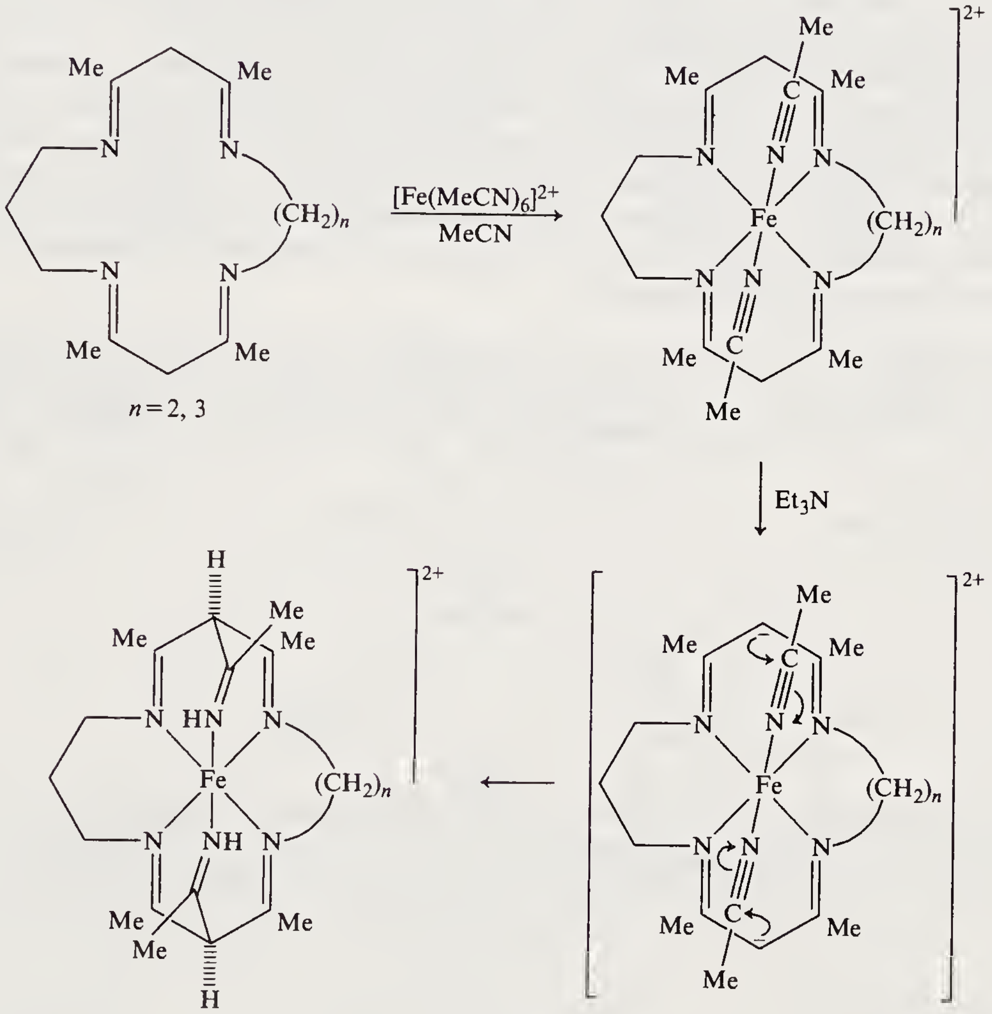

Scheme 61

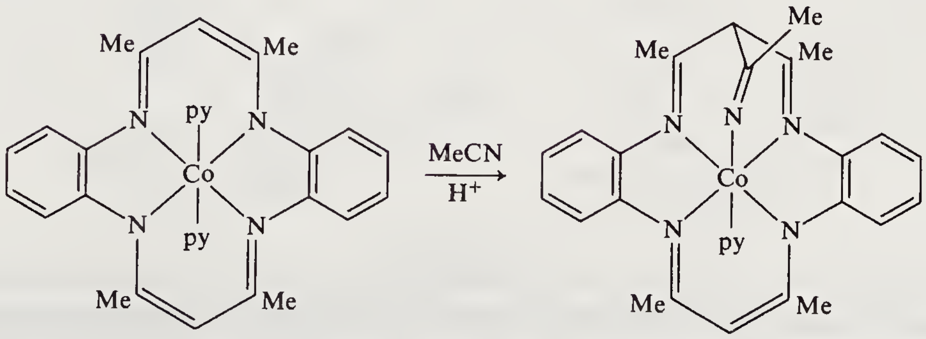

(56)

Numerous kinetic template reactions have been employed in the formation of porphyrins, corrins and phthalocyanins (see Section 61.1.3). The most instructive examples from a mechanistic point of view are those employed by Eschenmoser and his coworkers in the formation of corrins and

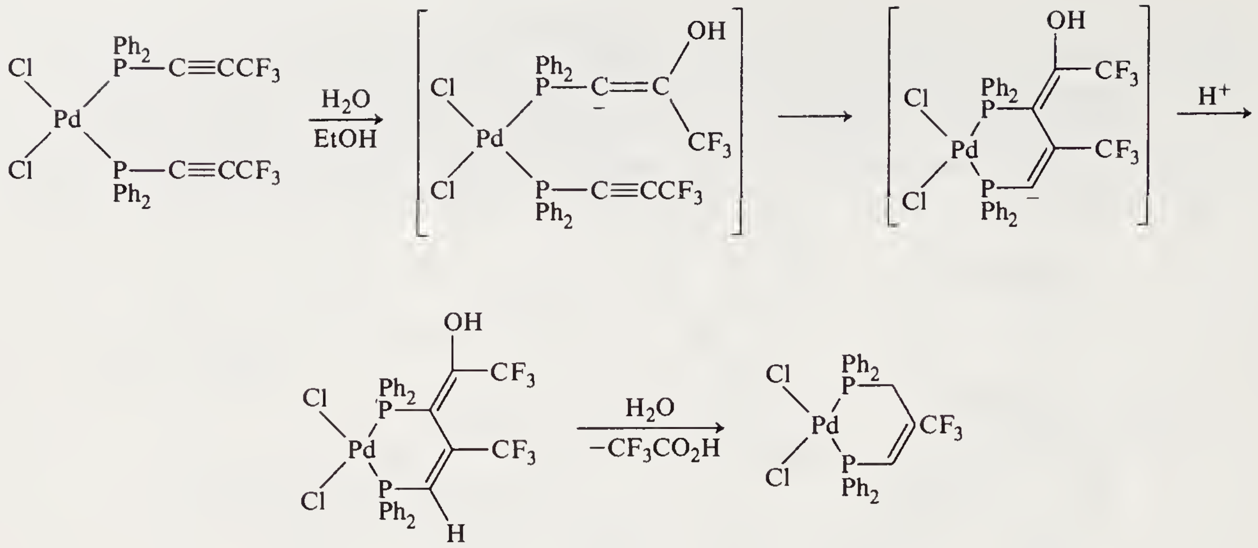

Scheme 62

vitamin B_{12}. Cyclization can be achieved most notably by enamine addition to an imino ester or thioimino ester, and by a light-induced 1,16-hydrogen transfer (Scheme 63).[192] The first cyclization proceeds for nickel(II), palladium(II) and dicyanocobalt(III) complexes, whereas the photochemical cyclization proceeds for lithium(I), magnesium(II), zinc(II), cadmium(II), palladium(II) or platinum(II) complexes, but not those of copper(II), cobalt(II), nickel(II) or manganese(II).[193] Both cyclization approaches have been used in total syntheses of vitamin B_{12}, the former in its thioimino ester version.[194] A more recent corrin cyclization is possibly of the aldol type involving the addition of an enolate anion on to an iminium salt (Scheme 64).[195] However, the transition state could also involve diradical character.

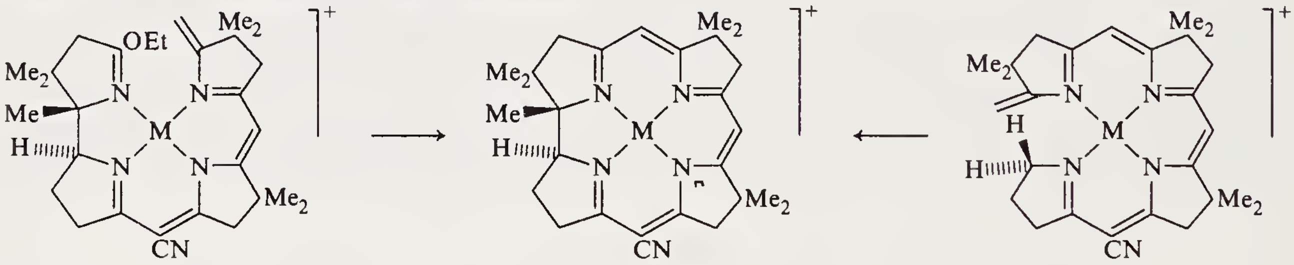

Scheme 63

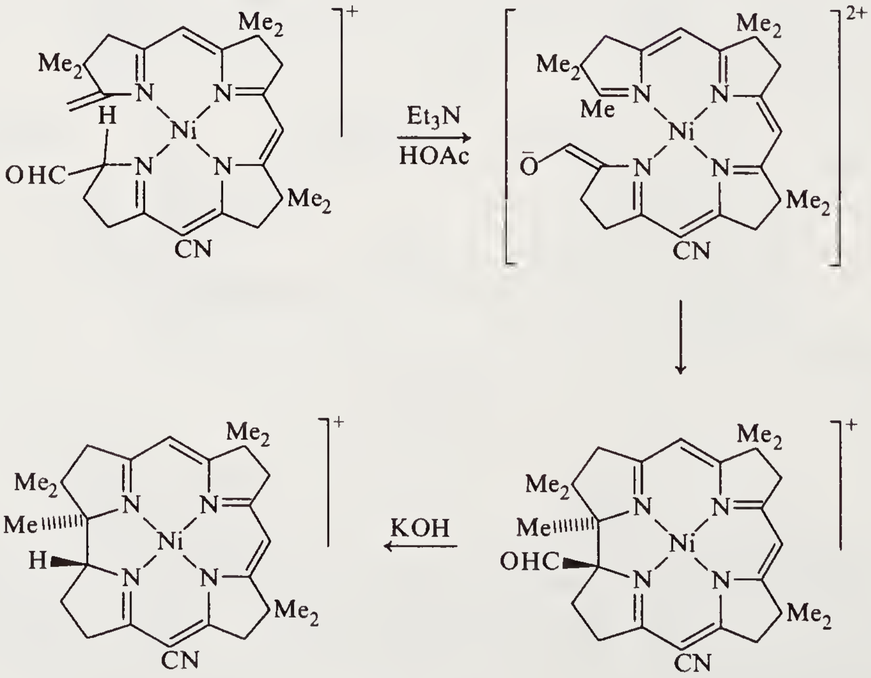

Scheme 64

The cyclization reaction developed by Scheffold, and shown in Scheme 65, makes use of the addition of an amidine to an iminium salt, and produces a product of reduced porphinoid character.[196,197]

Some of the numerous tetrapyrrole cyclizations and the occasional corrin cyclization give rise to the insertion of heteroatoms in the bridge. Some examples are shown in equation (57).[198]

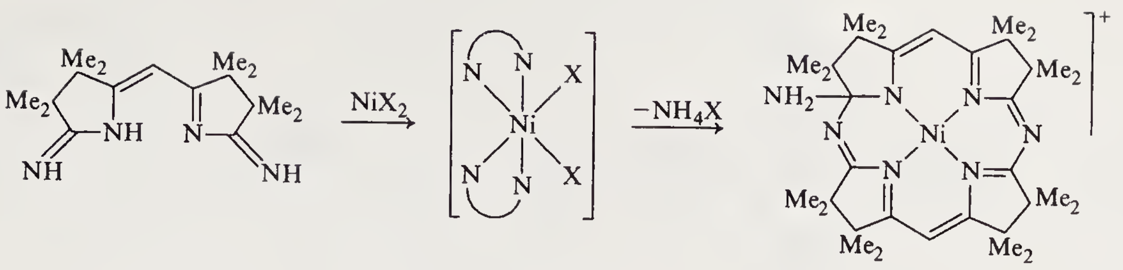

Scheme 65

Simpler insertion reactions have been demonstrated in the case of coordinated hydrazines and hydrazones, where the terminal amino group is still nucleophilic (equation 58).[199,200]

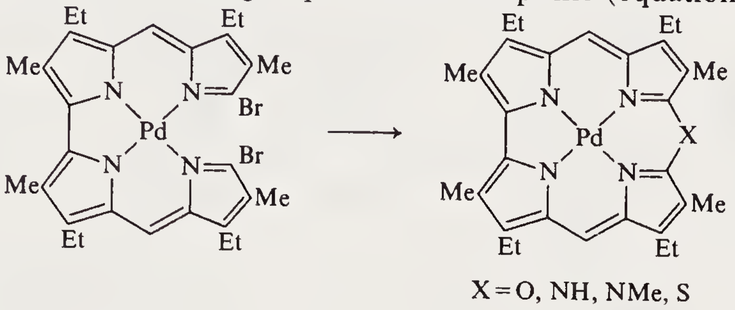

(57)

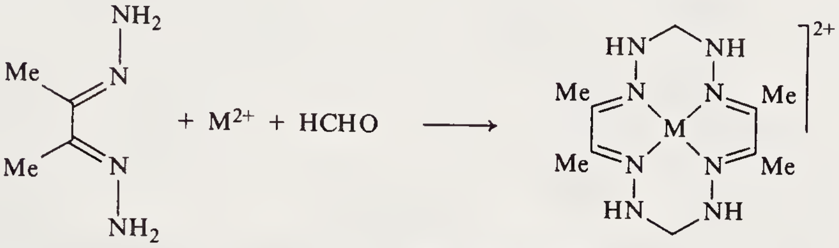

(58)

Replacement of the hydrogen bonds in oxime complexes with boron bridges leads to macrocyclic complexes such as those from dimethyl glyoxime (equation 59).[201,202] This kinetic template technique has been used for the encapsulation of metals inside cage ligands.[203,204]

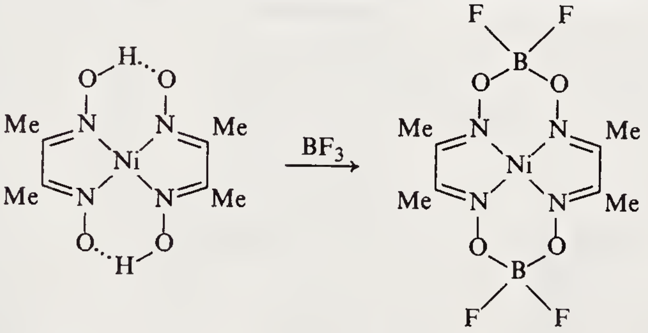

(59)

The most dramatic formation of cages has been provided by kinetic template reactions of ligands attached to cobalt(III). The deprotonated amine ligands undergo reaction with formaldehyde to produce bound imines which can be trapped by a variety of nucleophiles (Schemes 66 and 67).[205–208] The synthesis of cages of this type will be considered further in Section 61.1.2.

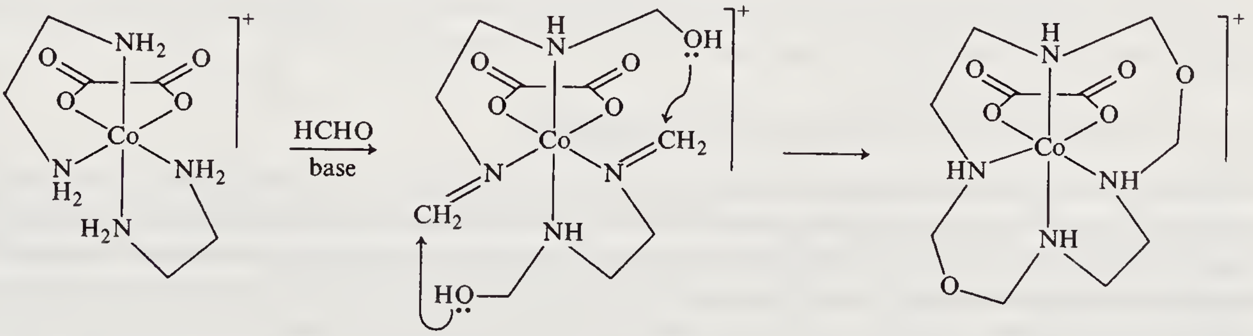

Scheme 66

Template syntheses have been reported for the preparation of so-called 'lacunar' complexes, in which a long strap bridges two sides of a bowl-shaped macrocyclic complex. Although the newly formed chelate ring is very large and therefore gains little or no stabilization from the chelate effect, the non-planar geometry of the precursor macrocycle encourages the intramolecular strap formation to occur in good yield. Two complementary methods can be used: one involves nucleophilic amine addition to an imidate and the other is a direct alkylation of an amidine (Scheme 68).[42,43]

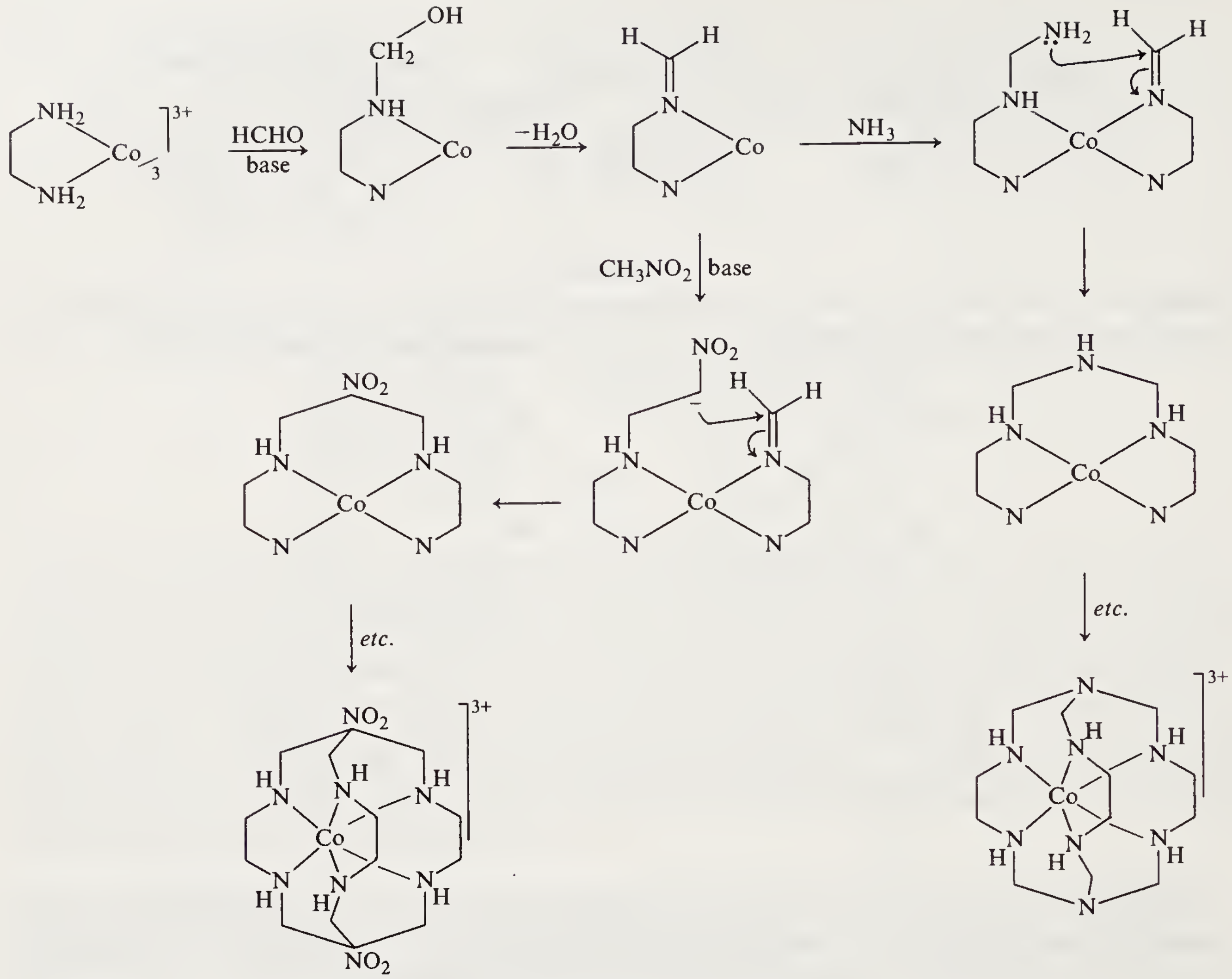

Scheme 67

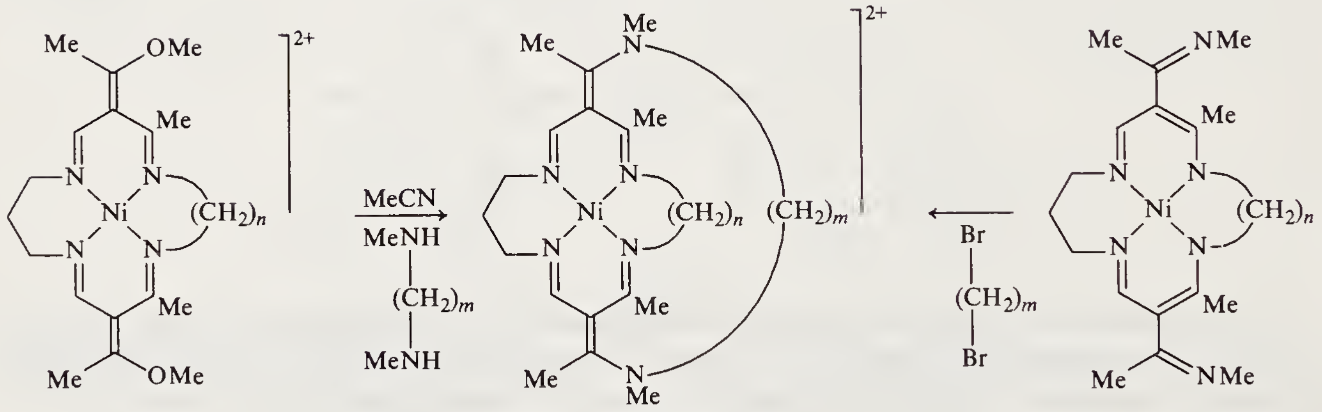

Scheme 68

A recently described oxygen migration reaction could proceed *via* a transition state incorporating a new chelate ring, but the actual mechanism is obscure (Scheme 69).[177]

7.4.4 CHELATE RING-MODIFYING REACTIONS

Although reactions of coordinated ligands can effect changes on the periphery of a ligand, or can construct new chelate rings, they can also result in modification of existing chelate rings. Some aspects of these reactions, particularly those involving nucleophilic attack on chelate rings, have already been considered. However, hydrogenation, dehydrogenation and rearrangement processes require brief mention here.

In general, coordinated imines undergo smooth reduction by sodium borohydride or lithium aluminum hydride as well as by catalytic hydrogenation. The metal does not appear to play a significant part in these reactions, in contrast to the dehydrogenation and oxidation of saturated chelate rings. One of the most useful features of both oxidative and reductive modification of chelate rings is that in many cases the final system would be inaccessible by direct synthesis. Furthermore, the free ligands would often be hydrolytically, oxidatively or reductively unstable. A typical example of the above processes is presented by the work of Curtis[183] and Busch[209]

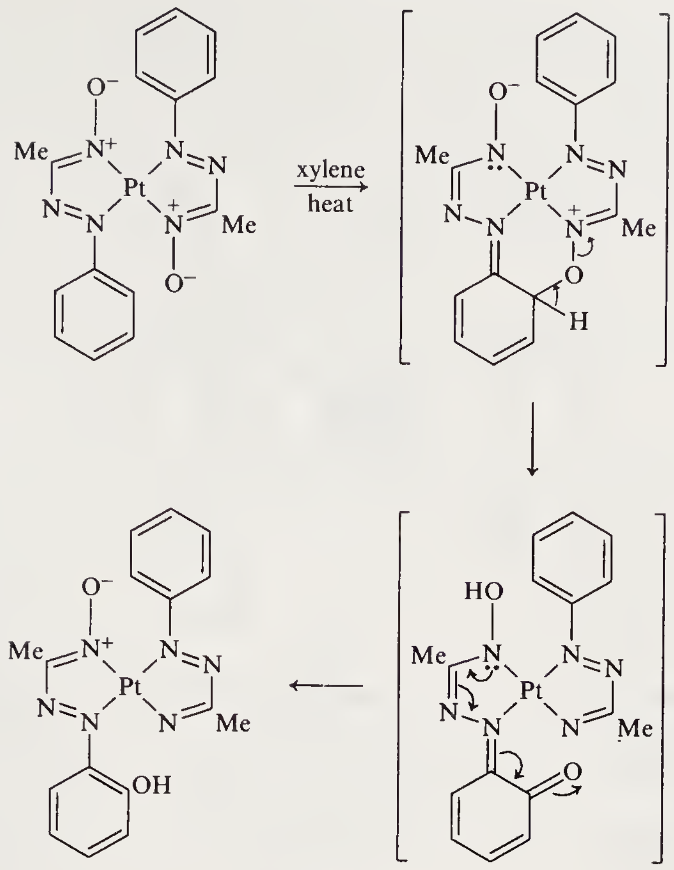

Scheme 69

(Scheme 70). The precise position of oxidative dehydrogenation can vary for the same ligand associated with different metals such as nickel(II) and iron(II).[210–212] Ruthenium(II) and iron(II) are particularly effective for the oxidative dehydrogenation of 1,2-diamine ligands[213,214] and even more simple amines.[215,216]

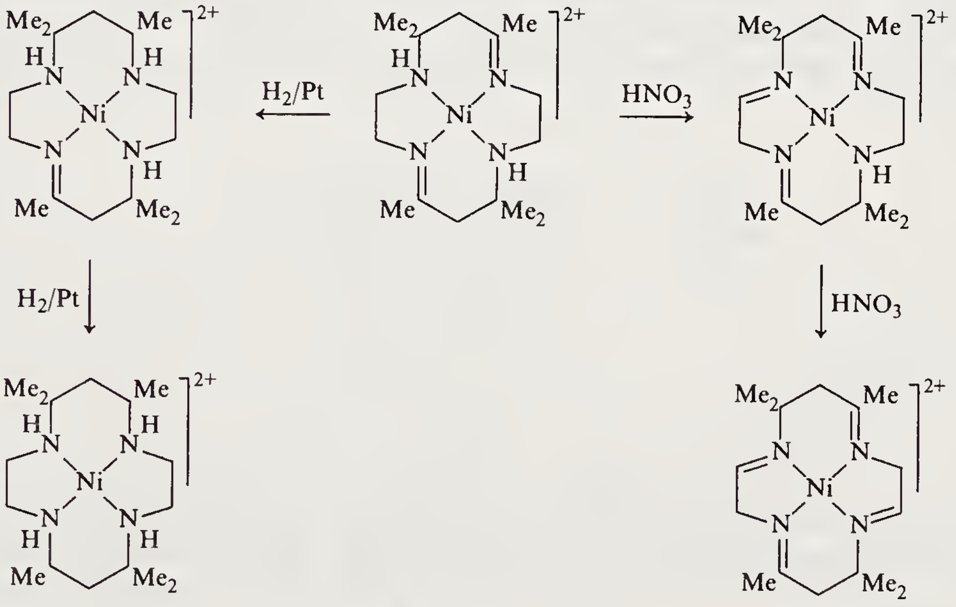

Scheme 70

1,3-Diamino ligands have been shown to undergo oxidative dehydrogenation to vinylogous amidines as exemplified in equations (60)[217] and (61).[9] In the second example, oxidation of aromatic amines is a very easy process and the metal ion appears to play only a supporting role as a substituent. Even cobalt(II) complexes allow the dehydrogenation to occur, a situation which does not arise in the case of ligands constructed from aliphatic amines. With such ligands it seems to be necessary for the metal ion to undergo oxidation to a relatively unstable state, unlike cobalt(III), and then suffer reduction at the expense of the ligand. Some related ligands, derived from hydrazones and formaldehyde, undergo spontaneous oxidation (equation 62).[199,200]

Oxygenation of ligands has also been observed. An α-diimine iron(II) complex has been effectively hydroxylated as a result of oxidation by cerium(IV) (equation 63).[218] Aerial oxidation in dimethylformamide of an iron(III) acetate complex results in the conversion of an ethano linkage to dioxo (equation 64).[219] During the formation of the related nickel(II) complex (**64**), the modified complex (**65**) was isolated.[220] It is likely that the product arose by reaction of 1,2-diaminoethane

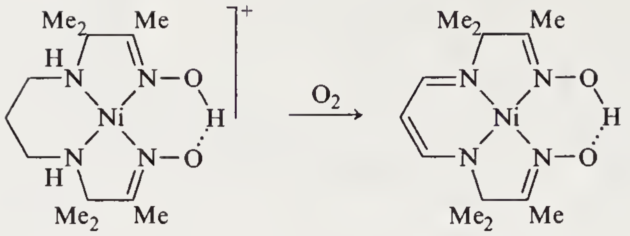

(60)

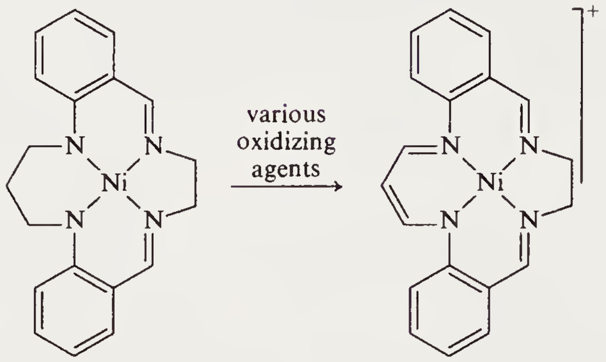

(61)

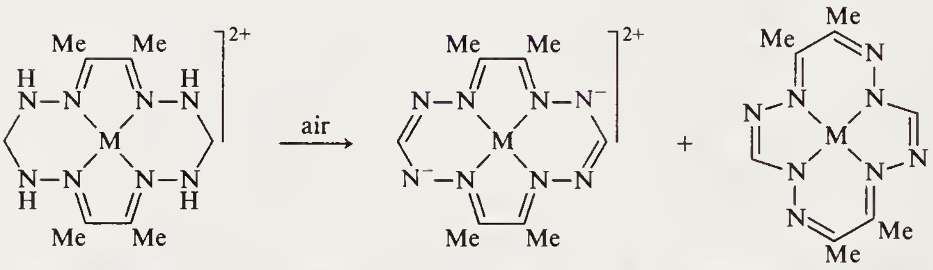

(62)

with an oxamide-type complex, formed by oxidation of (**64**). Radical intermediates have been postulated in the above examples. Indeed, good evidence has been found for a radical intermediate in a related base-promoted oxidation which leads to both oxygenation and oxidative dimerization products, (**66**) and (**67**) respectively (Scheme 71).[221,222] Electrochemical oxidation of related nickel(II) complexes yields dimers of the same type as compound (**67**).[223] The alkane dimer (**67**) has shown to undergo dehydrogenation with oxygen or iron(III) chloride to the corresponding alkene dimer (**68**).[224]

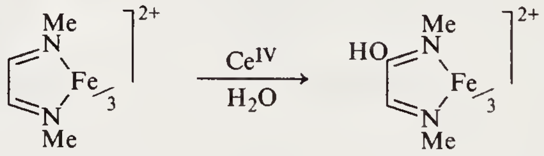

(63)

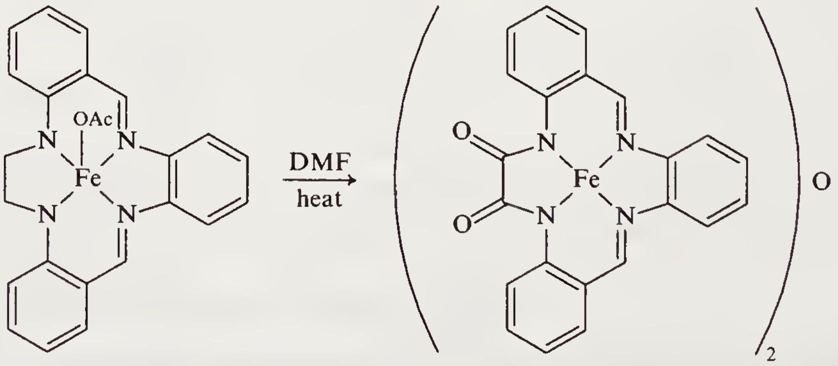

(64)

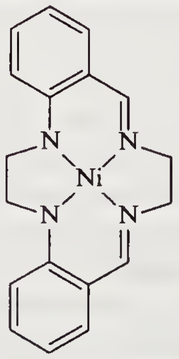

(64)

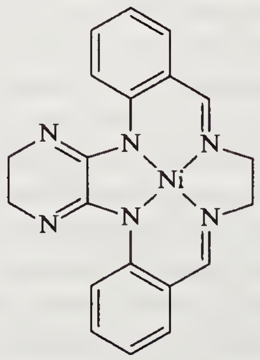

(65)

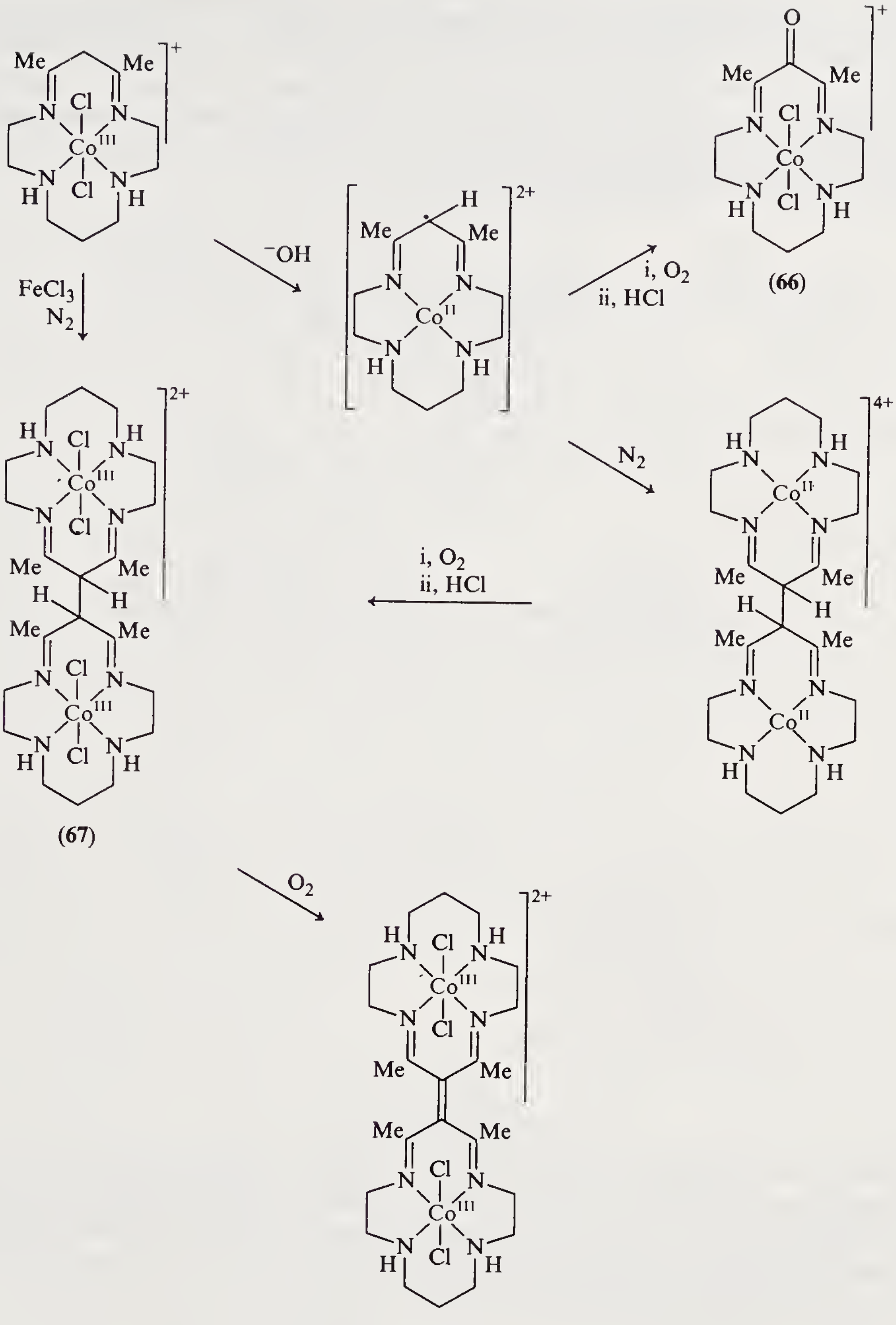

Scheme 71

The oxygenation of the β-diimine complex to give compound **(66)** (Scheme 71) could be a more general process as both the diheteroarylmethanes **(69)** and **(70)** undergo metal-catalyzed oxygenation to the related products **(71)** and **(72)** respectively.[225,226]

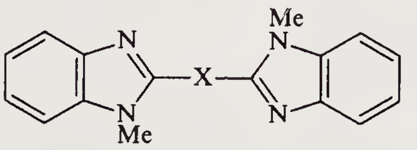

(69) X = CH$_2$
(71) X = CO

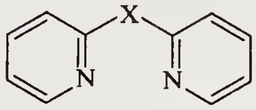

(70) X = CH$_2$
(72) X = CO

An unusual oxygenation of the mercapto acetate ligand of a chromium(III) complex has also been reported (equation 65).[227]

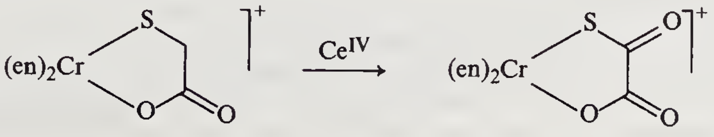

(65)

Modification of existing chelate rings has been observed in the metal-promoted rearrangement of 2,2′-pyridil into metal complexes of 2,2′-pyridilic acid (Scheme 72).[228] The tridentate chelate (**73**) has been shown to be an intermediate in the rearrangement and provides support for the mechanism outlined. The intermediate complexes (**73**), which contain five-, six- and seven-membered chelate rings, are stable at low temperature but undergo molecular rearrangement, with migration of a pyridyl group to the final product, which contains three six-membered chelate rings. Thus both ring contraction and ring expansion occur.

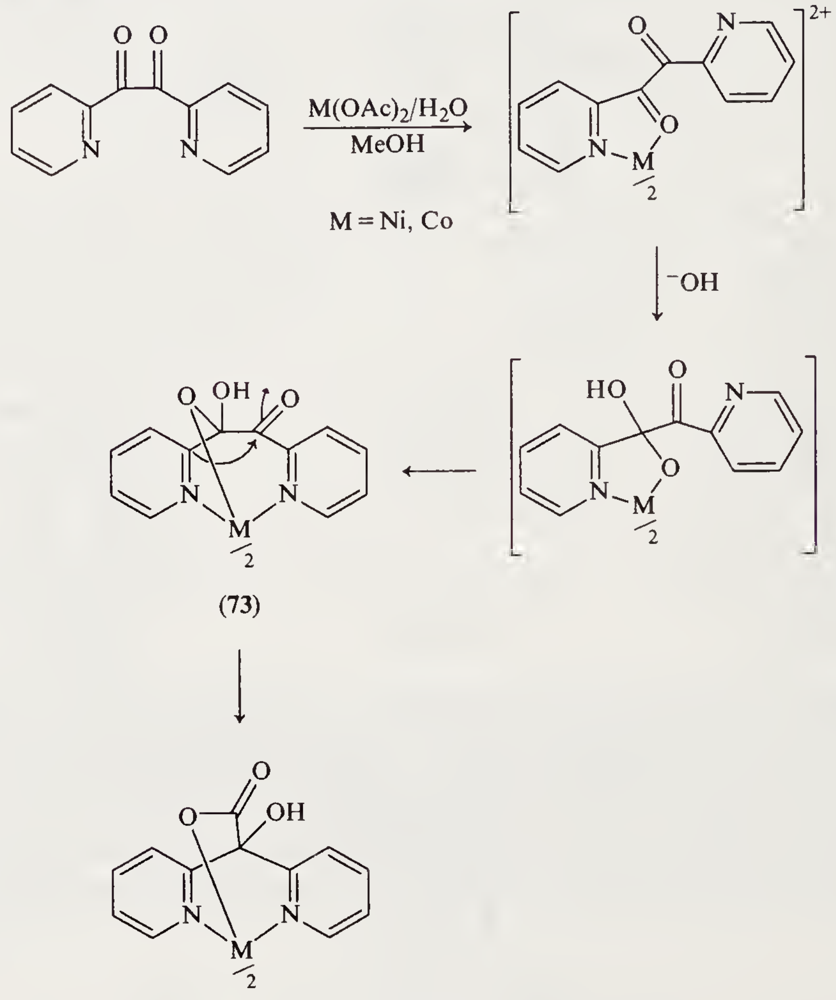

Scheme 72

A different type of rearrangement involves cycloaddition of dimethyl acetylenedicarboxylate on to a copper complex which serves to activate the ligand (Scheme 73).[229] The reaction is similar in some respects to that shown in equation (42), and indicates the difficulty in the categorization of many of the reactions of coordinated ligands according to mechanism. Consequently, the above account is of necessity somewhat subjective.

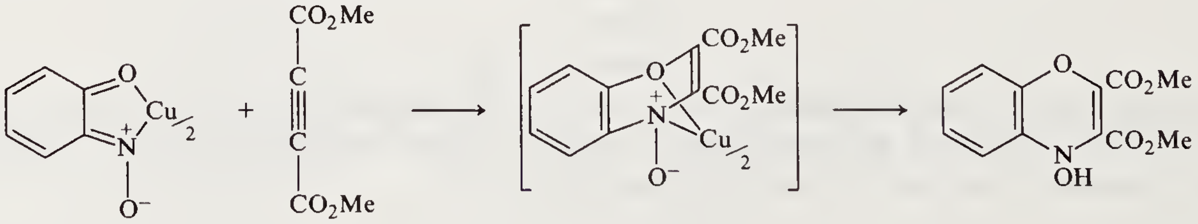

Scheme 73

7.4.5 REFERENCES

1. D. H. Busch, in 'Reactions of Coordinated Ligands and Homogeneous Catalysis' *(Advances in Chemistry Series, No. 37)*, American Chemical Society, Washington, 1963, p. 1.
2. F. P. Dwyer, in 'Chelating Agents and Metal Chelates', ed. F. P. Dwyer and D. P. Mellor, Academic, New York, 1964, p. 335.
3. D. St. C. Black and E. Markham, *Rev. Pure Appl. Chem.*, 1965, **15**, 109.
4. J. P. Collman, in 'Transition Metal Chemistry', Dekker, New York, 1966, vol. 2, p. 1.
5. M. D. Healy and A. J. Rest, *Adv. Inorg. Chem. Radiochem.*, 1978, **21**, 1.
6. Y. N. Kukushkin, *Russ. J. Inorg. Chem. (Engl. Transl.)*, 1965, **10**, 848.
7. I. I. Chernyaev, O. N. Adrianova and N. S. Leites, *Russ. J. Inorg. Chem. (Engl. Transl.)*, 1961, **6**, 252.
8. D. St. C. Black, A. J. Hartshorn, M. Horner and S. Hünig, *Aust. J. Chem.*, 1977, **30**, 2493.

9. R. V. G. Ewens and C. S. Gibson, *J. Chem. Soc.*, 1959, 431.
10. D. H. Busch, J. A. Burke, D. C. Jicha, M. C. Thompson and M. L. Morris, in 'Reactions of Coordinated Ligands and Homogeneous Catalysis' *(Advances in Chemistry Series, No. 37)*, American Chemical Society, Washington, 1963, p. 135.
11. D. H. Busch, D. C. Jicha, M. C. Thompson, J. W. Wrathall and E. Blinn, *J. Am. Chem. Soc.*, 1964, **86**, 3642.
12. G. W. Watt and P. W. Alexander, *Inorg. Chem.*, 1968, **7**, 537.
13. F. Wagner, M. T. Mocella, M. J. D'Aniello, A. H. J. Wang and E. K. Barefield, *J. Am. Chem. Soc.*, 1974, **96**, 2625.
14. M. J. D'Aniello, M. T. Mocella, F. Wagner, E. K. Barefield and I. C. Paul, *J. Am. Chem. Soc.*, 1975, **97**, 192.
15. A. E. Arbuzov and V. M. Zoroastrova, *Dokl. Akad. Nauk SSSR*, 1952, **84**, 503.
16. E. Fink, *C. R. Hebd. Seances Acad. Sci.*, 1885, **101**, 164.
17. F. Seel, K. Ballreich and R. Schmutzler, *Chem. Ber.*, 1961, **94**, 1173.
18. R. Schmutzler, in 'Reactions of Coordinated Ligands and Homogeneous Catalysis', *(Advances in Chemistry Series, No. 37)*, American Chemical Society, Washington, 1963, p. 150.
19. K. D. Maguire and M. M. Jones, *J. Am. Chem. Soc.*, 1962, **84**, 2316.
20. C. Bostic, Q. Fernando and H. Freiser, *Inorg. Chem.*, 1963, **2**, 232.
21. J. C. Taft and M. M. Jones, *J. Am. Chem. Soc.*, 1960, **82**, 4196.
22. W. C. Drinkard, H. F. Bauer and J. C. Bailar, *J. Am. Chem. Soc.*, 1960, **82**, 2992.
23. R. N. Hurd, G. De La Mater, G. C. McElheny and L. V. Pfeiffer, *J. Am. Chem. Soc.*, 1960, **82**, 4454.
24. R. A. Krause, D. C. Jicha and D. H. Busch, *J. Am. Chem. Soc.*, 1961, **83**, 528.
25. G. R. Brubaker and D. H. Busch, *Inorg. Chem.*, 1966, **5**, 2110.
26. A. Rosowsky and J. E. Wright, *J. Org. Chem.*, 1983, **48**, 1539.
27. K. Pedersen, *Acta Chem. Scand.*, 1948, **2**, 252.
28. K. Pedersen, *Acta Chem. Scand.*, 1948, **2**, 385.
29. J. P. Collman, *Angew. Chem., Int. Ed. Engl.*, 1965, **4**, 132.
30. Z. Yoshida, H. Ogoshi and Y. Shimidzu, *Tetrahedron Lett.*, 1969, 2255.
31. T. Mukaiyama, K. Narasaka and H. Hokonok, *J. Am. Chem. Soc.*, 1969, **91**, 4315.
32. L. F. Lindoy, H. C. Lip and W. E. Moody, *J. Ghem. Soc., Dalton Trans.*, 1974, 44.
33. D. St. C. Black and R. C. Srivastava, *Aust. J. Chem.*, 1971, **24**, 287.
34. J. G. Martin and S. C. Cummings, *Inorg. Chem.*, 1973, **12**, 1477.
35. J. G. Martin, R. M. C. Wei and S. C. Cummings, *Inorg. Chem.*, 1972, **11**, 475.
36. E. Jäger, *Z. Chem.*, 1968, **8**, 392.
37. C. J. Hipp and D. H. Busch, *J. Chem. Soc., Chem. Commun.*, 1972, 737.
38. J. A. Streeky, D. G. Pillsbury and D. H. Busch, *Inorg. Chem.*, 1980, **19**, 3148.
39. C. J. Hipp and D. H. Busch, *Inorg. Chem.*, 1973, **12**, 894.
40. P. W. R. Corfield, J. D. Mokren, C. J. Hipp and D. H. Busch, *J. Am. Chem. Soc.*, 1973, **95**, 4465.
41. W. P. Schammel, L. L. Zimmer and D. H. Busch, *Inorg. Chem.*, 1980, **19**, 3159.
42. D. H. Busch, D. J. Olszanski, J. C. Stevens, W. P. Schammel, M. Kojima, N. Herron, L. L. Zimmer, K. A. Holter and J. Mocak, *J. Am. Chem. Soc.*, 1981, **103**, 1472.
43. K. J. Takeuchi, D. H. Busch and N. Alcock, *J. Am. Chem. Soc.*, 1983, **105**, 4261.
44. E. Bayer, *Angew. Chem.*, 1964, **76**, 76.
45. E. Bayer, *Angew. Chem.*, 1961, **73**, 533.
46. D. A. Buckingham, L. G. Marzilli and A. M. Sargeson, *J. Am. Chem. Soc.*, 1967, **89**, 5133.
47. A. Pasini and L. Casella, *J. Inorg. Nucl. Chem.*, 1974, **36**, 2133.
48. M. Sato, K. Okawa and S. Akabori, *Bull. Chem. Soc. Jpn.*, 1957, **30**, 937.
49. J. C. Dabrowiak and D. W. Cooke, *Inorg. Chem.*, 1975, **14**, 1305.
50. Y. Ikutani, T. Okada, M. Sato and S. Akabori, *Bull. Chem. Soc. Jpn.*, 1959, **32**, 203.
51. D. C. Berndt, *J. Org. Chem.*, 1970, **35**, 1129.
52. M. Murakami and K. Takahashi, *Bull. Chem. Soc. Jpn.*, 1959, **32**, 308.
53. J. R. Brush, R. J. Magee, M. J. O'Connor, S. B. Teo, R. J. Geue and M. R. Snow, *J. Am. Chem. Soc.*, 1973, **95**, 2034.
54. G. Blaschke, *Angew. Chem., Int. Ed. Engl.*, 1980, **19**, 13.
55. B. T. Golding, G. J. Gainsford, A. J. Herlt and A. M. Sargeson, *Tetrahedron*, 1976, **32**, 389.
56. W. E. Keyes, R. E. Caputo, R. D. Willett and J. I. Legg, *J. Am. Chem. Soc.*, 1976, **98**, 6939.
57. Y. N. Belokon', V. M. Belikov, S. V. Vitt, T. F. Savel'eva, V. M. Burbelo, V. I. Bakhmutov, G. G. Aleksandrov and Y. T. Struchkov, *Tetrahedron*, 1977, **33**, 2551.
58. K. Harada and J. Oh-Hashi, *J. Org. Chem.*, 1967, **32**, 1103.
59. J. R. Fischer and E. H. Abbott, *J. Am. Chem. Soc.*, 1979, **101**, 2781.
60. T. Ichikawa, S. Maeda, Y. Araki and Y. Ishido, *J. Am. Chem. Soc.*, 1970, **92**, 5514.
61. T. Ichikawa, T. Okamoto, S. Maeda, S. Ohdan, Y. Araki and Y. Ishido, *Tetrahedron Lett.*, 1971, 79.
62. Y. N. Belokon', I. E. Zel'tzer, V. I. Bakhmutov, M. B. Saporovskaya, M. G. Ryzhov, A. I. Yanovsky, Y. T. Struchkov and V. M Belikov, *J. Am Chem. Soc.*, 1983, **105**, 2010.
63. W. G. Jackson, A. M. Sargeson, P. A. Tucker and A. D. Watson, *J. Am. Chem. Soc.*, 1981, **103**, 533.
64. W. G. Jackson, G. M. McLaughlin, A. M. Sargeson and A. D. Watson, *J. Am. Chem. Soc.*, 1983, **105**, 2426.
65. R. D. Gillard and D. A. Phipps, *Chem. Commun.*, 1970, 800.
66. E. Gelles and R. W. Hay, *J. Chem. Soc.*, 1958, 3673.
67. A. Wood, *Trans. Faraday Soc.*, 1966, 1231.
68. R. W. Hay and S. J. Harvie, *Aust. J. Chem.*, 1965, **18**, 1197.
69. G. Kubala and A. E. Martell, *J. Am. Chem. Soc.*, 1982, **104**, 6602.
70. R. Steinberger and F. H. Westheimer, *J. Am. Chem. Soc.*, 1951, **73**, 429.
71. J. E. Prue, *J. Chem. Soc.*, 1952, 2331.
72. H. Kroll, *J. Am. Chem. Soc.*, 1952, **74**, 2036.
73. D. A. Buckingham, J. P. Collman, D. A. R. Happer and L. G. Marzilli, *J. Am. Chem. Soc.*, 1967, **89**, 1082.
74. Y. Wu and D. H. Busch, *J. Am. Chem. Soc.*, 1972, **94**, 4115.
75. D. A. Buckingham, J. Dekkers, A. M. Sargeson and M. Wein, *J. Am. Chem. Soc.*, 1972, **94**, 4032.
76. A. Y. Girgis and J. I. Legg, *J. Am. Chem. Soc.*, 1972, **94**, 8420.
77. R. Nakon and R. J. Angelici, *J. Am. Chem. Soc.*, 1973, **95**, 3170.
78. R. P. Houghton and D. J. Pointer, *J. Chem. Soc.*, 1965, 4214.

79. M. D. Alexander and D. H. Busch, *J. Am. Chem. Soc.*, 1966, **88**, 1130.
80. R. W. Hay and P. J. Morris, *Chem. Commun.*, 1968, 732.
81. R. P. Houghton and R. R. Puttner, *Chem. Commun.*, 1970, 1270.
82. E. J. Corey and R. L. Dawson, *J. Am. Chem. Soc.*, 1962, **84**, 4899.
83. T. H. Fife, T. J. Przystas and V. L. Squillacote, *J. Am. Chem. Soc.*, 1979, **101**, 3017.
84. M. M. Jones, T. J. Cook and S. Brammer, *J. Inorg. Nucl. Chem.*, 1966, **28**, 1265.
85. R. W. Hay and P. J. Morris, *Chem. Commun.*, 1969, 1208.
86. R. L. Gustafson and A. E. Martell, *J. Am. Chem. Soc.*, 1962, **84**, 2309.
87. R. W. Hay, C. R. Clark and J. A. G. Edmonds, *J. Chem. Soc., Dalton Trans.*, 1974, 9.
88. C. R. Clark, R. W. Hay and I. C. M. Dea, *Chem. Commun.*, 1970, 794.
89. B. Anderson, R. M. Milburn, J. M. Harrowfield, G. B. Robertson and A. M. Sargeson, *J. Am. Chem. Soc.*, 1977, **99**, 2652.
90. J. P. Fackler, D. Coucouvanis, W. C. Seidel, R. C. Masek and W. Holloway, *Chem. Commun.*, 1967, 924.
91. D. J. Creighton, J. Hajdu and D. S. Sigman, *J. Am. Chem. Soc.*, 1976, **98**, 4619.
92. R. P. Hanzlik and A. Hamburg, *J. Am. Chem. Soc.*, 1978, **100**, 1745.
93. R. D. Gillard and G. Wilkinson, *J. Chem. Soc.*, 1964, 2835.
94. B. N. Storhoff and H. C. Lewis, *Coord. Chem. Rev.*, 1977, **23**, 1.
95. I. I. Creaser, J. M. Harrowfield, F. R. Keene and A. M. Sargeson, *J. Am. Chem. Soc.*, 1981, **103**, 3559.
96. I. I. Creaser and A. M. Sargeson, *J. Chem. Soc., Chem. Commun.*, 1975, 974.
97. N. J. Curtis, N. E. Dixon and A. M. Sargeson, *J. Am. Chem. Soc.*, 1983, **105**, 5347.
98. R. D. Gillard, *Coord. Chem. Rev.*, 1975, **16**, 67.
99. N. Serpone, G. Ponterini, M. A. Jamieson, F. Bolletta and M. Maestri, *Coord. Chem. Rev.*, 1983, **50**, 209.
100. V. W. Skopenko and E. Hoyer, *Z. Anorg. Allg. Chem.*, 1965, **339**, 214.
101. D. Kutscher and E. Hoyer, *Z. Chem.*, 1963, **3**, 68.
102. S. Chaberek and A. E. Martell, 'Organic Sequestering Agents', Wiley, New York, 1959, p. 433.
103. R. P. Houghton, *J. Chem. Soc. (C)*, 1967, 2030.
104. D. P. N. Satchell, *Chem. Soc. Rev.*, 1977, **6**, 345.
105. L. F. Lindoy, S. E. Livingstone and T. N. Lockyer, *Inorg. Chem.*, 1967, **6**, 652.
106. C. A. McAuliffe, *Inorg. Chem.*, 1973, **12**, 2477.
107. S. G. Murray and F. R. Hartley, *Chem. Rev.*, 1981, **81**, 365.
108. G. J. Gainsford, W. G. Jackson and A. M. Sargeson, *J. Am. Chem. Soc.*, 1979, **101**, 3966.
109. M. C. Thompson and D. H. Busch, *J. Am. Chem. Soc.*, 1962, **84**, 1762.
110. M. C. Thompson and D. H. Busch, *J. Am. Chem. Soc.*, 1964, **86**, 3651.
111. D. St. C. Black and A. J. Hartshorn, *Coord. Chem. Rev.*, 1973, **9**, 219.
112. M. C. Thompson and D. H. Busch, *J. Am. Chem. Soc.*, 1964, **86**, 213.
113. L. F. Lindoy, *Q. Rev. Chem. Soc.*, 1971, **25**, 379.
114. G. A. Melson and D. H. Busch, *J. Am. Chem. Soc.*, 1964, **86**, 4834.
115. G. A. Melson and D. H. Busch, *J. Am. Chem. Soc.*, 1965, **87**, 1706.
116. J. S. Skuratowicz, I. L. Madden and D. H. Busch, *Inorg. Chem.*, 1977, **16**, 1721.
117. M. D. Timken, R. I. Sheldon, W. G. Rohly and K. B. Mertes, *J. Am. Chem. Soc.*, 1980, **102**, 4716.
118. A. J. Jircitano, W. G. Rohly and K. B. Mertes, *J. Am. Chem. Soc.*, 1981, **103**, 4879.
119. D. St. C. Black and M. J. Lane, *Aust. J. Chem.*, 1970, **23**, 2055.
120. D. St. C. Black and N. E. Rothnie, *Aust. J. Chem.*, 1983, **36**, 1149.
121. A. R. Cutler and D. Dolphin, *J. Coord. Chem.*, 1976, **6**, 59.
122. A. R. Cutler and D. Dolphin, *Can. J. Chem.*, 1977, **55**, 3062.
123. F. A. L'Eplattenier and A. Pugin, *Helv. Chim. Acta*, 1975, **58**, 917.
124. F. A. L'Eplattenier and A. Pugin, *Helv. Chim. Acta*, 1975, **58**, 2283.
125. R. Hayes and O. Meth-Cohn, *Tetrahedron Lett.*, 1982, **23**, 1613.
126. D. S. Eggleston and S. C. Jackels, *Inorg. Chem.*, 1980, **19**, 1593.
127. V. Katovic, L. T. Taylor and D. H. Busch, *J. Am. Chem. Soc.*, 1969, **91**, 2122.
128. L. T. Taylor, F. L. Urbach and D. H. Busch, *J. Am. Chem. Soc.*, 1969, **91**, 1072.
129. P. F. B. Barnard, *J. Chem. Soc.(A)*, 1969, 2140.
130. S. Suzuki, M. Nakahara and K. Watanabe, *Bull. Chem. Soc. Jpn.*, 1971, **44**, 1441.
131. R. Breslow and M. Schmir, *J. Am. Chem. Soc.*, 1971, **93**, 4960.
132. H. Shivi, S. Yano, K. Toriumi, T. Ito and S. Yoshikawa, *J. Chem. Soc., Chem. Commun.*, 1983, 201.
133. P. Pfeiffer, W. Offerman and H. Werner, *J. Prakt. Chem.*, 1942, **159**, 313.
134. H. S. Verter and A. E. Frost, *J. Am. Chem. Soc.*, 1960, **82**, 85.
135. M. A. Wells and T. C. Bruice, *J. Am. Chem. Soc.*, 1977, **99**, 5341.
136. J. P. Collman and D. A. Buckingham, *J. Am. Chem. Soc.*, 1963, **85**, 3039.
137. C. J. Boreham, D. A. Buckingham and F. R. Keene, *J. Am. Chem. Soc.*, 1979, **101**, 1409.
138. D. S. Sigman and C. T. Jorgensen, *J. Am. Chem. Soc.*, 1972, **94**, 1724.
139. J. Suh, M. Cheong and M. P. Suh, *J. Am. Chem. Soc.*, 1982, **104**, 1654.
R. P. Houghton and C. S. Williams, *Tetrahedron Lett.*, 1967, 3929.
141. J. T. Groves and R. M. Dias, *J. Am. Chem. Soc.*, 1979, **101**, 1033.
142. R. Breslow, D. E. McClure, R. S. Brown and J. Eisenach, *J. Am. Chem. Soc.*,1975, **97**, 194.
143. D. A. Buckingham and L. M. Engelhardt, *J. Am. Chem. Soc.*, 1975, **97**, 5915.
144. C. J. Boreham, D. A. Buckingham, D. J. Francis, A. M. Sargeson and L. G. Warner, *J. Am. Chem. Soc.*, 1981, **103**, 1975.
145. J. M. Harrowfield and A. M. Sargeson, *J. Am. Chem. Soc.*, 1979, **101**, 1514.
146. P. J. Lawson, M. G. McCarthy and A. M. Sargeson, *J. Am. Chem. Soc.*, 1982, **104**, 6710.
147. A. R. Gainsford, R. D. Pizer, A. M. Sargeson and P. O. Whimp, *J. Am. Chem. Soc.*, 1981, **103**, 792.
148. J. M. Harrowfield, D. R. Jones, L. F. Lindoy and A. M. Sargeson, *J. Am. Chem. Soc.*, 1980, **102**, 7733.
149. G. J. Gainsford, W. G. Jackson and A. M. Sargeson, *J. Am. Chem. Soc.*, 1977, **99**, 2383.
150. G. J. Gainsford, W. G. Jackson and A. M. Sargeson, *J. Chem. Soc., Chem. Commun.*, 1981, 875.
151. D. A. Buckingham, B. M. Foxman, A. M. Sargeson and A. Zanella, *J. Am. Chem. Soc.*, 1972, **94**, 1007.
152. J. Springborg, R. J. Geue, A. M. Sargeson, D. Taylor and M. R. Snow, *J. Chem. Soc., Chem. Commun.*, 1978, 647.

153. D. A. Buckingham, A. M. Sargeson and A. Zanella, *J. Am. Chem. Soc.*, 1972, **94**, 8246.
154. J. Dale and P. O. Kristiansen, *Acta Chem. Scand.*, 1972,.**26**, 1471.
155. L. Mandolini and B. Masci, *J. Am. Chem. Soc.*, 1977, **99**, 7709.
156. G. Ercolani, L. Mandolini and B. Masci, *J. Am. Chem. Soc.*, 1983, **105**, 6146.
157. R. N. Greene, *Tetrahedron Lett.*, 1972, 1793.
158. G. W. Gokel, D. J. Cram, C. L. Liotta, H. P. Harris and F. L. Cook, *J. Org. Chem.*, 1974, **39**, 2445.
159. M. Chastrette and F. Chastrette, *J. Chem. Soc., Chem. Commun.*, 1973, 534.
160. M. D. Healy and A. J. Rest, *J. Chem. Soc., Chem. Commun.*, 1981, 149.
161. R. W. Kluiber and G. Sasso, *Inorg. Chim. Acta*, 1970, **4**, 226.
162. M. S. Elder, G. M. Prinz, P. Thornton and D. H. Busch, *Inorg. Chem.*, 1968, **7**, 2426.
163. E. L. Blinn and D. H. Busch, *Inorg. Chem.*, 1968, **7**, 820.
164. N. J. Rose, C. A. Root and D. H. Busch, *Inorg. Chem.*, 1967, **6**, 1431.
165. G. N. Schrauzer, R. K. Y. Ho and R. P. Murillo, *J. Am. Chem. Soc.*, 1970, **92**, 3508.
166. J. R. Baker, A. Hermann and R. M. Wing, *J. Am. Chem. Soc.*, 1971, **93**, 6486.
167. E. Uhlemann and M. Plath, *Z. Chem.*, 1969, **9**, 234.
168. G. J. Grant and D. J. Royer, *J. Am. Chem. Soc.*, 1981, **103**, 867.
169. T. A. Del Donno and W. Rosen, *J. Am. Chem. Soc.*, 1977, **99**, 8051.
170. B. N. Diel, R. C. Haltiwanger and A. D. Norman, *J. Am. Chem. Soc.*, 1982, **104**, 4700.
171. U. Thewalt and J. Weiss, *Z. Anorg. Allg. Chem.*, 1967, **352**, 225.
172. I. P. Evans, G. W. Everett and A. M. Sargeson, *J. Am. Chem. Soc.*, 1976, **98**, 8041.
173. D. A. Buckingham, J. M. Harrowfield and A. M. Sargeson, *J. Am. Chem. Soc.*, 1973, **95**, 7281.
174. V. M. Dziomko, U. A. Tomsons and Y. S. Ryabokobylko, *Khim. Geterotsikl. Soedin.*, 1976, 968.
175. V. M. Dziomko, M. N. Stopnikova and Y. S. Ryabokobylko, *Khim. Geterotsikl. Soedin.*, 1980, 837.
176. G. Hesse and M. Maurer, *Liebigs Ann. Chem.*, 1962, **658**, 21.
177. P. Bandyopadhyay, D. Bandyopadhyay, A. Chakravorty, F. A. Cotton, L. R. Falvello and S. Han, *J. Am. Chem. Soc.*, 1983, **105**, 6327.
178. D. W. Allen, I. W. Nowell, L. A. March and B. F. Taylor, *Tetrahedron Lett.*, 1982, **23**, 5479.
179. N. W. Alcock, B. T. Golding, D. R. Hall, U. Horn and W. P. Watson, *J. Chem. Soc., Perkin Trans. 1*, 1975, 386.
180. H. Kogen, K. Tomioka, S. Hashimoto and K. Koga, *Tetrahedron Lett.*, 1980, **21**, 4005.
181. A. I. Meyers, *Acc. Chem. Res.*, 1978, **11**, 375.
182. N. F. Curtis and D. A. House, *Chem. Ind. (London)*, 1961, **42**, 1708.
183. N. F. Curtis, *Coord. Chem. Rev.*, 1968, **3**, 3.
184. D. A. Widdowson, G. H. Wiebecke and D. J. Williams, *Tetrahedron Lett.*, 1982, **41**, 4285.
185. B. J. Banks, A. G. M. Barrett, M. A. Russell and D. J. Williams, *J. Chem. Soc., Chem. Commun.*, 1983, 873.
186. H. L. Finkbeiner, *J. Am. Chem. Soc.*, 1965, **87**, 4588.
187. H. L. Finkbeiner and M. Stiles, *J. Am. Chem. Soc.*, 1963, **85**, 616.
188. K. Bowman, D. P. Riley, D. H. Busch and P. W. R. Corfield, *J. Am. Chem. Soc.*, 1975, **97**, 5036.
189. D. P. Riley, J. A. Stone and D. H. Busch, *J. Am. Chem. Soc.*, 1976, **98**, 1752.
190. M. C. Weiss and V. L. Goedken, *J. Am. Chem. Soc.*, 1976, **98**, 3389.
191. A. J. Carty, S. E. Jacobson, R. T. Simpson and N. J. Taylor, *J. Am. Chem. Soc.*, 1975, **97**, 7254.
192. Y. Yamada, D. Miljkovic, P. Wehrli, B. Golding, P. Löliger, R. Keese, K. Müller and A. Eschenmoser, *Angew. Chem., Int. Ed. Engl.*, 1969, **8**, 343.
193. A. Eschenmoser, *Chem. Soc. Rev.*, 1976, **5**, 377.
194. A. Eschenmoser and C. E. Winter, *Science*, 1977, **196**, 1410.
195. A. Pfaltz, N. Buhler, R. Neier, K. Hirai and A. Eschenmoser, *Helv. Chim. Acta*, 1977, **60**, 2653.
196. J. Löliger and R. Scheffold, *Helv. Chim. Acta*, 1977, **60**, 2644.
197. L. Walder, G. Rytz, K. Meier and R. Scheffold, *Helv. Chim. Acta*, 1978, **61**, 3013.
198. A. W. Johnson, I. T. Kay and R. Rodrigo, *J. Chem. Soc.*, 1963, 2336.
199. N. W. Alcock and P. A. Tasker, *J. Chem. Soc., Chem. Commun.*, 1972, 1239.
200. V. L. Goedken and S. M. Peng, *J. Am. Chem. Soc.*, 1973, **95**, 5773.
201. G. N. Schrauzer, *Chem. Ber.*, 1962, **95**, 1438.
202. F. Umland and D. Thierig, *Angew. Chem.*, 1962, **74**, 388.
203. J. E. Parks, B. E. Wagner and R. H. Holm, *J. Am. Chem. Soc.*, 1970, **92**, 3500.
204. D. R. Boston and N. J. Rose, *J. Am. Chem. Soc.*, 1968, **90**, 6859.
205. R. J. Geue, M. R. Snow, J. Springborg, A. J. Herlt, A. M. Sargeson and D. Taylor, *J. Chem. Soc., Chem. Commun.*, 1976, 285.
206. S. M. Peng and V. L. Goedken, *Inorg. Chem.*, 1978, **17**, 820.
207. G. J. Gainsford, R. T. Geue and A. M. Sargeson, *J. Chem. Soc., Chem. Commun.*, 1982, 233.
208. I. I. Creaser, R. J. Geue, J. M. Harrowfield, A. J. Herlt, A. M. Sargeson, M. R. Snow and J. Springborg, *J. Am. Chem. Soc.*, 1982, **104**, 6016.
209. E. K. Barefield and D. H. Busch, *Inorg. Chem.*, 1971, **10**, 108.
210. V. L. Goedken and D. H. Busch, *J. Am. Chem. Soc.*, 1972, **94**, 7355.
211. G. G. Christoph and V. L. Goedken, *J. Am. Chem. Soc.*, 1973, **95**, 3869.
212. E. K. Barefield, F. V. Lovecchio, N. E. Tokel, E. Ochiai and D. H. Busch, *Inorg. Chem.*, 1972, **11**, 283.
213. V. L. Goedken, *J. Chem. Soc., Chem. Commun.*, 1972, 207.
214. D. F. Mahoney and J. K. Beattie, *Inorg. Chem.*, 1973, **12**, 2561.
215. V. E. Alvarez, R. J. Allen, T. Matsubara and P. C. Ford, *J. Am. Chem. Soc.*, 1974, **96**, 7686.
216. F. R. Keene, D. J. Salmon and T. J. Meyer, *J. Am. Chem. Soc.*, 1976, **98**, 1884.
217. E. G. Vassian and R. K. Murmann, *Inorg. Chem.*, 1967, **6**, 2043.
218. H. L. Chum and P. Krumholz, *Inorg. Chem.*, 1974, **13**, 514.
219. S. Gözen, R. Peters, P. G. Owston and P. A. Tasker, *J. Chem. Soc., Chem. Commun.*, 1980, 1199.
220. E. N. Maslen, L. M. Engelhardt and A. H. White, *J. Chem. Soc., Dalton Trans.*, 1974, 1799.
221. B. Durham, T. J. Anderson, J. A. Switzer, J. F. Endicott and M. D. Glick, *Inorg. Chem.*, 1977, **16**, 271.
222. J. A. Switzer and J. F. Endicott, *J. Am. Chem. Soc.*, 1980, **102**, 1181.
223. F. C. McElroy and J. C. Dabrowiak, *J. Am. Chem. Soc.*, 1976, **98**, 7112.
224. J. A. Cunningham and R. E. Sievers, *J. Am. Chem. Soc.*, 1973, **95**, 7183.

225. C. A. Sprecher and A. D. Zuberbühler, *Angew. Chem.*, 1977, **89**, 185.
226. F. L. Urbach, U. Knopp and A. D. Zuberbühler, *Helv. Chim. Acta*, 1978, **61**, 1097.
227. C. J. Weschler, J. C. Sullivan and E. Deutsch, *J. Am. Chem. Soc.*, 1973, **95**, 2720.
228. D. St. C. Black and R. C. Srivastava, *Aust. J. Chem.*, 1969, **22**, 1439.
229. A. McKillop and T. S. B. Sayer, *J. Org. Chem.*, 1976, **41**, 1079.

7.5

Reactions in the Solid State

H. EUGENE LeMAY, JR.
University of Nevada, Reno, NV, USA

7.5.1 INTRODUCTION

A large number of coordination compounds undergo either thermal or photochemical reactions in the solid phase. These reactions include ligand exchanges, isomerizations of various types, redox reactions and reactions of coordinated ligands. Some have been known since the time of Werner. However, very few systematic studies were performed prior to the 1960s. At that time, several research groups began to apply a variety of physical techniques, particularly thermogravimetric analysis (TGA), differential thermal analysis (DTA) and differential scanning calorimetry (DSC), to these reactions. At first these studies focused mainly on thermal stability and reaction stoichiometry; however, kinetic and thermodynamic studies were also often reported. Presently, there is a sizeable number of kinetic studies that have been reported in the literature. Nevertheless, the basic mechanisms by which coordination compounds react in the solid phase remain largely obscure. One difficulty is the identification, description and control of experimental parameters such as particle surface area, defect structure and sample atmosphere. Another difficulty is finding appropriate kinetic models. Unfortunately, investigators often fail to consider kinetic models appropriate to solids and instead uncritically apply procedures from solution kinetics. As a result, many kinetic studies of questionable reliability have appeared.

In this review our focus will be largely on thermal ligand exchange and isomerizations. Other reactions, including photochemical ones, will be dealt with only briefly. Most examples will come from studies of cobalt(III) and chromium(III) compounds merely because the chemistry of these metals is more fully developed.

7.5.2 GENERAL CHARACTERISTICS OF SOLID-STATE REACTIONS

Several reviews deal with the solid-state reactions of simple inorganic salts and of organic compounds.[1–8] The essential differences between solid-state reactions and reactions in solution can be ascribed to the fact that solid-state reactions occur within the constraining environment of the crystal lattice. The reactant crystal lattice can control both the kinetic features of a reaction, and the nature of the products. In many solid-phase reactions the separation distances and mutual orientations of reactants in the solid determine the product. Such reactions are said to be topochemically controlled.[9] Topochemical control of a reaction product is analogous to kinetic control in solution. The product is not necessarily the thermodynamically most stable product available to the system, but is rather the one dictated by the reaction pathway available in the constraining environment of the solid.

Regardless of whether or not topochemical control is evident in a reaction, there is often a coherence, on the molecular level, between the lattice of the product and that of the reactant; the reaction is then described as being topotactic. In other instances, the growth of the product phase proceeds in a less orderly manner, producing a product that is amorphous to X-rays. This situation seems to arise when the product lattice so fractures and disrupts the host lattice that long-range coherence between the crystal lattices is lost.

The geometric aspect of solid-state reactions can also manifest itself in the way the reaction commences and ensues throughout the solid. The products first formed, imbedded in the matrix of the reactant, may retain the molecular volume and lattice type of the reactant. Consequently, local deformation of the lattice must occur, a condition referred to generally as 'strain'. If the strain is sufficiently great, small collections of product molecules are unstable and tend to revert back to reactant. Only collections that reach a critical size are able to adopt their own lattice; thus, larger fragments are stable. Consequently, unless the product molecule can comfortably adopt the lattice of the host reactant, the reaction tends to begin at certain localized spots in the reactant and to spread from these. Thus, solid-state reactions tend to be heterogeneous processes in which distinct boundaries between reactant and product phases exist. The initial onset of the heterogeneous reaction is referred to as the nucleation stage. Once nucleation has occurred, the reaction takes place at the boundary between reactant and product phases as the nuclei grow, a process referred to as the growth stage of the reaction.

Nucleation often begins at the surface, where the product is not totally surrounded by reactant molecules. It may, however, occur at special sites either on the surface or in the bulk of the solid. The method of compound preparation and handling influences both surface area and the number and type of defects. Consequently, the rates of solid-phase reactions can depend on the history of the solid.

Nuclei may grow at different rates in different directions through the solid; however, most simple kinetic models assume isotropic growth of nuclei. Furthermore, the rate at which nuclei grow is influenced by the geometry of the sample. Thus, two samples of the same compound with the same crystal structure may react at different rates merely because of differences in the morphologies of the crystals. Studies of single crystals offer the advantages of allowing the growth of nuclei to be followed microscopically and also permitting complete description of the crystal geometry. Unfortunately, very few studies of the solid-state reactions of coordination compounds have been performed on single crystals.

Because reactions in solids tend to be heterogeneous, they are generally described by rate laws that are quite different from those encountered in solution chemistry. Concentration has no meaning in a heterogeneous system. Consequently, rate laws for solid-phase reactions are described in terms of α, the fraction of reaction (α = quantity reacted ÷ original quantity in sample). The most commonly encountered rate laws are given in Table 1. These rate laws and their application to solid-phase reactions are described elsewhere.[1–4,10–12] Unfortunately, it is often merely assumed that solid-phase reactions are first order. This uncritical analysis of kinetic data produces results that must be accepted only with great caution.

Table 1 Some Common Rate Laws

Description	*Integrated form of rate law*
Diffusion control, one dimension	$\alpha^2 = (k/x^2)t$
Diffusion control, two dimensions	$(1-\alpha)\ln(1-\alpha) + \alpha = (k/r^2)t$
Diffusion control, three dimensions	$(1-2\alpha/3)-(1-\alpha)^{2/3} = (k/r^2)t$
Phase boundary control, two dimensions	$(1-\alpha)^{1/2} = 1-kt$
Phase boundary control, three dimensions	$(1-\alpha)^{1/3} = 1-kt$
First order (random nucleation)	$\ln(1-\alpha) = -kt$
Nucleation and growth, two dimensions	$\ln(1-\alpha) = -kt^2$
Nucleation and growth, three dimensions	$\ln(1-\alpha) = -kt^3$

The method of varying initial concentrations of reactants in order to establish rate laws, which are of great importance in solution studies, is not possible for solid-state studies. The choice of rate law is therefore difficult, especially because the curve fit to experimental data is not always unique for a particular rate expression. Some of the general approaches that can be taken in obtaining a correct kinetic rate law are summarized by O'Brien.[12] Because rate constants and activation parameters depend to such a large extent on the kinetic model selected, kinetic data should be accompanied as much as possible by supporting observations involving techniques such as optical microscopy, scanning electron microscopy and X-ray diffraction. Unfortunately, such supporting studies are not always performed.

Mechanisms for solid-state reactions of coordination compounds have often been formulated based merely on comparisons of activation parameters within a series of compounds. There are, however, many potential problems associated with the use and interpretation of activation parameters in solid-state reactions.[4] Some of these are related to the problem of finding valid kinetic descriptions. The choice of rate law can have a dramatic effect on activation parameters. However, even where the question of rate law is satisfactorily resolved, there still remains the question of the meaning of these parameters, whether they reflect the chemical processes inherent to the sample, or are dependent on experimental conditions such as sample-bed thickness, particle size or atmosphere. Activation parameters obtained by non-isothermal methods, in particular, are often suspect because these questions are generally left unresolved.

In spite of all these complications, some very fine studies have been performed. Several recent studies have made very effective use of X-ray crystallography and it is hoped that there will be many more such studies in the future. Even where kinetic studies are suspect, general features may emerge that help clarify some mechanistic aspects of certain reactions.

7.5.3 LINKAGE ISOMERIZATION

Perhaps the most familiar solid-state reactions of coordination compounds are the linkage isomerization reactions of compounds containing NO_2^- and SCN^- ligands.[13] Nitrito-to-nitro isomerization was first noted in 1893 by Jørgensen and later studied extensively by many workers. This isomerization generally occurs 10–100 times faster in solution than in the solid state. In the case of $[Co(NH_3)_5ONO]X_2$ salts, the rate of the reaction in the solid state appears to be dependent on the anion, X^-.[14] Presumably a similar observation could be made for other complexes. It is to be anticipated that the nature of the interactions between the coordinated nitrito ligand and the surrounding lattice can determine the ease of linkage isomerization in the solid phase.

Nearly all nitrito compounds that isomerize in solution also isomerize in the solid state. This observation suggests that little or no change occurs in the crystal lattice during reaction. Consequently, there is a retention of crystallinity during the reaction, making this isomerization an excellent one to study by X-ray crystallography. Grenthe and Nordin have used X-ray diffraction to examine the isomerization of *trans*-$[Co(en)_2(NCS)(ONO)]X$ ($X^- = I^-$ or ClO_4^-)[15] and $[Co(NH_3)_5ONO]Cl_2$.[16] In the case of the *trans*-$[Co(en)_2(NCS)(ONO)]X$ compounds, the crystal structures of the nitrito and nitro isomers are essentially identical and indicate that the isomerization occurs intramolecularly by rotation of the NO_2^- group. The rotation path is not restricted by steric hindrance from the surrounding environment since no short van der Waals contact distances are obtained during the course of the reaction. Because only a single phase is observed throughout the reaction, it is reasonable to assume that the transformation occurs *via* formation of a solid solution (*i.e.* the reaction is homogeneous). Interestingly, the crystal structures of the nitro compounds formed in the solid-state reaction are not the same as those that are prepared from solution. The product lattice formed in a solid-state reaction is often determined by the reactant lattice and is not necessarily the lowest energy arrangement available to the system.

The isomerization of $[Co(NH_3)_5ONO]Cl_2$ also occurs by an intramolecular rotation of NO_2^-. However, in this case the isomerization is followed by a slow 90° rotation of half of the cations to give a change of space group from $P2_1nb$ to $C2/c$. This change appears to be caused by van der Waals repulsions between oxygen atoms in the first formed nitro structure and its immediate surroundings. This isomerization also appears to proceed homogeneously. However, in this case the final product is identical with that obtained from solution, except for possible slight disorder.

Snow and Boomsa have examined the linkage isomerization of $[Co(NH_3)_5SCN]Cl_2$ by X-ray diffraction studies.[17] The reaction is topotactic, but the product lattice is disordered such that a cobalt atom at 0,0,0 has 5/6 of an NH_3 group and 1/6 of an NCS^- group oriented along (100). In this case a simple intramolecular rotation of the SCN^- is prohibited by intermolecular contacts and the product structure can be explained in terms of Co—S bond rupture followed by acceptance by the $Co(NH_3)_5^{3+}$ intermediate of the N end of NCS^- from any direction. Labeling studies on solid $[Co(NH_3)_5SCN](S^{14}CN)_2$ reveal that the linkage isomerization occurs by scrambling of ionic and covalent SCN^-, consistent with an intermolecular ligand exchange process.[18] Interestingly, no Cl^-–SCN^- exchange was observed during the isomerization of $[Co(NH_3)_5SCN]Cl_2$. Labeling studies in solution indicate that $[Co(NH_3)_5SCN]^{2+}$ incorporates very little $N^{14}CS^-$, and the isomerization is proposed to occur intramolecularly.[19] That the isomerization occurs intramolecularly in solution and intermolecularly in the solid state is noteworthy, since it may imply that ion separations and ligand exchanges can occur more readily in solids than we might naively have expected. It could be, however, that the isomerization involves $Co(NH_3)_5^{2+}$ and SCN radicals, which could explain the lack of SCN^- and Cl^- exchange. In that case the mechanism could be viewed as involving a thermally induced solid-state redox reaction.

Numerous additional examples of linkage isomerization in solids have been reported.[13] Most studies have focused on elucidating the relative roles played by steric and electronic effects in determining the bonding mode of the nitrite or thiocyanate ligand. Interestingly, the bonding mode of thiocyanate has been found to be subject to counter-ion control in the solid state.[20]

7.5.4 RACEMIZATIONS

A variety of racemizations are known to be induced by heating or applying pressure to solids. O'Brien has reviewed these reactions.[12] Most studies to date have focused on tris-chelate complexes.

The earliest mention of solid-phase racemization involved $K_3[Cr(C_2O_4)_3]\cdot 2H_2O$, and the strychnine salts of $[Cr(C_2O_4)_3]^{3-}$ and $[Co(C_2O_4)_3]^{3-}$.[21] It was demonstrated that the anhydrous compounds could racemize, but that they did so at a much slower rate than the hydrated compounds. A more recent study of $K_3[Cr(C_2O_4)_3]\cdot 2H_2O$ by Chowdhury and Harris is in agreement on this matter; rapid racemization was observed during dehydration of the complex.[22] It was noted that water could be a nucleophile toward chromium, displacing one end of the oxalate or expanding the coordination shell. Subsequent deaquation could then be accompanied by racemization. The kinetic data of Chowdhury and Harris have been reinvestigated by O'Brien.[12] While O'Brien's interpretation of the kinetic data provides a reasonable model of how the reaction proceeds through the solid, it does not really allow any decision concerning the mode of racemization of the $[Cr(C_2O_4)_3]^{3-}$ ion itself.

One of the most thorough studies to date has been that by Kutal and Bailar on $[Co(en)_3]^{3+}$ salts.[23] Two features common to many other solid-phase reactions are found: the reaction is quite sensitive to anion, and it proceeds faster for hydrated salts than for anhydrous ones. Kutal and Bailar observe that the rate of racemization decreases in the order $I^- > Br^- > NCS^- > Cl^-$, which they explain in terms of the hydrogen bonding strength between anions and protons on the amine nitrogens. They argue for a trigonal-twist mechanism, suggesting that as the strength of the hydrogen bonds that must be broken decreases, the energy of activation for the twist process similarly decreases. House[24] notes that the anion effect also parallels the expected lattice energies, racemization being slower for the solid with the highest lattice energy. This correlation is also consistent with a trigonal-twist mechanism if formation of the transition state involves a volume expansion that must take place against the forces of the surrounding crystal lattice. Presumably, the weaker the lattice energy the more readily the lattice can accommodate this expansion. However, it is not clear whether formation of a trigonal-prismatic transition state would be accompanied by volume expansion for the $[Co(en)_3]^{3+}$ ion. Calculations for $[Co(C_2O_4)_3]^{3-}$ lead to a predicted volume decrease if the $C_2O_4{}^{2-}$ ligand is assumed to be rigid.[25]

The fact that the racemization of $[Co(en)_3]X_3\cdot nH_2O$ salts proceeds more rapidly for the hydrated complexes than for the anhydrous ones cannot be due to the nucleophilicity of H_2O toward the cobalt atom because $[Co(en)_3]I_3\cdot H_2O$ is found to racemize faster in the solid state than in solution![23] Instead, the dehydration process is thought to produce an open crystal structure with many defects in which inversion can occur in a less restricted fashion than is possible in the presumably more compact and defect free anhydrous compound. Interestingly, $[Co(en)_3]Cl_3\cdot H_2O$, which does not change crystal structure upon dehydration, does not racemize either as the hydrate or anhydrous compound. It is further observed (based on X-ray powder patterns) that the racemic compounds obtained from solution have different crystal structures than those obtained by solid-phase racemization.

Fujiwara and Yamamoto have studied the racemization of anhydrous compounds of the type $[M(phen)_3]X_2$ and $[M(bipy)_3]X_2$ where M = Fe or Ni and X = Cl^-, Br^-, I^- or $ClO_4{}^-$.[26] The rates of racemization of the nickel compounds were found to depend on the identity of the anion; racemization rates for the iron compounds were anion-independent. However, the kinetic analysis has been called into question.[27,28] If valid, the kinetic anion effect for the nickel compounds follows an order that is opposite that found by Kutal and Bailar[23] for the racemization of $[Co(en)_3]X_3$ salts: $ClO_4{}^- < I^- < Br^- < Cl^-$. It was proposed[25] that the iron compounds racemize by a twist mechanism and that the nickel compounds racemize by nucleophilic attack by lattice anions to form a seven-coordinate transition state.

More recently, Fujiwara has investigated the racemization of anhydrous salts of the type $[Co(phen)_{3-n}(en)_n]X_3$ where n = 0, 1 or 2 and X^- = Cl^-, Br^- or I^-.[29] All compounds exhibit anion effects. For $[Co(phen)_3]^{3+}$ the rates varied $Cl^- > Br^-$, whereas for $[Co(phen)_2(en)]^{3+}$ and $[Co(phen)(en)_2]^{3+}$ the sequence $I^- > Br^- > Cl^-$ was observed. The anion effects were interpreted in terms of the chemical interactions due to the donicity and hydrogen bonding ability of the anions. However, the kinetic analysis is open to criticism because a first-order rate law was assumed.

The pressure-induced racemizations of $K_3[Co(C_2O_4)_3]\cdot nH_2O$,[25,30] $[Ni(phen)_3](ClO_4)_2\cdot nH_2O$[31,32] and $[Fe(phen)_3](ClO_4)_2\cdot nH_2O$[31] have been studied at pressures on the order of 10000 atm. Because increasing pressure has an accelerating influence, it was suggested that the transition state in the racemization process is of smaller volume than the initial or final state. This behavior is consistent with the trigonal-twist mechanism. An associative process involving lattice water would also appear to be consistent with the negative activation volumes, but in the case of $K_3[Co(C_2O_4)_3]\cdot nH_2O$, water of hydration seemed to decrease the rate of racemization.[30]

Although the results do not appear consistent with a dissociative mechanism, such a mechanism cannot be completely ruled out. The negative activation volumes could arise from lattice changes or distortions rather than volume changes of the complex ion alone. The importance of the nature of the crystal lattice in such reactions is suggested by preliminary studies that indicate that $[Ni(phen)_3]I_2\cdot nH_2O$ cannot be made to racemize at a pressure of 3.81×10^4 atm for 70 h even though the corresponding perchlorate salt does racemize under such conditions.[33] Preliminary studies also indicate that $[Co(en)_3]I_3$ cannot be caused to racemize by application of high pressure,[31,33] although it does undergo racemization when heated.

Only one study of a *cis*-diacidobis(chelate) complex has been reported, that of *cis*-$[Cr(en)_2Cl_2]Cl\cdot H_2O$, although *cis*-$[Co(en)_2Cl_2]Cl$ has been shown to undergo solid-phase racemization.[34] The *cis*-$[Cr(en)_2Cl_2]Cl\cdot H_2O$ is reported to racemize only during dehydration, but unpublished studies suggest that the anhydrous compound may undergo slow racemization when heated.[35] The racemization of the hydrate was proposed to proceed through the *cis*-$[Cr(en)_2(H_2O)Cl]Cl_2$ intermediate. It has been observed that *cis*-$[Co(en)_2(H_2O)Cl]Cl_2$ undergoes deaquation and anation with accompanying racemization,[36] and presumably the same reaction would occur with the chromium analog. Studies of the *trans*-to-*cis* isomerization of $[Cr(en)_2Cl_2]Cl$ and similar compounds may also be pertinent to further studies on this system.[37] In the isomerization of anhydrous compounds of this sort, one-ended dissociation of coordinated amine is proposed.[38,39]

Although racemization of *cis*-$[Co(en)_2Cl_2]Cl$ has not been studied in any detail,[34] it has been observed that the racemic compound undergoes chloride exchange when heated.[40,41]. In the exchange studies, Cl^- vacancies in the crystal lattice were found to be of primary importance in determining reaction rate. The rate of Cl^- exchange was increased by irradiation with X-rays or with ^{60}Co γ-rays, which increased the number of Cl^- vacancies.

7.5.5 *CIS – TRANS* ISOMERIZATION

Many cobalt(III) and chromium(III) compounds of the dihalotetraammine[42–45] or dihalobis(diamine) type,[38,39,46] $[MN_4X_2]X$, have been found to undergo *trans*-to-*cis* or *cis*-to-*trans* isomerization in the solid phase. The amines studied include ethylenediamine, ±-propylenediamine, 1,3-propanediamine, ±-2,3-butanediamine, ±1,2-cyclohexanediamine and ±-2,4-pentanediamine. The *cis*-α-to-*cis*-β isomerization of $[Co(trien)Cl_2]Cl$ (trien = triethylenetetramine) has also been reported.[47] Although kinetic studies have been performed for most of these isomerization reactions, the data have generally been interpreted by assuming a first-order kinetic model; microscopic and other supporting studies are largely lacking.

Nevertheless, some general features of these reactions have emerged from studies to date. The cobalt compounds normally isomerize most readily during dehydration (or, in the case of compounds of the type *trans*-$[Co(AA)_2X_2](H_5O_2)X_2$, during dehydration–dehydrohalogenation). The anhydrous compounds may also isomerize, but at a much slower rate. By contrast, isomerization of chromium complexes generally occurs mainly after dehydration and requires somewhat higher temperatures than for the isomerization of the hydrated cobalt complexes. An aquation–anation pathway involving lattice water is generally invoked to explain the isomerization of the cobalt complexes. A twist mechanism has been proposed for the *cis*-α-to-*cis*-β isomerization of $[Co(trien)Cl_2]Cl$.[47] There is little substantiating evidence for these proposals. In the case of the chromium complexes, one-ended dissociation of amine is proposed to occur, and evidence has been presented for intermediates of the type $[Cr(AA)_2X_3]$, which possess an amine ligand coordinated through one end.[38,39] Calorimetric studies indicate that *cis*-to-*trans* isomerization of $[Co(en)_2X_2]X$ (X^- = Cl^- or Br^-)[48] and *trans*-to-*cis* isomerization of $[Co(NH_3)_4Cl_2]Cl$[49] proceed in the direction expected on thermodynamic grounds.

The best studied isomerizations are those of *trans*-$[Co(pn)_2Cl_2](H_5O_2)Cl_2$ and related compounds.[49–57] The dehydration–dehydrohalogenation of this compound and similar ethylenediamine compounds follows contracting-cube or contracting-square kinetics.[49,51] The dehydration–dehydrobromination of single crystals of *trans*-$[Co(en)_2Br_2](H_5O_2)Br_2$ is anisotropic, proceeding most slowly normal to the (100) faces. This behavior correlates well with the crystal structure of the complex.[51] The enthalpy change for the dehydration–dehydrohalogenation reaction has been measured for several compounds in this series and generally falls in the area of 150 kJ mol^{-1}.[51,53,56] The highly endothermic nature of the reaction causes sample self-cooling during rapid dehydration–dehydrohalogenation.[51] This effect led to early reports of activation energies that were erroneously low.[49] Once the self-cooling problem was recognized, the dehydration–dehydrohalogenation process was found to have an activation energy, E_a, approximately equal to the enthalpy change for the reaction, 150 kJ mol^{-1}.[51,53] Kinetic studies of the isomerization of *trans*-$[Co(pn)_2Cl_2](H_5O_2)Cl_2$ suggest that there is a linear correlation between percent isomerization and percent dehydration–dehydrochlorination for samples heated in thick sample beds.[50] However, the extinction coefficients used to analyze *cis*/*trans* mixtures are in error.[54] Furthermore, the activation energy reported for this isomerization, 96 kJ mol^{-1}, may be low due to self-cooling (the associated ΔH for dehydration–dehydrochlorination is reported in this same study as 42 kJ mol^{-1}, a value that is clearly too small).[50]

Radiochloride exchange studies reveal that the dehydration–dehydrochlorination of *trans*-$[Co(pn)_2Cl_2](H_5O_2)Cl_2$ is accompanied by scrambling of ionic and covalent chlorides.[52] Heating *trans*-$[Co(pn)_2Cl_2](H_5O_2)^{36}Cl_2$ at 120 °C results in loss of 25% of the chlorine-36 as HCl, and incorporation of 50% into the coordinate-covalent positions; thus the chlorides are completely scrambled. About 40% of the chloride exchanges lead to isomerization. By contrast, neither isomerization nor chloride exchange occurs when *trans*-$[Co(en)_2Cl_2](H_5O_2)Cl_2$ is treated under the same conditions.[52] To rationalize this difference it was proposed that the facile chloride exchange (and consequent isomerization) in *trans*-$[Co(pn)_2Cl_2](H_5O_2)Cl_2$ results from steric crowding at the reaction site caused by the methyl group of the propylenediamine ligand. This steric crowding can be relieved by passing through a transition state of reduced coordination number *via* loss of a chloride ion. To test this idea, several *N*-substituted ethylenediamine compounds were studied.[55] The *N*,*N*′-dimethylethylenediamine complex, *trans*-$[Co(dimeen)_2Cl_2](H_5O_2)Cl_2$, undergoes chloride scrambling to an extent somewhat less than that of the propylenediamine complex; isomerization is precluded by strong steric interactions between methyl groups in the *cis* isomer. The *N*-methylethylenediamine and *N*-ethylethylenediamine complexes do isomerize, but experimental difficulties have precluded radiochloride exchange studies.

Comparison of the crystal structures of *trans*-$[Co(en)_2Cl_2](H_5O_2)Cl_2$[58] and *trans*-$[Co(pn)_2Cl_2](H_5O_2)Cl_2$[59] reveals another factor that may be significant in explaining the different chloride exchange behavior of these compounds. In the ethylenediamine complex the closest distance between a covalent chloride and an ionic one is 4.21 —, whereas the corresponding distance in the propylenediamine complex is shorter, 3.80 —. Further crystal structures of other compounds of this sort together with accompanying chloride exchange studies are needed to determine whether this chloride–chloride distance or any other crystallographic feature of the solids is important in determining chloride exchange and isomerization behavior.

Complexes of other metal ions have also been observed to undergo *cis*–*trans* isomerization in the solid state. For example, *cis*-$[Cu(glycinato)_2]\cdot H_2O$ undergoes *cis*-to-*trans* isomerization upon dehydration at temperatures above 180 °C.[60] Thermal isomerization of compounds of the sort *trans*-$[PtLAX_2]$, where L is a ligand with a strong *trans* influence, is reportedly a widespread phenomenon.[61,63] The *cis*-to-*trans* isomerization of PtA_2X_2 (A = dimethyl sulfide and diethyl sulfide, X = Cl or Br) and the *trans*-to-*cis* isomerization of PtT_2Br_2 (T = thiopane) have also been reported.[62] No kinetic or other mechanistic studies have been reported for these reactions.

7.5.6 LIGAND EXCHANGE AND ANATION

A variety of ligand exchange reactions have been reported to take place in the solid state. Several of these accompany isomerization and have been referred to in earlier sections. For example, linkage isomerization of $[Co(NH_3)_5SCN](S^{14}CN)_2$ involves scrambling of ionic and covalent SCN^-.[18] The *trans*-to-*cis* isomerization of *trans*-$[Co(pn)_2Cl_2](H_5O_2)^{36}Cl$ involves chloride exchange.[52] Halogen exchange also occurs when *trans*-$[Co(pn)_2Cl_2](H_5O_2)Br_2$ and *trans*-$[Co(pn)_2Br_2](H_5O_2)Cl_2$ are heated.[52] The anhydrous *trans*-$[Co(en)_2Cl_2]{}^*Cl$, *trans*-$[Co(en)_2Br_2]{}^*Br$ and *cis*-$[Co(en)_2Cl_2]{}^*Cl$ also undergo halide exchange between ionic and covalent positions, but to a lesser extent and at higher temperatures than *trans*-$[Co(pn)_2Cl_2](H_5O_2){}^*Cl_2$.[40,41] Virtually identical rates and activation energies are exhibited for the halide exchange in these three anhydrous compounds, suggesting that bond making or bond breaking is not rate determining. Rather, it is proposed that anion vacancies are of primary importance in determining reaction rate.[40,41]

The isomerization of $[Co(en)(NH_3)_2Cl_2]SCN \cdot H_2O$ from the *cis*-dichloro-*trans*-diamine configuration to the *cis,cis* configuration is accompanied by chloride–thiocyanate exchange.[64] Several compounds of the type *cis*-$[Co(en)_2XY]SCN \cdot nH_2O$ similarly undergo halide–thiocyanate exchange. However, no racemization or isomerization is observed in these cases.[65] Kinetic studies of a rather superficial nature were performed on these reactions. Because activation energies for dehydration and ligand exchange in *cis*-$[Co(en)_2ClBr]SCN \cdot H_2O$ differ greatly (109 kJ mol^{-1} *versus* 226 kJ mol^{-1}), it was concluded that an aquation–anation pathway is not involved in these reactions.[65] Instead, an associative mechanism involving attack of the complex cation by SCN^- was postulated. However, there seems to be no strong reason why the mechanism could not equally well involve a dissociative loss of halide to form a square-based pyramidal transition state or intermediate.

A number of studies of anion exchange between coordination compounds and ammonium salts have been reported.[66,67] For example, *cis*-$[Co(en)_2(H_2O)_2](NO_3)_3$ is reported to react with NH_4Cl to form *trans*-$[Co(en)_2Cl_2]NO_3$.[66]

The most common and widely studied ligand exchange reactions are those that occur when a volatile ligand such as H_2O or pyridine is displaced from the coordination sphere of a complex ion and is replaced by an anion from the crystal lattice. Thus, heating $[Co(NH_3)_5(H_2O)]Cl_3$ produces $[Co(NH_3)_5Cl]Cl_2$; similarly, heating $[Co(en)_2(py)Br]Br_2$ produces $[Co(en)_2Br_2]Br$. Numerous kinetic studies have been performed on reactions of this sort. In particular, the deaquation–anation of the aquapentaammine complexes of cobalt(III) and chromium(III) have received considerable attention.[68,69] These reactions are reported to exhibit an entering-group (or anion) effect, with activation parameters varying with anion. The usual interpretation of this apparent anion effect is that it signifies an S_N2 (associative) ligand exchange between the leaving H_2O and the entering anion. However, it has been pointed out that an anion effect in such reactions can arise from differences in crystal lattices even if the ligand-exchange mechanism is S_N1 (dissociative).[24,68] Furthermore, the activation parameters reported by different research groups for such deaquation–anations are in poor agreement.[68] For example, the activation parameters reported for $[Cr(NH_3)_5(H_2O)]X_3$ salts show variations for any given anion that are as large as the variations between anions.

The differences in the results reported by different research groups may arise in part from the use of different rate laws in treating data. However, it has been suggested that the activation parameters for these reactions are strongly influenced by experimental conditions that have not been specified nor controlled in these experiments. Such factors include particle size, sample-bed thickness and the nature of the atmosphere around the sample. Indeed, studies on $[Co(NH_3)_5(H_2O)]X_3$ salts reveal that these factors strongly affect activation parameters.[69] Interestingly, all data reported for both $[Cr(NH_3)_5(H_2O)]X_3$ and $[Co(NH_3)_5(H_2O)]X_3$ ($X^- = Cl^-$, Br^-, I^- or NO_3^-) show a linear correlation of ΔH^+ and ΔS^+. (This relationship is referred to as the isokinetic effect; the related linear correlation of E_a and log A is called the kinetic compensation effect.) The isokinetic behavior of the chromium and cobalt complexes is statistically indistinguishable.[69] If the correlation is taken to mean that a common mechanism is operative throughout the series, then, we must conclude that the rate is not determined by either bond making or bond breaking. It could be that the rate is determined merely by diffusion of water from the reaction interface. Indeed, for reactions involving evolution of a gaseous product, adsorption phenomena or the back-reaction of the gaseous product with the solid product can affect kinetics.[70]

An anion effect is also reported for the solid-state anations of *cis*-$[Co(en)_2(py)X]Y_2$ ($X^- = Cl^-$ or Br^-; $Y^- = Br^-$ or I^-). Experimental conditions affect activation parameters, and the kinetic compensation effect is observed (that is, E_a is linearly correlated with log A). However, the correlation is different for $[Co(en)_2(py)X]Br_2$ than for $[Co(en)_2(py)X]I_2$.[71] This result suggests that the chemical process of importance is anion-dependent. It is proposed that the Co—py bond strength is affected by polarization effects due to the surrounding ionic halides.

The stereochemical course of anations has been examined in some systems. The deaquation and anation of *cis*- and *trans*-$[Co(en)_2(H_2O)_2]X_3$ ($X^- = Cl^-$ or Br^-) have been studied.[72] When $X^- = Cl^-$, the product in each case is *cis*-$[Co(en)_2Cl_2]Cl$; a mixture of *cis* and *trans* isomers forms when $X^- = Br^-$. The deaquation–anation of a series of compounds of the type *cis*-$[CoN_4(H_2O)X]Y_2$, where $X^- = Cl^-$ or Br^-, N_4 is tetraammine or bis(ethylenediamine) and $Y^- = Cl^-$, Br^- or NO_3^-, has also been investigated. When $X^- = Y^- = Cl^-$ the anation occurs with retention of configuration; the *trans* isomer forms when $X^- = Y^- = Br^-$.[73]

Another system that has been widely studied is the thermal deamination and anation of $[Cr(en)_3]X_3$ complexes.[74–80] Of these, the SCN^- and Cl^- salts have been most extensively studied.

Deamination of $[Cr(en)_3](NCS)_3$ produces *trans*-$[Cr(en)_2(SCN)_2]SCN$, whereas deamination of $[Cr(en)_3]Cl_3$ produces *cis*-$[Cr(en)_2Cl_2]Cl$. These reactions are catalyzed by NH_4SCN and NH_4Cl, respectively, although other acidic salts are effective catalysts as well. The role of the catalyst appears to be protonation of one end of the ethylenediamine ligand, thereby aiding in removal of the ethylenediamine from the coordination sphere. It is reported that HCl gas also catalyzes deamination of $[Cr(en)_3]Cl_3$, supporting the idea that the ammonium salt catalyst, NH_4X, functions by dissociation to form HX.[77] Efforts to correlate the thermal behavior of these compounds with their crystal structures have not provided much insight.[78–80]

7.5.7 OTHER THERMAL REACTIONS

Quite a number of interesting solid-state reactions have been observed that do not quite fit into the categories of earlier sections. These include reactions of coordinated ligands, changes of coordination number or geometry and polymerization reactions. Limitations of space do not permit detailed discussions of these reactions.

Few accounts of the reactions of coordinated ligands have been published. One recent report indicates that the copper complex of *S*-methylmethionine yields the copper complex of α-amino-γ-butyrolactone and dimethyl sulfide upon heating.[81]

A series of papers by Ohashi and coworkers has dealt with the racemization (actually epimerization) of complexes of *R*-α-cyanoethylbis(dimethylglyoximato)cobalt(III).[82–85] Exposure of these compounds to X-rays causes racemization of the cyanoethyl group without degradation of crystallinity. Extensive X-ray studies have been performed in which the effects of the reaction cavity around the cyanoethyl group have been examined. The reaction rate for these reactions shows a positive correlation with the volume of the cavity. The proposed mechanism involves formation of a planar cyanoethyl radical produced by Co—C bond cleavage. The radical rotates around the Co—C═N axis and then recombines with cobalt to give the racemic complex. Corresponding compounds containing the methoxycarbonylethyl group have also been examined.[85]

The chemistry of nickel(II) affords a number of interesting solid-state reactions in which the nickel changes either coordination number or geometry. When compounds of the type $[Ni(AA)_2(H_2O)_2]X_2$ (where AA is ethylenediamine or a *C*- or *N*-substituted ethylenediamine and X is a uninegative anion such as Cl^- or ClO_4^-) are heated in the solid state, they may undergo deaquation–anation with formation of an octahedral product, $[Ni(AA)_2X_2]$. However, they may merely undergo deaquation with the formation of a square-planar product, $[Ni(AA)_2]X_2$. The reaction path depends on the nature of both the amine and the anion. In general, more bulky amines produce a square-planar product as do anions such as ClO_4^- that are poor nucleophiles toward metals.[86–88]

Some square-planar compounds of the type $[Ni(AA)_2]X_2$ are reported to undergo reversible thermochroic behavior when heated beyond the temperature range for dehydration. This behavior has been attributed to reversible square-planar to octahedral conversion.[87,88] However, the thermochroic behavior of the similar copper compound, $[Cu(AA)_2](ClO_4)_2$ (where AA is *N,N*-diethylethylenediamine), does not involve a change in coordination number; rather, a change in the in-plane field strength appears to be the cause.[89]

The compounds $[NiBr_2R_2]$, where R = $PEtPh_2$ or PPr^iPh_2, undergo a change from square-planar to tetrahedral at room temperature.[90] The compound $[Et_4As]_4[Ni(NCS)_4]$ undergoes a change from an octahedral form (with thiocyanate bridges) to an approximately tetrahedral geometry at 155 °C.[91] The isomerization of $[NiL_6][NiCl_4]$ into NiL_3Cl_2 (where L is *N,N′*-dimethylurea) has also been reported.[92]

$NiX_2[P(CH_2CH_2CN)_3]_2$ (where $X^- = Cl^-$, Br^- or I^-) undergoes an isotropic solid-phase polymerization in which the square-planar complex is converted into an octahedral one with bridging cyanoethylphosphine groups. The reaction has been examined by optical microscopy and X-ray crystallography. Three unique monomer phases have been identified. Each behaves differently as the polymerization progresses. However, all lead to the same polymeric product phase. The polymerization proceeds topotactically, and the product is topochemically controlled.[93,94]

Finally, we wish to call attention to a kinetic study of the addition of HCl gas to solid $[IrClCO(PPh_3)_2]$ to form the *trans*-chloro complex $[Ir(H)Cl_2CO(PPh_3)_2]$.[95]

7.5.8 PHOTOCHEMICAL REACTIONS

Most solid-state photoreactions that have been reported involve photoredox, although examples of photoisomerization and photoaquation involving lattice water have also appeared. For example, photolysis of $[Co(NH_3)_5(H_2O)]X_3$ salts ($X^- = Cl^-$, Br^- or I^-) produces cobalt(II).[96] The photoreduction of $K_3[Fe(C_2O_4)_3]\cdot 3H_2O$ has also been investigated; in this case a mechanism with electron–hole pairs and radical ions as intermediates is suggested.[97]

Excitation of the charge-transfer transition of $[Co(NH_3)_5SCN]Cl_2$ in KBr pellets leads to linkage isomerization without redox decomposition.[98] It is proposed that the isomerization involves formation of $Co(NH_3)_5^{2+}$ and SCN radicals followed by geminate recombination of the radicals. Salts of $[Co(NH_3)_5NO_2]^+$ are also photosensitive, undergoing nitro-to-nitrito isomerization.[15,16,99] Some $[Cr(en)_3]X_3$ salts ($X^- = Cl^-$, Br^- or SCN^-) undergo photochemical loss of ethylenediamine accompanied by anation by lattice anions to give $[Cr(en)_2X_2]X$ species.[100,101]

Photoaquation involving lattice water has been observed for *trans*-$[Cr(en)_2X_2]X\cdot H_2O$ (where $X^- = Cl^-$ or Br^-). The quantum efficiency is very similar to that for the aquation in water solution, and the photoaquation apparently obeys the same photostereochemical selection rules that apply in solution.[102]

7.5.9 CONCLUSIONS

Coordination compounds have been found to undergo a wide variety of solid-state reactions. Although kinetic studies have been reported for many of these reactions, their mechanisms are not generally well understood. There appears to be much data collection, but little critical hypothesis testing. Furthermore, kinetic data often appear to be of poor quality owing to improper choice of rate law and incomplete description of experimental details, particularly details concerning the condition of the solid sample. Basic data are lacking in many articles, hampering reevaluation of experimental results.

The studies to date have been successful in providing patterns of reactivity and in pointing out certain general features of reactions. For example, it is frequently found that reactions occur more rapidly for hydrated compounds than for anhydrous ones. Two general explanations have been put forth: the water may act as a nucleophile; this mechanism is often referred to as the aquation–anation mechanism. The second idea is that loss of water provides lattice defects that permit more facile rearrangements. Another general observation is that many reactions of cations are sensitive to the identity of the accompanying lattice anions. In some cases this anion effect has been ascribed to anion nucleophilicity. On other occasions it has been related to the lattice rigidity (as measured by lattice energies), to the general openness of the lattice (in terms of the spaciousness of reaction cavities), to the distances between reactive centers, to the ease with which defects are generated, or to intermolecular interactions such as hydrogen bonding between a complex and its surrounding ions.

Further X-ray studies would be helpful in many systems. However, products are sometimes amorphous to X-rays, limiting the application of this technique. Optical and electron microscopy studies on single crystals could be useful, but such studies have been relatively rare. It is hoped that further studies focus not only on finding new examples of solid-state reactions, but that imaginative application of these tools and other physical techniques applicable to solids will be applied increasingly to these reactions in the future.

7.5.10 REFERENCES

1. W. E. Garner (ed.), 'Chemistry of the Solid State', Butterworths, London, 1955.
2. D. A. Young, 'Decomposition of Solids', Pergamon, London, 1966.
3. C. H. Bamford and C. F. H. Tipper (eds.), 'Comprehensive Chemical Kinetics', Elsevier, New York, 1980, vol. 22.
4. P. D. Garn, *CRC Crit. Rev. Anal. Chem.*, 1972, **3**, 65.
5. M. D. Cohen, *Angew. Chem., Int. Ed. Engl.*, 1975, **14**, 386.
6. I. C. Paul and D. Y. Curtin, *Science*, 1975, **187**, 19.
7. I. C. Paul and D. Y. Curtin, *Acc. Chem. Res.*, 1973, **6**, 217.
8. A. Gavezotti and M. Simonetta, *Chem. Rev.*, 1982, **82**, 1.
9. See, for example, J. M. Thomas, S. E. Morsi and J. P. Desvergne, *Adv. Phys. Org. Chem.*, 1977, **15**, 63; J. M. Thomas, *Philos. Trans. R. Soc. London, Ser. A*, 1974, **277**, 251.
10. W. L. Ng, *Aust. J. Chem.*, 1975, **28**, 1169.
11. C. J. Keattch and D. Dollimore, 'An Introduction to Thermogravimetry', 2nd edn., Heyden, New York, 1975, chap. 4 and 5.
12. P. O'Brien, *Polyhedron*, 1983, **2**, 233.
13. R. J. Balahura and N. A. Lewis, *Coord. Chem. Rev.*, 1976, **20**, 109.
14. B. Adell, *Z. Anorg. Allg. Chem.*, 1952, **271**, 49; B. Adell, *ibid.*, 1956, **284**, 197; I. R. Beattie and D. P. N. Satchell, *Trans. Faraday Soc.*, 1956, **52**, 1590.
15. I. Grenthe and E. Nordin, *Inorg. Chem.*, 1979, **18**, 1109.
16. I. Grenthe and E. Nordin, *Inorg. Chem.*, 1979, **18**, 1869.
17. M. R. Snow and R. F. Boomsa, *Acta Crystallogr., Sect. B*, 1972, **28**, 1908.
18. M. R. Snow and R. J. Thomas, *Aust. J. Chem.*, 1974, **27**, 1391.

19. D. A. Buckingham, I. I. Creaser and A. M. Sargeson, *Inorg. Chem.*, 1970, **9**, 655.
20. J. L. Burmeister, R. L. Hassel, K. A. Johnson and J. C. Lim, *Inorg. Chim. Acta*, 1974, **9**, 23.
21. C. H. Johnson and A. Mead, *Trans. Faraday Soc.*, 1933, **29**, 626; C. H. Johnson, *ibid.*, 1935, **31**, 612; C. H. Johnson and A. Mead, *ibid.*, 1935, **31**, 1621.
22. D. M. Chowdhury and G. M. Harris, *J. Phys. Chem.*, 1969, **73**, 3366.
23. C. Kutal and J. C. Bailar, Jr., *J. Phys. Chem.*, 1972, **76**, 119.
24. J. E. House, Jr., *Thermochim. Acta*, 1980, **38**, 59.
25. J. Brady, F. Dachille and C. D. Schmulbach, *Inorg. Chem.*, 1963, **2**, 803.
26. T. Fujiwara and Y. Yamamoto, *Inorg. Chem.*, 1980, **19**, 1903.
27. P. O'Brien, *J. Chem. Soc., Dalton Trans.*, 1982, 1173.
28. T. Fujiwara and Y. Yamamoto, *J. Chem. Soc., Dalton Trans.*, 1982, 1174.
29. T. Fujiwara, *Bull. Chem. Soc. Jpn.*, 1983, **56**, 122.
30. C. D. Schmulbach, J. Brady and F. Dachille, *Inorg. Chem.*, 1968, **7**, 287.
31. C. D. Schmulbach, F. Dachille and M. E. Bunch, *Inorg. Chem.*, 1964, **3**, 808.
32. G. E. Humiston and J. E. Brady, *Inorg. Chem.*, 1969, **8**, 1773.
33. J. Brady, Ph.D. Thesis, Pennsylvania State University, 1963, pp. 38–40.
34. H. E. LeMay, Jr. and J. C. Bailar, Jr., *J. Am. Chem. Soc.*, 1968, **90**, 1729.
35. J. C. Bailar, Jr., University of Illinois, personal communication.
36. J. P. Mathieu, *Bull. Soc. Chim. Fr.*, 1937, **4**, 687.
37. C. Sato and S. Hatakeyama, *Bull. Chem. Soc. Jpn.*, 1972, **45**, 646.
38. S. Mitra, T. Yoshikuni, A. Uehara and R. Tsuchiya, *Bull. Chem. Soc. Jpn.*, 1979, **52**, 2569.
39. R. Tsuchiya, A. Uehara and T. Yoshikuni, *Inorg. Chem.*, 1982, **21**, 590.
40. G. B. Schmidt and K. Rossler, *Radiochim. Acta*, 1966, **5**, 123.
41. K. Rossler and W. Herr, *Angew. Chem., Int. Ed. Engl.*, 1967, **6**, 993.
42. G. W. Watt and D. A. Butler, *Inorg. Chem.*, 1966, **5**, 1106.
43. H. E. LeMay, Jr. and J. C. Bailar, Jr., *J. Am. Chem. Soc.*, 1967, **89**, 5577; H. E. LeMay, Jr., J. R. Sheen and M. W. Babich, *J. Inorg. Nucl. Chem.*, 1972, **34**, 149.
44. R. Tsuchiya, A. Uehara and T. Nokayama, *Bull. Chem. Soc. Jpn.*, 1983, **56**, 3284.
45. K. Nagase and N. Tanaka, *Bull. Chem. Soc. Jpn.*, 1972, **45**, 1097.
46. R. Tsuchiya and A. Uehara, *Thermochim. Acta*, 1981, **50**, 93.
47. A. Sault, F. Fry and J. C. Bailar, Jr., *J. Inorg. Nucl. Chem.*, 1980, **42**, 201.
48. R. Tsuchiya, A. Uehara and Y. Muramatsu, *Bull. Chem. Soc. Jpn.*, 1982, **55**, 3770.
49. H. E. LeMay, Jr., *Inorg. Chem.*, 1968, **7**, 2531.
50. R. Tsuchiya, K. Murai, A. Uehara and E. Kyuno, *Bull. Chem. Soc. Jpn.*, 1970, **43**, 1383.
51. H. E. LeMay, Jr., *J. Phys. Chem.*, 1970, **74**, 1345.
52. H. E. LeMay, Jr., *Inorg. Chem.*, 1971, **10**, 1990.
53. H. E. LeMay, Jr. and P. S. Nolan, *Inorg. Nucl. Chem. Lett.*, 1971, **7**, 355.
54. H. E. LeMay, Jr. and D. L. Aalbers, *Inorg. Nucl. Chem. Lett.*, 1973, **9**, 469.
55. H. E. LeMay, Jr. and J. C. Seher, *J. Inorg. Nucl. Chem.*, 1977, **39**, 1965.
56. R. Tsuchiya, Y. Natsume, A. Uehara and E. Kyuno, *Thermochim. Acta*, 1975, **12**, 147.
57. T. Yoshikuni, R. Tsuchiya, A. Uehara and E. Kyuno, *Bull. Chem. Soc. Jpn.*, 1978, **51**, 113.
58. J. Roziere and J. M. Williams, *Inorg. Chem.*, 1976, **15**, 1174.
59. Y. Saito and H. Iwasaki, *Bull. Chem. Soc. Jpn.*, 1962, **35**, 1131.
60. B. W. Delf, R. D. Gillard and P. O'Brien, *J. Chem. Soc., Dalton Trans.*, 1979, 1301.
61. Y. N. Kukushkin, V. F. Budanova and G. N. Snedova, *Russ. J. Inorg. Chem. (Engl. Transl.)*, 1976, **21**, 768.
62. Y. N. Kukushkin, V. N. Budanova, G. N. Snedova, V. G. Pogareva, Y. N. Fadeov and M. S. Soboleva, *Russ. J. Inorg. Chem. (Engl. Transl.)*, 1976, **21**, 689.
63. E. A. Andronov, Y. N. Kukushkin, T. M. Lukicheva, L. V. Konovalov, S. I. Konovalov, S. I. Bakhireva and E. S. Postnikova, *Russ. J. Inorg. Chem. (Engl. Transl.)*, 1976, **21**, 1343.
64. R. Tsuchiya, M. Suzuki and E. Kyuno, *Bull. Chem. Soc. Jpn.*, 1971, **44**, 709.
65. R. Tsuchiya, T. Murakami and E. Kyuno, *Bull. Chem. Soc. Jpn.*, 1973, **46**, 3119.
66. F. C. Chang and W. W. Wendlandt, *J. Inorg. Nucl. Chem.*, 1970, **32**, 3535.
67. G. Grassini–Strazza, C. M. Polcaro, V. Carunchio and A. Messina, *Inorg. Chim. Acta*, 1978, **29**, L265.
68. H. E. LeMay, Jr., *Thermochim. Acta*, 1978, **23**, 349.
69. H. E. LeMay, Jr. and M. W. Babich, *Thermochim. Acta*, 1981, **48**, 147.
70. H. R. Oswald, A. Reller and M. Maciejewski, *Thermochim. Acta*, 1984, **72**, 139.
71. J. Zsako, G. Marcu and M. Varhelyi, *Rev. Roum. Chim.*, 1982, **27**, 815.
72. F. C. Chang and W. W. Wendlandt, *J. Inorg. Nucl. Chem.*, 1970, **32**, 3775.
73. R. Tsuchiya, M. Suzuki and E. Kyuno, *Bull. Chem. Soc. Jpn.*, 1972, **45**, 3105.
74. J. E. House, Jr. and J. C. Bailar, Jr., *J. Am. Chem. Soc.*, 1969, **91**, 67.
75. J. E. House, Jr., G. L. Jepsen and J. C. Bailar, Jr., *Inorg. Chem.*, 1979, **18**, 1397.
76. A. Uehara, Y. Nishiyama and R. Tsuchiya, *Inorg. Chem.*, 1982, **21**, 2422.
77. M. A. Hughes, *J. Therm. Anal.*, 1975, **8**, 99.
78. K. Akabori and Y. Kushi, *J. Inorg. Nucl. Chem.*, 1978, **40**, 625.
79. K. Akabori and Y. Kushi, *J. Inorg. Nucl. Chem.*, 1978, **40**, 1317.
80. K. Akabori, *J. Inorg. Nucl. Chem.*, 1981, **43**, 677.
81. P. O'Brien, *Inorg. Chim. Acta*, 1981, **55**, L27.
82. Y. Ohashi, K. Yanagi, T. Kurihara, Y. Sasada and Y. Ohgo, *J. Am. Chem. Soc.*, 1981, **103**, 5805.
83. Y. Ohashi, K. Yanagi, T. Kurihara, Y. Sasada and Y. Ohgo, *J. Am. Chem. Soc.*, 1982, **104**, 6353.
84. Y. Ohashi, A. Uchida, Y. Sasada and Y. Ohgo, *Acta Crystallogr. Sect. B*, 1983, **39**, 54.
85. T. Kurihari, A. Uchida, Y. Ohashi, Y. Sasada, Y. Ohgo and S. Baba, *Acta Crystallogr., Sect. B*, 1983, **39**, 431.
86. Y. Ihara, E. Izumi, A. Uehara, R. Tsuchiya, S. Nakagawa and E. Kyuno, *Bull. Chem. Soc. Jpn.*, 1982, **55**, 1028.
87. H. Nishimoto, T. Yoshikuni, A. Uehara, E. Kyuno and R. Tsuchiya, *Bull. Chem. Soc. Jpn.*, 1978, **51**, 1068.
88. Y. Ihara, T. Kamishima and R. Tsuchiya, *Thermochim. Acta*, 1983, **67**, 23.
89. I. Grenthe, P. Paoletti, M. Sandström and S. Glikberg, *Inorg. Chem.*, 1979, **18**, 2687.
90. R. G. Hayter and F. S. Humiec, *Inorg. Chem.*, 1965, **4**, 1701.

91. D. Forster and D. M. L. Goodgame, *Inorg. Chem.*, 1965, **4**, 823.
92. J. P. Barbier and R. P. Hugel, *Inorg. Chim. Acta*, 1977, **24**, 1.
93. B. M. Foxman, P. L. Goldberg and H. Mazurek, *Inorg. Chem.*, 1981, **20**, 4368.
94. K. Cheng and B. M. Foxman, *J. Am. Chem. Soc.*, 1977, **99**, 8102.
95. M. C. Ball and J. M. Pope, *J. Chem. Soc., Dalton Trans.*, 1973, 1802.
96. S. T. Spees and P. Z. Petrak, *J. Inorg. Nucl. Chem.*, 1970, **32**, 1229.
97. H. E. Spencer and M. W. Schmidt, *J. Phys. Chem.*, 1971, **75**, 2986.
98. A. Vogler and H. Kunklly, *Inorg. Chim. Acta*, 1975, **14**, 247.
99. D. A. Johnson and K. A. Pashman, *Inorg. Nucl. Chem. Lett.*, 1975, **11**, 23.
100. C. H. Strembridge and W. W. Wendlandt, *J. Inorg. Nucl. Chem.*, 1965, **27**, 129.
101. G. Sartori, F. Castelli and E. Cervone, *Gazz. Chim. Ital.*, 1971, **101**, 32.
102. A. D. Kirk and P. A. Warren, *Inorg. Chem.*, 1985, **24**, 720.

8.1

Electrochemistry and Coordination Chemistry

CHRISTOPHER J. PICKETT
University of Sussex, Brighton, UK

8.1.1 INTRODUCTION

Electrochemistry and coordination chemistry overlap in many important areas of fundamental and technological interest, for example in understanding the redox chemistry of metal centres of biological significance; in defining the photoredox chemistry of coordination compounds of relevance to solar energy conversion; in elucidating mechanisms of corrosion and its inhibition; and in the design of electrochemical devices such as power sources, sensors and displays.

The coordination chemist may be interested in the electrosynthesis of compounds, the generation and detection of unstable species in unusual oxidation states and the study of their mechanisms of decay or their spectroscopic properties, or in simply obtaining thermodynamic data. These, and related topics such as using electrogenerated metallo intermediates to catalyze the transformation of inert molecules, modifying the properties of an electrode surface by adsorbing or otherwise binding a coordination compound to it, or fundamental aspects of electron-transfer kinetics, are readily studied by the application of modern electrochemical techniques.

8.1.2 CYCLIC VOLTAMMETRY

Cyclic voltammetry is one such electrochemical technique which has found considerable favour amongst coordination chemists. It allows the study of the solution electron-transfer chemistry of a compound on the sub-millisecond to second timescale; it has a well developed theoretical basis and is relatively simple and inexpensive. Cyclic voltammetry is a controlled potential technique; it is performed at a stationary microelectrode which is in contact with an electrolyte solution containing the species of interest. The potential, E, at the microelectrode is varied linearly with time, t, and at some pre-determined value of E the scan direction is reversed. The current which flows through the cell is measured continuously during the forward and reverse scans and it is the analysis of the resulting i–E response, and its dependence on the scan rate $\mathrm{d}E/\mathrm{d}t$, which provides a considerable amount of information. Consider, for example, the idealized behaviour of a compound, M, in an inert electrolyte at an inert microelectrode (Scheme 1).

$$\mathrm{M} \; \underset{\substack{+ne \\ E^{\circ\prime}}}{\overset{-ne}{\rightleftharpoons}} \; \mathrm{M}^{n+} \xrightarrow{k} \text{Product}$$

Scheme 1

Cyclic voltammetry can: (i) determine the electrochemical reversibility of the primary oxidation (or reduction) step; (ii) allow the formal potential, $E^{\circ\prime}$, of the reversible process to be estimated; (iii) provide information on the number of electrons, n, involved in the primary process; and (iv) allow the rate constant for the decomposition of the M^{n+} species to be measured. Additional information can often be obtained if intermediates or products derived from M^{n+} are themselves electroactive, since peaks associated with their formation may be apparent in the cyclic voltammogram. The idealized behaviour illustrated by Scheme 1 is a relatively simple process; more complicated processes such as those which involve further electron transfer following the chemical step, pre-equilibria, adsorption of reactants or products on the electrode surface, or the attack of an electrogenerated product on the starting material, are also amenable to analysis.

There are several excellent articles which deal with the theory and practice of cyclic voltammetry.[1–4] Foremost among these is the comprehensive treatise by Bard and Faulkner which gives a thorough description of the theory of controlled potential microelectrode techniques, including cyclic voltammetry.[1] Particularly readable accounts of cyclic voltammetry and related techniques are given in Adams' book, 'Electrochemistry at Solid Electrodes',[2] in Pletcher's review[3] and in a series of articles which appeared in *J. Chem. Educ.*[4]

Whilst cyclic voltammetry is an informative technique, quantitative studies, particularly on the kinetics of decay of an electrogenerated intermediate, are often best made using other controlled potential techniques. In particular, potential-step and rotating ring-disc measurements give high-quality data.[1]

8.1.3 SPECTROELECTROCHEMICAL METHODS

Spectroelectrochemical methods provide the coordination chemist with a means of generating unstable species and examining their spectroscopic properties.[1,5] In addition, such methods can provide kinetic and mechanistic information complementary to that derived by electrochemical techniques alone. Two spectroelectrochemical techniques have found widespread use in the area of coordination chemistry: transmission UV–visible spectroscopy, using optically transparent electrodes (OTE) or optically transparent thin layer electrodes (OTTLE); and *in situ* electrolysis–EPR methods. The former technique relies on the use of transparent thin films of metals deposited on glass, conducting glasses such as antimony-doped tin oxide, or so-called 'mini-grids' of gold or platinum wires. The potential at the OTE or OTTLE is controlled, and the optical response recorded as a function of time and wavelength during the generation of intermediates.

In situ electrolysis–EPR methods usually employ a wire or grid electrode contained in a conventional flat or tube EPR cell. The constraints on the geometric configuration are such that secondary and reference electrodes are usually remote from the generating electrode, which often leads to problems in the control of the potential; nevertheless it is a valuable technique for recording spectra of EPR active intermediates. These and related spectroelectrochemical techniques have been reviewed by Robinson.[5]

8.1.4 SYNTHESIS

The coordination chemist can use controlled potential methods to synthesize compounds. Typically electrolyses are performed at large electrodes in a divided cell; products of electrolysis at the controlled electrode are isolated from the (undesirable) products generated at the counter electrode by a porous glass frit or semi-permeable membrane. The course of a preparative-scale electrolysis can be monitored by a variety of techniques: the current-decay can be measured as a function of charge passed (coulometry), the consumption of starting material, or the generation of stable intermediates, and the formation of products can be followed by *ex situ* spectroscopic techniques or indeed by *in situ* methods such as cyclic voltammetry. There are two clear advantages which controlled potential methods can have over chemical oxidation or reduction methods. The first is that fairly precise thermodynamic control of the process can be achieved: in a suitable electrolyte the energy of the electrode (its oxidizing or reducing power) can be infinitely varied about ±3 V *versus* the standard hydrogen electrode. The second advantage is that electrochemical oxidations or reductions can be performed in 'clean' systems. In using Cl_2 as an oxidizing agent, for example, there is the distinct possibility of producing chloro compounds; with NO^+, nitrosyl complexes may result. There are disadvantages; diffusion-controlled heterogeneous reduction or oxidation at an electrode surface takes longer than corresponding homogeneous chemical processes. Electrolysis times can be minimized by efficient stirring and by maximizing the electrode area/solution volume ratio. Controlled potential electrolysis methods have been reviewed and a discussion of the practical aspects of cell design, electrolytes and electrodes is given in a book by Sawyer.[1,6,7]

This chapter has confined itself to a brief description of the common controlled potential methods which can be employed by the coordination chemist, but it is worth pointing out that far less sophisticated constant current methods, a DC supply and two electrodes in an undivided cell, have been used very successfully to electrosynthesize a wide range of coordination compounds, notably by anodic dissolution of a metal, *i.e.* metal ions are 'sprayed' into an electrolyte solution containing an appropriate ligand.[7] It must also be remembered that virtually all industrial-scale electrosyntheses are performed by controlling current density rather than potential.[8] Nevertheless, understanding the fundamental nature of an electrochemical process, and using this knowledge to design new and improve old electrosyntheses, demands the more sophisticated techniques, and this underpins the electrochemical science.

8.1.5 REFERENCES

1. A. J. Bard and L. R. Faulkner, 'Electrochemical Methods', Wiley, New York, 1980.
2. R. N. Adams, 'Electrochemistry at Solid Electrodes', Dekker, New York, 1969.
3. D. Pletcher, *Chem. Soc. Rev.*, 1975, **4**, 471.
4. Various authors, *J. Chem. Educ.*, 1983, **60**, 248–340.
5. J. Robinson, in 'Electrochemistry', ed. D. Pletcher, Specialist Periodical Report, The Royal Society of Chemistry, London, vol. 9, pp. 101–160.
6. D. T. Sawyer and J. L. Roberts, Jr., 'Experimental Electrochemistry for Chemists', Wiley-Interscience, New York, 1974.
7. F. F. Said and D. G. Tuck, *Can. J. Chem.*, 1980, **58**, 1673.
8. D. Pletcher, 'Industrial Electrochemistry', Chapman and Hall, London, 1984.

8.2

Electrochemical Properties in Aqueous Solutions

DAVID H. VAUGHAN
Paisley College of Technology, Paisley, UK

8.2.1 WATER AS AN ELECTROCHEMICAL SOLVENT

To the coordination chemist who wishes to study the electrochemistry of any new complex, water should be the first choice of solvent since it is more convenient to use than any other solvent. The restrictions on the use of water are that the compound must be soluble in water to give a solution of concentration preferably $\geqslant 10^{-4}-10^{-3}$ mol dm^{-3}, and also it must not react with water during, at least, the time taken to perform the measurements.

The region of thermodynamic stability of inorganic species in aqueous solution is determined by the thermodynamics of the decomposition of water for which the relevant electrode reactions are

$$2H^+ + 2e^- \rightleftharpoons H_2 \qquad \text{at the cathode} \qquad (1)$$

$$H_2O \longrightarrow \tfrac{1}{2}O_2 + 2H^+ + 2e^- \qquad \text{at the anode} \qquad (2)$$

$$(\text{The net reaction is } H_2O \longrightarrow H_2 + \tfrac{1}{2}O_2)$$

For reaction (1) the electrode potential is given, assuming the temperature is 298 K, by

$$E = 0 + \frac{0.0592}{2}\log\frac{(H^+)^2}{pH_2}$$

and for reaction (2) by

$$E = 1.229 + \frac{0.0592}{2}\log\frac{(pO_2)^{1/2}(H^+)^2}{(H_2O)}$$

where the quantities in brackets refer to the activities of the species in solution or the (partial) pressures if the species are gaseous. Assuming $pO_2 = pH_2 = 1$ atm for the purpose of calculation and $(H_2O) = 1$, then O_2 is evolved at the anode if $E_{\text{anode}} > 1.229 + 0.0592\log(H^+)$, *i.e.* $E_{\text{anode}} > 1.229 - 0.059$ pH; and H_2 is evolved at the cathode if $E_{\text{cathode}} < -0.0592$ pH.

If one of the electrodes can undergo an alternative reaction then this may impose a different limit on the available potential range. Thus mercury, a common electrode material, undergoes anodic oxidation according to reaction (3):

$$2Hg \rightleftharpoons Hg_2{}^{2+} + 2e^- \qquad (3)$$

for which the potential is $E = 0.799 + \dfrac{0.0592}{2}\log(Hg_2{}^{2+})$.

This reaction will become significant when $(Hg_2{}^{2+}) > 10^{-5}$ mol dm^{-3}, *i.e.* when the anode potential is more positive than *ca.* 0.65 V. The presence of ligands which complex the mercury will reduce the anodic limit even further; chloride, for example, forms the insoluble Hg_2Cl_2 so that now the anodic reaction is (4):

$$2Hg + 2Cl^- \rightleftharpoons Hg_2Cl_2 + 2e^- \qquad (4)$$

for which $E = 0.27 + (0.0592/2)\log(1/(Cl^-)^2) = 0.27 - 0.0592\log(Cl^-)$. Thus when $(Cl^-) = 0.1\ \text{mol dm}^{-3}$ the anode potential cannot be very much to the positive side of 0.3 V before dissolution of mercury occurs.

Similarly, the presence of oxygen in the aqueous solution should be avoided (by flushing the solution with nitrogen prior to investigation) as reaction (5) occurs:

$$O_2 + 2H^+ + 2e^- \rightleftharpoons H_2O_2 \qquad (5)$$

for which the potential is

$$E = 0.680 + \frac{0.0592}{2}\log\frac{(H^+)^2(pO_2)}{(H_2O_2)} = 0.680 - 0.0592\,\text{pH} + 0.0296\log\frac{(pO_2)}{(H_2O_2)}$$

Thus at pH = 7, $pO_2 = 0.2$ atm, the (H_2O_2) becomes $> 10^{-5}\ \text{mol dm}^{-3}$ when $E < 0.393$ V.

The thermodynamic region of stability of a coordination complex in aqueous solution is thus within the limits of the decomposition of water, but this is usually extended because of kinetic factors as the oxidation and reduction of water is normally a slow process. The region of stability can be extended by varying amounts depending on the supporting electrolyte and electrode used. Thus with a mercury electrode the overpotential for the discharge of hydrogen is very large so that the practical potential range on the negative side is extended by *ca.* 0.7 V, the exact value depending on the pH. At values of pH less than 2–3 it is normally this reduction of hydrogen ion that limits the negative (cathodic) range, but at values of pH greater than *ca.* 2–3 it is generally the reduction of the cation of the supporting electrolyte that limits the range as hydrogen ions are reduced in this pH range at more negative values; the anodic range is limited, not by the oxidation of water but, as mentioned above, by the dissolution of mercury. In the case of a platinum electrode the overpotentials for oxidation and reduction of water are a lot smaller so that the cathodic potential range is nearly always determined by the reduction of water. Similarly, the anodic limit is determined by the oxidation of water, unless the oxidation of the anion of the supporting electrolyte interferes, which thus extends the anodic limit compared to that when mercury is the electrode.

Table 1 gives a short list of approximate potential ranges available in various aqueous solutions and for different electrodes. The values of the potentials quoted are, for practical convenience, relative to an aqueous saturated calomel electrode (SCE) as this is one of the most common and convenient reference electrodes used in aqueous electrochemical studies.

Table 1 Approximate Potential Ranges in Aqueous Solution

Electrode	*Supporting electrolyte*	*Potential range (V vs. SCE)*		
Mercury	0.1 M $NaClO_4$	+0.4	to	−1.9
	0.1 M $NaNO_3$	+0.4	to	−1.9
	0.1 M Me_4NClO_4	+0.4	to	−2.8
	0.1 M NaCl, KCl	0	to	−1.9
	0.1 M Me_4NCl	0	to	−2.8
	0.1 M HCl	0	to	−1.2
	0.1 M NaOH	−0.1	to	−1.9
Platinum	0.1 M NaCl, $NaClO_4$, Me_4NClO_4	+1.0	to	−0.7
	0.1 M $HClO_4$	+1.2	to	−0.3
	0.1 M NaOH	+0.7	to	−0.9
Carbon	0.1 M HCl	+1.12	to	−0.32
	0.1 M NaOH	+0.68	to	−0.34
	0.1 M KCl	+1.0	to	−1.3

It can be seen from Table 1 that by a variation of the electrode and supporting electrolyte a very wide range of potentials is available for the study of coordination compounds in aqueous solution. However, as a note of caution, the use of tetraalkylammonium salts in aqueous solution allows the use of potentials as negative as −2.8 V (relative to a SCE) but, at these negative potentials, the reduced species formed in the electrochemical process may be able to react rapidly with the water to regenerate the original species, hence giving rise to a catalytic process and this may limit the use of these negative potentials.

8.2.2 OBTAINING ELECTROCHEMICAL INFORMATION IN PRACTICE

For the coordination chemist wishing to undertake an electrochemical study of a metal complex, probably the most convenient and simplest technique with which to commence is DC polarography. The polarogram of the complex indicates, by the existence of waves, whether any redox processes are occurring and at what potentials. Extensions to other potentials not accessible to polarography are also obtained rapidly and easily *via* voltammetry using such electrodes as a rotating platinum electrode. The presence of waves in the polarogram or voltammogram, apart from indicating the existence of a redox reaction, can yield, from measurements of the wave, information on both the concentration of the electroactive species and the number of electrons involved in the redox process. In general the height of the wave is proportional to both the concentration of the electroactive species and the number of electrons involved in the redox process. In DC polarography at a dropping mercury electrode, for example, the relationship is given by the Ilkovic equation:

$$i_d = 607\, n\, D^{1/2}\, m^{2/3}\, t^{1/6}\, C$$

where i_d = the average limiting diffusion current, n = the number of electrons involved in the redox process, D = the diffusion coefficient of the electroactive species, m = rate of flow of mercury from the capillary, t = drop time and C = concentration of the electroactive species.

Thus for a given mercury capillary with given characteristics, *i.e.* constant values of m and t, i_d depends only on n, C and $D^{1/2}$. Diffusion coefficients of most coordination complexes do not vary greatly and for chemically similar species, *i.e.* similar complexes of the same or different metals, or complexes of the same metal in different oxidation states, the differences in $D^{1/2}$ are quite small. In general, for not too dissimilar complexes, the height of the polarographic wave obtained from solutions of equal concentration can be taken as being proportional to n. Thus the polarogram of Cu^{II} in an aqueous medium of NH_3/NH_4Cl shows two waves of equal height which are due to the successive reduction of Cu^{II} to Cu^{I} and Cu metal. Similarly the polarogram of $[Co(en)_3]^{3+}$ in KCl solution shows two waves, the second of which is twice the height of the first and this is due to the reduction of Co^{III} first to Co^{II} and then further reduction of the Co^{II} to Co metal.

However, the redox potential for the couple is not so readily obtained *via* polarography. Polarographic theory states that for a reversible couple (reversible in the electrochemical sense means that the electron transfer processes are rapid so that the oxidized and reduced forms of the couple are always in equilibrium, *i.e.* the relationship between the concentrations of the oxidized and reduced forms is given by the Nernst equation) the half-wave potential, $E_{1/2}$, is approximately equal to the redox potential. The half-wave potential is the potential at the point exactly half-way up the wave where i, the current flowing at the electrode, is $\frac{1}{2}i_d$. Unfortunately, the establishment of the reversibility or not of a couple by polarography is not always easy; if both forms of the couple are available then the polarographic wave obtained is a composite cathodic–anodic wave with little or no displacement between the two regions. Alternatively, if only one half of the redox couple is available then an analysis of the wave shape must be undertaken to establish reversibility. A quick but not very exact method is to measure the difference in potentials between two points corresponding to a quarter and three quarters of the way up the wave, and this for a reversible cathodic wave is given by $E_{1/4} - E_{3/4} = 56/n$ mV at 25 °C. A more accurate procedure is to plot E *vs.* $\log(i_d - i)/i$ which should be linear with a slope of $59.1/n$ mV at 25 °C if the wave is reversible. This method relies however upon a prior knowledge of n, and if this is not known then the method is not completely reliable as theory predicts that when the electron transfer process itself is slow, so that equilibrium at the electrode between the oxidized and reduced forms of the couple is established slowly and the Nernst equation cannot be applied, then an irreversible wave is obtained and a similar plot will also yield a straight line but of slope $54.2/\alpha n_a$ mV at 25 °C (α = transfer coefficient, *i.e.* the fraction of the applied potential that influences the rate of the electrochemical reaction, usually *ca.* 0.5; n_a = the number of electrons transferred in the rate-determining step). Thus a slope of 59.1 mV at 25 °C could be interpreted either as a reversible one-electron process or an irreversible two-electron process with $\alpha = 0.45$. If the wave is irreversible in DC polarography then it is not possible to obtain the redox potential of the couple.

In addition to the information that can be obtained from DC polarography as indicated above, polarography can also be used to study solution equilibria of coordination compounds. Thus from measurements of the shift of $E_{1/2}$ with solution environment, such as pH or concentration of complexing agent, it is possible to ascertain both the stoichiometry and values of the equilibrium constants of the species formed. For example, *cis*-$[Ru^{II}(bipy)_2(H_2O)_2]^{2+}$ was found[1] to undergo four successive one-electron oxidations at a glassy carbon or carbon paste electrode and the values of $E_{1/2}$ for each of the four redox couples was dependent on pH such that $E_{1/2}$ decreased linearly with increasing pH, with slope = 0.059 V pH^{-1}. This was interpreted as the loss of a single proton for each oxidation step according to, for example

$$cis\text{-}[Ru^{II}(bipy)_2(H_2O)_2]^{2+} \overset{-e}{\rightleftharpoons} cis\text{-}[Ru^{III}(bipy)_2(H_2O)(OH)]^{2+} + H^+$$

Cyclic voltammetry provides a very convenient method for determining the redox potentials of couples as the peak potentials for the cathodic, E_{pc}, and anodic, E_{pa}, processes of a reversible couple are related, at 25 °C, to the redox potential by $E_{pa} = E_{pc}/2 = E° + 0.285/n$ volts and $E_{pc} = E_{pa}/2 = E° - 0.285/n$ volts. $E_{pc}/2$ and $E_{pa}/2$ are the potentials at a point half-way up the wave; at these points the current is half the maximum value, *i.e.* i_{pc} for the cathodic wave or i_{pa} for the anodic wave. Again, this technique will yield redox potentials only if the couple is reversible in the electrochemical sense, but this is now very readily established through the above relationship that $E_{pa} - E_{pc} = \Delta E_p = 57/n$ mV and by the requirement that $i_{pc}/i_{pa} = 1$. In addition it should be established that E_p is independent of the scan rate, ν, and that the process is diffusion controlled by showing $i_p/\nu^{1/2}$ to be constant.

One advantage of the cyclic voltammetry technique is that, to some extent at least, the lifetime of the experiment may be controlled through the scan rate, *i.e.* the rate at which the potential range is scanned and then reversed. This means that if one of the components of the couple is not very stable it may still be possible, by increasing the scan rate, to observe reversibility and hence determine $E°$. Thus[2] the μ-superoxo/μ-peroxo-dicobalt(III) couples in the complexes of the type $[(NH_3)_5Co(\mu\text{-}O_2)Co(NH_3)_5]^{5+,4+}$ can be determined readily even though the peroxo complex is not very stable and decomposes rapidly under conditions where the superoxo is stable. However, the scan rate must not be increased too much as at fast scan rates the rate of the electrochemical process becomes slow relative to the scan rate and irreversible behaviour ($\Delta E_p > 57/n$ mV) will be obtained. In fact, this is the basis of a method for obtaining the heterogeneous rate constants of reversible couples.

In addition to providing redox potentials, cyclic voltammetry can provide a tremendous amount of information about the reactions occurring prior or subsequent to the actual redox processes. This is obtained by monitoring the change in, for example, peak potentials and/or peak currents with scan rate and also by noting the appearance or disappearance of peaks with variation in scan rate or when the potential range is scanned successively.

The cyclic voltammetry of the complexes *trans*-$[Ru^{III}LX_2]^+$, where L = $4NH_3$ or 2en, X = Cl or Br *etc.*,[3] illustrates the application of the technique for obtaining detailed mechanistic information on reactions occurring subsequent to the initial redox process. At moderately fast scan rates, *ca.* 1 V s^{-1}, the redox behaviour is typical of a single reversible one-electron couple corresponding to the couple Ru^{III}/Ru^{II}. At slower scan rates, *ca.* 0.1 V s^{-1}, a wave corresponding to the same complex again appears but on the second and subsequent scans two additional waves appeared at potentials positive to the original wave. These two additional waves were characterized as reversible one-electron processes. A similar pattern of behaviour was observed for all the complexes studied and it was found that the peak potential of one of the two waves observed on subsequent scans was independent of the nature of X for a given L. Controlled potential electrolysis of the starting complex followed by air oxidation identified the resulting product as *trans*-$[Ru^{III}L(H_2O)_2]^{3+}$, and the cyclic voltammetry of this gave a peak at the same potential as that found for the peak in the cyclic voltammetry of *trans*-$[RuLX_2]^+$ whose position was independent of the nature of X. A mechanistic scheme consistent with these observations is

$$\begin{tikzcd}
trans\text{-}[RuLX_2]^+ \arrow[r, shift left, "+e"] & trans\text{-}[RuLX_2] \arrow[l, shift left, "-e"] \arrow[d, "H_2O"', "k_1"] \\
trans\text{-}[RuLX(H_2O)]^{2+} \arrow[r, shift left, "+e"] & trans\text{-}[RuLX(H_2O)]^+ \arrow[l, shift left, "-e"] \arrow[d, "H_2O"', "k_2"] \\
trans\text{-}[RuL(H_2O)_2]^{3+} \arrow[r, shift left, "+e"] & trans\text{-}[RuL(H_2O)_2]^{2+} \arrow[l, shift left, "-e"]
\end{tikzcd}$$

Also, from the variation of i_{pc}/i_{pa} with scan rate for the peak corresponding to the original complex *trans*-$[RuLX_2]^+$, the value of k_1 was determined. It was found that the half life for the aquation of *trans*-$[Ru(NH_3)_4Cl_2]$ was *ca.* 0.7 s at 25 °C; hence the absence of peaks for the aqua complexes at relatively fast scan rates.

Although the techniques of DC polarography and cyclic voltammetry are used quite extensively, in order to obtain a complete and detailed picture of the overall mechanism occurring at the electrode these two techniques are usually supplemented by other techniques such as chronoamperometry, chronocoulometry, AC polarography, rotating disc voltammetry and controlled potential electrolysis and coulometry. In addition, non-electrochemical techniques, such as spectroscopic methods, are commonly used in conjunction with these electrochemical methods to assist in the elucidation of the overall electrode reaction. The use of controlled potential electrolysis was mentioned previously in connection with the complexes *trans*-$[RuLX_2]^+$. This technique is used extensively as a preparative method because it has the advantages that (a) by controlling the potential of the electrode it is possible to control the amount of energy introduced into the system and even, in very many cases, the number of electrons transferred, and (b) the addition or subtraction of electrons is chemically clean in that no other possible chemical contaminants are involved. As a word of caution, however, controlled potential electrolysis and coulometry are usually carried out over a longer time and at higher concentrations of electroactive material than other techniques so that if, for example, there are slow homogeneous reactions subsequent to the electron transfer process, then conflicting results may be obtained. Thus the cyclic voltammetry at pH 12 of *trans*-$[Rhen_2Cl_2]^+$ revealed[4] a reduction peak at *ca.* −0.65 V relative to a sodium chloride SCE, but controlled potential electrolysis at −0.70 V ceased after the passage of only a relatively small amount of electricity. This was explained as arising from the initial product of the electrode reaction, a Rh(I) species, catalyzing the conversion of the remainder of the *trans*-$[Rhen_2Cl_2]^+$ to *trans*-$[Rhen_2Cl(OH)]^+$ which was electroinactive at this potential.

8.2.3 FACTORS AFFECTING THE REDOX POTENTIAL $E°$

The approach adopted here has been to report on attempts to predict variations of $E°$ from semiempirical or semiquantitative relationships rather than to inquire into the fundamental reasons for variations of $E°$ in coordination complexes. Thus the electrode potential of a given couple in a series of complexes can be made more positive by (a) stabilizing the reduced form of the couple, (b) destabilizing the oxidized form of the couple and (c) both (a) and (b). The factors that can bring this about are as follows.

(i) The relative σ-donating and π-accepting ability of the ligands

A good σ-donating ligand, a measure of which is the pK_a of the ligand, stabilizes the oxidized form of the couple and hence makes it more difficult to reduce (negative shift in $E°$) and, providing π-bonding is possible between the metal and ligand, a good π-acid (electron accepting) ligand stabilizes the reduced form of the couple more than the oxidized form, hence giving rise to a positive shift in $E°$. Thus in a series of complexes of the type[5] *cis*-$[RuLCl_2]^{+/0}$, a change in the four ligating atoms in L from saturated nitrogen to the π-acid sulfur causes an anodic shift of *ca.* 1.0 V in $E°$. Similarly, if a series of σ-donating ligands are considered then the variation in $E°$ for the complexes with the same metal can be explained by inductive effects alone. This is especially true if the variation in the ligand occurs at a site fairly remote from the metal, so the $E°$ can be linearly correlated with the familiar Hammett[6] or Taft[7] parameters *via* a relationship of the form:

$$E°_X - E°_H = n\sigma\rho$$

where $E°_H$ = redox potential of the parent couple, *i.e.* when X = H, $E°_X$ = redox potential of the couple when the H in the parent couple is replaced by X, σ = Hammett substituent constant, n = number of substituents, X, in complex and ρ = 'reaction constant', characteristic of the series of complexes being studied. Numerous examples of relationships of this type[8,9] or variations of it, such as linear plots of $E°$ *vs.* pK_a of the ligand, have been reported for series of complexes where inductive effects are dominant and other effects such as mesomeric (resonance) and steric are either constant or unimportant.

Chatt *et al.*[10] have developed a different LFER for closed shell octahedral metal complexes. They defined a ligand constant P_L as $P_L = E°[Cr(CO)_5L] - E°[Cr(CO)_6]$ volts. The values of P_L so obtained had the same sign as the Hammett σ in that the more electron releasing was L the more negative was P_L. Thus a series of values of P_L for several ligands was established, with the strong π-acids, *e.g.* NO^+, having high positive values (*N.B.* $P_{CO} = 0$ by definition) and pure σ-donors, *e.g.* H^-, and σ- and π-donors, *e.g.* OH^-, having large negative values. Although the values of P_L were established in a non-aqueous solution, they apply to aqueous solutions; thus a good linear correlation was found for the redox potentials of the couples $[Ru^{III/II}(NH_3)_5L]$ *vs.* P_L.

(ii) Steric and solvational effects

Pure steric effects operate in a metal complex when the ligand, because of its geometry, is prevented from acquiring its most favoured orientation around the metal. Examples of this occur in complexes with macrocyclic ligands which usually have a preferred cavity size. This means that for a given macrocyclic ligand with a particular metal, one oxidation state of the metal may be favoured relative to all others and this will be reflected in the redox couples involving this oxidation state. An illustration of this effect is found with cobalt complexes containing macrobicyclic (hexaamine) ligands,[11] where the redox potential for the Co^{III} complex formed with the ligand which has a preferred cavity size that matches Co^{III} is more negative than that for a similar complex formed with a ligand whose preferred cavity size is different. The origin of this effect must clearly be associated with the ligand achieving a preferred metal–ligand bond length and/or the ligand adopting a preferred conformation in the complex.

Sometimes it is not possible to distinguish a steric effect from solvational effects. Thus the introduction of sterically bulky groups, like alkyl groups, while altering the steric requirements of the ligands also alters the solvation of the ligand and this can alter the redox potential of the couple. Replacement of H by R in a ligand will result in desolvation of the complex and this will be relatively greater for the higher charged half of the redox couple. It seems very likely that the positive shift in the reduction potential of Ru^{III}/Ru^{II} couples[12] in couples of the type *trans*-$[RuLCl_2]^{+/0}$, where L is a saturated amine, when L becomes increasingly chelated, *e.g.* $4NH_3$-2en-cyclam, is due, at least in part, to solvation effects.

(iii) Miscellaneous effects

Other factors, for example the charge on the complex or outer sphere effects such as ion pairing, will also have an effect on $E°$ but it is not possible to predict the exact relationship of $E°$ to these factors. Nevertheless, they should always be borne in mind.

One important result arising from a consideration of these factors affecting the redox potential is that it is now possible, in many cases, to prepare a complex of a given type and then 'tune' its redox potential to a required value by altering the ligands in accordance with the above effects.

8.2.3.1 Relationships between $E°$ and Other Parameters

Numerous examples exist in the literature[8] of relationships between $E°$ and another parameter obtained by some other experimental technique. These may be given in the form of LFER such as the relationship between $E°$ and the Hammett constants mentioned previously. Other examples of such relationships are correlations between $E°$ and various spectroscopic parameters, such as the energy of the first spin-allowed d–d band in the complex, the energy of the metal to ligand charge transfer band (*i.e.* the energy separation between the HOMO on the metal and the LUMO on the ligand), the energy of the ligand to metal charge transfer band (this is similar to the Hammett $E°$ *vs.* σ relationship) and NMR chemical shifts.

A consideration of these relationships reveals[8] that because $E°$ is a thermodynamic parameter and represents an energy difference between two oxidation states and in many cases the spectroscopic or other parameter refers to only one half of the couple, then some special conditions must exist in order for these relationships to work. The special conditions under which these relationships work are that (a) steric effects are either unimportant or approximately the same in both halves of the redox couple and (b) changes in $E°$ and the spectroscopic or other parameters arise mainly through electronic effects. The existence of many examples of these relationships for series of closely related complexes is perhaps not too unexpected as it is likely that, for such a series, the solvational contribution to the enthalpy change, and the total entropy change, for the redox reaction will remain constant, thus giving rise to the above necessary conditions.

8.2.3.2 Relationships involving Irreversible Couples

As noted earlier, the polarographic half-wave potential $E_{1/2}$ for an irreversible couple is not related in a simple manner to the standard redox potential of the couple because $E_{1/2}$ is governed by kinetic as well as thermodynamic parameters, so that attempts to correlate $E_{1/2}$ for irreversible couples with structural features of the complex have been very difficult to obtain. One moderately successful correlation, however, was obtained by Vlcek[13] and by Crow[14] for a fairly extensive series of complexes of Co^{III}, Cr^{III} and Rh^{III}. It was suggested that before reduction of the metal complex could occur at the electrode, an orbital on the metal complex with sufficient electron affinity must be available to accept the electron from the electrode. It is possible that the particular orbital is not empty in the ground state of the complex so that prior to the actual rapid electron transfer the complex must undergo an activation process. If this is the case then a significant contribution to the total activation energy for the overall process may arise from this change in the electronic energy of the metal complex. For the kinetically inert complexes of Co^{III}, Cr^{III} and Rh^{III} the lowest unoccupied orbital is an antibonding e_g orbital which has a low electron affinity so that a change in electronic configuration that results in a t_{2g} orbital, which possesses a much higher electron affinity, becoming vacant is necessary before electron transfer can occur. The electron that is removed from the t_{2g} orbital is presumed to enter the e_g orbital: this electronic change is very similar to that observed spectroscopically where the energy involved will depend on the ligand field stabilization energy of the complex. This hypothesis was supported by the observation that a linear correlation was found between the half-wave potential of the complexes $[M(NH_3)_5X]^{2+}$ (X is a variety of ligands such as H_2O, halogen, NO_3^-) and the difference in the position of the main d–d absorption band of these complexes and that of the parent complex $[M(NH_3)_6]^{3+}$. Other similar series of complexes also gave linear correlations.

More recently it has been found[15] that a correlation exists between spectroscopic parameters of the divalent aqua ions of the metals Cr to Ni, and the polarographic $E_{1/2}$. A linear relationship was found between Δ_0 and $(\alpha n E_{1/2} - E^\circ)$ where Δ_0 is the crystal field splitting parameter, α the transfer coefficient, n the number of electrons transferred in the reduction, $E_{1/2}$ the polarographic half-wave potential and E° the standard electrode potential. The use of the crystal field splitting parameter would seem to be a more sensible parameter to use than the position of λ_{max} for the main absorption band as the measured λ_{max} may not be a true estimate of the relevant electronic transition. This arises because the symmetry of the complex is less than octahedral so that the main absorption band in octahedral symmetry $({}^1A_{1g} \rightarrow {}^1T_{1g})$ is split into at least two components with the result that the position of the maximum of the composite band envelope may not correspond to any one particular transition. In addition, it was found that the quantity $(Q_{1/2} + \Delta_0)$ was approximately constant for the same series of ions, where $Q_{1/2}$ was the activation energy of the electrochemical process. It was suggested that for these labile ions the reduction mechanism was the same so that $Q_{1/2}$ was the energy requirement in excess of Δ_0 for the electrochemical reduction process. Conversely, when a series of complexes of the same metal ion are considered the total energy for the electrochemical reduction will vary, but provided the relative values of $Q_{1/2}$ and Δ_0 are not greatly altered, then a positive dependence of $Q_{1/2}$ on Δ_0 is predicted, as has been observed.

A study[16] of the irreversible reduction of several Co^{III}, Rh^{III} and Ir^{III} complexes revealed no correlation between the polarographic $E_{1/2}$ and several spectroscopic parameters but, interestingly, it was found that a linear correlation existed for several of the Co^{III} complexes between the $E_{1/2}$ and $\ln k_{ex}$, where k_{ex} was the rate constant for homogeneous electron transfer, when $[Ru(NH_3)_6]^{2+}$ was used as reductant. The theoretical foundation for this relationship is that $E_{1/2}$ is linearly related to $\ln k_s$ (the heterogeneous rate constant for electrochemical reduction) and, from the theories of Marcus and Hush, the ratio of k_s for a series of compounds is the same as the ratio of the rate constants k_{ex} for a constant reductant provided both pathways are outer sphere. The mechanistic implication of the relationship is not clear; it may simply mean that both pathways proceed *via* an outer sphere mechanism as no correlation was found between $E_{1/2}$ and the values of k_{ex} for reduction by V^{2+}, which can undergo homogeneous electron transfer by an inner sphere mechanism.

8.2.4 ELECTROCHEMISTRY OF COMPLEXES CONTAINING MORE THAN ONE REDOX CENTRE

There is increasing interest in the study of multi-metallic systems for several reasons. They are potential catalysts in many industrial processes and, because of the common occurrence of multimetallic species as active sites in many metalloenzymes, they may be used as models for these molecules. In addition, these complexes offer the possibility of studying multi-electron charge transfer and magnetic coupling phenomena.

In general, when a complex contains n equivalent and non-interacting sites then the electrochemical behaviour is governed by purely statistical factors.[17] Thus, with two identical noninteracting sites which undergo a one-electron redox process, the predicted separation of the two formal potentials is $2RT/F \ln 2$, *i.e.* 35.6 mV at 25 °C. Deviations from the purely statistical relationships will occur if (a) the redox centres undergo slow electrode kinetics, (b) structural changes accompany the electron transfer including such effects as ion pairing and solvational changes, (c) the reactants or products are adsorbed or precipitated at the electrode, (d) the diffusion coefficients of the electroactive species alter when charge transfer occurs or (e) interactions occur between the redox centres.

Of particular interest are the cases where, by a suitable design of the complex, the factors (a) to (d) above can be eliminated so that the departure of the electrochemical response from the purely statistical behaviour arises solely from cause (e). Two examples of such complexes which have been well studied are binuclear ruthenium complexes bridged by 4,4′-bipyridyl type ligands,[18] and binuclear complexes $[\mathrm{M_A}^{\mathrm{II}}\mathrm{M_B}^{\mathrm{II}}\mathrm{L}]^{2+}$ where L, the binucleating macrocyclic ligand, is a symmetric Schiff base and $\mathrm{M_A}$ and $\mathrm{M_B}$ may be different or identical metals.[19] An examination of these systems has revealed that the mixed valence species are relatively more stable than the two isovalent constituents. A consideration of the reasons for this stability suggests that it arises from several phenomena: (1) electrostatic interactions, *i.e.* an ion of charge $n(+)$ is more easily reduced than one with a charge $(n-1)(+)$; (2) with species containing two or more paramagnetic centres, magnetic superexchange effects between the metal centres may stabilize, or destabilize, the mixed valence species; (3) electron delocalization in mixed valence species will enhance their stability; and (4) electronic effects arising from a change in the electron accepting/donating power of the bridging ligand as the valency of the attached metal alters.

The relative importance of these effects will differ from one series of complexes to another. Thus the stability of the mixed valence species $[\mathrm{Cu^{II}Cu^{I}L}]^{3+}$ is thought[19] to arise from electron delocalization so that the ground state of the mixed valence species experiences significant delocalization (possibly class III in the Robin and Day scheme[20]). The origin of the delocalization stabilization probably arises from several contributing factors, namely (a) covalent effects (the single electron now occupying a three-centre molecular orbital), (b) simple charge redistribution within the complex which thus results in a decrease in both internuclear and interelectronic repulsion and (c) greater solvation of the delocalized state relative to the completely localized state. However, for the binuclear ruthenium complexes[18] it was thought that electronic effects were the most significant in giving rise to the stability of the mixed valence species. More recent studies[21] based on a consideration of the thermodynamic parameters of the electron transfer steps also indicate that, in similar binuclear ruthenium complexes, the two ruthenium centres act as two structurally independent redox centres.

For systems which undergo reversible sequential redox steps, as in (6) below

$$\mathrm{A} \xrightleftharpoons{n_1e,E_1^\circ} \mathrm{B} \xrightleftharpoons{n_2e,E_2^\circ} \mathrm{C} \qquad (6)$$

the difference in the two reduction potentials, ΔE, has a thermodynamic significance in that for the comproportionation equilibrium (7) below

$$n_2\mathrm{A} + n_1\mathrm{C} \overset{K_c}{\rightleftharpoons} (n_1 + n_2)\mathrm{B} \qquad (7)$$

the following relationship (8) holds

$$K_c = \frac{[\mathrm{B}]^{n_1+n_2}}{[\mathrm{A}]^{n_2}[\mathrm{C}]^{n_1}} = \exp\left\{\frac{\Delta E \ n_1n_2F}{RT}\right\} \qquad (8)$$

In the case of two equivalent non-interacting metal ions, undergoing successive one-electron reductions, ΔE should be 35.6 mV, *i.e.* $K_c = 4$. Values of $K_c > 4$ are thus a reflection of the stabilization of mixed valence species.

Although most of the binuclear metal complexes appear to undergo sequential steps, *i.e.* $(E_1^\circ - E_2^\circ) > 0$, a few examples are known[22] where a concerted two-electron charge transfer occurs, *i.e.* $(E_1^\circ - E_2^\circ) < 0$, so that addition of the second electron is easier than the first.

The majority of the work in this field has been restricted mainly to bimetallic systems, although there is some work on multi-metallic centres such as[23] $(\mathrm{Mo^{IV}})_3$ and $(\mathrm{Mo^{III}})_3$. However, the electrochemistry of transition metal clusters has received fairly wide attention.[24] This latter field would appear to be an interesting area of development as these species have the ability to participate in cooperative transport phenomena due to (a) their ability to exist in a range of oxidation states and their tendency to undergo reversible one-electron redox reactions, and (b) an arrangement of upper bonding levels which enables them to function as electron reservoirs (or sinks). It is this field and the study of the stability of mixed valence species in general that is of great interest, as these mixed valence species may represent special oases of stability and it is conceivable that Nature may have used these thermodynamic sinks to adjust redox potentials in such molecules as metalloenzymes.

8.2.5 MODIFIED ELECTRODES

A study of the electrochemistry of metal complexes is invariably carried out with the aid of electrodes. These electrodes are usually made of a chemically relatively simple substance, *e.g.* platinum, graphite, mercury, or TiO_2. One of the most significant advances in electrochemistry in the past ten years has been the introduction and study of electrochemical systems with the aid of modified electrodes.[25] Modified electrodes (or chemically modified electrodes, CME, as they are also called) can be prepared by several methods and are sometimes called by different names according to the method of preparation, *e.g.* derivatized, functionalized, electrostatically bound and polymer coated. In all cases a monomolecular layer or multimolecular layers of electrochemically reactive substances are attached to an electrode. The attachment of these molecules to the electrode may involve strong chemisorption, covalent bond formation or the deposition of a polymer layer on the electrode by dipping the electrode into a solution of the dissolved polymer, removing the electrode from the solution and allowing the solvent to evaporate, thus leaving a film of polymer on the electrode surface. In the case of polymer-coated electrodes the polymer itself may be electroactive, *e.g.* poly(vinylferrocene), or it may be electroinactive but is a polyelectrolyte so that an electroactive substance, which is ionic, can be partitioned into the polymer matrix by an ion exchange mechanism. For more details concerning the preparation and characterization of these electrodes, the references at the end of the section should be consulted. However, some characteristics of modified electrodes and two important applications of these electrodes will be mentioned briefly.

The redox sites in the mono- and multi-layers attached to the electrode can be oxidized or reduced by the electrode and one of the most convenient techniques for studying these modified electrodes is cyclic voltammetry. It is generally found that the formal potentials of these immobilized redox couples are very near those of analogous couples 'free' in solution. The amount of electrochemically active material on the electrode can be obtained from the area under the cyclic voltammetric wave. For monomolecular films and relatively slow scan rates the cyclic voltammetric behaviour obtained is characteristic of a species strongly adsorbed on the electrode and undergoing rapid electron transfer, *i.e.* the separation in the peak potentials of the waves for the reduction and oxidation of the immobilized redox couple, ΔE_p, is zero, and the current corresponding to the peak of the wave, i_p, is proportional to the potential sweep rate, v. For thicker layers this ideal behaviour is usually lost with ΔE_p no longer equal to zero and i_p becoming dependent on $v^{1/2}$. The reason for this is associated with the rather complicated process of electron transfer through the multilayers called electrochemical charge transport,[26] which involves electron transport through the layers by exchange between neighbouring redox sites. The original site is generated at the electrode, a flow of counterions through the layers is also necessary to maintain electroneutrality and, in the case of polymer films, there may in addition be polymer lattice motions to accommodate the counterion and solvent flow, and possibly the motions of neighbouring sites towards one another as this may be necessary before electron transfer can occur. An understanding of the factors involved in electrochemical charge transport is essential before efficient electrocatalysts using modified electrodes can be devised.

In this particular use of modified electrodes, *i.e.* electrocatalysis, the immobilized redox couple acts as an electron transfer mediator cycling between the reactive (catalyst) state and its non-catalytic state, as shown schematically in Figure 1.

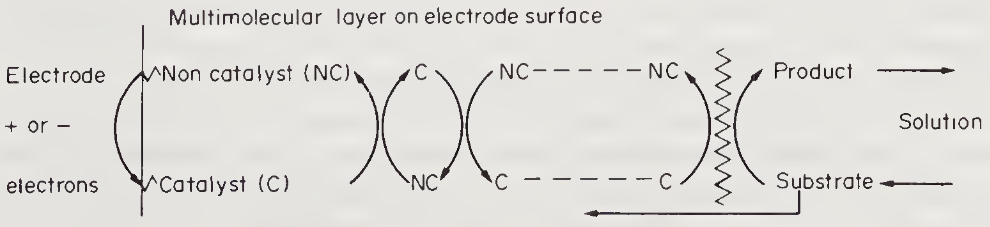

Figure 1 Electrocatalytic mechanism when a multimolecular layer film is present on the electrode

If monolayers are involved then the substrate probably reacts with catalytic sites directly on the electrode surface. However, when multilayers are involved the substrate is denied access to the surface and movement of electrons is by the previously described process of electrochemical charge transport; the substrate also diffuses through the multilayers. Under certain circumstances the presence of multilayers and hence of an increased number of catalytic sites may increase the rate of reaction.

One such reaction that has been studied is the electrocatalytic reduction of oxygen directly to water.[25,27] The electrocatalysts for this process are often based on metal porphyrins and phthalocyanins. Thus a graphite electrode whose surface was modified by the irreversible adsorption of a cofacial dicobalt porphyrin dimer was able to reduce oxygen under conditions where the reduction did not occur on the bare electrode itself. Similarly, a catalytic chemically modified electrode for the oxidation of chloride to chlorine has been prepared[28] where the active catalyst was reported to be a ruthenium dimer, $[(bipy)_2(OH)Ru^{IV}ORu^{V}O(bipy)_2]^{4+}$, which was reduced to the corresponding $[Ru^{III}{-}Ru^{IV}]$ dimer during the reaction.

Chemically modified electrodes can also be used in the mediation of biological redox components that normally undergo very slow heterogeneous electron transfer with the bare electrode. Thus the reduction of cytochrome *c* and its subsequent re-oxidation are accelerated on a platinum electrode *via* a covalently attached ferrocene derivative.[27] The electrocatalytic application described here is very similar to the use of mediator compounds for the electrochemical study of biological redox species.[29] A mediator is an electroactive species which is added to the solution of the biocomponent being studied, *e.g.* the electrochemical reduction of cytochrome *c* was irreversible in the electrochemical sense at some electrodes or even electroinactive at other electrodes at potentials close to its standard electrode potential, but the addition of the mediator 4,4′-bipyridyl produced quasi-reversible behaviour. It is thought that the mediator acts as an electron shuttle to provide redox coupling between the electrode and the redox centre in the biological component (Figure 2); hence the formal redox potential of the mediator should be close to that of the biocomponent being studied. The mode of action of the mediator is very similar to that of a chemically modified electrode but, in the case of the mediator, the electrode is not modified prior to use.

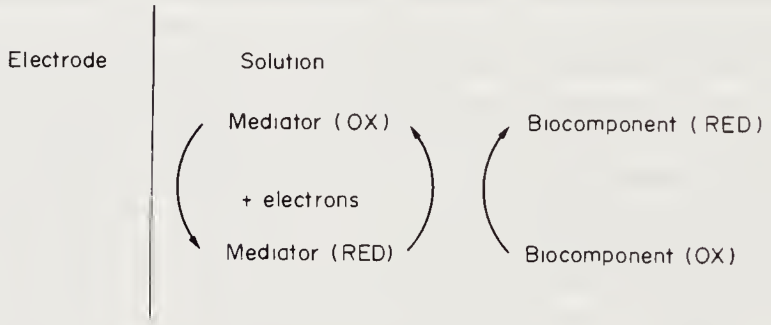

Figure 2 Action of a mediator in electron transfer to a biological molecule

Research into the use of modified electrodes for electrocatalysis continues to be a very active and promising area of research, as it seems very probable that electrocatalysis *via* chemically modified electrodes can be achieved for a large number of reactions.

Another important application of modified electrodes is in the field of analysis. This arises because molecules may become preferentially extracted from solution into the surface layer on the electrode with the result that the molecules of interest become concentrated in the surface layers. A pyrolytic graphite electrode coated with poly(vinylpyridine) (PVP) is initially electroinactive but on immersion in a solution of, for example, $[Ru^{II}(edta)]$ as dilute as 5×10^{-8} mol dm^{-3}, the cyclic voltammogram begins to show peaks, that grow with time, due to the incorporation of the ruthenium species into the polymer layer where it is thought the ruthenium becomes covalently attached to the pyridines in the polymer.[30] It is also possible to incorporate two different complexes of the same metal so that voltammetric peaks due to the two different complexes can be obtained. Thus if a PVP coated electrode was dipped first into a solution of $[Ru(NH_3)_5(H_2O)]^{2+}$ and then into a solution of $[Ru^{III}(edta)]$, the resulting cyclic voltammogram revealed the presence of two different ruthenium species. By a similar procedure two different metal ions can also be incorporated; a PVP coated electrode dipped successively into aqueous solutions of $CuCl_2$ and $[Ru^{III}(edta)]$ showed peaks in the resulting cyclic voltammogram due to copper and ruthenium species.

A recent development[31] is the preparation of metal polymer complexes directly on the electrode *via* the electrochemically induced polymerization of the metal complex. Ruthenium(II) and osmium(II) complexes with ligands containing aromatic amines, *e.g.* 3- or 4-aminopyridine or 5-amino-1,10-phenanthroline, are electrochemically polymerized to yield a film of the metal polymer on the electrode surface. The polymerization involves free radicals, which are formed *via* the initial oxidation of the metal complex to a radical cation and subsequent reaction of the radical cation with a base to yield the free radical.

8.2.6 REDOX PROPERTIES OF SPECIES IN EXCITED ELECTRONIC STATES

So far we have been considering the redox properties of species which are in their ground electronic state. However, as will be shown below, the redox properties of these species when they are excited to an upper electronic state are quite different from the ground state properties. In general, if an electron in a molecule is excited to a higher-energy orbital it leaves a vacancy in a low-energy orbital; thus the molecule is then expected to be able to lose an electron more readily, *i.e.* act as a reducing agent, and also to be able to accept an electron more readily, *i.e.* act as an oxidizing agent, than the molecule in its ground electronic state. As a general rule, then, we would expect the excited state of a molecule to be both a better oxidizing agent and reducing agent than the ground state molecule.

The lifetimes[32] of the lowest spin-allowed excited states of transition metal complexes are generally too short for them to undergo any bimolecular electron transfer reactions due to their high chemical reactivity and/or rapid intersystem crossing to the lowest spin-forbidden excited state, and it is normally only these states with their longer lifetimes that can participate in bimolecular reactions. Thus in the case of a d^6 octahedral complex, *e.g.* $[\mathrm{M^{III}L_6}]$, with a singlet ground state, it is the lowest triplet state that is of prime interest among the many excited states.

$$\mathrm{M^+ + e^- \rightleftharpoons M} \qquad (9)$$

For the simple redox couple (9) shown above, the relationship between the redox potentials of the ground and excited states is easily derived with reference to the energy diagram (Figure 3), where $^1\mathrm{M}$ and $^1\mathrm{M}^+$ are the ground states of metal and cation and $^3\mathrm{M}$ is the lowest excited triplet state of M. The potential, E, of any couple relative to a given reference electrode such as the normal hydrogen electrode is given by

$$-neF = \Delta G = \Delta H - T\Delta S$$

For the couple above, $n = 1$, and if it is assumed that the difference in geometry and solvation of the excited triplet state and ground state is small (the Stokes shift between absorption and emission is small) then the difference in entropy between the two states may be considered approximately zero. If ΔG and ΔH are expressed in volts then

$$-E = \Delta G \approx \Delta H$$

and

$$\Delta G(^1\mathrm{M}/^1\mathrm{M}^+) - \Delta G(^3\mathrm{M}/^1\mathrm{M}^+) = \Delta H(^1\mathrm{M}/^1\mathrm{M}^+) - \Delta H(^3\mathrm{M}/^1\mathrm{M}^+)$$

where $\Delta G(^1\mathrm{M}/^1\mathrm{M}^+)$ *etc.* represents the free energy change for the process $^1\mathrm{M} \rightarrow {}^1\mathrm{M}^+ + \mathrm{e}^-$.

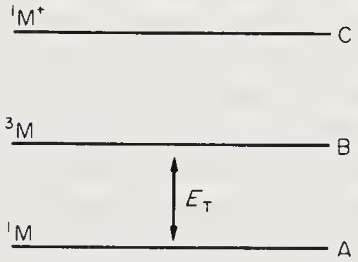

Figure 3 Energy diagram to show the relationship between the redox potentials of the ground and excited states of M

Referring to Figure 3:

$$\Delta H(^1\mathrm{M}/^1\mathrm{M}^+) - \Delta H(^3\mathrm{M}/^1\mathrm{M}^+) = \mathrm{CA} - \mathrm{CB} = \mathrm{AB} = E_\mathrm{T}$$

where E_T is the energy of the triplet state, expressed in volts, relative to the ground state. E_T is normally obtained spectroscopically as it is the zero–zero spectroscopic energy of the triplet state. Thus

$$-\Delta H(^1\mathrm{M}^+/^1\mathrm{M}) + \Delta H(^1\mathrm{M}^+/^3\mathrm{M}) = E_\mathrm{T}$$
$$E^\circ(^1\mathrm{M}^+/^1\mathrm{M}) - E^\circ(^1\mathrm{M}^+/^3\mathrm{M}) = E_\mathrm{T}$$
$$E^\circ(^1\mathrm{M}^+/^3\mathrm{M}) = E^\circ(^1\mathrm{M}^+/^1\mathrm{M}) - E_\mathrm{T}$$

where $E^\circ(^1\mathrm{M}^+/^1\mathrm{M})$ *etc.* is the reduction potential for the process $^1\mathrm{M}^+ + \mathrm{e}^- \rightleftharpoons {}^1\mathrm{M}$.
Thus, in general, for any excited state M* which has an energy E^* above the ground state:

$$E^\circ(\mathrm{M}^+/\mathrm{M}^*) = E^\circ(\mathrm{M}^+/\mathrm{M}) - E_*$$

Similar arguments can be used to derive the relationship for the redox couple $M + e^- \rightleftharpoons M^-$, *i.e.*

$$E^\circ(M^*/M^-) = E^\circ(M/M^-) + E^*$$

A series of complexes that has received particular attention in the past few years is of the type $[M^nL_3]^{n+}$, where M = Ru, Os or Cr and L = phen or bipy. One compound especially has been well studied and that is $[Ru^{II}(bipy)_3]^{2+}$. The energy level diagram for this compound is given in Figure 4.

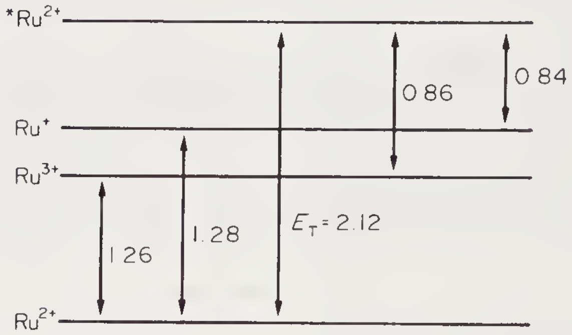

Figure 4 Energy level diagram for the redox states of $[Ru(bipy)_3]^{n+}$; energy separations are given in volts

For this system, $E^\circ(Ru^{2+}/Ru^+) = -1.28$ V and $E^\circ(Ru^{3+}/Ru^{2+}) = 1.26$ V; the zero–zero spectroscopic energy of $^*Ru^{2+}$ is 2.12 V. Using the previous expressions, the following values of the redox properties of the excited state $[Ru^{*II}(bipy)_3]^{2+}$ are obtained.

$$E^\circ(^*Ru^{2+}/Ru^+) = 0.84\ V$$

$$E^\circ(Ru^{3+}/^*Ru^{2+}) = -0.86\ V$$

Thus as mentioned previously, the couple $(^*Ru^{2+}/Ru^+)$ is a better oxidizing agent than the ground couple, and similarly the couple $(Ru^{3+}/^*Ru^{2+})$ is a better reducing agent than the ground state couple.

Complexes of this type, $[M^nL_3]^{n+}$, are particularly useful in that the excited state can be populated with a high efficiency irrespective of the wavelength of the incident radiation, the Stokes shift between absorption and emission is small so that the entropy difference between the ground and lowest excited state is very small, and the lifetime of the excited state is relatively long so that the excited state can undergo bimolecular electron transfer reactions. It is the short lifetime of many excited states that limits the usefulness of many potentially good redox reagents. However, because the ion $[Ru^{II}(bipy)_3]^{2+}$ possesses these favourable properties it has received considerable attention in solar energy conversion through the photodissociation of water;[33] thus the electronically excited state of the ion is energetically able to split water. However, due to the kinetic inertness of the reactions, the efficient use of the ion for the photodissociation of water is *via* the intermediacy of relay species and catalysts. A whole series[34] of complexes of the type $[Ru^{II}L'_{3-n}L''_n]^{2+}$ (n = 0–3; L′ = L″ = bipy, 2,2′-bipyrimidinyl or 2,2′-bipyrazyl) has been synthesized and although the chromophoric character of the complexes is approximately constant, both the ground state and excited state redox properties vary over a wide range, thus making available a series of similar complexes whose excited state potentials can be varied quite considerably.

Finally, in complexes of this type, where $[Ru^{II}(bipy)_3]^{2+}$ is one of the most studied, the lowest spin-forbidden excited state $[^*Ru^{II}(bipy)_3]^{2+}$ is responsible for the chemiluminescence produced when solutions of $[Ru^{III}(bipy)_3]^{3+}$ are mixed with suitable reducing agents. This same excited state can be produced electrochemically[35] in a process whereby electrical energy is converted into light — electrogenerated chemiluminescence (ECL). Thus if cyclic square waves are applied to a solution of $[Ru^{II}(bipy)_3]^{2+}$ between the potentials of formation of $[Ru^{I}(bipy)_3]^+$ and $[Ru^{III}(bipy)_3]^{3+}$, then ECL is observed *via* the following mechanism:

$$[Ru(bipy)_3]^{2+} + e^- \rightarrow [Ru(bipy)_3]^+$$
$$[Ru(bipy)_3]^{2+} - e^- \rightarrow [Ru(bipy)_3]^{3+}$$
$$[Ru(bipy)_3]^{3+} + [Ru(bipy)_3]^+ \rightarrow [Ru^*(bipy)_3]^{2+} + [Ru(bipy)_3]^{2+}$$
$$[Ru^*(bipy)_3]^{2+} \rightarrow [Ru(bipy)_3]^{2+} + h\upsilon$$

8.2.7. REFERENCES

1. K. J. Takeuchi, G. J. Samuels, S. W. Gersten, J. A. Gilbert and T. J. Meyer, *Inorg. Chem.*, 1983, **22**, 1407.
2. D. T. Richens and A. G. Sykes, *J. Chem. Soc., Dalton Trans.*, 1982, 1621.
3. C. K. Poon, C. M. Che and Y. P. Kan, *J. Chem. Soc., Dalton Trans.* , 1980, 128.
4. J. Gulens, D. Konrad and F. C. Anson, *J. Electrochem. Soc.*, 1974, **121**, 1421.
5. C. K. Poon, S. S. Kwong, C. M. Che and Y. P. Kan, *J. Chem. Soc., Dalton Trans.*, 1982, 1457.
6. L. P. Hammett, 'Physical Organic Chemistry', 2nd edn., McGraw-Hill, New York, 1970; P. Zuman, 'Substituent Effects in Organic Polarography', Plenum, New York, 1967.
7. R. W. Taft, *J. Am. Chem. Soc.*, 1953, **75**, 4231.
8. A. M. Bond, S. W. Carr, R. Colton and D. P. Kelly, *Inorg. Chem.*, 1983, **22**, 989 and refs. therein.
9. K. Das, K. M. Kadish and J. L. Bear, *Inorg. Chem.*, 1978, **17**, 930.
10. J. Chatt, *Coord. Chem. Rev.*, 1982, **43**, 337.
11. A. M. Bond, G. A. Lawrance, P. A. Lay and A. M. Sargeson, *Inorg. Chem.*, 1983, **22**, 2010.
12. C. K. Poon, C. M. Che and Y. P. Kan, *J. Chem. Soc., Dalton Trans.*, 1980, 128.
13. A. A. Vlcek, *Prog. Inorg. Chem.*, 1963, **5**, 211–384.
14. D. R. Crow, 'Polarography of Metal Complexes', Academic, New York, 1969, pp. 147–157.
15. D. R. Crow and J. G. Sharp, *J. Inorg. Nucl. Chem.*, 1980, **42**, 863.
16. N. J. Curtis, G. A. Lawrance and A. M. Sargeson, *Aust. J. Chem.*, 1983, **36**, 1327.
17. J. B. Flanagan, S. Margel, A. J. Bard and F. C. Anson, *J. Am. Chem. Soc.*, 1978, **100**, 4248.
18. (a) D. E. Richardson and H. Taube, *Inorg. Chem.*, 1981, **20**, 1278; (b) J. E. Sutton and H. Taube, *Inorg. Chem.*, 1981, **20**, 3125.
19. R. R. Gagné, C. L. Spiro, T. J. Smith, C. A. Hamann, W. R. Thies and A. K. Shiemke, *J. Am. Chem. Soc.*, 1981, **103**, 4073.
20. M. B. Robin and P. Day, *Adv. Inorg. Chem. Radiochem.*, 1967, **10**, 247.
21. J. E. J. Schmitz and J. G. M. van der Linden, *Inorg. Chem.*, 1984, **23**, 117.
22. L. S. Hollis and S. J. Lippard, *Inorg. Chem.*, 1983, **22**, 2605 and refs. therein.
23. M. T. Paffett and F. C. Anson, *Inorg. Chem.*, 1983, **22**, 1347.
24. P. Lemoine, *Coord. Chem. Rev.*, 1982, **47**, 55.
25. R. W. Murray, *Acc. Chem. Res.*, 1980, **13**, 135.
26. R. W. Murray, *Philos. Trans. R. Soc. London, Ser. A*, 1981, **302**, 253.
27. J. Zak and T. Kuwana, *J. Electroanal. Chem.*, 1983, **150**, 645.
28. C. D. Ellis, J. A. Gilbert, W. R. Murphy Jr. and T. J. Meyer, *J. Am. Chem. Soc.*, 1983, **105**, 4842.
29. M. L. Fultz and R. A. Durst, *Anal. Chim. Acta*, 1982, **140**, 1.
30. N. Oyama and F. C. Anson, *J. Am. Chem. Soc.*, 1979, **101**, 3450.
31. C. D. Ellis, L. D. Margerum, R. W. Murray and T. J. Meyer, *Inorg. Chem.*, 1983, **22**, 1283.
32. M. Julliard and M. Chanon, *Chem. Br.*, 1982, **18**, 558.
33. A. Harriman, *Platinum Met. Rev.*, 1983, **27**, 102.
34. D. P. Rillema, G. Allen, T. J. Meyer and D. Conrad, *Inorg. Chem.*, 1983, **22**, 1617.
35. J. Gonzales-Velasco, I. Rubinstein, R. J. Crutchley, A. B. P. Lever and A. J. Bard, *Inorg. Chem.*, 1983, **22**, 822.

8.3

Electrochemical Properties in Non-aqueous Solutions

CHRISTOPHER J. PICKETT
University of Sussex, Brighton, UK

8.3.1 APROTIC ELECTROLYTES

The principal advantage of aprotic electrolytes is that they provide the electrochemist with a wide potential domain within which to examine the electron-transfer chemistry of molecules or ions in solution.[1–3]

The electrochemical 'window' in aqueous electrolytes is limited by proton discharge and water oxidation. The negative domain can be stretched by working at high pH and by using an electrode material which has a high overpotential for proton discharge, *e.g.* mercury. The positive domain can be extended by working at low pH. Nevertheless, electrochemistry in water is still rather limited. The interesting domains in which highly reactive species can be generated and characterized, negative of about −1.5 V and positive of about 1.5 V *versus* the standard hydrogen electrode, are not accessible. In addition, water is a rather reactive solvent with electrophilic, nucleophilic and ligating properties. The same arguments apply to a greater or lesser extent with other hydroxylic solvents such as ethanol. However, trifluoroacetic acid containing $[NBu_4][BF_4]$ is of particularly low nucleophilicity and has been successfully used to stabilize electrogenerated metallo cations.[4]

The ideal aprotic electrolyte will have the widest possible potential window, be highly conducting and inert, yet a good solvent for neutral and ionic compounds. Perhaps the electrolyte which comes closest to the ideal is MeCN containing 0.2 M $[NBu_4][BF_4]$; MeCN does have the disadvantage that it can function as a rather good ligand at a wide variety of metal centres and in some conditions serve as a proton source. Other common aprotic electrolytes which can be frequently used with advantage are CH_2Cl_2, dimethylformamide (DMF) or tetrahydrofuran (THF) solutions of tetraalkylammonium $[BF_4]^-$ or $[ClO_4]^-$ salts: THF electrolytes are particularly useful for reductions at extreme negative potentials although the solutions are rather resistive. Less familiar electrolytes with interesting properties are liquid SO_2–0.1 M$[NBu_4][ClO_4]$, which has a good positive window *ca.* 0 to +3.5 V, liquid NH_3 – 0.1 M KCl, which is useful in the range *ca.* 0 to −3.0 V,[3] and $[NBu_4][BF_4]\cdot 3$ toluene, an ionic liquid which has a wide window of *ca.* ±3.0 V and is of low reactivity.[5]

8.3.2 SINGLE ELECTRON-TRANSFER REACTIONS, ELECTRON-TRANSFER SERIES AND LINKED REDOX CENTRES

The simplest electrochemical reaction which a compound can undergo at an electrode in an electrolyte is single, reversible electron transfer; there are innumerable examples of coordination compounds which show this type of behaviour. Figure 1 shows a cyclic voltammogram of one such example, the reversible one-electron oxidation of *trans*-$[Mo^{II}Cl_2(Ph_2PCH_2CH_2PPh_2)_2]$ (equation 1).

$$trans\text{-}[MoCl_2(Ph_2PCH_2CH_2PPh_2)_2] \underset{+e}{\overset{-e}{\rightleftharpoons}} trans\text{-}[MoCl_2(Ph_2PCH_2CH_2PPh_2)_2]^+ \qquad (1)$$

Preparative scale controlled potential electrolysis of the Mo^{II} species generates the stable cation, *trans*-$[Mo^{III}Cl_2(Ph_2PCH_2CH_2PPh_2)_2]^+$. An X-ray crystallographic analysis of the two redox partners shows that there is little structural change upon removal of one electron. The average Mo—Cl distance decreases by about 0.01 Å whilst the average Mo—P distance increases by about 0.1 Å; the basic octahedral geometry is retained.[6] This illustrates a general rule that reversible electron-transfer chemistry usually results in minimal structural change.[3] This is not a hard and fast rule, since there are examples where facile isomerization accompanies electron transfer, but the cyclic voltammetric behaviour is unperturbed, *i.e.* $E°$ values of the two isomeric pairs are essentially identical.[7] The diagnostic criteria of a reversible (Nernstian), diffusion-controlled, one-electron transfer process have been thoroughly documented for a wide range of electrochemical techniques[1–3] and will not be discussed here.

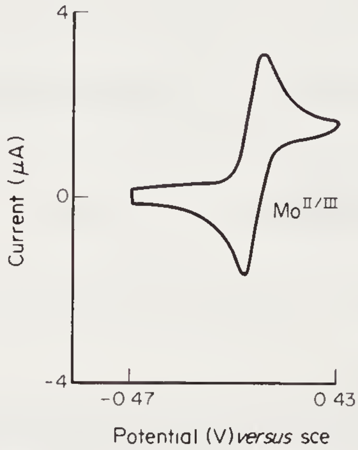

Figure 1. Oxidation of *trans*-$[MoCl_2(Ph_2PCH_2CH_2PPh_2)_2]$ (0.8 mmol dm^{-3}) in THF – 0.2 mol dm^{-3} $[NBu_4][BF_4]$ at a platinum electrode, scan rate 0.1 V s^{-1}.

Cyclic voltammetric and related techniques are particularly valuable for determining $E°$ values in cases where one member of the redox couple is unstable. At a microelectrode in electrolytes of low resistivity, cyclic voltammograms can be recorded at scan rates up to about 100 V s^{-1} and at low temperatures. This allows the detection of reversibility when the unstable partner has a life-time of the order of a millisecond or so. Ultra-microelectrode techniques promise to lower this limit even further.[1–3]

Several classes of coordination compound undergo several successive, reversible one-electron-transfer reactions. These comprise a so-called 'electron-transfer chain' or 'series'.[8] Cyclic voltammetry is particularly useful for recognizing such behaviour and an example is illustrated by Figure 2. This shows the four members of the electron-transfer chain $[Fe_4S_4(SPh)_4]^{n-}$, $n = 1–4$.[5] An electron-transfer series provides the coordination chemist with a means of examining the consequence of systematic addition (or removal) of electrons from a nominally fixed geometry: thermodynamic, kinetic and spectroscopic relationships between members of a series can be explored.[9]

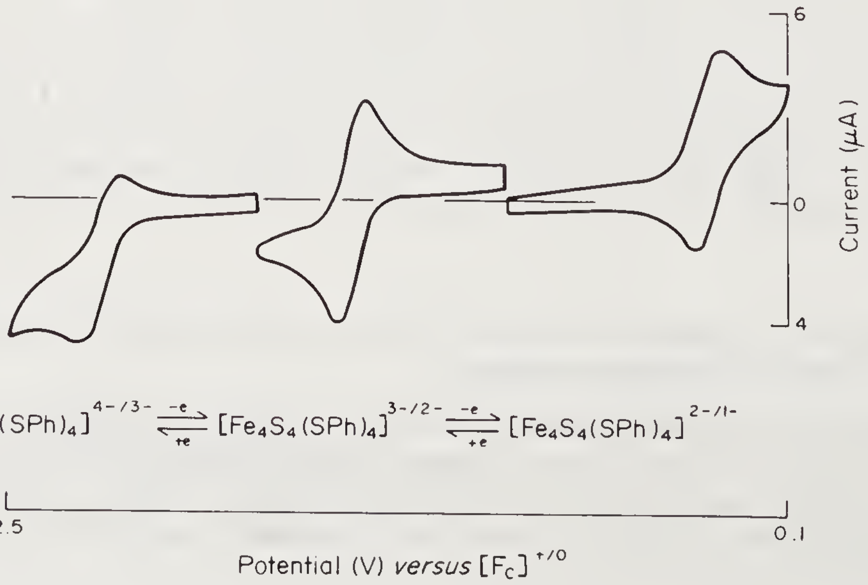

Figure 2 Electron-transfer series $[Fe_4S_4(SPh)_4]^{4-/3-/2-/1-}$ (3.8 mmol dm^{-3}) in 3:1 toluene:$[NBu_4][BF_4]$ at 23 °C, using platinum electrode and scan rate of 0.1 V s^{-1}

A question of particular interest is whether or not the redox orbitals are essentially metal or ligand based and how this varies as one traverses the series. For example, $[\text{Ru}(\text{bipy})_3]^{2+}$ (bipy = 2,2′-bipyridyl), a complex much studied for its photoredox chemistry, has been shown by electrochemical and spectroelectrochemical studies to undergo a series of reversible, ligand-localized electron-transfer reactions 'about' the reversible metal-centred $\text{Ru}^{\text{II}}/\text{Ru}^{\text{III}}$ couple (reaction 2).[9,10]

$$\begin{tikzcd}
{[\text{Ru}^{\text{II}}(\text{bipy})_3]^{2+}} \arrow[r, shift left, "-e"] \arrow[d, shift right, "-e"'] & {[\text{Ru}^{\text{III}}(\text{bipy})_3]^{3+}} \arrow[l, shift left, "+e"] \arrow[r, shift left, "-e"] & {[\text{Ru}^{\text{III}}(\text{bipy})_2(\overset{\cdot +}{\text{bipy}})]^{4+}} \arrow[l, shift left, "+e"] \\
{[\text{Ru}^{\text{II}}(\text{bipy})_2(\overset{\cdot -}{\text{bipy}})]^{+}} \arrow[u, shift right, "e"'] \arrow[r, shift left, "e"] & {[\text{Ru}^{\text{II}}(\text{bipy})(\overset{\cdot -}{\text{bipy}})_2]^{0}} \arrow[l, shift left, "-e"] \arrow[r, shift left, "e"] & {[\text{Ru}^{\text{II}}(\overset{\cdot -}{\text{bipy}})_3]^{-}} \arrow[l, shift left, "-e"]
\end{tikzcd} \tag{2}$$

Such electron-transfer processes have been referred to as 'ligand-based mixed-valency'.[11] Porphyrin, phthalocyanine and related complexes frequently show ligand-centred redox chemistry but with the spin-density delocalized over the macrocycle. A rather interesting example of this, which also demonstrates the importance of axial ligation, is shown by the electrochemistry of a ruthenium(II) octaethylporphyrin (OEP) complex.[12] With a carbonyl and a pyridine ligand occupying the two axial positions, this complex undergoes reversible one-electron oxidation which is ligand centred. Replacing both the carbonyl and the pyridine groups by two PPh_3 ligands induces an intramolecular electron transfer, generating a Ru^{III} centre (reaction 3).

$$\left[\text{Ru}^{\text{II}}(\text{OEP})(\text{CO})(\text{py})\right] \underset{e}{\overset{-e}{\rightleftharpoons}} \left[\text{Ru}^{\text{II}}(\overset{\cdot +}{\text{OEP}})(\text{CO})(\text{py})\right]^{+} \xrightarrow{\text{PPh}_3} \left[\text{Ru}^{\text{III}}(\text{OEP})(\text{PPh}_3)_2\right]^{+} \tag{3}$$

Cyclic voltammetric methods, or other related techniques such as differential pulse polarography and AC voltammetry,[3] provided a convenient method for the estimation of equilibrium constants for disproportionation or its converse, comproportionation. In this respect, the experimentally measured quantity of interest in a cyclic voltammetric experiment is $E_{½}$, the potential mid-way between the cathodic and anodic peak potentials. For a one-electron process, $E_{½}$ is related to the thermodynamic standard potential $E°$ by equation (4).[13] In practice, $E_{1/2} = E°$ is usually a good approximation.

$$E° = E_{½} - \frac{RT}{F} \ln(D_R/D_O)^{½}(\gamma_O/\gamma_R) \tag{4}$$

(D_R and D_O are the diffusion coefficients for the reduced and oxidized species; γ_O and γ_R are their respective activity coefficients.)

Suppose a compound, M, is observed to undergo two successive one-electron reduction steps (equation 5). The comproportionation constant K_c for reaction (6) is simply given by expression (7). At 298 K, with $\{E°_1 - E°_2 = \Delta E°\}$ expressed in mV, then expression (7) reduces to $K_c = \exp \Delta E/25.69$.

$$\text{M} \underset{-e}{\overset{\overset{E°_1}{e}}{\rightleftharpoons}} \text{M}^- \underset{-e}{\overset{\overset{E°_2}{e}}{\rightleftharpoons}} \text{M}^{2-} \tag{5}$$

$$\text{M} + \text{M}^{2-} \overset{K_c}{\rightleftharpoons} 2\text{M}^- \tag{6}$$

$$K_c = \exp\left[\frac{(E°_1 - E°_2)F}{RT}\right] \tag{7}$$

The study of mixed-valence species with two identical metal centres linked by a bridging ligand, *e.g.*

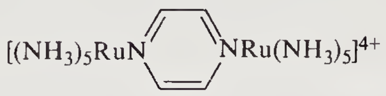

has played a central role in understanding the energetics of intramolecular electron transfer.[14] Estimation of K_c for such systems provides a measure of the degree of interaction of the metal centres. For two non-interacting metal centres, such as those linked by an 'insulating' bridge, $K_c = 0$ and the separation of the cathodic and anodic peak potentials in the reversible two-electron cyclic voltammogram is close to 36 mV at 298 K.[15] With K_c values greater than 0, then more or less interaction of the metal centres obtains. Such interaction may be a consequence of an electrostatic (field) effect, or reflect delocalization of charge across the two metal centres. Whilst electrochemical measurements alone cannot determine the relative importance of factors such as these, in combination with an analysis of electronic transitions, a knowledge of the inter-metal distance and EPR data, K_c values contribute the overall understanding of the electronic condition of a mixed-valence species.[16]

8.3.3 REDOX POTENTIALS AND STRUCTURE

Much information can be gained by examining trends in redox potentials within series of compounds. Let us consider such a series of coordination compounds, M_0, M_1, M_2 ... M_n, which undergo reversible, one-electron oxidation reactions at potentials $E°_0$, $E°_1$, $E°_2$, ... $E°_n$ respectively, with respect to the same reference electrode. If we define the oxidation of M_0 as our standard reaction (equation 8), then we can examine the variation of the free energy difference, $F(E°_0 - E°_n)$, in terms of the structural difference between M_0 and each other member M_n. Such an analysis is directly comparable to the classic approach of Hammett[17] which relates a free energy difference term, $\log(K_H/K_X)$, for equilibrium reactions such as (9) and (10), to the nature of the aryl substituent, X.

$$M^+_0 + e \rightleftharpoons M_0\ ;\ E°_0 \qquad (8)$$

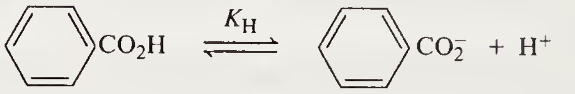

(9)

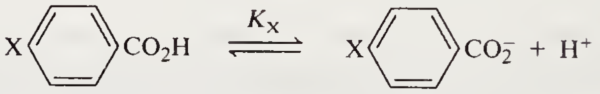

(10)

As with the Hammett analysis, we are primarily interested in the electronic contribution to $F(E°_0 - E°_n)$ rather than with the contribution of outer-sphere free-energy terms, *i.e.* solvation and ion-pairing effects. In practice, the outer-sphere terms for couples which involve the same overall change in net charge, *e.g.* $M_n^{0/+}$, are usually quite similar and therefore self-cancelling in the subtraction $(E°_0 - E°_n)$. (The same approximation is of course assumed in the Hammett analysis.) Even in cases where one desires to compare $E°$ values for couples which differ in the overall change in net charge, *e.g.* a couple $M^{0/+}$ with a couple $M^{-/0}$, the outer-sphere terms can often be neglected. Where the coordination compound has a radius of several ångströms and the redox potentials are measured in an aprotic electrolyte with weak solvation and ion-pairing properties, outer-sphere terms are often relatively small. Where they are not, some account of solvation energy contributions can be made using the Börn equation.[18]

With the above considerations in mind, we can now treat $F(E°_0 - E°_n)$ as a measure of inner-sphere electronic effects and relate it to the structural aspects such as the nature of the metal centre, the ligands and the redox orbital involved in the electron-transfer reaction. For an oxidation process, $F(E°_0 - E°_n)$ provides a reasonable measure of the change in energy of the Highest Occupied Molecular Orbital (HOMO); for a reduction process, we are dealing with relative changes in the energy of the Lowest Unoccupied Molecular Orbital (LUMO). There is a rather good pictorial illustration of this concept in the book of Bard and Faulkner to which the reader is referred.[19] Strictly speaking, $F(E°_0 - E°_n)$ is related to the energy difference between the oxidized and reduced states of the species; nevertheless, as discussed by Fenske, [20] trends in $E°$ should be expected to follow trends in HOMO (or LUMO) energy levels. Indeed, molecular orbital calculations for the reversible one-electron oxidations of a series of aromatic compounds,[21] and for the series $[Mn(CO)_{6-n}(CNMe)_n]$, $n = 0-6$,[20,22] correlate linearly with $E_{1/2} (\approx E°)$ data.

Correlation of gas-phase ionization potential data with solution redox potentials for series of organic, organometallic and coordination compounds[21-23] underlines the relationship between $F(E°_0 - E°_n)$ and orbital energies. For example, Cr 3*d* binding energy data for the first ionization process of complexes $[Cr(CO)_5L]$ correlate reasonably linearly with the $(E°_0 - E°_n)$ parameter, P_L,[23] as is illustrated by Figure 3.

Figure 3 also illustrates the considerable effect a single ligand change exerts on $(E°_0 - E°_n)$: values for the $[Cr(CO)_5(MeCN)]^{0/+}$ and $[Cr(CO)_6]^{0/+}$ couples differ by about 0.6 V, corresponding to about 60 kJ mol^{-1}. The influence of ligands on redox potentials is of course of considerable interest in many areas of coordination chemistry. On the one hand, we may be interested in the design of a compound with 'tailored' redox orbitals, or on the other, in understanding how ligands control the redox properties of metal centres in enzymes.

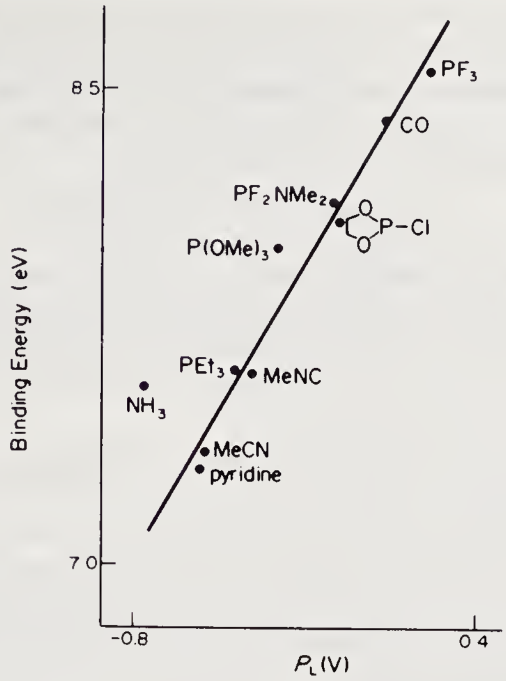

Figure 3 The relationship between photoelectron binding energy of $3d$ electrons of chromium and P_L for a range of ligands L in the complex $[Cr(CO)_5L]$

Ligands which possess a substituted aryl ring, *e.g.* p-XC_6H_4NC (X is a substituent), provide a convenient means of systematically perturbing the redox orbitals of a metal centre to which they are bound. Inductive or mesomeric influences on the redox orbitals can be probed by correlating $E°$ data with Hammett substituent constants such as σ_p or σ_p^+. There are numerous series which show linear correlations of $E°$ data with such constants,[24-26] usually σ_p. The ability of the $\{LC_6H_4X\text{-}p\}$ group to transmit its influence to the redox orbital(s) is reflected by the magnitude of the Hammett reaction constant, ρ. For an oxidation series with a correlation of $E°$ with σ_p, ρ is given by relationship (11).

$$\frac{F}{2.303RT}(\mathrm{d}E°/\mathrm{d}\sigma_p) = -\rho \tag{11}$$

Whilst such correlations of $E°$ with Hammett constants are interesting, the perturbations are usually small, X being remote from the valence orbitals of the metal centre. Of more consequence is changing the nature of a ligating atom or group, L, in a more dramatic fashion; for example, changing an O ligand for an S (Figure 4).[27]

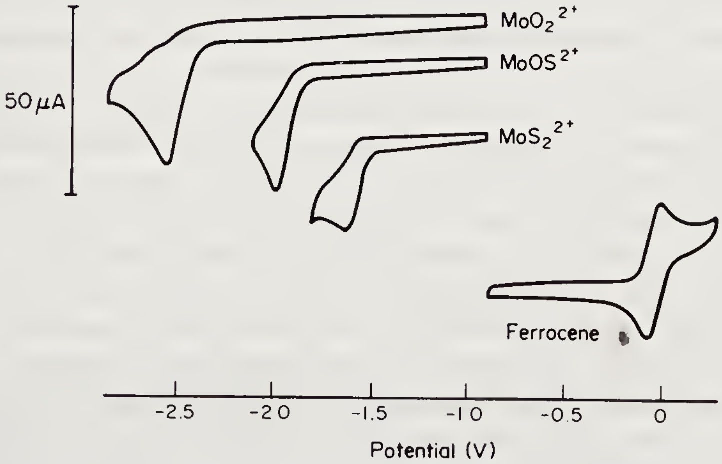

Figure 4 Cyclic voltammograms of the complexes *cis*-$[MoY_2(C_5H_{10}NO)_2]$ (Y = O and/or S) in a solution of 0.2 mol dm^{-3} $[NBu_4][BF_4]$ in DMF at 298 K and at a vitreous carbon electrode, scan rate 0.3 V s^{-1}

One approach to quantifying ligand effects on the oxidation potentials of closed-shell complexes is to define a scale of ligand constants for a 'standard' series, which are based on the free-energy difference $F(E°_0 - E°_n)$. This is analogous to the basis of the Hammett σ-scales. The standard series $[Cr(CO)_5L]$ has been used to define the ligand constant, P_L, according to the relationship (12).[28] L is a neutral or anionic two-electron donor ligand; when L = CO, $P_L = 0.0$ (*cf.* when X = H, $\sigma_p = 0.0$). P_L is found to correlate reasonably linearly with $E°$ data for the reversible oxidations of other series of octahedral closed-shell complexes which possess a ligand L; such relationships have been used diagnostically to identify unstable species.[28] From the linear correlations of P_L with E° data it is possible to determine a constant β, dE°/dP_L, analogous to the Hammett reaction constant, ρ. It provides a measure of the efficiency of the transmission of the ligand influence to the energy of the HOMO. The success or failure of such correlations presumably depends upon the HOMO being isolated from the valence orbitals on L.

$$P_L = E_{1/2}\{[Cr(CO)_5L]\} - E_{1/2}\{[Cr(CO)_6]\} \tag{12}$$

The redox potentials of many metalloporphyrin complexes are sensitive to the nature of the electrolyte in which they are measured. This is because one or both axial positions are coordinated by either solvent or anionic ligands. Such dependencies of E° values have been extensively studied by Kadish and coworkers;[29] notably good correlation between E° data and Donor/Acceptor Number properties of solvents have been observed.

Several studies have dealt with the 'additivity' of ligand influence on redox potentials, particularly for series such as $[Mn(CO)_{6-n}(CNMe)_n]$, $n = 0$–6. To a first approximation, successive replacement of one CO ligand by a CNMe group results in an incremental decrease in E°.[30,31] In detail when $n = 2$ or 3 the *cis* and *trans* and the *mer* and *fac* isomers in such series can deviate considerably from the linear trend of E° with n. Such deviation has been elegantly analyzed by Bursten, who has provided an empirical relationship between the HOMO energy of such complexes and $E_{1/2}$ data for their reversible one-electron oxidation.[32] This has the form shown by equation (13), where A, B and C are empirically determined parameters, n is the number of ligands, as in $[Cr(CO)_{6-n})(CNMe)_n]$, and x the number of those ligands which interact with the d_π orbital comprising the HOMO of the complex.

$$E_{1/2} = A + B_n + C_x \tag{13}$$

Whilst ligand effects can produce substantial changes in $F(E^\circ_0 - E^\circ_n)$, an overriding influence on the free-energy difference results when isostructural, isoelectronic species differ in net charge.[30,33] The $E^{\circ\prime}$ of the $d^{1/0}$ couples, $[WF_6]^{1-/0}$ and $[TaF_6]^{2-/1-}$, differ by about 3.2 V (of course the Ta couple occurs at the more negative potential): solvation energy changes account for no more than about 0.1 V of this difference.[33] A difference in E° potentials of a similar magnitude is observed between the oxidation potentials of $[WF_6]^{2-}$ and its isostructural, isoelectronic analogue $[ReF_6]^{1-}$ for the $d^{2/1}$ couples. However, the lower-valent couples *trans*-$[WCl_2(Ph_2PCH_2CH_2PPh_2)_2]^{1-/0}$ and *trans*-$[ReCl_2(Ph_2PCH_2CH_2PPh_2)_2]^{1+/0}$, $d^{5/4}$, differ by only 1.5 V. In this context it is interesting to compare cogeners. The $d^{1/0}$ couples $[WF_6]^{1-/0}$ and $[MoF_6]^{1-/0}$ differ in E° values by about 1.0 V, the heavier metal complex being the easier to oxidize; a similar difference in ease of oxidation is observed with the $[OsF_6]^{3-/2-}$ and $[RuF_6]^{3-/2-}$ $d^{5/4}$ couples. In contrast, the oxidation potentials for *trans*-$[WCl_2(Ph_2PCH_2CH_2PPh_2)_2]$ and its molybdenum analogue differ by a mere 0.1 V. Evidently the π-acceptor ligands, $Ph_2PCH_2CH_2PPh_2$, level the effect of the change in the central metal on the energy of the redox orbital: ligands such as F, which are incapable of π-acceptor behaviour, expose the dominant influence of the charge on the metal core.[33]

Redox potential data frequently correlate with parameters obtained by other spectroscopic measurements. The correlation of E° potentials with gas-phase ionization potentials has already been briefly discussed. Electronic transitions observed by UV-visible spectroscopy involve the promotion of an electron from one orbital to another and this can be viewed as an intramolecular redox reaction. If the promotion involves the displacement of an electron from the HOMO to the LUMO, then the redox potentials for the reduction of the compound, E°_{RED}, and for its oxidation, E°_{OX}, are of importance. For a closely related series of compounds, trends in oxidation and reduction potentials can be related to shifts in the absorption frequency, ν. If the structural perturbation causes the HOMO and the LUMO to rise or fall in energy in tandem, then $(E^\circ_{RED} - E^\circ_{OX})$ will remain constant; in such cases the HOMO–LUMO frequency (energy) will be essentially independent of the structural perturbation. Where there is a differential influence of the perturbation on the HOMO and the LUMO, then $(E^\circ_{RED} - E^\circ_{OX})$ will vary as will the energy of the electronic transition. In such cases a linear correlation of E°_{RED} or E°_{OX} may result. In the limit the energy of the HOMO, or more usually the LUMO, will be unaffected by structural perturbation; where the acceptor orbital is pinned, direct linear correlation of E°_{OX} with ν should be apparent. With E°_{OX} and ν in a common energy unit, the plot E°_{OX} *versus* ν should have a slope close to one.[33–36]

Infrared vibrational energies of ligating groups such as CO, N_2, NO or RNC (R = alkyl or aryl) have been extensively correlated with redox potential data.[28,37–41] For a series of closely related mononuclear complexes it is generally observed that as E° (or $E_{1/2}$) for the oxidation of members of the series becomes increasingly positive, then ν, the infrared stretching frequency for the (terminally bound) ligand (CO *etc.*), shifts to higher values. In many cases, reasonably good linear correlation between E°_{OX} and v is observed. The basis of such relationships can be visualized in the following way. As the effective nuclear charge on the metal is increased (by a structural perturbation), valence and redox orbital electrons are held more tightly by the metal centre, E°_{OX} becomes more positive, in parallel ligand to metal σ-donation is enhanced and metal to ligand $d\pi-\pi^*$ back-donation is decreased, thereby increasing ν.

Some attempt has been made to establish relationships between chemical shifts, measured by nuclear magnetic resonance spectroscopy and redox potential data.[42]

Finally, trends correlating the reactivity of coordination compounds towards nucleophiles or electrophiles and their redox potentials have been noted.[28,43]

8.3.4 CHEMISTRY FOLLOWING SINGLE ELECTRON TRANSFER

A single electron-transfer reaction of a coordination compound may result in the generation of an unstable or reactive species which decays to a more stable product, *i.e.* the primary species generated by electron transfer undergoes further chemistry.

Cyclic voltammetry provides a convenient method of recognizing such processes provided the lifetime of the intermediate is less than a minute or so. Consider an idealized reaction pathway (14) which involves the reversible one-electron reduction of a compound M. Of primary interest in the cyclic voltammetric experiment is the ratio of the back- and forward-peak currents, $i_\mathrm{p}{}^\mathrm{b}/i_\mathrm{p}{}^\mathrm{f}$, and the dependence of this ratio upon the scan rate, v.

$$\mathrm{M} \underset{-\mathrm{e}}{\overset{\mathrm{e}}{\rightleftharpoons}} \mathrm{M}^- \xrightarrow{k} \text{Product} \tag{14}$$

If M⁻ is unstable then $i_\mathrm{p}{}^\mathrm{b}/i_\mathrm{p}{}^\mathrm{f}$ will be less than unity. Its magnitude will depend upon the scan rate, the value of the first-order constant k, and the conditions of the experiment. At fast scan rates the ratio $i_\mathrm{p}{}^\mathrm{b}/i_\mathrm{p}{}^\mathrm{f}$, may approach one if the time gate for the decomposition of M^- is small compared with the half-life of M^-, ($\ln 2/k$). As the temperature is lowered, the magnitude of k may be sufficiently decreased for full reversible behaviour to be observed. The decomposition of M^- could involve the attack of a solution species upon it, *e.g.* an electrophile. In such cases, $i_\mathrm{p}{}^\mathrm{b}/i_\mathrm{p}{}^\mathrm{f}$, will of course be dependent upon the concentration of the particular substrate (under pseudo-first-order conditions, k is k_apparent). Quantitative cyclic voltammetric and related techniques allow the evaluation of the rate constants for such electrochemical–chemical, EC, processes. At the limit, the electron-transfer process is completely 'irreversible' if k is sufficiently large with respect to the rate of heterogeneous electron transfer; the electrochemical and chemical steps are concerted on the time-scale of the cyclic voltammetric experiment.[1–3]

The simplest example of an EC process is one in which structural isomerization follows single electron transfer, *e.g.* reaction (15),[44] and many examples of this type of reaction have been reported.[28,45–46]

$$\begin{tikzcd}
\textit{cis}\text{-}[\mathrm{Cr(CO)_2Ph_2PCH_2PPh_2)_2}] \arrow[r, shift left, "-\mathrm{e}"] & \textit{cis}\text{-}[\mathrm{Cr(CO)_2(Ph_2PCH_2PPh_2)_2}]^+ \arrow[l, shift left, "+\mathrm{e}"] \arrow[d] \\
 & \textit{trans}\text{-}[\mathrm{Cr(CO)_2(Ph_2PCH_2PPh_2)_2}]^+
\end{tikzcd} \tag{15}$$

There is, of course, a considerable diversity in the type of chemical reaction which follows electron transfer. The making or breaking of metal–ligand or metal–metal bonds, ligand-centred chemistry, disproportionation, and catalytic or stoichiometric oxidation or reduction of a solution substrate represent some of the types of reaction which are preceded by electron transfer. In many cases the following chemistry is quite complex; if, for example, the product of the chemical step is itself electroactive (at or near the potential necessary for the primary electron-transfer process to occur) then further electron transfer will result (an ECE process).[1–3] Usually such processes involve electron transfer in the same direction as the primary process, *i.e.* an oxidation followed by a chemical step leads to an intermediate which is itself oxidized. However, there are several examples where electron transfer involving an oxidation results in a product which is then reduced and *vice versa*: this is the basis of electron-transfer catalyzed substitution reactions such as (16).[47,49] In this reaction there is little current flow and the passage of merely 0.13 electrons per molecule of starting material gives a 98% conversion to product.

$$[W(MeCN)(CO)_5] \xrightarrow[\substack{\text{Pt electrode} \\ \text{MeCN electrolyte} \\ PPh_3}]{-1.0\ \text{V}} [W(PPh_3)(CO)_5] \qquad (16)$$

Modern electrochemical methods provide the coordination chemist with a powerful means of studying chemical reactions coupled to electron transfer and exploiting such chemistry in electrosynthesis. In addition, the electrochemical generation of reactive metallo intermediates can provide routes for the activation of otherwise inert molecules, as in the reduction of N_2 to ammonia,[50] and for electrocatalyzing redox reactions, such as the reduction of CO_2 to formate and oxalate,[51] the oxidation of NH_3 to NO_2^-,[52] and the technologically important oxidation of water to O_2 or its converse, the reduction of O_2 to water.[53] Electrochemical reactions involving coordination compounds and organometallic species have been extensively reviewed.[54–60]

8.3.5 REFERENCES

1. R. N. Adams, 'Electrochemistry at Solid Electrodes', Dekker, New York, 1969.
2. D. T. Sawyer and J. L. Roberts Jr., 'Experimental Electrochemistry for Chemists', Wiley-Interscience, New York, 1974.
3. A. J. Bard and L. R. Faulkner, 'Electrochemical Methods', Wiley, New York, 1980.
4. C. J. Pickett and D. Pletcher, *J. Chem. Soc., Dalton Trans.*, 1976, 636; see also S. N. Milligan, I. Tucker and R. D. Riecke, *Inorg. Chem.*, 1983, **22**, 987.
5. C. J. Pickett, *J. Chem. Soc., Chem. Commun.*, 1985, 323.
6. T. Al-Salih and C. J. Pickett, *J. Chem. Soc., Dalton Trans.*, 1985, 1255; T. Al-Salih, D. L. Hughes and C. J. Pickett, unpublished data.
7. A. M. Bond, D. J. Darensbourg, E. Mocellin and B. J. Stewart, *J. Am. Chem. Soc.*, 1981, **103**, 6827.
8. J. A. McCleverty, in 'Reactions of Molecules at Electrodes', ed. N. S. Hush, Wiley-Interscience, New York, 1971, p. 363 and refs. therein.
9. J. G. Gaudiello, P. R. Sharp and A. J. Bard, *J. Am. Chem. Soc.*, 1982, **104**, 6373.
10. P. S. Braterman, G. A. Heath and L. J. Yellowlees, *J. Chem. Soc., Chem. Commun.*, 1981, 287.
11. P. S. Braterman, G. A. Heath and L. J. Yellowlees, *Chem. Phys. Lett.*, 1982, **92**, 646.
12. M. Borley, J. Y. Becker, G. Domazetis, D. Dolphin and B. R. James, *J. Chem. Soc., Chem. Commun.*, 1981, 982; see also C. W. G. Ansell, J. Lewis, M. C. Liptrot, P. R. Raithby and M. Schroeder, *J. Chem. Soc., Dalton Trans.*, 1982, 1593.
13. P. Delahay, 'New Instrumental Methods in Electrochemistry', Interscience, New York, 1954, p. 56.
14. H. Taube, *Ann. N. Y. Acad. Sci.*, 1978, **313**, 481.
15. J. B. Flanagan, S. Murgel, A. J. Bard and F. C. Anson, *J. Am. Chem. Soc.*, 1978, **100**, 4248.
16. D. E. Richardson and H. Taube, *Inorg. Chem.*, 1981, **20**, 1278.
17. L. P. Hammett, 'Physical Organic Chemistry', McGraw-Hill, New York, 1940.
18. M. Born, *Z. Phys.*, 1920, **1**, 45.
19. A. J. Bard and L. R. Faulkner, 'Electrochemical Methods', Wiley, New York, 1980, pp. 4–5.
20. A. C. Sarape and R. F. Fenske, *Inorg. Chem.*, 1975, **14**, 247.
21. K. M. Kadish, L. A. Bottomley, J. G. Brace and N. Winograd, *J. Am. Chem. Soc.*, 1980, **102**, 431.
22. R. J. Klinger and J. K. Kochi, *J. Am. Chem. Soc.*, 1980, **102**, 5741.
23. C. J. Pickett, in 'Electrochemistry', ed. D. Pletcher, Specialist Periodical Report, The Royal Society of Chemistry, London, vol. 9, p. 94.
24. D. A. Bohling, J. F. Evans and K. R. Mann, *Inorg. Chem.*, 1977, **16**, 800.
25. K. M. Kadish, K. Das, D. Schaeper, C. L. Merrill, B. R. Welch and L. J. Wilson, *Inorg. Chem.*, 1980, **19**, 2816.
26. W. Hussain, G. J. Leigh, H. Mohd-Ali, H. Neukomm, C. J. Pickett and D. A. Rankin, *J. Chem. Soc., Dalton Trans.*, 1984, 1703; see also ref. 36.
27. S. Bristow, C. D. Garner and C. J. Pickett, *J. Chem. Soc., Dalton Trans.*, 1984, 1617.
28. J. Chatt, C. T. Kan, G. J. Leigh, C. J. Pickett and D. R. Stanley, *J. Chem. Soc., Dalton Trans.*, 1980, 2032.
29. S. L. Kelly and K. M. Kadish, *Inorg. Chem.*, 1982, **21**, 3631.
30. P. M. Triechel, G. E. Dureen and H. J. Mueh, *J. Organomet. Chem.*, 1972, **44**, 339.
31. C. J. Pickett and D. Pletcher, *J. Organomet. Chem.*, 1975, **102**, 327.
32. B. E. Bursten, *J. Am. Chem. Soc.*, 1982, **104**, 1299 and refs. therein.
33. J. A. Connor, E. M. Jones, G. A. McEwen, M. K. Lloyd and J. A. McCleverty *J. Chem. Soc., Dalton Trans.*, 1972, 1246.
34. J. G. Gandiello, P. R. Sharp and A. J. Bard, *J. Am. Chem. Soc.*, 1982, **104**, 6373.
35. D. F. Shriver and J. Posner, *J. Am. Chem. Soc.*, 1966, **88**, 1672.
36. G. Butler, J. Chatt, G. J. Leigh and C. J. Pickett, *J. Chem. Soc., Dalton Trans.*, 1979, 113.
37. A. A. Vlcek, *Electrochim. Acta*, 1968, **13**, 1063.
38. J. Masek, *Inorg. Chim. Acta Rev.*, 1969, **3**, 99.
39. N. G. Connelly, Z. Devnidowicz and R. L. Kelly, *J. Chem. Soc., Dalton Trans.*, 1975, 2335.
40. D. de Montauzon and R. Poilblanc, *J. Organomet. Chem.*, 1976, **104**, 99.
41. W. Hussain, G. J. Leigh, H. Mohd-Ali, C. J. Pickett and D. A. Rankin, *J. Chem. Soc., Dalton Trans.*, 1984, 1703.
42. A. M. Bond, S. M. Carr, R. Colton and D. P. Kelly, *Inorg. Chem.*, 1983, **22**, 989.
43. J. Chatt, G. J. Leigh, R. H. Morris, C. J. Pickett and D. R. Stanley, *J. Chem. Soc., Dalton Trans.*, 1981, 800.
44. A. M. Bond, R. Colton and J. J. Jackowski, *Inorg. Chem.*, 1975, **14**, 274.
45. F. L. Wimmer, M. R. Snow and A. M. Bond, *Inorg. Chem.*, 1974, **13**, 1617.
46. A. M. Bond, B. S. Grabaric and J. J. Jackowski, *Inorg. Chem.*, 1978, **17**, 2153 and refs. therein.
47. G. J. Bezems, P. H. Rieger and S. Visco, *J. Chem. Soc., Chem. Commun.*, 1981, 265.
48. J. W. Hershberger and J. K. Kochi, *J. Chem. Soc., Chem. Commun.*, 1982, 212.
49. J. W. Hershberger, R. J. Klinger and J. K. Kochi, *J. Am. Chem. Soc.*, 1982, **104**, 3034.

50. C. J. Pickett and J. Talamin, *Nature (London)*, 1985, **316**, 652.
51. M. Tezuka, T. Yatima, A. Tsuchiya, Y. Matsumoto, Y. Uchida and M. Hidai, *J. Am. Chem. Soc.*, 1982, **104**, 6834.
52. T. J. Meyer and M. S. Thompson, *J. Am. Chem. Soc.*, 1981, **103**, 5577.
53. J. A. McCleverty, in 'Reactions of Molecules at Electrodes', ed. N. Hush, Wiley-Interscience, New York, 1971, p. 460.
54. R. E. Dessy and L. A. Banes, *Acc. Chem. Res.*, 1972, **5**, 415.
55. L. K. Denisovitch and S. P. Gubin, *Russ. Chem. Rev. (Engl. Transl.)*, 1977, **46**, 27.
56. D. de Montauzon, R. Poilblanc, P. Lemoine and M. Gross, *Electrochim. Acta*, 1978, **23**, 1247.
57. C. J. Pickett, in 'Electrochemistry', ed. D. Pletcher, Specialist Periodical Report, The Royal Society of Chemistry, London, 1983, vol. 8, p. 81.
58. C. J. Pickett, in 'Electrochemistry', ed. D. Pletcher, Specialist Periodical Report, The Royal Society of Chemistry, London, 1984, vol. 9, p. 162.
59. N. G. Connelly and W. E. Geiger, *Adv. Organomet. Chem.*, 1984, **23**, 1.
60. C. J. Pickett in 'The Chemistry of the Metal–Carbon Bond', ed. F. R. Hartley and S. Dubai, Wiley, Chichester, 1985, vol. 2, p. 1.

9

Quantitative Aspects of Solvent Effects

DAVID H. VAUGHAN
Paisley College of Technology, Paisley, UK

9.1 THE SOLVENT EFFECT AND RATES OF REACTIONS

Probably the most familiar parameter used by the coordination chemist investigating the effect of solvent on rates of reaction of coordination complexes is the relative permittivity ε_R (dielectric constant) of the medium. If the solvent can be regarded as an inert medium then the effect of the solvent can be evaluated, semiquantitatively at least, if only electrostatic forces are considered.

For a reaction between two polar molecules A and B, the application of the transition state theory to the reaction $A+B \rightleftharpoons X^* \rightarrow$ Products, where X^* represents the transition state, and an expression for the free energy of a dipole in a medium of dielectric constant ε_R, derived by Kirkwood,[1] leads to equation (1):

$$\ln k = \ln k_0 - \frac{(\varepsilon_R - 1)}{4\pi\varepsilon_0 kT(2\varepsilon_R + 1)} \left[\frac{\mu_A^2}{r_A^3} + \frac{\mu_B^2}{r_B^3} - \frac{\mu_*^2}{r_*^3} \right] \tag{1}$$

where k is the rate constant in a medium of dielectric constant ε_R, k_0 is the rate constant in a condensed medium of dielectric constant unity, ε_0 is the permittivity of free space and μ and r represent the dipole moment and radius of the given species respectively. Equation (1) predicts that if the activated complex, X^*, is more polar than the reactants, as would be the case if the products were ions, then the rate of the reaction would increase as ε_R increased. In addition, equation (1) predicts that if the dielectric constant can be varied by conducting the reaction in a mixture of two solvents of variable composition, then a linear plot of $\ln k$ *versus* $(\varepsilon_R - 1)/(2\varepsilon_R + 1)$ should be obtained.

If a reaction is studied in a variety of different pure solvents then it is found that equation (1) is not very reliable, and quite commonly a group of similar solvents tend to lie on one straight line whereas another group of solvents may lie on a different straight line. Thus a plot of $\log k$ for the solvolysis of Cl in *trans*-$[Co(DH)_2(NH_3)Cl]$ (DH is a dioximine) against $(\varepsilon_R - 1)/(2\varepsilon_R + 1)$ gave two straight lines,[2] one for protic solvents and one for dipolar aprotic solvents. Interestingly however, a single straight line was obtained when $\log k$ was plotted against E_T, where E_T is the energy of the charge transfer band of the $I^- \rightarrow \pi$ (N-heterocycle) of 1-ethyl-4-methoxycarbonylpyridine iodide in these different solvents. The reason for this behavior is that the dielectric constant does not characterize the specific intermolecular interactions between particles present in the solution, and a better characteristic of such interactions is E_T: the energy of the charge transfer band.

Expressions similar to equation (1) can also be derived from simple electrostatic arguments for reaction between two ions of charge Z_A and Z_B, the rate constant k (presumed to be measured at zero ionic strength) in a medium of dielectric constant ε_R is given by equation (2):

$$\ln k = \ln k_0 - \frac{e^2}{8\pi\varepsilon_0\varepsilon_R kT} \left[\frac{(Z_A + Z_B)^2}{r_*} - \frac{Z_A^2}{r_A} - \frac{Z_B^2}{r_B} \right] \tag{2}$$

where k_0 is the rate constant in a medium of infinite dielectric constant, and r_A, r_B and r_* are the radii of the ions A, B and the activated complex respectively.

Equation (2) is usually employed in a simpler form, equation (3), obtained by letting $r_A = r_B = r_*$:

$$\ln k = \ln k_0 - \frac{Z_A Z_B e^2}{4\pi\varepsilon_0\varepsilon_R kT r_*} \tag{3}$$

which predicts a linear plot of $\ln k$ against $1/\varepsilon_R$ with a positive slope if the ions are of opposite charge, and a negative slope if the ions have the same sign. For a reaction between an ion and a polar molecule *i.e.* $Z_B = 0$, then equation (2) becomes (4):

$$\ln k = \ln k_0 + \frac{Z^2 e^2}{8\pi\varepsilon_0\varepsilon_R kT}\left[\frac{1}{r} - \frac{1}{r_*}\right] \tag{4}$$

Because r_* is larger than r then a linear plot of $\ln k$ *vs.* $1/\varepsilon_R$ with a positive slope will be obtained irrespective of the charge on the ion. The observation[3] that a positive slope of $\log k$ *vs.* $1/\varepsilon_R$ was obtained for the oxidation of triphenylmethane and diphenylmethane by $[Fe(CN)_6]^{3-}$ in various mixtures of aqueous acetic acid was taken as proof that the rate determining step was of the ion dipole type, *i.e.* involved $[Fe(CN)_6]^{3-}$ and the arylalkane molecule.

A study[4] of the base hydrolysis of $[M^{III}(NH_3)_5(NCS)]^{2+}$ (M = Co, Cr, Rh) in aqueous organic mixed solvents illustrates the use of these equations in the elucidation of the mechanism. It was deduced that the reaction proceeded through an ion pair formed between the substrate complex and OH^-. Values of the rate constants for the conversion of the ion pair to the products were determined and it was found that the plots of $\log k$ *vs.* $1/\varepsilon_R$ were linear with positive slopes. The values of the slope indicated that OH^- was the attacking nucleophile and not H_2O, which would have resulted in a numerically smaller slope. It was also argued that if there was significant M—NCS bond dissociation synchronous with the M—OH bond formation, then this would reduce the magnitude of the slope of the plot of $\log k$ *vs.* $1/\varepsilon_R$. The observed order of the slopes was found to be Co > Rh ≫ Cr, which indicates that there was a significant difference in the relative degree of M—NCS bond breaking and M—OH bond formation for the three metals, with bond breaking being largest for Cr and bond making relatively larger for Co and Rh.

In general these equations would appear to be more applicable to solvent mixtures than to different solvents. The reason is probably because under the first set of conditions the nature of the solvation process, *i.e.* the size and structure of the solvated solute, as well as the structure of the solvent (which may well be modified by the solute) may stay approximately constant over a limited range, at least, of composition. This point is especially important where ions are involved as these make special demands on the solvent because of the magnitude of the interaction. Because it is recognized that in many circumstances the solvent may participate quite actively in the reaction as well as possibly acting as a nucleophile, attempts have been made to correlate kinetic parameters with various solvent parameters. One such parameter, a solvatochromatic shift in the electronic spectrum of a given molecule, which is believed to quantify the solvating ability of various solvents or mixtures of solvents, was mentioned earlier in connection with the aquation of the cobalt dioximine complex. Other parameters that have been used are, for example, fluidity,[5] enthalpy of evaporation,[5b,6] donor number[7] and solubility parameter.[7a,b]

An approach to studying solvent effects attempting to correlate reaction rates with parameters designed to measure ion solvation is that employed by Grunwald and Winstein.[8] Their original work was concerned with studying organic solvolysis. They argued that as the rate-determining step for S_N1 (limiting) aquation is the ionization of the substrate, *i.e.* equations (5) and (6):

$$M—X \xrightarrow{\text{slow}} M^+ + X^- \tag{5}$$

$$M^+ + H_2O \xrightarrow{\text{rapid}} MH_2O \tag{6}$$

then the most important factor for such an aquation should be the ion solvating power of the medium. Thus it should be possible to measure this and certain other specific factors, *e.g.* hydrogen bonding, electrophilic catalysis, by the way changes in solvent composition affect the rate of aquation of a substrate known to aquate by a S_N1 (limiting) mechanism. Choosing as a standard the known S_N1 (limiting) solvolysis of *t*-butyl chloride in 80% ethanol–20% water (v/v) mixture, Grunwald and Winstein applied this reasoning to the solvolysis of other organic halides in various mixed solvents by using the two-parameter linear free energy relationship (equation 7):

$$\log k/k_0 = mY \tag{7}$$

where k_0 = rate constant in 80% ethanol–20% water; k = rate constant in a particular mixed solvent; Y = solvent parameter which gives a quantitative measure of its ionizing power, *i.e.* $Y = \log[k(\text{solvent})/k(80\%\ \text{ethanol})]$ for *t*-butyl chloride; and m = substrate dependent parameter independent of the solvent, which measures the sensitivity of the substrate to changes in the ionizing power of the solvent relative to the way it affects *t*-butyl chloride in the same solvent (*N.B.* m = 1 for *t*-butyl chloride). Furthermore, since in S_N2 reactions the rate-determining step is the formation of a transition state of increased coordination number, the rates of such associative processes should not depend greatly on the ionizing power of the medium. Consequently, Grunwald and Winstein postulated that plots of log*k* *vs.* *Y* could be used to distinguish between S_N1 and S_N2 mechanisms. Indeed with organic reactions it was found that, for S_N1 solvolyses, plots of log*k* *vs.* *Y* gave good linear correlations with slopes, *i.e.* values of *m*, of around unity for a range of water-rich solvents (to eliminate ion-pair effects which cause departures from linearity). In contrast, known S_N2 solvolyses were found to give curved plots with tangential slopes of around 0.25–0.5.[9]

One of the first extensions of this type of analysis to coordination complexes was made by Langford,[10] who examined the solvolysis of Cl and Br in *trans*-$[Co(en)_2Cl_2]^+$ and *trans*-$[Co(en)_2(NO_2)Br]^+$ in aqueous methanol mixtures. He obtained good correlations of log*k* *vs.* *Y* at 25 °C for water-rich ranges, with values for *m* of 0.25 and 0.18, respectively. These values of *m*, smaller than those obtained for the solvolysis of *t*-butyl chloride, showed that the organic substrate was much more sensitive to solvent ionizing power.

This result by comparison with the organic substrate might suggest that the hydrolysis of the Co^{III} halide is not dissociative or S_N1. However, it was argued [10,11] that the differences arose because the Co^{III}—halide bond was more ionic than the C—halide bond. Thus the results were consistent with a common dissociative S_N1 mechanism, with the larger value of *m* for the organic substrate arising from the fact that the increase in anion solvation in the transition state relative to the ground state was greater in *t*-butyl chloride than in the Co^{III} halide, *i.e.* the solvation of $[Co(en)_2Cl]^{2+}$ was less significant than that of Me_3C^+. Several other transition metal centres have been analyzed using the Grunwald–Winstein solvent *Y* values and examples of such results are given in Table 1.

Table 1 Values of Grunwald–Winstein *m* for Substitution at some Transition Metal Centres[a]

Bond involved	*Complex*	m
Co^{III}—Cl	*cis*-$[Co(en)_2Cl_2]^+$ (and several other examples)	*ca.* 0.3
Cr^{III}—Cl	$[Cr(NH_3)_5Cl]^{2+}$ *cis*-$[Cr(en)_2Cl_2]^+$ [b]	0.12
Rh^{III}—Cl	*trans*-$[Rh(dmgH)_2(NO_2)Cl]^-$	0.32
	trans-$[Rh(en)_2Cl_2]^+$ [c]	0.25–0.3
Ir^{III}—Cl	*trans*-$[Ir(en)_2Cl]^+$	0.3
Ru^{II}—Cl	$[Ru(NH_3)_5Cl]^+$	0.23
Pd^{II}—Cl	$[Pd(Et_4dien)Cl]^+$ $[Pd(dien)Cl]^+$ $[Pd(ieda)Cl]^+$ [d] $[Pd(iea)Cl]^+$	*ca.* 0.4

[a] M. J. Blandamer and J. Burgess, *Pure Appl. Chem.*, 1979, **51**, 2087.
[b] V. V. Udovenko, L. G. Reiter and I. Beran, *Russ. J. Inorg. Chem. (Engl. Transl.)*, 1977, **22**, 168.
[c] K. W. Bowker, J. Burgess, E. R. Gardner and F. M. Mekhail, *J. Inorg. Nucl. Chem.*, 1979, **41**, 1215.
[d] ieda = iminobis(ethylenediethylamine); iea = iminobis(ethylenamine).

Several points emerge from these results in Table 1. Although the results quoted were not all determined at the same temperature it is thought that temperature has only a small effect on the value of *m*.[12] The low values of *m* of *ca.* 0.3 which have been obtained for several Co^{III} complexes suggest that dissociative aquations in Co^{III} are characterized by a value of *m* of this magnitude. Extension to aquations of Co^{III} bromide revealed values of *m* of *ca.* 0.2, which are slightly lower than the values for analogous chloride complexes. These values are consistent with the anticipated lower solvent requirements of the larger Br^-, and a parallel situation was found in the organic substitution where $m = 0.92$ for *t*-butyl bromide.[8]

The analysis seems to work only if halides are the leaving group, as attempts to extend the Grunwald–Winstein analysis to thiocyanate as the leaving group in a series of complexes of Cr^{III} resulted[13] in quite scattered values of *m* (−0.01 to 0.4). The lower value of *m* obtained for Cr^{III} compared with Co^{III} can be taken to indicate more associative character during the aquation of Cr^{III} than in Co^{III}.

The square planar palladium complexes which give values of *m* of *ca.* 0.4 (Table 1) are known to react *via* a mainly associative mechanism so that the values of *m* are taken to indicate that Pd—Cl bond cleavage and leaving Cl solvation were both important in determining the reactivity trend for these complexes, *i.e.* there is a greater degree of M—Cl bond breaking in the transition state of palladium compared with cobalt.

Burgess[14] studied the kinetics of reaction (8) in a variety of mixed aqueous organic solvents:

$$[Fe(B)_2(CN)_2] + 3\ phen \longrightarrow [Fe(phen)_3]^{2+} + 2B + 2CN^- \qquad (8)$$

where B = 2,2′-bipyridyl or the Schiff base *N*-(2-pyridylmethylene)-3,4-dimethylaniline and phen = 1,10-phenanthroline or various substituted phenanthrolines. Since the original substrates used by Grunwald–Winstein had no charge then the uncharged low-spin, d^6, $[Fe(B)_2(CN)_2]$ complexes might be better suited for a Grunwald–Winstein treatment, even though a Cl is not the leaving group, than the cationic Co^{III} complexes. However, scattered plots of $\log k$ *vs.* Y with low values of m in the region 0–0.2 were obtained, suggesting that some degree of associative character was present during the aquation of these Fe^{II} complexes. Similarly a study[15] of reaction (9)

$$[Fe(bipy)_3]^{2+} + 2CN^- \longrightarrow [Fe(bipy)_2(CN)_2] + bipy \qquad (9)$$

revealed that the pseudo-first-order rate constant k_{obs} depended on $[CN^-]$ according to $k_{obs} = k_1 + k_2[CN^-]$, and that a Grunwald–Winstein analysis of the second order rate constant k_2 gave a family of curves, one for each cosolvent and all with tangents less than one, which was taken to indicate again that there was some considerable associative character with this pathway.

In summary it may be concluded that while the Grunwald–Winstein analysis m values may be useful in delineating the broad mechanistic features of octahedral complexes, attempts to probe the precise degree of associative and dissociative character in the reaction are not feasible.

A disturbing feature of the Grunwald–Winstein analysis is that quite often different values of m are obtained for the same complex with different solvent pairs. This has been attributed to variation in the nucleophilicity, N, of the organic component of the solvent and a more complex relationship (10) has been proposed[16] to account for the variation of rates in different solvents:

$$\log \frac{k}{k_0} = mY + lN \qquad (10)$$

In equation (10), Y is the ionizing power of the solvent and N its nucleophilic power with m and l measuring the sensitivity of the substrate to these factors. By selecting model compounds, *e.g.* *t*-butyl chloride, where only Y should be important and methyl chloride, where both N and Y would be important, then it is possible to obtain values of Y and N for various solvent mixtures. An examination of the variation of the rate of reaction of a given substrate in these solvents according to equation (10) would then reveal the relative importance of the associative and dissociative character to the reactions.

Equation (10) is only one example of several multiparametric equations[17] that may be used to forecast the effect of variation of solvent on rates of reaction. One such equation[18] that has been applied in organic chemistry is that of Kamlet and Taft (equation 11):

$$\log \frac{k}{k_0} = s\pi^* + a\alpha \qquad (11)$$

where α is a measure of the ability of the solvent to donate a proton (hydrogen bond donor acidity) and π^* is a measure of the solvent's polarity. Both α and π^* have been measured for various solvent mixtures. There does not appear to have been an extensive application of these equations to reactions of coordination complexes. One such example,[19] however, is the reaction of equation (12):

$$mer\text{-}[RhL(L')Cl_2X] \longrightarrow trans\text{-}[RhL_2Cl_2]^+ + X^- \qquad (12)$$

where L and L′ are (*o*-dimethylaminophenyl)dimethylarsine-*NAs* and -*As* respectively; $X^- = SCN^-, SeCN^-, N_3^-$ or NO_2^-. An analysis of the reaction using equation (11) yielded values of s and a which measure the susceptibility of the reaction to a change in the solvent polarity and hydrogen bond donor acidity. The positive value of a obtained in this analysis suggests that the outgoing X^- is similarly solvated in the activated complex and the final product. Similarly, the positive value of s was attributed to the increased stabilization of the polar transition state on increasing the polarity of the solvent. Thus the values of s and a yield information on the relative amounts of associative and dissociative character of the reaction in the same way as equation (10).

The success of equations such as (7), (10) and (11) depends on the validity of linear free energy relationships and of the applicability to these of the variation of the solvent as a perturbation.

One other consideration should always be borne in mind when attempting to correlate quantitatively the rate of reaction with solvent parameters, which is that the mechanism of the reaction must remain constant. Indeed, the breakdown of the linear plot of $\ln k$ *vs.* $1/\varepsilon_R$ for ionic reactions at low values of ε_R may arise, at least in part, from this fact, although one should always be aware that at sufficiently low values of ε_R the simple approximations made in deriving this and similar relationships will fail. The reaction between Fe^{3+} and SCN^- is believed[20] to have an associative mode of activation in water; however, in a bulky solvent like dimethyl sulfoxide the mode of activation is found to be dissociative. Thus in general when a reaction has an associative mode of activation in water, then caution must be exercised in attempting to correlate rates of the reaction with various solvent parameters. Likewise when investigating the reactions of solvated species, *e.g.* $[M(S)_6]^{n+}$ (S = solvent molecule), varying the solvent composition will invariably result, at some stage in the solvent composition range, in formation of mixed solvent species, *e.g.* $[M(S)_5(S')]^{n+}$. This again, naturally, leads to difficulty in interpretation of the results for rate variation with solvent composition.

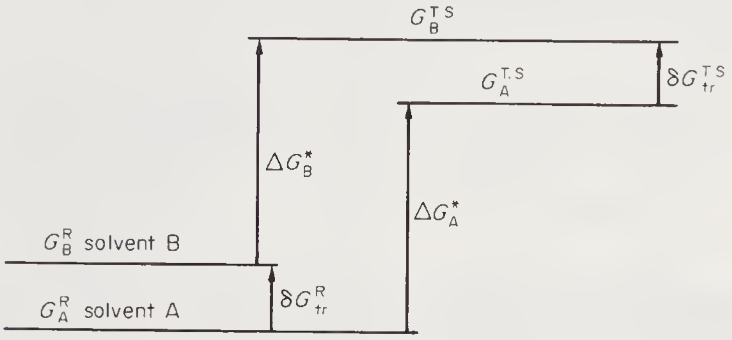

Figure 1 Relationship between free energies of reactants (initial state) and transition state in two solvents A and B for the same reaction, and the transfer free energy of the reactants and transition state. $G_A{}^R$, $G_B{}^R$ = free energy of reactant in solvents A and B respectively; $G_A{}^{TS}$, $G_B{}^{TS}$ = free energy of transition state in solvents A and B respectively; $\Delta G^*{}_A$, $\Delta G^*{}_B$ = free energy of activation for the process in solvents A and B respectively; $\delta G_{tr}{}^R$ = free energy of transfer of reactant from solvent A to B; and $\delta G_{tr}{}^{TS}$ = free energy of transfer of transition state from solvent A to B

An approach to the problem of trying to quantify the effect of changes in the solvent structure, as the composition of the solution is varied, with the rates of reaction has developed from the recognition that ΔG^* (the free energy of activation) represents the difference in free energy between the reactants and transition state, and that these two states may be affected differently by the change in solvent. Thus there is a need to bisect the solvent effect into its effect on the initial state and on the transition state and this can be accomplished through the use of thermodynamic transfer functions.[21] The principle of the method can be seen by referring to Figure 1, which portrays the relationship between the free energies of the reactants and transition state for the same reaction in two solvents A and B. If the free energy of the reactant R in solvents A and B is $G_A{}^R$ and $G_B{}^R$, respectively, then the difference in free energy of the reactant in the two solvents is defined (equation 13) as the transfer free energy $\delta G_{tr}{}^R$

$$\delta G_{tr}{}^R = G_B{}^R - G_A{}^R \tag{13}$$

A similar transfer free energy can be defined for the transition state (equation 14):

$$\delta G_{tr}{}^{TS} = G_B{}^{TS} - G_A{}^{TS} \tag{14}$$

$\delta G_{tr}{}^R$ can be obtained, in principle, from measurements of activity coefficients (equation 15):

$$\delta G_{tr}{}^R = -RT \ln \frac{\gamma_B}{\gamma_A} \tag{15}$$

which themselves can be measured by several standard methods, *e.g.* solubility and vapour pressure methods. By referring to Figure 1 it can be seen that the difference in the free energy of activation for the same process in the two different solvents, $\delta\Delta G^*$, is given by equation (16):

$$\delta\Delta G^* = \Delta G^*{}_B - \Delta G^*{}_A = (G_B{}^{TS} - G_B{}^R) - (G_A{}^{TS} - G_B{}^R) = \delta G_{tr}{}^{TS} - \delta G_{tr}{}^R \tag{16}$$

Now $\delta\Delta G^*$ can be evaluated from measurements of the rates of the process in the two different solvents; thus $\delta G_{tr}{}^{TS}$ can be evaluated if $\delta G_{tr}{}^R$ is known *via* equation (15).

Similar transfer functions can be defined for other thermodynamic state functions, *e.g.* *H*. However, if these functions are to be combined to yield other state functions, *e.g.* *S*, then care must be exercised to ensure that, as in the use of equation (15), the same standard state is always used.

The application of these principles to kinetic processes in general has been considered by Buncel and Wilson,[21] who were mainly concerned with organic reactions. They considered the various possible cases that could arise from the relative signs of $\delta G_{tr}{}^R$ and $\delta G_{tr}{}^{TS}$. Thus $\delta G_{tr}{}^R$ could be positive or negative, *i.e.* destabilization or stabilization respectively of reactant in solvent B relative to solvent A, or zero, which means that the solvent has no effect on the stability of the reactant. Also, if $\delta G_{tr}{}^{R}$ and $\delta G_{tr}{}^{TS}$ had the same sign it was termed a balancing situation, and when they had opposing signs it was termed a reinforcing situation. This leads to a convenient system for classifying solvent effects on rates of reaction (Table 2), where a rate increase or decrease is denoted by + or −, respectively, and by 0 if there is no effect. In addition, if $\delta G_{tr}{}^{R} = 0$ the effect is classified as transition state controlled, and when $\delta G_{tr}{}^{TS} = 0$ as reactant controlled.

Table 2 Classification of Reaction Types in Terms of Transfer Free Energies of Reactants, $\delta G_{tr}{}^{R}$, and Transition State, $\delta G_{tr}{}^{TS}$, and the Resulting Solvent Effect on the Rate of the Reaction[a]

Case	$\delta G_{tr}{}^{R}$	$\delta G_{tr}{}^{TS}$	*Effect on rate*	*Reaction type*
1	−	−	+, 0, −	Balanced
2	+	−	+	Positively reinforced
3	0	−	+	Positive transition state controlled
4	−	0	−	Negative initial state controlled
5	+	0	+	Positive initial state controlled
6	0	0	0	Solvent independent
7	−	+	−	Negatively reinforced
8	+	+	+, 0, −	Balanced
9	0	+	−	Negative transition state controlled

[a] +, − indicates a rate increase or decrease respectively; 0 indicates no effect on rate.

The extension of these ideas to reactions of coordination compounds is hampered by the fact that the majority of coordination compounds are charged and many of the common nucleophiles may also be charged. This presents the problem of determining a thermodynamic transfer parameter for a single ion. There are, broadly speaking, two ways[22] in which this has been done. One such way is to calculate the value for a given ion. Alternatively, the transfer parameter of a given salt is divided into a value for the cation and the anion using certain assumptions, *e.g.* the free energy of transfer of the ions Ph_4B^- and Ph_4As^+ are equal. Unfortunately there is still some uncertainty regarding the value for ions.

$$cis\text{-}[PtLCl_2] + tu \longrightarrow cis\text{-}[PtLCltu]^+ + Cl^- \tag{17}$$

L = bipy or (4-cyanopyridine)$_2$; tu = thiourea

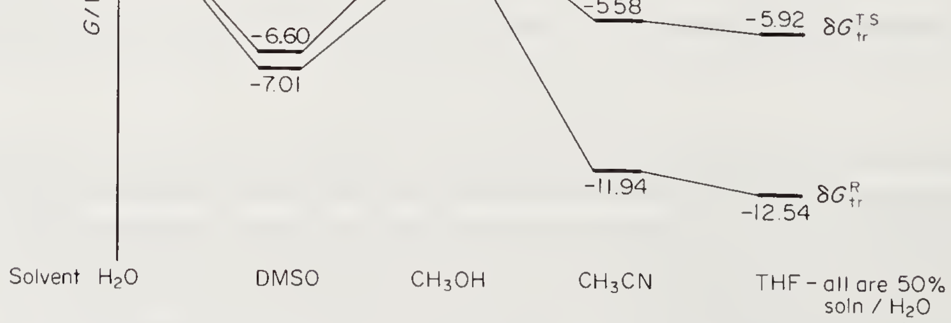

Figure 2 Initial state–transition state analysis of the reaction *cis*-$[Pt(4\text{-}CNpy)_2Cl_2]$/tu (equation 17). δ(Δ*G**) represents the change in the free energy of activation for the reaction in that particular solvent mixture relative to the value in water. Numerical values are from ref. 23. All values of *G* are relative to water

An example[22–24] of the use of this approach applied to neutral coordination complexes is the reaction given in equation (17), which was studied in aqueous dioxane and aqueous THF. An analysis of the reaction (the reaction is bimolecular and follows second order kinetics) revealed that increasing the organic component of the solution resulted in an increase in ΔG^*, *i.e.* a decrease in the rate, and this was due, in the case of L = bipy, to stabilization of the reactants with very little change in the stability of the transition state, *i.e.* a negative initial state controlled type reaction (Table 2). This result was explained as arising from the hydration characteristics of the platinum complex being dominated by the hydrophobic bipy. The introduction of a polar group into the hydrophobic aromatic ligand, *i.e.* L = (4-cyanopyridine)$_2$, results as expected in an increase in the solubility of the platinum complex in the aqueous organic solvents. An analysis of the variation in the rate of reaction (17) in different organic cosolvents revealed that in this case the solvation of the reactants, although very sensitive to the solvent, is relatively less important because the transition state parallels the behaviour of the initial state as shown in Figure 2, *i.e.* a balanced reaction type, but because $|\delta G_{tr}{}^{R}| > |\delta G_{tr}{}^{TS}|$ there is a decrease in the rate (see Table 2). The difference in behaviour of the two compounds is possibly due to direct interaction of the solvent with the ligand in the latter case, which thus makes the platinum complex more sensitive to its solvent environment. However, the importance of this approach to the effects of solvent variation is that it does indicate in a quantitative manner where the reasons for the difference of rates occur even if the particular causes for this are not too clear.

An example[24,25] of a reaction where ions are involved is shown in equation (18); the mechanism is dissociative (*D*) and the reaction was studied in aqueous methanol of varying composition.

$$[\mathrm{Fe(CN)_5(4\text{-}CNpy)}]^{3-} + \mathrm{CN}^- \longrightarrow [\mathrm{Fe(CN)_6}]^{4-} + 4\text{-}\mathrm{CNpy} \qquad (18)$$

4-CNpy = 4-cyanopyridine

It was found that the rate was very little affected by the variation in solvent composition, but an analysis of the initial state and transition state contributions in terms of the free energy (Figure 3) reveals that both the initial state and transition state are affected quite markedly by the varying solvent composition, but because they run parallel to one another there is very little change in ΔG^* (a balanced situation; see Table 2). This example thus illustrates the power of this approach in that important and large solvational changes may be disguised if composite quantities like only k or ΔH^* are used to investigate the variation of solvent composition.

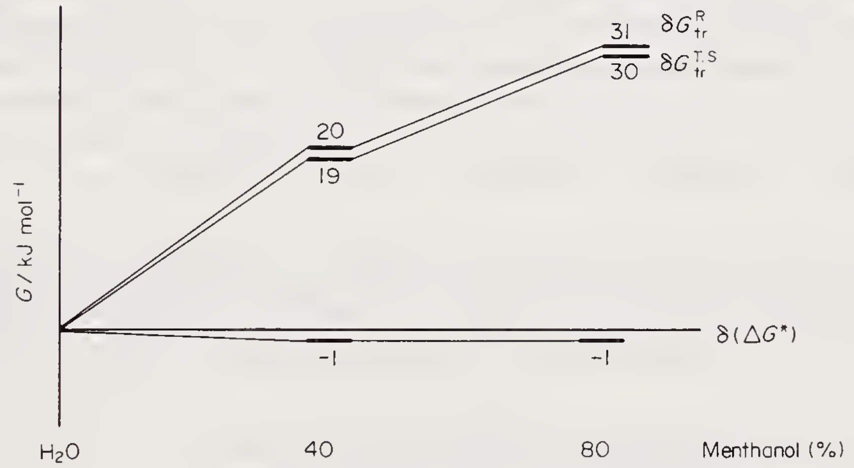

Figure 3 Initial state–transition state analysis of the reaction $[\mathrm{Fe(CN)_5(4\text{-}CNpy)}]^{3-}/\mathrm{CN}^-$ (equation 18). $\delta(\Delta G^*)$ represents the change in free energy of activation for the reaction in that particular solvent mixture relative to the value in water. Numerical values are from ref. 25. All values of *G* are relative to water

In applying the initial state–transition state analysis it is obviously important, as mentioned previously when considering other solvent parameters, to ensure that the mechanism remains the same, *i.e.* the same products are formed and the transition state remains the same as the solvent composition is altered. Sometimes it is possible that a different pathway to the same product may exist in the two solvents, or that the difference in the transition state in the two solvents represents a small structural modification such as an ion pair and an ion pair in which the two ions are separated by a solvent molecule. Under such circumstances, $\delta G_{tr}{}^{TS}$ would be measuring the difference in free energy of two different species, which makes the interpretation of such parameters more difficult, although possibly of greater fundamental interest. In addition to ensuring that the transition state remains the same it is of course essential to know the mechanism of the reaction before undertaking an analysis of this kind, otherwise quite erroneous conclusions can be drawn. Thus Wells[26,27] has investigated the aquation of a number of chloroamine complexes of $\mathrm{Co^{III}}$ and quantitatively analyzed the trends in terms of initial state and transition state components in a variety of aqueous organic solvents assuming the mechanism to be dissociative (*D*), even though in many cases the mechanism may be I_d, *i.e.* he has assumed the transition state to be $\{[\mathrm{CoL_4Cl^{2+}}]+\mathrm{Cl^-}\}$ where L represents a variety of amine type ligands. The result of this assumption is probably to overemphasize the importance of the solvation of the leaving Cl but the general conclusions reached in the analysis are probably not affected greatly by this assumption. However, other assumptions made in the analysis regarding the free energies of transfer of ions have been criticized.[28]

Because no assumptions regarding the nature of the transition state were made in this treatment, $\delta G_{tr}{}^{TS}$ by itself yields no information regarding its nature. However, it is possible to obtain some information concerning the properties of the transition state by comparing the value of $\delta G_{tr}{}^{TS}$ with δG_{tr} for stable solutes that are potential models of the transition state. Thus in the previous reaction (equation 18) it was found[25] that for this dissociative (D) reaction the transition state, *i.e.* $\{(CN)_5Fe\cdots L\}^{3-}$, was modelled reasonably well as far as free energies were concerned by $\{[Fe(CN)_6]^{3-} + L\}$, where L was 4-cyanopyridine.

One example[24] of where this treatment can yield mechanistic information based on modelling of the transition state is in the *cis→trans* isomerization of *cis*-$[Pt(PEt_3)_2(m\text{-}C_6H_4Me)Cl]$. Assuming a dissociative mechanism with Cl^- as the leaving group, and that the transfer of Cl^- alone was responsible for the variation of the isomerization rate in different solvents, then by estimating the value for the free energy of transfer of Cl^- in the various solvents it was possible to calculate the corresponding variation of the rate constant. Comparison between these calculated and experimental values was good and thus lends considerable support to the dissociative mechanism for isomerization in this compound at least.

When the mechanism of the reaction is more complex then an analysis of the initial state and transition state must take account of all the individual steps. A reaction which involves more than one step is the base hydrolysis of complexes of Co^{III}, Rh^{III} and Cr^{III}, which are believed to react *via* the S_N1(cb) mechanism.[29] This mechanism involves an initial pre-equilibrium to form the conjugate base, illustrated for $[Co(NH_3)_5Cl]^{2+}$ in equation (19):

$$[Co(NH_3)_5Cl]^{2+} + OH^- \xrightleftharpoons{K_{cb}} [Co(NH_3)_4(NH_2)Cl]^+ + H_2O \qquad (19)$$

The conjugate base undergoes a dissociative loss of Cl^- to give a five-coordinate intermediate which then reacts rapidly with solvent to give the product. Balt[30] has examined similar reactions in liquid NH_3 and found the rates to be faster. One factor contributing to the faster rates in liquid NH_3 was the greater value of K_{cb} in this solvent, and this was due to the more favourable enthalpy of solution of the proton, *i.e.* the enthalpy of transfer of the proton from water to liquid ammonia was large and negative. The application of transfer functions to equilibria will be mentioned again later.

Thus although the use of transfer functions can explain, in a quantitative manner, the reason for differences in rates of reaction in various solvents so that the mechanism can be defined fairly completely, this method, at this stage of development, is unable to predict how a solvent will affect the rate of a given reaction, *i.e.* we are unable to predict the solvent in which the rate will be fastest.

9.2 THE EFFECT OF SOLVENT ON REDOX POTENTIALS

The standard redox potential, $E°$, for a reduction process (equation 20)

$$\text{Ox} + ne \rightleftharpoons \text{Red} \qquad (20)$$

(where Ox and Red are the oxidized and reduced species respectively of the redox couple, and n is the number of electrons, e, taking part in the process) is related to the standard free energy change, $\Delta G°$, of that process through equation (21), where F is the Faraday constant.

$$\Delta G° = -nE°F \qquad (21)$$

In any chemical reaction involving the transfer of electrons there will be two couples involved, one of which undergoes oxidation and the other reduction, so that it will not be possible to study the above reaction (equation 20) in the absence of a second redox couple. To overcome this difficulty of not being able to measure the absolute value of $\Delta G°$ or $E°$ for equation (20), a scale of relative values of $E°$ can be obtained by measuring the potential of a redox couple relative to a common redox couple which is assigned an arbitrary value. In aqueous solution this common redox couple is the standard hydrogen electrode (equation 22), in which the $H^+(aq)$ and $H_2(g)$ are at unit activity and fugacity, respectively.

$$H^+(aq) + e^- \rightleftharpoons \tfrac{1}{2}H_2(g) \qquad (22)$$

At 298 K this couple is assigned a value of zero volts. Potentials of other redox couples are thus a measure of the free energy change associated with the reaction in equation (23):

$$\text{Ox} + \tfrac{n}{2}\text{H}_2(\text{g}) \longrightarrow \text{Red} + n\text{H}^+ \tag{23}$$

with the convention that the reaction is written with the $H_2(g)$ on the left-hand side, *i.e.* E° refers to a reduction process. Potentials for other couples can thus be obtained from measurements of the EMF of cells in which the cell reaction is equation (23), *i.e.* the cell incorporates the standard hydrogen electrode as one half-cell and the redox couple of interest, equation (20), as the other half-cell. In practice, the standard hydrogen electrode is not the most convenient electrode to use and other more convenient reference electrodes, *e.g.* the saturated calomel electrode, are used which have been accurately calibrated against the standard hydrogen electrode. Alternatively, where practical difficulties prevent direct measurements of cell EMFs, values of E° may possibly be obtained by determination of Gibbs free energy changes for reactions such as equation (23).

Values of E° by definition refer to conditions under which all species are in their standard states at 298 K. For non-standard conditions the electrode potential, E, of a redox reaction is given by the familiar Nernst expression (equation 24), where

$$E = E^\circ + \frac{RT}{nF}\ln\frac{\{\text{Ox}\}}{\{\text{Red}\}} \tag{24}$$

{Ox} and {Red} are the activities or fugacities of the oxidized and reduced forms, respectively. Tables of standard redox potentials are usually presented with the couples written as in equation (20), or abbreviated to Ox/Red, in which the symbol *n*e can be taken to indicate that the reaction $(n/2)H_2(g) \rightleftharpoons nH^+$ is to be added to the reaction for the redox couple, and the $H_2(g)$ and H^+ are at unit fugacity and activity, respectively. With the convention that E° refers to reduction potentials then strongly oxidizing couples have large positive values and strongly reducing couples have large negative values in aqueous solution.

It is a relatively simple process to set up a scale of redox potentials in a non-aqueous medium using the standard hydrogen electrode in that medium as the fundamental reference electrode. Thus in liquid ammonia, which is a well studied non-aqueous solvent and for which there exists a considerable amount of thermodynamic information,[31] the scale of standard electrode potentials is referred to the standard hydrogen electrode in liquid ammonia (equation 25), which is assigned the value of zero volts, and in which the H^+ exists as a solvated species, *i.e.* NH_4^+.

$$\text{NH}_4^+(\text{liq NH}_3\,;\, a = 1) + \text{e}^- \rightleftharpoons \tfrac{1}{2}\text{H}_2(\text{g}\,;\, f = 1) + \text{NH}_3(\text{l}) \tag{25}$$

The symbol for the electron in tables of values of E° in liquid ammonia is thus equivalent to $NH_3(l) + \frac{1}{2}H_2(g; f=1) \rightleftharpoons NH_4^+(\text{liq } NH_3; a=1)$. As for aqueous solutions, several secondary reference electrodes have proved more convenient for the actual measurement of E° in liquid ammonia, *e.g.* silver/silver chloride. This procedure has been applied to other inorganic solvents and numerous organic solvents, and tables of values are readily available.[32]

However, it is not an easy matter to relate these scales of E° to the standard electrode potentials in water. This is because of the unknown liquid junction potential that is inevitably introduced when one attempts to calibrate the potential of a reference electrode in a given non-aqueous solution against a common reference electrode, such as the standard hydrogen electrode or saturated calomel electrode in aqueous solution.

As a result, an alternative and more convenient approach to setting up scales of redox potentials is to measure polarographic halfwave potentials or peak potentials from cyclic voltammetry (see Chapter 8.2). The potentials are measured relative to the potential for a given couple which is assigned the value of zero volts. This approach thus avoids the difficulty of the unknown liquid junction potential which, as mentioned above, would be present if an aqueous reference electrode were to be used as a reference point. There is unfortunately, as yet, no universal agreement on the choice of this couple but it should be one whose redox potential does not vary from one solvent to another. In order for a couple to possess the property it has been recognized[33] that it should consist of large spherical and isostructural substrates with a low charge and a low peripheral charge density. Such couples that have been used are ferricinium/ferrocene,[33,34] bis-biphenylchromium(I)/bis-biphenylchromium(0),[33,34] Rb^+/Rb,[35] perylene[34] and cobalticinium/cobaltocene.[36]

In Figures 4a and 4b are shown the thermodynamic factors responsible for the redox potentials of the couples M^{z+}/M and $M^{(z+1)+}/M^{z+}$. From this it can be seen that differences in redox potentials in various solvents arise from differences in the solvation of M^{z+} in case (a), or relative differences of solvation of $M^{(z+1)+}$ and M^{z+} in case (b); the other terms appearing in the thermodynamic analysis are independent of solvent. A consideration of redox couples involving anions, *e.g.* Cl_2/Cl^- or

$[Fe(CN)_6]^{3-}/[Fe(CN)_6]^{4-}$, arrives at similar conclusions. Generally, it is found that approximately the same order of redox potentials is followed in the various non-aqueous solvents as in aqueous solution. In the case of non-aqueous solutions like alcohols the values of the redox potentials are also similar to the values in water, which is due to the comparable solvating properties of water and alcohols.

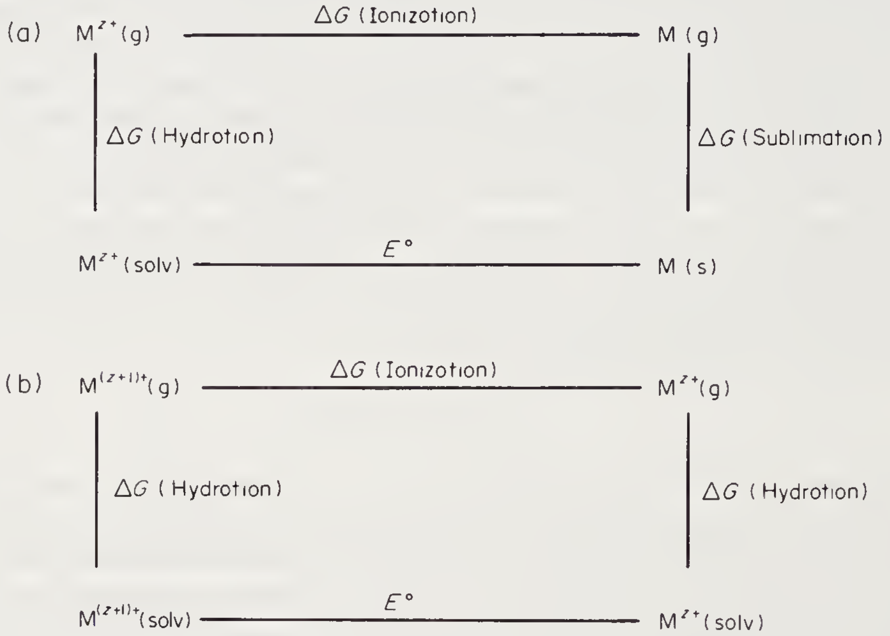

Figure 4 Thermodynamic analysis of the redox potentials for (a) M^{z+}/M and (b) $M^{(z+1)+}/M^{z+}$

Although the redox potentials in various non-aqueous solvents follow, as just mentioned, roughly the same order as in water, there may be minor differences when comparing couples with similar potentials which will give rise to differences in the redox chemistry of these couples in the different solvents. Sometimes, however, quite big differences in behaviour may be observed on transferring from one solvent to another. Copper(I) is unstable with respect to disproportionation in water[37] but in acetonitrile[38] and liquid ammonia[31] it is stable, as revealed by the relevant redox potentials in Figure 5a. Similarly, mercury(I) ion in water[37] is stable with respect to disproportionation but is very unstable with respect to disproportionation in liquid ammonia (Figure 5b).[31] These differences in behaviour arise because of the quite different solvational energies of the various cations in the different solvents.

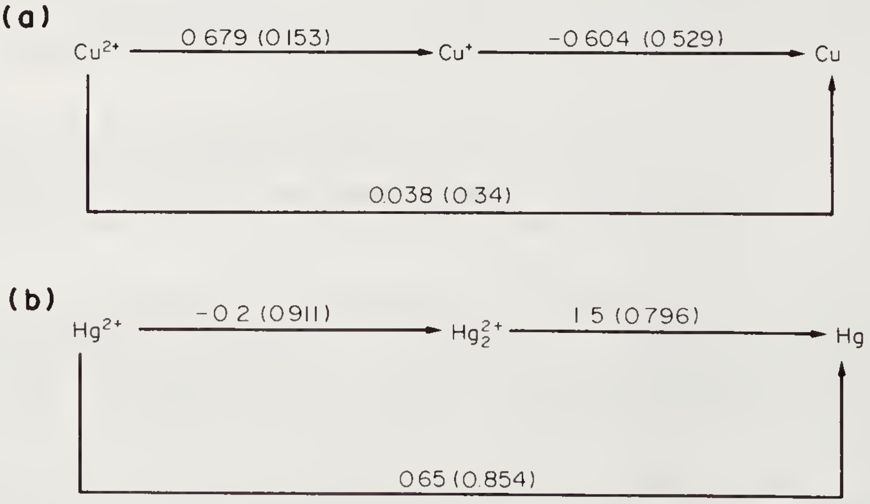

Figure 5 (a) Redox potentials for copper in acetonitrile (potentials measured relative to a standard silver electrode; T = 298 K); values in brackets are $E°$ in water. (b) Redox potentials for mercury in liquid ammonia (potentials measured relative to a standard hydrogen electrode in liquid ammonia; T = 298 K); values in brackets are $E°$ in water. Potentials quoted are all in volts

The thermodynamic cycle (Figure 4) showed that changes in redox potential in various solvents were a consequence of the different interaction of the solvent with the dissolved redox couple. One model that has been used to quantify these changes is the electrostatic model, which is based on treating the ion as an ideal sphere in a continuous dielectric; the model ignores the effect of any transfer of charge that may occur. The Born expression[39] for the free energy of solvation of an ion, ΔG_{solv} (equation 26), which is derived using this model, can be used to derive an expression for the difference in redox potential for a given redox couple in two different solvents, A and B:[34]

$$\Delta G_{\text{solv}} = \frac{-NZ^2e^2}{8\pi\varepsilon_0 r}\left[1 - \frac{1}{\varepsilon_R}\right] \tag{26}$$

where Z = charge on the ion, ε_0 = permittivity of free space, r = radius of the ion, ε_R = dielectric constant of the medium, N = Avogadro's number and e = charge on a proton. Thus for the couple M^{z+}/M consisting of a metal cation and the respective metal, equation (27) can be derived for the difference in E° in two solvents whose dielectric constants are ε_A and ε_B:

$$E^\circ_A - E^\circ_B = \frac{Ze}{8\pi\varepsilon_0 r}\left[\frac{1}{\varepsilon_B} - \frac{1}{\varepsilon_A}\right] \tag{27}$$

Similarly, in the case of two soluble anions, *e.g.* $[Fe(CN)_6]^{3-}/[Fe(CN)_6]^{4-}$, the expression for the difference in E° derived for such systems using Born's equation is (28):

$$E^\circ_A - E^\circ_B = \frac{e}{8\pi\varepsilon_0 n}\left[\frac{Z^2_{\text{ox}}}{r^2_{\text{ox}}} - \frac{Z^2_{\text{red}}}{r^2_{\text{red}}}\right]\left[\frac{1}{\varepsilon_B} - \frac{1}{\varepsilon_A}\right] \tag{28}$$

where Z_{ox} and Z_{red} = charge on the oxidized and reduced ion respectively, r_{ox} and r_{red} = ionic radius of the oxidized and reduced forms respectively, and n = number of electrons involved in the redox couple. Application of equations (27) and (28) to a series of redox couples of these types, *e.g.* $M^{z+}/M(Hg)$ (M = alkali metal, Tl^+, Cd^{2+}, Pb^{2+}, Cu^{2+}, Be^{2+} or Zn^{2+}) and $[M(CN)_6]^{3-}/[M(CN)_6]^{4-}$ (M = Fe or Mn) in formamide, *N*-methylformamide and *N*,*N*-dimethylformamide,[34] revealed that the Born equation was not successful in correlating the solvent effects on redox potentials, probably because of the inability of the Born equation to calculate the smaller variations in energy on transfer of an ion from one solvent to another compared with the case where an ion is transferred from the gas phase to solution.

Attempts [34] to improve on the simple Born expression by allowing for ion–dipole interactions and consideration of the solvent structure in the case of a redox couple of the type M^{z+}/M led to extensions of equation (27) to such as (29), which included terms for these factors:

$$E^\circ_A - E^\circ_B = \frac{Ze}{8\pi\varepsilon_0}\left[\frac{1}{(r+2r_B)}\left(1-\frac{1}{\varepsilon_B}\right) - \frac{1}{(r+2r_A)}\left(1-\frac{1}{\varepsilon_A}\right)\right] + \frac{C}{4\pi\varepsilon_0}\left[\frac{k_B\mu_B}{(r+r_B)^2} - \frac{k_A\mu_A}{(r+r_A)^2}\right] + W_A - W_B \tag{29}$$

where r_A and r_B = radius of solvent A and B respectively, k_A and k_B = solvation number of A and B respectively, μ_A and μ_B = dipole moment of A and B respectively, C = constant (= 3.33564×10^{-30} C m Debye^{-1}) and W_A and W_B = terms including solvent–solvent interactions and solvent structures. Whereas equations (27) and (28) require knowledge of the radii of ions in solution which may not be easy to obtain, equation (29) contains in addition several terms which are either difficult or impossible to obtain because of the present lack of knowledge of solvent structure for non-aqueous solutions. The application of equation (29), in which the terms in W were ignored, was attempted with redox couples of the type M^{z+}/M but again the agreement with theory was poor.

A theoretical model using the Born equation was developed to account for the variation of redox potentials of iron–sulfur clusters with solvent.[40] In addition to considering the simple charging of the ions in a medium of uniform dielectric, which is given by an expression similar to equation (28), the changes in the electrostatic free energy within the cluster accompanying the redox process were considered. This involved estimating the dielectric constant of the medium between the charges. Also, because the Fe—S cluster was thought to be well shielded from the solvent in proteins like ferredoxin, the local dielectric constant of the environment may be different and the effect on the Born equation of a spherical shell of different dielectric constant surrounding the cluster was considered. The final agreement between the experimental and theoretical values was not good but the results did indicate that these factors were partly responsible in accounting for the observed changes. The major difficulty in the treatment was assigning an appropriate value to the dielectric constant of the peptide environment around the cluster.

From these results it would therefore appear that the bulk electrostatic parameters of the solvent, *e.g.* dielectric constant and dipole moment, do not predict accurately the changes in redox potential that occur in different solvents.

An approach to quantifying the interaction between solute and solvent and hence to solvent effects on redox potentials is that developed by Gutmann.[41] Interactions between solvent and solute are treated as donor–acceptor interactions, with each solvent being characterized by two independent parameters which attempt to quantify the electron pair donor properties (donor number) and electron pair acceptor properties (acceptor number) of the solvent. The donor number of a solvent was defined as the negative value of the enthalpy change (in kJ mol^{-1}) for the interaction of the electron pair donor solvent with $SbCl_5$ in a highly dilute solution of CH_2Cl_2. The acceptor number of a solvent was deduced from ^{31}P NMR measurements on triethylphosphine oxide in different solvents; the values of the chemical shift were then used to obtain the acceptor numbers with $SbCl_5$ in CH_2Cl_2 being assigned a value of 100 and hexane, the reference solvent, a value of zero. According to Gutmann's concept, solvent molecules will act as electron donors to acceptors, *e.g.* cations in solution, and as acceptors to electron donors, *e.g.* anions in solution. In the case of cations, the stronger the interaction the more negative the charge transferred to the cation, thus making the cation more difficult to reduce, *i.e* accept further electrons. Applying this argument to a redox couple involving a metal ion and the metal or metal amalgam, then only the cations will be affected by the solvent so that the redox potential should shift to more negative values as the donor properties, *i.e.* the donor number, of the solvent increases. A similar argument applied to a redox couple involving two soluble cationic species, *e.g.* $[Co(en)_3]^{3+}/[Co(en)_3]^{2+}$, predicts that as the interaction of the higher charged species with the donor solvent would be relatively greater than that of the lower charged species, the higher charged species is relatively more stabilized by solvation. Thus the difference in solvational energies of the two ions would increase as the donor number of the solvent increased, hence giving rise again to a negative shift in the redox potential as the donor number of the solvent increased. Numerous examples[33,34,36,42] can be found to substantiate the argument and in the majority of cases the relationship between the redox potential and donor number is linear. Although a small amount of scatter is found in some of the plots, this is not too surprising as donor numbers are based on enthalpy measurements whereas redox potentials are equivalent to Gibbs' free energies.

If the interaction between the solvent and the ion is very strong then the solvent may actually coordinate with both partners in the redox couple. However, this will not affect the above arguments and consequent predictions of the variation of the redox potential. The potentials involving a series of Rh^{II} dimers of the type $[Rh_2L_4]$, where L represents a variety of bridging ligands, and their one-electron oxidation products were measured in different solvents.[43] A good linear correlation between the redox potential and the donor number of the solvent was found with the redox potential becoming more negative as the donor number of the solvent increased. In this case it was suggested that the dimers were complexed with solvents to form species $[Rh_2L_4S_{1\text{ or }2}]$ and $[Rh_2L_4S_{1\text{ or }2}]^+$ where S represents a solvent molecule. The solvents with the bigger donor number stabilize the cationic species more than the neutral species, leading to a negative shift in the redox potential as the donor number of the solvent increases.

For redox couples involving anions, *e.g.* $[M(CN)_6]^{3-}/[M(CN)_6]^{4-}$ (M = Fe, Mn), the anion acts as an electron-pair donor to the solvent so that the bigger the acceptor number of the solvent the stronger the interaction between the two. The more negatively charged ion, *i.e.* the reduced form of the couple, interacts more strongly with the solvent so that on going to a solvent of increased acceptor number the reduced form is relatively more stabilized by solvation than the oxidized form, leading to a positive shift in redox potential as the acceptor number of the solvent increases. Not only is this shift observed for redox couples of this type but a linear correlation between redox potential and acceptor number of the solvent is also found.[34,44]

Thus this model is capable of explaining the variation of redox potential with solvent in terms of the coordinative interactions between the ions of the redox couple and the solvent, *i.e.* redox potentials are determined by the donor or acceptor properties of the solvents. An important point of this model is that the nature of the binding forces between the solute and solvent are not specified. It should therefore be possible, once the linear relationship between the redox potential and the donor number or acceptor number of the solvent is established, to predict the value of the redox potential of that same couple in another solvent.

The Born equation, modified by the inclusion of empirical correction terms for the radii of the solvated ions, was used to calculate shifts in the polarographic halfwave potentials of the alkali metal ions in different solvents.[35]

Although the agreement with the experimental values was reasonable (in contrast to a similar study reported above, though the range of solvents in the two cases was quite different) it was also found that there was a correlation between the polarographic halfwave potentials and the donor number of the solvents. In this particular case it would appear that both approaches to estimating solvent effects on redox potentials are equally viable. As noted previously, the application of the Born equation, *i.e.* the electrostatic model, is not in general very successful. The apparent success here may arise because the alkali metal ions are relatively simple and approximate more closely to an ideal sphere than other ions. In this context it is interesting to note that a linear relationship between log(dielectric constant) and a linear combination of the donor number and acceptor number of a number of aprotic solvents has been reported.[41c] Thus the two different approaches to estimating changes in the redox potential with solvent variation may not be as different as initially thought.

If the number of ligands coordinated to the metal ion changes during the redox process, then it becomes difficult to separate the effect of ligand and solvent; if the stoichiometry of the process is known, then it may be possible to rationalize the observed changes in redox potential. For the couples $M^{III}L/M^{II}L$, where M = Ni or Cu and L was a polypeptide, the variation of redox potential with solvent composition was in opposite directions for the two metals.[45] Decreasing the percentage of water by adding a poor coordinating solvent, *i.e.* low donor number, caused the redox potential for Ni to become more positive and that for Cu more negative. This was explained as arising from the changes in solvent coordination accompanying the redox process; these are shown in equations (30) and (31), where charges have been omitted for clarity:

$$Cu^{III}L + 2H_2O + e \rightleftharpoons Cu^{II}L(H_2O)_2 \tag{30}$$

$$Ni^{III}L(H_2O)_2 + e \rightleftharpoons Ni^{II}L + 2H_2O \tag{31}$$

For the copper couple, increasing the amount of a poor coordinating solvent results in a decrease in the solvation energy of the reduced species, *i.e.* Cu^{II}, whereas the Cu^{III} is relatively unaffected so that it becomes more difficult to reduce the Cu^{III} to the Cu^{II}, *i.e.* a negative shift in the redox potential. The reverse occurs for the nickel couple with the Ni^{III} becoming less stabilized by the poor coordinating solvent and hence easier to reduce, *i.e.* a positive shift in the redox potential.

More subtle changes in redox potential with changing solvent composition occur in, for example, complexes with large hydrophobic groups, *e.g.* iron–sulfur clusters[46] which also contain a sizeable peptide chain. These molecules are used as models of iron–sulfur proteins like the ferredoxins. On changing the solvent it has been suggested that a change in the tertiary structure of the molecule may occur, possibly through an alteration of the hydrogen bonding in the peptide, which thus results in an alteration of the redox potential.

Finally, an interesting electrochemical application of varying the solvent and hence the solvating ability of the solvent was reported[47] for a series of $[\text{bis(arene)ruthenium(II)}]^{2+}$ complexes which undergo an overall two-electron reduction process. In good solvating solvents like acetonitrile a single two-electron reduction wave was generally observed. This means that the first reduction is more difficult than the second or else very close to the second ($E°_2 > E°_1$). On going to a less solvating solvent like dichloromethane the difference in the solvation energies of the Ru^{2+} and Ru^+ would be decreased, thus making the reduction of Ru^{2+} to Ru^+ easier with the result that the first reduction may become easier than the second ($E°_2 < E°_1$). The electrochemical behaviour of the complexes in dichloromethane was indeed found to be two one-electron reductions, *i.e.* the single two-electron wave in acetonitrile was separated in dichloromethane into two-component one-electron waves.

9.3 THE EFFECT OF SOLVENT ON EQUILIBRIUM CONSTANTS

It has long been recognized that the solvent can influence the value of the equilibrium constant and, through altering the mechanism, the nature of the products of a reaction. In general, polar solvents favour the formation of ionic species whereas non-polar solvents favour the formation of covalent species.[48] A well studied case concerns the *cis–trans* isomerization of square planar compounds of Pt^{II} and Pd^{II}. The phosphine catalyzed isomerization of $[PtX_2L_2]$ (where X = halide or pseudohalide and L = a neutral ligand such as a phosphine) was found[49] to proceed through a consecutive displacement mechanism in polar solvents and involved the ionic intermediate $[PtL_3X]^+$; the *cis* isomer, which has a dipole moment, was the favoured product in polar solvents. Nonpolar solvents tended to favour the *trans* isomer with the isomerization proceeding *via* a pseudo rotation mechanism. Similarly, a detailed study[50] of the *cis–trans* isomerization of $[PdCl_2P_2]$ ($P = PhMe_2P$ or Ph_2MeP) in a wide range of solvents revealed that in the vast majority of cases the *cis* isomer was the thermodynamically favoured product and that the proportion of *trans* isomer increased as the dipole moment of the solvent decreased. In addition, there was a trend in the values of the thermodynamic parameters for the equilibrium with the dipole moment of the solvent, but no correlation with the dielectric constant.

Addition of O_2 to Co^{II} Schiff base complexes[51] and porphyrins[52] was favoured in polar aprotic solvents due to the polar nature of the Co—O bond in the product. Likewise, the addition of HX, *e.g.* HCl, to Vaska's compound and analogues (*trans*-$[Ir(CO)YL_2]$, Y = halogen, L = tertiary phosphine) gave a *trans* product in polar solvents and a *cis* product in non-polar solvents as well as from the gas phase.[53] This arose through the different mechanisms in the two types of solvents. In polar solvents the mechanism involved initial dissociation of HX, whereas in non-polar solvents HX was so little dissociated that the mechanism was a concerted one in which the HX added on as one entity to give the *cis* product.

A related example[54] was the decrease in the value of the comproportionation constant with increasing dielectric constant of the medium for the system $[Ru(NH_3)_5(4,4'\text{-bipyridyl})\text{-}Ru(NH_3)_5]^{6+,5+,4+}$, which was attributed to the decrease in the electrostatic contribution to the stability of the mixed valence species as the dielectric constant increased.

There have been few attempts to quantify the effect of solvent on the equilibrium constant of a reaction for inorganic systems. Application of the electrostatic model *via* Born's expression,[39] equation (26), leads to the prediction that a linear relationship should exist between log(equilibrium constant) and the reciprocal of the dielectric constant of the medium. Such linear relationships or analogous relationships derived from the Born expression have been observed, for example, in equilibria involving cadmium complexes with thiocyanate, chloride and bromide,[55] copper(II) chelates of 1,3-diketones,[55] iron(III) with 2,2′-bipyridyl[56] and 1,10-phenanthroline,[57] and nickel(II) and copper(II) complexes with alanine.[58] In the majority of cases the linear relationship held only over a limited range of solvent composition. The failure of the simple electrostatic approach to predict the variation of the equilibrium constant over a wide range of solvent composition was similar to the failure[59] of this theory to account for the solvent dependence of the pK_a of weak acids, and arises because the dielectric constant is not the major factor affecting the equilibrium constant in many cases, the main factor being solute–solvent interactions. One approach[58,60] used to try and account for solute–solvent interactions has been to evaluate the overall equilibrium constant in which the activity, or concentration, of the solvent molecules was included as a variable in the equilibrium. Provided only one component of the solvent mixture solvated the solute, *i.e.* there was selective solvation as in water–dioxane mixtures where only the water was presumed to solvate the polar or ionic solutes, then a linear relationship was predicted between the log of the overall equilibrium constant and log(water activity) or log(concentration). The slopes of such plots should yield information on the number of solvent (water) molecules released. For the nickel(II) and copper(II) complexes with alanine[58] a good linear relationship was found in water–dioxane mixtures, but in water–methanol mixtures deviations from linearity were observed indicating that methanol–solute interactions were also important.

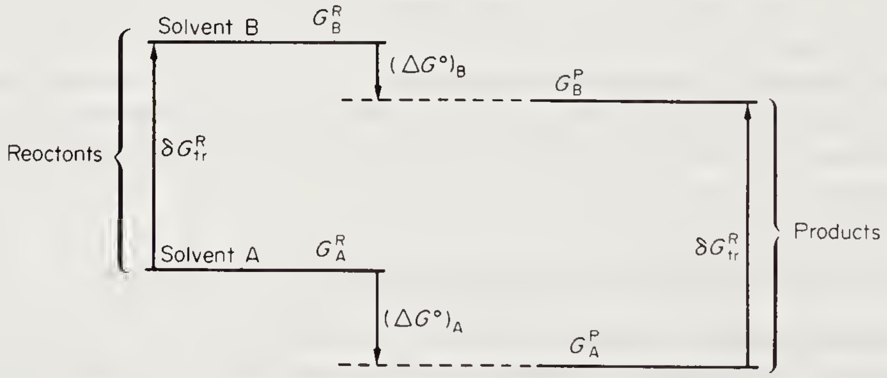

Figure 6 Relationship between standard free energy change for a given reaction in two solvents A and B, and the transfer free energy of reactant and product. $G_A{}^R$, $G_B{}^R$ = free energy of reactant in solvents A and B respectively; $G_A{}^P$,$G_B{}^P$ = free energy of product in solvents A and B respectively; $(\Delta G°)_A$, $(\Delta G°)_B$ = standard free energy change for the reaction in solvents A and B respectively; and $\delta G_{tr}{}^R$, $\delta G_{tr}{}^P$ = free energy of transfer of reactant and product respectively from solvent A to solvent B

A more exact analysis of the effect of solvent variation and hence of solvent–solute interactions could be obtained through the thermodynamic transfer functions.[21] The application of these to the equilibrium situation can be seen by referring to Figure 6. $\delta\Delta G_{tr}$ is defined as the difference in standard free energy of reaction between the two solvents A and B (equation 32), which by reference to Figure 6 leads to equation (33):

$$\delta\Delta G_{tr} = (\Delta G°)_B - (\Delta G°)_A \tag{32}$$

$$= (G_B{}^P - G_B{}^R) - (G_A{}^P - G_A{}^R) = (G_B{}^P - G_A{}^P) - (G_B{}^R - G_A{}^R)$$

$$= \delta G_{tr}{}^P - \delta G_{tr}{}^R \tag{33}$$

Thus, in principle, by measuring the transfer free energies of reactants and products it should be possible to evaluate the effect of solvent on the equilibrium constant through equation (33). There appears to have been little work done in this area on inorganic systems, probably because of the paucity of data on free energies of transfer of ions which require for their determination an extrathermodynamic assumption. As mentioned previously, the acidity of ammonia coordinated to metals like Co^{III} was larger in liquid ammonia than in water[30] and this has been attributed to the stronger interaction of the proton with liquid ammonia than with water. This was reflected in the favourable free energy of transfer (and enthalpy of transfer) of the proton from water to liquid ammonia.[30,31] Although a complete analysis of the equilibrium was not possible because of the lack of knowledge of the transfer functions for the other species, it seemed reasonable to assume that the energetics of solvation of the proton would dominate the equilibrium in different solvents. Quite commonly, because of the lack of data on transfer functions of ions, the tendency has been to adopt this approach, *i.e.* to try and identify the solute which is likely to be the most strongly solvated and account for the variation in equilibrium constant with solvent composition as arising, mainly, from the differing solute–solvent interactions of that same species.[61]

The use of the Gutmann[41] donor and acceptor numbers for describing solvent effects on rates, equilibria and other physicochemical properties has met with some success in organic chemistry.[62,63] However, because the donor and acceptor numbers of mixtures of solvents can not be inferred from the values of the pure solvents but must be determined experimentally, and also because the relationships describing the effects of solvent on chemical reactions were found to apply to non-associated solvents of medium to high dielectric constant, there has been very little attempt to introduce this approach into inorganic systems where the commonly used solvents are protic, *i.e.* associated. However, one such reaction that has been studied was[63] equation (34):

$$CoCl_3^- + Cl^- \rightleftharpoons CoCl_4^{2-} \tag{34}$$

for which $\Delta(\Delta G)$, the change in the standard free energy of reaction in a particular solvent measured relative to a reference solvent, was given by equation (35) where ΔDN and ΔAN were the changes in the donor number and acceptor number respectively of the solvent, again measured relative to the same reference solvent.

$$\Delta(\Delta G) = a\Delta \mathrm{DN} + b\Delta \mathrm{AN} + \text{constant} \tag{35}$$

The values of a and b could be accounted for in terms of the relative degrees of interactions of the solvent with the ions participating in the equilibrium.

Equation (35) is an example of a multiparametric equation[17,18,64] for describing solvent effects on equilibria and is similar to the multiparametric equations used to describe solvent effects on rates. The use of these equations in describing solvent effects on equilibria involving coordination compounds is, like their application to reaction rates of coordination compounds, not common. Equilibrium (36), where L, L′ and X are the same as in reaction (12),

$$mer\text{-}[RhL(L')Cl_2X] \rightleftharpoons trans\text{-}[RhL_2Cl_2] + X^- \tag{36}$$

has been analyzed[19] using equation (37) where π^* and α are the same as in equation (11).

$$\log K = \log K_0 + s\pi^* + a\alpha \tag{37}$$

Several alcohols were used as solvent for studying equilibrium (36). It was found that equation (37) predicted quite accurately the variation of the equilibrium constant and the values of s and a yielded, through a comparison with the values obtained in the kinetic analysis of reaction (12), information on the relative degrees of solvation of the products, reactants and transition state.

The equilibria considered up to now have all involved inner sphere complexes. There is the possibility that an inner sphere complex may react with free ligands in solution; this includes the solvent itself, to give an outer sphere complex where the ligand enters the secondary solvation shell of the inner sphere complex. If the two species involved in this type of interaction are of opposite sign, which is the situation where this type of complex formation is expected to be most effective, the outer sphere complex is called an ion pair. Fuoss[65] has derived an expression (equation 38) for the ion pair formation constant, K_{IP}, from electrostatic arguments:

$$K_{IP} = \frac{4\pi N a^3}{3000} \frac{\exp U}{kT} \tag{38}$$

where N = Avogadro's number, k = Boltzmann's constant, a = distance apart of the ions in the ion pair, usually assumed to be *ca.* 5 Å and U = Coulomb's energy for interaction between oppositely charged ions, given by equation (39):

$$U = \frac{Z_1 Z_2 e^2}{4\pi\varepsilon_0\varepsilon_R a} \tag{39}$$

A similar equation holds for association of ions with neutral ligands or similarly charged ions;[66] also the case where the ion size is smaller than or comparable to the size of the solvent has been considered.[67]

In general, the agreement between experimental and theoretical values in aqueous and non-aqueous solution is reasonable, but the estimation of K_{IP} does require certain assumptions which detract from the apparently reasonable agreement. It can be seen from equations (38) and (39) that a linear relationship between $\log K_{IP}$ and $1/\varepsilon_R$ is predicted and this has been observed in several instances.[4,68]

9.4 REFERENCES

1. J. W. Moore and R. G. Pearson, 'Kinetics and Mechanism', 3rd ed., Wiley, New York, 1981, chap. 7.
2. N. M. Samus and A. V. Ablov, *Coord. Chem. Rev.*, 1979, **28**, 177.
3. A. K. Bhattacharjee and M. K. Mahanti, *Gazz. Chim. Ital.*, 1983, **113**, 1.
4. M. N. Bishnu, B. Chakravarti, R. N. Banerjee and D. Banerjea, *J. Coord. Chem.*, 1983, **13**, 63.
5. (a) E. F. Caldin and H. P. Bennetto, *J. Chem. Soc.(A)*, 1971, 2191; (b) E. F. Caldin and H. P. Bennetto, *J. Solution Chem.*, 1973, **2**, 217.
6. (a) E. F. Caldin and H. P. Bennetto, *J. Chem. Soc.(A)*, 1971, 2198; (b) M. Tanaka, *Inorg. Chim. Acta*, 1981, **54**, L129 ; (c) M. Tanaka, *Inorg. Chem.*, 1976, **15**, 2325.
7. (a) M. Tanaka, *Inorg. Chem.*, 1980, **19**, 3205; (b) M. Tanaka, *Inorg. Chim. Acta*, 1983, **76**, L243; (c) S. Funahashi and R. B. Jordan, *Inorg. Chem.*, 1978, **16**, 1301; (d) L. L. Rusnak, E. S. Yang and R. B. Jordan, *Inorg. Chem.*, 1978, **17**, 1810.
8. E. W. Grunwald and S. Winstein, *J. Am. Chem. Soc.*, 1948, **70**, 846.
9. A. H. Fainberg and S. Winstein, *J. Am. Chem. Soc.*, 1956, **78**, 2770.
10. C. H. Langford, *Inorg. Chem.*, 1964, **3**, 228.
11. J. Burgess, *J. Chem. Soc. (A)*, 1970, 2703.
12. P. R. Wells, *Chem. Rev.*, 1963, **63**, 171.
13. J. Burgess, *J. Chem. Soc., Dalton Trans.*, 1973, 825.
14. J. Burgess, *J. Chem. Soc., Dalton Trans.*, 1972, 203.
15. M. J. Blandamer, J. Burgess and J. G. Chambers, *J. Chem. Soc., Dalton Trans.*, 1976, 606.
16. S. Winstein, A. H. Fainberg and E. Grunwald, *J. Am. Chem. Soc.*, 1957, **79**, 4146.
17. C. Reichardt, *Angew. Chem., Int. Ed. Engl.*, 1979, **18**, 98 and refs. therein.
18. (a) M. J. Kamlet and R. W. Taft, *J. Am. Chem. Soc.*, 1976, **98**, 377; (b) M. J. Kamlet and R. W. Taft, *J. Am. Chem. Soc.*, 1976, **98**, 2886; (c) M. J. Kamlet and R. W. Taft, *J. Chem. Soc., Perkin Trans. 2*, 1979, 337, 342, 349, 1723.
19. A. Peloso, *J. Chem. Soc., Dalton Trans.*, 1982, 2141.
20. K. Ishihara, S. Funahashi and M. Tanaka, *Inorg. Chem.*, 1983, **22**, 3589.
21. (a) E. Buncel and H. Wilson. *Acc. Chem. Res.*, 1979, **12**, 42; (b) E. Buncel and H. Wilson, *J. Chem. Educ.*, 1980, **57**, 629.
22. M. J. Blandamer and J. Burgess, *Coord. Chem. Rev.*, 1980, **31**, 93.
23. M. J. Blandamer, J. Burgess and S. J. Hamshere, *J. Chem. Soc., Dalton Trans.*, 1979, 1539.
24. M. J. Blandamer and J. Burgess, *Pure Appl. Chem.*, 1982, **54**, 2285.
25. M. J. Blandamer, J. Burgess, K. W. Morcom and R. Sherry, *Transition Met. Chem.*, 1983, **8**. 354.
26. C. F. Wells, *J. Chem. Soc., Faraday Trans. 1*, 1977, **73**, 1851.
27. I. M. Sidahmed and C. F. Wells, *J. Chem. Soc., Dalton Trans.*, 1983, 1035 and refs. therein.
28. M. V. Twigg (ed.), 'Mechanisms of Inorganic and Organometallic Reactions', Plenum, New York, 1983, pp. 148–151, 162–164 and refs. therein.
29. J. McGilly and D. H. Vaughan, *J. Chem. Soc., Dalton Trans.*, 1984, 385 and refs. therein.
30. S. Balt and A. Jelsma, *Inorg. Chem.*, 1981, **20**, 733 and refs. therein.
31. (a) W. L. Jolly, *J. Phys. Chem.*, 1954, **58**, 250; (b) W. L. Jolly, *J. Chem. Educ.*, 1956, **33**, 512.
32. J. Burgess, 'Metal Ions in Solution', Ellis Horwood, Chichester, 1978, chap. 8.
33. U. Mayer, A. Kotocova and V. Gutmann, *J. Electroanal. Chem.*, 1979, **103**, 409.
34. G. Gritzner, *J. Electroanal. Chem.*, 1983, **144**, 259.
35. N. Matsuura, K. Umemoto, M. Waki, Z. Takeuchi and M. Omoto, *Bull. Chem. Soc. Jpn.*, 1974, **47**, 806.
36. H. Elzanowska, Z. Galus and Z. Borkowska, *J. Electroanal. Chem.*, 1983, **157**, 251.
37. F. A. Cotton and G. Wilkinson, 'Advanced Inorganic Chemistry' 4th edn., Wiley, New York, 1980.
38. (a) J. K. Senne and B. Kratochvil, *Anal. Chem.*, 1971, **43**, 79; (b) J. K. Senne and B. Kratochvil, *Anal. Chem.*, 1972, **44**, 585.
39. M. Born, *Z. Phys.*, 1920, **1**, 45.
40. R. J. Kassner and W. Yang, *J. Am. Chem. Soc.*, 1977, **99**, 4351.
41. (a) V. Gutmann, *Electrochim. Acta*, 1976, **21**, 661; (b) V. Gutmann, 'The Donor Acceptor Approach to Molecular Interactions', Plenum, New York, 1978; (c) V. Gutmann, G. Resch and W.Linert, *Coord. Chem. Rev.*, 1982, **43**, 133.
42. G. Gonzalez, U. Mayer and V. Gutmann, *Inorg. Nucl. Chem. Lett.*, 1979, **15**, 155.
43. (a) J. L. Bear, T. P. Zhu, T. Malinski, A. M. Dennis and K. M. Kadish, *Inorg. Chem.*, 1984, **23**, 674; (b) K. Das, K. M. Kadish and J. L Bear, *Inorg. Chem.*, 1978, **17**, 930.

44. (a) G. Gritzner, K. Danksagmuller and V. Gutmann, *J. Electroanal. Chem.*, 1976, **72**, 177; (b) G. Gritzner, K. Danksagmuller and V. Gutmann, *J. Electroanal. Chem.*, 1978, **90**, 203; (c) A. Messina and G. Gritzner, *J. Electroanal. Chem.*, 1979, **101**, 201.
45. M. P. Youngblood and D. W. Margerum, *Inorg. Chem.*, 1980, **19**, 3068.
46. (a) N. Ueyama, T. Terakawa, M. Nakata and A. Nakamura, *J. Am. Chem. Soc.*, 1983, **105**, 7098; (b) K. Tanaka, T. Tanaka and I. Kawafune, *Inorg. Chem.*, 1984, **23**, 516; (c) C. L. Hill, J. Renaud, R. H. Holm and L. E. Mortenson, *J. Am. Chem. Soc.*, 1977, **99**, 2549.
47. R. G. Finke, R. H. Voegeli, E. D. Laganis and V. Boekelheide, *Organometallics*, 1983, **2**, 347.
48. E. Cesarotti, L. Kaplan and R. Ugo, *Coord. Chem. Rev.*, 1982, **43**, 275.
49. (a) J. A. Davies and V. Uma, *J. Electroanal. Chem.*, 1983, **158**, 13; (b) G. K. Anderson and R. J. Cross, *Chem. Soc. Rev.*, 1980, **9**, 185.
50. D. A. Redfield and J. H. Nelson, *Inorg. Chem.*, 1973, **12**, 15.
51. E. Cesarotti, M. Gullotti, A. Pasini and R. Ugo, *J. Chem. Soc., Dalton Trans.*, 1977, 757.
52. H. C. Stynes and J. A. Ibers, *J. Am. Chem. Soc.*, 1972, **94**, 5125.
53. R. G. Pearson and C. T. Kresge, *Inorg. Chem.*, 1981, **20**, 1878 and refs. therein.
54. J. E. Sutton and H. Taube, *Inorg. Chem.*, 1981, **20**, 3125.
55. D. R. Crow, 'Polarography of Metal Complexes', Academic, New York, 1969, pp.164–166 and refs. therein.
56. (a) D. K. Hazra and S. C. Lahiri, *Anal. Chim. Acta*, 1975, **79**, 335; (b) S. Aditya, G. Biswas and S. C. Lahiri, *J. Inorg. Nucl. Chem.*, 1978, **40**, 1069.
57. S. Aditya, A. Bhattacharyya, G. Biswas and S. C. Lahiri, *J. Indian Chem. Soc.*, 1977, **54**, 1137.
58. A. Gergely and T. Kiss, *J. Inorg. Nucl. Chem.*, 1977, **39**, 109.
59. (a) K. Kalfus, Z. Friedl and O. Exner, *Collect. Czech. Chem. Commun.*, 1984, **49**, 179; (b) R. G. Bates, *J. Electroanal. Chem.*, 1971, **29**, 1.
60. A. S. Quist and W. L. Marshall, *J. Phys. Chem.*, 1968, **72**, 1536.
61. R. Seeber, P. Zanello, A. Cinquantini and G. A. Mazzocchin, *J. Chem. Soc., Dalton Trans.*, 1979, 1274.
62. A. J. Parker, U. Mayer, R. Schmid and V. Gutmann, *J. Org. Chem.*, 1978, **43**, 1843.
63. U. Mayer, *Pure Appl. Chem.*, 1979, **51**, 1697 and refs. therein.
64. W. R. Fawcett and T. M. Krygowski, *J. Am. Chem. Soc.*, 1975, **97**, 2143.
65. (a) R. M. Fuoss, *J. Am. Chem. Soc.*, 1958, **80**, 5059; (b) M. Eigen, *Z. Elektrochem.*, 1960, **64**, 115.
66. M. Eigen, W. Kruse, G. Maass and L. de Maeyer, *Prog. React. Kinet.*, 1964, **2**, 287.
67. R. M. Fuoss, *J. Am. Chem. Soc.*, 1978, **100**, 5576.
68. R. A. Howard, D. R. Underdown and J. L. Bear, *J. Inorg. Nucl. Chem.*, 1977, **39**, 105.

10

Applications in Analysis

HARRY M. N. H. IRVING
University of Cape Town, South Africa

10.1 INTRODUCTION

10.1.1 Preliminary Observations

If we accept Cotton and Wilkinson's definition of a coordination compound (or complex) as embracing all species, charged or uncharged, in which a central atom is surrounded by a set of other atoms, ions, or small molecules called ligands,[1] we immediately encounter an *embarras de richesses* in considering their analytical applications. Not only is the variety of such applications so wide, but even in a quite arbitrarily restricted field (*e.g.* organic reagents for the absorptiometric determination of iron) research has thrown up such a superabundance of material that it is difficult to see the wood for the trees.

It is often not too difficult to synthesize a novel organic reagent or to modify an existing one... and to achieve another publication! But has the introduction of this new reagent sufficient advantages over an established one to justify, indeed to ensure, its replacing the established reagent? All too often the critical appraisal of a newly prepared reagent is entirely lacking and the magnitude of the problem can best be appreciated by scanning a recent review by K. Ueno[2] which lists many new organic reagents (specifically azo compounds, β-diketones, 'ferroins', arylhydroxylamines, Schiff's bases and various heterocyclics) that had been reported in the comparatively short period from 1968 to 1981.

In what follows no attempt can be made to be truly comprehensive (despite the title of this series), but examples of the use of coordination compounds in analytical chemistry will be drawn from the main fields of contemporary interest and these will be supplemented by references to selected publications, to books and to review articles where these are available.

10.1.2 Brief Historical Introduction

One of the earliest references to a reaction in solution, which, as we now realize, depends upon the formation of a coordination compound, was recorded by Pliny who stated that the adulteration of copper sulfate by iron sulfate could be detected by testing with a strip of papyrus soaked in gall-nuts, when a black colour developed if iron were present. A. Libavius (1540–1616) noted how ammmonia present in water could be detected by the blue colour formed with a copper salt and A. Jacquelain (1846) actually determined copper salts in terms of the blue colour formed on adding ammonia. Later developments used coordination compounds formed from ethylenediamine and other polyamines.[3] T. J. Herapath determined iron(III) as its red isothiocyanate complex in 1852 and the basic procedure is used today.[3]

The solubility of the complex anion $Ag(CN)_2^-$ in contrast to the high insolubility of neutral silver cyanide (AgCN) was exploited for the determination of silver (and/or cyanide) by Justus von Liebig as long ago as 1851: this procedure may well be cited as the best established complexometric titration preceding the great developments brought about by G. Schwarzenbach in 1940 when he pioneered the use of ethylenediaminetetraacetic acid, EDTA, and other aminopolycarboxylic acids as titrants[4] and opened up new vistas in titrimetry (see Section 10.6).

In the field of gravimetry the nitrosonaphthols were introduced by Illinsky in 1884 and Knorre in 1885 when α-nitroso-β-naphthol was found to give a very insoluble precipitate with cobalt ions which could be used to determine that element even in the presence of nickel: unfortunately the precipitate did not possess a stoichiometric or reproducible composition and ignition to a stable weighing form (such as Co_3O_4) was obligatory. In contrast, L. H. Tschugaeff reported in 1905 that dimethylglyoxime (DMG) formed, with nickel ions, a very insoluble red complex of reproducible and stoichiometric composition such that 'one part in 400000 parts of water is readily detected'.

The reaction was applied to the quantitative determination of nickel two years later (O. Brunck, 1907) and thereby initiated a new era in gravimetry.[5] Since DMG gave highly insoluble precipitates only with nickel and palladium, it was the first specific (strictly speaking, selective) organic reagent and sponsored a hope of finding a whole series of organic reagents which would react with only one element or, at least, with only a very small number. While the serendipitous discovery of DMG has promoted a great deal of research work, nothing comparable to it has emerged and the utopian dream now seems unrealizable.

Cupferron, the ammonium salt of *N*-nitrosophenylhydroxylamine, introduced by O. Baudische in 1909, acts as a precipitant for copper and iron in weakly acid solution. 8-Hydroxyquinoline (Berg, 1938) forms insoluble chelate complexes with quite a large number of cations but it can be made reasonably selective by controlling the pH and the use of masking agents (see Section 10.3). Unlike oxine (8-hydroxyquinoline) 2-methyl-8-hydroxyquinoline was found independently by Irving and by Merritt and Walker (1944) not to give a precipitate with aluminum although, like oxine, it still precipitates magnesium and beryllium thus permitting some useful separations in the determination of light alloys. This showed that steric hindrance could play a decisive role in the design of organic reagents for metals (see Section 10.2.2.3).

Since many metal chelates are strongly coloured they lend themselves to absorptiometric procedures (see Section 10.5) and since formally uncharged chelates are commonly insoluble in water but soluble in an immiscible organic solvent they lend themselves to liquid–liquid extraction and various preconcentration techniques the same is often true of ion-pairs formed from bulky chelated cations (or anions) with suitable anions (or cations).

Combined with steric factors which inhibited tris coordination to divalent transition metals these features led to the virtually serendipitous discovery of the reagent biquinolyl (Hoste, 1938) specific for copper(I). The many-faceted uses of 2,2′-bipyridyl, 1,10-phenanthroline, and their analogues are described later (see Section 10.5.2).

While the liquid–liquid extraction of inorganic elements as coordination complexes with thiocyanate ions can be traced back to Skey (1867), the extraction from hydrochloric acid into ether of iron(III) (J. W. Rothe, 1892) or gallium (E. H. Swift, 1924) depends on the formation of solvated acido complexes derived from $HMCl_4$; extractions of metal complexes from nitric, thiocyanic, hydrofluoric, hydrochloric and hydrobromic acids were studied exhaustively by Bock and his collaborators (1942–1956).[6]

The first metal complex used in liquid–liquid extraction appears to be that formed from 1,5-diphenylcarbazide and chromium(III). P. Cazeneuve (1900), and F. Feigl and F. L. Lederer (1925) later used the procedure for certain separations.[5] However, the most pregnant discovery was made by Helmuth Fischer (1925) when he pioneered the analytical applications of dithizone, PhNHNHCSN═NPh. Here both the reagent and its metal complexes are intensely coloured, soluble in organic solvents but insoluble in water. Only a small number of metals react and the procedures can readily be made highly selective.[7,8]

That a number of metal chelate complexes are intensely fluorescent did not escape attention and the use of morin by E. B. Sandell (1940) for the quantitative determination of traces of beryllium in the presence of aluminum is a noteworthy landmark.[5]

When J. C. Warf (1949) noted that tributyl phosphate (TBP) was highly effective in the solvent extraction of thorium and cerium(IV) from nitric acid, a new reagent of immense importance became available both in the laboratory and in chemical technology. TBP and its analogues coordinate to a very wide range of inorganic species and the extractability of the adducts varies markedly with their nature and increases with their charge (see Section 10.4.3.1). Interest in the separation of the heavier and radioactive elements and the growing interest in the trans-uranium elements led to extensive studies of the analytical potential of coordination compounds derived from mono- and di-phosphoric acids, trialkylphosphine oxides and many other types of phosphorus compounds (see Section 10.4.3.2).

The exigencies of research current around that time in the chemistry and separation of radionuclides led Calvin and his associates (1950) to introduce trifluorothenoylacetone (TTA), a reagent systematically and specifically designed for the solvent extraction of highly charged cations which had to be carried out from acidic solutions in order to avoid hydrolysis.

The deliberate use of coordination compounds for ion-exchange separations[9] may be traced to J. van R. Smit (1959), and C. S. G. Phillips (1940) seems to have been the first to use one as a substrate for gas chromatography (Section 10.7.3.3). If the chloride ion in such long-chain quaternary ammonium salts as Aliquat-336(Cl) is replaced by the complex ion $[Co(NH_3)_2(NO_2)_4]^-$ of Erdmann's salt,[10] a coloured liquid anion-exchanger of obvious potential is obtained (W. E. Clifford and H. M. N. H. Irving, 1964).

Although we must not underestimate the importance of coordination compounds such as ammonium phosphomolybdate (for the determination of phosphorus and more recently as an inorganic ion-exchanger see ref. 9), probably the greatest impact came from the introduction of organic reagents into analytical chemistry.[5]

10.2 GRAVIMETRY

10.2.1 Basic Requirements

To be of use in gravimetric analysis a compound should have a stoichiometric (or at least a strictly reproducible) composition and possess a low solubility in water (although the precipitating reagent itself should be relatively easily soluble). It must be precipitated in a physical form that is readily filterable, free from occlusions and adsorbed material, and capable of being washed and dried to constant weight without decomposition. Stability against the effects of changing pH and auxiliary complexing agents will assist in increasing selectivity, and a large gravimetric factor will clearly facilitate the determination of small amounts of analyte.

10.2.1.1 Factors governing solubility in water

If a substance is to dissolve in water, the highly associated structure of this solvent, brought about by strong hydrogen bonding between individual polar molecules, must be broken up. This can be achieved by aquation of any ionic species, especially by cations of increasing positive charge; structure breaking also comes about by competitive hydrogen bonding to suitable atoms in the solute. Whereas nitrogen forms hydrogen bonds almost as well as oxygen, replacement of these atoms by phosphorus or sulfur (or donor atoms still lower in the periodic table) will lead to a reduction in solubility.

Comparing the very soluble salt $Fe(ClO_4)_2$ with the sparingly soluble $Fephen_3(ClO_4)_2$ shows the effect of increasing the bulk of the cation so that the charge density at the surface, and hence the tendency to form ion dipoles with water molecules, is reduced. With cations of high positive charge the same effect is brought about by coordination with suitable anions: thus M^{3+} will yield MCl_6^{3-} (M = Sb, Ga, Tl) and Au^{3+} will give $AuCl_4^-$ which form precipitates with large cations derived from dyestuffs such as rhodamine.

A formally neutral molecule produced by chelation, *e.g.* copper glycinate (**1**), may yet be soluble because of hydrogen bonding to atoms in the periphery. Insolubility is favoured by aliphatic chains of increasing length and aromatic rings of increasing number. We can contrast (**1**) with the sparingly soluble chelate complex with quinaldinic acid (**2**). With aluminum trisoxinate (**3**) the charge is reduced to zero and only aromatic rings are exposed to the solvent leading to a complex highly insoluble in water.

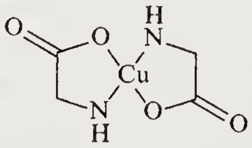

(**1**)

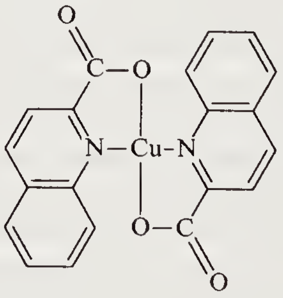

(**2**)

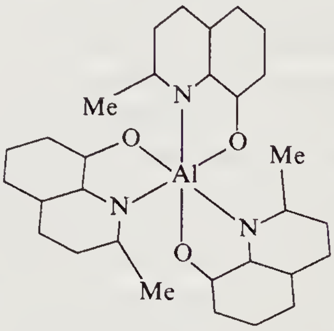

(**3**)

The introduction of a sulfonic acid (or other strongly ionized) group into a ligand will confer solubility: thus the tris complex of 8-hydroxyquinoline-5-sulfonic acid with iron(III) is readily soluble while the iron(III) analogue of (**3**) is not. While undesirable in a reagent designed for gravimetry, this solubilizing effect is required in a reagent for use in absorptiometry (see Section 10.5) or as a masking agent (see Section 10.3).

Another factor that leads to insolubility in water is the possibility of polymerization. Whereas pyrocatechol and many other *o*-dihydroxyphenols can form stable chelate rings and so participate in stoichiometric compounds, it is sterically impossible for all three oxygen atoms in pyrogallol (1,2,3-trihydroxybenzene) to coordinate simultaneously with the same metal atom (*e.g.* Sb, Bi). Two atoms engage in chelation but the third is linked to another metal atom which in turn is joined to other pyrogallol molecules. Since the degree of polymerization is determined by a number of factors, this ligand will certainly give rise to a precipitate, but one of irreproducible composition and thus unsuitable for gravimetry. On the other hand similar reagents, notably tannic acid, can play an important role as collectors of readily hydrolysable metals such as aluminum, chromium and iron, titanium and tungsten.

Coordination polymers can also play a useful role as stationary phases in chromatography (see Section 10.7.3.3).

10.2.1.2 Lattice energy

The solubility of a substance in a solvent is the result of the competition between the energy required to break down the crystal lattice and that acquired by solvation of the substance or its component ions.

The high solubility of lithium chloride and the low solubility of barium sulfate are familiar examples of the antagonism of these factors in inorganic salts. With formally uncharged coordination compounds differences in packing and intermolecular bonding may have dramatic effects which are best illustrated by the case of complexes of dimethylglyoxime (DMG). Although the stability of the complexes $M(DMG)_2$ increase normally following the Irving–Williams rule[11] in the order $M = Mn < Fe < Co < Ni < Cu$, nickel can be precipitated as $Ni(DMG)_2$ even in the presence of much copper.

The nickel complex (**4**) is essentially planar and there are two remarkably short hydrogen bonds ($O—H—O = 2.44$ Å), which undoubtedly explains why these hydrogen atoms are very difficult to remove and do not react with the solvent, thus contributing to a low solubility in water. But the most striking feature is the existence of metal–metal bonds ($Ni—Ni = 3.25$ Å) shown schematically in (**5**). Due then to nickel's tendency to form octahedral complexes the lattice structure actually involves what can be thought of as infinitely long columns of intermolecularly bonded $Ni(DMG)_2$ units.[12] Surprisingly perhaps, the individual molecule of $Cu(DMG)_2$ is not very different dimensionally although the planes of the two chelate rings are inclined at 21° 44′. However, the copper atom is somewhat displaced from the plane of the four nitrogen atoms in the directions of an oxygen atom in a nearby unit leading to a pyramidal arrangement with a long fifth bond ($Cu—O = 2.43$ Å). Two $Cu(DMG)_2$ units are associated in this way (*cf.* **6**) and there is a long spacing (3.76 Å) along this Cu—O direction before a methyl group of the next molecule is encountered.[13] The specificity of DMG towards Ni is thus due to its peculiar crystal structure.

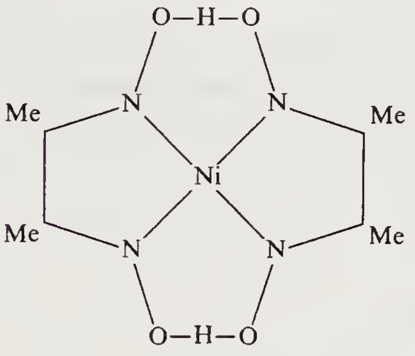

(**4**)

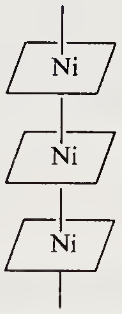

(**5**)

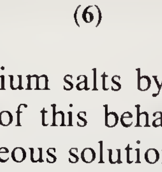

(**6**)

Whereas it is quite common to release carboxylic acids from their potassium salts by adding hydrochloric acid and extracting with ether, there is a complete reversal of this behaviour if catecholdiacetic acid (o-$C_6H_4(OCH_2COOH)_2$; H_2CDA), is added to an aqueous solution of potassium chloride. That hydrochloric acid is set free and the salt $KHCDA,H_2CDA$ precipitates is due to its peculiar structure: the potassium ion is encapsulated in a sandwich of two molecules of the H_2CDA which provide eight of the ten oxygen atoms, the coordination shell being completed by an oxygen atom from each of the two catecholdiacetic acid molecules. The driving force of the reaction is clearly the high lattice energy of the potassium compound and it is stated that Li^+, Na^+, NH_4^+ and Cs^+ do not react in this way.[14]

Although we shall see that it is now possible to synthesize cage compounds which will form coordination compounds with cations with ionic radii lying within prescribed limits (see Section 10.7.2), theory and computational facilities have not yet advanced to the stage when it is possible to predict the crystal structure of any new compound, and certainly not to the stage of being able to design a ligand which would ensure for a particular cation a crystal structure of exceptionally high lattice energy leading to characterizing solubility. We must be grateful for an occasional vagary of structure which can be put to good use — and explain it by hindsight!

10.2.1.3 Equilibrium conditions

Equation (1) represents the course of a reaction between a cation M^{n+} and the conjugate acid of a ligand L, represented for simplicity as monobasic: the same principles will apply *pari passu* to polybasic ligands.

Complex formation:

$$M^{n+}(aq) + nL^{-} = ML_n(aq) + nH^{+} \tag{1a}$$

Precipitation:

$$ML_n(aq) \rightleftharpoons ML_n(s) \tag{1b}$$

Clearly the position of the homogeneous reaction (1a) will depend on the concentration of the free metal ions which can be modified by an auxiliary complexing (or masking) agent (see Section 10.3). It will move increasingly to the right as the (overall) stability constant of the complex, ML_n, increases and to the left as the solution becomes more acidic. Increase of pH should lead to more complete reaction but since this implies a concomitant increase in hydroxyl ion concentration there will now be increasing competition between the tendencies of L^- and OH^- to coordinate to the cation; basic species and even metal hydroxides may form and precipitate.

Since the ligand is basic, various protonated species may occur in solution. Specifically, if C_L is the total concentration of ligand in solution then, ignoring any small amount present as any water-soluble metal complex, and omitting charges for the sake of generality:

$$C_L = L + HL + H_2L + \ldots\ldots. H_nL$$

whence

$$[L] = C_L/\{1 + \beta_1^H[H] + \beta_2^H[H]^2 + \ldots\ldots \beta_n^H[H]^n\} \tag{2}$$

where $\beta_n^H = [H_nL]/[L][H]^n$. Clearly the *effective* amount of ligand will increase with increase in pH and as the overall formation constant β_n^H of the acidic species H_nL decreases.

Similarly in the presence of an auxiliary complexing agent A (*e.g.* NH_3, en, phen, halogen$^-$, Ac^-, CN^-, *etc.*) the effective amount of cation M^{n+} will be less than the total amount C_M in solution. Specifically:

$$[M] = C_M/\{1 + \beta_1^A[A] + \beta_2^A[A]^{2+} \ldots\ldots \beta_n^A[A]^n\} \tag{3}$$

where $\beta_n^A = [MA_n]/[M][A]^n$ is the overall formation constant of the species MA_n. Equilibria based on these considerations are fully treated in a number of textbooks where the use of 'conditional constants' and 'α-coefficients' is introduced to facilitate calculations.[15,16]

10.2.1.4 Stability of complexes

Since

$$-2.303RT \log [ML_n]/[M][L]^n = -RT \ln \beta_n = \Delta G = \Delta T - T\Delta S \tag{4}$$

for the generalized reaction

$$M(\text{solvated}) + nL(\text{solvated}) = ML_n(\text{solvated}) + x \text{ mol of solvent} \tag{5}$$

the stability of the complex will clearly depend on the solvent, the temperature and the entropy and enthalpy of the reaction represented by equation (4), charges again being omitted in the interests of generality.

For a given ligand in water the Irving–Williams order for divalent transition metal cations (Mn < Fe < Co < Ni < Cu > Zn) is very widely obeyed although spin-pairing, stereochemical factors and ligand-field effects may disturb the normal sequence.[11] The nature of the donor atoms (stability O < N; O—O < O—N < N—N for chelates) does not perturb the order. With other cations the situation is more involved and it is scarcely surprising that no inflexible order of stability applies to all types of ligand. Nevertheless the behaviour of halide complexes where the stability order may be $F^- \gg Cl^- > Br^- > I^-$ or $F^- < Cl < Br^- < I^-$ depending on the cation involved and its oxidation state has been systematized and interpreted by Ahrland, Chatt and Davies.[17]

Although the whole question of the thermodynamics of metal complexes in solution is dealt with in Chapter 5 of this series and specific ligands are treated exhaustively in Chapters 12 to 21, it will not be inappropriate to call attention to an excellent book by D. D. Perrin[18] which considers the structure and behaviour of organic ligands especially from the point of view of their application to inorganic analysis. Chapter 14, dealing with the search for new organic reagents, is particularly stimulating.

Whatever theoretical explanation of the ‘chelate effect’ is adopted, there is no doubt as to the extra stability conferred by polydentate ligands capable of forming one or more chelate rings. This is of especial importance in titrimetry (see Section 10.6) and, as we shall see shortly, bidentate ligands play a significant role in the formation of precipitates of value in gravimetry.

10.2.2 Gravimetry with Metal Oxinates

10.2.2.1 8-Hydroxyquinoline–metal complexes

8-Hydroxyquinoline (**7b**; 8-quinolinol, HOx) readily protonates to give (**7a**; H_2Ox^+) and by loss of a proton yields (7c; Ox^-) which is the effective bidentate ligand involved in chelation.

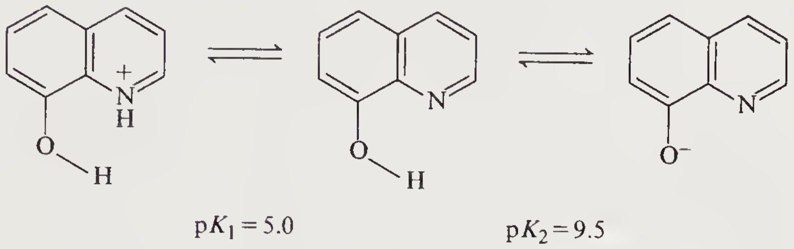

(7a) **(7b)** **(7c)**

Since the reaction with the reagent (**7b**) in homogeneous solution proceeds according to

$$M^{n+}(aq) + nHOx \rightleftharpoons MOx_n(solution) + nH^+ \tag{6a}$$

followed by:

$$MOx_n(solution) \rightleftharpoons MOx_n(precipitate) \tag{6b}$$

the position of equilibrium in equation (6a) will depend on the pH and the basicity of the ligand (as indicated quantitatively by pK_1 and pK_2), and on the formation (stability) constant for the complex $\beta_n(ML_n)$, and on the total amounts of ligand and metal ion, C_L and C_M, from which the actual amounts not involved in complex formation can be calculated from equations (2) and (3) given above. The extent of precipitation is then controlled by the solubility product $K_S = [M^{n+}][Ox^-]^n$ where concentrations are used rather than activities to simplify the equations.

If C_L, C_M and pH are kept the same for a series of different cations, the position of equilibrium in equation (6a) would depend on the value of the formation constant, β_n, for the metal complex in question and the extent of precipitation on its solubility product, K_S. The more stable the complex and the lower its solubility in water, the greater the extent of precipitation. Essentially there is a competition between cations M^{n+}, and protons, H^+, for the free ligand anion Ox^-.

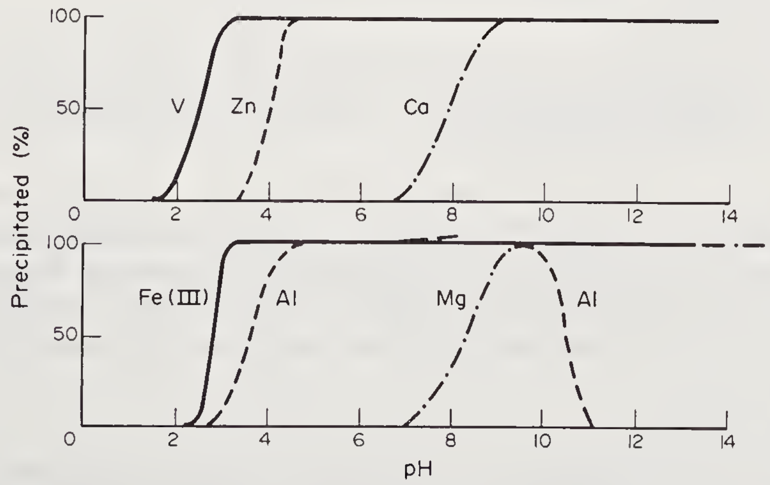

Figure 1 The percentage precipitation of several metal oxinates at increasing pH values

If two cations are present together, the one forming the more stable complex will generally precipitate at a lower pH, for differences in stability are usually more significant than differences in solubility. Anomalous and overriding solubility effects such as those noted with the copper and nickel chelates of DMG (see Section 10.2.1.2) are the exception rather than the rule.[19] Under favourable conditions clean separations are possible by control of pH reinforced by the addition of masking agents. The above points are illustrated in Figure 1.

Thus aluminum can be separated from beryllium in an acetic acid–ammonium acetate buffer and magnesium from alkaline earths in ammoniacal buffers. Table 1 gives the pH values at which precipitation commences and the range over which it is complete. Although the five-membered chelate rings are formed in each case by the phenolic oxygen and heterocyclic nitrogen atoms to give normal complexes with coordination numbers 4 (Be, Cu, Cd, Pb), 6 [*e.g.* iron(III), bismuth, aluminum, indium, gallium and thallium(III)], or 8 (thorium and zirconium), there are some exceptions shown in Table 1 and of particular interest is the precipitation of adducts such as $ThOx_2 \cdot HOx$, $UO_2Ox_2 \cdot HOx$, and $PuO_2Ox_2 \cdot HOx$. The liquid–liquid extraction of such adducts is commonplace, especially in the presence of excess ligand. Magnesium is somewhat exceptional as it achieves octahedral coordination by aquation, forming $MgOx_2 \cdot 2H_2O$, although the anhydrous complex $MgOx_2$ is chloroform soluble: similar hydrates are formed by Fe^{II} and Zn^{II}.

Table 1 Metal Oxinates

	pH for precipitation[a]		
Metal complex	*(a) Incipient*	*(b) 100% range*	*Solubility in chloroform*
$AlOx_3$	2.9	4.2–9.8	S
$BiOx_3$	3.7	4.8–10.0	S
$CdOx_2$	4.5	5.4–14.0	S
$CaOx_2$	6.8	9.2–13.0	I
$CoOx_2$	3.6	4.8–13.0	S
$CuOx_2$	3.0	> 5.3	S
$FeOx_3$	2.5	2.8–12	S
$GaOx_3$	—	—	S
$InOx_3$	—	Acetic buffer	S
$PbOx_2$	4.8	8.4–12.3	S
$MgOx_2 \cdot 2H_2O$	7.0	9.4–12.7	I
MoO_2Ox_2	2.0	3.6–7.3	S
$MnOx_2$	4.3	5.9–10	S
$NiOx_2$	3.5	4.6–10	S
$PdOx_2$	—	Dilute HCl	S
$PuO_2Ox_2 \cdot HOx$	—	3.5–9	S
$ScOx_3$	—	—	S
$TiOOx_2$	3.6	4.8–8.6	S
$TlOx_3$	—	Acetate buffer	S
$ThOx_4 \cdot HOx$	3.9	4.4–8.6	S
$UO_2Ox_2 \cdot HOx$	3.7	5.0–9.8	S
$V_2O_3Ox_4$	1.4	2.7–6.1	S
WO_2Ox_2	3.5	5.0–5.7	S
$ZnOx_2 \cdot 2H_2O$	3.3	4.4–13.5	I

[a] The pH values are indicative only, for incipient precipitation is often delayed by supersaturation. Mg and Zn oxinates are only extracted in their anhydrous forms.

Details of procedures for the use of particular metal oxinates in gravimetric analysis must be sought in the appropriate textbooks[20,21] but owing to difficulties of achieving reproducibly stoichiometric precipitates in some cases it may be preferable to ignite the precipitate to some other weighing form or to use a different finish altogether.[3] Uses of metal oxinates in absorptiometric procedures or in liquid-liquid extraction will appear later (see Sections 10.5.4 and 10.4.4.4).

10.2.2.2 Substituted oxinates

Many derivatives of 8-hydroxyquinoline have been prepared with substituents in the benzene and/or pyridine ring and examined for their analytical potential.[22] The substitution of a halogen atom in the 5- or 7-position reduces the solubility and Berg[20] made good use of 5,7-dichloro(or dibromo)-8-hydroxyquinoline for the precipitation of iron(III) and titanium(IV) in quite acidic solutions and reported a number of useful separations. Introducing a methyl group increases the value of pK_2: the nitrogen atom is more basic and stronger metal complexes are formed. This has been demonstrated experimentally for several chelate complexes (notably those of Mg^{2+}, Zn^{2+} and

UO_2^{2+}) which, though very sparingly soluble in water, are sufficiently soluble in 50% aqueous dioxan for potentiometric studies to be feasible.[23]

10.2.2.3 2-Methyl-8-hydroxyquinoline and sterically hindered reagents

In 1944 Merritt and Walker[24] reported that 2-methyl-8-hydroxyquinoline closely resembled the parent oxine in forming insoluble chelate complexes with all the same metal ions with the notable exception of aluminum which failed to give a precipitate. This exceptional behaviour was exploited in a procedure for determining aluminum in the presence of zinc or magnesium. An explanation was given as follows: 'Probably because of its increased size, it (8-hydroxyquinaldine) is a more selective reagent. If the size of the molecule is the determining factor, the larger molecule might be expected not to react with the smaller ions because of the difficulty of grouping three large molecules around the small ion. If a complex is formed it might be less stable.'

The exceptional behaviour of aluminum had been noted independently by Irving *et al.* who showed that the precipitation of chelates was not inhibited by alkyl or other substituents in the 4-, 5-, 6-, or 7-positions although it was inhibited by 2-phenyl-, 2-(1-ethylpropyl)- and a wide variety of 2-methyl- or halogen-substituted 8-hydroxyquinaldines, by 1-hydroxyacridine and by 9-hydroxy-1,2,3,4-tetrahydroacridine in which the 2-position has been involved in annelation.[23] This seemed to confirm that steric hindrance to the packing of such molecules around the small aluminum ion (radius 0.50 Å) was indeed the explanation of its exceptional behaviour and indeed Ga^{3+} and Tl^{3+} (ionic radii 0.62, 0.81 and 0.95 Å) all behaved 'normally' to give insoluble tris chelate complexes. The possibilities of steric hindrance in octahedral complexes can be visualized as in Figures 2 and 3 where the tris complex is shown in the *fac*-form: crowding in the *mer*-form would be even less favourable to coordination. Despite earlier statements that beryllium (ionic radius Be^{2+} = 0.31 Å) is incompletely precipitated by 8-hydroxyquinaldine, it does in fact form a well-characterized bis chelate which has been exploited for the determination of beryllium, titanium and iron in the presence of aluminum.[25] This is clearly the result of beryllium using $2s2p^3$ hybridization to form a tetrahedral complex in which there is no steric hindrance to coordination caused by bulky 2-substituents, since the two coordinating ligands now lie in planes at right angles as shown in Figure 3. This assumption has been fully confirmed by X-ray crystallography.[26]

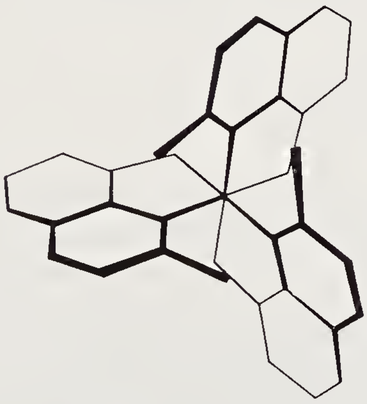

Figure 2 Steric hindrance in an octahedral metal complex of, for example, 2-methyl-8-hydroxyquinoline. Atoms are omitted for clarity

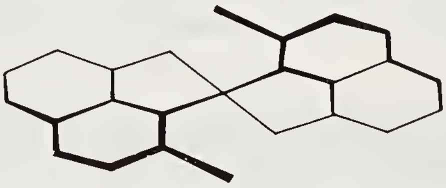

Figure 3 Absence of steric hindrance in a tetrahedral complex of, for example, beryllium and 2-methyl-8-hydroxyquinoline

It is noteworthy that the Be—O distance (1.60 Å) is of the same order as that found for other coordination compounds of beryllium and leads to the value of 1.0–1.1 Å for the covalent radius of beryllium in this type of coordination.[26] Clearly arguments based on relative ionic radii are invalid. Thus the dihydrate of zinc oxinate has been shown to form a distorted tetrahedron with two long $Zn—H_2O$ bonds while the lengths Zn—O and Zn—N to the ligand are 2.05 and 2.06 Å respectively, whence the zinc radius is 1.38 Å. Clearly the use of an ionic radius ($Zn^{2+} = 0.74$ Å) would be misleading. Similarly the Cu—N bond in compounds of Cu^{II} with ammonia and ethylenediamine (1.99, 2.05, 2.01 Å) implies a radius of 1.3–1.4 Å in these coordination compounds, a value considerably larger than the ionic radius of 0.7 Å.[23]

Clearly arguments based on differences in ionic radii are suspect and we should look for other factors to account for the anomalous behaviour of Al^{3+}. If K_{eq} is the equilibrium constant of equation (6a) we can see that

$$\log K_{eq} = \log \beta_n - npK_2 \tag{7}$$

There is abundant evidence that steric hindrance to coordination will decrease the formation constant of any complex formed and may even inhibit complex formation altogether. Numerical data are available for transition metals and substituted ethylenediamines,[27] or substituted oxines,[23] for 1,10-phenanthroline and its 2- and 2,9-methyl-substituted derivatives[28] and for other systems.[29] Since the introduction of a 2-methyl substituent into oxine diminishes β_n while increasing pK_2, it is not surprising that the effective concentration $[Al(2\text{-}MeOxine)_3]$ may not be great enough to cause precipitation, although this is achieved in non-aqueous media such as ethanol.

If a solution containing metal ions is gradually made alkaline, the hydroxide will precipitate when the solubility product $K_S(M(OH)_n) = [M^{n+}][OH^-]^n$ is exceeded. If a chelating agent L^- is present, the formally neutral complex will precipitate when its solubility product $K_S(ML_n) = [M^{n+}][L^-]^n$ is exceeded and provided $K_S(ML_n) < K_S(M(OH)_n) \times ([L^-]/[OH^-])^n$. If the converse is true the hydroxide will be thrown down preferentially. Table 2 shows the pH for incipient precipitation for aluminum and two similar relevant cations. In the case of gallium(III) and indium(III) precipitation of the three yellow trisoxine complexes occurs at a lower pH than that of the metal hydroxides, whereas pure white $Al(OH)_3$ precipitates at pH 4.2 even in the presence of 2-methyl-8-hydroxyquinoline. The effect of introducing a basifying methyl group can be seen in Figure 4, which shows the percentage of ionization for oxine and two of its analogues as a function of pH. To achieve the same concentration of ligand, $[L^-]$, it will be clear that a higher pH will be needed in the case of the more basic 2-methyl derivative.

Table 2 pH of Incipient Precipitation of Metal Oxinates

		Metal alone			*Metal and reagent*		
		Al	*Ga*	*In*	*Al*	*Ga*	*In*
	4.4	4.2	2.9	4.1	3.2	1.8	2.2
5-Methyloxine	5.3	4.2	2.9	4.1	3.6	2.0	2.5
2-Methyloxine	5.5	4.2	2.9	4.1	4.2[a]	2.8	2.9

[a] Pure $Al(OH)_3$ is precipitated.

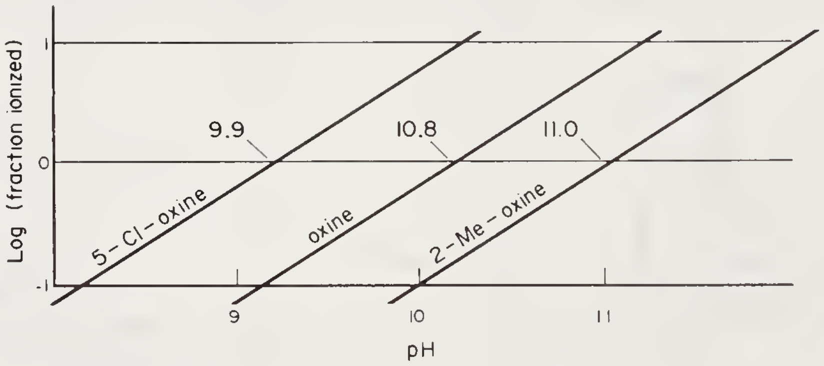

Figure 4 Plots of log (fraction ionized) *versus* pH for oxine and two of its derivatives showing the need for a higher pH in the case of 2-methyloxine to attain the same fractional amount of coordinating ligand

So far no comparable cases of this steric effect have been identified with other metals or other types of ligands.

10.2.3 Reagents Forming Five-membered Chelate Rings through Nitrogen and Oxygen

The possibility of forming a five-membered ring through N and O shown by 8-hydroxyquinoline (**7**) is shared by quinaldinic acid (**2**) which forms well defined complexes $Cu(C_{10}H_6NO_2)_2{\cdot}H_2O$ from relatively acid solutions whence the more soluble complexes of Cd and Zn can be separated. Like oxine it is unselective and reacts with very many cations so that pH and other reaction conditions must be carefully controlled. Anthranilic acid (**8**) is so unselective that its use is confined to the quantitative precipitation of a single cation from a solution containing only Cd, Co, Cu, Ni or Zn.

On the other hand, α-benzoinoxime (cupron, PhCH(OH)C(Ph)═NOH) gives a green insoluble 1:1 complex with copper(II) (probably as **9**) in dilute ammoniacal solution, weighable as $Cu(C_{14}H_{11}O_2N)$ after drying at 110 °C. In the presence of tartrate copper may readily be separated from Al, Cd, Co, Pb, Ni, Zn and small amounts of iron. From fairly acid solutions cupron precipitates molybdates, tungstates, vanadates and uranyl salts as complexes of uncertain composition (possibly involving six-membered rings chelated through oxygen): ignition to reproducible

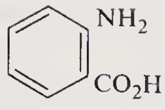

(8)

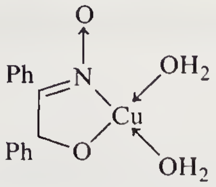

(9)

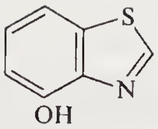

(10)

oxides as weighing forms is desirable. Many acyloin oximes analogous to cupron but without aryl rings behave similarly but give rise to less stable chelate complexes.

Hydroxybenzothiazole (**10**) has the same chelating group as oxine (**7**) and forms insoluble complexes with Cu, Ni, and Zn, which are relatively more soluble, probably because the sulfur atom tends to form hydrogen bonds with the solvent.

10.2.4 Reagents Forming Six-membered Chelate Rings through Nitrogen and Oxygen

It has been mentioned above that α-nitroso-β-naphthol was introduced early on as a precipitant for cobalt with which it gives (**11**). It is relatively unselective and reacts similarly with Fe^{III}, Cr^{III}, Zr^{IV}, W^{VI} and other cations of high charge. An interesting feature is that once formed, the Co^{III} complex is kinetically inert so that strong acidification leaves it untouched while complexes of other metals dissociate and pass into solution. Though valuable for separating Co from large amounts of Ni, the precipitate has not got a reliably stoichiometric composition and ignition in the presence of oxalic acid to Co_3O_4 or thence to $CoSO_4$ is recommended.

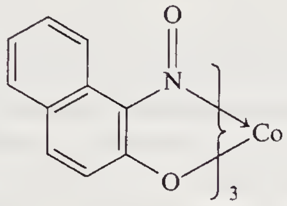

(11)

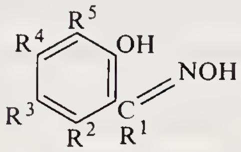

(12)

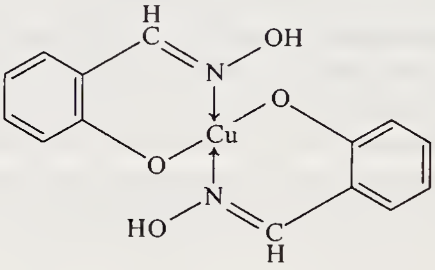

(13)

Salicylaldoxime (**12**; R_n = H) forms chelates with many divalent metals. Bonding takes place between the phenol oxygen and the nitrogen of the oxime grouping to form again a five-membered ring. Alkylation of the phenolic group completely destroys its ability to chelate.

At pH 2.6–3.3 it is a selective precipitant for Cu^{II} yielding (**13**) but as the pH is increased Ni, Pb, Hg^{II}, Co^{II}, Ag^{I}, Zn^{II}, Cd^{II}, Bi^{III}, Fe^{II}, Mn^{II} and Mg^{II} are precipitated. Under certain circumstances 1:1 complexes are formed with Pb, Zn and Cu^{III}, but their structures are uncertain and they have little interest analytically.

As suggested by (**12**) a large number of analogues of salicylaldoxime have been synthesized with such substituents as Me, OMe, CO_2H and NO_2: positions 2,3 and 3,4 have been made part of a second aromatic ring. Provided the α-configuration of the oxime is retained they all give precipitates with copper but are not notably more selective.

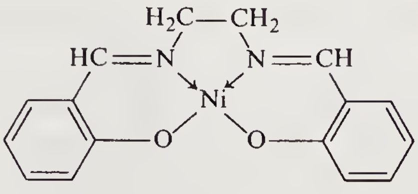

(14)

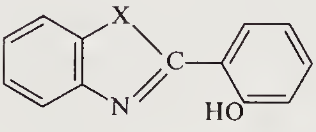

(15a) X = O
(15b) X = NH

Schiff's bases formed from *o*-hydroxyaldehydes often form reagents of service in analysis. For example, the base formed with ethylenediamine forms an insoluble complex with nickel (**14**) which has been used for its gravimetric determination. 2-(*o*-Hydroxyphenyl)benzoxazole (**15a**) has been proposed for the quantitative determination of cadmium, and 2-(*o*-hydroxyphenyl)benzimidazole (**15b**) for mercury.

10.2.5 Reagents Forming Five-membered Chelate Rings through Two Oxygen Atoms

Cupferron, the ammonium salt of *N*-nitroso-*N*-phenylhydroxylamine, was so called by O. Baudisch (1907) because it precipitates both copper and iron. In strong mineral acids (5% v/v HCl or H_2SO_4) it precipitates iron(III), cerium(IV), gallium(III), niobium(V), tantalum(V), tin(IV), titanium(IV), tungsten(VI), vanadium(V) and zirconium(IV), enabling separations from aluminum, barium, beryllium, calcium, chromium, cobalt, manganese, nickel, strontium, zinc and uranium to be carried out. It is necessary to work with an excess of this reagent and in the cold, and to ignite the precipitate to yield an oxide of reproducible composition and to burn off excess of precipitant. A pure metal complex can be formulated as (**16**; Ar = Ph).

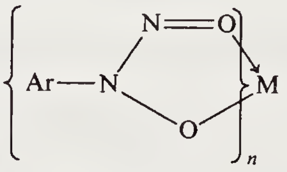

(16)

Complexes of neocupferron, the ammonium salt of *N*-nitroso-*N*-2-naphthylhydroxylamine (**16**; Ar = naphthyl) are less soluble and bulkier than those of cupferron and can be used to determine copper and iron from the sea and natural waters without a preliminary concentration stage.

Benzoyl-*N*-phenylhydroxylamine (**17**; $R^1 = R^2 =$ Ph) is one of a general class of reagents that forms insoluble complexes with those elements that prefer to bond through oxygen, such as Al, Be, Fe, Nb, Sc, Sn, Mo^{VI}, Ta, Ti^{IV}, U^{VI}, V and Zr. They are very unselective but can be made less so by a careful control of the pH of precipitation and the addition of appropriate masking reagents (see Section 10.3). Much work has been done on a wide variety of hydroxamic acids and of the few reagents where donation is through a sulfur atom, *trans*-2-thiophene-*trans*-aldoxime (**18**) can be used to determine palladium gravimetrically.

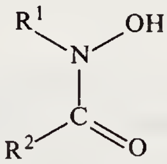

(17)

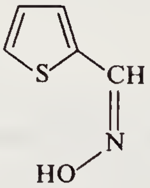

(18)

Mandelic acid, PhCH(OH)CO_2H, is a sensitive and highly selective reagent for zirconium with which it gives insoluble tetrakis complexes from hydrochloric acid. Owing to the large excess of reagent that must be used and the difficulty of removing this, the 4-chloro or 4-bromo derivative is preferred. Again it is preferable to ignite the precipitate and weigh the residual ZrO_2.[21,30]

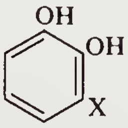

(19)

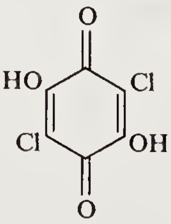

(20)

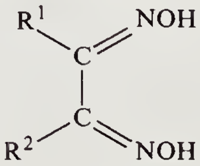

(21)

Pyrogallol (**19**; X = OH) is able to form a five-membered chelate ring by using two adjacent hydroxy groups and it forms insoluble complexes with bismuth and antimony which can be used for their quantitative determination alone or in the presence of arsenic, cadmium, lead or zinc. It is more than likely that although the third adjacent oxygen atom cannot take part in chelation for steric reasons, it can link molecules together as a polymer and so promote insolubility. The basic structure of catechol (**19**; X = H) does not occur in many gravimetric reagents but is of great significance in water-soluble complexes used in absorptiometry (see Section 10.5) and in metallochromic indicators (see Section 10.6.4).

Although chloranilic acid (**20**) forms sparingly soluble complexes with many cations by way of chelation through pairs of phenolic and adjacent quinonoid oxygen atoms, these are seldom used as a weighing form. More usually the insoluble chloranilate is collected, washed and treated with a more powerful chelating agent: the liberated red chloranilate ion is then determined spectrophotometrically.[13] Chloride can be determined by shaking with a suspension of sparingly soluble mercury(II) chloranilate whereupon the chloranilate ion is displaced quantitatively as the more stable mercury—chloride complex forms. In a similar procedure lanthanum chloranilate has been used to determine phosphate and fluoride.

10.2.6 Reagents Forming Five-membered Chelate Rings through Two Nitrogen Atoms

The classical case here is that of dimethylglyoxime (**21**; $R^1 = R^2 = Me$), which forms such a useful insoluble complex with nickel (**4**) and can be used to determine this element in the presence of copper. Reasons for this have been put forward in Section 10.2.1.2. A great number of variants on (**21**) have been prepared and tested with a view to increasing the solubility of the reagent in water without increasing the solubility of the nickel complex. This is of considerable practical importance, for the low solubility of H_2DMG in water (0.4 g dm^{-3}) means it must be used as a 1% (w/v) solution in ethanol and the mass of the precipitate is reduced by prolonged washing with alcohol—water mixtures.

α-Furildioxime (**22**) is a slightly stronger acid than H_2DMG so that the optimum pH can be reduced from about 5.1 to 4.3. The nickel complex is even more insoluble than $Ni(DMG)_2$ and the gravimetric factor is much more favourable. Perhaps its greatest advantage is the solubility of the reagent in water which enables the precipitate to be washed free of any excess. Both cyclohexane-1,2-dioxime (nioxime, **23**; R = H) and cycloheptane-1,2-dioxime (heptoxime, **24**) are more soluble in water than H_2DMG. The tendency of the former to coprecipitate with the metal complex is avoided in 4-methylcyclohexane-1,2-dione dioxime (**23**; R = Me), which precipitates nickel quantitatively down to pH 3, is readily washed, and filters well.

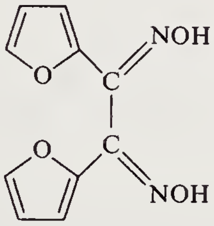

(22)

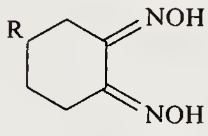

(23)

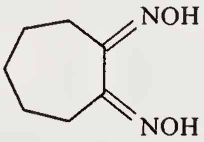

(24)

All reagents of this dioxime type are equally suitable for the gravimetric determination of palladium(II) and the very sparingly soluble yellow bis chelate complexes also have axial intermolecular metal—metal bonds. Oxamidoxime (**21**; $R^1 = R^2 = NH_2$) forms an insoluble bis complex with nickel but a soluble one with cobalt. Somewhat similar to DMG in their reactions are 2-pyridylmethylketoxime and 2-pyridylphenylketoxime where the five-membered chelate ring is formed between the nitrogen of the oxime group and the nitrogen of the heterocyclic ring.

10.2.7 Reagents Coordinating through Sulfur

The tendency to combine more strongly with sulfur than with oxygen (as instanced by the precipitation of many sulfides from aqueous solutions) is characteristic of many metals and can be explained theoretically.[17] It could therefore be expected that chelate complexes of familiar ligands with a donor oxygen atom replaced by a donor sulfur would be more stable and more selective.

The 8-SH analogue of oxine has been studied extensively as a precipitant but its use is severely restricted because of its ease of oxidation. On the other hand thionalide (thioglycollic-β-aminonaphthalide; **25**) is similar to hydrogen sulfide in its reactions and forms precipitates with most metals of the hydrogen sulfide group in acid solution. It can be used for determining Cu in the presence of Cd, Co, Fe^{II}, Mn, Ni, Pb, Tl and Zn, but chloride ions interfere. In a sodium hydroxide—cyanide—tartrate medium only Tl is precipitated. Most thionalide complexes have a definite composition and can be dried and weighed at 105 °C. However solutions of the reagent (in ethanol or ethanoic acid) are only stable for a few hours and it is prone to oxidation, *e.g.* by iron(III), a disability which can be minimized by adding hydroxylamine sulfate. Dithizone (**26**) forms highly insoluble metal complexes but these are only used in liquid–liquid extraction procedures (Section 10.4.4.5) and in absorptiometric procedures (Section 10.5.3). Dithiooxamide (rubeanic acid; **27**) has been used as a precipitant for Cu, Ni and Co in weakly acidic or ammoniacal media. It readily undergoes hydrolysis to H_2S so that it precipitates Ag, Cd, Hg, Pb and Zn as their sulfides. Mercaptobenzothiazole (**28**) precipitates many metals from weakly acidic (*e.g.* Cu) or ammoniacal solution (*e.g.* Cd) but most precipitates must be ignited to achieve weighable forms. Bis(allythiocarbamido)hydrazine (dalzin, $C_3H_5NHCSNHNHCSNHC_3H_5$) forms insoluble 1:1 complexes (**29**) with Cu, Hg, Ni, Pb, Pd and Zn, and has been recommended for their gravimetric determinations. On the other hand although toluene-3,4-dithiol (**30**) forms many metal chelate complexes, the solubility of these in organic solvents makes this a reagent of choice for procedures involving liquid–liquid extraction (Section 10.4.4.5). The extreme ease of oxidation is a major disadvantage of many reagents with sulfur–donor atoms (another is their pronounced odour) and militates against their greater use.

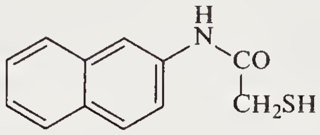

(25)

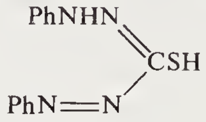

(26)

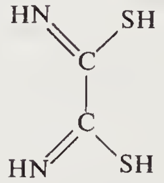

(27)

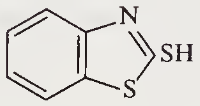

(28)

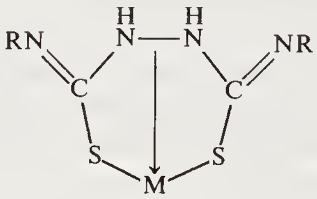

(29) $R = C_3H_5$

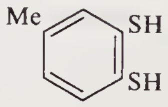

(30)

10.2.8 Purely Inorganic Coordination Compounds

Bridging the gap between the use for gravimetric analysis of entirely inorganic coordination compounds and those described above where organic ligands, usually bidentate anions, form hydrophobic chelate complexes of formally neutral charge, are a group of compounds introduced by Spacu and his coworkers. Here organic bases such as pyridine, quinoline, isoquinoline and benzidine are used to increase the coordination number (and displace water) in thiocyanates of, for example, cadmium, copper, zinc and other divalent metals to give sparing soluble compounds such as $Cd(CNS)_2 \cdot 2py$.[31]

A considerable number of coordination compounds existing as bulky cations or anions have been introduced as more or less selective precipitants. Sodium tetraphenylborate is a convenient source of the ion BPh_4^- which gives insoluble salts with K^+. Rb^+, Cs^+ and NH_4^+. The older and cheaper reagent dipicrylamine has similar properties. Picrolonic acid, 1-(3′-nitrophenyl)-3-methyl-4-nitropyrazole-5-one, forms slightly soluble crystalline precipitates with Ca, Pb and Th, and has been used in gravimetry though many other metals interfere. Nitron (1,4-diphenyl-3,5-endanilo-4,5-dihydro-1,2,4-triazole) is a classic reagent for the precipitation of nitrate though its use in gravimetry is fraught with problems.[32] The tetraphenylarsonium ion, $AsPh_4^+$, the methyltriphenylammonium ion, $MePh_3N^+$, and various alkyltin cations are among the host of reagents proposed for gravimetry for which details will be found in major publications.[30,33]

A case deserving special mention is the determination of phosphorus (as phosphate) for which the classical methods have been (a) precipitation as ammonium magnesium phosphate and weighing after ignition as magnesium pyrophosphate, and (b) precipitation as ammonium molybdophosphate. Double precipitation is essential if accurate results are to be obtained by (a) and the procedures are slow. Now the formula for ammonium molybdophosphate is approximately $(NH_4)_3[PO_4 \cdot 12MoO_3] \cdot nH_2O$ and it tends to drag down and hold tenaciously other ions and even acids. The literature abounds with 'formulae', *e.g.* $(NH_4)_3PO_4 \cdot 12MoO_3 \cdot 2HNO_3 \cdot H_2O$ and

$(NH_4)_{14}(PO_4)_4SO_4{\cdot}53MoO_3$ purporting to represent the composition of the precipitate formed under various conditions and it was common to use a 'factor' to correct the weight of precipitate to the percentage of phosphorus.

In a definitive series of experimental investigations H. N. Wilson showed that the quinolinium salt, $(C_9H_8N)_3{}^+[PO_4{\cdot}12MoO_3]^{3-}$ was anhydrous, contained exactly 12 moles of molybdenum trioxide per mole of phosphate, that the precipitate had a negligible solubility and could be dried to constant weight in two hours at 105 °C. This precipitate also lent itself to a precise alkalimetric titration. In the presence of citric acid interference by silica was inhibited so that the method was admirably suitable for the analysis of basic slags or fertilizers.[34]

10.2.9 Scavenging

The lack of selectivity of 8-hydroxyquinoline (Section 10.2.2.1) can be turned to good advantage when the problem is one of collecting a wide spectrum of cations from a dilute solution—a problem of increasing importance in studying environmental pollution. Vanderborgh and Van Grieken argued that although active charcoal will absorb many cations directly (capacity ~1 mg per g for Zn^{2+} or Cu^{2+}) it has a greater capacity for neutral organic substances. They found the capacity of an active charcoal for metal oxinates (where the strength of interaction was doubtless enhanced by the π-orbitals of the aromatic rings) was some 30 times greater than for the metals alone and by using an excess of oxine (2.5–25 p.p.m. at pH ~8) they could collect from natural works 90–100% of transition metals, Cd, Hg, Hf and lanthanides, 80–90% of Cu and Pb, 30% Ag, 0-2% Sb, <10% alkaline earths.[35] Metal chelate complexes are often effective and selective by themselves. Thus if tris(pyrrolidinedithiocarbamato)cobalt(III) is precipitated *in situ* it takes up >90% of Cr^{VI}, Cd, Ni and Pb from initial concentrations of 0.1 mg l^{-1}; adsorption of Cu, Fe^{II} and Fe^{III} is poorer and that of Cr^{III}, Mn and Zn is quite poor.[36]

10.2.10 Concluding Remarks

Unless they can be regarded primarily as gravimetric reagents it has seemed appropriate to relegate many other coordination compounds to sections where they are more appropriately located, *e.g.* absorptiometry (Section 10.5.4), liquid–liquid extraction (Section 10.4), titrimetry (Section 10.6) or chromatography (Section 10.7.3). Nevertheless a steady stream of new organic reagents continues to appear in the current literature and it has been decided not to yield to the temptation of adding to the above list of reagents simply in an attempt to appear up-to-the-minute. For what is very rarely established (and often tacitly ignored by authors) is how far the newcomers present cogent advantages (from the point of sensitivity, selectivity, cost, practical considerations, *etc.*) over existing reagents. Despite the need and obvious value of such work little kudos would accrue to compensate for the tremendous expenditure of time, experimental effort and critical experience needed. Even the criteria for making such a select list of gravimetric reagents have yet to be established!

10.3 MASKING

10.3.1 Introduction

It will be apparent from the examples quoted in Section 10.2 that most organic reagents are very unselective and react with a wide spectrum of cations. Where the complexing agent is used in the form of the conjugate acid of the effective ligand (*cf.* equation 6a), and if it is a weak acid, careful control of the pH can substantially increase the selectivity and may permit of satisfactory separations in certain cases. In addition auxiliary complexing or masking agents may be needed. If the resulting metal complexes are sufficiently stable, the concentration of the interfering ion may well be reduced sufficiently to prevent reaction with a reagent added later. The metal is then said to be 'masked'.

A familiar example is the reaction of dilute ammonium hydroxide with silver ions to give $Ag(NH_3)_2{}^+$, which reduces the concentration of free Ag^+ to a value below that needed to exceed the solubility product of AgCl (but not that of AgBr or AgI). If ammonia is replaced by cyanide ions, which form more stable complexes, only the more insoluble AgI can be precipitated. Hence by choice of the masking agent used a cation can be selectively masked towards some reagents but not others.

In a different field thallium(I) can be separated from lead by adding ethylenediaminetetraacetic acid (EDTA; H_4Y) in an ammonium acetate buffer. The lead complex is very stable, K_{PbY} =

$10^{18.3}$, compared to that of thallium(I), $K_{\text{TlY}} = 10^{6.5}$, and so lead is masked while only the thallium is precipitated as its sparingly soluble iodide, TlI.

10.3.2 Quantitative Treatment of Masking

If [L′] is the apparent ligand concentration, *i.e.* the concentration of ligand *not* bound to the central metal ion M (though it may exist free or in protonated forms), we adapt equation (2) to read

$$[L'] / [L] = 1 + \beta_1{}^{H}[H] + \ldots\ldots \beta_n{}^{H}[H]^n = \alpha_{L(H)} \tag{8}$$

where $\beta_n{}^{H} = [H_nL]/[L][H]^n$. $\alpha_{L(H)}$ is termed the α-coefficient (or side-reaction coefficient) and in this instance specifies the effect of $[H^+]$ upon [L′]. Since $\alpha_{L(H)}$ is a function of all the proton stability constants $\beta_n{}^{H}$ and the pH, its numerical value ($\geqslant 1$) can be calculated from tabulated data.[29] Similarly if [M′] is the apparent free metal ion concentration, *i.e.* the concentration of cation that has *not* reacted with the complexing agent (but may have done so with an auxiliary complexing agent, A), then analogous to equation (3) we can write

$$[M'] / [M] = 1 + \sum \beta_n{}^{A}[A]^n = \alpha_{M(A)} \tag{9}$$

where the α-coefficient now specifies numerically the influence of the given concentration of auxiliary complexing agent on the apparent free metal ion concentration.

Finally for the formation of the complex ML_n under practical conditions we can define an overall conditional stability constant by

$$\begin{aligned} \beta'_n &= [ML_n] / [M'][L']^n \\ &= \beta_n / \alpha_{M(A)}\, \alpha^n{}_{L(H)} \end{aligned} \tag{10}$$

where β_n is the tabulated stoichiometric formation constant.

If M is involved in more than one side reaction, we have

$$\alpha_{M(A,B,C\ldots)} = \alpha_{M(A)} + \alpha_{M(B)} + \alpha_{M(C)} + \ldots\ldots - (i-1) \tag{11}$$

where i is the number of side reactions. If no side reactions are involved, $\alpha = 1$ and $[M] = [M']$, $[L] = [L']$. In other cases α can be as large as 10^{20} and the term $(i-1)$ is generally negligible. Graphs of log $\alpha_{M(OH)}$ *vs.* log[OH] or log $\alpha_{M(NH_3)}$ *vs.* log$[NH_3]$ for typical metals, and of log $\alpha_{L(H)}$ *vs.* pH for most of the common masking agents have been published.[16]

10.3.3 Treatment of Precipitation

If $S_O = [M]^m[L]^l$ is the stoichiometric solubility product for the species M_mL_l at a given ionic strength, precipitation will not take place unless this ion product is exceeded. However if M or L undergoes side reactions, the analytical concentrations of the free ions left in solution will be reduced such that $[M'] < [M]$ and $[L'] < [L]$ and the effective or conditional solubility product, S'_O, is now given by

$$S'_O = S_O \alpha_n{}^m \alpha_L{}^l \tag{12}$$

i.e. it will be increased. The net effect may be that precipitation of metal M by the ligand L cannot now take place, whereas that of metal N will. Metal M has been masked preferentially to N. Thus the precipitation of hydroxides of Ni^{2+}, Cu^{2+}, Zn^{2+} and Cd^{2+} can be prevented by adding excess ammonia while other cations, *e.g.*, Fe^{3+}, Al^{3+}, precipitate. Tartrates and citrates are commonly used to 'hold up' Mn^{2+}, Pb^{2+}, Al^{3+} and In^{3+} under conditions where other metal hydroxides precipitate. Tartrate will reduce the concentration of Cu^{2+} below that at which it can be reduced and precipitated as Cu_2O by aldose sugars.

A widely applicable masking agent is sodium triphosphate, $Na_5P_3O_{10}{\cdot}6H_2O$, which readily complexes with a very wide variety of cations in all groups of the Periodic Table, preventing their precipitation by alkali hydroxide, ammonia, phosphate, carbonate or borate. It is used commercially as Calgon to mask calcium which cannot then form precipitates with citrate, fluoride or oxalate ions and in many other instances (see Table 3).

Anions can be masked too. Cyanide ions are masked by mercury(II) since $Hg(CN)_4{}^{2-}$ and $Hg(CN)_2$ are very stable.

Mercury(II) is also a very effective masking agent for Cl^-, Br^- and I^- as well as SO_3^-. Masking of fluoride ions is important analytically and this can be done effectively by transforming it into a variety of stable coordination compounds, *e.g.* boric acid yields BF_4^-, beryllium gives BeF_4^{2-} and a number of stable octahedral complexes are formed with Al, Fe, Ti, Zr, Nb and Ta.

Table 3 Common Masking Agents

Element	*Masking agent*
Ag	OH^-, Cl^-, Br^-, I^-, NH_3, $S_2O_3^{2+}$, thioglycollic acid
Al	Acetylacetone, acetate, citrate, glyconate, tartrate, oxalate, OH^-, F^-, sulfosalicylate, BAL, triethanolamine, EDTA
As	OH^-, BAL, S^{2-}
Au	Br^-, CN^-, $S_2O_3^{2-}$
B	F^-, hydroxy acids, 1,2-diols
Ba	Citrate, tartrate, SO_4^{2-}, DHG, NTA, EDTA
Be	Citrate, tartrate, F^-
Bi	Citrate, tartrate, Cl^-, I^-, DHG, NTA, EDTA, triethanolamine, thiourea, thioglycollic acid, BAL
Ca	Citrate, tartrate, F^-, DHG, NTA, EDTA, $P_2O_7^{4-}$
Cd	Citrate, tartrate, I^-. CN^-, SCN^-, $S_2O_3^{2-}$, unithiol, thioglycollic acid, DHG, NTA, EDTA
Ce	Citrate, tartrate, F^-, tiron
Cl^-	Hg
CN^-	Hg, transition metals, formaldehyde, chloral
Co	Citrate, tartrate, NO_2^-, NH_3, en, tren, penten, CN^-, H_2O_2, $S_2O_3^{2-}$, SCN^-, BAL, DHG, NTA, EDTA
Cr	Citrate, tartrate, ascorbic acid, triethanolamine, NTA, EDTA
Cu	Citrate, tartrate, I^-, NH_3, en, tren, penten, CN^-, S^{2-}, $S_2O_3^{2-}$, SCN^-, thiourea, cysteine, BAL, DTC, thioglycollic acid, triethanolamine, DHG, NTA, EDTA
F^-	Borates, Be, Al, Fe, Hg, Ti, Zr, Nb, Ta
Fe	Acetylacetone, citrate, gluconate, tartrate, oxalate, ascorbic acid, F^-, CN^-, bipy, phen, PO_4^{3-}, $P_2O_7^{4-}$, S^{2-}, SCN^-, $S_2O_3^{2-}$, thiourea, thioglycollic acid, BAL, sulfosalicylic acid, tiron, triethanolamine, DTG, NTA, EDTA
Ga	Acetate
Ge	Oxalate, F^-
Hf	Citrate, tartrate, oxalate, F^-, H_2O_2, SO_4^{2-}, PO_4^{3-}, $P_2O_7^{4-}$, triethanolamine, DHG, NTA, EDTA,
Hg	Citrate, tartrate, Cl^-, I^-, CN^-, tren, penten, SO_3^{2-}, cysteine, thioglycollic acid, semicarbazide, unithiol, BAL, triethanolamine, DHG, NTA, EDTA
I^-	Hg
In	Thioglycollic acid
Ir	Citrate, tartrate, SCN^-, thiourea
Mg	Citrate, tartrate, oxalate, F^-, OH^-, glycols, $P_2O_7^{4-}$, DHG, NTA, EDTA
Mn	Citrate, tartrate, oxalate, F^-
Mo	Citrate, tartrate, oxalate, H_2O_2, SCN^-, tiron, NTA, EDTA
Nb	Citrate, tartrate, oxalate, OH^-, F^-, H_2O_2, tiron
Ni	Citrate, tartrate, CN^-, NH_3, tren, penten, SCN^-, NTA, EDTA
Os	CN^-, SCN^-
Pb	Acetate, citrate, tartrate, Cl^-, I^-, SO_4^{2-}, $S_2O_3^{2-}$, urithiol, BAL, thioglycollic acid, 3-mercaptopropionic acid, DHG, NTA, EDTA
Pd	Acetylacetone, citrate, tartrate, I^-, CN^-, NO_2^-, NH_3, SCN^-, $S_2O_3^{2-}$, triethanolamine, DHG, NTA, EDTA
Pt	Citrate, tartrate, I^-, CN^-, NO_2^-, NH_3, SCN^-, $S_2O_3^{2-}$, DHG, NTA, EDTA
Rh	Citrate, tartrate, thiourea
Sb	Citrate, lactate, tartrate, I^-, F^-, OH^-, S^{2-}, BAL
Sc	F^-, I^-, citrate, tartrate, reducing agents
Sc (and anions)	S^{2-}, SO_3^{2-}, diaminobenzidine
Sn	Citrate, lactate, tartrate, oxalate, OH^-, F^-, I^-, PO_4^{3-}, thioglycollic acid, BAL, triethanolamine
SO_3^{2-}	Hg^{2+}, formaldehyde
Sr	Citrate, tartrate, SO_4^{2-}, DHG, NTA, EDTA
Ta	Citrate, tartrate, F^-, OH^-
Th	Acetate, citrate, tartrate, F^-, SO_4^{2-}, triethanolamine, DHG, NTA, EDTA
Tl	Citrate, tartrate, Cl^-, CN^-, thioglycollic acid, triethanolamine, NTA, EDTA
U	Acetylacetone, carbonate, citrate, tartrate, oxalate, F^-, H_2O_2
V	F^-, CN^-, H_2O_2, triethanolamine, tiron, EDTA
W.	Tartrate, F^-, H_2O_2, SCN^-, tiron
Zn	Citrate, tartrate, OH^-, glycols, CN^-, NH_3, tren, penten, SCN^-, thioglycollic acid, unithiol, BAL, DHG, NTA, EDTA
Zr	Citrate, tartrate, oxalate, F^-, H_2O_2, SO_4^{2-}, PO_4^{3-}, $P_2O_7^{4-}$, triethanolamine, DHG, NTA, EDTA

Abbreviations: DHG = *N,N*-di(2-hydroxyethyl)glycine; NTA = nitrilotriacetic acid; EDTA = ethylenediaminetetraacetic acid; tiron = pyrocatechol-3,5-disulfonic acid; BAL = 2,3-dimercaptopropanol; unithiol = sodium 2,3-dimercaptopropane sulfonate; tren = triaminatriethylamine; penten = tetrakis(aminoethyl)ethylenediamine; bipy = 2,2′-bipyridyl; phen = 1,10-phenanthroline.

Although in no sense comprehensive, Table 3 indicates a range of applications which can be supplemented by the specific uses of EDTA[4] and ways in which the reactions of particular ligands can be made more selective.

10.3.4 Kinetic Masking

This is a special case where the replacement of groups already coordinated to a cation by a new ligand is a slow process. In the case of chromium(III) this can be attributed to losses of ligand-field stabilization energy whether a five- or a seven-coordinate reaction intermediate is involved and the classical example is the slow reaction with EDTA at room temperature. This makes it possible to titrate a mixture with other metals (*e.g.* Fe^{III}) which react quickly without interference from Cr^{III}.

10.3.5 Demasking

The term 'demasking' is used rather broadly to describe any process which reverses the process of masking. Control of the pH can be used to mask calcium ions in admixture with copper(II) whereby, in sufficiently acid solution, the latter is precipitated by oxine whereas the concentration of Ox^- is reduced sufficiently by protonation to prevent the precipitation of calcium oxinate. Raising the pH will increase $[Ox^-]$ and both metals can now be precipitated. A more obvious example is the addition of fluoride ions to form the very stable complex anion $SnF_6{}^{2-}$ and so to mask tin(IV) against its precipitation as SnS_2. Addition of boric acid will give $BF_4{}^-$ and so demask the tin.

Masking of Zn or Cd as their very stable cyanide complexes $Zn(CN)_4{}^{2-}$ or $Cd(CN)_4{}^{2-}$ enables the precipitation (and titration) of many other cations to be effected without their interfering. Demasking is carried out by warming with formaldehyde or chloral. Precipitation of $Ti(OH)_4$ in alkaline solution is masked by adding hydrogen peroxide: demasking is effected by adding reducing agents such as formaldehyde (or urotropine), $SO_3{}^-$ or $NO_2{}^-$. In an alkaline medium cobalt(II) is masked against complexation with diethyldithiocarbamate by a slight excess of EDTA. If an excess of calcium ions is now added this will displace cobalt from its complex and the demasked cobalt then reacts with the sulfur ligand.

10.4 LIQUID–LIQUID EXTRACTION

10.4.1 Basic Principles

Factors leading to insolubility in water were discussed in Section 10.2.1.1. Provided they are not highly polymerized, such hydrophobic substances are generally soluble in non-aqueous solvents. In a two-phase system formed by an aqueous phase and a second phase immiscible with it a solute will partition between them until its activity is the same in both. The Nernst partition isotherm quantifies this relationship in the form

$$K_{D(A)} = \{A\}_1 / \{A\}_2 \approx [A]_1 / [A]_2 \tag{13}$$

where K_D is the partition coefficient and the two phases are distinguished by the subscripts 1 and 2. For many analytical discussions it is convenient and not unreasonable to use K_D to represent a ratio of concentrations rather than of activities but a precise treatment will be found in many specialist articles and books.[6,37–40]

The Nernst partition isotherm applies to each individual species in an equilibrium mixture. The analyst is more directly concerned with the experimentally determinable distribution ratio, D, defined as

$$D_A = \frac{\text{(total analytically determined concentration of A in all its forms in the organic (water-immiscible) phase)}}{\text{(total analytically determinable concentration of A in all its forms in the aqueous phase)}} \tag{14}$$

This distinction is important and best illustrated by an example such as the equilibrium distribution of Co^{2+} between an aqueous buffer containing a bidentate chelating agent acetylacetone ($acac^-$) and pyridine (py) and a water-immiscible (organic) phase such as hexane in which only formally uncharged species such as $Co(acac)_2$ and any adducts with pyridine, uncharged pyridine and the conjugate acid of the ligand (Hacac) will be extracted. The aqueous phase will contain each of these species together with Hpy^+, Co^{2+}, $Co(acac)^+$, $Co(acac)_3{}^-$ and possibly adducts with one or more molecules of pyridine. The distribution of cobalt can be written

$$D(Co) = \sum[Co(acac)_2(py)_y]_{org} / \sum[Co(acac)_x(py)_y]_{aq} \tag{15}$$

where $x = 0, 1, 2, 3...$ and $y = 0, 1, 2...$; analysis for total cobalt will not distinguish between the various components.

Similarly

$$D(\mathrm{py}) = \frac{[\mathrm{py}]_{\mathrm{org}} + y\sum[\mathrm{Co(acac)_2(py)}_y]_{\mathrm{org}}}{[\mathrm{py}]_{\mathrm{aq}} + [\mathrm{Hpy}^+]_{\mathrm{aq}} + y\sum[\mathrm{Co(acac)}_x(\mathrm{py})_y]_{\mathrm{aq}}} \tag{16}$$

The relationship between D and the percentage of material extracted into an equal volume of an organic phase, $E = 100D/(1+D)$, is shown in Table 4.

Table 4 Relationship Between Distribution Ratio and Percentage Extraction for Equal Phase Volumes

log D	−3	−2	−1	0	1	2	3
D	0.001	0.01	0.1	1	10	100	1000
E (%)	0.1	1.0	9.1	50	90.9	99.0	99.9

Clearly if log $D > 3$, a single extraction will effect an almost quantitative extraction when the phase volumes are equal. If the aqueous phase were as much as 100 times larger than the extracting organic phase, the same efficiency would be achieved if log $D > 5$: successive extractions with fresh portions of solvent is another solution.

One important analytical use of liquid–liquid extraction is to achieve a desired degree of concentration of a desired material. Conversely it can be used to reduce the concentration of an unwanted, interfering substance to a suitable low value.

For two substances A and B separation is possible if $D_A \neq D_B$: the greater the difference the easier and more effective the separation. Much of the art of exploiting liquid–liquid extraction in analytical chemistry lies in choosing the appropriate ligands and masking agents (Section 10.3) to achieve the desired relative magnitudes of distribution coefficients for the procedure in hand. Back-washing is commonly used to improve the degree of separation and successive extractions may be needed to increase the overall efficiency. Counter-current separations[6] are not often needed in laboratory analytical determinations but for quantitative work it is often necessary to 'strip' the extracted solute before applying an appropriate finish.

10.4.1.1 Classification of extraction systems

The extraction of iron(III) from hydrochloric acid in ether, first exploited by Rothe (1892), was the prototype of a large number of procedures in which a solvated halometallic acid, *e.g.* $(\mathrm{H^+aqS}_n)\mathrm{FeCl_4}^-$ partitions favourably into a donor solvent S. Another large group of extractions involves adducts such as $\mathrm{UO_2(NO_3)_2S_{org}}$. Acidic extractants such as di-2-ethylhexylphosphoric acid have been very extensively studied together with other chelating phosphorus acids. The extraction of non-solvated ion pairs has assumed considerable importance too.

10.4.2 Extraction of Acido- and Halo-metallic Complexes

Several metals (*e.g.* tervalent iron, gallium, indium and thallium) can be extracted from mineral acids in the form of the conjugate acids of coordination complexes (*e.g.* $\mathrm{H^+Mhal_4}^-$) provided the acidic proton is aquated and also coordinated by a donor organic solvent which is generally an ether, dichlorodiethylether, pentyl acetate, or a water-immiscible ketone such as isobutyl methyl ketone (hexone; MIBK). The percentage extracted varies characteristically with the metal concerned, with the concentration of mineral acid, and with its concentration as illustrated in Figures 5, 6 and 7. Changes in the halogen acid have a profound effect because the position of the equilibrium in the aqueous phase reaction

$$\mathrm{M^{3+} + 4hal^- \rightleftharpoons Mhal_4^-} \tag{17}$$

is critical: thus, for indium, the overall formation constant for the 4:1 species increases in the order F < Cl < Br < I whereas the reverse would be true for the first member of the series (Al) and progressive changes reflect the changing 'hardness' of the cation.[17] Superimposed on this is the increased tendency of the acido complex to partition into the organic phase as the anion $\mathrm{Mhal_4}^-$ becomes bulkier. Obvious analytical separations are tervalent Fe, Ga and Ti from indium in hydrochloric acid, and indium from these elements in hydriodic acid (where $\mathrm{Fe^{III}}$ is reduced to $\mathrm{Fe^{II}}$ and does not extract at all). Another point to note is that the concentration of halogen acid at which maximum extraction occurs decreases in the order HCl > HBr > HI. Change of organic solvent does not greatly improve the separability of different metals in a particular mineral acid.

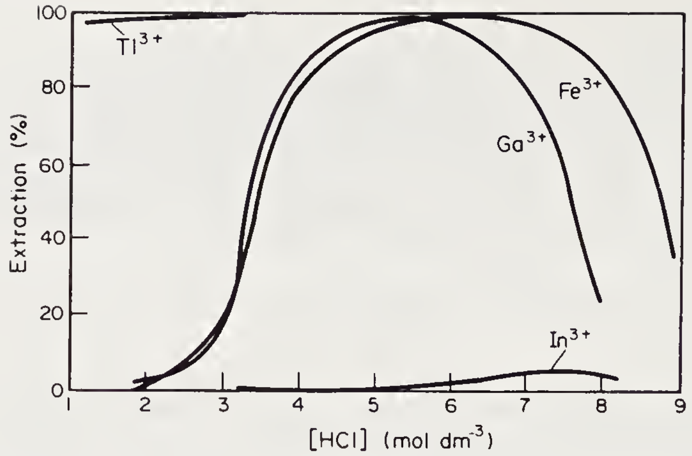

Figure 5 The extraction of some tervalent cations dissolved in hydrochloric acid into an equal volume of diethyl ether

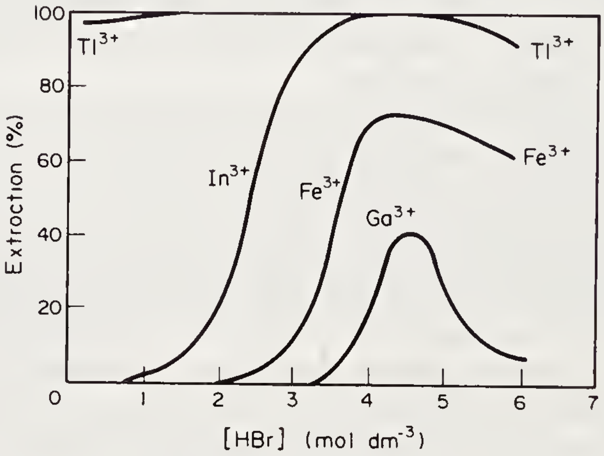

Figure 6 The extraction of some tervalent cations from hydrobromic acid into an equal volume of diethyl ether

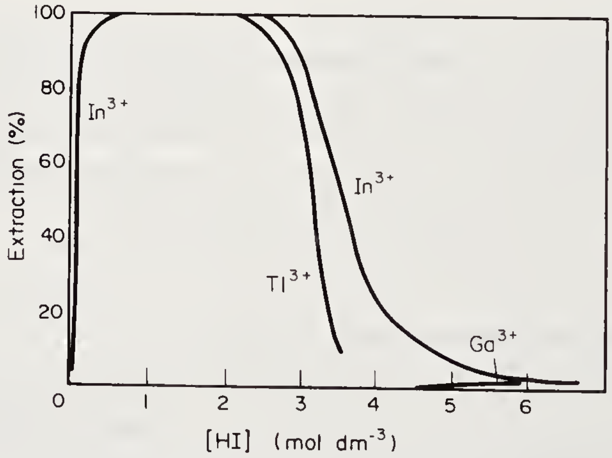

Figure 7 The extraction of some tervalent cations from hydriodic acid into an equal volume of diethyl ether

As might be expected from the quite different types of complexes formed by metals with F^-, extractions from hydrofluoric acid (despite the experimental difficulties and hazards) can lead to useful separations within a quite different set of metals as indicated in Figure 8.

In much the same way extractions from thiocyanic acid and from nitric acid (also comprehensively studied by Bock and his collaborators[41]) lend themselves to numerous analytic separations. Although the basic facts of equilibrium conditions in such systems were worked out many years ago, subsequent research has been largely confined to elucidating the difficult problems of the physical chemistry involved and is less relevant to their analytical application.[37]

10.4.3 Solvated Acids and Salts

The partition of HCl and HNO_3 into oxygen donor solvents almost invariably involves the partition of a solvated species and many salts (notably perchlorates and thiocyanates) extract well into the higher alcohols and ketones. Complex nitrates such as that of Ce^{IV} may extract as

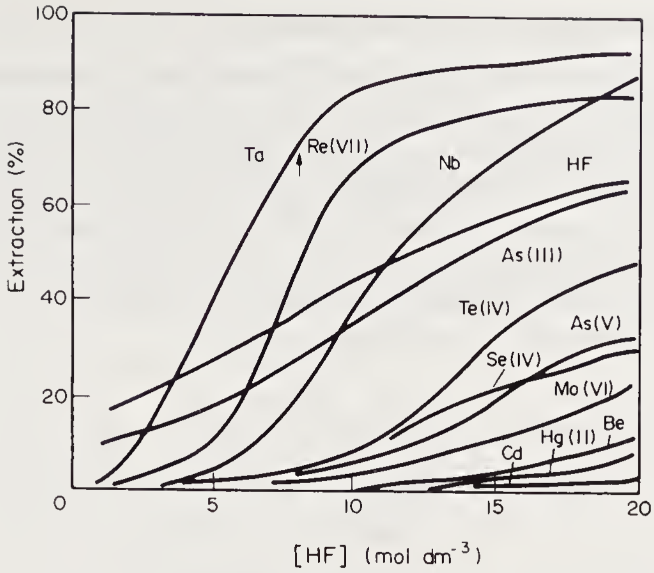

Figure 8 The extraction of various cations from hydrofluoric acid into an equal volume of diethyl ether

$[H(solvated)]_2^+[Ce(NO_3)_6]^{2-}$ or more probably as $[Ce(ether)_2(NO_3)_4]$. Interference by phosphate ions can be eliminated by making the aqueous solution acidic with H_2SO_4 and extracting liberated H_3PO_4 into ether.

10.4.3.1 Extraction of adducts with neutral phosphorus and other ligands

Tributylphosphate (TBP; $(BuO)_3PO$) has become one of the most important analytical reagents for the liquid–liquid extraction of salts, especially nitrates, and there is an extensive literature.[37,38] It has a relatively high dielectric constant (8.0), a high dipole moment (3.0 Debye units), and has a low solubility in water (1.25 mM at 25 °C) but is seldom employed alone but rather when dissolved in a diluent such as hexane or kerosene. TBP readily hydrates to give $TBP{\cdot}H_2O$ and hydrohalic acids Hhal (hal = Cl, Br, I), perchloric acid, and nitric acid extract as species containing TBP with or without water according to the conditions.[37] Chlorides, perchlorates, nitrates of tetravalent elements such as Zr, Hf and Th, of the lanthanides and actinides, of the platinum metals, of cobalt, iron, gold and very many other elements have been exhaustively studied,[37,42] particularly in view of the great interest attaching to the processing of nuclear fuels and the ease with which uranium(VI) is extracted as $UO_2(NO_3)(TBP)_2$ although the solvated trinitratouranyl acid $[H(TBP)_2]^+[UO_2(NO_3)_3]^-$ occurs in highly concentrated nitric acid. In most cases, the nature of the extracted species varies with the conditions, *e.g.* with the kinetically robust complexes of nitrosylruthenium both $Ru(NO)(NO_3)_3(TBP)_3$ and $[H(TBP)_n]_2^+[Ru(NO)(NO)(NO_3)_5]^{2-}$ occur, while rhenium extracts from nitric acid as $H(TBP)_n^+ReO_4^-$ and chromium as $H_2CrO_4{\cdot}3TBP$. The analytical applications have not been summarized and reviewed since 1960 but fresh uses still appear in the literature.

It will be appreciated that if liquid–liquid extraction is used primarily as a means of concentration or separation the actual formula of the extracted species is of little importance. However, for quantitative determinations of extracted material it is essential to set up conditions such that the nature of the extractable species and its distribution coefficient do not vary from sample to sample.

The great range of differences in extracting cations of different type and charge when all other conditions remain the same is illustrated by Figure 9, which applies to the extraction of various nitrates from 1 M nitric acid by a 20% solution of TBP in an inert diluent. Ions of the highest charge show the greatest extractability although oxy cations such as UO_2^{2+} or PuO_2^{2+} extract better than other formally divalent ions. The order $Ca^{2+} > Sr^{2+} > Ba^{2+}$ and $Li^+ > Na^+ > K^+ > Cs^+$ is that of decreasing deforming power.

Figure 9 The extraction of various metal nitrates from 1 M nitric acid by a solution of tributylphosphate (TBP) in an inert diluent (20% v/v)

10.4.3.2 Phosphonates, phosphinates and phosphine oxides

Since the solvating power of TBP originates in the P=O group, compounds in which the basicity of this group has been increased should be still better extractants. If the butyl group of TBP is replaced by chloroalkyl or phenyl groups there is a decrease in extracting power. On the other hand the residual replacement of BuO by Bu leads, as shown in Figure 10, to a progressive improvement in log *D*. Here again the feasibility of separation recurs. What has been shown for uranium(VI) has been demonstrated experimentally for plutonium, neptunium and thorium and probably sets a general pattern. All values of log *D* can be enhanced if salting-out agents like aluminum nitrate are incorporated in the aqueous phase.

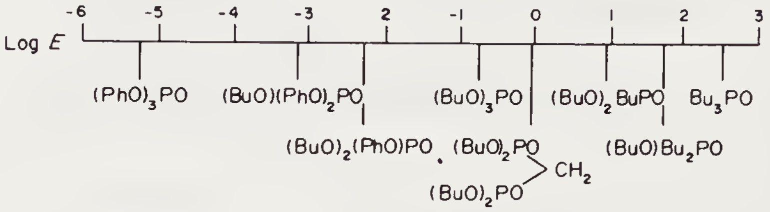

Figure 10 The extraction of uranyl nitrate $UO_2(NO_3)_2$, from 1 M nitric acid by a number of different phosphorus extractants

Tri-*n*-octylphosphine oxide (TOPO) has been the most popular phosphine oxide to be used as an extractant for the determination of iron, uranium, plutonium, molybdenum, titanium and thorium among other metals.[43,44]

Elements that form stronger bonds with sulfur than oxygen are extracted well by trialkyl thiophosphates, and triphenyl phosphite has been used to extract copper(I) into CCl_4 as the trimer $(PhO)_3PCuA_3$ where A = Cl, Br, I or SCN.

10.4.3.3 Phosphorus acids

Round about 1950, values reported by different groups of workers for distribution coefficients of various actinides where TBP was used as an extractant showed considerable discrepancies. These were traced to the presence of hydrolysis products in the samples used and it became obvious that mono- and dibutyl-phosphoric acids are good extractants themselves. A wide range of synthetic dialkylphosphoric acids has been studied but most work has centred on the use of di-2-ethylhexylphosphoric acid HDEHP.[45] These dialkyl acids are normally dimeric: dimerization is strongest in an inert solvent such as hexane but decreases with more strongly hydrogen-bonding solvents and there is the added complication of association with the diluent which is strongest with hexol, but diminishes in the order TBP, diisopropyl ether, chloroform, carbon tetrachloride and hexane.[46,47] The general mechanism for the extraction of metals by a dialkyl phosphate is

$$M^{m+} + m(HX)_2(\text{org}) \longrightarrow M(HX_2)_m(\text{org}) + mH^+ \tag{18}$$

where a formally uncharged coordination compound (**31**) is extracted.[48] HDEHP has proved to be of special importance for the extraction of the trivalent lanthanides and actinides[49] but is also valuable for elements like Be, Zn, Nb, Pa, Mo and of course U^{VI}.[37,38] Monobasic phosphorus acids such as the phosphoric acids, (RO)(R′O)PO(OH), the phosphonic acids (RO)R′PO(OH), and the phosphinic acids RR′PO(OH) are also generally polymeric in organic solvents though quite effective extractants.[37,38] Like the dialkylphosphoric acids their effectiveness would appear to be due to their ability to form very stable chelates with the metal to be extracted combined with their ability to solvate these chelates further. Rates of complexation are quite dependent on reaction conditions and they have been reported on by Coleman and Roddy.[50]

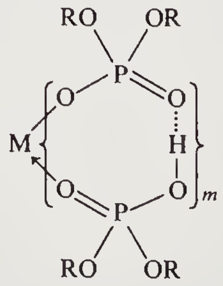

(31)

10.4.4 Formally Neutral Complexes: General Comments

If HL is the conjugate acid of a chelating ligand L^- the reaction with a metal ion proceeds as follows

$$M^{m} + m\text{HL(org)} \rightleftharpoons \text{ML}_m\text{(org)} + m\text{H}^+ \tag{19}$$

and if K_{ex} is the extraction constant

$$K_{ex} = [\text{ML}_m]_{org}[\text{H}^+]^m / [\text{M}^{m+}][\text{HL}]_{org}{}^m \tag{20}$$

It follows that the distribution constant, defined as

$$\begin{aligned} D &= [\text{ML}_m]_{org} / [\text{M}^{m+}]_{aq} \\ &= K_{ex}[\text{HL}]_{org}{}^m / [\text{H}^+]^m \end{aligned}$$

whence

$$\log D = \log K_{ex} + m[\text{HL}]_{org} + m\text{pH} \tag{21}$$

The value of K_{ex} is, of course, fixed for any given cation–extracting agent–solvent system. Analytically important distribution coefficients, D, can be varied by changing the concentration of ligand relative to that of the metal and more significantly by adjusting the pH; for 50% extraction $D = 1$ and equation (21) reduces to

$$0 = \log K_{ex} + m \log [\text{HL}]_{org} + m\text{pH}_{1/2} \tag{22}$$

If $\Delta\text{pH} = (\text{pH}_{1/2} - \text{pH})$ it has been shown[51] that

$$E = 50(1 - \tanh 1.1513\, m\, \Delta\text{pH}) \tag{23}$$

Figure 11 shows such sigmoid curves for a hypothetical system where curve (a) is drawn for complex ML_2 with $[\text{HL}]_{org} = 10^{-3}$ M and $K_{ex} = 10^2$. Curves (b), (c) and (d) are drawn for $[\text{HL}]_{org} = 10^{-5}$ M, $K_{ex} = 10^2$ for complexes ML, ML_2 and ML_3 respectively. Curve (e) represents a complex ML_2 for which $[\text{HL}]_{org} = 10^{-5}$ M but $K_{ex} = 10^{-2}$. The control that can be exercised by change of $[\text{HL}]_{org}$ and pH will be obvious and separations will always be possible if values of K_{ex} for two metals are different, for besides the variables mentioned above auxiliary complexing agents may be included in the aqueous phase to mask one or more of the unwanted cations (Section 10.3). Specific examples will be described for only one particular extractant (dithizone) to illustrate the general principle (Section 10.4.4.5).

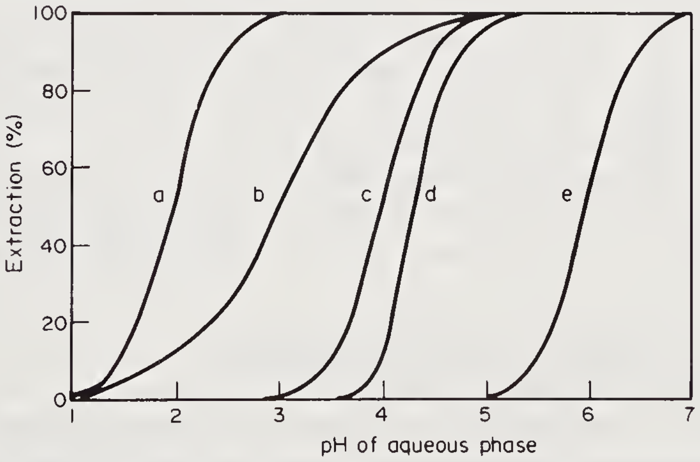

Figure 11 Sigmoid curves illustrating the effect of changing values of the extraction constant, K_{ex}, the concentration of ligand, $[\text{HL}]_{org}$, and the pH on the percentage of the neutral complex ML_m extracted into an equal volume of immiscible solvent. Details in text

Besides their uses in separation and preconcentration many of the extractable metal chelates are coloured and can be used directly for quantitative spectrophotometric determinations.

10.4.4.1 Extraction with 1,3-diketones

Acetylacetone and analogous 1,3-diketones (**32**) have been extensively used as extracting agents: in their enolic form they behave as monobasic acids and give rise to formally neutral complexes with stable five-membered rings. Very often the complexes are coloured and can be used for quantitative determinations by spectrophotometry.

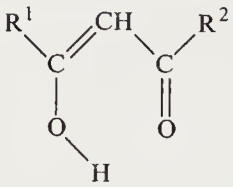

(32)

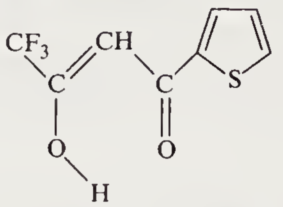

(33)

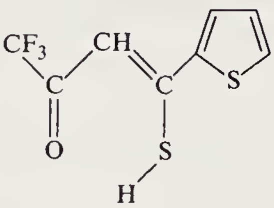

(34)

To meet the problems encountered in the early days of the atomic energy industry it became necessary to find a reagent which could be used to extract metals in high oxidation states which were prone to hydrolysis. Calvin and his collaborators arrived at thenoyltrifluoroacetone (**33**; HTTA) as a more versatile reagent than acetylacetone since in view of the strongly electronegative groups the chelating enol form is a strong acid and its metal complexes can be extracted from solutions of quite low pH. Because of the thiophene moiety, solubility in water is reduced and HTTA partitions well into benzene. The stability constants of its complexes increase with the charge on the metal ion and with increasing atomic number in any column in the Periodic Table. Examples are listed in Starý's book[52] and in reviews.[2,49,53,54] Monothio analogues of acac have been studied in the expectation that they would be more selective for soft metal ions. 1,1,1-Trifluoro-4-(2-thienyl)-4-mercaptobut-3-en-2-one (**34**; STTA) has been found to have certain advantages over dithizone (Section 10.4.4.5) for the coloured complexes with Cd, Co, Cu, Pb, Hg^{II}, Ni, Pd and Zn are more stable and the extraction can be carried out from more acidic solutions.[2] Other newer reagents are selenium analogues of acac and TTA, *viz.* selenoylacetone (**32**; $R^1 = Me$, R^2 = selenophen-2-yl) and 4,4,4-trifluoro-1-(selenophen-2-yl)butane-1,3-dione, recommended as extraction reagents for neodymium.[55]

10.4.4.2 Extractants bonding through two oxygen atoms

Cupferron has already been cited in Section 10.2.5 and gives complexes (**16**) which, though insoluble in water, extract readily into chloroform, benzene, and many other organic solvents.[52] Ease of extraction follows the sequence Fe^{III}, Ga, Sb^{III}, Ti^{IV}, Sn^{IV}, Zr, V^{V}, U^{IV} and Mo^{VI} which can be extracted into chloroform from 2 to 3 M H_2SO_4 > Bi, Cu^{II}, Th > Pb, Zn, Co^{II}, Ni > Mn^{II} > Mg, while Al can only be extracted at pH ~3.5–4.0. Neocupferron shows a number of practical advantages.[52]

Benzoylphenylhydroxylamine (**17**; $R^1 = R^2 = Ph$) forms complexes with V, Sn, Ti and Zr in 5 to 9 M HCl but only that of vanadium is extractable into chloroform, permitting a selective determination of that element in chrome ores. *N*-Cinnamoyl-*N*-phenylhydroxylamine is even more sensitive. In less acid solutions solvent extractable complexes are formed with a number of other cations and, for example, an orange-red complex of uranium(VI) is extracted by *N*-benzoyl-*N*-phenylhydroxylamine into chloroform.[52]

Of the many hydroxamic acids $R^1CONR_2^2(OH)$ (*cf.* Section 10.2.5) which give five-membered chelate rings, that with R^1 = thienyl and R^2 = phenyl or *p*-tolyl are reported to be highly selective extractants for vanadium(V).[52,56] The literature up to 1966 has been reviewed by A. D. Shendrikar.[57]

10.4.4.3 Extractants bonding through two nitrogen atoms

Red coloured complexes of Ni^{II} with dioximes (Section 10.2.6) can be extracted into chloroform, values of the maximum absorption decreasing from furildioxime (**22**; $\lambda_{max} = 435$) ≫ heptoxime (**24**) > DMG (**4**). The sensitivity for nickel is high (~0.1 p.p.m. with nioxime, **23**, R = H) but the specificity is poor since dioximes of copper and other metals can be extracted. Palladium can be determined spectrophotometrically with furildioxime preferred to DMG. An important and prolific group of reagents forming five-membered chelate rings through two nitrogen atoms comprises 2,2′-bipyridyl (bipy) and 1,10-phenanthroline (phen) which form complex cations with a wide variety of metals. Since salts such as $[Fe(phen)_3]Cl_2$ are highly coloured and water soluble it will be more appropriate to discuss this important group in the section on absorptiometry (Section 10.5.2). However, whereas salt formation with long-chain alkyl sulfates or alkane sulfonates (*e.g.* Teepol) is needed to render complexes with bipy and phen extractable into chloroform, the complex of iron(II) with bathophenanthroline (4,7-diphenyl-1,10-phenanthroline) is extracted well by chloroform or pentanol and as little as 0.25 μg of iron can be determined in the presence of $H_2PO_4^-$.[58]

Among numerous Schiff bases that have been studied, *N,N′*-bis(*o*-aminoacetophenone)ethylenediimine (**35**; R = Me) has been used as a photometric extraction agent for palladium ($\varepsilon_{max} = 3700$ at 470 nm after extraction at pH 7.0 into 2-methylbutanol) and the benzophenone analogue (**35**; R = Ph) serves for nickel (pH 8, $\varepsilon_{max} = 8700$ at 496 nm in chloroform).

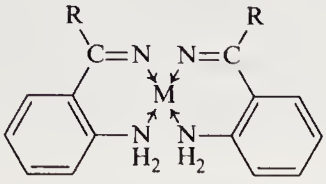

(35)

10.4.4.4 Extractants bonding through nitrogen and oxygen

Since α-nitroso-β-naphthol (**11**; p*K* = 7.70) and β-nitroso-α-naphthol (p*K* 7.22) are weaker acids than nitrosophenylhydroxylamine (**16**; p*K* = 4.15), complex formation and solvent extraction require more alkaline solutions. Tris complexes of Fe^{III} or Co^{III} are formally uncharged octahedral species extractable into light petroleum like the uncharged square planar complex of Pd^{II}. On the other hand the bis complexes of Fe^{III}, Ni^{II} and Co^{II} require two water molecules to complete their coordination sphere and though extractable into diethyl ether are insoluble in the non-polar ligroin.

Oximes of the type $R^1COCr^2{=}NOH$ behave as monobasic acids and form complexes such as (**36**). Those with Fe^{II} as blue and extractable into organic solvents, and coloured complexes with Co^{III}, Ni^{II}, Cu^{II}, Zr, Cd and Hg^{II} are extractable into ether.[18,52]

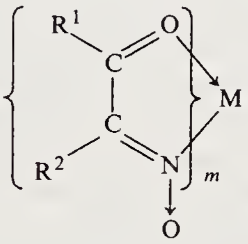

(36)

Virtually all chelate complexes of the type $M(Ox)_m$ derived from the cation M^{m+} are extractable into chloroform and, being coloured, form the basis of spectrophotometric determinations. The extractions can be made more selective by controlling the pH (*cf.* Section 10.2.2.1) and/or by using suitable masking agents. Thus extraction of the yellow aluminum trisoxinate can be made almost specific at pH 8.5–9.0 if EDTA, cyanide ions and sulfite ions (to reduce Fe^{III} to Fe^{II}) are present. Since the range for extraction of individual metal oxinates extends from pH 1.6 to 14, separation of individual species is facilitated.[52,59]

Whereas Co, Ni and Cu^{II} form planar (or tetragonal) complexes with weakly bonded water molecules and are extractable into chloroform, Fe^{II}, Zn and Mg prefer octahedral coordination and the firmly attached water in, for example, $MgOx_2(H_2O)_2$ makes it hydrophilic and incapable of being solvent extracted. However, in the presence of excess oxine it, and other alkaline earth complexes, become soluble in chloroform as the water is displaced by the more hydrophobic oxine molecules. Anhydrous $ZnOx_2$ dissolves easily in chloroform but on equilibration with water $ZnOx_2(H_2O)_2$ separates at the interface.

As previously stated (Section 10.2.2.2) the introduction of halogens into the 5 and 7 positions reduces the solubility in water and the corresponding metal oxinates are extracted at lower pH values.

Owing to steric hindrance (Section 10.2.2.3) the tris complex of aluminum with 2-methyl-8-hydroxyquinoline cannot form in aqueous solution so that this reagent can be used to solvent extract other metals from aluminum, which can then be solvent extracted in its turn and determined with unsubstituted 8-hydroxyquinoline.[24,25,52]

Diphenylcarbazide, PhNHNHCONNHPh, or its dehydro derivative diphenylcarbazone, have long been known to form a water-soluble red-violet complex with chromium(VI) but this can be extracted into organic solvents in the presence of long-chain alkyl sulfates or sufficient acetate, chloride or perchlorate ions.

The introduction of 1-(2-pyridylazo)-2-naphthol (PAN; **37**) as a metallochromic indicator by K. L. Cheng and R. H. Bray in 1955 led to the synthesis of a very large number of heterocyclic arylazo compounds[2,60] all capable of chelating through an *o*-hydroxyazo grouping. Of the dozens of analogues containing thiazole, benzothiazole, imidazole and triazole rings in place of pyridine and the hydroxyl group forming part of a chromotropic acid, phenanthrene, or quinoline moiety several are commended as specially suitable for the determination of particular elements by extractive photometric procedures.[2] Unfortunately the preference seems largely to be subjective and no comprehensive yet critical review exists, although Savvin[61] and Budesinsky[62] have covered part of the literature up to 1968.

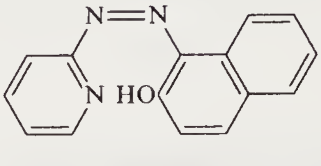

(**37**) PAN

10.4.4.5 Extractants bonding through nitrogen and sulfur

Dalzin (bis(allylthiocarbamido)hydrazine) forms sparingly soluble complexes (**29**) in which it is bonded through sulfur and nitrogen atoms (Section 10.2.7) but the bright orange-red bismuth complex can be extracted into chloroform for a spectrophotometric determination provided cyanide is present to mask copper. 1,4-Diphenylthiosemicarbazide PhNHNC(SH)NHPh can be used for the spectrophotometric determination of ruthenium after extraction of its violet-red complex into chloroform.

The classic reagent for the absorptiometric determination of trace metals is dithizone (3-mercapto-1,5-diphenylformazan, H_2Dz; **26**; Ar = Ph) introduced by Helmuth Fischer in 1925. This forms water insoluble complexes ('primary dithizonates') of stoichiometric composition $M(HDz)_m$ with a number of elements grouped in the centre of the Periodic Table, *viz.* Mn^{II}, Fe^{II}, Co, Ni, Cu^{I} and Cu^{II}, and Zn; Pd, Ag, Cd, In and Sn^{II}; Pt, Au, Hg^{I} and Hg^{II}, Tl^{I}, Pb^{II}, Bi and Po[7,8,40,52] as well as with organometallic cations such as R_3Sn^+, R_2Sn^{2+}, RHg^+, R_2Tl^+, R_3Pb^+ and R_2Pb^{2+} (where R = alkyl or aryl groups).[8] All are readily extracted into chloroform (less so into CCl_4, benzene,...hexane). The conditions for quantitative extraction range from $pK < 0$ for mercury(II) to $pH > 12$ for thallium(I) and since dithizone is a weak acid ($pK_I = 4.5$), separations can be realized by careful control of pH and selectivity achieved by adding masking agents to the aqueous phase (Table 5).[7,40,52] $Te(HDz)_2$ is extracted when Te^{IV} reacts oxidatively with dithizone but details of the course of its reactions with Se^{IV}, Au^{III} and Tl^{III} are still unresolved.[8]

Table 5 Use of Masking Agents in the Extraction of Metal Dithizonates[7,8]

Conditions	*Metals still reacting with dithizone*
(a) Slightly acidic solutions	
(i) Containing cyanide	Ag, Cu, Hg^{II}, Pd^{II}
(ii) pH 5 containing thiosulfate	Cd, Sn^{II}, Zn, (Cd, Co, Ni)
(iii) pH 4–5.5 containing thiosulfate and cyanide	Sn^{II}, Zn
(b) Dilute acidic solutions	
(i) Containing thiocyanate	Au, Cu, Hg
(ii) Contaning thiocyanate and cyanide	Cu, Hg
(iii) Containing bromide or iodide	Au, Cu, Pd
(iv) Containing EDTA	Ag, Hg
(c) Alkaline solutions	
(i) Basic solutions containing cyanide	Bi, Pb, Sn^{II}, Tl^{I}, (In)
(ii) Strongly alkaline solutions containing citrate and tartrate	Ag, Cd, Co, Cu, Ni, Tl
(iii) Slightly alkaline solutions containing bis(2-hydroxyethyl) dithiocarbamate	Zn

X-ray crystallography shows that bonding is through nitrogen and sulfur as shown in (**38**) and (**39**), square planar complexes being formed by Cu^{II}, Ni and Pd, tetrahedral by Zn and Hg, and octahedral by Bi. Indium is unusual in having two dithizone residues chelated normally while the third is effectively monodentate through sulfur in a trigonal bipyramidal arrangement.[63]

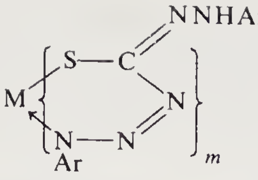

(38)

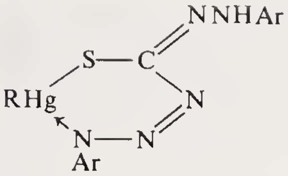

(39)

In addition to the organic-extractable primary complexes dithizone also forms secondary complexes such as Ag_2Dz, $Cu^I{}_2Dz$, HgDz which are very sparingly soluble in organic solvents and of as yet undetermined structure: they are of no value in analysis.[8]

10.4.4.6 Extractants bonding through two sulfur atoms

Toluene-3,4-dithiol (dithiol; **30**) gives complexes with many metals (*e.g.* Bi, Sb^{III}, Co, Cu, Ni and Pb in acid solution; Mn, Fe, Tl, V and Ru in alkaline, aqueous pyridine solution). The yellow-green tris complex with molybdenum can be separated from tungsten(VI) by extraction into pentyl acetate from 3.7 M HCl. The blue-green tungsten complex extracts if the acidity is lowered. Sn^{II} also gives a yellow-red complex.

The great drawback to this reagent is its proneness to oxidation and it is often stored as the zinc complex from which it is released by dissolving in acid or alkali. The analogous quinoxaline-2,3-dithiol has been recommended for the determination of Ni and Co, and 2-mercaptobenzothiazole (**28**) for cadmium through extraction of its complex into chloroform.[52]

The most versatile reagent of this group is diethyldithiocarbamic acid (**40**), which forms coloured and extractable complexes with very many metals, selectivity being assured by control of the pH and the presence of masking agents.[52] Here again the practical disadvantages stem from the ease of oxidation and many alternate carbamic acids derived from pyrrolidine and other dialkylamines have been studied.

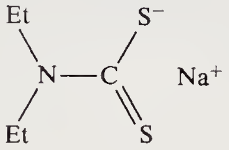

(40)

10.4.5 Synergic Effects in Liquid–Liquid Extraction

Synergism in liquid–liquid extraction refers to the phenomenon where two reagents cooperate in the extraction of a particular species in such a way that the distribution ratio D is greater than that calculated from a simple summation of the effect of each extractant acting alone.[6,64] The classical system of U^{VI} in nitric acid with (HA + B) where HA is HDEHPA and B is a neutral phosphorus extractant such as Bu_3PO, $(BuO)Bu_2PO$, $(BuO)_2BuPO$, and $(BuO)_3PO$ was reported by Baes in 1963 though an earlier example had been noted by Cuninghame, Scargill and Willis in 1954.[65] Irving and Edgington showed that the phenomenon was common to many systems in which the neutral metal complex is coordinatively unsaturated. In addition to the classical example illustrated in Figure 12, synergism was demonstrated among chelate complexes of the actinides, thorium, the lanthanides and even the first row transition metals.[6,49] The second component is not necessarily a phosphorus compound, for amines and sulfoxides also show the phenomenon though to less striking extents. The chemistry of extraction by sulfoxides has recently been reviewed[66] and C. Madic has reviewed examples of synergism involving TTA in combination with other compounds.[67]

The explanation of the synergic effect is not entirely clearcut in every case. Often one component (*e.g.* TBP) acts simply as a Lewis base displacing water from an already coordinatively saturated and extractable species, thereby both making it less hydrophilic and increasing its bulk: sometimes adduction through hydrogen bonding seems to be involved. It is interesting that the weak complex of manganese(II) with dithizone is rendered more stable and extractable by adding pyridine[8] and that the addition of 1,10-phenanthroline greatly increases the rate of extraction of nickel by dithizone to give a blue adduct $Ni(HDz)_2phen$ which forms the basis of a very sensitive extractive–photometric determination.[8]

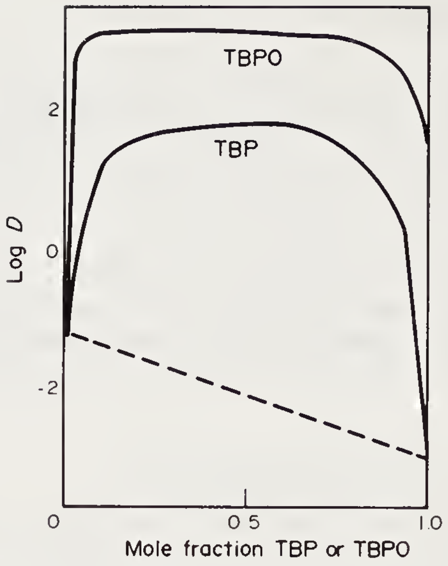

Figure 12 Synergism shown in the distribution of U^{VI} between 0.1 M HNO_3 and mixtures of HTTA and TBP (or TBPO) of constant molarity 0.02 M in cyclohexane. After H. Irving and D. N. Edgington, *Proc. Chem. Soc.*, 1959, 160

10.4.6 Extraction of Heteropolyacids

The determination of phosphorus after precipitation and solvent extraction as molybdophosphoric acid (MPA) and reduction to 'molybdenum blue' is a classical procedure,[30,40] while cerium can be determined directly as molybdocerophosphoric acid (MCPA; ε_{max} 7300 at 318 nm). A more selective method is to strip excess of MPA by extraction with chloroform, then to decompose residual MCPA and determine the phosphate liberated therefrom as MPA after extraction into isobutyl acetate. Alternatively AAS can be used to determine the amount of molybdenum.

Molybdogermanic, molybdoniobic, molybdoarsenic and molybdosilicophosphoric acids and other heteropolyacids have been used in liquid–liquid extraction procedures which also permit the resolution of mixtures.[68] A comprehensive review has been published.[69]

10.4.7 Extraction of Ion-pairs

Large symmetrical ions with a uniformly distributed charge tend to become extractable into organic solvents of relatively large dielectric constants if they form ion association aggregates with similar ions of opposite charge.

Classical papers in this field are those of Tribalat[70] who showed that tetraphenylarsonium or tetraphenylphosphonium cations would extract, *e.g.* perrhenate (but not molybdate) anions into chloroform. About the same time Smith and Page[71] drew attention to the uses of long-chain tertiary amines or quaternary ammonium salts which are nowadays called liquid anion exchangers because they form ion-pairs soluble in organic solvents and can exchange their anions for other anions, and more relevant in the present context, for anionic metal complexes. A wide range of reagents such as Alamine-336 $(C_{8-10}H_{17-21})_3N$, or Aliquat-336 $(C_{8-10}H_{17-21})_3MeN^+Cl^-$, are commercially available. Thus iron can be extracted as $FeCl_4^-$, gold as $AuCl_4^-$, cobalt as $Co(CNS)_4^{2-}$ (in the presence of nickel) and zinc as $Zn(CNS)_4^{2-}$. Most metals including the alkaline earths, lanthanides, divalent Mn, Fe, Co, Ni, Cu, Zn, Cd, Hg, Pb and Pd together with Mn^{III}, Fe^{III}, Cu^{III}, V^{IV} and V^V form anionic complexes with EDTA (and other complexones such as NTA, IMDA, CDTA) which can be extracted into 1,2-dichloroethane by Aliquat-336; this is the basis of procedures for preconcentration, separation (assisted by pH control and the presence of auxiliary complexing agents) and determination as most of the complexes are strongly coloured.[72]

The interaction of metallochromic indicators (Section 10.6.4) with metals has received a lot of attention since the resulting complexes are often solvent extractable. C. Woodward and H. Freiser[73] have examined complexes of metals with sulfonated azo dyes with a view to their extraction by Aliquat-336. Vanadium in sea water can be determined at the 2 p.p.b. level by complexation with PAR (4-(2-pyridylazo)resorcinol) in the presence of CDTA and extracting the anion so formed into Zephiramine (tetradecyldimethylbenzylammonium chloride).[74] The field has been reviewed up to 1971 by Ueno.[2]

As a single example of the use of a long-chain amine in analytical determinations one could cite the separation and determination of U, ^{237}Pu and Np in human urine.

The three nuclides are collected on calcium phosphate, wet oxidized and taken to dryness. The residue is taken up in 10 M HCl and extracted with 10% Alamine-336 chloride in xylene as $(R_3NH)_2UO_2Cl_4$, $(R_3NH)_2PuCl_6$ and $(R_3NH)_2NpO_2Cl_2$. Pu is then stripped at 80 °C with 10 M HCl containing NH_4I, Np at 80 °C with 4 M HCl containing HF, and finally U with 0.1 M HCl.[75]

10.5 ABSORPTIOMETRY

10.5.1 Introduction

Quantitative analytical procedures based on the uses of absorption spectra are generally fast and lend themselves to routine measurements since the necessary skills are simple and easily acquired and there is currently available a wide range of instrumentation at all levels of sophistication.

Clearly the coordination complex must obey the Beer–Lambert Law, $A = \varepsilon cl$, which implies a sufficiently large formation constant unless a large excess of ligand is acceptable. It should absorb preferably in the visible region, or at least well away from the region at which the solvent itself begins to absorb. It must of course exist in true solution. While iron(III) can be determined as its trisoxinate in chloroform, measurements in water would prefer 7-iodo-8-hydroxyquinoline-5-sulfonic acid ('ferron') for the 7-iodo group produces a bathochromic shift while the 5-sulfonic group confers water solubility.

High sensitivity requires a high value for the molecular extinction coefficient. For the 'forbidden' *d–d* transitions, which are responsible for the colours of most transition metal ions, values of ε range from 0.01 to 10 $mol^{-1}\ m^2$; for tetrahedral complexes MX_4^{2-} (M = Co, Cu, Ni; X = Cl, Br, I) that lack a centre of inversion ε_{max} is much larger (20 to 120 $mol^{-1}\ m^2$). It would be inappropriate here to elaborate on charge-transfer and other spectra[18] but it may be useful to recall the relationship $\varepsilon \approx 10^4 Pa$ where P is the transition probability and a the area of the chromophoric group (in cm^2). 'Allowed' transitions, regarded as those for which $\log\varepsilon \geqslant 3$, lead to high intensity absorption but values of ε_{max} rarely exceed $10^4\ mol^{-1}\ m^2$. On the other hand $\log\varepsilon_{max}$ for Rhodamine B chloroantimonate or the zinc complex of 2-naphthylthiocarbazone is round about 4 implying that an absorbance of 0.1 in a 1 cm cell corresponds to a metal content of 0.1 p.p.m. for a metal complex of molar mass 100.

For the most part reagents used in absorptiometric procedures are those containing both chelating and chromophoric groupings which form stable complexes whose favourable absorption characteristics (*i.e.* λ_{max} and ε_{max}) differ as widely as possible from those of the reagent. If the reagent is colourless so much the better, and examples are given later under the reactions of bipy, phenan and analogous substances (Section 10.5.2). Coloured ligands that give rise to coloured complexes are typified by dithizone (Section 10.5.3). Many reagents giving rise to water insoluble complexes can be adapted to procedures in aqueous solution by incorporating solubilizing groups (*e.g.* CO_2H, SO_3H) into the reagent.

10.5.2 Ligands of the 2,2′-Bipyridyl Type

The low-spin tris complexes $Fe(bipy)_3^{2+}$ and $Fe(phen)_3^{2+}$ owe their stability to the possiblity of electron delocalization from the t_{2g} orbital of the iron to the π orbital of the ligand and they have long been used for its spectrophotometric determination (l_{max} = 870 and 1100 $mol^{-1}\ m^2$). Whereas the Irving–Williams stability order[11] Mn < Fe < Co < Ni < Cu < Zn > Cd is followed for 1:1 and 1:2 complexes of bipy, phenan, and 5-methylphenan and by 1:1, 1:2 and 1:3 complexes of 2-methylphenan (save that Cu^{II} only forms a 1:2 complex), the change from high- to low-spin configuration in the case of iron with phenan and bipy when the third ligand is coordinated leads to a very stable diamagnetic complex and the 'anomalous' order Mn < Co < Cu < Ni < Fe > Zn > Cd.[78] Models show that substituents adjacent to the nitrogen atoms inhibit sterically the formation of octahedral complexes of the divalent transition metal ions but not that of the tetrahedral (sp^3) complex of copper(I). Figures 2 and 3 illustrate this point. So whereas 'neocuproine' (2,9-dimethyl-1,10-phenanthroline; **41**; X = Me, Y = H) forms a purple complex ion $Cu(2,9\text{-}Me_2phen)_2^+X^-$ extractable into isopentyl alcohol, this reagent does not react with iron(II), so enabling copper to be determined in its presence. A favoured alternative is to use 'cuproine' (2,2′-biquinolyl; **42**; Y = H) in which steric hindrance to coordination in octahedral complexes is caused by fusing on to bipy aromatic rings across positions 5 and 6 (and 5′,6′). If the extra rings are at positions 4,5 (and 4′,5′), the resulting bi-isoquinolyl forms complexes with both Fe^{II} and Cu^{I}. If fused at 3,4 (and 3′,4′), complexes can still result from coordination uninhibited by steric factors: but now interference between the aromatic rings remote from the metal atom (or strictly between the hydrogen atoms 3,3′) prevent coplanarity of the entire resonance structure and the value of ε_{max} is reduced considerably.

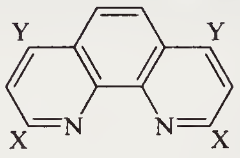

(41)

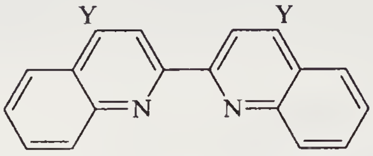

(42)

If phenyl groups are introduced into positions 4 and 7 of phen (bathophenanthroline; **41**; X = H, Y = Ph) the sensitivity is roughly doubled (ε_{max} = 2200 mol m^{-2} for Fe^{II}). So too ε_{max} increases from 541 to 902 in the case of 4,4′-diphenyl-2,2′-biquinolyl (**42**; Y = Ph). Introducing 4- and 7-phenyl groups into cuproin produces bathocuproine (**41**; X = Me, Y = Ph) for which ε_{max} = 1420 mol m^{-2} at λ_{max} = 479 nm and Cl^-, ClO_4^-, NO_3^-, PO_4^{3-}, SO_4^{2-}, *etc.* do not interfere in the determination of copper in the presence of iron.[79]

Dozens of compounds with the so-called ferroin-specific grouping N=C—C=N incorporated in pyridine, quinoline, benzimidazole, benzoxazole, *etc.* have been investigated and the most sensitive reagents for iron(II) are 2,4,6-tripyridyl derivatives of 1,3,5-triazine (**43**), the complexes of which have values of ε_{max} = 2260 (R = H), 2440 (R = Et) and 2520 mol m^{-2}(R = Ph). The whole field has been exhaustively reviewed.[79,80]

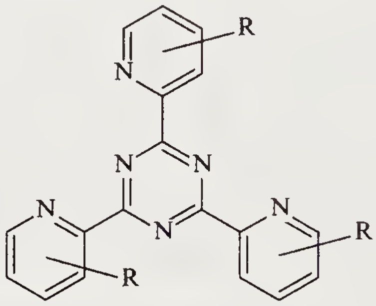

(43)

10.5.3 Dithizonates

When a metal complex $M(HDz)_n$ is extracted into an organic solvent (say CCl_4) together with an excess of reagent dithizone, a ‘mixed colour’ results. The system may be reduced to a ‘monocolour’ system if the metal complex is sufficiently stable to remain unaffected while excess dithizone is ‘stripped’ into the aqueous phase as yellow dithizonate ion by equilibrating the mixed organic phase with dilute ammonium hydroxide.[7,8] Most metal dithizonates have a single peak at λ_{max} 463–530 nm and scarcely absorb at 640 nm where that of the reagent is greatest: in any case from the measured absorbance of any excess reagent at 640 nm that at λ_{max} for the metal complex can readily be calculated and subtracted from the experimentally observed absorbancy. The general method would be to measure the absorbance of the ‘mixed colour’ at two wavelengths λ_1 and λ_2 chosen so that differences in molecular extinction coefficients between reagent and complex are maximal. Since $A_1 = C_d\varepsilon_{d,1} + C_C\varepsilon_{C,1}$ at λ_1 with a similar equation for A_2 at λ_2, determination of C_d = $[H_2Dz]$ follows readily to give C_C the concentration of complex. The method can be generalized and Henderson and Snyder analyzed mixtures of $Pb(HDz)_2$ (red, λ_{max} 520), $Et_2Pb(HDz)_2$ (orange, λ_{max} 487) and $Et_3Pb(HDz)$ (yellow, λ_{max} 435) from measurements at 424, 500 and 540 nm. The reversion method can also be used in appropriate cases.[8]

10.5.4 Summary of Absorptiometric Determinations

Strictly specific procedures are unknown and interferences must be minimized by control of conditions (pH, addition of masking agents) according to the nature of the matrix.

Table 6 merely lists reagents such as xylenol orange (**44**) and arsenazo(III) (**45**) which are often used absorptiometrically, and morin (**46**) used also in fluorimetric procedures, together with other reagents for the commoner metals. It would be pointless to give practical details of procedures which can be found in standard text books[3,7,22,30,33] or specialist publications.[76,77] IUPAC have published absorptiometric data on compounds used for the colorimetric determination of elements.[81]

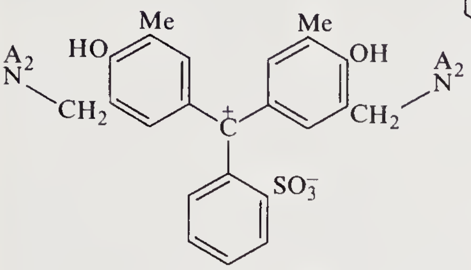

(**44**) A = $—CH_2CO_2H$

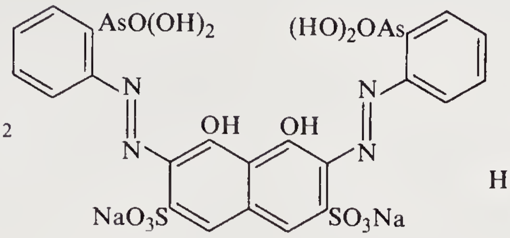

(**45**)

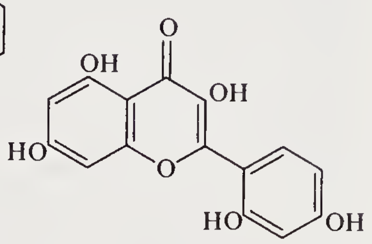

(**46**)

Table 6 Absorptiometric and Fluorimetric Determination of Metals through Coordination Complexes

Element	*Reagent used*
Al	Aluminon,[a] haematoxylin,[a] eriochiome cyanine B,[a] alizarin S,[a] quinalizarin,[a] oxine,[b] morin,[c] pontachrome blue black R[c]
Sb	Rhodamine B,[b] malachite green,[b] AgDDC
As	AgDDC, dithiol
Ba	Sulphonazo III
Be	Acac,[b] morin,[c] aluminon,[a] thorin
Bi	Dithizone,[b] XO, HQBA,[b] oxine,[b] NaDDC[b]
B	Carminic acid, curcumin, dianthrimide
Cd	Dithizone
Ca	GBHA, oxine,[b] murexide
Ce	Oxine,[b] TTA[b]
Cr	Diphenylcarbazide, CTA, TTA[b]
Co	1-Nitroso-2-naphthol,[b] 2-Nitroso-1-naphthol,[b] nitroso-R salt, 5-Cl-PADAB, NaDDC,[b] PAN[b]
Cu	Dithizone,[b] oxalic acid bis(cyclohexylidene) hydrazide, cuproine,[b] neocuproine,[b] bathocuproine,[b] bathocuproinedisulfonate, NaDDC,[b] NH_2Et_2DDC,[b] HQBA,[b] oxine[b]
Ga	Aluminon, morin,[c] rhodamine B,[c] XO
Ge	Phenylfluorone[a]
Au	Rhodamine,[b] rhodamine B,[b] dithizone[b]
Hf	Arsenazo III, quercitin[c]
In	Dithizone,[b] oxine,[b] morin[c]
Fe	Bathophen,[b] bathophen sulfonic acid, TPT,[b] bipy, phen, variamine blue
Li	Oxine[c]
Pb	Dithizone,[b] NaDDC,[b] PAR
Mg	Eriochrome black T, oxine,[b] xylidyl blue, HQBA,[b] quinalizarin[a]
Mn	Formaldoxime, NaDDC,[b] triethanolamine
Hg	Dithizone,[b] TMK, TAM,[b] diphenylcarbazide
Mo	Dithiol,[b] chloranilic acid, quercitin,[b] tiron
Ni	DMG, furildioxime,[b] NaDDC,[b] oxine,[b]
Nb	PAR
Os	Diphenylcarbazide[b]
Pd	Bismuthiol I, nitrosonaphthol,[b] TMK,[b] dithizone,[b] furildioxime[b]
Pt	Dithizone,[b]
Rare earths	Arsenazo III, alizarin S, oxine
Re	Furildioxime
Rh	PAN,[b] NaDDC
Ru	Diphenylurea, TPT
Sc	Alizarin S
Ag	Dithizone,[b] rhodamine
Ta	Phenylfluorone, pyrogallol
Te	NaDDC
Th	Brilliant green,[b] rhodamine B,[b] dithizone,[b] NaDDC[b]
Th	Arsenazo III, thorin
Sn	Dithiol, phenylfluorone, pyridylfluorone, morin[c]
Ti	Tiron, oxine
W	Dithiol[b]
U	GBHA, PAN,[b] 2-(5-bromo-2-pyridylazo)-5-(diethylamine)phenol,[b] TTA,[b] thorin
V	*N*-Benzoyl-*N*-phenylhydroxylamine, variamine blue, vanadox, PAN,[b] PAR,[b] TTA[b]
Yt	Arsenazo III, alizarin S[b]
Zn	Dithizone,[b] zincon, HQBA,[b] NaDDC[b]
Zr	XO, arsenazo III, PV, phenylfluorone

---

[a] Lake formation or stabilized colloid.
[b] Solvent extraction precedes absorptiometry.

(continued)

[c] Fluorescence reaction. Abbreviations (supplementary to those of Table 3 or given in text): Acac (**32**); AgDDC (**40**); alizarin S, 1,2-dihydroxyanthraquinone-3-sulfonic acid, sodium salt; aluminon, ammonium aurintricarboxylic acid; arsenazo III, 1-(2-arsonophenylazo)-2-hydroxy-3,6-naphthalenedisulfonic acid, sodium salt (**45**); bismuthiol I, 2,4-dimercapto-1,3,4-thiadiazole, dipotassium salt; bathocuproine (**41**, X = Me, Y = Ph); CTA, chromotropic acid, 4,5-dihydroxy-2,7-naphthalenedisulfonic acid; chloranilic acid (**20**); 5-Cl-PADAB, 4-(5-chloro-2-pyridylazo)-*m*-phenylene diamine; cuproine, 2,2′-biquinolyl (**42**); dianthrimide, 1,1′-dianthraquinonyl amine; dithiol (**30**); dithizone (**26**) *cf.*(**38**,**39**); eriochrome black T (52); eriochrome cyanine R (**55**); furildioxime (**22**); GBHA, glyoxal bis(2-hydroxyanil); HQBA, methyl *N*-[α-(8-hydroxy-7-quinolyl)benzyl]anthranilate; malachite green, bis(dimethylaminophenyl)phenylmethane salt; morin (**46**); murexide (**50**); NaDDC (**40**); neocuproine (**42**, X = Me, Y = H); nitrosonaphthol (**11**); nitroso-R salt, 2-hydroxy-1-nitroso-3,6-naphthalene disulfonic acid, disodium salt; oxine (**7**); PAN (**37**); PAR, 4-(2-pyridylazo)resorcinol monosodium salt; phenylfluorone, 2,6,7-trihydroxy-9-phenyl-3*H*-xanthen-3-one; 3-pyridylfluorone (as preceding with 3-pyridyl in the 9-position); pontachrome blue black R, 1-(2′-hydroxynaphthylazo)-2-hydroxynapthalene-4-sulfonic acid, sodium or zinc salt; PV, pyrocatechol violet (**54**); quercitin, 3,5,7,3′,4′-pentahydroxyflavone; quinalizarin, 1,2,5,8-tetrahydroxyanthraquinone; rhodanine, 5-(4-dimethylaminobenzylidene) rhodanine; rhodamine B, tetraethylrhodamine; sulfonazo III, 2,7-di-(2′-sulfophenylazo)-1,8-dihydroxynaphthalene-3,6-disulfonic acid; thorin, see arsenazo III; TMK, thio-Michler's ketone, 4,4′-bis(dimethylamino)thiobenzophenone; TAM, 4-methoxy-2-(2-thiazolylazo)phenol; TPT, 2,4,6-tri(2-pyridyl)-1,3,5-triazine (**43**); TTA (**33**); variamine blue, 4-amino-4′-methoxydiphenylammonium chloride; vanadox, 2,2′-dicarboxydiphenylamine; XO, xylenol orange (**44**); zincon, 2-{[α-(2-hydroxy-3-sulfophenylazo)benzylidene]-hydrazino}benzoic acid, monosodium salt (**57**).

10.5.5 Mixed Complexes

It has already been noted (Section 10.4.5) that the addition of phen to nickel dithizonate (ε_{max} = 3400 mol m^{-2}) gives a more intensely coloured blue complex, $Ni(HDz)_2phen$ (ε_{max} = 4900). Very many such mixed complexes have been introduced into analytical practice[79] and the literature has been surveyed by Babko[82] and Ueno[2]: there have been several attempts to place the subject on a sound theoretical basis.[79] Some typical examples are shown in Table 7.

Table 7 Typical Examples of Mixed Complexes

Element	*In aqueous media*[b]	*After solvent extraction*[b]
Ag	$[Ag(BPR)(phen)_2]$	—
Cd	$[Cd(BPR)_x(phen)_y]$	—
M = Cd, Co, Cu^{II}, Mn, Pb, Zn	—	$[M(RBE)(phen)_2]$
Cu^{I} [a]	—	$[\{Cu^{I}(phen)_2\}_2(RBE)]$
Fe^{III}	$[Fe(oxine)_3py]$	—
Ga	—	$[Ga(XO)(oxine)_2]$
Halides and CN^-	$[Hg^{II}(MTB)X]^{5-}$	—
Lanthanides	$[Ln(salf)_2(phen)]$	$[Ln(TTA)_2(OH)(DHC)]$, $[Ln(sal)_2(phen)_2][Hsal]$
Ni	$[NiLa(ALC)_2]^{n-}$	$[Ni(HDz)_2(phen)]$

[a] Fluorescence measurement.

[b] Abbreviation as in Table 6 with BPR = bromopyrogallol red; RBE = rose bengal extra, tetrachlorotetraiodofluorescein; MTB = methylthymol blue; salf = salicylfluorenone; DHC = dihydroxychromenol; Hsal = salicylic acid; ALC = alizarin complexan.

10.5.6 Spot Tests

The precipitation (Section 10.2) and extraction (Section 10.4) of coordination compounds under controlled conditions and their optical characteristics (Section 10.5) have been exploited, together with a miscellany of other procedures, for detecting selectively small traces of elements in very small volumes of a test sample. Such 'spot reactions' have been painstakingly collected, refined and recorded by Fritz Feigl.[83]

10.6 TITRIMETRIC ANALYSIS

10.6.1 Basic Considerations

There are several minimum requirements for a successful titration: (a) the reaction taking place must proceed quantitatively according to a particular stoichiometric equation; (b) the reaction must be sufficiently rapid; (c) there must be a satisfactory way of locating the equivalence point; and (d) it must be possible to prepare (and maintain) a standard solution of the titrant of precisely known concentration, although this restriction is overcome in other ways in the practice of coulometric titrations. Clearly condition (a) implies that the titrant must not enter into any side reactions and that no extraneous material is present that could alter the stoichiometry of the desired titration reaction.

Although coordination compounds have sometimes been used as titrants, *e.g.* ferrocyanide ions for the titration of zinc(II), and permanganate or dichromate ions in redox titrations, probably the only outstanding reaction in classical titrimetry that involves the reversible formation of a coordination compound is the Liebig–Deniges reaction.

$$Ag^+ + 2CN^- \rightleftharpoons Ag(CN)_2^- \tag{24}$$

with its extension to Ni and Co^{II}.[84]

10.6.2 Titrations with Polyamines

If ammonia is added to a solution of copper(II), a blue colour develops and equilibrium is rapidly established between up to six cations of formula $Cu(NH_3)_n^{2+}$. The average formula can be written as $Cu(NH_3)_{\bar{n}}^{2+}$ where $\bar{n}$, the degree of formation, is a function of $\log[NH_3]$. Generalizing, the effect of mixing concentrations C_M and C_L of metal and ligand is to produce a mixture of average composition $ML_{\bar{n}}$ where

$$\bar{n} = (C_L - [L]) \Big/ C_M = \sum_0^n n\beta_n[L]^n \Big/ \sum_0^n \beta_n[L]^n \tag{25}$$

The plot of $\bar{n}$ against $p(NH_3)$ for the titration of Ni^{2+} is not a smooth curve, showing that the complexation reaction procedes in discrete steps. Even when six equivalents of ammonia have been added, $\bar{n}$ has only reached 2.89 and at that stage only 0.13% of a solution initially 0.01 M in Ni^{2+} is in the form $Ni(NH_3)_6^{2+}$: the stoichiometric end-point is far from being reached. Thanks to the greater stability of the complexes $Nien^{2+}$, $Nien_2^{2+}$ and $Nien_3^{2+}$ (arising from the 'chelate effect') a corresponding titration of 0.01 Ni^{2+} with ethylenediamine gives $\bar{n} = 2.94$ when $C_{en} = 3C_{Ni}$ and 93.8% is present as the tris complex. Only a slight excess of titrant causes virtually complete complexation. With a terdentate ligand such as diethylenetriamine ($NH_2CH_2CH_2NHCH_2CH_2NH_2$; 'dien') still higher stability constants are involved and the complexation reaction to $Ni(dien)_2^{2+}$ is virtually complete when only two equivalents have been added.

However the reagent of choice is pentaethylenehexamine ($(H_2NCH_2CH_2)_2NCH_2CH_2N(CH_2CH_2NH_2)_2$; 'penten') where coordination of a single molecule produces a 1:1 complex (**47**) containing no less than five chelate rings: since $\log K_{Nipenten} = 19.3$, the addition of just one equivalent is 100% effective. Titration can be carried out with other elements that show a preference for coordination through donor nitrogen atoms, *viz.* Cd (16.8), Co (15.8), Cu (22.4), Hg (>22), Ni (19.3) and Zn (16.2), where the decadic logarithms of the respective formation constants are shown in brackets.

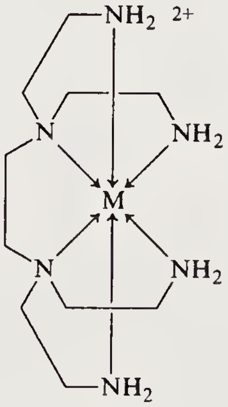

(47)

But even here there is a snag, for the very basic titrating agent is able to take up protons competitively and, since it exists in solution predominantly as $H_4penten^{4+}$, the effective reaction is

$$H_4penten^{4+} + Ni^{2+} \rightleftharpoons Ni(penten)^{2+} + 4H^+ \tag{26}$$

with an effective or conditional constant of 4.9×10^9.

Nevertheless conditions have been worked out for using polyamines as relatively selective titrants.[4]

10.6.3 Complexones

Complexing agents that are less selective but nevertheless capable of forming strong metal complexes with both cations that prefer to bond to oxygen and those that prefer nitrogen donors are illustrated by nitrilotriacetic acid ($N(CH_2CO_2H)_3$; NTA), iminodiacetic acid and ethylenediaminetetraacetic acid (**48**; EDTA). Although many analogues of these complexones have been synthesized and sometimes found to give even more stable complexes,[85] only EDTA (**48**; H_4Y) in the form of its commercially available disodium salt $Na_2H_2Y{\cdot}2H_2O$, and *trans*-cyclohexanediaminetetraacetic acid (**49**) are widely used in practice. The anionic complexes are always formed in the molar ratio 1 : 1 and the ligand is generally sexidentate but sometimes water enters the coordination sphere as in $[MgY(H_2O)]^{2-}$, $[FeY(H_2O)]^-$, $[LnY(H_2O)_{2\,\mathrm{or}\,3}]^-$ or $[Cr^{III}(H_2O)Y]^-$ in which the ligand is pentadentate with an uncoordinated carboxyl group. Details of this class of compounds appear in Chapter 20.3.

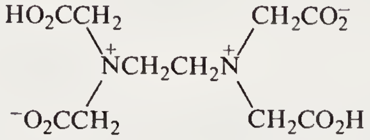

(48)

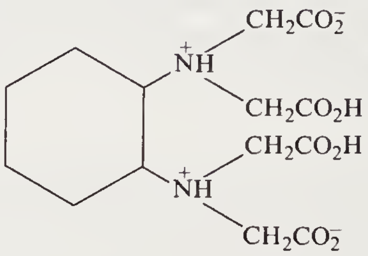

(49)

As shown in Table 8 the stability of metal complexes of EDTA increases as the charge on the cation M^{m+} increases and it is greater for transition metals than for the alkaline earths. If an element exists in more than one valency state, that in the higher oxidation state forms the more stable complex. The position of equilibrium in the reaction

$$M^{m+} + H_2Y^{2-} \rightleftharpoons MY^{(m-4)} + 2H^+ \tag{27}$$

can always be made to go effectively completely to the right by using an appropriate buffer and the equivalence point will then be marked by an abrupt increase in pM.

Table 8 Formation Constants of Metal Complexes of EDTA[a]

Metal	$\log K_{MY}$	*Metal*	$\log K_{MY}$	*Metal*	$\log K_{MY}$	*Metal*	$\log K_{MY}$	*Metal*	$\log K_{MY}$
Ag	7.3	Be	~9	Mn	13.8	Al	16.1	Zn	29.5
Tl^I	5.3	Mg	8.7	Fe^{II}	14.3	Sc	23.1	Hf	~19
		Ca	10.7	Co^{II}	16.3	Y	18.1	Ce^{IV}	24.2
		Sr	8.6	Ni	18.6	La	15.5		
		Ba	7.8	Cu^{II}	18.8	Ce	15.9		
		Ra	7.1			Lu	19.8		
				Zn	16.5	Ga	20.3		
		Sn^{II}	22	Cd	16.5	In	24.9		
		Pb^{II}	18.0	Hg^{II}	21.8	Tl^{III}	21.5	Pu^{III}	18.1
						Bi^{III}	27.9	Am^{III}	18.2
				Changes in oxidation state					
		Tl^I	5.3	Fe^{II}	14.3	Eu^{II}	7.7	Ce^{III}	15.9
		Tl^{III}	21.9	Fe^{III}	25.1	Eu^{III}	17.0	Ce^{IV}	24.2
		V^{2+II}	12.7	VO_2^{+V}	15.6	TiO^{2+IV}	17.3	UO_2^{2+VI}	~10
		V^{3+III}	18.8	VO^{2+IV}	18.8	Ti^{3+III}	21.3	U^{4+IV}	25.5

[a] Values of $\log K_{MY}$ at 20 °C and I = 0.1 M.

10.6.4 Metallochromic Indicators

Although changes in pM can readily be followed by physical means (*e.g.* potentiometrically), following colour changes associated with the formation and dissociation of metal coordination complexes visually or spectrophotometrically is a more versatile and convenient procedure. The serendipitous discovery of so-called metallochromic indicators made by G. Schwarzenbach (1945) led immediately to the introduction of murexide (**50**) as an indicator in calcium titrations and initiated the search for indicators for other metal–EDTA systems. It will be realized that the chosen metal indicator must be considerably less stable than the metal–EDTA complex, but not so weak as to dissociate appreciably in the vicinity of the end-point when the concentration of free metal ions becomes very small. Further conditions are that the formation of the metal–indicator complex (MIn) should be reversible, that the indicator and its metal complex should be soluble in water and ideally that the combination should be specific or at least selective under the conditions of the titration.[4,87,88]

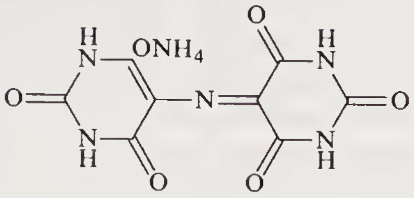

(50)

10.6.4.1 *Murexide*

Murexide is the ammonium salt of purpuric acid (**50**) and the red-violet anion H_4In^- can lose protons or combine with Ca^{2+} as shown in Figure 13 which indicates how pCa at that point where there is a marked colour change varies with pH. By working in a solution ~0.1 M with respect to NaOH the end-point is marked by a sharp colour change from red to blue. In this strongly alkaline solution $Mg(OH)_2$ is so sparingly soluble as not to interfere, thus affording a method for determining Ca alone in hard water. The indicator–metal complex presumably has the structure shown in (**51**) with two chelate rings. The colour change ('pink' to 'red-violet') can be improved by adding a screening dye as an inner filter but it is not very satisfactory, unlike the excellent change from yellow to violet in the titration of nickel in strongly ammoniacal solution.[8,86]

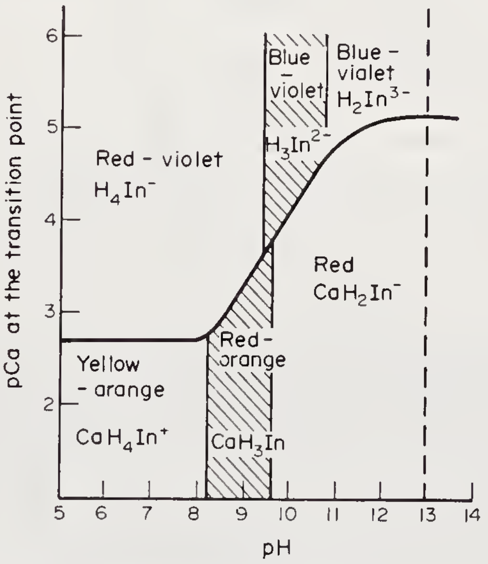

Figure 13 Colour changes in the titration of Ca^{2+} with EDTA using murexide as indicator. The effect of pH on pCa at the colour transition point

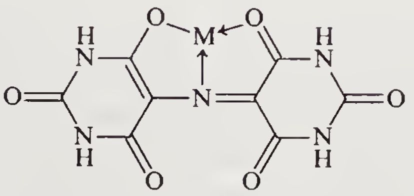

(51)

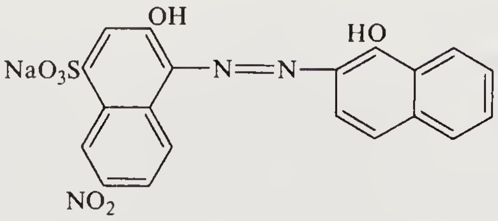

(52)

10.6.4.2 *Hydroxyazo dyestuffs*

The first indicator in this group was proposed by Schwarzenbach and Biedermann in 1948. This was eriochrome black T (solochrome black T, erio T, **52**) which behaves as an acid–base indicator with changes from H_2In^- (red) to HIn^{2-} (blue) to In^{3-} (orange) at pH 6.5 and 11.5, respectively. However in a buffer of pH ~ 10 erio T forms a wine-red 1:1 complex with cadmium, calcium, magnesium, manganese and zinc; the colour change is well marked at as low as 10^{-6} to 10^{-7} M Mg^{2+}. Erio T cannot be used for the direct titration of Al, Co, Cu or Ni because it is 'blocked' by these ions, *i.e.* kinetically stable complexes are formed which do not react sufficiently rapidly with EDTA.

More than 50 such dyestuffs have been proposed as indicators,[8] but they have in common at least one *o*-hydroxy group from which the titratable metal displaces a hydrogen atom and forms a five-membered chelate ring with the azo nitrogens (*cf.* **51**): most have two *o*-hydroxy groups and can form two chelate rings. Of the few that are still used calcon (eriochrome blue black R; 1-(2′-hydroxynaphthylazo)-2-naphthol-4-sulfonic acid, sodium salt) can be used to determine 10^{-2} M Ca in the presence of an equal concentration of Mg. Cal-red (Patton–Reader's indicator, 2-hydroxy-1-(2-hydroxy-4-sulfo-1-naphthylazo)-3-naphthoic acid) resembles erio T, but calmagite (1-(2-hydroxy-3-methyl-1-phenylazo)-2-naphthol-4-sulfonic acid) has the virtue of being more stable in aqueous solution. Acid alizarin black SN (1-hydroxy-2-(2-hydroxy-6-sulfo-1-naphthylazo)-6-(2-hydroxy-1-naphthylazo)benzene-4-sulfonic acid, sodium salt) has been used for the titration of Ca, Cd, Mn, Sr and Zn in alkaline medium and of Th in an acetate buffer. Since it has two coordinating centres, a considerable variety of metal complexes may be formed.[87]

Calcichrome IREA produced by self-coupling of diazotized H-acid has been assigned a cage structure (**53**) by Close and West (1960) and an open-chain structure with an entirely different molecular formula by Lukin, Zavarikhina and Syslev (1957). Whatever the actual structure may be, this complexing ligand forms red chelates with barium, cadmium, calcium, lanthanum, magnesium and zinc at pH 11.5 and with calcium only at pH 13, detecting as little as 0.25 p.p.m.[87]

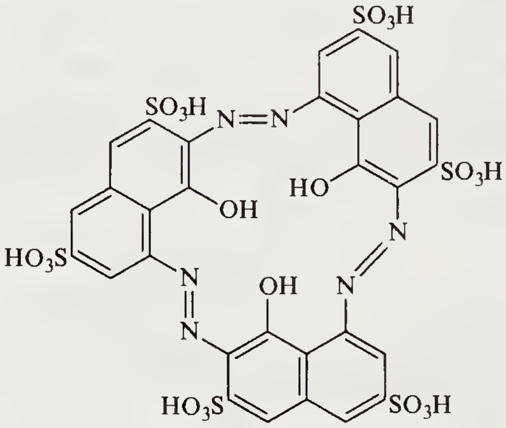

(**53**)

PAN (**37**) has already been mentioned (Section 10.4.4.4), but owing to the sparing solubility of its chelates very slow titration at an elevated temperature and the addition of 25–50% of organic solvent is recommended. A superior indicator is PAR (4-(2-pyridylazo)resorcinol) where the second carboxyl group produces increased solubility of the reagent and its metal complexes. It is one of the best reagents for titrating metals at pH 5–7 using a hexamine buffer. Bismuth can even be titrated selectively at pH 1. Again many analogues (*e.g.* derivatives of thiazole) have been synthesized but have shown little positive advantage over PAR.

10.6.4.3 Triphenylmethane dyestuffs

The most important metallochromic indicators are probably those derived from familiar acid–base indicators of the phenolphthalein or sulfonphthalein series. Although themselves unable to form chelate complexes, this facility can be incorporated by introducing a grouping such as $-OH$, $-CO_2H$, $-CH_2NHCH_2CO_2H$ or $-CH_2N(CH_2CO_2H)$ *ortho* to the phenol group.

Pyrocatechol violet (**54**; PV) is soluble in water forming a yellow solution of H_3In^- and forms intensely blue chelate complexes through the two adjacent phenolic OH groups with bismuth, copper and thorium (red colour) and is a good compleximetric indicator for acidic media. Al, Fe, In and Ti can be determined in back-titrations. Pyrogallol red differs in structure by an oxygen atom bridging the two catechol residues. Bromopyrogallol red (with bromine atoms *ortho* to the OH and :O group) can be used for the titration of Bi in acidic solution, lanthanons in ammonium acetate, and Cd, Co, Mg and Ni in an ammoniacal medium. Eriochrome cyanine R (**55**) which can form a six-membered metal chelate, *viz.* through adjoining OH and CO_2H groups, has been suggested for the determination of zirconium (back-titration), but chrome azurol S (2,6-dichloro-3′,3″-dimethyl-3-sulfofuchsondicarboxylic acid, trisodium salt), which is identical with (**55**) in respect of the chelating groupings, has been used for the determination of alkaline earths, aluminum, cerium, copper, iron(III), nickel, thorium and zirconium.[87]

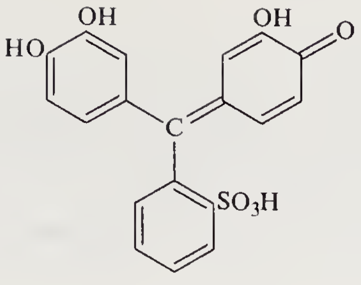

(54)

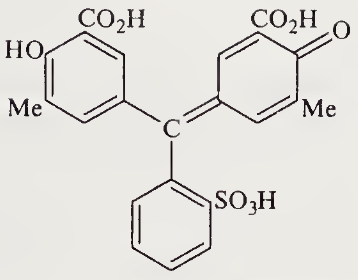

(55)

The most valuable class of metallochromic indicators comprises those containing one or two chelating groups —$CH_2N(CH_2CO_2H)$; they are synthesized from phthalein or sulfonphthalein acid–base indicators by carrying out a Mannich reaction with formaldehyde and iminodiacetic acid. The first 'metal-phthalein' was prepared by Schwarzenbach *et al.* from *o*-cresolphthalein in 1954 and named cresolphthalexone or phthalein purple (**56**). In ammoniacal solution it gives the pink ion H_2In^{4-} and this reacts with Ca, Sr or Ba to give intensely violet chelate complexes. Most heavy metals do not form coloured complexes although Mn and Cd block this indicator.

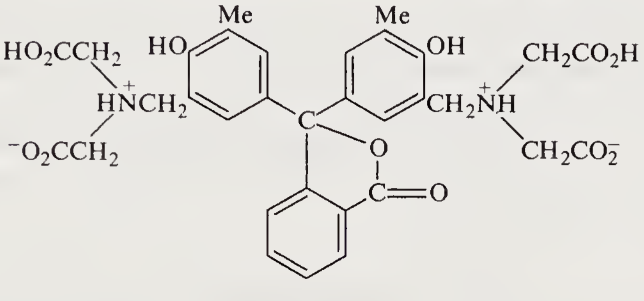

(56)

Phenolphthalexene is identical with (**56**) save for the absence of the two methyl groups. In titrating zinc with EDTA in alkaline solution a change from colourless to violet occurs at the end-point. Thymolphthalexone (**56** but with Me replaced by $CHMe_2$ and methyl groups *meta* to the phenolic OH) gives intensely blue complexes with Ca, Sr and Ba and on titration with EDTA the colour change is from blue to smoky grey or colourless.

The best indicator for use in acidic media from 0.1 M HNO_3 up to pH 5.6 is xylenol orange (XO; **44**). Direct determinations can be made of cadmium and cobalt (at 60 °C), copper (in the presence of phen), lead and zinc, scandium, indium, yttrium and the lanthanons, zirconium, hafnium and thorium. Many other elements that block the indicator can be determined indirectly. Consecutive titrations such as Bi (at pH 2) and Pb (at pH 5.5) can be carried out in the same solution and the colour change for the latter is particularly sharp from an intense reddish violet to lemon yellow. The extensive literature on this indicator is reviewed in several places.[2,4,76,87]

Methylthymol blue and methylxylenol blue, prepared by the Mannich reaction from thymolsulfonphthalein and *p*-xylenol blue respectively, have been intensively studied and resemble xylenol orange in many respects. If only one chelating group is introduced into cresol red, semi-xylenol orange results which is a common contaminant in XO and proves to be a more sensitive reagent for zirconium.

Another group of metallochromic indicators comprises those prepared by the Mannich reaction using formaldehyde and glycine and which therefore contain the chelating group —$CH_2NHCH_2CO_2H$ adjacent to a phenolic group. Typical are glycinethymol blue, glycinecresol red (with a particularly intensely coloured red copper complex), and semi-glycinecresol red. Of numerous other indicators of different types mention should be made of glyoxal bis(2-hydroxyanil), dithizone (**26**) and zincon (**57**) which is used particularly for the determination of zinc in buffered ammoniacal solution. The colour change (blue to yellow) is very sharp.

10.6.4.4 Alizarin complexone

The condensation product of dihydroxyanthraquinone with formaldehyde and iminodiacetic acid was introduced by Belcher, Leonard and West (1958) under the name alizarin complexan (**58**), though the names alizarin complexone or (nowadays) alizarin fluorine blue are preferred. It greatly resembles xylenol orange in its general behaviour though its complexes with thorium and the lanthanons are more stable than these EDTA complexes. However, the most interesting

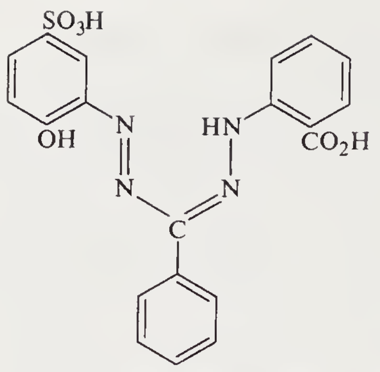

(57)

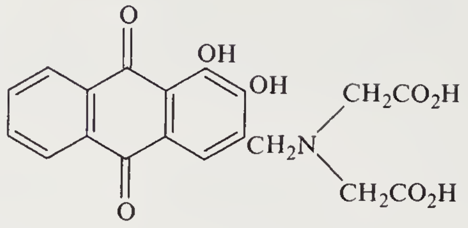

(58)

feature of this indicator lies in the behaviour of the red complexes it forms with cerium, lanthanum or praseodymium, for these form a striking blue ternary complex with fluoride ions enabling this element to be determined spectrophotometrically.[87]

10.6.4.5 Metallofluorescent indicators

By introducing the complexing moiety $—CH_2N(CH_2CO_2H)_2$ into fluorescein or umbelliferone metallochromic indicators termed calcein or fluorexone, and calcein blue or umbellicomplexone are formed. These indicators exhibit green (and blue) fluorescence in dilute alkali which disappears at pH 12 but reappears on the addition of calcium, strontium, or barium. Problems arise from the difficulty of freeing the indicators from fluorescent impurities, from self-fluorescence, and from the quenching effect of copper ions.

Table 9 Masking in EDTA Titrations

Conditions	*Masking agent*	*Cations masked*	*Cations now titratable*
Acid solutions	Thiosemicarbazide	Hg^{II}	Bi, Cd, Pb, Zn
pH 5–6	1,10-Phenanthroline	Cd, Co, Cu^{II}, Mn, Ni, Zn	Al, Pb
Alkaline	BAL(2,3-dimercaptopropanol)	As, Bi, Cd, Hg^{II}, Pb, Sb^{III}, Sn^{II}, Zn	Ca, Mg
	Triethanolamine	Al, Fe^{III}, Mn	Ca, Ni
	Tiron	Al, Fe^{III}, Ti^{IV}	Alkaline and rare earths
	Acetylacetone	Al, Be, Fe^{III}, Pd^{II}, UO_2^{2+}	Pb, Zn
pH 10	Fluoride	Al, Ca, Mg, Nb, Ta, Ti, lanthanides	Cd, Co, Ni, Zn
Strong alkali	H_2O_2	Ti^{IV}	

Details of masking by potassium cyanide, triethanolamine, thioglycollic acid, mercaptopropionic acid, BAL, unithiol, dimercaptosuccinic acid, NH_4F, H_2O_2, KOH, K_2SO_4, KI, $Na_2S_2O_3$, thiourea, thiosemicarbazide, phen, acac and demasking reactions are given by Pribil.[87]

As with all other titrations by a non-selective reagent the analysis of one metal present in admixture with others can only be encompassed with the assistance of auxiliary complexing agents. Table 9 gives an indication of what can be done in this direction but standard texts are needed to give precise operational details.[4,86,87]

10.7 OTHER ANALYTICAL APPLICATIONS OF COORDINATION COMPOUNDS

Grouped in this concluding section are brief accounts of some other analytical fields in which coordination compounds play a considerable role.

10.7.1 Redox Indicators

'Ferroin', $Fe(phen)_3^{2+}$, has been used since 1933 as a redox indicator because with the first excess of oxidant $Fe(phen)_3^{3+}$ is immediately formed with a concomitant colour change from red to blue: this redox reaction is reversible. By introducing substituents the redox potential is altered to give a range of indicators from which the correct one can be chosen for each situation. Values of E_o (volts) in 1 M H_2SO_4 are as follows: 5-nitro (1.25), 5-sulfono (1.20), ferroin itself (1.06), 5-methyl (1.02), 5,6-dimethyl (0.97), 4,7-dimethyl (0.88), and 3,4,7,8-tetramethyl (0.81).[88] 2,3,4-Substituted phenanthroline complexes of Fe^{II} and Cu^{II} show a linear relationship between E_o and the dissociation constant of the ligand.

$V(phen)_3^{2+}$ has been used as a redox indicator in the titration of $FeCl_3$ by Cr^{II} and E_o for $Ru(bipy)_3^{2+}$ is very high (1.33 V at pH = 0) and the colour change (colourless to yellow) is well marked in the titration of oxalate in 2 M perchloric acid with ceric nitrate.

The couple formed by $K_2[Fe(CN)_4phen]\cdot 4H_2O$ (λ_{max} 462) and $H[Fe(CN)_4phen]\cdot H_2O$ has the potential $E_o = 0.656$ V almost independent of pH.

Reductants such as quinol, ascorbic acid, hydroxylamine, hydrazine, $K_4Fe(CN)_6$ and tannin, and oxidants such as Ce^{IV}, Cr^{VI}, MnO_4^- can be determined spectrophotometrically at 462 nm.[89]

10.7.2 Ion Selective Electrodes

If an electrode surface comprises a film containing a weak organic ligand acid, HL, and if the aqueous phase contains ions M^{n+} which can form an extractable metal chelate ML_n, the electrode potential will be given by

$$E = E_o + (RT/nF)\left(\ln K_{ex} + \ln n - \ln C_{HL}\right) + (RT/nF)\ln\left[M^{n+}\right] \tag{28}$$

provided the value of the extraction constant, K_{ex}, is large enough for all the reagent to be transformed into its metal complex so that $C_{HL} = n[ML_n]$. Under certain circumstances equation (28) reduces to

$$E = \text{constant} + (0.059/n)\log\left[M^{n+}\right] \tag{29}$$

and the electrode will show a Nernstian slope response independent of pH.

Practical considerations call for a liquid of high viscosity and low vapour pressure and a low solubility in water. A solution of a calcium complex with a dialkylphosphoric acid (*e.g.* $((RO)_2POO)_2Ca$, where R = C_8H_{17} to $C_{16}H_{33}$) in a very polar solvent such as di-*n*-octylphenyl phosphate can be used in an ion-selective electrode that gives a linear response over $10^{-1} \gtrsim [Ca^{2+}] \geqslant 5\times10^{-5}$. Solutions of $Ni(phen)_3^{2+}$ nitrate (or perchlorate, or tetrafluoroborate) in nitrobenzene of *p*-nitrocymene have been used as specific ion electrodes for nitrate (or perchlorate, or tetrafluoroborate).[90] A mercury dithizonate electrode can be prepared which is ion-specific for mercury(II) and replaces the mercury drop electrode for the titration of Al, Ca, Cu, Hg^{II}, Ni and Zn with EDTA. Silver, lead and palladium dithizonates have also been used in titrimetry.[91]

Intense activity has also been centred on the design of neutral carriers after Stafanac and Simon had shown in 1967 that macrocyclic antibiotics such as valinomycin (**59**) showed a high sensitivity and selectivity for potassium. Apart from naturally occurring and synthetic macrotetrolides, the crown ethers (*cf.* **60**) coordinate around cations with oxygen atoms directed towards the centre, thus forming cavities whose volume can be designed to accommodate ions of specific ionic radius: in this way highly selective electrodes can be prepared from an appropriate coordination compound.[92]

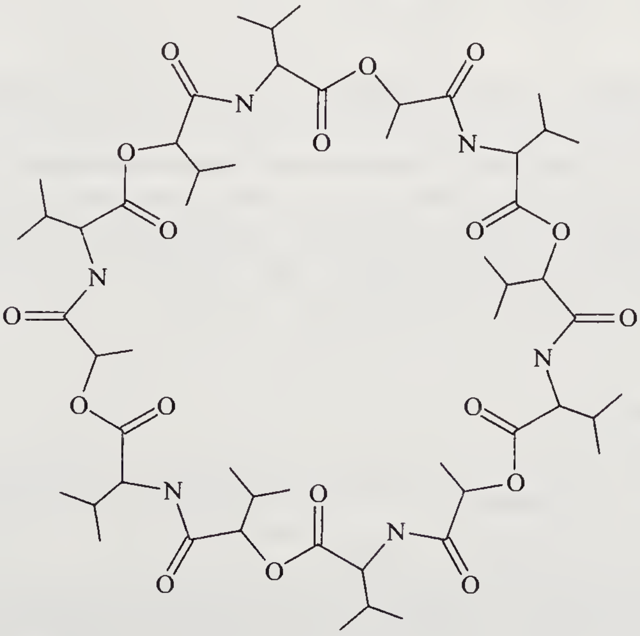

(59)

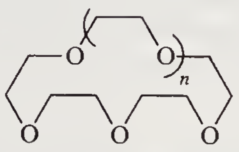

(60)

10.7.3 Gas Chromatography

10.7.3.1 Volatile metal chelates

The main problem here is to obtain suitable coordination compounds that can be vaporized at reasonably low temperatures at which they are thermally stable. To this end a great deal of work has been published on the gas chromatography of β-diketone complexes such as (**61**; $R^2 = H$).[93] Volatile complexes of the rare earths with dipivaloylmethane (**61**; $R^1 = R^3 = CMe_3$; $R^2 = H$) were first prepared in 1965 but while the separation of pairs of neighbouring metals (*e.g.* Eu and Sm) has been reported, the complete separation of the whole group has not been successfully achieved. Attempts to use columns longer than 70–75 cm result in peak-broadening and inefficient separation.[94]

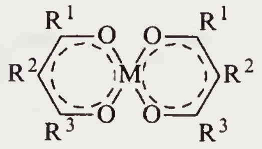

(61)

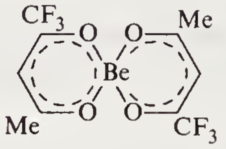

(62)

More success has been achieved with fluorinated analogues of (**61**).[2,94,95] For example, beryllium bistrifluoroacetylacetone (**62**) has been gas-chromatographed in a procedure for determining traces of beryllium down to 4 × 10^{-4} g in 10–100 mg samples of lunar dust and rock.[96]

The gas chromatography of complexes with mixed ligands (*e.g.* 1,1,1,2,2,6,6,7,7,7-decafluoroheptane-3,5-dione with neutral donors such as dibutylsulfoxide, TBP and tributylphosphine oxide) has been extensively studied but the results leave much to be desired with respect to their use in analytical separations.

10.7.3.2 Ligands containing oxygen, sulfur or nitrogen

Belcher and his colleagues examined bis chelates of $R^1CSCH_2COR^2$ and found them to be mainly monomeric.[95] Hexafluorothioacetylacetone formed a number of volatile chelates (**63**; M = Cd, Cu, Fe^{II}, Ni, Pb, Pt and Zn) with quite low melting points ranging from 108 °C (Cd) to as little as 54.5 °C (Zn), and many satisfactory separations are reported. Monothiotrifluoroacetylacetone has been used to determine Ni down to 10^{-11} g.[97]

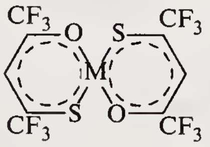

(63)

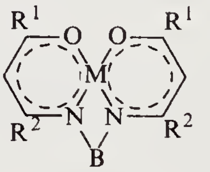

(64)

$B = (CH_2)_2$, $(CH_2)_3$ or CH_2CHMe ; $R^1 = Me$; $R^2 = Me$ or CF_3

β-Ketoiminates also form chelate complexes and tetradentate ligands form complexes such as (**64**; M = Ni, Cu, Pd and Pt). The vapour pressures of these compounds are low and chromatography must be carried out up to 250 °C. On the other hand their thermal stability is high so that there is virtually no decomposition on the column.[94] Cu and Ni have been determined down to 10^{-13} g.

Chelate complexes of diethyldithiocarbamic acid, $Et_2NCS(SH)$, with Ag and Cu^{II} are stable up to 240 °C and those of Co, Ni, Pd and Pt up to 300 °C. Complexes of Fe^{III}, Co^{III}, Ni and Zn proved to be highly stable thermally and many elegant separations have been reported.

10.7.3.3 Stationary phases: steric hindrance

A coordination polymer such as (**65**) proves to have exemplary thermal and chemical stability and it has been used as the solid phase for separating a variety of aliphatic and heterocyclic bases. Retention volumes remained constant after many hours use at 100 °C.[98]

The use of a silver salt in the stationary phase for the GLC of alkenes was one of the earliest examples of exploiting stereoselective features in coordination,[99] and dicarbonylrhodium(I)-3-trifluoroacetylcamphorate (**66**) has been shown to provide an excellent stationary phase for the GC of monoalkenes, for complex formation is stronger and the effects of structural differences between *cis* and *trans*, and between positional isomers, is more decisive.

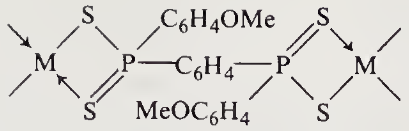

(65)

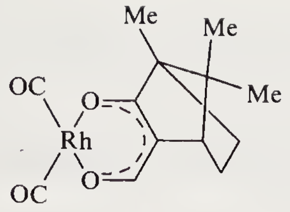

(66)

Stereochemical effects have also been exploited by using a substrate which can interact chemically to increase its coordination number. Figure 14 illustrates the separation of a number of substituted pyridines using a stationary phase containing cobalt(II)phthalocyanine (5% on Sterling F.T.G.). Since the coordination of 2-methyl (but not 3- or 4-methyl) substituted pyridines is sterically hindered, they are eluted before pyridine even though they have higher molecular masses and boiling points.[100]

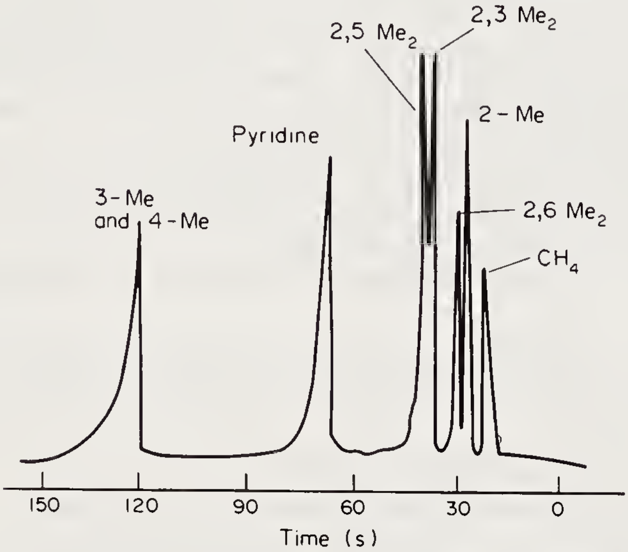

Figure 14 Separation of some pyridine bases on 5% cobalt(II) phthalocyanine supported on Sterling F.T.G. 10 m column at 175 °C with N_2 and NH_3 as carrier gas

10.8 REFERENCES

1. F. A. Cotton and G. Wilkinson, 'Advanced Inorganic Chemistry', 3rd edn., Wiley-Interscience, New York, 1972.
2. K. Ueno, in 'MTP International Review of Science', ed. T. S. West, Butterworth, London, 1973, vol. 13, chap. 2, pp. 43-69.
3. E. B. Sandell and H. Onishi, 'Photometric Determinations of Traces of Metals', 4th edn., Wiley-Interscience, New York, 1978.
4. G. Schwarzenbach and H. Flaschka, 'Complexometric Titrations', 2nd English edn., translated and revised by H. M. N. H. Irving, Methuen, London, 1969.
5. H. M. N. H. Irving, *Analyst (London)*, 1974, **99**, 787.
6. H. M. N. H. Irving, in 'Treatise on Analytical Chemistry', 2nd. edn., Wiley, New York, 1977, part 1, vol. 5, chap. 11.
7. G. Iwantscheff, 'Das Dithizon und seine Andwendung in der Mikro- und Spurenanalyse', Verlag Chemie, Weinheim, 1972.
8. H. M. N. H. Irving, 'Dithizone', 'Analytical Science Monograph', No. 5, The Chemical Society, London, 1977.
9. C. B. Amphlett, 'Inorganic Ion Exchange Materials', Elsevier, Amsterdam, 1964.
10. H. M. N. H. Irving and J. Hapgood, *Anal. Chim. Acta*, 1980, **119**, 207.
11. H. Irving and R. J. P. Williams, *Nature (London)* 1948, **162**, 746; *J. Chem. Soc.*, 1953, 3192.
12. L. E. Godycki and R. E. Rundle, *Acta Crystallogr.*, 1953, **6**, 487.
13. E. Frasson, R. Bondi and S. Bezzi, *Acta Crystallogr.*, 1959, **12**, 201.
14. E. A. Green, W. L. Duax, G. M. Smith and F. Wudl, *J. Am. Chem. Soc.*, 1975, **97**, 6689.
15. A. Ringbom, 'Complexation in Analytical Chemistry', Wiley-Interscience, New York, 1963.
16. J. Inczedy, 'Analytical Applications of Complex Equilibria', Ellis Horwood, Chichester, 1976.
17. S. Ahrland, J. Chatt and N. R. Davies, *Q. Rev., Chem. Soc.*, 1958, **12**, 265; *cf.* B. G. F. Carleson and H. Irving, *J. Chem. Soc.*, 1954, 4390.
18. D. D. Perrin, 'Organic Complexing Reagents: Structure, Behaviour, and Application to Inorganic Analysis', Wiley, New York, 1964.
19. M. L. Salutsky 'Precipitates: Their Formation, Properties, and Purity', in 'Treatise in Analytical Chemistry', ed. I. M. Kolthoff and P. J. Elving, Interscience, New York, 1959, part I, vol. I, pp. 723–764.
20. R. Berg, 'Die analytische Verwendung von o-Oxychinolin (Oxin) und seiner Derivate', 2nd edn., Enke, Stuttgart, 1938.
21. L. Erdey, 'Gravimetric Analysis', vol. I, Macmillan, London, 1963, vol. II, Pergamon, Oxford, 1964, vol. III, Pergamon, Oxford, 1965.
22. R. G. W. Hollingshead, 'Oxine and its Derivatives', Butterworth, London, 1954-6, vols. I-IV.
23. H. Irving and L. D. Pettit, *Anal. Chem.*, 1962, **122**, and refs. therein.

24. L. L. Merritt and J. K. Walker, *Ind. Eng. Chem., Anal. Ed.*, 1944, **16**, 387.
25. K. Motojima, *Bull. Soc. Chem. Jpn.*, 1956, **29**, 29, 71 and 75.
26. J. C. van Niekerk, H. M. N. H. Irving and L. R. Nassimbeni, *S. Afr. J. Chem.*, 1979, **32**, 85.
27. H. Irving and J. M. M. Griffiths, *J. Chem. Soc.*, 1954, 213.
28. H. Irving, M. J. Cabell and D. H. Mellor, *J. Chem. Soc.*, 1953, 3417; H. Irving and D. H. Mellor, *J. Chem. Soc.*, 1962, 5237; *cf.* W. A. E. McBryde, D. A. Brisbin and H. Irving, *J. Chem. Soc.*, 1962, 5222, 5245.
29. 'Stability Constants of Metal-Ion Complexes', ed. L. G. Sillén and A. E. Martell, *Chem. Soc. Spec. Publ.*, 1964, No. 17, and 1971, No. 25.
30. C. L. Wilson and D. W. Wilson (eds.), 'Classical Analysis', in 'Comprehensive Analytical Chemistry', Elsevier, Amsterdam, 1962, vol. Ic.
31. G. Spacu and J. Dick, *Z. Anal. Chem.*, 1927, **71**, 97, 442; 1928, **74**, 188; 1929, **76**, 273; *cf.* A. E. Spakowski and H. Freiser, *Anal. Chem.*, 1949, **21**, 986.
32. M. Williams, *Ind. Chemist*, 1954, 594.
33. W. J. Williams, 'Handbook of Anion Determination', Butterworth, London, 1979.
34. H. N. Wilson, *Analyst (London)*, 1951, **76**, 65; 1954, **79**, 535.
35. B. M. Vanderborght and R. E. Van Grieken, *Anal. Chem.*, 1977, **49**, 311.
36. K. V. Krishnamurty and M. M. Reddy, *Anal. Chem.*, 1977, **49**, 222.
37. Y. Marcus, *Chem. Rev.*, 1963, **63**, 139, and refs. therein.
38. T. Sekine and Y. Hasegawa, 'Solvent Extraction Chemistry', Dekker, New York, 1977.
39. R. M. Diamond and D. G. Tuck, *Prog. Inorg. Chem.*, 1960, **2**, 109 and refs. therein.
40. G. H. Morrison and H. Freiser, 'Solvent Extraction in Analytical Chemistry', Wiley, New York, 1957.
41. R. Bock, *Z. Anal. Chem.*, 1951, **133**, 110; R. Bock and E. Bock, *Z. Anorg. Allg. Chem.*, 1950, **263**, 146; W. Fischer and R. Bock, *Z. Anorg. Allg. Chem.*, 1942, **249**, 146; R. Bock and M. Herrmann, *Z. Anorg. Allg. Chem.*, 1956, **284**, 288; R. Bock, H. Kursche and E. Bock, *Z. Anal. Chem.*, 1953, **138**, 157.
42. T. Ishimori and K. Watanabe, *Bull. Chem. Soc. Jpn.*, 1960, **33**, 1443.
43. J. C. White and W. J. Ross, *Natl. Acad. Sci. Nucl. Sci.*, NAS-NS-3102, 1961 (U.S. Atomic Energy Commission).
44. B. Martin, D. W. Ockenden and J. K. Foreman, *J. Inorg. Nucl. Chem.*, 1961, **21**, 96.
45. K. Kimura, *Bull. Chem. Soc. Jpn.*, 1960, **33**, 1038; 1961, **34**, 63.
46. D. H. Liem, 'On the Solvent Extraction of Organophosphorus Extractants in the Organic Phase', Inaugural Dissertation, Stockholm, 1976.
47. Z. Kolarik, *Solvent Extr. Rev.*, 1971, **1**, 1.
48. D. F. Peppard, W. J. Driscoll, R. J. Sironen and S. McCarty, *J. Inorg. Nucl. Chem.*, 1957, **4**, 326.
49. S. Ahrland, J. O. Liljenzin and J. Rydberg, 'Actinide Solution Chemistry', in 'Comprehensive Inorganic Chemistry', Pergamon, Oxford, 1973, vol. 5.
50. C. F. Coleman and J. W. Roddy, *Solvent Extr. Rev.*, 1971, **1**, 63.
51. H. Irving and R. J. P. Williams, *J. Chem. Soc.*, 1941, 1841.
52. J. Starý, 'The Solvent Extraction of Metal Chelates', Pergamon, New York, 1964.
53. K. I. Pashkevich, V. I. Saloutin and I. Ya. Postovskii, *Russ. Chem. Rev.*, 1981, **50**, 180.
54. A. M. Poskanzer and B. M. Foreman, *J. Inorg. Nucl. Chem.*, 1961, **16**, 323.
55. V. M. Peshkova, I. P. Efimov and N. N. Magdesieva, *Zh. Anal. Khim*, 1966, **21**, 499.
56. S. G. Tandon and S. C. Bhattacharyya, *Anal. Chem.*, 1961, **33**, 1267.
57. A. D. Shendrikar, *Talanta*, 1969, **16**, 542.
58. A. T. Pillipenko and E. R. Falendysh, *Russ. Chem. Rev.*, 1972, **41**, 991.
59. C. H. R. Gentry and L. G. Sherrington, *Analyst (London)*, 1950, **75**, 17.
60. R. G. Anderson and G. Nickless, *Analyst (London)*, 1967, **92**, 207.
61. S. B. Savvin, *Talanta*, 1968, **15**, 1494.
62. B. Budesinsky, 'Chelates in Analytical Chemistry', ed. H. A. Flaschka and A. J. Barnard, Jr., Dekker, New York, 1969.
63. J. McB. Harrowfield, C. Pakatwatchai and A. H. White, *J. Chem. Soc., Dalton Trans.*, 1983, 1109.
64. H. Irving, in 'Solvent Extraction Chemistry', ed. D. Dyrssen, J. O. Liljenzin and J. Rydberg, North Holland, Amsterdam, 1967.
65. T. V. Healy, in 'Solvent Extraction Research', Proceedings of the 5th ISEC, ed. A. S. Kertes and Y. Marcus, Wiley-Interscience, New York, 1969.
66. Yu. E. Nikitin, Yu. I. Murinov and A. M. Rozen, *Russ. Chem. Rev.*, 1976, **45**, 1155.
67. C. Madic, *Chim. Anal.*, 1972, **54**, 102.
68. H. Irving, *Chem. Ind.* (*London*), 1974, 639.
69. E. N. Dorokhova and I. P. Alimarin, *Russ. Chem. Rev.*, 1979, **48**, 502.
70. S. Tribalat, *Anal. Chim. Acta*, 1949, **3**, 113; 1950, **4**, 228.
71. E. L. Smith and J. E. Page, *J. Soc. Chem. Ind.*, 1948, **67**, 48.
72. H. M. N. H. Irving and R. H. Al-Jarrah, *Anal. Chim. Acta*, 1971, **55**, 135; 1973, **63**, 79; and unpublished results.
73. C. Woodward and H. Freiser, *Talanta*, 1973, **20**, 417.
74. M. Nishimura, K. Matsunaga, T. Kudo and F. Obara, *Anal. Chim. Acta*, 1973, **65**, 466.
75. H. M. N. H. Irving, *J. Radioanal. Chem.*, 1976, **33**, 287.
76. W. C. Johnson (ed.), 'Organic Reagents for Metals', Hopkin and Williams, Essex, 1955, vol. 1, 1964, vol. 2.
77. J. Fries and H. Getrost, 'Organic Reagents for Trace Analysis', Merck, Darmstadt, 1977.
78. H. Irving and D. H. Mellor, *J. Chem. Soc.*, 1962, 5222, 5237.
79. A. T. Pilipenko and E. R. Faiendysh, *Russ. Chem. Rev.*, 1972, **41**, 991.
80. A. A. Schilt, 'Analytical Applications of 1,10-Phenanthroline and Related Compounds', Pergamon, Oxford, 1969.
81. 'IUPAC Tables of Spectrophotometric Absorption Data of Compounds used for the Colorimetric Determination of Elements', Butterworth, London, 1963.
82. A. K. Babko, *Talanta*, 1968, **15**, 721.
83. F. Feigl and V. Anger, 'Spot Tests in Inorganic Analysis', 6th edn., translated R. E. Oesper, Elsevier, Amsterdam, 1982.
84. I. M. Kolthoff and V. A. Stenger, 'Volumetric Analysis', Interscience, New York, 1942, vol. 1, 1947, vol. 2.
85. A. E. Martell and R. M. Smith, 'Critical Stability Constants', Plenum, New York, 1974, vol. 1.
86. R. Pribil, 'Analytical Applications of EDTA and Related Compounds', Pergamon, Oxford, 1972.
87. R. Pribil, 'Applied Complexometry', Pergamon, Oxford, 1982.

88. T. H. Whitehead and C. C. Willis, Jr., *Chem. Rev.*, 1941, **29**, 69.
89. A. A. Schilt and A. M. Gresswell, *Talanta*, 1968, **15**, 911.
90. W. E. Van der Linden, 'Ion Selective Electrodes', in 'Comprehensive Analytical Chemistry', ed. G. Svehla, Elsevier, Amsterdam, 1981, vol. XI, chap. 3.
91. H. M. N. H. Irving, *CRC Crit. Rev. Anal. Chem.*, 1980, **8**, 321.
92. J. Vesely, D. Weiss and K. Stulik, 'Analysis with Ion-Selective Electrodes', Ellis Horwood, Chichester, 1978.
93. R. W. Moshier and R. E. Sievers, 'Gas Chromatography of Metal Chelates', Pergamon, Oxford, 1965.
94. D. N. Sokolov, *Russ. Chem. Rev.*, 1977, **46**, 388.
95. R. Belcher, *Pure Appl. Chem.*, 1973, **34**, 13.
96. K. J. Eisentraut, D. J. Gries and R. E. Sievers, *Anal. Chem.*, 1971, **43**, 2003.
97. E. Bayer, H. P. Muller and R. Sievers, *Anal. Chem.*, 1971, **43**, 2012.
98. J. Delventhal, H. Keck and W. Kuchen, *Angew. Chem.*, 1972, **84**, 435, 832.
99. B. W. Bradford, D. Harvey and D. E. Chalkley, *J. Inst. Petroleum (London)*, 1955, **41**, 80; *cf.* D. L. Schmitt and H. B. Jonassen, *Anal. Chim. Acta*, 1970, **49**, 580.
100. E. Gil-Av and V. Schurig, *Anal. Chem.*, 1971, **43**, 2030.

Subject Index

Formula Index